Texas Water Resources Institute TR-436
February 2013

2012 International SWAT Conference Proceedings

Dan Kiniry, Texas A&M University
Courtney Smith, Texas A&M AgriLife Resesarch
Raghavan Srinivasan, Texas A&M AgriLife Research

Texas Water Resources Institute
make every drop count

2012 International SWAT Conference Proceedings

Indian Institute of Technology Delhi

SWAT 2012
IIT Delhi, India

Texas Water Resources Institute

TR-436, 2013

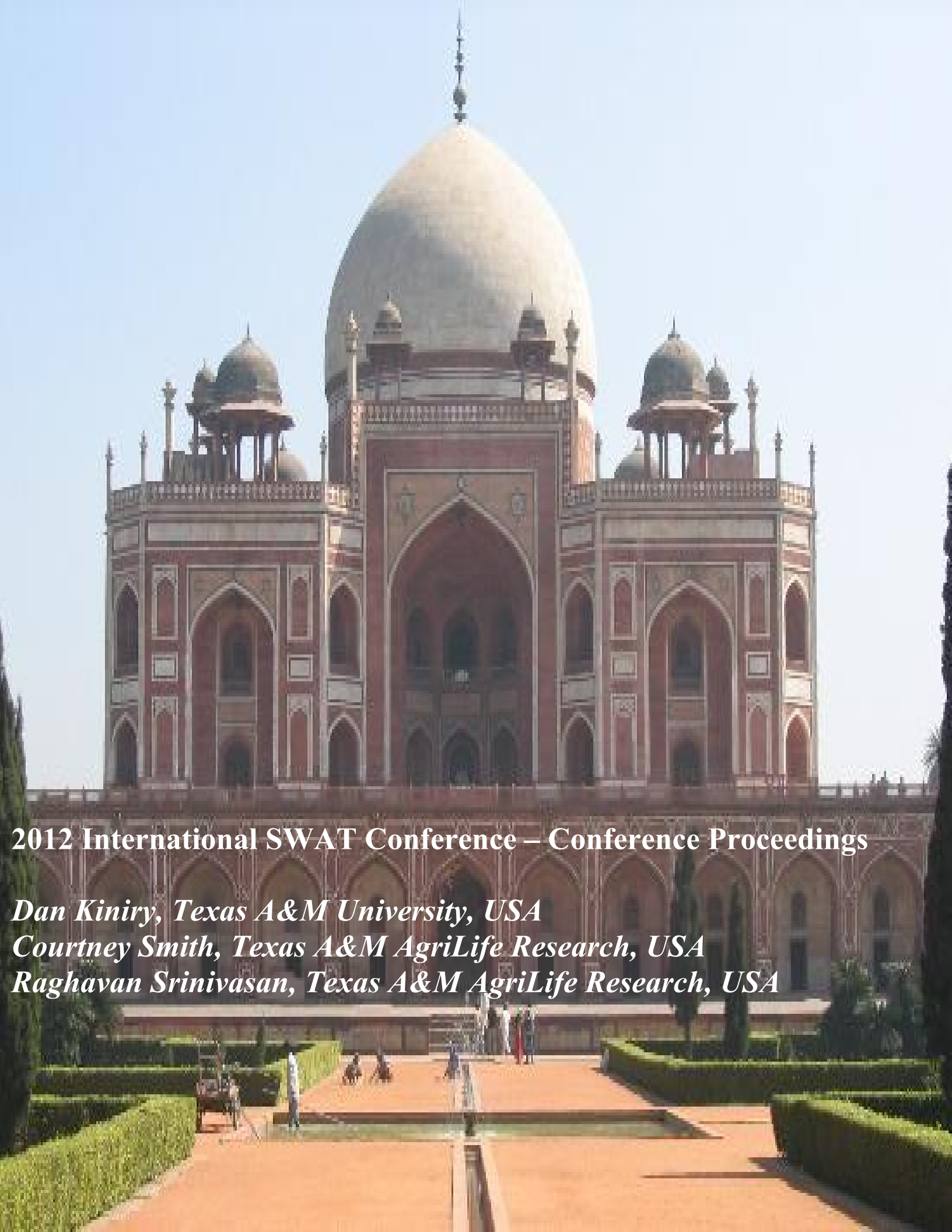

2012 International SWAT Conference – Conference Proceedings

Dan Kiniry, Texas A&M University, USA
Courtney Smith, Texas A&M AgriLife Research, USA
Raghavan Srinivasan, Texas A&M AgriLife Research, USA

Organizing Committee

Dr. A.K. Gosain, Indian Institute of Technology, Delhi
Dr. Balaji Narasimhan, Indian Institute of Technology, Madras
Dr. Jeff Arnold, U.S. Department of Agriculture-Agricultural Research Service, USA
Dr. R. Srinivasan, Texas A&M AgriLife Research, Texas A&M University, USA
Courtney Smith, Texas A&M AgriLife Research, USA

Scientific Committee

Karim Abbaspour, EAWAG, Switzerland

A. K. Gosain, Indian Institute of Technology Delhi

R. Srinivasan, Texas A&M University, USA

Eldho Iype, Indian Institute of Technology, Bombay

Valentina Krysanova, PIK, Germany

Sue White, Cranfield University, United Kingdom

Sandhya Rao, INRM Consultants, India

Fred F. Hattermann, Potsdam Institute for Climate Impact Research, Germany

Xuesong Zhang, Pacific Northwest National Laboratory, USA

P. P. Mujumdar, Indian Institute of Science

N. H. Ravindranath, Indian Institute of Science, Bengaluru

Karim Abbaspour, EAWAG, Switzerland

Ann van Griensven, UNESCO-IHE, The Netherlands

Indrajeet Chaubey, Purdue University, USA

Xuesong Zhang, Pacific Northwest National Laboratory, USA

K. P. Sudheer, Indian Institute of Technology, Madras

Jeff Arnold, USDA-ARS, USA

Pramod Aggarwal, International Water Management Institute, Delhi, India

Philip Gassman, Iowa State University, USA

Nicola Fohrer, Christian-Albrechts-University, Kiel, Germany

José M. Sánchez-Pérez, ECOLAB, France

Martin Volk, Helmholtz Centre for Environmental Research - UFZ, Germany

Mike White, USDA-ARS, USA

Scientific Committee

Arvind K. Nema, Indian Institute of Technology, Delhi C. Allan Jones, Texas AgriLife Research, USA

Antonio Lo Porto, IRSA, Italy

Mike White, USDA-ARS, USA

Pushpa Tuppad

Amit Garg, Public Systems Group

Narendra Signh Raghuwanshi, Indian Institute of Technology, Kharagpur

Muthiah Perumal, Indian Institute of Technology Roorkee, India

Antonio Lo Porto, IRSA, Italy

Jose Maria Bodoque Del Pozo, UCLM, Spain

D. Nagesh Kumar, Indian Institute of Science, Bangalore

Kapil Dev Sharma, Government of India

Dhrubajyoti Sen, Indian Institute of Technology, Kharagpur

Nicola Fohrer, Christian-Albrechts-University, Kiel, Germany

Ann van Griensven, UNESCO-IHE, The Netherlands

Balaji Narasimhan, Indian Institute of Technology, Madras

P. Rajendra Prasad, Andhra University, Visakhapatnam, India

Subashisa Dutta, Indian Institute of Technology, Guwahati

Jeff Arnold, USDA-ARS, USA

R. Srinivasan, Texas A&M University, USA

José M. Sánchez-Pérez, ECOLAB, France

Virginia Jin, USDA-ARS, USA

A. K. Mittal, Indian Institute of Technology Delhi, India

Nicola Fohrer, Christian-Albrechts-University, Kiel, Germany

Ann van Griensven, UNESCO-IHE, The Netherlands

Jaehak Jeong, Texas AgriLife Research, USA

Scientific Committee

Arup Kumar Sarma, Indian Institute of Technology, Guwahati

Ann van Griensven, UNESCO-IHE, The Netherlands

R. Srinivasan, Texas A&M University, USA

Pedro Chambel Leitão, IST-MARETEC, Portugal Dharmendra Saraswat,

University of Arkansas, USA

C. Allan Jones, Texas AgriLife Research, USA

Jaehak Jeong, Texas AgriLife Research, USA

Amit Garg, Public Systems Group

Kapil , Indian Institute of Technology, Bombay Gupta

Valentina Krysanova, PIK, Germany

Martin Volk, Helmholtz Centre for Environmental Research - UFZ, Germany

Pedro Chambel Leitão, IST-MARETEC, Portugal

Scientific Committee

Jaehak Jeong, Texas AgriLife Research, USA

José M. Sánchez-Pérez, ECOLAB, France

D. R. Kaushal, Indian Institute of Technology Delhi, India

Pranab Mohapatra, University of South Carolina

Balaji Narasimhan, Indian Institute of Technology - Madras

A. K. Gosain, Indian Institute of Technology Delhi

Sandhya Rao, INRM Consultants, India

B. S. Murty, Indian Institute of Technology Madras, India

B. R. Chahar, Indian Institute of Technology Delhi, India

Subashisa Dutta, Indian Institute of Technology, Guwahati

Dharmendra Saraswat, University of Arkansas, USA

Indrajeet Chaubey, Purdue University, USA

Balaji Narasimhan, Indian Institute of Technology - Madras

A. K. Gosain, Indian Institute of Technology Delhi

D. Nagesh Kumar, Indian Institute of Science, Bangalore

Sharad Jain, Indian Institute of Technology, Roorkee

Kapil Dev Sharma, Government of India

Balaji Narasimhan, Indian Institute of Technology, Madras

D. Nagesh Kumar, Indian Institute of Science, Bangalore

Rakesh Khosa, Civil Engineering Department, IIT Delhi, Hauz Khaz, New

Foreword

It was such a satisfying experience to host at the Department of Civil Engineering, IIT Delhi, New Delhi, the 2012 SWAT Conference and Workshops during July 16-20, 2012. Over the years, this event has become globally a very coveted and eagerly awaited event.

The untiring efforts of Jimmy, Jeff, Srini (as Drs. J. R. Williams, J. G. Arnold, R. Srinivasan are known to the SWAT community) with many other workers of their team saw the initial versions of SWAT (Soil and Water Assessment Tool) to reach a status in later part of nineties where the user and developer community of hydrological modelling across the Globe started accepting the SWAT as a product worth using. The popularity was not only due to the fact that it was a very robust model, which indeed it is, but also because of the fact that they were very sincere in extending a helping hand to whosoever wanted to use it and even participate in its enhancement. While doing so they not only have helped tens of hundreds of scientists but also championed the philosophy of collective development of the mathematical models that are essential to solve many of the recent problems of water resources in a transparent manner where everybody is welcome to participate in any capacity. I still remember like yesterday, although it was in 1996, when I approached Srini and Jeff that IIT Delhi shall like to use the model, the reply was so positive and warm that a bond was created that is still going strong till today.

The SWAT workshops have also become a part and parcel of these events where many of the budding researchers are inducted into the use of SWAT model to solve the problems being faced in their countries.

For those who are still not connected to the model, SWAT is developed by a group of scientists from the United States Department of Agriculture - Agricultural Research Service (USDA-ARS); the United States Department of Agriculture - Natural Resources Conservation Service (USDA-NRCS) and Texas AgriLife Research. It was developed to predict the impact of land management practices on water, sediment and agricultural chemical yields in large complex watersheds with varying soils, land use and management conditions over long periods of time.

Over one hundred and twenty papers were presented in SWAT 2012. It is for the first time that Non-SWAT papers were also allowed in the conference to enable researchers working in the area of water resources to interact with the SWAT community.

I take this opportunity to thank all the participants who participated in the conference and made it a grand success. I am sure that they would have gone satisfied with the opportunity they got to interact with the best researchers in the world and to listen to them. However, the total proceedings of the conference are available at http://swat.tamu.edu/conferences/2012/ in the form of videos of the presentations. The present volume of the full paper proceedings shall provide an opportunity to the researchers to access all the papers ranging over a large cross section of the water resources problems being faced by the society. It shall also inspire an enthusiasm in new entrants into the modelling by widening their understandings in the field of hydrologic modelling. I wish everyone a very fruitful reading.

Dr. A. K. Gosain,
Professor,
Department of Civil Engineering
Indian Institute of Technology Delhi, New Delhi - 110016, India

Table of Contents

Session A4: SWAT Applications and Development in India

Session B1: Hydrology

Session B2: Large Scale Applications

Session B3: Database and GIS Application & Development

Session C1: Climate Change Applications

Session C2: Irrigation Water Management

Session C4: Hydrology

Session D1: Hydrology

Session D2: Sediment, Nutrients & Carbon

Session D3: Climate Change Application

Session E1: SWAT Applications and Development in India

Session E2: Irrigation Water Management

Session E3: Environmental Applications

Session E4: Hydrology

Session F1: Sensitivity Calibration and Uncertainty

Session F2: Climate Change Applications

Session F3: Hydrology

Session F4: Large Scale Applications

Session G1: Resources Applications

Session G2: Sensitivity Calibration and Uncertainty

Session G3: SWAT Applications and Innovations from the CGIAR Global Spatial Analysis and Modeling Topic Working Group (SAM)

Session H1: Ganga River Basin Management

Session H4: Database and GIS Applications & Development

Session J1: Model Development

Session J3: Poster Session

Session J4: Environmental Applications

Impact of recharge sources on isotopic composition and microbiological quality of groundwater- a case study from Punjab, India

Saroj Kumari
Gurukul Kangri Vishvavidyalaya, Haridwar
M S Rao
Hydrological Investigation Division, National Institute of Hydrology, Jalvigyan Bhawan, Roorkee Uttarakhand 247 667, India
Shyam Lal
Hydrological Investigation Division, National Institute of Hydrology, Jalvigyan Bhawan, Roorkee Uttarakhand 247 667, India
Padma Singh
Gurukul Kangri Vishvavidyalaya, Haridwar
Gopal Krishan
Hydrological Investigation Division, National Institute of Hydrology, Jalvigyan Bhawan, Roorkee Uttarakhand 247 667, India
Corresponding Author: drgopal.krishan@gmail.com

Abstract

A study was conducted to find out the impact of recharge sources on isotopic and microbiological quality of groundwater in a transect of Hoshiapur district of Punjab, India. The water samples were collected from deep and shallow regions and were subjected to isotopic and microbiological analysis.

The groundwater salinity in deep aquifer follows a narrow range (510 μS/cm to 660 μS/cm) compared to that at shallow aquifer groundwater (760 μS/cm to 1960 μS/cm).The results of microbiological analysis show that deep water contains higher number of bacterial population than shallow water. The isotopic composition in shallow groundwater ranged from -4.49‰ to -5.87‰ for $\delta^{18}O$ & -35.24‰ to -39.57‰ for δ D and in deep groundwater the values of $\delta^{18}O$ ranged from -4.79‰ to -7.01‰ and δ D ranged from -38.50‰ to -43.24‰. The isotopic values of the deeper aquifers were more depleted than the shallow aquifers.

The integrated studies clearly show that (i) using isotopes groundwater recharge source and interaction between shallow and deep aquifer can be monitored, (ii) bacteriological colonies can infilterate and contaminate even deep aquifers whenever there is interaction between shallow and deep groundwater., (iii) the pollution due to anthropological influence changes groundwater salinity and also cause bacteriological contamination of groundwater and (iv) natural freshwater recharge freshens the quality of water and the length over which freshening results depends upon level of pre-contamination and fresh water recharge conditions.

Keywords: Stable isotopes, bacteriological analysis, groundwater, recharge sources, Punjab

Introduction

Groundwater is a vital element to sustain life and is widely used for drinking, irrigation and industrial purposes. The primary resource of groundwater recharge is precipitation. In addition to precipitation, other surface water sources such as canal, pond, drain, also contribute over a time depending upon its transverse in the area of recharge, however decreasing availability of groundwater due to rapid growth of population, urbanization and agricultural activities is increasingly placing stress on both human communities and surrounding environmental

system. Moreover, the groundwater quality is also deteriorating due to geogenic and anthropogenic activities. The quality deterioration may be physical, chemical or microbiological. Microbial contamination of groundwater is increasing due to an increase in number of point and nonpoint sources of pollution.

Groundwater is found in aquifers, which are the layers below the ground with the capability of both storing and transmitting the water. Most rainwater is absorbed by the ground and fills the tiny spaces between soil particles. The excess water which is not absorbed runs over the top of the soil until it reaches a river, stream, or reservoir. The absorbed water in the ground trickles down through soil pores until it touches to the water table. The sub-surface water containing zone is called aquifer. The aquifer stores and transmits water from the recharge region to the discharge zone. Water can be pumped out from an aquifer. Aquifers are of two types unconfined and confined aquifer. Unconfined aquifer is those into which water seeps from ground surface directly above the aquifer. Confined are those in which an impermeable dirt/rock layer exists preventing water from seeping into aquifer from the ground surface.

We are mostly concerned about unconfined aquifers because they are not "protected" by an impermeable layer. This means that if anything leaks or spills into the soil above the unconfined aquifer, it will seep into and contaminates the water. This is why we wouldn't want to drill our drinking water well in an unconfined aquifer.

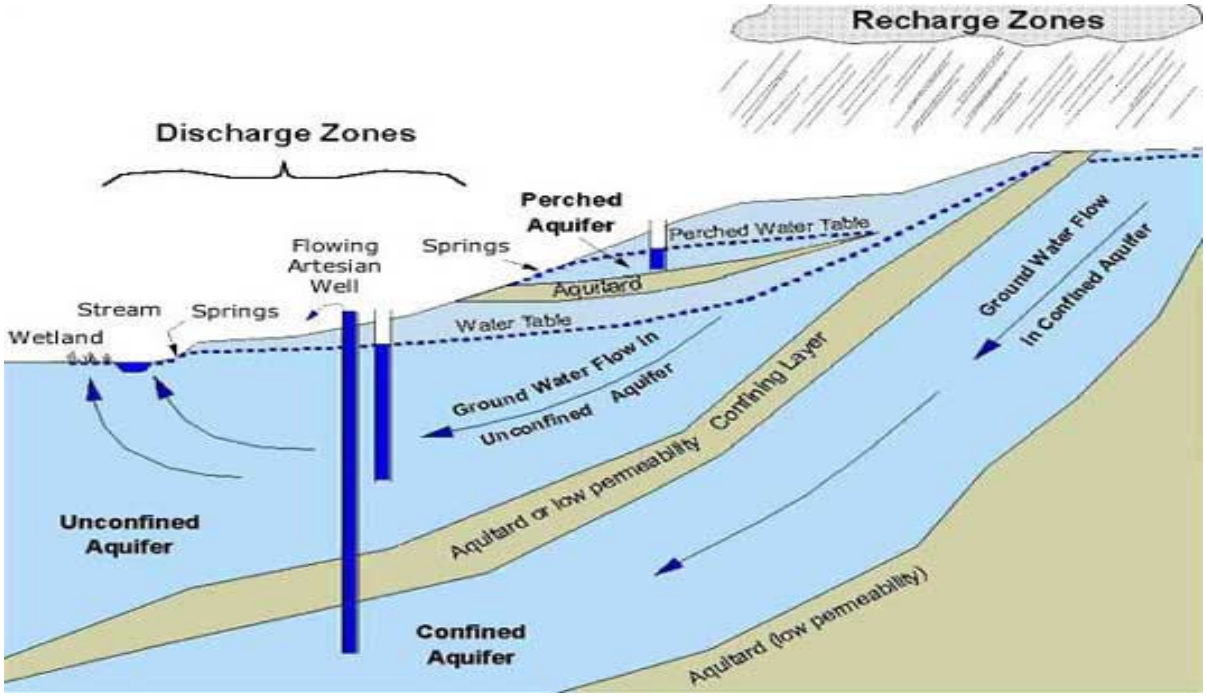

Fig. 1: schematic flow of aquifer in groundwater

Groundwater can be contaminated in many ways. If surface water that recharges the aquifer is contaminated, the groundwater will also become contaminated. This can, in turn, affect the quality of surface water at discharge areas. Groundwater can also be contaminated by liquid hazardous substances (or solids that

can dissolve in water) that filter through the soil into groundwater, by saltwater moving in from the ocean, or by minerals that are naturally present in the area.

Until the 1970's, scientific concepts and methods limited our knowledge of groundwater microbiology. First, it was common to assume that the ground- water environment was devoid of life. Second, methods for sampling ground- water environments for microbes were very limited. Third, it was generally assumed that water passing through the soil was purified by active microbial processes and by filtration; therefore, there was little concern with ground- water contamination. As ground-water contamination became more and more evident during the 1980's, the motivation for understanding ground-water environments increased and new methods in microbiology, based on advances in molecular biology, provided microbiologists with new tools to explore this difficult-to-sample microbial habitat.

Isotopes are useful in tracing the groundwater flow paths and in analyzing the mixing ratio quantitatively for multiple recharging sources forming the groundwater. Isotope ratio provides information on the rate of chemical reaction, evaporation effects, condensation process, diffusive processes etc. similar to DNA fingerprinting, Isotope provides fingerprint indexing to the recharge sources. However the microbiological and chemical quality in groundwater are compared in several previous reports (Jimenez *et al*., 2006; Munoz *et al*., 2004; Pacheco *et al*., 2004; Perez and Pacheco, 2004; Ramirez *et al*., 2009, 2010; Robles *et al*., 2009, 2010) but there was no study carried out using the isotopic techniques and microbiological quality to know impact of recharge sources on groundwater.

Therefore, the present study are carried out with an objective to investigate the impact of recharge sources on isotopic and microbiological quality of groundwater in a transect of Hoshiarpur district of Punjab.

Study area

Present study is taken up in the Hoshiarpur district located in the Beas-Satluj Doab region of the Punjab state. Hoshiarpur district falls in the eastern part of the Punjab State and is bounded by North latitudes $30^0$58’30’’ and $32^0$08’00’’and East longitudes $75^0$28’00’’ and $76^0$30’00’’. The district is drained by the river Beas in the north and northwest and Satluj in the south. The area comprises three distinct geomorphologic units, viz, hilly area in the northeast, piedmont zone belt and the alluvial plains occurring south western part of the district.

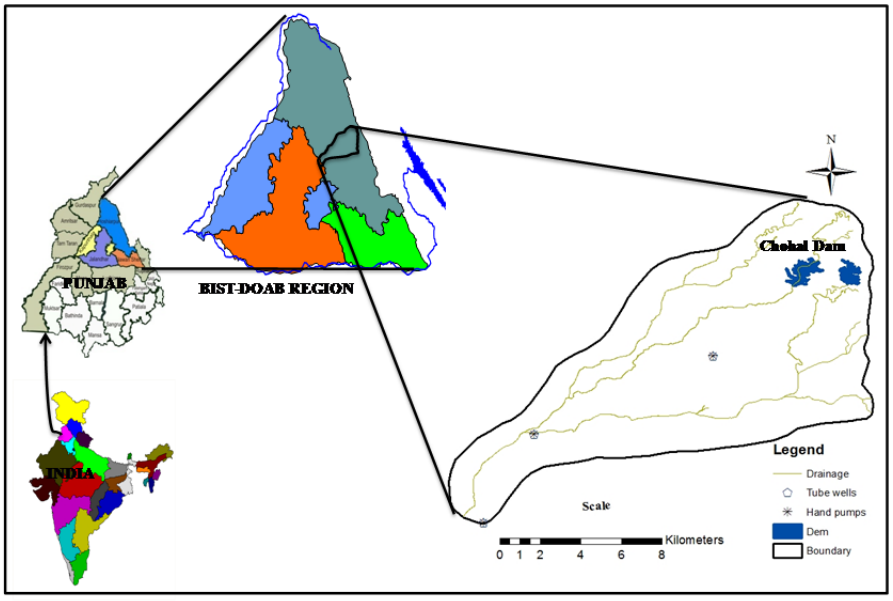

Fig. 2: Study area

The study of exploratory boreholes drilled by of Central Ground Water Board (1999, 2000) indicated presence of three aquifer group's up to 425m depth below ground level. A total of 3 distinct aquifer groups as under were deciphered.

Aquifer Group	General Depth Range (m bgl)	Nature
I	0 to 55	Unconfined consisting of individual sand & clay layers
II	160 to 225	Semi-confined/ confined consisting of Individual sand and clay layers.
III	380 to 425	Confined, consisting of thin sand layers alternating with thicker clay layer.

In the rest of the area the ground water likely to occur under unconfined conditions in shallow aquifers and under semi-confined to confined condition in deeper aquifers. The depth to water level is deeper in the south-eastern and shallow in north eastern parts and central and south-western parts. The depth to water level during post monsoon period ranges between 4.41m bgl to 19.84m bgl.

Materials and methods

3.1 Sample collection

The groundwater samples were taken from the Tube wells and Hand pump of the irrigated lands at a depth of 137 m to 231 m and at the shallow region of 18 m to 30 m from the ground level (Table 1). The ground water samples were collected from 3 locations Adamwal, Hoshiarpur and Nusrala and from two different depths at each location. All the samples were collected in clean sterile plastic containers after flushing out pre-stored

groundwater in order to collect pure dynamic aquifer water. The samples were transported to the laboratory using ice-box for analysis of physic-chemical parameters and bacteriological quality.

Table 1: Physiographical details of the groundwater samples

S.No	Sample code	Location of sample	Altitude (m)	Latitude	Longitude	Source of sample	Depth (m)
1	2, 2	Hoshiarpur	313	31° 31'56.2"	75°51'13.3"	Tube well	231.64
2	1, 1					Hand pump	30.48
3	3, 1	Adamwal	323	31°34'01.8"	75°55'59.8"	Tube well	228.6
4	4, 2					Hand pump	24.38
5	5, 1	Nusrala	267	31°29'34.8"	75°49'53.6"	Tube well	137.16
6	6, 2					Hand pump	18.28

3.2 Microbiological analysis

The bacteriological enumeration was done by plate count, pour plate, serial agar plate methods and isolation by streak plate method. The serial dilution technique is one of the most routinely used procedure because of the enumeration of the viable cells by this method .This method is based on the principle that when material containing bacteria is cultured ,every viable bacterium develops into a visible colony on a nutrient agar medium**.** The no. of colonies, therefore, are same as the number of the organism contained in the sample.

The bacterial concentration is calculated using the following formula

$$\text{No. of cells / ml or g} = \frac{\text{No. of colonies } \mathbf{x} \text{ dilution factor}}{\text{Quantity of water samples}}$$

(In the present study, 1 ml of water sample is taken for the analysis)

Therefore, the above equation reduces to;

No. of cells / ml = no. of colonies **x** dilution factor

In the present analysis dilution factor 10^1 to 10^5 is used.

The gram stain test was performed to identify bacteria as gram positive or gram negative and it is also used to determine bacterial shape. The catalase activity test and starch hydrolysis tests were also carried out for identification of bacteria on the basis of differential metabolism.

Isotopic analysis

Oxygen and hydrogen isotopic analyses were carried out using a dual-inlet isotope ratio mass spectrometer (Isoprime with Masslynx software Ver. 4.0). For statistical consistency, three aliquots of each sample were taken. $\delta^{18}O$ analysis was carried out using a CO_2 equilibration method (Epstein and Mayeda, 1953) whereas measurement of the deuterium/hydrogen (D/H) ratio was performed with hydrogen gas in the presence

of platinum (Pt catalyst, marketed as Hokko Beads). Secondary standards used in the batch were pre-calibrated using the primary standards and pre-analysed samples procured from the International Atomic Engery Agency, Vienna. The precision of estimated $\delta^{18}O$ and δD was within ±0.1‰ and ±0.1‰, respectively. Ratios of the standard originated from the Vienna Standard Mean Ocean Water (VSMOW) for water. Triplicate measurements of water for $\delta^{18}O$ of water yielded a standard deviation of ±0.05‰.

Results and discussion

4.1 Microbiological analysis

Plate count method was used to determine the total no. of the cells in per ml of the sample. Water samples are diluted to the 10^{-1} to 10^{-6}. By pour plate method bacterial colonies are grown on the Nutrient Agar Plate (NAM). Different types of the bacterial colonies are appeared on the NAM plates. We counted these colonies by standard plate count method. The average no. of colonies found in each dilution is described in the table 2.

Table2. Enumeration of bacterial population from Hoshiarpur, Adamwal and Nusrala (average triplicates)

Hoshiarpur

Dilutions	**sample_1 (deep region) average no. of colony**	**sample_2 (shallow region) average no. of colony**
10^{-4}	102×10^{-4}	63×10^{-4}
10^{-5}	95×10^{-5}	35×10^{-5}
10^{-6}	91×10^{-6}	35×10^{-6}

Adamwal

Dilutions	**sample _1 (deep region) average no. of colony**	**sample_2 (shallow region) average no. of colony**
10^{-4}	110×10^{4}	65×10^{4}
10^{-5}	57×10^{5}	31×10^{5}
10^{-6}	44×10^{6}	24×10^{6}

Nusrala

Dilutions	**sample _1 (deep region) average no. of colony**	**sample_2 (shallow region) average no. of colony**
10^{-4}	110×10^{4}	76×10^{4}
10^{-5}	65×10^{5}	30×10^{5}
10^{-6}	30×10^{6}	26×10^{6}

As evident from the table 2, the no. of the bacterial population is decreasing with the increase in dilution. This variation of the colonies in increasing the dilutions is due to the fragmentation of the parental bacterial colonies into its finer colonies. While increasing the dilutions the bacterial colonies start breaking itself up to the stage

when each colony breaks into individual bacteria. So at this stage dilution show the exact size counting of the bacteria but due to their size it is not possible to count them. That is why the dilutions are limited to 10^{-1} to$10^{-6.}$

Standard plate count method is much useful in the comparison of the two samples than the counting of the absolute no. of the bacterial colonies. The other reason of using this method is that it is the faster method. In process of the dilution method sample vigoursaly shaken for the uniform dispersion of the bacteria in the sample.

For the identification of the bacterial species pure cultured is isolated from the mixed culture. By the streak plate method on the NAM plates.

Isolated pure bacterial culture is identified for the particular bacterial species by Gram's staining and some biochemical tests like catalase test and starch hydrolysis tests. Bacterial species which are identified are ***Bacillus spp., Staphylococcus aureus, E.coli, Streptococcus lactis, and Micrococcus luteus.*** Biochemical test and Morphological characteristics' of the identified bacterial colonies are shown in the table 3.

Table 3. Morphological and biochemical characterization of bacteria from Hoshiarpur, Adamwal and Nusrala region

Hoshiarpur

CHARACTERSTICS	**DEEP REGION**	**SHALLOW REGION**	
Morphological characteristics	**E.coli**	**Bacillus sp.**	**E.coli**
Growth	Moderate	Slight, Waxy growth	Moderate
Form	Circular	Circular	Circular
Margins	Entire	Entire	Entire
Pigmentation	Yellow	White	Yellow
Biochemical tests			
Gram staining	-ve rods	+ve rods	-ve rods
Catalase test	+	+	+
Starch hydrolysis test	-	+	-

Adamwal

Nusrala

After microbiological analysis of the collected water samples of different depth of the tube

CHARACTERSTICS	DEEP REGION		SHALLOW REGION	
Morphological characteristics	**E.coli**	**Bacillus**	**Streptococcus lactis**	**Micrococcus**
Growth	Moderate	Slight, waxy growth	moderate	Abundant
Form	Circular	circular	Circular	Circular
Margins	Entire	Entire	Entire	Entire
Pigmentation	Yellow	White	Yellow	Creamish
Biochemical tests				
Gram staining	-ve rods	+ve rods	+ve coccus	+ve coccus
Catalase test	+	+	-	+
Starch hydrolysis test	-	+	-	-

CHARACTERSTICS	DEEP REGION		SHALLOW REGION
Morphological characteristics	**Staphylococcus aureus**	**Streptococcus lactis**	**Staphylococcus aureus**
Growth	Moderate	moderate	moderate
Form	Circular	Circular	Circular
Margins	Entire	Entire	Entire
Pigmentation	White	Yellow	white
Biochemical tests			
Gram staining	-ve rods	+ve coccus	-ve rods
Catalase test	+	-	+
Starch hydrolysis test	-	-	-

wells and hand pump has different bacterial concentration in different places. In the deeper region the bacterial concentration is higher than that of the shallow region and in some places common bacterial species are found in both deeper and shallow region. This shows that it may be possible that water flow in same direction. The reason of the different bacterial species in different places may be due to environmental variation and the factors which are responsible for the growth of the bacteria.

Some common bacteria found in the different places show that there is a connection between the places like *E.coli* and *Bacillus* is found in both the places Hoshiarpur and Nusrala, same is in the case of the case of the *Streptococcus lactis* is found in both Nusrala and Adamwal. So it is concluded that the flow of the water of Nusrala is linked with both the Hoshiarpur and Adamwal. Another cause is may be due to the hydrochemistry

and nutrient chemistry which is dependent on the nutrients present in the land use and the quality of the rechargeable water. Recharge sources of the groundwater are may be due to the rainfall and the rivers.

4.2 Isotopic analysis

Stable isotopic variation in groundwater from Adamwal to Nusrala is shown in the figure 3. The stable isotopic composition of shallow groundwater at Adamwal (-4.49‰) can be assumed to represent the isotopic composition of the local rainfall as this location is far away from any surface drains or reservoir. On the other hand, groundwater in deeper aquifer at Adamwal is highly depleted (-7.01‰) with respect to the isotopic composition of shallow groundwater (at the same location) indicating recharge to deep groundwater from much higher altitude such as that taking place from the Chohal dam that receives water from catchment from much higher average altitude. At Hoshiarpur, the isotopic difference between shallow and deep groundwater gets reduced. The shallow groundwater gets depleted (from -4.49 to -5.87‰) while, deep groundwater gets enriched to -6.39‰. This probably indicates recharge from drain carrying depleted water to shallow aquifer and also recharge to deep aquifer from the overlying shallow aquifer through partial connectivity. At Nusrala, both shallow and deep aquifer shows enriched isotopic composition. This probably indicates overall decrease in dam contributed recharge to groundwater with respect to the total precipitation recharge on the catchment. This can also be seen from the fact that beyond Hoshiarpur other drains that do not carry dam water also join to form a single stream and that the Nusrala represents catchment outlet representing overall catchment characteristic.

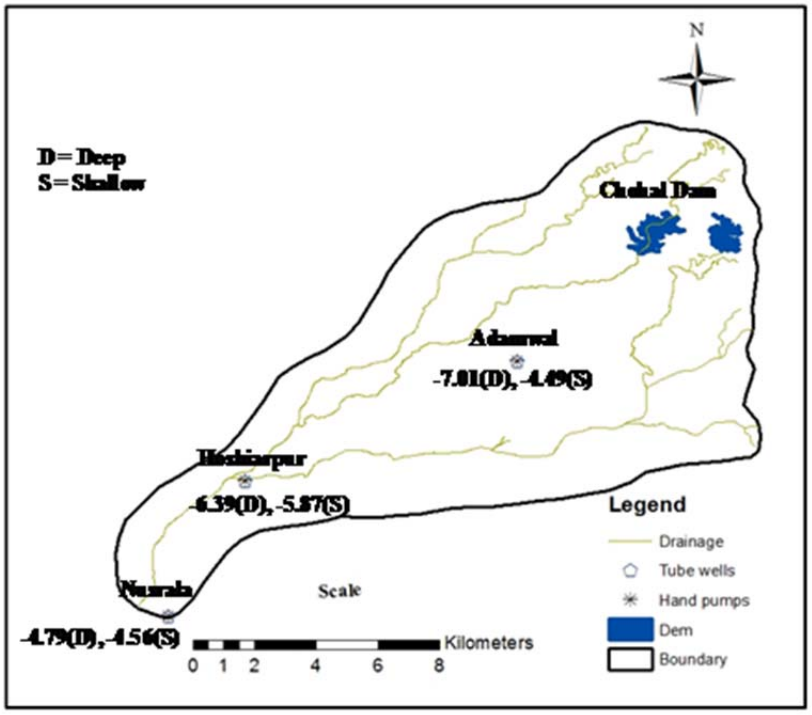

Fig. 3. Variation in isotopic composition of groundwater in the study area

Chemical analysis

As evident from the table 4 that the groundwater salinity in deep aquifer is in general much low at all sites and follows a narrow range (510 μS/cm to 660 μS/cm) compared to that at shallow aquifer groundwater (760 μS/cm to 1960 μS/cm). From Admawal to Hoshiarpur, the salinity in shallow groundwater abruptly increases from 760 μS/cm to 1960 μS/cm. Such an abrupt increase indicates anthropogenic source of contamination. It is also seen that the anthropogenic effects are confined to shallow groundwater as no such increase is observed in deeper aquifer. Beyond Hoshiarpur, freshwater recharge to shallow aquifer from local catchment resulted in dilution of salinity from 1960 μS/cm to 1270 μS/cm. A minor increase in salinity in deeper aquifer is also observed (510μS/cm to 660 μS/cm) indicating recharge to deeper aquifer through shallow groundwater. Thus, salinity wise, shallow and deep groundwater in Admawal is fresh, at Hoshiarpur the shallow groundwater is contaminated due to anthropogenic pollution which is partially recovered at Nusrala.

Location of sample	Source of sample	Depth (m)	EC (μs/cm)
Adamwal	Tube well	228.6	530
	Hand pump	24.38	760
Hoshiarpur	Tube well	231.64	510
	Hand pump	30.48	1960
Nusrala	Tube well	137.16	660
	Hand pump	18.28	1270

Table 4: EC details of the collected water samples

Conclusions

Some common bacteria found in the different places show that there is a connection between the places like *E.coli* and *Bacillus* is found in both the places Hoshiarpur and Nusrala, same is in the case of the case of the *Streptococcus lactis* is found in both Nusrala and Adamwal. So it is concluded that the flow of the water of Nusrala is linked with both the Hoshiarpur and Adamwal. Another cause is may be due to the hydrochemistry and nutrient chemistry which is dependent on the nutrients present in the land use and the quality of the rechargeable water. Recharge sources of the groundwater are may be due to the rainfall and the rivers.

A minor increase in salinity in deeper aquifer is also observed (510μS/cm to 660 μS/cm) indicating recharge to deeper aquifer through shallow groundwater. Thus, salinity wise, shallow and deep groundwater in

Admawal is fresh, at Hoshiarpur the shallow groundwater is contaminated due to anthropogenic pollution which is partially recovered at Nusrala.

The integrated studies clearly show that (i) using isotopes groundwater recharge source and interaction between shallow and deep aquifer can be monitored, (ii) bacteriological colonies can infilterate and contaminate even deep aquifers whenever there is interaction between shallow and deep groundwater., (iii) the pollution due to anthropological influence changes groundwater salinity and also cause bacteriological contamination of groundwater and (iv) natural freshwater recharge freshens the quality of water and the length over which freshening results depends upon level of pre-contamination and fresh water recharge conditions.

References

Central Ground Water Board, Northern Region, 1999. Hydrogeology and deep Ground water exploration in Ganga basin.

Central Ground Water Board. 2000. Water balance studies in upper YamunaBasin – terminal report - project findings and recommendations. Chandigarh:Central Ground Water Board

Epstein, S., and Mayeda, T., 1953. Variation of ^{18} O content from natural sources. Geochimica et Cosmochimica Acta 4, 213–224.

Jimenez, G., Baez, T. M. and Sanchez, M.M. (2006): Mineralización del agua subterranean en la ciudad de Puebla. XV Congreso Nacional de Ingeniería Sanitaria y Ciencias Ambientales. FEMISCA, 6th – 10th April 2006. Proceeding Booklet, 125-133.

Munoz, H., Armienta, M. A. Vera, A. and Ceniceros, N. (2004): Nitrato en el agua subterránea del Valle de Huamantla, Tlaxcala, México. *Rev*. *Int*. *Contam*. *Ambie*., 20: 91-97.

Pacheco, A. J., Cabrera, S. A.and Pérez, C. R. (2004): Diagnóstico de la calidad de agua subterránea en los sistemas municipales en el Estado de Yucatán, México. Ing., 8: 165-179.

Perez, C. R. and Pacheco, J. A. (2004): Vulnerabilidad del agua subterránea a la contaminación de nitratos en el estado de Yucatán. *Ing*., 8: 33-42.

Ramirez, E., Robles, E., Sáinz, M. G., Ayala, R. and Campoy, E. (2009): Calidad microbiológica del acuífero de Zacatepec, Morelos. México. *Rev*. *Int*. *Contam*. *Ambie*., 25: 247-255.

Ramirez, E., Robles, E., Gonzalez, M. E. and Martinez, M. E. (2010): Microbiological and physicochemical quality of well water used as a source of public supply. *Air*, *Soil*, *Water Res*., 3: 105-112.

Robles, E., Ramírez, E., Ayala R., Durán A., Sáinz, M. G., Martínez, B., Martínez, M. E.and González, M. E. (2010): Calidad del agua de tres pozos de la zona centro del acuífero Cuautla-Yautepec, Morelos, México. BIOCYT, 3: 159-175.

Robles, E., Ramírez, E., Durán, A., Ayala, R.,Sáinz, M. G. and González, M.E. (2009):Estudio fisicoquímico y bacteriológico de la calidad del agua en pozos del acuífero de Cuernavaca, Morelos. *Rev*. *Latinoamer*. *Rec*. *Nat*., 9: 114-122.

Hydrological Modelling of small watersheds of South Ponnaiyar Basin in the Soil and Water Assessment Tool (SWAT)

Dr. B.S. Polisgowdar
Associate Professor, Department of Soil and Water Engineering, College of Agricultural Engineering, Raichur 584102 (Karnataka)
E Mail: polisgowdar61@yahoo.com

Dr. S. Santhana Bosu
Dean Agricultural Engineering College and Research Institute,
TNAU, Coimbatore, Tamil Nadu
E Mail: ssbosu@hotmail.com

Abstract

A widely tested SWAT model was applied to the monthly runoff and sediment yield of two gauged agricultural watersheds of Tamil Nadu. The watershed and subwatershed boundaries, drainage networks, slope, soil series and texture maps were generated using a geographical information system (GIS). A supervised classification method was used for land-use/cover classification from satellite imageries. The calibration and validation of SWAT for prediction of runoff and sediment yield at Poyyapatti (7445.07 hectare area) and testing the validity of the calibrated model to Nallur watershed (2150.58 hectares area) of South Ponnaiyar river basin in Tamil Nadu was performed. The input parameters viz., Curve number for AMC-II, Soil available water capacity, Universal soil loss equation C factor & P factor, Mannings' n for tributary channel and main channel, Effective hydraulic conductivity for tributary channel alluvium and Effective hydraulic conductivity for main channel alluvium were selected for calibration of runoff and sediment. The Coefficient of Determination, Nash-Sutcliffe Coefficient, Root Mean Square Error and Percent Deviation were used to test the validity of predicted monthly values of runoff and sediment yield rates. The model performance was very good in simulating runoff and sediment yield during calibration and validation period (2005-08) at Poyyapatti. The validated model performance was observed to be good for simulating monthly runoff and sediment yield at other watershed during the period 2004-08. Therefore, it can be concluded that the SWAT model could be used for developing a multiple year management plan for the critical erosion prone areas of a small watershed.
KEY WORDS GIS; hydrological modelling; runoff; sediment yield; SWAT model

Introduction

Extensive soil erosion and its attendant ill effects have already contributed very significantly to the impoverishment of the land and people of India. Sheet erosion exists throughout almost the whole country (Anon, 1996).Out of total geographical area of 328.6 M ha in India, 103.16 M ha is affected by severe erosion due to water and wind which accounts about 33.4 per cent of total geographical area. In Tamil Nadu out of total geographical area of 13.006 M ha, 5.334 M ha (41%) is degraded under different categories and degradation due to water erosion alone is 4.926 M ha (92% of degraded area) (*Source:indiastat.com*). The problem of sedimentation in reservoirs has become alarming, since the silt deposited in the reservoirs or tanks decreases the capacity of the reservoirs and reduces the utility and life. The studies on the sedimentation problems carried out in 33 reservoirs in Tamil Nadu reveal that there is a loss in capacity of more than 50% in two reservoirs and more than 30% capacity loss in 8 reservoirs (*source: tn.nic.in*).

Field studies for prediction and assessment of soil erosion are expensive, time-consuming and need to be collected over many years. Though providing detailed understanding of the erosion processes, field studies have limitations because of complexity of interactions and the difficulty of generalizing from the results. Soil erosion

models can simulate erosion processes in the watershed and may be able to take into account many of the complex interactions that affect rates of erosion.

The intensive study of individual watersheds is necessary to enable management plans to be developed and also to apply the results of one watershed, to another with similar characteristics. Effective control of soil and nutrient losses requires implementation of best management practices in critical erosion prone areas of the watershed. It can be enhanced by the use of physically based distributed parameter models, remote sensing technique and geographic information system that can assist management agencies in both identifying most vulnerable erosion prone areas and selecting appropriate management practices.

Several physically based distributed parameter models (ANSWERS, AGNPS, SHE, SWRRB and SWAT) have been developed to predict runoff, erosion, sediment and nutrient transport from agricultural watersheds under various management regimes. Among these models, Soil and Water Assessment Tool (SWAT) is the most recent one used successfully for simulating runoff, sediment yield and water quality of small watersheds. The SWAT model is a distributed parameter, continuous model developed by the USDA-ARS (Arnold et al. 1998). Limited research work on identification of critical sub-watersheds and assessment of the impact of management practices on runoff and sediment yield using SWAT has been reported in India.

Owing to all above, information on existing land uses, runoff and sediment yield are required at micro level in the design of soil and water conservation measures to control non-point source pollution. The study reported here was attempted to assess, calibrate and validate SWAT for estimating runoff and sediment yields, from a watershed and to test the validity of the calibrated model for another watershed of South Ponnaiyar catchment of Tamil Nadu.

Description of the Study Area

The study was conducted in two of the sub-watersheds namely Nallur and Poyyapatti of South Ponnaiyar river basin of undivided Dharmapuri district and presently in Krishnagiri and Dharmapuri districts respectively. The location maps of both watersheds is presented in Fig.1. Agro-climatically both Nallur and Poyyapatti watersheds come under North Western Zone of Tamil Nadu. The total area of the Nallur watershed taken up for the study is 2150.58 hectares. It lies between 12° 42′ N to 12° 45′N latitudes and between 78°3′E to 78°7′E longitudes. It is covered under Survey of India (SOI) topo-sheet No. 57 L/2. The watershed receives average annual rainfall of 1042.14 mm and average maximum and minimum temperature are 39°C and 18°C respectively. Poyyapatti watershed lies between 11°59′ N to 12° 7′ 4''N latitudes and between 78° 32′E to 78° 36′E longitudes. It is covered under Survey of India (SOI) toposheet nos. 57 L/12 and 57 I/9. The total area of the watershed taken up for the present study is 7445.07 hectare. The watershed receives average annual rainfall of 986 mm and average maximum and minimum temperature are 38.5°C and 19°C respectively.

Agriculture is mostly rainfed (85-90% of the area) in both the watersheds. The remaining 10-15 per cent receives irrigation mainly from wells. This together with the prevalence of conventional cultivation practices, characterized by conventional tillage or no tillage, low fertilize/ manure consumption and local crop verities, is mainly responsible for the low crop productivity in the area.

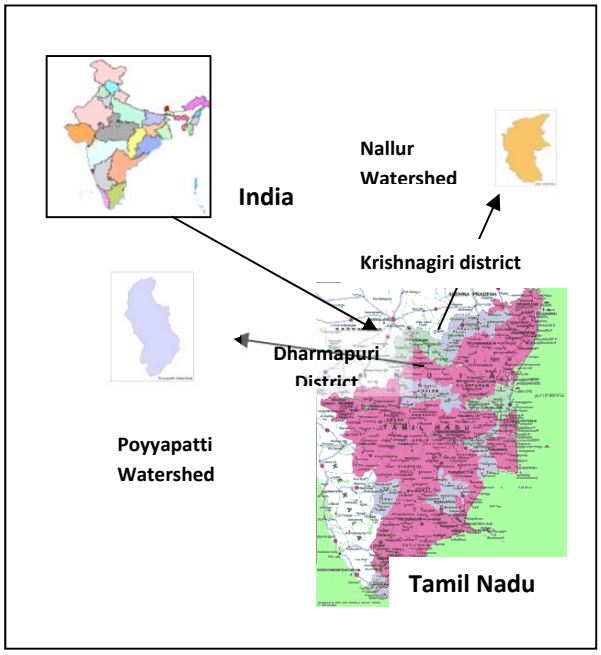

Fig.1. Location map of selected watersheds

Materials and Methods

Preparation of Data Base Required for the Model

Nallur watershed consists of a Hi-Tech weather station with a recording type and a non-recording type rain gauge to record hourly and cumulative daily rainfall respectively. The weather station also records daily maximum and minimum temperature, relative humidity and wind velocity. These data are available since 11.05.2004 and for the present study weather data up to 31.12.2008 have been used.

Poyyapatti watershed consists of a non-recording type rain gauge which records cumulative daily rainfall. The rainfall data is available since 01.07.2005 and for the present study rainfall data up to the year 31.12.2008 has been used. As the temperature data for this watershed is not available temperature data for the above period was taken from Regional Research Station, Paiyur of Tamil Nadu Agricultural University situated at about 40 kilometres from the study area. Statistical parameters needed for preparing weather generator input file were estimated.

Runoff and silt monitoring stations have been installed by the state Agricultural Engineering Department under River Valley Project (RVP) for each of the selected watersheds at the outlets. Daily runoff and sediment data were collected for the period 2005-08 for Poyyapatti watershed and 2004-08 for Nallur watershed.

Land use map of Nallur watershed is shown in Fig. 2. and the distribution of various classes is presented in Table.1. The major land use categories of the watershed are Waste Land With Scrub (WLWS) is 57.43 per cent, Agricultural crops (AGRR) 20.06 percent, orchard crops(ORCD) 14.27, Built-up area(URLD) 1.05, Waste Land Without Scrub(WLOS) 0.97 and water bodies(WATR) 0.23 per cent of the total area of the watershed. Among the agriculture crops row crops like ragi, bajra, maize and sorghum forms major per cent area and the rest of the area is covered by groundnut, paddy under well irrigation, vegetables and tapioca. The orchard crops mainly are coconut and mango.

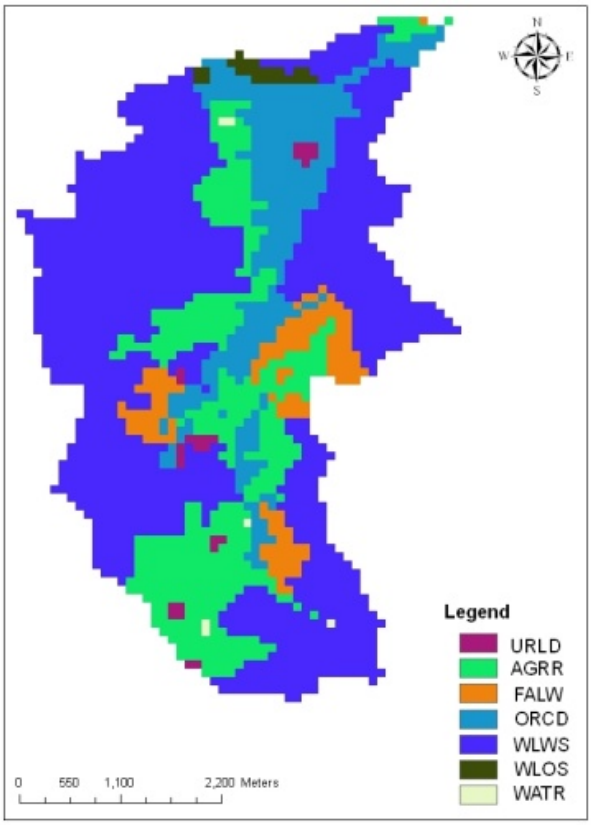

Fig.2. Land use map of Nallur watershed

Sl. No.	Land use	Area (ha)	% area
1	Builtup (URLD)	22.58	1.05
2	Agriculture land (AGRR)	431.45	20.06
3	Fallow (FALW)	128.77	5.99
4	Orchard (ORCD)	306.87	14.27
5	Waste Land With Scrub (WLWS)	1234.99	57.43
6	Waste Land Without Scrub (WLOS)	20.90	0.97
7	Water bodies (WATR)	5.02	0.23
Total		2150.57	100

Table 1. Landuse distribution for Nallur watershed

Land use map of Poyyapatti watershed is shown in Fig.3. and the distribution of various classes is presented in Table.2. The major land use category of the watershed is Deciduous Forest (FRSD) 45.84 per cent and the other land uses are Agricultural crops (AGRR) 29.93, Waste Land With Scrub (WLWS) 11.15, orchard crops(ORCD) 10.14, Waste Land Without Scrub(WLOS) 2.54, builtup area(URLD) 0.35 and water bodies(WATR) 0.04 per cent of the total area of the watershed. Among the agriculture crops row crops like ragi, bajra, maize and sorghum forms major per cent area and the rest of the area is covered by groundnut, vegetables, sunflower and tapioca. The orchard crops mainly are coconut and mango.

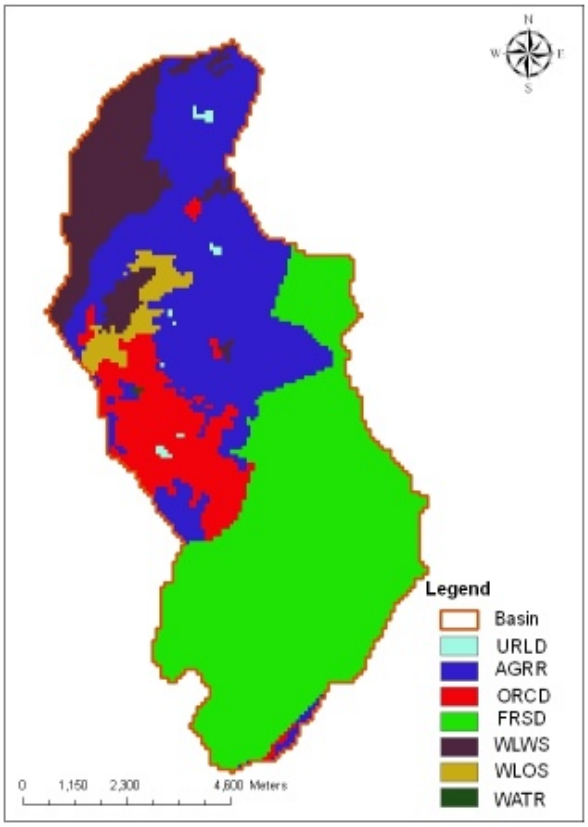

Fig. 3. Land use map of Poyyapatti watershed

Sl. No.	Land use	Area (ha)	% area
1	Builtup (URLD)	25.92	0.35
2	Agriculture land (AGRR)	2228.34	29.93
3	Orchard (ORCD)	755.04	10.14
4	Forest-Deciduous (FRSD)	3413.16	45.84
5	Waste Land With Scrub (WLWS)	830.30	11.15
6	Waste Land Without Scrub (WLOS)	188.97	2.54
7	Water bodies (WATR)	3.35	0.04
Total		7445.07	100

Table 2. Landuse distribution for Poyyapatti watershed

Slope Nallur watershed map is shown in Fig. 4. It is observed from figure that slope class of 1-6 per cent forms 44.71 per cent of the total area followed by 10-25 per cent(26.71%), 6-10 per cent (16.64 %), 25 per cent and above (9.02%) and 0-1 per cent (2.92 %).

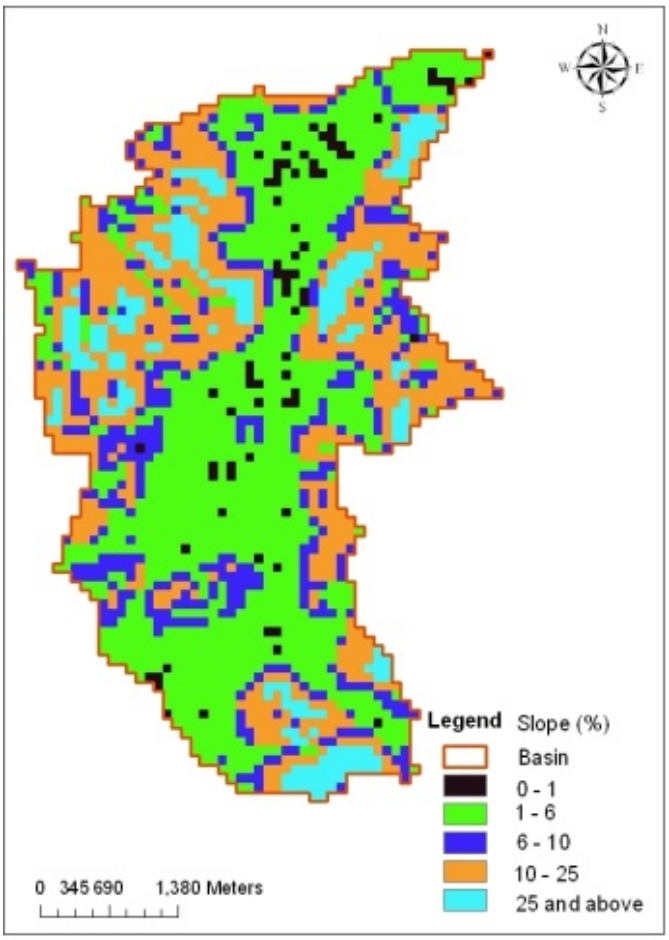

Fig. 4. Slope class for Nallur watershed

Slope map of Poyyapatti watershed are presented in Fig. 5. Slope class 1-6 per cent forms the major part (61.30 %) of the watershed followed by slope class 25 per cent and above (14.42 %), 10-25 per cent (12.81 %), 0-1 per cent (6.02 %) and slope class 6-10 per cent (5.45 %).

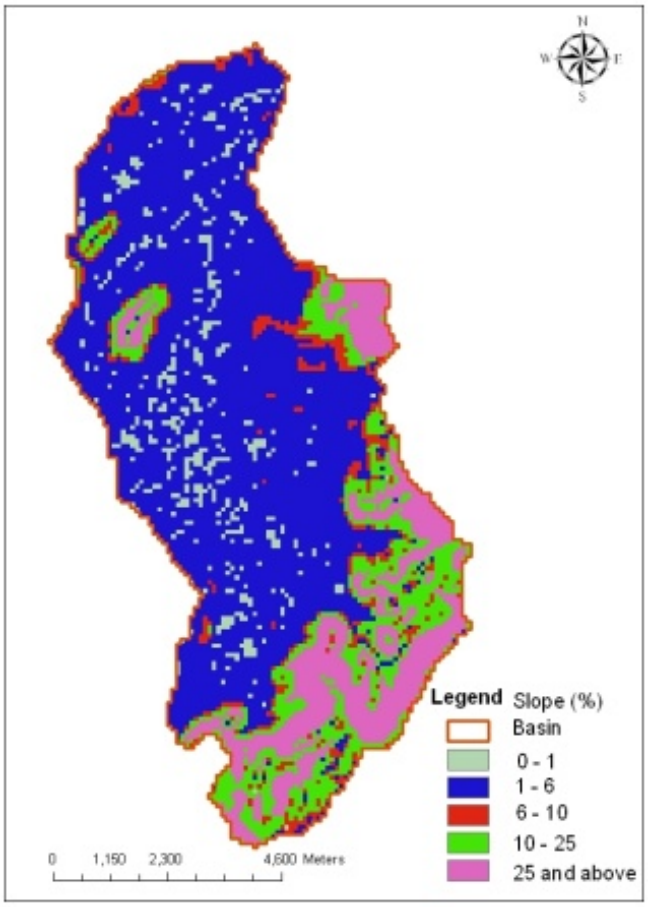

Fig. 5. Slope class for Poyyapatti watershed

GIS layers pertaining to soil for both watersheds in 1:50000 scale were collected from the Department of Soil Science and Agriculture Chemistry, Tamil Nadu Agricultural University, Coimbatore. The soil layer was overlaid on the topo-sheet No. 57 L/2 for Nallur and 57 L/12 and 57 I/9 for Poyyapatti (1:50000 scale) of Survey of India (SOI).The latitude and longitudes of the representative locations of the soil mapping units were identified. The location of the mapping units were tracked out in the field using GPS meter and soil samples was collected and were analysed. A complete soil data base of both watersheds required for the model was prepared in dBASE IV and was linked to the respective images of soil as attributes.

Based on the textural classification at Nallur watershed sandy clay loam soil covers 84.56 per cent, sandy clay 13.88 per cent and sandy loam covers 1.56 per cent of the total area (Table 3). The physical characteristics of the soils of Poyyapatti watershed (Table 4) indicates that clay loam soil covers an area of 39.66 per cent followed by sandy clay loam soil 28.07 per cent and sandy loam 24.24 per cent. The rest is covered by sandy clay (5.37 %), silty clay (1.24 %), loamy sand (1.13 %) and clay (0.29%).

Table 3. Physical characteristics of soils for Nallur watershed

Soil series	Coarse sand 0.1-2 mm (%)	Fine sand 0.05-0.1 mm (%)	Total sand (%)	Silt (%)	Clay (%)	Texture	Organic matter (%)
Alagappapuram	41.90	13.30	55.20	15.20	29.60	Sandy clay loam	0.40
Katripatti	64.35	12.85	77.20	15.40	7.40	Sandy loam	0.70
Maryappatti	54.00	8.20	62.20	14.93	22.87	Sandy clay loam	0.90
Periyapatti	36.40	10.10	46.50	18.20	35.30	Sandy Clay	0.50
Tulukkanur	49.70	25.50	75.20	3.60	21.20	Sandy clay loam	0.60

Soil series	Coarse sand 0.1-2 mm (%)	Fine sand 0.05-0.1 mm (%)	Total sand (%)	Silt (%)	Clay (%)	Texture	Organic matter (%)
Devadanappatti	30.90	11.20	42.10	19.28	38.62	Clay loam	0.78
Dharapuram	68.00	9.20	77.20	10.00	12.80	Sandy loam	0.80
Indali	46.10	5.00	51.10	18.00	30.90	Sandy clay loam	0.82
Kadiripuram	68.33	8.67	77.00	6.00	17.00	Sandy loam	0.70
Kalugachalapuram	24.65	10.35	35.00	22.00	43.00	Clay	0.65
Kollattur	49.27	15.50	64.77	14.34	20.89	Sandy clay loam	0.62
Matathari	10.30	2.00	12.30	43.20	44.50	Silty clay	0.43
Misal	45.27	34.20	79.47	2.88	17.65	Sandy loam	0.60
Mohanavaram	37.55	10.95	48.50	13.00	38.50	Sandy clay	0.91
Ooty	30.70	9.50	40.20	24.70	35.10	Clay loam	1.50
Paranur	61.50	19.50	80.65	8.88	10.47	Loamy sand	0.61

Table 4. Physical characteristics of soils for Poyyapatti watershed

Model set up

The watershed and sub-watershed boundaries were delineated from a digital elevation model (DEM) generated from basic 20 m contour data (1:50000 scale) for both the study watersheds. This led to 13 sub-watersheds in the Poyyapatti watershed and 5 in the Nallur watershed. To capture the homogeneity in soil, land use and slope class of the study watersheds, each sub-watershed within it was further divided into one or more of hydrologic response units (HRU), representing a unique combination of the land use, soil type and slope class. This resulted in a total of 50 and 63 HRUs each for Poyyapatti and Nallur watersheds respectively. All the input files required to run the model were generated sequentially through the interface and was run for the calibration and validation periods. Hargreaves method was selected for computation of ET as the combination of CN method with Hargreaves ET estimation method gives good results than any other combination (Kannan et al.2007a).

Results and Discussion

Model Calibration and Validation

Calibration was done mannually for Poyyapatti watershed (during 2005 and 2006) by varying the input parameters viz., Curve number for AMC-II, Soil available water capacity, Universal soil loss equation C factor & P factor, Mannings' n for tributary channel and main channel, Effective hydraulic conductivity for tributary channel alluvium and Effective hydraulic conductivity for main channel alluvium. These calibrated parameters were then used for the test and validation on the input data for the remaining years (2007 and 2008). The calibrated parameters at Poyyapatti watershed were applied at Nallur watershed to test the validity of the model (at a site other than where it was calibrated) for the period 2004 and 2005. The Coefficient of Determination (Leagates and McCabe Jr.1999)., Nash-Sutcliffe Coefficient(Nash and Sutcliffe, 1970), Root Mean Square Error(Thomann, 1982) and Percent Deviation (Martinec and Rango 1989) statistical measures were used for assessing the monthly runoff and sediment yield predicting efficiency of the model.

Surface runoff calibration at Poyyapatti watershed

Different range of curve numbers (CN) for various land uses of the watersheds were tried as specified in the SWAT users manual. The model was run with different curve numbers for each HRU of each sub-watershed. The model was over predicting the surface runoff during default run , therefore, reduced values of the curve numbers were used. The final calibrated CN values were presented in Table.5.The values are the weighted mean for each sub-watershed. Further the surface runoff values were fine tuned by using another tuning parameter SOL_AWC (soil available water capacity). This parameter was increased by a value 0.02 only for clay, silty clay and sandy clay soils of the watershed.

Table .5. Calibrated curve number (CN) for the sub-watersheds of Poyyapatti watershed

Sub-watershed	Default CN(weighted)	Calibrated CN(weighted)
1	84.12	74.80
2	82.05	77.10
3	81.27	73.52
4	82.18	73.42
5	81.62	74.69
6	82.22	77.95
7	80.40	75.38
8	75.82	68.25
9	78.28	72.86
10	67.92	58.12
11	83.00	77.00
12	71.08	61.58
13	78.12	70.68

The comparison of monthly observed runoff and simulated surface runoff by model is presented in Fig.6. The overall model performance was found to be satisfactory as indicated by close relation between observed and simulated runoff.

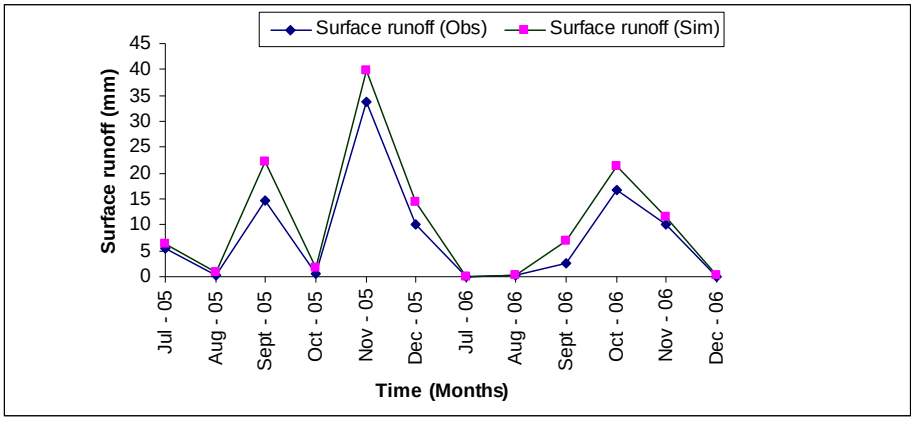

Fig. 6. Observed (Obs) and Simulated (Sim) surface runoff (mm) at Poyyapatti watershed during calibration period (2005 and 2006)

Table 6: Statistical comparison between observed and simulated monthly surface runoff at Poyyapatti during calibration period (2005-06)

Statistical Parameters	Surface Runoff		Sediment Yield	
	Observed (mm)	Simulated (mm)	Observed ($t\ ha^{-1}$)	Simulated ($t\ ha^{-1}$)
Mean (mm)	7.89	10.46	0.646	0.833
Standard Deviation (mm)	7.59	9.066	0.960	1.213
Sum (mm)	94.74	112.5	7.76	9.17
Coefficient of determination (r^2)	0.966		0.997	
Deviation, D (%)	-18.746		-18.17	
Simulation Efficiency (E)	0.785		0.882	
RMSE (mm)	2.275		0.212	

Table 6. shows all statistical analysis for observed and simulated surface runoff and sediment yield for the watershed. The coefficient of determination (r^2) values of 0.97 and Nash-Sutcliffe simulation efficiency values of 0.78 indicated very good agreement between the observed and simulated values. The root mean square values of 2.27mm reflect close agreement between observed and simulated values. The overall deviation values of -18.75 per cent indicated slightly over prediction of runoff but it is within 20 per cent limit and is considered as the acceptable level of accuracy for the simulation (Pandey et. al 2005).

Sediment yield calibration at Poyyapatti watershed

The Universal Soil Loss Equation (USLE) P factor was uniformly kept as 1 for all the land uses, soils and slopes in the model as default. Field observations in the watershed indicated that the farmers were following the contour cultivation. The land holding being very small in the area the boundary bunds were existing which limits the slope lengths. Looking into these aspects P value for agriculture fields (existing in 0-1% and 1-6% slope areas) was replaced with 0.8 as specified in Weichmeir and Smith (1978). This parameter solved the over prediction of sediment yield to some extent.

In order to simulate the physical processes affecting the flow of water and transport of sediment in the channel network of the watershed, SWAT requires information on the physical characteristics of the main channel within each sub-watershed. The main channel input file (.rte) summarizes the physical characteristics of the channel which affect water flow and transport of sediment. Mannings 'n' value for the main channel (CH_N2) and effective hydraulic conductivity in the main channel (CH_K2) are the main parameters which decides the flow and sediment transport. These values were kept 0.014 and 0 respectively for CH_N2 and CH_K2 as model default. Chow (1959) has given values of Mannings "n" values for natural streams. Looking into the condition of the main channel in the area 'n' value of 0.05 applicable for natural streams with few trees, stones or brush was selected for calibration of sediment yield. Effective hydraulic conductivity (CH_K2) of value 6 mm hr^{-1} was adopted based on the channel alluvium in the area (Lane 1983). In order to model sub-watersheds and the HRUs the physical characteristics of the tributary channels needs to be looked into at the sub-watershed level. Minnings 'n' of tributary channel (CH_N1) was 0.014 in the default model run which was very low as observed from the vegetation conditions of the tributary channels of the area. A value of 0.075 (Chow 1959) was selected for calibration of sediment yield from the HRUs. The effective hydraulic conductivity of tributary channel alluvium (CH_K1) was 0 for default model run and a value of 4.5mm hr^{-1} was selected for calibration based on the field observations.

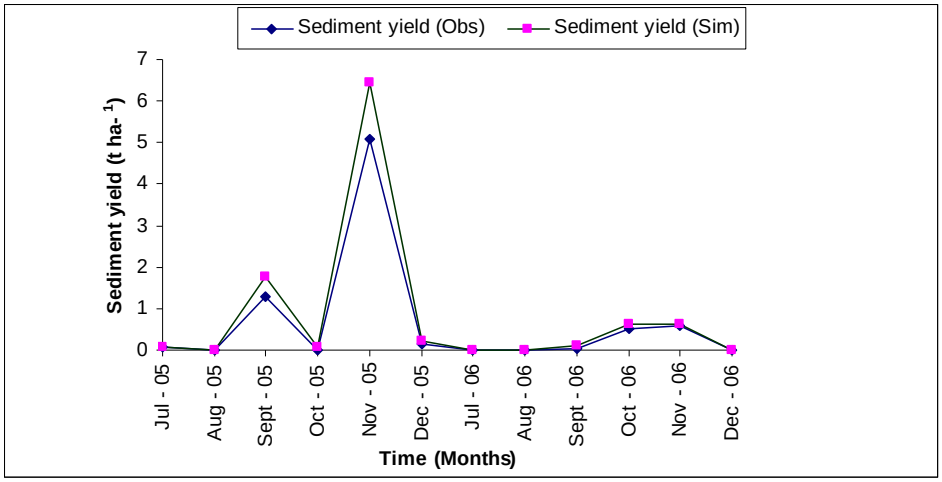

Fig. 7. Observed (Obs) and Simulated (Sim) sediment yield (t ha^{-1}) at Poyyapatti watershed during calibration period (2005 and 2006)

The model was run with the above calibrated values for the years 2005 and 2006 and the annual values of observed and simulated values were checked statistically and graphically. After getting satisfactory results the model was run for monthly values. The comparison of monthly observed and simulated sediment yield is presented in Fig.7. The model gives quite well prediction for sediment yield. The model performance was found to be satisfactory as indicated by close relationship between the observed and simulated values. Table 6 gives the results of statistical tests between observed and simulated sediment yield for the calibration period. The coefficient of determination (r^2) value of 0.997, Nash-Sutcliffe simulation efficiency values of 0.88 indicated a close agreement between observed and simulated sediment yields. A per cent deviation of -18.17(within 20% limit) and root mean square error 0.21shows a good agreement during calibration period.

Surface runoff validation at Poyyapatti watershed

The observed and simulated monthly runoff during the validation period (2007-08) was compared graphically (Fig. 8). It was observed a fairly good match between observed and simulated surface runoff.

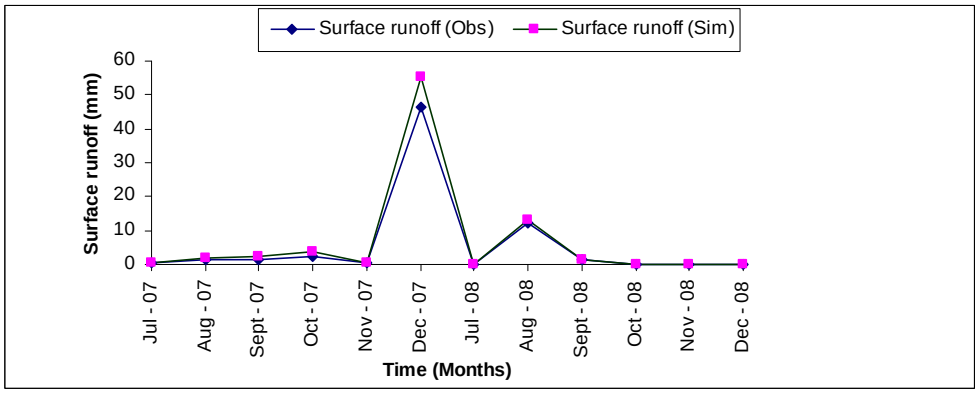

Fig. 8 Observed (Obs) and Simulated (Sim) surface runoff (mm) at Poyyapatti watershed during validation period (2007 and 2008)

Table 7 shows all statistical analysis for observed and simulated monthly surface runoff and sediment yield for validation period. The coefficient of determination (r^2) values of 0.95 and Nash-Sutcliffe simulation efficiency values of 0.95 indicated good agreement between the observed and simulated values. The root mean square values of 0.21mm and overall deviation values of -18.8 per cent (within acceptable limit) and reflects good agreement between observed and simulated values.

Table 7 Statistical comparison between observed and simulated monthly surface runoff at Poyyapatti during validation period (2007-08)

Statistical Parameters	Surface Runoff		Sediment Yield	
	Observed (mm)	Simulated (mm)	Observed (t ha^{-1})	Simulated (t ha^{-1})
Mean	4.74	5.63	0.17	0.22
Standard Deviation	7.79	9.21	0.35	0.46
Sum	56.83	67.56	2.07	2.47
Coefficient of determination (r^2)	0.951		0.965	
Deviation, D (%)	-18.893		-19.321	
Simulation Efficiency (E)	0.950		0.866	
RMSE (mm)	0.21		0.081	

Sediment yield validation at Poyyapatti watershed

The observed and simulated monthly sediment yield values were compared graphically (Fig. 9) and the model prediction was observed to be good.

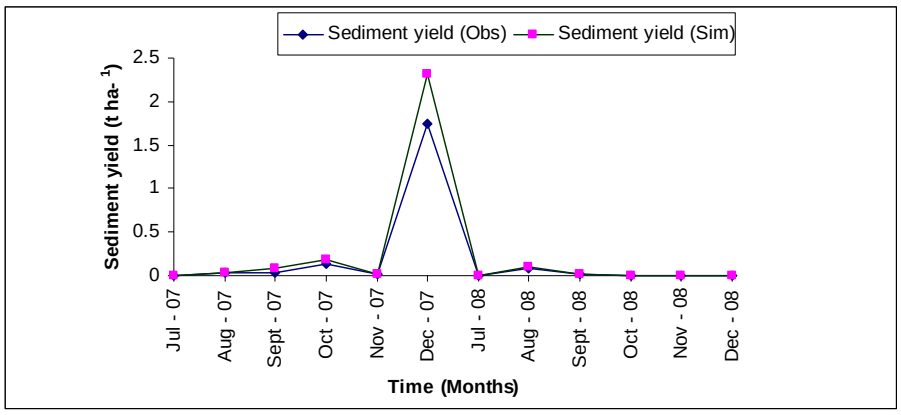

Fig. 9 Observed (Obs) and Simulated (Sim) sediment yield (t ha^{-1}) at Poyyapatti watershed during validation period (2007 and 2008)

Table 7shows all statistical analysis for observed and simulated monthly sediment yield during validation period. The coefficient of determination (r^2) values of 0.965 and Nash-Sutcliffe simulation efficiency vales of 0.87 indicated good agreement between the observed and simulated values. The root mean square values of 0.081 t ha^{-1} and overall deviation values of -19.32 per cent reflects good agreement between observed and simulated values.

Model Validation for Nallur watershed

The purpose of this model validation is to establish whether the model can estimate output for locations, time periods or conditions other than those that the parameter values were calibrated to fit.

Surface runoff validation

The comparison of land use of both Nallur and Poyyapatti watershed indicated a close resemblance with respect to agriculture, waste land with scrub and horticulture crops. Further the comparison of soils of both watersheds indicated a sizable area of Nallur (84.56%) and Poyyapatti (28.07 %) consists of sandy clay loam soils.Therefore the curve number (CN) values and soil available water capacity (SOL_AWC) values that were calibrated for Poyyapatti watersheds were tested for validation of surface runoff at Nallur watershed.

The observed and simulated monthly runoff during the validation period was compared graphically (Fig. 9). It was observed a fairly good match between observed and simulated surface runoff during these months.

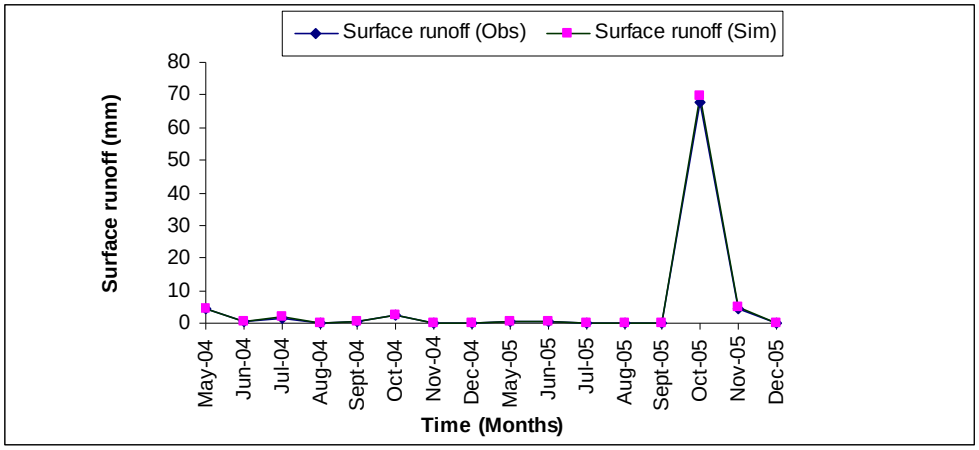

Fig. 9 Observed (Obs) and Simulated (Sim) surface runoff (mm) at Nallur watershed during validation period (2004 and 2005)

The coefficient of determination (r^2) values of 0.91 and Nash-Sutcliffe simulation efficiency values of 0.89 indicated good agreement between the observed and simulated values. The root mean square values of 0.38mm and overall deviation values of -4.7 per cent also reflected good agreement between observed and simulated values (Table 8).

Table 8 Statistical comparison between observed and simulated monthly surface runoff (May-December) at Nallur during validation period (2004-05)

Statistical Parameters	Surface Runoff		Sediment Yield	
	Observed (mm)	Simulated (mm)	Observed ($t\ ha^{-1}$)	Simulated ($t\ ha^{-1}$)
Mean	5.74	6.01	1.95	2.06
Standard Deviation	12.38	12.77	4.18	4.32
Sum	45.94	48.10	15.59	16.48
Coefficient of determination (r^2)	0.91		0.89	
Deviation, D (%)	-4.70		-12.78	
Simulation Efficiency (E)	0.89		0.98	
RMSE (mm)	0.38		0.08	

Sediment yield validation

Upon field verification of both the study watersheds indicated that the type and extent of vegetation in the main channel and tributary channels resembled fairly. Also the channel alluvium was almost same. Looking into the field conditions of both the watersheds the parameters namely, Mannings 'n' for main channel (CH_N2), effective hydraulic conductivity of the main channel alluvium (CH_K2), Mannings 'n' for tributary channel (CH_N1) and effective hydraulic conductivity of the tributary channel alluvium (CH_K1) calibrated for Poyyapatti watershed were tested for Nallur watershed. The comparison of monthly observed and simulated sediment yield is presented in Fig.10. The model gives quite well prediction for sediment yield. Table 11 gives the results of statistical tests between observed and simulated sediment yield for the validation period.

The coefficient of determination (r^2) value of 0.89, Nash-Sutcliffe simulation efficiency values of 0.98 indicated a close agreement between observed and simulated sediment yields. A per cent deviation of -12.78 (within the acceptable limit of 20%) and root mean square error 0.08 $t\ ha^{-1}$ shows a good agreement during validation period (Table 8).

The above results of the simulated surface runoff and sediment yield at Nallur watershed using the parameters calibrated for Poyyapatti watershed indicated that the SWAT model could predict the runoff and sediment yield to a fairly reasonable extent at a location other than where it was calibrated and validated. This result is very significant in the context of establishment of gauging stations in all the watersheds being very costly and that the requirement of more skilled persons for monitoring the gauging instruments. The calibrated model could be applied for an un-gauged watershed with similar agro-climatic conditions to predict runoff and soil loss and in turn help in prioritizing the watershed based on which suitable soil and water conservation measures could be planned.

Conclusions

The present study was aimed at modelling, calibration and validation of distributed parameter, continuous model, 'Soil and Water Assessment Tool (SWAT)' for estimation of surface runoff and sediment yield at one watershed (Poyyapatti) and testing the validity of the calibrated model to another watershed (Nallur) of South Ponnaiyar river basin in Tamil Nadu.

The model performance was tested graphically and statistically and was found to be good in predicting surface runoff and sediment yield both during calibration and validation period at Poyyapatti watershed. The calibrated model at Poyyapatti watershed was tested for its validity in estimating surface runoff and sediment yield at Nallur watershed. The model performance was found to be good. This shows that the SWAT model can be applied for estimating monthly surface runoff and sediment yield for another watershed having similar agro-climatic conditions as that of Poyyapatti watershed.

References

Anon, 1996. Working group report, IX Plan for HADP, NGDP, Planning Commission, Government of India.

Arnold, J.G., R. Srinivasan, R.S. Muttiah, and J.R. Williams. 1998. Large area hydrologic modeling and assessment part I: Model development. J. Amer. Water Resour. Assoc., 34(1): 73-89.

Leagates, D.R and C.J. McCabe Jr. 1999. Evaluating the use of "goodness-of-fit" measures in hydrologic and hydroclimatic model validation. Water Resour. Res., 35: 233-241.

Nash, J.E and J.V. Sutcliffe. 1970. River flow forecasting through conceptual models, Part I: A discussion of principles. J. Hydrol., 10(3): 282-290.

Thomann, R.V., 1982. Verification of water quality models. J. Environ. Engg. Div. 108: 923-940.

Martinec, J and A.. Rango. 1989. Merits of statistical criteria for the performance of hydrological models. Water Resour. Bull., AWRA. 25: 421-432.

Wischmeier, W.H and D.D Smith. 1978. Predicting rainfall erosion losses- a guide to conservation planning. U.S. Department of Agriculture, Agriculture Handbook No. 537.

Chow, V.T. 1959. Open-channel hydraulics. McGraw-Hill, New York.

Lane, L.J. 1983. Chapter 19: Transmission Losses. p.19-1–19-21. *In* Soil Conservation Service. National engineering handbook, section 4: hydrology. U.S.Government Printing Office, Washington, D.C.

Assessment of groundwater resources and quality in Bist Doab region, Punjab, India

Anju Pant
Hydrological Investigation Division, National Institute of Hydrology, Jalvigyan Bhawan, Roorkee Uttarakhand 247 667, India

M S Rao
Hydrological Investigation Division, National Institute of Hydrology, Jalvigyan Bhawan, Roorkee Uttarakhand 247 667, India

Y S Rawat
Hydrological Investigation Division, National Institute of Hydrology, Jalvigyan Bhawan, Roorkee Uttarakhand 247 667, India

P. Purushothaman
Hydrological Investigation Division, National Institute of Hydrology, Jalvigyan Bhawan, Roorkee Uttarakhand 247 667, India

Gopal Krishan

Hydrological Investigation Division, National Institute of Hydrology, Jalvigyan Bhawan, Roorkee Uttarakhand 247 667, India

Corresponding Author: somesh@nih.ernet.in

Abstract

The long term groundwater level trend indicates increasing groundwater stress in Bist-Doab region of Punjab with maximum stress in central zone of the region and in central part of piedmont zone (locally known as Kandi). The rate of decline in groundwater is as much as 0.9m/year in some locations of the region whereas, favored hydrogeology and relatively low use of groundwater has led to moderate to high groundwater potential along the flood plains of the rivers Satluj and Beas. Depletion of groundwater has resulted mainly due to increase in irrigation demand, domestic requirement and reduction in surface water-bodies. These have resulted in highest groundwater abstraction per unit area in Jalandhar followed by Kapurthala district. In some parts of Kandi region, groundwater utilization is also less mainly due to hilly terrain and occurrence of groundwater at levels exceeding 50m bgl. The net groundwater availability in Bist-Doab region is 333,656ha-m, which is much smaller than the total groundwater draft of which the draft for irrigation itself constitutes 571,549ha-m. Except hard terrain zone, which is thinly populated, almost entire Bist Doab region comes under dark category with groundwater utilization exceeding 300%. Regionally, groundwater quality is fairly good except at few locations showing salinity, hardness, heavy metals and fluoride concentrations above the safe drinking limit. Various measures can be adopted to improve groundwater resource, which include augmentation of groundwater resource through artificial recharge, conjunctive use of surface water and groundwater system, use of blending technique in irrigation practices in areas where groundwater quality is poor. The present paper provides a comprehensive account of stage of water resources of Beas-Satluj Doab region.

Keywords: Bist Doab region, groundwater, water availability, water level, groundwater quality

Introduction

Groundwater is an essential resource for drinking, irrigation and industrial purposes. However, groundwater resources are under stress due to rapid population growth, urbanization, industrialization and agriculture activities. Groundwater quality is also influenced by geogenic and anthropogenic activities. In general, the irrigation sector remains the main consumer of groundwater. Withdrawal of groundwater for other uses and evapotranspiration from shallow water table areas also adds up to the groundwater depletion.

Punjab State, located in northwestern part of India, is also facing severe groundwater stress due to its intensive use in agriculture and other activities. The economy of the state is primarily depend on agricultural. About 85% of geographical area of Punjab is under agriculture of which 97% area is irrigated (Gupta, 2011). The surface water resources of the state are limited and completely utilized, therefore to meet the increasing demand for agriculture, population and industries, dependency on groundwater has been increasing day-by-day. Based on cropping pattern and practices, the total demand of water for agriculture is 4.38 mham against the total availability of 3.13 mham (Tiwana et al., 2007). Therefore, the shortage of 1.25 mham is met through over-exploitation of groundwater reserves, resulting in rapid decline of water table in the entire state except south western parts due to limited extraction because of its brackish and saline quality (Tiwana et al., 2007). Moreover, the area under irrigation by groundwater through tube wells had increased from 55 to 72 percent during 1970-2006 with the corresponding decrease in the area under irrigation by canals (Vashisht, 2008). The annual average rainfall has also decreased from 739.1 mm in 1980 to 529.2 mm in 2008 (Statistical Abstracts, 2009), which is putting extra pressure on groundwater resources.

Bist Doab region, the interfluves of Rivers Sutlaj and Beas, in Punjab is also experiencing severe groundwater depletion due to increasing agricultural activities and physiology of the region. In general, water levels are declining in region on a long term basis. However, in some parts, groundwater utilization is less due to hilly terrain. The net groundwater availability in Bist-Doab region is much smaller than the total groundwater draft (CGWB, 2007 a-d). In some parts of the region, groundwater quality is also deteriorating. Thus, the pressure on groundwater resources is continuously increasing. Therefore, to maximize production per unit of resources, it is emphasized to utilize every drop of water available sensibly and carefully. Hence, it becomes imperative to understand the availability of water resources, water level behaviour and measures that can be adopted to improve groundwater resource in the region. The present paper provides a comprehensive account of stage of water resources of Beas-Satluj Doab region.

Study Area

The Bist Doab is a triangular region and covers an area of 9060 km^2. The area lies between 30°51' and 30°04' N latitude and between 74°57' and 76°40' E longitude. The region comprises Hoshiarpur, Kapurthala, Jalandhar and Nawan Shahar districts of Punjab State, India (Fig. 1). It is bounded by Siwaliks in the north-east, the river Beas in the north east-south west and the river Satluj in south east-south west. The area is drained by the perennial rivers Satluj and Beas and their tributaries. They coalesce at the Harike. The drainage density is high in the north east strip bordering the Siwaliks, but it is moderate to low in the rest of the area with sub-parallel and sub-dendritic patterns. The climate of the area is influenced by the Himalayas in the north. The region receives an average of 543 mm annual rainfall (Statistical Abstracts, 2009). The area nearest the Siwaliks receives maximum rainfall.

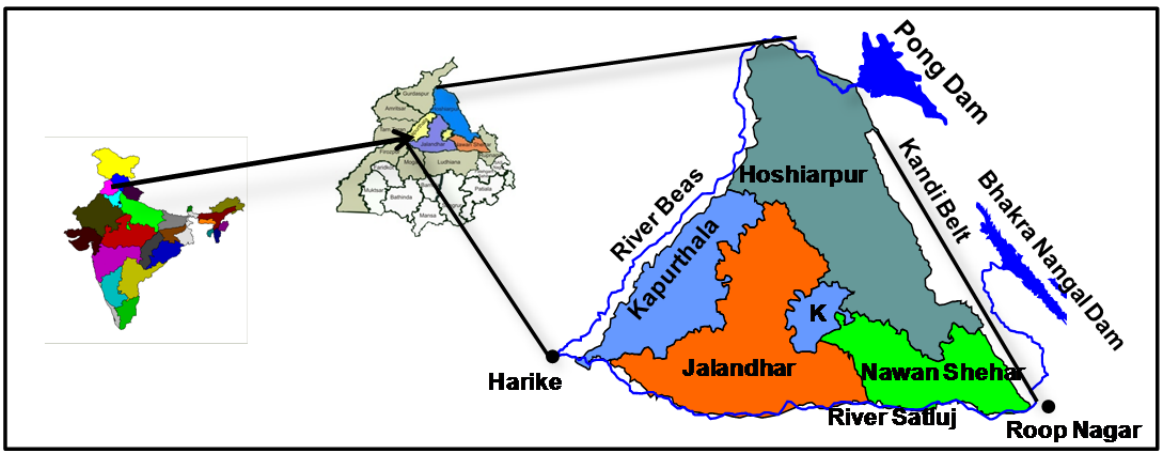

Fig. 1. Bist Doab Region

Demography

According to 2011 Census of India, Bist Doab region has a population of 5,196,575, which is 18.75% of the total population of Punjab State. The density of population is 529 per square kilometer (Census, 2011). Central part (district Jalandhar and Kapurthala) has the highest population density in the region. The eastern parts (Hoshiarpur and Nawanshehar districts) have a low population density because these regions have choe–ridden hilly tracts. According to the latest Census, nearly 63% of the region's population lives in rural areas where the overall growth rate of population has declined and nearly 37% of the region's population lives in urban areas. Agriculture is the main occupation of the people of the region.

Climatic condition

Bist Doab region has a continental climate. The most significant climatic elements involved in shaping the region in the present form are temperature and rainfall, their amount, periodicity and fluctuation. Temperature

in summers ranges from 30 to 32 ºC while the maximum can go up to 45 ºC. Winters are moderately cold with normal temperatures falling between 10 and 15 ºC. The month of June is the hottest and January is the coolest month. Hot and dry winds in the summers and frost in the winters are common features. The average rainfall of the region is 543.3mm. The highest normal monthly rainfall is obtained in August and the lowest in October. A large amount of rainwater goes waste as runoff causing floods and large scale soil erosion in some parts of the region.

Drainage and Canal System

The Satluj river and Beas river are the major natural drainage channels observed in the region. The Satluj river flows westwards and registers the southern boundary of the region (Jalandhar and Nawan Shahar districts) and the Beas river flows on the northwestern boundary (Hoshiarpur and Kapurthala districts). East/White Bein and West/Black Bein flowing in the north-east to south-west direction are the other natural drainage channels present in the area. In addition to these major drainage channels, the area is also drained by numerous *choes* (seasonal rivulets). The north part (Hoshiarpur district) of the region comprises of two nearly equal portions of hills and plain area. The *Kandi* area comprising of hills and piedmont is rainfed. There are four canals (Shah Nehar, Shahpur, *Kandi* and Bist Doab canals) in the region providing water for irrigation. Banga distributary and Hardibad, Uchapind, Ibban and Kalupur minors also irrigate some areas of the region. For most parts of the year, the seasonal streams do not carry any water and when the discharge is full, especially in monsoon season, they erode the surrounding area and degrade the cultivated land. Some active flood plains and old channels have high water table due to their lower topographic position and flooding during the monsoon season.

Land use

Punjab Remote Sensing Centre, Ludhiana assessed the land use pattern of the region. Land use/Land cover of Bist Doab region is divided into following six major land use classes – built-up land, agricultural land, forest, wasteland, water bodies and wetlands (Fig. 2). The maximum area of the region is covered by agricultural land, which constitutes crop land, fallow, agricultural plantations, horticultural plantations and orchards and covers 708075.38 ha (79.63% of Total Geographical Area (TGA) of the region). Out of this, crop land covers 702429.9 ha (78.99% of TGA of the region). The piedmont and alluvial plain area is intensively cultivated. Therefore, the region is dependent upon heavy water requirement for agriculture. In 2008-09, 97 percent of the total cropped area was under wheat and paddy crops in the region (Statistical Abstracts, 2009). The groundwater over exploitation in the region is mainly due to the agricultural activities. Long term trend for water utilization for agriculture in the region shows that the water utilized per unit area is highest in Jalandhar district followed by Kapurthala district (Fig. 3). Water is the major limitation to crop production in Kandi area of the region. The

area has low inherent fertility of soil and the groundwater development extremely difficult as well as uneconomical due to hilly terrain.

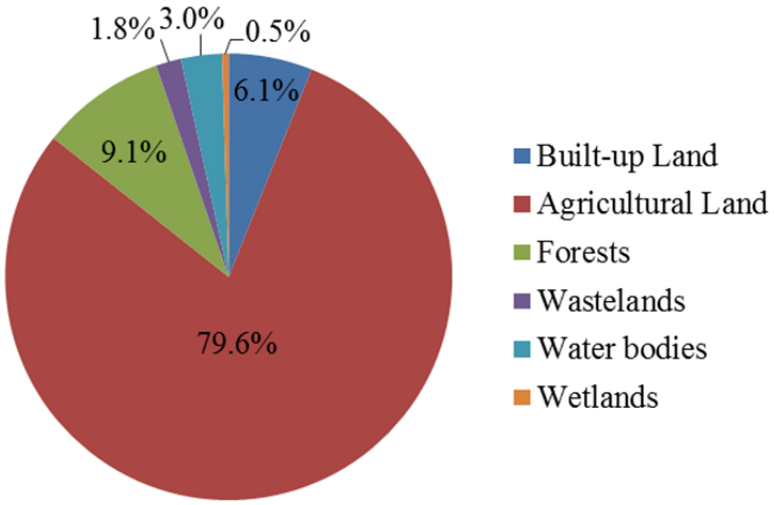

Fig. 2: Land use of Bist Doab region (Source: Punjab Remote Sensing Centre, Ludhiana, 2008)

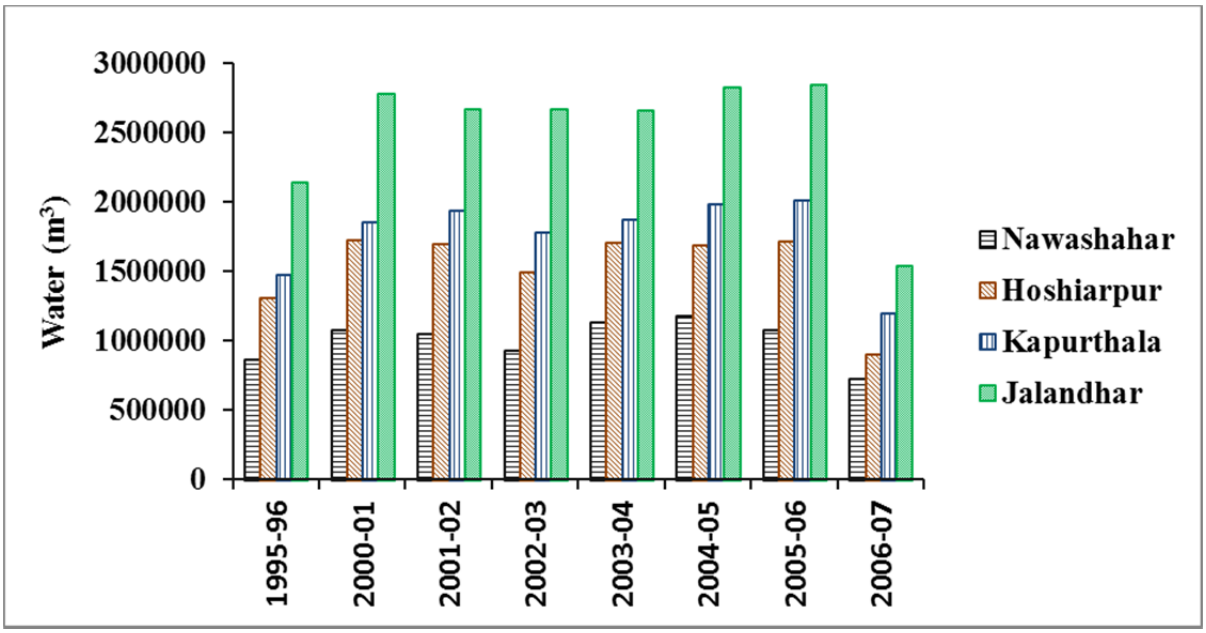

Fig. 3 Water utilization per unit area for irrigation in Bist-Doab region

Hydrogeology

In the northeastern part of the region, sediments of recent origin are deposited in an area running parallel to the Siwalik range, locally called Kandi and forms major recharge zone to the underlying aquifers in the lower reaches of the Bist-Doab. Groundwater occurs largely under unconfined conditions in this belt. Sand mixed together with clay beds is predominant in the area. Sediments in the lower reaches are mainly fluvial. Sand and gravel horizon coupled with intercalating clay beds are the main lithological units in the region. Multi layered aquifer system in the region has been divided into two aquifer groups. The top layer of aquifer group I consist

of coarse sand beds. The sand beds are generally thick separated by small, thin clay beds that are not regionally extensive. The prevalence of clay beds increases considerably and thickness ranges from 72m to 94m. The average top layer is 72m in Hoshiarpur district, 76m in Nawanshahr district, 81m in Jalandhar district and 94m in Kapurthala district (CGWB, 2009). Aquifer group I separates from underlying aquifer group II by a regionally extensive clay layer with varying thickness from 16 to 32m. The maximum 32m thickness of confining clay layer is in Hoshiarpur district towards north. Whereas, this clay layer thickness is only 16m in Kapurthala district, 21m in Nawan Shahar and 24m in Jalandhar district (CGWB, 2009). Underlying aquifer group II consists of thick layers of sand separated by thin clay beds that are not regionally extensive. The major sediments of this group are sand, clay, gravel and occasional kankar. A thickness of this aquifer below the confining layer upto 250m ranges between 81m and 105m in the region. The thickness of aquifer is 81m in Hoshiarpur district, 85m in Kapurthala district, 87m in Jalandhar district and 105 m in Nawanshahr district (CGWB, 2009).

Water Resources

For any particular region, available water sources comprise: (1) rainfall (2) surface water and (3) the groundwater. Present status of these water resources in Bist Doab region is discussed below:

Rainfall

In Bist Doab region, the annual average rainfall is 543.3mm, which is highly inconsistent in distribution in time and space. Around 80% of the total rainfall is received during 3 to 4 months of the monsoon period.

The monthly rainfall data taken for the period 2000-2010 for the region were obtained from Statistical Abstracts (2009) and Indian Meteorological Department (2011). The annual rainfall of different districts of the Bist Doab region are shown in Fig. 4. Nawanshahar district received the maximum mean annual rainfall followed by Hoshiarpur and Jalandhar, whereas Kapurthala district received the minimum mean annual rainfall. Nawanshahar and Hoshiarpur districts received mean rainfall above 600mm, whereas district Jalandhar received above 500mm and Kuparthala above 400mm. The rainfall is erratic and non-uniformly distributed over the region.

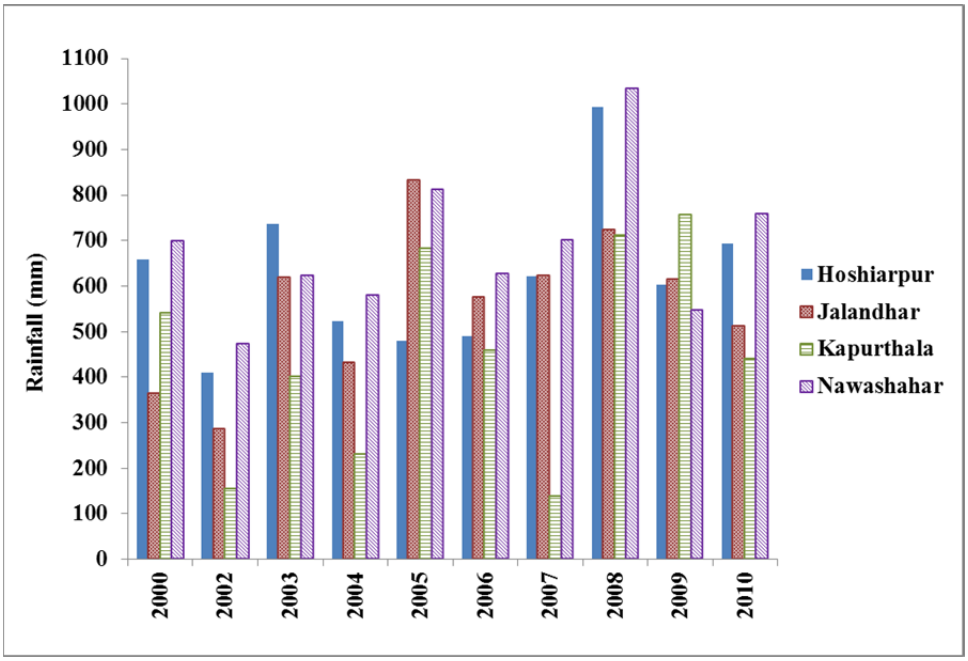

Fig. 4 Rainfall pattern in Bist Doab region

Trends of annual rainfall variations show non-uniformity and the magnitude of trend varies from one district to another in the region. The increase was, in general, higher in north-east and smaller in south-west. The districts, Nawanshahar and Hoshiarpur are among the highest rainfall districts of the region and Jalandhar and Kapurthala experience the lowest rainfall. Average annual rainfall in the Kandi zone (Hoshiarpur and Nawanshahar) is 1100 mm. Much of the rainfall is wasted in the form of surface runoff. This zone is severely affected by soil and water erosion due to steep slope of the Siwalik foothills and high rainfall.

Changes in rainfall patterns could have a direct impact on water resources. Part of rainfall also contributes towards surface runoff and groundwater recharge. The changes in precipitation levels will be accompanied by increased evaporation rates with temperatures rise. The combination of these changes will have profound effects on availability of water for agriculture production, ultimately resulting in groundwater stress due to overdrafting.

Surface Water

In general, the availability of surface water is assessed by the Directorate of Water Resources, Punjab. As mentioned above, the Satluj river and Beas river are the major natural drainage channels in the region. There are four canals (Shah Nehar, Shahpur, *Kandi* and Bist Doab canals) in the region providing water for irrigation. Out of total surface water resources available, river Satluj contributes 29380 ha-m and river Beas contributes 44870 ha-m (Gupta, 2011). The surface water utilization through canal network depends upon the water released from

the reservoirs in the region. Canals in the region contributes approximately 14038 ha-m of water for irrigation in the region (Aggarwal et al., 2009, 2010, 2011)

Ground Water

The replenishable groundwater is mainly generated from the following sources: Infiltration due to rainfall; seepage from canals system; and return flow from surface irrigation. Rainfall and seepage from canal networks contribute 165 ha-m of water to groundwater in Punjab (Aulakh, 2004).

The groundwater draft has been continuously increasing in the Bist- Doab region. The net groundwater availability in the region is 333,656 ha-m whereas gross groundwater draft of the region is 608,297 ha-m resulting in an overdraft of 274,641 ha-m (Fig. 5). Out of which, the draft for irrigation itself constitutes 571,549ha-m. The groundwater availability decreases from central zone to central region of Kandi. The maximum amount of groundwater draft of 3000000 ha-m per year is in Jalandhar district. Most of the blocks in the region are over exploited (22 out of 30 blocks). Stages of groundwater development in districts Nawan Shahar is 175%, Kapurthala is 204%, Jalandhar is 254% and Hoshiarpur is 85% (Vashisht, 2008). The safe category blocks fall all along the foothills where water levels are deep.

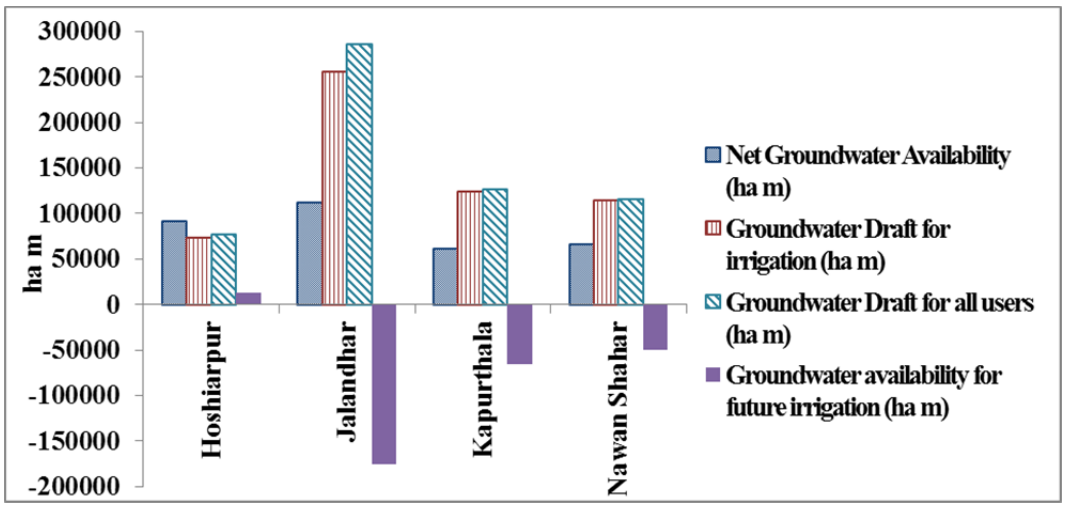

Fig. 5 Ground water availability in Bist Doab region (Source: CGWB, 2007)

Available Water Resources for Irrigation

The available water resource for irrigation in the Jalandhar, Kapurthala and Nawan Shahar districts were 167655 ha-m, 116501 ha-m, and 72160 ha-m respectively (Aggarwal et al., 2009 , 2010, 2011). A total of 654 mm water is available in Jalandhar district, out of which groundwater, rainfall and canal water contributes 74%, 21% and 5%, respectively (Aggarwal et al., 2009). A total of 573 mm water is available in Kapurthala district,

out of which groundwater, rainfall and canal water contributes 86.9%, 12.5% and 0.6%, respectively (Aggarwal et al., 2011). In terms of depth, 569 mm of total water is available in Nawan Shahar district, out of which groundwater, rainfall and canal water contributes 67.7%, 25.7% and 6.6%, respectively (Aggarwal et al., 2010).

Ground Water Level Behavior

The depth to water table in the Bist- Doab region varies from near surface to 50m below surface. Water level is deeper in the Kandi region and water logging conditions prevail at the southwestern part of the Bist- Doab region. The shallow groundwater is in unconfined state and deeper aquifer exists at confined state with master groundwater slope is towards southwest.

The depth of pre monsoon water level is moderate (5-10 m bgl) in a large part of the region. The water level is deep along the eastern fringe of Hoshiarpur district, underlain by Kandi formations. Depth to water level in post monsoon is 5-10 m bgl in a large part in the eastern half of the basin and shallow (3-5 m bgl) in the western half (CGWB, 2007 a-d). Though, groundwater quality of Siwalik foothill zone is excellent, however, water level is fairly deep in most parts of the zone and not easy to explore and pump due to hilly terrain. The central part is experiencing the maximum decline in water table because of the over exploitation of groundwater for cropping. According to CGWB (2007 c), the declining trend is seen in several patches in Hoshiarpur district. Water levels deeper than 50 m occur in the Plateau region of Hoshiarpur district. The decadal fluctuation in water level show fall in water levels is between less than 2 meters to more than 4 meters. The groundwater gradient is steep in the NE foothill region of Hoshiarpur district being of the order of 3.3m/km (CGWB, 2007 c).

Seasonal fluctuation shows that in general there is an overall rise in the water level except in the central part and few isolated patches. The water table elevation is highest in the north-eastern part (Kandi area) and lowest in the south-western part, which in turn reflects the topographic gradient. According to CGWB (2007, a-d), the long-term (10 years) water level trend indicates that there is a decline in water level ranging from 0.2m/yr to 1.0 m/yr during pre-monsoon and 0.3 m/yr to 0.9 m/yr during post-monsoon. However, long-term net change of water levels in central part (Jalandhar district) indicates a general decline (negative change) up to 8.18m (CGWB, 2007 a).

Groundwater Quality

In Bist Doab region, groundwater quality is fairly good except at few locations. In parts of Hoshiarpur and Kapurthala districts, shallow aquifers are alkaline in nature and salinity is low to medium (EC ranges between 280 and 1050 μS). Most of the chemical parameters are well within the permissible limits for safe drinking waters in the region except nitrate concentration (permissible limit is 45 mg/L) is high in some places of Kapurthala, Hoshiarpur, Nawan Shahar and Jalandhar districts (CGWB, 2010), iron concentration (permissible

limit is 1.0 mg/L) is higher in two blocks of Hoshiarpur district (CGWB, 2010), high fluoride concentration (permissible limit is 1.5 mg/L) in Jalandhar district (CGWB, 2010), while arsenic is higher than the permissible limit of 0.01 mg/l in Kapurthala and Hoshiarpur districts (CGWB, 2007 a, b). The suitability of ground water for irrigational uses is generally ascertained by considering salinity (EC), Sodium Adsorption Ratio (SAR) and Residual Sodium Carbonate (RSC), which are within permissible range in the region. Such waters cause neither salinity nor sodium hazards when used for customary irrigation (CGWB, 2007 a- d). In general, the groundwater quality of the region is suitable for both domestic and irrigation purposes.

Water Management Strategies

The Bist Doab region is facing a problem of declining groundwater levels due to over-exploitation of the resource for the domestic and agriculture purposes. The main cause of water scarcity in the region is to maintain the present level of crop production. Water scarcity results in over exploitation of groundwater resources that further deteriorates the groundwater quality, increase soil salinity due to irrigation with poor quality water and consequently reduction in yields. Various water management measures can be adopted to reduce water withdrawal and to increase recharging of groundwater in water declining zones.

Reducing water withdrawal

In the region, paddy and wheat utilize maximum water due to cropping pattern and evapotranspiration. Therefore, the traditional cropping pattern needs to be changed to utilize less water, such as during Kharif season, paddy may be replaced with cotton, maize, pulses and oilseeds (Vashisht, 2008). Additionally, for higher productivity per unit use of water, better technologies related to soil and agronomic management are needed that save water without a loss of crop yields (Hira, 2004). These technologies include planting and transplanting time of crops, irrigation scheduling, irrigation methods, straw mulching and tillage.

Optimization of irrigation applications

In general, there is a false impression among farmers that higher application of irrigations lead to higher crop yields. To maximize the use of irrigation, there is a need of water application system that is suitable for the crop and the soil. Ridge and furrow system of irrigation is used worldwide for crops like cotton, maize, sugarcane and sunflower, which helps in preventing the crops from excess water damage during rainy season and save about 30 to 40% of irrigation water. So, there is a need to introduce ridge and furrow irrigation system in the region to reduce excess utilization of the irrigation water.

Artificial Groundwater Recharge

Various measures for enhancing artificial groundwater recharge can be adopted to reduce the groundwater decline in the region. A network of available surface water drains in the region can be utilized for artificial groundwater recharge using surplus runoff water during rainy season through canal network (Khepar, 2003). The check dams may be constructed across the drains at suitable intervals to enhance the groundwater recharge through surface drains.

Kandi zone of the region receive average annual rainfall of 1100 mm. Out of which, a substantial amount of rainfall is wasted in the form of surface runoff. This zone is also severely affected by soil and water erosion due to steep slope of the Siwalik foothills and high rainfall. By adopting different soil and water conservation practices, a reduction in runoff may be achieved, which may increase water level in central part of the region. These conservation measures include construction of water harvesting structures, slope management through terracing, land leveling and contour bunding (Vashisht, 2008).

Recharge from east and west Beins of the region may also be developed. Presently, these Beins are not utilized appropriately. East Bein is used for draining untreated polluted water from industries and West Bein is covered with waterweeds, thus hampering the natural flow. These Beins may be suitably utilized by constructing seepage tanks on the banks of Beins in sandy formations along their courses (Vashisht, 2008).

Groundwater recharge may also be enhanced by diverting the water flow of the major rivers Satluj and Beas during the monsoon or rest of the year towards natural and artificial drains by constructing barrages at appropriate locations. Tube wells may be used as recharge wells by constructing efficient filtering device. The abandoned dug wells could also be used for groundwater recharge by diverting runoff or rooftop water towards these wells.

Conjunctive use of surface water and groundwater system

In general, the water quality of Bist Doab region is good. Wherever there is a poor quality, then such groundwater may be blended with good quality canal water for reducing the salinity or sodicity hazards of the problematic waters. Such blended may be used for irrigation purposes.

Summary and Conclusions

The over exploitation of groundwater and further deterioration in quality needs proper attention and priority in the Bist Doab region. Bist Doab region is experiencing severe groundwater depletion due to increasing agricultural activities. The maximum area (79%) of the region is covered by agricultural land that require higher

amount of water for irrigation. Long term trend for water utilization for agriculture in the region shows that the water utilized per unit area is highest in Jalandhar district followed by Kapurthala district. The rainfall is erratic and non-uniformly distributed over the region. Although, Kandi zone receives maximum rainfall, however, much of the rainfall is wasted in the form of surface runoff due to hilly terrain. The groundwater draft has been continuously increasing in the Bist- Doab region. The net groundwater availability in the region is 333,656 ha-m whereas gross groundwater draft of the region is 608,297 ha-m resulting in an overdraft of 274,641 ha-m. Out of which, the draft for irrigation itself constitutes 571,549ha-m. The groundwater availability decreases from central zone to central region of Kandi. Most of the blocks in the region are over exploited (22 out of 30 blocks). The rate of decline in groundwater is as much as 0.9m/year in some locations of the region whereas, favored hydrogeology and relatively low use of groundwater has led to moderate to high groundwater potential along the flood plains of the rivers Satluj and Beas. The groundwater quality of the region is good except few locations of the region and water is suitable for domestic and irrigation purposes. There is an urgent need for proper water management. The adoption measures like reducing water withdrawal by changing cropping pattern, optimization of irrigation, artificial groundwater recharge by utilizing natural surface drains, surface runoff in Kandi zone, utilizing east and west Beins appropriately, by diverting the water flow of the major rivers Satluj and Beas towards natural and artificial drains by constructing barrages, by blending of brackish groundwater with good quality canal water.

Acknowledgement

The present work is part of the research project funded by the World Bank under Purpose Driven Study of HP II, Ministry of Water Resources, Government of India, (GoI), initiated by the Hydrological Investigations Division of NIH, Roorkee, India. Hence, the financial support from the World Bank is acknowledged.

References

Aggarwal, R., S. Kaur, and P. Miglani. 2009. Blockwise assessment of water resources in Jalandhar district of Indian Punjab. *Journal of Soil and Water Conservation* 8(3): 69-73.

Aggarwal, R., S. Kaur, and P. Miglani. 2010. Assessment of water resources in Shaheed Bhagat Singh Nagar- A case study. *Journal of Soil and Water Conservation* 9(4): 288-300.

Aggarwal, R., S. Kaur, and P. Miglani. 2011. Study at micro level of water resources in Kapurthala district. *Journal of Soil and Water Conservation* 10(2): 104-107.

Aulakh, K. S. 2004. Resource conservation and sustainability under Punjab conditions. In *National symposium on Resource Conservation and Agricultural Productivity, Nov., 22-25, 2004, Ludhiana.*

Census 2011. Punjab Data Sheet - Census. Available at: http://censusindia.gov.in/2011-prov-results/data_files/punjab/Final%20Data2.pdf. Accessed 3 January 2012.

CGWB (2009). Methodology for assessment of development potential of deeper aquifers. http://www.cgwb.gov.in/Documents/Report_methodology%20deeper%20aquier.pdf

CGWB. 2007 a. Ground water scenario of Jalandhar District, Punjab. Central Ground Water Board North Western Region, Chandigarh, 2007, pp- 15.

CGWB. 2007b. Groundwater Information Booklet Kapurthala District Punjab. Central Ground Water Board, North Western Region, Chandigarh, 2007, pp- 20.

CGWB. 2007c. Ground Information Booklet Hoshiarpur District, Punjab. Central Ground Water Board North Western Region, Chandigarh, 2007, pp- 15.

CGWB. 2007d. Groundwater Information Booklet Nawan Shahar District, Punjab. Central Ground Water Board North Western Region, Chandigarh, 2007, pp- 20.

CGWB. 2009. Methodology for assessment of development potential of deeper aquifers, Report of the Working Group. Available at: http://www.cgwb.gov.in/Documents/Report_methodology%20deeper%20aquier.pdf. Accessed 10 January 2012.

CGWB, 2010. Ground water quality in shallow aquifers of India. Central Ground Water Board, Faridabad. Available at: http://cgwb.gov.in/documents/Waterquality/GW_Quality_in_shallow_aquifers.pdf. Accessed 10 January 2012.

Gupta, S. 2011. Ground Water Management in Alluvial Areas. Available at: www.nass.usda.gov.http://cgwb.gov.in/documents/papers/incidpapers/Paper%2011-%20sushil%20gupta.pdf. Accessed 4 December 2011.

Hira, G. S. 2004. Status of water resources in Punjab and management strategies. Groundwater use in North-West India-Workshop papers. Centre for Advancement of Sustainable Agriculture, New Delhi, pp. 202.

Indian Meteorological Department, 2011. District wise rainfall information, Monthly Rainfall Punjab. Available at: http://www.imd.gov.in/section/hydro/distrainfall/punjab.html. Accessed 6 December 2011.

Khepar, S. D. 2003. Integrated approach for combating water table decline in rice-wheat systems. In *Water Management for sustainable rice-wheat production system in Indo-Gangatic plains* (Hira, G. S., Haer, H.S., and Chawla, A. eds.) Tech. Bull. No. 1/2003, Dept. of Soils, PAU, Ludhiana.

Statistical Abstracts of Punjab, 2009. Economic & Statistical Organisation, Government of Punjab.

Tiwana, N. S., N. Jerath, S. S. Ladhar, G. Singh, R. Paul, D. K. Dua, and H. K. Parwana. 2007. State of Environment; Punjab-2007, Punjab State Council for Science & Technology, pp 243.

Vashisht A. K. 2008. Status of water resources in Punjab and its management strategies. *Journal of Indian Water Resources* 28(3): 1-8.

Precision orchard management system and erosion control

Attila Nagy,
University of Debrecen, Centre for Agricultural and Applied Economic Sciences, Faculty of Agricultural and Food Sciences and Environmental Management, Institute of Water and Environmental Management, Böszörményi str. 138. H-4032 Debrecen, Hungary. E-mail: attilanagy@agr.unideb.hu

János Tamás
University of Debrecen, Centre for Agricultural and Applied Economic Sciences, Faculty of Agricultural and Food Sciences and Environmental Management, Institute of Water and Environmental Management, Böszörményi str. 138. H-4032 Debrecen, Hungary E-mail: tamas@agr.unideb.hu

Abstract

Modern geographical information programmes and databases make possible to create such data systems with more detailed data than earlier, which can be analysed for precision agriculture, erosion control point of view. By using applied GIS methods, the spatial distribution of physical and water management properties of soils were surveyed in this study, in order to examine erosion risks in orchards and to supply complex research evaluation activities in precision farming.
The research field was an 338.52 hectare pear, peach, apricot, walnut, sweet and sour cherry orchard at Siófok, situated in the South Western part of Hungary. Row distance is grassed, and the orchard is irrigated. In the course of the field work the spatial position and individual extent of all pear trees was defined to set up a detailed GIS data base. The established geographical information system of the pear plantation contains the name of species, data of plantation circumstances, soil parameters, and the properties of the fruit trees. This datasets are appropriate tool for precision irrigation and nutrition system. To evaluate the effect of erosion, three dimensional digital terrain models were produced and GPS based soil samples were taken from the surface. Both soil physical (soil plasticity) and chemical (pH, NPK and soluble microelement contents of soils) characteristics of the samples were measured in the laboratory.
This study integrated site spatial data sets became the basis for a precision spatial decision support system. Therefore those sites were determined where erosion risk is high, the increasing intensity of runoff caused faster nutrient and microelement leaching, liming is needed.

Keywords: precision agriculture, erosion control, SWAT input data

Introduction

From a sustainable development and production point of view, soil conservation has become more and more highlighted in agriculture. However, the scientific surveys and examinations of soil degradation and erosion were started in the last century (Browning, 1977). On world scales man's non-agricultural activities which accelerate erosion are hardly significant. On the other hand, agriculture is so widespread that agricultural activities which materially alter the speed of the erosion process are much more important. Nearly all agricultural operations do tend to encourage erosion (Hudson, 1995). Water is probably the most important single agent of erosion (Morgan, 1996).
Spatial variability of soil properties may appear in yield variation within a single field even in areas considered to be homogeneous from soil survey point of view. Effects of various sources of soil heterogeneity on the annual or long-term average soil water budget appear to differ markedly (*Kim, 1995*). Furthermore the negative water balance in the Carpathian Lowland: 450-600 mm precipitation vs. 680-720 mm potential evapotranspiration is equilibrated by horizontal inflow (on the surface as runoff, in the unsaturated zone as seepage; and in the saturated zone as groundwater flow), which leads to the accumulation of the weathering products of the large catchment area. In Hungary, resulting from water erosion is about 100 million t/year. Due to the effect of possible climate change, Mediterranean and semi arid climatic characteristics are becoming more intensive in Hungary (Kertész, 1995). As a result of the change, short rainfalls with high intensity are

going to determine and affect the extent of water erosion in Hungary. The more influencing effect of semi-arid and Mediterranean type rainfalls make the reassessment of the erosion risk actual (László and Rajkai, 2003; Jolánkai 2010). In addiction to the hardly predictable atmospheric precipitation pattern, the two additional reasons of extreme soil moisture regime (the simultaneous hazard of waterlogging or overmoistening and drought sensitivity) are:
the heterogeneous microrelief of the „flat" lowland;
the highly variable, sometimes mosaic-like soil cover and the unfavourable physical and hydrophysical properties of some soils (mainly due to heavy texture, high clay and swelling clay content, or high sodium saturation: ESP).

Materials and methods

The aims of our study were to survey the spatial distribution of physical and water management properties of soils in order to examine erosion risks in orchards and to supply complex research evaluation activities for precision farming.The main goal was to establish such a precision decision support system, with which the water management properties of soil can be meliorated, and can be reduced the effect of high precipitation intensity on orchards.
The research field was at Siófok, in Hungary, which is situated in the South East side of Lake Balaton. Topographical maps with 1:10.000 scale in Hungarian EOV coordinate system were used as a basis of the vectorization. The methods used survey point elevations and contour lines digitized from existing maps describing terrain surface. Upper limit of soil plasticity according to Arany, soil density, acidity, $CaCO_3$, humus, N and P content, main microelements of soils were measured to obtain appropriate information on the physical and water management properties of the soil. The detailed goals were the followings:

- mapping and analyzing of physical properties of the soil in water management point of view,
- mapping the acidity and $CaCO_3$content of soil for precision liming,
- measurement of humus the element content.

Due to the heterogeneous terrain surface special attention has to be paid to places with different location in order to examine all of the different soil varieties. The coordinates of the sampling points were collected by GPS. Systematic sampling strategy was carried out based on the number of the rows and apple trees to collect as much information as possible with possibly the least number of samples. Geoinformatics calculations were made in ArcGIS 10 environment.

Results and discussion

The 3-dymensional digital elevation model (DEM) was interpolated from vectorized topographic maps and field measurements. Then the orthophoto of the examined site was added to the DEM by 10 times exaggeration factor, in order to emphasize the surface differences (Figure 1.). The vectorization and kriging interpolation was based on contour lines, considering altitude attributes. At the examined site, the lowest point was 101 m above sea level, while the highest point was 162 m.

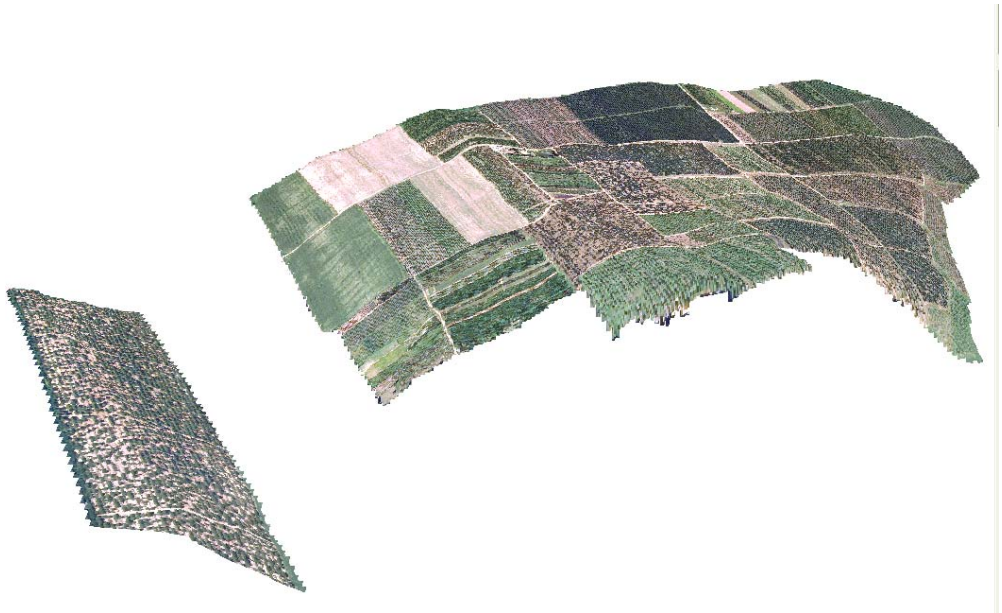

Figure 1. Masked DEM + orthophoto image of the examined site (rotated by 45°).

Based on the DEM model, the slope characteristics are more or less homogeneous at the examined site; the aspect is North Eastern oriented within 30 % and South Western oriented within 24,8 of the orchard (Figure 2.) due to geologically formed valleys .

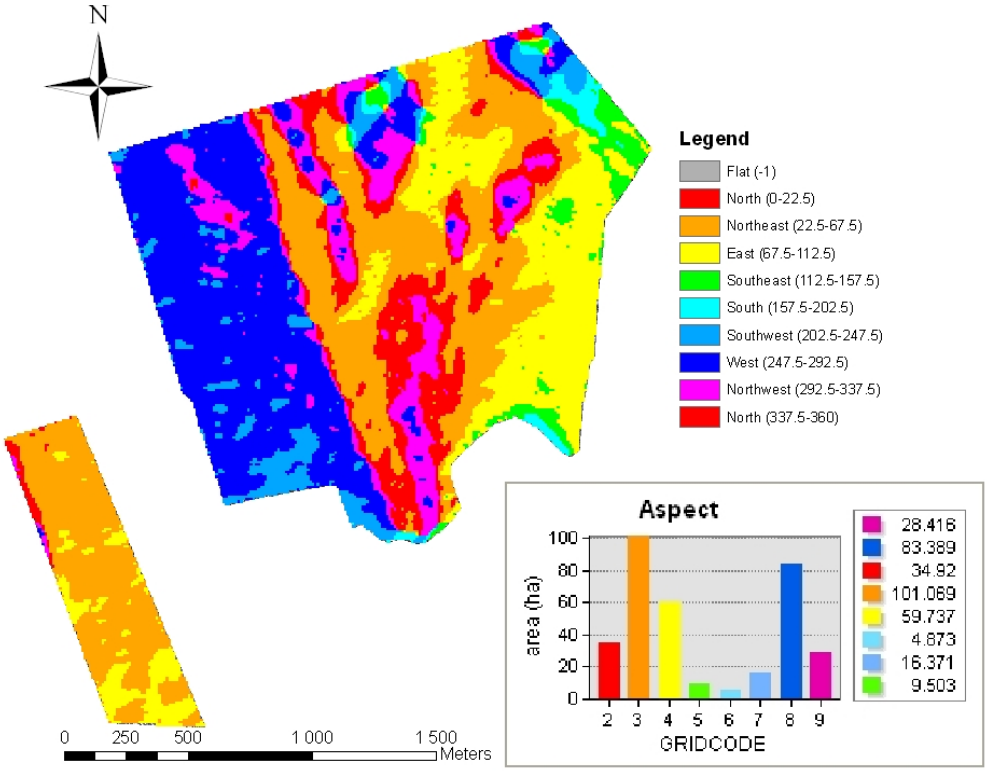

Figure 2. Aspects of the orchard

North Eastern slopes is not advantageous from a plant and environmental protection point of view, because these slopes are shaded at dawn and in the morning, therefore the dew and vapor dry up later, which can cause an increase in fungous diseases and pesticide output. On the other hand, pear trees requires at least 65% relative humidity, therefore these slope aspects of the site are quite appropriate for the pear orchard. On Southern slopes faster snowmelt and intensive rainfalls can cause greater amounts of erosion.

Risk of sheet erosion is considered within 24,4% of the site (slopes steeper than 5%). Besides sheet erosion, considerable risk of rill erosion appears at the steepest slopes (12 % or more), which comprise only 1,18 % of the orchard (slopes greater than 25 % steepness is not detected) (Figure 3). Fortunately the grassed row space reduces the erosion risk but no contour bands and stormwater drains were constructed, which can effectively control erosion. Another problem is that micro terraces would have to be constructed at 17 % or steeper slopes in order retain water. At present, it is recommended to enhance soil cover with mulch, utilize more manure instead of artificial fertilizers (to achieve better soil structure as well), or cultivate individual platforms, only small spots which surround the pear trees and vegetate other surfaces. Sheet eroded plots in areas with these kinds of slopes and North Western aspect can be easily found on the ortophoto as well. Even rows are mainly directed to valleys, so the row directions of the orchard also strengthen the effect of erosion.

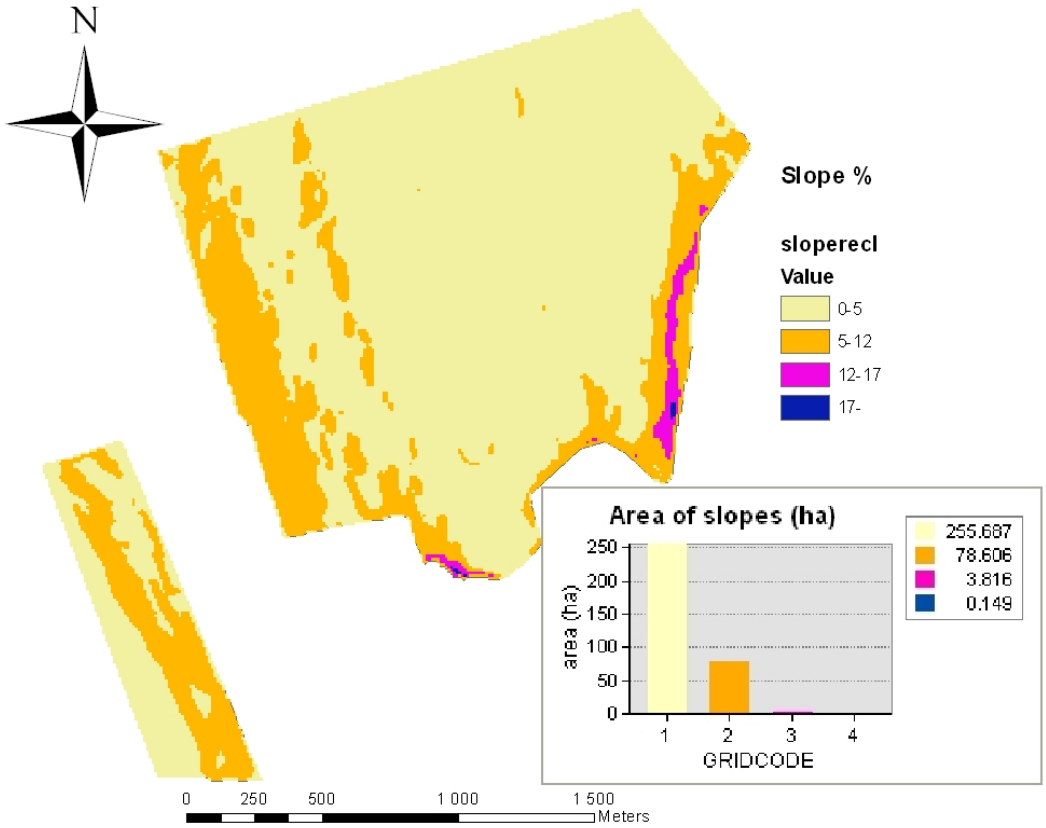

Figure 3. Slope categories of the examined site.

In order to reduce the effect of erosion and the amount of runoff the slope length has to be decreased. Utilizing the potential of farm roads and tracks in erosion control, the levels of the existing farm tracks should be developed with reverse slope to control the collection and channeling of runoff. Open side, vegetated, mowable drains are required only on the upper side of the roads. Vegetated stormwater drains are also required, leading water from the drains through culverts and drop inlets.

Based on soil plasticity, according to Arany, sites with different physical characteristics (from sandy loam to loamy clay) could be distinguished. The spatial variability of soil plasticity, thus the physical features of the soil appeared differently (Figure 4.). Since the maximal saturation percentage (K_A=48,05) measured at the sampling point with the highest altitude, it was possibly caused by erosion processes. Concerning the humus content, the same spatial distribution can be found as the soil plasticity. The reason for this is that besides the possible increase of clayminerals, the increasing rate of colloidal humus content contributes to larger soil plasticity. Statistics also proved positive and moderate correlation (r=0.701) between the soil plasticity and humus content. Moderate correlation (p=0.705) was found between K and humus content, which shows the higher adsorption capacity of soils rich in humus.

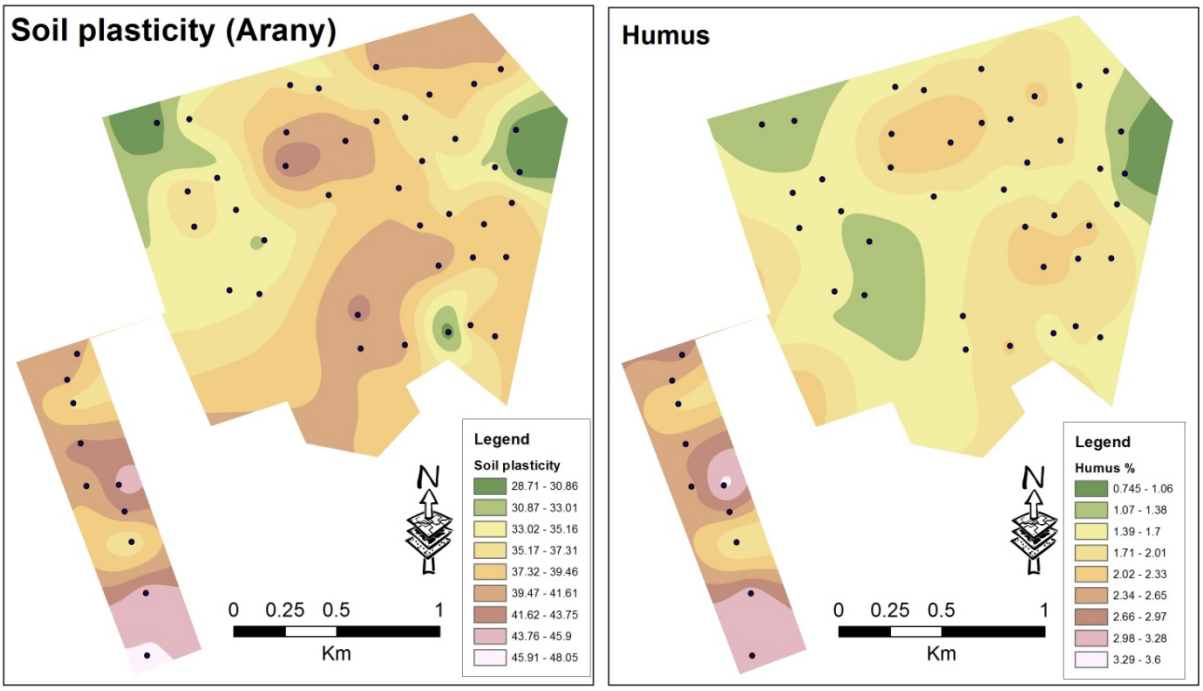

Figure 4. Spatial distribution of soil plasticity and humus

Although the spatial distribution of pH and calcium carbonate show positive moderate correlation (r=0.689) as it was supposed, the results can be used in precision agriculture (Figure 5). In the case of pH, only a small part of the orchard is has to be limed, since most of the orchard has neutral pH, which is advantageous for nuts and stone fruits. It has to be mentioned, that the $CaCO_3$ supply is also appropriate for the stone fruits. The measured extremities are probably due to sampling errors.

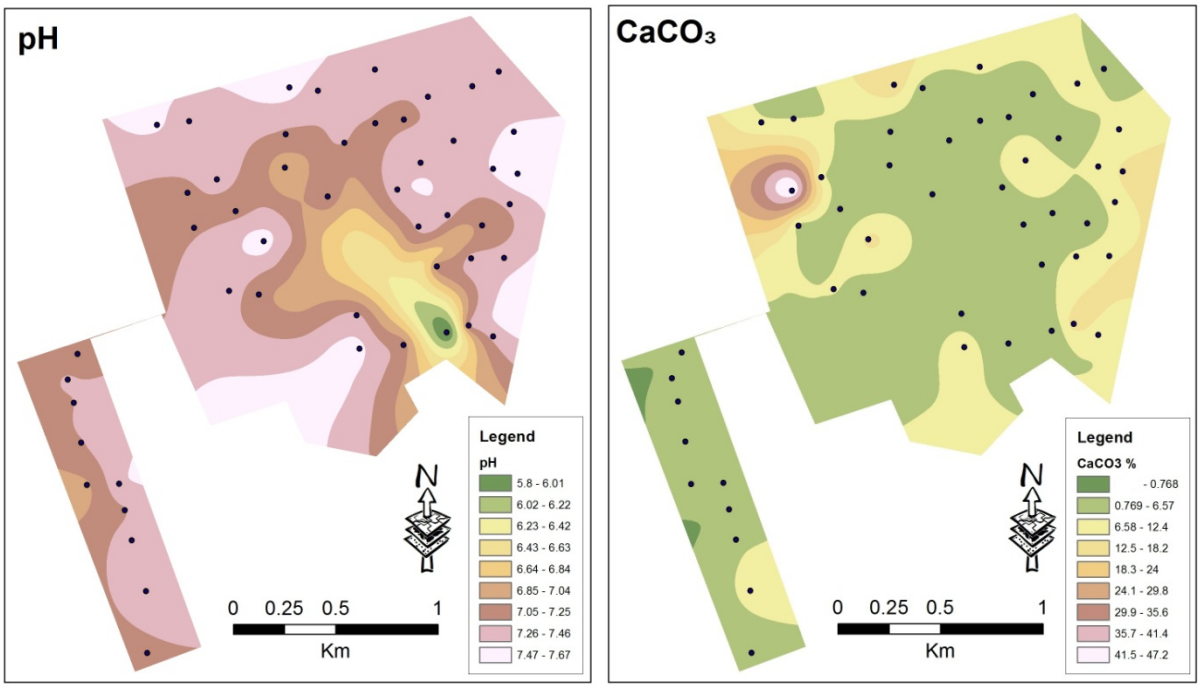

Figure 5. Spatial distribution of pH and $CaCO_3$

The spatial distribution of nutrients and microelements was also investigated. Based on nutrient distribution, erosion risk and soil type maps, locations were defined where considerable nutrient loss can occur. With the present situation, distributing small doses of fertilizer should be utilized at the ridge spots, while in the case of convex parts of the valley, smaller doses of nutrient should be used.

Conclusion

As a conclusion, in the case of a possible replantation of the orchard, trees should be planted along the contour lines, so as to avoid erosion and tree damage caused by water erosion. The rrigation of the orchard would be much easier in this case due to better establishment of the irrigation system and lower pipe-line pressure lost. To decrease the effect of erosion, the levels of the existing farm tracks have to be developed with reverse gradient. With the present situation, distributing small doses of fertilizer should be utilized at the ridge spots, while in the case of convex parts of the valley, smaller doses of nutrients should be used. These digital data can be the basis for a precision spatial decision support system.

Acknowledgement

This study is funded by TECH_08-A3/2-2008-0373 and TECH_08-A4/2-2008-0138 projects.

References

Browning, G. M. 1977. Developments that led to the universal soil loss equation: a historical review. In: Soil Erosion: Prediction and Control. (ED.: FOSTER, G. R.) 3–5. Soil Conservation Society of America. Ankeny, Iowa.

Hudson, N. 1995. *Soil conservation*. 3rd ed. London, B.T. Batsford Ltd.

Jolánkai M. 2010. Agriculture, soil management and climate change. In: *Climate change and Hungary: Mitigating the hazard and preparing for the impacts (The "VAHAVA" report)*, 38-45. Budapest, Hungary.

Kertész, Á. 1995. Aridification in a region adjacent to the Mediterranean. Objectives and outline of a scientific programme, MEDALUS Working Paper 65. King's College. London.

Kim R. (1995): The water budget of heterogeneous areas. Doctoral thesis. Wageningen Agricultural University. Wageningen, The Netherlands.

László, P., and K. Rajkai. 2003. A talajerózió modellezése. (Modeling of soil erosion) *Agrokémia és Talajtan* 52(3-4): 427-442.

Morgan, R.P.C. 1996. Soil Erosion and Conservation 2nd ed. London, Cranfield University.

Evaluating the change of hydrological processes and sediment yield considering the impact of climate change

Dao Nguyen Khoi*
Interdisciplinary Graduate School of Medicine and Engineering, University of Yamanashi
4-3-11 Takeda, Kofu, Yamanashi 400-8511, Japan
Email: dnkhoi86@gmail.com

Tadashi Suetsugi
Interdisciplinary Graduate School of Medicine and Engineering, University of Yamanashi
4-3-11 Takeda, Kofu, Yamanashi 400-8511, Japan
Email: dnkhoi86@gmail.com

* Corresponding author

Abstract

In this study, we investigated the impact of climate change on hydrology and sediment yield in Be River Catchment using SWAT hydrological model. The calibration and validation results indicate that SWAT model is a reasonable tool to simulate the impact of environmental change on hydrology and sediment yield for this catchment. Based on the calibrated model, the responses of hydrology and sediment yield to climate change were simulated. Climate change scenarios (A1B and B1) were developed from four GCM simulations (CGCM3.1 (T63), CM2.0, CM2.1, and HadCM3). Under the climate change impacts, the simulated results exhibit that the annual streamflow is expected to decrease by 0.7% to 5.1%, and the annual sediment yield is projected to change by -5.5% to 4.5% in the future. It is indicated that changes in sediment yield due to climate change are larger than the corresponding changes in streamflow. In addition, climate change causes changes in annual evapotranspiration (-0.6% – 2.8%) and decreases in groundwater discharge (3.0% – 8.4%) and soil water content (2.0% – 4.8%).

Keywords: Be River Catchment; Climate change; Hydrology; Sediment yield; SWAT model

Introduction

The Intergovernmental Panel on Climate Change (IPCC) report reaffirms that "global warming" is occurring (IPCC 2007). This global warming leads to changes in precipitation and temperature, thence affects the hydrological cycle, and thus changing in the streamflow and also modifying the transformation and transport characteristics of sediment as well as water pollutants (Tu 2009). Therefore, climate change is an important factor influencing hydrological conditions and sediment yield. Understanding the hydrologic and sediment responses to climate change is a necessity for water resource planning and management. In recent decades, the potential impacts of climate change on hydrological processes have gained considerable attention from many hydrologists. A variety of studies have been investigated the impact of climate change on hydrology (e.g. Christensen and Lettenmaier, 2007; Zhang et al., 2007; Githui et al., 2009; Boyer et al., 2010; Ruelland et al., 2012; Kienzle et al., 2012) and sediment yield (e.g. Thodsen et al., 2008; Li et al., 2011). In most of these studies, the hydrological model is first calibrated against observed data, and then run with future climate scenarios using calibrated parameters. Global climate models (GCM) are the main tool used to build the climate change scenarios in hydrological impact studies. Kingston et al. (2011) emphasized the importance of multi-GCMs evaluations in the climate change impacts because the future precipitation simulated from different GCMs often disagree even in the direction of change.

Literature review shows that there are many hydrological and soil erosion models such as AGNPS (Agricultural Non-Point Source) model, HSPF (Hydrological Simulation Program Fortran) model, SWAT (Soil and Water Assessment Tool) model, WEPP (Water Erosion Prediction Project) model, and WaTEM/SEDEM model. These models are used presently to simulate hydrological and sediment processes at catchment scale. Among these models, the SWAT model is frequently used to evaluate hydrology and sediment yield in many catchments around the world (e.g. Xu et al., 2009; Wang et al., 2010; Betrie et al., 2011; Oeurng et al., 2011).

Vietnam has experienced changes in climate that include rising air temperatures and more variation in precipitation. In the period of 1958-2007, the annual average temperature increased about 0.5-0.7°C. The annual precipitation decreased in Northern part while increased in Southern part. On an average for the whole country, the rainfall over past 50 years (1958-2007) decreased approximately 2% (MONRE 2009). These changes have been led to significant changes in the availability of water resources and sediment yield in Vietnam. Some previous studies have been performed to evaluate the impact of climate change on water resources in Vietnam (e.g. Kawasaki et al., 2010; Phan et al., 2010; Thai and Thuc, 2011). However, few studies have investigated future climate change impacts on sediment yield in Vietnam. For instance, Phan et al. (2011) studied changes in sediment yield for Song Cau watershed in northern Vietnam under the climate change scenarios obtained from Vietnam Ministry of Natural Resources and Environment (MONRE) and have reported that the streamflow and sediment yield are expected to increase by 1.0% to 3.0% and 1.2% to 4.0% under the impact of climate change (B1, B2, and A2 emission scenarios).

The specific objective of this study is to assess the impact of climate change on hydrological processes and sediment yield of Be River Catchment in Vietnam using the SWAT hydrological model. For this purpose, plausible climate scenarios are developed from the GCMs based on the IPCC AR4 database. The results achieved from this study provide decision-makers important information that they need to help water resources planning efforts and sustainable development.

Study area

The catchment selected for study from the Dong Nai River Basin in the south of Vietnam lies between latitudes $11^{o}10'$ to $12^{o}16'$ N and longitudes $106^{o}36'$ to $107^{o}30'$ E (Fig. 1). It is located in Dak Nong, Binh Phuoc, Binh Duong, and Dong Nai provinces and has a catchment area of about 7500 km^2. The altitude varies from 1000m in the highland area to 100m in the plain area with the direction from the northeast to southwest and south. The origin of the branched tree drainage system of Be River lies in the Tuy Duc at the international border of Vietnam and Cambodia in Dak Nong province. The study area is located in the steep area. The degree of slope can be divided into three levels, a slope from 0-7% accounts for 45% of the total area, one of 8 to 15% accounts for 33% of the area, and one greater than 15% accounts for 22% of the area. The climate is tropical monsoon. The annual rainfall varies between 1800 and 2800 mm with an average of 2400 mm. This area has two seasons: the rainy season and the dry season. The rainy season lasts from May to October and accounts for 85 to 90% of the total annual precipitation. The average temperature is about 25.9ºC, the highest temperature is 36.6ºC and the lowest temperature is 17.3 ºC. This area has relatively fertilized land (75% basalt soil) consistent with agricultural development. The total population in 2010 was approximately 1 million people. Be River Catchment has been assessed as having the most abundant water resources in Dong Nai River Basin and large hydropower potential. Furthermore, this catchment provides water for urban water supplies, agriculture, and the industrial sector not only in this area but also in surrounding provinces such as Binh Duong, Tay Ninh, Ho Chi Minh, and Long An. In addition, this catchment supplies water for preventing salinity intrusion into the Sai Gon and Dong Nai Rivers in the dry season. Therefore, any changes in the supply of rainfall due to climate change could have serious consequences for the agricultural, industrial, and environmental sectors.

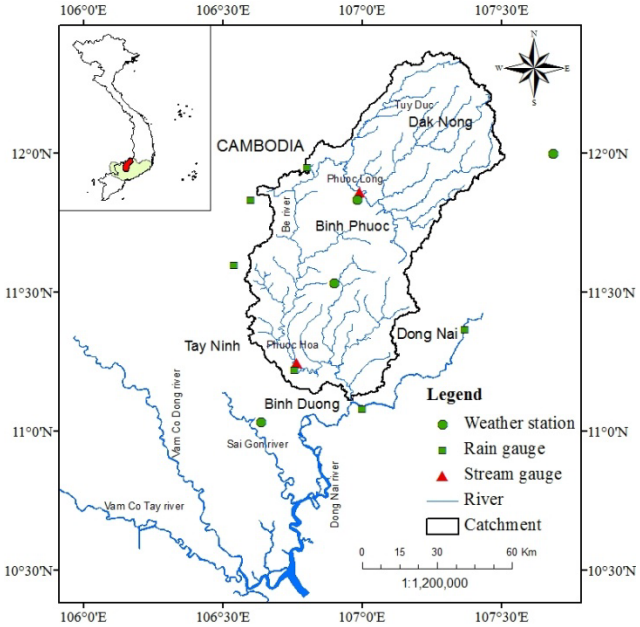

Figure 1. Location map of Be River Catchment

Methodology

SWAT model

The SWAT model is a physically based distributed model designed to predict the impact of land management practices on water, sediment and agricultural chemical yields in large complex watersheds with varying soils, land-use and management conditions over long periods of time (Neitsch et al., 2011). In the SWAT model, a catchment is divided into a number of sub-watersheds or sub-basins. Sub-basins are further partitioned into hydrological response units (HRUs) based on soil types, land-use and slope classes that allow a high level of spatial detail simulation. The model predicts the hydrology at each HRU using the water balance equation:

$$SW_t = SW_0 + \sum_{i=1}^{t} \left(R_{day} - Q_{surf} - E_a - w_{seep} - Q_{gw} \right) \qquad (1)$$

where SW_t is the final soil water content (mm), SW_0 is the initial soil water content on day i (mm), t is the time (days), R_{day} is the amount of precipitation on day i (mm), Q_{surf} is the amount of surface runoff on day i (mm), E_a is the amount of evapotranspiration on day i (mm), w_{seep} is the amount of water entering the vadose zone from the soil profile on day i (mm), and Q_{gw} is the amount of return flow on day i (mm).

The SWAT model provides two methods for estimating surface runoff: the SCS curve number procedure (USDA-SCS, 1972) and the Green and Ampt infiltration method (Green and Ampt, 1911). SWAT calculates the peak runoff rate using a modified rational method. The evapotranspiration is estimated in the SWAT model using three methods: the Penman-Monteith method (Monteith, 1965), the Priestley-Taylor method (Priestley and Taylor, 1972), and the Hargreaves method (Hargreaves et al., 1985). Channel routing is simulated using the variable storage coefficient method (William, 1969) and the Muskingum method (Chow, 1959).

The SWAT model uses the Modified Universal Soil Loss Equation (MUSLE) to simulate sediment yield for each HRU. MUSLE is a modified version of the Universal Soil Loss Equation (USLE) developed by Wischmeier and Smith (1965, 1978). The MUSLE (William, 1995) is given as:

$$sed = 11.8 \times \left(Q_{surf} \times q_{peak} \times area_{HRU} \right)^{0.56} \times K_{USLE} \times C_{USLE} \times P_{USLE} \times LS_{USLE} \times CFRG \qquad (2)$$

where sed is the sediment yield on a given day (tons), Q_{surf} is the surface runoff volume (mm/ha), q_{peak} is the peak runoff rate (m^3/s), $area_{HRU}$ is the area of the HRU (ha), K_{USLE} is the USLE soil erodibility factor, C_{USLE} is

the USLE cover and management factor, P_{USLE} is the USLE support practice factor, LS_{USLE} is the USLE topographic factor, and CFRG is the coarse fragment factor.

The sediment channel routing model consists of two components – deposition and degradation, which simulate simultaneously. The amount of sediment that can be transported from a reach segment is a function of the peak channel velocity. Once the amount of deposition and degradation has been calculated, the amount of sediment in the reach is determined:

$$sed_{ch} = sed_{ch,i} - sed_{dep} + sed_{\deg} \quad (3)$$

where sed_{ch} is the amount of suspended sediment in the reach (tons), $sed_{ch,i}$ is the amount of suspended sediment in the reach at the beginning of the time period (tons), sed_{dep} is the amount of sediment deposited, and sed_{deg} is the amount of sediment re-entrained (tons). Further details can be found in the SWAT Theoretical Documentation (Neitsch et al., 2011).

SWAT model set-up

The input data required for SWAT include weather data, a land-use map, a soil map, and a Digital Elevation Map (DEM), as listed in Table 1. Discharge data were also used in the simulation of surface runoff for calibration and validation purposes. The ArcGIS interface of the SWAT 2009 version was used to delineate a watershed and extract the SWAT input files. The Be River Catchment was delineated and sub-divided into 104 sub-basins using a 90m DEM (http://gisdata.usgs.gov/website/HydroSHEDS/). Sub-basin parameters such as the slope gradient and slope length of the terrain were derived from the DEM.

Land-use/Land-cover is one of the most important factors affecting runoff, erosion, recharge, and evapotranspiration in the watershed (Shimelis et al., 2010). This study obtained land-use data in 2005 from Sub-National Institute of Agricultural Planning and Projection, Vietnam (Sub-NIAPP). The main land-use types of the area are forest land, shrubland, agricultural land, urban, and water.

The soil types of the study area were extracted from SOIL-FAO databases from the Food and Agriculture Organization of the United Nations (FAO, 1995). The data are provided at 10km spatial resolution along with a database of soil properties for two soil layers. The top layer is created at a default of 0 to 30cm, and the subsequent layer is set at 30 to 100cm (effective plant root depth). Soil properties for particle size distribution, bulk density, organic carbon content, and available water capacity were obtained using Reynolds et al. (1999). Major soil types in the catchment are Pellic Vertisols, Rhodic Ferrasols, Gleyic Acrisols, and Ferric Acrisols.

SWAT requires the climatic data at daily time step which can be obtained from a measured dataset or generated by a weather generator algorithm. The required climatic variables include rainfall, minimum and maximum temperatures, relative humidity, wind speed, and solar radiation. In this study, data taken at six rain gauges and three weather stations located within and around the catchment for 1978 to 2007, obtained from Hydro-Meteorological Data Center of Vietnam, were used (Fig. 1). Daily rainfall and minimum and maximum temperatures were available from all six rain gauges and three weather stations, while relative humidity, wind speed, and solar radiation were available from all the weather stations at monthly level.

Daily river flow data measured at Phuoc Long (1981 to 1993) and Phuoc Hoa (1981 to 2000) gauging stations (Fig. 1) were used for the model calibration and validation of streamflow simulation. Monthly sediment load data measured at Phuoc Hoa station (1999-2004) were used for calibration and validation of sediment simulation.

Table 1. SWAT model input data for Be river catchment

Data type	*Description*	*Resolution*	*Source*
Topography map	Digital Elevation Map (DEM)	90 m	SRTM
Land-use map	Land-use classification	1 km	Sub-NIAPP
Soil map	Soil types	10 km	FAO
Weather	Daily precipitation, minimum and maximum temperature	9 stations	Hydro-Meteorological Data Center (HMDC)

The model set-up consists of five steps: (1) data preparation, (2) sub-basin discretization, (3) HRU definition, (4) parameter sensitivity analysis, and (5) calibration and validation. Sensitivity analysis was carried out to identify the most sensitive parameters for the model calibration using Latin Hypercube One-factor-At-a-Time (LH-OAT), an automatic sensitivity analysis tool implemented in SWAT (Van Griensven *et al.* 2006). Those sensitive parameters were calibrated using the Auto-calibration Tool that is currently available in the SWAT interface (Van Liew *et al.* 2005).

SWAT model evaluation

In order to evaluate the performance of hydrological model, three statistical measures were applied for calibration and validation periods: Nash-Sutcliffe efficiency (NSE), percent bias (PBIAS), and ratio of the root mean square error to the standard deviation of measured data (RSR).

The ratio of root mean squared error to observations standard deviation (RSR) is calculated as the ratio of the RMSE and standard deviation of measured data, as shown in Eq. 4 (Moriasi et al., 2007):

$$RSR = \frac{RMSE}{STDEV_{obs}} = \frac{\sqrt{\sum_{i=1}^{N}(O_i - P_i)^2}}{\sqrt{\sum_{i=1}^{N}(O_i - \overline{O})^2}} \quad (4)$$

where O_i is the observed value, P_i is the simulated value, $\overline{O}$ is the mean of the observed data, and N is the total number of observations.

According to Moriasi et al. (2007), the values of NSE greater than 0.5 and the values of RSR less than 0.7 indicate the satisfactory model performance for both flow and sediment simulation. The values of PBIAS which are considered satisfactory are less than 25% for flow simulation and 55% for sediment simulation.

Climate change scenarios

The outputs of four GCMs driven by A1B and B1 emission scenarios were used for building climate change scenarios in three future periods: 2020s (2010-2039), 2050s (2040-2069), and 2080s (2070-2099). The four selected climate models are CGCM3.1, CM2.0, CM2.1, and HadCM3 (Table 2). These models were chosen because they showed the good performance in reproducing historical rainfall for Be River Catchment (Khoi & Suetsugi 2011).

GCMs represent accurately climate at a global scale, but are inaccurate when simulating climate at regional scale (Kienzle et al., 2012). In order to apply the GCMs on a regional scale and create future climate scenarios for local hydrological impact assessment, the delta change method was used to downscale GCM output to regional level. The delta change method has been widely used in previous climate change studies (e.g., Kim and Kaluarachchi, 2009; Boyer et al., 2010; Van Roosmalen et al., 2010; Kienzle et al., 2012) because its simplicity enables rapidly generating a wide range of plausible climate scenarios from a group of GCMs which is an important aspect of this study. In essence, this method modifies the observed historical time series by adding the difference between the future and the baseline periods as simulated by a GCM. The monthly differences

between the future and the reference periods are calculated for temperature (maximum and minimum) and precipitation over the region covering at least one grid point depending on the resolution of each GCM. Regional differences obtained with more grid points give more physically representative results than a value calculated with just one grid point (Wilby et al., 2004; Boyer et al., 2010). The differences are then added to the observed daily maximum and minimum temperature during the baseline period while the ratio is applied for precipitation.

Table 2. Description of GCMs used

Center, country	*Center abbreviation*	*Model identify*	*Model resolution*	
			Longtitude	*Latitude*
Canadian Centre for Climate Modelling and Analysis, Canada	CCCMA	CGCM3.1(T63)	3.750000	3.711136
Geophysical Fluid Dynamics Laborary, USA	GFDL	CM2.0	2.500000	2.022471
		CM2.1	2.500000	2.022471
UK Met. Office, UK	UKMO	HadCM3	3.750000	2.500000

Results and discussion

Calibration and validation

The most sensitive parameters for flow simulations were curve number (CN2), soil evaporation compensation factor (ESCO), threshold water depth in the shallow aquifer for flow (GWQMN), baseflow alpha factor (ALPHA_BF), soil depth (SOL_Z), available water capacity (SOL_AWC), channel effective hydraulic conductivity (CH_K2), groundwater "revap" coefficient (GW_REVAP), Manning's value for main channel (CH_N2), and saturated hydraulic conductivity (SOL_K). The most sensitive parameters for sediment simulations were linear re-entrainment parameter for channel sediment routing (SPCON), exponent of re-entrainment parameter for channel sediment routing (SPEXP), and USLE support practice factor (USLE_P). Those flow and sediment parameters were used to calibrate the simulated runoff and sediment with the observed data. These parameters and their calibrated values are presented in Table 3. Calibration and validation efforts were performed to improve the model performance at main gauging stations. The calibration for streamflow was carried out using daily simulations, while sediment calibration was performed using monthly simulations because of a lack of daily sediment load data. The flow calibration was conducted first and then sediment calibration.

The SWAT flow simulations were calibrated against daily flow from 1981 to 1989 and validated from 1990 to 1993 at Phuoc Long gauging station, as shown in Figure 2. The simulated daily flow fit well the observed data for the calibrated period with NSE, PBIAS, and RSR equal to 0.75, 14.30%, and 0.50, respectively. For the validation period, the values of NSE = 0.78, PBIAS = 14.40%, and RSR = 0.47 suggest that there was a good agreement between the simulated and observed streamflow during this period, based on the performance criteria given by Moriasi et al. (2007). The aggregated monthly average flow values from daily flow values improved the fit between model predictions and observed flows. More detail can be seen in Table 4. Figure 3 shows a hydrograph of the simulated and observed daily flow for calibration and validation period at Phuoc Hoa station. The statistical evaluations shown in Table 4 also suggest that there was a good agreement between the daily measured and simulated streamflow during these periods according to Moriasi et al. (2007). This agreement is shown by NSE = 0.80, RSR = 0.44, and PBIAS = -1.20% for the calibration period and NSE = 0.70, RSR = 0.55, and PBIAS = -6.00% for validation period. In case of the aggregated monthly average flow values, the match between simulated flow values and observed values was improved. This match is shown in Table 4. Although the simulated and observed streamflow were in the same trend, the peak flow was overestimated for

Phuoc Long station and underestimated for Phuoc Hoa station. This may have resulted from the precipitation data. Generally speaking, these results reveal that hydrologic processes in SWAT are modeled realistically for the Be River Catchment which is important for simulation of sediment.

Table 3. SWAT sensitive parameters and calibrated values

*Parameter value is replaced by given value.

**Parameter value is added by given value.

***Parameter value is multiplied by (1 + a given value).

Process	*Parameter*	*Description of parameter*	*Calibrated value*	
			Phuoc Long	*Phuoc Hoa*
Flow	CN2	Initial SCS CN II value***	0.692	0.860
	ESCO	Soil evaporation compensation factor*	0.405	0.743
	GWQMN	Threshold water depth in the shallow aquifer for flow**	1674	2177
	ALPHA_BF	Baseflow alpha factor*	0.268	0.565
	SOL_Z	Soil depth***	0.266	0.055
	SOL_AWC	Available water capacity***	0.334	0.023
	CH_K2	Channel effective hydraulic conductivity**	184	249
	GW_REVAP	Groundwater "revap" coefficient**	0.213	0.193
	CH_N2	Manning's value for main channel*	0.035	0.263
	SOL_K	Saturated hydraulic conductivity***	0.165	-0.051
Sediment	SPCON	Linear re-entrainment parameter for channel sediment routing*	0.003	
	SPEXP	Exponent of re-entrainment parameter for channel sediment routing*	1.825	
	USLE_P	USLE support practice factor*	0.032	

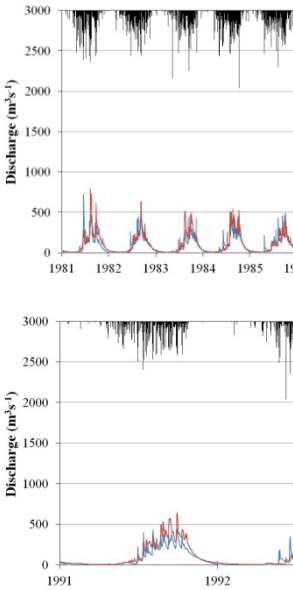

Figure 2. Observed and simulated daily flow hydrograph at the Phuoc Long station, calibration (left) and validation (right)

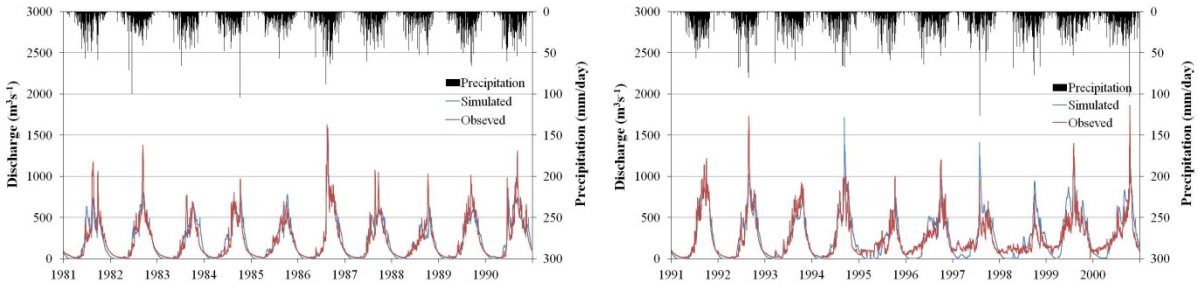

Figure 3. Observed and simulated daily flow hydrograph at the Phuoc Hoa station, calibration (left) and validation (right)

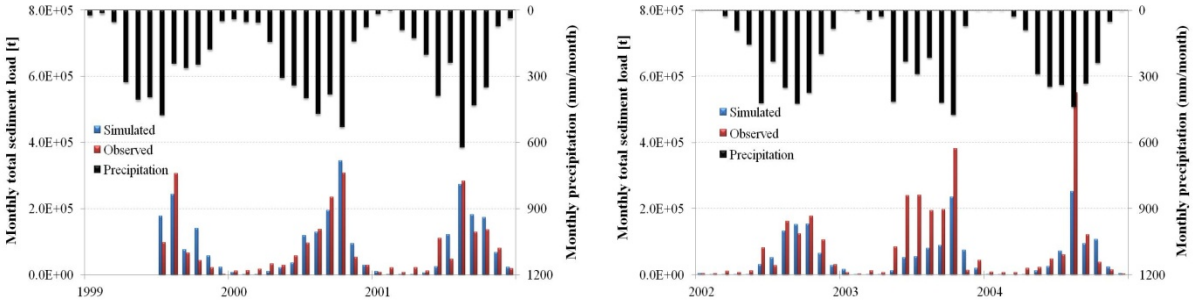

Figure 4. Observed and simulated monthly sediment hydrograph at the Phuoc Hoa station, calibration (left) and validation (right)

Table 4. Model performance for the simulation of runoff

Phuoc Long station					*Phuoc Hoa station*				
Period	*Time step*	*NSE*	*PBIAS*	*RSR*	*Period*	*Time step*	*NSE*	*PBIAS*	*RSR*
Calibration (1981-1990)	Daily	0.75	14.30%	0.50	Calibration (1981-1990)	Daily	0.80	-1.20%	0.44
	Monthly	0.85	14.30%	0.39		Monthly	0.92	-1.20%	0.28
Validation (1991-1993)	Daily	0.78	14.40%	0.47	Validation (1991-2000)	Daily	0.70	-6.00%	0.55
	Monthly	0.88	14.40%	0.34		Monthly	0.79	-6.00%	0.46

Table 5. Model performance for the simulation of sediment yield at Phuoc Hoa station

Period	*Time step*	*NSE*	*PBIAS*	*RSR*
Calibration (07/1999-2001)	Monthly	0.80	-6.72%	0.44
Validation (2002-2004)	Monthly	0.54	-39.72%	0.67

The simulated sediment load were calibrated against monthly observed data from 07/1999 to 2001 and validated from 2002 to 2004 at Phuoc Hoa station, as presented in Figure 4. The fit between simulated and observed sediment load was acceptable according to Moriasi *et al.* (2007). The fit indicated by the values of the NSE = 0.80, RSR = 0.44, and PBIAS = -6.72% for calibration period and NSE = 0.54, RSR = 0.67, and PBIAS = 39.72% for validation period (Table 5). Although an overestimation of monthly sediment yield by the model for the validation period was within the satisfactory level of acceptance, it generally can be said that the simulated result was acceptable.

From the results of calibration and validation, it is reasonable to conclude that the SWAT model could simulate well the hydrology and sediment yield in this catchment. The calibrated parameters were accepted for the scenario simulations.

Climate change scenarios

The baseline and future scenarios of temperature and precipitation under the A1B and B1 scenario are shown in Figures 5a and b. The gray bands provide the range of projections from the four GCMs: CGCM3.1(T63), CM2.0, CM2.1, and HadCM3 while the dashed line represents the ensemble mean GCM projections. The figures show an obvious increase in temperature in the future, while the temperature change amplitude is uncertain due to various climate models. Annual temperature of four GCMs increases range from 1.0ºC to 1.4ºC in 2020s with the ensemble average of 1.1ºC, from 1.8ºC to 2.3ºC in 2050s with the average of 2.1ºC, and from 2.4º to 3.3ºC in 2080s with the average of 2.9ºC for the A1B scenario. Considering the B1 scenario, the mean annual temperature is projected to increase by 1.0°C (the range of 0.8°C – 1.3ºC) in the 2020s, 1.6ºC (1.3°C –

1.8°C) in the 2050s, and 2.0°C (1.6°C – 2.4º) in the 2080s. Increases in temperature showed more variation at monthly time step, with a range from 0.3ºC to 2.2ºC in 2020s, 0.9ºC to 2.9ºC in 2050s, and 1.3ºC to 4.2ºC in 2080s for the A1B scenario. Under the B1 scenario, the temperature rise ranges from 0.2°C to 1.8ºC, 0.6ºC to 2.6ºC, and 1.1ºC to 3.1ºC for the 2020s, 2050s, and 2080s, respectively. Generally, the climate has more warming from the mid-dry season to the early wet season and the temperature rise is predicted higher in the A1B scenario than in the B1 scenario.

In case of precipitation, the precipitation changes show more uncertainty due to various climate models compared with the temperature changes (Figures 5a and b). Averaged over all GCMs ("ensemble average"), the average annual precipitation decreases slightly in the 2020s and 2050s for both scenarios; there is a decrease of 1.2% (the range of -4.2% – 1.7%) in the 2020s and 1.2% (-4.4% – 0.3%) in the 2050s for the A1B scenario, and 4.0% (-5.9% – -0.3%) and 2.4% (-5.4% – 0.8%) for the 2020s and 2050s under the B1 scenario. By the 2080s, the annual precipitation increases about 0.7% (-4.9% – 5.4%) for the A1B scenario and 0.7% (-0.8% – 3.0%) for the B1 scenario. There could be many reasons for precipitation decreasing in the 2020s and 2050s but increasing in the 2080s. However, this is most likely attributed to the GHG emission scenarios. In terms of seasonal change, the precipitation significantly decreases in the dry season. The decrease in dry-season precipitation is 12.8, 10.5 and 11.8% for the A1B scenario, and 19.7, 16.7 and 8.3% for the B1 scenario for the 2020s, 2050s and 2080s, respectively. In the wet season, the precipitation increases slightly in the A1B scenario, with increases of 0.7, 0.4 and 2.8% for the 2020s, 2050s and 2080s, respectively. Under the B1 scenario, the wet-season precipitation decreases slightly in the 2020s, but increases in the 2050s and 2080s. The wet-season precipitation in the B1 scenario is -1.4, 0 and 2.2% for the 2020s, 2050s and 2080s, respectively.

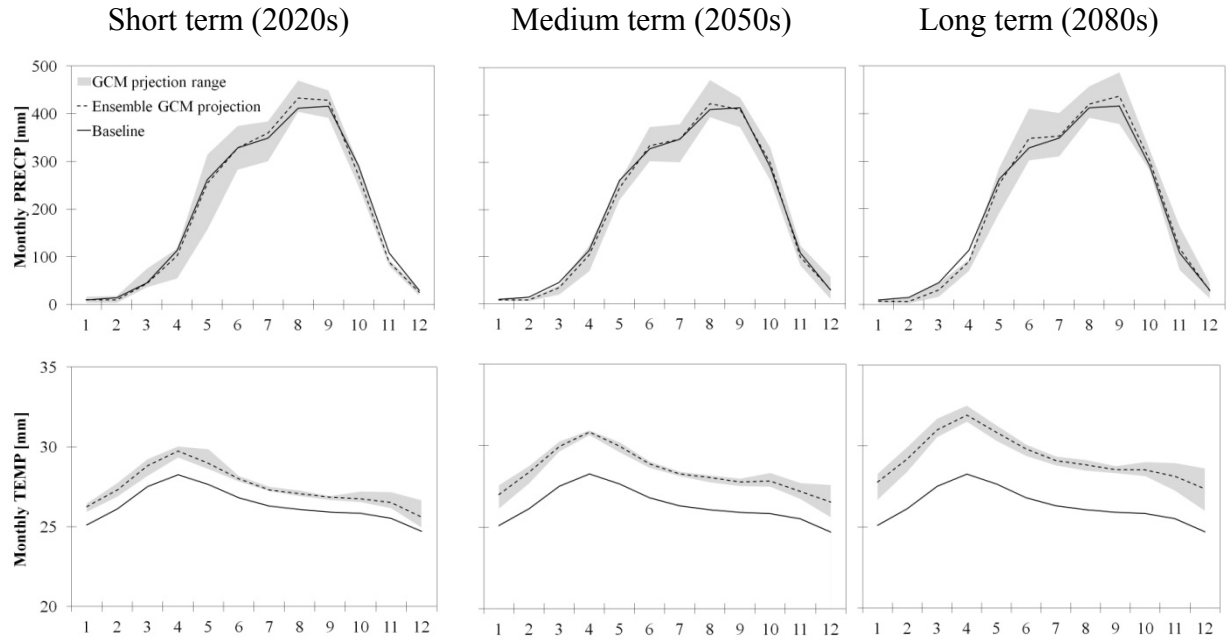

Figure 5a. Monthly changes in climate variables for the 2020s, 2050s, and 2080s in A1B scenario

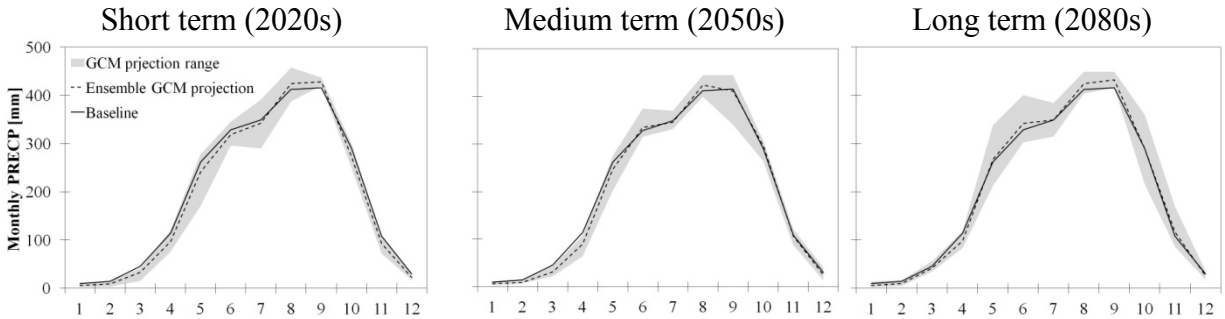

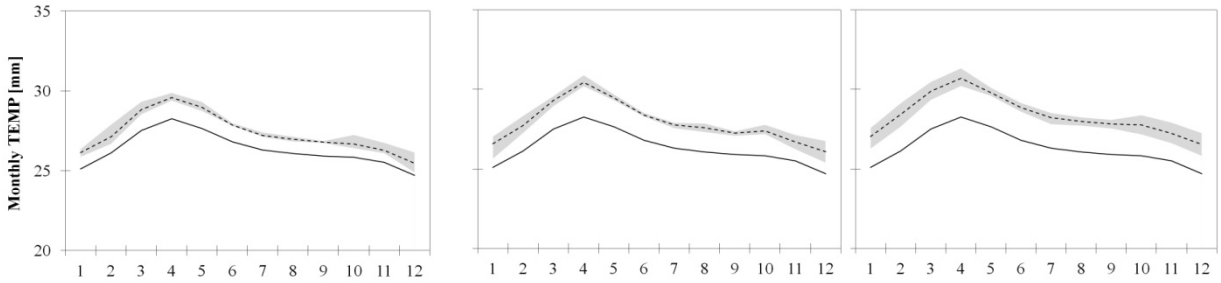

Figure 5b. Monthly changes in climate variables for the 2020s, 2050s, and 2080s in B1 scenario

Regarding both temperature and precipitation, the changes are clear. However, there is much uncertainty associated with the extent of the change under various possible climate change conditions. This would indicate that future streamflow response predictions are also uncertain.

Impacts of climate change on water balance components

Table 6 shows the changes in water balance components such as evapotranspiration (ET), the amount of groundwater discharge (GW_Q), and soil water content (SW) compared with the baseline periods. In general, climate change causes increases in evapotranspiration in most simulations, except for the 2020s in the B1 scenarios. Under the A1B scenario, average increases in evapotranspiration are projected to be 0.8%, 2.1%, and 2.8% for the periods of 2020s, 2050s, and 2080s, respectively. By the B1 scenario, evapotranspiration is simulated to decrease by 0.6% for the 2020s but increase by 0.5% for the 2050s and 2.3% for the 2080s. The changes in evapotranspiration may be the result of increases in the future temperature and changes in precipitation in those periods. The mean annual groundwater discharge is estimated to decrease, on average, by 4.4%, 6.1%, and 5.7% for the A1B scenario and 8.4%, 6.9%, and 3.0% for the B1 scenario for the periods of 2020s, 2050s, and 2080s, respectively. It has been suggested that the increases in evapotranspiration when temperature increases could result in the reduction of groundwater discharge. Besides that, the increases in evapotranspiration may also lead to decreases in soil water content. Indeed, the mean annual soil water content is projected to decrease by 2.0% in the 2020s, 3.4% in the 2050s, and 4.8% in the 2080s for the A1B scenario. In the B1 scenario, the decrease in soil water content is 3.8%, 4.0%, and 2.7% in the periods of 2020s, 2050s, and 2080s, respectively.

Table 6. Percent change of water balance components

Period		A1B scenario			B1 scenario		
		ET	GW_Q	SW	ET	GW_Q	SW
2020s	Min	-1.7	-10.7	-4.7	-2.7	-11.9	-6.2
	Max	1.5	-1.5	-1.1	0.3	-7.0	-3.4
	Ensemble	0.8	-4.4	-2.0	-0.6	-8.4	-3.8
2050s	Min	-0.6	-9.6	-6.1	-0.9	-12.8	-5.2
	Max	2.6	-3.2	-2.9	1.9	-4.7	-2.3
	Ensemble	2.1	-6.1	-3.4	0.5	-6.9	-4.0
2080s	Min	0.7	-12.7	-7.6	1.1	-6.8	-4.2
	Max	3.6	-1.1	-3.4	3.3	-1.3	-1.8
	Ensemble	2.8	-5.7	-4.8	2.3	-3.0	-2.7

Impact of climate change on streamflow and sediment load

Figures 6a and b show the mean monthly discharge and sediment load for the baseline and future climate of three periods of 2020s, 2050s, and 2080s under the A1B and B1 scenarios. Under the impact of climate change scenarios, mean annual streamflow is predicted to decrease during the three future periods. The mean annual decrease of four GCMs is 2.8% (-6.9% – 1.7%), 4.4% (-9.0% – 0.7%), and 2.4% (-10.1% – 4.4%) in the A1B scenario and 7.0% (-11.5% – -3.8%), 5.1% (-12.2% – -3.1%), and 0.7% (-5.3% – 2.7%) in the B1 scenario for the 2020s, 2050s, and 2080s, respectively. The decreases of streamflow can be explained by increases in evapotranspiration and decreases in precipitation. In the 2080s, the precipitation will increase, but the

streamflow is simulated to decrease. It may be explained that an increase in streamflow caused by increase in precipitation will be compensated by a decrease caused by increase in evapotranspiration. In the case of seasonal change, the wet season streamflow decreases slightly in a range from 0.9% to 5.1% and 3.3% to 3.7% for the 2020s and 2050s, respectively. In the dry season, the predicted streamflow decreases considerably varied from 18.3% to 22.8% and 13.5% to 16.2% for the 2020s and 2050s, respectively. In the 2080s, the predicted seasonal streamflow changes slightly, ranging from -1.4 to 0.1% in the wet season, but decreases significantly within a range from 7.0% to 10.5% in the dry season. The reason that declining dry season streamflow is rapidly can be explained by the fact that the runoff in the dry season is more sensitive to the changes in evapotranspiration than in the wet season (Kim and Kaluarachchi, 2009).

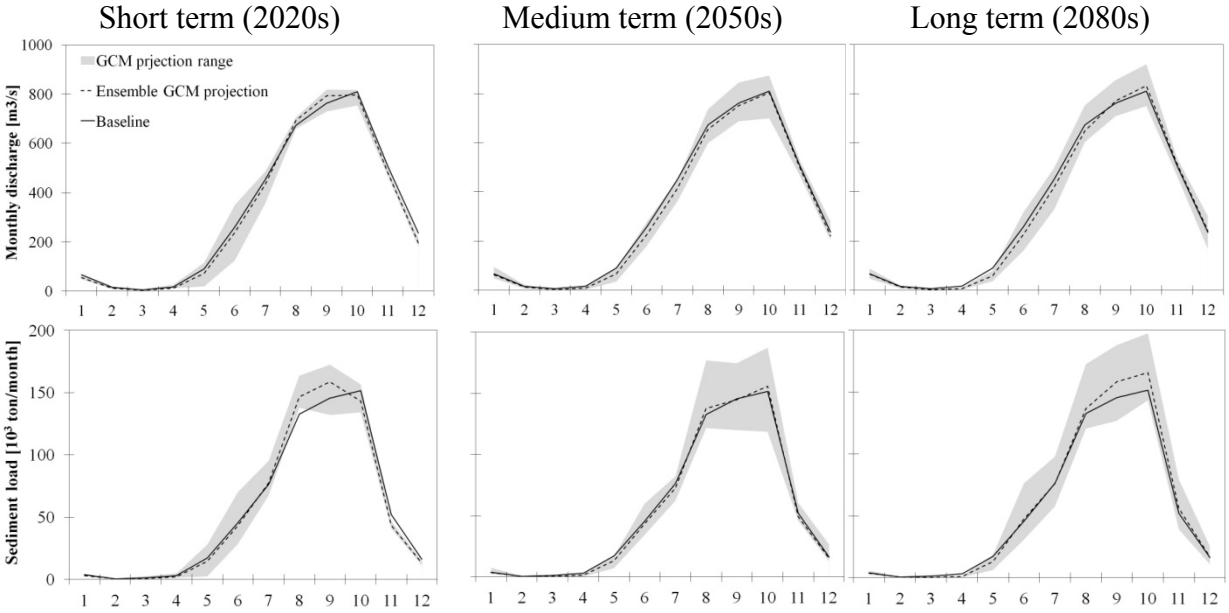

Figure 6a. Monthly changes in streamflow and sediment yield for the 2020s, 2050s, and 2080s in A1B scenario

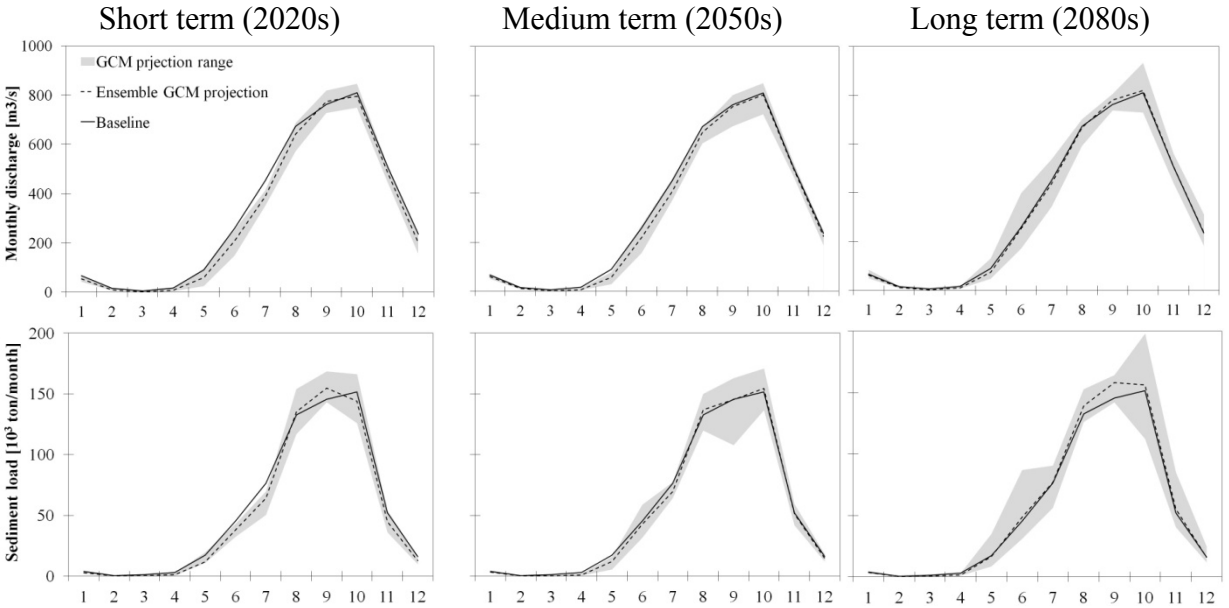

Figure 6b. Monthly changes in streamflow and sediment yield for the 2020s, 2050s, and 2080s in B1 scenario

Considering the impact of climate change on sediment yield, the mean annual sediment yield is predicted to change by 0.1% (-2.1% – 6.3%) in the 2020s, -1.4% (-11.3% – 9.8%) in the 2050s, and 4.5% (-8.4% – 18.9%) in the 2080s for A1B scenario. By the B1 scenario, the changes in annual sediment yield are -5.5% (-14.0% – 3.3%), -2.3% (-12.7% – 2.8%), and 4.1% (-1.0 – 12.6%) for the 2020s, 2050s, and 2080s, respectively. In general, it is interesting to note that the trends of sediment yield and streamflow do not occur in the same

direction. It is shown clearly in the 2080s that the sediment yield will increase even though the streamflow decreases. For this period, the increase in soil erosion is most likely attributed to the increase in precipitation. Besides that, the increase in temperature could influence soil erosion rate through plant growth rate in the region. When the temperature exceeds the optimum temperature, the plant growth rates begin to slow, which is results in soil erosion (Li *et al.* 2011). In terms of seasonal change, sediment yield is projected to change by 1.4%, -0.1%, and 6.0% for the A1B scenario and -3.8%, -0.7%, and 5.0% for the B1 scenario for the periods of 2020s, 2050, and 2080s, respectively in the wet season. In the dry season, the sediment yield is predicted to decrease rapidly by 19.8%, 19.0%, and 17.5% in the A1B scenario and 30.4%, 25.6%, and 8.9% in the B1 scenario for the 2020s, 2050, and 2080s, respectively. Overall, the changes in streamflow and sediment yield are not same with the findings of the study on impacts of climate change in northern Vietnam carried out by Phan *et al.* (2011). In that study, it is indicated that increasing in the streamflow will increase sediment yield and vice versa.

Generally speaking, different seasons will show different change patterns in streamflow and sediment yield. In addition, the changes in annual and wet season flow and sediment load are not dramatic (less than ±20%) in the future. Furthermore, the uncertainty in sediment load is greater than the uncertainty in flow (Figures 6a and b). Because the sediment yield is calculated in the SWAT model based on the surface runoff using MUSLE equation, it will inherit the uncertainty in flow simulation.

Conclusion

The SWAT model was applied to simulate hydrology and sediment processes under the impact of climate change in Be River Catchment, Vietnam. The calibration and validation for streamflow and sediment simulations suggest that the SWAT model could simulate streamflow and sediment yield well for the catchment. The calibrated model can be used for investigating the impact of different climate change scenarios on streamflow and sediment yield.

Two emission scenarios (A1B and B1) and four GCMs (CGCM3.1(T63), CM2.0, CM2.1, and HadCM3) were used to build future climate scenarios in three periods (2020s, 2050s, and 2080s). The projected climate scenarios show that the climate in the study area would generally become warmer under most scenarios and drier in the 2020s and 2050s, but wetter the 2080s. Climate change in the catchment leads to increases in evapotranspiration, decreases in groundwater discharge, soil water content, and streamflow, and changes in sediment yield. The impact of climate change on sediment yield is more variation than on streamflow and the responses of streamflow and sediment yield do not always occur in the same way. In general, an increase in temperature combined with variable rainfall causes variations of hydrological processes over the year. Furthermore, the impacts of climate change also would exacerbate serious problems related to water shortage in the dry season.

In order to improve the simulated results, collecting the additional data should be considered to improve the model calibration and validation. While hydrological modeling is calibrated and validated at daily time step for the long period, sediment simulation is calibrated and validated at monthly time step for the short period. This is a limitation of simulated results. Besides that, the impact of land-use change is not considered in this study and land-use in the basin is assumed to keep the same in the future. In addition, although it is possible to generate realistic future climate scenarios quickly for four selected GCMs, the delta change method still has the limitation. It does not modify the temporal and spatial pattern of the observed data (Boyer et al., 2010). Although there are some limitations as mentioned above, the modeling results are considered reasonable in the prediction of climate change impact on hydrology and sediment yield in the catchment. The results obtained in this study could be useful for planning and managing water resources strategies as well as sediment strategies in this region through enhancing the understanding of the impact of various climate change scenarios on hydrology and sediment.

Acknowledgement

The authors acknowledge the Global Center of Excellent (GCOE) program, University of Yamanashi that funded this study.

References

Betrie, G. D., Y. A. Mohamed, A. Van Griensven, and R. Srinivasan. 2011. Sediment management modelling in the Blue Nile Basin using SWAT model. *Hydrol. Earth Syst. Sci.* 15: 807-818.

Boyer, C., D. Chaumont, I. Chartier, and A. G. Roy. 2010. Impact of climate change on the hydrology of St. Lawrence tributaries. *J. Hydrol.* 384: 65–83.

Chow, V.T. 1959. *Open Channel Hydraulics*. New York: McGraw-Hill.

Christensen, N. A. and D. P. Lettenmaier. 2007. A multimodel ensemble approach to assessment of climate change impacts on the hydrology and water resources of the Colorado River Basin. *Hydrol. Earth Syst. Sci.* 11: 1417-1434.

FAO. 1995. Digital Soil Map of the World and Derived Soil Properties. Rome: Food and Agriculture Organization of the United Nation.

Githui, F., W. Gitau, F. Mutua, and W. Bauwens. 2009. Climate change impact on SWAT simulated streamflow in western Kenya. *Int. J. Climatol.* 29: 1823-1834.

Green, W. H. and G. A. Ampt. 1911. Studies on soil physics: Part I. The flow of air and water through soils. *J. Agr. Sci.* 4: 1-24.

Hargreaves, G. L., G. H. Hargreaves, and J. P. Riley. 1985. Agricultural benefits for Senegal River Basin. *J. Irrig. Drain. E.-ASCE* 111(2): 113-124.

IPCC. 2007. *Climate change 2007: The Physical Science Basic: Contribution of working group I to the fourth assessment report of the Intergovernmental Panel on climate change*. Cambridge, United Kingdom: Cambridge University Press.

Kawasaki, A., M. Takamatsu, J. He, P. Rogers, and S. Herath. 2010. An integrated approach to evaluate potential impact of precipitation and land-use change on streamflow in Srepok River Basin. *Theory and Application of GIS* 18 (2): 9-20.

Khoi, D. N. and T. Suetsugi. 2011 Assessment of climate change impact on streamflow in Be River Catchment, Vietnam. *Proceedings of International Conference on Water Resources Management and Engineering*. Zhengzhou, China.

Kienzle, S. W, M. W. Nemeth, J. M. Byrne, and R. J. MacDonald. 2012. Simulating the hydrological impacts of climate change in the upper North Saskatchewan River Basin, Alberta, Canada. *J. Hydrol.* 412-413: 76-89.

Kim, U. and J. J. Kaluarachchi. 2009. Climate change impacts on water resources in the upper Blue Nile river basin, Ethiopia. *J. Am. Water Resour. Assoc.* 45(6): 1361-1378.

Kingston, D.G., J. R. Thompson, and G. Kite. 2011. Uncertainty in climate change projections of discharge for the Mekong River Basin. *Hydrol. Earth Syst. Sci.* 15: 1459-1471.

Li, Y., B. M. Chen, A. G. Wang, and S. L. Peng. 2011. Effects of temperature change on water discharge, and sediment and nutrient loading in the lower Pearl River basin based on SWAT modeling. *Hydrol. Sci. J.* 56(1): 68-83.

MONRE. 2009. *Climate change, sea level rise scenarios for Vietnam*. Hanoi: Vietnam Ministry of Natural Resources and Environment.

Monteith, J. L. 1965. Evaporation and the environment. In: *The State and Movement of Water in Living Organisms, XIXth Symposium on the Society of Experimental Biology*. Cambridge: Cambridge University Press, 205-234.

Moriasi, D. N., J. G. Arnold, M. W. Van Liew, R. L. Bingner, R. D. Harmel, and T. L. Veith. 2007. Model evaluation guidelines for systematic quantification of accuracy in watershed simulations. *Trans. ASABE* 50: 885-900.

Neitsch, A. L., J. G. Arnold, J. R. Kiniry, and J. R. Williams. 2011. Soil and Water Assessment Tool Theoretical Documentation Version 2009. Technical Report No. 406. Texas A&M University, Texas: Texas Water Resources Institute.

Oeurng, C., S. Sauvage, J. M. Sánchez-Pérez. 2011. Assessment of hydrology, sediment and particulate organic carbon yield in a large agricultural catchment using the SWAT model. *J. Hydrol.* 401: 145-153.

Phan, D. B, C. C. Wu, and S. C. Hsieh. 2011. Impact of climate change on stream discharge and sediment yield in northern Vietnam. *Water Resources* 38(6): 827-836.

Phan, T. T. H., K. Sunada, S. Oishi, and Y. Sakamoto. 2010. River discharge in the Kone River basin (Central Vietnam) under climate change by applying the BTOPMC distributed hydrological model. *Journal of Water and Climate Change* 1(4): 269-279.

Priestley, C. H. B. and R. J. Taylor. 1972. On the assessment of surface heat flux and evaporation using large-scale parameters. *Mon. Weather Rev.* 100: 81-92.

Reynolds, C. A., T. J. Jackson, and W. J. Rawl. 1999. Estimating available water content by linking the FAO soil map of the World with global soil profile databases and pedo-transfer functions. *Proceedings of the AGU 1999 spring conference*, Boston, MA.

Ruelland, D., S. Ardoin-Bardin, L. Collet, and P. Roucou. 2012. Simulating future trends in hydrological regime of a large Sudano-Sahelian catchment under climate change. *J. Hydrol.* 424-425(6): 207-216.

Shimelis, G. S., S. Ragahavan, M. M. Assefa, D. Bijan. 2010. SWAT model application and prediction uncertainty analysis in the Lake Tana Basin, Ethiopia. *Hydrol. Process.* 24: 357-367.

Thai, T. H. and T. Thuc. 2011. Impacts of climate change on the flow in Hong-Thai Binh and Dong Nai River Basins. *VNU Journal of Science, Earth Sciences* 27: 98-106.

Thodsen, H., B. Hasholt, and J. H. Kjærsgaard. 2008. The influence of climate change on suspended sediment transport in Danish rivers. *Hydrol. Process.* 22: 764-774.

Tu, T. 2009. Combined impact of climate and land use changes on streamflow and water quality in eastern Massachusetts, USA. *J. Hydrol.* 379: 268-283.

USDA-SCS. 1972. National Engineering Handbook: Section 4. Hydrology. Washington, DC: USDA.

Van Griensven, A., T. Meixner, S. Grunwald, T. Bishop, M. Diluzio, and R. Srinivasan. 2006. A global sensitivity analysis tool for the parameters of multi-variable catchment models. *J. Hydrol.* 324: 10-23.

Van Liew, M. W., T. L. Veith, D. B. Bosch, and J. Arnold. 2005. Problems and potential of auto-calibrating a hydrologic model. *Trans. ASABE* 48(3): 1025-1040.

Van Roosmalen L., J. H. Christensen, M. B. Butts, K. H. Jensen, J. C. Refsgaard. 2010. An intercomparison of regional climate model data for hydrological impact studies in Denmark. *J. Hydrol.* 380(3-4): 406-419.

Wang, X., S. Shang, W. Yang, C. R. Clary, and D. Yang. 2010. Simulation of land-use soil interactive effects on water and sediment yields at watershed scale. *Ecological Engineering* 36: 328-344.

Wilby, R. L., S. P. Charles, E. Zorita, B. Timbal, P. Whetton, and L. O. Means. 2004. Guidelines for Use of Climate Scenarios Developed from Statistical Downscaling. IPCC Task Group on Scenarios for Climate Impact Assessment (TGCIA).

William, J. R. 1969. Flood routing with variable travel time or variable storage coefficients. *Trans. ASABE* 12: 100-103.

William, J. R. 1995. Chapter 25: The EPIC model. In *Computer models of watershed hydrology*, Singh VP (ed.). Water Resources Publications; 909-1000.

Wischmeier, W. H. and D. D. Smith. 1965. Predicting rainfall-erosion losses from cropland east of the Rocky Mountains. Agriculture Handbook 282. USDA-ARS.

Wischmeier, W. H. and D. D. Smith. 1978. Predicting rainfall-erosion losses: a guide to conservation planning. Agriculture Handbook 282. USDA-ARS.

Xu, Z. X., J. P. Pang, C. M. Liu, and J. Y. Li. 2009. Assessment of runoff and sediment yield in the Miyun Reservoir catchment by using SWAT model. *Hydrol. Process.* 23: 3619-3630.

Zhang, X., R. Srinivasan, and F. Hao. 2007. Predicting hydrologic response to climate change in the Luohe River Basin using the SWAT model. *Trans. ASABE* 50(3): 901-910.

Hydrological response to climate change in the Krishna basin

B. D. Kulkarni *
Indian Institute of Tropical Meteorology, Pune 411008
bdkul@tropmet.res.in

S. D. Bansod

Abstract

In this study, impacts of climate change on water balance components in the Krishna river basin are investigated. Semi-distributed hydrological model namely Soil and Water Assessment Tool (SWAT) has been used. The outputs from RCM, viz. PRECIS ("Providing REgional Climates for Impacts Studies") are applied to generate daily monthly time series of precipitation, surface flow, water yield, ET and PET. The framework predicts the impact of climate change on the hydrological regime with the assumption that the land use shall not change over time and any manmade changes are not incorporated. Simulation at 23 sub-basins of the Krishna basin has been conducted with 30 years of data belonging to control (present) , for the remaining 60 years data (2011-2040) and (2041-2070) were corresponding to GHG (future) climate scenario. Quantification of climate change impact has been done through the use of SWAT hydrological model. The initial analysis has been predicted,the increase in precipitation in almost half of the month of the year and decrease in precipitation in the remaining months. The future annual discharge, surface runoff and base flow in the basin show increases over the present as a result of future climate change.

Key words: Climate change, simulation, Krishna river basin, SWAT, PRECIS

Introduction

Climate variability and change are expected to alter regional hydrologic conditions and result in variety of impacts on water resource systems throughout world. Potential impacts may include changes in hydrological processes such as evaportranspiration, soil moisture, water temperature, streamflow volume, timing and magnitude of runoff, and frequency and severity of floods. Such hydrologic changes will affect almost every aspect of human well-being, from agricultural productivity and energy use to flood control, municipal and industrial water supplies, and fish and wildlife management. Quantitative estimation of the hydrological effects of climate change will be helpful for appropriate design and management of water resources in this region. The general impacts of climate change on water resources have been brought out by the Third Assessment Report of the Intergovernmental Panel of Climate Change (IPCC), 2001). Observed warming over several decades has been linked to changes in the large-scale hydrological cycle such as, increasing atmospheric water vapor content; changing precipitation patterns, intensity and extremes; reduced snow cover and widespread melting of ice; and changes in soil moisture and runoff. Precipitation changes show substantial spatial and temporal variability. The frequency of heavy precipitation events (or proportion of total rainfall from heavy falls) has increased over most areas. (Goswami et. al. 2006). Changes in the total amount of precipitation as well as in its frequency and intensity have been predicted which shall in turn affect the magnitude and timing of runoff and soil moisture status. The impacts of climate change are also predicted to be dependent on the baseline condition of the water supply system and ability of water resource managers to respond not only to climate change but also to population growth and changes in demands technology, as well as economic, social and legislative conditions.

Thus, impact of climate change is going to be most severe in the developing countries, because of their poor capacity to cope with and adapt to climate variability. This paper presents detailed results of predicted water balance components in the Krishna river basin of the country on account of climate change

The main objective of this study is to evaluate the climate change effect on the future water balance components at different sub-basins of the Krishna river basin. In order to accomplish this objective, SWAT (Soil and Water Assessment Tool), a distributed hydrologic model has been used. The feature projected precipitation and temperature changes projected by PRECIS ("Providing REgional Climates for Impacts

Studies") regional model under A1B scenario was input into SWAT to predict future streamflow changes. The results obtained in this study are expected to provide more insight into the availability of future streamflow, and to provide local water management authorities with a planning tool.

Study Area

This study was carried out in the Krishna river basin. The Krishna River and its tributaries form an important integrated drainage system in the central portion of the Indian Peninsula. As per the Khosla (1949) classification, the entire basin has been divided into 5 sub-catchments (No. 306 to 310) .The drainage area of the entire basin is about 2,58,948 km^2 of which 26.8% lies in Maharashtra, 43.8% in Karnataka and 29.4% in Andhra Pradesh. By considering the orography, geographic location and rainfall characteristics, the entire basin has been divided in 5 sub-basis (see Fig.1). Details of sub-catchments and number of raingauge stations in each of the sub-basin are given in Table-1. However, in this study the Krishna basin has been divided in to 23 sub-basins (Fig. 3) for computation of hydrological parameters.

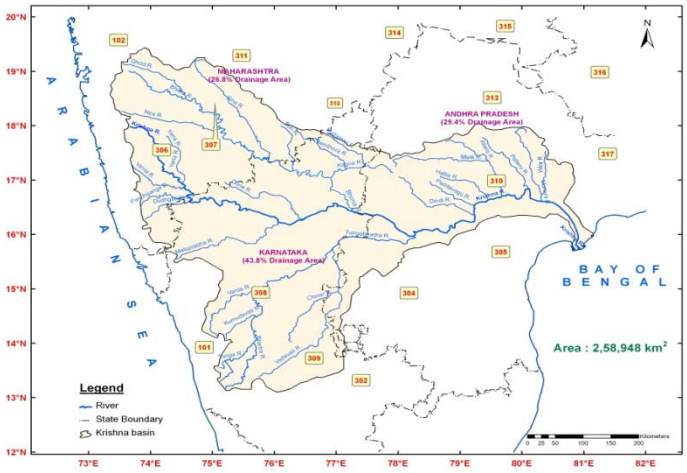

Fig. 1: Locations of sub-catchments in and around the Krishna basin

Table 1. Sub-catchments of the Krishna river basin

Sub-basin	Name of sub/zone	No of Stations in each catchment
306	River Krishna up to its confluence with River Bhima, excluding river Bhima	60
307	River Bhima	62
308	Tungabhadra up to Tungabhadra dam site	49
309	Vedavati up to confluence with Tungabhadra	75

Materials and Methods

SWAT (Soil and Water Assessment Tool) water balance model has been used to carry out the hydrologic modelling of the Krishna river basin. The SWAT model is a physically based, continuous-time model, developed by Dr. Jeff Arnold for UDSA-ARS (Agricultural Research Service; Arnold and Fohrer, 2005). It is used in many countries (Rosenberg et al. 1999). In India also this model has been extensively used for climate change study of Indian River basins by Indian Institute of Technology (IIT) Delhi (Gosian et al 2006). The model has capability of being used for watersheds as well as the major river basin systems. The study determines the present water availability in space and time without incorporating any man made changes like dams, diversions etc. The same framework then used to predict the impact to climatic change on the availability

of water resources (future) by using the predicted data of a PRECIS with assumption that the land use shall not change over time.

Data inputs for Hydrological modelling

The SWAT model requires data on terrain, land use, soil weather for the assessment of water-resources availability at desired locations of the drainage basin. To create a SWAT dataset, the interface needs to access ARC GIS with spatial analyst extension and data set files, which provide certain types of information about the watershed. The following maps and database files were prepared prior to making the simulation runs.

Digital Elevation Model (DEM)

DEM represents a topographic surface in terms of a set of elevation values measured at a finite number of points. DEM for study area have downloaded from ASTER GDM., ASTER Global Digital Elevation Model (ASTER GDEM) .The Ministry of Economy, Trade and Industry of Japan (METI) and the National Aeronautics and Space Administration (NASA) are collaborating on a project to develop ASTER Global Digital Elevation Model (ASTER GDEM), a DEM data which is acquired by a satellite-borne sensor "ASTER" to cover all the land on earth. The resolution of data is 30 seconds and it is downloaded in degree tiles and then mosaic using ARC GIS tool box. The stream layer and watershed layer have been generated using above mentioned data set.

Land Cover/Land Use Layer

Classified land cover data produced using remote sensing by the University of Maryland Global Land cover Facility (13 categories) with resolution of 1 km grid cell size has been used (Hansen et al., 1999).

Soil Data

The published paper maps of soil layer have been procured from the National Bureau of Soil Survey and Land Use Planning (NBSS&LUP, 2002), Nagpur, a premier Institute of the Indian Council of Agriculture Research (ICAR). These soil maps were first digitized and various soil properties viz .Hydrological Group, Maximum routing Depth (mm), Depth of soil at various layers, Water holding capacity of the soil, Texture of the soil, Bulk Density, Moist soil Albedo, Erosion factor of the soil have been worked out. Fig 2 shows the soil layer of the Basin

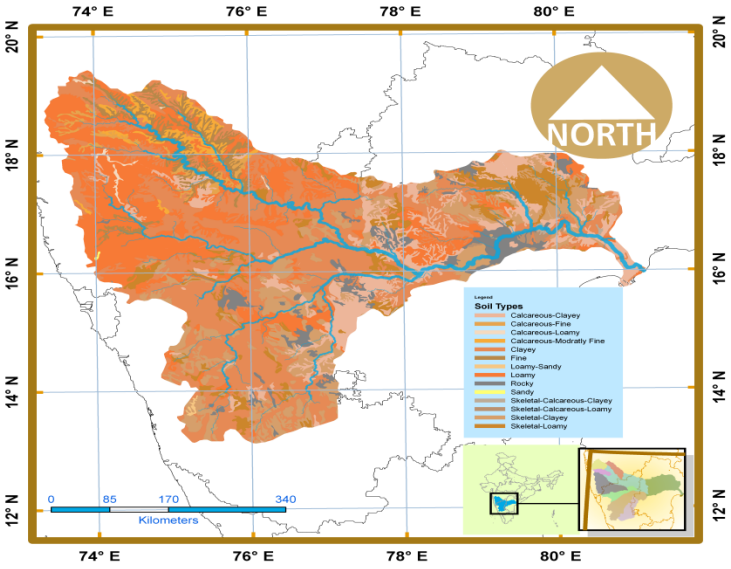

Fig. 2: Soil layer of the Krishna basin

Delineation of the River Basin

Automatic delineation of the Krishna river basin is done by using the DEM as input and the final outflow point on the river basin as the final drainage point. Fig.3 depicts the modelled river basin (automatically delineated

using ARCGIS). The river basin has been further divided into sub-basins depending on the selection of the threshold value.

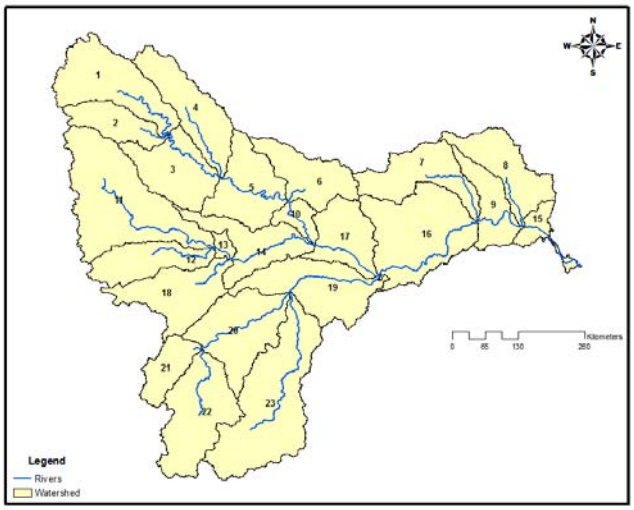

Fig. 3: Delineated sub-basins of the Krishna basin by SWAT

Weather Data

Observed Weather Data

SWAT requires daily values of precipitation, maximum and minimum temperature, solar radiation, relative humidity and wind speed. For generating this data, daily grided observed precipitation and temperature values published by India Meteorological Department (IMD) for the period 1901-2005 and 1950-2000 respectively have been used. Climatic data for solar radiation, wind and humidity published by IMD has also been used.

Weather Data (Climate Model Data)

The data generated in transient experiments PRECIS (("**P**roviding **RE**gional **C**limates for **I**mpacts **S**tudies"), at a resolution 0.44°x 0.44°latitue by longitude RCM grid points has been obtained from Indian Institute of Tropical Meteorology (IITM),Pune, India. PRECIS is an atmospheric and land surface model of limited area and high resolution which is locatable over any part of the globe. PRECIS is forced at its lateral boundaries by the simulations of high resolution global model (HadAM3H). The daily weather data on temperature (maximum and minimum), rainfall, solar radiation, wind speed and relative humidity at all the grid locations were processed. The centroid of each grid point is then taken as the location of weather station to be used in the SWAT model. The procedure has been used for processing the control/present (representing series (1960-1990) and the GHG (Green House Gas) A1B scenarios, (representing series 2011-2040 and 2041-2070).

Hydrological modelling of the basin

The ARCSWAT distributed hydrologic model has been used for simulation of water balance components. The basin has been sub-divided in to 23 sub-basins using the threshold value to adopt to divide the basin into a reasonable number of sub-basins so as to account for the spatial variability. After mapping the basin for terrain, land use and soil, simulated imposing the weather conditions predicted for control and GHG climate

Control Climate Scenario

The Krishna basin has been simulated using ARCSWAT model firstly using generated daily weather data by PRECIS control climate scenario (1960-1990). Although the SWAT model does not require elaborate

calibrations, yet in the present case , any calibration was not meaningful since the simulated weather data is being used for the control period which is not historical data corresponding to the recorded runoff. An evaluation of the PRECIS model, skills and biases is well comparable with observed precipitation and temperature patterns with those in the baseline simulation. (Rup Kumar et al., 2006). The SWAT model has been used on various Indian catchments of varied sizes and it has been observed that the model performs very well without much calibration (Gosain and Sandhya Rao, 2007). Presently, the model has been used with the assumption that river basin is a virgin area without any manmade changes. The model generates the detailed outputs on flow at sub-basin outflow points, actual evapotranspiration and soil moisture status at monthly intervals. Further sub-divisions of the total flow into components such as surface and subsurface runoff, recharge to the ground water can be made on daily basis. The monthly average precipitation, actual evapotranspiration and water yield as simulated by the model over the Krishna basin as whole for control scenario as well as for two A1B Scenarios has been depicted in Fig 4.

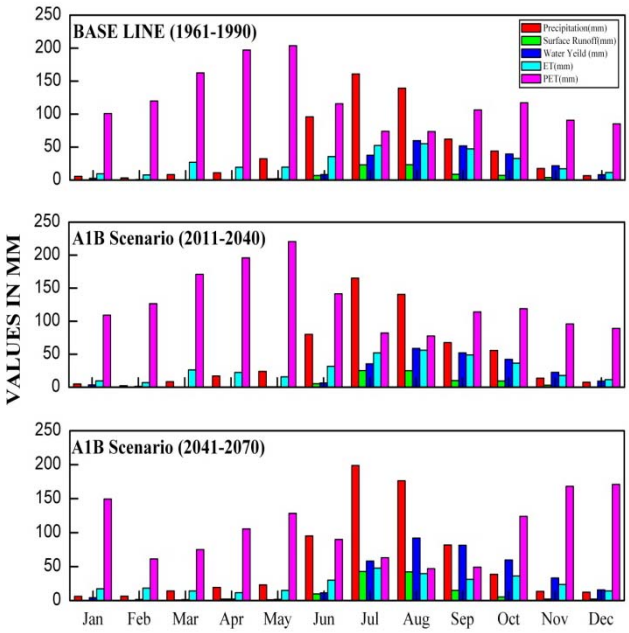

Fig.4 Mean monthly water balance components for A1B Scenarios (2011-2040 and 2041-2070)

PRECIS Climate Scenario

The model has been then run on the Krishna river basin using GHG climate scenarios (for the years, 2011-2040 and 2041- 2070) data but without changing the land use. The outputs of these two scenarios have been made available at sub-basin levels for the Krishna river basin. Detailed analyses have been performed on the problem basin to demonstrate the impacts at the sub-basin level. The monthly average simulated precipitation, actual evapotranspiration, potential evapotranspiration, surface flow and water yield have been depicted in Fig. 4. All annual water balance components have been normalized, by using mean and standard deviation of respective water balance components for the base line period (Fig. 5). The variation in mean annual water balance components from current to GHG scenarios shows that there has been increase in the annual precipitation. The increase in precipitation has been found more prominent for the period 2041-2070. For the period 2011-2040 there is slight decrease in soil moisture storage and surface runoff, where as for the period 2041-2070, surface runoff as well as annual water yield and actual evapotranspiration also likely to be increased. However, there is a decrease in soil moisture storage.

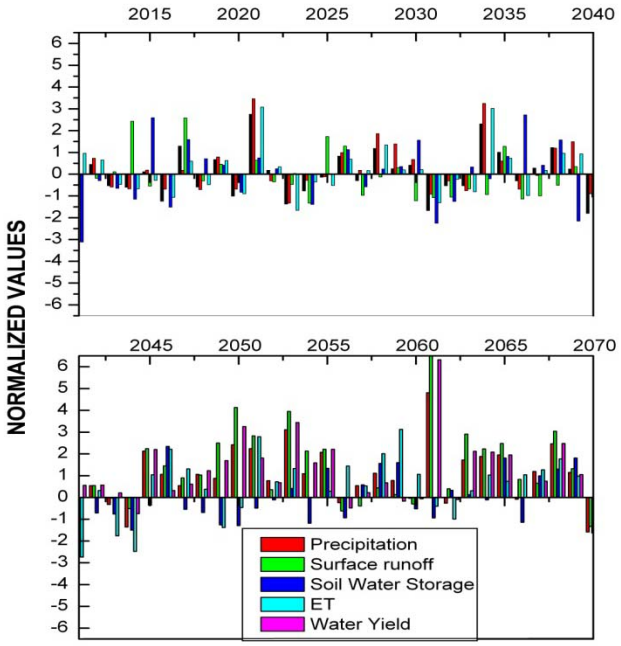

Fig. 5: Normalized annual Water balance components

Changes in Water Balance Components

As mentioned above, the monthly average precipitation, actual evapotranspiration, potential evapotranspiration, surface flow and water yield as simulated over the Krishna basin as a whole for control and two Scenarios (A1B PRECIS) has been obtained. Fig 6 shows the variation in mean monthly water balance components from control to GHG scenario, both in terms of change in individual values of these components as well as percentage of change over control.

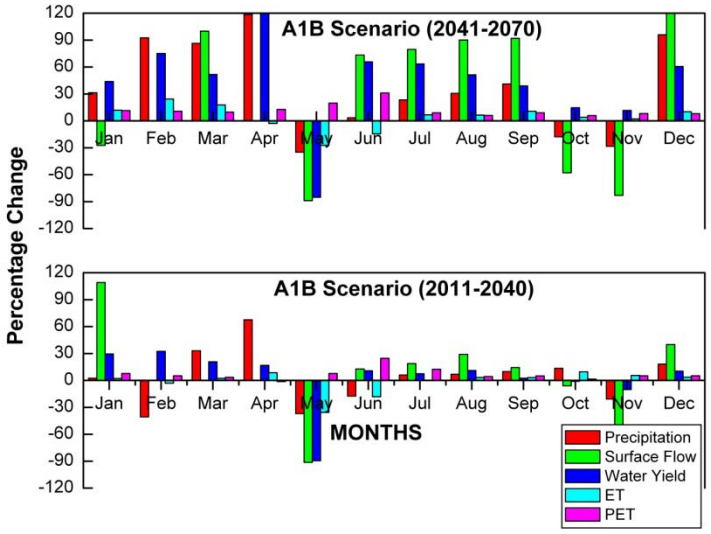

Fig 6: Percentage change in mean monthly water balance components from control to A1B Scenario

It may be observed from the above figures that increase in precipitation has been predicted in almost more than half of the months the year, while remaining months decrease in precipitation has been predicted. The magnitude of this increase/decrease in precipitation over the Krishna basin has been variable over various months. Also the monthly average precipitation, actual evapotranspiration and water yield as simulated by the model over the basin is seems to be increased during the period 2041-2070.

Limitations of the Study

It also should be noted that future flow conditions cannot be projected exactly due to uncertainty in climate change scenarios and GCM outputs. However, the general results of this analysis should be identified and incorporated into water resources management plans in order to promote more sustainable water use in the study area. Climate change impact assessment on water availability for the study watershed considered two model analyses and out puts, which are depends on simplified assumptions. Hence, it is unquestionable that the uncertainties presented in each of the models and model outputs kept on cumulating while progressing towards the final output. These Uncertainties include: Uncertainty Linked to Data quality, General Circulation Model (GCM), Emission scenarios. The model simulations considered only future climate change scenarios assuming all other things constant. But change in land use scenarios, soil, management activities and other climate variables will also contribute some impacts on water availability and crop production.

CONSULISIONS

In this study projections of precipitation and evaporation change and their impacts on stream flow were investigated in the Krishna river basin for the 21st century. The SWAT model is well able to simulate the hydrology of the Krishna river Basin. The future annual discharge, surface runoff and baseflow in the basin show increases over the present as a result of future climate change. However, water resources in the basin will be less reliable in the future.

This study used future climate series for one of the RCM, PRECIS for the impact analysis. Due to uncertainties in climate forecasting, the use of climate model ensembles and multiple scenarios will be useful for understanding the range of climate change impact that can be expected on the water resources in the Krishna river basin.

Acknowledgments

Authors are thankful to Prof. B. N. Goswami, Director, IITM, Pune, Dr K. Krishna Kumar , Programme Manager "Climate Variability and Dynamics", for their keen interest and encouragement for carrying out this study.

REFERENCES

Arnold, J.G., Fohrer, N., (2005) SWAT2000 current capabilities and research opportunities in applied watershed modelling. Hydrological Processes
19, pp. 563-572.

Gosain, A. K. Sandhya Rao and Debajit Basuray (2006) Climate change impact assessment on hydrology of Indian River basins Current Sciences Vol. 90 No. 3, pp. 346-353

Gosain, A. K. and Sandhya Rao (2007) Impact Assessment of Climate Changes on Water Resources of two River systems of India. Jalvigyan Sameeksha, Vol22, 2007,
pp. 1-19

Goswami B.N**.,** Venugopal V., Sengupta D., Madhusoodanan M.S., Xavier Prince K., (2006) Increasing trend of Extreme Rain Events over India in a Warming Environment, Science, 314, 5804, 1 December, 1442-1445

Hansen. M. C., DeFries, R. S., Townshend, J. R. G. and Sohlberg, R. (1999) *1 km Global Land Cover Data Set Derived from AVHRR.* Global Land Cover Facility, University of Maryland institute for Advanced Computer Studies, College Park, Maryland, USA, 1999.

IPCC 2001: Climate Change (2000) ,The science of climate change. Assessment report of the IPCC (Intergovernmental Panel for Climate Change) Working Group I (Eds J. T. Houghton et al) and WMO/UNEP, Cambridge University Press, Cambridge.

Khosla A. N. (1949) , Appraisal of Water Resources Analysis and Utilization of data, Proc. United Nations Scientific Conference on conservation and utilization of resources. Sept 1949.

NBSS and LUP (2002), National Bureau of Soil & Land use Planning , Nagpur *Soils of India* NBSS Publ. No. 94 pp. 1-129

Rosenberg, N.J., Epstein, D.J., Wang, D., (1999) Possible impacts of global warming on the hydrological of the Ogallala aquifer region. Climatic Change 42 (4), pp. 677-692

Rupa Kumar, K., Sahai, A. K., Krishna Kumar, K. , Patwardhan, S. K., Mishra, P. K., Revadekar, J. V., Kamala, K. & Pant, G. B. (2006) High- resolution climate change scenarios for India for the 21st century. Current Science. Vol. 90 No. 3 Feb. 2006 pp.334-345

Management Scenario for the Critical Sub-watersheds of Small Agricultural Watershed using SWAT model and GIS Technique

M. P. Tripathi*
Indira Gandhi Krishivishwavidyalaya, Raipur (C.G.) India
drmpt64@hotmail.com

M. K. Verma**
Indian Institute of Technology, Raipur (C.G.) India
mkseem670@rediffmail.com

and Narendra Agrawal*
Indira Gandhi Krishivishwavidyalaya, Raipur (C.G.) India
agrawal2002in@yahoo.co.in

ABSTRACT

A distributed parameter model, the Soil and Water Assessment Tool (SWAT) was tested on monthly and seasonal basis and used for developing management scenarios for the critical sub-watersheds of a small agricultural watershed (Chhokranala) of Raipur in Chhattisgarh (India). The watershed and sub-watershed boundaries, drainage networks, slope and soil texture maps were generated using GIS. Supervised classification method was adopted for land use/cover classification from satellite imagery using ERDAS Imagine. Manning's 'n' for overland and channel flow and Fraction of Field Capacity (FFC) were calibrated for monsoon season of the years 2002 to 2003. The model was validated for the years 2004 to 2005. Results revealed that the model was predicting the monthly and seasonal surface runoff and sediment yield satisfactorily. Simulation results of nutrients including organic N and P in sediment and NO_3-N and soluble P in runoff were also compared with observed data for several events and found satisfactory. The critical sub-watersheds were identified on the basis of average annual sediment yield and nutrient losses during the study period. Out of seven sub-watersheds, SWS-5, SWS-6 and SWS-7 were found to be critical. Several combinations of treatment options were considered including four crops, five tillage and three levels of fertilizer. The existing management practice was considered as the base for evaluating other management practices for rice. The results showed other crops couldn't replace rice since these crops resulted in higher sediment yield as compared to rice. Considering both sediment and nutrient losses together the zero tillage, conservation tillage and field cultivator with half dose of fertilizer (40:30 of N:P kg/ha) were found to be better than the other treatments considered for evaluating their impact on sediment yield and nutrient losses for sub-watershed (SWS-5).Similar results were also noticed for other critical sub-watersheds i.e. SW-6 and SW-7.

KEYWORDS: Effective Management Plan, GIS, Nutrient Losses, Remote Sensing, Surface Runoff, Sediment Yield, SWAT Model and Weather Generator.

INTRODUCTION

Effective control of soil erosion and sediments requires implementation of best management practices in critical erosion prone areas. This effort can be enhanced by the use of physically based computer simulation models, remote sensing and Geographic Information Systems (GIS) that can assist management agencies in both identifying most vulnerable erosion prone areas and selecting appropriate management practices. Among several computer models, the SWAT is recent one and it has been used most widely for simulating the runoff, sediment yield and water quality of the small watersheds (Arnold et al. 1996). It has capability to simulate the long-term effectiveness of Best Management Practices (BMPs).

The review of the research on SWAT model inferred that the model was tested on daily, monthly or annual basis for both runoff and sediment yield by the most of the researchers (Srinivasan et al. 1993; Srinivasan and Arnold, 1994; Rosenthal et al., 1995; Cho et al., 1995; Tripathi et al., 2003). Very little work has been done to know the impact of management practices on runoff, sediment yield and nutrient losses. The compilation and input of hydrologic and other data that are required by the SWAT model is often cumbersome. However, through the use of GIS and the associated software such data can be compiled and processed with relative ease.

This study gives an approach to use physically based model (SWAT), GIS (GEOMETICA) and image processing software (ERDAS Imagine) to estimate the surface runoff, sediment yield and nutrient from the small watershed of Chhattisgarh. Critical sub-watersheds were identified on the basis of average annual sediment yield and nutrient losses during the study period. The calibrated and validated model was used for planning and management of critical sub-watersheds.

MATERIALS AND METHODS

Study area

The Chhokranala watershed was selected for the study, which is located between 81^0 42'to 81^0 46' E longitude and $21^0$13'to $21^0$14' N latitude and covers an area of 1731 ha. The altitude of the watershed varies from 290 to 310m above MSL. The part of the research farm of the Indira Gandhi Agricultural University, Raipur comes under the selected watershed. The Chhokranala is third order watershed and comprises of 6 villages. Location map of Chhokranala watershed in Chhattisgarh along with contours and drainage lines is shown in Fig. 1.

The topography of the watershed is almost flat. The slope ranges from 1% to 2% and the weighted average slope of the watershed is 1.6%. The watershed receives an average annual rainfall of 1420 mm, out of which the monsoon season (June to October) contributes more than 90% rainfall. The monthly mean temperature ranges from a maximum of 37^0C in the month of May to a minimum of 7^0C in the month of December. The monthly mean relative humidity varies from a minimum of 38% in the month of April to a maximum of 83% in the month of August. Overall climate of the area can be classified as sub-humid tropical. Major crops grown in the area are paddy, maize and vegetables in *kharif* season and gram, mustered and vegetables in *rabi* season.

SWAT Model

The major goal of the SWAT model development was to predict the impact of management measures on water, sediment and agricultural chemical yields in large ungauged basins. The SWAT model simulates the surface runoff using the SCS curve number method (USDA-SCS, 1972). Sediment yield is computed for each sub-basin with the Modified Universal Soil Loss Equation (MUSLE) (Williams and Berndt, 1977). The model predicts sub-basin nutrient yield and nutrient cycling using EPIC model (Williams *et al.*, 1984). The SWAT model uses a command structure for routing runoff and chemicals through a watershed similar to the structure of HYMO model (Williams and Hann, 1973). The crop model is a simplification of the EPIC crop model (Williams *et al.*, 1984). Crop yield is estimated using the harvest index concept. The SWAT tillage component was designed to incorporate surface residue into the soil. Fertilizer applications can also be scheduled by the user or automatically applied by the model.

Theoretical consideration

A brief description of sub-basin components and the mathematical relationships used to simulate the processes

and their interactions in the model as described by Arnold et al. (1996) are considered in this study. The mathematical relationships used in the model for simulating runoff volume and sediment yield are described below.

Runoff Volume

SWAT predicts surface runoff for daily rainfall by using the Soil Conservation Service (SCS) Curve Number (CN) method (USDA-SCS, 1972). The model adjusts curve numbers based on Antecedent Moisture Condition (AMC). The basic equations used in SCS curve number method are as follows;

$$Q = \frac{(\mathrm{P} - 0.2S)^2}{P + 0.8S}, \quad P > 0.2S \qquad \ldots.(1)$$

$$Q = 0.0, \qquad R \leq 0.2S \qquad \ldots.(2)$$

Where, Q is the daily runoff, P is the daily rainfall, and *S* is the retention parameter. The retention parameter varies in space because of varying soil, land use, management, and slope; and in time because of changes in soil water content. The parameter *S* is related to CN as follows;

$$S = 254 \left(\frac{100}{CN} - 1\right) \qquad \ldots.(3)$$

The constant, 254, in equation 3 gives *S* in mm. Thus, P and Q are also expressed in mm. The curve number for average moisture condition II (CN_2) (USDA-SCS, 1972) is appropriate for a slope of 5% and can be adjusted for other slopes using the following formula;

$$CN_{2s} = \frac{1}{3}\left(CN_3 - CN_2\right)\left[1 - 2\exp\left(-13.86s\right)\right] + CN_2 \qquad \ldots.(4)$$

Where CN_{2s} is the handbook CN_2 value adjusted for slope, CN_3 is the curve number for moisture condition III (wet), and *s* is the average slope of the watershed. Curve numbers for moisture conditions I (CN_1) and III (CN_3) can be estimated using CN_2 as follows;

$$CN_1 = CN_2 - \frac{20\left(100 - CN_2\right)}{100 - CN_2 + \exp\left[2.533 - 0.0636\left(100 - CN_2\right)\right]} \qquad \ldots.(5)$$

$$CN_3 = CN_2 \exp\left[0.00673\left(100 - CN_2\right)\right] \qquad \ldots.(6)$$

Eq. (7) describes change in retention parameter based on fluctuations in soil water content:

$$S = s_1\left(1 - \frac{FFC}{FFC + \exp\left[w_1 - w_2(FFC)\right]}\right) \qquad \ldots.(7)$$

Where, s_1 is the value of *S* associated with CN_1, w_1 and w_2 are the shape parameters and FFC is the fraction of field capacity and can be computed using Eq. (8):

$$FFC = \frac{SW - WP}{FC - WP} \qquad \ldots.(8)$$

Where, SW is the soil water content in the root zone, WP is the wilting point water content and FC is the field capacity water content.

Values for w_1 and w_2 can be obtained from a simultaneous solution of Eq. 7 according to the assumptions that $S = s_2$ when FFC = 0.6 and $S = s_3$, when (SW-FC)/(PO-FC) = 0.5;

$$w_1 = \ln\left(\frac{60}{1 - s_2/s_1} - 60\right) + 60\,w_2 \qquad \text{....(9)}$$

$$w_2 = \frac{\ln\left(\frac{60}{1 - s_2/s_1}\right) - \ln\left(\frac{POFC}{1 - s_3/s_1} - POFC\right)}{POFC - 60} \qquad \text{....(10)}$$

Where, s_3 is the CN_3 retention parameter and POFC is the porosity-field capacity ratio and can be computed with the following equation;

$$POFC = 100 + 50\left(\frac{\sum_{l-1}^{M}\left(PO_l - FC_l\right)}{\sum_{l-1}^{M}\left(FC_l - WP_l\right)}\right) \qquad \text{....(11)}$$

Where, PO is the porosity of soil layer l. Eqs. (9) and (10) assure that CN_1 corresponds with the wilting point and that the curve number can not exceed 100.

The FFC value obtained in Eq. (8) represents soil water uniformly distributed through the top 1.0 m of soil. Runoff estimates can be improved if the depth distribution of soil water is known. The model estimates daily water content of each soil layer and thus the depth distribution is available. The effect of depth distribution on runoff is expressed in the depth weighting function;

$$FCC^* = \frac{\sum_{l-1}^{M} FCC_l \frac{Z_l - Z_{l-1}}{Z_l}}{\sum_{l-1}^{M} \frac{Z_l - Z_{l-1}}{Z_l}}, \qquad Z_l \le 1.0\ m \qquad \text{....(12)}$$

Where, FFC^* is the depth weighted FFC value for use in Eq. (7), Z is the depth in m to the bottom of soil layer l, and M is the number of soil layers.

Sediment yield

Sediment yield is computed for each sub-basin with the Modified Universal Soil Loss Equation (MUSLE) (Williams and Berndt, 1977);

$$Y = 11.8\left(V\ q_p\right)^{0.56}(K)(C)(PE)(LS) \qquad \text{.... (13)}$$

Where, Y is the sediment yield from the sub-basin in tonnes, V is the surface runoff volume for the sub-basin in m^3, q_p is the peak flow rate for the sub-basin in $m^{3}\cdot s^{-1}$, K is the soil erodibility factor, C is the crop management factor, PE is the erosion control practice factor and LS is the slope length and steepness factor.

The LS factor is computed with the equation (Wischmeier and Smith, 1978);

$$LS = \left(\frac{\lambda}{22.1}\right)^{\xi}\left(65.41S^2 + 4.465S + 0.065\right) \quad \ldots.(14)$$

Where, λ is the average slope length and S is the average slope of the sub-basin.
The exponent ξ varies with slope and is computed with the equation;

$$\xi = 0.6\left[1 - \exp\left(-35.835S\right)\right] \quad \ldots.(15)$$

The crop management factor, C, is evaluated for all days when runoff occurs using the equation;

$$C = \exp\left[\left(-0.2231 - CVM\right)\exp\left(-0.00115\,CV\right) + CVM\right] \quad \ldots.(16)$$

Where, CV is the soil cover (above ground biomass + residue) in kg·ha^{-1} and CVM is the minimum value of C. The value of CVM is estimated from the average annual C factor using the equation;

$$CVM = 1.463\ln\left(CVA\right) + 0.1034 \quad \ldots.(17)$$

The value of average annual C factor CVA for each crop and PE factor for each sub-basin can be determined from tables and information prepared by Wischmeier and Smith (1978).

Model Testing

The SWAT model was tested and used for identifying the critical sub-watershed of the Chhokranala watershed. The validation of a calibrated model is an essential part of the model testing. Therefore, the model was validated using the observed daily rainfall discharge and temperature data. The observed runoff and sediment yield were analyzed and compared with the simulated results for the evaluation of model validation performance. The performance of the model was evaluated on the basis of test criteria recommended by the ASCE Task Committee (1993). The numerical and graphical performance criteria used in this study are described below:

Martinec and Rango (1989) recommended that the criteria should be as simple as possible. The deviation of runoff volumes, D_V, is one goodness-of-fit criterion.

$$D_V(\%) = \frac{V - V'}{V}100$$

where V is the measured yearly or seasonal runoff volume; V' is the model computed yearly or seasonal runoff volume. D_V can take any value; however, smaller the number better the model results are. D_V would equal zero for a perfect model. The use of D_V provided an immediate compliment to a visual inspection of the continuous hydrographs.

The second basic goodness-of-fit criterion recommended by ASCE Task Committee (1993) is the Nash-Sutcliffe coefficient or coefficient of simulation efficiency (COE) (Nash and Sutcliffe, 1970):

$$COE = 1 - \frac{\sum_{i=1}^{n}\left(Q_i - Q'_i\right)^2}{\sum_{i=1}^{n}\left(Q_i - Q\right)^2}$$

where Q_i is the measured daily discharge; Q'_i is the computed daily discharge; Q is the average measured discharge values. The COE values can be varies from 0 to 1, with 1 indicating a perfect fit. A value of COE = 0 indicates that the model was simulating no better than using the average of the observed data. Martinec and Rango (1989) recommended using Q for the year or season to avoid unrealistically high values of COE in low runoff years.

Weather generator of SWAT model

The weather variables necessary for running the SWAT model are the daily values of rainfall, air temperature (maximum and minimum), solar radiation, wind speed and relative humidity. If daily rainfall and air temperature data are not available or data are not adequate, the weather generator component of the model can simulate daily rainfall and temperature.

The precipitation model developed by Nicks (1974) is a first-order Markov chain model. Input for this model includes monthly probabilities of receiving precipitation if the previous day was dry and if the previous day was wet. Given the wet-dry state, the model determines stochastically if precipitation occurs or not. A random number (0-1) is generated and compared with the appropriate wet-dry probability. If the random number is less than or equal to the wet-dry probability, precipitation occurs on that day. Random numbers greater than the wet-dry probability give no precipitation. Since the wet-dry state of the first day is established, the process can be repeated for the next day and so on throughout the simulation period. If wet-dry probabilities are not available, the average monthly number of rainy days may be substituted (Arnold et al., 1996). The probability of a wet day is calculated directly from the number of wet days:

$$PW = \frac{NWD}{ND} \tag{1}$$

where *PW* is the probability of a wet day, *NWD* is the number of rainy days, and *ND* is the number of days, in a month. The probability of a wet day after a dry day can be estimated as a fraction of PW.

$$P(W/D) = \beta\ PW \tag{2}$$

where P(W/D) is the probability of a wet day following a dry day and where β is a fraction usually in the range of 0.6 to 0.9. For many locations, β = 0.75 gives satisfactory estimates *of P(W/D)*. The probability of a wet day following a wet day *P(W/W)* can be calculated directly by using the equation:

$$P(W/W) = 1.0 - \beta + P(W/D) \tag{3}$$

When precipitation event occurs, the amount is generated from a skewed normal daily precipitation distribution

$$R_i = \left(\frac{\left(\left(SND_i \frac{SCF_k}{6.0} \right) \left(\frac{SCK_k}{6.0} \right) + 1 \right)^3 - 1}{SCF_k} \right) RSDV_k + \overline{R}_k \tag{4}$$

where *R* is the amount of rainfall on day *i*, in mm, *SND* is the standard normal deviate for day *i*, *SCF* is the skew coefficient, *RSDV* is the standard deviation of daily rainfall in mm, and *R* is the mean daily rainfall in month *k*.

If the standard deviation and skewness coefficient are not available, the model simulates daily rainfall by using a modified exponential distribution.

$$R_i = \frac{(-\ln(\mu))^{\zeta}\ \overline{R}_k}{\int_{0.0}^{1.0} (-\ln(\chi))^{\zeta}\ dx} \tag{5}$$

where μ is a uniform random number (0.0-1.0) and ζ is a parameter usually in the range of 1.0 to 2.0. The modified exponential is usually a satisfactory substitute and requires only the monthly mean of daily precipitation as input. Amount of daily precipitation is partitioned between rainfall and snowfall using average daily air

temperature.

Data collection and Processing

Rainfall and runoff data for the years 2002 through 2005 were collected at the outlet of Chhokranala watershed. The cloud free geocoded digital data of IRS-1C (LISS-III) satellite with date of pass of 5th October 2002 were collected and used for land use/land cover classification. Topographic maps on 1:50,000 scales collected from Survey of India, Raipur. The maps were traced, scanned and exported to the GEOMETICA for registration, digitization and further processing. Digitizing the contour map of Chhokranala watershed using topographic map of Survey of India having 2m contour intervals. Digitized contour map was then used for preparing the DEM. The DEM of the watershed was prepared in 30m by 30m resolution. Many researchers have also used DEM of 30m by 30m resolution and found satisfactory results (Bingner, 1996; Sharma et al., 1996; Tiwari et al., 1997; Wang and Hjelmfelt, 1998).

Watershed can be subdivided on the basis of natural topographic boundaries, smaller relatively homogenous areas and grids or cell (Arnold et al. 1998). The SWAT model can work on sub-watershed basis, so that the watershed was divided into 7 sub-watersheds on the basis of drainage and elevation information of corresponding watershed. Sub-watershed boundaries were carefully digitized using GIS and area corresponding to different sub-watersheds of Chhokranala watershed was determined (Fig. 2). The watershed and sub-watersheds boundary, drainage networks and slope map were generated using the procedure described by Jenson and Domingue (1988).

Accuracy of image classification was judged after performing the land use/cover classification. A high value of overall accuracy 89.0% and Kappa coefficient (KHAT) of 0.87 for Chhokranala watershed indicated that the land use/cover classification was appropriate for the study watershed. Land use/cover classification (Fig. 3) was matched well with the land use/cover actually mentioned in the field. In many previous studies similar range of classification accuracy and Kappa coefficient were observed and accepted for further use (Yifang et al., 1995; Pratt et al., 1997; Tiwari et al., 1997; Tripathi et al., 2003).

Sub-watershed wise land use information was used for determining the runoff Curve Number (CN) for each sub-watershed (Dhruva Narayana, 1993). Other input parameters of the delineated sub-watersheds, such as overland and channel slope, channel length and average slope length were extracted using the various maps including contour map, sub-watershed map, slope map and drainage map. Sub-watershed wise input parameters were analyzed using the standard procedure and are given in Table 1.

Soil texture maps (Fig. 4) and soil resources data for the watershed was collected from Department of Soil and Water Engineering, Indira Gandhi Agricultural University, Raipur. In the study watershed there are mainly four series of soil. They are the Bhata, Matasi, Dorsa and the Kanhar series, which occupied 203.88, 655.50, 231.33 and 640.39 ha area, respectively. The predominant soil of watershed is sandy clay loam. Sandy loam, loam and clay are also found in this watershed.

The observed surface runoff and sediment yield for monsoon season (June to October) were analyzed and used for evaluation of model calibration performance. The input parameters in the calibration run were given for the each sub-watershed. Most of the parameters showed negligible variation in monthly surface runoff and sediment yield therefore those were not calibrated and taken as suggested in the User's Manual (Arnold et al., 1996). The weighted average values for the parameters such as curve number, surface slope, channel length, average slope length, channel width, channel depth, soil erodibility factor and other soil layer data were taken for each sub-watersheds. Initial soil water storage and Manning's 'n' value for overland flow and channel flow were calibrated and sensitivity analysis were also performed to observe the effect of these parameters on runoff and sediment yield. After calibration, validation of model was performed. Various methods such as graphical and linear regression method, statistical tests of significance and Nash-Sutcliffe simulation efficiency (Nash and Sutcliffe, 1970) were used for model testing.

Identification and Prioritization of Critical Sub-watersheds

Identification and prioritization of critical sub-watersheds based on actual sediment yield rates may be possible only when sediment data is available. In this context, annual sediment yields were simulated for each sub-watersheds of the Chhokranala watershed using SWAT model. Priorities were fixed on the basis of ranks assigned to each critical sub-watershed according to ranges of soil erosion classes described by Singh et al.

(1992) (Table 2). Also for nutrient losses a threshold value of 10 mg/l for nitrate nitrogen and 0.5 mg/l for dissolve phosphorous as described by EPA (1976) was considered as criterion for identifying the critical sub-watersheds. Identified critical sub-watersheds were arranged in descending order and then priorities were fixed for their management.

Effective Management of the Watershed

For evaluating the management scenarios of the critical sub-watersheds the recorded rainfall and temperature data for the year 2003-2005 were used. Several simulations were performed considering 70 combinations of the different treatments for the management of the critical sub-watersheds. Four numbers of crops, three fertilizer doses and five tillage practices were considered (Table 3). Major parts of the watershed are under agronomic practices, which are feasible. Therefore crop based agronomic measures were only considered for management purpose. Justifications for each treatment are presented below:

Tillage: These treatments were selected on the basis of previous studies for evaluating management practices by the researchers all over the world. Tillage treatments and their respective mixing efficiencies are given in Table 4. Mixing efficiencies were considered as suggested by Arnold et al. (1996) for all the tillage treatments except for country plough for which it was determined on the basis of other tillage implements.

Crops: The rice (*Oryza sativa*) crop in the Chhokranala watershed is mostly grown under both upland and low land situations with high seed rate (150-200 kg/ha) and low doses of fertilizer (20-25 kg N/ha and 10-15 kg P/ha). This crop predominantly occupied maximum area (about 36% of the total area) in the watershed. The crop is normally sown during June-July and harvested during September-October. Maize (*Zea mays*) was the second crop occupying about 8% area of the watershed. Maize is generally grown during monsoon season (June to October) in upland situation only. Some of the farmers are also growing groundnut (*Arachis*) in few patches of uplands. Soybean (*Glycine max*) may be suitable for the prevailing agro-climatic condition of the study watershed. This is a cash crop, therefore considered in this study. Selected crops along with fertilizer level considered were shown in Table 3.

Fertilizer levels: All soils of the watershed are low in fertility in terms of availability of nitrogen and phosphorus. Soils of the watershed are acidic in nature; availability of phosphorous is limited due to fixation in acidic soils. Organic manure in conjunction with different chemical sources of nutrients for various crops was evaluated to identify suitable combinations to maintain soil fertility and productivity on a sustained basis under various tillage practices. Fertilizer levels along with manure for different crops are given in Table 3.

RESULTS AND DISCUSSION

Model Calibration

Input data for each sub watersheds were entered into the respective files and the model was run to get the daily output. Different values of input parameters were tried and several simulations were performed to get the model adequately calibrated model. Surface runoff and sediment yields simulated by the SWAT model were compared with their observed counterparts using various methods such as mathematical, graphical, linear regression and statistical tests of significance. The calibrated values for hydraulic conductivity of alluvium for surface and channel were found to be 25.0 and 1.0, respectively, and roughness coefficient for channel and over land flow were found to be 0.040 and 0.025, respectively.

Daily distribution: The results of the daily model calibration (Table 5) for the Chhokranala watershed indicated that the observed and simulated daily runoff and sediment yield was matched quite well for the calibration period (June to October 2003). The coefficient of determination (r^2) of 0.97 and 0.93 for runoff and sediment yield respectively indicated a close relationship between measured and predicted runoff and sediment yield (Fig. 5 & 6). The Nash-Sutcliffe simulation efficiency of 0.96 and 0.92 for runoff and sediment yield,

respectively also corroborated the same fact. Comparison of means using Students t-test revealed that the means of observed and predicted runoff and sediment yield were not significantly different at 95 per cent confidence level. The overall percent deviation (Dv) of 6.37 and 9.81 per cent for runoff and sediment yield respectively indicated that the model was predicting satisfactorily.

Monthly distribution: Graphical and statistical methods of test showed that the observed and simulated monthly runoff and sediment yield for the calibration period (June to October 2002-2003) matched quite well (Table 5). The coefficient of determination (r^2) of 0.96 and 0.94 for runoff and sediment yield, respectively, indicated a close relationship between measured and predicted runoff and sediment yield (Fig. 7 & 8). Comparison of means using Students t-test revealed that the means of observed and predicted runoff and sediment yield were not significantly different at 95 per cent confidence level. The overall percent deviation (Dv) of 9.80 and 2.27 per cent for runoff and sediment yield respectively indicated that the model was predicting satisfactorily.
Developer of the SWAT model and it's users also reported similar results (Srinivasan et al., 1993; Srinivasan and Arnold, 1994; Rosenthal et al., 1995; Bingner, 1996; Peterson and Hamlett, 1998; Srinivasan et al., 1998). Overall prediction of daily and monthly surface runoff and sediment yield by the SWAT model during the calibration period was satisfactory and was accepted for further analysis.

Sensitivity Analysis: Sensitivity analysis revealed that the sediment yield was more sensitive as compared to the surface runoff to both overland flow and channel 'n' values. Calibrated values of Manning's 'n' for overland flow and channel flow were found to be 0.040 and 0.025, respectively. The annual sediment yield increased with decrease in the channel 'n' value. Both, annual runoff and sediment yield increased by increasing Fraction of Field Capacity (FFC) value.

Model Validation
The calibrated SWAT model was validated using the observed daily rainfall and temperature data. The observed runoff and sediment yield were analyzed and compared with the simulated results for the evaluation of model validation performance. Thereafter, the observed and simulated daily and monthly surface runoff and sediment yield were compared graphically. All the calibrated and known parameters were considered for model validation.

Daily distribution: The calibrated model was validated for the monsoon season of the year 2004. The results indicated that the observed daily runoff and sediment yield was matched well with the simulated daily runoff and sediment yield (Table 6). The coefficient of determination (r^2) of 0.98 and 0.95 and the Nash-Sutcliffe simulation efficiency of 0.93 and 0.94 for runoff and sediment yield, respectively also indicated a close relationship between measured and predicted runoff and sediment yield (Fig. 9 & 10). Similarly the Students t-test revealed that the means were found to be statistically different at 95% level of confidence. The values of Dv indicating that the model was over predicting daily runoff by 7.38% and sediment yield by 7.29%.

Monthly distribution: Graphical representation showed that the observed and simulated monthly runoff and sediment yield for the validation period (June to October 2004-2005) matched quite well (Table 6). The coefficient of determination (r^2) of 0.94 and 0.91 for runoff and sediment yield respectively, indicated a close relationship between measured and predicted runoff and sediment yield (Fig. 11 & 12). The Students t-test for the watershed revealed that the means of observed and predicted runoff and sediment yield were not significantly different at 95 per cent confidence level. The overall percent deviation (Dv) indicated that the model was over predicting by 5.2 and 19.5 per cent, respectively for runoff and sediment yield.
Based on the above results, it can be concluded that the model was accurately validated for predicting both daily and monthly surface runoff and sediment yield. On the basis of calibration and validation results, it is inferred that the SWAT model can successfully be used for effective planning and management of the Chhokranala watershed.

Nutrient losses: The observed and simulated nutrient losses were tested for the seventy events during the

monsoon season of the years 2003 to 2005. The Student's t-test was showing similarity in means of observed and simulated organic N at 95 % confidence level (Table 7), also a high value of r^2 of 0.92 indicated very good agreements between observed and simulated organic N. The Dv value was found to be 12.6 % indicated that the model was under predicting organic N. The coefficient of determination 0.95 also showed good agreements between observed and simulated organic P. Both the means were found to be statistically similar at 95 % level of confidence in case of organic phosphorous also (Table 5). Percent deviation (Dv) indicated that the model was over predicting organic phosphorous by 11.9 %.

Similarity in means of observed and simulated values at 95 % confidence level indicated that there were good agreements between observed and predicted values of NO_3-N. Moreover, an r^2 value of 0. 83 indicated a good agreement between observed and simulated values of nitrate-nitrogen. The Dv indicated that the model was under predicting NO_3-N by about 12.3 %. Also r^2 value of 0.80 indicated good agreement between observed and simulated values of soluble P. The means of observed and simulated values were also found similar at 95 % confidence level in case of soluble P; the Dv value (15.3 %) indicated that the model was predicting soluble P satisfactorily for the selected rainfall events during validation period.

Generation of Rainfall

To develop long-term management scenarios for the critical areas of the watershed, rainfall and temperature and other weather parameters are also required by the model. Therefore, the model was tested with respect to generation of daily rainfall. The daily surface runoff and sediment yield from the watershed were also simulated using generated rainfall. The observed and simulated rainfall, runoff and sediment yields were compared on daily as well as monthly basis for evaluating the performance of the weather generator.

Daily distribution: The SWAT model generates rainfall using first order Markov chain model. The results of daily rainfall simulations for the five years (2001-2005) are given in Table 8. The coefficients of determination were found to be 0.98 where as Dv values was found to be 14.5 %.

Monthly distribution: The monthly simulations were performed for four years (2002-2005) and the results are given in Table 8. The coefficients of determination were found to be 0.82 where as Dv values were found to be 14.1 %. Similarities in means and standard deviation indicated that the frequency distribution of predicted rainfall was similar to the observed rainfall during the period of simulation. The mean values of observed rainfall (96.80 mm) and simulated rainfall (83.13 mm) were compared statistically by applying Student's t-test. It was found that the means of monthly observed and simulated rainfall were comparable at 95 % level of confidence because t-cal (1.546) was found to be less than the t-critical (2.012). The standard deviation for the observed and simulated monthly rainfall was found to be 145.54 and 133.15 respectively.

Monthly distribution for monsoon period: The model performance was also tested for the monsoon period of the year 2002-2005 (Table 9). Results showed that the model could predict monthly rainfall values close to the observed values for the monsoon period. The coefficients of determination were found to be 0.67, 0.85 and 0.86, respectively for monthly rainfall, runoff and sediment yield. Dv values of 10.0 %, 1.2 % and 6.7 %, respectively for monthly rainfall, runoff and sediment yield indicated that model was predicted monthly rainfall and thereby runoff and sediment yield satisfactorily. On the basis of these results it can be concluded that the model can be used for long-term simulation of hydrological parameters and for assessing their impact on agricultural activities in the watershed.

Identification and Prioritization of Critical Sub-watersheds

Out of seven sub-watersheds, only SWS-5 sub-watershed fell under very high soil loss group (20 to 40 t/ha/yr). Sub-watersheds SWS-6 and SWS-7 fell under high soil loss group (10 to 20 t/ha/yr). Other sub-watersheds fell under moderate soil loss group (5 to 10 t/ha/yr) and also not exceeding the prescribed permissible limit of soil loss (11.20 t/ha/yr). On the basis of annual sediment yield and nutrient losses, sub-watersheds SWS-5, SWS-6 and SWS-7 were found to be critical. As a result the critical sub-watersheds SWS-5, SWS-6 and SWS-7 were assigned first, second and third priority, respectively, to adopt the management measures in that order for minimizing the sediment losses and conserve rainwater for sustainable crop production (Table 10).

Management of critical sub-watershed (SWS-5): Results showed the similar trend in terms of runoff,

sediment yields and nutrient losses for all the critical sub-watersheds, therefore results of only one critical sub-watershed (SWS-5) are discussed (Table 11 & 12). Results revealed that none of the crop could replace the rice because maize, groundnut and soybean were yielding high rate of sediment yield as compare to rice. Therefore, simulation results of all the treatments considered for rice were compared with the conventional tillage and existing fertilizer (N:P kg/ha) level.

The results indicated that very little increase and decrease in runoff was there in case of all the tillage treatments and fertilizer levels. The decrease in sediment yield as compared to conventional tillage with existing fertilizer dose was found to be about 63.2%, 35.3% and 26.2 %, respectively for zero tillage, conservation tillage and field cultivator. Similar trends of sediment yield were observed in case of all the tillage with half and full dose of fertilizer levels.

Considering the existing fertilizer dose, the losses of NO_3-N were found to increase by about 3.9%, 3.8% and 1.9%, respectively for zero tillage, conservation tillage and field cultivator whereas it was decreased by 2.5% in case of M. B. plough. However, NO_3-N losses were found to be increased in the range of 12 to 43% for both the cases of fertilizer dose. Losses of soluble P were found to be similar in case of all the fertilizer levels with respective tillage. For all doses of fertilizer, soluble P losses were increased by about 17-50% for both zero tillage and conservation tillage. At all the fertilizer levels organic N and P losses were found to be higher in case of M. B. plough as compare to other tillage.

Considering both sediment and nutrient losses collectively the zero tillage, conservation tillage and field cultivator with half dose of fertilizer were found to be better than the other treatments considered for evaluating their impact on sediment yield and nutrient losses for sub-watershed (SWS-5). Therefore, zero tillage, conservation tillage and field cultivator with half dose of fertilizer (40:30 of N:P kg/ha) could be used for the management of the critical sub-watersheds. Sediment losses in these cases were found to be less than the conventional tillage and within the average soil loss (16.35 t/ha/yr) of the country. These tillage practices also yielded nutrient losses within the permissible limit. Hence these practices can be recommended to adopt in the critical sub-watersheds of the study watershed.

CONCLUSIONS

Manning's 'n' values for overland flow and channel flows are 0.040 and 0.025, respectively for the Chhokranala.

The annual sediment yield is inversely proportional to the overland and channel 'n' values whereas; annual runoff and sediment yields are directly proportional to the FFC.

The SWAT model accurately simulates monthly runoff and sediment yield from the watershed. The SWAT model accurately simulates nutrient losses from the watershed on daily event basis.

The SWAT model can successfully be used for identifying critical sub-watersheds for management purpose.

The weather generator can be used to simulate monthly rainfall and thereby runoff and sediment yield. The model can be used for planning and management of the small agricultural watersheds on long-term basis.

The sub-watershed SWS-5, SWS-6 and SWS-7 was found to be critical.

Crops like maize, groundnut and soybean can not replace the existing rice crop, on the basis of sediment and nutrient losses reduction criteria.

The zero tillage, conservation tillage and field cultivator along with 40:30 kg/ha of N:P can be recommended because these tillage practices reduce sediment yield as compared to existing tillage and nutrient losses being within the permissible limit.

REFERENCES

ASAE Task Committee 1993. Criteria for evaluation of watershed models. J. Irri. and Drain. Engg., ASCE, 119 (3): 429-442.

Arnold, J. G., Williams, J. R., Srinivasan, R. and King, K. W. 1996. In Soil and Water Assessment Tool, Use's Manual. USDA, Agriculture Research Service, Grassland, Soil and Water Research Laboratory, 808 East Blackland Road Temple, TX 76502.

Arnold, J. G., Srinivasan, R., Muttiah, R. S. and Williams, J. R. 1998. Large area hydrologic modeling and assessment Part I: Model development. J. of the Am. Water Resour. Asso., AWRA 34(1): 73-89.

Bingner, R. L. 1996. Runoff simulation from Goodwin Creek watershed using SWAT. Trans. of the ASAE 39(1): 85-90.

Bingner, R. L., Garbrecht, J., Arnold, J. G. and Srinivasan, R. 1997. Effect of watershed division on simulation of runoff and fine sediment yield. Trans. of the ASAE 40: 1329-1335.

Cho, S. M., Jennings, G. D., Stallings, C. and Devine, H. A. 1995. GIS-based water quality model calibration in the Delaware river basin. ASAE Microfiche No. 952404, ASAE, St. Joseph, Michigan.

Dhruva Narayana, V. V. 1993. In Soil and Water Conservation Research in India. Indian Council of Agricultural Research, Krishi Anusandhan Bhavan, Pusa, New Delhi; 146-151.

EPA, 1976. "Quality Criteria for Water", Environmental Protection Agency, Washington,

Jenson, S. K. and Domingue, J. O. 1988. Extracting Topographic Structure from Digital Elevation Data for Geographic Information System Analysis. Photogrammetric Engineering and Remote Sensing, 54 (11): 1593-1600.

Martinec, J and Rango, A. (1989). Merits of statistical criteria for the performance of hydrological models. Water Resour. Bull., AWRA, Vol. 25 (20): 421-432.

Nash, J. E. and Sutcliffe, J. V. 1970. River flow forecasting through conceptual models, part 1- A discussion of principles. J. of Hydrology, Vol. 10 (3): 282-290.

Nicks, A. D. 1974. Stochastic generation of the occurrence, pattern, and location of maximum amount of daily rainfall. In: Proc. Symp. Statistical Hydro, Aug.-Sept. 1971, Tucson, AZ. U.S. Dept. Agric., Misc. Publ. No. 1275, pp.154-171.

Narayana, V.V.D., 1993. "Soil and Water Conservation Research in India", Indian Council of Agricultural Research, Krishi Anusandhan Bhavan, Pusa, New Delhi, 146-151.

Pratt, N. D., Bird, A. C., Taylor, J. C. and Carter, R. C. 1997. Estimating area of land under small-scale irrigation using satellite imagery and ground data for a study area in N. E. Nigeria. The Geographical J., 163(1): 65-77.

Peterson, J. R. and Hamlett, J. M. 1998. Hydrological calibration of the SWAT model in a watershed containing fragipan soils. J. of the Am. Water Res. Asso., 34 (3): 531-544.

Rosenthal, W.D., Srinivasan, R. and Arnold, J.G., 1995. "Alternative River Management Using a Linked GIS-Hydrology Model", Transactions of the ASAE, Vol.38 (3), pp. 783-790.

Singh, G., Ram Babu, Pratap Narain, Bhushan, L.S. and Abrol, I. P., 1992. "Soil Erosion Rate in India", J. of Soil and Water Cons., Vol.47 (1), pp. 97-99.

Srinivasan, R., Arnold, J.G., Rosenthal, W., and Muttiah, R.S., 1993. "Hyrologic Modeling of Texas Gulf Basin Using GIS.", In: Proceedings of Second International GIS and Environmental Modeling, Breckinridge, Colorado, pp. 213-217.

Srinivasan, R. and Arnold, J. G., 1994. "Integration of a Basin Scale Water Quality Model with GIS", Water Resources Bulletin, Vol.30 (3), pp. 453-462.

Sharma, K. D., Menenti, M., Huygen, J. and Vich, A. 1996. Modeling spatial sediment delivery in an arid region using thematic mapper data and GIS. Trans. of the ASAE, Vol. 39(2): 551-557.

Srinivasan, R., Ramanarayanan, T. S., Arnold, J. G. and Bednarz, S. T. 1998. Large area hydrologic modeling and assessment part II: model application, J. of the Am. Water Res. Asso., Vol.34, No.1, 91-101.

Tiwari, K. N., Kanan, N., Singh, R and Ghosh, S. K. 1997. Watershed parameters extraction using GIS and remote sensing for hydrologic modelling. ASIAN-PACIFIC Remote Sensing and GIS J., Vol. 10(1): 43-52.

Tripathi, M.P., Panda, R.K. and Raghuwanshi, N.S., 2003. "Calibration and Validation of SWAT Model for Predicting Runoff and Sediment Yield of a Small Watershed in India", Int. Agril. Engg. Journal, AIT, Bangkok, Thailand. Vol.12 (1 & 2), pp. 95-118.

USDA-SCS, 1972. "National Engineering Handbook", Hydrology Section 4, Chapters 4-10.

Williams, J.R. and Berndt, H.D., 1977. "Sediment Yield Prediction Based on Watershed Hydrology", Transactions of the ASAE, Vol.20(6), pp. 1100-1104

Williams, J.R. and Hann, R.W., 1997. "HYMO: Problem-Oriented Language for Hydrologic Modeling-User's Manual, USDA, ARS-S-9.

Williams, J.R., Jones, C. A. and Dyke, P.T., 1984. "A Modeling Approach to Determining the Relationship Between Erosion and Soil Productivity", Trans. of the ASAE, Vol.27 (1), pp. 129-144.

Wischmeier, W. H. and Smith, D. D. 1978. Predicting Rainfall Erosion Losses. USDA Hand book. 537. Washington, D. C.: 58.

Wang, M. and Hjelmfelt, A. T. 1998. DEM based overland flow routing. J. Hydro. Engg., 3(1): 1-8.

Yifang, B., Paul, M. T., Philip, J. H., Brian, B. and Ron, J. B. 1995. Improving the accuracy of synthetic aperature Radar analysis for agricultural crop classification. Can. J. of Remote Sensing, 21(2): 156-164.

Table 1: Sub-watershed wise data for Chhokranala watershed

Table 2: Area under different classes of soil erosion by water in India

Sub-watershed	Area (ha)	Slope (%)	Curve Numbers	Av. slope length (m)	Channel length (km)	Channel slope (%)	K value	P value
WS1	185.45	1.2	79.32	140.3	2.13	.001	0.18	0.60
WS2	290.71	1.6	88.16	143.8	3.75	.003	0.20	0.50
WS3	119.71	1.4	87.37	142.6	3.70	.002	0.14	0.50
WS4	316.71	1.3	89.52	145.4	3.15	.002	0.15	0.50
WS5	277.74	2.0	81.63	149.8	2.13	.005	0.21	0.60
WS6	280.71	1.8	89.23	142.3	3.70	.004	0.23	0.60
WS7	259.97	1.7	83.31	135.0	3.75	.003	0.21	0.50
WS	1731.00	1.6	85.02	146.7	6.10	.005	0.20	0.50

Soil erosion classes	Slight	Moderate	High	Very high	Severe	Very severe
Soil erosion range (t/ha/yr)	0-5	5-10	10-20	20-40	40-80	>80
Area (km^2)	801,350	1,405,640	805,030	160,050	83,300	31,895

Table 3: Level of N:P (kg/ha) of various crops taken for management

Fertilizer level (code)	Rice	Maize	G-nut	Soybean
Existing (F1)	25:15 (5:5)	20:15 (5:5)	10:20 (5:5)	10:20 (5:5)
1/2 of the recommended (F2)	40:30 (10:10)	50:30 (10:5)	20:40 (10:5)	30:30 (10:5)
Recommended (F3)	80:60 (20:20)	100:60 (20:10)	30:60 (15:10)	60:60 (15:10)

Table 4: Tillage treatments and their mixing efficiencies

Tillage treatments	Code	Mixing efficiency
Zero tillage	T1	0.05
Conservation tillage	T2	0.25
Field cultivator	T3	0.30
M. B. plough	T4	0.90
Country plough (Conventional)	T5	0.50

Table 5: Statistical analysis for daily and monthly observed and simulated runoff and sediment yield

Statistics	Daily (2003)				Monthly (2002-2003)			
	Runoff (mm)		Sediment (t/ha)		Runoff (mm)		Sediment (t/ha)	
	Obs.	Sim.	Obs.	Sim.	Obs.	Sim.	Obs.	Sim.
Mean	5.46	5.82	0.173	0.190	105.34	115.66	3.51	3.58
Standard deviation	13.78	14.20	0.387	0.458	115.67	120.10	3.07	3.64

Maximum peak	86.67	84.47	2.1	2.3	326.28	353.9	9.07	11.82
Total	835.8	889.1	26.49	29.09	1053.88	1156.61	35.02	35.82
Count	153	153	153	153	10	10	10	10
t-calculated	-1.670		-1.160		-1.344		0.069	
t-critical (two tailed)	1.975		1.975		2.262		2.262	
r^2	0.967		0.930		0.959		0.938	
% deviation	-6.373		-9.815		-9.800		-2.267	
COE	0.964		0.917		0.968		0926	

Table 6: Statistical analysis for daily and monthly observed and simulated runoff and sediment yield

Statistics	Daily (2004)				Monthly (2004-2005)			
	Runoff (mm)		Sediment (t/ha)		Runoff (mm)		Sediment (t/ha)	
	Obs.	Sim.	Obs.	Sim.	Obs.	Sim.	Obs.	Sim.
Mean	2.34	2.51	0.077	0.082	124.08	130.49	3.64	4.35
Standard deviation	11.20	13.58	0.319	0.446	103.31	109.61	2.81	3.29
Maximum peak	120.7	154.2	3.38	5.12	320.70	359.78	8.92	11.12
Total	357.7	384.1	11.79	12.65	1240.84	1304.98	36.41	43.5
Count	153	153	153	153	10	10	10	10
t-calculated	-0.698		-0.453		-0.789		-2.153	
t-critical (two tailed)	1.975		1.975		2.262		2.262	
r^2	0.976		0.949		0.946		0.910	
% deviation	-7.378		-7.294		-5.16		-19.46	
COE	0.926		0.935		0.924		0.937	

Table 7: Statistical analysis of the observed and simulated nutrient losses (2003-2005)

Statistical parameters	Organic N		Organic P		NO_3-N		Soluble P	
	Obs.	Sim.	Obs.	Sim.	Obs.	Sim.	Obs.	Sim.
Mean (kg/ha)	0.374	0.327	0.185	0.207	0.160	0.141	0.015	0.013
Standard deviation (kg/ha)	0.430	0.411	0.344	0.458	0.227	0.167	0.013	0.011
Maximum (kg/ha)	1.540	1.500	2.120	2.950	1.550	1.280	0.050	0.040
Total (kg/ha)	26.185	22.91	12.931	14.476	11.227	9.846	1.051	0.891
Count	70	70	70	70	70	70	70	70
t-calculated	1.655		0.391		1.470		1.145	
t-critical (two tailed)	2.201		2.201		2.201		2.201	
r^2	0.921		0.948		0.830		0.800	
% deviation	12.51		-11.95		12.30		15.29	

Table 8: Statistical results of the observed and simulated daily and monthly rainfall

Statistics	Daily Rainfall (mm) (2001-2005)		Monthly Rainfall (mm) (2002-2005)	
	Observed	Simulated	Observed	Simulated
Mean	3.17	2.71	96.80	83.13
Standard deviation	11.47	10.06	145.54	133.15
Maximum peak	173.4	162.8	543.70	465.00
Total	5783.6	4942.9	4646.40	3990.41
Count	1826	1826	48	48
t-calculated	10.52		1.546	
t-critical (two tailed)	1.96		2.012	
r^2	0.98		0.82	
% deviation	14.5		14.1	

Table 9: Statistical analysis for the monthly observed and simulated rainfall, runoff and sediment yield during the monsoon period (2002-2005)

Statistical parameters	Rainfall (mm)		Runoff (mm)		Sediment (t/ha)	
	Observed	Simulated	Observed	Simulated	Observed	Simulated
Mean	216.0	194.40	119.82	118.36	3.571	3.331
Standard deviation	161.34	146.44	105.32	107.39	2.871	3.205
Maximum	543.70	465.0	326.28	353.9	9.07	10.81
Total	4320.0	3888.08	2396.35	2367.26	71.43	66.63
Count	20	20	20	20	20	20
t-calculated	1.033		0.152		0.888	
t-critical (two-tail)	2.093		2.093		2.093	
r^2	0.67		0.85		0.86	
% deviation	10.0		1.2		6.7	

Table 10: Model output for identification of the critical sub-watersheds (2003-2005)

Sub-Watershed	Area (km^2)	Runoff (mm)	Sediment (t/ha)	Organic N (kg/ha)	Organic P (kg/ha)	NO_3-N (kg/ha)	Soluble P (kg/ha)	Erosion class	Priority
SWS 1	185.2	502.0	8.49	5.39	2.96	3.75	0.05	Moderate	-
SWS 2	290.8	491.1	9.44	5.83	3.26	3.72	0.05	Moderate	-
SWS 3	119.4	521.7	6.43	4.19	2.28	3.94	0.05	Moderate	-
SWS 4	316.8	444.2	8.76	6.36	3.34	3.24	0.05	Moderate	-
SWS 5	278.7	662.5	21.02	10.70	6.26	4.78	0.06	V. High	**I**
SWS 6	280.4	519.8	15.86	9.42	5.17	3.91	0.05	High	**II**
SWS 7	259.6	490.7	13.01	7.71	4.33	3.71	0.05	High	**III**
WS	1730.9	518.9	11.86	7.09	3.94	3.86	0.05	-	-

Table 11: Effect of crops on average annual sub-watershed (SWS 5) yield under existing practices during monsoon season (2003-2005)

Crop	Runoff (mm)	Sediment (t/ha)	Organic N (kg/ha)	Organic P (kg/ha)	NO_3-N (kg/ha)	Soluble P (kg/ha)	Grain yield (t/ha)
Rice	666.5	21.016	10.698	6.264	4.780	0.062	0.601
G-nut	657.5	24.769	11.461	6.647	5.859	0.076	1.127
Maize	661.3	28.858	12.791	7.353	4.660	0.078	0.480
Soybean	662.4	24.230	11.259	6.544	6.194	0.087	0.838

Table 12: Effect of various tillage and fertilizer level on watershed yield of SWS 5 (2003-2005)

Treatments*	Runoff (mm)	Sediment (t/ha)	NO_3-N (kg/ha)	Soluble P (kg/ha)	Organic N (kg/ha)	Organic P (kg/ha)
F1+T1	662.70	07.74	4.97	0.07	03.85	02.06
F1+T2	662.62	13.60	4.96	0.07	07.23	03.89
F1+T3	662.59	15.52	4.87	0.06	07.29	04.15
F1+T4	662.34	26.86	4.66	0.05	12.79	07.35
F1+T5	662.49	21.02	4.78	0.06	10.70	06.26
F2+T1	662.79	07.75	5.51	0.08	06.07	03.90
F2+T2	662.77	13.61	5.49	0.08	11.67	07.15
F2+T3	662.76	15.53	5.48	0.07	11.78	07.23
F2+T4	662.65	26.87	5.36	0.06	17.51	11.93
F2+T5	662.75	21.02	5.44	0.07	13.01	07.84
F3+T1	663.39	07.75	6.81	0.09	09.63	06.92
F3+T2	663.34	12.61	6.78	0.09	18.51	13.31
F3+T3	663.28	15.53	6.76	0.08	19.68	13.56
F3+T4	663.20	26.86	6.62	0.07	30.85	23.01
F3+T5	663.22	21.03	6.72	0.08	20.74	14.55

* Tillage: Zero tillage (T1), conservation tillage (T2), field cultivator (T3), M. B. plough (T4) and conventional tillage (T5). Fertilizer level: Existing (F1), half of the recommended (F2) and recommended (F3)

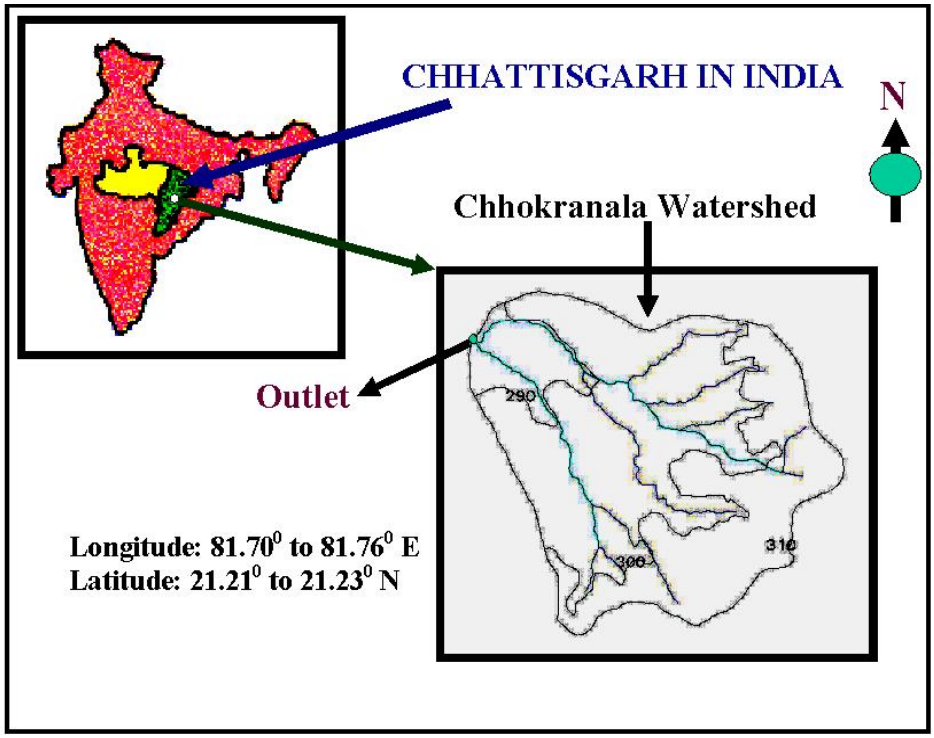

Fig. 1: Location map of the Chhokranala watershed

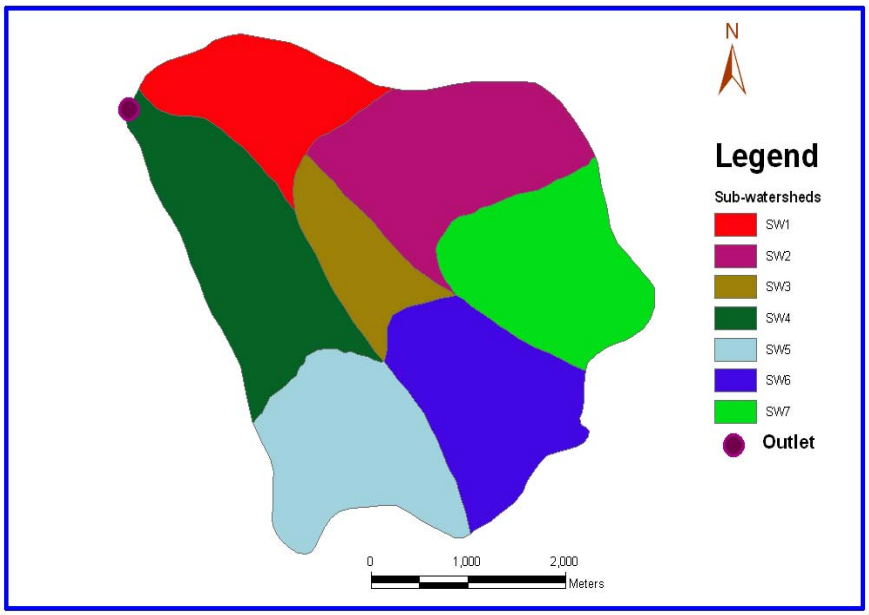

Fig. 2: Sub-watershed map of the Chhokranala watershed

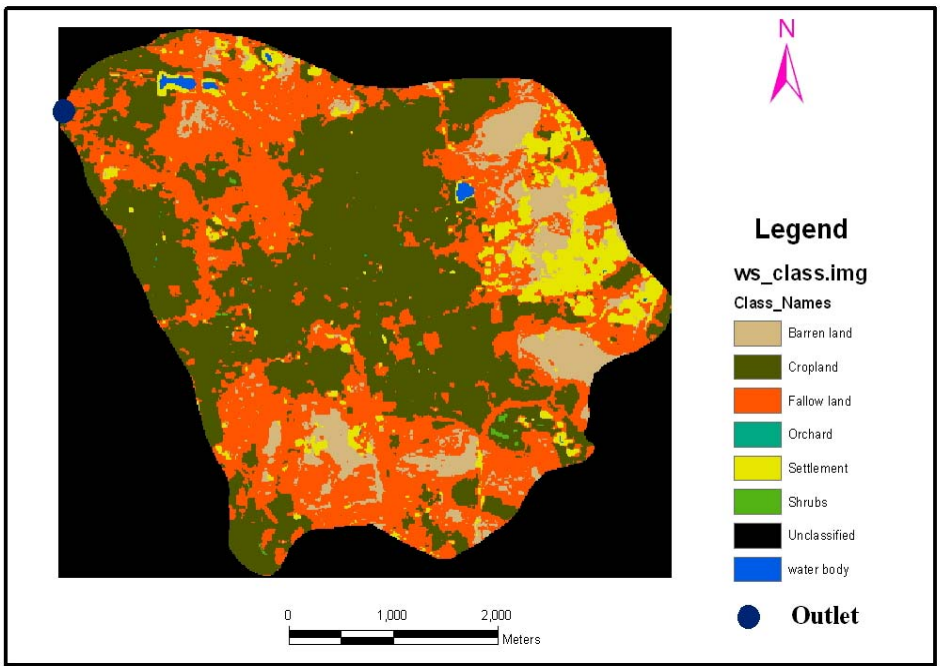

Fig. 3: Land use/cover map of the Chhokranala watershed

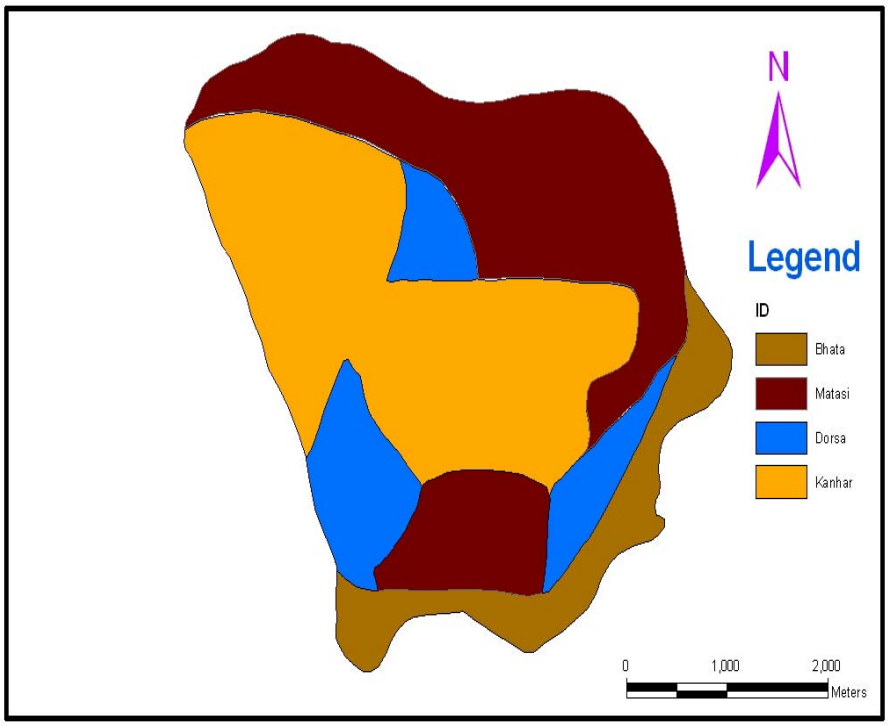

Fig. 4: Soil texture map of the Chhokranala watershed

Model Calibration

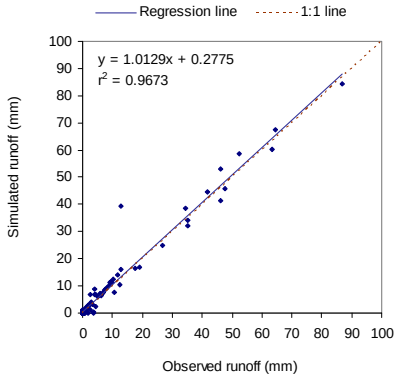

Fig. 5: Comparison of observed and simulated daily runoff (2003)

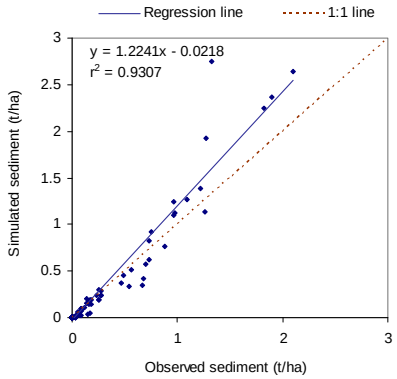

Fig. 6: Comparison of observed and simulated daily sediment yield (2003)

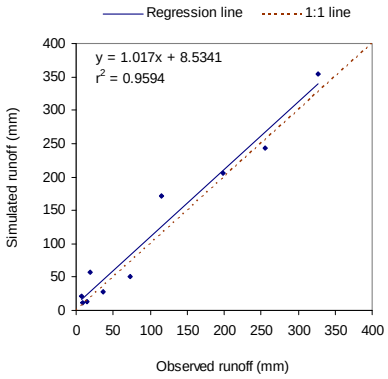

Fig. 7: Comparison of observed and simulated monthly runoff (2002-03)

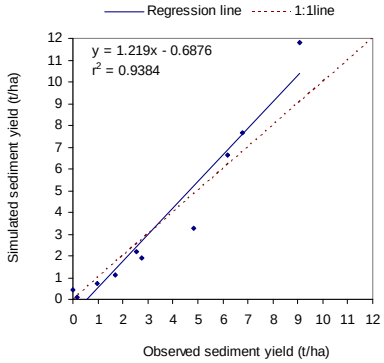

Fig. 8: Comparison of observed and simulated monthly sediment yield (2002-03)

Model Validation

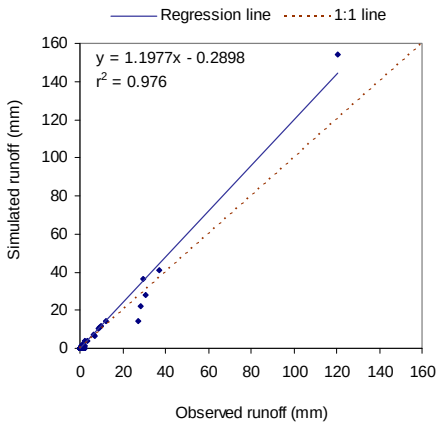

Fig. 9: Comparison of observed and simulated daily runoff (2004)

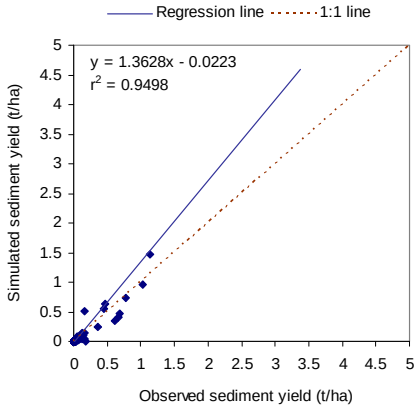

Fig. 10: Comparison of observed and simulated daily sediment yield (2004)

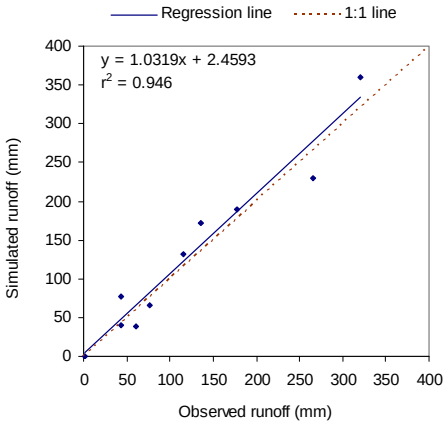

Fig. 11: Comparison of observed and simulated monthly runoff (2004-05)

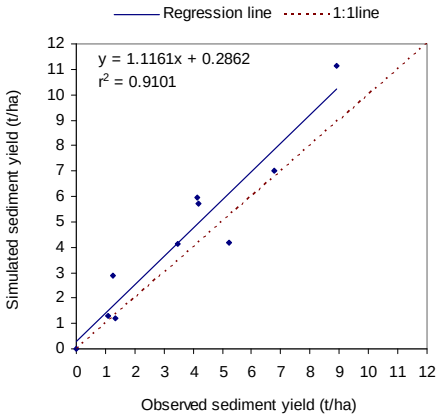

Fig. 12: Comparison of observed and simulated monthly sediment yield (2004-05)

HYDROLOGICAL CYCLE SIMULATION OF KODAVANAR RIVER (ATHUR BLOCK) WATERSHED USING SOIL AND WATER ASSESSMENT TOOL (SWAT)

K.Kaviya [a]
Research Scholar , IRS, Anna University, Chennai-25
kaviyaselva@gmail.com

M.Ramalingam[b],
Director, IRS, Anna University, Chennai-25
ramalingam:m1@gmail.com

Abstract

An adequately tested soil and water assessment tool (SWAT) model was applied to the runoff and sediment yield of a small agricultural watershed in India using rainfall. SWAT was used to simulate the transport of runoff and sediment into the Kodavanar River, Tamilnadu in this study. The main objective was to validate the performance of SWAT and the feasibility of using this model as a simulator of runoff. The investigation was conducted using a 10-year historical rainfall record from Jan'88-Jan'98 for calibration and validation. Based on the water balance study the surface runoff and evapotranspiration and sediment yield were calculated and the flow duration curve was drawn and the validation work has been carried out.
The SWAT generally performs well and could accurately simulate both monthly and yearly runoff. The simulated monthly and yearly runoff matched the observed values satisfactorily, with a correlation coefficient greater than 0.9 and coefficient of determination (R^2) greater than 0.95. Therefore, it can be concluded that the SWAT model could be used for developing a multiple year management plan for the critical erosion prone areas of a small watershed and planners in studying water quality problems and taking decisions.

(**Keywords:** Hydrological modeling; Runoff simulation; SWAT Model; watershed and sub Watershed; Geographic information system)

1.**Introduction**

Watershed is all the land and water area, which contributes runoff to a common point. In India the need of accurate information on basin runoff and silt yield has felt during the past two decades along with the acceleration of the watershed management for conservation and development of soil and water resources. The hydrologic behaviors of watershed play an important role in water resources planning and management. Advances in computational power and the growing availability of spatial data have made it possible to accurately describe watershed characteristics for modeling of watershed hydrology.
Geographic Information Systems (GIS) has become an indispensable tool for watershed-scale hydrologic analysis and modeling. The integrative capabilities of GIS can emulate real-world complexity, facilitating interdisciplinary research and communication.
Prediction of runoff and sediment yield is necessary for the design of conservation structures to reduce the ill effects of sedimentation and to select the priority watersheds for resource management programmes. The model study of Kodavanar watershed helps in evaluating and selecting the alternative land use and management practices. A number of simulation models have been developed to evaluate water quality parameters affected by agricultural land management at both field and watershed scale. Among these models, the SWAT model(Arnold et al., 1998), is the most recent one used successfully for simulating runoff, sediment yield and water quality of an agricultural watershed. SWAT divides the catchment into a number of sub-catchments each of which consists of a number of Hydrologic Response Units (HRU) (Leavesley et al., 1983). An HRU is a unit of area with unique land use and soil type without reference to their actual spatial position within each sub-catchment

1. a.Description of the model

A physically based continuous time model Soil and Water Assessment Tool (SWAT2000) (Arnold et al., 1998, 2001; Neitsch et al., 2001) are used to represent the hydrologic balance of the selected watershed. It is linked with raster-based geographical information system (GIS) to facilitate the input of the spatial data such as land use, soil maps and digital elevation models (DEM). The model itself based on the water balance equation:

$$W_t = Wo + \sum_{i=t-1}^{t}(R_{day,\,i} - Q_{surf,\,i} - E_{a,\,i} - W_{seep,\,i} - Q_{gw,\,i}) \qquad \text{------- (1)}$$

Where:
W_t is the final soil water content in mm;
W_o is the initial soil water content in mm;
t is the time in days;
R_{day},i is the amount of precipitation on day i in mm;
Q_{surf},i is the amount of surface runoff on day i in mm;
E_a,i is the amount of evapotranspiration on day i in mm;
W_{seep},i is the amount of water entering the vadose zone from the soil profile on day i in mm; and Q_{gw},i is the amount of return flow on day i in mm.

Surface runoff Q_{surf} is calculated by applying an improved Soil Conservation Service (SCS) curve number approach. Peak runoff predictions are based on Modified Rational Formula. The rainfall intensity during the watershed time of concentration is estimated for each storm as a function of total rainfall using a stochastic technique. Watershed time of concentration is estimated using Manning's formula considering both overland and channel flow. The percolation component W_{seep} consists of a linear storage up to 10 layers. The flow rate is governed by the hydraulic conductivity and the available water storage capacity of each layer. For subsurface flow, a kinematic storage model is used. Percolation from the root zone recharges a shallow aquifer, which is also connected from stream flow. The model offers three options for estimating potential evapotranspiration (PET): Hargreaves, Priestley–Taylor, and Penman–Monteith. The model calculates the evaporation and transpiration terms separately. The actual evaporation is a function of the soil water content and soil depth. Transpiration is computed as a linear function of potential plant evapotranspiration and leaf area index. Canopy storage for each crop is also included. The application of ArcView SWAT (AVSWAT) in the present study provides the capabilities to streamline GIS processes tailored towards hydrologic modeling and to automate data entry communication and editing environment between GIS and the hydrologic model. Fohrer et al. (1999) have calibrated and validated the SWAT for the gauged 'Aar' watershed with a land use map derived from satellite images of 1987. Fohrer et al. (2001) and Santhi et al. (2001) validated the SWAT modelling concept for watersheds with widely differing land use. Saleh et al. (2000) validated the SWAT for the baseline condition within Upper North Bosque River Watershed and the model output was compared to flow, sediment and nutrient measurements for 11 stream sites within the watershed for the period of October 1993–July 1995. Weber et al. (2001) suggested on the basis of SWAT results that land use has a significant influence on the water balance components of the catchment.

2. Methods and materials

2. a. Study area

The study area chosen for this study is Attur block in Dindigul district and it's traversed by Kodavanar River. This block is located in the southern side of dindugul district and bounded by Vadipatti and Nilakottai in south and south east, Dindugul block in the east, Reddiyapuram in the north and Kodaikannal in the west. The area lies between geographic co-ordinates, north latitude 10° 14'50'' to 10° 20'00'' and east longitude 77°37'45" to 77°46'00''. The extent of area is 321.44 sq km. The nearest rainfall station is at Viralipatti and the average annual rainfall is 820mm. The major rock type encounted in the area are basic metamorphic and charnochites.

The geomorphic units look of buried pediments (shallow and deep) pediments, Inselberg complex are noticed on the southern part of the block area fringing kodai hills. Structural hills (kodai hills). Bazada zones are available in the fringes of the hills in the western part. This block is comprised of crystalline metamorphic arcliaes occurs in water table and semi confined conditions. The block receives fairly uniform rain fall throughout the period. Area receives appreciable rainfall during September to December. Water level rise in January in the year 1988, 1990, 1991, 1994 and 1995. Declining trends are observed from January 1988, September1989December 1990, January 1991 to September 1992, 1993, 1994 and January 1995 to December 1996. Weathered thickness varies from 10 to 15m. Generally the quality of water is good and portable. Ec varies from 2000 to 4000 micro mhos/cm. The hydrological soil group 'C' with slow rate of infiltration is seen about three fourth of the area of the block. The rest of the area is covered by soil group 'B' with moderated rate. The terrain of the block varies between moderately sloping to strongly sloping category. About 66% of the total area is classified as Agricultural lands. Around 21% of the block area falls and forest lands, nearly 9% of the block area is represented by waste lands.

2.b. Data used

Rainfall data for 1988 to 1998 from a recording-type rain gauge were collected from the nearest rain gauge (Viralipatti) station. Other meteorological data such as maximum and minimum air temperature and relative humidity were collected from a meteorological observatory at Chennai. Measured monthly average values for 10 years (1988–1998) for the rainfall, temperature, relative humidity, wind velocity and solar radiation are given in Table I. Hydrological data in addition to rainfall were also collected for the study. The spatial data used by this model includes a SRTM 90m digital elevation model (DEM), IRS 1C- LISS III +PAN merged image, land use map, and soil map. In addition, time series of certain meteorological variables, Soil input data base, Urban data base, Fertilizer data base file, Tillage data base, Land cover/ Plant growth data base were also used.

3. Model implementation

Surface runoff occurs whenever the rate of water application to the ground surface exceeds the rate of infiltration. When water is initially applied to a dry soil, the application rate and infiltration rates may be similar. However, the infiltration rate will decrease as the soil becomes wetter. When the application rate is higher than the infiltration rate, surface depressions
begin to fill. If the application rate continues to be higher than the infiltration rate once all surface depressions have filled, surface runoff will commence.
SWAT provides two methods for estimating surface runoff: the SCS curve number procedure (SCS, 1972) and the Green & Ampt infiltration method (1911).

3.a.Runoff volume: SCS curve number procedure

The SCS runoff equation is an empirical model that came into common use in the
1950s. It was the product of more than 20 years of studies involving rainfall-runoff relationships from small rural watersheds across the U.S. The model was developed to provide a consistent basis for estimating the amounts of runoff under varying land use and soil types (Rallison and Miller, 1981).
The SCS curve number equation is (SCS, 1972):

$$Q_{Surf} = \frac{(R_{Day} - I_a)^2}{(R_{Day} - I_a + S)} \text{ ------- (2)}$$

where Q_{surf} is the accumulated runoff or rainfall excess (mm H_2O), R_{day} is the rainfall depth for the day (mm H_2O), I_a is the initial abstractions which includes surface storage, interception and infiltration prior to runoff (mm H_2O), and S is the retention parameter (mm H_2O). The retention parameter varies spatially due to changes in soils, land use, management and slope and temporally due to changes in soil water content. The retention parameter is defined as:

$$S = 25.4\left\{\left(\frac{1000}{CN}\right) - 10\right\} \text{ ---------- (3)}$$

where *CN* is the curve number for the day. The initial abstractions, I_a, is commonly approximated as 0.2*S* and equation (3) becomes

------- (4)

Runoff will only occur when $R_{day} > I_a$.

4. Results and discussion

Model performance was evaluated for generating the rainfall and thereby monthly averages of surface runoff and sediment yield from a small watershed. The average values of observed and simulated rainfall, runof were compared on a monthly basis for evaluating the performance of the weather generator. SWAT simulation for the period of 10 years (Jan'88-Jan'98), showed their goodness of fit and reproduced the same result as that of Santhi et al. (2001). This result showed the efficient surface runoff and evapotranspiration system. The results of the SWAT simulation in the BASINS system showed the reliability and efficiency of Kodavanar (Athur) watershed analysis. The calibration results are shown in the bar chart and the curves as below. The efficient runoff was calculated and the flow duration curve was drawn. The yearly runoff was calculated and displayed. The sub basin wise runoff was calculated through the simulation and explained in the form of bar chart as in figure 4.1

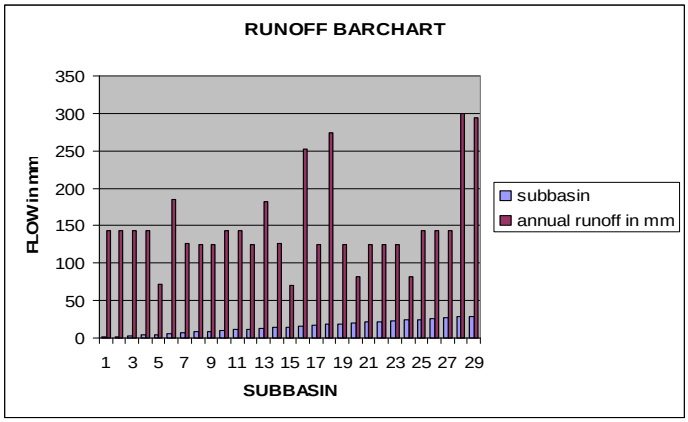

Figure 4.1 sub basin wise runoff

The simulated runoff result has been shown in the figure 4.2 through the flow duration curve for the entire sub basin in the watershed.

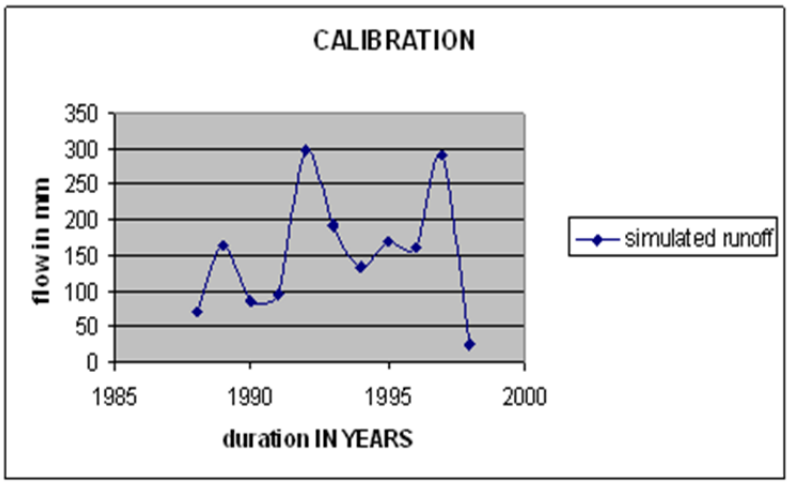

Figure 4.2 Simulated runoff curves

The tabulated value of the observed and the simulated runoff has been shown. The average yearly runoff is presented in the table 4.1 shown below

Table 4.1 Average annual runoff

Year	Simulated runoff(mm)	Observed Runoff(mm)	Difference in %age
1988	70.54	56.02	-20
1989	163.75	129.2	-26
1990	87.16	102.17	14
1991	96.1	78.89	-23
1992	300.25	289.51	-4
1993	193.5	154.35	-25
1994	134.5	128.9	-4
1995	169.08	182.2	7
1996	162.38	142.68	-14
1997	291.85	265.38	-9
1998	26.44	37.92	29
			Average %age Difference=-7.5

The simulated result was validated with the observed value collected from the direct methods as shown in figure 4.3.

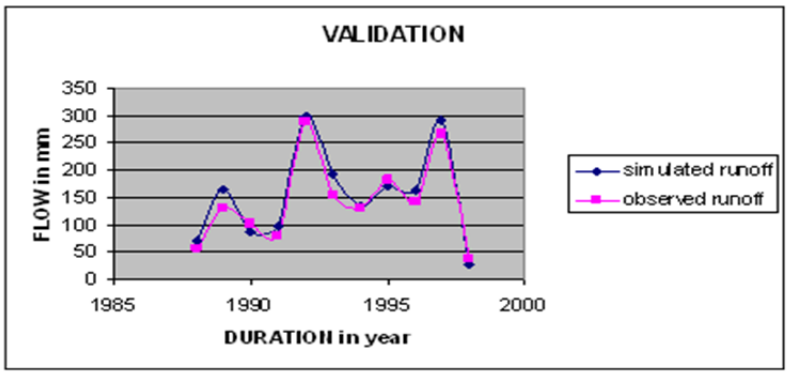

Figure 4.3 Validation curve for the runoff

The statistical validation also carried out and displayed in the table 4.2.

Table 4.2 Statistical averages of observed and simulated runoff

Yearly		
	Observed	Simulated
Mean	154.1409	142.4745
Std deviation	79. 29586	85.89632
Slope	0. 902385	
Correlation coefficient®		0.9774
Coefficient of determination(r2)		0.9555

The validation curve and the statistical validation show that the more of the values of the simulated is very close to the observed result.

The result of the calibration of the model will give many parameters. The evapotranspiration of the watershed also calculated based on the calibration. The monthly average evapotranspiration also listed in the table and the bar chart shows (figure 4.4) the monthly average PET (Potential Evapotranspiration) for the watershed.

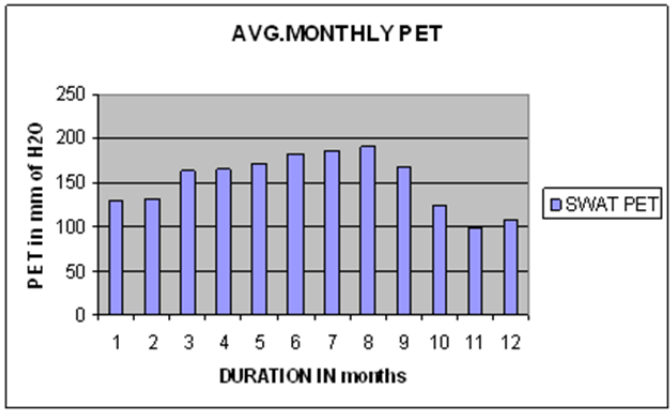

Figure 4.4 the monthly average PET

The result of the simulated PET was compared with the observed PET for validation. The computed and the observed values provided in the table 4.3.

Table 4.3 Observed and Simulated PET

Months	Observed PET	Simulated PET	Difference in %age
1	127.7	136	7
2	132	140	6
3	162.27	174	7
4	164.94	177	7
5	171.3	195	14
6	182.1	186	2
7	186.32	183	2
8	190.7	186	2
9	167.09	165	1
10	122.78	133	9
11	98.83	111	13
12	106.92	121	14
			Average %age=-6.16

The values are drawn as curve and the results are compared. The compared result was shown in figure 4.5.

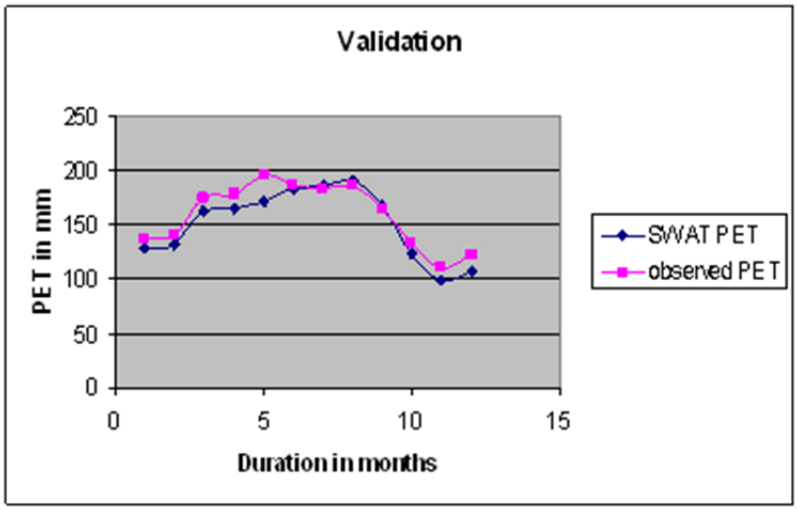

Figure 4.5 Comparison of observed and simulated PET

The statistical validation of the PET also shown in the table 4.4.The water balance study parameters are listed below which was obtained from the SWAT result.

Table 4.4 statistical average of observed and simulated PET

Monthly		
	Observed	Simulated
Mean	158.9167	151.07921
Std Deviation	28.96537	31.83488
Correlation coefficient®		0.96779
Coefficient of determination(r^2)		0.9366

The simulated data was listed in the table 4.5
The other results obtained from the calibration of the model are listed below
soil water content(Amount of water in the soil profile at the end of the time period)-6.610mm of H2O
Sediment yield ranges from 0-44.731t
Organic Nitrogen yield ranges from 0-18.453kg/ha
No3 in surface runoff ranges from 0-0.381kg/ha
Organic Phosphorus yield ranges from 0-1.811kg/ha

Table 4.5 Water balance study parameters listed

Subbasin No	Area(km2)	PERC(mm)	SURQ(mm)	ET(mm)	PET(mm)
1	6	1003.126	88.901	1570.004	119.403
2	5.024	992.273	88.874	1569.998	119.4
3	2.659	1003.131	88.9	1570.019	119.404
4	3.804	997.687	88.88	1570.003	347.89
5	16.005	2.368	72.51	1679.352	214.172
6	36.605	7.36	157.469	1680.24	116.605
7	0.9	995.862	73.149	1697.72	116.074
8	9.071	437.42	72.623	1697.503	116.58
9	7.397	963.896	73.01	1697.79	119.396
10	0.269	986.9	88.87	1569.99	119.411
11	5.655	1003.153	88.86	1569.83	116.606
12	2.861	1001.3	73.02	1697.89	214.177
13	6.059	217.360	157.51	1680.76	116.605
14	0.101	1001.319	73.02	1698.032	214.177
15	7.683	132.048	74.146	1683.37	116.605
16	19.304	5.295	215.837	1676.37	115.904
17	5.806	985.863	72.909	1697.98	212.775
18	12.585	7.36	153.544	1693.149	116.598
19	2.247	995.86	73.058	1698.007	213.25
20	5.461	907.357	43.744	1661.669	116.605
21	7.296	131.632	71.78	1697.658	119.078
22	4.014	985.064	74.036	1697.79	115.185
23	10.392	862.22	73.096	1697.62	116.603
24	5.360	955.95	43.58	1661.639	116.521
25	3.257	992.267	88.88	1570.088	119.099
26	12.909	133.58	87.367	1569.096	119.398
27	8.516	868.80	88.659	1569.556	117.521
28	25.405	7.56	153.56	1696.82	119.33
29	2.895	7.562	153.557	1697.26	213.233

researchers and planners in studying water quality problems and taking decisions.

5. Conclusions

In most instances simulated values were closer to the observed values during the calibration period, calibration should also be based on several years of simulation in order to appraise parameters under a wide range of climatic and soil conditions. In each case calibrated models were developed in identifying land use characteristics responsible for adverse impact in stream water quality. The Arc view interface was effective at reducing the spatial data into formatted input files for the models. SWAT, calibration and validation procedures presented in this case studies will be useful to

6.0. References

1. Arnold J G; Srinivasan R; Muttiah R S; Williams J R (1998). Large area hydrologic modeling and assessment, partI: model development. Journal of American Water Resources Association, 34(1), 73–89
2. Arnold J G; Srinivasan R; Di Luzio M; Neitsch(2001).SWAT2000— capabilities and improvements in watershed modeling. Proceeding of International SWAT Conference, SFB 299 and Justus-Liebig-University Giesen, Germany,August 13–17, 2001
3. Fohrer N; Eckhardt K; Haverkamp S; Frede H G (1999). Effects of land use changes on the water balance of rural a watershed in a peripheral regional. Journal of Rural Engineering Development, 40(5–6), 202–206
4. Fohrer N; Haverkamp S; Eckhardt K; Frede H G (2001). Hydrologic response to land use changes on the catchment scale. Pergamon, Physics and Chemistry of the Earth (B), 26(7–8), 577–582
5. Gassman, P.W., 1997. The national pilot program integrated modeling system: environmental baseline assumptions and results for the APEX model. In: Livestock Series Report 9. Center for Agriculture and Rural Development, Iowa State University, IA.
6. Green, W.H. and G.A. Ampt. 1911. Studies on soil physics, 1. The flow of air and water through soils. Journal of Agricultural Sciences 4:11-24.
7. Leavesley, G.H., Lichty, R.W., Troutman, B.M., Saindon, L.G., 1983. Precipitation-runoff modelling system: user's manual. United States Geological Survey, Water-Resources Investigation Report 83-4238, pp. 207.
8. Rallison, R.E. and N. Miller. 1981. Past, present and future SCS runoff procedure. p. 353-364. *In* V.P. Singh (ed.). Rainfall runoff relationship. Water Resources Publication, Littleton, CO.
9. Saleh A; Arnold J G; Gassman P W; Hauck L M; Rosenthal W D; Williams J R; McFarland A M S (2000). Application of SWAT for the Upper North Bosque River Watershed. Transaction of the ASAE, 43(5), 1077–1087
10. Santhi.C.,Arnold J G; Srinivasan R: Williams J R:A.Dugas:L.M.Hauck 2001,Valadation of SWAT model on a large river basin with point and non-point sources. Journal of American Water Resource Association, 37:1169-1188.
11. Santhi.C.,Arnold J G; Srinivasan R: Williams J R:A.Dugas:L.M.Hauck 2001,Valadation of SWAT model on a large river basin with point and non-point sources. Journal of American Water Resource Association, 37:1169-1188.
12. Soil Conservation Service. 1972. Section 4: Hydrology in National Engineering Handbook. SCS.

Impact of Climate Changes on Catchment Hydrology and Rainfall – Runoff Correlations in Karjan Reservoir Basin, Gujarat

Amit D. Bhatt
PG student, Civil Engg. Dept., Faculty of Technology and Engg., MSU

Geea S. Joshi , Ph.D. Associate Professor
Civil Engg. Dept., Faculty of Technology and Engg., MSU, rs_geera @yahoo.com

Gaurang I. Joshi, Assistant Professor
Civil Engg. Dept., Faculty of Technology and Engg., MSU,

Abstract

Since the start of industrialization, the use of fossil energy has created a additional source of carbon dioxide emission from the Earth into the atmosphere. The concentration of green house gases has been increased through mankind's activities. This has resulted into the significant climate changes. Human induced activities and intense human utilization of land causes land use and Land cover changes. The term 'climate changes' is used to summarize the changes in climatologically conditions and changes in land-use and land-cover conditions. The study has been taken to assess the climate change, to assess the impact of climate change on catchment hydrology and to assess the impact of climate change on rainfall-runoff correlations for the catchment area of Karjan reservoir project i.e. Karjan reservoir basin. The impact assessment of 'climate changes' in the catchment area of the Karjan reservoir project indicates that the runoff potential of the basin has increased significantly. The results of this study will prove beneficial to the Karjan project authorities for the better management of the water resources in the basin and to decide sustainable reservoir operating policy for both monsoon season and summer season.

Keywords: Climate change impact, Catchment hydrology , Rainfall-runoff correlations

Introduction

Since the start of industrialization, the use of fossil energy has created a new (additional) source of carbon dioxide emissions from the Earth into the atmosphere. i.e. the carbon dioxide concentration of the lower atmosphere has increased. Besides carbon dioxide, the concentration of other 'greenhouse gases' has been increased through mankind's activities. Carbon dioxide and the other 'greenhouse gases' affect the atmospheric absorption properties of longwave radiation, and changing the radiation balance. The most obvious impact of this altered radiation balance is the warming of the lower troposphere, which has been observed through an increase of global temperature. (Bronstert. 2004)

since the era of industrialization and rapid growth of population, land-use change phenomena have accelerated in many regions, such as deforestation of tropical forest. (LUCC, 2002) or urbanization of formerly agricultural or forested land (Krausmann *et al*., 2003).

In this study, the term 'climate change' summarize the changes in climatologically conditions and land-use and land-cover condition.

The rainfall runoff models can serve as a best tool for describing the impact of climate change on catchment hydrology, because it transform the meteorological forcing (in particular rainfall) and changed boundary conditions (land use and land cover) into the hydrological response of a catchment (in particular runoff).

Development of the Rainfall-runoff model is the only way to obtain some quantitative figures about the impact of such climate change. The hydrological processes and their interdependencies are represented by the rainfall-runoff model in such a way that possible system changes can be covered by the model. The rainfall-runoff models can serve as most adequate tools to assess the impacts of climate change on the hydrological cycle.

In recent years, a wide range of rainfall-runoff model have been used to assess the impacts of climate and land-use change on the hydrological cycle, e.g. see Bronstert *et al*. (2002) or Niehoff *et al*. (2003) for an overview.

Description of the study area

The Karjan river basin is one of the largest tributary basins of the Lower Narmada Valley, which joins it from the south. The Karjan river originates in the trappean Mandvi hills of Wankal Dungar near Bilwan. It flows northward from its origin and for the most of its 90 km length it traverses through trappean highlands and enters the alluvial plain near Jitnagar before meeting the Narmada river at Mota Bhilwada. The major part of the river is restricted to the hilly terrain of Mosda-Sagbara hills and Dediapada uplands. The Tarav and Daman Khadi are the main tributaries that meet Karjan river in the trappean highland on its right bank whereas Mohan Nadi is the only major tributary meeting on its left bank. Geomorphologically, the Karjan basin is divisible into two broad geomorphic zones; the Upland zone and the Alluvial zone.

The Karjan dam is constructed on Karajan river across the narrow gorge near village Jitgadh Taluka, Nadod and District Narmada at Lat. 21^0 – 49' N and Long. 73^0 – 32' E. It is located near 80 km. from Bharuch and is very near to Navagam dam site of Sardar Sarovar Project. The total catchment area of the dam site is 1403.78 Km^2, out of which 31.08 Km^2 lie in Maharashtra state and remaining lie in Gujarat state. The gross storage of the Karajan reservoir is 630 Mm^3 and usable storage is 581 Mm^3.

The study is taken up for analyzing the impact of climate changes on the catchment hydrology of the catchment of Karajan reservoir project i.e Karajan reservoir basin, and also to assess the impact of changs in the rainfall-runoff correlations in the Karajan reservoir basin. There are 6 raingauge stations installed in a Karajan reservoir basin, namely, Karajan, Dediapada Juna mosada, Bitada, Thava, Umarapada The rainfall data from year 1961 to 2010 are available from these raingauge stations since each one is installed, from State Water Data Centre (SWDC) Gujarat. The inflows data in the Karajan reservoir is also made available from Karajan reservoir Authority. The meteorological-temperature data at Karajan station is made available from State Water Data Centre from Year 2000 onwards.

Methodology

The Steps of Methodology adopted for this study are as follows:

Analysis of the meteorological data for climate change assessment
Assessment of impact of climate change on catchment hydrology
Assessment of impact of climate change on Rainfall-Runoff processes

Climate Change Assessment

Maximum daily rainfall intensity (mm/day) of each year is assessed to identify the evidence of changing climate from daily rainfall data of each rain gauge stations. The Fig. 1 shows the maximum daily rainfall intensity of

each year, average of maximum daily rainfall intensity and 5 year moving mean of maximum daily rainfall intensity from the year in which the concerned raingauge station is installed.

Analysis of data for Climate Change Assessment

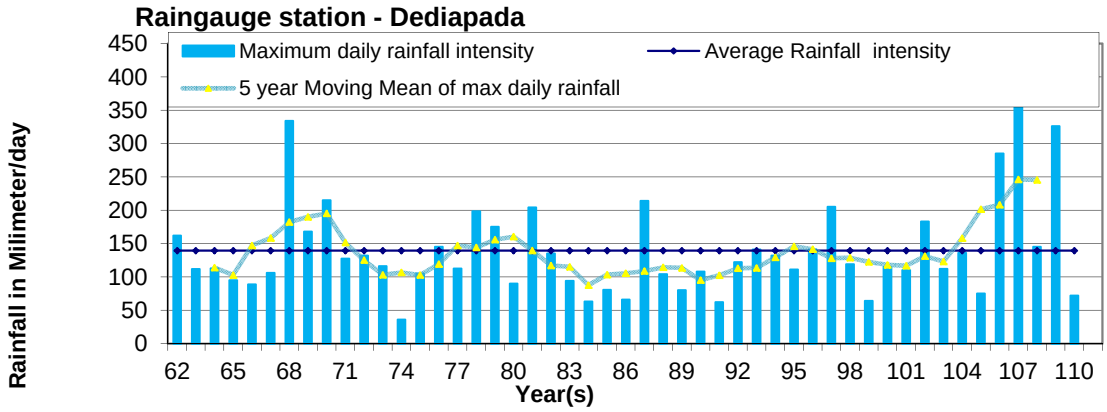

Fig. 1 Maximum daily rainfall intensity and its average and 5 year moving mean

It is seen from Fig. 1 that the abrupt increase in 5 year moving mean of max, daily rainfall intensity of the year is taking place from year 2000. Like this, the graphs have been prepared for other raingauge stations in reservoir basin namely, Karajan, Junamosada, Bitada, Thava, It is found that such abrupt change in the maximum daily rainfall intensity (mm./day) of the year takes place from year 2000.

The climate change is a continuous process, but in this study, the impact of climate change on rainfall – runoff process have been computed after year 2000, and it is compared with the impact of climate changes before year 2000. Because it is found that abrupt change in climate change has been taken place after year 2000. The scenario before year 2000 has been referred as reference scenario, while scenario after climate change has been referred as climate change scenario in this study. Since the temperature data are available from Karajan meteorological station only after year 2000 (i.e. for climate change scenario), the temperature as a parameter to identify the evidence of climate change could not be considered in this study. However, mean monthly temperature analysis of climate change scenario (year 2000-2010) indicates that the mean monthly temperature of winter season months December and February increases. This indicates the slight shifting of winter season extending till the end of February. Also, mean monthly temperature analysis indicates that the mean monthly temperature of May and June increases in comparison to March and April, This indicates the shifting of summer season concentrating in the months of May and June.

Assessment of Impact of Climate Change on Catchment Hydrology

The average rainfall over the Karajan reservoir basin have been computed by using Thession polygon method. Thession polygons have been drawn in AutoCad and area of each Thession polygon, covering each raingauge station have been computed. By weighing the rainfall value at each raingauge station depending upon the area covered, the average rainfall over the basin have been computed.

Now onwards, the rainfall referred in this study is the average rainfall over a Karajan reservoir basin computed by Thession Polygon method described as above.

Analysis of frequency of rainfall

The frequency curve for annual rainfall has been drawn for climate change scenario (year 2000 – 2010) and reference scenario (year 1961- 1999) , It is as shown in Fig. 2.

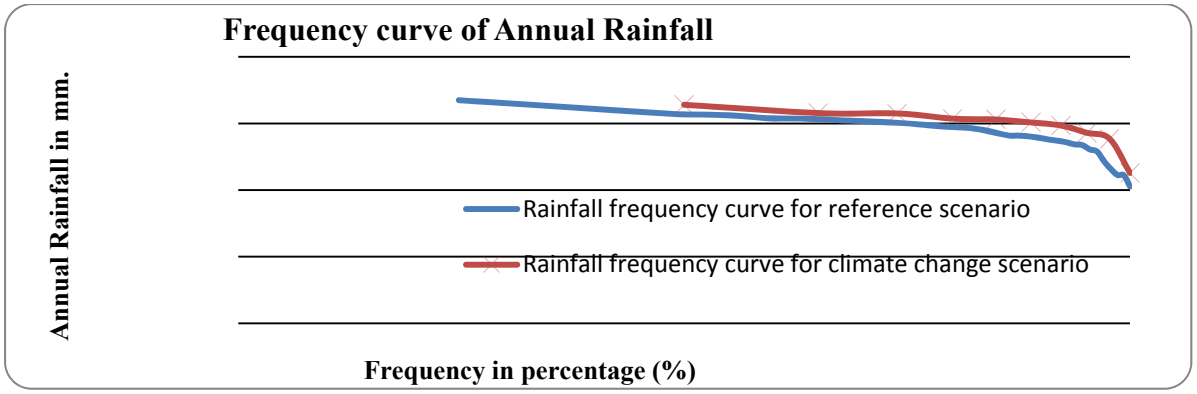

Fig. 2 Frequency curve for annual Rainfall

It is seen from Fig.2 that the frequency of magnitude of rainfall is higher in climate change scenario in comparison to reference scenario. This shows that the frequency of high rainfall magnitude has increased after year 2000.

Analysis of the number of rainy days of the season

Fig. 3 shows the number of rainy days of the season from year 1961 to year 2010. It is found that that the number of rainy days of the season have been significantly reduced after year 2000.

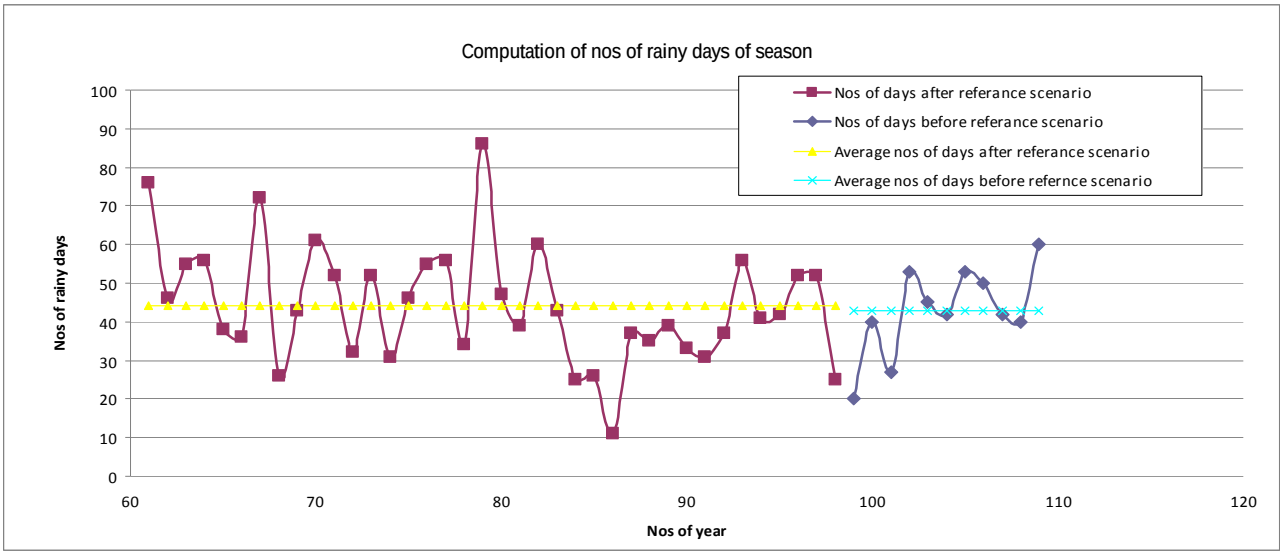

Fig, 3 Number of rainy days of the rainy season in the year

It is further analyzed that even the number of rainy days in a season have been reduced significantly after year 2000, the annual rainfall have been found to be increased after year 2000 as shown in Fig.2.. This is again justifying the climate change in the region after year 2000.

Analysis of the runoff from the basin at Karajan reservoir station

Fig. 4 shows the recurrence interval and frequency of a flow (runoff from the basin at Karajan reservoir station) for reference scenario (1961-1999) and for climate change scenario (2000-2010).

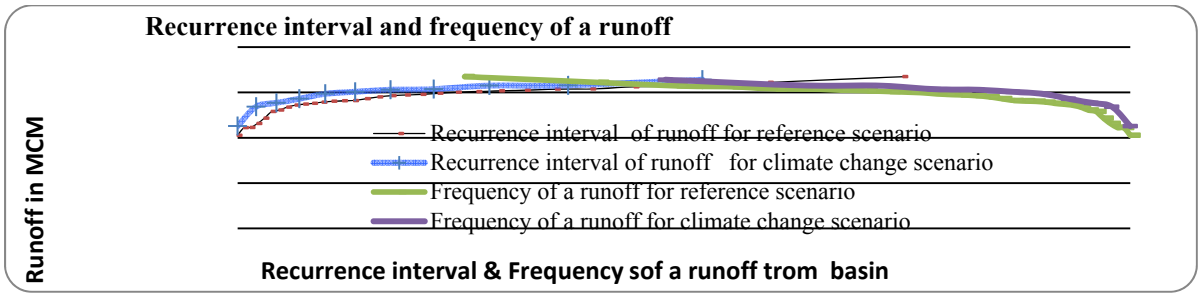

Fig. 4 Recurrence interval frequency of flow (runoff from the basin)

It is firther analyzed from Fig. 4 that frequency of occurrence of given magnitude of annual runoff (MCM) increases in climate change scenario in comparison to the reference scenario. Also the recurrence interval of the given magnitude of the annual runoff (MCM) reduces in climate change scenario in comparison to reference scenario. It is further analyzed from Fig. 2 and Fig. 3 that the frequency of higher magnitude of rainfall has increased and frequency of higher magnitude of inflows from the basin has also increased in climate change scenario in comparison to reference scenario.

The most important to know in rainfall-runoff process is that what is the effect of rainfall on runoff volume in climate change scenario in comparison to reference scenario This effect of rainfall on runoff will summarize the impact of climate changes on rainfall-runoff processes. The rainfall-runoff model will truly represent the impact of climate change and land use and land cover.

Analysis of Impact of Climate changes on Rainfall - Runoff Correlations

Impact of climate changes have been analyzed on monthly, monsoon season and annual rainfall –runoff correlations

The time series of annual rainfall (mm) and annual runoff from the basin (MCM) have been plotted and shown in Fig. 5.

Comparison of annual rainfall and runoff for reference and climate change scenario

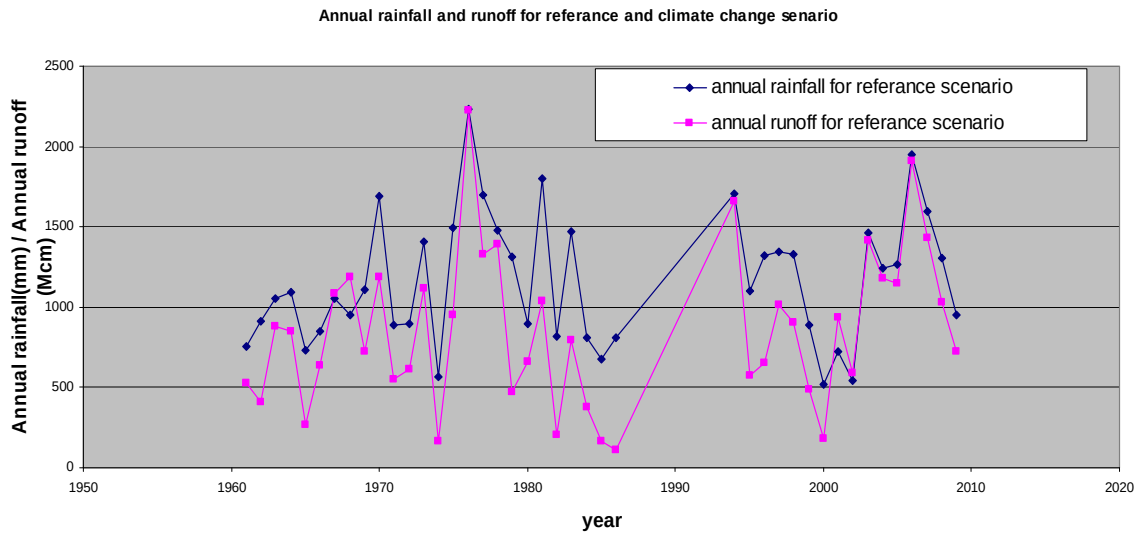

Fig. 5 Comparison of annual runoff of the basin with the rainfall

On comparing the annual rainfall in (mm) and runoff (MCM) from the basin, it is found that the annual runoff in (MCM) is higher with the annual rainfall in climate change scenario (year 2000- 2010) in comparison to reference scenario (1961-1999).

Annual rainfall runoff Correlations

The rainfall- runoff correlations have been developed using regression analysis. The annual rainfall – runoff correlations of reference scenario have been shown in Fig. 6, while annual rainfall – runoff correlations for climate change scenario have been shown in Fig. 7.

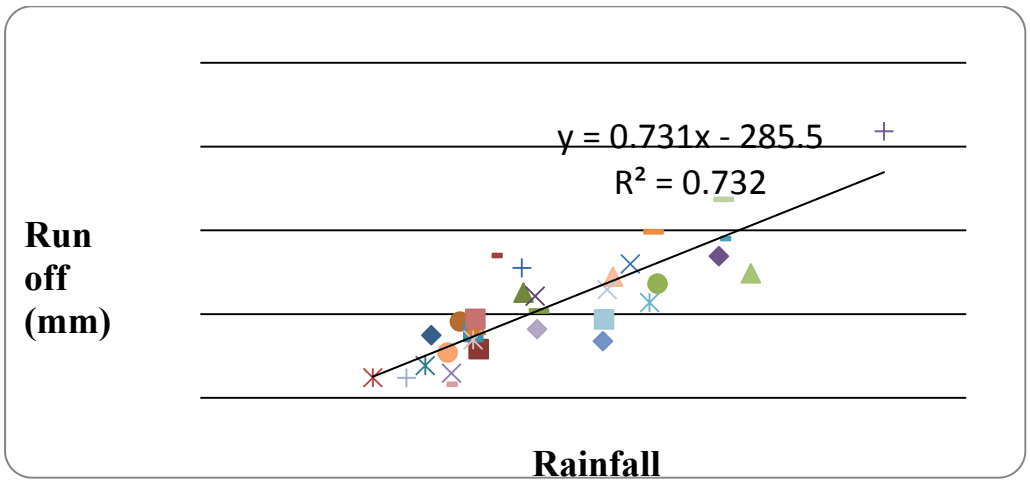

Fig. 6 Annual Rainfall-Runoff correlation for reference scenario in Karjan reservoir basin

It is found that developed equation between annual rainfall and runoff for reference scenario is as follows:

$R = 0.731\ P - 285.5$ Eq. (1)

Where, R = Annual runoff from the Karajan Reservoir basin (mm.), P = Annual Rainfall (mm). The coefficient of correlation (r^2) for this developed relationship is 0.732.

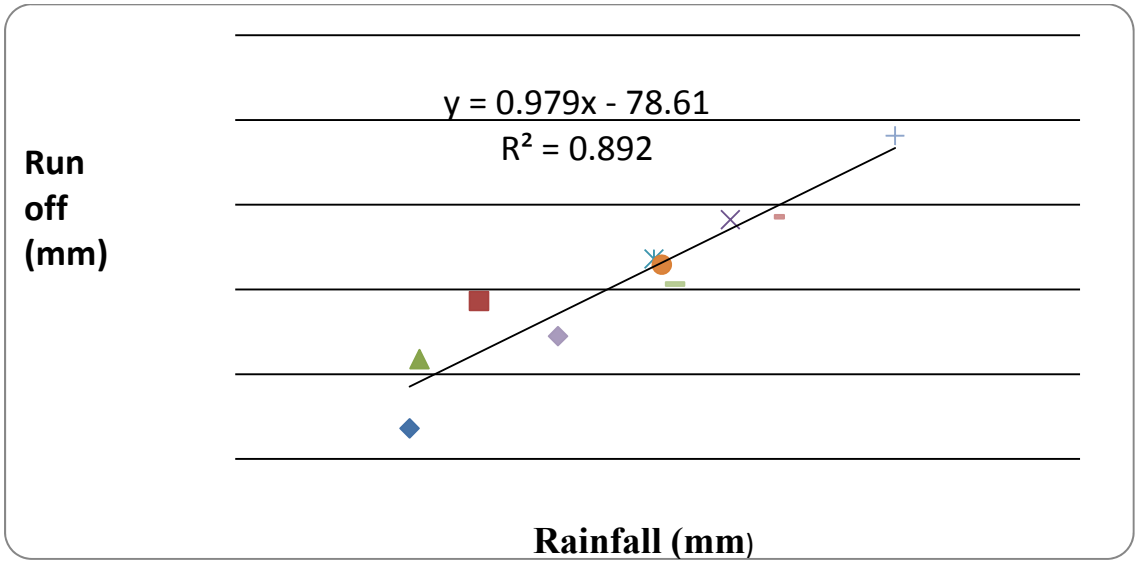

Fig. 7 Annual Rainfall-Runoff correlation for climate change scenario in Karajan Reservoir basin

It is found that developed equation between annual rainfall and runoff for climate change scenario is as follows:

$R = 0.979 P – 78.61$ Eq. (2)

Where, R = Annual runoff from the Karajan Reservoir basin (mm.), P = Annual Rainfall (mm). The coefficient of correlation (r^2) for this developed relationship is 0.892.

Comparison of annual rainfall – runoff correlations of reference and climate change scenario

Comparison of annual rainfall – runoff correlation for reference scenario and climate change scenario have been shown in Fig. 8.

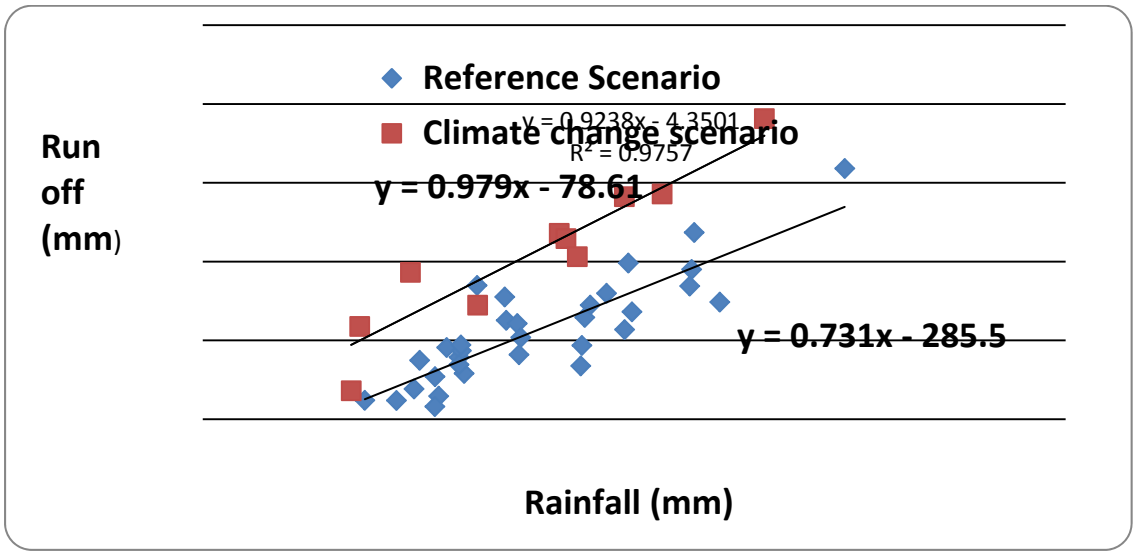

Fig. 8 Comparison of annual rainfall-runoff correlations of reference and climate change scenario

On comparisons of annual Rainfall - Runoff correlations of reference and climate change scenario, it is found that the runoff potential of the climate change scenario (after year 2000) increases significantly.

Monthly rainfall runoff Correlations

The monthly rainfall – runoff correlations of reference scenario have been shown in Fig. 9, while monthly rainfall – runoff correlations for climate change scenario have been shown in Fig. 10.

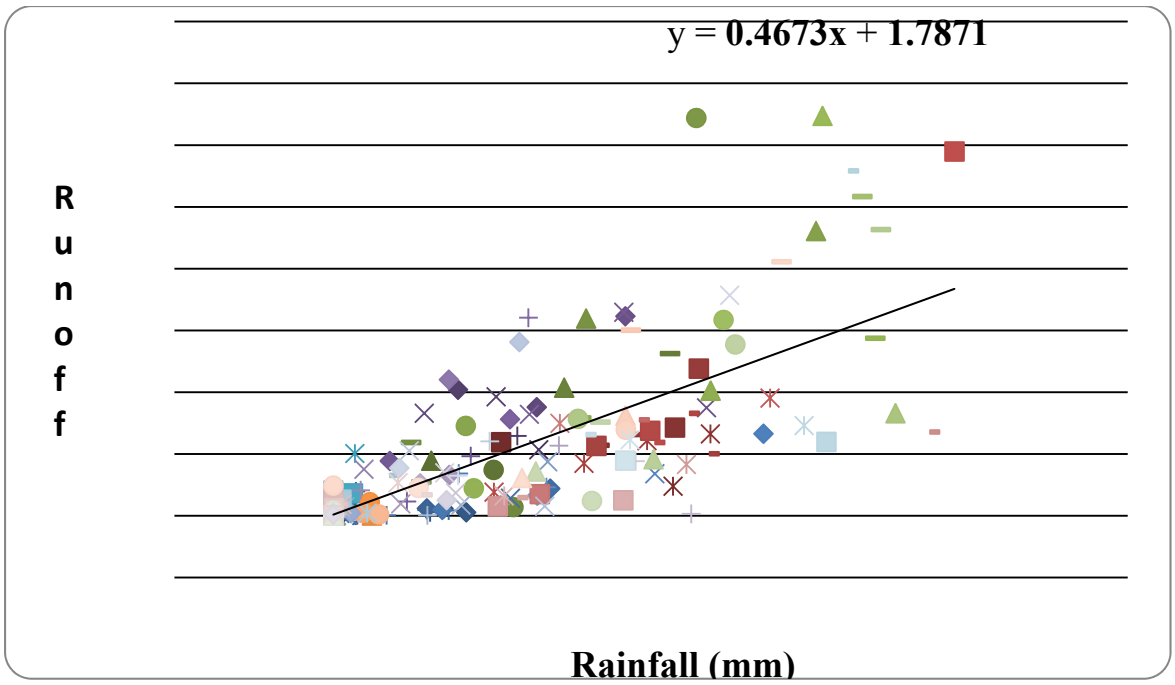

Fig. 9 Monthly rainfall-runoff correlations for reference scenario

It is found that the developed equation between monthly rainfall and runoff for reference scenario is as follows:

$R = 0.467\ P + 1.787$ Eq. (3)

Where, R = Monthly runoff from the Karajan Reservoir basin (mm.), P = Monthly Rainfall (mm). The coefficient of correlation (r^2) for this developed relationship is 0.639.

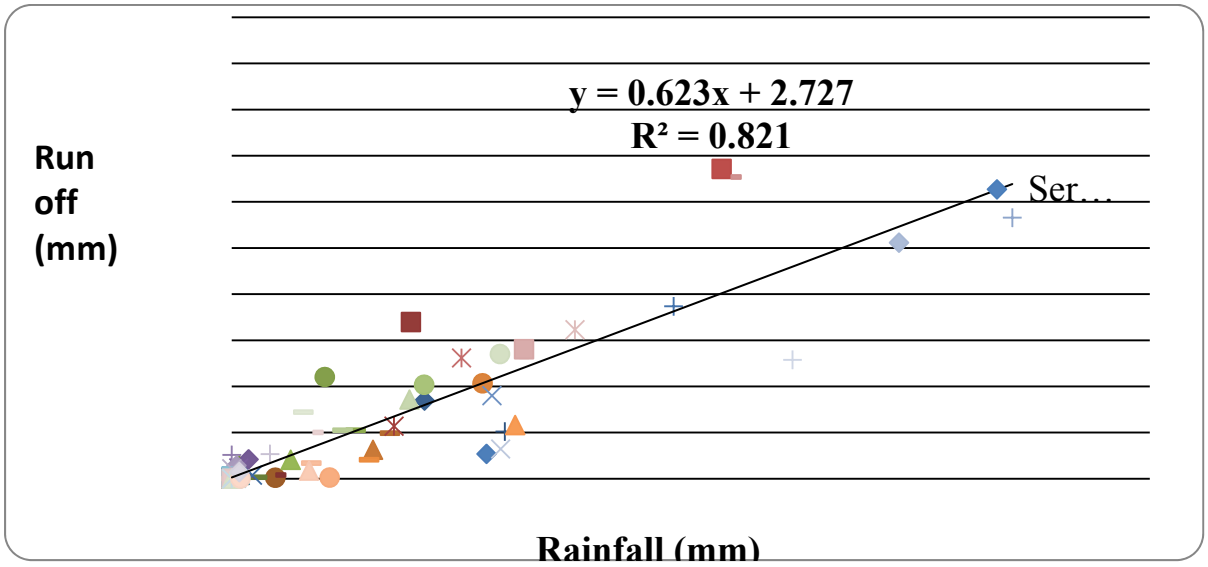

Fig. 10 Monthly rainfall-runoff correlations for climate change scenario

It is found that the developed equation between monthly rainfall and runoff for climate change scenario is as follows:

$R = 0.623\ P + 2.727$ Eq. (4)

Where, R = Monthly runoff from the Karajan Reservoir basin (mm.), P = Monthly Rainfall (mm). The coefficient of correlation (r^2) for this developed relationship is 0.821.

On comparisons of monthly Rainfall - Runoff correlations of reference and climate change scenario as shown in Fig. 11, it is found that the runoff potential of the climate change scenario (after year 2000) increases significantly.

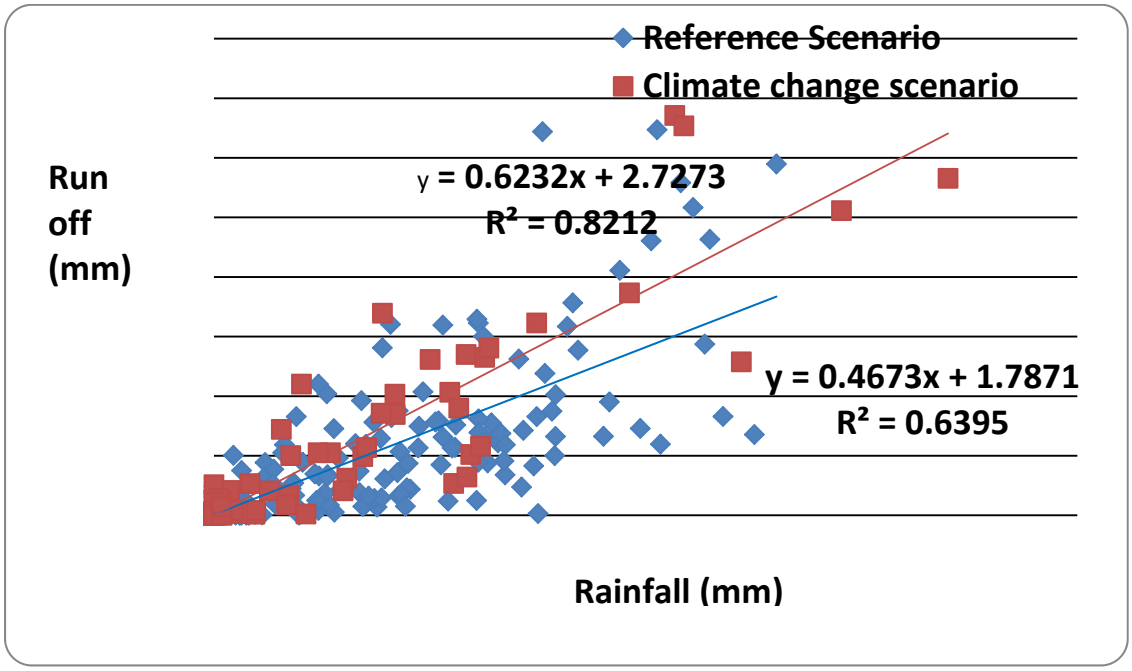

Fig. 11 Comparison of monthly rainfall-runoff correlations for reference scenario and climate change scenario

Monsoon seasonal rainfall runoff Correlations

The monsoon rainfall – runoff correlations of reference scenario have been shown in Fig. 12, while monsoon rainfall – runoff correlations for climate change scenario have been shown in Fig. 13.

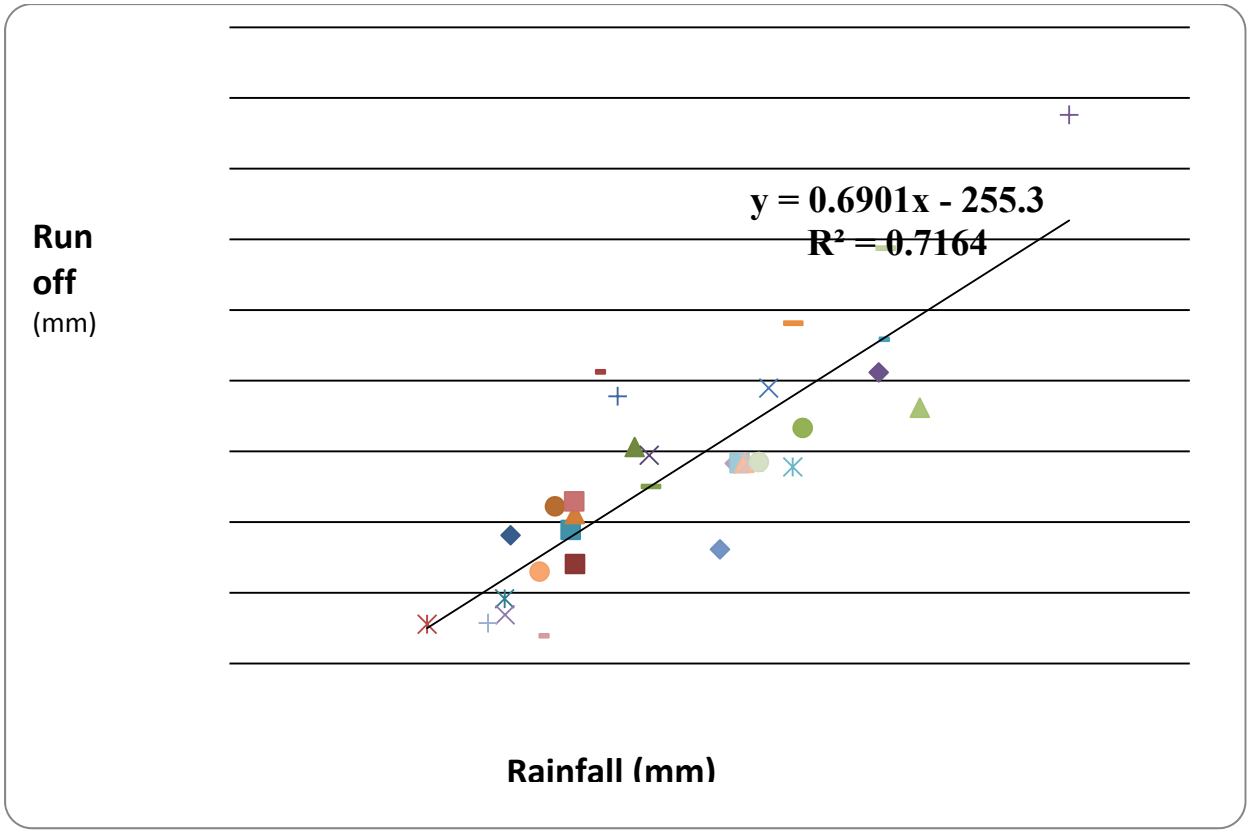

Fig. 12 Monsoon rainfall-runoff correlations for reference scenario

It is found that the developed equation between monsoon rainfall and runoff for reference scenario is as follows:

$R = 0.6901\ P - 255.3$ Eq. (5)

Where, R = Monsoon season runoff from the Karajan Reservoir basin (mm.), P = Monsoon season Rainfall (mm). The coefficient of correlation (r^2) for this developed relationship is 0.7164.

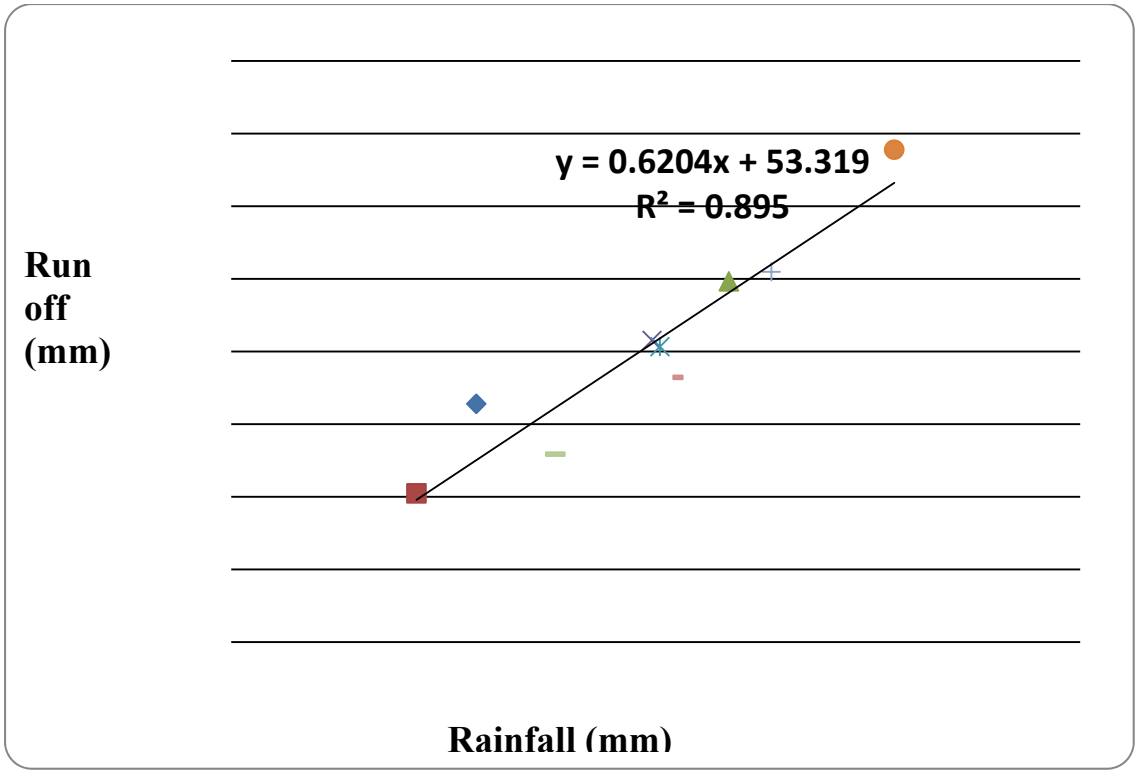

Fig. 13 Monsoon rainfall-runoff correlations for climate change scenario

It is found that the developed equation between monsoon rainfall and runoff for climate change scenario is as follows:

$R = 0.6204\ P + 53.319$ Eq. (6)

Where, R = Monsoon runoff from the Karjan Reservoir basin (mm.), P = Monsoon Rainfall (mm). The coefficient of correlation (r^2) for this developed relationship is 0.895.

On comparisons of monsoon Rainfall - Runoff correlations of reference and climate change scenario as shown in Fig. 14, it is found that the runoff potential of the climate change scenario (after year 2000) increases significantly.

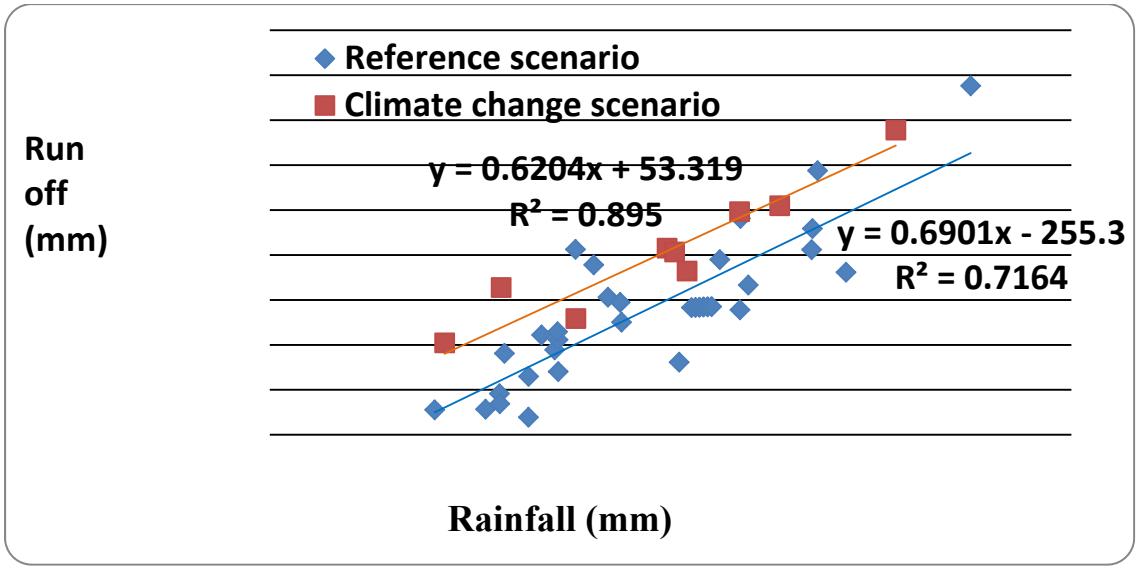

Fig. 14 Comparison of monsoon rainfall-runoff correlation for reference and climate change scenario

CONCLUSIONS

It is found from the climate change assessment that climate in the region (i,e, catchment area of Karajan reservoir project) has significantly changed from year 2000.

The effect of climate change on catchment hydrology indicates that frequency of high rainfall increases. Also, the frequency of higher runoff increases,

The annual rainfall-runoff, monsoon season rainfall-runoff and monthly rainfall-runoff model could be established satisfactorily with correlation coefficient reasonably good,

Further, it is analyzed that from the annual, monsoon season and monthly rainfall-runoff model that the impact of 'climate change' (after year 2000) in the basin (catchment of Karjan Reservoir Project) has increased the runoff potential of the basin.

The results of this study will prove beneficial to the Karjan project authorities for the better management of the water resources in the basin and to decide sustainable reservoir operating policy for both monsoon and summer season. The increased volume of runoff can be planned for supplying the urban water demand of the cities. The Surplus water can be planned to divert for hydropower generation through canal bed power house Thus results of this study will be useful towards preventing the cities against climate change impacts.

Acknowledgements

Authors are thankful to State Water Data Centre (SWDC), Gandhinagar for providing rainfall data. Also, thanks are to the Karjan reservoir authorities for providing runoff data.

REFERENCES

Bronstert, Axel (2004). Rainfall-runoff modelling for assessing impacts of climate and land-use change, *Hydrol. Process.* 18, 567–570 (2004)

Krausmann F, Haberl H, Schulz NB, Erb K-H, Darge E,,Gaube V. 2003. Land-use change and socio-economic metabolism
in Austria—part I: driving forces of land-use change:
1950–1995. *Land-use Policy* 20(1): 1–20.

LUCC.2002. New estimates of tropical deforestation and terrestrial carbon fluxes: result of two complementary studies. *LUCC Newsletter* (December).

.

EVALUATION OF REVISED SUBSURFACE TILE DRAINAGE ALGORITHMS IN SWAT FOR A COLD CLIMATE

D. N. Moriasi
P.H. Gowda
J.G. Arnold
D.J. Mulla
S. Ale

Abstract

Subsurface tile drains in agricultural systems of Midwest U.S. are a major contributor of nitrate loadings to hypoxic conditions in the Gulf of Mexico. Strategies to reduce nitrate loadings from these agricultural systems require better understanding of role of subsurface tile drain flows. In this study, long-term (1983-1996) monitoring data on subsurface tile drain flow was used to evaluate the extensively used Soil and Water Assessment Tool (SWAT) model. Tile flow computations in SWAT are heavily driven by water table depth that is a function of soil water movement. This traditional method used in the SWAT that computes the retention parameter as a function of soil profile water content generally over predicts runoff in poorly drained soils such as those in the Mid-western U.S. The retention parameter is used to compute daily curve number (CN) for estimating surface runoff. This paper presents 1) modifications made to potential maximum soil moisture retention parameter algorithms to account for the effects of tile drainage on the computation of surface runoff using the CN method in poorly drained agricultural watersheds and 2) calibration and validation of the SWAT for subsurface tile drain flow for poorly drained soils in a cold climate using long term monitoring data. The retention parameter was increased to account for the effect of tile drainage, which is not accounted by the CN tables. Comparison of monthly tile drain flows from the SWAT to measured data indicated excellent agreement. Calibration and validation of revised SWAT model for flow gave Nash-Sutcliffe efficiency (NSE) values of 0.77 and 0.78, respectively, the percent bias (PBIAS) values of -1% and 5%, respectively, and root mean square error (RMSE) values of 2.9 mm and 2.0 mm, respectively. Predicted annual water budget was found similar to those reported in the literature. The validated tile flow algorithms in SWAT will be useful for modeling the impacts of tile drain spacing and depth on nitrate losses in poorly drained soils of Upper Midwest U.S.

Keywords: SWAT, Tile drain, Curve number, Retention parameter

INTRODUCTION

Expanding hypoxic zones in the Gulf of Mexico is a serious environmental issue and has been attributed to the nutrient enriched waters entering the Gulf from the Mississippi River. The Upper Mississippi River Basin contributes one-third of the total Nitrate-N loading on the Mississippi River (Alexander et al., 1995). Higher nitrate-N loadings in the Upper Mississippi River Basin are associated with tributaries from agricultural areas of state of Minnesota, Iowa, and Illinois where high percentage of croplands equipped with subsurface tile drainage systems. Subsurface tile drainage system is a commonly used agricultural practice in the Midwest to enhance crop yield in poorly drained but highly productive soils. It improves aeration, increases the availability of plant nutrients (Lal and Taylor, 1970), and enhances crop productivity (Cannell, 1979) by facilitating timely farm operations. It also reduces crop diseases, soil erosion, and surface runoff (Fausey et al., 1986). Two long-term monitoring studies on clay soils in northern Ohio have shown that subsurface drainage substantially improved average corn and soybean yields and helped to reduce year-to-year variability in yields (Brown et al., 1998). More than 30% of the crop lands in the Midwest U.S. are equipped with subsurface drainage systems and expected to exceed 40% by year 2000 (Zucker and Brown, 1998). Research has shown that presence of tile

drainage systems expedite the transport of plant nutrients to streams and lakes through subsurface drainage and often contains significant amount of nitrate-N (Baker, 1994; Logan et al., 1994).

Monitoring quantity and quality of subsurface drainage can be useful in assessing the impact of agricultural management practices on surface and ground water quality (Kanwar et al., 1988; Randall and Schmitt, 1993). It can be used to identify alternative agricultural Best Management Practices (BMPs) to reduce nutrient loadings to streams and rivers while enhancing the crop yield. The subsurface tile drainage configuration, varying soil properties, topography, and climatic conditions have a major impact on pattern and magnitude of nutrient losses. Better understanding of the role of these parameters is required to identify alternative agricultural BMPs. For this reason, many long-term water quality-monitoring studies have been conducted throughout the Midwest U.S. and Canada with more emphasis on tile spacing and depth, N-application rates and timing, crop rotation, and climatic variability. Most of these studies have been conducted either at plot or field scales to describe the effect of specific farming practices. However, there are only a few such watershed-scale studies, as they require all farmers within a watershed to follow prescribed farming practices. This requires incentive payments for farmers to adopt new practices. In addition, it is difficult to evaluate more than one or two farming practices, as it is economically not viable.

Computer simulation models have proved to be an efficient and effective tool to analyze water resource problems. Consequently, a wide variety of surface and subsurface water quality simulation models such as AGNPS (Young et al., 1994; He et al., 2001), CREAMS (Knisel, 1980), GLEAMS (Leonard et al., 1987), DRAINMOD (Skaggs, 1982), NLEAP (Shaffer et al., 1991), LEACHM (Hutson and Wagenet, 1992), RZWQM (USDA-ARS, 1992), ADAPT (Ward et al., 1993), and SWAT (Arnold et al. 1998; Arnold and Fohrer, 2005) have been developed and are being used to evaluate the impact of agricultural management practices on water quality. However, these models need to be calibrated and validated for all the major hydrologic processes to build users' confidence in the model. There are two algorithms used to compute tile drainage in SWAT. The first algorithm calculates tile flow as function of water table depth, tile depth, and the time required to drain the soil to field capacity (Arnold et al., 1999) assuming that the tile systems have already been designed with regard to tile spacing and size. The second algorithms computes tile flow using the Hooghoudt's (1940) steady-state and Kirkham (1957) tile drain equations that are a function of water table depth, tile drain depth, size, and spacing (Moriasi et al., 2012). The water table depth is a function of soil water movement. However, the traditional method, which computes the retention parameter in SWAT as a function of soil profile water content, generally over predicts runoff in poorly drained soils equipped with tile drains. This paper presents 1) modifications made to potential maximum soil moisture retention parameter algorithms to account for the effects of tile drainage on the computation of surface runoff using the CN method in poorly drained agricultural watersheds, and 2) calibration and validation of the modified SWAT for subsurface tile drain flow for a cold climate using long term monitoring data. The retention parameter was increased to account for the effect of tile drainage, which is not accounted by the CN tables.

METHODS AND MATERIALS

Modifications to Soil Moisture Retention Parameter Algorithms in SWAT:

According to Walker et al. (2000), the CN method was developed to predict the initial or "quick" response of a watershed to a storm event. In the case of tile-drained watersheds, total watershed response may be the sum of base flow or water flowing directly in through the sides and bottom of the ditch or stream channel, flow entering the ditch via field tile systems, and surface runoff. Quick response may be predominantly tile-flow, with any surface runoff being passed to the low lying areas of the watershed to exit as base flow or tile flow. Therefore, they concluded that conceptually, the CN method can be applicable to tile-drained watersheds, with possible modification of (1) CN used to estimate potential maximum soil retention (S) and (2) potential maximum retention (S) associated with initial abstractions (I_a).

In SWAT simulations, modification of the CN is usually accomplished by calibration. In this study, we focused on modifying the potential maximum retention associated with initial abstractions. With SWAT, users are allowed to select between two methods for calculating the retention parameter (Neitsch et al., 2009). The traditional method allows the retention parameter to vary with soil profile water content. An alternative added in SWAT allows the retention parameter to vary with accumulated plant evapotranspiration. Calculation of the daily CN as a function of plant evapotranspiration was added, because the soil moisture method was predicting too much runoff in shallow soils. In this study, we modified the traditional soil moisture method for mildly-sloped tile-drained watersheds by increasing the retention parameter (Eq. 1) to account for tile flow, which is the predominant subsurface water budget component.

$$S = 8.0 * S_{\max} \cdot \left(1 - \frac{SW}{\left[SW + \exp\left(w_1 - w_2 \cdot SW \right) \right]} \right) \quad (1)$$

where S is the retention parameter for a given day (mm), S_{max} is the maximum value the retention parameter can achieve on any given day (mm), SW is the soil water content of the entire profile excluding the amount of water held in the profile at wilting point (mm H_2O), and w_1 and w_2 are shape coefficients. This modification is allowed as a third alternative method for computing the retention parameters.

***Study Area**:* In this study, long-term (1983-1996) monitoring data on subsurface tile drain flow was used to evaluate the extensively used SWAT model. Measured tile drain flow used in this study was collected from three continuous corn plots located in the University of Minnesota's Agricultural Experiment Station near Waseca, southern Minnesota. Water, crop, and nutrient management practices on these plots were typical of the Upper Mid-western USA, where tile drains are essential for agricultural production by draining water from the shallow water tables to allow timely tillage and planting operations. Field measurements of soil and crop properties were made as a part of a tile drainage study (Randall et al., 1997; Randall and Iragavarapu, 1995; Buhler et al., 1993). The size of each plot was 13.5 x 15.0 m. These plots were designed to simulate a tile drain spacing of 27 m. Tile drains were installed at a depth of 1.2 m with a gradient of 0.1%. Diameter of the tile drain was 100 mm. Since 1982, these plots were planted with continuous corn under moldboard plow tillage. Tile drain flows were measured daily and summed to calculate monthly and yearly values.

Model Input: Weather data including daily values of precipitation, average air temperature, solar radiation, wind speed, and average relative humidity recorded at a weather station located at about 0.5 km from the experimental plots was used in the simulation. The soil input data and subsurface tile drainage system parameter values for the study location are presented in tables 1 and 2. These parameters were held constant for all simulations unless otherwise stated. Soil properties such as depth of each horizon, particle size distribution, and organic matter content reported in Cully (1986) was used in the simulations. The SCS runoff curve number of 78 was estimated for the hydrologic group rating of the Webster soil (B/D rating – poor drainage improved by tiling) under a straight row cropping system (Natural Resources Conservation Service, 1994). The values of hydraulic conductivity and depth to impermeable layer were obtained from Davis et al. (2000). Initial N content of the soil was obtained from Randall (1983). Although both tile drain algorithms in SWAT can be used with the maximum soil moisture retention parameter, the Hooghoudt's (1940) steady-state and Kirkham (1957) tile drain equations were used in this study because tile spacing and size were available. A depth to impervious layer of 2.00 m and Priestley-Taylor PET method were used.

Table 1. Soil input data (Davis et al., 2000). WP is the wilting point.

Layer	Thickness (mm)	Clay (%)	Silt (%)	Sand (%)	Organic Carbon (%)	WP (mm mm^{-1})	Hydraulic Conductivity (mm hr^{-1})	Porosity (mm mm^{-1})	Initial Soil N (mg kg^{-1})
1	310	33	38	29	6.10	0.23	48	0.45	6.70
2	310	31	33	36	2.10	0.21	48	0.41	6.40
3	310	30	31	39	1.00	0.19	48	0.39	5.50
4	870	29	32	39	1.00	0.19	48	0.39	4.60

Table 2. Values used for subsurface drainage systems in the study plot (Davis et al., 2000).

Parameter	Description	Value
DDRAIN	Depth to subsurface tile (mm)	1200
Size	- Diameter of tile drain (mm)	100
SDRAIN	Distance between two drain or tile tubes (mm)	27000

Model Calibration and Validation: The Modified SWAT model was manually calibrated and validated for tile flow. In addition, simulated water budget was compared with available measured data to evaluate SWAT's ability to predict individual components of the budget. Also simulated crop yields were compared with available measured data. Calibration and validation of the SWAT model consisted of predicting and comparing monthly subsurface tile drainage with measured data between April and August. For calibration, the measured data for the years 1983, 1985, 1987, 1989, 1991, 1993, and 1995 were used. The selection of odd years for calibration was made in order to improve model performance across a wide range of climatic conditions. Years 1989 and 1993 were the driest and wettest years, respectively, in the last 40 years. If we had simply used the first seven years for model calibration, the model would have been biased toward the driest year. If we had used the last six years for calibration, it would have been biased toward the wettest year.

According to Davis et al. (2000) study on the same plot using the ADAPT model, the most sensitive water budget components for the study plots were ET, surface runoff and subsurface tile flow. Based on this information, the following parameters were varied during manual calibration: the plant uptake compensation factor (EPCO) and leave area index (LAI) for ET and drainage coefficient (DRAIN-CO; mm day^{-1}), multiplication factor to determine lateral saturated hydraulic conductivity (k_{sat}) from SWAT vertical hydraulic conductivity (k_{sat}) input values for each HRU (LATKSATF), effective radius of tile drain (RE; mm) Surface runoff parameters such as CN2 were not calibrated since the modified soil profile retention parameter simulated average annual surface runoff value close to the measured average annual surface runoff for the study plot (Davies et al., 2000). All other parameters (Neitsch et al. 2009) were kept at the SWAT default values.

Model Evaluation: In addition to the graphical methods, the percent bias (PBIAS) (Gupta et al., 1999), Nash-Sutcliffe efficiency (NSE) (Nash and Sutcliffe, 1970), coefficient of determination (R^2), and the root mean square error (RMSE, in the units of the simulated component) model performance measures were used to determine the performance of the modified SWAT. According to Moriasi et al. (2007), a model is considered satisfactorily calibrated if monthly NSE $\geq$ 0.65 and PBIAS $\leq \pm$10.0% and validated if NSE > 0.50 and PBIAS $\leq \pm$25.0%. According to Singh et al. (2004) RMSE values less than half the standard deviation of the measured data may be considered low.

RESULTS AND DISCUSSION

The calibrated values for the ESCO, LAI, DRAIN-CO, LATKSATF and RE are 0.001, 2.10, 51.0 mm, and 50.0 mm, respectively Details about the range of values for the calibration parameters are given by Neitsch et al. (2009). Table 3 compares the predicted and measured average water budgets for the period 1983 – 1996 during the growing season of April through August. The predicted average tile drainage was 39% of the precipitation total precipitation during the growing season, which is equivalent to the measured value of 39%. Although not measured, the predicted average ET was 68% of the rainfall, which was comparable to measured values of 64% to 70% in 1994 on a fine-textured tile-drained soil cropped with corn located in central Iowa (Moorman et al., 1999). This means that surface runoff simulated by the modified SWAT was about 1% of the total rainfall during the growing season. Although surface runoff was not measured, the simulated surface results were in agreement with Randall and Iragavarapu (1995) who considered surface runoff to be minimal on the same Waseca plots. This result is also in the same order of magnitude with the value of 5.4% average annual surface runoff of average annual precipitation obtained by Nangia et al. (2009) on a nearby commercial field equipped with tile drains managed by the Minnesota Department of Agriculture. This implies that the modified SWAT model simulates surface runoff amount and indicates that it is partitioning water reasonably well.

Table 3. Model predicted and field measured components for the years 1983 to 1996.

Component	Mode predictions		Field observations	
	Depth (cm)	Percent of precipitation	Depth (cm)	Percent of precipitation
Precipitation	52.8		52.8	
Evapotranspiration	35.9	68	-	-
Tile Drainage	20.3	39	20.7	39

Model Calibration and Validation Performance for Tile flow:

The calibration and validation model performance results for predicting monthly tileflow are presented in Table 4. Supporting time-series graphical plots of monthly tile flow for the calibration and validation periods are illustrated in figures 1 and 2, respectively. During the calibration period, the monthly NSE value was 0.77 while the PBIAS value was ±1.1% (table 3). According to Moriasi et al. (2007), a model is considered calibrated for streamflow if monthly NSE $\geq$ 0.65 and PBIAS $\leq$ ±10%. Therefore, the Modified SWAT model was well calibrated as shown by the statistics in table 4 and supported by the monthly hydrograph (figure 1). The statistical results during the validation period were as good as during the calibration period (table 4 and figure2). The simulated RMSE of 2.86 mm and 1.97 mm, were 0.47 and 0.46 of the standard deviation of the observed tile flow during the calibration and validation periods, respectively. Both of these values are below the 0.5 value recommended by Singh et al. (2004), therefore, the simulated RMSE values during the calibration and validation periods are low.

Table 4. Simulation performance: Monthly streamflow calibration and validation statistics of the measured and simulated data.

Statistic	Calibration	Validation
NSE	0.77	0.78
PBIAS (%) -	-1.1	5.4
RMSE (mm)	2.86	1.97

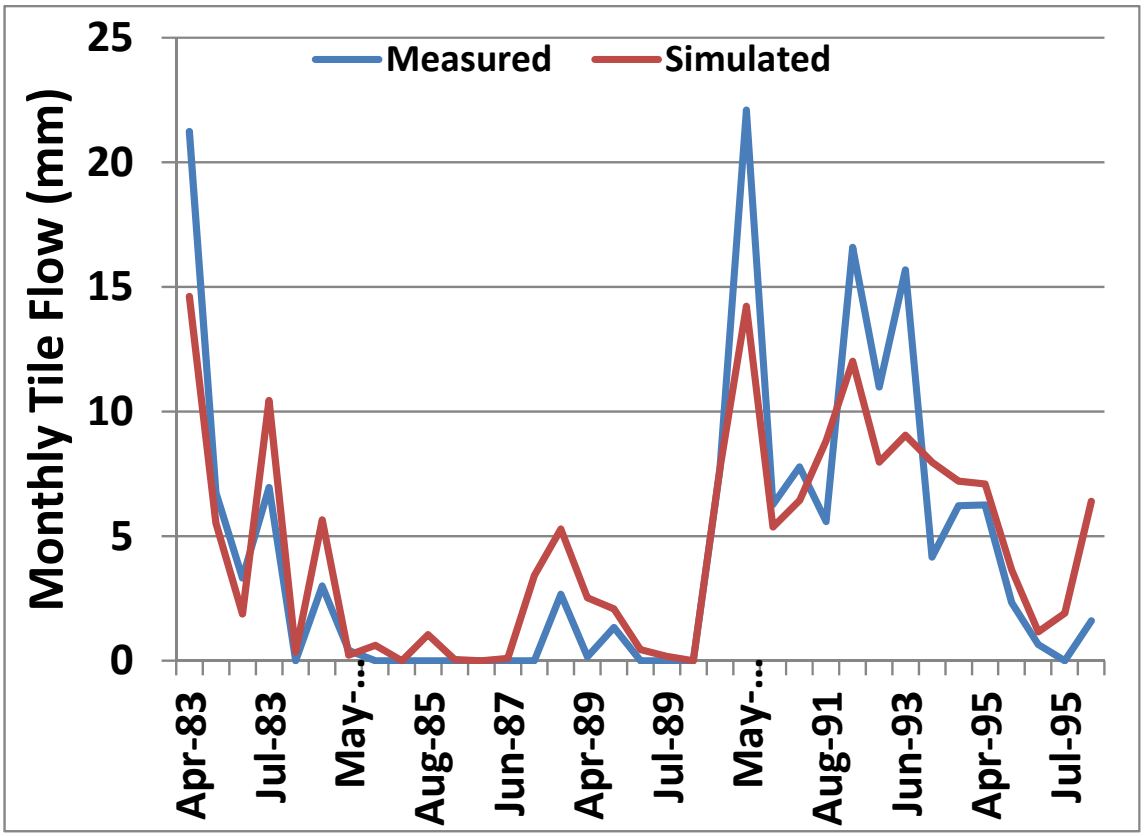

Figure 1. Monthly observed and simulated tile flow for the calibration period

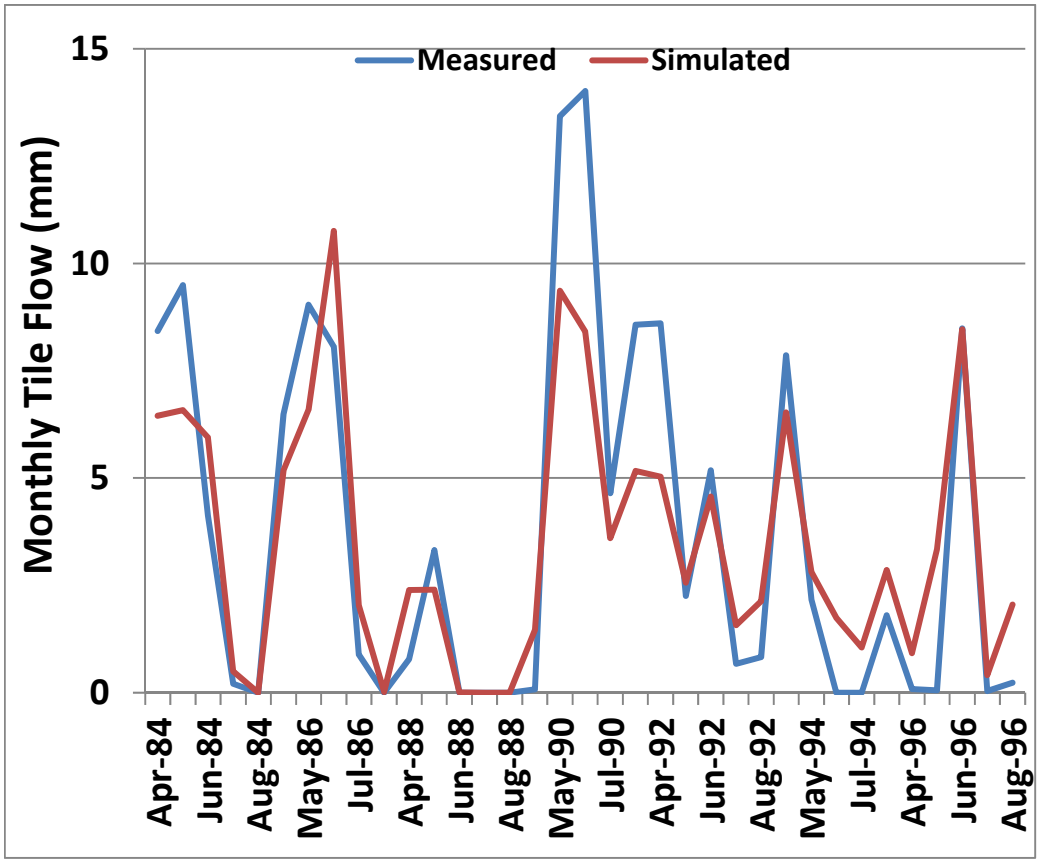

Figure 2. Monthly observed and simulated tile flow for the validation period

SUMMARY

In this study, the SWAT model was modified to increase the retention parameter to account for the effect of tile drainage, which is not accounted by the CN tables. Long-term monitoring data on subsurface tile drain flow from three plots located in Waseca, Minnesota USA were used to evaluate the modified SWAT model. Based on the water budget results, the modified SWAT model simulates surface runoff amount and indicates that it is partitioning water reasonably well. The calibration and validation results showed that the modified SWAT simulated tile flow reasonably well on a monthly time step. The validated tile flow algorithms in SWAT will be useful for modeling the impacts of tile drain spacing and depth on nitrate losses. Additional studies are underway to further test the modified SWAT on how well it simulates water quality components.

ACKNOWLEDGEMENT

The authors are grateful to Alan Verser for his invaluable assistance with building, calibrating and validating the modified SWAT.

REFERENCES

Alexander, R. B., R. A. Smith, and G. E. Schwarz. 1995. The regional transport of point and nonpoint source nitrogen to the Gulf of Mexico. Proceedings of the Hypoxia Management Conference, Gulf of Mexico Program, New Orleans, LA.

Arnold, J.G., R. Srinivasan, R.S. Muttiah, and J.R. Williams. 1998. Large-area hydrologic modeling and assessment: Part I. Model development. J. Amer. Wat. Res. Assoc. 34(1):73-89.

Arnold, J.G., P.W. Gassman, K.W. King, A. Saleh, and U. Sunday. 1999. Validation of the Subsurface Tile Flow Component in the SWAT Model. Presented at the ASAE/CSAE-SCGR Ann. Intl. Meeting. ASAE Paper No. 992138. St. Joseph, Mich.: ASAE.

Arnold, J.G. and N. Fohrer. 2005. SWAT2000: current capabilities and research opportunities in applied watershed modeling. Hydrol. Process. 19(3):563-572.

Baker, D. B. 1994. Long-term water quality monitoring in the Lost Creek watershed: A data synthesis. Water Quality Laboratory, Heidelberg College, Tiffin, OH.

Baker, J. L., and H. P. Johnson. 1981. Nitrate-nitrogen in tile drainage as affected by fertilization. Journal of Environmental Quality, 10:519-522.

Baker, J. L., and S. W. Melvin. 1994. Chemical management, status, and findings. *In* Agricultural drainage well research and demonstration project - Annual report and project summary, Iowa Department of Agriculture and Iowa State University, pp. 27-60.

Brown, L. C., B. M. Schmitz, M. T. Batte, C. Eppley, G. O. Schwab, R. C. Reeder, and D. J. Eckert. 1998. Historic drainage, crop rotation, and yield studies on clay soils in Ohio. Proceedings of the 7th Annual Drainage Symposium, "Drainage in the 21st Century: Food production and the environment," ASAE, Orlando, FL, pp. 456-464.

Buzicky, G. C., G. W. Randall, R. D. Hauck, and A. C. Caldwell. 1983. Fertilizer losses from a tile drained mollisol as influenced by rate and time of 15-N depleted fertilizer application. In: Agronomy Abstracts, American Society of Agronomy, Madison, WI, p.213.

Cannell, R. G. 1979. Effects of soil drainage on root growth and crop production. In soil physical properties and crop production in the tropics. R. Lal and D. J. Greenland (eds.), J. Wiley & Sons, Chichester, U. K., pp. 183-187.

Chung, S. O., A. D. Ward, N. R. Fausey, and T. J. Logan. 1991. Evaluation of the pesticide component of the ADAPT water table management model. Transactions of ASAE, 35(2):571-579.

Chung, S. O., A. D. Ward, and C. W. Schalk. 1992. Evaluation of the hydrologic component of the ADAPT water table management model. Transactions of ASAE, 35(2):571-579.

Davis, D. M. 1998. Simulation of tile drain flow and nitrate loss from a clay loam soil. M.S. Thesis, Department of Soil, Water, and Climate, University of Minnesota, pp 1-69.

Davis, D.M., P.H. Gowda, D.J. Mulla, and G.W. Randall. 2000. Modeling nitrate nitrogen leaching in response to nitrogen fertilizer rate and tile drain depth or spacing for southern Minnesota, USA. J. Environ. Qual. 29:1568-1581.

Desmond, E. D., A. D. Ward, N. R. Fausey, and T. J. Logan. 1995. Nutrient component evaluation of the ADAPT water management model. Proceedings of the International Symposium on Water Quality Modeling, Orlando, FL, pp. 21-30.

Desmond, E. D., A. D. Ward, N. R. Fausey, and S. R. Workman. 1996. Comparison of daily water table depth prediction by four simulation models. Transactions of ASAE, 39(1):111-118.

Doorenbos, J. and W. O. Pruitt. 1977. Guidelines for predicting crop water requirements, 144. Irrigation and Drainage Paper 24. New York: FAO United Nations.

Fausey, N. R., G. S. Taylor, and G. O. Schwab. 1986. Sub-surface drainage studies in a fine textured soil with impaired permeability. Transactions of ASAE, 29:1645-1653.

Fausey, N. R., L. C. Brown, H. W. Belcher, and R. S. Kanwar. 1995. Drainage and water quality in great lakes and cornbelt states. Journal of Irrigation and Drainage Engineering, 121(4):283-288.

Geohring, L. D., P. E. Wright, and T. S. Steenhuis. 1988. Preferential flow of liquid manure to subsurface drains. Proceedings of the 7th Annual Drainage Symposium "Drainage in the 21st Century: Food production and the environment," ASAE, Orlando, FL, pp. 1-8.

Gordon, R., A. Madani, K. Caldwell, S. Welling, P. Harvard, and L. Cochrane. 1998. Leaching characteristics of nitrate-N in a subsurface drained soil in Atlantic Canada. Proceedings of the 7th Annual Drainage Symposium "Drainage in the 21st Century: Food production and the environment," ASAE, Orlando, FL, pp. 567-573.

Gowda, P. H. 1996. An integrated spatial-process model to predict agricultural nonpoint source pollution. Ph. D. Dissertation. Department of Food, Agricultural and Biological Engineering, The Ohio State University, Columbus, OH.

Gowda, P. H., A. D. Ward, D. A. White, and J. G. Lyon. 1996. Using GIS with a field scale model to describe agricultural impacts on Rock Creek watershed. ASAE Paper No. 96-3090, American Society of Agricultural Engineers, Pheonix, AZ.

Gowda, P. H., A. D. Ward, D. A. White, D. B. Baker, and T. J. Logan. 1998. Modeling drainage practice impacts on the quantity and quality of stream flows for an agricultural watershed in Ohio. Proceedings of the 7th Annual Drainage Symposium "Drainage in the 21st Century: Food production and the environment," ASAE, Orlando, FL, pp. ASAE, Orland, FL, pp. 145-154.

Gupta, H. V., S. Sorooshian, and P. O. Yapo. 1999. Status of automatic calibration for hydrologic models: Comparison with multilevel expert calibration. J. Hydrologic Eng. 4(2): 135-143.

Haan, C. T., B. J. Barfield, and J. C. Hayes. 1994. Design Hydrology and Sedimentology for small catchments. Academic Press, San Diego, CA.

Hooghoudt, S. B. 1940. Bijdragen tot de kenins van enige natuurkundige grootheden van de ground. No. 7. Versl. Landbouwk. Onderz. (Contributions to the knowledge of some physical constants of the soil. No.7. Report Agric. Res.). 46: 515-707.

Hutson, J. L., and R. J. Wagenet. 1992. LEACHM: Leaching estimation and chemistry model: A process based model of water and solute movement, transformations, plant uptake and chemical reactions in the unsaturated zone. Version 3. Department of Agronomy, Cornell University, Ithaca, NY.

Kanwar, R. S., D. E. Stotenberg, R. Pfeiffer, D. L. Karlen, T. S. Colvin, and M. Honeyman. 1991. Long-term effects of tillage and crop rotation on the leaching of nitrate and pesticides to allow groundwater. In Ritter, W. F. (ed.), Irrigation and Drainage Proceeding. Conference of ASCE Irrigation and Drainage Division. ASCE. New York. pp. 655-661.

Kanwar, R. S., J. L. Baker, and D. G. Baker. 1988. Tillage and split N-fertilization effects on subsurface drainage water quality and crop yields. Transactions of ASAE, 31:453-460.

Kanwar, R. S., J. L. Baker, and J. M. Laflen. 1985. Nitrate movement through the soil profile in relation to tillage system and fertilization application method. Transactions of ASAE, 28:1802-1807.

Kirkham, D. 1957. Theory of Land Drainage, In "Drainage of Agricultural Lands Agronomy Monograph No. 7, American Soc. Agron", Madison, Wisconsin.

Kitur, B. K., M. S. Smith, R. L. Blevins, and W. W. Frye. 1984. Fate of 15N-depleted ammonium nitrate applied to no-tillage and conventional tillage corn. Agronomy Journal, 76:240-242.

Kladivko, E. J., G. E. Van Scoyoc, E. J. Monke, K. M. Oats, and W. Pask. 1991. Pesticide and nutrient movement into subsurface tile drains on a silt loam soil in Indiana. Journal of Environmental Quality, 20:264-270.

Kladivko, E. J., J. Grochulska, R. F. Turco, G. E. Van Scoyoc, and J. D. Eigel. 1999. Pesticide and nitrate transport into subsurface tile drains of different spacings. Journal of Environmental Quality, 28:997-1004.

Knisel, W. G. 1980. CREAMS: A field-scale model for chemicals, runoff, and erosion from agricultural management systems. USDA Conservation Research Report 26. USDA, Washington, D. C.

Lal, R., and N. R. Fausey. 1998. Drainage and tillage effects on leaf tissue nutrient contents of corn and soybeans on crosby-kokomo soils in Ohio. Proceedings of the 7th Annual Drainage Symposium, ASAE, Orlando, FL.

Lal, R., and G. S. Taylor. 1970. Drainage and nutrient effects on a field lysimeter study. II. Mineral uptake by corn. Soil Science Society of America Proceedings, 34:245-248.

Leonard, R. A., W. G. Knisel, and D. A. Still. 1987. GLEAMS: Groundwater loading effects of agricultural management systems. Transactions of ASAE, 30(5):1403-1418.

Logan, T. J., D. J. Eckert, and D. G, Beak. 1994. Tillage, crop, and climatic effects on runoff and tile drainage losses of nitrate and four pesticides. Soil & Research, 30:75-103.

Moriasi, D.N., C.G. Rossi, J.G. Arnold, and M.D. Tomer. 2012. Evaluating hydrology of SWAT with new tile drain equations. Journal of the Soil and Water Conservation Society. Accepted on April 6, 2012.

Moriasi, D.N., J.G. Arnold, M.W. Van Liew, R.L. Bingner, R.D. Harmel, and T.L. Veith. 2007. Model evaluation guidelines for systematic quantification of accuracy in watershed simulations. Trans. ASABE 50:885-900.

Nangia, V., P. H. Gowda, D. J. Mulla, and G. R. Sands. 2009. Modeling impacts of tile drain spacing and depth on nitrate-nitrogen losses. Vadose Zone J. 9:61–72.

Nash, J. E., and J. V. Sutcliffe. 1970. River flow forecasting through conceptual models: Part 1. A discussion of principles. J. Hydrology 10(3): 282-290.

Neitsch, S. L., J. G. Arnold, J. R. Kiniry, and J. R. Williams. 2009. Soil and Water Assessment Tool theoretical documentation version 2009. Texas Water Resources Institute Technical Report 406. Texas A&M University System. College Station, Texas:

Parsons, R. L., J. W. Pease, and D. J. Bosch. 1995. Simulating nitrogen losses from agricultural land: Implications for water quality and protection policy. Water Resources Bulletin, 31(6):1079-1087.

Randall, G. W. 1998. Implications of dry and wet cycles in nitrate loss to subsurface tile drainage. Proceedings of the 7th Annual Drainage Symposium, ASAE, Orland, FL, pp. 53-60.

Randall, G. W. and T. K. Iragavarapu. 1995. Impact of long-term tillage systems for continuous corn on nitrate leaching to tile drainage. Journal of Environmental Quality, 24:360-366.

Randall, G. W., and M. A. Schmitt. 1993. Best management practices for nitrogen use statewide in Minnesota. University of Minnesota, Minnesota Extension Service, AG-FO-6125.

Ritchie, J. T., 1972. A model for predicting evaporation for a row crop with incomplete cover. Water Resources Research, 8(5):1204-1213.
Schwab, G. O., N. R. Fausey, E. D. Desmond, and J. R. Holman. 1985. Tile and surface drainage of clay soils. Research Bulletin 1166, OARDC, The Ohio State University & ARS-USDA, pp. 1-21.

Shaffer, M. J., A. D. Halvorson, and F. J. Pierce. 1991. Nitrate leaching and economic analysis package (NLEAP): Model description and application. *In* R. F. Follet, D. R. Keeney, and R. M. Cruse (ed.) Managing nitrogen for ground-water quality and farm profitability. Soil Science Society of America, Madison, WI.

Singh, J., H. V. Knapp, and M. Demissie. 2004. Hydrologic modeling of the Iroquois River watershed using HSPF and SWAT. ISWS CR 2004-08. Champaign, Ill.: Illinois State Water Survey. Available at: www.sws.uiuc.edu/pubdoc/CR/ISWSCR2004-08.pdf. Accessed 8 September 2005.

Skaggs, R. W. 1982. Field evaluation of a water management simulation model. Transactions of ASAE, 25(3):666-674.

Tim, U. S. 1995. Coupling vadose zone models with GIS: Emerging trends and potential bottlenecks. Applications of GIS to the modeling of nonpoint source pollutants in the vadose zone, ASA-CSSA-SSSA Bouyoucos Conference, Riverside, CA.

USDA-ARS. 1992. Root zone water quality model. (RZWQM) V. 1.0, Technical documentation, GPSR technical report no. 2. USDA-ARS Great Plains Systems Research Unit, Ft. Collins, CO.

Walker, S., K. Banasik, J. K. Mitchell, W. J. Northcott, Y. Yuan, and N. Jiang. 2000. Applicability of the SCS Number Method to Tile-Drained Watersheds. Land Reclamation No 30: 3-14.

Ward, A. D., E. Desmond, N. R. Fausey, T. J. Logan, and W. G. Logan. 1993. Development studies with the ADAPT water table management model. 15th International Congress on Irrigation and Drainage. The Hague, The Netherlands.

Weed, D. A. J., and R. S. Kanwar. 1996. Nitrate and water present in and flowing from root-zone soil. Journal of Environmental Quality, 25:709-719.

Yildririm, Y. E., C. J. Skonard, J. Arumi, D. L. Martin, and D. G. Watts. 1997. Evaluation of best management practices using an integrated GIS and SWAT model for field sized areas. Paper No. 97-2162, ASAE Annual International Meeting, Minneapolis, MN.

Young, R. A., C. A. Onstad, D. D. Bosch, and W. P. Anderson. 1994. Agricultural Nonpoint Source Pollution Model, Version 4.03 AGNPS User's Guide. USDA-ARS, MN.

Zucker, L. A, and L. C. Brown (eds.). 1998. Agricultural drainage - Water quality impacts and subsurface drainage studies in the Midwest. Bulletin 871, The Ohio State University, 40 p.

EXPERIMENTAL INVESTIGATION OF RAINFALL RUNOFF PROCESS

Ankit Chakravarti
Research Scholar, Department of Civil Engineering, Indian Institute of Technology Roorkee, Roorkee – 247667
Email: ankitchakravarti@gmail.com

M.K.Jain
Assistant Professor, Department of Hydrology, Indian Institute of Technology Roorkee, Roorkee – 247667, India.
Email: jain.mkj@gmail.com

Kapil Rohilla
Research Scholar, Department of Civil Engineering, Indian Institute of Technology Roorkee, Roorkee – 247667,

Abstract

For mathematical simulation of rainfall-runoff process, controlled rainfall - runoff experiments were conducted on Advanced Hydrologic System to obtain runoff hydrograph data. The experiments were carried out over a non-cohesive sediment layer having sediment particle size of 0.5 mm to 1 mm placed over an impermeable plane surface (smooth metal sheet), with a uniform rectangular cross section of dimension one meter wide and two meter long. The generated experimental data were simulated using a one-dimensional finite difference numerical model of kinematic wave equation for overland flow to investigate the effects of variation of rainfall intensity and surface slope on overland flow roughness. Data was observed for catchment slope between 1 % to 4 % and rainfall intensity between 30 to 90 mm/hr. The comparison of observed and simulated runoff hydrograph reveals that the kinematic wave model simulates the rising, equilibrium discharge and upper part of recession limb of observed hydrograph reasonably well. However, the lower portion of the recession limb of observed hydrograph remained under predicted. The study further reveals that the resistance due to flow decrease linearly with increase in slope for a given rainfall intensity. Also for a given slope of overland flow plane, the resistance to flow decreases with increase in the rainfall intensity. It was observed that for a given rainfall intensity, an increase in the overland plane slope, reduces the time to peak.

Keywords: Rainfall, Runoff, Kinematic wave model, overland flow roughness, Simulation.

Introduction

Transformation of Rainfall into runoff is an important aspect in hydrological analysis. Many climatic and physiographic factors affect significantly the transformation of rainfall into runoff in a catchment. The rain

falling on a catchment undergoes numerous transformations under the influence of these factors before it emerges as runoff at the catchment outlet. A number of models such as physically based and conceptual models have been used to simulate the rainfall runoff process. However, due to its complexity and spatio-temporal variation, few models can accurately simulate this highly non-linear process. Rainfall simulation has become a very effective technique for modeling overland flows, soil erosion and rainfall runoff processes (Turner, 1965; Tossell et al., 1987; Bryan and poesen, 1989; Cerda at al., 1997). Rainfall simulation makes it possible to control the spatial and temporal characteristics of precipitation. It employs a watershed experimentation system as a tool for collection of experimental data to understand the behavior of the system under varying conditions. Chief advantage of using experimental setup is that it gives ability to repeat experiments for predefined set of conditions.

Rainfall simulation experiments provides control on the spatial and temporal characteristics of precipitation, at both field and laboratory scale (Willems, 2001). The data collected using rainfall simulators can be analysed to understand the processes involved in rainfall-runoff transformation. Flood wave propagation in overland flow may be described by the hydrodynamic equations continuity and momentum, popularly known as the St. Venant equations. These equations constitute a relatively accurate physical representation of the flow, (Ponce and Simons, 1978) both for overland flow and channel flow routing. Henderson (1966) noted that kinematic wave approximation of the St. Venant equations behave closely to observed natural flood waves in steep rivers (slopes > 0.002).

Smith and Woolhiser (1971) used a kinematic wave approximation to model the unsteady overland flow. The model was tested by comparisons to data from laboratory experiment and a field plot. The study found good agreement between measured and predicted hydrographs, but differences in the recession limb were noted. The influence of slope was not examined in this study. de Lima and Singh (2002) studied the importance of spatial rainfall intensity patterns of moving rainstorms on overland flow by conducting laboratory experiments on an impermeable smooth plane surface with a movable sprinkling-type rainfall simulator to simulate a moving storm. They used a simple numerical model, based on the non-linear kinematic wave, for comparing the results for hypothetical storms moving up and down on an impervious plane surface. The results indicate considerable

differences in runoff volumes and peaks and in overland flow hydrograph shapes, for storms moving upstream and downstream at differing velocities. de Lima and Singh (2003) conducted laboratory experiments on an impermeable smooth plane surface with a movable sprinkling-type rainfall simulator, simulating a moving storm. the only parameters that were varied were storm velocity and direction. The results indicate considerable differences in runoff volumes, peaks and in overland flow hydrograph shapes, for storms moving-upstream and downstream at different velocities. Bronstert and Bardossy (2003) reported a case study using data from an experimental hill slope in a loess catchment. Willems (2001) studied that the rainfall simulation provides control of the spatial and temporal characteristics of precipitation, in both field and laboratory studies.

The experimental investigations could be performed to understand surface, sub-surface or ground water runoff generation mechanism. Runoff is generated by rainstorms and its occurrence and quantity are dependent on the characteristics of the rainfall event, i.e. intensities, duration and distribution. The mechanism of surface runoff generation due to different rainfall intensity and overland slopes is however the focus of the present investigation.

Description of the Experimental Set-up

All experimental testing for the investigation of overland flow simulation described herein were conducted in the watershed laboratory in the Department of Hydrology, IIT Roorkee.

2.1 The rainfall simulator

The rainfall simulator used in present study is designed to simulate the rainfall event over the small rectangular catchment. The basic components of the simulator are tilting flume for slope adjustment, continuous spray nozzles, pumping system, and flow regulators for generating variable rainfall over the catchment. The pumping system gives a stable pressure to avoid variations in rainfall intensity during the simulated rainfall events. Pressure gauges monitored the pressure at the pump and nozzle. Although the rainfall simulator permits the use of several rows of spray nozzles, the experiments described in this study used eight nozzles, at a fixed height. Fig. 1 gives a photographic view of the laboratory set-up for the present study.

2.2 The flume

The impermeable plane surface (smooth stainless steel metal sheet) had a uniform rectangular cross-section 1 m wide and 2 m long, with slope adjustment mechanism which allow slope variation up to 5% slope. The flume is filled with sediment having particle size ranges between 0.5 to 1.0 mm.

2.3 The runoff recording system

The purpose of runoff recording system is to measure rate of runoff coming out of the experimental catchment with time. The runoff recording system uses a high sensitivity pressure transducer (depth sensor) connected to a data logger which records the water level in the collector tank from which runoff water is passing through a properly calibrated rectangular notch and the controlling system software converts water depth in to water discharge rate instantly.

2.4 Rainfall intensity pattern

A recent study has emphasized the importance of spatial rainfall intensity patterns of moving storm s on the shape of the runoff hydrographs, times to peak and peak discharges (e.g. de Lima and Singh, 2002). However, in this study, the simulated rainfall pattern is used having three different pattern of rainfall intensity i.e. 30 mm/hr. to 90 mm/hr.

Fig.1 S-12 MKII-50 Advanced Hydrologic Systems (rainfall simulator).

3.0 KINEMATIC WAVE FORMULATION

The Kinematic wave (KW) theory was developed by Lighthill and Whitham (1955), ever since then kinematic wave theory has been widely used for modeling overland and stream flow. Kinematic wave formulation uses physiographic parameters such Overland roughness, slope, drainage area, length, and soil characteristics for computation of overland flow. The KW approximation of Saint-Venant's equation can be written as

$$\frac{\partial A}{\partial t} + \frac{\partial (vA)}{\partial x} = q_l \qquad (1)$$

$$Q = \alpha A^{m} \qquad (2)$$

Where v is the flow velocity (L T^{-1}); A is the water flow area (L^2), Q is flow rate (L^3 T^{-1}), q_l is lateral inflow rate (L^2 T^{-1}), t is time (T), x is the distance measured positive in the direction of flow (L), and α and m are parameters of the kinematic wave model which are closely related to the characteristics of the flow **(**Singh 1996). Equation (1) and (2) are the governing partial differential equation of the kinematic wave model which may be written in the combined form as follows:

$$\frac{\partial A}{\partial t} + \alpha m A^{m-1} \frac{\partial A}{\partial x} = q_l \qquad (3)$$

Assuming an overland strip of unit width, the water area A can be replaced with the overland flow depth h , and lateral flow by rainfall excess intensity (i.e. $q_l = r - f$). Where f is infiltration rate, however in the present case, the experiments were conducted in non-infiltrating conditions, hence f is taken as zero. Thus, the resulting kinematic wave equation for overland flows is as follows:

$$\frac{\partial h}{\partial t} + \alpha_o m_o h^{m_o - 1} \frac{\partial h}{\partial x} = r \qquad (4)$$

$$q_o = \alpha_o h^{m_o} \qquad (5)$$

Where r = rainfall intensity (L T^{-1}), and $\alpha_o = s_o^{1/2} / n_o$ and $m_o = 5/3$.

Equations (4) and (5) can be solved using analytic method for simple configurations (Chow et. al., 1988), however, in present study, the governing differential equation were solved numerically using a explicit numerical method. From equation (1) and (2) using explicit finite difference method,

$$\frac{h_{i+1}^{t+1} - h_{i+1}^{t}}{\Delta t} + \frac{q_{i+1}^{t+1} - q_{i}^{t+1}}{\Delta x} = (r)_{i+1}^{t+1} \tag{6}$$

$$q_{i+1}^{t+1} = \alpha \left(h_{i+1}^{t+1}\right)^{m} \tag{7}$$

$$q_{i}^{t+1} = \alpha \left(h_{i}^{t+1}\right)^{m} \tag{8}$$

After simplifying the these equation,

$$f\left(h_{i+1}^{t+1}\right) = \frac{\Delta t}{\Delta x}\alpha\left(h_{i+1}^{t+1}\right)^{m} - \left(\frac{\Delta t}{\Delta x}\alpha\left(h_{i}^{t+1}\right)^{m} + h_{i+1}^{t} + \Delta t(r)_{i+1}^{t+1}\right) + h_{i+1}^{t+1} \tag{9}$$

By solving the above equation using Newton-Raphson iterative method,

$$\left(h_{i+1}^{t+1}\right)_{k+1} = \left(h_{i+1}^{t+1}\right)_{k} - \frac{f\left(h_{i+1}^{t+1}\right)_{k}}{f^{/}\left(h_{i+1}^{t+1}\right)_{k}} \tag{10}$$

Where

$$f^{/}\left(h_{i+1}^{t+1}\right) = 1 + \frac{\Delta t}{\Delta x}\alpha\, m\left(h_{i+1}^{t+1}\right)^{m-1} \tag{11}$$

The most commonly used initial condition for overland flow is a dry surface. For overland flow, the initial and boundary conditions are prescribed keeping in mind the fact that the overland flow in small watersheds has negligible base flow. Considering these conditions the initial and boundary conditions have been defined as follow:

$h_o^i = 0$ for every x at $t = 0$ (12a)

$q_{oi}^o = 0$ for every x at $t = 0$ (12b)

$h_o^o = 0$ for every t at $x = 0$ (12c)

$q_{o0}^j = 0$ for every t at $x = 0$ (12d)

3.1 Nash sutcliffe criterion

The closeness of reproduction of the observed data with those computed using kinematic wave model solution were evaluated using the well known Nash-Sutcliffe efficiency criterion (Nash-Sutcliffe, 1970). It is experssed as;

Nash-Sutcliffe Efficiency in (%),

$$NES = \left(1 - \frac{\sum_{i-1}^{n}(Y_o - Y_c)^2}{\sum_{i-1}^{n}(Y_o - Y_m)^2}\right) \times 100 \quad (13)$$

Where, Y_o = Observed flow (Experimental rainfall flow) value at time t.

Y_c = Computed flow (kinemaic flow) value at time t.

Y_m = Mean of observed values.

3.2 Error in Runoff Volume Computation

The error in runoff volume was estimated as,

$$\text{Volumetric error, in \%} = \left(1 - \frac{Y_c}{Y_o}\right) \times 100 \quad (14)$$

Where, Y_c = volume computed

Y_o = volume observed

4.0 ANALYSIS AND DISCUSSION OF RESULTS

Experimental data obtained from Advanced Hydrologic System (rainfall simulator) were analysied using one dimentional kinematic wave overland flow simulation model. The code for one dimentional kinematic wave model for overland flow was developed in Fortran programming language. The simulation was done using time step Δt of 5 sec and spatial grid size Δx is taken as 1 cm. Experimental data were simulated using developed model in order to study the change in overland flow roughness due to variation of slope and rainfall intensity on the catchment. Data was observed for catchment slope between 1 % to 4 % and intensity of rainfall varied between 30 to 90 mm/hr.

Developed kinematic wave model was calibrated using Manning's roughness coefficient "n" as fitting parameter such that the sum of the squared error between observed and simulated runoff is minimum. Plots between observed and model computated hydrograph for 30 mm/hr internsity of rainfall are shown in Fig. 2 and 3 for slope of 2% and 4%. The statiscal comparison between the volume of observed and simulated hydrograph, its volumetric error, time to peak and Nash-Sutcliffe efficiency at different values of surface slope and calibrated manning's roughness coefficient is shown in Table 1. Further, the plots between observed and

computed runoff hydrographs for rainfall intensity of 60 mm/hr and slope of the overland plane from 3% and 4% are shown in Figs. 4 and 5 respectively. The comparison between the observed and computed runoff volume, time to peak, volumetric error, calibrated manning's roughness coefficient and Nash-Sutcliffe efficiency is given in Table 2. For rainfall intensity of 90 mm/hr and slope of the overland plane from 1% and 2%, the observed and simulated overland flow hydrographs by the kinematic wave model are shown in Figs. 6 and 7 respectively. The comparison between the observed and computed runoff volume, time to peak, volumetric error, calibrated manning's roughness coefficient and Nash-Sutcliffe efficiency are shown in Table 3. As can be seen from these plots the kinematic wave model could reproduce resonably well rising limb of the observed hydrograph as well as steady state discharge. In case of falling limb of the hydrograph, two segments are clearly visible. On where only surface runoff domainates which is reproduceed well by kinematic wave model and second the release of water from sand bed, which the kinematic wave model has not simulated because the mechanism of release of water from sand bed was not incorporated in the kinematic wave model.

It is observed from Tables 1 to 3 that for a given rainfall intensity, an increases in the overland plane slope, reduces the time to peak. This may be due to raipd draining of the water due to increased surface slope. For a given rainfall intensity, the observed data were simulated very well at higher values of surface slope as compaired to lower value of surface slope. This indicate that for a given rainfall intensity the kinematic wave model give a better fit for a steeper value of surface slope. Simillarly, for a given surface slope, the observed data showed good agreement for higher values of rainfall intensity.

Visual comparison depicted between observed and model simulated hydrographs presented in Figs. 1 to 7 reveals that the nummerical model simulates the rising limb of the observed hydrograph very well, but the the falling limb of the hydrograph was underestimated. This may be due to fact that, when water moves on the surface in response to slope, it is postulated that two phenomena will act in conjuction to effectively alter the hydrodynamics of the soil water. Firstly, water moving on the soil surface will exert a small pull on pore water by applying an upward suction force that is proportional to $V^2/2g$, where V is the average surface water velocity which is several orders of magnitude larger than the pore water velocity. Due to this suction force water from the pores are drained out and thus contirbute to the surface runoff which is not estimated by the one-dimentional kinematic wave model. Secondly, while applying the water on the catchment, after stoping the rainfall intensity, some amount of water is still stored in the overhead pipe. This volume of water is then released subsequently from the nozzle due to the gravity. This amount of water, is not included in the numerical model.

The values of Manning's 'n' obtained through calibration for different overland plane slope were plotted against slope of the plain for different intensity of rainfall and are given in Fig. 8, 9 and 10 for rainfall intensity 30 mm/hr, 60 mm/hr and 90 mm/hr respectively. It can be seen that the value of manning's 'n' decreases linearly with increase in overland plane slope. The effect of rainfall intensity on calibrated value of manning's

roughness coefficient ‘n’ was also studied for different overland flow plane slopes. From Fig. 11 to 14 depicits the plots of rainfall intensity with manning’s roughness coefficient ‘n’ for overland slope 1% to 4%. It is evident from these plots that the value of manning’s ‘n’ decreases with increase in rainfall intensity for all slopes studied herein. It is therefore revealed that rainfall intensity as well as the slope of the overland flow plane affects the resistance to flow.

Table 1 Pertinent characteristics of observed and computed hydrograph for 30 mm/hr intensity of rainfall and Area = $2m^2$.

S.No	Slope (%)	Volume			Time to Peak			NSE (%)
		Observed (lit)	Computed (lit)	Error (%)	Observed (min)	Computed (min)	Error (%)	
1	1	9.3	7.9	4.3	2.7	2.4	11.1	98
2	2	6.3	5.9	6.3	2.3	2.1	8.6	97.2
3	3	8.3	7.9	4.8	2.1	2	4.7	91
4	4	7.6	7.3	3.9	2	1.8	5	93.2

Table 2 Pertinent characteristics of observed and computed hydrograph for 60 mm/hr intensity of rainfall and Area = $2m^2$.

S.No	Slope (%)	Volume			Time to Peak			NSE (%)
		Observed (lit)	Computed (lit)	Error (%)	Observed (min)	Computed (min)	Error (%)	
1	1	12.5	12.2	2.4	3.9	3.5	10.2	97.8
2	2	10.4	10.1	2.8	3.2	2.9	9.3	96.6
3	3	16.2	15.8	2.4	2.8	2.6	7.1	97
4	4	12.5	12.1	3.2	2.5	2.4	4	92.6

Table 3 Pertinent characteristics of observed and computed hydrograph for 90 mm/hr intensity of rainfall and Area = $2m^2$.

S.No	Slope (%)	Volume			Time to Peak			NSE (%)
		Observed (lit)	Computed (lit)	Error (%)	Observed (min)	Computed (min)	Error (%)	
1	1	16.1	15.7	2.4	3.6	3.3	8.3	96
2	2	18.3	17.9	2.1	3.1	2.9	6.4	97
3	3	15.4	14.9	3.2	3.2	3	6.2	96.1
4	4	15.1	14.7	2.6	2.6	2.5	3.8	96.7

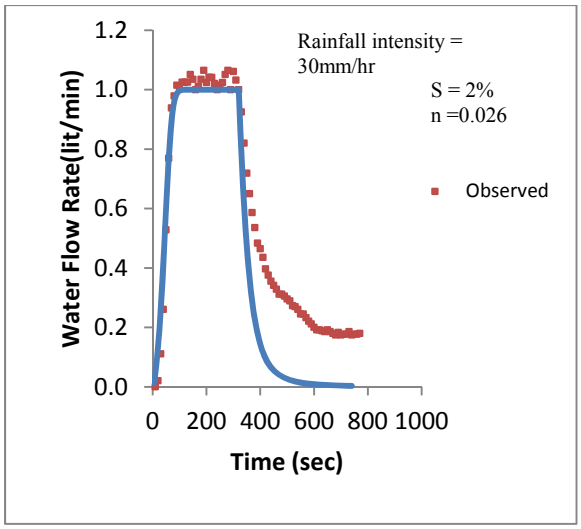

Fig 2 Comparison of observed and computed hydrograph for rain fall intensity 30 mm/hr at 2 % slope of the plane.

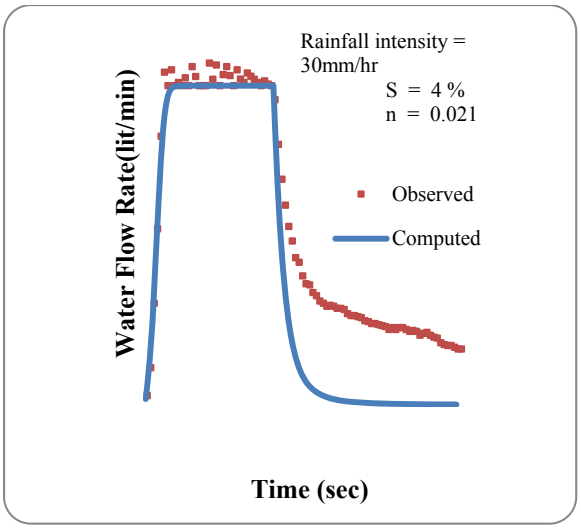

Fig 3 Comparison of observed and computed hydrograph for rainfall intensity 30mm/hr at 4% slope of the plane.

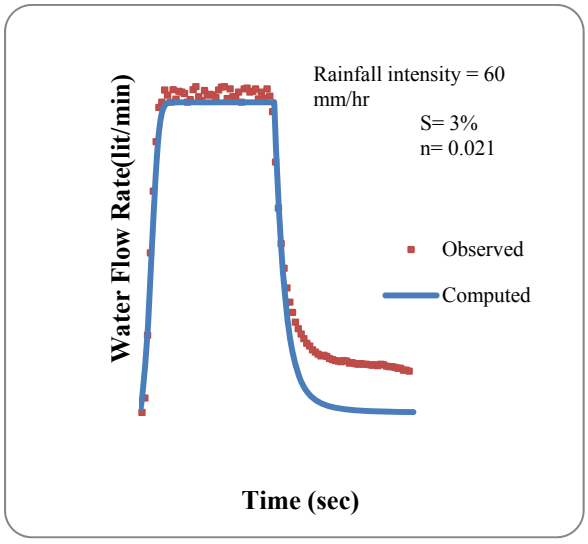

Fig 4 Comparison of observed and computed hydrograph for rainfall intensity 60mm/hr at 3% slope of the plane.

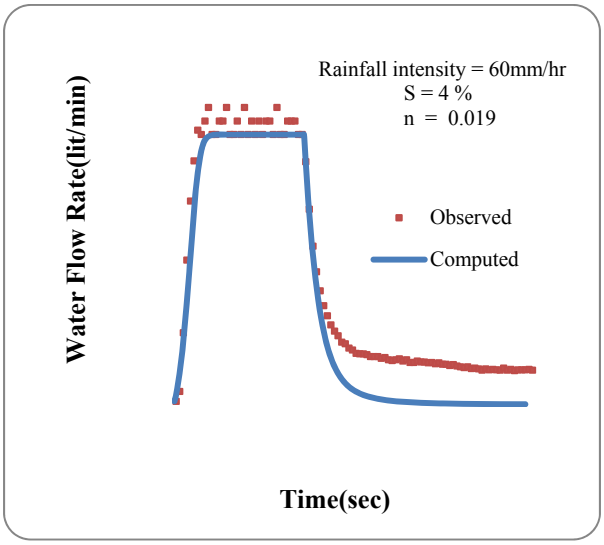

Fig 5 Comparison of observed and computed hydrograph for rain fall intensity 60 mm/hr at 4% slope of the plane.

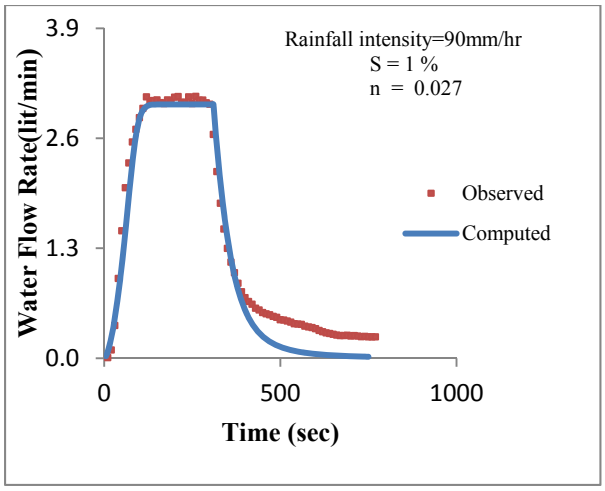

Fig 6 Comparison of observed and computed hydrograph for rainfall intensity 90mm/hr at 1% slope of the plane

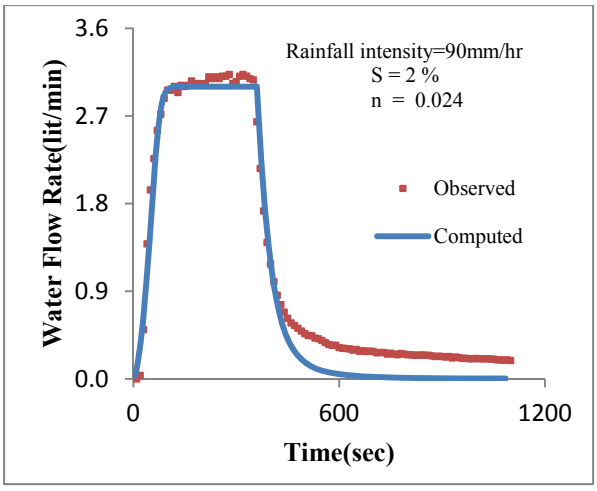

Fig 7 Comparison of observed and computed hydrograph for rainfall intensity 90mm/hr at 2% slope of the plane.

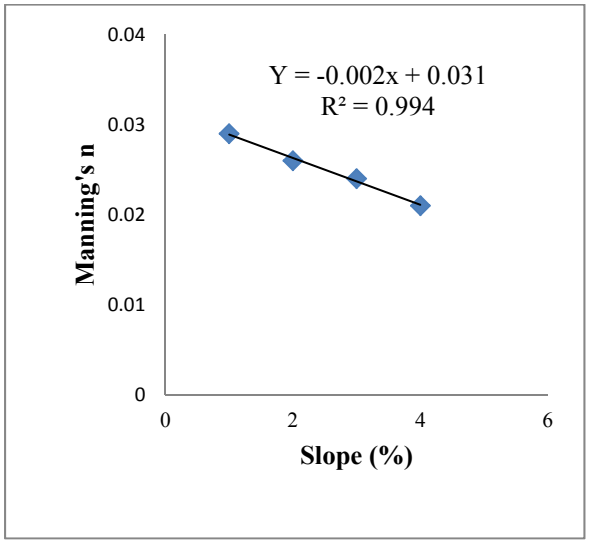

Fig 8 Variation of Manning's roughness with overland flow plane slope for rainfall intensity 30 mm/hr.

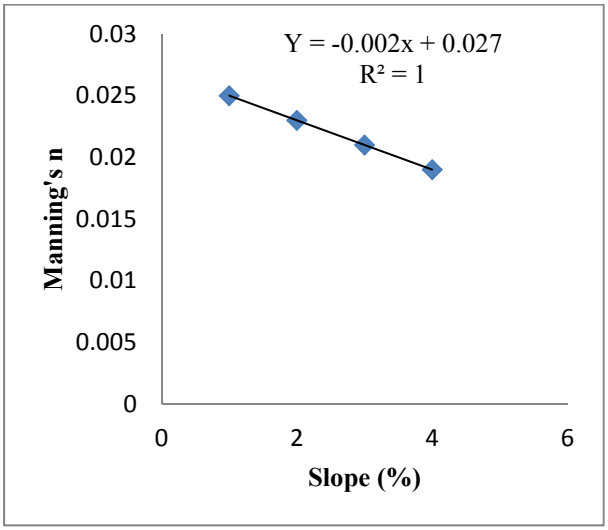

Fig 9 Variation of Manning's roughness with overland flow plane slope for rainfall intensity 60 mm/hr.

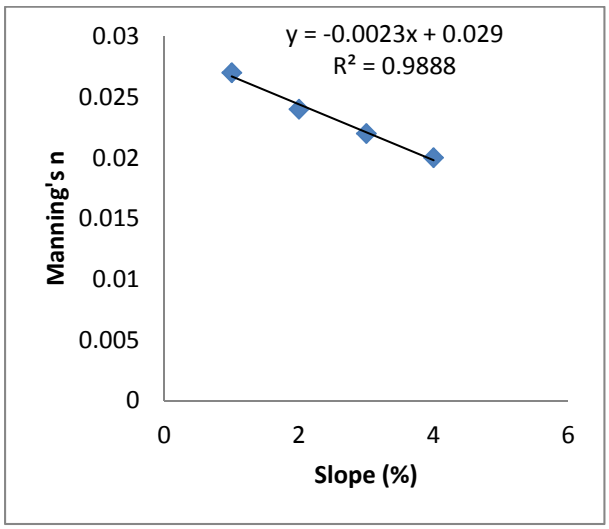

Fig 10 Variation of Manning's roughness with overland flow plane slope for rainfall intensity 90 mm/hr.

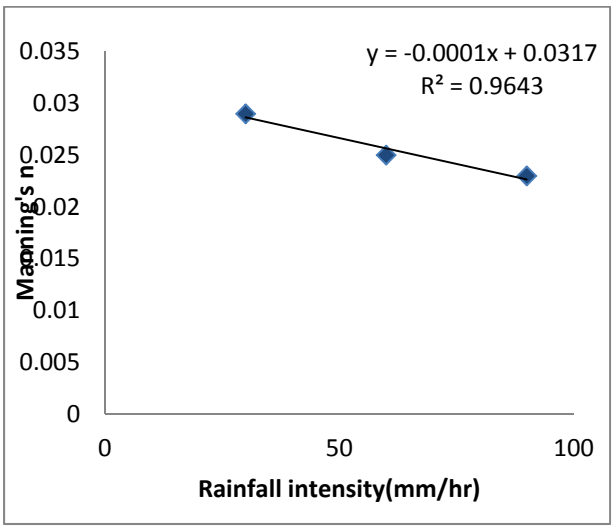

Fig 11 Variation of Manning's roughness with rainfall intensity for 1% slope of the plane.

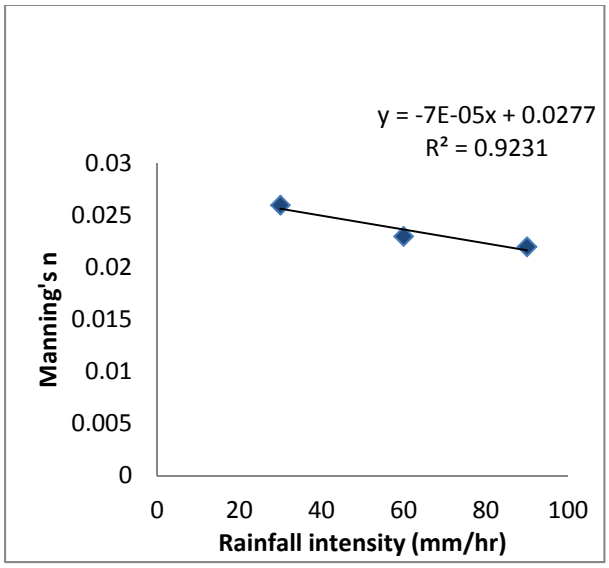

Fig 12 Variation of Manning's roughness with rainfall intensity for 2% slope of the plane.

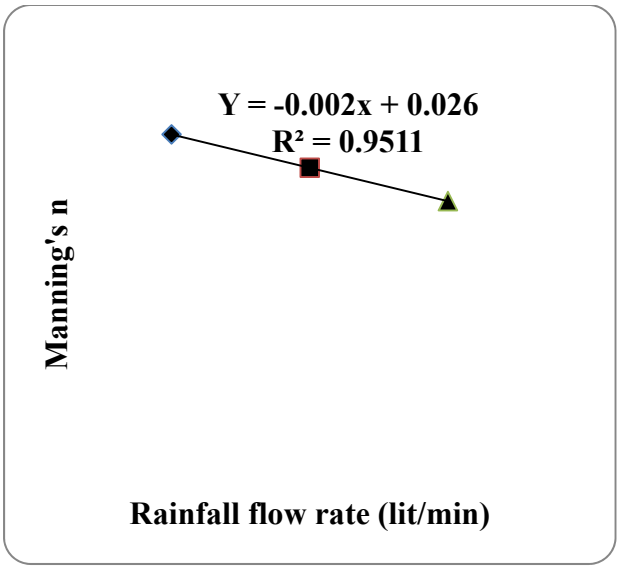

Fig 13 Variation of Manning's roughness with rainfall intensity for 3% slope of the plane.

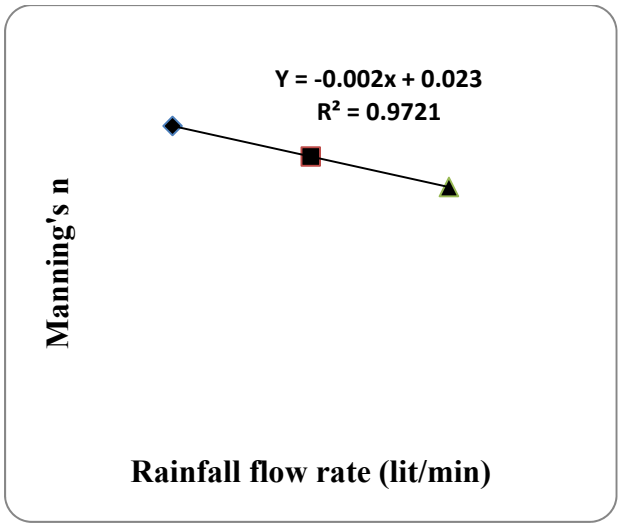

Fig 14 Variation of Manning's roughness with rainfall intensity for 4 % slope of the plane.

5.0 Conclusion

A one-dimensional kinematic wave model for overland flow routing was developed to study the effect of slope and rainfall intensity on overland flow roughness. The study reveals that the kinematic wave model reproducell reasionably well rising and study state and upper part of recession limb of hydrographs for all slopes and rainfall intensity but conderable differences where observed in the lower part of recession limb between observed and simulated runoff hydrograph patterns. The possible reason for such difference could be explained by the fact that in the present investigation, a sand bed was used as overland flow plain, which release water even after rainfall is stopped. The resistance due to flow decreases lineraly due to increase in overland plain slope for a given rainfall intensity and for a given slope the resistance due to flow decreases lineraly with increases in rainfall intensity.

Acknowledgements

The laboratory experiments described herein were conducted in the Watershed Laboratory of the Department of Hydrology, Indian Institute of Technology, Roorkee-247667 (India). Authors thank the Prof.& Head of the department for permission to conduct experiments in the laboratory of the Department.

List of notations

$A =$ *Area* (m^2)

$D =$ *Hydraulic depth (m)*

$g =$ *Acceleration due to gravity* (m/s^2)

$h =$ *Depth of overland flow (m)*

$i =$ *Integeer for space increment (mm)*

$j =$ *Integer for time increment (s)*

$k =$ *Kinematic wave number*

$L =$ *Maximum length of flow(m)*

$m =$ *Kinematic wave parameter*

NES = Nash-Sutcliffe Efficency (%)

n = *Manning's roughness coefficient*

Q = *Discharge in* (m^3/s)

q_l = *Lateral inflow rate (m/s)*

q_0 = *Overland flow*(m^3/s)

r = *Rainfall intensity (mm/hr)*

S = *Slope of the catchment (%)*

t = *time increment (s)*

Y_c = *Volume computed (%)*

Y_o = *Volume observed (%)*

Y_m = *Mean of observed value (%)*

Δt = *time step (s)*

Δx = *Space step (cm)*

α = *Kinematic wave parameter*

α_o = *Kinematic wave parameter for overland flow*

References

Bryan, R.B., and J. Poesen. 1989. Laboratory experiments on the influence of slope length of runoff, percolation and rill development. *Earth Surface processes and Landforms*, (14): 211-231.

Bronstert A., Bardossy A. 2003. Uncertainty of runoff modelling at the hillslope scale due to temporal variations of rainfall intensity. *Physics and Chemistry of the Earth*, (28): 283–288.

Chow, V. T., Maidment, D. R., and Mays, L. W. 1988. *Applied Hydrology*, New York Book Co., Singapore, McGraw-Hill.

Cerda, A.S. Ibanez and A. Calvo. 1997. Design and operation of a small and portable rainfall simulator for rugged terrain. *Soil Technology*, (11): 163-170.

de Lima, J.L.M.P., Singh, V.P. 2002. The influence of the pattern of moving rainstorms on overland flow. *Advances on Water Resources* 25 (7): 817–828.

de Lima, J.L.M.P., Singh, V.P. 2003. Laboratory experiments on the influence of storm movement on overland flow. *Physics and Chemistry of the Earth* 28 (2003): 277-282.

F.M. Henderson.1966. *Open Channel Flow*. New York, The MacMillan Company.

M.J. Lighthill, G.B. Whitham. 1955. On Kinematic Waves I. Flood movement in long rivers. *Proc. Royal Soc. Lond.,* Series A 229 (1178): 281–316.

Nash, J.E., and Sutcliffe, J.V. 1970. River flow forecasting through conceptual model. Part 1-A discussion of principles. *Journal of Hydrology*. (10): 282-290.

Smith, R.E., Woolhiser, D.A. 1971. Overland flow on infiltrating surface. *Water Resources Research* 7(4): 899-913.

Tossell, R.W., W.T. Dickinson, R.P. Rudra and G.J. Wall. 1987. A portable rainfall simulation. *Can.Agric.Eng.,* Vol. (29): 155-162.

Turner, A.K. 1965. The simulation of rainfalls studies in overland flow. *Journal Inst.Eng.Austr.,* Vol. (39): 9-15.

V.M. Ponce, D.B. Simons 1978. Applicability of kinematic and diffusion models. *Journal Hydr. Div., ASCE* Vol. 104 (3): 353–360.

Willems, P. 2001. A spatial rainfall generator for small spatial scales. *Journal of Hydrology* vol.252: 126–144.

Application of GIS-based SWAT tool water management of irrigation project under rotational water supply

S.D. Gorantiwar
Head, Dept. of Irrigation and Drainage Engineering
Dr. A. S. College of Agril Engg., Mahatma Phule Krishi Vidyapeeth, Rahuri,
Dist. Ahmednagar, Maharashtra State, INDIA
sdgorantiwar@rediffmail.com

R.T. Thokal
Ph D student and Chief Scientist, AICRP on Water Management,
Dr. B.S. Konkan Krishi Vidyapeeth, Dapoli, Dist.Ratnagiri, Maharashtra State, INDIA
rtt1966@yahoo.com

Mahesh Kothari
Assistant Professor, Department of Soil & Water Engg.
College of Technology & Engineering
Maharana Pratap University of Agri. & Tech., Udaipur, Rajasthan State, INDIA

S.R. Bhakar
Head, Department of Soil & Water Engg.
College of Technology & Engineering
Maharana Pratap University of Agri. & Tech., Udaipur, Rajasthan State, INDIA

R.C. Purohit
Head, Department of Soil & Water Engg.
College of Technology & Engineering
Maharana Pratap University of Agri. & Tech., Udaipur, Rajasthan State, INDIA

Abstract

Forecasts of water withdrawals on a global scale predict sharp increases in future demand to meet the needs of the urban, industrial and environmental sectors. India's efforts to increase food grain production have been achieved through promoting large-scale crop intensification by extending the area under irrigation. The expansion of irrigation has resulted in several undesirable consequences like low output from the stored water in the reservoirs and improper water distribution throughout the irrigation command. The objective of the present paper is to select the best compromise irrigation operation rule on the regional scale. This paper presents the developed framework tool using SWAT, GIS and irrigation model with a case study on Sina Medium Irrigation Project of Maharashtra State, India. A tool developed using hydrological model (SWAT) combined with GIS was used to simulate water movement and availability over a wide range crops, and soil conditions. The tool determines crop yield and profitability of irrigation project for the different combinations of operation rules on the regional scale. Once, developed, a decision support system or expert system can be applied to identify those regions of greatest need for irrigation, based on predicted increases in crop yield and profitability.

Keywords: SWAT, deficit irrigation, operation rules, GIS, irriation model, water allocation, irrigation command, rotational irrigation system

Introduction

Irrigated agriculture is the primary user of diverted water globally, reaching a proportion that exceeds 70-80% of the total in the arid and semi-arid zones. It is therefore not surprising that irrigated agriculture is perceived in those areas as the primary source of water, especially in emergency situations. Currently, irrigated agriculture is caught between two perceptions that are contradictory; some perceive that agriculture is highly insufficient by growing 'water-guzzling crops' (Postel *et al*., 1996), while others emphasize that irrigation is essential for production of sufficient food in the future, given the anticipated increases in food demand due to world population growth and changes in diets (Dyson, 1999). Globally, food production from irrigation represents more than 40% of the total and uses only about 17% of the land area devoted to food production (Fereres and Connor, 2004). Nevertheless, irrigated agriculture is still practiced in many areas in the world with complete disregard to basic principle of resource conservation and sustainability. Therefore, irrigation water management in an era of water scarcity will have to be carried out most efficiently, aiming at saving water and at maximizing its productivity. Given the high costs of irrigation development, until now the paradigmatic irrigation strategy has been to supply irrigated areas with sufficient water so that the crops transpire at their maximum potential and the full evapotranspiration (ET) requirements are met throughout the season. This approach is increasingly challenged by segments of society in regions where water is scarce, because of both the large amounts of water required by irrigation and the negative effects that such diversions and use have on nature. Thus, a strategic change in irrigation management is taking place, one that limits the supply available for irrigation to what is left after all other sectors of higher priority satisfy their needs. Under such situations, farmers often receive water allocations below maximum ET needs, and either have to concentrate the supply over a smaller land area or have to irrigate the total area with levels below full ET. Thus, the water demand for irrigation can be reduced and the water saved can be diverted for alternate uses. If water saving strategy is not applied, the insufficient water supply for irrigation will be the norm rather than the exception, and irrigation management will shift from emphasizing production per unit area towards maximizing the production per unit water consumed, the water productivity. To cope

with the scarce supplies, deficit irrigation, defined as the application of water below full crop-water requirements, is an important tool to achieve the goal of reducing irrigation water use. Fereres and Soriano (2006) reviewed deficit irrigation and concluded that the level of irrigation supply should be 60-100% of full evapotranspiration needs in most cases to improve water productivity. Under conditions of scarce water supply and drought, deficit irrigation can lead to greater economic gains than maximizing yields per unit of water for a given crop. Gorantiwar and Smout (2003) revealed that practicing deficit irrigation enables the irrigation area and total crop production in the irrigation scheme used for the case study to be increased by 30-45% and 20-40%, respectively, over the existing rule and by 50 and 45%, respectively, over the adequate irrigation. The objective of the present paper is to evaluate the crop yield for deficit irrigation, and to select the most suitable and sustainable irrigation planning strategy under rotational irrigation system in the irrigation command.

Development and application of simulation models could be one of the solutions for improving water use efficiency in irrigation commands. Several irrigation scheduling models have been produced that aim at aiding farm managers and irrigation engineers to determine and design for their irrigation needs, for a given crop-field combination. A few commonly used irrigation models include: CROPWAT (Smith, 1992), ISAREG (Pereira *et al*., 2003), SCHED (Harrington and Heermann, 1981) and WATSCHED (Horward and Benn, 1986). However, none of these models are designed to look at the highly variant conditions found over a given command area, and simultaneously identify the potential net benefit of irrigation for each area, thereby prescribing priority use for limited water resources.

A tool developed using hydrological model Soil and Water Assessment Tool (SWAT) (Arnold *et al*., 1998; Neistsch *et al*., 2002) combined with GIS was used to simulate water movement and availability over a wide range crops, and soil conditions. This information was then supplied to irrigation model to determine whether irrigation is scheduled on prescribed day, and integrate this information into a complete hydrological model. The tool can determine crop yield and profitability of irrigation project for the different combinations of operation rules on the regional scale. Once, developed, a decision support system or expert system can be applied to identify those regions of greatest need for irrigation, based on predicted increases in crop yield and profitability.

Material and Methods

Development of tool framework

Proposed GIS-based tool framework for irrigation scheduling with deficit irrigation under rotational distribution system is presented in Fig. 1. This tool framework mainly comprises three modules: allocation rules, SWAT modules and economic module. The water allocation formulated initially depending upon water availability in the reservoir at the beginning of season, is the additional input to SWAT. The canal network, their commanded areas, deficit ratio, canal releases are also additional inputs to SWAT. The SWAT runs over growth periods of crops under study and estimates output parameters such as Potential Evapotranspiration (ETo), Actual Evapotranspiration (ETa), etc. The yields of various crops under different pre-specified allocation rules were than estimated by using water production function model given by Stewart *et al*. (1976).

$$\frac{Y_a}{Y_m} = 1 - \sum_{s=1}^{ns} K_{y_s} \left(\frac{ET_{o_s} - ET_{a_s}}{ET_{o_s}} \right) \quad \ldots 1$$

This module utilizes ETo and ETa values obtained from SWAT and estimates the reduction in crop yield compared to potential yield due to pre-specified allocation rule. The tool eventually estimates the total crop production, yield reduction due to specific water allocation, benefits from the crops under study, grown on all soils, in all allocation units in the irrigation command. The tool framework is able to estimate daily updates of the reservoir storage on the basis of inflow to reservoir, outflow (water release) and losses from reservoir. The model runs daily for maximum 365 days, for crop season and each soil type. After 365 days cycle of run, it terminates and estimates the carry over storage in the reservoir. It also terminates if the reservoir storage is less than the dead storage or predefined stage. The model is able to give spatial output such as Allocation Unit (AU) wise area, irrigation amount, actual crop yield, crop economics, net benefit, etc.

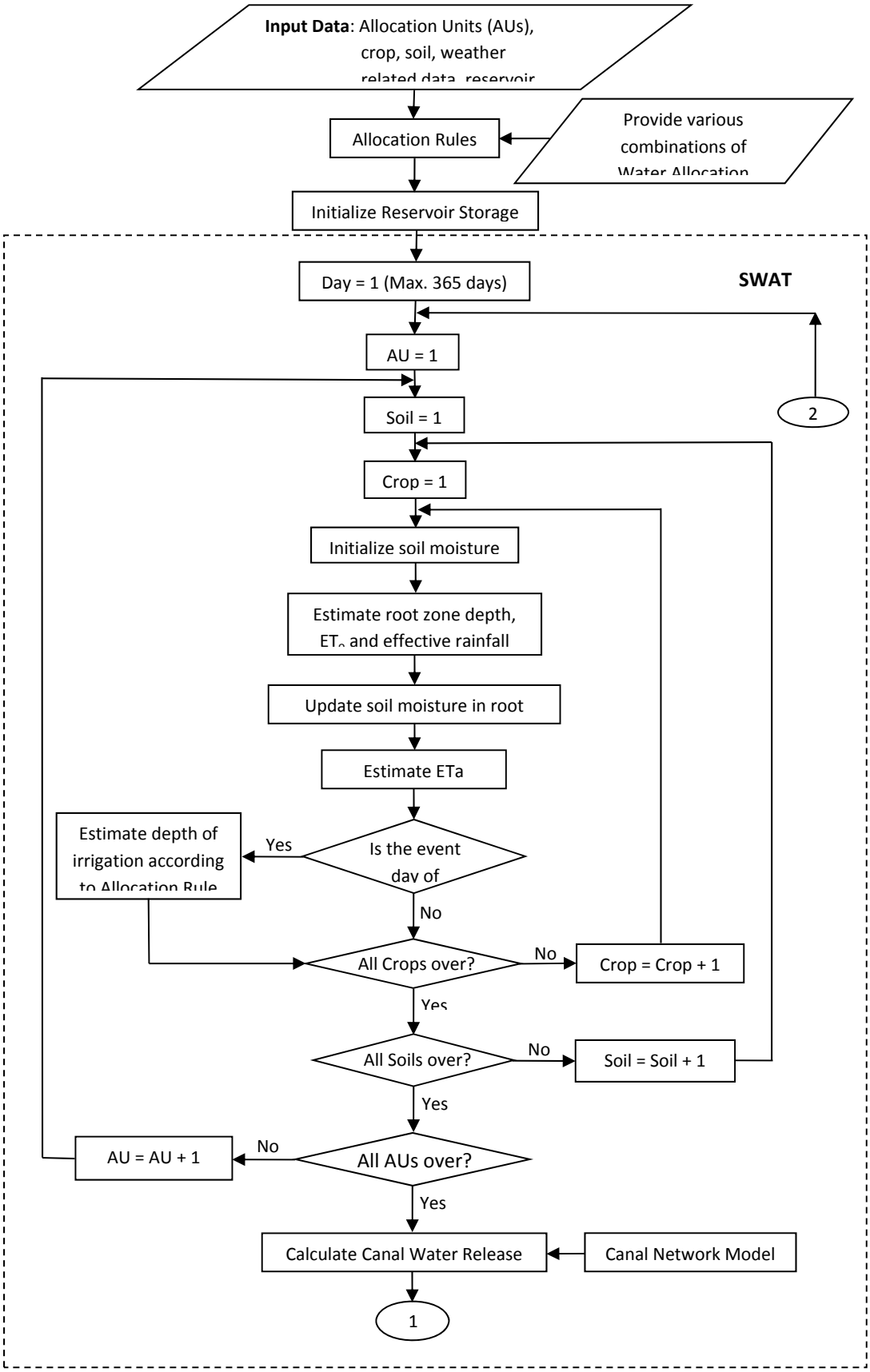
Input Data: Allocation Units (AUs), crop, soil, weather related data, reservoir
Provide various combinations of Water Allocation
Allocation Rules
Initialize Reservoir Storage
SWAT
Day = 1 (Max. 365 days)
AU = 1
Soil = 1
Crop = 1
2
Initialize soil moisture
Estimate root zone depth, ET0 and effective rainfall
Update soil moisture in root
Estimate ETa
Is the event day of
Yes
Estimate depth of irrigation according to Allocation Rule
No
All Crops over?
No
Crop = Crop + 1
Yes
All Soils over?
No
Soil = Soil + 1
Yes
All AUs over?
No
AU = AU + 1
Yes
Calculate Canal Water Release
Canal Network Model
1

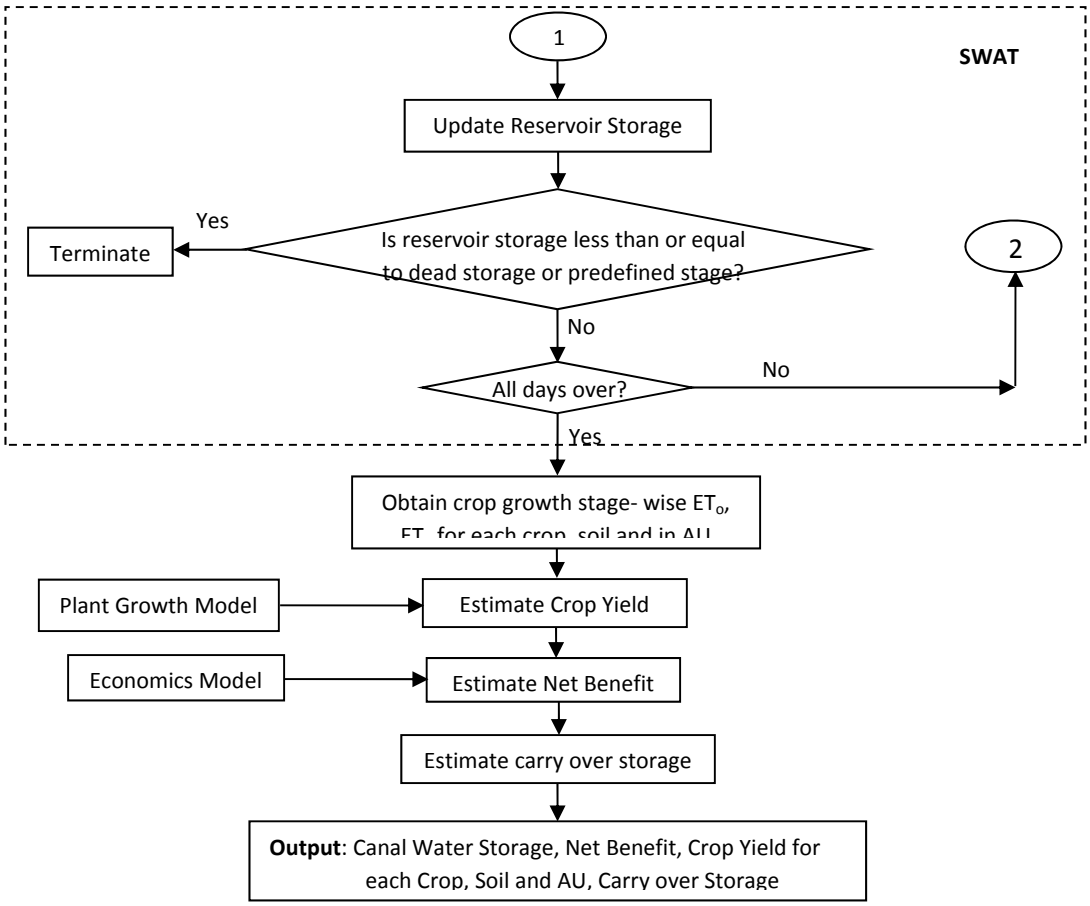

Fig. 1. Schematic flowchart of the conceptual tool framework proposed in the study

Allocation Rules

The allocation rules are mainly based on the storage in reservoir at the start of October month. The major aim of the allocation rules was to increase the storage longevity and increase the net project benefit without much compromise with the crop productivity. Depending upon the storage availability in the reservoir, crops and their distribution in the irrigation command, combinations of release rate, irrigation depth and area to be irrigated were given as allocation input to the framework. The tool framework was run for the different combinations of operation rules using the SWAT module and the results from SWAT module were used for estimating the crop yields under different scenarios.

SWAT module

The proposed framework uses a GIS-based hydrological simulation model, Soil and Water Assessment Tool (SWAT) (Arnold *et al*., 1998; Neitsch *et al*., 2002,

www.brc.tamus.edu/swat), developed by the USDA Agricultural Research Service (USDA-ARS). SWAT is a physically based simulation model operating on a daily time step. It was developed to simulate land management processes and rainfall-runoff processes with a high level of spatial detail by allowing watershed to be divided into sub-basins. Each sub-basin is divided into several land use and soil combinations, called hydrologic response units (HRUs). The sub-basin simulation processes of SWAT include major components such as hydrology, weather, erosion, soil temperature, crop growth, and agricultural management.

As the study is related to irrigation management, the watershed was treated as the irrigation command, area commanded by each outlet was treated as one sub-basin and the HRUs were treated as Allocation Units (AUs).

Economic module

Once the crop yields were estimated by using the daily outputs of ETo and ETa from SWAT module, the profitability of crops for each combination of operation rule was worked out by the standard procedures. This task was completed in economic module and the net project benefit was calculated to take a decision for irrigation allocation for crops under each outlet and for the certain storage in the reservoir.

Description of Study Area

A case study for Sina Medium Irrigation Project was selected to describe the ability and applicability of the framework. The project is located on river Sina, a tributary of river Bhima in Krishna basin, at Nimgaon Gangarda village of Ahmednagar district, Maharshtra state, India (latitude 18°49'0"N and longitude 74°57'0"E) spread over the topo-sheets of 47 J/13, 47 J/14, 47 N/1 and 47 N/2. The location map is shown in Fig. 2.

Water Distribution in Study Area

The rotational water supply is being followed in the canal command area of Sina Irrigation Project with an irrigation rotation of 10 days. The rotation is based on 5 days on and 5 days off period. As a routine practice, water demand for each rotation is estimated by collecting the demand of water on the basis of cops grown by the farmers in the command area. The total amount of water release is decided after considering demands of water from each sub-division, before the start of each rotation. Tail to Head water distribution system is followed in the outlet

command i.e. the tail end farmers receive water first, then water is delivered to farmers whose lands are located towards the head of the outlet. This type of water distribution is called as *Shejpali* system and is generally adopted in all the irrigation projects of Maharashtra State. In this system, the concerned authorities display the water distribution schedules before the release of each rotation. Each farmer in the command gets prior intimation of water delivery i.e. date, time and amount of water according to his request for water demand. The water demand is mainly estimated by the thumb rule and is not based on the soil and crops type. Thus, it leads to either excess water to some crops and soils and sometimes the crops remain under stress in certain soils. This in turn leads to either more release of water, which empties the reservoir earlier or low water releases lead to non-uniformity of water distribution in the irrigation command.

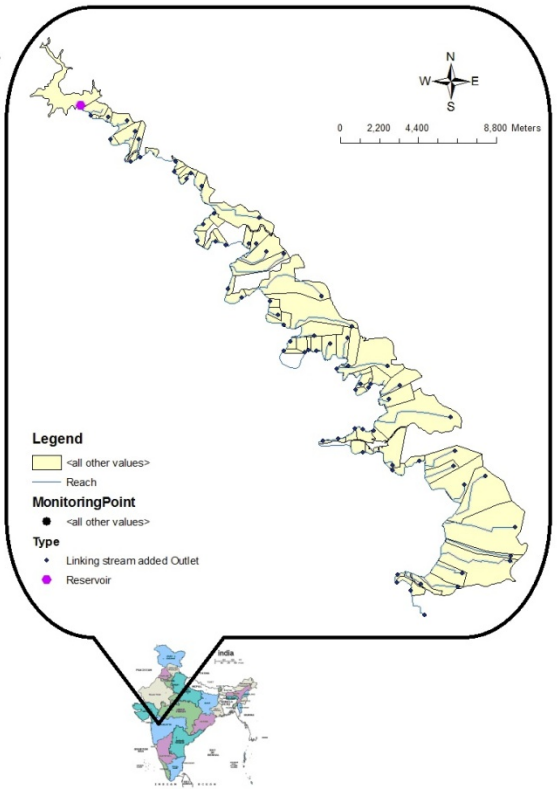

Fig. 2. Stream network and command area with location map of Sina Medium irrigation project

Input to Tool Framework

The study was conducted for a canal irrigation system using a hydrologic modeling approach with spatial distribution capability for extracting model inputs. The spatial inputs like

reservoir, irrigation canal network, area commanded by each outlet, topography, soils and existing cropping pattern in the irrigation command were used for the study.

GIS Input Files

The basin layout, soil, land use, topography and discretize maps were incorporated into ArcGIS® and then applied to the SWAT model, through the use of the SWAT ArcView interface.

Elevation data: Topo-sheets of 1:50000 ratio were available for the study area and the contour lines passing through the area of interest were of larger intervals, only few lines could be digitized to form the Digital Elevation Map (DEM), which were insufficient to get the elevation data. Thus, images downloaded from Spectral Radar Topographic Mission (SRTM) were used as DEM in this study. As the area of interest was divided in two images of SRTM, these images (SRTM_51_091 and SRTM_52_091) were downloaded and mosaiced to form one DEM input for the project.

Land Cover/Land Use File: Information on land use and land cover for the study was obtained from Regional Remote Sensing Centre (RRSC), Nagpur. The shape file of the imagery taken from LISS III with a 23x23 metre resolution and a date of pass (DOP) during the study period was used in this study. The GIS files and other input data required for this study obtained from various governmental agencies are listed in Table 1.

Table 1. Various inputs and sources of information for the required data set of Sina Irrigation Project

Subject area	*Data basis*	**Source and map scale**
Basic data	Boundaries of the command area, administrative boundaries, stream network	Survey of India (SoI); 1:50,000
Climatic data	Mean monthly and daily precipitation, maximum and minimum temperature, relative humidity, wind speed, evaporation	Meteorological observatory, Irrigation Department, Sina Irrigation Project, Mirajgaon
Soil-physical data	Soil series map, soil characteristics (silt, sand, clay, rocks), field capacity, wilting point, hydraulic conductivity, depth to water table, properties for different soil layers varying with depth,	National Bureau of Soil Survey and Land Use Planning (NBSS&LUP); 1:2,50,000 and its reports from Command Area

	organic content, EC, pH, etc.	Development Authority (CADA), Ahmednagar
Land use data	Ground cover, seasonal cropping pattern, land use data imageries	CADA, SoI, State Agriculture Department, IRRSSC, Nagpur
Topography data	Elevation contours, digital elevation map (DEM)	SRTM data (SRTM_51_091 and SRTM_52_091)
Command area	Irrigation canal network	Irrigation Research & Development Wing, Pune
Reservoir storage data	Gauge readings at dam	Sina Irrigation Project, Mirajgaon
Canal release data	Gauge readings at the head of canal network	Sina Irrigation Project, Mirajgaon

Soil Data: Soil map and data for area of interest were obtained from Command Area Development Authority (CADA), Ahmednagar and reports of NBSSLU&P, Nagpur. The shape file of command area was prepared from the map and detailed information on classification in the attribute was added from available data. The soil classification was based on National Bureau of Soil Survey and Land Use Planning (NBSS&LUP) land use.

SWAT is capable of calculating estimated stream positions with the use of an elevation grid file alone, however, the limited resolution of the file, particularly with low lying flat areas, makes the incorporation of the stream delineation of added advantage. Also the canal network may not follow all-the-way the same path as per the elevation grid. For this reason, the "user-defined watersheds and stream" option was chosen for delineation process to define accurately the areas commanded under each canal outlet.

The soil database for the irrigation command was created with the information on soil properties including texture, bulk density, water holding capacity, organic carbon content, and horizon depths.

User-defined and Canal/Stream Network File: Shape file of canal/stream network was prepared by using the map procured from Irrigation Research & Development Wing (IRDW), Pune.

Climate Record File: The weather data of 19 years record procured from meteorological observatory, was used to calculate statistical parameters for weather generator input file. The

meteorological observatory for study area is located at Nimgaon Gangarda village in the command area with the location of 18°49'1.24" N latitude, 74°57'31.62" E longitude and altitude of 585.945m. Other input files for climatic parameters were also created for SWAT.

Canal Irrigation Component

A canal irrigation routine of SWAT model was used to simulate canal irrigation. In this framework approach, area under each outlet was considered as a sub-watershed. The crop fields within the sub-basin were represented by HRUs within the sub-watershed. In this module, SWAT estimates evaporation and seepage losses on daily basis.

Crop Irrigation Scheduling

The user can input a schedule (specifying the depth of irrigation, time, and source of irrigation) for irrigating the crop in an AU, in which the irrigation schedule was planned with the irrigation depth of 50mm, 70mm and 90mm and the irrigation frequency was varied according to the season i.e. 14 days interval for summer, 21 days interval for winter and 28 days interval for monsoon season. The management operations like planting, irrigation, fertilizer application, harvest and kill (termination) were scheduled by date. The potential evapotranspiration (PET) was estimated with SWAT by using modified Penman-Monteith (Monteith, 1965; Allen, *et al*., 1989). Irrigation water applied to a crop AU was used to fill the soil layers to field capacity beginning with the soil surface layer and working downward until all the water applied was used or the soil profile reached field capacity. Soil depth was based on soil horizon and irrigation water was applied only to rooting depth maximum up to depth of soil horizon.

Framework Calibration for Reservoir Storage and Canal Conveyance Efficiency

The framework was simulated from 1990 through 2008 (19 years). The major water losses in an irrigation system are canal conveyance losses (seepage and evaporation). The reservoir storage was also simulated. Hence, the framework was verified for these two parameters. Simulated reservoir storage values from 1985-86 through 2008-09 were compared with the actual storage values reported for the region. Similarly, the model was calibrated for the conveyance losses reported for the distribution network.

Net Benefit Calculations

The daily potential and actual ET data through output of simulation for different combinations of allocation rules were analyzed for estimating the crop yields under and net benefit calculations of the project. For these calculations, cost of cultivation of each crop under study, crop economic returns and actual sale price as well as the cost of water were considered.

Allocation Scenario

The calibrated framework was used to assess the net project benefit from different allocation rules on release rate, irrigation depth and area to be irrigated. These scenarios were analyzed by simulating the system hydrology using daily historical weather information for the year 1998-1999 during which the reservoir was completely filled. The allocation rules were mainly concentrated on the sustainable storage in the reservoir and better uniformity in the water distribution system.

Three types of allocation rules were formed comprising depth of irrigation, release rate and area to be irrigated during the year with available reservoir storage. The irrigation depths were selected as 90mm, 70mm and 50mm; release rates were selected as $5m^3$/sec, $4m^3$/sec, $3m^3$/sec, $2m^3$/sec and $1.5m^3$/sec and area to be irrigated as 100% Irrigable Command Area (ICA), 80% ICA, 60%ICA, 40% ICA and 20%ICA.

Results and Discussion

Allocation Units Analysis

The total area also included the area occupied by the reservoir (373ha). Thus, the irrigable command area is 7656ha. SWAT created total 305 AUs within 72 sub-basins, the first sub-basin is allocated as the reservoir. The existing cropping pattern in the irrigation command has maximum area during the *kharif* season occupied under pearl millet (41.34%), while that in *rabi* season under wheat (51.81%). This cropping pattern is obviously deviated from the approved cropping pattern for the area.

The combination of the distribution of crop-soil and slope in the ICA of the study area created by SWAT is presented in Table 2. The area occupied in the irrigation command by Mirajgaon soil series (clay), Ghumari soil series (clay loam), Ratanjan soil series (silt clay) and Nagalwadi soil series (silt loam) are 1566ha, 3084ha 1821ha, and 1185ha, respectively. The distribution of slope among the sub-basins showed that the irrigation command has a gentle slope varying from 0-3%

and more than 99% area is occupied under this category of slope, while very few area (0.49%) is having stiff slope (3% and above).

Table 2. Distribution of combination of crop-soil and slope created by SWAT

Soil series / class	Slope					
	0-0.5%	0.5-1%	1-3%	3-5%	Above 5%	Total
Mirajgaon (clay)	39.6	491.9	1034.4	0.0	0.0	1565.9
Ghumari (clay loam)	11.4	358.3	2714.2	0.3	0.0	3084.2
Ratanjan (silt clay)	21.0	328.5	1433.0	36.4	1.9	1820.8
Nagalwadi (silt loam)	2.8	97.6	1083.8	1.1	0.0	1185.3
Total	74.8	1276.3	6265.4	37.8	1.9	7656.2
Soil	Crop					
	Wheat	Sugarcane	Pearl millet	Mung bean	Sorghum	Total
Mirajgaon (clay)	1206.5	22.4	337.1	0.0	0.0	1566.0
Ghumari (clay loam)	1204.8	5.3	1874.0	0.0	0.0	3084.1
Ratanjan (silt clay)	1499.9	46.7	23.1	26.5	14.4	1820.7
Nagalwadi (silt loam)	243.2	3.7	875.9	62.6	0.0	1185.4
Total	4154.4	78.1	3110.1	89.1	14.4	7656.2
Slope	Crop					
	Wheat	Sugarcane	Pearl millet	Mung bean	Sorghum	Total
0-0.5%	62.3	2.8	9.7	0.0	0.0	74.8
0.5-1%	874.4	8.6	393.2	0.0	0.0	1276.2
1-3%	3186.4	58.7	2916.8	89.1	14.4	6265.4
3-5%	31.4	6.2	0.3	0.0	0.0	37.9
Above 5%	0.0	1.9	0.0	0.0	0.0	1.9
Total	4154.5	78.2	3320.0	89.1	14.4	7656.2

The SWAT distributed the crop, soil, and slopes among the 305 AUs. The data indicated that more that 80% of the area lies under the slope category of 1-3% followed by 0.5-1% slope. The distribution of wheat was maximum in both clay and clay loam soils. The sugarcane crop was more concentrated in silt clay followed by clay soil. The maximum pearl millet was grown in clay loam followed by silt loam soil. However, the crops like mung beans and sorghum (*rabi*) are very less in the irrigation command and are more concentrated in silt clay and silt loam soils. Most of the crops are more concentrated in the slope category of 1-3% followed by 0.5-1% slope.

Reservoir Storage Scenario

The allocation rules with the combination of release rate, irrigation depth and percentage of irrigable area were analyzed and selected in such a way that the stored water in the reservoir

should be sufficient to irrigate the crops during three seasons in the year. The hypothesis is that even if the crop productivity with lower depth of irrigation is less and project net benefit is compensated by the increase in irrigated area, that strategy can be selected as the best allocation rule. The reservoir storage analysis was mainly based on the balance of available live storage remained in the reservoir from start of October till the end of summer season.

The longevity in live storage of reservoir after it is filled up to its full capacity from 1st October for the different allocation rules is briefed in Fig. 3. It is obvious that the retention in storage can be increased with decrease in the release rate, irrigation depth and the irrigated area. The decrease in release rate from 5 to 1.5m^3/sec for 90mm irrigation depth resulted in increase in longevity of live storage from 121 to 191 days when the 100%ICA was irrigated. Similarly, it increased from 133 to 241 days for 80% ICA and 141 to more than 243 days for 60% ICA. The live storage in reservoir for the release rates from 5 to 1.5m^3/sec and 70mm irrigation depth resulted as 134 to 225 days for 100%ICA, 142 to more that 243 days for 80%ICA and 146 to more than 243 days for 60%ICA. Similarly live storage in reservoir for the release rates from 5 to 1.5m^3/sec and 50mm irrigation depth lasted from 142 to more than 243 days for 100%ICA, 147 to more that 243 days for 80%ICA and 154 to more than 243 days for 60%ICA. For 40% and 20%ICA irrigated with 90 to 50mm irrigation depth and release rates from 5 to 1.5m^3/sec the longevity in live storage of reservoir ranged from 152 to more than 243 days. The allocation rules for which the live storage lasted more than 243 days, may be proper operation rule as far as the adequacy is concerned, however, irrigating very less area may not be beneficial for the project.

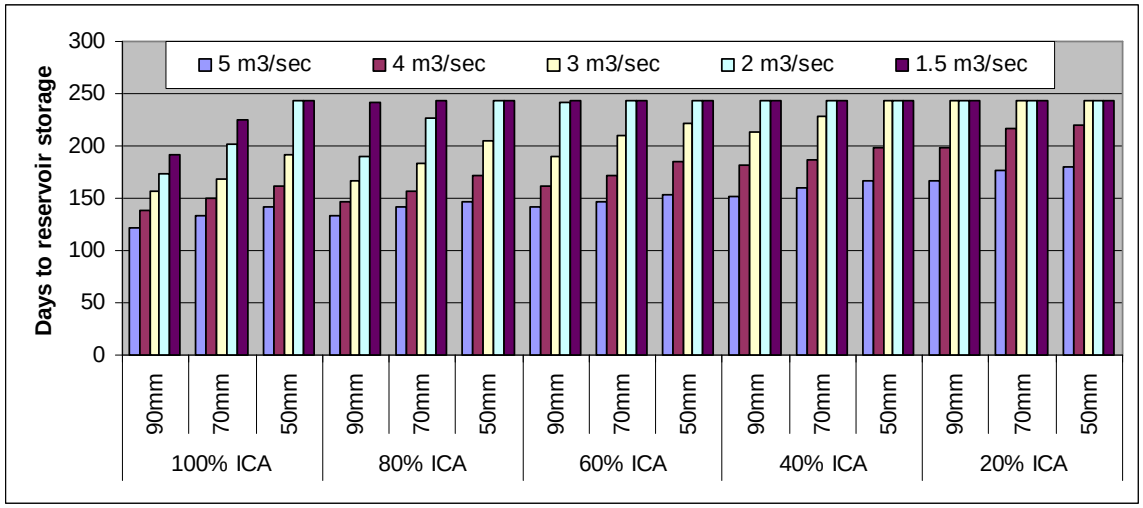

Fig. 3. Longevity (days) of reservoir live storage from 1st October for different allocation rules

Water Distribution Uniformity in Irrigated Area:

The uniformity in water distribution was analyzed for different release rates from reservoir so as to assess how best uniformly the irrigation water can be distributed along the canal network in the irrigation command when the crop was irrigated at different depths and area to be irrigated. The canal network was divided into three reaches according to the area commanded under each outlet. The percentage of release rate (RR) for head, middle and tail reaches in distribution system under different operational rules is presented in Fig. 4.

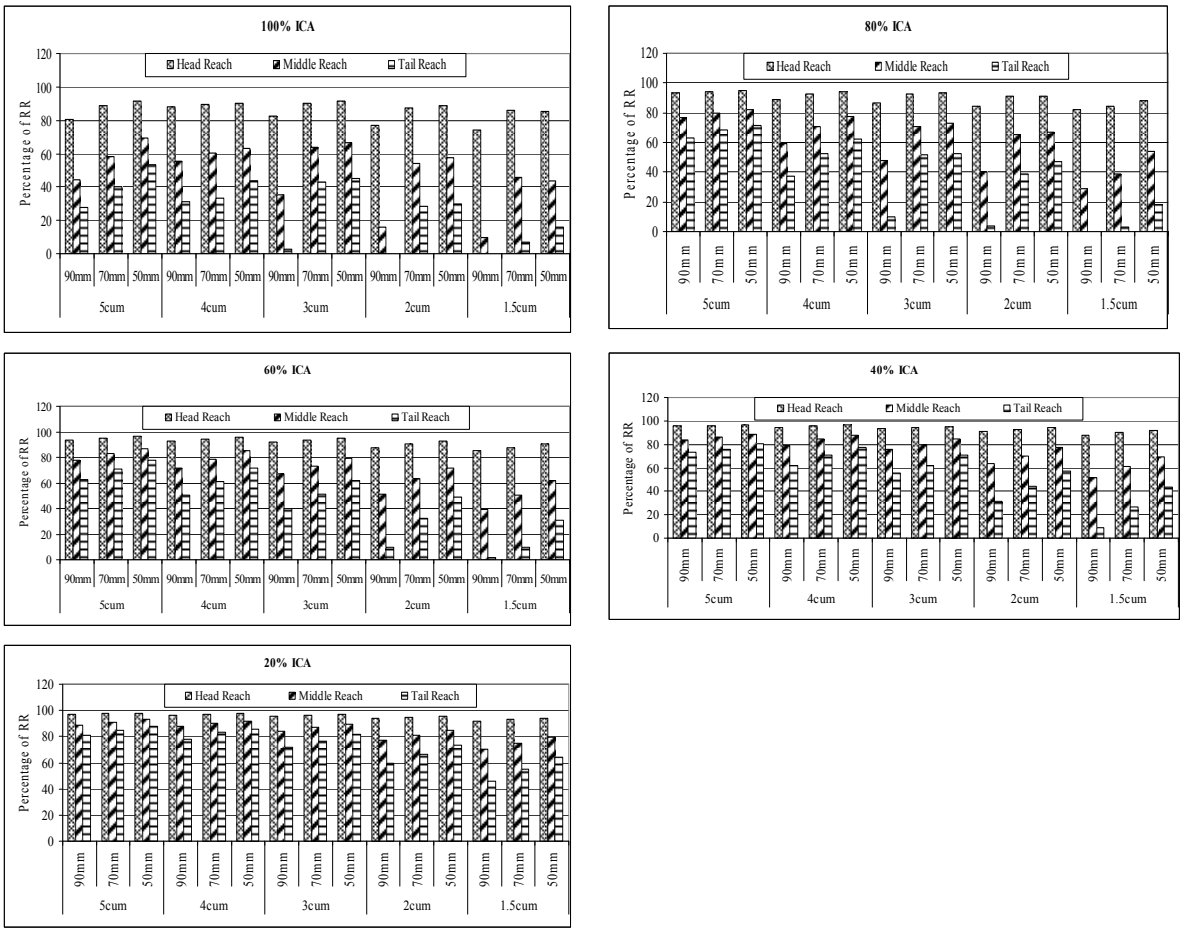

Fig. 4. Percentage of release rate (RR) in head, middle and tail reaches of distribution system

The results reveal that the reduction in release rate in the middle and tail reaches is very fast when the aim is to irrigate more area with more depth of irrigation. Area in tail reach of distribution network can not be irrigated when the target is to irrigate area more than 60% ICA

with irrigation depth of 90mm and release rate of 2m^3/sec and less. For higher areas under irrigation (above 60% ICA) with irrigation depth as 90mm, the release rates reduced to zero in the tail reach, ultimately affecting the uniformity in distribution system i.e. more water in head reach and no water in tail reach, which may affect the overall yields of crops as well as project net benefit. These results also corroborate that the operation rule with medium range of irrigation depth and release rate with targeted area under irrigation between 60 to 80% ICA may result in better net project benefits.

Conveyance Efficiency in Canal Network

The conveyance efficiency (accounting both seepage and evaporation losses from canal network) was determined for different allocation rule and is presented in Fig. 5. The seepage losses are more prominent as compared to the evaporation loss. In all the combinations, seepage loss was about seven times as that of the evaporation loss. The results clearly indicate that the conveyance efficiency was constant for the release rate of 5m^3/sec. The conveyance efficiency was observed to be increasing with the decrease in irrigation depth; however, it decreased with the decrease in release rate. The conveyance efficiency was in the range of 66% to 78%.

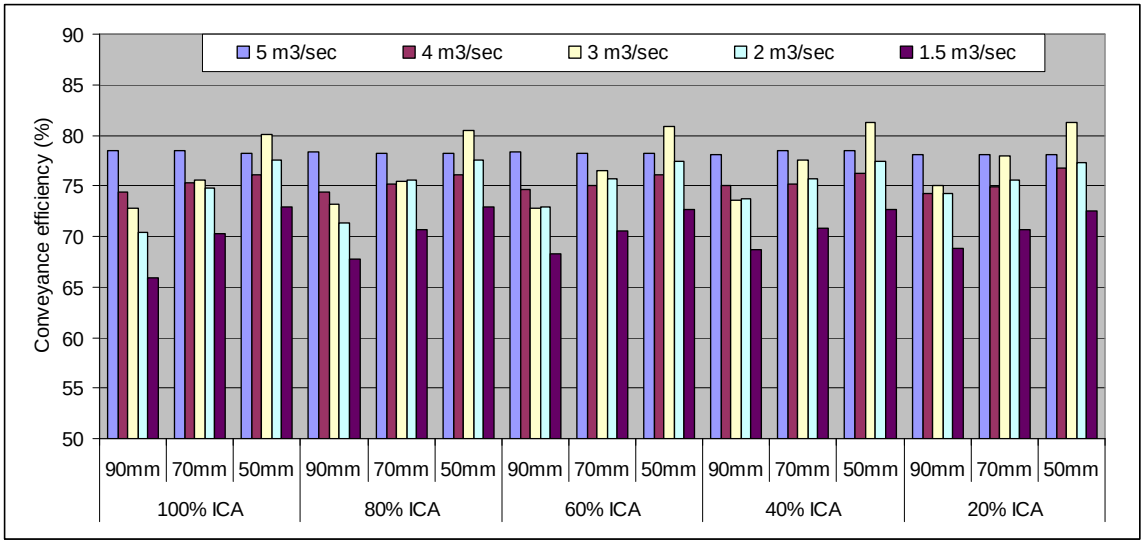

Fig. 5. Conveyance efficiency in canal network for different allocation rules

Project Net Benefit

The crop yields under 305 allocation units comprising different soil were estimated for the different water allocation rules. The benefits from production of each crop were worked out taking into consideration the cost of water for crop production. The cost of water was calculated

from known prices as per Government rules for each crop. The Govt. costs for irrigation water is based on the crop per ha. This cost was converted into cost of irrigation water on volumetric basis applied to each crop under each depth of irrigation so as to view how much cost of irrigation water is required for production of each crop. In case the water in excess of water required by the crops is released, the cost of excess water going out of irrigated command was also considered and was added to the net benefit of the project. In this way, the net project benefit was worked out for each combination of water allocation rule by considering the area under each crop as well as area of each soil type in each allocation unit. The net project benefit for all the combinations is presented in Fig. 6.

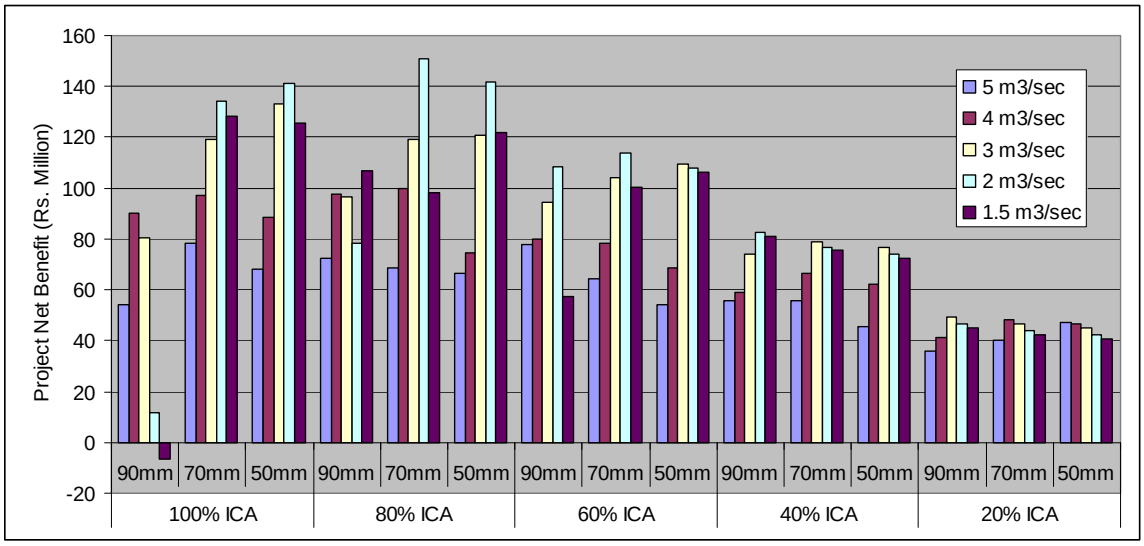

Fig. 6. Project net benefit for different water allocation rules

The results of net project benefit (Table 6) are very promising, which indicate that the area to be irrigated below 60% ICA results tremendous decrease in net project benefit. The net project benefit was negative only in case of allocation rule with 90mm depth of application and release rate of 1.5m^3/sec when the target area to be irrigated is 100% ICA. This was due to the non-uniformity of distribution of water in the canal network. Many times, the area in the tail reach could not get the sufficient water for irrigation with this release rate and depth of irrigation, which hampered the crop productivity and in turn it reflected in the net project benefit. The highest net project benefit of Rs. 151.06 Million could be fetched in case of the water allocation rule with release rate of 2m^3/sec, depth of irrigation of 70mm and area of 80%ICA could be irrigated. In this allocation rule, total 6208.76 ha area could be irrigated during *kharif* season and 6196.09 ha area could be irrigated during the *rabi* and summer seasons. The longevity of storage

in the reservoir was up to 15th May. The net benefit from production of crops was observed to be Rs. 71.05 Millions during *kharif* season and Rs. 78.41 Millions during *rabi* and summer seasons. The exchequer of Rs. 1.60 Million could be fetched from 22.03 Million m^3 excess water, which was additional benefit to the project. The conveyance efficiency in distribution system for this allocation rule was observed to be 76%.

Based on the highest net project benefit, the water release during different irrigation rotation plan was prepared for the total irrigation command. An example of water release during different irrigation rotations to outlets located in the head (Minor 1), middle (DO 17) and tail (DO 34) regions of the distribution system are presented in Fig. 7. The irrigation water can be supplied to the irrigation command during 21 rotations from October to the end of summer season. Total 63.36 ha area can be irrigated through Minor 1, which is located in the region. The crops grown in the area are sugarcane, wheat and *rabi* sorghum. The outlet DO 17 located in the middle reach of the distribution system has area of 5.70 ha that can be irrigated and the crops grown in the area are only wheat and sugarcane. The outlet DO 34 located in the tail reach of the distribution system has total irrigated area of 11.61 ha and the crops grown in the area are wheat and groundnut.

In this way, the water release pattern was obtained for the irrigation command. These are useful for management of water in reservoir for irrigation purpose.

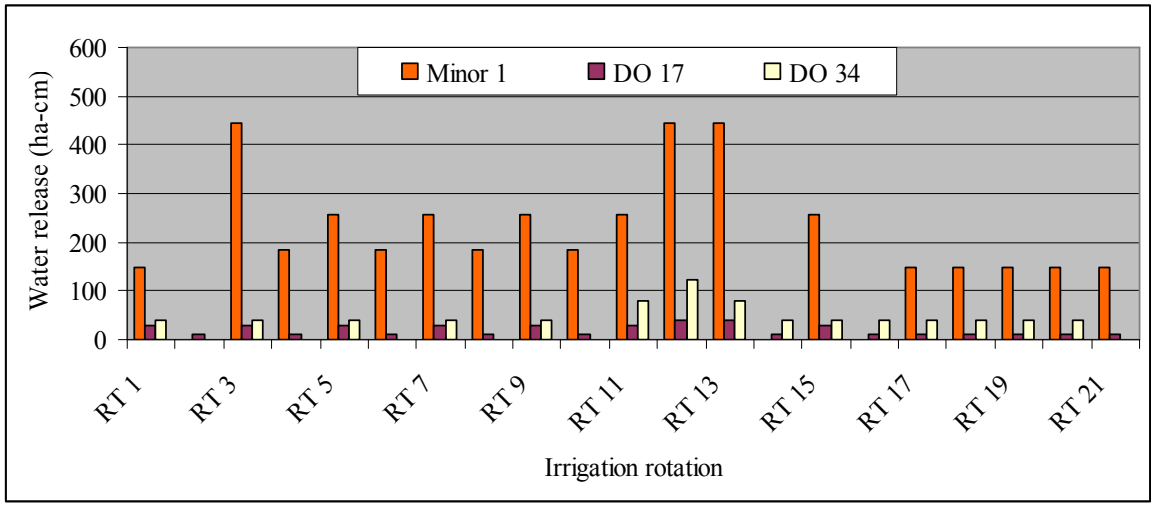

Fig. 7. Water release during different irrigation rotations to outlets located in the head, middle and tail regions of the distribution system

Conclusions:

The GIS based water allocation tool framework was formulated by using SWAT model for increasing the water productivity and net project benefit based on storage availability in the reservoir at the beginning of season. This tool framework mainly comprises three modules: allocation rules, SWAT modules and economic module. The allocation rules with the combination of release rate, irrigation depth and percentage of irrigable area were analyzed and selected in such a way that the stored water in the reservoir should be sufficient to irrigate the crops during three seasons in the year. The reservoir storage analysis was mainly based on the balance of available live storage remained in the reservoir from start of October till the end of summer season. Sina irrigation project in Maharashtra state of India was selected as a case study with irrigable command area of 7656ha. Total 305 AUs were created within 72 sub-basins, the first sub-basin was allocated as the reservoir. As per existing cropping pattern, maximum area during the *kharif* season was occupied by pearl millet (41.34%), while that in *rabi* season under wheat (51.81%). Area occupied by clay loam, silt clay, clay and silt loam soils are 3083ha, 1821ha, 1571ha and 1185ha, respectively. The maximum area (more than 99%) in irrigation command has a gentle slope varying from 0-3%. The highest net project benefit of Rs. 151.06 Million could be fetched in case of the water allocation rule with release rate of $2m^3$/sec, depth of irrigation of 70mm and area of 80%ICA could be irrigated. In this allocation rule, total 6208.76 ha area could be irrigated during *kharif* season and 6196.09 ha area could be irrigated during the *rabi* and summer seasons. The longevity of storage in the reservoir was up to 15th May. The net benefit from production of crops was observed to be Rs. 71.05 Millions during *kharif* season and Rs. 78.41 Millions during *rabi* and summer seasons. The exchequer of Rs. 1.60 Million could be fetched from 22.03 Million m^3 excess water, which was additional benefit to the project. The conveyance efficiency in distribution system for this allocation rule was observed to be 76%.

References:

Allen, R.G.; Jenson, M.E.; Wright, J.L. and Burman, R.D. 1989. Operational estimates of evapotranspiration. *Agron. J.* **81**: 650-662.

Anonymous. 1997. Second Revised Project Report of Sina Medium Irrigation Project. *Report of Irrigation Department, Ahmednagar Irrigation Circle,* Government of Maharashtra – 1996-1997. Vol. I.

Arnold, J. G., Srinivasan R., Muttiah R.S., and Williams, J. R. 1998. Large-area Hydrologic modeling and assessment: Part I. Model development. *J. Am. Water Resour. Asso*. **34**: 73-89.

Dyson, T. 1999. World food trends and prospects to 2025. *Proceedings of the National Academy of Sciences*, USA. 96: 5929-5936.

Fereres, E. and Connor, D.J. 2004. Sustainable water management in agriculture. In Canbera E, Cobacho R, eds. *Challenges of the new water policies for XXI century*. Lisse, The Netherlands: A.A. Balkema, 157-170.

Fereres, E. and Soriano, M.A. 2007. Deficit irrigation for reducing agricultural water use. *J. Exp. Botany* Vol. 58(2): 147-159.

Gorantiwar, S.D. and Smout, I.K. 2003. Allocation of scarce water resources using deficit irrigation in rotational systems. *J. Irrig. & Drain. Engg.* **129**: 155-163.

Harrington, G.J. and Heermann, D.F. 1981. State of art irrigation scheduling computer program. In: *Irrigation Scheduling for Water and Energy Conservation in the 80's*. ASAE Publication 23-81: 171-178.

Howard, S.E. and Benn, J.R. 1986. Computer modelling for water management on smallholder irrigation schemes. Report No. OD 74, *Hydraulics Research* Wallingford, UK.

Monteith, J.L. 1965. Evaporation and environment. In: The state and movement of water in living organisms. *19th Symposium, Soc. for Environmental Biology*. Cambridge, UK, Cambridge University Press. 205-234.

Neitsch, S.L.; Arnold, J.G.; Williams, J.R.; Kiniry, J.R. and King, K.W. 2002. Soil and Water Assessment Tool (Version 2000). *Model documentation. GSWRL 02-01, BREC 02-05,TR-191*. College Station, Texas: Texas Water Resources Institute.

Pereira, L.S.; Teodoro, P.R.; Rodregues, P.N. and Teixerira, J.L. 2003. Irrigation scheduling simulation: the model ISAREG. In *Tools for Drought Mitigation in Mediterranean Regions*. Eds. G. Rossi, A. Cancelliere, L.S. Pereira, T. Oweis, M. Shatanawi and A. Zairi. 161-180. Netherlands: Kluwer Academic Publishers.

Postel, S.L.; Daily, G.C. and Ehrlich, P.R. 1996. Human appropriation renewable freshwater. *Science* **271**: 785-788.

Smith, M. 1992. CROPWAT, A computer program for irrigation planning and management. *FAO Irrigation & Drainage paper 24*. Rome, Italy.

Stewart, J.L.; Hagen, R.M. and Pruit, W.O. 1976. Water production functions and predicted irrigation programs for principal crops as required for water resources planning and increased water use efficiency. University of California. *Dep. Land, Air and Water Resources*, Davis, and USDI/Br, Denver, Co.

Variability in Normalized Difference Vegetation Index (NDVI) in relation to south west monsoon, western ghats, India

T.V. Lakshmi Kumar
Atmospheric Science Research Laboratory, SRM University, Kattankulathur, Tamilnadu, India

R. Uma, Humberto Barbosa
Universidade Federal de Alagoas – UFAL, Maceió, AL – Brasil

K. Koteswara Rao
Climatology & Hydrometeorology Division, Indian Institute of Tropical Meteorology, India

Abstract

Eleven years (2000 to 2010) of Normalized Difference Vegetation Index (NDVI) data, derived from Moderate Imaging Spectroradiometer (MODIS) Terra with 250m resolution are used in the present study to discuss the changes in the trends of vegetal cover. The interannual variability of NDVI over western ghats (number of test sites are 17) showed increasing trend and the pronounced changes are resulted due to the monsoon variability in terms of its distribution (wide spread/fairly wide spread/scattered/isolated) and activity (vigorous/normal/weak) and are studied in detail. The NDVI progression is observed from June with a minimum value of 0.179 and yielded to maximum at 0.565 during September/October, on average. The study then relates the NDVI with the no of light, moderate and heavy rainfall events via statistical techniques such as correlation and regression to understand the connection in between the ground vegetation and the south west monsoon.

The results of the study inferred i) NDVI, Antecedent Precipitation Index (API) are in good agreement throughout the monsoon which is evidenced by correlation, ii) NDVI maintained good correlation with no of Light Rainy and Moderate Rainy alternatively but not with no of Heavy Rainy days, iii) Relation of NDVI with Isolated, Scattered distributions and active monsoons is substantial and iv) Phenological stages captured the Rate of Green Up during the crop season over western ghats.

Author for correspondence :

Dr.T.V. Lakshmi Kumar
Atmospheric Science Research Laboratory
Dept of Physics, Faculty of Engineering & Technology
SRM University, Kattankulathur, Tamilnadu
India – 603 203

Email : lkumarap@hotmail.com

INTRODUCTION

Southwest (SW) monsoon is considered to be the principal rainy season in India and its role in country's economy is remarkable. The crops, those grow in this season mainly use the rain water from the monsoon to produce better yields. Thus, the SW monsoon can decide the crop fate that is going to be failure or success. There are several studies carried out in studying the crop/Agriculture in relation to weather, monsoon in particular (Mathews et al, 1997; Lakshmi Kumar et al 2011). These studies made use of model derived outputs/ insitu measurements to understand and monitor the crops. Sarma & Lakshmi Kumar 2006 used crop growing periods, soil moisture adequacy to study the different growth stages of crops over Andra Pradesh. Al-Bakri & Suleiman, 2004; Sarma & Lakshmi Kumar 2006a, Sarma and Lakshmi Kumar 2008 used rainfall, soil moisture and growing degree days to study the same phenomenon. But these studies have limitations that are unable to asses over large areas due to lack of sufficient point observations and model interpretations.

With the advent of satellite era, Scientist started using satellite derived indices to study the crops directly from space. National Oceanic and Atmospheric Administration (NOAA) Advanced Very High Resolution Radiometer, MODIS, SPOT VGT are a few satellites provide vegetation indices to study the vegetation/crop/agriculture over large areas as well as yet fine resolution levels. NOAA AVHRR vegetation index, known as Normalized Difference Vegetation Index (NDVI) has been widely used to relate the synoptic meteorology/Climatology to understand the vegetation dynamics, vegetation response to climate and climate vegetation feedback mechanism

(Cihlar et al 1991, Devanport & Nicholson 1993, Barbosa & Lakshmi Kumar 2011, Barbosa et al 2011). The studies of Kogan 1997, Unganai & Kogan 1998 and Ramesh et al 2003 concluded that AVHRR NDVI is one of the best tools to monitor / asses the large area agricultural droughts.

Wan et al 2004, Knight et al 2006 and Funk et al 2009 used NDVI derived from MODIS to understand the crop stages and long term disasters at fine resolution level. MODIS TERRA facilitates to provide NDVI at 250 m resolution level from which one can make studies from a particular point location where ever required. Narasimhan & Stow 2010 studied the early season dynamics using MODIS NDVI across Alaska to understand the greening patterns of Artic vegetations. Schnur et al 2010 estimated the root zone soil moisture at distant sites using MODIS NDVI & EVI in a semi – arid region of southwestern USA and found the growth correlation between NDVI & soil moisture.

In the present investigation, an attempt is made to study the NDVI variations

In view of this back ground, present investigation is an attempt to study the NDVI variations during a season as well as in different years. The trend analysis of NDVI during SW monsoon is of priority to understand vegetation growth for the past 11 years from 2000 over Western Ghats India. also, attempts were made to see these variations in relation to light, moderate and heavy rainy days. The study also focuses in quantifying the relations of NDVI with monsoon distribution (isolated/scattered/fairly wide spread/wide spread) and monsoon activity (weak/normal/active/vigorous).

STUDY AREA

The present study is focussed to Western Ghats which is located in peninsular region of India. The Western Ghats extends along the West coast of India from Lat ... with an area of 160,000 sq km. Western Ghats has got climatologically significance in India which is considered to be all time humid region. The mean annual rainfall and temperatures are 1200 mm and 20°C - 22° C respectively. The SW monsoon contributes nearly 80% of the annual rainfall. Paddy and maize are the major crops that grow during SW monsoon season. Six (6) Test sites those wide spread in

Western Ghats are selected for the present study of which latitude & longitude are given in Table 1.

Test Site	District	Latitude	Longitude
Madikeri	Kodagu	12.42°N	75.73°E
Mangalore	Dhakshin Kannada	12.91°N	74.85°E
Puttur	Dhakshin Kannada	12.75°N	75.19°E
Udupi	Udipi	13.33°N	74.76°E
Haliyal	Uttar Kannada	15.32°N	74.75°E
Kumta	Uttar Kannada	14.42°N	74.41°E

DATA AND METHODOLOGY

MODIS NDVI pictures are available on the website ftp://e4ft1010.ecs.nasa.gov/MOLT/MODO9Q1.0051 supplied by National Aeronautics and Space Administration.The time interval of these pictures is eight (8) days and accessible for peninsular region of India. The pictures are downloaded and processed for SW monsoon season for 11 years ie from 2000 -2010 and NDVI values for the six test sites are obtained. ERDAS 9.3 is used for the image analysis and the procedure for deriving NDVI is given below in the form of flow chart.

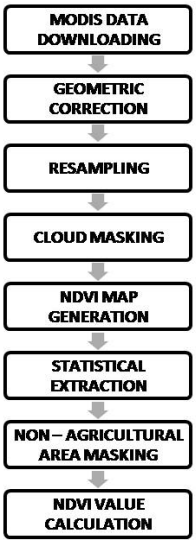

Daily rainfall data from ground rain gauges for the test sites have collected from Karnataka State Natural Disaster Monitoring Centre (KSNDMC), Bangalore, Karnataka, India.

The authors have made an attempt to understand the relation between NDVI and rainfall. For this purpose using daily rainfall, Antecedent Precipitation Index (API**)** for the selected six test sites has been calculated. Antecedent Precipitation Index is an essential parameter of the rainfall. It is reported that API plays a key role in assessing runoff and soil moisture of a region. The formulation of API given below as suggested by Rosenthal et al 1982

$API(j) = API(j-1)*C + P_t$

Where

j - current week

j-1 - previous week

$C^t = (P_t/P_o)$;

Where

P_t - t th week rainfall

P_o – initial rainfall

Pearson correlation is used to relate NDVI with API over the test sites of this study.

Based on the amount of rainfall, categorization suggested by India Meteorological Department (IMD) is followed to distinguish the rainy days. Based on the number of sites recording rainfall and long term normal, IMD also suggested one criterion to explain the monsoon distribution and monsoon activity during south west monsoon season.

IMD Criterion

Categorization of Rainy days

Light Rainy Day (LR)	- Rainfall is less than 7.4mm
Moderate Rainy Day (MR)	- Rainfall is fro, 7.5mm to 34.4mm
Heavy Rainy Day (HR)	- Rainfall is above 34.5mm

Monsoon distribution

Isolated (I)	- No of sites recording rainfall of 2.5mm and above should of 25% of total number of sites.
Scattered (S)	- No of sites recording rainfall of 2.5mm and above should of 25% to 50%of total number of sites.
Fairly wide spread (F)	- No of sites recording rainfall of 2.5mm and above should of 50% to 75%of total number of sites.
Wide spread (W)	- No of sites recording rainfall of 2.5mm and above should of above 75% of total number of sites.

Monsoon activity

Weak (W) - Actual rainfall should be below one and half of the normal

Normal (N) - Actual rainfall should be half and one and half of the normal

Active (A) - Actual rainfall should be one and half to four times of the normal. At least two places should get rain above 30mm rainfall and rainfall distribution should be fairly wide spread.

Vigorous (V) - Actual rainfall should be above four times the normal. At least two places should get rainfall above 50mm and rainfall distribution should be fairly wide spread to wide spread.

NDVI IMAGE ANALYSIS

The crop/vegetation reflects high energy in the near infrared band due to its canopy geometry and health of the standing crops / vegetation and absorbs high in the red band due to its biomass and photosynthesis. Using these contrast characteristics of vegetation in near infrared and red bands, which indicate both the health and condition of the crops/ vegetation; Normalized Difference Vegetation Index (NDVI) is derived by the difference of these measurements and divided by their sum. The vegetation index was generated from each of the available satellite data irrespective of the cloud cover present.

The vegetation index maps for the particular boundaries overlaid and are given in specific colors for the vegetation index ranges. The various colors in the NDVI map: yellow through green to violet indicate increasing green leaf area and biomass of different vegetation types. Cloud and water are represented in black and blue colors, respectively. The bare soil, fallow and other non-vegetation categories are represented in brown color.

NDVI images were generated for each time interval (8 days) by removing the non agricultural area (forest, fallow lands etc). About 80-90% of non agricultural area was excluded in different districts of the Western Ghats. The agricultural area mask thus generated can be used for drought assessment studies.

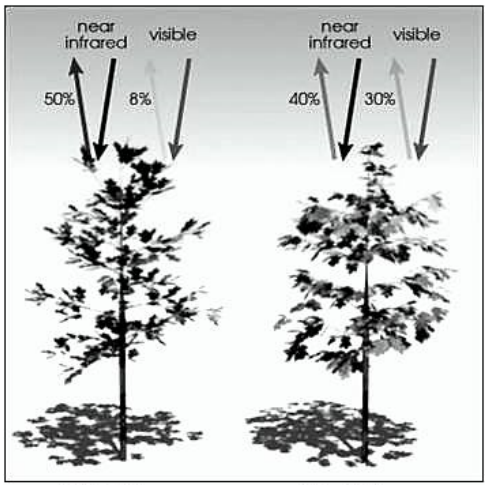

Fig.1. Vegetation response to solar radiation

NDVI is calculated from the visible and near-infrared light reflected by vegetation. Healthy vegetation (left) absorbs most of the visible light that hits it, and reflects a large portion of the near-infrared light. Unhealthy or sparse vegetation (right) reflects more visible light and less near-infrared light. The numbers on the figure above are representative of actual values, but real vegetation is much more varied.

Nearly all satellite Vegetation Indices employ this difference formula to quantify the density of plant growth on the Earth — near-infrared radiation minus visible radiation divided by near-

infrared radiation plus visible radiation. The result of this formula is called the Normalized Difference Vegetation Index (NDVI). Written mathematically, the formula is:

NDVI = (NIR — RED)/(NIR + RED)

Calculations of NDVI for a given pixel always result in a number that ranges from minus one (-1) to plus one (+1); however, no green leaves gives a value close to zero. A zero means no vegetation and close to +1 (0.8 - 0.9) indicates the highest possible density of green leaves. MODIS makes use of 645nm for red and 857nm for near Infra-Red to obtain the NDVI (Yingxin et al 2007)

RESULT AND DISCUSSIONS

NDVI IMAGE ANALYSIS

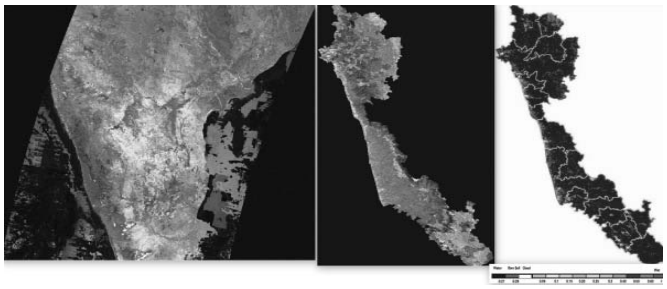

Fig.2. a) MODIS TERRA Raw Image, b) Western Ghats region & c) NDVI over Western Ghats

To understand the various steps involved in deriving NDVI from MODIS a sample picture is given in Fig 2. (a, b & c). Fig. 2a is the raw image obtained from MODIS which is available in the website. This picture has been downloaded and on this a toposheet of Western Ghats was imposed which can be seen in Fig 2b. Fig 2b illustrates the vegetation status including agricultural & non-agricultural area. To monitor the different stages of agricultural droughts, it

ought to focus only on the agricultural regions. The information of agricultural area has been collected from Agricultural Commission, Karnataka and the same is imposed on the vegetation status in agricultural areas of Western Ghats. The Fig 2c is in full fledged form that reveals the vegetation conditions through NDVI values. The figure is made by applying taluk boundaries from where the NDVI values have obtained for the six selected sites and used in present study.

CROP PHENOLOGICAL STAGES

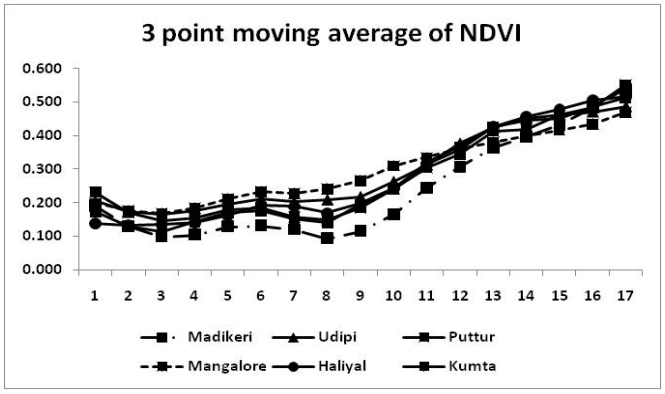

Fig.3. Crop phenological stages at the test sites

Fig.3 infers the three point moving averages of eight days NDVI during June to October of eleven years (2000 – 2010) for the six test sites. Since NDVI pictures are available for 8 days, we denoted these NDVI pictures with number from 1 to 19 corresponding to each 8 days from June to October. The moving averages have been done to smooth out the NDVI time series. It

can be inferred from the figure that the six stations recorded a value 0.31 on average during initial conditions. The NDVI variation is not in order till it enters August. This shows that the vegetation / crops are in preparatory period and inconsistent to changes weather. Also, crops initial conditions vary from site to site because of site specific synoptic topographic conditions. From the first week of August, NDVI started increasing in all stations and reached optimum in the last week of October with an average of 0.51. This orderly increment of NDVI resembles the rate of green up with a steep slope of 0.03.The Fig.3 could able to capture the crop phenology stages such as start of season and rate of green up only. Since our analysis is restricted to June to October, it is not possible to say about rate of senescence and end of season.

RELATION BETWEEN NDVI AND API

Authors of the paper attempted to see the relation between NDVI & rainfall. For this, Pearson correlation technique has been used which resulted in poor correlation when the values are taken on 8 days basis. It is also attempted to correlate NDVI & rainfall with one month cumulation, seasonal totals, one – two months lags. Even then the relation did not show strong correlation. So, this comparative study has taken using NDVI and rainfall derived index called API of which formulation is mentioned in methodology.

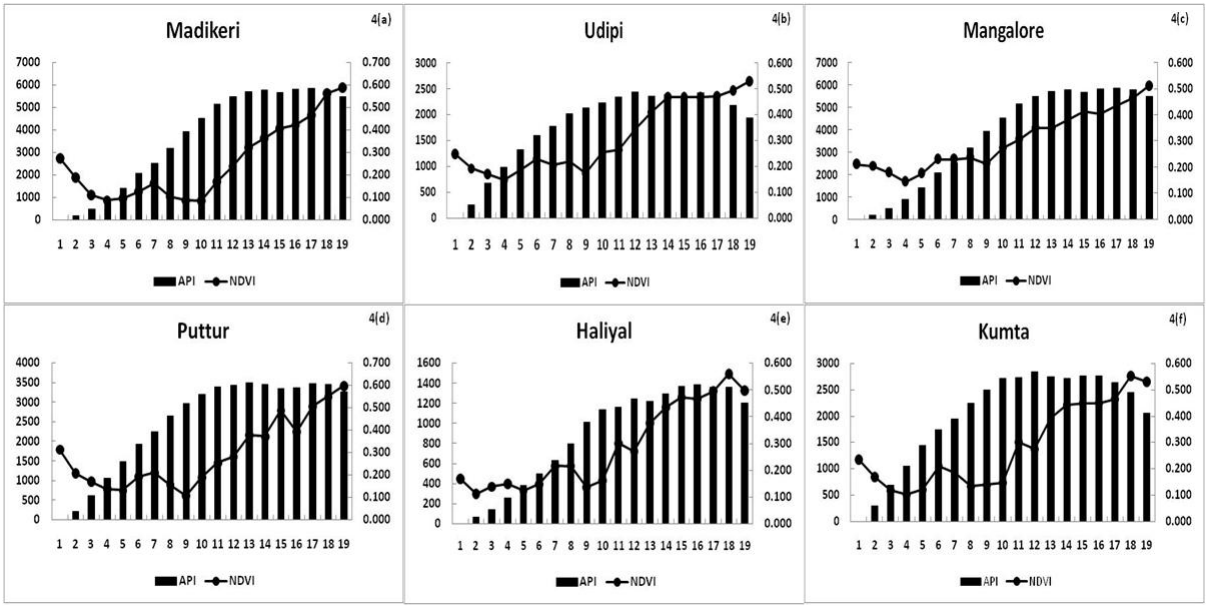

Fig.4. Time series of NDVI and API at a) Madikeri, b) Udipi, c) Mangalore, d) Puttur, e) Haliyal & f) Kumta.

Fig. 4 (a, b, c, d, e & f) show the variation of NDVI with API for the six test sites for the long term 2000 – 2010. The API has progressed from June and reached maximum in the month of September which signifies the monsoon activity over these test sites. NDVI also scaled up as discussed in the first part during this session along with API. It is clear from the figure that all the stations utilized the rainfall proportionality, thus the rate of green up during this season is explicable. It is to worth mention that in all stations, NDVI increased and recorded higher values in October where as corresponding API values in October are digressed. The decline in API features the end of SW monsoon season while NDVI represents the matured status.

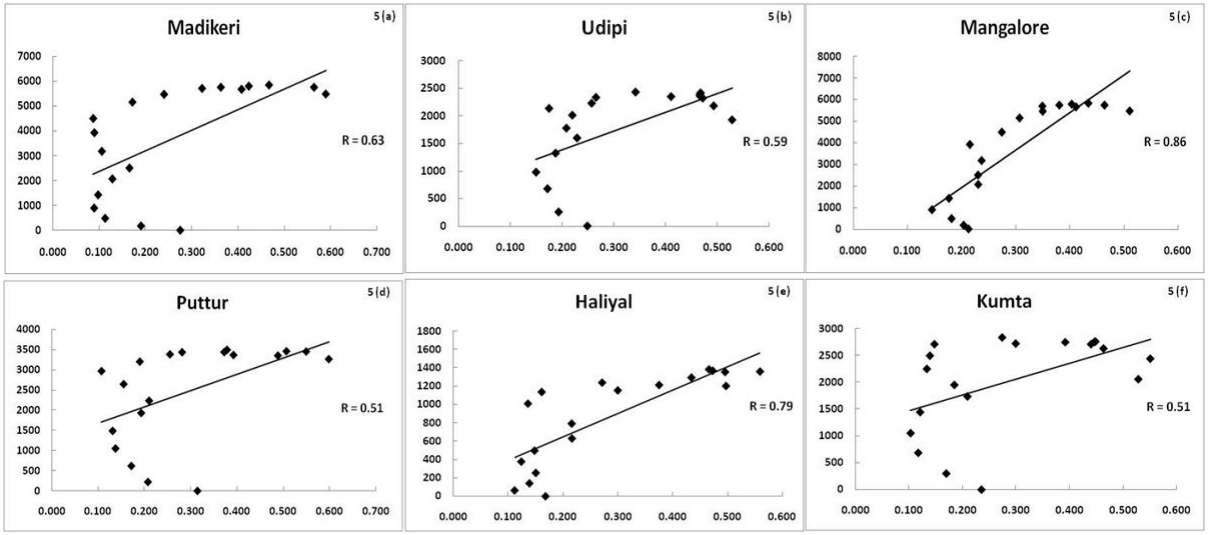

Fig.5. Scatter plots of NDVI and APT at a) Madikeri, b) Udupi, c) Mangalore, d) Puttur, e) Haliyal & f) Kumta.

The scatter plots (Fig 5 (a, b, c, d, e & f) of the six test sites supported the above study with substantial correlations of 0.63, 0.59, 0.86, 0.51, 0.79, 0.51, 0.79, 0.51 for Madikeri, Udipi, Mangalore, Puttur, Haliyal and Kumta respectively.

RELATION OF NDVI WITH DIFFERENT RAINY DAYS

Table 2 & 3 show the correlations of NDVI with LR, MR and HR and with Monsoon distribution and monsoon activity. The NDVI is correlated with Isolated/scattered/fairly wide spread/wide spread days of western ghats and Weak, normal, active and vigorous monsoonish days in western ghats.

Table.2. Correlation of NDVI with LR, MR and HR days

Station Name	Correlation		
	LR	MR	HR
Madikeri	0.10	0.11	-0.36
Mangalore	-0.06	-0.03	-0.02
Puttur	0.28	0.10	-0.24
Udipi	0.40	0.13	-0.34
Haliyal	-0.14	0.14	-0.39
Kumta	-0.33	0.56	-0.63

Table.3. Correlation of NDVI with Monsoon distribution and monsoon activity

YEAR	Correlation							
	Monsoon Distribution				Monsoon Activity			
	I	S	F	W	W	N	A	V
2000	0.3	0.3	0.1	-0.2	0.1	0.1	0.2	-0.3
2001	0.5	0.4	0.2	-0.3	0.2	-0.1	0.1	-0.5
2002	0.6	0.1	-0.1	-0.3	0.1	0.0	+0.3	-0.4
2003	0.3	0.6	0.1	-0.2	0.1	0.0	+0.4	-0.3
2004	0.5	0.3	-0.1	-0.2	0.2	-0.1	-0.2	-0.4
2005	0.3	0.2	0.0	-0.1	0.1	0.0	0.0	-0.2
2006	0.4	0.2	0.2	-0.2	0.1	-0.1	0.4	-0.2
2007	0.3	0.0	0.2	-0.1	-0.2	0.0	0.6	-0.2
2008	0.0	0.0	0.2	-0.1	0.0	0.0	0.3	-0.4
2009	0.4	0.4	0.1	-0.3	0.1	0.1	0.7	-0.5
2010	0.4	-0.1	0.2	-0.1	-0.1	0.1	0.4	-0.4

From the table, it can be inferred that NDVI maintained strong negative correlation with the heavy rainy days. The correlation is maximum at Kumta (-0.63) and minimum at Mangalore (-0.02). NDVI also maintained good relation either with LR or with MR days. Udupi has shown a correlation of +0.40 with LR days where as it is +0.1 with MR days. Similarly, Kumta has displayed a negative correlation of -0.33 with LR days and in the case of MR days, it is +0.56.

Table 3 shows the correlation values of NDVI with different events of monsoon distribution and monsoon activity. Form the table of monsoon distribution, we can understand that NDVI yielded to good correlation during isolated and scattered days of monsoon in western

ghats. The fairly wide spread and wide spread do not give any meaningful correlation. In the same way, the correlation table with weak, normal, active and vigorous monsoonish days of western ghats display the good correlation with the active monsoonish days rather with weak, normal and vigorous monsoon. NDVI maintained negative correlation with the number of vigorous monsoon days which is unfavorable to vegetation growth.

CONCLUSIONS

The paper mainly focused on establishing the relation between NDVI and rainfall over Western Ghats. Since, western ghats is al-time humid region, extracting relation between the above is a crucial task. It is obvious that the vegetation cannot show immediate response to rainfall when plenty of moisture is already available in the soil which can be utilized by the vegetation for its sustenance. In this case, the amount of rainfall for that particular period will have significance in addition to the antecedent rainfall. Here, in this study, we made same attempt to see the relation between NDVI and API at six test sites in Western Ghats which has come out with good agreement evidenced by strong positive correlations. The plots show that vegetation green up rate is followed by the consistent API from August. The NDVI values showed lower and higher values during the season which is the replicate of Khariff season. The study is of immense help to understand some of the crop phonological stages as well as the relation between rainfall and NDVI in humid climatic regions. The relation of NDVI with isolated, scattered distributions and active monsoons is substantial.

REFERENCES

Al-Bakri, J.T & Suleiman, A.S (2004) *NDVI response to rainfall in different ecological zones in Jordan*, International Journal of Remote Sensing, .25(19), 3897-3912.

Cihlar, J., St. Laurent, L & Dyer, J.A (1991) *The relation between normalized difference vegetation index and ecological variables*, Remote sensing of Environment, 35, 279-298.

Chris Funk & Michale E. Budde (2009), *Phenologically – tuned MODIS NDVI based*

production anomaly estimates for Zimbabwe. Remote Sensing Environment. 113, 115 – 125.

Davenport M.L & Nicholson, S.E (1993) *On the relation between rainfall and the Normalized Difference Vegetation Index for diverse vegetation types in East Africa*, International Journal of Remote Sensing, 14, 2369.

Humberto A Barbosa, Michel d S Mesquita & Lakshmi Kumar, T V (2011) *What do vegetation indices tell us about the dynamics of the Amazon evergreen forests?*, Geophysical Research Abstracts, 13, EGU 2011, 12894.

Humberto Barbosa & Lakshmi Kumar, T.V (2011) *Strengthening regional capacities for providing remote sensing decision support in dry lands in the context of climate variability and change*, In:Young,SS and S.E.Silvern (Org) International Perspective of Global Environmental Change, In Tech.

Kogan F., (1997) *Global Drought Watch From Space*. Bulletin of the American Meteorological Society, 78, pp. 621-36.

Knight, J.K., Lunneta, R.L., Ediriwickerma, J. & Khorram, S (2006) *Regional scale land cover characterization using MODIS – NDVI. 250 m multi- temporal imagery: A phenology based approach*. GIScience and Remote Sensing (Special issue on Multi-Temporal Imagery Analysis), 43(1), 1-23

Lakshmi Kumar, T.V., Humberto Barbosa, K. Koteswara Rao & Emily Prabha Jothi (2011) *Studies on the frequency of extreme weather events over India*, Journal of Agriculture Science & Technology, Accepted for publication.

Mathews R.B, Kropff M.J, Horie T. Bachelet D (1997) *Simulating the impact of climate change on rice production in Asia and evaluating options for adaptation*, Agricultural Systems, 54, 399 – 425.

Raghuram Narasimhan and Douglas Stow (2010) *Daily MODIS products for analyzing*

Ramesh, P.S., Sudipa, R., and Kogan, F., (2003). *Vegetation and temperature condition indices from NOAA AVHRR data for drought monitoring over India*. International Journal of Remote Sensing, 24, pp. 4393-4402.

Sarma, A.A.L.N & Lakshmi Kumar, T.V (2006) *Studies on crop growing period and NDVI in relation to water balance components*, Indian Journal of Radio & Space Physics, 35, 424-434.

Sarma, A.A.L.N & Lakshmi Kumar, T.V (2006a) *Studies on the agroclimatic elements and soil wetness estimation using MSMR data*, Journal of Agrometeorology, .8(1), 19-27.

Sarma, A.A.L.N & Lakshmi Kumar, T.V & Koteswara Rao (2008) *Development of an agroclimatic model for the estimation of rice yield,* Journal of Indian Geophysical Union, .12(2), 88 – 96.

Unganai, L.S. and Kogan, F.N., (1998). *Southern Africa's Recent Droughts From Space*. Advance in Space Research, 21, No. 3, pp. 507-511.

Wan, Z., P.Wang, and X.Li (2004), *Using MODIS land surface temperature & normalized vegetation index for monitoring drought in the sourthern Great Plains, USA*, Int. J. Remote Sens., 25, 61 – 72

Rainfall runoff variability over semi-urban catchment, Maharashtra, India

Dipak R. Samal*

IIT Bombay, Research Scholar, Centre of Studies In Resources Engineering.

Shirish S. Gedam

IIT Bombay, Associate Professor, Centre of Studies In Resources Engineering.

Abstract

Long-term rainfall and associated runoff characteristics are good indicators of catchment response over time. Present study is being carried out for the upper Bhima catchment, a part of Krishna basin, India. It receives an average annual rainfall of about 1180 mm. Its landscape has been changing continuously due to various anthropogenic activities, which is more rapid in recent times. Keeping this view in background, rainfall and runoff data since last two decades (1985-2004) were analysed to find out whether any alteration in these phenomena has occurred significantly. Moreover, availability of daily rainfall and stream flow records from 16 rain gauge and 10 river gauge stations in the catchment gives an opportunity to study such anthropogenic effects. Linear Regression analysis and Mann-Kendall (MK) test is applied for studying temporal rainfall trend in the area, along with the runoff trend observed near outlet. Inter-annual variability, seasonal and decadal rainfall pattern are studied statistically, whereas the spatial pattern of rainfall analyzed through geo-spatial interpolation technique. The study period is divided into two decades i.e. D1 (from year 1985 to 1994) and D2 (from year 1995 to 2004) to analyze rainfall-runoff process. The study revealed that overall rainfall pattern in the area was nearly constant, whereas a drastic decline rate (-1285m^3/s per year) of stream flow is being observed during study period. The mean annual rainfall during period D1 and D2 was about 1213 mm and 1164 mm respectively, where as runoff was almost doubled during period D1, with respect to D2. Growing agricultural activities supported by construction of reservoirs, increasing demand of domestic and industrial water in upstream areas are main factors behind runoff alteration during the study period.

Key words: MK test, Interpolation, Bhima catchment, runoff

Introduction

Basin/ catchment/ watershed is a hydrological unit, where various natural resource conservation and management practices can be carried out through proper management of water resources. In this approach the development is not only confined but also diversified. The growing population and industrialization have a great impact on this natural unit. In addition, climate change and anthropogenic pressure contributes a major share in modifying its hydrological environment. According to Dinar et al., 2010, anthropogenic-induced climate change is expected to influence water resource cycles significantly. Many authors have stated that runoff is the residual of rainfall and study of long term rainfall and runoff pattern reflects the impact of climate change over the area. Long-term stream flow analysis is essential for effective water resources management and therefore has immense socio-economic significance (Klavins et al., 2002).

Catchment hydrological modelling and historical hydrological data analysis are two broad approaches to study rainfall runoff variability. Hydrological modelling deals with various physical parameters to model various catchment hydrological processes whereas historical data analysis deals with statistical analysis of time series hydrological datasets. The latter approach is considered to be very important in terms of response of catchment over different time period. Any activity in the catchment will directly or indirectly affect the runoff process, whether it is forestation /deforestation, construction of reservoirs or growing of urban settlement. The effects of these factors will be prominent if the area is small but in case of large basin, sometimes it is difficult to detect such changes. At the same time it is very difficult to separate out the effects of climate change from anthropogenic pressure on rainfall runoff process. In the present paper an attempt has been made to study rainfall runoff pattern in the upper Bhima catchment during 1985 to 2004. The study is solely based on availability of rainfall runoff data along with ancillary information about the area.

Study area

The study area is upper Bhima catchment, covering geographical area of 6381 sq. km in Pune district of Maharashtra, India (Fig. 1). The maximum and minimum elevation of the catchment is ranging from 1298 to 499 m. above sea level. The higher elevation act as barrier to monsoon wind and causes heavy rainfall (more than 3000 mm) in the adjacent areas near to the Western ghat ranges. Its geographical location lies in between 73^0 $20'$ 11E″- 74^0 $33'$ $42''$E longitude and 18^0 $17'$ $38''$N - 19^0 $5'$ $26''$N latitude. The Bhima is the major river originates and drains through the catchment. Mean annual rainfall in the catchment is about 1180 mm. Pune city which is one of the fastest growing cities in India is within this region and is well connected to Mumbai, financial capital of India, through efficient road, rail and airways. It attracts many industries due to good transport system in the region.

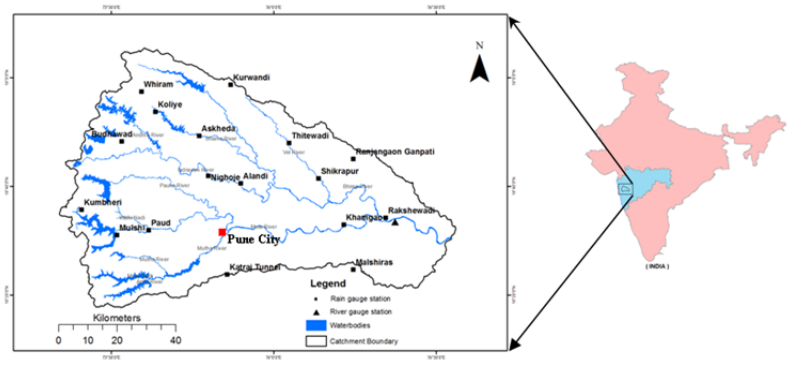

Figure 1. Bhima catchment and hydro-meteorological stations

Data and Methodology

Daily rainfall and runoff records from 16 rain gauges and river gauge stations are used in the study. The location of these rain gauge and river gauge stations are shown in figure 1. Rain gauge stations are very well distributed throughout the catchment and height of these rain gauge stations are ranging from 955 m. near the Katraj Tunnel to 526m near Rakshewadi. A suitable study period is selected on the basis of availability of common rainfall and resulting runoff data for the catchment. The rainfall and runoff datasets during 1985-2004 is found to be continuous with very less data gaps and considered as study period.

Both parametric and non-parametric statistical techniques as well as GIS based spatial interpolation techniques are incorporated to study the spatio-temporal variability of rainfall pattern throughout catchment. Daily rainfall data are available for all months, whereas, daily runoff data are available only from June to October. According to data providing agency (NHP project, Nasik, India), river flow is very insignificant during rest months of the year. Daily rainfall and runoff records are aggregated to monthly, seasonal and annual datasets. Regression analysis followed by MK test is applied for each rain gauge station to study temporal variability of rainfall pattern. The computational procedure for MK test is given as:

Where Y_i and Y_j are the sequential data, N is the total number of data in the time series.

The runoff pattern near the catchment outlet is being observed carefully. Student's t-test is imposed to detect statistical significant trend in rainfall datasets. The impact of serial correlation

for each rain gauge station analyzed thoroughly before applying MK test, because only serial uncorrelated datasets are eligible to perform MK test.

Results and Discussion

The favourable geographical location of catchment, which lies very close proximity to the eastern margin of the Western ghats and causes heavy rainfall in surrounding areas. The spatial distribution of rainfall pattern for the entire catchment is prepared by taking mean annual rainfall over each station and represented by 300 mm isohyet (Fig 2) in GIS environment. Some of rain gauge stations outside the catchment boundary are also taken into consideration during interpolation process in GIS. From the figure it is very clear that rainfall magnitude is declining as one goes from west to east. Most of the areas in the catchment are under isohyet of less than 600mm. Near Kumbheri the rainfall magnitude is very high due to Western ghat hill ranges and decreases gradually towards catchment outlet. A clear spatial trend exists in the study catchment, which prevails from west to east direction. Station wise mean maximum and minimum rainfall is recorded as 3362 mm at Kumbheri and 310 mm at Malshiras (Figure 3) respectively.

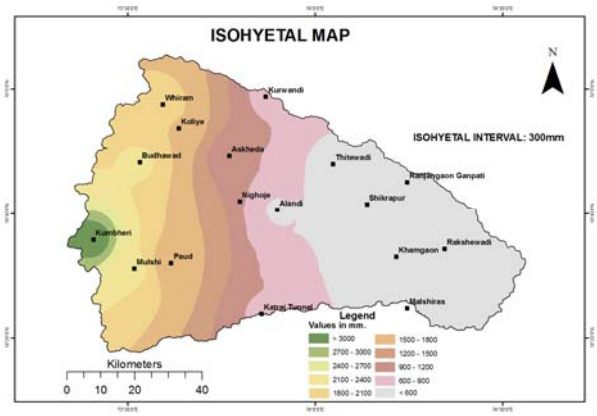

Figure 2. Spatial distribution of Rainfall pattern in the study catchment

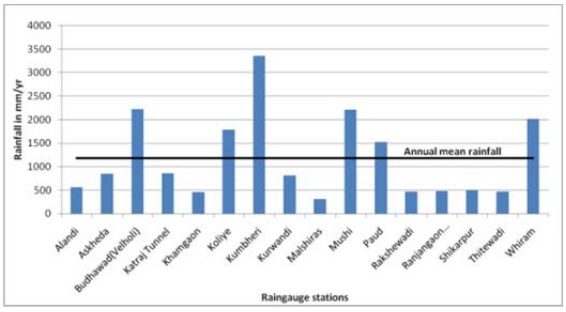

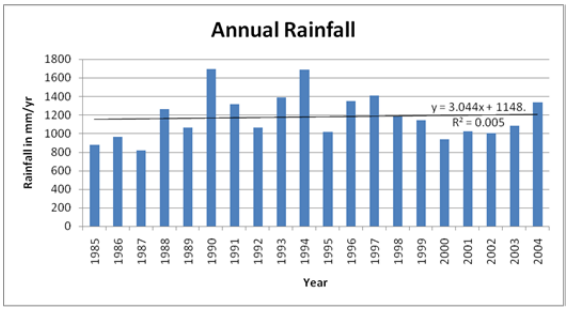

Figure 3. Mean rainfall over each station **Figure 4.** Mean annual rainfall

The mean annual rainfall in catchment is about 1180 mm/yr and only six out of the sixteen stations crossed the catchment average level. These stations are mainly confined to hilly western

region. Most of rainfall in the catchment is occurred during South-West monsoon period (~90%), whereas very insignificant amount of rainfall is being recorded during pre-monsoon (~2%) and winter season (<1%).

Annual rainfall for each rain gauge station is plotted against time and a linear trend line fitted through OLS (ordinary least square) method. Slope of this trend line is given in the table-1, which signifies the rate of increase or decrease of rainfall trend over the particular station during study period. However, these values should be statistically significant to draw any valid conclusion about the rainfall trend. In statistical terms, trend is a determination of whether the probability distribution from which they arise has changed over time (Helsel and Hirsch, 2002).We found that none of these slope values qualify t-test at 5% level of significance. Then MK test is being applied to time series rainfall datasets for each station. MK test is a non-parametric test for identifying trends in time series dataset to detect monotone trends in time series (Mann, 1945; Kendall, 1975). It compares the relative magnitudes of sample data rather than the data values themselves (Gilbert, 1987). One merit of this test is that the data need not to confirm any particular type of distribution. This test imposed on the time series annual rainfall over each rain gauge station. The test revealed that only one station i.e. Koliye has significant trend (Table-1) in the catchment, however its surrounding station doesn't have any trend. This isolated increasing rainfall pattern might be influenced by strong local weather phenomena rather than overall increase in rainfall in the region.

Table 1. Regression and MK test parameters

RG stations	MK test				Regression test		
	τ	S_{MK}	P	R_T	S_R	t_{tat}	R_T
Alandi	0.12	24	0.461	NT	5.11	0.528	NT
Askheda	0.05	10	0.773	NT	2.34	0.32	NT
Budhawad	0.06	12	0.725	NT	22.11	0.87	NT
Katraj	-0.08	-16	0.631	NT	-5.64	-0.67	NT
Khamgaon	-0.04	-8	0.823	NT	0.003	0.0005	NT
Koliye	0.34	66	0.034	T	-6.97	-0.613	NT
Kumbheri	-0.07	-14	0.677	NT	-27.5	-0.613	NT
Kurwandi	0.1	20	0.542	NT	3.92	0.325	NT
Malshiras	0.74	-14	0.677	NT	-0.63	-0.136	NT
Mulshi	0.1	-19	0.559	NT	-13.7	-0.588	NT
Paud	0.07	14	0.677	NT	12.36	0.70	NT
Rakshewadi	-0.19	-36	0.26	NT	-3.56	-0.624	NT
Ranjangaon	0	0	0.974	NT	2.35	0.289	NT
Shikrapur	-0.1	-19	0.559	NT	-4.52	-0.611	NT
Thitewadi	0.1	19	0.559	NT	6.7	0.89	NT
Whiram	-0.02	-4	0.924	NT	2.3	0.098	NT

*τ:Kandell's tou, R_T: Rainfall Trend NT: No trend, T: Trend, p value at 5% significance level S_R:Slope of regression, S_{MK}: MK stat value

From these parametric and non-parametric statistical tests we found that there is no such significant temporal

trend exists over the catchment during the study period or in other words it is more or less constant.

The discharge pattern in catchment is studied near the outlet of Bhima river in the catchment. In the year 1990 and 1994 there was good amount of rainfall followed by high stream flow (Fig. 5). The overall discharge pattern shows very high interannual variation, specifically a decreasing pattern during study period. The interannual variation of stream flow is highly influenced by construction of reservoirs and diversion of water for agricultural and domestic purpose. The decreasing pattern is more prominent after the year 1994. The duration of the whole study year is divided into two decades and named as D1 (1985-1994) and D2 (1995-2004) to study decadal variation of rainfall runoff pattern. A significant declining of runoff is being observed during D2, which is less than half of the stream flow during D1. There are number of reservoirs that have come up during the study period, specifically in D2 period which are meant only for domestic and agricultural activities. The Pune city, which is located in central part in the catchment also influence the steam flow in catchment. The city extent covers less than 10% of total catchment and influences more than half of the catchment areas due to various anthropogenic activities. The population of Pune city is growing at a growth rate of more than 50 percent (2001 census), which receives water from reservoirs built in the upstream areas of catchment. After 1990, substantial expansion of Pune city has been observed. The growing tourism in the Western ghat region also imposes a threat to the water resources in the region. In recent activities, the Temghar Dam was built-up to fulfill growing domestic and industrial water demand, Chaskaman and Askheda dam was built in the year 1999 and 2000 respectively to support agricultural and power sector in the region.

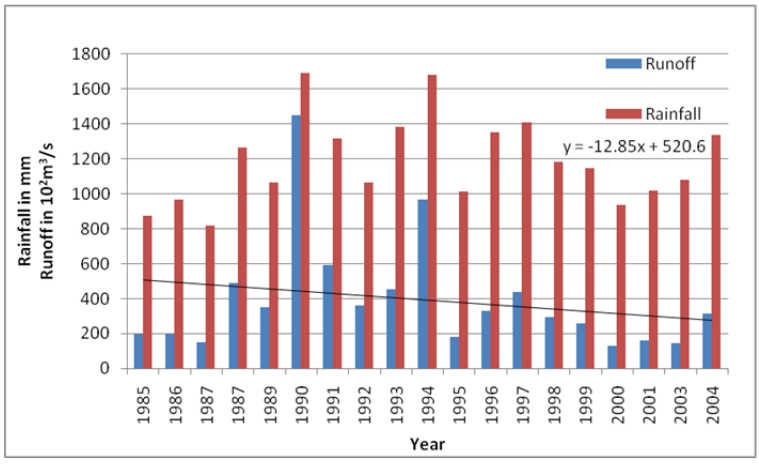

Figure 5. Annual rainfall and runoff over Bhima catchment

Conclusion

From the study it is evident that a clear spatial rainfall trend prevails in the region whereas temporal trend is not significant. Some isolated patches show some sign of increasing trend due

to some strong local influence where as the overall rainfall pattern was constant during study period. The rainfall and resulting runoff indicates decreasing trend of runoff which is resulted due to the construction of reservoirs, increasing demand of domestic water resource in the region. The agricultural activities supported by construction of dams/reservoirs also responsible for decline in runoff in the region. The hard rock basement of catchment discourages groundwater potential in the region. A single dry year could cause a severe water scarcity problem for the entire region. The decreasing trend of runoff will affect the downstream areas because most of water arrested through dams and reservoirs in the heavy rainfall region. An alternative source of water resource as well as suitable water conservation technique in low rainfall region should be adapted to enhance water resource and fulfill future water demand in the catchment.

Future scope of study

The entire catchment can be modeled through SWAT to study land use change on catchment hydrological processes, as the catchment has undergone a rapid land use change in recent years. Validation, calibration, sensitivity analysis and efficiency test should be carried out before applying the model for field application.

Acknowledgements

Authors are thankful to Ministry of Human Resource Development (MHRD) for providing financial assistance to carry out this research work in Centre of Studies In Resources Engineering (CSRE) at Indian Institute of Technology Bombay. India

References

Dinar, A., Blankespoor, B., Dinar, S, and Kurukulasuriya, P. 2010. Does precipitation and runoff variability affect treaty cooperation between states sharing international bilateral rivers? Ecological Economics, 69, 2568-2581.

Gilbert, R.O., 1987. Statistical methods for environmental pollution monitoring. Van Nostrand Reinhold, New York.

Helsel, D.R., Hirsch, R.M., 2002. Statistical methods in water resources. USGS, Book 4, Chapter A3, pp-324.

Kendall, M.G., 1975. Rank Correlation Methods. Griffin, London, (202pp.).

Klavins, M., Bried, A., Rodinov, V., Kokorite, I, and Frisk, T. 2002. Long term changes of the river runoff in Latvia. Boreal environmental research, 7, 447-456.

Mann, H.B., 1945. Nonparametric tests against trend. Econometrica 13, 245–259.

Sharma, R. H, and Shakya, N. M. (2006). Hydrological changes and its impact on water resources of Bagmati watershed, Nepal. Journal of Hydrology, 327, 315- 322.

GIS based Distributed Modelling of Soil Erosion and Sediment Yield for Isolated Storm Events - A Validation Study of DREAM

RAAJ Ramsankaran
Department of Civil Engineering, Birla Institute of Technology and Science Pilani, Pilani-333031, Rajasthan, India. Email: ramsankaran_raaj@yahoo.co.in

Umesh Chandra Kothyari
Department of Civil Engineering, Indian Institute of Technology Roorkee, Roorkee-247667, Uttarakhand, India. Email: umeshfce@iitr.ernet.in

Abstract

This article presents a validation study conducted for a Geographical Information Systems (GIS) based process oriented physically based distributed (PBD) hydrological model called Distributed Runoff and Erosion Assessment Model (DREAM) in the semi-forested watershed of Pathri Rao, located in Garhwal Himalayas, India. DREAM is capable of handling watershed heterogeneity in terms of landuse, soil type, topography, rainfall, etc. and generates runoff and sediment yield estimates in spatial and temporal domains. Unlike other PBD models, all the inputs of DREAM can be measured in field. The model is based on simultaneous solution of flow dynamics followed by soil erosion dynamics. The flow dynamics is based on the well accepted kinematic wave theory. As the storm rainfall proceeds, the process of generation of overland depth is a dependent function of interception storage and infiltration rates. These have been taken care of by the use of modified Merriam (1960) and Smith and Parlange (1978) infiltration approaches. The components of the soil erosion model have been modified for better prediction of sediment flow rates and sediment yields (Ramsankaran 2010). The model validation study conducted to test its performance in simulating soil erosion and sediment yield during different storm events registered in the study watershed shows the model results are satisfactory. It is worthy to mention here that the distributed nature of the model combined with the use of GIS techniques allows computation and presentation of spatial distribution of sediment yield for the simulated storm events.

Introduction

The prediction potential of soil loss rates has improved steadily, from the average annual estimations using the Universal Soil Loss Equation approach (Wischmeier and Smith, 1978) to increasingly complex soil erosion models capable of estimating the consequences of single rainfall events (Favis-Mortlock et al., 2001; Toy et al., 2002). Recent event-based models include DREAM (Ramsankaran et al., 2012), CASC2D-SED (Johnson et al., 2000), EUROSEM (Morgan et al., 1998), KINEROS (Smith et al., 1995), LISEM (de Roo et al., 1996) and WEPP (Flanagan and Nearing, 1995). Detailed list is available elsewhere and also can be found in Ramsankaran (2010). Though there are many more models available, it is not always clear when and where to use which type of model (Singh and Woolhiser, 2002). Comparison of some of the models shows that no one model works well in every situation of runoff and sediment yield generation in the watersheds (Bingner et al., 1989). Many of the models require enormous data for parameterization and calibration which is not feasible to obtain for most of the watersheds, subsequently preclude their use universally.

It is in this background, a relatively simple process oriented PBD model called Distributed Runoff and Soil Erosion Assessment Model (DREAM), has been developed by keeping in mind that the model should be applicable to un-gauged watersheds too. As the DREAM model is relatively new, only few validation studies are available. Hence to popularize and to highlight the capability of the DREAM model, brief details of the DREAM and its validation study conducted using real world data are therefore presented in this article.

Dream Model Description

The developed water induced soil erosion model consists of two components that are linked together to allow computations of soil erosion and sediment yield from watersheds. The first part comprises surface flow dynamics and the second pertains to soil erosion dynamics. Flow dynamics provides inputs such as velocity of flow, depth of flow, and discharge rate, which in turn serve as the components of soil erosion dynamics. The approach assumes that the sediment concentration in the overland flow is sufficiently small so that it does not affect the flow regime. Under such an assumption, both the processes, viz., rainfall–runoff and the soil erosion so caused can be solved independently. The flowchart depicting all the processes (both hydrodynamics and soil erosion dynamics) considered in the DREAM model is illustrated in Fig. 1. All the processes have been coded in to a modular computer program using FORTRAN 90 programming language (Ramsankaran, 2010). All the model inputs and outputs are compatible with standard GIS data formats so that they can be viewed and analyzed in any GIS platform.

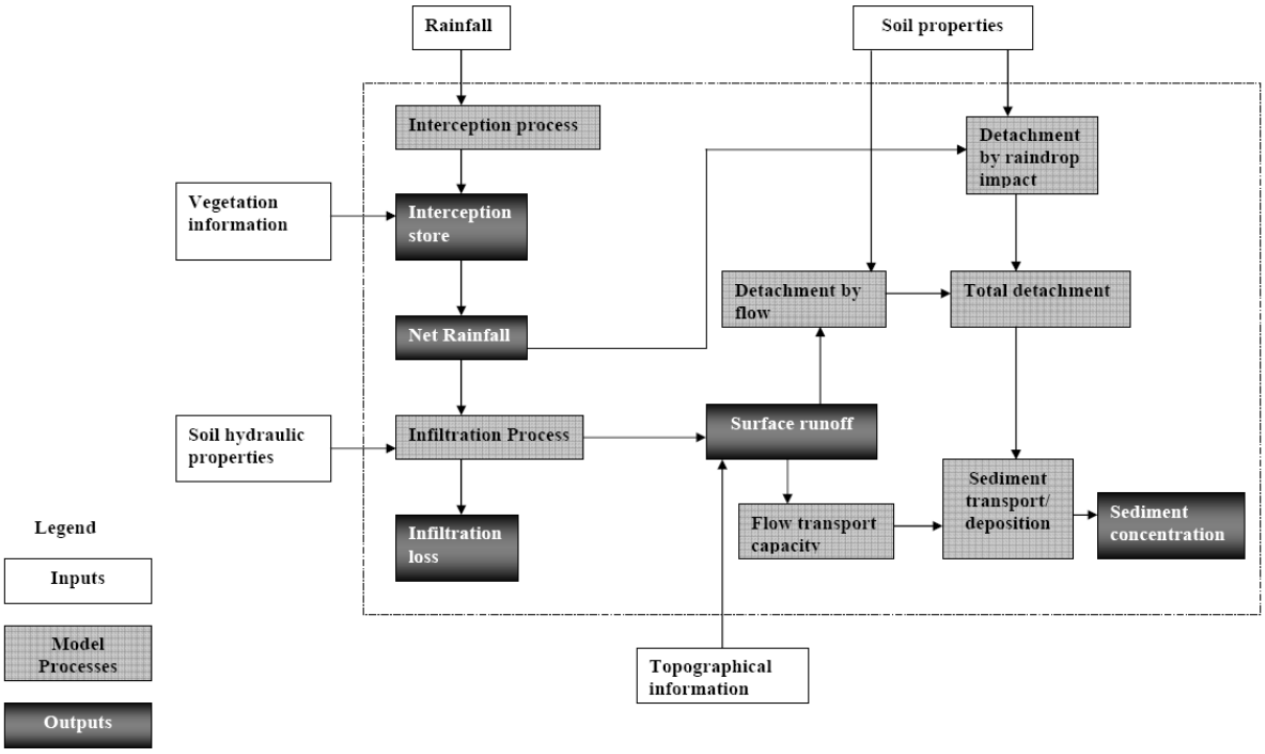

Figure 1. Flowchart depicting the processes considered in DREAM

Model Application

To test the predictive ability and performance of the proposed model, it has been applied for simulating few storm events observed in the Pathri Rao watershed located in Shivalik ranges of Garhwal Himalayas, India.

Study Area Description

The study watershed selected for validating the developed model is located at about 17 km north-east of Roorkee town, Uttarakhand, India. It lies between the latitude of 28° 55' N to 30° 05' N and longitude of 78° to 78° 05'. The location of the watershed is depicted in Fig. 2. The catchment area of the watershed up to the gauging station at watershed outlet is about 38 km^2. Elevation of the watershed ranges between 272 m and 730 m. The lower tracts of the watershed area are having flat slopes and are therefore, densely habituated while the upland areas consists of mostly hilly terrain having steep slopes. These are densely forested and form a part of Rajaji National park which falls in the Shivalik foothills of Garhwal Himalayas. In the lower part of the watershed wheat–maize crop rotation is being followed. The watershed receives an average annual rainfall of 1300 mm with an average of 50 rain days with more than 90% of it occurring during the monsoon season, i.e. between June to September. High intensity and short duration storms are very common in the area. The mean minimum and maximum temperatures in the region are 3°C and 42°C, respectively. The mean relative humidity varies from a minimum of 40% in April to a maximum of 85% in the month of July. The overall climate of the area can be classified as semi-arid to humid sub-tropical region.

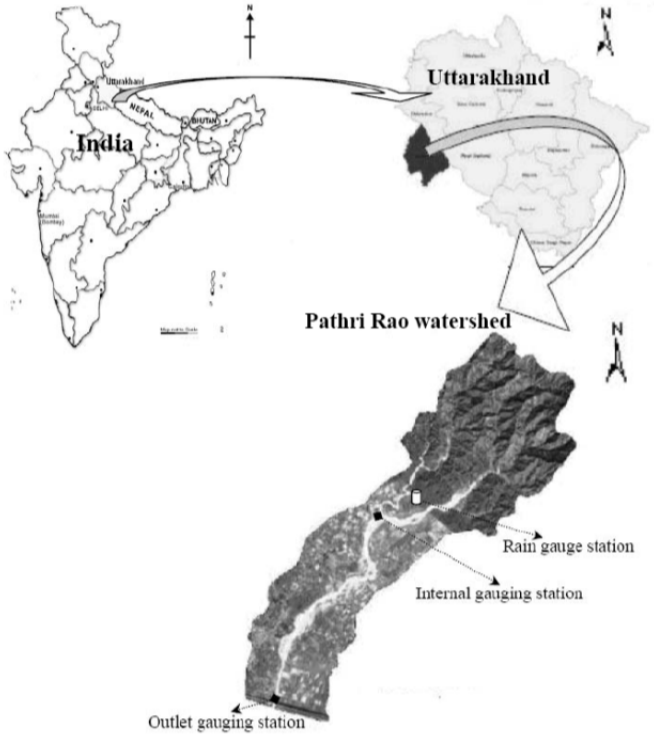

Figure 2. Location map of the Pathri Rao watershed

The major soil groups found in the watershed are loam, sandy loam, loamy sand, coarse sandy loam and silt loam. The average soil depth ranges from 0 cm to 100 cm. The river is of influent type which has flows only during the storm events. The watershed has never been gauged earlier. For the purpose of present study, field observations on rainfall, runoff and sediment yield have been made during the monsoon storm events of the year 2005 (Kothyari and Ramsankaran, 2010; Kothyari et al., 2010; Ramsankaran, 2010).

Model Parameterization

The DREAM model requires several parameters related to rainfall, soil and landuse characteristics in a spatially distributed form. Table 1 shows those spatially distributed parameters required by DREAM. The spatial information can be given directly or supplied by appropriate surrogate maps, such as soil maps for texture and hydraulic properties and land-use maps for the remaining parameters. Model parameterization comprises calibration of the model for various set-ups. Accordingly, six parameters viz., initial soil moisture index, Manning's overland/channel roughness index, saturated hydraulic conductivity, soil porosity, soil cohesion and soil detachability were chosen for calibration due to their sensitivity to rates of runoff and soil loss and timing of the peak flow and sediment discharge (Ramsankaran et al., 2012; Ramsankaran, 2010). Out of the available five storms, two storms were arbitrarily chosen for the calibration exercise varying both in terms of intensity and duration (Table 2). Five equal-span values, which were within the ranges suggested by Morgan et al. (1998), Woolhieser et al. (1990), and Rawls and Braunswiek (1989), were assigned to each parameter. All combinations of parameter values were used to run the model simulation. The best combination of parameter values was determined based on the visual fit of hydrographs and sedimentographs, Pearson's correlations between simulated and measured measurements, root mean square error (Smith et al., 1996), and the mean difference between measurement and simulation (Addiscott and Whitmore, 1987), etc.

The results of the calibration exercise are given in Table 3. For illustration purpose, the sedimentographs for one of the calibration storm events representing a successful calibration is shown in Fig. 3. From Table 4 that shows the statistical estimates, it is clear that except the sediment yield for 23 July 2005 storm event, other variables like peak sediment discharge and time to peak sediment discharge for both the calibration events have the PE values ranged only between -5% and +12%. Further, it may be noted that for 6 August 2005 event the PE in predicting the sediment yield, peak sediment discharge and time to peak sediment discharge is less than ±5%. Such accuracy is considered to be excellent, because even the more elaborated process based soil erosion models are found to produce results with still larger errors (Foster, 1982; Jain, 2002; Wicks and Bathurst, 1996; Wu et al., 1993).

Table 1. Spatially Distributed Parameters Required by DREAM.

Input parameter description	Units	Source of information used in this study	Description/Remarks
Meteorological forcing			
Rainfall Intensity	mm hr^{-1}	Field measurements	Break point rainfall data.
Landuse/cover parameters			
Canopy cover fraction(c_f)	%	Woolhiser et al. (1990) and Sunil Chandra (personal communication)	As per growth stage of the vegetation.
Maximum interception storage capacity (s_c)	mm	Morgan et al. (1998)	As per canopy cover and the size, shape and roughness of its leaves.
Manning's overland roughness index (n_o)	-	Engman (1986) and Vieux (2001)	-
Manning's channel bed roughness index (n_c)	-	Arcement and Schneider (1992)	-
Soil texture based parameters			
Soil infiltration parameters			
Initial Soil moisture Index (S_{ini})	%	Antecedent daily rainfall records	Storm event dependent
Saturated hydraulic conductivity (K_s)	mm hr^{-1}	Rawls and Brakensick (1989)	-
Capillary Drive (G)	mm	Rawls and Brakensick (1989)	-
Porosity(η)	-	Rawls and Brakensick (1989)	-
Soil erosion dynamics parameters			
Soil detachability (K)	g J^{-1}	Morgan et al. (1998)	-
Soil cohesion(J)	kPa	Morgan et al. (1998)	-
Particle median size (d_{50})	□m	USDA (1975) and Munõz-Carpena and Parsons (2000)	-

Table 2. Hydro-meteorological parameters of the selected storm events.

Date of the storm event	Rainfall depth (mm)	Duration (hr)	Initial soil moisture index (%)*
26.06.05 (v)	36.07	2.5	0.20 -0.30
23.07.05 (c)	40.34	2.5	0.50 - 0.60
04.08.05 (v)	39.04	3	0.15 - 0.40
06.08.05 (c)	24.87	1.5	0.70 - 0.80
10.09.05 (v)	17.93	1	0.25 - 0-50

* A likely initial estimate based on antecedent daily rainfall records

Table 3. Model results on sedimentograph variables for the calibration and validation storm events in Pathri Rao watershed.

Storm events	Sediment yield (tonnes)		Peak sediment discharge (kg s^{-1})		Time to peak sediment discharge (min)	
	Obs.	Comp.	Obs.	Comp.	Obs.	Comp.
(a)Calibration events						
23 July 2005	916.20	1221.68	169.56	190.12	195	218
6 August 2005	744.80	706.51	115.89	110.02	180	183
(b)Validation events						
26 June 2005	278.33	226.38	37.61	25.72	255	288
4 August 2005	731.18	746.13	115.25	118.10	195	203
10 September 2005	113.61	101.89	22.21	14.58	210	233

Table 4. Summary of parametric statistical results on sedimentograph variables for the calibration and validation storm events in Pathri Rao watershed.

Storm events	Percentage error in prediction			R^2	wR^2	NS-EF (%)
	SY_{storm}	$Q_{(s)peak}$	$T\text{-}Q_{(s)peak}$			
(a)Calibration events						
23 July 2005	+ 33.34	+12.12	+11.79	0.76	0.64	73.82
6 August 2005	-5.14	-5.07	+1.67	0.99	0.93	99.22
(b)Validation events						
26 June 2005	-18.66	-31.61	+12.94	0.61	0.42	54.16
4 August 2005	+2.04	+2.47	+4.10	0.98	0.95	97.79
10 September 2005	-10.32	-34.35	+10.95	0.76	0.45	70.25

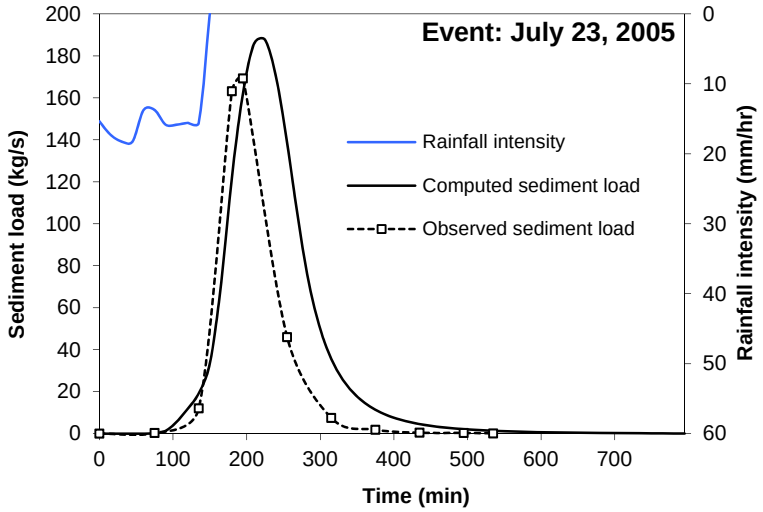

Fig. 3. Comparison of computed and observed sedimentographs of July 23, 2005 storm event in the Pathri Rao watershed.

Model Validation

The parameter file resulting from the calibration was used for the validation exercise using data of three of the remaining rainfall events (Table 2). Simulated values of runoff rate, cumulative runoff, sediment concentration, soil loss rate and cumulative soil loss were compared graphically with observations (Ramsankaran 2010). It can be seen from Tables 3 and 4 that the computed sediment yield, peak sediment discharge and time to peak sediment discharge compares well with their corresponding observed values for the validation storm events as well. Visual inspection of two of the simulated and observed sedimentographs shown in Figs. 4 and 5 and the summary of the statistical results for all the validated storm events reveal that the model performance and efficiency are generally good. Keeping in view the complex nature of the process of soil erosion and sediment yield and relatively larger size of the study watershed, the results presented here indicate that the proposed DREAM model realistically simulates the overall shape of the sedimentographs for all the three validation storm events.

With the use of GIS techniques, the distributed nature of the present model allows generation and presentation of spatial distribution of sediment yield resulting from a storm event. Such maps, however, would be extremely useful in identifying the sediment source areas so that the areas producing more sediment could be given top priority for implementation of appropriate soil conservation measures. Pattern of spatial distribution of sediment yield has been studied for all the storm events in the study watershed. For illustration purpose, one such spatial distribution map of sediment yield for the storm event occurred on 10 September 2005 have been generated and presented in Fig.6. This and other such figures (Ramsankaran, 2010) indicate that the high sediment source areas are mainly lying in the overland plane areas that have less vegetation and steep slopes. Such results are understandable and are on expected lines.

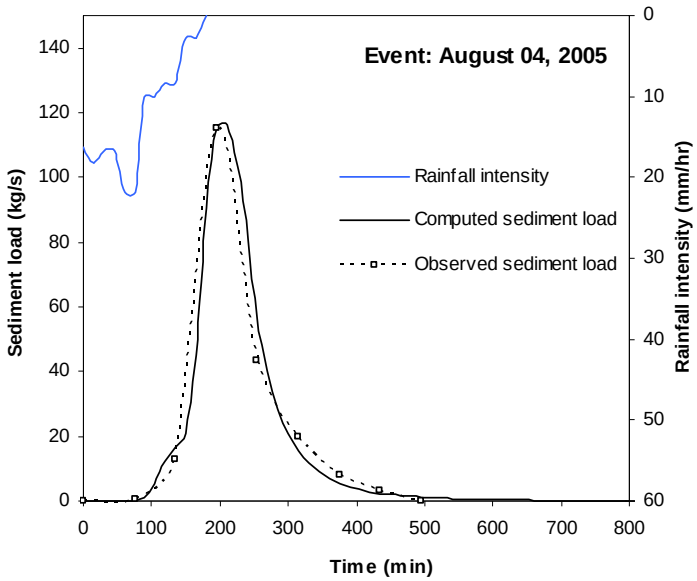

Fig. 4. Comparison of computed and observed sedimentographs of August 04, 2005 storm event in the Pathri Rao watershed.

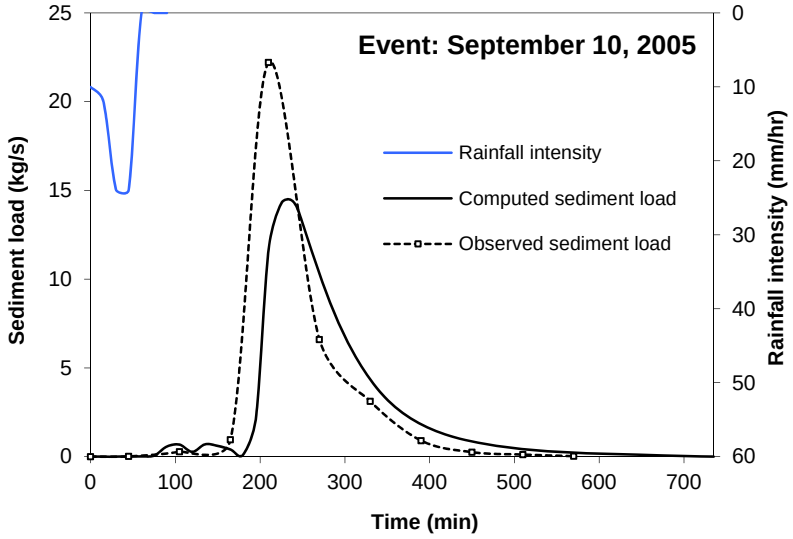

Fig. 5. Comparison of computed and observed sedimentographs of September 10, 2005 storm event in the Pathri Rao watershed.

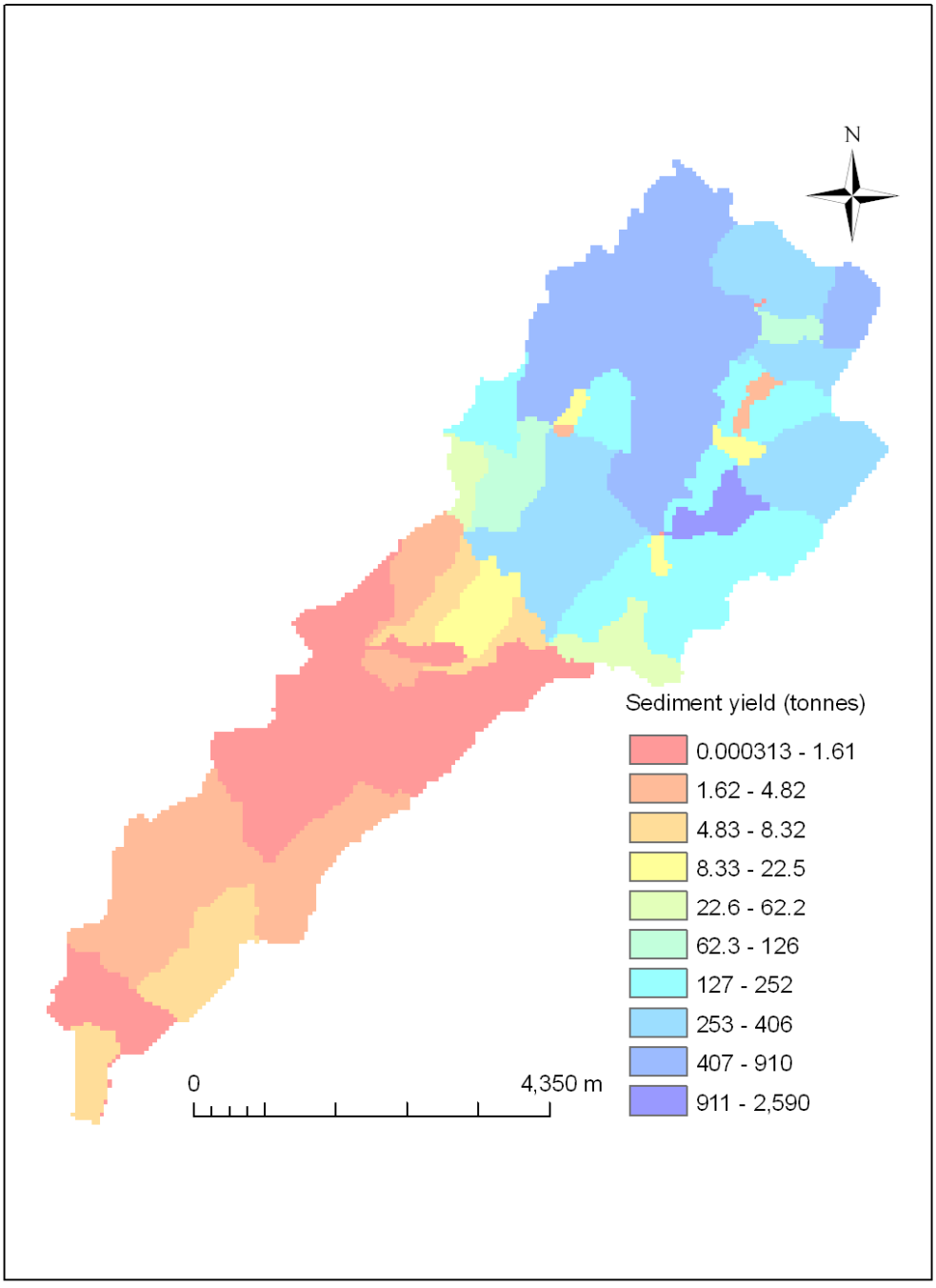

Fig. 6. Spatial distribution of computed sediment yield for September 10, 2005 storm event in the Pathri Rao watershed.

Conclusions

The results reported in this paper indicate that DREAM can simulate soil erosion and sediment yield reasonably well for individual storm events. Considering the complex nature of the soil erosion and sediment yield processes and the inbuilt errors in the numerous hydrologic interrelationships used in the simulation of soil erosion dynamics under natural conditions, the deviation of ±30% may not be considered high. Hence the DREAM stands validated yet under simplified conditions. It is encouraging to be able to say that this study did indicate that the DREAM can work under certain conditions in the Pathri Rao watershed. However many more validation studies need to be carried out for many sites under various scenarios to establish the model performance trends and its consistency.

References

Addiscott, T. M., A. P. Whitmore. 1987. Computer simulation of changes in soil mineral nitrogen and crop nitrogen during autumn, winter and spring. *J. Agric. Sci. Camb.* 109: 141-157.

Arcement Jr., G. J., and V. R. Schneider. 1992. Guide for selecting Manning's roughness coefficients for natural channels and flood plains. *USGS Water Supply Paper* 2339: 38.

Bingner, R. L., C. E. Murphree, and C. K. Mutchler. 1989. Comparison of sediment yield models on watersheds in Mississippi. *Trans. Am. Soc. Agric. Biol. Eng.* 32: 529-534.

de Roo, A. P. J., C. G. Wesseling, and C. J. Ritsema. 1996. LISEM: a single event physically-based hydrological and soil erosion model for drainage basins: I—theory, input and output. *Hydrol. Process.* 10(8): 1107-1117.

Engman, E. T. 1986. Roughness coefficients for routing surface runoff. *J. Irrig. Drainage, ASCE* 112: 39-53.

Favis-Mortlock, D., J. Boardman, and V. MacMillan. 2001. The limits of erosion modeling: why we should proceed with care. In *Landscape Erosion and Evolution Modeling*, 477-516.Harmon, R. S., and W. W. Doe, eds. New York: Kluwer Academic/Plenum Publishers.

Flanagan, D. C., and M. A. Nearing. 1995. *USDA Water Erosion Prediction Project: Hillslope profile and watershed model documentation. NSERL Report no. 10*. West Lafayette: USDA-ARS National Soil Erosion Research Laboratory.

Foster, G. R. 1982. Modelling the erosion processes. In *Hydrologic Modelling of Small Watersheds, ASAE Monograph No. 5*, 295–380. C. T. Haan, H. Johnson and D. L. Brakeniek, eds. St. Joseph, Michigan: American Society of Agricultural Engineers.

Jain, M. K. 2002. Distributed modelling of runoff and sediment yield using remote sensing and GIS. Unpublished PhD diss. Indian Institute of Technology Roorkee, Roorkee, India.

Johnson, B. E., P. Y. Julien, D. K. Molnar, and C. C. Watson. 2000. The two-dimensional upland soil erosion model CASC2D-SED. *J. Am. Water Res. Assoc.* 36: 31-42.

Kothyari, U. C., and RAAJ. Ramsankaran. 2010. Application of distributed hydrologic modelling in Pathri Rao and Khulgad watershed for watershed evaluation, runoff harnessing and soil erosion abatement. Final Project Report submitted to NRDMS Division, Department of Science and Technology (DST) New Delhi (Unpublished).

Kothyari, U. C., RAAJ. Ramsankaran, D. Sathish Kumar, S. K. Ghosh, and N. Mendiratta. 2010. Geospatial based automated watershed modeling in Garhwal Himalaya. *IWA J. Hydroinform.,* 12(4): 502-520.

Morgan, R. P. C., J. N. Quinton, R. E. Smith, G. Govers, J. W. A. Poesen, K. Auerswald, G. Chisci, D. Torri, M. E. Styczen, and A. J.V. Folly. 1998. *The European Soil Erosion Model (EUROSEM): Documentation and User Guide*. Silsoe College, Cranfield University.

Muñoz-Carpena, R., and J. E. Parsons. 2000. *VFSMOD User's Manual*, vol. 1.04. North Carolina State University, Raleigh, NC, USA.
Ramsankaran, RAAJ. 2010. Distributed modelling of runoff and sediment yield based on geospatial techniques. Unpublished PhD diss. Indian Institute of Technology Roorkee, Uttarakhand, India.
Ramsankaran, RAAJ., U. C. Kothyari, S. K. Ghosh, A. Malcherek, and K. Murugesan.2012. Physically based distributed modelling of soil erosion and sediment yield for isolated storm events. *Hydrol. Sci.* (Accepted)
Rawls, W. J., and Brakensiek, D. L. 1989. Estimation of soil water retension and hydraulic properties. In *Unsaturated Flow in Hydrologic Modeling: Theory and Practice*, 275-300. Morel-Seytoux, ed. Boston: Kluwer Academic Publisher.
Singh, V. P., and D. A. Woolhiser. 2002. Mathematical modeling of watershed hydrology. *J. Hydrol. Eng.* 7: 270-292.
Smith, R. E., D. C. Goodrich, and J. N. Quinton. 1995. Dynamic, distributed simulation of watershed erosion: the KINEROS2 and EUROSEM models. *J. Soil Water Conserv.* 50, 517-520.
Smith, J., P. Smith, and T. Addiscott. 1996. Quantitative methods to evaluate and compare soil organic matter (SOM) models. In *Evaluation of Soil Organic Matter Models Using Existing Long-Term Datasets. NATO ASI Series I*, Vol. 38, 181-199. Powlson, D. D., P. Smith, and J. U. Smith, eds. Heidelberg: Springer-Verlag.
Toy, T. J., G. R. Foster, and K. G. Renard. 2002. *Soil Erosion: Processes, Prediction, Measurement, and Control*. New York: John Wiley & Sons, Inc.
U.S. Department of Agriculture (USDA). 1975. *Soil Taxonomy. Hand book 436* p. 752. Washington, DC: USDA, DC.
Vieux, B. E. 2001. *Distributed Hydrologic Modeling Using GIS*. Dordrecht, The Netherlands: Kluwer Academic Publishers.
Wicks, J. M., and J. C. Bathurst. 1996. SHESED: a physically based, distributed erosion and sediment yield component for the SHE hydrological modeling system. *J. Hydrol.* 175: 213-238.
Wischmeier, W. H., and D. D. Smith. 1978. Predicting rainfall erosion losses. In *Agricultural Research Service Handbook*, vol. 537, 1-58. Washington, DC: USDA.
Woolhiser, D. A., R. E. Smith, and D. C. Goodrich.1990. *KINEROS: A Kinematic Runoff and Erosion Model: Documentation and User Manual*. USDA Agricultural Research Service ARS-77.
Wu, T. H., J. A. Hall, and J. V. Bonta. 1993. Evaluation of runoff and erosion models. *J. Irrig. Drainage Eng. Am. Soc. Civil Eng.* 119, 364-382.

Hydrologic Modelling of the Eastern Contributing Basins of Vembanad Lake using SWAT

Raktim Haldar
Department of Civil Engineering, Indian Institute of Technology, Delhi
Hauz Khas, New Delhi -110016, India
rhaldar.iitd@gmail.com

Rakesh Khosa
Department of Civil Engineering, Indian Institute of Technology, Delhi
Hauz Khas, New Delhi -110016, India
rakesh.khosa@gmail.com

A K Gosain
Department of Civil Engineering, Indian Institute of Technology, Delhi
Hauz Khas, New Delhi -110016, India
akgosain@gmail.com

Abstract

Modelling plays a very important role in arriving at the diagnosis of past behaviour as well as a prognosis of the likely future states of a given basin's hydrology. It is indeed important to objectively evaluate impacts of past or proposed anthropogenic intervention on the natural system's hydrologic and/or hydraulic responses. In this study rainfall runoff models have been developed for the five principal contributing river basins of the Vembanad Wetland System in the state of Kerala in India and further, within this derived hydrologic framework, the likely future impacts of various water resources development initiatives have also been assessed.
Flow from the five rivers namely Muvattupuzha, Meenachil, Manimala, Pamba and Achenkovil debouch into the southern part of the lake system. Hydrologic models, duly calibrated and validated using available record of observations, were developed for these latter systems using ArcSWAT. Simulations were performed for the presently existing development scenario as well as the likely future scenario by incorporating all known developmental proposals in addition to the proposal that entails a trans-basin-boundary export to the Vaippar basin in the neighbouring state of Tamil Nadu. The impact on the flow in terms of percentage reduction was found to be greater during non-monsoon season when the rainfall is relatively meagre thus rendering the system more vulnerable to possible degradation of the riverine and the connected lake environments.

Keywords: Hydrology, SWAT, Rainfall-Runoff Modelling, Kuttanad, Vembanad Lake

Introduction

Water is a precious natural resource and its management determines its prospective capability to sustain growth and development related aspirations of the society and its balance with the need to maintain the ecological integrity of its hydrologic crucible. In order to keep pace with the global economic growth and industrial development, drainage basins all over the world are in the process of alteration by man. The last few decades have seen a lot of change in the field of water resources development. In the blind run for economic development a lot of anthropogenic influences have been imposed upon the natural systems raising the question of sustainability. Hence, it has now become a practice to study the probable impacts of any proposed water resource development with the help of hydrologic modelling. The importance of hydrologic modelling can be easily felt through the visible direct and indirect impacts that anthropogenic influences have already had in the past (Plan, R., 2005; Leichenko and Wescoat Jr, 1993; Caliandro et al., 1992; Goldsmith and Hildyard, 1986; Ji et al., 2006).

Out of the various natural water bodies lakes and wetlands have an important position. The importance of wetlands, specially, came to light lately, before which, they were thought to be wastelands. Lots of wetlands were harmed in satisfying the acute needs of human requirements such as progressive industrialisation, enhanced food production and recreation raising need of concern for the present day scientists (Menon et al., 2000). Water resources development of any area serves one or more of the purposes such as irrigation, flood control, hydro power development, soil conservation, water distribution, pollution control, sediment control, salinity control, water exports to neighboring basins, etc. At the same time they have also created many side effects due to man's interference with the environment (Kannan, 1979). Similarly construction of artificial structures like dams may pose serious problems in both the upstream and downstream areas (Limbe, 1998).

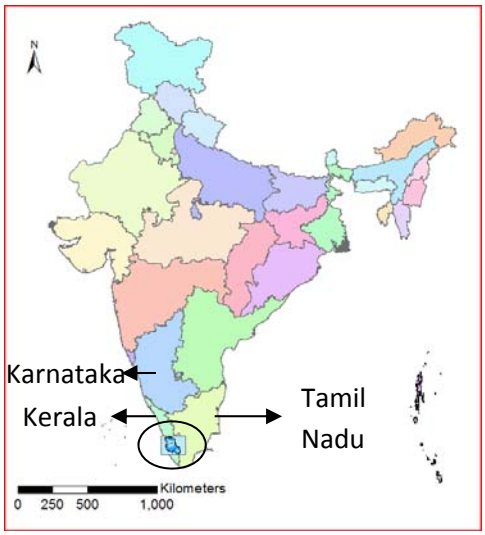

Figure 1: Location of study area in Kerala, India

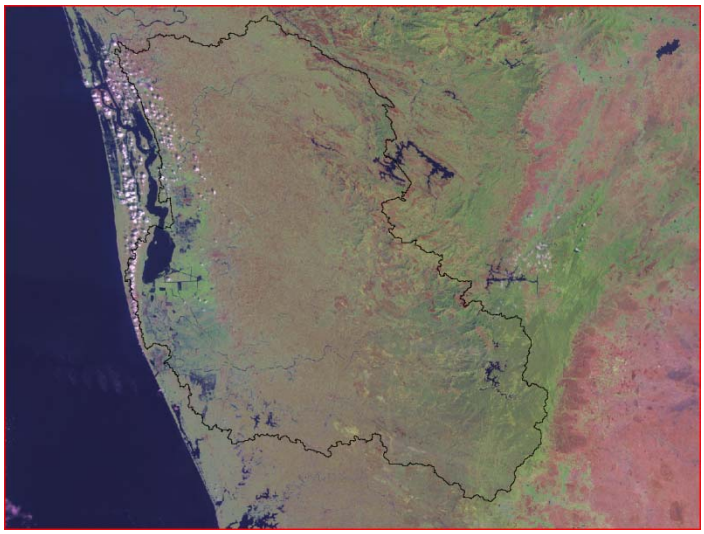

Figure 2: Pseudo colour LANDSAT imagery of the study area

The present study consists of a rainfall-runoff modelling for five river basins along with the calibration and validation for flow in each of the rivers, and then using the same models for predicting the impact of different upcoming or proposed projects that are going to be individually or collectively responsible to change the flow regime of the rivers. The study area consisting of the five river basins of Muvattupuzha, Meenachil, Manimala, Pamba and Achenkovil lying in Kerala receives a high average annual rainfall of about 3000 mm. Kerala is one of the southern states of India, being surrounded by Tamil Nadu on the east, the Arabian Sea on the west and Karnataka in the North. The state receives two monsoon rains, the southwest monsoons in the months of June to September and the northeast monsoons in the month of October and November (Simon and Mohankumar, 2004). However the basins have a peculiar geometry that provides special attribute to the runoff characteristics of the area. The upper reaches of the basins are steep sloped and the downstream parts of the rivers join the Vembanad Lake and wetland system where the terrain is almost flat. Also, the rivers are only rain-fed, that is, there is no contribution from snow melt. So, the upper reaches practically run out of water in the non-monsoon period. Two centuries ago the Vembanad Lake and wetland system covered an area of almost 363 km^2. However, on account of the excessive wetland reclamation the water-spread as well as volume has reduced by more than 60% of what it was earlier in order to facilitate paddy cultivation bi-annually and also establish industries in the low-lying regions (Swaminathan et al., 2007). The present lake area is separated from the adjacent plains by manually constructed bunds. These bunds are either concrete retaining wall type or temporary mud-wall type strengthened by coir geo-textile membranes (Sarma and Jose, 2008).

Another interesting feature of the region is the Western Ghats which forms a boundary between the states of Kerala and Tamil Nadu, affecting the rainfall pattern in the area. The part of Tamil Nadu which falls in the leeward zone gets lesser rainfall. Figures 3 to 5 present the comparison of rainfall at four grid locations, two each on both sides of the Western Ghats. Figures 3 and 4 show the location of four points on the map and the intervening topography (altitude above MSL). Two of the points on the eastern side of the Western Ghats (9.5°N, 77°E and 9°N, 77°E) receive lesser precipitation than the other two (9.5°N, 77.5°E and 9°N, 77.5°E), which lie on the eastern side. Figure 5 shows the plot of the annual rainfall for the years 1969-2005. The average annual rainfall at the four grid locations are summarised in Table 1 calculated over 37 years (1969-2005).

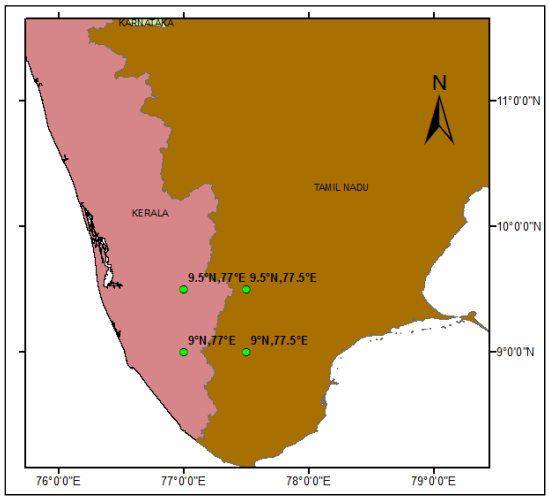

Figure 3: Location of four grid points with the states Kerala and Tamil Nadu

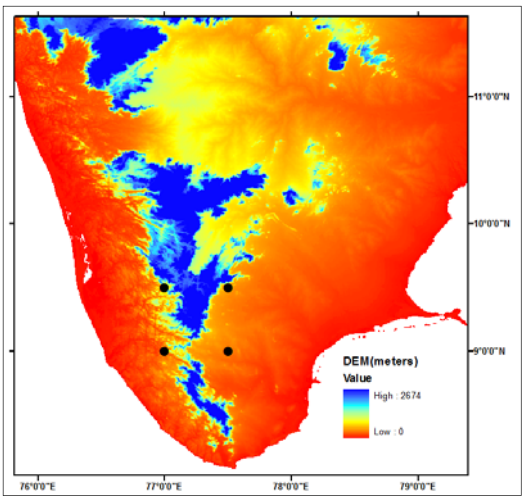

Figure 4: Topography showing a portion of the Western Ghats

The National Water Development Agency (NWDA) proposed, as a part of the interlinking plan of Indian rivers, inter basin water transfer from the rivers Achenkovil and Pamba to Vaippar basin with the construction of three reservoirs and pipeline system for transferring water. The Pamba Achenkovil- Vaippar Link Project (PAVLP) proposed an annual diversion of 634M cu.m of water from Pamba and Achenkovil rivers in Kerala to irrigate areas in the Vaipar river basin in Tamil Nadu. Apart from this, the project envisioned generation of 508 MW of power and providing regulated releases of 150 M cu.m of water during seasons of lean flow in the rivers Pamba and Achencoil to improve the lean season flows and combat salinity intrusion (NWDA Report, 1995).

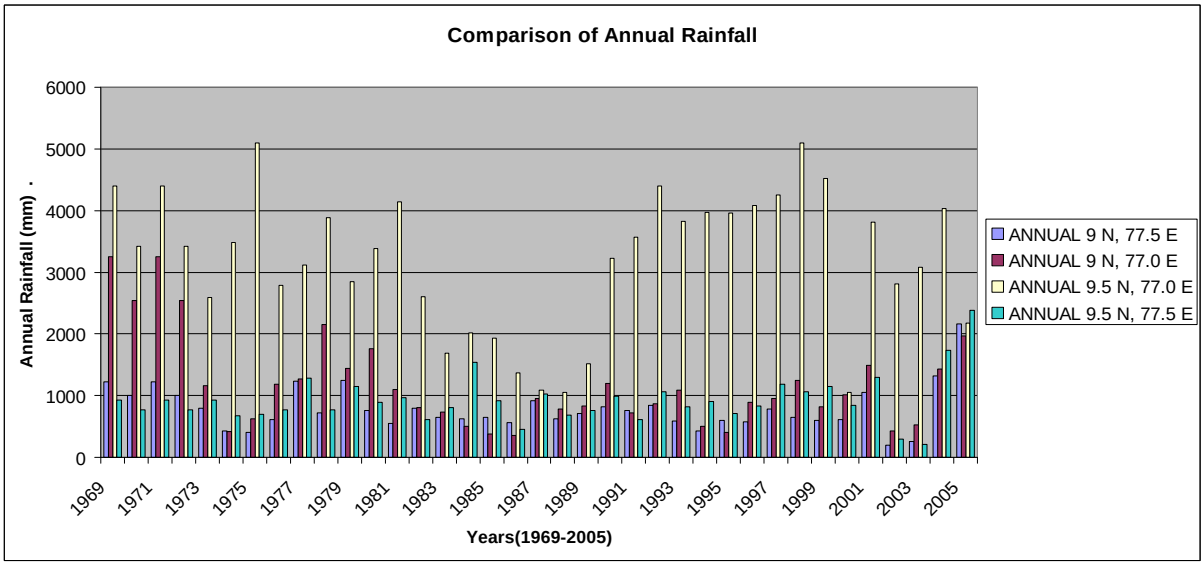

Figure 5: Plot of Annual rainfall for the years 1969-2005

Table 1: Average annual rainfall

Location	Average Annual Rainfall (mm)
9 N, 77.5 E	783.3051351
9 N, 77.0 E	1177.429459
9.5 N, 77.0 E	3191.878108
9.5 N, 77.5 E	929.3027027

The current study attempts to find the implications of this and two other upcoming projects, the Perunthenaruvi Small hydroelectric project and the Ranni-Perunad small hydroelectric project, on the flow conditions in the Pamba and Achenkovil rivers. The Soil and Water Assessment Tool (SWAT) model was selected for this study owing to its dependability based on its broad usage all around the globe for hydrologic modelling and water quality simulation for large as well as small catchments. The SWAT model has been extensively tested for hydrologic modeling at different spatial scales (Zhang et al., 2008) as can be seen clearly from the works of Gollamudi et al. (2007), Spruill et al. (2000), Chu and Shirmohammadi (2004), Santhi et al. (2001a), Zhang et al. (2007), Srinivasan et al. (1998) and Arnold et al. (1999). The suitability of the SWAT model in Indian conditions has been assessed by Kaur et al., (2003).

SWAT is a physical process based model to simulate continuous-time hydrological processes at a catchment scale (Arnold et al., 1998; Neitsch et al., 2005). The catchment is divided into subbasins as per spatial distribution of tributaries and further into hydrological response units (HRUs) based on soil type, land use and slope classes that allows a high level of spatial detail simulation. The major model components include hydrology, weather, soil erosion, nutrients, soil temperature, crop growth, pesticides agricultural management and stream routing. The historical development and application areas of SWAT have been discussed by Gassman et al. (2007).

Materials and Methods

Description of the modelled area

The coastal boundary of Kerala has a continuous chain of lagoons or backwaters. These water bodies are fed by rivers and drain into the Lakshadweep Sea through small openings in the sandbars called 'azhi', if permanent or 'pozhi', if temporary (Swaminathan et al., 2007). The largest among these backwater systems is the Vembanad wetland system. The latitudinal and longitudinal extent of the five study river basins along with other their corresponding area modelled in SWAT and their maximum elevations with respect to mean sea level (MSL) are given in Table 2.

The total catchment area contributing to the lake consisting partly wetlands and partly the five river basins Muvattupuzha, Meenachil, Manimala, Pamba and Achenkovil is approximately 7400 km^2. Also a part of the Periyar River joins the northern estuary which drains its water partly through the Azhikode outlet and partly through the Kochi outlet. However, the basin area of Periyar has not been included as a contributing basin to the Vembanad wetland because (i) a significant fraction of the Periyar water is diverted to the neighbouring Vaigai system from the Mullaperiyar Dam located in the upstream part of the Periyar river; and (ii) it joins the wetland system in the Azhikode estuary quite north of the main lake body and discharges a major part of its water through the Azhikode outlet near Munambam, thus having negligible influence on the part of Vembanad Lake south of Thanneermukkom Bund. The Thanneermukkom bund or salt water barrier was constructed in 1975 to prevent the intrusion of saline water from the Cochin estuary into the southern part of the Vembanad Lake and hence allow paddy cultivation in the Kuttanad region more than once a year.

The area through which these five rivers flow just before joining the Vembanad Lake is known as the Kuttanad region. The region is the deltaic formation of the west flowing river systems called the rice bowl of Kerala. The Kuttanad is a low-lying region extending over an area of about 1100 km^2 in Kottayam and Allepey districts of Kerala and much of the area are below the sea level (Thampatti and Padmakumar, 1999). The somewhat higher area in the south-east of Kuttanad is called upper Kuttanad and the elevations here range from 0.5m below to 6.0m above MSL. The core area of Kuttanad is lower Kuttanad and the land levels here are 1.5m below to 1m above MSL.

Table 2: Spatial details of the five basins

Sl. no	Basin	Latitudinal Extent	Longitudinal Extent	Approximate Area (sq.km.)	Maximum Elevation (m)
1	Muvattupuzha	9° 41' N to 10° 8' N	76° 22' E to 77° 00' E	1593.14	1257
2	Meenachil	9° 26' N to 9° 52' N	76° 22' E to 77° 57' E	777.15	1182
3	Manimala	9° 19' N to 9° 41' N	76° 22' E to 77° 00' E	996.92	1379
4	Pamba	9° 10' N to 9° 20' N	76° 22' E to 77° 18' E	1744.84	1916
5	Achenkovil	9° 0' N to 9° 20' N	76° 25' E to 77° 17' E	1188.20	1881

The Vembanad-Kol Wetland was included in the list of wetlands of international importance, as defined by the Ramsar Convention for the conservation and sustainable utilization of wetlands in 2002, where its area is mentioned as 151,250 ha. It is home to more than 20,000 waterfowls in India. Major livelihood activities include agriculture, fishing, tourism, inland navigation, coir retting, lime shell collection.

Due to the orographic influence of the Western Ghats the annual rainfall at different locations in the area vary from 2000 mm to 5000 mm. That is to say, the range of spatial variation of annual rainfall in the catchment area may be as high as 3000 mm in a particular year. The climate is typical of tropical features with monsoon (June–September) yielding 60–65% of the total rainfall (Menon et al., 2000). The temperatures from March to May are hot (30–34°C) and lowest in December (22–24°C). The soil types present in the region are clay, gravelly clay, loam, gravelly loam and sandy.

SWAT Model

The present study concerns the application of a physically based watershed model SWAT2005 in the Vembanad Lake Basin to model flows and examine the influence of the proposed projects on stream flow. The application of the model involved calibration, validation and simulation of proposed scenarios. For this purpose manual calibration was performed.

SWAT divides the total watershed into a number of subbasins depending on the number of reach outlets (generally, tributaries). Further the subbasins may be discretized into number of parts called Hydrologic Response Units (HRUs) using the landuse, soil type and slope

classification. HRU forms a basic computational unit assumed to have homogeneous hydrologic response. The computed results of the various physical processes on the HRU scale are integrated to the subbasin level and then into the basin level.

Model Inputs

The spatially distributed data (GIS input) needed for the ArcSWAT interface include the Digital Elevation Model (DEM), soil data, land use and stream network layers. Data on weather and river discharge were also used for prediction of streamflow and calibration and validation process.

Topography was defined by a Digital Elevation Model (DEM) that contains the elevation information of all points in a given area at a specific spatial resolution arranged in a gridded form. A 90 m by 90 m resolution DEM (Figure 6) based on SRTM (Shuttle Radar Topography Mission) data sets (Jarvis et al., 2008) was used as a basis for the delineation of the river basins. To strengthen the flow direction and accumulation algorithms stream network layer obtained from the office of ISW, Government of Kerala were used. Subbasin parameters such as slope gradient, slope length of the terrain, and the stream network characteristics such as channel slope, length, and width were derived from the DEM.

The land use map gained from the open-source Global Land Cover Facility (GLCF) (Tucker et al., 2004) was used to estimate vegetation and their parameters for input into the SWAT model. The soil map used for the model was obtained from the published dataset by Food and Agriculture Organisation of the United Nations (Batjes, 1997). It holds more than 5000 soil types.

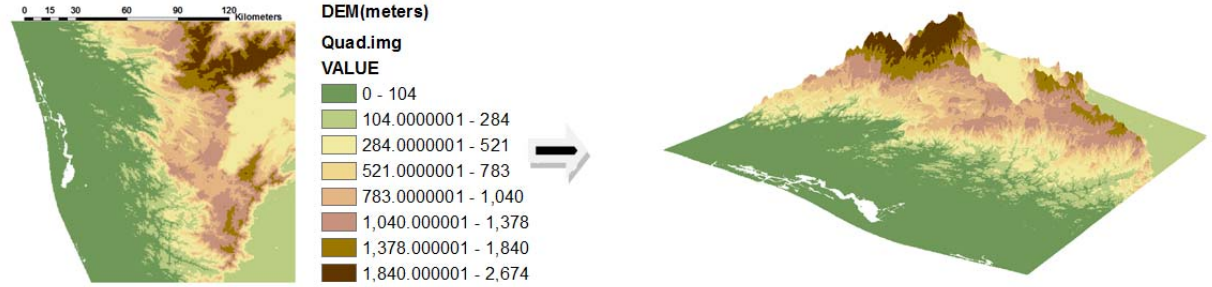

Figure 6: 3-Dimensional view of the study region showing the Western Ghats

Daily precipitation data for 21 stations, daily discharge data for 5 stations and water use data obtained with the help of the Chief Engineer, ISW, Government of Kerala were used for modelling purpose. Details of Muvattupuzha Irrigation Scheme, Pamba Irrigation Scheme, details of various dams and reservoirs, hydroelectric schemes and water use were obtained from the office of ISW, Government of Kerala. Daily precipitation in form of gridded data obtained from India Meteorology Department (IMD) was used for comparing rainfall between study area and neighbouring regions. Temperature data (gridded) from IMD was used in SWAT input.

The five basin models were set up using different thresholds for drainage calculation. Then subbasins and HRUs were formed. Figure 7 shows the delineated watershed of the Achenkovil Basin.

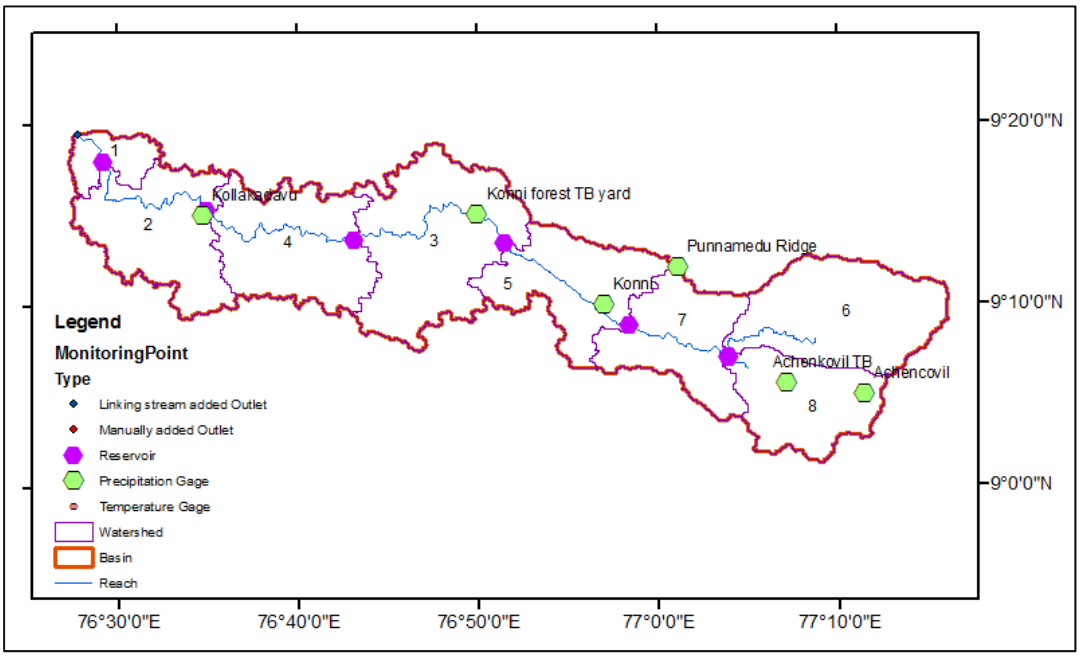

Figure 7: Delineated watershed of the Achenkovil basin

Model Calibration

Hydrologic models for five rivers were prepared on the ArcSWAT 2005 interface implemented in the ArcGIS software version 9.2. The most influential parameters governing the stream-flow were identified using the sensitivity analysis tool in ArcSWAT which uses the combination of Latin Hypercube (LH) and One-factor-At-a-Time (OAT) sampling (Van Griensven, 2006).

Calibration was done manually by changing the model parameters influencing the surface water and ground water flows. One parameter at a time was changed to see the improvement in the model results. The main parameters, changes in which improved the model performance are CN2, SURLAG, GW_DELAY, GWQMN, RCHRG_DP, GW_REVAP, OV_N and ALPHA_BF.

Modelling under different development scenarios

After the SWAT model was calibrated and validated for the existing scenario of development, proposed changes were included in the model by adding reservoirs to the specific subbasins and changing the water uses of few subbasins where new projects and diversions are proposed.

Results and Discussion

Calibration and Validation

Five separate models were prepared for the five rivers. For each of the basin models calibration and validation of streamflow was done at one discharge gauging location. The five discharge locations can be found marked in Figure 22Figure 8. The details of the discharge locations are given in Table 3. Manual calibration for daily-step streamflow was done. Following pre-processing, model derived runoff simulations were iteratively refined by adjusting model parameters till the discrepancy between these simulations and actual observations are reduced to a minimum.

A list of the parameters, their range of values and the final parameter values achieved after the manual calibration of the SWAT model for Pamba river basin are shown in Table 4. For the other four river models the parameters assumed similar values.

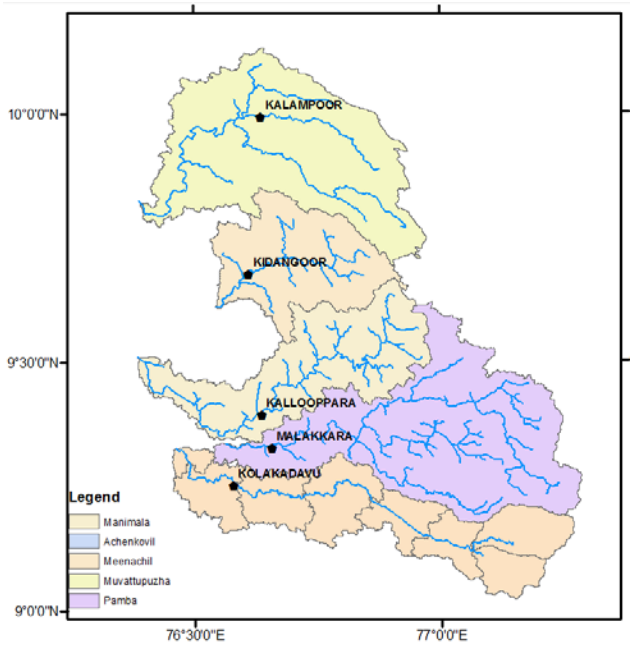

Figure 8: The five modelled river basins with the gauge measuring locations

Table 3: Calibration and Validation periods of five river basins

Sl. no.	Basin	Discharge Gauge for Calibration	Calibration Period	Validation Period
1	Muvattupuzha	Kalampoor	1st Feb to 31st Dec 1997	1st Jun to 10th Aug 2001
2	Meenachil	Kidangoor	1st Jan to 31st Dec 1997	1st Jan to 31st Dec 1998
3	Manimala	Kallooppara	1st Jan to 31st Dec 1995	1st Jan to 31st Dec 1996
4	Pamba	Malakkara	1st Jan to 31st Dec 1996	1st Jan to 31st Dec 1997
5	Achenkovil	Kollakadavu	1st Jan to 31st Dec 1997	1st Jan to 31st Dec 1998

Table 4: List of parameters, their range of appropriate values and final calibrated values for the Pamba SWAT model

Parameter	Name	Range	Final Value
ALPHA_BF	Baseflow alpha factor	0–1.0	0.05
CN2	Curve number	0–100	60.9-80.15*
GW_DELAY	Ground water delay time, days	0–100	130
GW_REVAP	Ground water revap coefficient	0.02–0.20	0.01
OV_N	Manning's n for overland flow	0.01-30	0.1
RCHRG_DP	Deep aquifer percolation fraction	0–1.0	0.001
SURLAG	Surface runoff lag coefficient	0–10	0.25

* The parameter has different values for different HRUs

In Figures 9 and 10 the simulated daily discharges for the Pamba basin generated from SWAT model are compared with the corresponding measured data for the calibration period.

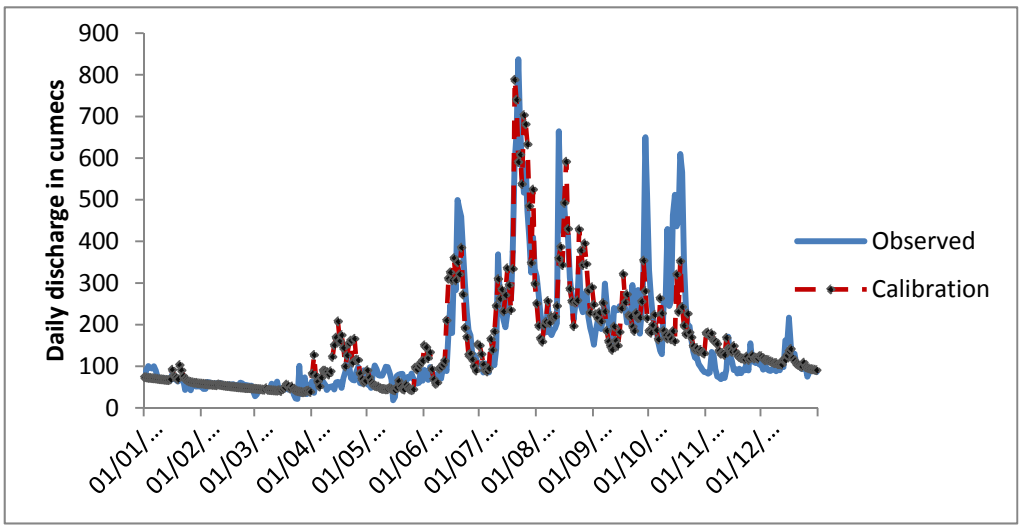

Figure 9: Observed and simulated mean daily discharges at Malakkara, Pamba for calibration period

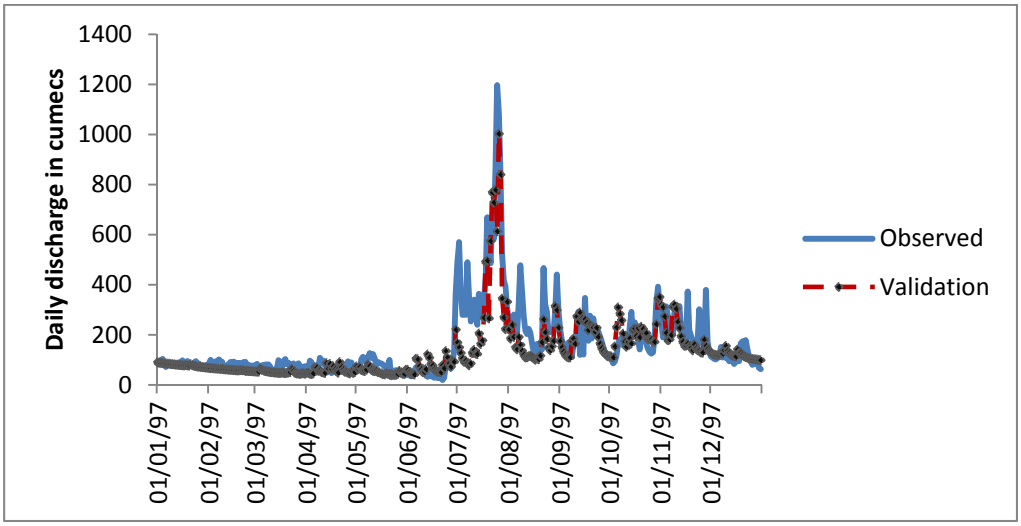

Figure 10: Observed and simulated mean daily discharges at Malakkara, Pamba for validation period

Model performance was evaluated using the coefficient of determination (R^2) and Nash-Sutcliffe model efficiency (Nash and Sutcliffe, 1970) indices. The other parameters for checking model performance such as RSR (Moriasi et al., 2007) and percentage bias (PBIAS) (Gupta et al., 1999) were also calculated. The RSR is defined as the ratio of the RMSE to the standard deviation of measured data. RMSE is the root mean square error (Singh et al., 2004). As per guidelines described by Moriasi et al., (2007) model performance can be evaluated as satisfactory if NSE > 0.5, RSR ≤ 0.7, PBIAS < ± 25% for streamflow, at a monthly time step. In

this case calibration was done on a daily time step and the values of these parameters are found to be within the acceptable limits. R^2 ranges from 0 to 1, and typically values greater than 0.5 are considered acceptable (Santhi et al., 2001). The values of the four model efficiency parameters for the five models are given in Table 5.

Table 5: Model performance of the five river models

Monitoring stations	NSE	R^2	RSR	PBIAS (%)
Acceptable Limits	$> 0.5_a$	$> 0.5_b$	$< 0.7_a$	$\pm 25_a$
Kalampoor (Muvattupuzha)	0.805549	0.817319	0.440966	1.559381
Kidangoor (Meenachil)	0.605457	0.69074	0.628127	0.705749
Kallooppara (Manimala)	0.806507	0.822214	0.439879	6.289268
Malakkara (Pamba)	0.724427	0.727976	0.52495	0.840595
Kollakadavu (Achenkovil)	0.685099	0.811673	0.56116	22.13738

a (Moriasi et al., 2007) **b(Santhi et al., 2001)**

Results for scenarios

There are two existing major irrigation projects in the study region, the Muvattupuzha Valley Irrigation Project and the Pamba Irrigation Project. The Pamba River has a few major and minor hydro-electricity production stations throughout its length. There are a number of developments related to hydel-power plants proposed in the Pamba basin region. Along with these, there is the PAVLP proposal which consists of construction of three reservoirs, canal system as well as tunnels for irrigation, hydel production and diversion of water.

The available details of the existing and proposed projects have been entered into the model. The Achenkovil and Pamba basin models have been simulated for the existing scenario and proposed scenario of development for the 10 years 1996-2005 keeping the other inputs such as precipitation and temperature as the same.

Figure 11 and Figure 12 show the simulated monthly results for two scenarios of water resources development.

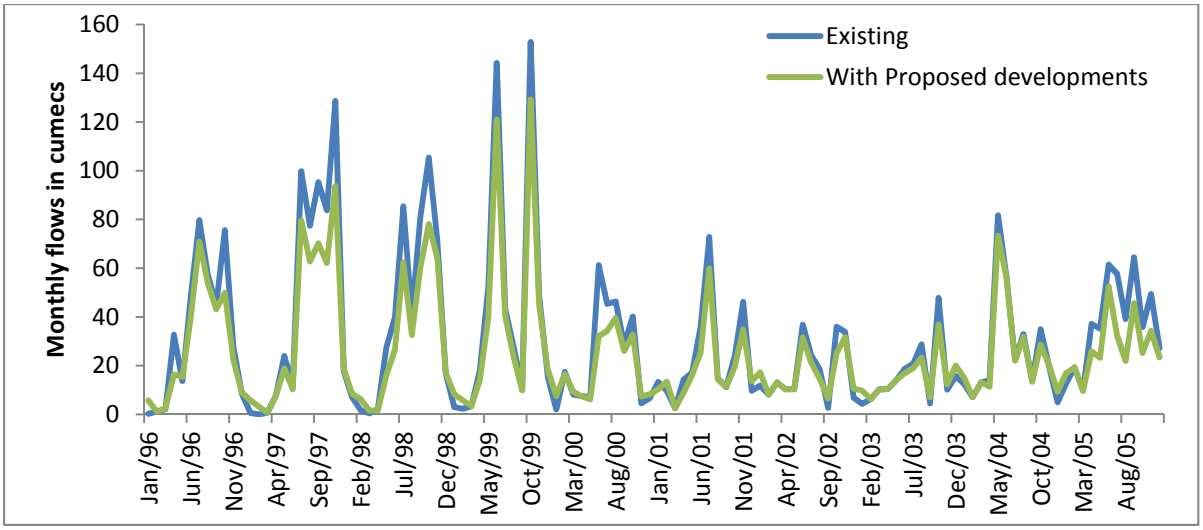

Figure 11: Comparison of simulated monthly flows for Achenkovil River before and after proposed developments

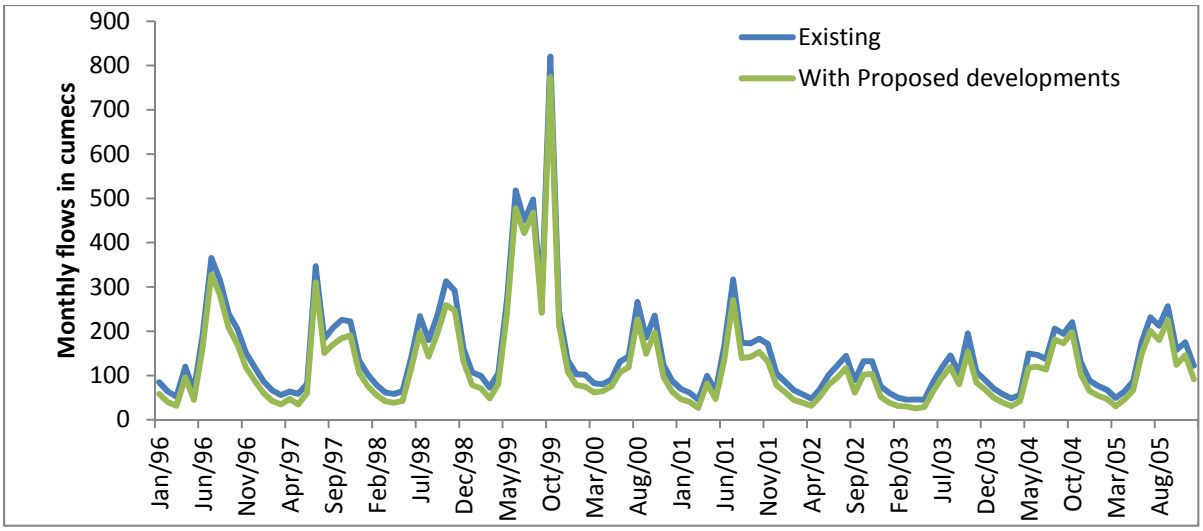

Figure 12: Comparison of simulated monthly flows for Pamba River before and after proposed developments

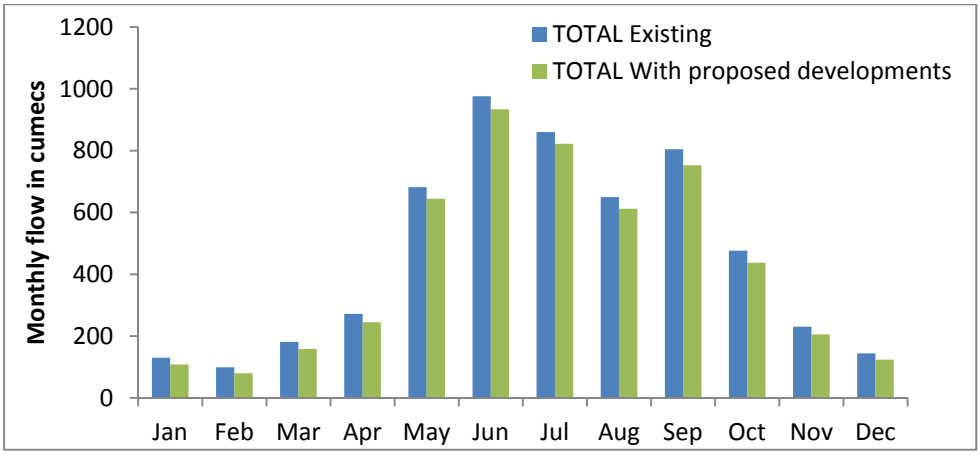

Figure 13: Comparison of average (1996-2005) simulated total monthly flows for the five rivers before and after development

As seen in Figure 11, a reduction is found in the flow in Achenkovil River in most of the months. According to the NWDA feasibility report a regulated release of 5.72 m^3/s will be allowed from the Achenkovil Kal Ar reservoir, that is proposed on the Achenkovil Kal Ar branch of the Achenkovil River, into the downstream reach during the lean season months of October to May for environmental concerns. The slight increase observed in the flows in November – April months is due to this allowance. However it was seen that the Achenkovil Kal Ar reservoir is not able to support the proposed constant flow. The effect on the flow in the Pamba River can be seen in Figure 12. Similarly, for the Pamba River, NWDA proposed a regulated flow of 1.43 m^3/s from the Punnamedu Reservoir that is proposed on the Pamba Kall River, a tributary of the Pamba River.

Figure 13 shows the simulated average monthly total flow of the five rivers taken over the ten years, 1996-2005. Further Figure 14 shows the percentage reduction in total flow of the system as a result of the proposed projects. As observed, there is greater reduction in flow in the non-monsoon period when the flow in the rivers is already less.

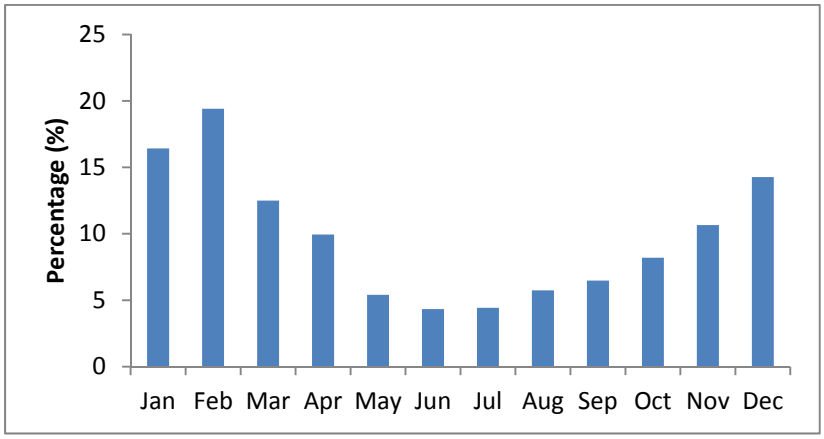

Figure 14: Percentage reduction in total flow of five rivers averaged for ten years modeled (1996-2005)

Conclusion

This paper summarizes the effect of various water resources development in the study region. The study establishes that the impact of these latter initiatives on the natural river regime, both in quantity as well as quality terms is expected to be significant. The natural consequence of these impacts is its adverse effect on the connected wetland system along with its resident biota.

The inferences from the study can be concluded as:

- The riverine environment might be significantly impacted on the execution of the proposed water resources developments.
- The alteration of the Pamba and Achenkovil hydro-systems introduce a change of 5 – 20 % in the total flow volumes entering into the Vembanad Wetland system.
- The higher impacts can be seen in the low –flow months during which the rivers have meagre flow and become almost stagnant.
- This can be another serious problem to the already depleted lake environment.

Hence it is very important that the decisions related to water resources development be taken after deliberate research and attention to previously witnessed fate of so many river and wetland systems in the world. Further, it is suggested that the environmental impacts of anthropogenic influences on the Vembanad Lake be studied and modelled.

Acknowledgements
The present work was performed a part of 'Water Balance Study of Vembanad Wetland System', funded by Irrigation Department, Kerala. The authors would like to thank Smt. P. Lathika, Chief

Engineer, Inter-State Water (ISW) and Sri Abraham Koshy (Assistant Executive Engineer), Irrigation Department, Government of Kerala for their valuable support.

References

Arnold, J. G., R. Srinivasan, R. S. Muttiah and P. M. Allen. 1999. CONTINENTAL SCALE SIMULATION OF THE HYDROLOGIC BALANCE. JAWRA Journal of the American Water Resources Association, 35:1037-1051.

Arnold, J. G., R. Srinivasan, R. S. Muttiah and J. Williams. 1998. Large area hydrologic modeling and assessment part I: Model development. JAWRA Journal of the American Water Resources Association, 34:73-89.

Batjes, N. 1997. A world dataset of derived soil properties by FAOâ€“UNESCO soil unit for global modelling. Soil use and management, 13:9-16.

Caliandro, A., A. Hamdy, C. Lacirignola and M. CATALAN. 1992. Environmental impacts of water resource development and management. CIHEAM-IAMB.

Chu, T. and A. Shirmohammadi. 2004. Evaluation of the SWAT model's hydrology component in the Piedmont physiographic region of Maryland. Transactions of the ASAE, 47:1057-1073.

Gassman, P. W., M. R. Reyes, C. H. Green and J. G. Arnold. 2007. The Soil and Water Assessment Tool: Historical development, applications, and future research directions.

Goldsmith, E. and N. Hildyard. 1986. The social and environmental effects of large dams. Volume 2: case studies. Wadebridge Ecological Centre.

Gollamudi, A., C. Madramootoo and P. Enright. 2007. Water quality modeling of two agricultural fields in southern Quebec using SWAT. Transactions of the Asabe, 50:1973-1980.

Gupta, H. V., S. Sorooshian and P. O. Yapo. 1999. Status of automatic calibration for hydrologic models: Comparison with multilevel expert calibration. Journal of Hydrologic Engineering, 4:135-143.

Jarvis, A., H. Reuter, A. Nelson and E. Guevara. 2008. Hole-filled seamless SRTM data V4, International Centre for Tropical Agriculture (CIAT). Cali, Columbia.

Ji, X., E. Kang, R. Chen, W. Zhao, Z. Zhang and B. Jin. 2006. The impact of the development of water resources on environment in arid inland river basins of Hexi region, Northwestern China. Environmental Geology, 50:793-801.

Kannan, K. 1979. Ecological and socio-economic consequences of water-control projects in the Kuttanad region of Kerala. Sadhana, 2:417-433.

Kaur, R., R. Srinivasan, K. Mishra, D. Dutta, D. Prasad and G. Bansal. 2003. Assessment of a SWAT model for soil and water management in India. Land Use and Water Resources Research, 3:1-7.

Leichenko, R. M. and J. L. Wescoat Jr. 1993. Environmental impacts of climate change and water development in the Indus Delta region. International Journal of Water Resources Development, 9:247-261.

Limbe, W. 1998. Water resources development and vector borne diseases in Malawi. Water resources development and vector-borne diseases in Malawi:38.

Menon, N., A. Balchand and N. Menon. 2000. Hydrobiology of the Cochin backwater systemâ€“a review. Hydrobiologia, 430:149-183.

Moriasi, D., J. Arnold, M. Van Liew, R. Bingner, R. Harmel and T. Veith. 2007. Model evaluation guidelines for systematic quantification of accuracy in watershed simulations.

Nash, J. E. and J. Sutcliffe. 1970. River flow forecasting through conceptual models part Iâ€”A discussion of principles. Journal of hydrology, 10:282-290.

Neitsch, S., A. Arnold, J. Kiniry, J. Srinivasan and J. Williams. 2005. Soil and Water Assessment Tool Userâ€™s Manual: Version 2005. Texas Water Resources Institute. TR-192, College Station, Texas.

NWDA Report. 1995. Feasibility Report of Pamba-Achankovil-Vaippar Link Project, National Water Development Agency, Ministry of Water Resources, New Delhi, India.

Plan, R. 2005. Narail Sub-project Bangladesh: Southwest Area Integrated Water Resources Planning and Management Project, June.

Ritchie, J. T. 1972. Model for predicting evaporation from a row crop with incomplete cover. Water resources research, 8:1204-1213.

Santhi, C., J. G. Arnold, J. R. Williams, W. A. Dugas, R. Srinivasan and L. M. Hauck. 2001. Validation of the Swat Model on a Large Rwer Basin with Point and Nonpoint Sources. JAWRA Journal of the American Water Resources Association, 37:1169-1188.

Sarma, U. and A. Jose. 2008. Application of a coir geotextile reinforced mud wall in an area below sea level at Kuttanad, Kerala. p. 18-22.

Simon, A. and K. Mohankumar. 2004. Spatial variability and rainfall characteristics of Kerala. Journal of Earth System Science, 113:211-221.

Singh, J., H. Knapp and M. Demissie. 2004. Hydrologic modeling of the Iroquois River watershed using HSPF and SWAT. ISWS CR 2004-08. Champaign, Ill.: Illinois State Water Survey.

Spruill, C., S. Workman and J. Taraba. 2000. Simulation of daily and monthly stream discharge from small watersheds using the SWAT model. Transactions of the ASAE, 43:1431-1439.

Srinivasan, R., J. Arnold and C. Jones. 1998. Hydrologic modelling of the United States with the soil and water assessment tool. International Journal of Water Resources Development, 14:315-325.

Swaminathan, M.S. et al., 2007. Measures to Mitigate Agrarian Distress in Alappuzha and Kuttanad Wetland Systems. A Study Report by Swaminathan Research Foundation, Union Ministry of Agriculture.

Thampatti, K. C. M. and K. Padmakumar. 1999. Nature watch. Resonance, 4:62-70.

Tucker, C., J. Pinzon and M. Brown. 2004. Global inventory modeling and mapping studies (GIMMS) satellite drift corrected and NOAA-16 incorporated normalized difference vegetation index (NDVI), monthly 1981-2002. Global Land Cover Facility, University of Maryland.

Van Griensven, A. and W. Bauwens. 2003. Multiobjective autocalibration for semidistributed water quality models. Water resources research, 39:1348.

Zhang, X., R. Srinivasan and F. Hao. 2007. Predicting hydrologic response to climate change in the Luohe River basin using the SWAT model. Transactions of the Asabe, 50:901-910.

Zhang, X., R. Srinivasan and M. Van Liew. 2008. Multi-site calibration of the SWAT model for hydrologic modeling. Transactions of the ASAE, 51:2039-2049.

Estimation of Wavelet Based Spatially Enhanced Evapotranspiration Using Energy Balance Approach

V.Gowri
Associate Professor, Dept of Civil Engineering, Jerusalem College of Engineering, Chennai, India
gowrisenthilkumar@gmail.com

D.Thirumalaivasan
Professor, Institute of Remote Sensing, Anna University, Chennai, India
dtvasan@annauniv.edu

Abstract

Evapotranspiration (ET) is one of the major components of the hydrologic cycle which links the water cycle and energy balance together. Conventional techniques that are based on the point measurements are representative only at local scales. The problem of actual ET estimation over a large area can be solved using remote sensing methods that provide ET on pixel-by-pixel basis. The objective of this paper is to estimate spatial distribution of actual ET from satellite remote sensing images at high spatial resolution. This study has been carried out using Landsat 7 Enhanced Thematic Mapper + sensor. The Surface Energy Balance Algorithm for --Land (SEBAL) was used to estimate actual ET. The Thermal Infrared (TIR) remote sensing data is very essential in the estimation of the actual ET. The spatial resolution of the resulting ET maps is determined by the pixel resolution of the TIR sensor. Data fusion techniques take advantage of the complementary spatial/spectral resolution characteristics of imaging sensors to spatially enhance the acquired image. The fusion scheme should preserve the spectral characteristics of the original low resolution TIR image. Hence to satisfy this criterion the Multi Resolution Analysis (MRA) technique based data fusion was used in this study. The Discrete Wavelet Transforms (DWT) was adopted in this research work to spatially enhance the TIR image. The ET information is estimated using this spatially enhanced TIR images. Further the distributed values of actual evapotranspiration obtained from the developed methodology could be utilized directly in the hydrological and crop models for addressing various hydrological and agricultural problems.

Keywords: Thermal infrared, actual evapotranspiration, SEBAL, Wavelet transforms, Spatial enhancement, image fusion

Introduction

Fresh water has become our most precious natural resource and the wise management of this resource is one of our greatest challenges. Future water resource utilization requires the determination of the components of the hydrological cycle. is the evapotranspiration. Evapotranspiration (ET) is one of the important components of the hydrological cycle. Conventional methods of ET estimation are based on point measurements. With the advancements in the field of satellite remote sensing various models concerning the derivation of evapotranspiration using satellite data have been published (Carlson and Buffum 1989; Carlson et al 1995; Kustas and Norman 1996) which provides with spatial estimation of ET.

Among the current remote sensing based models, the Surface Energy Balance Algorithm for Land (SEBAL) has been designed to calculate the energy partitioning at regional scale with minimum ground data (Bastiaanssen 1998). Thermal infrared imagery (TIR) is very important for the model. However, spatial resolution of the thermal data is coarser than the shortwave bands. Spatial enhancement of the thermal data with the spatial resolution of shortwave bands can increase fidelity of the energy balance and subsequent ET estimates.

The current ET estimating methods using coarse spatial thermal bands are of little use for analyzing its spatial distribution. Thus a practical spatial limit is reached that prevents the straight forward implementation of the evapotranspiration monitoring by satellite imagery at high spatial resolution. Considering these challenges this research is designed to spatially enhance the low spatial resolution TIR image and to analyze the spatial variation of actual Evapotranspiration (ETact) estimated from the enhanced TIR image.

The objective of providing better evapotranspiration information can be achieved by using spatially enhanced TIR image. This leads to the research question addressed in this research to find out, how to benefit from the high spatial resolution data from the same sensor which provides low spatial resolution of TIR data. Hence this study aims at enhancing the low resolution TIR image, deriving the spatial details at the spatial resolution of the visible/near infrared images. The research work also focuses on the satellite derived surface temperature and evapotranspiration to characterize the spatial variability.

Materials and Methods

Description of Study Area

The study area is located in the state of Tamil Nadu, India (Figure 1). The study area is a part of Periyar-Vaigai irrigation system. It spreads out in the Madurai district. Geographically the study area extends from 10˚ 03’ 46” N to 9˚ 57’ 43” N and 78˚ 00’ 38” E to 78˚ 14’ 20” E. The total extent of the study area is 284.50 Sq Km. The study area covers the branch canal 3 to branch canal 9 of Periyar Vaigai irrigation system. The area is generally a plain terrain with gentle undulations. The area has a tropical monsoon climate.

2.2 Satellite Data Processing

In this study Landsat 7 ETM+ imagery is used for ET estimation. Cloud free images were selected from the archive. The WRS path and row of the images acquired is 143 and 053 respectively. The header file of the satellite image contains important information that is necessary for processing the images. Table 2 lists the details of images used in the research study.

Table 1 List of Landsat 7 ETM+ images used in the study

No	Acquisition data	Julian day	Over pass time	Sun elevation (degrees)	Sun azimuth (degrees)
2	4 Dec 1999	338	10:28:21.89	49.60179	143.26033
3	19 Oct 2000	293	10:25:40.71	58.59446	129.34565

2.3 Spatial Enhancement

Image enhancement at pixel level is aimed from which the low spatial resolution of TIR band is enhanced with the details derived from available 30m spatial resolution optical images. The spatial enhancement scheme should preserve the spectral characteristics of the original data. The multiresolution image enhancement techniques merge the spatial information from a high resolution image with the spectral information from a low resolution image. Discrete Wavelet Transforms are adopted in this research work.

The image similarity assessment was conducted to identify the high resolution image from which the spatial details were extracted. The high resolution bands at 30m spatial resolution were reduced to 60m spatial resolution in the MATLAB 7.0 environment. The reduced image at 60m spatial resolution was compared with the original TIR image at 60m resolution. The spectral similarity assessments were conducted by means of correlation coefficient matrix. The high correlation was studied from the correlation matrix, which revealed the band from which the spatial details were to be derived. The following section describes about the multi resolution analysis methods of spatial enhancement adopted in the present study.

2.4 Wavelet Based Spatial Enhancement

Figure 1 shows the schematic diagram of the basic structure for the wavelet based spatial enhancement adopted in the research. The basic idea was the same as for the wavelet based enhancement algorithm developed by Li et al (1995). The two dimensional Discrete Wavelet Transform (2D-DWT) enhancement was carried out with substitution method.

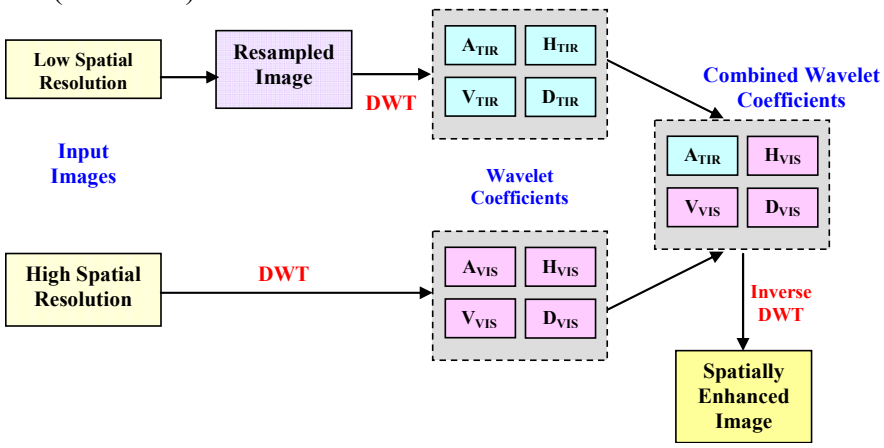

Figure 1 Frame Work for Wavelet Based Spatial Enhancement of TIR Image

Wavelet based spatial enhancement involves three steps: forward transform, fusion rule and inverse transform. With reference to Figure 1 both the high resolution image and the low resolution TIR image were decomposed by the one level 2D-DWT. The low resolution TIR image has been previously expanded by 2 in order to process the low resolution image having the

same spatial scale as the high resolution image. For this purpose, the 7 taps pyramid generating low pass Gaussian filter was applied along the rows and columns, after upsampling by 2.
Spatial enhancement has been carried out with the biorthogonal wavelet family. Two sets of wavelet coefficients were obtained, approximation and detail images of the original image. The high spatial details of the high resolution image were contained in the detail wavelet coefficients of high resolution image. For each pixel (i,j) the detail coefficients of TIR image was substituted with the corresponding detail coefficients of the high spatial resolution. And then the inverse DWT was performed. The obtained enhanced image was a fused product at high spatial resolution TIR image with high spatial details. The main objective of merging high-resolution image and low resolution TIR satellite images was to keep maximum spectral information from the low resolution image while increasing the spatial resolution. This was ascertained by performing the quantitative metrics analysis.

2.5 Image Quality Assessment Technique
Quality refers to both the spatial and spectral quality of images (Wald et al 1997). The subjective quality assessment was done by visual comparison. The spectral quality and spatial quality of the enhanced images were evaluated based on quality metrics.
2.5.1 Visual Evaluation
Qualitative approach involved the visual comparison between original TIR image and enhanced TIR image. For visual evaluation, if the comparison is not conducted under the same visualization condition, the comparison will not provide reliable results (Mansour and Guangdao 2007). The resampled TIR image and spatially enhanced TIR images were displayed under the same display conditions and were compared with each other.
2.5.2 Quantitative Evaluation
The spatially enhanced images are quantitatively evaluated for spectral and spatial qualities based on some indices. During enhancement process the spectral information from the original image should be retained and at the same time the spatial detail from the high resolution image should be absorbed by the enhanced image. Hence, in this study Wald's properties are proposed to be used to test the enhanced image quality. The indices like Root Mean Square (RMSE), Correlation Coefficient (CC), ERGAS and Image Quality Assessment (Q) were used to perform the spectral quality assessment. To perform the spatial quality assessment indices like Standard Deviation (SD), Mean Gradient (MG), Correlation Coefficient (CC) and High Pass Correlation Coefficient (HPCC) were used.

2.6 SEBAL
The surface energy balance for land (SEBAL) is used to estimate the evapotranspiration and other energy balance terms. The processing of the SEBAL model has been done after the standard method described in Bastiaanssen et al (1998) to calculate energy partitioning at the regional scale with an effort to use minimum ground data.
In the SEBAL model, ETa is calculated from satellite images and local weather station data using surface energy balance equation. Since the satellite image provides information for the satellite overpassing time only, the SEBAL computes an instantaneous ET flux for the image time. The instantaneous ET flux is calculated for each pixel of the image as a residual of the surface energy balance equation:

$$\lambda E = R_n - G_0 - H \qquad (1)$$

where;λE is the latent heat flux (measure of evapotranspiration) in W/m^2, R_n is the net radiation flux at the surface in W/m^2, G_0 is the soil heat flux in W/m^2 and H is the sensible heat flux to the air in W/m^2.

The net radiation flux at the surface (R_n) is the actual radiant energy available at the surface. It is given by the surface radiation balance equation:

$$R_n = (1-\alpha)R_S\downarrow + R_L\downarrow - R_L\uparrow - (1-\varepsilon_0)R_L\downarrow \quad (2)$$

where; $R_S\downarrow$ is the incoming shortwave radiation (Wm-2), α is the surface albedo (dimensionless), $R_L\downarrow$ is the incoming longwave radiation (Wm-2), $R_L\uparrow$ is the outgoing longwave radiation (Wm-2), and ε_0 is the surface thermal emissivity (dimensionless).

Soil heat flux is the rate of heat storage into the soil and vegetation due to conduction. In the SEBAL, the ratio G/Rn is calculated using the following empirical equation developed by Bastiaanssen:

$$\frac{G}{R_n} = \frac{T_S}{\alpha}\left(0.0038\alpha + 0.0074\alpha^2\right)\left(1 - 0.98NDVI^4\right) \quad (3)$$

where Ts is the surface temperature (in ˚C); α is the surface albedo and NDVI is the Normalized Difference Vegetation Index.

Sensible heat flux is the rate of heat loss to the air by convection and conduction due to temperature difference. The computation of H requires more attention because of the strong dependence upon the type of surface and height of vegetation and local meteorological conditions. It is computed using the following equation for heat transport:

$$H = \frac{\left(\rho_a \times C_p dT\right)}{r_{ah}} \quad (4)$$

where ρ_a is air density (1.15 kgm-3), C_p is air specific heat (1004.16 Jkg-1K-1), dT is the temperature difference ($T_S - T_a$) and r_{ah} is the stability corrected aerodynamic resistance to heat transport (s/m). r_{ah} varies with wind speed, and intensity and direction of the H. Therefore, rah could be determined through several iterations.

$$r_{ah} = \frac{\ln\left(\frac{Z_h - d}{Z_{oh}}\right) - \psi_h}{u_* \times k} \quad (5)$$

$$u_* = \frac{k \times u_z}{\ln\left(\frac{Z_m - d}{Z_{om}}\right) - \psi_m} \quad (6)$$

where Z_m and Z_h are heights in meters above the zero plane displacement (d) of the vegetation, u_* is the friction velocity (m/s) which quantifies the turbulent velocity fluctuations in the air and k is von karman's constant (0.41), k is von Karman's constant, u_z is the wind speed (m/s) at height Z_m and Z_{om} is the momentum roughness length (m). ψ_m and ψ_h are stability correction factors for momentum and heat transfer, respectively which are functions of Monin-Obukhov stability parameters.

The actual evapotranspiration, ETa (mm/day) is determined as

$$ET_a = 8.64x10^7 \Lambda \left(\int_0^{24} R_n \right) / \left(\lambda \rho_w \right) \quad (7)$$

where Λ = evaporative fraction $\left[\Lambda = \lambda E / (\lambda E + H) \right]$ on the instantaneous time basis (-) ; λ are latent heat of vaporization (J/Kg) and ρ_w = density of water (Kg/m3).

Results and Discussion

Image Quality Assessment

The evaluation of spatial enhancement results is an important process, and it mostly includes qualitative evaluation and quantitative calculation analysis. The wavelet based spatial enhancement of the TIR images has been carried out on spatially degraded TIR image. The qualitative and quantitative metrics of spatially enhanced images were compared with the metrics of resampled TIR image to evaluate the quality of the image enhancement.

3.1.1 Spectral Quality

As discussed by Wald's 1st property the enhanced TIR image when degraded to its original image should be as identical as possible to the original TIR image. Table 2 shows the spectral quality assessment for the spatially enhanced image obtained at 30m spatial resolution. The wavelet enhanced images had lower RMSE and the CC and Q4 values were also higher (nearing towards 1). Spectral ERGAS values were within the range of 3. From the above discussion it can be concluded that the wavelet enhancement method has optimum preservation of spectral information from the original TIR image.

Table 2 Spectral Quality Assessment

Image	TIR_{RES}			
	RMSE	CC	ERGAS	Q4
04-Dec-99	0.916	0.928	1.473	0.959
19-Oct-00	0.852	0.964	1.372	0.974
Image	TIR_{WAV}			
	RMSE	CC	ERGAS	Q4
04-Dec-99	0.591	0.949	2.644	0.915
19-Oct-00	0.778	0.989	2.853	0.928

3.1.2 Spatial Quality

The goal of the enhancement techniques is to increase the spatial resolution of the low resolution image. After spatial resolution enhancement some information is added to or lost during the process. This assessment checks how much of the spatial detail information gets absorbed to the low spatial resolution image to improve on the spatial resolution of TIR image. The spatial quality of the spatially enhanced image at 30m spatial resolution is compared with the original image at 30m spatial resolution. This is carried out to analyze the variability of spatial quality.

Table 3 reports the spatial quality assessment for the spatially enhanced image obtained at 30m spatial resolution with the original visible band at 30m spatial resolution. The standard deviation (SD) indicates the amount of information change that has occurred in the enhanced image. The standard deviation for the resampled image has no change indicating that there is no addition or loss of information. The SD is low for wavelet based method indicating that the wavelet

enhanced images have low deviation of the pixel values. As stated by Wehrmann et al (2005) SD index increases or decreases depending on the detail information that is absorbed by the low resolution image. SD increases when more information is added which distorts the spatial resolution. When the mean gradient is observed the wavelet enhancement technique has got a higher mean gradient compared to the ELP enhancement technique. However the SD and MG alone do not define the ability of methods for enhancement.

Table 3 Spatial Quality Assessment for Enhanced Images (at 30m Spatial Resolution)

Images	Standard Deviation (SD)		Mean Gradient (MG)	Correlation Coefficient (CC)	HighPass Correlation Coefficient (HPCC)
	TIR_{WAV}	TIR_{RES}	TIR_{WAV}	TIR_{WAV}	TIR_{WAV}
04-Dec-99	4.919	2.844	4.690	0.894	0.954
19-Oct-00	5.256	2.870	4.849	0.925	0.981

The closer the correlation coefficient is to one, the more closely the spatial data of the fused image matches the spatial data of the high resolution image, indicating better spatial quality. The HPCC which involves the high frequency component of the enhanced images have a value closer to one indicating a good quality of spatial enhancement undergone by wavelet method. The high pass correlation coefficient which indicates the correlation coefficient between the high pass details gives a good insight into the evaluation techniques (Pradhan 2005). HPCC and CC for the wavelet enhancement method is high compared to ELP enhancement method. The correlation coefficient denotes the similarity between the images. It is high for wavelet enhancement method.

It is inferred from the assessment of the spectral and spatial metrics that the wavelet enhancement method enhances spatial resolution with spectral preservation.

3.2 SEBAL Results

The actual evapotranspiration is calculated from SEBAL by combination of satellite images and ground data from meteorological station. The input parameters in the process of estimating actual evapotranspiration from resampled image and wavelet enhanced image are named with subscripts RES and WAV respectively. The resulting images at each stage of the SEBAL analysis are discussed in the following section.

3.2.1 Normalised Difference Vegetation Index

NDVI values close to 1 indicate very dense vegetation, while values near 0 indicate bare soil or very sparse vegetation. Negative values of NDVI usually correspond to water bodies or urban areas (Caparrini and Manzella 2009). The NDVI is a sensitive indicator of the amount and condition of green vegetation. The NDVI image estimated for the images are shown in Figure 2.

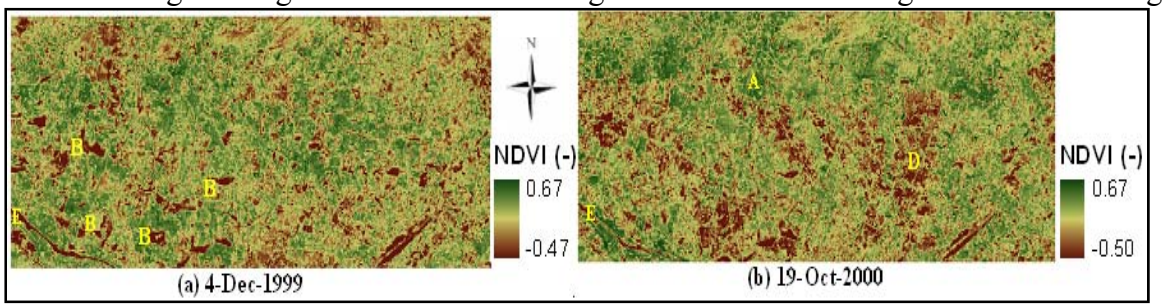

Figure 2 Spatial variation of NDVI image

A color gradation of brown (low NDVI) to dark green (high NDVI) is provided to depict the spatial variability of NDVI values in the NDVI image. The agricultural areas have the higher NDVI value, hence these areas appear to be in the shades of green. The intensity of green color also reflects the condition of the crops.

The water surface, urban and bare lands have low NDVI. The water surface indicated by the letter B has very low NDVI value, mostly less than 0. The dark brown color (indicated by letter B) in the NDVI image of 4-Dec-1999 show that the open water surface has low NDVI. It is observed that in all the images the bare land area and the rivers indicated by the letter E also have low NDVI values due to the absence of vegetation. The spatial variation of bare land is also clearly visible in the NDVI image.

3.2.2 Surface temperature

The retrieval of surface temperature is one of the essential parameter for estimation of evapotranspiration. The surface temperature images are computed from the atmospherically corrected radiance of TIR image. The estimated surface temperature images were validated with the data obtained from the meteorological station located within the study area. The observed temperature data at the meteorological station are given in Table 4.

Table 4 Observed Temperature Value at Meteorological Station

Images	Temperature (K)		
	Min	Max	Mean
4-Dec-1999	294.66	301.36	298.01
19-Oct-2000	298.76	308.16	303.46

The surface temperature images for resampled TIR images and wavelet enhanced TIR images are reported in Figure 4. The color scale of blue to red was used to show the spatial variation of temperature within the image. The blue color implies the low temperature region and red color implies the high temperature region. This indicated that the agricultural area with vegetation cover and open water surface have low surface temperature value

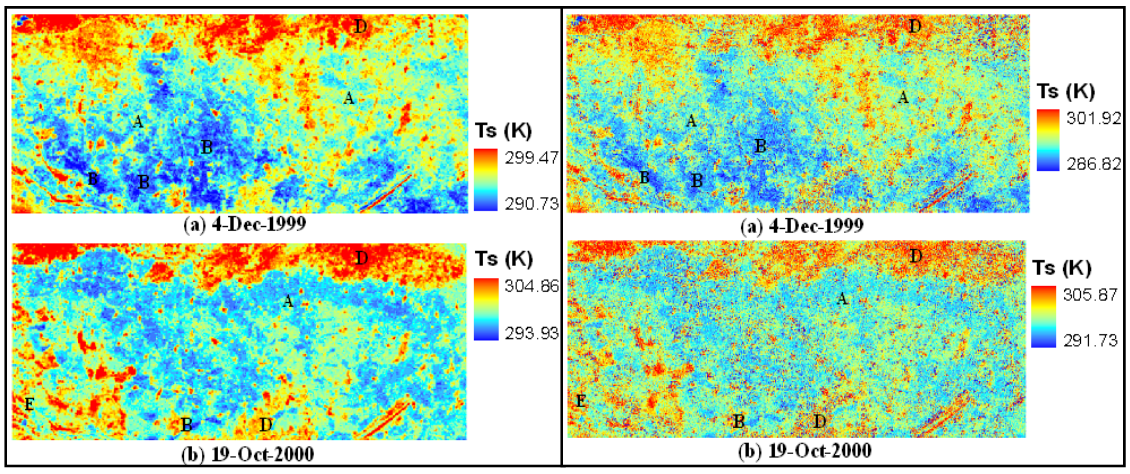

Figure 4 Surface Temperature Images from TIR_{Res} and TIR_{WAV} Image

3.2.3 Net Radiation

The essential inputs to derive net radiation are surface albedo, NDVI and surface temperature images. Generally net radiation value ranges from 100-700W/m2 (Morse et al 2000). Table 5 reports the statistics of the estimated net radiation. Generally net radiation value ranges from 100-700W/m2 (Morse et al 2000). From the observation of the statistics of Table 5 it is noticed that the estimated mean value for resampled TIR image and wavelet enhanced TIR image for

each image does not vary much. The net radiation is high for water surface since the incident radiation is absorbed by the water and outgoing longwave radiation is not radiated as much as the land surface.

Table 5 Statistics of Estimated Net Radiation

Images	Rn with TIR_{RES} (W/m2)			Rn with TIR_{WAV} (W/m2)		
	Min	Max	Mean	Min	Max	Mean
4-Dec-1999	172.37	410.03	330.16	169.37	412.29	331.42
19-Oct-2000	180.87	454.58	374.55	183.13	460.96	374.40

3.2.4 Soil Heat Flux

Soil heat flux is estimated using surface albedo, temperature and NDVI. According to Murray and Verhoef (2007), for relatively sparse vegetation, G can consume a significant proportion of R_n. Table 6 reports the statistics of the estimated soil heat flux. The estimated G values tend to be lower in crop covered condition and higher in bare soil condition (Tasumi 2003a). The soil heat flux decreased with the growth and development of the crop during the growing season as the crop canopy cover increased. The bare land areas have the high soil heat flux value. Water bodies also have high soil heat flux value.

Table 6 Statistics of Estimated Soil Heat Flux

Images	G with TIR_{RES} (W/m2)			G with TIR_{WAV} (W/m2)		
	Min	Max	Mean	Min	Max	Mean
4-Dec-1999	23.18	39.20	31.27	20.04	41.86	31.37
19-Oct-2000	20.49	51.82	41.76	20.14	55.83	41.67

3.2.5 Sensible Heat Flux

The sensible heat flux is estimated using the surface temperature derived from resampled TIR image and wavelet enhanced TIR image. Table 7 reports the statistics of the sensible heat flux values of the images. When the surface is warmer than the air above, heat is transferred upwards into the air as a positive sensible heat transfer. If the air is warmer than the surface, heat is transferred from the air to the surface creating a negative sensible heat transfer. For the surface of the water bodies the H value is very low (negative). This is mainly explained by the relative higher value of daily net radiation at the water bodies. The agriculture fields also have low sensible heat flux, because the difference between air and surface temperature is low as compared to the bare land (Sarwar and Bill 2007).

Table 7 Statistics of Estimated Sensible Heat Flux

Images	H with TIR_{RES} (W/m2)			H with TIR_{WAV} (W/m2)		
	Min	Max	Mean	Min	Max	Mean
4-Dec-1999	-18.43	294.78	110.63	-22.43	306.64	119.26
19-Oct-2000	-18.63	297.41	134.28	-11.25	269.05	128.90

3.2.6 Evaporative Fraction

Prior to the estimation of actual evapotranspiration image, evaporative fraction images were derived. The value of evaporative fraction usually varies from 0 to 1 (Sarwar and Bill 2007; Ambast et al 2008). Several studies have shown that this technique is reasonable with differences in daily evapotranspiration less than 1 mm/day (Kustas et al 1994). The low evaporative fraction is observed for dry uncultivated areas, whereas the high evaporative fraction for water bodies. Table 8 shows the statistical value of the evaporative fraction obtained for the images derived from both resampled TIR image and wavelet enhanced TIR image.

Table 8 Statistics of Estimated Evaporative Fraction

Images	Evaporative fraction with TIR_{RES} (-)			Evaporative fraction with TIR_{WAV} (-)		
	Min	Max	Mean	Min	Max	Mean
4-Dec-1999	0	0.96	0.69	0	0.98	0.78
19-Oct-2000	0	0.98	0.68	0	0.97	0.79

3.2.7 Daily Actual Evapotranspiration

The estimation of actual evapotranspiration (ETact) is the final step in the SEBAL process. The spatial distribution of ETact over the study area is discussed based on the derived ETact using surface temperature obtained from resampled TIR image and wavelet enhanced TIR image. Table 9 reports the statistics of ETact for the analyzed images.

Table 9 Statistics of Actual Evapotranspiration Estimation

Images	ETact with TIR_{RES} (mm/day)			ETact with TIR_{WAV} (mm/day)		
	Min	Max	Mean	Min	Max	Mean
4-Dec-1999	0	5.37	3.24	0	4.97	2.41
19-Oct-2000	0	4.98	2.89	0	5.09	2.62

Figure 6 depict the spatial variation of the actual evapotranspiration estimated using the surface temperature image derived from resample TIR image and wavelet enhanced TIR image. It is observed from the ETact images that the spatial variation has a similar pattern with the corresponding evaporative fraction images. The spatial variation of the ETact estimated using resampled TIR image ranges from minimum of 0 to maximum of 5.67 mm/day and for ETact estimated using wavelet TIR image the value ranges from 0 to 5.79 mm/day. The distribution pattern of actual evapotranspiration for different land covers are presented in Table 10.

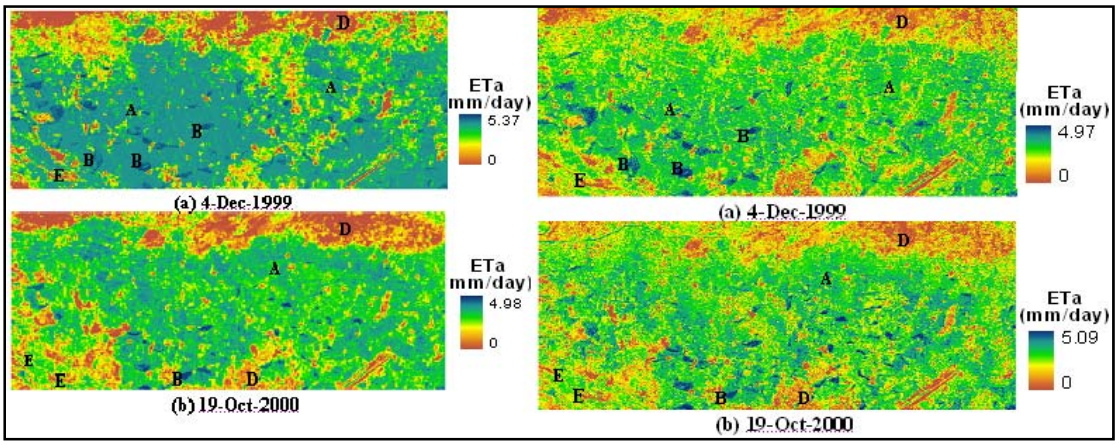

Figure 6 Spatial Distribution of ETact Using Resampled TIR Image and Wavelet Enhanced TIR Image

3.2.8 Comparison of Sebal Results to Reference ET

The daily estimates of ET_{act} results estimated by SEBAL were compared with the reference evapotranspiration estimated by conventional approaches. The comparison is targeted on three scales point to point, with the spatial average of vegetated area and also with the spatial average of the whole study area. The results are displayed in Table 11. It is evident from Table 11 that the spatial average of SEBAL results for ET_{act} -WAV estimated from wavelet enhanced TIR

image were lower than the reference ET of the two approaches compared to ET_{act} -RES estimated from resampled TIR image.

Table 11 Summary of SEBAL Estimates at Different Scale and the Point Estimate of Reference ET

Images	ET_o Penman-Monteith (mm/day)	ET_o (Pan evaporation) (mm/day)	ET_{act} Station Pixel (mm/day)		ET_{act} Vegetation (mm/day)		ET_{act} (whole scene) mm/day	
			ETact-RES	ETact-WAV	ETact-RES	ETact-WAV	ETact-RES	ETact-WAV
4-Dec-99	4.32	3.19	4.17	4.12	3.56	4.18	3.24	2.41
19-Oct-00	4.65	4.4	4.27	4.24	3.71	4.27	2.89	2.62

The percentage difference in the estimation of actual evapotranspiration was also analyzed. The penman-Monteith derived ET_o was compared with the actual evapotranspiration of the agricultural landuse. Table 12 shows the percentage difference in the estimation of actual evapotranspiration. It is well explained from the Table 12 that the ET_{act} estimated from the wavelet enhanced TIR image has a reliable estimate of ET_{act}.

Tsouni et al., (2008) has discussed that, the Penman-Monteith method is useful as it sets an upper limit to evapotranspiration which should not be exceeded by the actual evapotranspiration. The estimation of reference evapotranspiration (Penman-Montieth model) calculated from climatic data using CROPWAT (Smith et al 1990) and satellite estimation based on surface energy balance approach show that generally evapotranspiration values from satellite information are lower than computed using the CROPWAT model (Table 11). The comparison made with the spatial average of the agricultural area with the point estimate also shows a good agreement. This comparison is done mainly starting from the definition point of view (Allen et al 1998), reference ET is for a hypothetical grass with optimum supply, extensive surface of green, completely shading the ground and albedo of about 0.2.

Table 12 Percentage Difference between ET Estimates for Agricultural Land Type

Images	ETo Penman-Monteith (mm/day)	ET_{act} Vegetation (mm/day)		Percentage Difference (%)	
		$ET_{act\text{-}RES}$	$ET_{act\text{-}WAV}$	$ET_{act\text{-}RES}$	$ET_{act\text{-}WAV}$
4-Dec-99	4.32	3.56	4.18	17.59	3.24
19-Oct-00	4.65	3.71	4.27	20.22	8.17

Conclusions

The analysis on relation between actual evapotranspiration and surface temperature reveals that at higher temperature, the sensible heat flux is high and hence evapotranspiration is also high and vice versa. The same relation was found with parameters calculated using both resampled TIR image and wavelet enhanced TIR image. Even though there was no ground truth data for validation of the actual evapotranspiration derived from SEBAL, it was also attempted to compare it with the conventional approaches which are considered to be the upper limit of the remote sensing result (Ambast et al 2008). The comparison was made between the daily actual evapotranspiration (ETact-RES and ETact -WAV) values obtained from SEBAL, Penman-Monteith approach. The reference ET method provided point estimates and was influenced by the surrounding microclimate. But the RS approach gives spatial estimation with pixel size of 30m over a large area. The evapotranspiration and vegetation index have a high agreement in

terms of spatial distribution based on the positive relation of vegetation index and evapotranspiration.
The resulting ET information has a great potential to the water management, especially irrigation management. The largest advantage of the SEBAL is that it is an operationally usable model that can be applied with a minimum amount of ground data. Further the distributed values of actual evapotranspiration obtained from the developed methodology could be utilized directly in the hydrological and crop models for addressing various hydrological and agricultural problems.

References

Allen, R.G., Pereira, L.S., Raes, D. and Smith M. 1998. Crop evapotranspiration. *guidelines for computing crop water requirements, FAO Irrigation and Drainage, Paper No. 56, Rome, Italy.*

Ambast, S.K., Keshari, A.K. and Gosain, A.K. 2008. Estimating Regional Evapotranspiration Using Remote Sensing: Application to Sone Low Level Canal System, India. Journal of Irrigation and Drainage *Engineering,134 (13): 13-25.*

Bastiaanssen, W.G.M., Menenti, M., Feddes, R.A. and Holtslag, A.A.M. 1998.A remote sensing surface energy balance algorithm for land (SEBAL)-1. Formulation. Journal of Hydrology,212-213: 198-212.

Caparrini, F. and Manzella, F. 2009. Hydrometeorological and vegetation indices for the drought monitoring system in Tuscany Region, Italy. Advances in Geosciences 17:105-110.

Carlson. T.N. and Buffum. M.J. 1989. On estimating total evapotranspiration from remote surface temperature measurements. Remote Sensing of Environment, 29:197-207.

Carlson, T.N., Gillies, R.R. and Schmugge, T.J. 1995. An interpretation of methodologies for indirect measurements of soil water content. Agricultural and Forest Meteorology, 77:191-205.

Kustas, W.P., Moran, M.S., Humes, K.S., Stannard, D.I., Pinte,r P.J., Hipps, L.E., Swiatek, E. and Goodrich, D.C. 1994. Surface energy balance estimates at local and regional scales using optical remote sensing from an aircraft platform and atmospheric data collected over semiarid rangelands. Water Resources Research, 30(5):1241-1259.

Kustas, W.P. and Norman, J.M. 1996. Use of remote sensing for evapotranspiration monitoring over land surface. Hydrological Sciences Journal. 41(4):495-516.

Li, H., Manjunath, B.S. and Mitra, S.K. 1995. Multisensor Image Fusion Using the Wavelet Transform', Graphical Models and Image Processing. 57(3):235-245.

Mansour, S.A. and Guangdao, H. 2007. Using remote sensing data to improve geological interpretation mapping in Heqing Area, Northwestern Yunnan Province, China. Asian Journal of Information Technology. 6(4):495-501.

Morse, A., Tasumi, M., Allen, R.G. and Kramber, W.J. 2000. Application of the SEBAL methodology for estimating consumptive use of water and streamflow depletion in the Bear River basin of Idaho through remote sensing. Final Report, Phase I, Submitted to The Raytheon

Systems Company, Earth Observation System Data and Information System Project, by Idaho Department of Water Resources and University of Idaho.

Murray, T. and Verhoef, A. 2007. Moving towards a more mechanistic approach in the determination of soil heat flux from remote measurements II, Diurnal shape of soil heat flux. Agricultural and Forest Meteorology, 147:88-97.

Pradhan, P. 2005. Multiresolution based, Multisensor, Multispectral image fusion', Ph.D. dissertation, Mississippi State University, Mississippi.

Sarwar A. and Bill R. (2007), 'Mapping evapotranspiration in the Indus river basin using ASTER data', International Journal of Remote Sensing, Vol. 28, No. 22, pp. 5037-5046.

Smith, M., Clark, D. and El-Askari, K. 1990. CROPWAT 4 Windows, Land and Water Development Division. Food and Agriculture Organization, Rome, Italy.

Tasumi, M. 2003. Progress in operational estimation of regional evapotranspiration using satellite imagery. Ph.D. Dissertation, University of Idaho, Moscow, Idaho.

Tsouni, A., Kontoes, C., Koutsoyiannis, D., Elias, P. and Mamassis, N. 2008. Estimation of actual evapotranspiration by remote sensing: Application in Thessaly Plain, Greece. *Sensors*, 8:3586-3600.

Wald, L., Ranchin, T. and Mangolini, M. 1997. Fusion of satellite images of different spatial resolutions: Assessing the quality of resulting images. *Photogrammetric Engineering and Remote Sensing* 63(6):691-699.

Wehrmann, T., Colditz, R.R., Bachmann, M., Steinnocher, K. and Dech, S. 2005 Evaluation of Image Fusion Techniques. Remote Sensing & GIS Environmental Studies 113:296-302.

Estimating Sediment and Nutrient loads of Texas Coastal Watersheds with SWAT

A case study of Galveston Bay and Matagorda Bay

Nina Omani
Spatial Sciences Laboratory, Texas A&M University, Texas AgriLife Research, USA,
ninaomani@gmail.com

Raghavan Srinivasan
Spatial Sciences Laboratory, Texas A&M University, Texas AgriLife Research, USA,
r-srinivasan@tamu.edu

Taesoo Lee
Chonnam National University. Gwangju, S. Korea, Department of Geography,
taesoo@chonnam.ac.kr

Abstract

The SWAT (Soil and Water Assessment Tool) model was used to estimate terrestrial sediment and nutrients loads to Galveston and Matagorda bays from their contributing watersheds. In this report, the term "terrestrial loads" represents the sum of gauged loads from gauged subbasins and model-generated loads from ungauged subbasins. Municipal WWTPs and industrial point source discharges are not included in this calculation of water quality variables. This information, however, would be required to calculate the total nutrient load actually reaching a bay. Due to the lack of information of sedimentation and contributed nutrient load from the watersheds it was impossible to compare the SWAT outputs with estimated loads from literatures.

In this study, two watersheds, Galveston Bay and Matagorda Bay, were selected for a pilot study because one represents an urbanized watershed (Galveston Bay) and the other a rural watershed (Matagorda Bay). The project consists of two parts. Hydrologic simulation was performed in the first phase, and the second phase focuses on the estimation of sediment and nutrient loads. We used the USGS LOAD ESTimator (LOADEST) program to extrapolate the water quality samples into monthly data. Modeled monthly sediment showed very good agreement when compared with observed TSS with R2 ranging from 0.76 to 0.93 and NSE ranging from 0.70 to 0.93. Estimated monthly total nitrogen and total phosphorus showed good to acceptable correlation with observed values with R2 ranging from 0.69 to 0.80 and NSE ranging from 0.49 to 0.79, while predicted monthly nitrate was not satisfactory.

Keywords: Coastal, Texas, Sediment, Nutrient, SWAT

Introduction

The TWDB recently requested that the Soil and Water Assessment Tool (SWAT) be used to estimate surface inflows and sediment and nutrient loads to the bays with up-to-date technology and data. Accordingly, this project was initiated to develop and apply the SWAT model to two Texas estuaries in order to estimate sediment and nutrient loads and to evaluate model performance when compared with TWDB reports. Freshwater inflow from ungauged and gaged watersheds to coastal bays was predicted using SWAT in the first phase of this project. SWAT estimated total bay sediment and nutrient loads for both gauged and ungauged subbasins using a calibrated model setting for gauged subbasins in the second phase of the project.
Although not considered, municipal WWTPs and industrial point source discharges from the subbasins would be required to calculate the total nutrient loads actually reaching a bay. The objectives of this study were to: 1) apply the SWAT model using up-to-date technology such as Geographic Information System (GIS) data, satellite imagery and NEXt generation RADar (NEXRAD) weather data for two watersheds, 2) estimate sediment and nutrient loads to the estuary by including gauged and ungauged subbasins, and 3) develop methodologies and procedures for estimating terrestrial sediment and nutrient loads to the estuaries as required by the TWDB.

Methodology

To avoid repetition of the common sections we did not include the study area description, soil, land use, DEM and streamflow data collection, SWAT model description or initial model settings in this paper. For more information refer to the first phase (Lee et al., 2011).

Sediment and nutrient samples at USGS gauging stations

The USGS (U.S. Geological Survey) provided sediment sample data at stream gauging stations, 85 of which were available in the watersheds (Figure 1). Of those stations, only two in Galveston Bay watershed and one in Matagorda Bay watershed were used for sediment calibration. Nutrient samples were available at three gauging stations in Galveston Bay watershed and two gauging stations in Matagorda Bay watershed. All other stations were eliminated because they had either too much missing data or the gauging stations were located in a minor tributary and could not be analyzed.
Table 1 and Table 2 summarize the available gauging stations for sediment and nutrients, respectively.
Gauging stations 08066500 and 08162500 are inlets for the Galveston Bay and Matagorda Bay watersheds, respectively. Due to the lack of sediment and nutrient data, delivered loads from the inlet to the Galveston watershed were ignored. However, that information would be required to calculate total sediment and nutrient loads actually reaching a bay. The monthly sediment and total N from the inlet to the Matagorda are estimated at Gauging Station 08162000, which is located upstream of the Matagorda inlet point (Gauge 08162500).

Project Setup

In SWAT, two separate projects were set up for each watershed. The modeled period for sediment load at Galveston and Matagorda watersheds lasted from 1984 to 2000 and 1980 to 2000, respectively, and they included two-year model warm-up periods. All data used in the SWAT model were projected to Albers Equal Area with North American 1983 for datum. This section explains the setup and parameters of the two SWAT projects. Watershed delineation, subbasins, HRUs and NEXRAD data are available in the report on the first phase.

Table 1. List of USGS gauging stations used for sediment calibration in both watersheds

Watershed	Station #	Note
Galveston Bay Watershed	08069000	Subbasin 30 106 samples 1965-1975, 2005-2010
	08070000	Subbasin 16, 15* 109 samples 1976-1990, 2004-2008
Matagorda Bay Watershed	08164000	Subbasin 2, 7 97 samples 1977-1993

*Subbasin numbers indicate the contributing subbasins for each gauging station.

Table 2. List of USGS gauging stations used for nutrients calibration in both watersheds

Watershed	Station #	Note
Galveston Bay Watershed	08067650	Subbasin 7 282 samples 1983-2004
	08069000	Subbasin 30 (only used for validation) 333 samples 1983-1999, 2008
	08070000	Subbasin 16, 15* 231 samples 1996-1999, 2005-2010
	08070500	Subbasin 1, 3, 5, 12 423 samples 1984-1999, 2005-2010
Matagorda Bay Watershed	08164000	Subbasin 2, 7 402 samples 1972-1993
	08162600	Subbasin 10 330 samples 1970-1981

* Subbasin numbers indicate the contributing subbasins for each gauging station.

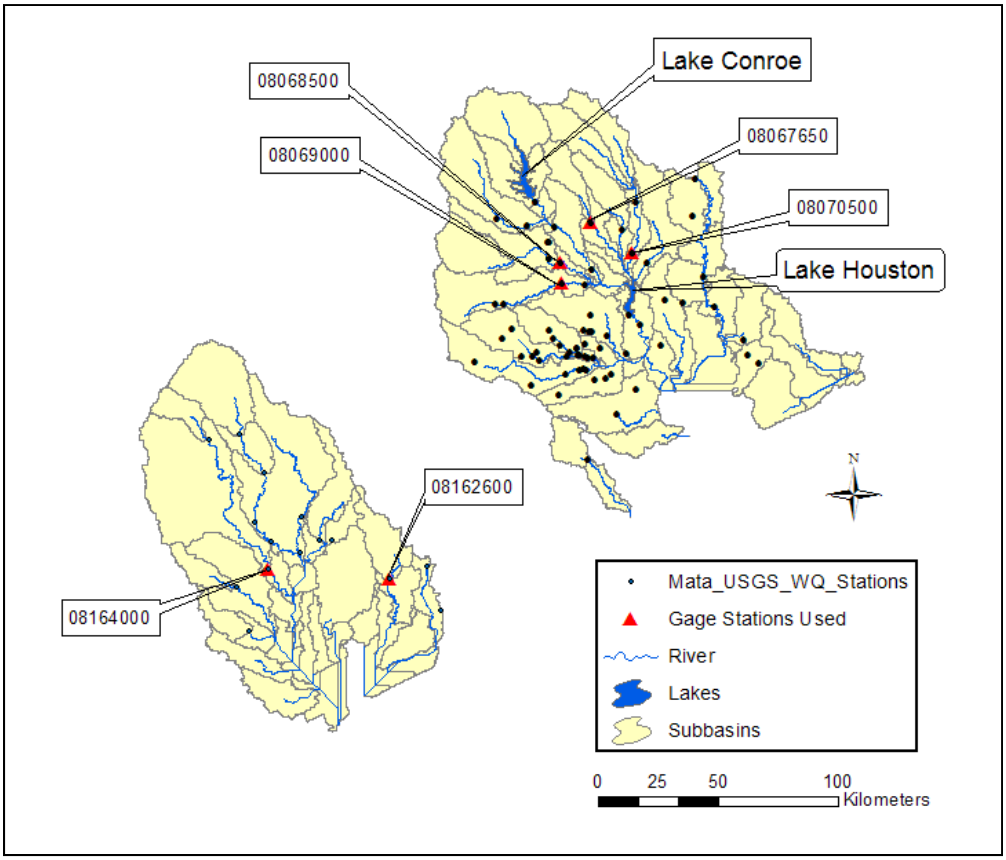

Figure 1. USGS gauging stations available in both watersheds

Land use distribution in each gauged watershed

Table 3 shows the percentage of each land use category in each gauged subbasin and contributing subbasins that lie above the gauging station in both Galveston and Matagorda watersheds. The land use percentages are portions of the total area from each contributing subbasin and are not from the original land cover dataset but from the SWAT-processed HRUs. This means any land use categories covering less than 5% of the total subbasin area were not included in this distribution.

Most subbasins with gauging stations are located in the upper part of the watershed in both Galveston and Matagorda bays, and the land use categories within these subbasins consist mainly of forest and hay (Table 3).

Point sources

This study did not include point sources, but they were set up in most modeled subbasins for future use. All outputs from point sources were set to zero during this study.

Table 3. Land use distributions in each gauged subbasin. The total area includes the gauged subbasins and contributing subbasins that lie above the gauged subbasin.

Land Use	Gauging stations in Galveston			
	08067650 7*	08070500 1, 3, 5, 12	08068500 16, 15	08069000 30
Water	0%	0%	0%	0%
Urban	8%	2%	20%	32%
Forest	32%	51%	33%	9%
Agricultural	0%	0%	0%	14%
Hay	23%	11%	21%	45%
Rangeland	21%	15%	16%	0%
Wetland	16%	21%	11%	0%
Total	100%	100 %	100%	100%

Land Use	Gauging stations in Matagorda	
	08164000 2,7	08162600 10
Water	0%	0%
Urban	0%	0%
Forest	20%	0%
Agricultural	0%	58%
Hay	61%	42%
Rangeland	19%	0%
Wetland	0%	0%
Total	100%	100%

* Subbasin numbers

Agricultural practices

One of the important factors affecting sediment and nutrient loads is agricultural practices. Non-point source pollution, such as fertilizer and pesticide, has important effects on the surface and underground water quality through irrigation and rainfall runoff, soil infiltration and percolation.

In this project, simplified assumptions are made to describe agricultural practices. Agricultural land in the watersheds is simulated as row-crop agriculture land (AGRR) with automatic irrigation and fertilization operations. The presented agricultural practices and rates are only for the purposes of annual nutrient load estimation; it is not applicable for daily or weekly simulation. Agricultural practices in the AGRR class are defined as follows:

Practices	Heat Units
Conservation tillage	0.15
Planting	0.15
Auto fertilization (1 kg mineral N/kg fertilizer)	0.16
Auto irrigation (Auto water stress: 85%)	0.16
Harvest and kill operation	1.2

Soil supporting practice factor

The soil support practice factor was reduced from one to 0.3 in plain areas to 1 in uplands. For urban areas it was reduced to 0.3. The USLE_P value was set to 0.7 and 0.3 for agricultural lands and urban areas, respectively.

Sensitivity Analysis

Parameter sensitivity analysis was performed using the SWAT Calibration and Uncertainty Program (SWAT-CUP) (Abbaspour, 2004). SWAT-CUP is a computer program that calibrates SWAT models. It enables sensitivity analysis, calibration, validation and uncertainty analysis of SWAT models. The current version, SWAT-CUP 4.3.2, enables us to calibrate parameters of all soil layers, management methods and crops. In this project, Sequential Uncertainty Fitting (SUFI2), one of the SWAT-CUP calibration methods, was used to perform global and one-at-a-time sensitivity analysis. Table 4 shows the results of global sensitivity for suspended sediment, Nitrate, organic Nitrogen and Phosphorus.

Six parameters were sensitive to sediment only. From 18 parameters influencing water quality variables, six parameters were sensitive to organic N, four parameters were sensitive to Nitrate and seven parameters were sensitive to organic and mineral P. Sensitivity analysis was performed for the observed suspended sediment and nitrate at Reach 7 of Matagorda watershed and organic N, organic P, and mineral P at Reaches 7, 12 and 30 of Galveston watershed.

Table 4. List of sensitive SWAT parameters

Sediment	Nitrate	Organic	Mineral P	Organic
CH_N2	CDN	ERORGN	PSP	PSP
SPCON	NPERCO	BIOMIX	ERORGP	ERORGP
PRF	SDNCO	BC3	CDN	CDN
SPEXP	CMN	NPERCO	SDNCO	SDNCO
CH_COV2		CDN	PHOSKD	BIOMIX
CH_COV1		RS4	RCN	

Model Calibration and Validation

Calibration and validation for each gauging station

Grab samples of water quality data including suspended sediment, nitrate, organic N, total N, orthophosphate P, and total P were extrapolated into monthly data using the LOADEST program. In this project, orthophosphate is referred to as mineral P and for calibration purpose it is assumed that organic P is difference when observed mineral P is subtracted from total P.

After initially configuring SWAT, model calibration was performed. Calibration refers to the adjustment or fine-tuning of modeling parameters to reproduce observations. This section of the report presents the process that was used to calibrate the model both for water quality. Modeling results are also summarized.

Monthly sediment was calibrated against USGS gauging station data. Time periods with available data, however, varied among the gauging stations (Table 5). Calibration and validation

periods were determined based on the streamflow calibration (1991-2000) and validation periods (1977-1990; Table 5).

Table 5. USGS gauging station data and the period of calibration and validation. The calibration period was selected for the latter half of the entire data period.

Galveston watershed

Water quality	Subbasin	Gauging stations	Data period	Calibration period	Validation period
TSS	15	08069000	1985-2000	1991-2000	1985-1990
	30	08069000	1985-2000	1991-2000	1985-1990
TN	7	08067650	1984-2000	1991-2000	1984-1990
	12	08070500	1984-2000	1991-2000	1984-1990
	30*	08069000	1984-2000	1991-2000	1984-1990
TP	7	08067650	1985-2000	1991-2000	1985-1990
	12	08070500	1985-2000	1991-2000	1985-1990
	30*	08069000	1991-2000	1991-2000	-
ORGN	7	08067650	1984-2000	1991-2000	1984-1990
	12	08070500	1984-2000	1991-2000	1984-1990
	30	08069000	1984-2000	1991-2000	1984-1990
ORGP**	7	08067650	1991-2000	1991-2000	-
	12	08070500	1991-2000	1991-2000	-
	30*	08069000	1991-2000	1991-2000	-
MINP	7	08067650	1991-2000	1991-2000	-
	12	08070500	1991-2000	1991-2000	-
	30*	08069000	1991-2000	1991-2000	-
NO_3	30*	08069000	1984-1992	-	1984-1992
	12	08070500	1991-2000	1991-2000	-

* Subbasin 30 was considered for calibrating local parameters affecting the nutrient load only

Matagorda watershed

Water quality	Subbasin	Gauging stations	Data period	Calibration period	Validation period
TSS	7	08164000	1980-2000	1991-2000	1980-1990
TN	7	08164000	1980-1993	1986-1993	1980-1985
	10*	08162600	1977-1981	-	1977-1981
TP	7	08164000	1980-1993	1986-1993	1980-1985
	10*	08162600	1977-1981	-	1977-1981
ORGN	7	08164000	1980-1993	1986-1993	1980-1985
	10*	08162600	1977-1981	-	1977-1981
ORGP**	7	08164000	1980-1993	1986-1993	1980-1985
MINP	7	08164000	1980-1993	1986-1993	1980-1985
NO_3	7	08164000	1980-1993	1986-1993	1980-1985

*Subbasin 10 was considered for calibrating local parameters affecting the nutrient load only

**Due to the lack of data it is assumed that ORGP=TP-MINP

The streamflow calibration period for some of the gauging stations was taken from 1991 to 2008, but the plotted graphs and statistics revealed that the predicted streamflow at selected gauging stations for sediment and nutrient calibration matched well to the observed streamflow for years before 2000. Therefore, sediment and nutrients were calibrated from 1991 to 2000.

It should be mentioned that Subbasin 30 (Galveston watershed) was not considered for basin-wide parameter determination, and only the parameters affecting the subbasin nutrient load were determined by calibration. This subbasin was only selected to show the model performance in an urbanized area and was not used to calibrate the parameters affecting nutrient loads from other gauged subbasins.

Due to the lack of data, Subbasin 10 in Matagorda was used for validation purposes only. The basin-wide parameters were determined using the nutrient data at Reach 7. After determining the basin-wide parameters, these parameters remained constant and local parameters of Subbasin 10 were determined. Municipal WWTPs and industrial point source discharges were not included in this study.

Table 6 and Table 7 list parameters calibrated for sediment and Table 8 and Table 9 list parameters calibrated for nutrients and their default and adjusted value.

Table 6. Parameter values for sediment calibration (gauging stations) used in the Galveston Bay watershed SWAT project

Parameters	Subbasin #	Default Value	Input Value
CH_N2.rte	30	0.014	0.032
CH_N2.rte	16, 15	0.014	0.059
SPCON.bsn	15, 16, 30	0.0001	0.005
PRF.bsn	15, 16, 30	1	0.445
SPEXP.bsn	15, 16, 30	1	1.219
CH_COV1.rte	15, 16, 30	0	0.005
CH_COV2.rte	15, 16, 30	0	0.715

Table 7. Parameter values for sediment calibration (gauging stations) used in the Matagorda Bay watershed SWAT project

Parameters	Subbasin #	Default Value	Input Value
CH_N2.rte	2, 7	0.014	0.070
SPCON.bsn	2, 7	0.0001	0.004
PRF.bsn	2, 7	1	0.430
SPEXP.bsn	2, 7	1	1.260
CH_COV1.rte	2, 7	0	0.005
CH_COV2.rte	2, 7	0	0.715

Table 8. Parameter values for nutrient calibration (gauging stations) used in the Galveston Bay watershed SWAT project

Parameters	Default value	Subbasins 1,3,5,12	Subbasin 7	Subbasin 30*
RS4.swq	0.05	0.022	0.09	0.063
BC3.swq	0.21	0.19	0.21	0.26
RS3.swq	0.5	0.77	0.72	0.37
RS2.swq	0.05	0.016	0.020	0.051
BC4.swq	0.35	0.06	0.025	0.64
RS5.swq	0.05	0.008	0.065	0.061
ERORGP.hru	0	0.91	0.98	2.19
ERORGN.hru	0	3.71	0.69	0.76
BIOMIX.mgt	0.2	0.96	0.96	0.92
NPERCO.bsn	0.2	0.12		-
CMN.bsn	0.0003	0.001		-
RSDCO.bsn	0.05	0.04		-
CDN.bsn	1.4	2.99		-
PPERCO.bsn	10	10.86		-
PHOSKD.bsn	175	170		-
PSP.bsn	0.4	0.31		-
SDNCO.bsn	0.05	0.083		-
RCN.bsn	1	0.44		-

Table 9. Parameter values for nutrient calibration (gauging stations) used in the Matagorda Bay watershed SWAT project

Parameters	Default value	Subbasin 2, 7	Subbasin 10*
RS4.swq	0.05	0.011	0.087
BC3.swq	0.21	0.27	0.37
RS3.swq	0.5	0.97	0.72
RS2.swq	0.05	0.083	0.046
BC4.swq	0.35	0.13	0.63
RS5.swq	0.05	0.097	0.085
ERORGP.hru	0	0.39	0.81
ERORGN.hru	0	2.22	0.44
BIOMIX.mgt	0.2	0.54	0.99
NPERCO.bsn	0.2	0.37	-
CMN.bsn	0.0003	0.001	-
RSDCO.bsn	0.05	0.056	-
CDN.bsn	1.4	1.26	-
PPERCO.bsn	10	13.23	-
PHOSKD.bsn	175	165	-
PSP.bsn	0.4	0.35	-
SDNCO.bsn	0.05	0.86	-
RCN.bsn	1	0.78	-

Determination of the SWAT parameters at ungauged subbasins

Identical to the applied method in Phase I, comparison of sediment and nutrient loads from the ungauged and gauged subbasins of Galveston and Matagorda bays was conducted by extending and applying parameter settings from the calibration of gauged subbasins to ungauged subbasins. In addition, for each watershed, SWAT's sediment and nutrient output was compared with TWDB's estimated sediment and nutrient loads from some of the subbasins. For this comparison, parameters were adjusted only in ungauged subbasins which were not considered during calibration (see previous section). Based on the TWDB's estimated annual average sediment loads from Subbasin 5 (Station 08070000) in Galveston watershed the higher CH_N2 values from 0.1 to 0.15 were applied to ungauged subbasins in Galveston Bay watershed. When applying parameter values to ungauged subbasins, the parameter values of gauged subbasins were applied based on land cover similarity. The ungauged subbasins in Galveston Bay watershed were classified into three classes, urbanized, forested, and semi-urbanized subbasins. The parameter values from the calibration of the urbanized subbasin were applied to the ungauged urbanized subbasins and the average parameter value from calibration of all gauged subbasins was applied to semi-urbanized ungauged subbasins. The parameter values of ungauged subbasins are presented in Table 10 and Table 11.
The dominant land covers in the Matagorda Bay watershed are agricultural and hay, so the ungauged subbasins were classified in three classes, agricultural, non-agricultural (hay and rangelands), and semi-agricultural. The parameter values from gauged agricultural subbasin 10 were applied to ungauged agricultural subbasins in the Matagorda Bay watershed.

Table 10. Parameter values for ungauged subbasins used in the Galveston Bay SWAT project

Parameters	Default value	Urbanized subbasins*	Forested subbasins**	Semi-urbanized subbasins***
CH_N2.rte	0.014	0.032	0.059	0.1-0.15
CH_COV1.rte	0	0.005	0.005	0.005
CH_COV2.rte	0	0.715	0.715	0.715
RS4.swq	0.05	0.063	0.022-0.09	0.058
BIOMIX.mgt	0.2	0.922	0.960	0.946
ERORGN.hru	0	0.756	0.69-3.71	1.719
RS2.swq	0.05	0.051	0.016-0.02	0.029
BC4.swq	0.35	0.644	0.025-0.060	0.243
RS5.swq	0.05	0.061	0.007-0.065	0.044
ERORGP.hru	0	2.190	0.91-0.98	1.359
BC3.swq	0.21	0.263	0.19-0.21	0.221
RS3.swq	0.5	0.372	0.77-0.72	0.621

*Parameter values from gauged Subbasin 30 were applied for ungaugegauged urbanized subbasins
** Parameter values from gauged Subbasin 7 or 12 were applied for forested subbasins
***Average parameter values from calibrated gauged Subbasins 7, 12, 30 were applied for ungauged subbasins

Table 11. Parameter values for ungauged subbasins used in the Matagorda Bay SWAT project

Parameters	Default value	Agricultural subbasins*	Non-agricultural subbasins**	Semi-agricultural subbasins***
CH_N2.rte	0.014	0.07	0.07	0.07
CH_COV1.rte	0	0.005	0.005	0.005
CH_COV2.rte	0	0.715	0.715	0.715
RS4.swq	0.05	0.087	0.011	0.049
BIOMIX.mgt	0.2	0.99	0.54	0.76
ERORGN.hru	0	0.44	2.22	1.33
RS2.swq	0.05	0.046	0.083	0.065
BC4.swq	0.35	0.63	0.13	0.38
RS5.swq	0.05	0.085	0.097	0.091
ERORGP.hru	0	0.81	0.39	0.6
BC3.swq	0.21	0.37	0.98	0.675
RS3.swq	0.5	0.72	0.267	0.49

*Parameter values from gauged Subbasin 10 were applied for ungauged agricultural subbasins
** Parameter values from gauged Subbasin 7 were applied for non-agricultural subbasins
***Average parameter values from calibrated gauged Subbasins 7 and 10 were applied for ungauged subbasins

Results

Monthly Suspended Sediment at gauging stations

Table 12 summarizes monthly suspended sediment calibration and validation results from gauged subbasins. Model performance statistics used to assess calibration efforts indicate that SWAT model estimates are good, with a range of 0.75 to 0.93 for R^2 and NSE ranging from 0.70 to 0.93 for both watersheds. Validation results also correlate well, ranging from 0.59 to 0.80 for R^2 and from 0.34 to 0.79 for NSE. Removing the single high pick from the predicted monthly sediment of Subbasin 15 reduced the R^2 and NSE from 0.93 to 0.77 and 0.55, respectively, in the calibration period.

Figure 2 shows the observed and predicted monthly sediment loads for calibration and validation periods at Subbasin 30 in the Galveston Bay watershed. The graphs show in both calibration and validation periods that the peaks do not fit well. One of the reasons could be streamflow mismatches; the monthly predicted streamflow for Subbasin 30, however, was accurate enough to calibrate monthly sediment load. The mismatch in June 1992 is related to a mistake in rainfall or streamflow measurement; the observed streamflow was recorded as negligible for June 1992 even though there was a considerable amount of precipitation.

Table 12. Model performance in estimating monthly sediment (calibration and validation)

Watershed	Station #	Subbasin #	Calibration		Validation	
			R^2	NSE*	R^2	NSE
Galveston Bay watershed	08068500	16, 15	0.93(0.77)	0.93(0.55)	0.59	0.46
	08069000	30	0.75	0.70	0.79	0.34
Matagorda Bay watershed	08067650	2, 7	0.76	0.71	0.8	0.79

*NSE: Nash Sutcliffe model efficiency

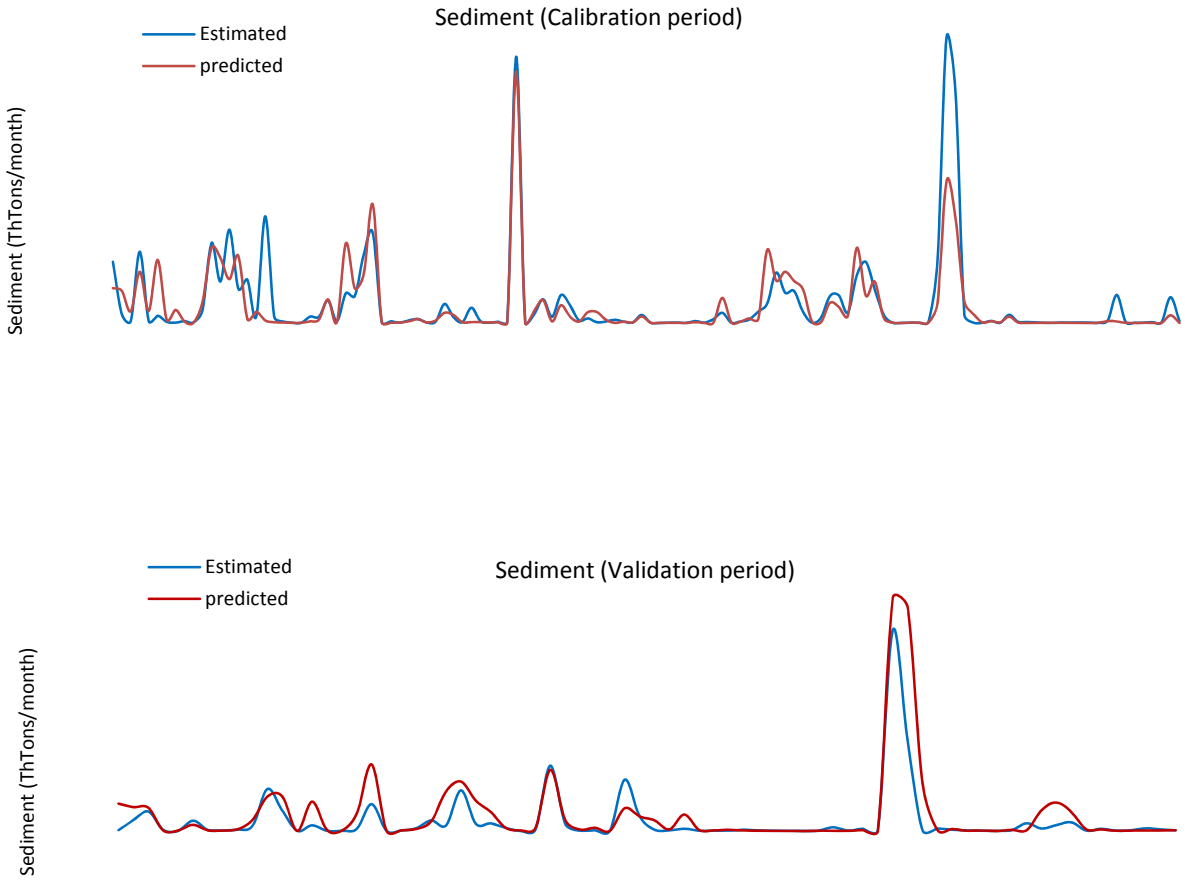

Figure 2. Observed and predicted monthly sediment for calibration and validation periods at Subbasin 30, Galveston Bay watershed

Monthly Nutrients at gauging stations

Table 13 summarizes monthly nutrient calibration and validation results from gauged subbasins. Model performance statistics used to assess calibration efforts indicate that SWAT model estimates are good in rural subbasins and poor in urbanized subbasins (Subbasin 30 of Galveston). It should be mentioned that data of municipal WWTPs and industrial point source discharges in the subbasins were not considered in nutrient load calibration. The uncalibrated model failed to predict total Nitrogen and Phosphorus components, however, it well predicted the total Nitrogen and total Phosphorus with R^2 and NSE about 0.80.

The model performed well in predicting all nutrient loads except nitrate; the table shows poor performance in nitrate prediction in Subbasin 12. The main reason is uncertainty in nitrate contribution from agricultural fertilizers. Nitrate load from Subbasin 12 in the Galveston Bay watershed was less than 10% of the total nitrogen load, so the effect of poorly predicting NO_3 was negligible in predicting the total nitrogen load.

Total N and total P, organic P and mineral P from Subbasin 30 in the Galveston watershed were not predicted well. The SWAT model underestimated the total N and total P from Subbasin 30 by about 47,000 kg and 15,500 kg per month, respectively; this indicates that point sources contribute constant Nitrogen and Phosphorus loads throughout the year. More than 30% of subbasin area is urban land. Eliminating the constant load from the Nitrogen and Phosphorus data of Subbasin 30 improves NSE from – 0.30 to 0.57 and – 0.40 to 0.69, respectively while the R^2 remains unchanged. It should be mentioned that due to the high uncertainty in nutrient loads from point sources, Subbasin 30 was considered for local parameter calibration only. Correlation for the validation period was poor in Subbasin 7 in Galveston Bay watershed; one of the reasons can be rapid urbanization of the Galveston Bay watershed since the 1980s. Figure 3 shows the observed and predicted monthly total N and total P loads for calibration and validation period at Reach 12 in Galveston Bay watershed.

The only poor result in Matagorda Bay watershed was related to prediction of Nitrate in Subbasin 7 for validation period. Single high pick in data series (January 1984) reduced R^2 from 0.39 to 0.03 and NSE from 0.37 to -3.54 for validation period, respectively. In fact, model output showed unexpected high increase in instream Nitrate load in January 1984, while there was considerable instream loss of Nitrate for other months during calibration and validation periods.

In general, the model did a better job at predicting the Matagorda nutrient load than it did predicting the Galveston nutrient load. As concluded in Phase I, correlation for the validation period was worse in the Galveston Bay watershed than in the Matagorda Bay watershed due to the fact that a much larger portion of the Galveston Bay watershed has urbanized since the 1980s while the Matagorda Bay watershed has experienced relatively little change in land use. The two important factors for improving simulation results are determining fertilization operation parameters and including point source loads in the model.

Table 13. Model performance in estimating monthly nutrients (calibration and validation)
Galveston

	Stations #	Subbasin #	Calibration		Validation	
			R^2	NSE	R^2	NSE
TN	08067650	7	0.81	0.49	0.47	-0.03
	08070500	12	0.85	0.63	0.77	0.57
	08069000	30*	0.71	-0.30(0.57)	-	-
TP	08067650	7	0.81	0.79	0.40	-0.06
	08070500	12	0.76	0.69	0.57	0.46
	08069000	30	0.71	-0.40(0.69)	-	-
ORGN	08067650	7	0.72	0.63	0.50	0.10
	08070500	12	0.70	0.60	0.44	0.29
	08069000	30	0.74	0.58	0.57	0.45
ORGP**	08067650	7	0.78	0.76	-	-
	08070500	12	0.64	0.60	-	-
	08069000	30	0.50	-0.15(0.53)	-	-
MINP	08067650	7	0.82	0.74	-	-
	08070500	12	0.80	0.62	-	-
	08069000	30	0.71	0.40 (0.67)	-	-
NO_3	08069000	30	-	-	0.28	-3.30
	08070500	12	0.51	0.08	-	-

Matagorda

	Stations #	Subbasin #	Calibration		Validation	
			R^2	NS	R^2	NS
TN	08164000	7	0.78	0.78	0.43	0.27
	08162600	10***	-	-	0.51	0.45
TP	08164000	7	0.70	0.68	0.65	0.55
	08162600	10	-	-	0.80	0.33
ORGN	08164000	7	0.84	0.70	0.55	0.51
	08162600	10	-	-	0.73	0.68
ORGP	08164000	7	0.71	0.63	0.62	0.49
MINP	08164000	7	0.68	0.60	0.63	0.52
NO_3	08164000	7	0.57	0.55	0.04 (0.38)	-3.5 (0.37)
	08162600	10	-	-	0.48	0.33

* Subbasin 30 was considered for calibrating local parameters affecting the nutrient load only
** Due to the lack of data it is assumed that ORGP=TP-MINP
*** Subbasin 10 was considered for calibrating local parameters affecting the nutrient load only

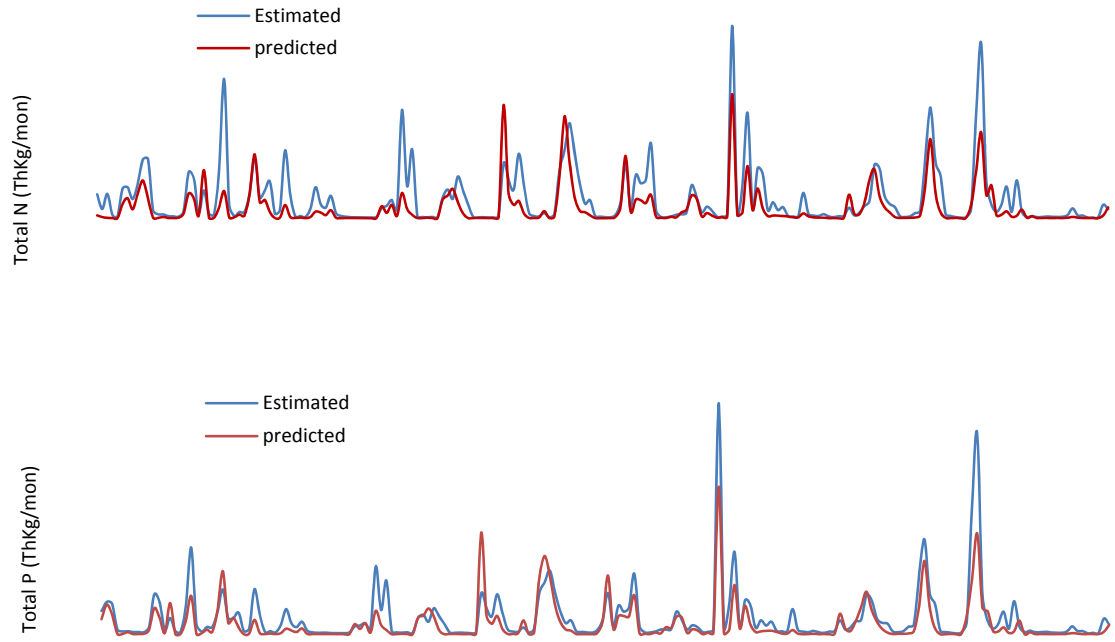

Figure 3. Observed and predicted monthly total N and total P for calibration and validation periods at Subbasin 12, Galveston Bay watershed.

Sediment and Nutrient Loads from Gauged and Ungauged Subbasins

Due to the lack of data at gauging stations at watershed inlets, the total sediment and nutrient loads from the Trinity River basin to Galveston Bay were ignored. However, that information would be required to calculate total sediment and nutrient loads actually reaching a bay. The monthly sediment and total N from the Colorado River basin to Matagorda were estimated at Gauging Station 08162000, which is located upstream of the Matagorda inlet point.
For more information, the total loads to the Matagorda Bay were estimated adding and eliminating the inlet loads. Annual average sediment and nutrient loads from 1977 to 2005 are summarized in Table 14. In this table, the contributed sediment and nutrient loads from HRUs are presented without considering instream processes such as deposition and erosion. Sediment routing processes dramatically affect the sediment load discharge and consequently nutrient loads from a reach. It was estimated that a certain portion of the contributed sediment from HRUs would be deposited at main channels, especially at head streams. Estimates of this transport loss ranged from 10 to 90 percent.
Due to the very limited available information about sediment and nutrient loads from Galveston Bay and Matagorda Bay watersheds over the model running period, it was not possible to compare simulated loads to estimated loads. Table 15 provides useful information about sedimentation and contributed nutrient loads from different land-uses calculated by SWAT_Check program. It should be mentioned that the values in this table are contributed loads from HRUs without considering sediment and nutrient routing process.

Table 14. Annual average sediment and nutrient loads over a 29-year period from 1977 to 2005

Variable name	Matagorda kg/ha	Galveston kg/ha	Matagorda kg	Galveston kg
Total sediment loading*	$4.60*10^3$	$3.5*10^3$	$5,366,71210^3$	$5,645,626*10^3$
Organic N	3.82	3.35	4,437,411	5,403,671
Organic P	0.31	0.65	360,104	1,048,473
NO_3 surface runoff	1.00	0.206	1,161,626	332,278
Soluble P Surface Runoff	0.134	0.066	55,757	155,654
NO_3 in rainfall	7.59	5.36	8,816,741	8,645,873

*The contributed sediment and nutrient loads from HRUs without considering instream processes

Table 15. Average sediment, surface runoff, NO_3 and ORGN
Galveston, 1977-2005

Land use	Area km^2	CN	Surface runoff mm	Sediment tons/ha	NO3 kg/ha	ORGN kg/ha
FRSE	1944	60	181	0.05	0.14	0.03
FRST	897	64	229	0.05	0.18	0.04
RNGE	618	70	277	2.87	0.19	2.22
HAY	3532	74	352	7.13	0.20	5.57
WETF	2553	77	398	0.00	0.24	0.00
RNGB	517	61	182	0.97	0.12	0.66
WATR	682	96	0	0.00	0.00	0.00
BERM*	3837	86	567	4.99	0.25	6.22
WETN	591	84	543	0.00	0.32	0.00
AGRR	942	79	434	10.49	0.31	9.23
FRSD	19	83	396	0.04	0.23	0.04

Matagorda, 1977-2005

Land use	Area km^2	CN	Surface runoff Mm	Sediment Tons/ha	NO3 Kg/ha	ORGN Kg/ha
HAY	5104	70	151	3.75	1.08	5.05
RNGB	991	71	210	2.19	0.68	1.78
FRSD	835	74	226	0.04	0.89	0.03
FRSE	249	61	162	0.03	0.58	0.02
AGRR	3042	84	450	10.58	1.50	5.54
WETF	0.5	78	182	0.00	0.59	0.00
WATR	1070	88	0.00	0.00	0.00	0.00
WETN	322	78	433	0.00	1.38	0.00

*Plant cover in urban areas

Figure 4 shows the accumulated monthly terrestrial sediment, total N and total P for each watershed. The average annual sediment and nutrient loads to Matagorda Bay and Galveston Bay from 1977 to 2005 are presented in Table 16. Finally, Table 17 and Table 18 show the average monthly loads from Galveston and Matagorda Bay watershed over 29 years.

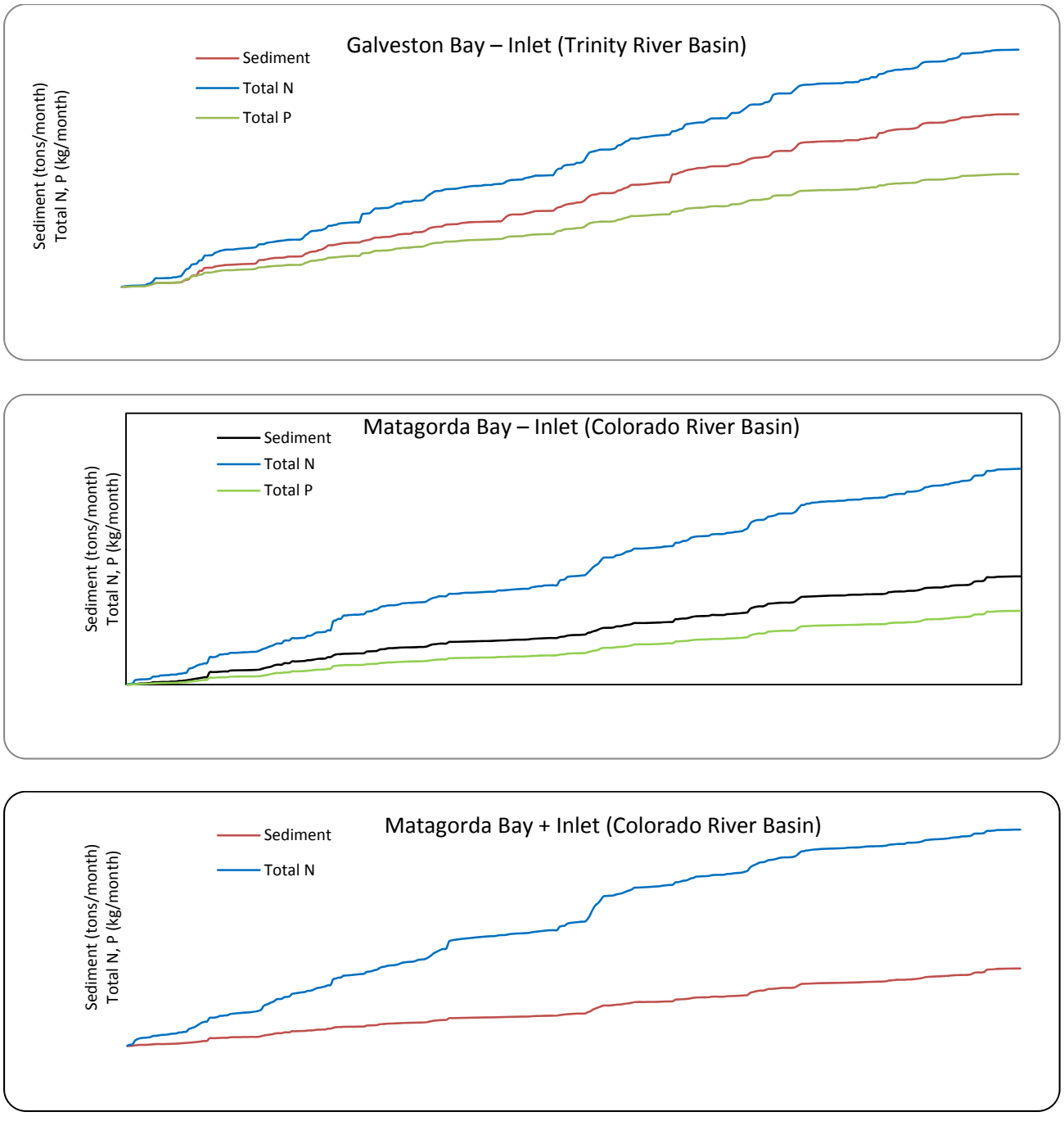

Figure 4. Accumulated monthly terrestrial sediment, total N and total P to the bay for each watershed.

Table 16. Average annual sediment and nutrient loads to Matagorda and Galveston Bays, 1977-2005

	Sediment ton/year	Total N kg/year	Total P kg/year
Galveston watershed	1,577,810	2,164,988	1,033,445
Matagorda watershed - Inlet	825,530	1,645,980	562,514
Matagorda watershed + Inlet	1,124,030	3,134,760	-*

*Total P data was not available at Matagorda inlet

Table 17. Average monthly loads from Galveston Bay watershed over 29 years.

	Sediment tons/month	Total N kg/month	Total P
January	205,074	364,986	163,514
February	143,459	287,569	125,915
March	115,166	175,949	87,221
April	99,251	140,159	70,942
May	114,699	102,496	65,310
June	182,308	138,207	82,132
July	94,413	70,198	33,200
August	59,726	80,210	36,481
September	132,079	213,002	94,502
October	158,359	212,029	98,826
November	132,748	195,583	92,528
December	140,637	184,685	82,925

Table 18. Average monthly loads from Matagorda Bay watershed over 29 years.

	Watershed+Inlet		Watershed-Inlet		
	Sediment ton/month	Total N kg/month	Sediment ton/month	Total N kg/month	Total P
January	43,421	235,870	41,914	221,278	36,014
February	57,330	147,581	55,829	140,271	35,357
March	74,020	148,719	71,774	143,163	42,225
April	51,019	154,176	49,646	149,795	36,247
May	84,855	136,136	82,189	128,678	58,217
June	89,278	149,127	86,562	140,915	60,108
July	46,129	61,339	44,566	57,990	25,414
August	25,568	45,591	24,802	43,338	18,096
September	114,276	218,263	110,663	193,520	75,016
October	118,331	169,508	115,058	158,916	73,858
November	104,619	193,466	101,345	183,305	72,499
December	42,810	90,182	41,191	84,820	29,459

Conclusion

This study was conducted to develop SWAT models for Galveston Bay and Matagorda Bay to estimate terrestrial sediment and nutrient loads. In gauged subbasins, SWAT was calibrated for sediment, nitrate, organic nitrogen, total nitrogen, organic phosphorus, mineral phosphorus and total phosphorus at USGS gauging stations, and the SWAT-estimated total output from each subbasin was estimated.

For both Galveston and Matagorda Bay watersheds, two separate projects were set up. Calibration was conducted for subbasins that were upstream from available gauging stations. The same parameter settings were then applied to the remaining subbasins based on land use similarity to calibrated subbasins, and in very limited cases, some parameters at ungauged subbasins were set considering the simulated loads in comparison to TWDB's estimated loads.

Monthly sediment calibration at each gauging station showed good correlation, with an R^2 ranging from 0.75 to 0.93 and an NSE ranging from 0.70 to 0.93. Validation results also correlate well, ranging from 0.59 to 0.80 for R^2 and from 0.34 to 0.79 for NSE. It should be mentioned that simulated sediment discharge is very sensitive to the instream process and sediment routing parameters should be selected carefully at ungauged subbasins; having enough information about channel deposition and erosion dramatically improves sediment load estimation at ungauged subbasins.

The uncalibrated model failed to predict total Nitrogen and Phosphorus components, however, it well predicted the total Nitrogen and total Phosphorus with R2 and NSE about 0.80. Comparison between observed and modeled monthly nutrient loads showed that the model had good performance in predicting all nutrient loads except nitrate. A possible reason is uncertainty in fertilizer applications and simulated nutrient loads shows high peaks when applying fertilizers in agricultural and hay fields.

Overall, model performance in prediction of Matagorda nutrient loads is better than for Galveston. A possible explanation is that the land use data created in 2001 may not have accurately represented the validation period, which included the 1980s. The two important factors should be determined to improve the simulation results are fertilization operations parameters and point source loads. The calibration results showed that model performance is poor in urban area unless point source loads are included in the model. Sediment and nutrient loads were estimated for Galveston and Matagorda-Colorado watersheds and due to the lack of data the loads from Galveston watershed inlet (Trinity River) was not considered. SWAT estimated average annual sediment into Galveston Bay at 1,577,810 tons. The estimated sediment load into the Matagorda Bay was 1,124,030 tons including loads from Reach 26 (Inlet) and would have been 825,530 tons without the discharge from the Colorado River basin.

SWAT is capable of building and evaluating scenarios including, but not limited to, BMPs, point source removal, land use change and climate change. Finally, using similar methodology and model setting, SWAT can be applied to other Texas coastal watersheds. These capabilities should be explored in future work.

References

Abbaspour, K.C. 2011. User Manual for SWAT-CUP4, SWAT Calibration and Uncertainty Analysis Programs. Dübendorf, , Switzerland: Swiss Federal Institute of Aquatic Science and Technology, EWAG.

Arnold, J.G., Srinivasan, R., Muttiah, R.S. and Williams, J.R., 1998. Large area hydrologic modeling and assessment, Part I: Model Development. Journal of the American Water Resources Association, 34(1): 73-89.

CRWR270. 1998. Suspended sediment yield in Texas watersheds. Bureau of Engineering Research. The University of Texas at Austin.

Di Luzio, M., R., Srinivasan, J.G., Arnold, and S.L., Neitsch. 2002. ArcView interface for SWAT2000 User's Guide. Texas Water Resources Institute, College Station, TX.

Lee, T., R., Srinivasan, N., Omani. 2011. Estimating the water balance of Texas coastal watersheds with SWAT.

Nash, J.E., and J.V., Sutcliffe. 1970. River flow forecasting through conceptual models: Part I - A discussion of principles. Journal of Hydrology, 10: 282-190.

USGS Water-Quality Data for USA, 2011, National Water Information System. Available at: http://waterdata.usgs.gov/nwis/qw. Accessed 10 June 2011.

Appendix

BIOMIX.mgt: Biological mixing efficiency

BC3.swq: Rate constant for hydrolysis of organic N to NH4

BC4.swq: Rate constant for mineralization of organic P

CDN.bsn: Denitrification exponential rate coefficient

CH_COV1.rte: Channel cover factor

CH_COV2.rte: Channel erodibility factor

CH_N2.rte: Manning's n value for the main channel

CMN.bsn: Rate factor for humus mineralization of active organic nutrients (N and P)

ERORGN.hru: Nitrogen enrichment ratio for loading with sediment

ERORGP.hru: Phosphorus enrichment ratio for loading with sediment

NPERCO.bsn: Nitrate percolation coefficient

PHOSKD.bsn: Phosphorus soil partitioning coefficient

PPERCO.bsn: Phosphorus percolation coefficient

PRF.bsn: Peak rate adjustment factor for sediment routing in the main channel

PSP.bsn: Phosphorus availability index

RS2.swq: Benthic P source rate coefficient

RS3.swq: Benthic NH4 source rate coefficient

RS4.swq: Organic N settling rate coefficient

RS5.swq: Organic P settling rate coefficient

RCN.bsn: Concentration of Nitrogen in rainfall

RSDCO.bsn: Residue decomposition coefficient

SPCON.bsn: Linear parameter for calculating the maximum amount of sediment that can be re-entrained during channel sediment routing

SDNCO.bsn: Denitrification threshold water content

SPEXP.bsn: Exponent parameter for calculating sediment re-entrained in channel sediment routing

Assessment of Climate Change Impacts on Environmental Flow Release from a Multi-purpose Dam of South Korea Using SWAT Model

R. Ha, Ph.D. Candidate
Konkuk University, Dept. of Civil and Environmental System Eng., 1 Hwayang dong, Gwangjin-gu, Seoul 143-701, South Korea

H. G. Jeong, Meteorological Research Scientist
Han River Flood Control Office CO.,LTD, 328 Dongjakdaero, Seocho-Gu, Seoul, 137-049, South Korea

M. S. Lee, researcher
National Institute of Environmental Research, Environmental Research Complex, Kyungseo-Dong, Seo-Gu, Incheon, 404-170, South Korea

S. J. Kim*, Professor
Konkuk University, Dept. of Civil and Environmental System Eng., 1 Hwayang dong, Gwangjin-gu, Seoul 143-701, South Korea

Abstract

This study is to evaluate the climate change impact on future environmental flow secured in a dam. For the purpose, the Soil Water Assessment Tool (SWAT) was adopted and it was prepared for a watershed including a multi-purpose dam. The model was tested using multi-sites observed data of upstream and downstream including dam release data. For future evaluation, the MIROC3.2 hires A1B and B1 scenarios were applied. After bias correction using the ground measured data, the climate data were temporally downscaled using LARS-WG method. For the 2040s and 2080s, the availability of environmental flows will be checked at first and briefly discuss the adaptation strategies by looking at the temporal variations of future dam inflow and water level management for proper water supply.In the future, the2080s dam inflow and storage showed decrease of -6.92% and -8.74%, respectively, basedon the 2002-2010 data. So, the control of reservoir release and environmental flow will be decrease in autumn and winter season in the future, especially.

Keywords: Climate Change; MIROC3.2 hires; LARS-WG; Multi-Purpose Dam; Reservoir Operation; SWAT

Introduction

Future uncertainty on water demand caused by future climate condition and water consumption leads a difficulty to determinethe reservoir operation rule for supplying sufficient water to users. It is, thus, important to operate reservoirs not only for distributingenough water to users using the limited water resources but also for preventing floods and drought under the unknownfuture condition.

There are only a few hydrological impact studies. Burn and Simonovic(1996)studied the potential impacts of climate change on the operationalperformance of the Shellmouth reservoir in Manitoba, Canada.Using two different 'warm' and 'cool' sets of climatic conditions,synthesized monthly streamflow sequences were input to a reservoiroperation model. The impacts from implementation of the reservoiroperating policy on the reliability of the reservoir for meetingthree purposes, viz. flood control, recreation and water supply were determined. The reservoir performance was determined to be sensitiveto the inflow data. Lettenmaier and Gan(1990) analyzed the hydrologic sensitivities of four catchments in the Sacramento and San Joaquin River basins to long-term global warming. Under carbon dioxide doubling scenarios from three GCMs, they showed that winter runoff increased while spring snowmelt runoff decreased in these catchments. The snowmelt and soil moisture accounting models also simulated large increases in the annual flood maxima, with the time of occurrence of many large floods shifting from spring to winter.

The main goal of this study is to assess the potential impact of climate change on the inflow and storage of multi-purpose dam and the downstream flowby the future climate data of MIROC3.2 hires A1B and B1 scenarios using SWAT model.For the above purpose, the8245.62 km2 watershed which has two multi-purpose dam within the watershed was adopted.

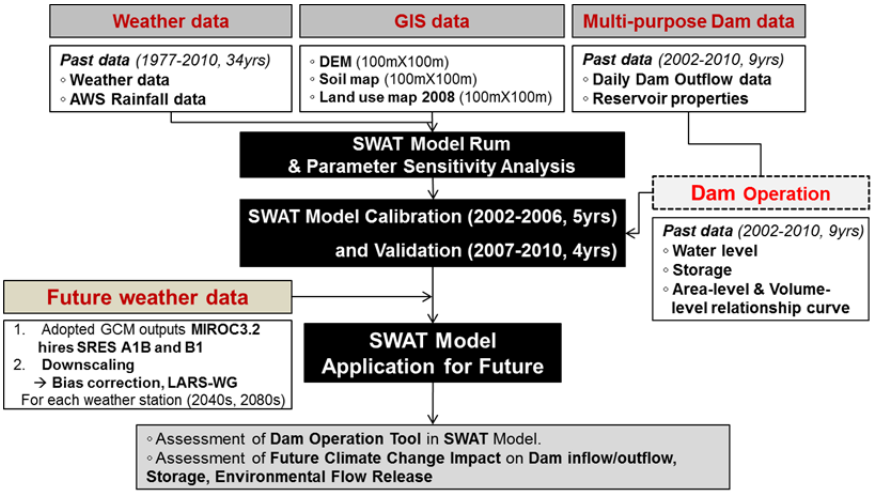

Fig. 1 A schematic diagram of this study.

Materials and Methods

Study Area and Data for Model Evaluation

The study watershed has a total area of 8245.62 km2 located in southeast Han river basin of South Korea (Fig. 2). The elevation ranges from 68 to 1556 m, the annual average precipitation

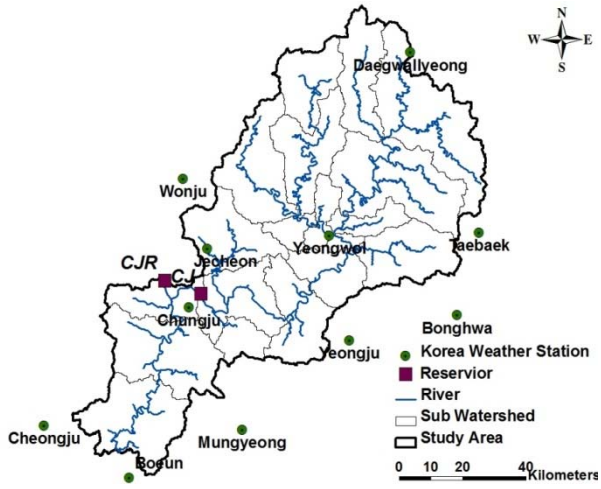

Fig. 2 The study area.

was1261 mm, and the mean temperature was 9.4°C over the last30 years. At the watershed outlet is the Chungju multipurposedam, which is 97.5 m in height, 447 m in length, and has avolume of 9.7 million m3. This important dam provides energy(412 MW capacity) and water for Seoul (metropolitan cityof South Korea) and adjacent urban areas, supplies irrigationfor 22,000 ha, protects rural areas from floods, and outlets334 million tons or water per year to maintain streamflow.More than 78.5% of the watershed area is forested,and 16% is cultivated.

Thirty years (1981-2010) of daily weather data obtainedfor the Korea Meteorological Administration were collectedfrom eleven ground stations. In addition, continuous dailystreamflow data were obtained from three gauging stations(YW: Yeongwol, CD: Chungju Dam and CRD: ChungjuRegualtion Damat the watershedoutlet) of the Han River Flood Control Office.The important two multi- purpose dam inflow and outflow data were obtained from the Korea Water Resources Corporation.The land use map (100 m spatial resolution) was prepared using a Landsat TM (Thematic Mapper) image of 2008 (Fig. 3c). Elevation data were rasterized from a vector map at a 1:5,000 scale that was supplied by the Korea National Geography Institute (KNGI) (Fig. 3b). Soil data were rasterized from a vector map at a 1:50,000 scale that were supplied by the Korea Rural Development Administration (KRDA). The soil type of the watershed is shown in Fig. 3d.

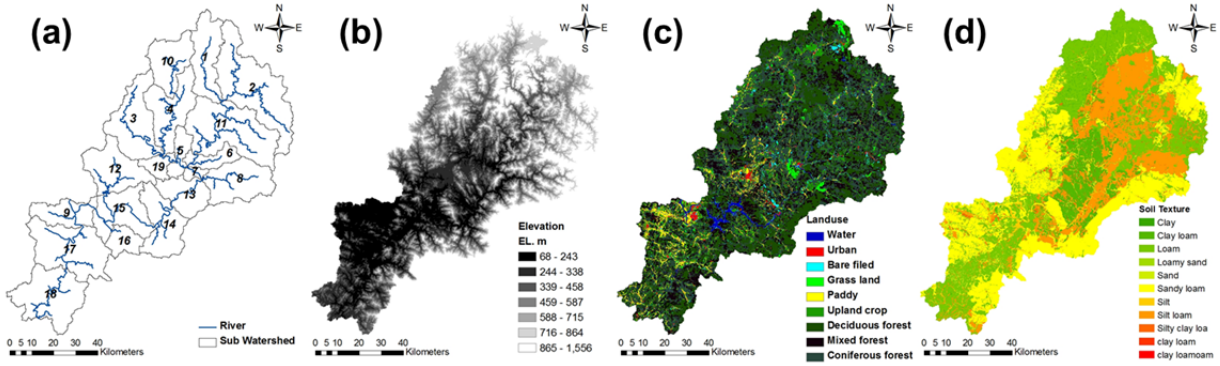

Fig. 3 GIS Data of Study Watershed: (a)Subwatershed, (b) DEM, (c) Landuse and (d) Soil.

Bias Correction and Downscaling of the GCM Climate Data

As GCM data, the MIROC3.2hires data from two SRESclimate change scenarios (A1B and B1) developed by the NationalInstitute for Environmental Studies of Japan wereadopted from the IPCC Data Distribution Center (www.mad.zmaw.de/IPCC_DDC/html/SRES_AR4/index.html).Here,A1B is a “middle” GHGs emission scenario and B1 is a “low”GHG emission scenario.

The MIROC3.2hires GCM data(30 years of data from 1971 to 2000) were downscaled by the biascorrectionmethod described by Alcamo et al. (1997). And daily rainfall amount and minimum (Tmin) andmaximum (Tmax) daily temperatures were estimated over100-year simulated periods using the LARS-WG stochasticweather generator. LARS-WG was chosen over WXGEN, theweather generator included in SWAT, so that the generated datacould be manipulated for climate change scenarios beforeSWAT input.

The SWAT Model

In this study, AVSWAT-X model version under AVSWAT 4.11 interface was used and reservoir operation. Impoundments play an important role in water supply and flood control. SWAT models four types of water bodies: ponds, wetlands, depressions/potholes, and reservoirs. So, two damswere operated by reservoir tool by SWAT model.Further details can be found in the SWAT theoretical documentation.

Results and Discussions

SWAT Model Calibration and Validation

In this study, eleven parameters were selected for calibrationof three subwatersheds, final values as followstable 1. And reservoir parameters were entered as followstable 2.

Table 1 Data sets for SWAT model parameterization

Parameter	Description	Range	YW	CD	CRD
CN2	SCS runoff curve number	± 20 %	-10%	-	-10%
GWQMN	Threshold water level in shallow aquifer for base flow (mmH2O)	0 ~	500	500	250
GW_DELAY	Groundwater delay time (days)	0 ~ 500	300	300	31
GW_REVAP	Revap coefficient	0.02 ~	0.02	0.02	0.2
REVAPMN	Threshold water level in shallow aquifer for revap (mmH2O)	0 ~ 500	250	250	200
CH_N	Manning coefficient for channel	0.01 ~	0.016	0.01	0.016
SFTMP	Snowfall temperature (℃)	-5 ~ 5	5	5	5
SMTMP	Snowmelt base temperature (℃)	-5 ~ 5	0.5	0.5	0.5
SMFMX	Maximum snow melt factor (mm H2O/ºC-day)	0 ~ 10	1	1	1
SMFMN	Minimum snow melt factor (mm H2O/ºC-day)	0 ~ 10	4.5	4.5	4.5
TIMP	Snow pack temperature lag factor	0 ~ 1	1	1	1

Table 2 Related SWAT calibration parameter values of reservoir

Watershed	IYRES	RES_ESA	RES_EVOL	RES_PSA	RES_PVOL	RES_VOL	RES_K
CD	2002	9634	261951	8775	225152	74211.5	0.5
CRD	2002	1194	5585	851	3373	2749.5	0.1

Summary of model calibration and verification is given in Table 3. The Nash-Sutcliffe efficiency ME (Nash and Sutcliffe, 1970), R^2 (coefficient of determination) and RMSE (root mean square error) were 0.69, 0.77, and 3.32 mm/day respectively. The best fit is at ME equals 1, becoming worse as ME departs from 1. The average value of ME, 0.69 means that the model predicted 69 % better respectively than simply using the average streamflow value during that period

(2002-2010). Figure 4 shows the observed versus simulated daily dam storage by model calibrated.

Table 3Statistical summary of the model calibration and validation results.

Note		Calivration					Verification			
Year		2002	2003	2004	2005	2006	2007	2008	2009	2010
P (mm)		1442.4	1763.3	1475.8	1385.8	1518.4	1452.0	959.6	1140.3	1228.0
Yeongwol										
Q (mm)	Obs.	777.0	1166.4	1075.7	937.8	972.8	1081.6	509.3	671.3	899.6
	Sim.	954.4	1282.6	1110.3	1071.4	1293.1	1205.3	726.0	937.6	1013.1
QR (%)		66.2	72.7	75.2	77.3	85.2	83.0	75.7	82.2	82.5
RMSE (mm/d)		3.89	3.11	3.35	3.03	4.64	2.62	2.08	3.61	3.09
R^2		0.82	0.73	0.79	0.73	0.85	0.83	0.82	0.73	0.72
ME		0.69	0.71	0.76	0.73	0.67	0.82	0.80	0.58	0.63
Chungju Dam										
Q (mm)	Obs.	985.6	1256.1	1027.8	840.0	1172.0	1016.5	462.4	613.2	809.1
	Sim.	889.5	1235.2	983.2	811.8	1062.3	1071.3	669.5	749.7	801.1
QR (%)		61.7	70.1	66.6	58.6	70.0	73.8	69.8	65.7	65.2
RMSE (mm/d)		8.92	4.10	4.48	2.62	9.16	3.08	4.42	3.23	3.73
R^2		0.62	0.62	0.72	0.67	0.57	0.70	0.72	0.82	0.90
ME		0.42	0.62	0.73	0.66	0.57	0.69	0.26	0.71	0.50
ChungjuRegualtion Dam										
Q (mm)	Obs.	850.8	1247.1	1075.2	854.3	1165.1	931.2	515.7	562.8	730.7
	Sim.	829.8	1186.4	1063.2	830.0	1131.4	852.6	535.3	596.7	728.6
QR (%)		57.5	67.3	72.0	59.9	74.5	58.7	55.8	52.3	59.3
RMSE (mm/d)		3.55	1.75	1.92	1.29	3.30	1.89	0.83	0.88	1.10
R^2		0.74	0.85	0.83	0.83	0.90	0.80	0.71	0.95	0.76
ME		0.73	0.83	0.81	0.75	0.88	0.79	0.65	0.94	0.77

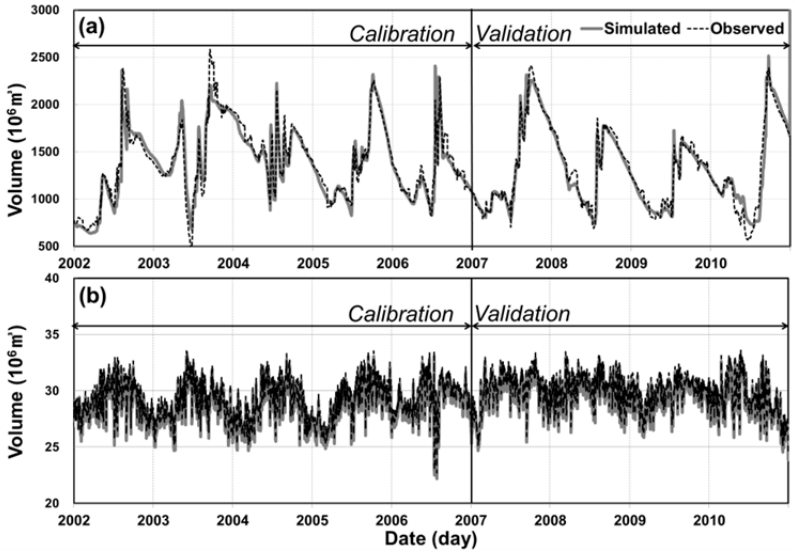

Fig.4Comparison of the measured versus simulated dam volume: calibration (2002-2006) and validation (2007-2010) - (a) Chungju Dam and (b) ChungjuRegualtion Dam.

Summary and Conclusions

The climate change impacts on dam inflow andstorage

The future climate change impacts on dam inflow andits temporal storage were evaluated for the 2040s and 2080s based on the 2010 data.The 2080sA1B and B1 temperatures were predicted to increase 4.5and 3.4℃, respectively. The future precipitation changeranged from -0.4 to +22.0% for the A1B scenario andfrom +7.5 to +10.7% for the B1 scenario. The future CD and CRD inflowsincreased in the winter (December to February) and springperiods (March to May), ranging from 3.38% (0.03 m^3/s)to 52.89% (0.52 m^3/s). The predominant trend of dam inflow for the summer (June to August) and autumn periods (September–November) decreasedranging from -3.42% (-0.12 m^3/s) to -36.07%(-1.43 m^3/s), and storages of autumn and winter periods decreased from -0.02 % to -42.77 %forthe A1B and B1 scenarios.

Table11. The Future Possible Changes (in percentage) in Seasonal and Annual Streamflow and Evapotranspiration for 2040s and 2080s A1B and B1 Scenarios

Component	Streamflow		Evapotranspiration	
Scenario	A1B	B1	A1B	B1
Spring (March – May)				
2040s	+14.48	+24.31	+38.92	+36.84
2080s	+15.97	+26.41	+50.28	+43.87
Summer (June – August)				
2040s	-14.08	-4.05	+61.76	+48.17
2080s	-3.34	-11.44	+73.47	+52.54
Autumn (September – November)				
2040s	-11.62	-20.70	+68.69	+59.91
2080s	-36.30	-14.66	+76.21	+59.99
Winter (December – February)				
2040s	+13.35	+10.14	+62.92	+53.76
2080s	+5.79	+10.88	+62.55	+56.75
Annual (January – December)				
2040s	-7.67	-5.67	+57.39	+48.27
2080s	-12.56	-6.29	+67.15	+52.26

Table10. The Future Possible Changes (in percentage) in Seasonal and Annual Dam Inflow and Storage for 2040s and 2080s A1B and B1 Scenarios

Component	Dam Inflow				DamStorage			
Dam	CD		CRD		CD		CRD	
Scenario	A1B	B1	A1B	B1	A1B	B1	A1B	B1
Spring (March – May)								
2040s	+26.82	+46.53	+19.37	+38.92	+1.78	+2.58	+0.46	+0.76
2080s	+35.26	+52.89	+22.9	+45.2	+2.14	+2.79	+0.59	+0.82
Summer (June – August)								
2040s	-17.54	-11.03	-4.96	-13.77	+6.98	+10.91	+18.40	+25.10
2080s	-3.42	-14.20	-17.47	-6.41	+13.96	+11.26	+27.08	+22.41
Autumn (September – November)								
2040s	-4.24	-12.56	-7.10	-17.95	-31.82	-39.54	-0.90	-0.34
2080s	-26.31	-7.43	-36.07	-10.67	-42.77	-31.51	-7.98	-0.91
Winter (December – February)								
2040s	+7.59	+5.01	+9.36	+6.30	-6.69	-9.27	-0.03	-0.02
2080s	+3.38	+5.24	+3.68	+7.50	-11.38	-7.25	-0.22	-0.06
Annual (January – December)								
2040s	-7.21	-5.12	-1.36	-1.96	-6.71	-8.01	-3.82	-5.01
2080s	-6.92	-4.45	-5.39	-2.36	-8.74	-5.57	-3.05	-4.66

Conclusions

This study was assessed the future potential impact of climate change on the dam inflow and storage by dam operation tool using SWAT Model, and the availability of environmental flows were checked for the 2040s and 2080s.From the evaluation results, the SWAT model simulation of the reservoir was estimated to be well.The predicted annual inflow to CD changed up to -7.21% while the CRD changed up to -1.36% in the 2040s A1B. The future decreased inflows in summer and autumn affected the dam storage for these periods and the following winter period.The future annual storage to CDchanged up to -6.71% while the CRD changed up to -3.82% in the 2040s A1B. So, the control of reservoir release will be decrease in autumn and winter seasonin the future. For additional adaptation strategies, there can be the reinforcement of bank height or will be decrease environmental flow release.The results of this research should be identified and incorporated into dam operation, water resources planning and management in order to promote more sustainable water demand and water availability for a mountainous watershed in our country.

Acknowledgement

This work was supported by the National Research Foundation of Korea (NRF) grant funded by the Korea government (MEST) (No. 2011-0029851).

References

Burn H.D., Simonovic S.P. 1996. Sensitivity of reservoir operation performance toclimatic change.*Water Resour Manage* J10(6):463-78.

Kaczmarek Z. 1990.Impact of climatic variations on storage reservoir systems.Working paper, WP-90-020, international institute for applied systemsanalysis (IIASA), Laxenburg, Austria p.35.

Alcamo, J., P. Do¨ ll, F. Kaspar,and S. Siebert.1997. Global change and global scenarios ofwater use and availability: an application of WaterGAP 1.0. Report A9701, Center for Environmental Systems Research, University ofKassel, Germany.

Nash, J. E., and J. V. Sutcliffe.1970.River flow forecasting through conceptual models, Part I - A discussion of principles.*Journal of Hydrology* 10: 283-290.

Lettenmaier DP, Gan TY. 1990. Hydrologic sensitivities of the Sacramento SanJoaquin River Basin, California, to global warming. *Water Resour Res*26(1):69-86.

Hydrologic Modelling of the Eastern Contributing Basins of Vembanad Lake using SWAT

Raktim Haldar
Department of Civil Engineering, Indian Institute of Technology, Delhi
Hauz Khas, New Delhi -110016, India
rhaldar.iitd@gmail.com

Rakesh Khosa
Department of Civil Engineering, Indian Institute of Technology, Delhi
Hauz Khas, New Delhi -110016, India
rakesh.khosa@gmail.com

A K Gosain
Department of Civil Engineering, Indian Institute of Technology, Delhi
Hauz Khas, New Delhi -110016, India
akgosain@gmail.com

Abstract

Modelling plays a very important role in arriving at the diagnosis of past behaviour as well as a prognosis of the likely future states of a given basin's hydrology. It is indeed important to objectively evaluate impacts of past or proposed anthropogenic intervention on the natural system's hydrologic and/or hydraulic responses. In this study rainfall runoff models have been developed for the five principal contributing river basins of the Vembanad Wetland System in the state of Kerala in India and further, within this derived hydrologic framework, the likely future impacts of various water resources development initiatives have also been assessed.
Flow from the five rivers namely Muvattupuzha, Meenachil, Manimala, Pamba and Achenkovil debouch into the southern part of the lake system. Hydrologic models, duly calibrated and validated using available record of observations, were developed for these latter systems using ArcSWAT. Simulations were performed for the presently existing development scenario as well as the likely future scenario by incorporating all known developmental proposals in addition to the proposal that entails a trans-basin-boundary export to the Vaippar basin in the neighbouring state of Tamil Nadu. The impact on the flow in terms of percentage reduction was found to be greater during non-monsoon season when the rainfall is relatively meagre thus rendering the system more vulnerable to possible degradation of the riverine and the connected lake environments.

Keywords: Hydrology, SWAT, Rainfall-Runoff Modelling, Kuttanad, Vembanad Lake

Introduction

Water is a precious natural resource and its management determines its prospective capability to sustain growth and development related aspirations of the society and its balance with the need to maintain the ecological integrity of its hydrologic crucible. In order to keep pace with the global economic growth and industrial development, drainage basins all over the world are in the process of alteration by man. The last few decades have seen a lot of change in the field of water resources development. In the blind run for economic development a lot of anthropogenic influences have been imposed upon the natural systems raising the question of sustainability. Hence, it has now become a practice to study the probable impacts of any proposed water resource development with the help of hydrologic modelling. The importance of hydrologic modelling can be easily felt through the visible direct and indirect impacts that anthropogenic influences have already had in the past (Plan, R., 2005; Leichenko and Wescoat Jr, 1993; Caliandro et al., 1992; Goldsmith and Hildyard, 1986; Ji et al., 2006).

Out of the various natural water bodies lakes and wetlands have an important position. The importance of wetlands, specially, came to light lately, before which, they were thought to be wastelands. Lots of wetlands were harmed in satisfying the acute needs of human requirements such as progressive industrialisation, enhanced food production and recreation raising need of concern for the present day scientists (Menon et al., 2000). Water resources development of any area serves one or more of the purposes such as irrigation, flood control, hydro power development, soil conservation, water distribution, pollution control, sediment control, salinity control, water exports to neighboring basins, etc. At the same time they have also created many side effects due to man's interference with the environment (Kannan, 1979). Similarly construction of artificial structures like dams may pose serious problems in both the upstream and downstream areas (Limbe, 1998).

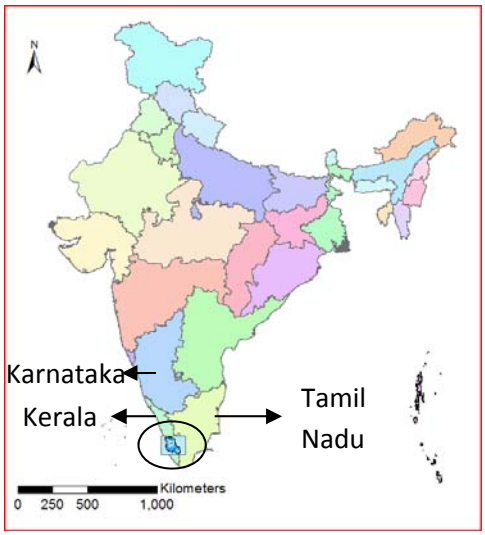

Figure 15: Location of study area in Kerala, India

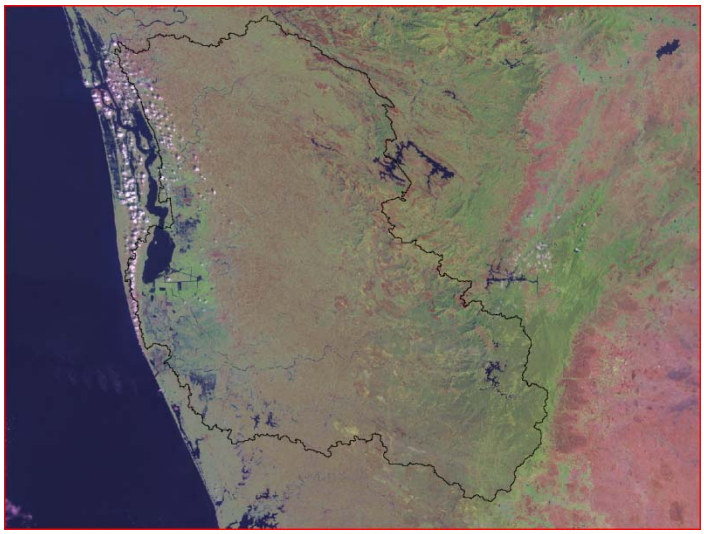
Figure 16: Pseudo colour LANDSAT imagery of the study area

The present study consists of a rainfall-runoff modelling for five river basins along with the calibration and validation for flow in each of the rivers, and then using the same models for predicting the impact of different upcoming or proposed projects that are going to be individually

or collectively responsible to change the flow regime of the rivers. The study area consisting of the five river basins of Muvattupuzha, Meenachil, Manimala, Pamba and Achenkovil lying in Kerala receives a high average annual rainfall of about 3000 mm. Kerala is one of the southern states of India, being surrounded by Tamil Nadu on the east, the Arabian Sea on the west and Karnataka in the North. The state receives two monsoon rains, the southwest monsoons in the months of June to September and the northeast monsoons in the month of October and November (Simon and Mohankumar, 2004). However the basins have a peculiar geometry that provides special attribute to the runoff characteristics of the area. The upper reaches of the basins are steep sloped and the downstream parts of the rivers join the Vembanad Lake and wetland system where the terrain is almost flat. Also, the rivers are only rain-fed, that is, there is no contribution from snow melt. So, the upper reaches practically run out of water in the non-monsoon period. Two centuries ago the Vembanad Lake and wetland system covered an area of almost 363 km^2. However, on account of the excessive wetland reclamation the water-spread as well as volume has reduced by more than 60% of what it was earlier in order to facilitate paddy cultivation bi-annually and also establish industries in the low-lying regions (Swaminathan et al., 2007). The present lake area is separated from the adjacent plains by manually constructed bunds. These bunds are either concrete retaining wall type or temporary mud-wall type strengthened by coir geo-textile membranes (Sarma and Jose, 2008).

Another interesting feature of the region is the Western Ghats which forms a boundary between the states of Kerala and Tamil Nadu, affecting the rainfall pattern in the area. The part of Tamil Nadu which falls in the leeward zone gets lesser rainfall. Figures 3 to 5 present the comparison of rainfall at four grid locations, two each on both sides of the Western Ghats. Figures 3 and 4 show the location of four points on the map and the intervening topography (altitude above MSL). Two of the points on the eastern side of the Western Ghats (9.5°N, 77°E and 9°N, 77°E) receive lesser precipitation than the other two (9.5°N, 77.5°E and 9°N, 77.5°E), which lie on the eastern side. Figure 5 shows the plot of the annual rainfall for the years 1969-2005. The average annual rainfall at the four grid locations are summarised in Table 1 calculated over 37 years (1969-2005).

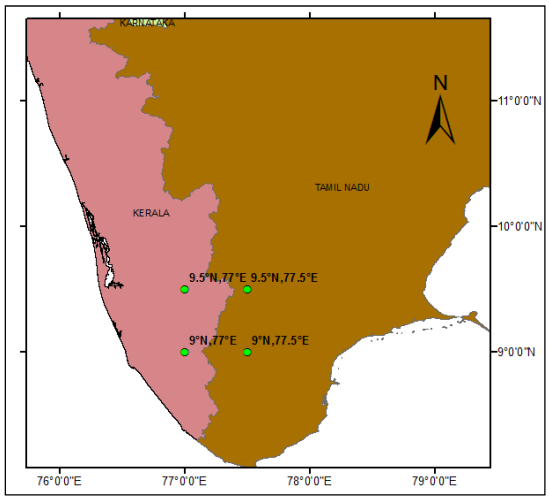

Figure 17: Location of four grid points with the states Kerala and Tamil Nadu

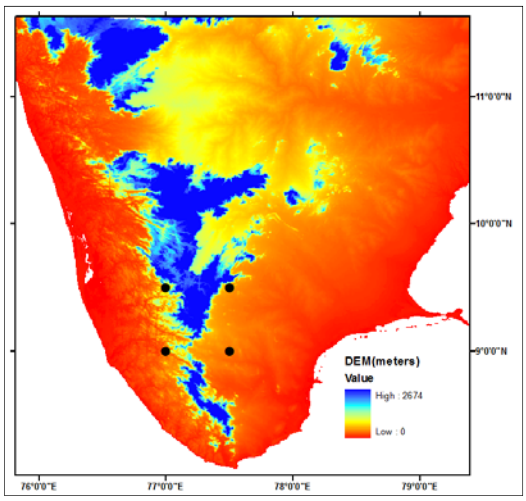

Figure 18: Topography showing a portion of the Western Ghats

The National Water Development Agency (NWDA) proposed, as a part of the interlinking plan of Indian rivers, inter basin water transfer from the rivers Achenkovil and Pamba to Vaippar basin with the construction of three reservoirs and pipeline system for transferring water. The Pamba Achenkovil- Vaippar Link Project (PAVLP) proposed an annual diversion of 634M cu.m of water from Pamba and Achenkovil rivers in Kerala to irrigate areas in the Vaipar river basin in Tamil Nadu. Apart from this, the project envisioned generation of 508 MW of power and providing regulated releases of 150 M cu.m of water during seasons of lean flow in the rivers Pamba and Achencoil to improve the lean season flows and combat salinity intrusion (NWDA Report, 1995).

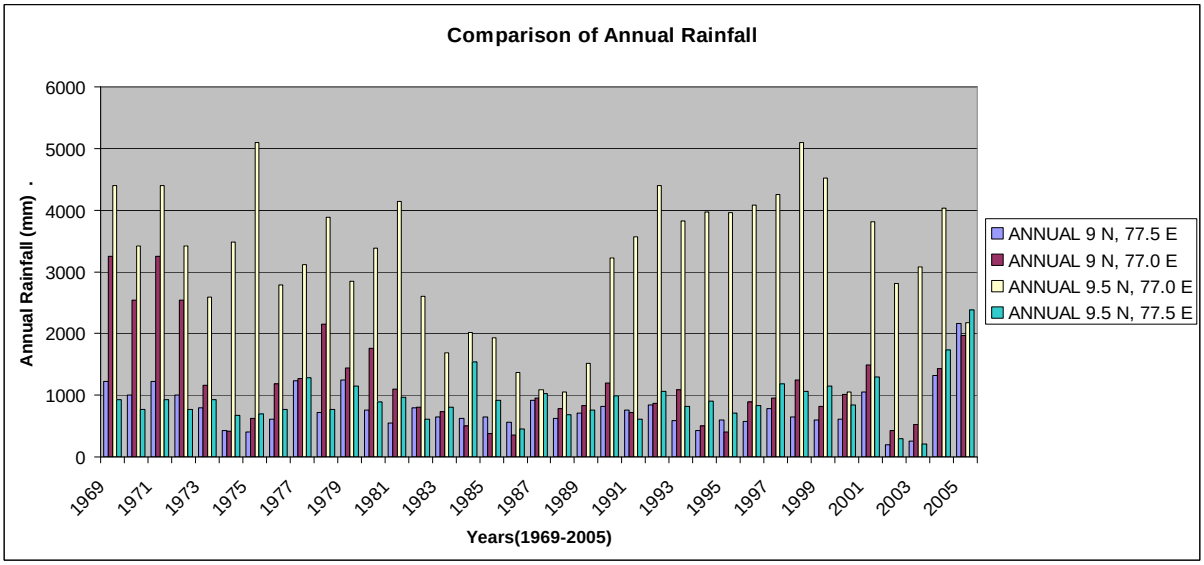

Figure 19: Plot of Annual rainfall for the years 1969-2005

Table 6: Average annual rainfall

Location	Average Annual Rainfall (mm)
9 N, 77.5 E	783.3051351
9 N, 77.0 E	1177.429459
9.5 N, 77.0 E	3191.878108
9.5 N, 77.5 E	929.3027027

The current study attempts to find the implications of this and two other upcoming projects, the Perunthenaruvi Small hydroelectric project and the Ranni-Perunad small hydroelectric project, on the flow conditions in the Pamba and Achenkovil rivers. The Soil and Water Assessment Tool (SWAT) model was selected for this study owing to its dependability based on its broad usage all around the globe for hydrologic modelling and water quality simulation for large as well as small catchments. The SWAT model has been extensively tested for hydrologic modeling at different spatial scales (Zhang et al., 2008) as can be seen clearly from the works of Gollamudi et al. (2007), Spruill et al. (2000), Chu and Shirmohammadi (2004), Santhi et al. (2001a), Zhang et al. (2007), Srinivasan et al. (1998) and Arnold et al. (1999). The suitability of the SWAT model in Indian conditions has been assessed by Kaur et al., (2003).

SWAT is a physical process based model to simulate continuous-time hydrological processes at a catchment scale (Arnold et al., 1998; Neitsch et al., 2005). The catchment is divided into subbasins as per spatial distribution of tributaries and further into hydrological response units (HRUs) based on soil type, land use and slope classes that allows a high level of spatial detail simulation. The major model components include hydrology, weather, soil erosion, nutrients, soil temperature, crop growth, pesticides agricultural management and stream routing. The historical development and application areas of SWAT have been discussed by Gassman et al. (2007).

Materials and Methods

Description of the modelled area

The coastal boundary of Kerala has a continuous chain of lagoons or backwaters. These water bodies are fed by rivers and drain into the Lakshadweep Sea through small openings in the sandbars called 'azhi', if permanent or 'pozhi', if temporary (Swaminathan et al., 2007). The largest among these backwater systems is the Vembanad wetland system. The latitudinal and longitudinal extent of the five study river basins along with other their corresponding area modelled in SWAT and their maximum elevations with respect to mean sea level (MSL) are given in Table 2.

The total catchment area contributing to the lake consisting partly wetlands and partly the five river basins Muvattupuzha, Meenachil, Manimala, Pamba and Achenkovil is approximately 7400 km^2. Also a part of the Periyar River joins the northern estuary which drains its water partly through the Azhikode outlet and partly through the Kochi outlet. However, the basin area of Periyar has not been included as a contributing basin to the Vembanad wetland because (i) a significant fraction of the Periyar water is diverted to the neighbouring Vaigai system from the Mullaperiyar Dam located in the upstream part of the Periyar river; and (ii) it joins the wetland system in the Azhikode estuary quite north of the main lake body and discharges a major part of its water through the Azhikode outlet near Munambam, thus having negligible influence on the part of Vembanad Lake south of Thanneermukkom Bund. The Thanneermukkom bund or salt water barrier was constructed in 1975 to prevent the intrusion of saline water from the Cochin estuary into the southern part of the Vembanad Lake and hence allow paddy cultivation in the Kuttanad region more than once a year.

The area through which these five rivers flow just before joining the Vembanad Lake is known as the Kuttanad region. The region is the deltaic formation of the west flowing river systems called the rice bowl of Kerala. The Kuttanad is a low-lying region extending over an area of about 1100 km^2 in Kottayam and Allepey districts of Kerala and much of the area are below the sea level (Thampatti and Padmakumar, 1999). The somewhat higher area in the south-east of Kuttanad is called upper Kuttanad and the elevations here range from 0.5m below to 6.0m above MSL. The core area of Kuttanad is lower Kuttanad and the land levels here are 1.5m below to 1m above MSL.

Table 7: Spatial details of the five basins

Sl. no	Basin	Latitudinal Extent	Longitudinal Extent	Approximate Area (sq.km.)	Maximum Elevation (m)
1	Muvattupuzha	9° 41' N to 10° 8' N	76° 22' E to 77° 00' E	1593.14	1257
2	Meenachil	9° 26' N to 9° 52' N	76° 22' E to 77° 57' E	777.15	1182
3	Manimala	9° 19' N to 9° 41' N	76° 22' E to 77° 00' E	996.92	1379
4	Pamba	9° 10' N to 9° 20' N	76° 22' E to 77° 18' E	1744.84	1916
5	Achenkovil	9° 0' N to 9° 20' N	76° 25' E to 77° 17' E	1188.20	1881

The Vembanad-Kol Wetland was included in the list of wetlands of international importance, as defined by the Ramsar Convention for the conservation and sustainable utilization of wetlands in 2002, where its area is mentioned as 151,250 ha. It is home to more than 20,000 waterfowls in India. Major livelihood activities include agriculture, fishing, tourism, inland navigation, coir retting, lime shell collection.

Due to the orographic influence of the Western Ghats the annual rainfall at different locations in the area vary from 2000 mm to 5000 mm. That is to say, the range of spatial variation of annual rainfall in the catchment area may be as high as 3000 mm in a particular year. The climate is typical of tropical features with monsoon (June–September) yielding 60–65% of the total rainfall (Menon et al., 2000). The temperatures from March to May are hot (30–34°C) and lowest in December (22–24°C). The soil types present in the region are clay, gravelly clay, loam, gravelly loam and sandy.

SWAT Model

The present study concerns the application of a physically based watershed model SWAT2005 in the Vembanad Lake Basin to model flows and examine the influence of the proposed projects on stream flow. The application of the model involved calibration, validation and simulation of proposed scenarios. For this purpose manual calibration was performed.

SWAT divides the total watershed into a number of subbasins depending on the number of reach outlets (generally, tributaries). Further the subbasins may be discretized into number of parts called Hydrologic Response Units (HRUs) using the landuse, soil type and slope classification. HRU forms a basic computational unit assumed to have homogeneous hydrologic response. The computed results of the various physical processes on the HRU scale are integrated to the subbasin level and then into the basin level.

Model Inputs

The spatially distributed data (GIS input) needed for the ArcSWAT interface include the Digital Elevation Model (DEM), soil data, land use and stream network layers. Data on weather and river discharge were also used for prediction of streamflow and calibration and validation process.

Topography was defined by a Digital Elevation Model (DEM) that contains the elevation information of all points in a given area at a specific spatial resolution arranged in a gridded form. A 90 m by 90 m resolution DEM (Figure 6) based on SRTM (Shuttle Radar Topography Mission) data sets (Jarvis et al., 2008) was used as a basis for the delineation of the river basins. To strengthen the flow direction and accumulation algorithms stream network layer obtained from the office of ISW, Government of Kerala were used. Subbasin parameters such as slope gradient, slope length of the terrain, and the stream network characteristics such as channel slope, length, and width were derived from the DEM.

The land use map gained from the open-source Global Land Cover Facility (GLCF) (Tucker et al., 2004) was used to estimate vegetation and their parameters for input into the SWAT model. The soil map used for the model was obtained from the published dataset by Food and Agriculture Organisation of the United Nations (Batjes, 1997). It holds more than 5000 soil types.

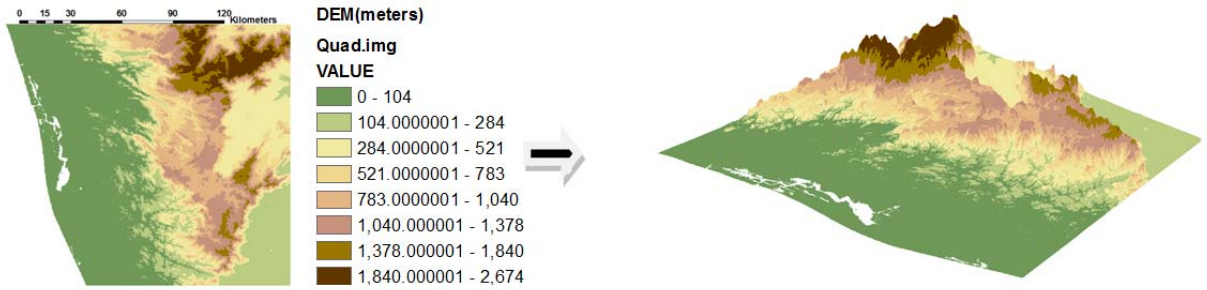

Figure 20: 3-Dimensional view of the study region showing the Western Ghats

Daily precipitation data for 21 stations, daily discharge data for 5 stations and water use data obtained with the help of the Chief Engineer, ISW, Government of Kerala were used for modelling purpose. Details of Muvattupuzha Irrigation Scheme, Pamba Irrigation Scheme, details of various dams and reservoirs, hydroelectric schemes and water use were obtained from the office of ISW, Government of Kerala. Daily precipitation in form of gridded data obtained from India Meteorology Department (IMD) was used for comparing rainfall between study area and neighbouring regions. Temperature data (gridded) from IMD was used in SWAT input.

The five basin models were set up using different thresholds for drainage calculation. Then subbasins and HRUs were formed. Figure 7 shows the delineated watershed of the Achenkovil Basin.

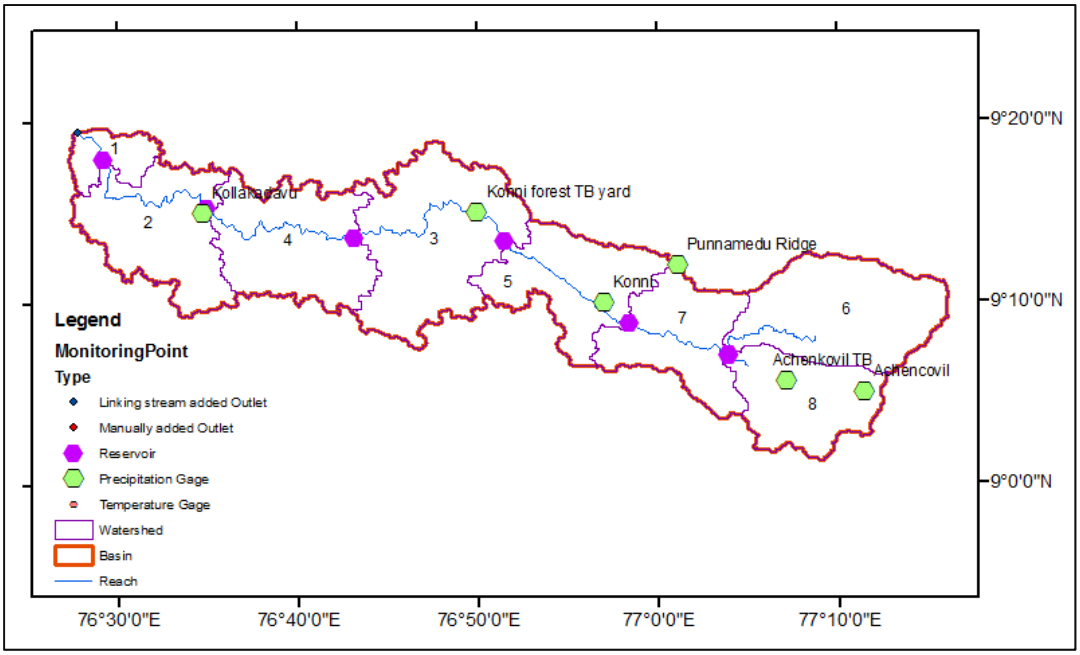

Figure 21: Delineated watershed of the Achenkovil basin

Model Calibration

Hydrologic models for five rivers were prepared on the ArcSWAT 2005 interface implemented in the ArcGIS software version 9.2. The most influential parameters governing the stream-flow were identified using the sensitivity analysis tool in ArcSWAT which uses the combination of Latin Hypercube (LH) and One-factor-At-a-Time (OAT) sampling (Van Griensven, 2006). Calibration was done manually by changing the model parameters influencing the surface water and ground water flows. One parameter at a time was changed to see the improvement in the model results. The main parameters, changes in which improved the model performance are CN2, SURLAG, GW_DELAY, GWQMN, RCHRG_DP, GW_REVAP, OV_N and ALPHA_BF.

Modelling under different development scenarios

After the SWAT model was calibrated and validated for the existing scenario of development, proposed changes were included in the model by adding reservoirs to the specific subbasins and changing the water uses of few subbasins where new projects and diversions are proposed.

Results and Discussion

Calibration and Validation

Five separate models were prepared for the five rivers. For each of the basin models calibration and validation of streamflow was done at one discharge gauging location. The five discharge locations can be found marked in Figure 22Figure 8. The details of the discharge locations are given in Table 3. Manual calibration for daily-step streamflow was done. Following pre-

processing, model derived runoff simulations were iteratively refined by adjusting model parameters till the discrepancy between these simulations and actual observations are reduced to a minimum.

A list of the parameters, their range of values and the final parameter values achieved after the manual calibration of the SWAT model for Pamba river basin are shown in Table 4. For the other four river models the parameters assumed similar values.

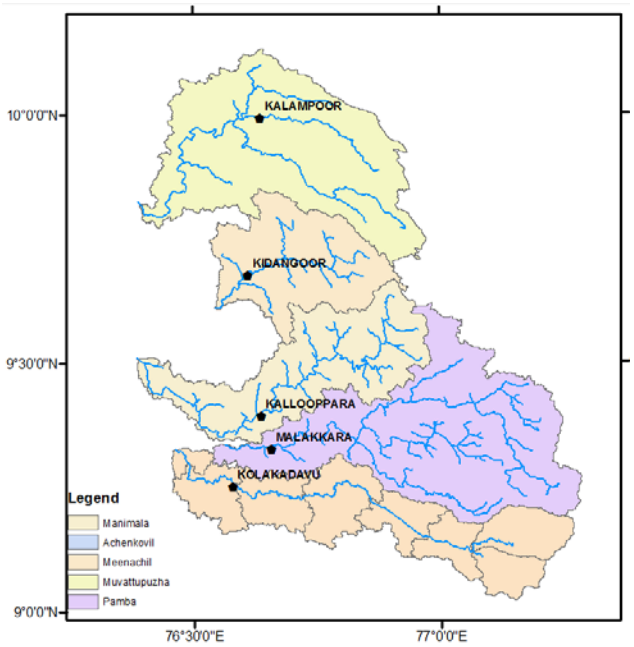

Figure 22: The five modelled river basins with the gauge measuring locations

Table 8: Calibration and Validation periods of five river basins

Sl. no.	Basin	Discharge Gauge for Calibration	Calibration Period	Validation Period
1	Muvattupuzha	Kalampoor	1st Feb to 31st Dec 1997	1st Jun to 10th Aug 2001
2	Meenachil	Kidangoor	1st Jan to 31st Dec 1997	1st Jan to 31st Dec 1998
3	Manimala	Kallooppara	1st Jan to 31st Dec 1995	1st Jan to 31st Dec 1996
4	Pamba	Malakkara	1st Jan to 31st Dec 1996	1st Jan to 31st Dec 1997
5	Achenkovil	Kollakadavu	1st Jan to 31st Dec 1997	1st Jan to 31st Dec 1998

Table 9: List of parameters, their range of appropriate values and final calibrated values for the Pamba SWAT model

Parameter	Name	Range	Final Value
ALPHA_BF	Baseflow alpha factor	0–1.0	0.05
CN2	Curve number	0–100	60.9-80.15*
GW_DELAY	Ground water delay time, days	0–100	130
GW_REVAP	Ground water revap coefficient	0.02–0.20	0.01
OV_N	Manning's n for overland flow	0.01-30	0.1
RCHRG_DP	Deep aquifer percolation fraction	0–1.0	0.001
SURLAG	Surface runoff lag coefficient	0–10	0.25

* The parameter has different values for different HRUs

In Figures 9 and 10 the simulated daily discharges for the Pamba basin generated from SWAT model are compared with the corresponding measured data for the calibration period.

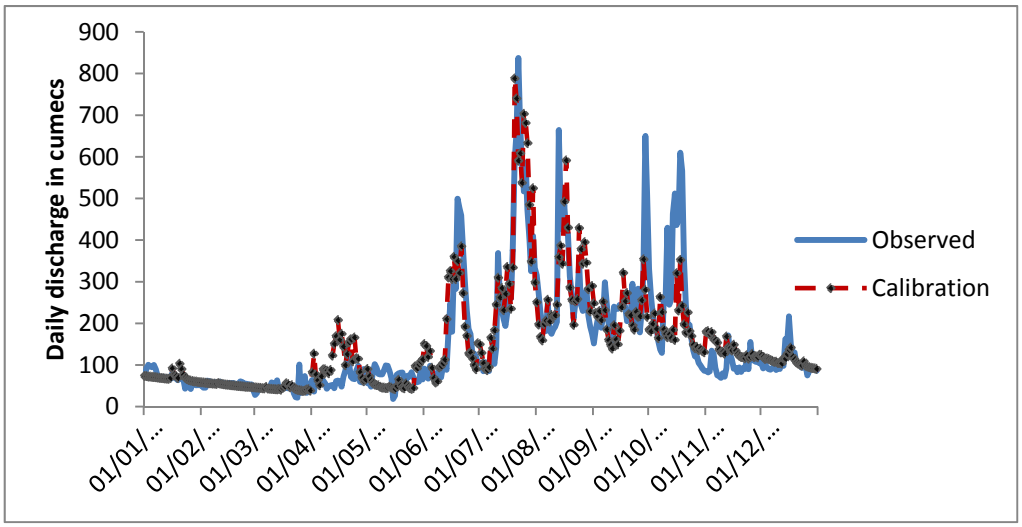

Figure 23: Observed and simulated mean daily discharges at Malakkara, Pamba for calibration period

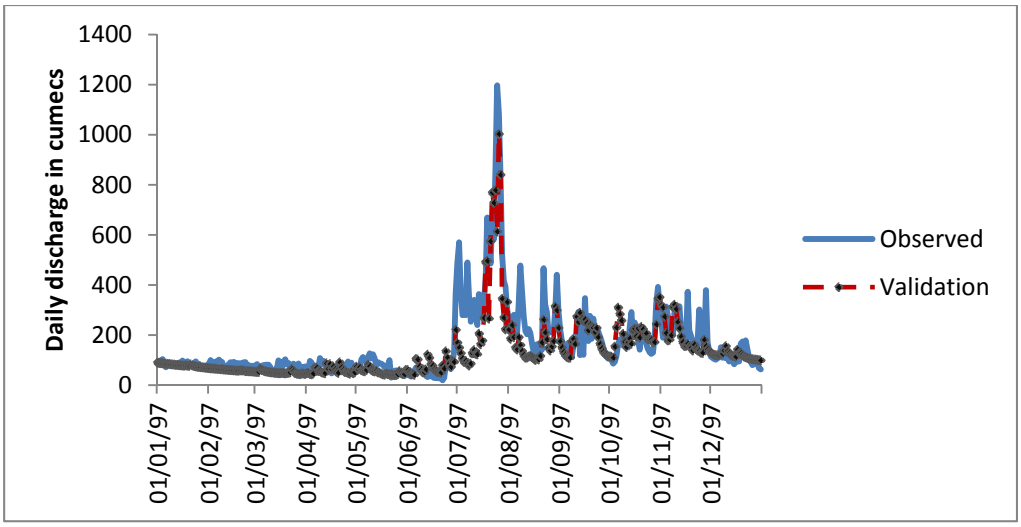

Figure 24: Observed and simulated mean daily discharges at Malakkara, Pamba for validation period

Model performance was evaluated using the coefficient of determination (R^2) and Nash-Sutcliffe model efficiency (Nash and Sutcliffe, 1970) indices. The other parameters for checking model performance such as RSR (Moriasi et al., 2007) and percentage bias (PBIAS) (Gupta et al., 1999) were also calculated. The RSR is defined as the ratio of the RMSE to the standard deviation of measured data. RMSE is the root mean square error (Singh et al., 2004). As per guidelines described by Moriasi et al., (2007) model performance can be evaluated as satisfactory if NSE > 0.5, RSR ≤ 0.7, PBIAS < ± 25% for streamflow, at a monthly time step. In this case calibration was done on a daily time step and the values of these parameters are found to be within the acceptable limits. R^2 ranges from 0 to 1, and typically values greater than 0.5 are considered acceptable (Santhi et al., 2001). The values of the four model efficiency parameters for the five models are given in Table 5.

Table 10: Model performance of the five river models

Monitoring stations	NSE	R^2	RSR	PBIAS (%)
Acceptable Limits	> 0.5[a]	> 0.5[b]	< 0.7[a]	± 25[a]
Kalampoor (Muvattupuzha)	0.805549	0.817319	0.440966	1.559381
Kidangoor (Meenachil)	0.605457	0.69074	0.628127	0.705749
Kallooppara (Manimala)	0.806507	0.822214	0.439879	6.289268
Malakkara (Pamba)	0.724427	0.727976	0.52495	0.840595
Kollakadavu (Achenkovil)	0.685099	0.811673	0.56116	22.13738

a (Moriasi et al., 2007) **b(Santhi et al., 2001**

Results for scenarios

There are two existing major irrigation projects in the study region, the Muvattupuzha Valley Irrigation Project and the Pamba Irrigation Project. The Pamba River has a few major and minor hydro-electricity production stations throughout its length. There are a number of developments related to hydel-power plants proposed in the Pamba basin region. Along with these, there is the PAVLP proposal which consists of construction of three reservoirs, canal system as well as tunnels for irrigation, hydel production and diversion of water.

The available details of the existing and proposed projects have been entered into the model. The Achenkovil and Pamba basin models have been simulated for the existing scenario and proposed scenario of development for the 10 years 1996-2005 keeping the other inputs such as precipitation and temperature as the same.

Figure 11 and Figure 12 show the simulated monthly results for two scenarios of water resources development.

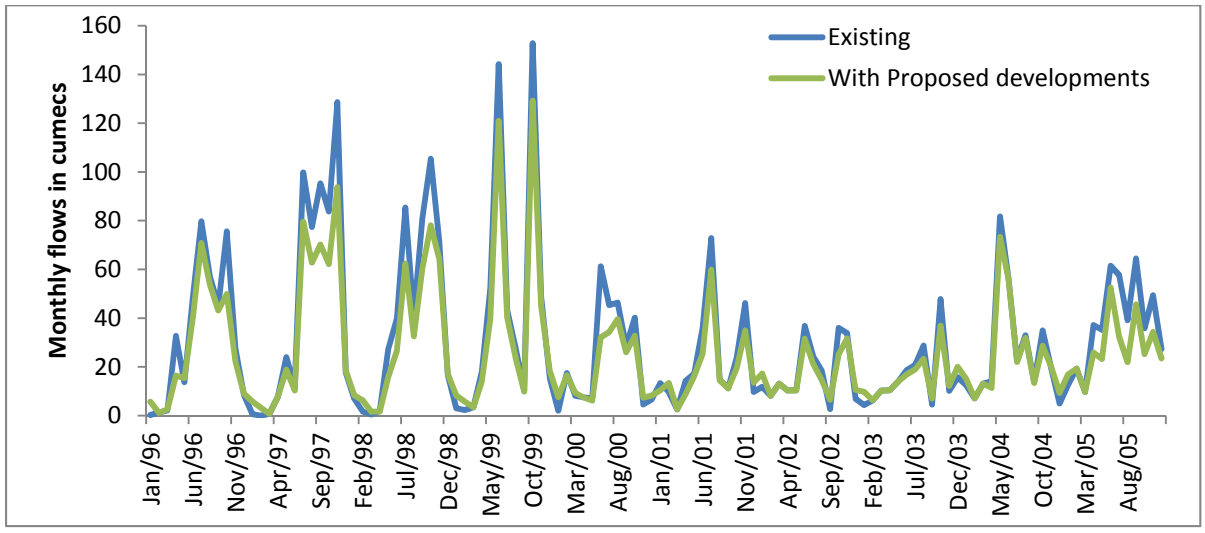

Figure 25: Comparison of simulated monthly flows for Achenkovil River before and after proposed developments

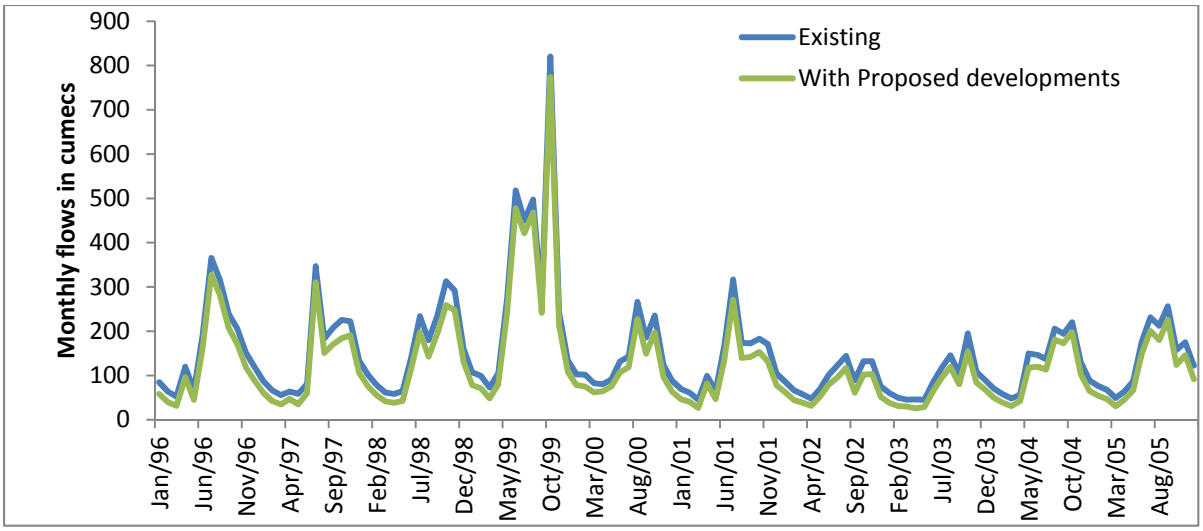

Figure 26: Comparison of simulated monthly flows for Pamba River before and after proposed developments

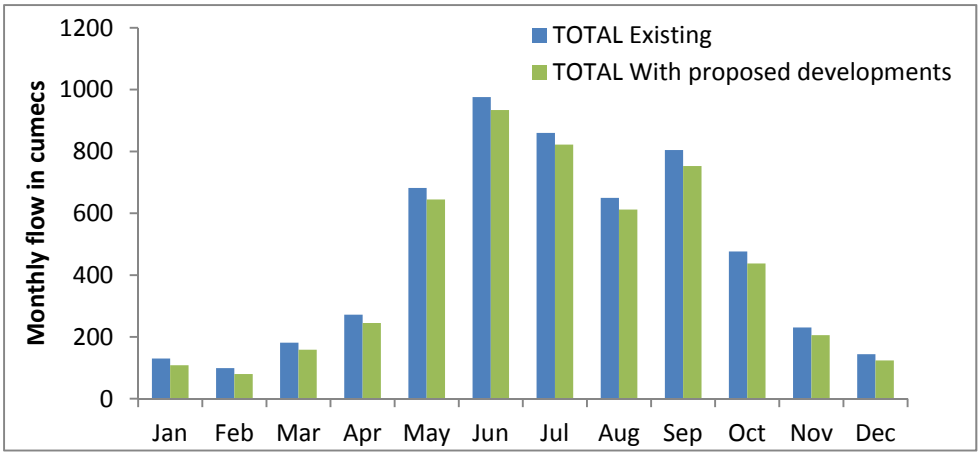

Figure 27: Comparison of average (1996-2005) simulated total monthly flows for the five rivers before and after development

As seen in Figure 11, a reduction is found in the flow in Achenkovil River in most of the months. According to the NWDA feasibility report a regulated release of 5.72 m^3/s will be allowed from the Achenkovil Kal Ar reservoir, that is proposed on the Achenkovil Kal Ar branch of the Achenkovil River, into the downstream reach during the lean season months of October to May for environmental concerns. The slight increase observed in the flows in November – April months is due to this allowance. However it was seen that the Achenkovil Kal Ar reservoir is not able to support the proposed constant flow. The effect on the flow in the Pamba River can be seen in Figure 12. Similarly, for the Pamba River, NWDA proposed a regulated flow of 1.43 m^3/s from the Punnamedu Reservoir that is proposed on the Pamba Kall River, a tributary of the Pamba River.

Figure 13 shows the simulated average monthly total flow of the five rivers taken over the ten years, 1996-2005. Further Figure 14 shows the percentage reduction in total flow of the system

as a result of the proposed projects. As observed, there is greater reduction in flow in the non-monsoon period when the flow in the rivers is already less.

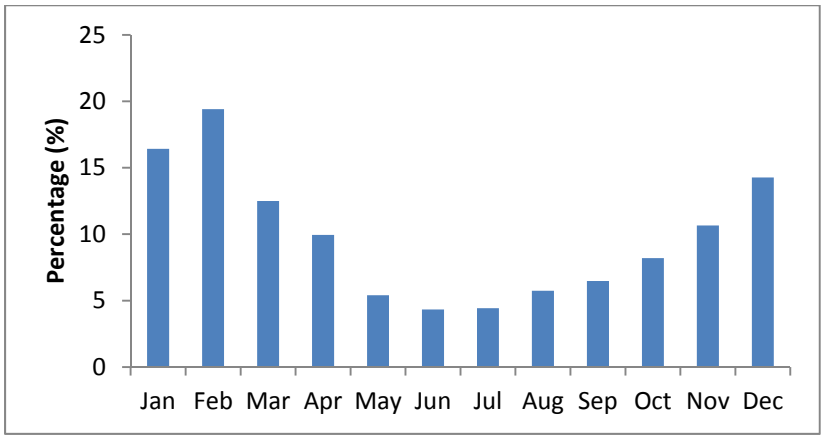

Figure 28: Percentage reduction in total flow of five rivers averaged for ten years modeled (1996-2005)

Conclusion

This paper summarizes the effect of various water resources development in the study region. The study establishes that the impact of these latter initiatives on the natural river regime, both in quantity as well as quality terms is expected to be significant. The natural consequence of these impacts is its adverse effect on the connected wetland system along with its resident biota.

The inferences from the study can be concluded as:

The riverine environment might be significantly impacted on the execution of the proposed water resources developments.
The alteration of the Pamba and Achenkovil hydro-systems introduce a change of 5 – 20 % in the total flow volumes entering into the Vembanad Wetland system.
The higher impacts can be seen in the low –flow months during which the rivers have meagre flow and become almost stagnant.
This can be another serious problem to the already depleted lake environment.
Hence it is very important that the decisions related to water resources development be taken after deliberate research and attention to previously witnessed fate of so many river and wetland systems in the world. Further, it is suggested that the environmental impacts of anthropogenic influences on the Vembanad Lake be studied and modelled.

Acknowledgements
The present work was performed a part of 'Water Balance Study of Vembanad Wetland System', funded by Irrigation Department, Kerala. The authors would like to thank Smt. P. Lathika, Chief Engineer, Inter-State Water (ISW) and Sri Abraham Koshy (Assistant Executive Engineer), Irrigation Department, Government of Kerala for their valuable support.

References

Arnold, J. G., R. Srinivasan, R. S. Muttiah and P. M. Allen. 1999. CONTINENTAL SCALE SIMULATION OF THE HYDROLOGIC BALANCE. JAWRA Journal of the American Water Resources Association, 35:1037-1051.

Arnold, J. G., R. Srinivasan, R. S. Muttiah and J. Williams. 1998. Large area hydrologic modeling and assessment part I: Model development. JAWRA Journal of the American Water Resources Association, 34:73-89.

Batjes, N. 1997. A world dataset of derived soil properties by FAOâ€“UNESCO soil unit for global modelling. Soil use and management, 13:9-16.

Caliandro, A., A. Hamdy, C. Lacirignola and M. CATALAN. 1992. Environmental impacts of water resource development and management. CIHEAM-IAMB.

Chu, T. and A. Shirmohammadi. 2004. Evaluation of the SWAT model's hydrology component in the Piedmont physiographic region of Maryland. Transactions of the ASAE, 47:1057-1073.

Gassman, P. W., M. R. Reyes, C. H. Green and J. G. Arnold. 2007. The Soil and Water Assessment Tool: Historical development, applications, and future research directions.

Goldsmith, E. and N. Hildyard. 1986. The social and environmental effects of large dams. Volume 2: case studies. Wadebridge Ecological Centre.

Gollamudi, A., C. Madramootoo and P. Enright. 2007. Water quality modeling of two agricultural fields in southern Quebec using SWAT. Transactions of the Asabe, 50:1973-1980.

Gupta, H. V., S. Sorooshian and P. O. Yapo. 1999. Status of automatic calibration for hydrologic models: Comparison with multilevel expert calibration. Journal of Hydrologic Engineering, 4:135-143.

Jarvis, A., H. Reuter, A. Nelson and E. Guevara. 2008. Hole-filled seamless SRTM data V4, International Centre for Tropical Agriculture (CIAT). Cali, Columbia.

Ji, X., E. Kang, R. Chen, W. Zhao, Z. Zhang and B. Jin. 2006. The impact of the development of water resources on environment in arid inland river basins of Hexi region, Northwestern China. Environmental Geology, 50:793-801.

Kannan, K. 1979. Ecological and socio-economic consequences of water-control projects in the Kuttanad region of Kerala. Sadhana, 2:417-433.

Kaur, R., R. Srinivasan, K. Mishra, D. Dutta, D. Prasad and G. Bansal. 2003. Assessment of a SWAT model for soil and water management in India. Land Use and Water Resources Research, 3:1-7.

Leichenko, R. M. and J. L. Wescoat Jr. 1993. Environmental impacts of climate change and water development in the Indus Delta region. International Journal of Water Resources Development, 9:247-261.

Limbe, W. 1998. Water resources development and vector borne diseases in Malawi. Water resources development and vector-borne diseases in Malawi:38.

Menon, N., A. Balchand and N. Menon. 2000. Hydrobiology of the Cochin backwater systemâ€“a review. Hydrobiologia, 430:149-183.

Moriasi, D., J. Arnold, M. Van Liew, R. Bingner, R. Harmel and T. Veith. 2007. Model evaluation guidelines for systematic quantification of accuracy in watershed simulations.

Nash, J. E. and J. Sutcliffe. 1970. River flow forecasting through conceptual models part Iâ€”A discussion of principles. Journal of hydrology, 10:282-290.

Neitsch, S., A. Arnold, J. Kiniry, J. Srinivasan and J. Williams. 2005. Soil and Water Assessment Tool Userâ€™s Manual: Version 2005. Texas Water Resources Institute. TR-192, College Station, Texas.

NWDA Report. 1995. Feasibility Report of Pamba-Achankovil-Vaippar Link Project, National Water Development Agency, Ministry of Water Resources, New Delhi, India.

Plan, R. 2005. Narail Sub-project Bangladesh: Southwest Area Integrated Water Resources Planning and Management Project, June.

Ritchie, J. T. 1972. Model for predicting evaporation from a row crop with incomplete cover. Water resources research, 8:1204-1213.

Santhi, C., J. G. Arnold, J. R. Williams, W. A. Dugas, R. Srinivasan and L. M. Hauck. 2001. Validation of the Swat Model on a Large Rwer Basin with Point and Nonpoint Sources. JAWRA Journal of the American Water Resources Association, 37:1169-1188.

Sarma, U. and A. Jose. 2008. Application of a coir geotextile reinforced mud wall in an area below sea level at Kuttanad, Kerala. p. 18-22.

Simon, A. and K. Mohankumar. 2004. Spatial variability and rainfall characteristics of Kerala. Journal of Earth System Science, 113:211-221.

Singh, J., H. Knapp and M. Demissie. 2004. Hydrologic modeling of the Iroquois River watershed using HSPF and SWAT. ISWS CR 2004-08. Champaign, Ill.: Illinois State Water Survey.

Spruill, C., S. Workman and J. Taraba. 2000. Simulation of daily and monthly stream discharge from small watersheds using the SWAT model. Transactions of the ASAE, 43:1431-1439.

Srinivasan, R., J. Arnold and C. Jones. 1998. Hydrologic modelling of the United States with the soil and water assessment tool. International Journal of Water Resources Development, 14:315-325.

Swaminathan, M.S. et al., 2007. Measures to Mitigate Agrarian Distress in Alappuzha and Kuttanad Wetland Systems. A Study Report by Swaminathan Research Foundation, Union Ministry of Agriculture.

Thampatti, K. C. M. and K. Padmakumar. 1999. Nature watch. Resonance, 4:62-70.

Tucker, C., J. Pinzon and M. Brown. 2004. Global inventory modeling and mapping studies (GIMMS) satellite drift corrected and NOAA-16 incorporated normalized difference vegetation index (NDVI), monthly 1981-2002. Global Land Cover Facility, University of Maryland.

Van Griensven, A. and W. Bauwens. 2003. Multiobjective autocalibration for semidistributed water quality models. Water resources research, 39:1348.

Zhang, X., R. Srinivasan and F. Hao. 2007. Predicting hydrologic response to climate change in the Luohe River basin using the SWAT model. Transactions of the Asabe, 50:901-910.

Zhang, X., R. Srinivasan and M. Van Liew. 2008. Multi-site calibration of the SWAT model for hydrologic modeling. Transactions of the ASAE, 51:2039-2049.

Application of SWAT model for Water Resources Management in Kopili River Basin in NE India

B.C.Kusre

Associate Professor

College of Agricultural Engg and PHT, Central Agricultural University, Ranipool, Sikkim- 737135 (INDIA); Email: kusrebharat@gmail.com

D. C. Baruah Professor

Department of Energy, Tezpur University, Napaam, Tezpur-784028 (INDIA); Email: baruahd@tezu.ernet.in

Abstract

Accurate estimation of water availability on spatial and temporal scale is prerequisite to water resource management. With the advances in hydrological models supported by GIS tools and remote sensing data, the constraints related to inaccessibility for assessment of water resources have significantly reduced in recent past. In the present study a semi distributed process oriented SWAT model was applied to Umkhen watershed of Kopili River basin in India to assess the spatial and temporal variation of water resources. The data requirements of SWAT model for this typical hilly watershed were fulfilled from locally available sources. The climatic data of Umkhen was taken from two well established meteorological stations. Similarly, the observed discharge data was taken from a gauging station located at the outlet of Umkhen. The data was available for the period of 1988-1993 and was used after testing the non-significant differences with the long time data pertaining to the study region. The sensitivity analysis indicated curve number as the most sensitive parameter affecting the hydrology of Umkhen watershed. The prediction performance of the model was assessed through multi-stage validation process. This was done to ensure the applicability of the model with minimum prediction error. As a validation procedure, observed and simulated water yield at the outlet were compared with satisfactory level of agreement. Coefficient of determination (R^2), Nash and Sutcliffe efficiency (*NSE)* and index of agreement (*d*) were also estimated while analysing the observed water yield and SWAT simulated water yield of Umkhen. Overall, the model was found validated. Analysis of spatial

and temporal variation of water yield was performed in the 13 delineated sub watersheds. The variability of input data (soil, land use and weather) has also been found appropriately reflected in model outputs at the outlets of 13 delineated sub-watersheds.

Key words: Hydrological modeling, northeastern region, SWAT, sensitivity analysis, calibration, validation.

Introduction

The North eastern region of India is a unique region in terms of its terrain, climate and biodiversity. The region consists of eight Indian states occupying around 26.22 Mha areas that constitute 8% of the country's land mass. The region is characterized by undulating terrain consisting of 70% hills and 30% plains. Wide variation in altitude coupled with abundance of rainfall (varying from 2000-4000 mm annual average rainfall) has given rise to wide variations in climatic conditions within the region which in turn has endowed the region with rich bio-diversity. Soil erosion due to high rainfall in the upper catchment has been another characteristics feature of north-eastern rivers. As a result of such soil erosion the river carries huge sediment load to the downstream areas. Chronically appearing flood has been another evil of this region. Huge amount of tangible and intangible losses are reported due to devastating flood every year in this region. Average annual loss incurred due to the recurring floods has been estimated as US$ 6000 million (GoA 2004).

It is therefore viewed that proper management of water resource is a prerequisite to ensure development based on optimal utilization of water resource. Water resource management can address the issues comprising (i) assessment of water resources with maximum possible precision, (ii) realistic planning for water resource development and (iii) implementation of water resource developmental plan. However, precise assessment of water availability on spatial and temporal level is a key step in effective integrated water resources management. More informed decisions for watershed planning and water allocation must rely on the better understanding of hydrology of upper catchment and the relationship between land use practice, flow generation process, and associated water distribution and use.

With the advent of latest computational techniques, use of process based hydrological models is gaining popularity to cater the problems associated with watershed planning and management

(Chen and Mackay, 2004). The process based models have capability to integrate different processes going on within the watershed to simulate the complete watershed hydrology. To reduce the uncertainties associated with the integration of individual processes, calibration becomes necessary (Kannan et al, 2007). The use of models for assessment of water resources, ongoing processes and management options have been reported by many researchers (Bhuyan, et al. 2003; Knebl et al. 2005; Gallart et al. 2007; Jang et al. 2007; Jia et al. 2007; Kiat et al. 2008). In the present study SWAT (Soil and Water Assessment tool) model has been used to simulate the various processes going on within a watershed in NE India. It is presumed that identification of dominating processes can help in prioritizing sub watershed and suggesting suitable measures for mitigating the impacts of floods and arresting soil erosion in the upper watershed. SWAT was considered for the present study because of two reasons. First, SWAT has been already successfully applied for water quantity and quality issues for a wide range of scales and environmental conditions around the globe. A comprehensive SWAT review paper summarizing the findings of more than 250 peer-reviewed articles is written by Gassman et al., (2007). Secondly as processes are represented by parameters in the model, in data scarce regions SWAT can run with a minimum number of parameters. As more is known about a region, more processes can be invoked for by updating and running the model again (Schoul, 2008).

Soil and Water Assessment Tool (SWAT2000)

SWAT is a basin scale, continuous time model that operates on a daily time step and is designed to predict the impact of management on water, sediment, and agricultural chemical yields in un-gauged watersheds (Arnold et al. 1993; Neitsch et al. 2001). It is a public domain model supported by the U.S. Department of Agriculture, Agricultural Research Service at the Grassland, Soil and Water Research Laboratory at Temple, TX, USA. The model is semi distributed process oriented, computationally efficient, and capable of continuous simulation over long time periods (Arnold et al. 1998). SWAT has the capability to simulate several physical processes involving (i) water movement, (ii) sediment movement, (iii) crop growth and (iv) nutrient cycling. The simulation process of SWAT is separated in two major divisions *viz*., land phase and routing phase. The land phase depicts the movement of amount of water, sediment, nutrient and pesticide loadings to the main channel in each sub basin. Whereas, the routing phase depicts the movement of water, sediment, nutrient and pesticides through the channel network of the watershed to the outlet. Specifically SWAT simulates different processes

such as surface runoff, transmission losses, evaoptranspiration, soil water movement (*viz*., percolation, by pass flow and lateral flow), ground water flow, nutrient and pesticide transport, sediment movement, channel routing and reservoir routing. In SWAT, a watershed is divided into multiple sub-watersheds, which are then further subdivided into hydrologic response units (HRUs) that consist of homogeneous land use, management, and soil characteristics. Thus, a watershed can be subdivided into sub-watersheds that are characterized by dominant land use, soil type, and prevailing management practices.

Although strength of SWAT has been reported by its users, there are some limitations associated with it. Considerable data requirements have been viewed as one of the major drawbacks of SWAT modeling (Abbot and Refsgaard, 1996; Gassman et al., 2007). Presence of several sub-models to mimic distinct hydrological processes has also been viewed as a weakness of SWAT. This is due to the fact that conflicting assumptions could result from sub-model integration, as each assumption may not be explicitly defined resulting unreliable simulation (Mackay and Robinson, 2000; Beven, 1995). However, uncertainty due to the above shortcomings could be minimized if (i) data requirement could be satisfied reliably and (ii) model could be calibrated and validated appropriately. Thus, in situations where historic gauged discharge data are not available for spatial mapping, SWAT model in conjunction with climate and land data could be an appropriate tool. In the present investigation, SWAT has been used to assess water resources in a hilly watershed located in the north-eastern region of India on the strength of such considerations.

Description of Study Area

Kopili river system is one of the major tributaries of the mighty Brahmaputra in the north-eastern region of India. The main river Kopili originates from Barail ranges near Jowai in Jaintia hills District of Meghalaya (India) at an altitude of 1800 m above mean sea level. The catchment area of Kopili River is 14,670 km^2, which is about 2.44% of the total catchment of Brahmaputra River. The river has its catchment in two Indian states *viz.,* Assam and Meghalaya. The Kopili river basin consists of five major sub basins *viz.,* Umiam, Umkhen, Diyung, Kopili and Jamuna. In the present study the Umkhen sub basin was considered.

Umkhen River originates near the South Western slope of the Shillong Peak, at an altitude of 1829 m near Shillong in the state of Meghalaya in India. The catchment lies between 25°30´N

and 26°00′N latitudes and 91°50′E and 92°35′E longitudes. The total area of the Umkhen watershed till its confluence in Kopili River is 2228 km^2. However, for the development of model, the outlet was taken at a downhill distance of 102 km from the origin due to availability of discharge data at the location. The discharge data was recorded by Assam Power Generation Company Limited (India) for planning hydroelectricity project. The catchment area till the selected outlet is 1204 km^2 (Fig 1).

The watershed is characterized by variety of forest cover viz., (i) evergreen and semi evergreen, (ii) deciduous, (iii) riverine and (iv) mixed deciduous bamboo forests are predominantly available. However, evergreen coniferous pine forest is dominantly available in the upper altitudes of the watershed (NBSSLUP 1999; Chetry & Saikia, 2002). It is further reported that the watershed is sparsely populated with scattered habitation. The tribes in the watershed follow a typical traditional agricultural practice known as shifting cultivation.

The climate of the watershed is variable with reference to distribution of rainfall, temperature and humidity. Average annual rainfall ranges from 2000 mm in the lower parts to 3000 mm in the upper parts. More than 80% of rainfall occurs during the monsoon months (June to September). Monthly mean temperature ranges from a maximum of 35 ^oC (May) to a minimum of 8 ^oC (January) in the lower altitude. In the higher altitudes the monthly mean temperature varies from 25 ^oC (May) to a minimum of 4 ^oC (January). The daily mean relative humidity varies from a minimum of 40% (April) to a maximum of 95% (July).

Methodology

Watershed Configuration

SWAT first of all divides the watershed into sub watershed and further into hydrologic response units (HRUs) that consist of homogeneous land use, management, and soil characteristics. In this study the threshold value was taken as 50 km^2 as it is considered as appropriate size for taking up watershed management programs in India. Based on the threshold value, the interface created 13 numbers of sub basins and 32 numbers of hydrological response units (HRU) of Umkhen watershed. HRU is the reference unit for hydrological balance which is further aggregated up to sub-basin and basin level. Primarily, Arc-View interfacing assisted delineation of the entire watershed into smaller units to enhance the computational efficacy of the model.

Data requirement

The application of SWAT2000 requires some specific data to simulate watershed hydrology. The requirements are fulfilled by types of data. Spatial thematic map covering the entire watershed has been one such type of data. On the other hand, discrete data corresponding to some specific locations of the study watershed has been other type of data. Spatial thematic maps used as model inputs were (i) digital elevation model (DEM), (ii) stream network, (iii) soil map and (iv) land use map. The input data corresponding to discrete points included (i) climatic data and (ii) discharge data of some specific locations of the study watershed. The detail descriptions of the data used in the present study are given below:

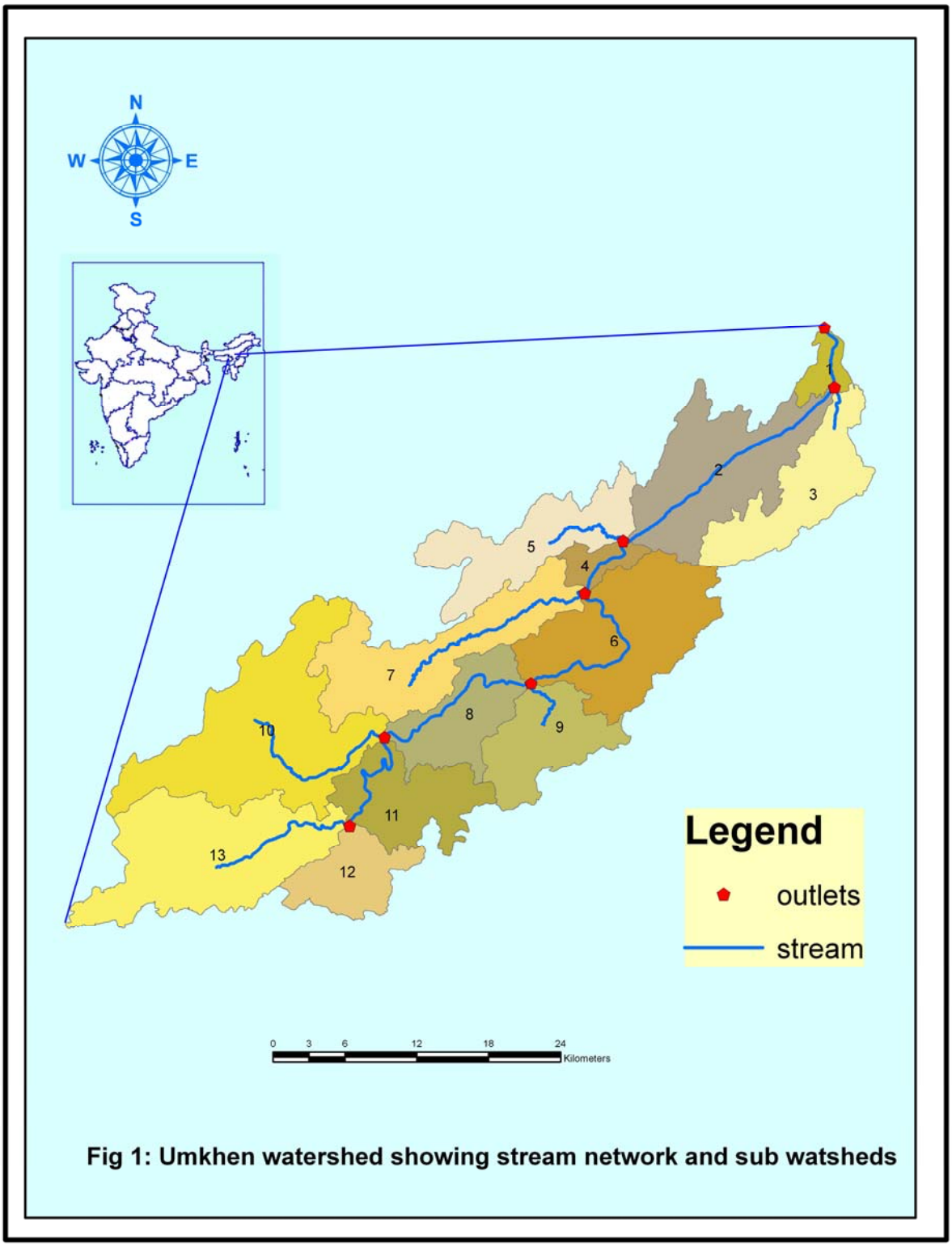

Fig 1: Umkhen watershed showing stream network and sub watsheds

Digital Elevation Model (DEM) and stream network

The digital elevation model was prepared by digitizing contours from the Survey of India (SOI) toposheets through ILWIS 3.3 GIS software. The toposheets are prepared by Survey of India under Department of Science and Technology, Government of India. SOI is India's principal mapping agency with its special responsibility to provide base map for expeditious and integrated development ensuring full utilization of its resources. The uses of SOI toposheets for hydrological studies of northeast India have been reported by some earlier research works (Dabral et al. 2008). The toposheets are available at 1: 50000 scale and have contours at 20 m interval. The digitized contour map was converted into raster map consisting pixels with known elevation representative of specific contour line. Elevations of intermediate pixels were determined through a standard linear interpolation technique (ILWIS, 2001). Realizing the importance of DEM for the preciseness of the present study, care was taken to minimize any possible deviation of DEM from existing topography in digitization process. Finally, stream network available in the study area was considered as reference to investigate the correctness of DEM. DEM generated streams were compared with streams available in toposheet and satellite imagery. For that purpose, the streams available in the toposheet were independently digitized to prepare stream network map and used as input. Similarly, the stream network available in the satellite imagery of Umkhen was also used to investigate correctness of DEM.

Soil map

District level soil maps (1: 250,000 scale) for the state of Assam and Meghalaya were obtained from National Bureau of Soil Survey and Land Use Planning (NBSSLUP), Government of India. Mapping of Indian soil resources is undertaken by NBSSLUP by standard procedure using extensive field survey, image and laboratory analysis (Sehgal et al. 1987 and Sarma et al. 1987) and has been considered as standard source for extracting soil information in India. The input soil maps taken from NBSSLUP were prepared with some standard grids of 10 km. The soil map obtained from NBSSLUP was scanned and geometrically transformed to the appropriate location on the blank raster. The mapping units of the study area were digitized in ILWIS 3.3 GIS software and 11 mapping units were available for the Umkhen watershed (Fig 2).

Values of some soil properties viz., soil depth and texture of Umkhen watershed are available from NBSSLUP. However, values of (i) Fraction of porosity (ii) moist bulk density, (iii) available water capacity of the soil layer and (iv) saturated hydraulic conductivity were not directly available for Umkhen. It is reported that these properties are functionally related with the texture of the soil which was known for Umkhen. The functional relationships used earlier by several sources were used in the present modeling (Clapp and Hornberger, 1978; Hanks and Ashcroft, 1980).

Water holding capacity and its movement is governed by soil texture and thus influences hydrology. Textural information of each soil class of Umkhen, obtained from NBSSLUP has been another input to the model. Model also required some other soil properties viz., (i) saturated hydraulic conductivity, (ii) porosity fraction and (iii) bulk density. These properties affect water movement in term of percolation, lateral flow and aquifer recharge.

Land use map

As mentioned earlier, Umkhen watershed lies in two neighboring states of India, *viz*., Assam and Meghalya. Two different sources were available for land use maps of the study watershed falling in Assam and Meghalaya. Land use map for the Assam portion was obtained from Assam Remote Sensing Application Centre (ARSAC). The land use maps were prepared by interpretation of Landsat TM images taken in the month of March and November 1987. The land use map for the Meghalaya portion of the watershed was not available with ARSAC. Therefore, another source was considered for the land use map for the Meghalaya portion (Saikia, 1990). The land use map of Meghalaya was prepared by Department of Geography, Cotton College under a project sponsored by Department of Science and Technology, Government of India. Land use maps prepared from the recent images would have been better. However, as recent maps were not available, it is assumed that a major change of land use pattern has not taken place since 1987. Being a hilly watershed with less human intervention, the assumption seems to be realistic (Fig 3).

The land use classification of the Umkhen watershed considered as input into the model is presented in Table 1. Different types of forests and abandoned shifting cultivation dominated the watershed. In Umkhen watershed the area under shifting cultivation was found about 33% of the

total area of the watershed. It has been reported that shifting cultivation causes accelerated erosion and quicker runoff due to denuding of the vegetation (Prasad *et al.,* 1990). Response to hydrology will vary with changing land use. For example forested catchment will have higher evapotranspiration, interception losses as compared to area under shifting cultivation and habitation.

Table 1: Land use pattern in the study area

Sl No	Type of land use	Area (km2)	Percentage area
1	Built up	0.39	0.03
2	Dense mixed forest	101.44	8.44
3	Evergreen/ semi forest	118.01	9.82
4	Fairly dense mixed forest	58.21	4.85
5	Open mixed forest	234.96	19.56
6	Pine forest	283.11	23.56
7	Shifting cultivation abandoned	399.17	33.22
8	Shifting cultivation current	9.22	0.77
	Total	1204.52	

Climate data

But for the present study, only two reliable data stations located 82 km apart could be identified for obtaining daily data of rainfall and air temperature recorded during 1988 to 1993. The period of climatic data was decided corresponding to the period of availability of reliable discharge data. The description of data stations is given in Table 2.

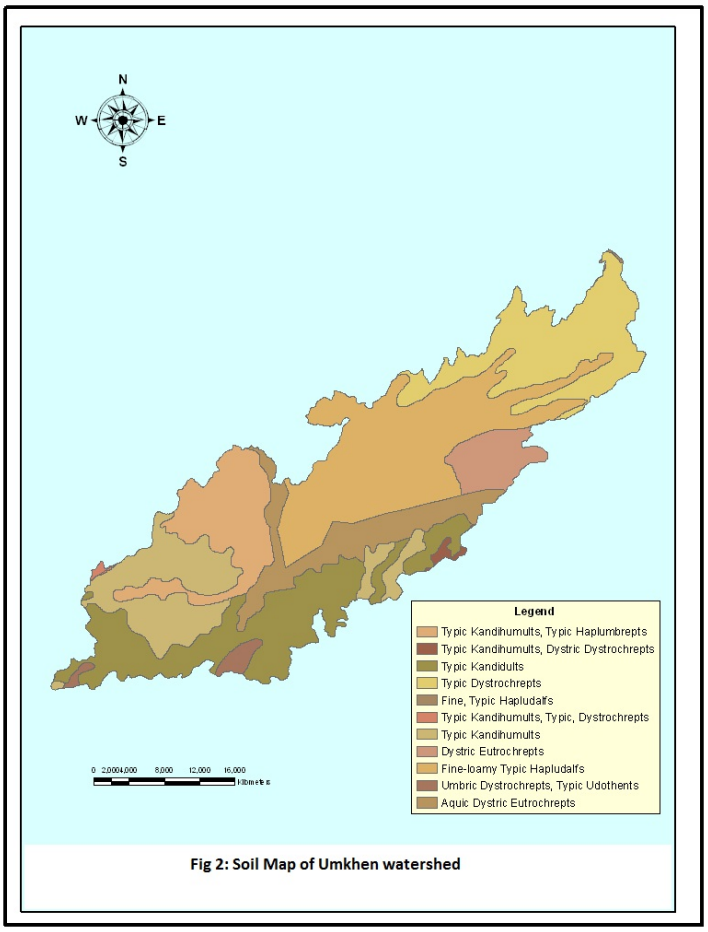

Fig 2: Soil Map of Umkhen watershed

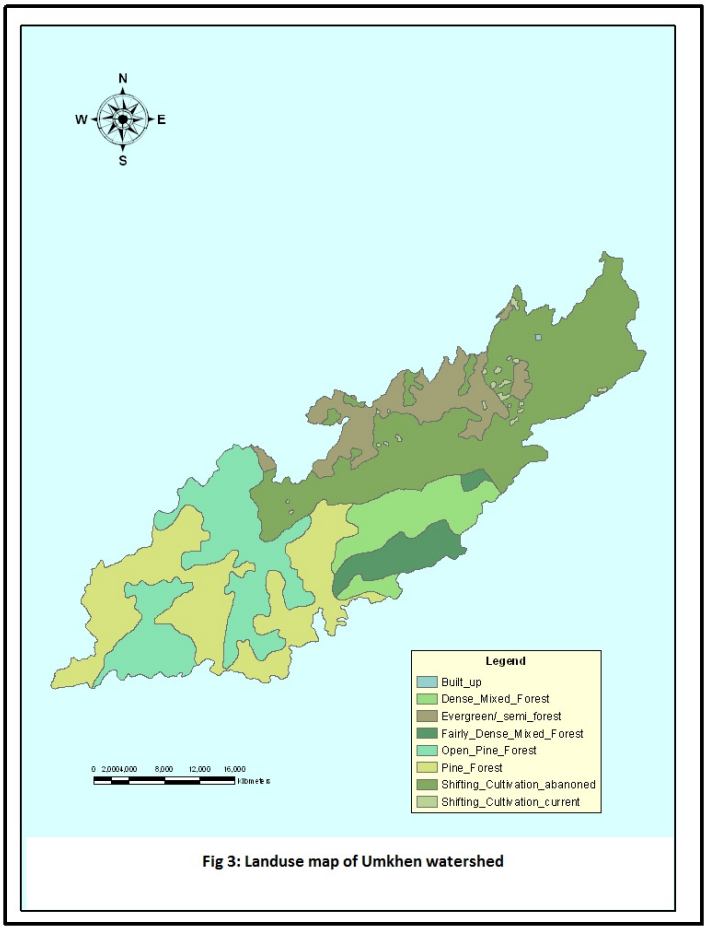

Fig 3: Landuse map of Umkhen watershed

Table 2: Description of climatic data stations

Sl No	Data stations	Description
1	Shillong	Locations: 25º30´30.09″ N, 91º49´30.02″ E; Elevation above msl : 1598 m
2	Baithalangso	Locations: 25º59´32.83″ N, 92º33´02.57″ E Near outlet of watershed; Elevation above msl : 81 m

Longer data period including recent climatic data would have been better to minimize the uncertainty and variability involved in modeling. It is assumed that shorter and relatively older data period would not reduce the usefulness of the present modeling work, considering minimum changes of watershed. Moreover, one of the objectives of the present work is to demonstrate the application of hydrological modeling for typical hilly watershed of northeast India. Thus, as reliability and authenticity of data are fully ensured, length of data period seems not to affect the output of the model and would be still applicable.

The validity of using the short term data as a substitute of long term data was tested through a statistical procedure. Long term data pertaining to annual rainfall event for two meteorological stations in the vicinity of the study area were available. The average values of long term annual rainfall data of Guwahati meteorological station recorded during 1971 to 2000 and Shillong meteorological station recorded during 1969 to 2000 were compared with their respective short-term averages recorded during 1988 to 1993. Failure to prove the difference as statistically significant would support the assumption for use of the available data.

Discharge data

The Assam Power Generation Company Limited (APGCL) is a state owned organization involved in planning and implementation of power project in Assam. APGCL establishes and manages gauge-discharge data station at prospective hydropower locations in Assam. One of the APGCL data stations was located nearby the outlet of Umkhen watershed (25º59´32.83″ N' 92º33´02.57″ E). The site was established for recording discharge data for hydro power project and subsequently a 100 MW power project was installed at that site. The discharge site was

located at sparsely populated location. Further, till the data station no competitive users of water could be found. Thus, the entire discharge from the watershed was recorded at the gauging station. The available data recorded during the period from 1988 to 1993 was considered for the present study.

Model outputs

With all the inputs mentioned above model was run was performed to develop SWAT for Umkhen watershed of north eastern region of India. Output of the model corresponding to final run was obtained after performing (i) sensitivity analysis, (ii) calibration and (iii) validation.

Sensitivity analysis

The identification of critical model parameters effecting the model predictions was done by sensitivity analysis. The SWAT modeling has inbuilt list of model parameters with prescribed ranges of values. Sensitivity analysis was performed running the model for output with varying a particular model parameter within the prescribed range keeping remaining parameters unaltered. This was repeated for all the parameters and most sensible parameters were identified.

Calibration and Validation

Daily observed rainfall and temperature data during 1988 to 1990 and corresponding observed discharge data were used for calibration of the model. Initially the model simulation was performed for annual values and after obtaining reasonably acceptable values, the simulation run was continued up to monthly discharge values.

After calibration of the model, it was also validated using another set of climatic and discharge data not used for calibration i.e. observed during 1991 to 1993. The values of simulated discharge at specified location have been compared with the observed discharge for validation of the model. The comparison was made through statistical criteria viz., (i) Coefficient of determination (R^2), (ii) Nash and Sutcliffe efficiency (*NSE*) and (iii) index of agreement (*d*). These indices used by earlier researchers for similar purposes (Krause et al. 2005; Gassman et al. 2007) have been used in the present study.

Results and discussion

The results of the present investigation corresponding to (i) input, (ii) sensitivity analysis, (iii) Calibration and validation, and (iv) water balance components are presented and discussed below.

Validity of rainfall data

The importance of input data for the present study has been fully realized and care is taken to ensure reliability of data. The reliability of short term data was analyzed through statistical analysis. The climatic and discharge data was available for five continuous years and used with the assumption that such data will be representative of the long term situation prevailed in the study watershed. To verify this assumption a statistical significance test was performed comparing the long duration climatic (rainfall) data with short duration data of two well established meteorological data stations neighboring to the study watershed. The calculated *t* values for Guwahati meteorological data stations (1.7904) and Shillong meteorological data stations (0.94058) were less than the tabulated value of 2.04 at 95% confidence level. Thus, no significant difference of long term (30 years) and short term (6 years) was found as indicated by the results of *t*-test. Therefore the use of six years data could be representative of long duration data.

Sensitivity Analysis

Altogether there were 27 model parameters of SWAT model describing watershed hydrology and related aspects such as sediment yield and quality of water. All the parameters are not equally effective and effectiveness of the parameters is considered as the characteristics of the watershed. Identification of the effective parameters is one aspect of hydrological modeling. The sensitivity analysis was performed to identify the effective model parameters for Umkhen watershed while modeling various processes. The in-built sub-routine of the model identified the 13 sensible parameters including (i) curve number, (ii) soil available water, (iii) soil evaporation compensation factor, (iv) threshold depth of water in shallow aquifer, (v) groundwater revap coefficient, (vi) threshold depth of water in shallow aquifer for revap to occur, (vii) Manning's roughness coefficient and (viii) overland flow length. The sensitive model parameters can be grouped based on relative sensitivities which has been defined and discussed in earlier work

(Abraham et al. 2007). The relative sensitivity (RS) is a measure of the absolute differences of model outputs corresponding to extreme values of model parameters. While using SWAT model for simulating watershed hydrology, Abraham et al. 2007 classified the model parameters on the basis of estimated values of RS. The categorization of sensible parameters on the basis of such classification for the present study is presented in Fig. 4.

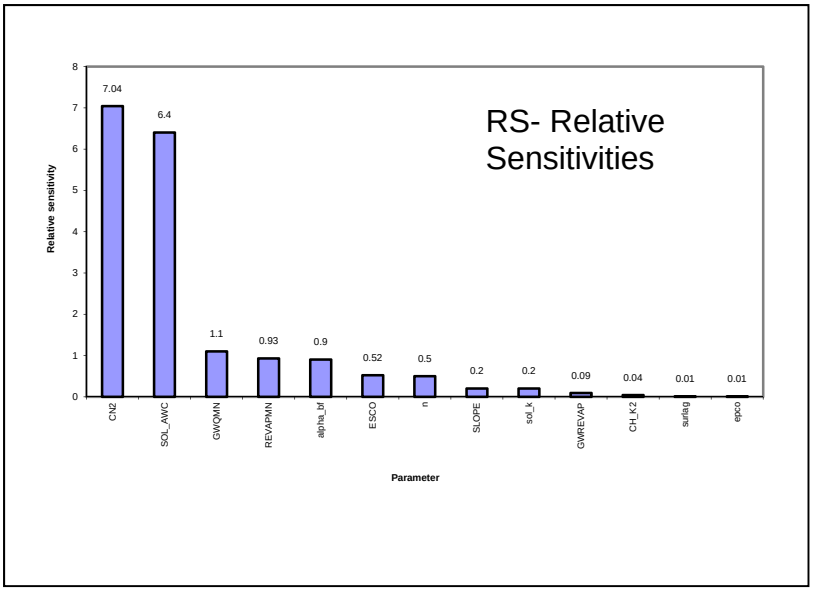

Parameters	Description
CN2	Initial CN II values
SOL_AWC	soil available water flow
GWQMN	threshold water flow in shallow aquifer for flow
REVAPMN	Threshold water depth in the shallow aquifer for flow (mm)
alpha_bf	Base flow recession alpha factor (days)
ESCO	soil evaporation compensation factor
N	Mannings N for tributary channel
SLOPE	average slope seetpness

Fig 4: Sensitive parameters and their relative sensitivities

Calibration and validation

The parameters with higher sensitivity were considered for calibration. The calibrated model was then validated. The results of calibration and validation are discussed below.

Calibration

Seven parameters which were identified as higher sensitivity could be calibrated for the present study. The calibration was continued till the difference between modeled water yield (calibrated) and corresponding observed water yield could not be minimized. The calibrated water yield (modeled) and observed water yield corresponding to spatial and temporal reference are plotted and presented in Fig. 5.

The calibrated parameters and their numerical values are presented in Table 3. The prescribed SWAT limits corresponding to the identified parameters are also given in the Table 3 for comparison (Neitsch et al. *2*001). As can be seen, the values of the calibrated parameters are within the prescribed limits.

Table 3: Parameters used for calibration of SWAT model for Umkhen watershed

Sl	Parameters	Results of calibration	Recommended range
1	Surface runoff curve number (CN2) for land use:		
(a)	Forest Evergreen	52	35-98
(b)	Forest mixed	50	
(c)	Pine	62	
2	Base flow recession alpha factor (days)	0.48	0-1
3	Threshold depth of water in the shallow aquifer	1.0	0-500
4	Soil evaporation compensation factor	0.1	0-1
5	Available water capacity of the soil layer (mm/mm soil)	0.2	0-1
6	Threshold water depth in the shallow aquifer for flow (mm)	20	0-5000
7	Manning 'n' for the tributary	0.1	0.01-0.12

The numbers of model parameters calibrated in earlier works were reported varying from situation to situation.

Validation

The calibrated model was used for assessment of spatial water yield of Umkhen watershed. However, the prediction ability of the model was judged using some well defined validation criteria before using it for water yield assessment. The validation procedure has been discussed earlier and results are discussed below.

Simulated and observed values of monthly water yield at outlet were plotted against the observed time period under reference (Fig. 6). Ideally, the two plots should be unique giving no difference between simulated and observed water yield. However, such an ideal results are difficult due to several reasons inherent to watershed characteristics and modeling features. Therefore, minimum difference between observed and simulated results will be considered acceptable for the present study as followed in earlier research works (Barlund et al. 2007; Tolson and Shoemaker, 2007).

The prediction pattern can be analyzed from Fig. 6. It is seen that differences of simulated water yield and observed water yield are more during rainy season (April to September) than during non rainy season (October to March). Moreover, overestimation of the rising (including peaks) sides and underestimation of the recession sides was also characteristics feature of model simulation in Umkhen watershed. Thus, prediction accuracy of the model may be considered temporally varying.

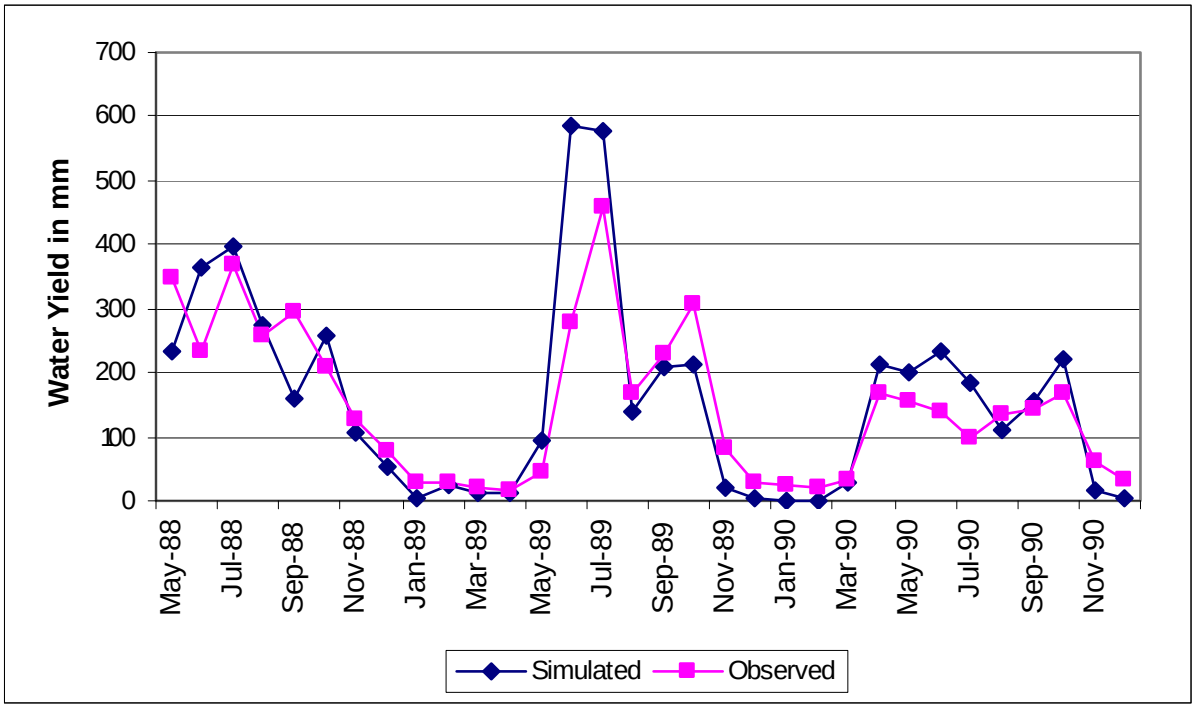

Fig 5: Simulated and observed monthly water yields at the watershed outlet during calibration (1988 to 1990).

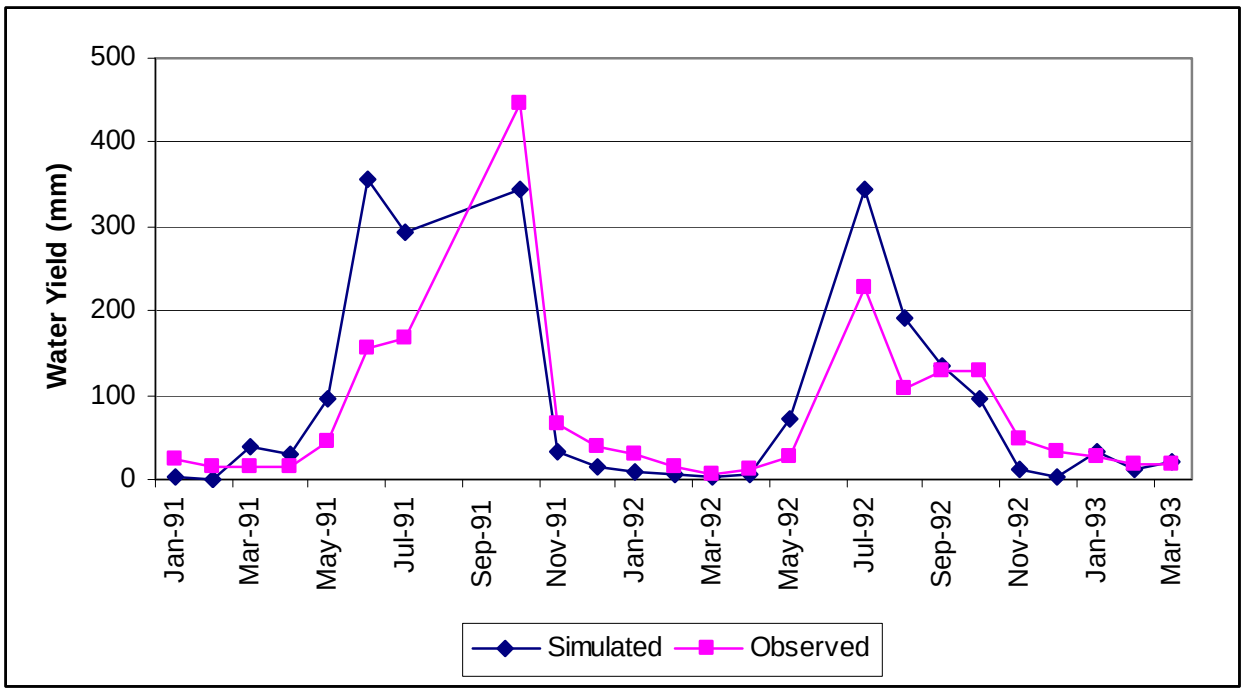

Fig 6: Simulated and observed monthly water yields at the watershed outlet during validation (1991 to 1993)

The reasons for such variation were further investigated consulting the previous hydrological modeling works. The variation in the simulated and observed values might be due to uncertainties in inputs, model uncertainty, parameter uncertainty and limitations associated with curve number method.

Apart from investigating the prediction accuracy as discussed above, the prediction accuracy of the model was also assessed through some "efficiency criteria". Efficiency criteria are defined as mathematical measures of how well model simulation fits with the observed results (Beven,

2000). The details about the statistical parameters are discussed earlier and the results are presented in Table 4.

Table 4: Values of validation parameters during different period

Sl No	Validation parameters	Entire period	Rainy period	Non rainy period
1	Coefficient of determination (*R2*)	0.70	0.68	0.93
2	Nash-Sutcliffe Efficiency (*E*)	0.64	0.0	0.86
3	Index of Agreement (*d*)	0.91	0.83	0.96

The coefficient of determination (R^2) estimated between the simulated and observed water yields for Umkhen watershed has been found as 0.70. The value of R^2 obtained in the present validation study was compared with earlier results relating to similar hydrological modeling. The Nash and Sutcliffe efficiency (*NSE)* value for prediction of water yield at the outlet of Umkhen watershed was found as 0.64. The values of *NSE* obtained by earlier researchers were consulted and found to vary between 0.41 to 0.80 (Sintondji, 2005; Bärlund *et. al.,* 2007; Tolson and Shoemaker, 2007). Moriasi et al. (2007) suggested that *NSE* values should exceed 0.5 for satisfactory prediction of hydrologic results. In addition to R^2 and *NSE*, the index of agreement (*d*) was also estimated to assess the model efficacy for the simulated results of Umkhen watersheds. The estimated value of *d* for the validation period was obtained as 0.91.

The model performance was also assessed separately during (a) rainy and (b) non rainy season through similar validation criteria as discussed above (Table 5). Considering the relative values of the efficiency criteria, better prediction ability is indicated during non-rainy season (R^2 = 0.93; *NSE* = 0.86 and d = 0.96) as compared to rainy season (R^2 = 644 0.68; *NSE* = 0 and *d* = 0.83). The reasons of such variability of predictions with reference to season could not be ascertained and needs further investigation.

No specific limits of R^2, *NSE* and *d* for validation of hydrological model could be consulted from the previous literature on watershed hydrological modeling. However, research works on modeling watershed hydrology could be consulted where simulated results were considered validated based on the similar values of the three indices as obtained in the present study

(Sintondji, 2005; Bärlund *et. al.,* 2007; Tolson and Shoemaker, 2007). Thus, the simulated results of Umkhen are also considered validated.

Water balance component

The predicted water balance components obtained from the model are shown in Table 5. The percentage of rainfall appearing as water yield was 54.45% at Umkhen outlet. Thus, about 45% of rainfall took different routes of hydrological cycle. Land use and topography are the major parameters effecting rainfall to water yield conversion as was evidenced from earlier works. The rainfall pattern was also indicated as an important factor governing the conversion.

Table 5: Predicted water balance components in Umkhen watershed

Sl No	Component	Total (mm)
1	Precipitation	2904.00
2	Surface runoff (mm)	715.98
3	Lateral flow contribution to stream flow (mm)	871.45
4	Revap (Shallow Aquifer water returning to root zone)	142.17
5	Deep aquifer recharge	29.55
6	Total aquifer recharge	597.56
7	Total water yield	1581.28
8	Percolation out of soil	619.80
9	Actual evapotranpiration	707.30
10	Potential evapotranpiration	1122.50
11	Transmission losses	6.15

In the present study the water balance component indicates that the conversion of rainfall to water yield from Umkhen accounted for more than half the precipitation received in the watershed. The water balance components indicated that surface runoff and lateral flow contribution to stream are the dominating process accounting to more than 50% of precipitation. The high conversion rate of precipitation into water yield in the present case might be attributed to the characteristics features of soil, land use, morphology and climate. The sloping terrain of the watershed coupled with a substantial area under shifting cultivation (33%) may be reason for such high conversion. Further, it was found that the hydro-geology of the study watershed indicated that the aquifer is mostly impervious with limited ground water prospects.

The results of the spatial variation of water yield of the watershed have been presented below in order to correlate the variable behavior of the spatial units with water balance components.

Spatial and temporal variation of water yield

There are 13 sub-watersheds of Umkhen viz, SW1, SW2 etc., delineated during the model development (Fig 1). The average annual water yields from these 13 sub watersheds were modeled using the SWAT200. The rainfalls to runoff conversion percentages of the sub-watersheds were estimated to assess the characteristics of the watershed. The ET components were also simulated by the model and precipitation components were generated based on the rainfall data provided as input. The modeled water yields along with other parameters such as rainfall, ET, runoff conversion percentage and area of sub-watersheds are presented in Table 6. The results are discussed below.

The spatial variations of the hydrological factors such as rainfall, soil characteristics, climate and topography contributed such variations of water yields amongst the sub-watershed. Rainfall seems to be the prominent factor responsible for generation of water yield, as southern parts of Umkhen experiences relatively higher rainfall then the northern part.

Further, investigation of the variation of water yield amongst the sub-watersheds lying in high rainfall southern part was made in light of the relevant input data and underlying hydrological processes. All the sub-watersheds are not identically converting precipitation into runoff. For example, the five sub-watersheds viz., SW6, SW8, SW9, SW11 and SW13 experiences identical rainfall situation (5277.84 mm). However, rainfall to runoff conversion percentages of SW6 (62.7%) and SW13 (63.2 %) were more than the remaining sub-watersheds viz., SW8 (52.9 %), SW9 (57.7%) and SW11 (49.9%). Though, receiving identical rainfall, these two groups of sub-watersheds differ in land uses and soil characteristics. In the higher runoff generating group, sub-watershed SW6 had mixed forest (68.12%) as dominating land use followed by pine forest (24.12%), evergreen (6.88%) and agricultural land use (0.84%). SW13 is dominated only by pine forest. Moreover, upper soil layers in of SW6 and in the entire profile in SW13 are dominated by sandy clay loam. The characteristic of this soil mapping unit is excessively well drained (NBSSLUP, 1999). Thus, characteristic features of soil type, land coverage coupled with higher elevation might have favoured the hydrological process in SW6 and SW13 to generate higher level of water yields. On the other hand, in the other group of low water yield sub watersheds (SW8, SW9 and SW11) clay and clay loam are the dominating soil type. Hydrologically clay and

clay loam soil do not favour higher water yield. This might be the reason for high storage within the watershed and thus resulting comparatively lower water yield within the group. Land uses of this group of sub-watershed do not differ much from the other group mentioned above. Thus, soil type might be the only influencing factor to cause differential water yields amongst the sub-watershed.

Table 6: Sub watershed wise water yield in Umkhen

Sub watershed	Watershed size	Rainfall	Average water Yield	Rainfall to run off conversion	ET
	(km2)	(mm)	(mm)	(%)	(%)
SW 1	17.13	1275.14	700.09	54.90	54.84
SW 2	126.98	1275.14	700.62	54.94	54.37
SW 3	82.47	1275.14	406.34	31.87	57.74
SW 4	88.81	1275.14	698.75	54.80	56.35
SW 5	19.09	1275.14	707.49	55.48	53.76
SW 6	119.12	5277.84	3309.82	62.71	10.45
SW 7	138.40	1275.14	379.26	29.74	60.90
SW 8	68.96	5277.84	2795.68	52.97	10.36
SW 9	71.20	5277.84	3047.95	57.75	10.47
SW 10	187.01	1681.94	625.68	37.20	40.15
SW 11	75.66	5277.84	2633.30	49.89	10.71
SW 12	157.05	1681.94	708.57	42.13	39.81
SW 13	52.11	5277.84	3336.72	63.22	10.64

Similarly, the processes dominating hydrological phenomena in the low water yielding northern sub-watersheds (SW1, SW2, SW3, SW4, SW5, and SW7) were also analyzed. Evapo-transpiration was the dominating process in these sub watersheds with ET exceeding 50% of precipitation. Higher temperature prevailing in the lower altitude of Umkhen might be the reason of higher ET of these sub-watersheds. The annual average temperature of northern side exceeds by about 10 $^{\circ}$C compared to southern side of Umkhen.

The variations of water yields amongst the sub-watersheds were also noticed in northern side of Umkhen in spite of receiving identical precipitation. Dominating clay loam soil in SW3 and

SW7 seems to cause reduced amount of runoff generation with only 31.87% and 29.74%, respectively. The runoff generation percentages of the remaining sub-watersheds viz., SW1, SW2, SW4, and SW5 were more than 54% due to presence of silty clay loam and sandy clay loam type soil.

Type of land coverage might not be the distinguishing cause of the variations of runoff generations in the northern sub-watersheds, as 28.01% (ever green forest), 75.70% (mixed forest), 1.37% (agricultural land) and 0.31% (residential) are more or less uniformly present in the entire northern side.

The seasonal variability of water yield was also estimated using the model for all the sub watersheds under study. Output of the model was used to compare the behavior of sub-watersheds during extreme wet and dry periods (Table 7). The rainfall pattern indicated that June is the wet period and February is the dry period. The water yields during wet and dry months were also exhibited similar spatial variation as observed with annual water yield which has been discussed above.

Table 7: Sub watershed wise water yield during dry and wet period

Sub watershed	Rainfall (mm)	Water Yield for the month of February (mm)	Water Yield for the month of June (mm)
SW1	1275.14	2.67	221.00
SW2	1275.14	2.69	221.38
SW3	1275.14	0.33	81.96
SW4	1275.14	2.74	222.20
SW5	1275.14	2.78	222.83
SW6	5277.84	14.38	790.01
SW7	1275.14	0.33	81.63
SW8	5277.84	10.64	672.17
SW9	5277.84	8.45	514.60
SW10	1681.94	3.30	149.35
SW11	5277.84	7.77	655.32
SW12	1681.94	3.51	170.13

SW13	5277.84	14.15	803.65

The present work attempted to model hydrology of a hilly watershed (Umkhen) of north-eastern India using SWAT2000 and available input data. The model successfully simulated water yield at the outlet of Umkhen watershed. Further, the variability of input data (soil, land use and weather) has also been found appropriately reflected in model outputs at the outlets of 13 delineated sub-watersheds. The results of the investigation will be useful for the development of water resources. However, the limitations discussed in the article should be fully appreciated while using the results of the present investigation.

Conclusion

Traditionally the assessment of hydrological parameters is done on the basis of observed data at the outlet of the watershed. Such assessments are site specific and would generally ignore the on-going hydrological processes within the watershed. Assessments at other alternative sites are not possible in absence of site specific observed values. In the inaccessible north-eastern region of India it is practically not feasible to set up gauging stations at number of places. Thus, need of alternative methods of water assessment has been felt. GIS based models have been widely used in most part of the world to mimic watershed hydrology in different situations including mountainous watershed. Spatial and temporal assessment of water has also been one of the aspects of watershed modeling. In the present study SWAT2000 hydrological model has been used for simulating hydrological processes of a hilly watershed located in north-eastern region of India. Integration of model components in GIS environment and satisfying the model for the extensive data requirements have been the major tasks. A number of data sources have been used for different types of data concerning Umkhen watershed viz., (i) terrain data, (ii) land use, (iii) soil data and (iv) meteorological data. Despite of ensuring reliability and authenticity of data sources, deficiency of data can not be ruled out and such deficiencies might have reflected in the model output in the form of simulation error. To ensure that error remains within the agreeable limit, the developed model has been calibrated and then validated using standard procedure. The specific conclusions of the present investigation are:

(i) SWAT2000 has been demonstrated to simulate water yield in a hilly watershed with the involvement of locally acquired data including observed water yield data.

(ii) The most sensitive parameters of SWAT2000 watershed modeling of Umkhen are curve number and soil available water.

(iii) The simulation ability of the Umkhen watershed model has been tested through standard procedure comparing with observed data. The model is capable to simulate water yield with reasonable degree of agreement. Prediction ability of the model is better during non-rainy period then rainy period.

(iv) The limitations of the Umkhen watershed modeling are mainly related to data deficiency. Non availability of meteorological data (temperature, rainfall) from a number of closely spaced data stations within the study watershed has been one of the major deficiencies. Similarly, the soil mapping was also done at a grid of 10 km which might have ignored the intermediate variability soil characteristics. These aspects might have attributed to simulation error of modeling. Apart from the limitations of the input data, the errors might have been induced during model parameterization. The mis-paramaterization might include non availability of equivalent definition of each parameter for Indian condition particularly the definition of land use and components of curve number methods.

(v) The variability of input data (soil, land use and weather) has also been found appropriately reflected in model outputs at the outlets of 13 delineated subwatersheds.

References

Abbot, M.B., and Refsgaard, J.C., 1996. Distributed Hydrological Modeling. Kluwer Academic Publishers Dordrecht, Netherlands. 321 p.

Abraham, L.Z., Roehrig, J, Chekol, D.A., 2007. Calibration and Validation of SWAT Hydrologic Model for Meki Watershed, Ethiopia. Conference on International Agricultural Research for Development, Organized by University of KasselWitzenhausen and University of Göttingen, October 9-11, 2007.

Arnold, J.G., Allen, P.M., Bernhardt, G., 1993. A comprehensive surface-groundwater flow model. Journal of hydrology 142, 47-69.

Arnold, J.G., Srinivasan, R., Muttiah, R.S., Williams, J.R., 1998. Large scale area hydrologic modeling and assessment part I: model development. Journal of American Water Resources Association 34(1), 73-89.

Ba¨rlund, I., Kirkkala, T. Malve, O. Ka¨ma¨ri J., 2007. Assessing SWAT model performance in the evaluation of management actions for the implementation of the Water Framework Directive in a Finnish catchment; Environmental Modeling & Software, 22, 719-724.

Beven, J.Keith., 2000. Rainfall-Runoff Modeling The Primer, John Willey & Sons Ltd, New York. P.360. Beven, K., 1995. Linking parameters across scales: sub grid parameterization and scale dependent hydrological models. Hydrological processes 9, 509-525.

Bhuyan, S.J., Koelliker, J.K., Marzen, L.J. and Harrington,Jr, J.A., 2003. An integrated approach for water quality assessment of a Kansas watershed. Journal of Environmental Modeling and Software, Vol. 18 (5), 473-484p.

Chen E. and D.S. Mackay. 2004. Effects of combining non-spatial simulation units and explicit models of sediment delivery on an agricultural nonpoint source pollution model. *Journal of Hydrology*, 295, 211-224.

Chetry, N.; Saikia, R., 2002. Atlas of resources, Infrastructure and development. An publication of the output of the Department of Science and Technology Sponsored Project on Integration and Management of Multi-Source Data Using GIS for Development Plan/ Strategy for Kathiatoli Development Block within Kopili Basin in North East India. ; Department of Geography, Cotton College Guwahati. 52p.

Clapp, R.B., and G.M. Hornberger., 1978. Empirical equations for some soil hydraulic properties. Water Resour. Res. 14:601–604.

Dabral, P.P., Baithuri, N and Pandey, A., 2008. Soil erosion assessment in a hilly catchment of north eastern India using USLE, GIS and remote sensing. Journal of Water Resources Management, Vol 22, 1783-1798.

Gallart, F., Latron, J, Llorens, P and Beven, K., 2007. Using internal catchment information to reduce the uncertainty of discharge and base flow predictions. Journal of Advances in Water Resources. Vol. 30 (4), 808-823p.

Gassman, P.W., Reyes, M. R., Green, C. H., Arnold J. G., 2007. The Soil and Water Assessment Tool: Historical Development, Applications, and Future Research Directions. Transactions of the ASABE., Vol. 50(4): 1211-1250.

GoA., 2004. Economic Survey of Assam. Published by Government of Assam. Chapter VIII, 34-37.

Hanks, R.J. and G.L. Ashcroft., 1980. Applied Soil Physics. Springer-Verlag, New York.

ILWIS., 2001. ILWIS 3.0 User Guide, International Institute for Aerospace Survey and Earth Sciences (ITC) Enschede, The Netherlands. 520p.

Jang, S., Cho, M., Yoon, J., Yoon, Y., Kim, S., Kim, L. and Aksoy, H., 2007. Using SWMM as a tool for hydrological impact assessment. J. Desalination, Vol. 212, issue 1-3, 344-356.

Jia, Y., Niu, C., and Wang, H., 2007. Integrated modeling and assessment of water resources and water environment in the Yellow River Basin. Journal of Hydro environment Research . Volume 1 (1) , September 2007, Pages 12-19.

Kannan, N., White, S.M., Worrall, F., Whelan, M.J., 2007. Hydrological modeling of a small catchment using SWAT-2000 – Ensuring correct flow partitioning for contaminant modeling. Journal of Hydrology, 334, 64– 72.

Kiat, C.C., Ghani, A.A., Abdullah, R. and Zakaria, N.A., 2008. Sediment transport modeling for Kulim River – A case study. Journal of Hydro-environment Research. Volume 2, (1), September 2008, Pages 47-59.

Knebl,M.R., Yang, Z.L., Hutchison, K and Maidment, D.R., 2005. Regional scale flood modeling using NEXRAD rainfall, GIS, and HEC-HMSRAS: a case study for the San Antonio River Basin Summer 2002 storm event. Journal of Environmental Management, Volume 75 (4), 325-336p.

Krause, P., Boyle, D.P., and B¨ase, F., 2005. Comparison of different efficiency criteria for hydrological model assessment, Advances in Geoscience (5), 89-97p.

Mackay, D.S., Robinson, V.B., 2000. A multiple criteria decision support system for testing integrated environmental models. Fuzzy set and system 113, 53-67.

Moriasi, D. N., J. G. Arnold, M. W. Van Liew, R. L. Binger, R. D.Harmel, and T. Veith., 2007. Model evaluation guidelines for systematic quantification of accuracy in watershed simulations. Trans. ASABE 50(3): 885-900.

NBSSLUP., 1999. Soils of Meghalaya for optimizing land use, National Bureau of Soil Survey and Land Use Planning Pub 52. Soils of India Series, 44p.

Neitsch, S.L., Arnold, J.G., Kiniry, J.R., Williams, J.R., 2001. Soil and Water Assessment Tool-Version 2000-user manual, Temple, TX, USA.

Prasad, R.N., Singh, A., Verma, A., 1990. Shifting cultivation and land degradation. In: Shifting cultivation. In North East India, Muzumdar, D.N. ed., Omsons Publications, Allahabad, 143-148p.

Saikia, R., 1990. Geomorphology of the Kopili Basin, North East India. Unpublished 957 Ph.D. thesis, Department of Geography, Gauhati University.

Sarma, V.A.K., Krishnan, P., Budhilal, S.L., 1987. Laboratory methods-Soil resources mapping of different states of India. Tech Bull, NBSS Pub 14, NBSS&LUP (ICAR), Nagpur (India), 49p.

Schuol, J., Abbaspour, K.C., Yang, H., Srinivasan, R., Zehnder, A.J.B., 2008. Modeling blue and green water availability in Africa. Water Research Resources, Vol 44, W07406, doi:10.1029/2007WR006609, 2008.

Sehgal, J.L., Saxena, R.K., Vadivelu, S., 1987. Field Manual-Soil resources mapping of different states of India. Tech Bull, NBSS Publ. 13, NBSSLUP, Nagpur (India), 73p.

Sintondji, Luc Oliver C., 2005. Modeling the Rainfall-runoff process in the upper Ouěmě catchment (Terou in Bĕnin Republic) in a context of global change: extrapolation from local to the regional scale. Ph.D. thesis, Mathematics and Natural Resources Department, University of Bonn, 205pp.

Tolson, B.A., Shoemaker, C.A., 2007. Cannonsville Reservoir Watershed SWAT2000 model development, calibration and validation; Journal of Hydrology, 337, 68– 86.

Development of a SWAT-based soil productivity index

Roberto de Jesús López Escudero
Instituto Nacional de Investigaciones Forestales, Agrícolas y Pecuarias (INIFAP)
e-mail: lopez.roberto@inifap.gob.mx

Héctor Daniel Inurreta Aguirre
Instituto Nacional de Investigaciones Forestales, Agrícolas y Pecuarias (INIFAP)

Jesús Uresti Gil
Instituto Nacional de Investigaciones Forestales, Agrícolas y Pecuarias (INIFAP)

Diana Uresti Durán
Instituto Nacional de Investigaciones Forestales, Agrícolas y Pecuarias (INIFAP)

Elibeth Torres Benítez
Colegio de Postgraduados (CP)

Abstract

The objective of this work was to develop and map a soil productivity index (SPI) for the State of Veracruz, México. The variables considered to integrate the SPI were depth, texture, organic matter content, internal drainage and slope. Each variable was divided into three categories: high, medium and low, mapping the resulting classification. Classified maps were overlaid, creating a new map containing all variables. Soil data was obtained from 829 descriptive soil profiles, well distributed along of the study area. Land slope was extracted from a 90x90m digital elevation model. Productivity was assessed through the dry grain yield of corn. The Soil and Water Assessment Tool (SWAT) model was used to simulate the total biomass and grain yield throughout the 7.18 million hectares of Veracruz. The map shows that the SPI categories high, medium and low cover an area of 5.45, 0.56 and 0.24 Mha with an average yield of grain of 6.0, 4.4 and 1.4 t ha-1 respectively. High SPI was described as a deep soil, with high organic matter content, slow internal drainage and any soil texture and slope. Medium SPI was described as a medium-depth soil, with organic matter content from medium to low, internal drainage from medium to fast and any soil texture and slope. Low SPI is described as shallow soils and any category of the other variables. SPI was mainly determined by soil depth, organic matter content and internal drainage.

Keywords: Corn, ArcSwat, Geographical Information Systems, Soil Productivity Index.

Introduction

Soils cover most lands of the earth, but regarding their service for humans they are a limited and largely nonrenewable resource (Blum,1993). On the globe about 3.2 billion hectares are used as arable land, which is about a quarter of the total land area (Scherr, 1999; Davis and Masten, 2003) and the total area with agricultural vocation covers about 40- 50 % of the global land area (Smith et al.,2007). The development and survival of civilizations has been based on the potential of soils to provide food and further essential goods for humans (Hillel, 2009). Global issues of the 21st century like food security, demands of energy and water, climate change and biodiversity are associated with the sustainable use of soils (Lal,2008,2009; Jones et al.,2009; Lichtfouse et al., 2009).. Agricultural development cannot be intensified at expense of the soil degradation, ecosystems and socio-economic environment. It has to be achieved using balanced strategies to develop multifunctional landscapes on our planet (Wiggering et al., 2006; Helming et al., 2008). Due of this, it is necessary to generate an index of soil productivity, to assist in the evaluation of different alternatives for land use.

Soil productivity refers to the capacity of soil to grow crops or plants under specified environmental conditions and is influenced by soil properties, climate conditions and management inputs. Crop Yields are useful in determining the suitability of any soil for agricultural use. Attempts have been made to relate the crop yield with a limited number of soil properties (Olson et al., 2000).

Many scientists have tried to find relationships between soil properties, climate, and crop yields, and soils have been grouped for comparison. Many studies like Olson (1985) and Olson (1986) have shown that crop yield response is correlated with soil properties. Silt and organic matter contents of a soil layer have a significant positive correlation with available water percentage; other soil properties of importance include texture, moisture conductivity, and depth. Other features associated with the land, such as the slope and shape of the ground surface, affect the quantity of rain that effectively recharge the supply of soil moisture.

Differences in crop yield and soil productivity may be represented by productivity indices. Productivity ratings are a good indicator of the suitability of soils for crop production and are useful to determining the best use and management of soils. It is necessary to generate accurate and reliable information about the productivity of soils, presented as crop yield estimations and productivity indices for each soil type. Consequently, information is required about the influence of soil properties in crop yields (Olson et al., 2000).

Corn is one of the most important crops in the state of Veracruz, Mexico, but according to the current problems related to land use, it is necessary to generate new technologies for more efficient land use.

In consideration with the situation described previously, the aim of this work was to develop and map a soil productivity index (SPI) of Corn for the total area of the state of Veracruz, México.

MATERIALS AND METHODS

The Studied area

Veracruz State is located in the center of the Gulf of Mexico with a littoral of 745 Km, and have boundary with seven Mexican states (Tamaulipas, San Luis Potosi, Hidalgo, Puebla, Oaxaca, Chiapas and Tabasco).It has 212 municipalities distributed in a total area of 78, 815 ha, representing 3.7% of the total area of Mexico. It is located between the 17º 00' and 22º 20' north latitudes and between the 93º 35' and 98 º 34' west longitudes. It presents five type of climates with annual means temperatures from 0° to 26° centigrade grades, the climate variation is mainly caused by altitudinal differences,(from the 0 to the 5,610 meters above sea level). (SEDECO 2011). In the Figure 1 shows the location of Veracruz, while in Figure 2 shows the geographical distribution of climates, soils, slopes and land use, respectively, according to digital maps of 1:250,000 scale obtained from INEGI (Instituto Nacional de Estadistica y Geografia)

Figure 1. Localization of the state of Veracruz, Mexico.

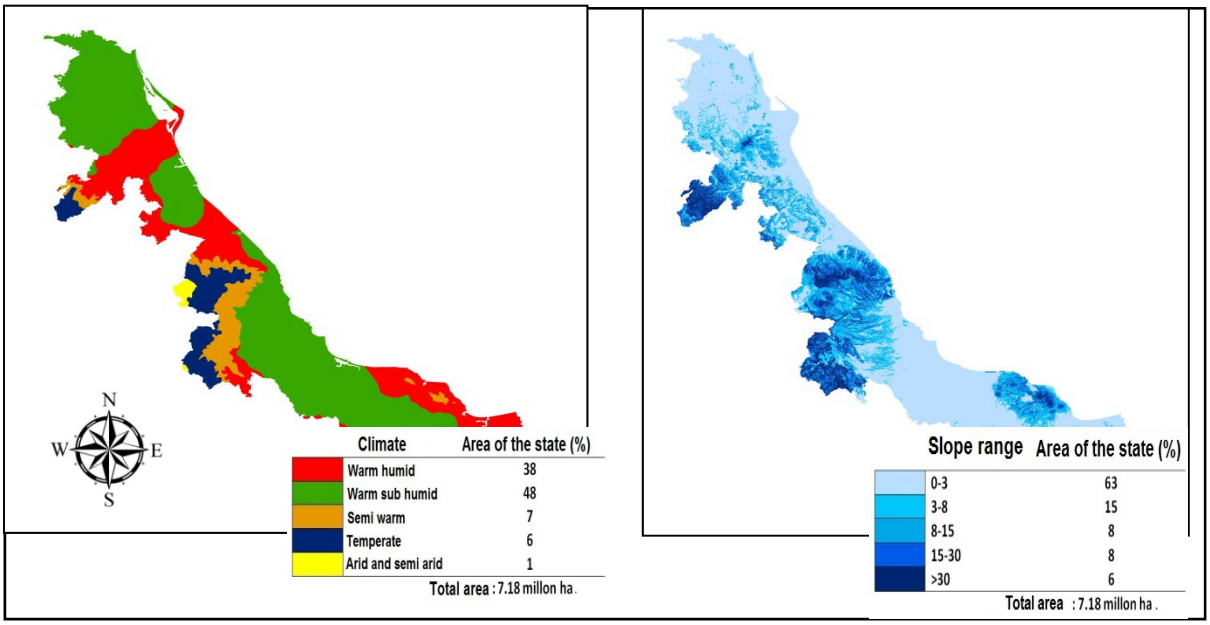

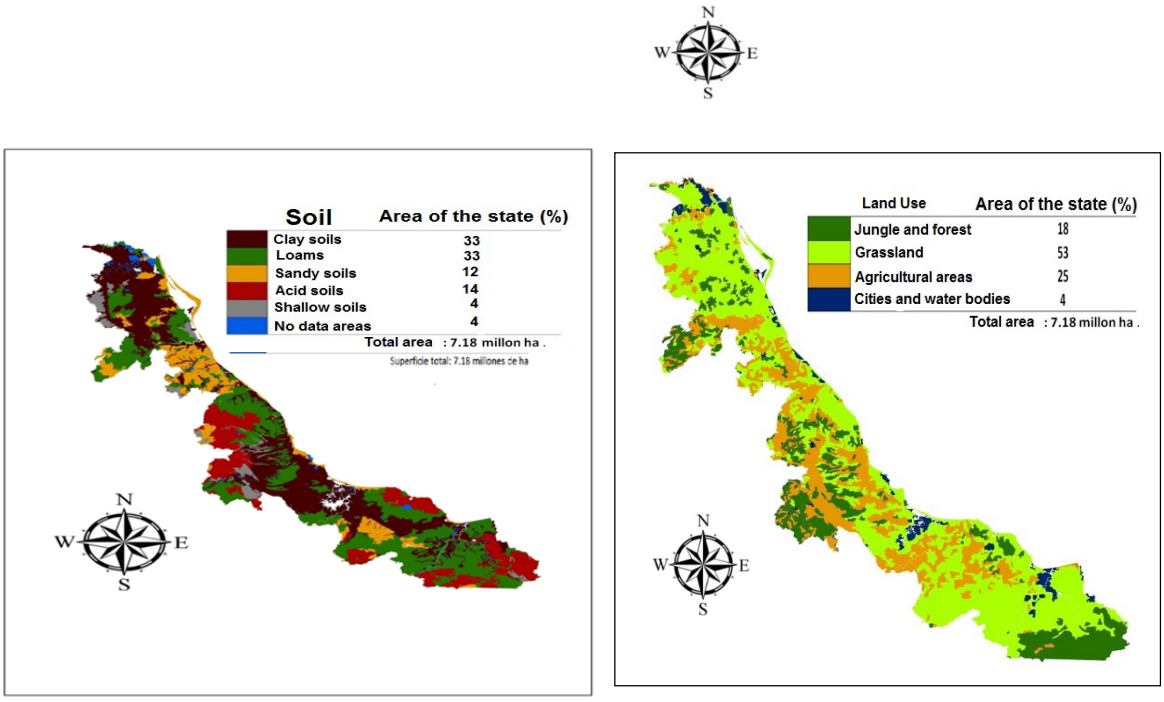

Figure 2. Geographical distribution of climates, soils, topography, and land use of the state of Veracruz, México.

Crop Yield calculation

To achieve the objectives of this work was first necessary to calculate grain yield of corn in different edafoclimatic conditions present in the study area. For that purpose the model SWAT (Soil and Water Assessment Tool) was used to simulate the crop growth and estimate the amount of corn grain produced.

The simulation process with SWAT can be divided in two phases, in the first the simulation units are created through the overlaying maps and in the second this units are parameterized with the information contained in the internal database of the program, this database can be supplemented and modified by the user with local information

Watershed delineation

The SWAT model works at basin level (Neitsch, et al. 2005 and Garg, et al. 2012), so first of all is necessary to delineate the watershed. The watershed delineation was performed using a digital elevation model (DEM) with a pixel size of 90x90 m acquired from INEGI, with a mask of an area larger than the State for assure that all of the study area were included in the simulation process. To increase the accuracy of the flow calculation in the basin, a river mask was added to the process. The flow direction and accumulation was carried out based on DEM. The stream network was created using the minimum mapping area. After that, the model splits

the basin in subbasins using the DEM and the newly prior generated information (Narasimhan, et al. 2005; Garg, etal. 2011; Du, et al. 2006; Akhavan,et al. 2010, Guzman et al. 2004). With this information, the model displays every point of water discharge and asks the user which of them want to consider. In this work, all available outlets were selected, with the intention of creating as many subbasins as possible. Finally 90 subbasins were created and parametrized.

Generation of Hydrological Response Units (HRU)

The unit of analysis and simulation of SWAT is the Hydrological Response Units (HRU), which is defined as an area who belongs to the same subbasin and share the same type of soil, land use and slope category (Narasimhan, et al. 2005; Garg, etal. 2011; Du, et al. 2006; Akhavan,et al. 2010, Guzman et al. 2004). The HRU were defined from five slope categories map (0-3, 3-8, 8-15, 15-30 and >30%), 46 soil sub-units (FAO soil classification) and one land use maps; assuming the entire state of Veracruz was cropped with corn. The slope categories were worked out from the DEM, while the soil and map of land use (Scale 1:250,000) were obtained from INEGI. The above process resulted in 4,053 HRU's.

Databases

The internal database of the model contains information of soil, climate, agronomic management and physiological parameters of different plant-species. This information influences the crop growth and determines their yield, and, as explained above, can be supplemented or modified with local information. In this work, because the conditions are different from those prevailing where the model was developed, the information was customized, developing a local database of soil and climate, changing physiological parameters of corn, according to the local varieties and developing an agronomic management appropriate to the surrounding conditions

Soils

The soil map used, divided study area in 49 classes of soil using the FAO-UNESCO classification, this map was modified according to the presence of lytic phase in some soil classes, creating 13 new soil classes. Using the data of 829 soil profiles from INEGI, well distributed in the Mexican Southeastern a typical profile was created for every soil class and then them were parameterized, averaging the corresponding values according to the soil class and to the horizon. However, soil profile data, did not contain all the information required by the model, so it was necessary obtained or estimated it from other sources. The Table 1 shows as an example the parameters of the typical soil profile of eutric Cambisol and the different sources of the used information.

Table 1. Features of eutric cambisol (Be) typical soil profile.

Horizon	Dep.	Text.	B.D.	A. M.	O.C.	S.H.C.	C.R.	Alb.	USLE K	E.C
A	200	17-32-51	1.45	0.12	3.01	14.5	0	0.06	0.23	1.22
B1	390	16-37-47	1.45	0.13	1.48	12.2	0	0.02	0.40	1.23
B2	1019	18-31-51	1.45	0.12	0.65	9.9	0	0.01	0.41	1.07

Dep: Depth in mm (INEGI), **Text:** texture in percentage in order of clay-silt-sand (INEGI), **B.D:** Bulk density in g cm^{-3} (Saxton *et al.* 1986), **A.M:** Available moisture in mm mm^{-1}. (Saxton *et al.* 1986), **O.C:** Organic carbon in percentage of the total soil (Neitsch *et al.* 2005) **S.H.C:** Saturated hydraulic conductivity in mm hr^{-1} (Saxton *et al.* 1986) **C.R:** Content of rock in percentage of the total soil (INEGI) **Alb:** Albedo (Harris equation, software Curve Expert 2.0) **USLE K:** "K" factor of the universal soil erosion equation (Neitsch *et al.* 2005) **E.C:** electrical conductivity in dS m^{-1} (INEGI).

Climate

To the climate data inputs required by the model were introduced historical data from 137 weather stations located within the state of Veracruz with daily data of precipitation and temperature (maximum and minimum) of at least 20 years in the period 1960- 2000. Due that the model requires certain monthly statistical parameters, and besides some weather stations had incomplete data, was necessary to simulate the climate using the EPIC weather generator (Sharply and Williams 1990). In Table 2 shows, as an example, the monthly statistics of the station Ver30153. Because the SWAT assigns to the entire basin, the climate of the nearest weather station to their centoide, only 95 wheater stations were considered by the model.

Physiological parameters and management inputs

To the simulation of growth of corn and calculate their grain production, the model requires the physiological parameters of this specie. SWAT contains an internal database with physiological parameters of several crops and this database includes corn. However these physiological parameters are for the varieties used in U.S.A, so it had to be adjusted to local varieties using peer-reviewed literature and local expert opinion. Table 3. shows the more important physiological parameters finally used by SWAT for simulated the corn growth.

Table 2. - Climate statistics of Ver30153 weather station.

	Month											
Feature	**J**	**F**	**M**	**A**	**M**	**J**	**J**	**A**	**S**	**O**	**N**	**D**
Tmax	24.70	27.80	30.10	32.50	32.50	32.00	32.80	32.30	29.80	28.30	25.80	24.70
Tmin	14.50	14.90	17.80	20.00	22.60	22.80	22.00	22.00	21.90	20.30	18.10	16.40
DETmax	5.90	5.30	4.90	4.00	3.00	2.80	2.60	2.90	3.60	4.00	4.80	5.20
DETmin	3.50	3.00	3.10	2.70	2.50	1.30	1.00	1.00	1.70	2.30	3.20	2.90
PPM	69.60	96.20	81.80	52.20	76.20	137.60	125.80	118.30	214.90	205.9	146.7	113.5
DEPPM	11.35	16.90	15.41	16.67	25.35	17.95	19.25	18.65	36.89	25.36	26.49	16.18
CAPPM	2.68	2.88	3.71	2.51	2.16	2.78	4.66	2.20	3.40	1.94	2.48	2.95
PDHDS	0.22	0.21	0.16	0.08	0.10	0.17	0.20	0.19	0.18	0.22	0.19	0.25
PDHDH	0.37	0.40	0.48	0.42	0.25	0.52	0.38	0.43	0.49	0.47	0.35	0.41
PDPM	8.00	7.30	7.40	3.70	3.60	8.00	7.60	7.60	7.80	9.10	6.70	9.30
PMMH	15.10	20.60	23.00	25.00	35.20	36.70	28.80	35.30	55.00	44.00	43.00	20.60
RS	12.00	14.00	16.00	19.00	19.00	20.00	20.00	21.00	19.00	17.00	15.00	13.00

Tmax: Maximum temperature, **Tmin**: Minimum temperature; **DETmax**: Standard desviation of the maximum temperature; **DETmin**: Standard desviation of minimum temperature,**PPM**: mean monthly precipitation; **DEPPM**: Standard desviation of the mean monthly precipitation; **ACPWP**: Coefficient of asymmetry of the mean monthly precipitation;**PDHDS**: Probability of a wet day after dry day**; PDHDH**: Probability of a wet day after wet day, **PDM**: average days with precipitation per month; **PMMH**: maximum rainfall in half an hour, **RS**: Solar radiation.

Table 3. Physiological parameters introduced to SWAT of Corn.

Species	**RUE ($Kgha^{-1}/Mjm^{-2}$)**	**2nd point RUE**	**LAI**	**HI**	**Canopy Height (m)**	**Root Depth (m)**	**Optimum Temp. °C**	**Base Temp °C**
Corn	35	42	3.5	0.45	2.5	1	25	10

RUE: Radiation use efficiency; **LAI:** Leaft area index; **HI:** Harvest index; **Temp:** Temperature.

Although SWAT contains several agronomic management operations, those considered to simulate corn were only planting dates, tillage and fertilization rates. The irrigation operations

was not used because de aim of the work was the productivity in dry conditions and the other operations were discriminated, because they did not have an impact in the simulated grain production. The Table 4 shows agronomic management operations used for the simulation.

Soil Productivity Index (SPI)

With the simulation results, a map of the potential yield of corn grain in the state of Veracruz was created. Because tropical varieties of corn, as the used in the simulation, do not grow at altitudes above 1,200 meters, all areas with higher altitude were removed. The procedure was the same with the areas occupied by cities, water bodies and protected areas. Once you create a map of potential grain yield of corn, the SPI was generated using five soil variables (depth, texture, organic matter content, internal drainage and slope) for each HRU.

Table 4. Corn management operations used introduced to SWAT.

Activity	Year	Operation	Input rate	Date
Land preparation	1	Slash-Blade	Blade 10 ft	14th May
	1	Sub-soiling	Disk Plow Ge 23 ft	24th May
	1	Harrowing	Finishing Harrow Ge 15 ft	29th May
	1	Harrowing	Finishing Harrow Ge	30th May
	1	Furrowing	Furrow Dicker	31th May
Corn establishment	1	Planting	CORN	1st June
Fertilization	1	1st Fertilization	25-65-00 NPK(Kg ha^{-1})	1st June
	1	2nd Fertilization	80-00-00 NPK(Kg ha^{-1})	1st june
	1	3th Fertilization	80-00-00 NPK(Kg ha^{-1})	27th june
Pesticide application	1	1st Chemical control	0.90 Atrazine (Lts ha^{-1})	4th June
	1	2nd Chemical control	0.20 Cypermethrin (Lts ha^{-1})	25th june
	1	3th Chemical control	0.68 2.4-D amine (Lts ha^{-1})	5th july
	1	4th Chemical control	1.00 Carbaryl (Lts ha^{-1})	15th july
	1	4th Chemical control	1.00 Carbaryl (Lts ha^{-1})	9th August
Harvest	2	1st Harvest		31th May

NPK: Nitrogen, Phosphorus, potassium

Each soil class was classified into three categories for each of the five aforementioned variables. The categories were created using the soil profile descriptions and the opinion of expert pedologist. The Table 5 shows this classification.

Table 5. Classification of soils according to the variables used to obtain the SPI.

Variable	Division	Soils (FAO classification)
1.- Depth	1. Shallow (<30 cm.)	I, E,
	2. Medium (30-70 cm.)	Vp(L), Hc(L), Hh(L), Lc(L), Lo(L), Bk(L), Bh(L), Re(L), Rd(L), Rc(L), To(L), Tm, Kh, We, Zo, Zg
	3. Deep (>70 cm.)	Rd, Vc, Bc, Gm, Bd, Hh, Th, Bg, Qc, Bk, Bf, Lc, To, Ao, Hc, Je, Be, Lg, Re, Rc, Hl, Gv, Gp, Lp, Ah, Bv, Ap, Lf, La, Lo, Ge, Jg, Kl, Kk, Lv, Jc, Vp, Nd
2.- Texture	1. Coarse	Bd, Hh, Rc, Rd(L), Re, Re(L), Th, Tm, Zo
	2. Medium	Be, Bg, Bk, Gm, Hc, I, Jc, Je, To
	3. Fine	Ah, Ao, Ap, Bc, Bf, Bh(L), Bk(L), Bv, E, Ge, Gp, Gv, Hc(L), Hh(L), Hl, Jg, Kh, Kk, Kl, La, Lc, Lc(L), Lf, Lg, Lo, Lo(L), Lp, Lv, Nd, Qc, Rc(L), Rd, Vc, Vp, Vp(L), We, Zg.
3.- Organic matter content	1. Low	Ao, Ap, Be, Bf, Bg, Bk(L), Bv, Ge, Gp, Gv, Hc, Hc(L), Hh, Hh(L), Hl, Jc, Je, Jg, Kk, Kl, Lg, Lv, Qc, Rc, Rd, Rd(L), Re, Re(L), Vc, Vp, Vp(L), We, Zg.
	2. Medium	Ah, Bc, Bd, Bh(L), Bk, Gm, La, Lc, Lc(L), Lf, Lo, Lo(L), Lp, Nd, Rc(L), Tm, To, Zo.
	3. High	E, I, Kh, Th.
4.- Internal drainage	1. Fast	E, I, Qc, Rc, Rc(L), Rd, Rd(L), Re, Re(L), Th, Tm, To.
	2. Medium	Ah, Ao, Ap, Bc, Bd, Be, Bf, Bh(L), Bk, Bk(L), Hc, Hc(L), Hh, Hh(L), Jc, Je, Kh, Kk, La, Lc, Lc(L), Lf, Lo, Lo(L), Lp, Nd, We, Zo.
	3. Slow	Bg, Bv, Ge, Gm, Gp, Gv, Hl, Jg, Kl, Lg, Lv, Vc, Vp, Vp(L), Zg.

Cm: centimeters

In the simulation process, the model parameterizes each HRU, within these parameters are included soil class and slope. Through the soil class it is possible to know the depth, texture, organic matter content and internal drainage of every HRU.

The results were mapped and successively overlaid in pairs creating different interactions, and using the map of the potential yield of corn grain, after that these different interactions were reclassified in three categories (high, medium and low). The Table 6 shows the different interactions created to generate the SPI.

Table 6. Different interactions to create the SPI.

Number of interaction	Variable 1	Variable 2
1	Depth	Texture
2	(Depth, Texture)	Organic Matter content
3	(Depth, Texture, Organic Matter Content)	Internal Drainage
4	(Depth, Texture, Organic Matter Content, Internal Drainage)	Slope

RESULTS

The Table 7 shows the average of grain corn yield in the interaction of soil depth (D) and soil texture (T), while the Table 8 shows the characteristics of the reclassification (D+T).

Table 7. Average of grain corn yield in different interactions of D and T.

	(D) Depth 0-30 cm.	(D) Depth 30-70 cm.	(D) Depth >70 cm.
(T) Texture Coarse	L ND	M 3.83 t ha^{-1}	H 5.73 t ha^{-1}
(T) Texture Medium	L 0.68 t ha^{-1}	M ND	H 5.86 t ha^{-1}
(T) Texture Fine	L 2.53 t ha^{-1}	M 4.74 t ha^{-1}	H 6.1 t ha^{-1}

ND: No data, **L:** Low, **M:** Medium, **H:** High, **cm:** centimeters

Table 8. Characteristics of the reclassification of D+T.-

CATEGORIES	DESCRIPTION
(D+T) High	• Deep soils > 70 cm. • Any kind of texture
(D+T) Medium	• Medium soils 30-70 cm. • Any texture
(D+T) Low	• Shallow soils < 30 cm. • Any texture

cm: centimeters

As seen in Table 7 and Table 8, the high yield potential of corn is strongly related with the soil depth, regardless their texture.

The Table 9 shows the average of grain corn yield in the interaction of D+T and organic matter content (O), while the Table 10 shows the characteristics of the reclassification (D+T+O).

Table 9. Average of grain corn yield in different interactions of D+T classification and O.

	(D+T) Low	(D+T) Medium	(D+T) High
(O) Low organic matter content	L ND	M 4.77 t ha^{-1}	H 5.9 t ha^{-1}
(O) Medium organic matter content	L ND	M 4.23 t ha^{-1}	H 5.91 t ha^{-1}
(O) High organic matter content	L 1.41 t ha^{-1}	H 5.24 t ha^{-1}	H 6.42 t ha^{-1}

DT: Depth-Texture, **ND:** No data, **L:** Low, **M:** Medium, **H:** High

Table 10. Characteristics of the reclassification of D+T+O.

CATEGORIES	DESCRIPTION
High	• Deep soils > 70 cm. • Any kind of texture • High organic matter content
Medium	• Medium soils 30-70 cm. • Any texture • Low and medium organic matter content
Low	• Shallow soils < 30 cm. • Any texture • Any organic matter content

cm: centimeters

As seen in Table 9 and Table 10, the high yield potential of corn was related with the D+T classification. High yields exist in a different class to "D+T High", only when the organic matter content was high.

The Table 11 shows the average of grain corn yield in the interaction of D+T+O and internal drainage (I), while the Table 12 shows the characteristics of the reclassification (D+T+O+I).

Table 11. Average of grain corn yield in different interactions of D+T+O classification and I.

	(D+T+O) Low	(D+T+O) Medium	(D+T+O) High
Slow Internal Drainage (I)	L ND	H 5.63 t ha^{-1}	H 6.39 t ha^{-1}
Medium Internal Drainage (I)	L ND	M 4.36 t ha^{-1}	H 5.70 t ha^{-1}
Fast Internal Drainage (I)	L 1.41 t ha^{-1}	M 4.45 t ha^{-1}	H 5.75 t ha^{-1}

DTO: Depth-Texture-Organic Matter Content, **ND:** No data, **L:** Low, **M:** Medium, **H:** High

CATEGORIES	DESCRIPTION
High	• Deep soils > 70 cm. • Any kind of texture • High organic matter content • Slow internal Drainage
Medium	• Medium soils 30-70 cm. • Any texture • Low and medium organic matter content • Fast and Medium internal Drainage
Low	• Shallow soils < 30 cm. • Any texture • Any organic matter content • Any internal Drainage

Table 12. Characteristics of the reclassification of D+T+O+I.
cm: centimeters

As seen in Table 11 and Table 12, the high yield potential of corn was related with the D+T+O classification. High yields exist in a different class to "D+T+O High", only when the internal drainage was low.

The Table 13 shows the average of grain corn yield in the interaction of D+T+O+I and land slope (S), while the Table 14 shows the characteristics of the reclassification (D+T+O+I+S).

Table 13. Average of grain corn yield in different interactions of D+T+O+I classification and S.

	(DTOI) Low	(DTOI) Medium	(DTOI) High
(S) 0-8% Slope	L 1.50 t ha^{-1}	M 4.40 t ha^{-1}	H 5.84 t ha^{-1}
(S) 8-15% Slope	L 1.34 t ha^{-1}	M 4.43 t ha^{-1}	H 5.96 t ha^{-1}
(S) > 15% Slope	L 1.33 t ha^{-1}	M 4.36 t ha^{-1}	H 6.21 t ha^{-1}

DTOI: Depth-Texture-Organic Matter Content- Internal Drainage, **ND:** No data, **L:** Low, **M:** Medium, **H:** High

Table 14. Characteristics of the reclassification of D+T+O+I+S.

CATEGORIES	DESCRIPTION
HIGH	• Deep soils > 70 cm. • Any kind of texture • High organic matter content • Slow internal Drainage • Any kind of slope
MEDIUM	• Medium soils 30-70 cm. • Any texture • Low and medium organic matter content • Fast and Medium internal Drainage • Any kind of slope
LOW	• Shallow soils < 30 cm. • Any texture • Any organic matter content • Any internal Drainage • Any kind of slope

cm: centimeters

The Tables 13 and 14 shows that land slope was not determinate on the grain corn yield.

As shows in Figure 3, 5.45 Mha are located in the area of high productivity, with an average of grain corn yield of 6.0 t ha^{-1}; 0.56 Mha located in the area of medium productivity, with an average of grain corn yield of 4.4 t ha^{-1} and 0.24 Mha are located in the area of low productivity, with an average of grain corn yield of 1.4 t ha^{-1}.

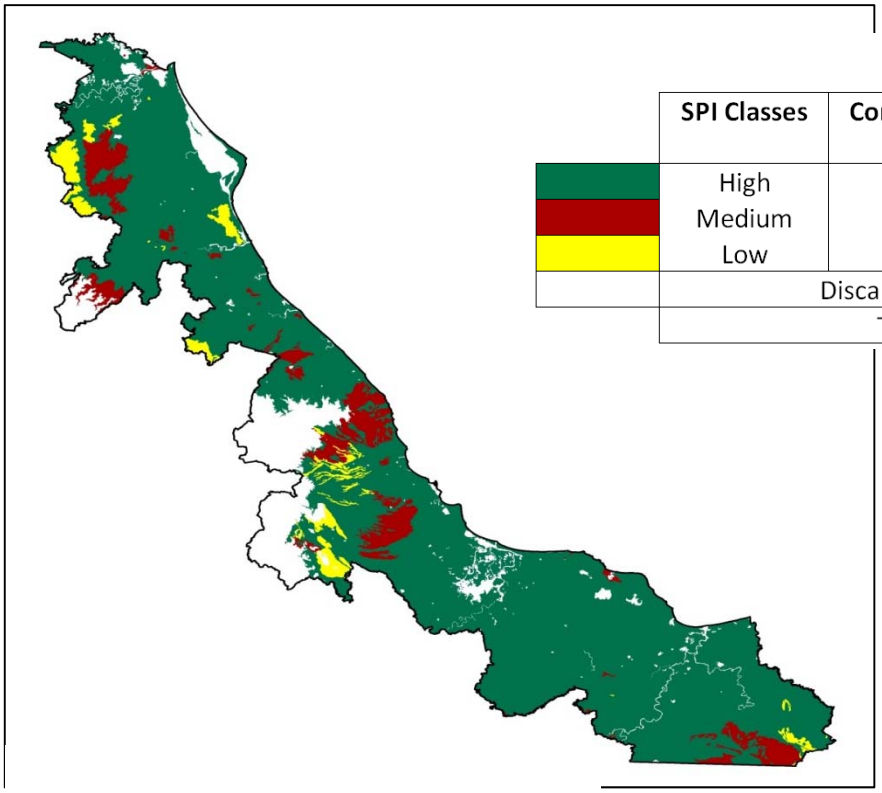

SPI Classes	Corn average corn yield t ha^{-1}	Surface Mha
High	6.0	5.45
Medium	4.4	0.56
Low	1.4	0.24
Discarded area		0.93
Total		7.18

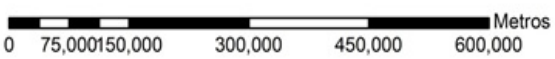

Figure 3. Soil productivity index (SPI) of corn generated using SWAT model

As seen in the Figure 3 most of the State presents a high SPI, so that the constraints on productivity would be related to climatic factors or management. Also the results of productivity presented in this work are consistent with the production statistics reported by the National Ministry of Agriculture.

REFERENCES

Akhavan S., L. Abedi-Koupai, S. F. Mousavi, M. Afyuni, S. S. Eslamianand K. C. Abbaspour. (2010). Applications of SWAT model to investigate nitrate leaching in Hamadan-Bahar Watershed, Iran. Ecosystems and Environment 139: 675-688.

Blum W.E.H. (1993) Soil Protection Concept of the Council of Europe and Integrated Soil Research, in: Eijsackers H.J.P., Hamer T. (Eds.), Integrated Soil and Sediment Research: A basis for Proper Protection, Soil and Environment, Dordrecht: Kluwer Academic Publishers, Vol. 1, pp. 37–47.

DavisM.L.,MastenS.J. (2003) Principlesof Environmental Engineering and Science, McGraw-Hill Professional, ISBN 0072921862, 9780072921861, 704 p.

Du B., A. Saleh, D. B. Jaynes, and J. G. Arnold. (2006). Evaluation of SWAT in Simulating Nitrate Nitrogen and Atrazine Fates in a Watershed with Tiles and Potholes. American Society of Agricultural and Biological Engineers 49: 949-959.

Garg K. K., L. Bharati, A. Gaur, B. George, S. Acharya, K. Jella, and B. Narasimhan. (2011). Spatial mapping of agricultural water productivity using the SWAT model in Upper Bhima Catchment, India. Irrigation and Drainage. Publicado en línea en Wiley On line Library.

Guzman E., J. Bonini, D. Matamoros. (2004). Aplicación del modelo hidrológico SWAT (Soil and Water Assessment Tool) para la predicción de caudales y sedimentos en una cuenca hidrográfica Caso de estudio: Cuenca del Rio Chaguana. Revista Tecnológica 17: 152-161.

Helming K.,Tscherning K.,KönigB.,Sieber S.,Wiggering H.,Kuhlman T., Wascher D., Perez-Soba M., Smeets P., Tabbush P., Dilly O., Hüttl R.F., Bach H. (2008) Ex ante impact assessment of land use change in European regions: the SENSOR approach, in: Helming K.,Pérez-Soba M.,Tabbush P. (Eds.), Sustainability impact assessment of land use changes, Berlin, Springer, pp. 77–105.

Hillel D.(2009) The mission of soil science in a changing world, J. Plant Nutr. Soil Sci. 172, 5–9.

Jones A., Stolbovoy V., Rusco E., Gentile A.-R., Gardi C., Marechal B., Montanarella L., (2009) Climate change in Europe. 2. Impact on soil. A review, Agron. Sustain. Dev. 29, 423–432.

Lal R. (2009) Soils and food sufficiency, A review, Agron. Sustain. Dev. 29, 113–133.

Lal R.(2008) Soilsandsustainable agriculture. Areview, Agron. Sustain. Dev. 28, 57–64.

Lichtfouse E.,Navarrete M.,Debaeke P.,Souchère V.,Alberola C.(2009) Sustainable Agriculture, Springer, 1st ed., 645 p., ISBN: 978-90481-2665-1.

Narasimhan B., R. Srinivasan., J. G. Arnold, and M. Di Luzio. (2005). Estimation of long-term soil moisture using a distributed parameter hydrologic model and verification using remotely sensed data. American Society of Agricultural Engineers 48: 1101-1113.

Neitsch S. L., J. G. Arnold., J. R. Kiniry, and J. R. Williams. (2005). Soil and Water Assessment Tool. Theoretical Documentation. Backland Research Center. Texas, U.S.A. 494p.

Olson, K.R., and G.W. Olson. 1985. A soil-climate index to predict corn yield. Agricultural Systems 18:227– 237.

Olson, K.R., and G.W. Olson. 1986. Use of multiple regression analysis to estimate average corn yields using selected soils and climatic data. Agricultural Systems 20:105–120.

Olson K.R., J.D. Garcia-Paredes., R.N. Majchrzak., C.I. Hadley., M.E. Woolery., R.M. Rejesus. (2000). University of Illinois.College of Agricultural, Consumer and Environmental Sciences. Average Crop, Pasture, and Forestry Productivity Ratings for Illinois Soil. Pp 89.

Saxton K. E., W. J. Rawls, J. S. Romberger, and R. I. Papendick. 1986. Estimating generalized soil-water characteristics from texture. Soil Science Society of America Journal 50: 1031-1036

Scherr S.J. (1999) Soil Degradation. A Threat to Developing-Country Food Security by 2020. Food, Agriculture, and the Environment Discussion Paper 27, International Food Policy Research Institute, Washington, DC 20006-1002, USA.

Sharpley A. N., and J. R. Williams. (1990). EPIC-Erosion/Productivity Impact Calculator. USDA. Agricultural Research Service, Technical Bulletin No. 1768, Washington, D.C. E.U.A. 235p.

Smith P., Martino D., Cai Z., Gwary D., Janzen H., Kumar P., McCarl B., Ogle S., O'Mara F., Rice C., Scholes B., Sirotenko O. (2007) Agriculture, In Climate Change 2007: Mitigation. Contribution of Working Group III to the Fourth Assessment Report of the Intergovernmental PanelonClimateChange, in:MetzB.,Davidson O.R., Bosch P.R., Dave R., Meyer L.A. (Eds.), Cambridge University Press, Cambridge, United Kingdom and New York, NY, USA.

Wiggering H., Dalchow C., Glemnitz M., Helming K., Mueller K., Schultz A., Stachow U., Zander P. (2006) Indicators for multifunctional land use: linking socio-economic requirements with landscape potentials, Ecol. Ind. 6, 238–249.

SWAT Application for Snow Bound Karkheh River Basin of Iran

Hamid R. Solaymani
PhD Scholar, Department of civil Engineering - IIT Delhi -New Delhi - 110016 -India
E-mail: h.solaymani@civil.iitd.ac.in or hrsolaymani@yahoo.com

A.K.Gosain
Professor and Head of Department of civil Engineering -IIT Delhi - New Delhi -110016 -India
(http://www.iitd.ac.in)
E-mail: gosain@civil.iitd.ac.in

Abstract

Main objective of this research is to simulate the snow bound KARKHEH River Basin (KRB) in Iran. The KRB is located in the south west with geographical coordinates between 30° to 35° northern latitude and 46° to 49° eastern longitudes with total area of about 50800 km^2. Most of the precipitation (about 65%) falls during the winter months from December to March and with almost no precipitation during summer season, i.e., June to September. Hydrological features of the KRB are peculiar and heterogeneous because of its diverse topography and natural settings of geology (Piedment fan and valley terrace deposits and metamorphic rocks e.g. karst), climate and ecology. Generally, the basin is characterized by a Mediterranean climate having cool and wet winters and hot and dry summers.

SWAT model has been used for simulation of KRB. The SWAT model has been set up using the data on terrain (90 meter resolution DEM), landuse (derived using 50 meter resolution ETM+ 2002 image), soil type (FAO) and local meteorological conditions (Iran Meteorological Organization). Two approaches have been used for calibration; i) the manual and ii) the auto-calibration. The One – factor- At – a- Time (OAT) sampling has been used for manual calibration. The Sequential Uncertainty Fitting (SUFI-2) algorithm in the SWAT-CUP program was used for parameter optimization. The evaluation of calibration has been done using Graphical Procedure, Nash–Sutcliffe Efficiency (NSE), Percent Bias (PBIAS), and Ratio of Root Mean Square Error (RMSE) - observations standard deviation (RSR).

KEY WORDS: SWAT Model; Snowbound; Auto Calibration; Sensitivity Analysis; Karkheh River Basin

Introduction

Hydrological modelling has great potential for advancement of the hydrologic science. Watershed models are essential for studying hydrologic processes and their responses to both natural and anthropogenic factors, but due to model limitations in the representation of complex natural processes and conditions, models usually must be calibrated prior to application to closely match reality (Bastidas et al., 2002). Stream-flow, which is known as integrated process of atmospheric and topographic processes, is of prime importance to water resources planning (Kahya and Dracup, 1993). An ideal hydrologic data set calibration should include combined climatic conditions of dry, average, and wet years. In practice, however, hydrologic models are calibrated based on average climate conditions, or the best available data (Van Liew and Garbrecht, 2003).

This becomes an essential task for heterogenous basins that are more susceptible to flooding (peak flows) and base flows; hence, subsequent water resources planning and management on such basin becomes a challenging task. Validation of the calibrated model is typically done by comparing simulated with measured stream-flow values. In addition to total stream-flow, the validation of several hydrologic components, especially surface and groundwater flow and their responses to climatic conditions, is also needed in the development of distributed hydrologic models, but such comparisons are not very common (Beven, 1995; Arnold and Allen, 1996; Chu and Shirmohammadi, 2004; White and Chaubey, 2005).

Differences between simulated and measured data often occur, especially during extreme years or seasons (Singh et al., 2005; Rosenthal et al., 1995; Srinivasan et al., 1998; Mapfumo et al., 2004; Chu and Shirmohammadi, 2004; Govender and Everson, 2005). Singh et al. (2005) found that two commonly used hydrologic models overestimated stream flow during drought years by about 39–49%, and underestimated flow during the wettest year by 14–7.2%. Kalin and Hantush (2006) report accurate surface runoff and stream flow results for the 120 km^2 Pocono Creek watershed in eastern Pennsylvania; their base flow estimates were weaker, but they state those estimates were not a performance criteria. Base flow and other flow components estimated with SWAT by Srivastava et al. (2006) for the 47.6 km^2 West Branch Brandywine Creek watershed in southwest Pennsylvania were found to be generally poor. Peterson and Hamlett (1998) also found that SWAT was not able to simulate base flows for the 39.4 km^2 Ariel Creek watershed in northeast Pennsylvania, due to the presence of soil fragipans. Chu and Shirmohammadi (2004) found that SWAT was unable to simulate an extremely wet year for a 3.46 km^2 watershed in Maryland. After removing the wet year, the surface runoff, base flow, and stream flow results were within acceptable accuracy on a monthly basis. Subsurface flow results also improved when the base flow was corrected.

Despite all the above mentioned discrepancies SWAT still remains one of the most popular and used model worldwide. The Soil and Water Assessment Tool (SWAT) is a process-based continuous hydrological model and the main components of the model include: climate, hydrology, erosion, soil temperature, plant growth, nutrients, pesticides, land management, channel and reservoir routing. The version ArcSWAT2009 working with the ArcGIS9.3 interface was selected for this research. The model divides the watershed into multiple sub-basins, which are then further sub-divided into hydrological response units (HRUs) which consist of homogeneous land use, management and soil characteristics. SWAT divides rainfall into different components which include evaporation, surface runoff, infiltration, plant uptake, lateral flow and groundwater recharge. Surface runoff from daily rainfall is estimated with a

modification of the SCS curve number method from the United States Department of Agriculture Soil Conservation Service (USDA SCS) and peak runoff rates using a modified rational method (Neitsch et al., 2005). The model estimates plant growth under optimal conditions, and then computes the actual growth under stresses inferred by water and nutrient deficiency.

MATERIAL AND METHODS

Study Area

The efficacy of calibration and validation process is dependent on the effectiveness of the characterization of the watershed characteristics through the hydrological model. In order to evaluate the general performances of different calibration methods, SWAT was applied to KARKHEH river basin (KRB). The KRB is located in the western part of Iran. The drainage area of the basin is about 50,764 km2, out of which 80% falls in the Zagros mountain ranges. The topography depicts large spatial variation with elevations ranging from 3 to more than 3,000 masl. The elevation of about 60% of the basin area is 1,000-2,000 masl and about 20% is below 1,000 masl (Ashrafi et al. 2004). The population living in the basin is about 4 million (in 2002), and about one third resides in the rural areas (JAMAB 1999; Ashrafi et al. 2004). Hydrological features of the KRB are complex and heterogeneous because of its diverse topography, and natural settings of geology, climate and ecology. The precipitation (P) pattern depicts large spatial and intra-and inter-annual variability across the basin. The mean annual precipitation ranges from 150 mm/yr. in the lower arid plains to 750 mm/yr. in the mountainous parts (JAMAB 1999). According to this variability KRB can be divided to three main sub-basins; Upper Karkheh, Middle Karkheh and Lower Karkheh. On average, the middle part receives higher P than the upper and lower parts as illustrated by the records of Kermanshah (450 mm/yr.), Khorramabad (510 mm/yr.) and Ahwaz (230 mm/yr.) synoptic stations. Most of the precipitation (about 65%) falls during the winter months from December to March and almost no P during summer season, i.e., June to September. In the mountainous parts during winter, due to temperatures often falling below 0°C, the winter P falls as snow and rain. The temperature shows large intra-annual variability, with January being the coolest and July the hottest month. The potential evapotranspiration (ET_p) largely follows a similar pattern as the temperature (T) with the highest in the southern arid plains and the lowest at the mountainous semi-arid region. There is a large gap between ET_P and P in most of the months, which widens as we move from upper northern semi-arid regions to the lower southern arid parts of the basin. The hydrological analysis and assessment of water resources in such semi-arid to arid regions with high climatic variability is a challenging task compared to humid areas where P exceeds the ET_P in most of the months (Sutcliffe 2004).

The water resources of the KRB comprise from both surface water and groundwater. The volume of water generated by the average annual rainfall in the basin is 24.9bm^3, of which 5.1 bm^3 is surface water, 3.4bm^3 infiltrates to ground and the remaining 16.4 bm^3 is lost directly to the atmosphere. The quality of river water is generally good, though it varies both seasonally and along the path downstream, reaching up to 3dsm^{-1} (decisiemens per meter) near the final outlet. The Karkheh basin comprises five major sub-basins, i.e. the Gamasiab, Qarasu, Seymareh, Kashkan and south-Karkheh as shown in Figure 1. Basic characteristics of these five sub-basins are given in Table (1).

Table 1- Basic characteristics of five sub-basins of the KRB (JAMAB Consulting Co. 2006)

Sub-basins	Total area (km^2)	Average annual rainfall (mm)	Mean annual Discharge (MCM/y)	Irrigated Area (km^2)
Gamasiab	11500	465	1080	1360
Qarasu	5350	435	722	276
Kashkan	8960	390	1639	543
Seymareh	16400	350	5827	490
south-Karkheh	8590	260	5153	1110

Groundwater exists in hard rock aquifers (often karst) and alluvial aquifers, both unconfined and confined conditions are present. The aquifers have large variations in area and thickness, which have largely been attributed to the tectonic factor, lithology, climate conditions and topography (e.g. JAMAB 1999; Tizro et al. 2007). Generally, subsurface water storage in porous aquifers in the northern mountainous regions of the basin is limited to valley floors characterised by relatively large depths, high infiltration and good water quality. In the southern arid plains, while the area for porous groundwater bodies increases, the thickness and infiltration decrease and the groundwater degrades. The KRB remained largely unregulated without any large storage dam during the twentieth century. However, the first large multipurpose dam, the Karkheh dam, was completed and commissioned in 2001.

Snow Role

In mountainous sub-basin of KRB, snow melt is the main surface water resource in spring and early summer period. The snowmelt also recharges groundwater aquifers and later contributes to the summer runoff flowing in the rivers. Most of precipitation in this region occurs in the cold season and a good portion is in the form of snow. Saghafian and Davtalab (2007) has shown that the snow water equivalent (SWE) for the mountainous parts of the KRB is about 75 mm/yr., which is about 17% of the long-term annual precipitation in the basin. The amount and distribution of snow are strongly influenced by elevation, varying from 44 mm/yr. for elevations less than 1,500 masl to 245 mm/yr. with elevation more than 3,500 masl. Other specific findings by them were; the widespread snowfall occurs over December to March period in the in mountainous sub-basin of KRB. Moreover, the correlation coefficient between the average annual/monthly SCs (snow coefficient that is equal to ratio of accumulated SWE to the total precipitation) and the elevation is not particularly strong.

Data

The Shuttle Radar Topography Mission (SRTM) Digital Elevation Model (DEM) of 90 m resolution was used for sub-basin definition. A threshold of 500 km^2 was used for the delineation of sub-basins. This threshold was interactively divide study area into a reasonable number of (49 in the present case) sub-basins (Figure 1).

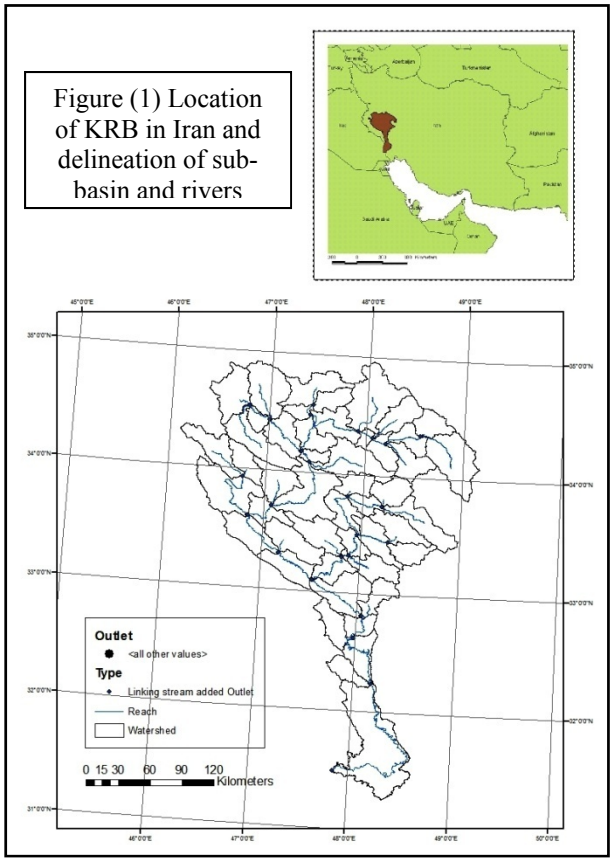

Figure (1) Location of KRB in Iran and delineation of sub-basin and rivers

The hydrological response units (HRUs) were defined based on information on landuse, soil and slope. The land use/land cover map was prepared using fine resolution Landsat ETM+ image 2002 (Mirghasemi et al, 2006). It distinguishes land use/land cover classes, with rain-fed farming (33%), forest (23%), rangelands (18%), and bare lands (15%) constituting about 90% of the study area. The soil map was obtained from the global soil map of the Food and Agriculture Organization of the United Nations (FAO,1995), which provides data for 5000 soil types comprising two layers (0–30 cm and 30–100 cm depth) at a spatial resolution of 10 km. The five categories of slope were defined to be used in the HRU definition, i.e., a) 0-5%; b)5-10%;c)10-20%;d) 20-30% and e) > 30%. Finally, the HRUs were defined using the land use, soil and slope information. A threshold value of 5% for land use, soil and slope was used in the HRU definition. A threshold value of 5 to 10% is commonly used in HRU definitions to avoid small HRUs, reduce total number of HRUs and improve the computational efficiency of the model (Starks and Moriasi 2009). Daily climatic data for the period from January 1982 to December 2005 were used for the model simulations. Precipitation and temperature data from 13 synoptic stations data were available. The missing data were regenerated by using data of other stations based on a regression analysis.

Sensitivity Analysis

Sensitivity analysis refers to the identification of some parameters that have important effects in the model. It is the prior step to model calibration. It demonstrates the impact that change to an individual input parameter has on the model response and can be performed using a number of different methods. The method in the Arc-SWAT Interface combines the Latin Hypercube (LH) and One-factor-At-a-Time (OAT) sampling. The sensitivity analysis tool in Arc-SWAT has the capability of performing two types of analyses. The first type of analysis uses only modelled data to identify the impact of adjusting a parameter value on some measure of simulated output, such as average streamflow. The second type of analysis uses measured data to provide overall "goodness of fit" estimation between the modelled and the measured time series. The first analysis may help to identify parameters that improve a particular process or characteristic of the model, while the second analysis identifies the parameters that are affected by the characteristics

of the study watershed and those to which the given project is most sensitive (Veith and Ghebremichael, 2009). The description of parameters used for sensitivity analysis and their relative sensitivity after the analysis is presented in Table (2). In this research, sensitivity analysis had done based on both the approaches; with and without observed data. The parameters were ranked based on their sensitivities. For example; curve number for wetting condition II (CN2) ranked first in both approaches; it means CN2 is most responsive in comparison to other parameters.

Table 2 – SWAT Sensitivity analysis results for KRB

No	Parameter	Description	Initial value	Rank No. *	Rank No. **
1	ALPHA_BF	Baseflow alpha factor (Days)	0-50	2	4
2	CANMX	Maximum canopy storage (mmH_2O)	0-10	10	16
3	CH_K2	Channel Effective Hydraulic Conductivity	0-150	4	15
4	CH_N2	Manning Coefficient for Channel	0.01-0.3	6	5
5	CN2	Initial SCS Runoff Curve number for Wetting Condition-2	±20%	1	1
6	EPCO	Plant uptake compensation factor	0-1	14	20
7	ESCO	Soil Evaporation Compensation Factor	0-1	3	3
8	GW_DELAY	Ground Water Delay Time	0-50	11	10
9	GW_REVAP	Ground Water "REVAP" Coefficient	0.02-0.2	15	19
10	GWQMN	Threshold Depth for shallow aquifer for flow	0-5000	13	2
11	RCHRG_DP	Deep Aquifer Percolation Factor	0-1	7	12
12	REVAPMN	Threshold Depth of water in shallow aquifer for "REVAP"	0-500	16	18
13	SFTMP	Snowfall temperature (°C)	-5-5	20	6
14	SLOPE	Slope steepness (m/m)	0-0.6	9	13
15	SMFMN	Melt factor for snow December 21 (MM H_2O/°C-day)	0-10	20	8
16	SMFMX	Melt factor for snow June 21 (mm H_2O/°C-day)	0-10	20	11
17	SMTMP	Snow melt base (°C)	-5-5	8	7
18	SOL _AWC	Soil Available Water Capacity	0.01-0.5	20	14
19	SURLAG	Surface Runoff Lag Time	0-10	5	5
20	TIMP	Snow pack lag temperature lag factor	0-1	12	9

*without observed data - **with observed data

Model Calibration and Validation

Calibration involve in tuning of model parameters based on checking model results against observations to ensure same response over time. This involves comparing the model results, generated with the use of historic meteorological data, to recorded stream flows. In this process, model parameters are varied until recorded flow patterns are accurately simulated. For this study,

two approaches have been used for calibration; i) the manual and ii) the auto-calibration. The One–factor-At–a-Time (OAT) sampling has been used for manual calibration. The Sequential Uncertainty Fitting (SUFI-2) algorithm in the SWAT-CUP program was used for parameter optimization. The evaluation of calibration has been done using Graphical Procedure, Nash–Sutcliffe Efficiency (NSE), Percent Bias (PBIAS) and Root Mean Square Error (RMSE)-observations standard deviation ratio (RSR).

NSE indicates how well the plot of observed versus simulated data fits the 1:1 line. NSE ranges between -∞ to 1 and NSE=1being to optimal value. According to Moriasi et al (2007); NSE values between 0.0 and 1.0 are generally viewed as acceptable levels of performance whereas values lower than 0.0 indicate that the mean observed value is a better predictor than the simulated value which indicates unacceptable performance. NSE is computed as shown in equation (1):

$$NSE = 1 - \left[\frac{\sum_{i=1}^{n} (Q_i^{obs} - Q_i^{sim})^2}{\sum_{i=1}^{n} (Q_i^{obs} - Q_i^{mean})^2} \right] \qquad (1)$$

Where Q_i^{obs} is the i^{th} observation for the constituent being evaluated, Q_i^{sim} is the i^{th} simulated value for the constituent being evaluated, Q_i^{mean} is the mean of observed data for the constituent being evaluated, and n is the total number of observations.

PBIAS measures the average tendency of the simulated data to be larger or smaller than their observed values (Moriasi et al 2007). Positive values indicate model underestimation bias, and negative values indicate overestimation bias (Gupta et al 1999), the optimal value of PBIAS being zero. PBIAS is computed as shown in equation (2):

$$PBIAS = \left[\frac{\sum_{i=1}^{n} (Q_i^{obs} - Q_i^{sim}) * 100}{\sum_{i=1}^{n} (Q_i^{obs})} \right] \qquad (2)$$

PBIAS values lower than 25% using SWAT are considered satisfactory, less than 10% are very good and between 10-15% are good. RMSE is a commonly used error statistic with model performance deceasing with increasing RMSE values. According to Singh et al (2005), RSR values can be considered low when they are less than half the standard deviation of the observed data. RSR is computed as shown in equation (3):

$$RSR = \frac{RMSE}{STDEV^{obs}} = \frac{\left[\sqrt{\sum_{i=1}^{n} (Q_i^{obs} - Q_i^{sim})^2} \right]}{\left[\sqrt{\sum_{i=1}^{n} (Q_i^{obs} - Q_i^{avg})^2} \right]} \qquad (3)$$

In RSR equation, 'n' is the number of years, months or days according the kind of time series. The study period was divided into a calibration period from 1994 to 1996 and a validation period from 1997 to 1999. A warm-up period of three years (1991 to 1993), were used to initialize the model for calibration period.

RESULTS AND DISCUSSION

Model Evaluation

General model evaluation guidelines, for a daily time step, were developed based on performance ratings for the recommended statistics and on project-specific considerations. As stated previously, graphical techniques provide visual model evaluation overviews and should be the first step in model evaluation. A general visual agreement between observed and simulated constituent data indicates adequate calibration and validation over the range of the constituent being simulated (Singh et al., 2004). As shown in Figure (2) simulated and observed hydrograph is demonstrated from 1994 to 1999. Based on magnifying portion in the graph, too little base flow, too high surface runoff and high fluctuated condition in simulated hydrograph has been found.

Figure 2 - Observed and simulated flow before calibration in Pay-e-pol flow gauge station (1994 to 1999)

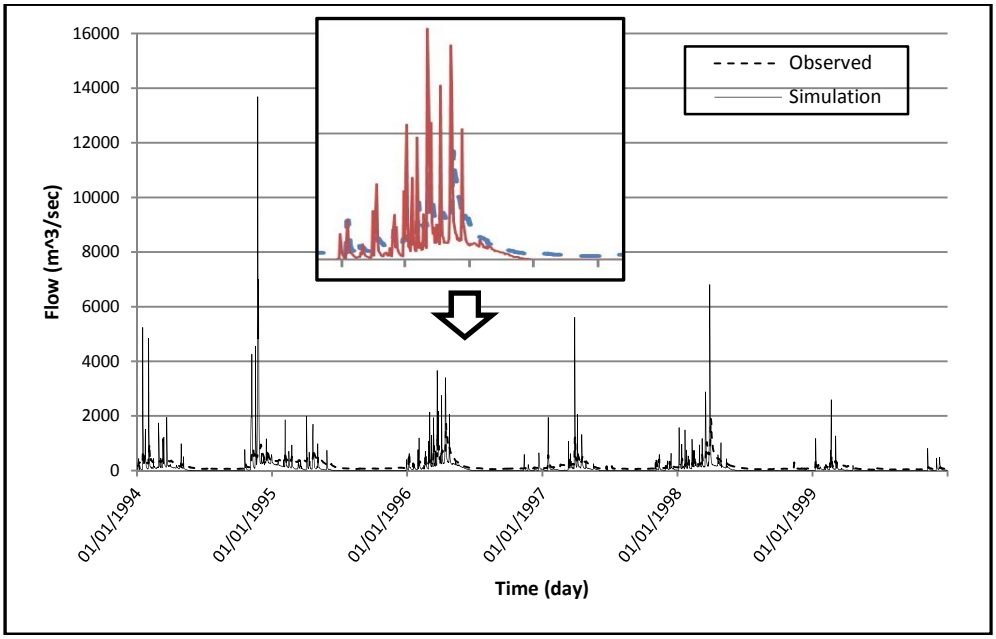

Based on parameters that had been shown in Table (2), the flow discharge has been simulated. As mentioned earlier, two approaches have been used for calibration; i) the manual and ii) the auto-calibration. The One – factor- At – a- Time (OAT) sampling has been used for manual calibration. The Sequential Uncertainty Fitting (SUFI-2) algorithm in the SWAT-CUP program was used for parameter optimization. The Figure (3) show the comparison between manual calibration and auto-calibration approaches in Pay-e-pol hydrometric flow gauge located at the outlet of KARKHEH dam.

Figure 3 - Comparing the Observed and calibrated simulated flow (Auto-calibration and manual calibration) in Pay-e-pol flow gauge station (1994 to 1996)

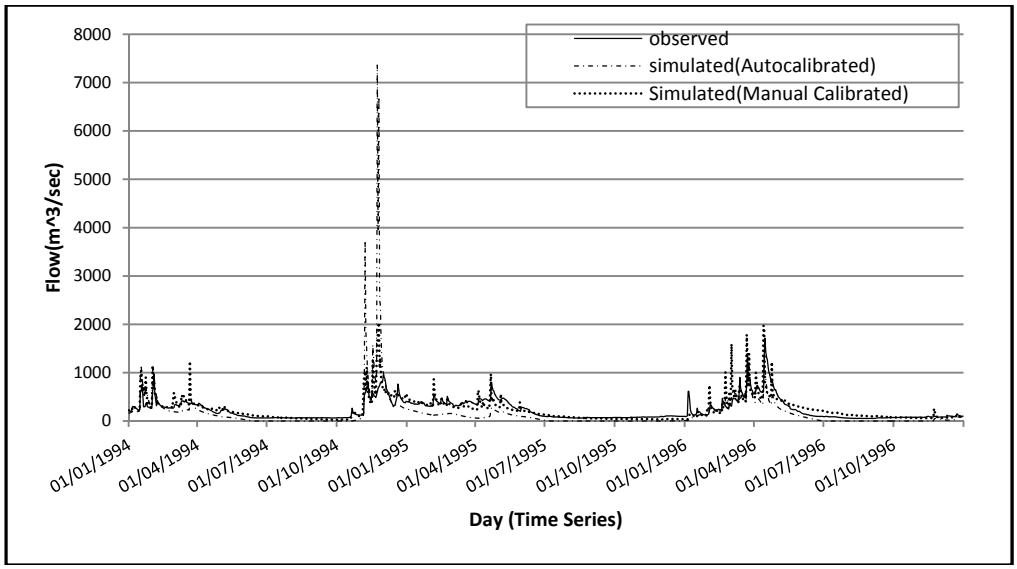

Graphical comparison based on two approaches indicates that manual calibration method result in better simulation under extreme conditions as well as for average values. In figure (4) the calibration and validation series using manual approach is shown.

Figure 4 - Observed and simulated flow after manual calibration in Pay-e-pol flow gauge station (Calibrated 1994 to 1996 and validated 1996 to 1999)

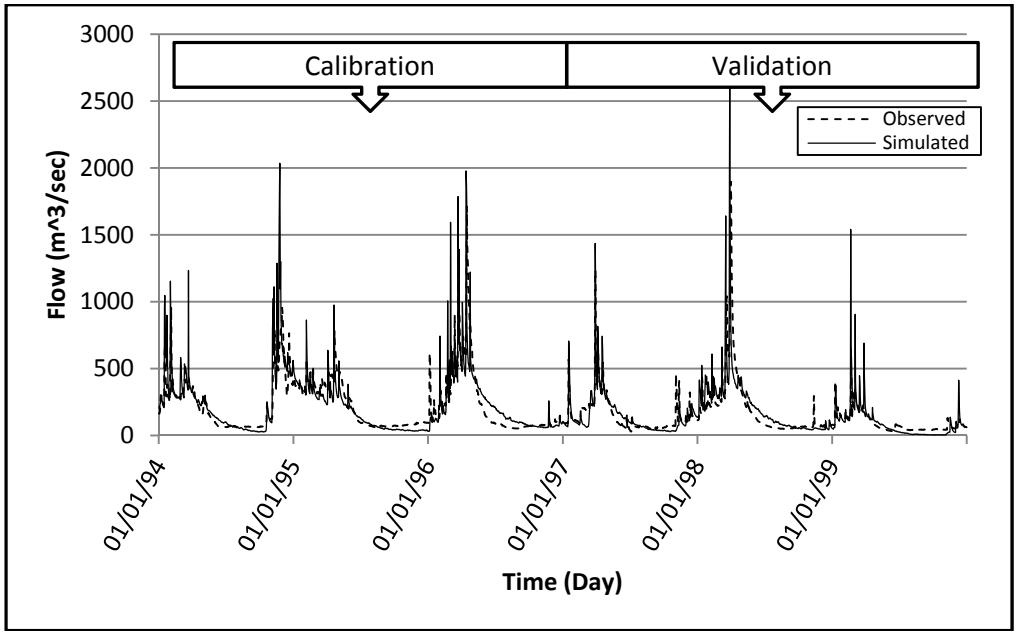

The next step was to calculate values for NSE, PBIAS, and RMSE. With these values, model performance can be judged based on general performance ratings (Table 3). Model performance can be evaluated as "satisfactory" with NSE > 0.50 and RSR < 0.70 and, for measured data of typical uncertainty, if PBIAS ± 25% for stream-flow. These ratings should be adjusted to be more or less strict based on project-specific considerations discussed in further. Additional consideration that the performance ratings presented in Table (3) for RSR and NSE statistics are

for a monthly time step; therefore, they need to be modified appropriately. Generally, as the evaluation time step increases, a stricter performance rating is warranted.

Table 3 - General performance ratings for recommended statistical parameters for a monthly time step (Moriasi, et Al, 2007)

Performance Rating	NSE	PBIAS	RSR
Very good	0.75<NSE<1.00	PBIAS<±10	0.00<RSR<0.50
Good	0.65<NSE<0.75	±10<PBIAS<±15	0.50<RSR<0.60
Satisfactory	0.60<NSE<0.65	±15<PBIAS<±25	0.60<RSR<0.70
Unsatisfactory	NSE≤0.50	PBIAS≥±25	RSR≥0.70

The goodness of fit achieved for the basin for both approaches; auto-calibration and manual calibration have been shown in Table (4).

According to the results of Table (4), the manual calibration has outperformed the automatic calibration procedure, e.g. NSE values equal 0.71 for manual calibration approach for calibration time series (1994 to 1996) is a much better than the auto-calibration for same time series. In comparing the PBIAS and RSR parameters also the trend is similar.

Table 4 - Outputs for statistical parameters with manual calibration and auto-calibration at Pay-e-pol flow gauge station (Daily-Base data)

Approach	NSE		PBIAS		RSR	
	Calibration	Validation	Calibration	Validation	Calibration	Validation
Manual Calibration	**0.71** (Good)	**0.60** (Satisfactory)	**-0.24** (Very good)	**0.96** (Very good)	**0.6** (Good)	**0.25** (Very good)
Auto-calibration	**0.31** (Unsatisfactory)	**0.32** (Unsatisfactory)	**30.7** (Unsatisfactory)	**0.50** (Very good)	**0.71** (Unsatisfactory)	**0.78** (Unsatisfactory)

In situations with conflicting performance ratings, for different criteria, performance on the conservative side should be attributed. For example, if simulation for one output variable in one watershed produces performance ratings of “very good” for PBIAS, “good” for NSE, and “satisfactory” for RSR, then the overall performance should be described conservatively as “satisfactory” for that one watershed. In the present case, the values of NSE, PBIAS and RSR for manual calibration approach respectively are 0.71(Good), -0.24(Very good) and 0.6(Good). Therefore, the overall result for “Manual calibration” for the watershed should be designated as “Good” and in the same manner for validation period is “Satisfactory”. Similar interpretation can be arrived at from the Table (4) for Auto- calibration results. Since majority of performance ratings are termed “Unsatisfactory” under calibration and validation periods, therefore, the overall results for the Automatic calibration is termed as “Unsatisfactory”.

Also it should be noted that the time step which was used for the performance analysis was daily. It was also decided to check the impact of the choice of interval on the performance of the model. Thus, performance was computed again by taking the interval as monthly and the results are shown in Table (5).

Table 5 - Outputs for statistical parameters with manual calibration and auto-calibration at Pay-e-pol flow gauge station (Using monthly data)

Approach	NSE		PBIAS		RSR	
	Calibration	Validation	Calibration	Validation	Calibration	Validation
Manual Calibration	**0.91** (Very good)	**0.85** (Very good)	**-0.001** (Very good)	**0.07** (Very good)	**0.31** (Very good)	**0.39** (Very good)
Auto-calibration	**0.31** (Unsatisfactory)	**0.32** (Unsatisfactory)	**0.002** Very good)	**0.77** (Very good)	**1.14** (Unsatisfactory)	**0.63** (Satisfactory)

It may be observed from Table 5 that overall the performance with respect to all the parameters have improved by taking the monthly interval. The overall performance under the "Manual calibration" for both calibration and validation period has improved to "Very good". The results under the "Auto-calibration" approach has also improved in comparison to the daily interval for some of the individual statistical parameters, for both calibration and validation time steps. However, the overall performance under "Auto-calibration" does not improve and remain "Unsatisfactory" to be on the conservative side.

Conclusions

The SWAT model has been used on the KRB basin which has heterogeneous climatic conditions.
The model has been calibrated and validated using manual and auto-calibration procedure It has been seen that the manual calibration procedure performs much better than the auto-calibration procedure. The performance further enhances if the calibration is done using the monthly interval rather than the daily interval.

References

Arnold, J.G., Allen, P.M., 1996. Estimating hydrologic budgets for three Illinois watersheds, Journal of Hydrology (Amsterdam) 176, 57–77.

Ashrafi, S.; Qureshi, A.S.; Gichuki, F. 2004. Karkheh Basin profile: Strategic research for enhancing agricultural water productivity. Draft Report. Challenge Program on Water and Food.

Bastidas, L.A., Gupta, H.V., Sorooshian, S., 2002. Emerging paradigms in the calibration of hydrologic models, In: Singh, V.J., Frevert, D. (Eds.), Mathematical Models of Large Watershed Hydrology, vol. 1. Water Resources Publications, LLC, Englewood, CO, pp. 25–56.

Beven, K.J., 1995. Linking parameters across scales: sub-grid parameterisations and scale dependent hydrological models. Hydrological Processes 9, 507–526.

Chu, T.W., Shirmohammadi, A., 2004. Evaluation of the SWAT models hydrology component in the Piedmont physiographic region of Maryland, Transactions of the ASAE 47, 1057– 1073.

Gupta, H. V., Sorooshian, S. and Yapo, P. O., 1999, Status of auotomatic calibration for hydrologic models; Comparison with multilevel expert calibration, J. Hydrologic Eng. 4(2): 135-143.

JAMAB. 1999. Comprehensive Assessment of National Water Resources: KARKHEH River Basin. JAMAB Consulting Engineers in association with Ministry of Energy, Iran. (In Persian)

JAMAB Consulting Engineers. 2006b. Water balance report of Karkheh River Basin area: Preliminary analysis. Tehran, Iran. (In Persian)

Kahya, E. and J.A. Dracup, 1993, US stream-flow patterns in relation to the El Nino/southern oscillation, Water Resources Research 28(8), pp.2491-2503.

Kalin, L., and M. H. Hantush. 2006. Hydrologic modeling of an eastern Pennsylvania watershed with NEXRAD and rain gauge data. J. Hydrol. Eng. 11(6): 555-569.

Mapfumo, E., Chanasyk, D.S., Willms, W.D., 2004. Simulating daily soil water under foothills fescue grazing with the Soil and Water Assessment Tool model (Alberta, Canada). Hydrological Processes 18 (15), 2787–2800.

Mirqasemi, S.A.; Pauw, E. De. 2007. Land use change detection in the Karkheh Basin, Iran by using multi-temporal satellite images. In: Extended abstracts. International Workshop on Improving Water Productivity and Livelihood Resilience in Karkheh River Basin, ed. Ghafouri, M. Soil Conservation and Watershed Management Research Institutes (SCWNRI), Tehran, Iran. September 10-11, 2007.

Moriasis, D.N., Arnold, J. G., Van Liew, M. W., Bingner, R.L., Harmel, R. D. and Veith, T. L. 2007. Model evaluation guidelines for systematic quantification of accuracy in watershed simulation, Transactions of the ASABE. Vol. 50(3): 885-900.

Peterson, J. R., and J. M. Hamlet. 1998. Hydrologic calibration of the SWAT model in a watershed containing fragipan soils. J. American Water Resour. Assoc. 34(3): 531-544.

Rosenthal, W.D., Srinivasan, R., Arnold, J.G., 1995. Alternative river management using a linked GIS-hydrology model, Transactions of the ASAE 38, 783–790.

Saghafian, B.; Davtalab, R. 2007. Mapping snow characteristics based on snow observation probability. International Journal of Climatology 27: 1277- 1286.

Singh, J., Knapp, H.V., Arnold, J.G., Demissie, M., 2004. Hydrological modeling of the Iroquois River Watershed using HSPF and SWAT, Journal of the American Water Resources Association 41, 343–360.

Srinivasan, R., Arnold, J.G., Jones, C.A., 1998. Hydrologic modeling of the United States with the soil and water assessment tool, International Journal of Water Resources Development 14, 315– 325.

Starks, P.J.; Moriasi, D.N. 2009. Spatial resolution effect of precipitation data on SWAT calibration and performance: Implications for CEAP. Transactions of the ASABE 52(4): 1171-1180.

Sutcliffe, J.V. 2004. Hydrology: A question of balance. IAHS special publication 7. Wallingford, UK: IAHS Press.

Tizro AT, Voudouris KS, Eini M (2007) Groundwater balance, safe yield and recharge feasibility in a semi-arid environment: a case study from western part of Iran. J Appl Sci 20:2967–2976.

Van Liew, M.W., Garbrecht, J., 2003. Hydrologic Simulation of the Little Washita River Experimental Watershed Using SWAT, Journal of the American Water Resources Association 39, 413–426.

Veith, T.L. and L.T. Ghebremichael. 2009. How to: applying and interpreting the SWAT Auto-calibration tools. In: Fifth International SWAT Conference Proceedings. August 5-7, 2009

White, K.L., Chaubey, I., 2005. Sensitivity analysis calibration and validations for multi-site and multivariable SWAT model, Journal of the American Water Resources Association 41, 1077–1089.

Quantification of Urbanization Effect on Water Quality Using Swat Model in Midwest US

Shashank Singh
Department of Agricultural Engineering, Marathwada Institute of Technology, India

Chetan Maringanti
Department of Agricultural and Biological Engineering, Purdue University, US

Abstract

Land use change from non-urban to urban land has social and economic benefits but can alter hydrologic processes significantly. Urban land cover provides more impervious surface causing higher hortonian runoff and less infiltration capacity affecting stream and river system. The objective of this study was to assess how increase in urban area (1560 km^2) and crop area affect runoff and water quality in Upper White river watershed (7043 km^2) in central Indiana. Of concern specifically is the potential impact of future developments in the watershed on the increase in stream flow and degradation of water quality. Anticipated increase in imperviousness, on the other hand, is expected to elevate flood risk and the associated environmental damage. The change in land use also has an effect on the hydrologic processes such as soil moisture, surface runoff and evapotranspiration. The study was divided into two components and various estimates were modeled using a distributed watershed level simulation model Soil and Water Assessment Tool (SWAT). Firstly, the impact of land use change (increased imperviousness) on surface runoff in the watershed was analyzed. Secondly, the impact of land use change (increased urban area and crop area) on surface runoff in the watershed was analyzed. The first objective was achieved by changing the curve number (CN) uniformly in the watershed. To accomplish the second objective, land use was reclassified with increase in urban area and crop area by forest land. The result showed a significant change in surface runoff due to change in imperviousness in watershed and also with increase in urban and crop area in watershed.

Keywords: Watershed modeling, Urbanization, Land use, Water quality, stream flow, sediment, SWAT

Introduction

Land use and land cover (LULC) change has been recognized as a critical factor in changing the environment and the climate. Land use denotes the human employment of the land whereas land cover implies conversion and modification (Meyer and Turner, 1994). Land use change drives land cover change and directly impacts the physical environment. Urbanization, which typically replaces a permeable vegetated land surface with impervious surface areas, significantly changes the hydrologic cycle of a drainage basin. Such changes affect surface water, groundwater and evapotranspirated water in the watershed. In agricultural fields land use changes are commonly

associated with tillage practice, crop sown, fertilizer application, irrigation, drainage, live stock pasturing etc. There can be social, economical or political factors that can lead to LULC change.

The land cover has changed as more land declared under conservation reserve program (CRP) protection is been utilized for corn production and also land use is changing with monoculture cropping of corn. Approximately, 4.6 million acres of land under existing CRP program will return to production by 2010 (USDA, 2007). The impact of change in land use/cover can be directly on water quality and indirectly upon climate (Meyer and Turner, 1994). Over the past 25 years, the population of the United States has grown over 30% which has lead to substantial increase in urbanized areas and results in a degradation and loss of forested and agricultural lands (USDC Census Bureau, 2005). Hydrologically, urbanization is accompanied by increased imperviousness in the landscape. Increase in imperviousness reduces soil permeability which in turn reduces infiltration rate, and increases surface runoff. When increased surface runoff is combined with the effect of reduced surface roughness, it results in more frequent and more intense local flood events.

Under this situation there is need to quantify the impact of land use / cover change in long term on surface runoff, water quality and climate factor like evapotranspiration associated with land use pattern changes. The objective of this research was to study the impact of land use change on stream flow, water quality and evapotranspiration. The specific tasks that were performed to address the issues were:

To quantify the change in imperviousness in watershed on stream flow
To quantify the change in urbanization and agricultural crop area on stream flow

Site description

The Upper White River (UWR) watershed, located in central Indiana, encompasses an area of 7043 km2 and includes Indianapolis. It extends across sixteen counties including significant portions of Hancock, Marion, Hendricks, Johnson, Hamilton, Morgan, Boone, Tipton, Madison, Henry, Delaware, and Randolph Counties. The UWR watershed is highly urbanized (22%) with a major area contributed by Indianapolis city (Figure 1). Bulk of the water demands in the urbanized areas of the watershed is supplied by four main reservoirs. Hamilton County is home for Morse Reservoir on White River and Geist Reservoir on Fall Creek; Eagle Creek Reservoir on Eagle Creek and Prairie reservoir area located in Marion and Delaware Counties respectively. Crops and Pasture are the predominant land use in the watershed. There are about 456 impaired streams covering total length of 177 km (Figure 1). About 61% of the streams in the watershed are impaired streams (303 (d) list, IDEM).

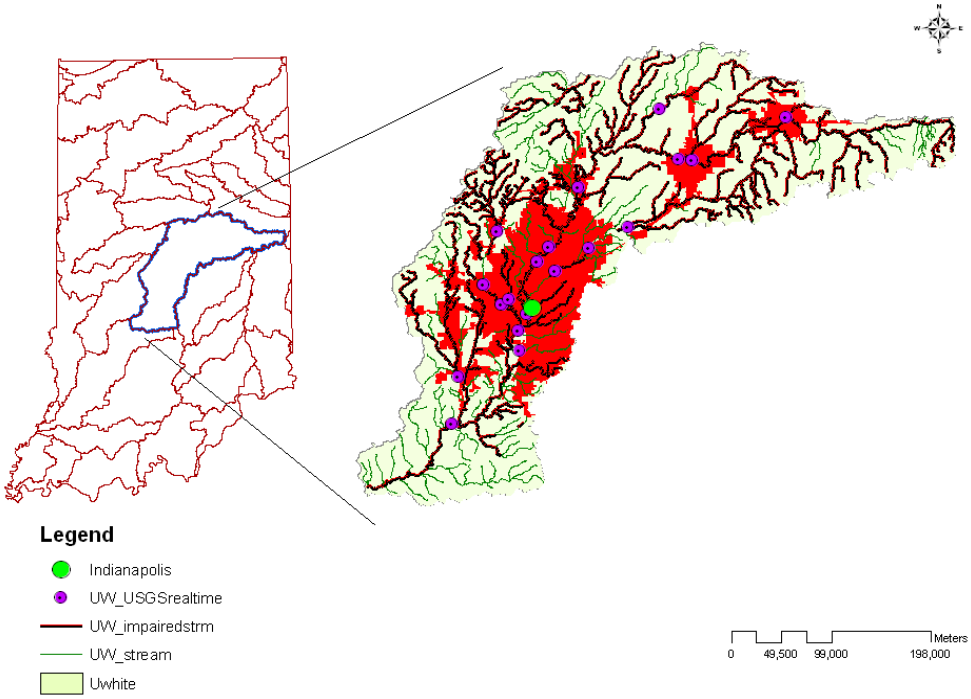

Figure 1: Location of Upper White Watershed in state of Indiana US

Data collection and analysis

The Soil and Water Assessment Tool (SWAT) is a physically based model which has been used as an effective tool to model impacts of climatic change on hydrologic and biogeochemical cycles in a variety of watersheds (Arnold et al., 1998). SWAT divides a watershed into subwatersheds and each subwatershed is connected through a stream channel which is further divided in to Hydrologic Response Unit (HRU). HRU is a unique combination of a soil and a vegetation type in a subwatershed, and SWAT simulates hydrology, vegetation growth, and management practices at the HRU level. The model estimates relevant hydrologic components such as surface runoff, evapotranspiration (ET), and soil moisture change for each HRU.SWAT assumes flows in streams and reservoirs are one-dimensional.

SWAT model setup required digital elevation map (DEM) of scale 1:24,000, land use land cover, soil, and climate data. DEM (30 m grid size) was obtained from USGS (www.seamless.usgs.gov). Land use land cover data was (30 m grid) was obtained from the National Land Cover Data – (NLCD 2001). The soil information was obtained in a feature format from the STATSGO. The surface flow in the watershed is monitored using 28 USGS real time gauge stations located at various streams in the watershed. The climate data was obtained in a 12 km grid format developed for the Variable Infiltration Capacity (VIC) model. The precipitation and temperature information was obtained for 64 grids in the watershed, for a period of 1915-2006.

Table 1 : Management information used to setup SWAT model

Corn-Soybean rotation			**Continuous Corn**		
Management type	Date	Rate of application	Management type	Date	Rate of application
Tillage	April 1	-	Tillage	April 1	-
Tillage	April 6	-	Tillage	April 6	-
Planting (Corn)	April 13	-	Planting (Corn)	April 13	-
Fertilizer (An. NH3)	May 25	145 kg/ha	Fertilizer (An. NH3)	May 25	145 kg/ha
Harvest and Kill	Oct. 30	-	Harvest and Kill	Oct. 30	-
Tillage*	Apr. 28	-	Tillage*	April 1	-
Fertilizer (P) *	May 2	32 kg/ha	Tillage*	April 6	-
Planting (Soybean) *	May 20	-	Planting (Corn) *	April 13	-
Harvest and Kill*	Oct. 1	-	Pesticide (Atrazine) *	April 16	1.5 kg/ha
Tillage*	Oct. 20	-	Fertilizer (An. NH3) *	May 25	145 kg/ha
			Harvest and Kill*	Oct. 30	-

*Year 2 of cropping and this process is repeated for five years

Methodology and Results

The SWAT model was calibrated for flow, as it is the most important component of the water balance and has a direct influence on the water quality. The gauge located at the watershed outlet (#0345400) was used to calibrate the SWAT model at a daily scale for the period of 1989-2001, the first three years of data was used as warm up information for the model and the simulation during this period were discarded. Therefore the calibration was performed for the period 1992-2001 (10 years). Before the SWAT model was calibrated, a sensitivity analysis was performed for the parameters for flow. Linear local, one at a time sensitivity analysis was performed to estimate the relative sensitivity of the parameters. The ranking of the parameters was done based on their relative sensitivity indices (Eq. 1). Table 2 describes the relative sensitivity and ranking of the parameters for flow. The daily performance measures for the calibration were RNS2 (Eq. 2) of 0.62 and R2 (Eq. 3) of 0.72 (Figure 3). Figure 4 describes the hydrograph of the simulated and observed flows in the watershed. The validation of the model was performed for the period of 2002-2004 (1999-2001 used as warm up years). The daily performance measures during the validation were RNS2 (Eq. 2) of 0.59 and R2 (Eq. 3) of 0.62 (Figure 4). Figure 3 details the hydrograph for simulated and observed flow during the validation period. The calibrated SWAT model was used to simulate daily surface flow and ET outputs for each of the subbasins in the watershed.

$$Sr = \frac{\overline{P}}{\overline{O}}\left(\frac{O_2 - O_1}{P_2 - P_1}\right) \quad \text{Eq. (1)}$$

$$R_{NS}^{\ 2} = \left[1 - \frac{\sum_{i=1}^{n}(O_i - P_i)^2}{\sum_{i=1}^{n}(O_i - O_{avg})^2}\right] \quad \text{Eq. (2)}$$

$$R^2 = \left[\frac{\sum_{i=1}^{n}(O_i - O_{avg})(P_i - P_{avg})}{\sum_{i=1}^{n}(O_i - O_{avg})^2 \sum_{i=1}^{n}(P_i - P_{avg})^2}\right]^2 \quad \text{Eq. (3)}$$

Table 2 : Ranking of parameters and the corresponding relative sensitivity indices during the sensitivity analysis (Sr)

Parameter	Sr	Ranking
Curve Number (CN-II)	1.6	1
Soil evaporation compensation factor (ESCO)	0.4	2
Soil available water content (SOL-AWC)	0.04	3
Groundwater "revap" coefficient (GW_REVAP)	0.03	4
Groundwater delay (GWDELAY)	0.01	5
Ground water threshold depth required in shallow aquifer for return flow (GWQMN)	0.007	6
Base flow factor (Alpha_bf)	0.0003	7

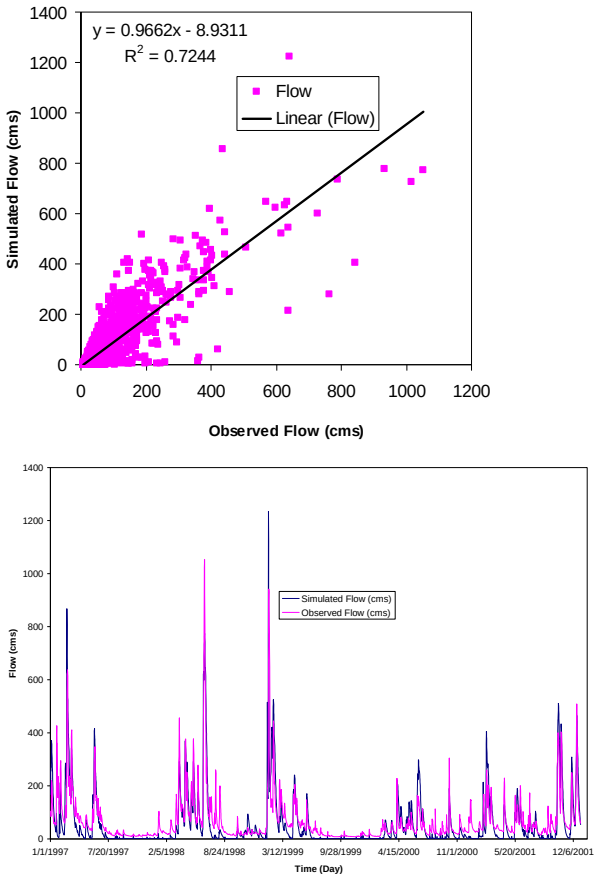

Figure 2(a) Linear regression fit between the simulated and observed flows showing the slope of the line and the regression coefficient R2 2(b) Observed and Simulated hydrograph during the calibration period (1997-2001)

The impact of land use change on the water quality and ET is estimated using SWAT. The management file in SWAT was provided with 5 years of crop rotation (corn-soybean-corn-soybean-corn). Curve number (CN) is presently considered most reliable method for estimating runoff, although it is based on empirical approach. Firstly, imperviousness of the entire watershed was changed uniformly by changing the curve number by -10%, -5%, 5%, and 10% of the original CN set up by SWAT as baseline. The stream flow was found to increase by 22 % with increase in 10% of CN from baseline CN. As expected increase in surface runoff showed increase in sediment yield from the watershed (Figure 3 and Figure 4).

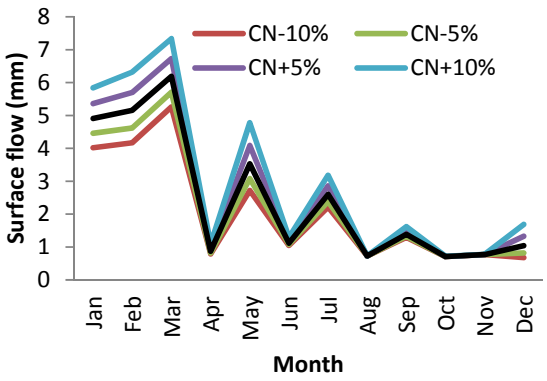

Figure 3: Monthly stream flow (mm) from watershed with changing curve number (CN)

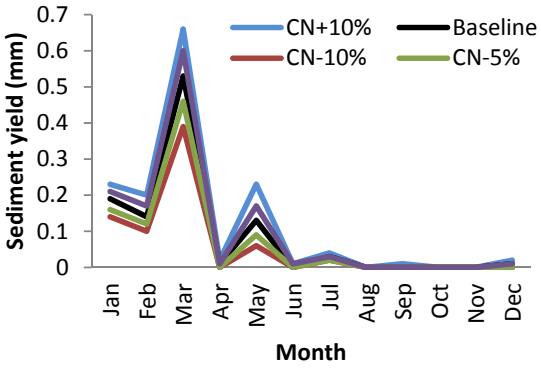

Figure 4 : Monthly sediment yield (mm) from watershed with changing curve number (CN)

To quantify the effect of increase in urban area on stream flow and sediment yield land use (NLCD, 2001) was reclassified by converting forested land (13%) to low density urban area. The reclassified land use was used to rerun the SWAT model. The result showed that there was significant increase in stream flow and sediment yield and as expected decrease in evapotranspiration. There is significant change in monthly stream flow with increase in urban area (Figure 5). Similarly, there is increase in sediment yield (76 % average annual) from the watershed with increase in urban area which is in consistent with increase in stream flow. The reason is forest land which was about 13 % areas in the watershed was classified as low density urban area thus there is loss in evapotranspiration from forest trees.

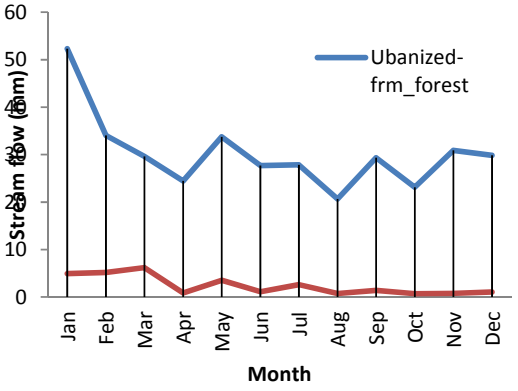

Figure 5 : Monthly stream flow (mm) from watershed with forest land classified as low

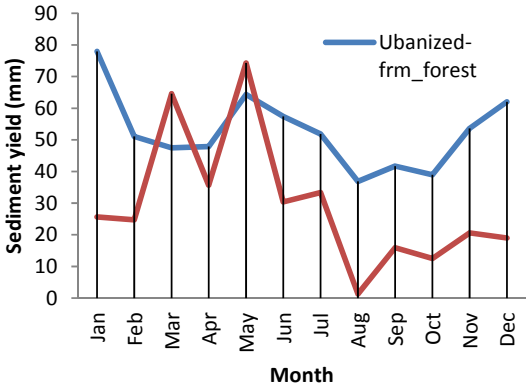

Figure 6 : Monthly sediment yield (mm) from watershed with forest land classified

density urban area **as low density urban area**

Conclusions

The impact of land use change due to increase in imperviousness, urbanization area and crop acreage to meet the biofuel demand on stream flow, sediment yield and ET was analyzed using the SWAT model to simulate the various parameters of concern. The SWAT model was calibrated for flow, which was used in the analysis. The results indicated that as the imperviousness in the watershed was increased, there was an increase in stream flow and sediment yields but no change was observed in evapotranspiration. Then the impact of increase in urban area from classifying forest areas as low density urban area was analyzed. It was seen that the stream flow and sediment yield are highly impacted due to increase in urban area. Ecohydrologicaly the watershed water balance is going to shift due to the change in land use and climate change and the plants in the region would be subjected to higher water stresses due to the increased temperatures and decreased precipitation.

References

Arnold, J. G., Srinivasan, R., Muttiah, R. S., and Williams, J. R.: Large area hydrologic modeling and assessment - Part 1: Model development, Journal of the American Water Resources Association, 34(1), 73-89, 1998.

Crawford, C. G.: Occurrence of pesticides in the White River, 1991-95, US Geological Service Fact Sheet, 95, 233-295, 1995.

Hill, J., Nelson, E., Tilman, D., Polasky, S., and Tiffany, D.: From the Cover: Environmental, economic, and energetic costs and benefits of biodiesel and ethanol biofuels, Proceedings of the National Academy of Sciences, 103(30), 11206, 2006.

Meyer, W. B., and Turner, B. L.: Changes in Land Use and Land Cover: A Global Perspective, Cambridge University Press, 1994.

USDA: Corn acres expected to soar in 2007, Press release 2007. Available online at http://www.nass.usda.gov/Newsroom/2007/03_30_2007.asp. Last accessed April 2008, 2007.

Assessing Climate change Impacts and Adaptation in Central Vietnam using SWAT and Community Based Approach: Case study in Vu Gia watershed, Quang Nam Province

Nguyen Kim Loi
Nong Lam University, Ho Chi Minh City, Vietnam
nguyenkimloi@gmail.com

Pham Cong Thien
Nong Lam University, Ho Chi Minh City, Vietnam

Nguyen Duy Liem
Nong Lam University, Ho Chi Minh City, Vietnam

Le Hoang Tu
Nong Lam University, Ho Chi Minh City, Vietnam

Le Van Phan
Nong Lam University, Ho Chi Minh City, Vietnam
Nguyen Van Trai
Nong Lam University, Ho Chi Minh City, Vietnam

Hoang Thi Thuy
Nong Lam University, Ho Chi Minh City, Vietnam

Le Anh Tuan
Can Tho University, Vietnam

Chinvanno
Southeast Asia START Regional Center, Bangkok, Thailand

Abstract

With the changes in climate, biophysical, socio-cultural, economic and technological components, paradigm shift in natural resources management are unavoidably adapt/modified to harmonize with the global changes and the local communities' needs. This research focused on climatic change risk, vulnerability and adaptation in Dong Giang district in response to climate change impacts as case study. The Soil and Water Assessment Tool (SWAT) model was applied to assess climate, land use change and practice impacts to soil and water resources in Dong Giang district as upstream of Vu Gia watershed, Quang Nam province. This part focuses on the relationship between upstream and downstream in Vu Gia watershed and using sustainable watershed management in response to climate change in Quang Nam province, Vietnam. The research also concerns with changes in ecological and socio-economic conditions driven by climate change and human activities in Dong Giang; and adaptation measures in agricultural production and livelihoods to suit the new conditions.

Keywords: Climate Change, SWAT, Community Base, Vu Gia watershed, Quang Nam

Introduction

Current climate change estimates indicate that major environmental changes are likely to occur due to climate change in practically every part of the world, with majority of these changes being felt through modification of hydrological cycle as e.g, floods, droughts and storms. Climate change impacts are also estimated to be particularly severe in many developing countries of the world and especially in Vietnam.. The recent studies (World Bank Study, Dasgupta et al.: 2007, IPCC, 2007) have concurred that Viet Nam will be one of most vulnerable countries to climate change in the world. Gradual changes such as sea level rises and higher temperatures, more extremes of weather such as drought, and more intense typhoons are all on the horizon and will have a potentially devastating impact on the country's people and economy.

Dong Giang District is one of eight mountainous districts that locate in western part of Quang Nam province – the centre of Vietnam, with 70 km far way from Da Nang city. The area often have tremendous catastrophically natural hazard by flood and typhoon. Recently, the number of events occurring such as landslide, drought, flash flood, etc. has increased rapidly. In addition, developing activities in the area such as hydropower construction, road building, and deforestation contributed to changing of ecosystem in Vu Gia watershed.

Hence, this research attempts to assess climate change impacts on ecosystems and livelihood in Dong Giang district, Quang Nam province and to make policy recommendations to decision maker on climate change impacts to adapt to the new context.

Study area description

Dong Giang District is one of eight mountainous districts located in western part of Quang Nam province and upstream Vu Gia watershed – the central Vietnam, with 107^{o} 30' to 107^{o}56' longitude and 15^{o}35' to 16^{o}10' latitude and 70 km west of Da Nang city. The region occupies an area of approximately 81,000 ha as shown in Figure 1. The Dong Giang district has been divided into 10 villages and 1 town. Dong Giang locates in mountainous area associated with small valleys and distributed by small and middle stream networks. The area is classified into 3 categories by height, i.e. the area of higher than 1000m over sea level accounts for approximately 22,600 ha which is 27.81% of the total; from 500m to 1000m height is about 38,400 ha (47.25%) and below 500m is 24.94%.

Statistically, the population of the district was 23,635 people in 2008, of which 73.21% were C'tu ethic-a minor group and the rest was Kinh people. Eighty percent of the local population relied on agricultural production and forestry activities for their livings. The value of Dong Giang district has been based on its diverse natural, cultural and historical resources including forest and its products, ethnic culture, etc.

On the other aspect, the area often suffers from tremendous catastrophically natural hazard causing by flash flood and typhoon. Recently, these disasters are in increasing trends. In addition to natural disasters, developing activities such as hydropower construction, road building, mining and stone exploitation have accelerate the hazard.

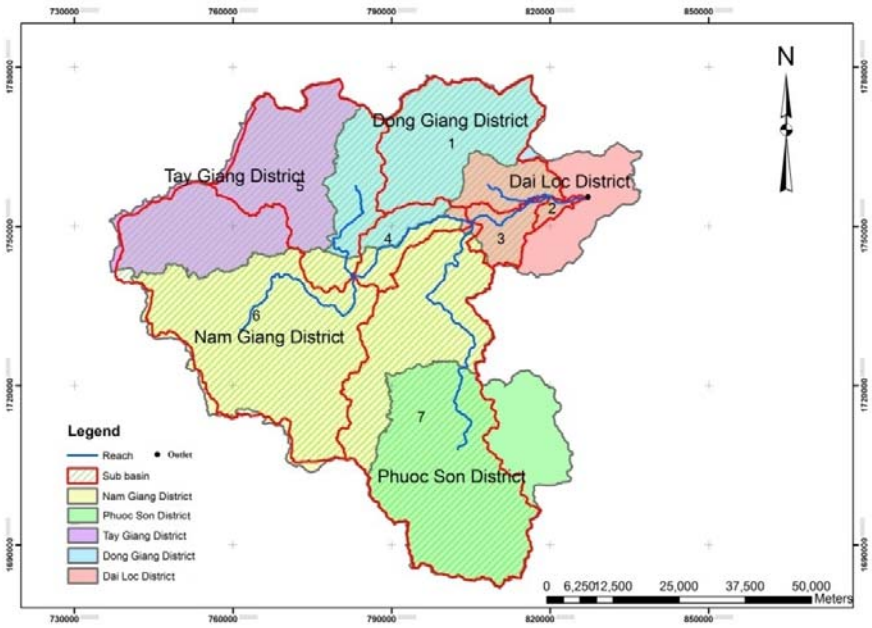

Figure 1. *Vu Gia watershed map*

Methodology

Brief description of SWAT model

The Soil and Water Assessment Tool (SWAT) has been widely applied for modeling watershed hydrology and simulating the movement of non-point source pollution. The SWAT is a physically – based continuous time hydrologic model with Arcview GIS interface developed by the Blackland Research and Extension Center and the USDA-ARS (Arnold et al., 1998) to predict the impact of land management practices on water, sediment, and agricultural chemical yields in large complex basins with varying soil type, land use and management conditions over long periods of time. The main driving force behind the SWAT is the hydrological component. The hydrological processes are divided into two phases, the land phase, which control amount of water, sediment and nutrient loading in receiving waters, and the water routing phase which simulates movement through the channel network. The SWAT considers both nature sources (e.g. mineralization of organic matter and N-fixation) and anthropogenic contributions (fertilizers, manures and point sources) as nutrient inputs (Somura, H. et.al. 2009). The SWAT is expected to provide useful information across a range of timescales, i.e. hourly, daily, monthly, and yearly time-steps (Neitsch et al., 2002).

The Scenario Planning Process for watershed and community approach

The SWAT Model

The principal planning task is aiming at the efficient planning of future in Vu Gia watershed. The objectives of each plan will assist in deciding upon the socio-economic, physical and environmental data that required formulating the different planning scenarios. The derived objectives are also used later in the methodology to evaluate the efficiency of each proposed planning scenario.

The next step of the planning process is to formulate climate change scenarios. Two scenarios are formulated for Vu Gia watershed as input of SWAT model.

Scenario A: Climate (1990s): The climate data were provided by Department of Meteorology and Hydrology in Central of Vietnam.
Scenario B: Future Climate (2030s): The climate data were provided by SEA-START Center.
Impact assessment of climate change in Vu Gia watershed on surface water, sediment yield. The SWAT model requires meteorological data such as daily precipitation, maximum and minimum air temperature, wind speed, relative humidity, and solar radiation data. Spatial data sets including digital parameter layers such as parameters (R, K, C, P) and topography (LS) was digitized from the associated maps. LS factor of the watershed is derived from digital elevation model (DEM) obtained from topography. The SWAT model was applied in Vu Gia watershed as shown in Figure 3, 4.

PRA (Participatory Rural Appraisal) Method

In order to conduct a comprehensive assessment of climate change impacts on ecosystem and livelihood in Dong Giang district, the PRA method (as shown in Figure 2) was applied to collect data for additional analysis. Specifically, the PRA method in combination with field visit were conducted in Dong Giang to collect information for an overall picture of the district regarding concerns in livelihoods (including agricultural productions and other living activities) in relation with climate change issues and natural disasters; and adaptation capacity of local people to the new context. Especially, the discussion also aimed to identify the perspectives of local people on climate change issues that affect their living conditions.

Participants in the PRA discussion comprised of research team members (from RCCC of Nong Lam University, Dragon Institute of Can Tho University and SEA-START Center, Thailand) who played a role of facilitators to guide the discussion and local authorities, other stakeholders (Social Unions and farmers).

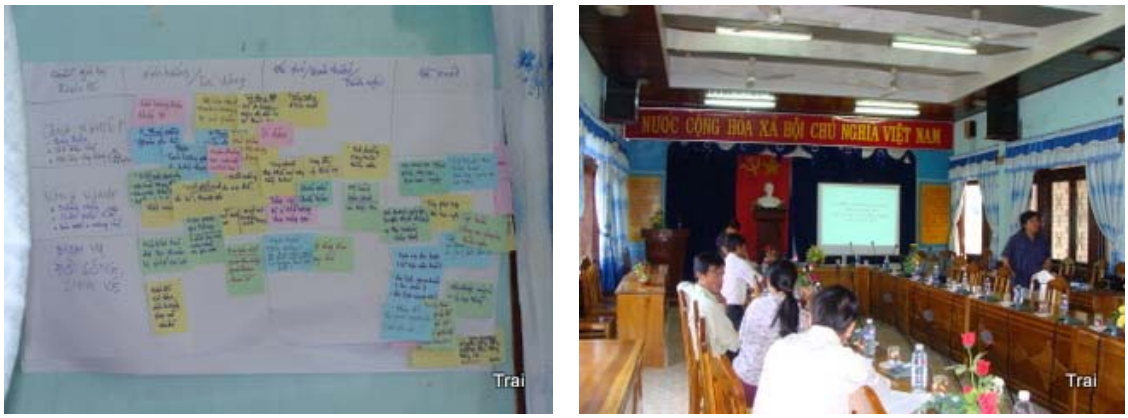

Figure 2. *Photos of PRA discussion in Dong Giang District, Quang Nam Province*

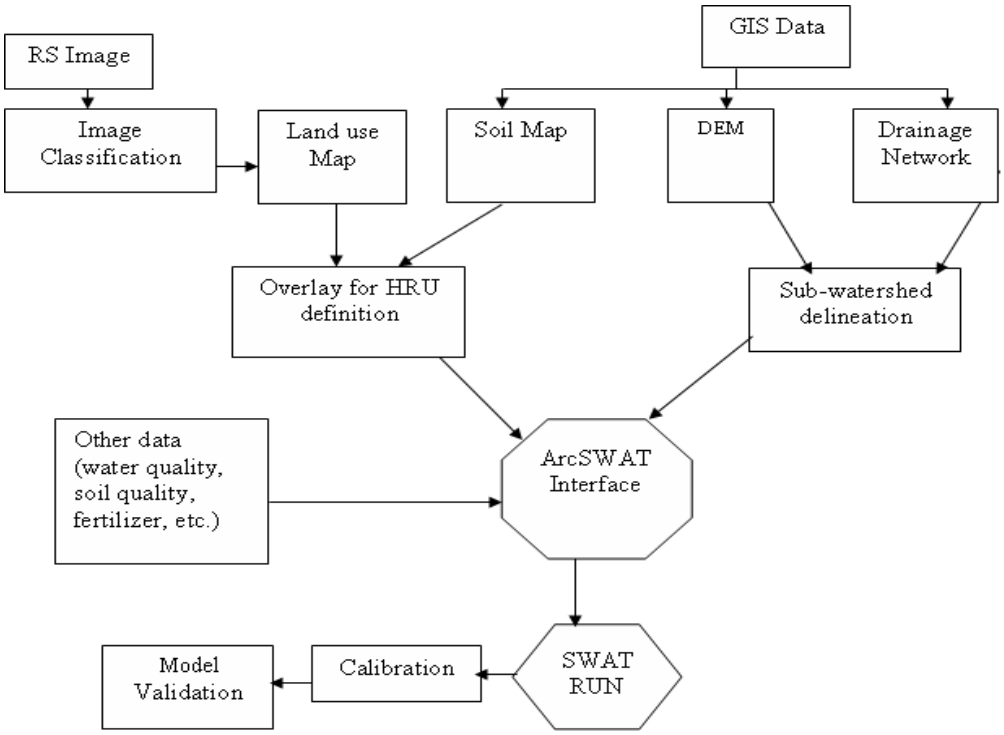

Figure 3. *The SWAT model*

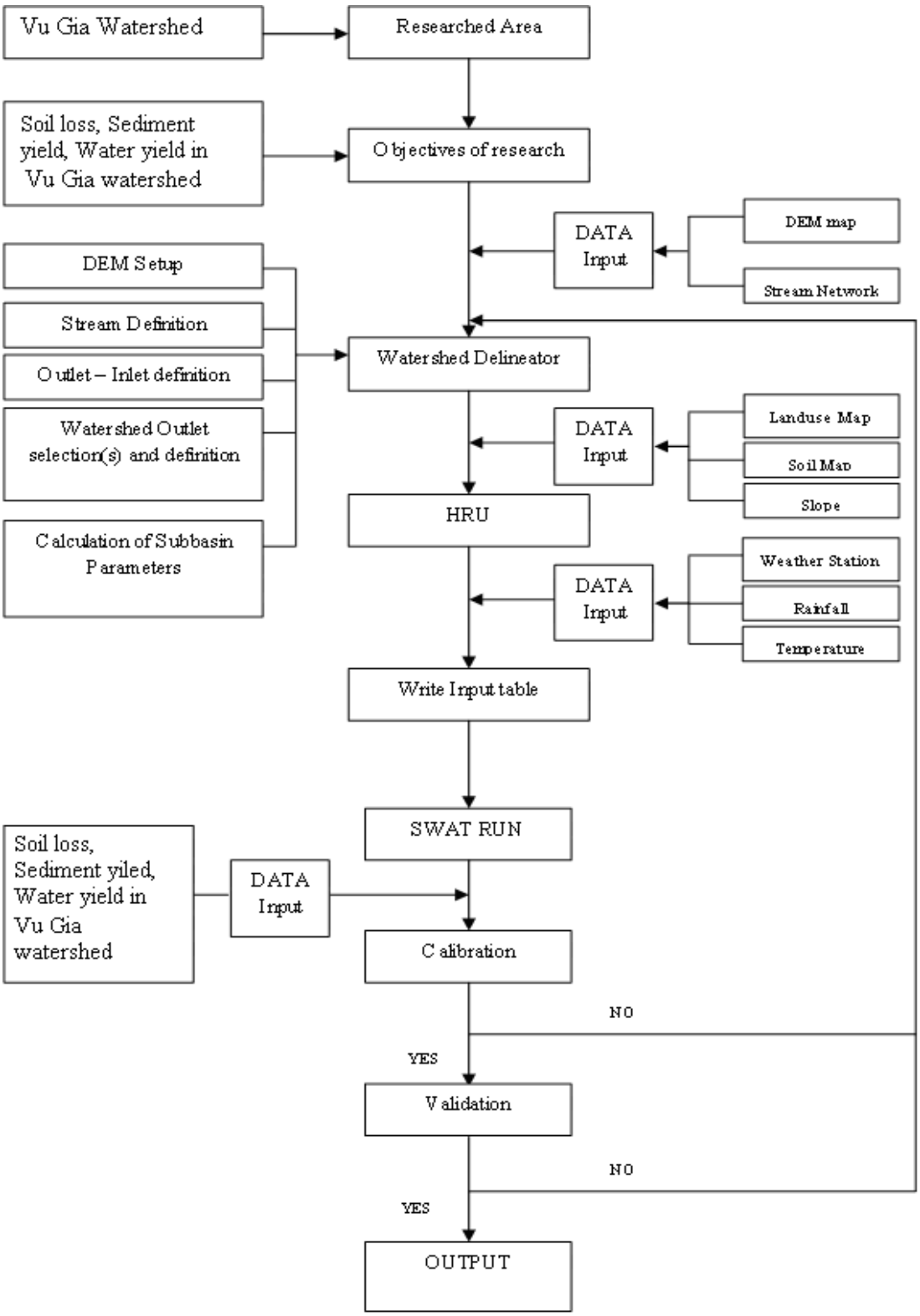

Figure 4. *Application of SWAT model in Vu Gia watershed*

Results and discussion

Evaluation of land use change effect on surface runoff and sediment yield

In Vu Gia watershed have 5 sub-basins as shown in Figure 5 based on SWAT model. In order to develop sound management schemes of protecting the Vu Gia watershed and to have clear picture of the impact of climate change specifically on surface runoff, and sediment yield. The calibrated model was run to simulate two climate change scenarios. Climate change scenarios are:

Scenario A: Climate (1990s)

Scenario B: Future Climate (2030s)

For developing the scenarios, the key processes and related model parameters such as P factor of USLE, infiltration rate were modified in the appropriate SWAT input files. An USLE P factor of 0.6 to 1.0 was used in simulations to reflect the condition of the watershed with and without soil conservation intervention. The predicted surface runoff and sediment yield in 1990s and 2030s were summarized in Table 1. The daily simulated surface runoff and sediment yield in the watershed is shown in Figure 6, 7.

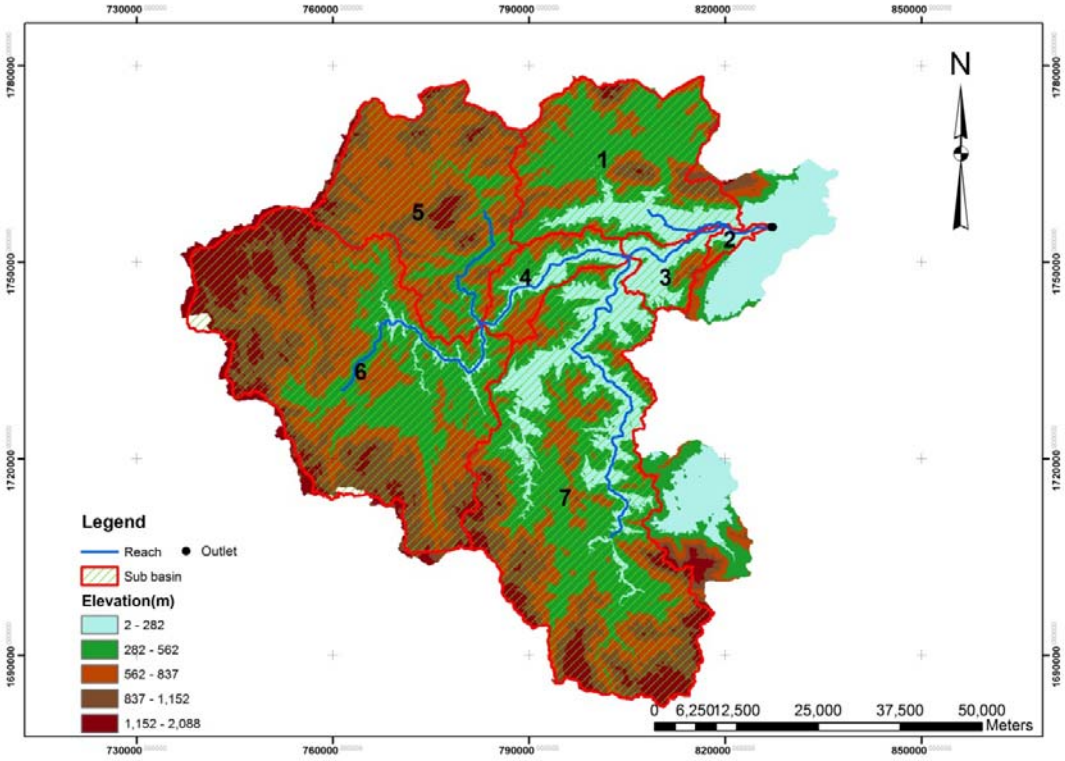

Figure 5. *The Vu Gia watershed along with its sub-basin automatically delineated*

Table 1. *The SWAT output (monthly) with different climate scenarios*

Month	Rainfall (mm)		Surface runoff Q (mm)		Sediment yield (ton/ha)	
	Scenario A	Scenario B	Scenario A	Scenario B	Scenario A	Scenario B
1	11.90	21.10	0.01	0.70	0.00	0.59
2	81.01	26.90	17.03	0.26	11.74	26.26
3	66.96	71.78	7.19	11.03	18.42	13.65
4	183.50	183.50	49.18	70.79	45.50	51.41
5	195.47	195.47	57.69	80.41	19.62	78.94
6	126.83	126.83	49.84	89.08	11.50	5.40
7	328.80	398.80	99.53	190.34	0.23	15.48
8	435.76	465.76	90.40	210.54	61.08	130.04
9	393.16	393.16	91.34	196.34	13.56	156.40
10	482.41	482.41	110.65	219.87	28.82	118.87
11	328.80	228.80	70.32	87.87	0.16	91.91
12	68.35	58.15	8.05	7.50	8.84	10.95

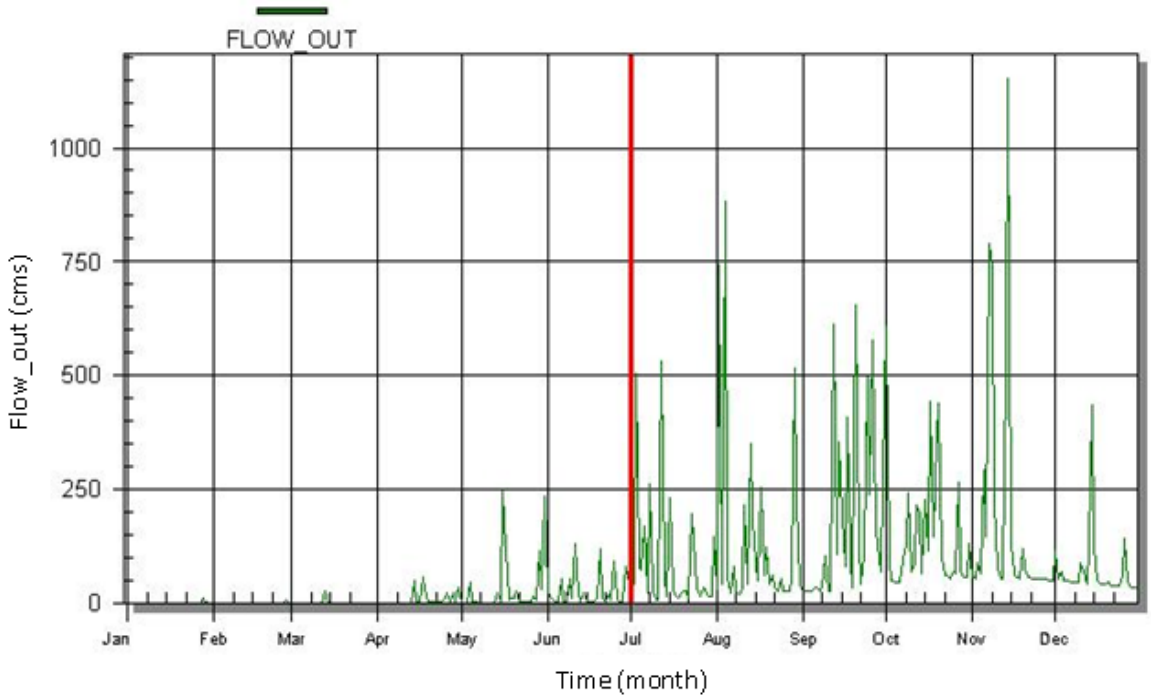

Figure 6. *Simulated surface flow in sub-basin 1 (Dong Giang district) in Vu Gia watershed*

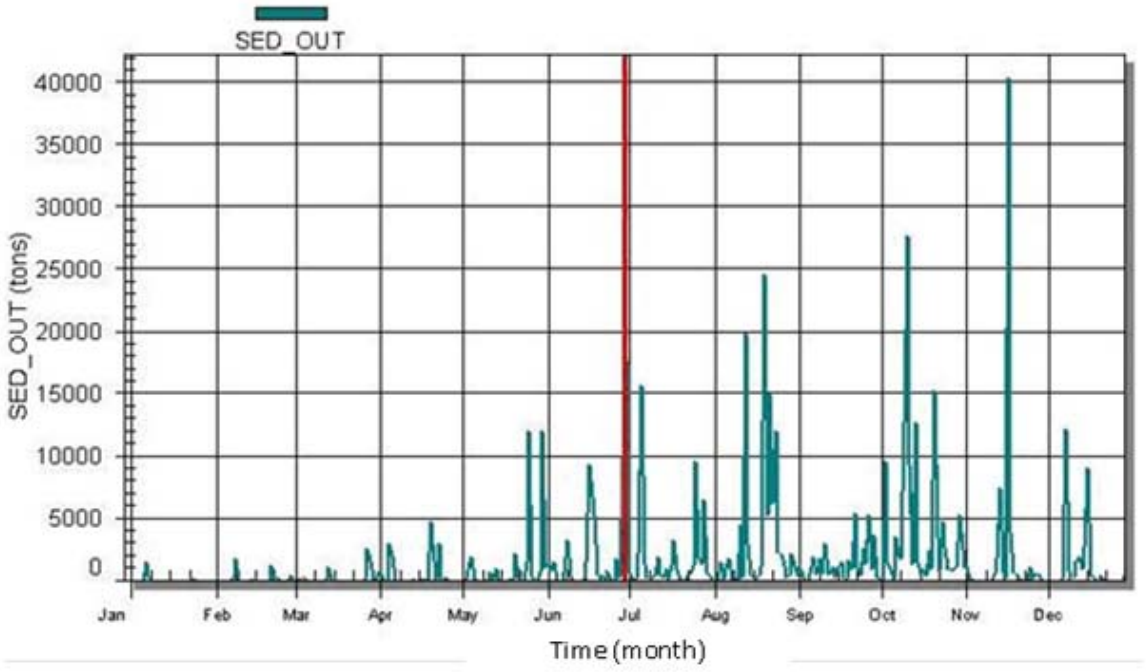

Figure 7. *Simulated Sediment yield loading to reservoir in Vu Gia watershed*

To assess the effects of climate change in the study area, the SWAT model was run to simulate two scenarios of climate change on surface runoff, sediment yield. Results of the simulation shown that surface runoff increase. An increase about 42.22% in surface runoff occurs compared between 1990s and 2030s. Meanwhile, sediment yield increase about 54.2% compared between 1990s (28.96 ton/ha) and 2030s 41.66 ton/ha).

Table 2. *The SWAT simulated statistics for Vu Gia watershed using climate scenario A (1990s) and climate scenario B (2030s)*

Scenario	Precipitation (mm)	Surface runoff (mm)	Sediment yield (ton/ha)
1990s	2652.66	41.89	41.66
2030s	2702.95	29.44	28.96

Effect of extreme weather phenomenon on natural and socio-economic conditions of Dong Giang District.

Result from the PRA discussion is presented in Figure 8.

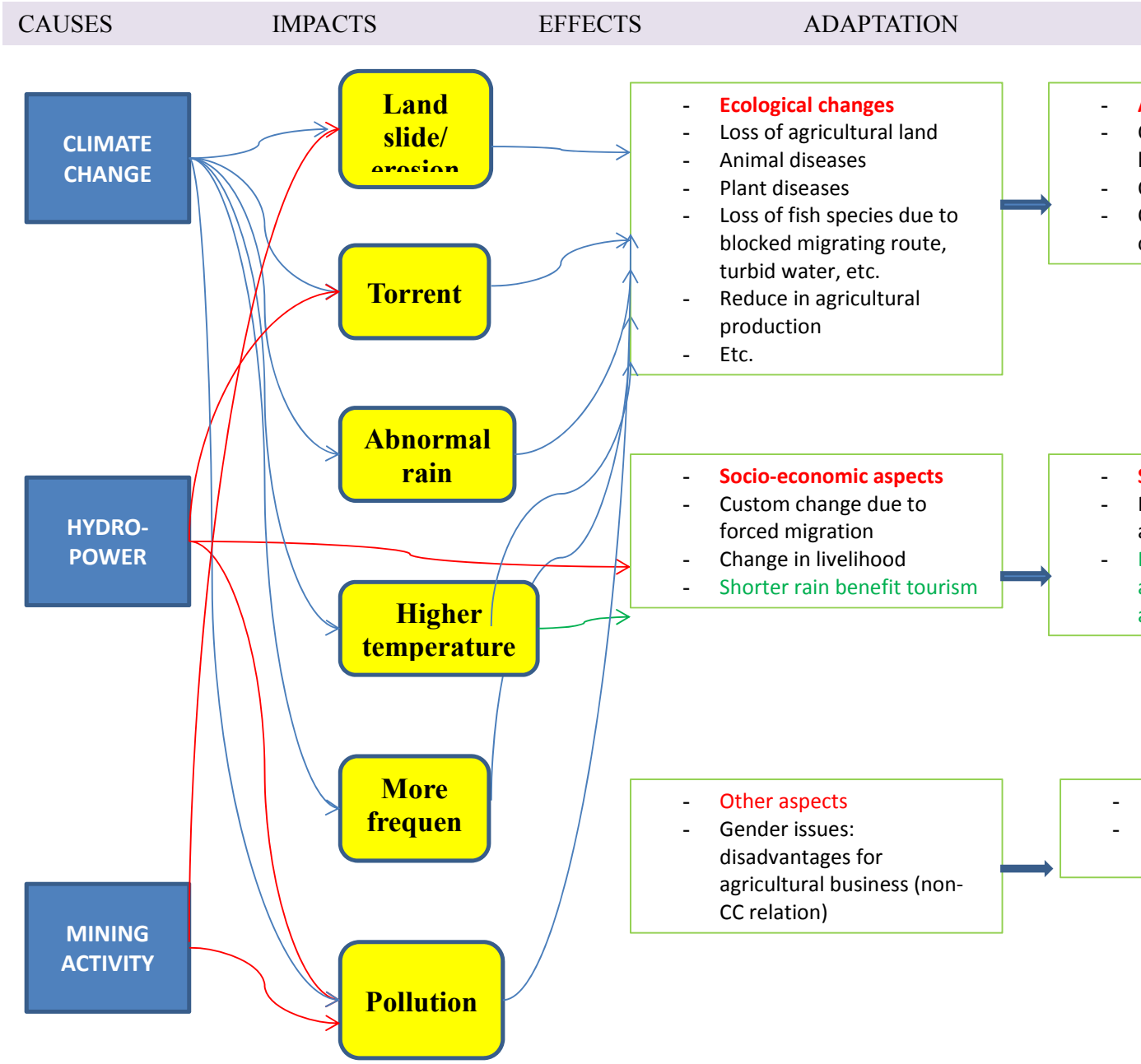

Figure 8. *Ecological and socio-economic changes caused by extreme weather conditions and adaptation to suit the new context*

The above flow chart conveys a key message that the destructive phenomena including extreme weather conditions that occurred recently in Dong Giang was partially caused by climate changes. For instance, more landslide incidences were due to heavier rainfall and torrent that occurred at higher frequency in the district recently. Similarly, higher temperature events and more frequent storm tend to increase in the last few years. In spite of human activities such as construction of hydropower plants and gold mining were also key sectors

caused adverse impacts on the environment, climate change phenomena are believed to significantly contribute to the livelihood changing.

Most of the mentioned phenomena caused adverse effects on local people in various aspects such as ecological changes, socio-economic disruption and some other gender issues. In terms of ecological changes, the most frequent reported events included loss of agriculture land, disease occurrence in human and agricultural productions, change in water quality and current pattern leading to loss of fish species. Other concerns were that custom and livelihood changes due to home loss and resettlement.

In order to adapt to new conditions, local people have adjusted their farming calendar and changed varieties for cultivation and husbandry. For example, cow has been raised instead of buffalo because it can tolerate better in hotter weather. However, eco-tourism has been further developed because it benefit from a longer dry season and drought which prompt tourists to searching such environment in the District.

Conclusions

This research is just the first step apply SWAT in Vu Gia watershed. The SWAT model performed well in simulating the general trend of surface runoff, sediment yield, at watershed over time for daily, monthly time intervals. The results shown that the climate change was affected surface runoff, sediment yield. Results of the simulation shown that surface runoff increase. An increase about 42.22% in surface runoff occurs compared between 1990s and 2030s. Meanwhile, sediment yield increase about 54.2% compared between 1990s (28.96 ton/ha) and 2030s 41.66 ton/ha). While simulation results are subject to further validation, this study showed that the Soil and Water Assessment Tool (SWAT) model can be a useful tool for modeling the impact of climate change in Vietnam watershed.

The recent adaptation to deal with changes in ecology and socio-economics requires further attention from the authority for more appropriate policies and strategies to support local people for better livelihoods.

Acknowledgements

The authors acknowledge the APN (Asia-Pacific Network for Global Change Research) funded “Building research capacity on assessing community livelihood vulnerability to climate change impact in central Vietnam and Mekong River delta” project for funding this research.

References

Arnold, J.G., Srinivasan, R., Muttiah, R.S. and Williams, J.R. 1998. Large area hydrologic modeling and assessment part I: model development. *J. American Water Resources Association* 34: 73-89.

Dasgupta, S., Laplante. B., Meisner, C., Wheeler, D., and Yan, J. 2007. The Impact of Sea Level Rise on Developing Countries. A Comparative Analysis. World Bank Policy Research Working Paper 4136, February 2007.

IPCC. 2007. Climate Change 2007: Impacts, Adaptation, and Vulnerability. The Fourth Assessment Report of the Intergovernmental Panel of Climate Change. Cambridge University Press.

Loi. N.K., and N. Tangtham. 2005. Decision support system for sustainable watershed management in Dong Nai watershed – Vietnam. Paper presented in International Seminar on "Synergistic Approach to Appropriate Forestry Technology for Sustaining Rainforest Ecosystem", March 7 - 9, 2005, Bintulu Kinabalu, Malaysia.

Neitsch, S.L., Arnold, J.G., Kiniry, J.R., Srinivasan, R. and Williams, J.R. 2002. Soil and Water Assessment Tool User's Manual Version 2000. GSWRL Report 02-02, BRC Report 2-06. Temple, Texas, USA.

Somura, H., Hoffman, D., Arnold, J.G., Takeda, I. and Mori, Y. 2009. Application of the SWAT Model to the Hii River Basin, Shimane Prefecture, Japan. In *Soil and Water Assessment Tool (SWAT) Global Applications. World Association of Soil and Water Conservation. Special Pub. No.4.*

RAINFALL-RUNOFF MODELING USING DOPPLER WEATHER RADAR DATA FOR ADYAR WATERSHED, INDIA

S. Josephine Vanaja
Research Scholar, Centre for Water Resources, Anna University, Sardar Patel Road, Chennai, Tamilnadu, India, 600025. Email: josephine.vanaja@yahoo.com

B V Mudgal
Associate Professor, Centre for Water Resources, Anna University, Sardar Patel Road, Chennai, Tamilnadu, India, 600025. Email: bvmudgal@annauniv.edu

Abstract

Precipitation is a significant input for hydrologic models; so, it needs to be quantified precisely. The measurement with rain gauges gives the rainfall at a particular location, whereas the radar obtains instantaneous snapshots of electromagnetic backscatter from rain volumes that are then converted to rainfall via algorithms. It has been proved that the radar measurement of areal rainfall can outperform rain gauge network measurements, especially in remote areas where rain gauges are sparse, and remotely sensed satellite rainfall data are too inaccurate. There are numerous papers showing the improvements in flood estimation and flood forecasting using radar rainfall as the input data to hydrological models. The research focuses on a technique to improve rainfall-runoff modeling based on radar derived rainfall data for Adyar watershed, Chennai, India. A hydrologic model called 'Hydrologic Engineering Center-Hydrologic Modeling System (HEC-HMS)' is used for simulating rainfall-runoff processes. CARTOSAT 30 m DEM is used for watershed delineation using HEC-GEOHMS. The Adyar Watershed is within 100 km radius from the Doppler Weather Radar Station, hence it has been chosen as the study area. The JAL Storm event from 4th November 2010 to 8th November 2010 period is selected for the study. The data for this

period are collected from the Statistical Department, and the Cyclone Detection Radar Centre, Chennai, India. The results showed that the radar over predicts the flow rate.

Key words: Rain gauge, Radar rainfall, Z-R relationship, Rainfall-Runoff Model, HEC-HMS Model.

INTRODUCTION

Precipitation is a significant input for hydrologic models; so, it needs to be quantified precisely. The measurement with rain gauges gives the rainfall at a particular location; with an assumption that it is uniform over an area. With this presumption many hydrological models were developed, and the prediction of the surface water potential was done. But it did not always match with the observed data due to spatial and temporal variations in rainfall.

Research has been carried on the Upper Bernam River Basin, Malaysia on rainfall-runoff modeling based on radar derived rainfall data. The results concluded that the watershed river flow can be better anticipated by using the radar derived rainfall data over the conventional rain gauge data (Waleed et al., 2009). A study was done using the Width Function Instantaneous Unit Hydrograph (WFIUH) model for the Treja river basin, Italy (Lopez et al., 2005). The results proved that the radar rainfall data is able to improve hydrograph reconstruction significantly. Todini (2001) conducted a case study on the upper Reno River close to Casalecchio, near Bologna (Italy), where several rain gauges and one C-band Doppler meteorological radar and stated that weather radar based rainfall estimates has a wide range of possible applications. Many researchers concluded that meteorological radars have several advantages over the conventional rain gauges, since a single site is able to obtain coverage over a wide area with high temporal and spatial resolution (Taffe and Kucera 2005; TSMS, 2005; Meischner, 2004; Borga 2002; Wyss et al., 1990).

Researches have been carried out in different countries using radar derived rainfall data. But there are only limited studies were carried out in India to utilize the weather radar products for hydrological purposes. So the present challenge in India is the utilization of Doppler Weather Radar (DWR) products for hydrological purposes similar to the rainfall-runoff models, flood forecasting, and Research and Development activities.

This study focuses on utilizing the radar derived rainfall data to predict the surface runoff of Adyar watershed, Chennai using HEC-HMS model. Research is to analyze and propose the prospects of using radar based rainfall-runoff estimation for Adyar watershed, Chennai, India.

CASE STUDY

The Chennai basin group the rivers, which are situated between latitudes 12o30’00’’ to 13o35’00’’ N and longitudes 79o15’00’’ to 80o22’30’’ E and is located in the northern part of Tamil Nadu, India. The Chennai basin comprises of eight watersheds such as Adyar, Araniyar, Cooum, Gummidipoondi, Kosasthalaiyar, Kovalam, Nagari, and Nandhiyar.

Figure 1: Study area and Rain gauge stations

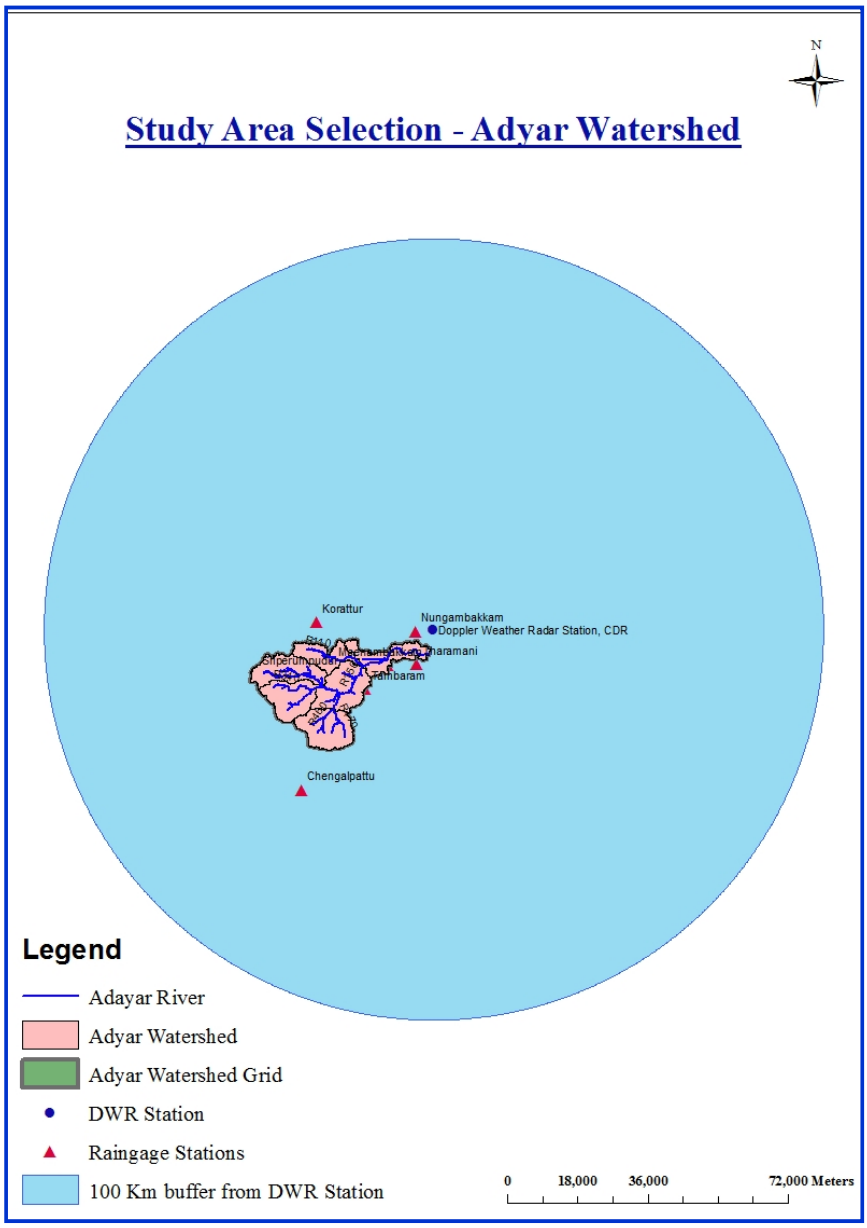

The Adyar watershed is a low-lying, flat, slightly undulating terrain with a general slope of 3–5º toward the E-ENE direction. The area is characterized by high temperature and high humidity and falls under the semi-arid tropical region. Average monthly minimum and maximum temperatures are about 19º C and 42º C respectively. The mean relative humidity is about 67.27 %, while the mean wind velocity is 4.84 km/hour. Average Sunshine

hours/day is 7.25, the mean annual evaporation is 165.03 mm and the average annual rainfall is about 1200 mm (Suriya et al. 2011).

There is one S-Band Doppler Weather Radar installed at Cyclone Detection Radar Centre (CDR), Chennai. The DWR derived products Surface Rainfall Intensity (SRI) and Precipitation Accumulation (PAC) are available only for 100 km radius circle from the DWR station, Chennai. The Adyar watershed is within 100 km radius from DWR Station, hence it has been chosen as the study area and it has an aerial extent of 1081.47 Km^2 (Figure 1).

METHODOLOGY

Rain gauge Rainfall Data

Based on the hydro meteorological features of the watershed, year in India is divided into Southwest monsoon period spanning from June to September (4 months), and Northeast monsoon period spanning from October to December (3 months), Winter period spanning from January to February (2 months) and Summer period spanning from March to May (3 months).

There are eight rain gauge stations in and around the Adyar watershed, but only two rain gauges are automatic. Based on the rainfall analysis, the annual rainfall of the Adyar watershed varies from 2111 mm to 753 mm. The watershed receives more rainfall in the northeast monsoon and it varies from 1171 mm to 274 mm. Southwest monsoon rainfall varies from 776 mm to 263 mm, winter rainfall varies from 307 mm to 0 mm and summer rainfall varies from 399 mm to 0.90 mm(Chennai Basin Report, 2007). The JAL Storm event from 4th November 2010 to 8th November 2010 period is selected for the study. The rain gauge data for this period is collected from the State Ground and Surface Water Resources

Data Centre, Tharamani, Chennai. Table 1 shows the radar and rain gauge rainfall data for the study period.

Table 1: Radar and Rain gauge rainfall data from 04-Nov-2010 to 08-Nov-2010

Radar Data (mm)								
Date	**Nungmbkm**	**Tharamani**	**Meenambkm**	**Tambaram**	**Chembarampkm**	**Koratur**	**Sriperum**	**Chengalpatu**
Distance from DWR (Km)	**10**	**10**	**20**	**30**	**30**	**40**	**40**	**60**
04-Nov-10	0.00	0.00	0.00	0.00	0.00	0.00	0.00	4.90
05-Nov-10	0.00	0.00	1.00	1.00	0.00	1.00	0.00	0.00
06-Nov-10	2.90	2.20	10.00	2.60	16.60	0.00	1.00	2.20
07-Nov-10	19.30	20.90	17.00	19.70	14.30	17.40	11.90	26.70
08-Nov-10	9.60	13.50	10.00	36.90	31.80	6.80	18.90	37.59
Sum	**31.80**	**36.60**	**38.00**	**60.20**	**62.70**	**25.20**	**31.80**	**71.39**
Rain gauge Data (mm)								
04-Nov-10	1.80	0.00	4.80	1.00	5.00	13.00	0.00	73.00
05-Nov-10	3.80	0.00	0.00	0.00	5.00	6.00	0.00	0.00
06-Nov-10	3.80	0.00	5.00	8.00	12.00	0.00	0.00	0.00
07-Nov-10	22.80	23.80	21.40	11.20	12.00	5.00	8.20	11.40
08-Nov-10	47.80	40.80	44.80	49.00	49.00	37.00	53.00	79.20
Sum	**80.00**	**64.60**	**76.00**	**69.20**	**83.00**	**61.00**	**61.20**	**163.60**

Radar Rainfall Data

The relationship between the rainfall rate and the reflectivity seems to be affected by the geography, seasonal variation, and the climatological conditions of the place. So, it is not possible to give a universal Z-R Relationship (Sen Jaiswal et al., 2009). The DWR operating at CDR, Chennai uses the following Z-R Relationship for the SRI computation and PAC is calculated as a second-level product based on the SRI (India Meteorological Department Report, 2010).

$$Z = 267 R^{1.345} \quad (1)$$

SRI images obtained at every 15 minutes interval and PAC is an accumulation of the SRI products per day to give the cumulative 24 hours rainfall. The DWR derived products SRI and PAC at 500 m resolution are used for the runoff estimation. The radar rainfall data is

collected from CDR, Chennai. Few software tools have been developed for reformatting the radar data into the format required by the HEC-HMS program and the radar data processing methodology is elucidated in Figure 2.

Figure 2: Radar Data Processing Methodology

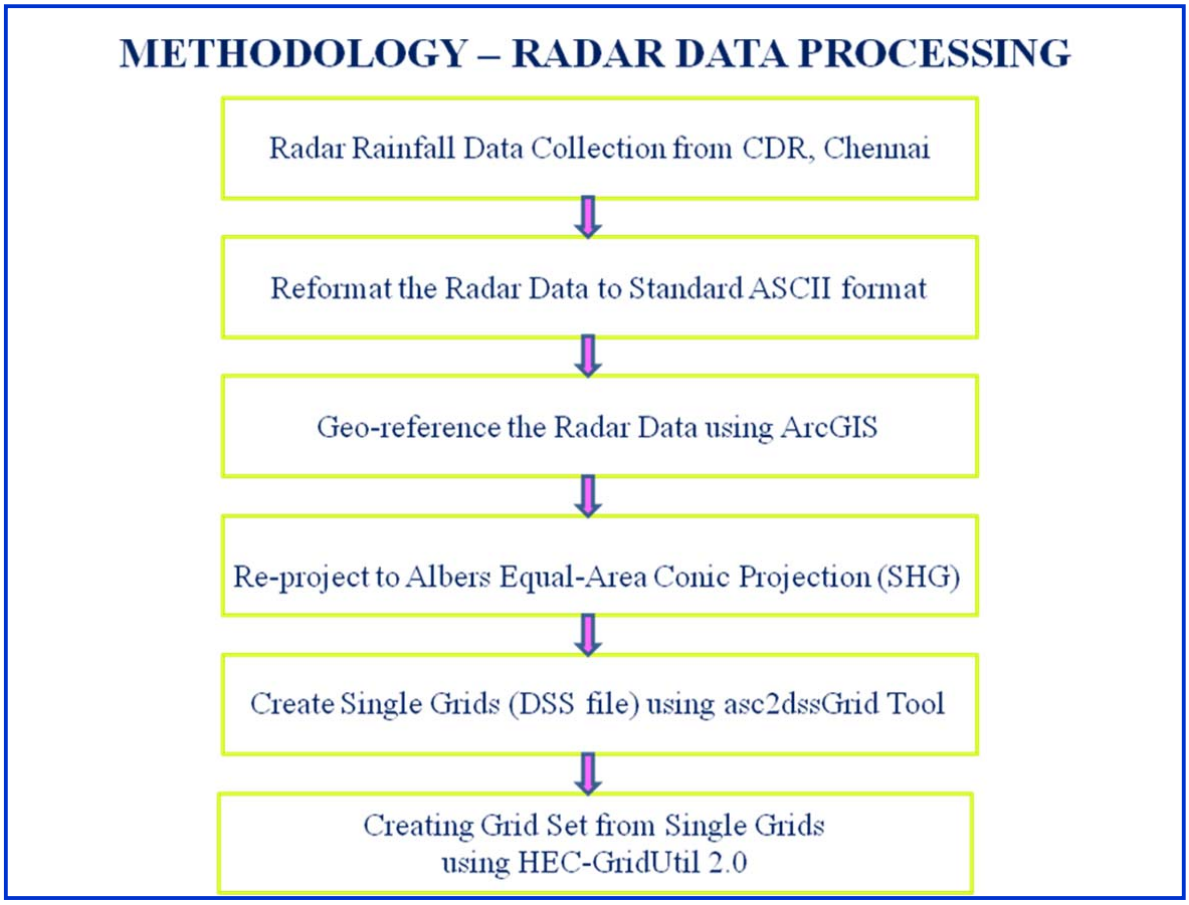

Radar Rainfall Adjustment Procedures

The weather radar does not measure rainfall directly; it acquires instantaneous snapshots of electromagnetic backscatter from rain volumes that are then converted to rainfall via algorithms (Lopez et al., 2005). So the radar data requires adjustment prior to using it as the input to any model. Figure 3 shows the scatter plot between original radar data and rain gauge data. A trend line is drawn to study the correlation between two different inputs and obtained

the linear trend equation y = 1.786 x with correlation coefficient 0.441 (i.e) Rain gauge data = 1.786 * radar data. Hence the radar rainfall calibration factor for the study area is identified as 1.786.

Figure 3: Radar Rainfall Calibration Model (Original Values)

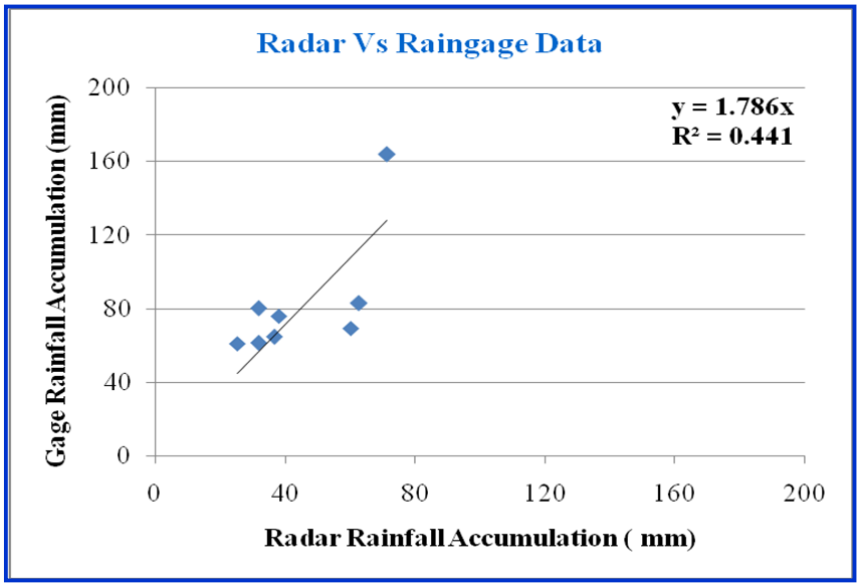

The adjustment of radar data is obtained by matching the accumulation of rain gauge rainfall data and radar rainfall data in the study area. The estimated radar derived rainfall data is adjusted by multiplying the original value by the calibration factor. Figure 4 shows the scatter plot between calibrated radar data and rain gauge data with linear trend equation y = 1.000 x

and correlation coefficient 0.441.

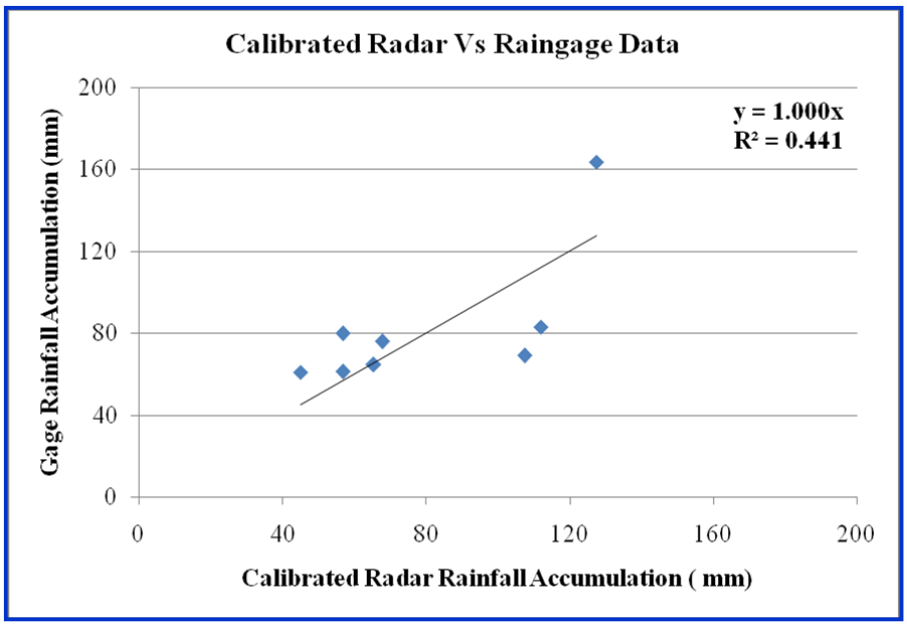

Figure 4: Radar Rainfall Calibration Model (Calibrated Values)

HEC-HMS Rainfall Runoff Model

The Adyar watershed is delineated using CARTOSAT 30 m Digital Elevation Model (DEM). Geographic Information System (GIS) pre-processing is done using HEC-Geo Hydrological Modeling System (HEC-GeoHMS) software. It uses ArcGIS tools such as ArcView and the Spatial Analyst extension, to develop a number of hydrologic modeling inputs for the HEC-HMS model. Parameters such as Initial Abstraction, Curve Number, Impervious %, Lag Time, Muskingum K, and Muskingum X are calculated using Adyar Soil and landuse maps. HEC-HMS program is designed for surface water hydrology simulation. It includes all the components of the hydrologic cycle like precipitation, evaporation, infiltration, surface runoff, and baseflow. HEC-HMS program can be adapted to fit almost any watershed. Figure 5 illustrates the framework of research methodology.

Figure 5: Framework of Research Methodology

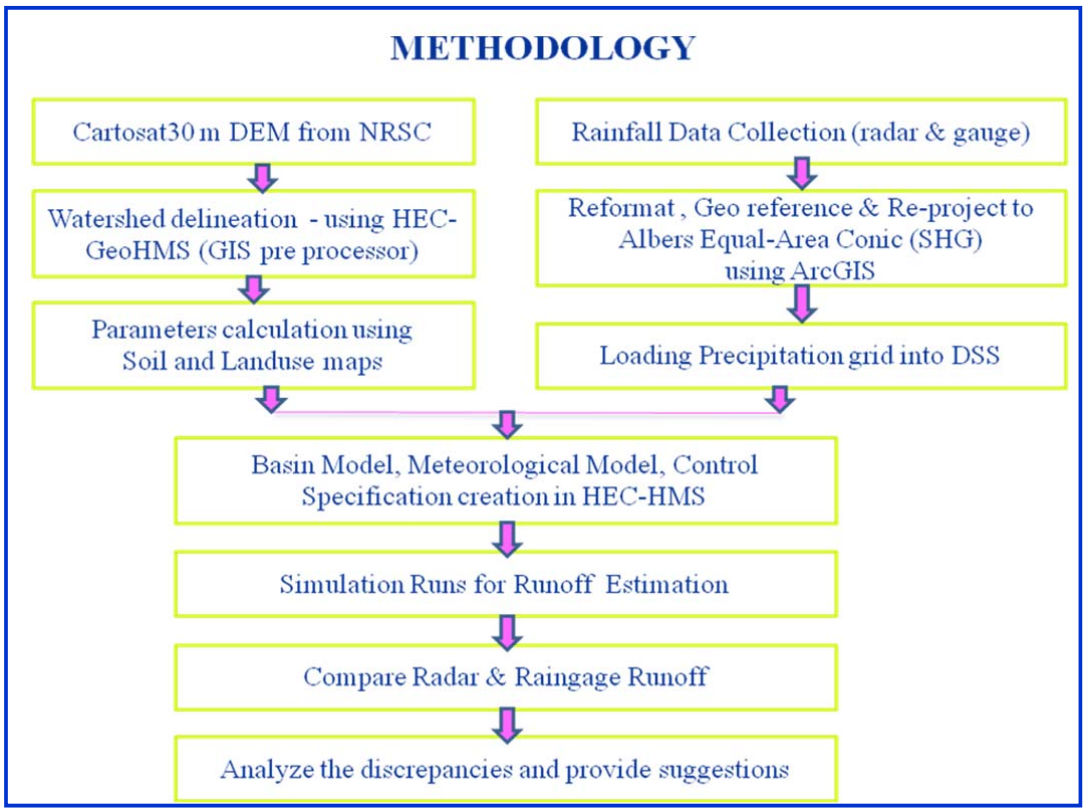

Basin models, meteorologic models, and control specifications are all main components used in simulation runs. Subbasins are the only elements that receive precipitation and other meteorologic inputs. The basin map is used to visualize a basin model component. Figure 6 shows the basin model of Adyar watershed in HEC-HMS.

Figure 6: Basin model of Adyar watershed in HEC-HMS Model

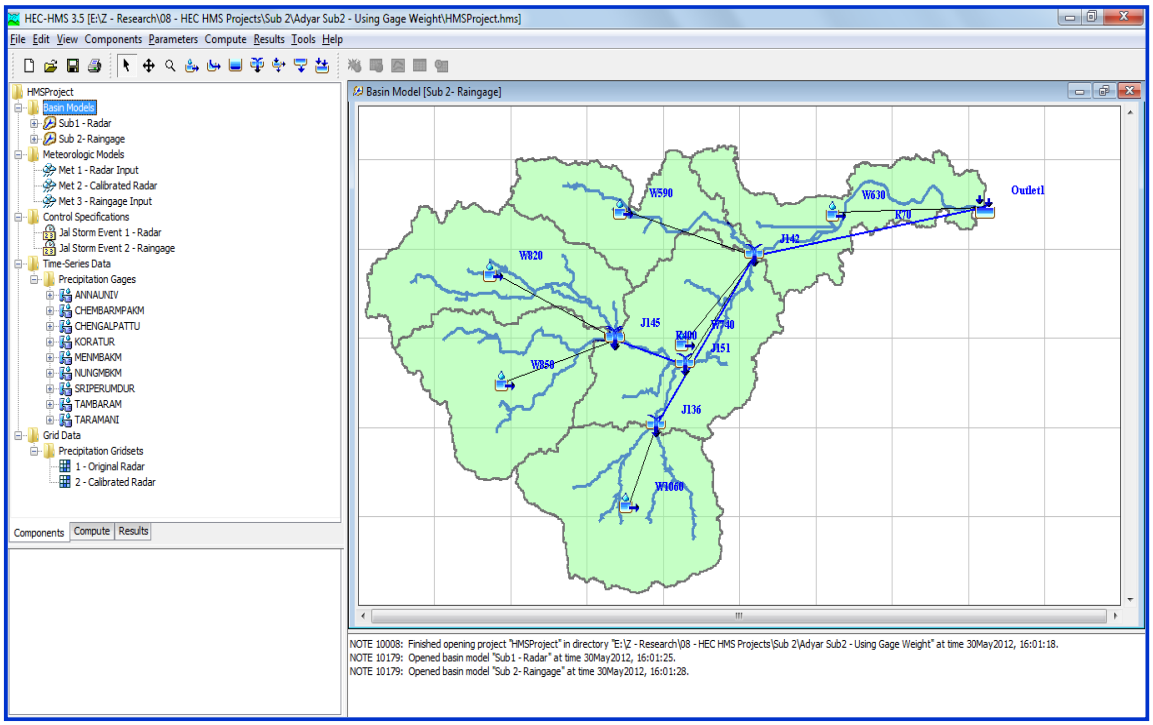

With HEC-GeoHMS inputs, basin model is created in the HEC-HMS. Excess rainfall is estimated using Soil Conservation Service-Curve Number (SCS–CN) method. SCS Unit Hydrograph transform method converts excess precipitation into runoff at the subbasin outlet. The routing method deals movement of the water in the reach. The Muskingum routing method is popular and relatively simple to use; hence it has been selected.

The meteorologic model deals all of the atmospheric conditions over the watershed. Meteorologic model is defined with type of precipitation analysis like gridded precipitation for radar and Thiessen polygon (Gage weight) for rain gauge. Control specifications are lightweight components. Time span is defined using control specification with start and end date and time.

A simulation run consists of one basin model, meteorologic model, and control specifications and it calculates the rainfall-runoff response. Three simultion runs are executed using rain

gauge rainfall, original radar rainfall and the calibrated rainfall data and results are stored in the output Data Storage System (DSS) file.

RESULTS AND DISCUSSION

The common way of assessing the accuracy of radar rainfall estimates is through the comparisons with observations from automatic rain gauge networks. Eight rain gauges are available in the study area, but only two rain gauges (Nungambakkam and Meenambakkam) are automatic. Hence all the eight rain gauges are considered for radar rainfall comparison and model calibration. The radar derived rainfall calibration factor is identified as 1.786 for Adyar Watershed. It is found that, the percentage error between rain gauge rainfall and radar rainfall reduced from 46% before calibration to 3% after calibration. Thus Radar-derived rainfall calibration model is successfully developed. Figure 7 and 8 shows the results of simultion runs using rain gauge data, original radar data and calibrated radar data.

Figure 7: HEC-HMS Result at the Adyar watershed outlet for rain gauge data

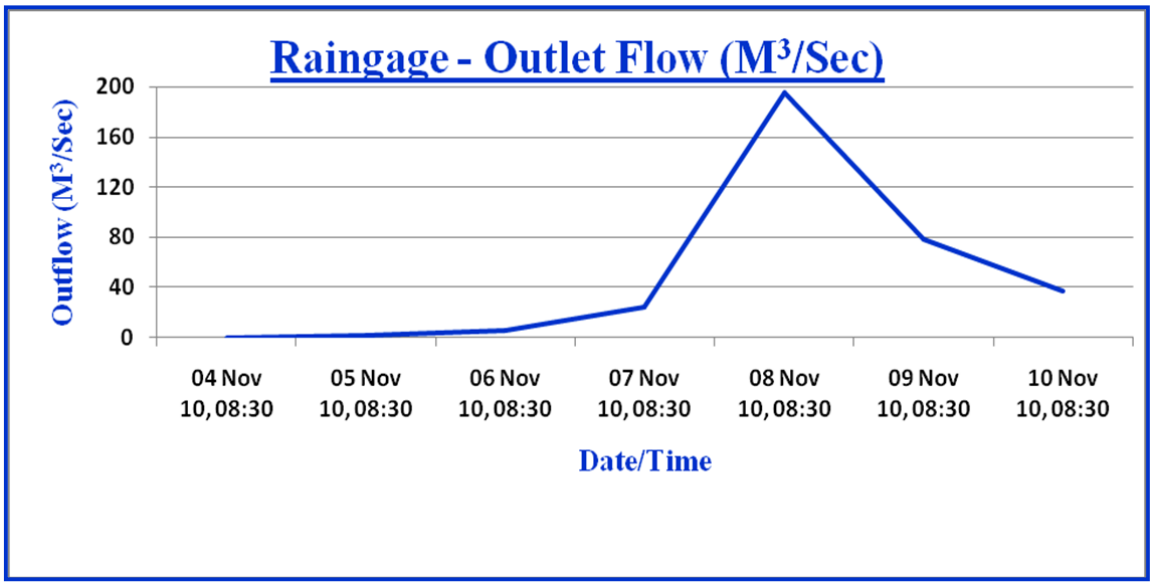

Figure 8: HEC-HMS Result at the Adyar watershed outlet for original and calibrated radar data

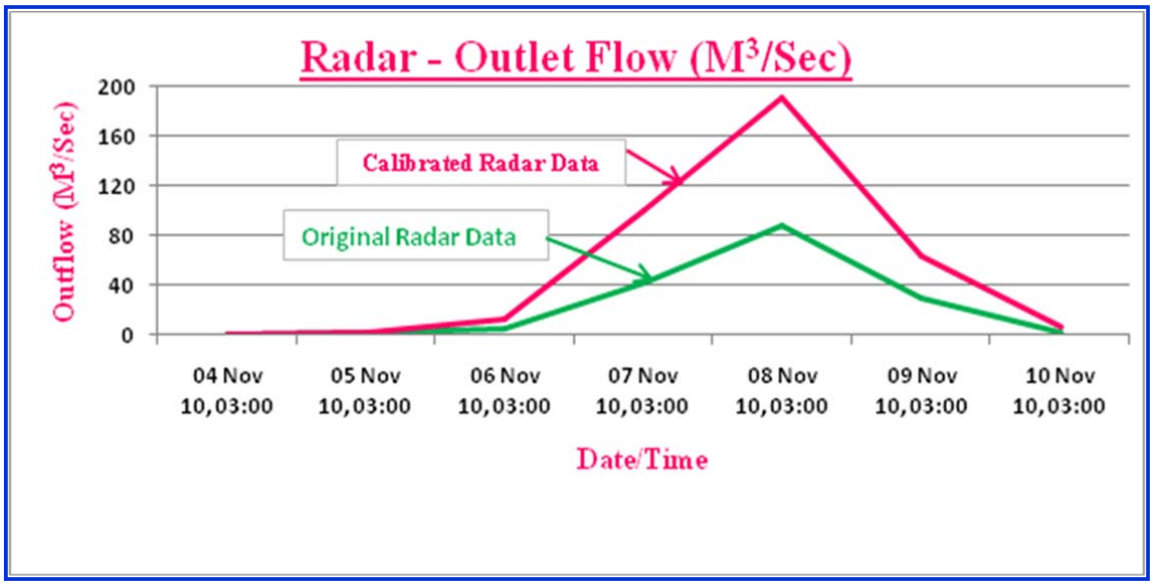

Calibrated radar and rain gauge results are compared at the outlet of the Adyar watershed and difference in peak outflow (m^3/sec) is 2.46 % and total outflow (MM) is 13.67 %. Radar shows slightly higher total outflow. The discrepancy might be due to the consideration of spatial and temporal variations in rainfall at the watershed.

ABBREVIATIONS

CDR	Cyclone Detection Radar Centre
DEM	Digital Elevation Model
DSS	Data Storage System
DWR	Doppler Weather Radar
GIS	Geographic Information System
HEC-GeoHMS	Hydrologic Engineering Center-Geo Hydrologic Modeling System
HEC-HMS	Hydrologic Engineering Center-Hydrologic Modeling System
IMD	India Meteorological Department
PAC	Precipitation Accumulation
SCS–CN	Soil Conservation Service-Curve Number
SRI	Surface Rainfall Intensity
WFIUH	Width Function Instantaneous Unit Hydrograph
Z-R	Radar measured reflectivity - Rainfall rate

REFERENCES

Borga Marco, Accuracy of radar rainfall estimates for stream flow simulation, Journal of Hydrology, 267, 26-39, 2002.

Chennai Basin Micro level study, Volume 1, Government of Tamilnadu Public Works Department, Water Resources Organization, 2007.

India Meteorological Department, National Seminar on Doppler Radar And Weather Surveillance (Draws-2010), Chennai, 2010.

Lopez, V., Napolitano, F., and Russo, F., Calibration of a rainfall-runoff model using radar and rain gauge data, Advances in Geosciences, 2, 41–46, 2005.

Meischner, P., Weather Radar Principles and Advanced Applications, Springer, 2004.

Sen Jaiswal, R., Uma, S., and Sathakumaran, A., Study of Z-R relationship over Gadanki for different rainfall rates, Indian Journal of Radio & Space Physics, 38, 159-164, 2009.

Suriya, S and Mudgal B V, Impact of urbanization on flooding: The Thirusoolam sub watershed - A case study, Journal of Hydrology, 412, 210-219, 2011.

Taffe, M. M., and Kucera, P. A., Radar Rainfall Estimation and Rain Gauge Comparison Studies at Wallops Island, Virginia, 2005.

Todini E, A Bayesian technique for conditioning radar precipitation esftimates to rain-gauge measurements, Hydrology and Earth System Science, 187-199, 2001.

TSMS, WMO, CIMO, Training Course on Weather Radar Systems, Module A – F, Turkey Radar Training 1.0/Alanya, 2005.

Waleed A. R. M., Amin, M. S. M., Abdul Halim, G., Shariff, A. R. M., and Aimrun, W., Calibrated Radar-Derived Rainfall Data for Rainfall-Runoff Modeling, European Journal of Scientific Research, 30, 608-619, 2009.

Wyss, Jonathan, Williams, E. R., and Bras, R. L., Hydrologic modeling of New England river basins using radar rainfall data, Journal of Geophysical Research, 95 (D3), 2143–2152, 1990.

Performance evaluation and uncertainty analysis of SWAT model for simulating hydrological processes in an agricultural watershed of India

[*] **Corresponding author: Ajai Singh**
Assistant Professor in Soil and Water Conservation, RRS (OAZ), Uttar Banga Krishi Viswavidyalaya, Majhian, Patiram – 733133, Dakshin Dinajpur, West Bengal, India, E-mail: ajai_jpo@yahoo.com, Phone: 91 3522 253898, Fax: 91 3522 253900

Mohd. Imtiyaz
Professor & Dean, Vauge School of Agricultural Engineering & Technology, SHIATS, Allahabad – 211007, UP, India

R. K. Isaac
Professor, Vauge School of Agricultural Engineering & Technology, Department of Soil Water Land Engg. and Mgt., SHIATS, Allahabad – 211007, UP, India

D. M. Denis
Professor, Vauge School of Agricultural Engineering & Technology, Department of Soil Water Land Engg. and Mgt., SHIATS, Allahabad – 211007, UP, India

Abstract

In the present study, Soil and Water Assessment Tool (SWAT), a river basin or watershed scale model was applied to predict the monthly stream flow and sediment yield of Nagwa watershed in Eastern India. The SWAT model was calibrated and validated with the measured stream flow and sediment yield, and quantification of the uncertainty in the SWAT model output was assessed using Sequential Uncertainty Fitting Algorithm (SUFI-2). Weather data, monthly stream flow and sediment yield data from meteorological station near the outlet of the watershed (1991 to 2007) were used for model set up, calibration and validation of the model. ArcGIS 9.3.1 was used to prepare spatial input data such as digital elevation model, land use land cover and soil maps. The coefficient of determination (R^2) and Nash-Sutcliffe simulation efficiency (*NSE*) values were found to be 0.77 and 0.75 during calibration, and 0.70 and 0.67 during validation periods for stream flow, respectively. R^2 and *NSE* values of 0.77 and 0.77 for the calibration, and 0.68 and 0.66 for the validation periods, respectively, were observed for simulated sediment yield. The values of R-factors were found to be 1.26 and 0.79 for stream flow and sediment yield simulation, respectively, which indicates a wider prediction interval. The values of P-factor show that the percentage of observed stream flow values bracketed by the 95PPU and the SWAT model successfully captured 87% of the measure stream flow data and 82% of the sediment yield data. In other words the SWAT model estimates the stream flow and sediment yield values accurately and with less uncertainty. The SWAT model predictions were quite good keeping in view the approximations and spatial variability involved in simulating the complex hydrological processes.

Keywords. SWAT, SUFI 2, Measured stream flow, Sediment yield, Simulation, Modeling.

Introduction

Pollutant concentrations in the downstream water are usually elevated due to sediment and nutrients derived from agricultural as well as urban areas. Excessive amounts of these pollutants because of mild to severe erosion from upstream watershed can deteriorate stream water quality and cause excessive biological growth. Minimization of the discharges of these pollutants and improved agricultural practices are the only solution to check non point source (NPS) pollution problem. Soil and Water conservationmeasures are adopted on watershed basis. Proper understanding of the watershed's hydrology is important to guide and evaluate the impacts of proposed or ongoing soil and water conservation measures. Since the hydrologic responses of the watersheds vary spatially and temporally, an intensive study of the individual watershed is necessary for developing the management practices and also for applying the results from one watershed to another watershed with the same characteristics. The Damodar Valley Corporation, Hazaribagh, India has taken several initiatives to restore and improve the hydrology, reduce sediment loads and nutrient concentrations, and improve habitat along the upper Sewani River and its watershed. Computer models for modeling the hydrological processes for a watershed are nowadays helping to people engaged in watershed development program. In conjunction with monitoring programs, modeling approach can identify the critical source areas of NPS pollution and accordingly corrective measures can be implemented.

Many watershed hydrological models are in use presently. In this study, Soil and Water Assessment Tool (SWAT) model was used. The SWAT model was developed by US Department of Agriculture – Agriculture Research Service (USDA-ARS). The current SWAT model is a modified and improved version of the Simulator for Water Resources in Rural Basins (SWRRB) model (Arnold and Williams, 1987) which was designed to simulate impacts of management on water and sediment movement. It is a conceptual model that functions on a continuous time step. The model components include weather, hydrology, erosion, sedimentation, plant growth, nutrients, pesticides, agricultural management, channel routing, and reservoir routing. Agricultural components in the model include fertilizer, crops, tillage options, irrigation methods, and grazing and have the capability to include point source loads. The SWAT model predicts the impacts of land management practices on constituent yields from a watershed. SWAT is the continuation of over 30 years of model development within the US Department of Agricultural Research Service. The robustness of SWAT model in predicting stream flow and sediment loads at different watershed scales has been shown in several studies. Srinivasan et al. (1998) concluded that SWAT sediment accumulation predictions were satisfactory for the 279 km^2 Mill Creek watershed located in North Central Texas. Arnold and Allen (1999) used SWAT to simulate average annual sediment loads for five major Texas river basins and concluded that the SWAT predicted sediment yields compared reasonably well with estimated sediment yields obtained from rating curves. Saleh et al. (2000) evaluated SWAT model for the 932.5 km^2 upper North Bosque River watershed in North Central Texas, and found that predicted monthly sediment losses matched with measured data well but SWAT daily output was found to be poor. Santhi et al. (2001a) found that SWAT simulated sediment loads matched with measured sediment loads well for two Bosque River (4277 km^2) sub watersheds, except in March. Tripathi et al. (2003) found that SWAT sediment predictions agreed closely with observed daily sediment yield for the watershed in Damodar-Barakar catchment. Kaur et al. (2004) concluded that SWAT predicted annual sediment yields reasonably well for a test watershed in Damodar-Barakar, India. Van Liew et al. (2005) investigated the effect of different cultivation patterns on reducing erosion in the Lake Creek watershed in southwestern of Oklahoma, USA by

using the SWAT model. Recently many works have been carried out on impact of best management practices scenario on simulation results of the SWAT model. Jacobs and Srinivasan (2005) simulated the impact of land use conversion from forest to cultivated land in the poorly equipped watershed of Upper Tana in Kenya by using the SWAT model. They concluded that sediment loads could be decreased by increasing the reforested areas up to 55%. Mishra et al. (2007) found that SWAT accurately replicated the effects of three check dams on sediment transport within the Banha watershed in northeast India. Cao et al. (2008) applied the SWAT model to simulate two land cover scenarios in the Motueka River catchment, New Zealand and observed that the annual total water yields, quick flow and base flow decreased moderately in the two scenarios when compared with the current land use. Setegnet al. (2010) tested the SWAT model successfully for prediction of sediment yield in Anjeni gauged watershed, Ethiopia.

Since models are playing a very important role in decision making about alternative land management strategies, it is essential to calibrate the model with careful uncertainty analysis. Sources of model structural uncertainty include processes not accounted for in the model such as unknown activities in the watershed, and model inaccuracy due to over-simplification of the processes considered in the model. Other uncertainties in distributed models may also arise due to the large number of unknown parameters and the errors in the data used for parameter calibration. Many uncertainty analysis techniques have been developed to accommodate these uncertainties in the last two decades and have been applied to various catchments. Researchers have developed several uncertainty analysis techniques for hydrological watershed models. These include Bayesian inference methods, such as: the Markov chain Monte Carlo (MCMC) method (Kuczera and Parent, 1998; Yang *et al*., 2008); generalized likelihood uncertainty estimation (GLUE) (Beven and Binley, 1992); parameter solution (ParaSol) (van Griensven and Meixner, 2006); and sequential uncertainty fitting (SUFI-2) (Abbaspour, 2007). GLUE, ParaSol, SUFI-2, and MCMC have been interfaced with SWAT into a single package, referred to as SWAT-CUP (SWAT Calibration Uncertainty Programs) (Abbaspour, 2007). This study aims to calibrate and validate the SWAT model for simulation of monthly stream flow and sediment yield. Uncertainties in the outputs of SWAT model will also be analyzed in this study. In the current study, we used SUFI-2 for a combined calibration and uncertainty analysis of our SWAT model.

Materials and methods

Study area

Keeping in view the objective and availability of hydrological and meteorological data, a small watershed named Nagwa, located in the Upper Damodar Valley, Hazaribagh Command, Jharkhand, India was selected. The watershed is approximately 92.46 km^2 of which about 30-40% is under shrubs and forest and the remaining under cultivation. The average elevation of the command is 540 m from the mean sea level. It is bounded by latitudes of 23^0 59' 08" N to 24 ^{0} 05' 41" N and longitudes of 85 ^{0}16' 35" E to 85 ^{0}23' 45" E.

Preparation of spatial data

The ArcGIS 9.3.1 was used for the analyses of satellite digital data, digitization of contours, construction of Digital Elevation Model (DEM), automatic extraction of watershed parameters and interpretation of results. The extracted watershed information was used to generate the input parameters of ArcSWAT 2009.93.4. The satellite data obtained from Thematic Mapper sensor for path no. 141 and row no 043 (spectral band: 0.45 - 2.35 μm) for October 14, 2006 was used in the present study to prepare the land use land cover maps of

the Nagwa watershed. All the layers were stacked and area of interest was taken out. Supervised method of classification was used to classify the land uses. The maximum likelihood was used as a parametric rule while performing the classification. The statistical probability of any pixel value to decide its particular land use class among the neighboring clusters is computed based on mean and co-variance matrices. The land use classes used mainly include agriculture, dense forest, water, fallow land and urban settlement. Classification accuracy was estimated by using a maximum likelihood report module, which simply compared ground truth pixels with the classified pixels through a confusion matrix. Kappa coefficient, which ranges from 0 to 1, is used for measuring overall accuracy. It was computed for each pixel class based on difference between the actual agreement of the classification and reference data through formation of confusion matrix. The overall classification accuracy of 96.23% and Kappa coefficient of 0.94 were achieved. The required rainfall, stream flow and sediemnt yield data were processed with the MS Excel 2003™.

Model description

SWAT Model

The SWAT model is a physically based, semi-distributed parameter and watershed-scale model that works on a continuous daily time step. It simulates hydrological processes, sediment yield, nutrient and pesticide losses into surface and groundwater, and the effects of land management practices on down stream water quality in large watersheds (Arnold et al., 1998). In the SWAT model, the watershed is partitioned into small sub-basins that are further subdivided into hydrological response units (HRU) based on unique land cover, soil and topographic conditions. The hydrology component of the model determines a soil water balance at each time step based on daily data of precipitation, runoff, evapotranspiration, percolation, and base flow. The SWAT model incorporates the effects of weather, surface runoff, evapotranspiration, crop growth, irrigation, groundwater flow, nutrient loading, pesticide loading and water routing as well as the long-term effects of varying agricultural management practices (Neitsch et al., 2002, 2005). In the hydrologic component, surface runoff is estimated separately for each sub-watershed or HRUs' of the total watershed area and routed to obtain the total runoff for the watershed. Runoff volume is estimated from daily rainfall using modified Soil Conservation Service-Curve Number (SCS-CN) method and Green–Ampt methods. The model requires input of DEM, land use and soil maps as well as weather data such as daily precipitation and temperature. The SWAT model can be used to simulate a single watershed or a system of multiple hydrologically connected watersheds. In this study, the SCS-CN method was used to estimate surface runoff. The SCS curve number is a function of the permeability of the soil, land use, and antecedent soil water conditions. SWAT calculates the surface erosion within each HRU with the Modified Universal Soil Loss Equation (MUSLE).

$$sed = 11.8\left(Q_{surf}.q_{peak}.area_{hru}\right)^{0.56}.K_{USLE}.C_{USLE}.P_{USLE}.LS_{USLE}.CFRG^{0.56} \quad \ldots\ldots\ldots(1)$$

where, sed is sediment yield (ton/day), Q_{surf} is surface runoff volume (mm/ha), q_{peak} is the peak runoff rate (m^3/s), $area_{hru}$ is the area of HRU (ha), K_{USLE} is the USLE soil erodibility factor, C_{USLE} is the USLE cover and management factor, P_{USLE} is the USLE support practice factor, LS_{USLE} is the USLE topographic factor and $CFRG$ is the coarse fragment factors. Further details of ULSE factors are available in Neitsch et al. (2005).

The SWAT model was calibrated against the monthly stream flow and sediment yield measured at the outlet of the watershed during the monsoon season (June to October) for the periods from 1991 to 2004. The input parameters of the model were extracted from the DEM analysis, satellite imagery, maps and field observation. SWAT model was run for several simulations with different values of the input parameters to achieve a well calibrated model. All the values of the input parameters were chosen within the defined limit of the parameter. The manual calibration procedure, based on sensitivity analysis findings on ranking of parameter, was used. After each parameter adjustment, the simulated and measured stream flows were compared to judge the improvement in the model prediction. Mainly stream flow at outlet of the reach which was carrying the outlet of the whole watershed was monitored. Single weather station data for the entire watershed has been taken due to the availability of only one gauging station in the entire watershed.

Uncertainty analysis of SWAT model using SWAT -CUP

As hydrological watershed models are increasingly being used for taking up the appropriate soil and water conservation measures and land management decision, it is logical to calibrate and validate the model with careful sensitivity and uncertainties analysis (Abbaspour, 2010). There are three major sources of uncertainty in the outputs of a hydrological model: structural uncertainty, input uncertainty and parameter uncertainty. The structural uncertainty stems due to several assumptions made to develop the model for simplifying the modeling of the desired process. The uncertainty in input and model parameter may be induced respectively by the error in various weather inputs like rainfall and temperature, and errors related to the non-uniqueness sets of model parameters (Abbaspour, 2008). In this present study, SUFI 2 algorithm was applied by using SWAT CUP. SWAT-CUP consists of five different uncertainty analysis and optimization programs such as Sequential Uncertainty Fitting ver. 2 (SUFI2), Generalized Likelihood Uncertainty Estimation (GLUE), Parameter Solution (ParaSol), Monte Carlo Markov Chain (MCMC), and Particle Swarm Optimization (PSO), which are linked with similar inputs to SWAT. This program allows comparing different optimization algorithms as well as the effect of different objective functions (only with SUFI2) on the final parameter sets. After each round of sampling, the range of each parameter is reduced until two conditions are met: (1) most of the observed variables are bracketed by the 95PPU and (2) the average distance between the upper and lower limits is small. Quantification of the aforementioned conditions depends on the quality of measured data (Talebizadeh, 2009).

The uncertainties are quantified by a measure known as the P-factor, which is the percentage of observed data bracketed by the 95% prediction uncertainty (95PPU). The 95PPU is calculated at the 2.5% and 97.5% levels of the cumulative distribution of an output variable obtained through Latin hypercube sampling. This is calculated by the 2.5^{th} and 97.5^{th} percentiles of the cumulative distribution of every simulated point. As all forms of uncertainties are reflected in the measurements, the parameter uncertainties generating the 95PPU account for all uncertainties. The goodness of fit is assessed by the uncertainty measures calculated from the percentage of measured data bracketed by the 95PPU band and the average distance *d* between the upper and the lower 95PPU can be determined from:

$$\bar{d}_x = \frac{1}{k}\sum_{l=1}^{k}\left(X_U - X_L\right)_l \qquad \text{.....(2)}$$

where, k is the number of measured data points. The best result shows 100% of the measurements are bracketed by the 95PPU and $\bar{d}$ is close to zero. Another measure quantifying the strength of a uncertainty analysis is the R - factor, which may be defined as the average thickness of the 95PPU band divided by the standard deviation of the observed data (Abbaspour, 2008). The R-factor expressed as:

$$R - factor = \frac{\bar{d}_x}{\sigma_x} \quad \text{.....(3)}$$

where σ_x is the standard deviation of the measured variable x. A value of less than 1 is a desirable measure for the R-factor. The goodness of fit and the degree to which the calibrated model accounts for the uncertainties are assessed by the above two measures. Theoretically, the value for P-factor ranges between 0 and 100%, while that of R-factor ranges between 0 and infinity.

Model evaluation techniques

Coefficient of determination (R^2)

It explains the proportion of the variance in measured data explained by the model. R^2 ranges from 0 to 1, with higher values indicating less error variance, and normally values greater than 0.5 are considered acceptable (Santhi et al., 2001a; Van Liew et al., 2003). Although R^2 has been widely used for model evaluation, but it is oversensitive to high extreme values and insensitive to additive and proportional differences between model predictions and measured data (Legates and McCabe, 1999). Coefficient of determination (R^2) can be determined by the following equation.

$$R^2 = \left[\frac{\sum_{i=1}^{n} \left(Y^{obs} - \bar{Y}^{obs} \right) \left(Y^{sim} - \bar{Y}^{sim} \right)}{\sqrt{\sum \left(Y^{obs} - \bar{Y}^{obs} \right)^2} \sqrt{\sum \left(Y^{sim} - \bar{Y}^{sim} \right)^2}} \right] \quad \text{.....(4)}$$

where, Y^{sim} and Y^{obs} are the simulated and observed values, $\bar{Y}^{obs}$ and $\bar{Y}^{sim}$ are the mean of n observed and simulated values.

Nash-Sutcliffe efficiency (NSE)

The Nash-Sutcliffe efficiency (NSE) is a normalized statistic that determines the relative magnitude of the residual variance compared to the measured data variance (Nash and Sutcliffe, 1970). NSE indicates how well the plot of observed versus simulated data fits the 1:1 line. NSE is computed as shown in the following equation:

$$NSE = 1 - \left[\frac{\sum_{i=1}^{n} \left(Y_i^{obs} - Y_i^{sim} \right)^2}{\sum_{i=1}^{n} \left(Y_i^{obs} - Y^{mean} \right)^2} \right] \quad \text{....(5)}$$

where, Y_i^{obs} is the i^{th} observation for the constituent being evaluated, Y_i^{sim} is the i^{th} simulated value for the constituent being evaluated, Y^{mean} is the mean of observed data for the constituent being evaluated, and n is the total number of observations. NSE ranges between $-\infty$ and 1.0, with NSE = 1 being the optimal value. NSE was used in this study for two main reasons: (1) it is recommended for use by ASCE (1993) and Legates and McCabe (1999), and (2) it is very commonly used, which provides extensive information on reported values.

Results and discussion

Stream flow

The Hargreave method of evapotranspiration computation and Muskingum method of routing were found to give best performance under sub-humid region and were adopted in the present study. The major parameters affecting stream flow and sediment yield were modified to increase agreement between the simulated and observed values. During the calibration processe, the curve number was adjusted within the range of ±10% from the curve number value for moisture condition II. These curve numbers were also adjusted for slopes greater than 4%. For simulation of the base flow in the watershed, the base-flow recession constant was adjusted to 0.05. It is directly proportional to groundwater flow response to changes in recharge. Groundwater delay time was adjusted to 43 days. This represents the lag between the times that water exits the soil profile and enters the shallow aquifer. This slightly reduced the overall stream flow and shifts the monthly timing. Groundwater revap coefficient that indicates the rate of transfer of water from the shallow aquifer to the root zone was adjusted to 0.002. The soil evaporation compensation factor was adjusted to 0.87. The calibrated values represent the response of land cover, land management practices, soil properties, and topographic condition of the watershed. The calibration process significantly reduced the difference between the measured and simulated stream flows. These parameters were adjusted to the level where they could represent the characteristics of the existing land use and topographic condition of the watershed. The final fitted values are listed in Table 1.

Table 1. Sensitive parameters for stream flow and sediment yield simulation and their calibrated values.

Parameter	Lower Bound	Upper Bound	Calibrated Value
Sub Initial SCS CN II value, CN2	-25	25	17.63
Baseflow alpha factor (days), Alpha_Bf	0	100	43
Plant uptake compensation factor, EPCO	0	1	0.73
Soil evaporation compensation factor, ESCO	0	1	0.87
GW_REVAP Groundwater "revap" coefficient	-0.036	0.036	0.002
REVAPMN Threshold water depth in the shallow aquifer for "revap" (mm)	-100	100	79.38
SOL_AWC Available water capacity (mm/mm soil)	-25	25	2.53

USLE equation support practice factor (USLE_P)	0	1.00	0.60
Channel erodibility factor (Ch_Erod)	0	1.00	0.14
Linear parameter for calculating the maximum amount of sediment that can be reentrained during channel sediment routing (Spcon)	0.0001	0.01	0.005
Channel cover factor (Ch_Cov)	0	1.00	0.72
Exponent parameter for calculating sediment reentrained in channel sediment routing (Spexp)	1	2.00	1.51
USLE C factor for land cover/plant (USLE_C)	-25	25.00	0.27

The scatter plots of the observed and simulated monthly stream flow for the calibration periods has been shown in Fig.1(top). The major portion of the scatter plot is well distributed about the regression line indicating the model capability of estimating stream flow for well-distributed normal rainfall events. The R^2 value during the calibration period shows a good correlation between observed and simulated values of runoff. The R^2 and NSE values were found to be as 0.77 and 0.75 respectively. Low NSE obtained in this case might be due to underestimated precipitation to the dominant soil type. The SWAT model over predicted almost all the years of validation except in 2007 when rainfall received was highest (Fig. 1 (down)). This year has seen more frequent and intense rainfall as compared to remaining years. Most of the compared points are unevenly distributed around the regression line except a few events of lower magnitudes of stream flow. The SWAT did not perform very well during validation period. This may be due to inconsistency in terms of normal, wet and dry year and anomalies in the observed data. SWAT model simulated stream flow as 2.58 m^3/s against the observed average stream flow of 2.43m^3/s during the calibration periods. During validation periods, SWAT model simulation of stream flow of 3.44m^3/s was found to be overestimated. This is the result of only one of the many similarly good simulations. It is appropriate to show the 95% model prediction uncertainty (95PPU) intervals of the last iteration. It is quite reasonable to judge the performance of the model as represented by the P-factor and the R-factor. In average 87% of the measured monthly stream flow values could be bracketed by the 95PPU and the average R-factor was 1.26 during calibration of SWAT model and P – factor and R – factor were found to be as 27% and 0.51 during validation. Few observed values were bracketed with 95PPU during validation periods. Fig. 2 shows large uncertainties in the years of high rainfall. There are still many other influencing processes which were neglected (e.g., water use, irrigation) or simplified approach (e.g., assigning the dominant soil and land use to represent the whole subbasin), and using generated daily weather parameter except rainfall and temperature due to the limited available information. SWAT does not simulate groundwater flow appropriately. Groundwater recharge is important in these regions. If base flow were better simulated, a larger P - factor as well as a smaller R - factor could be achieved for an overall calibration result.

Sediment yield

Sediment calibration is followed by hydrologic calibration and must be done before water quality calibration. The major sediment parameters are modified to increase agreement between the simulated and observed monthly sediment yield. The over production of total sediment is contributed mainly from the high rains during the month of August and September and also due to the sediment load estimation from rainfall quantity. The overall prediction of the monthly sediment yield during the whole calibration period was in close agreement with its observed values. The scatter plots between the observed and simulated monthly sediment yield along with the regression line are presented in Fig. 3 (top) for the calibration periods. The figure shows an even distribution of the simulated values about regression line for both lower and higher measured values. A close relationship between observed and simulated sediment yields are indicated by the value of R^2 and NSE as 0.77 and 0.77, respectively. The calibrated model was validated for the monsoon season (June to October) for the years 2005-2007. The scatter plots between the observed and simulated monthly sediment yield along with the regression line are presented in Fig. 3 (down). The simulated values are evenly distributed about regression line for both lower and higher measured values. The figure shows that the months receiving high rainfall are under predicted by the model and this is attributed to the quantitative approach of model in simulation rather

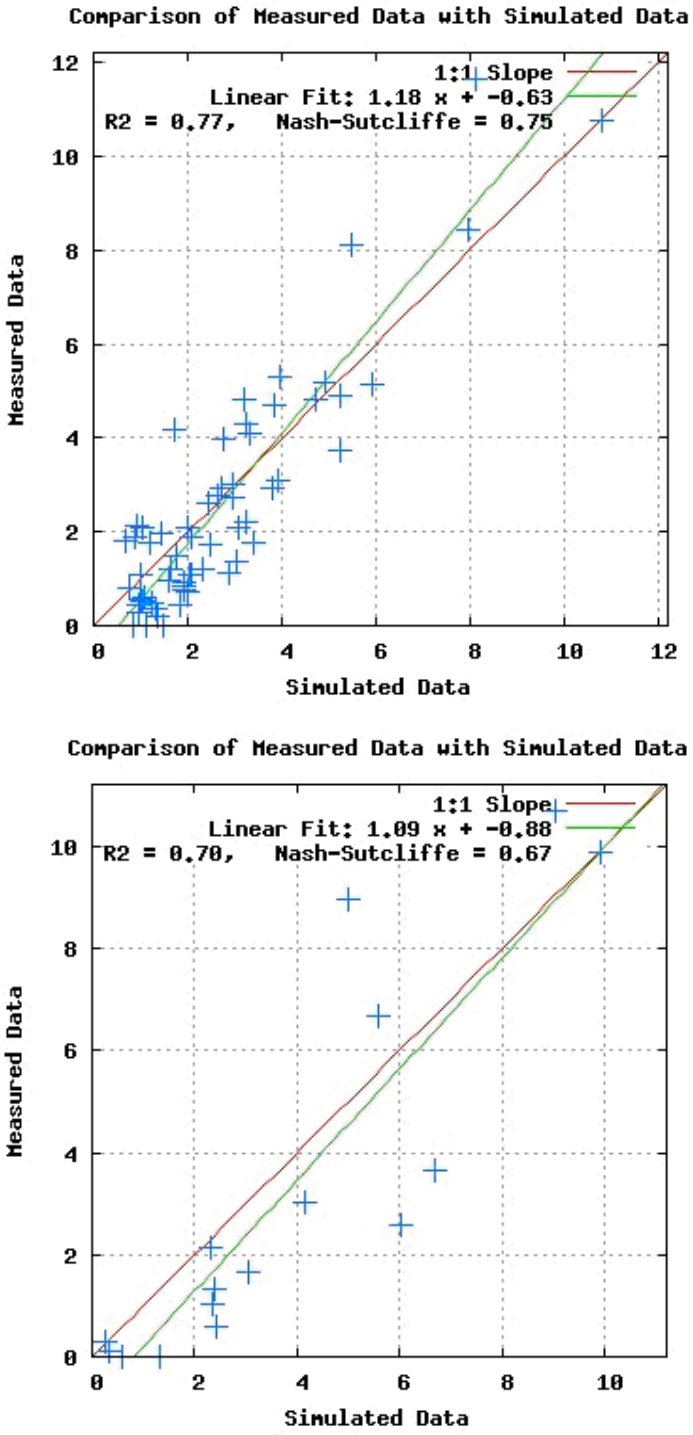

Fig. 1 Scatter plots of monthly measured and SWAT simulated stream flow (m^3/s) for calibration periods (top) and validation periods (down).

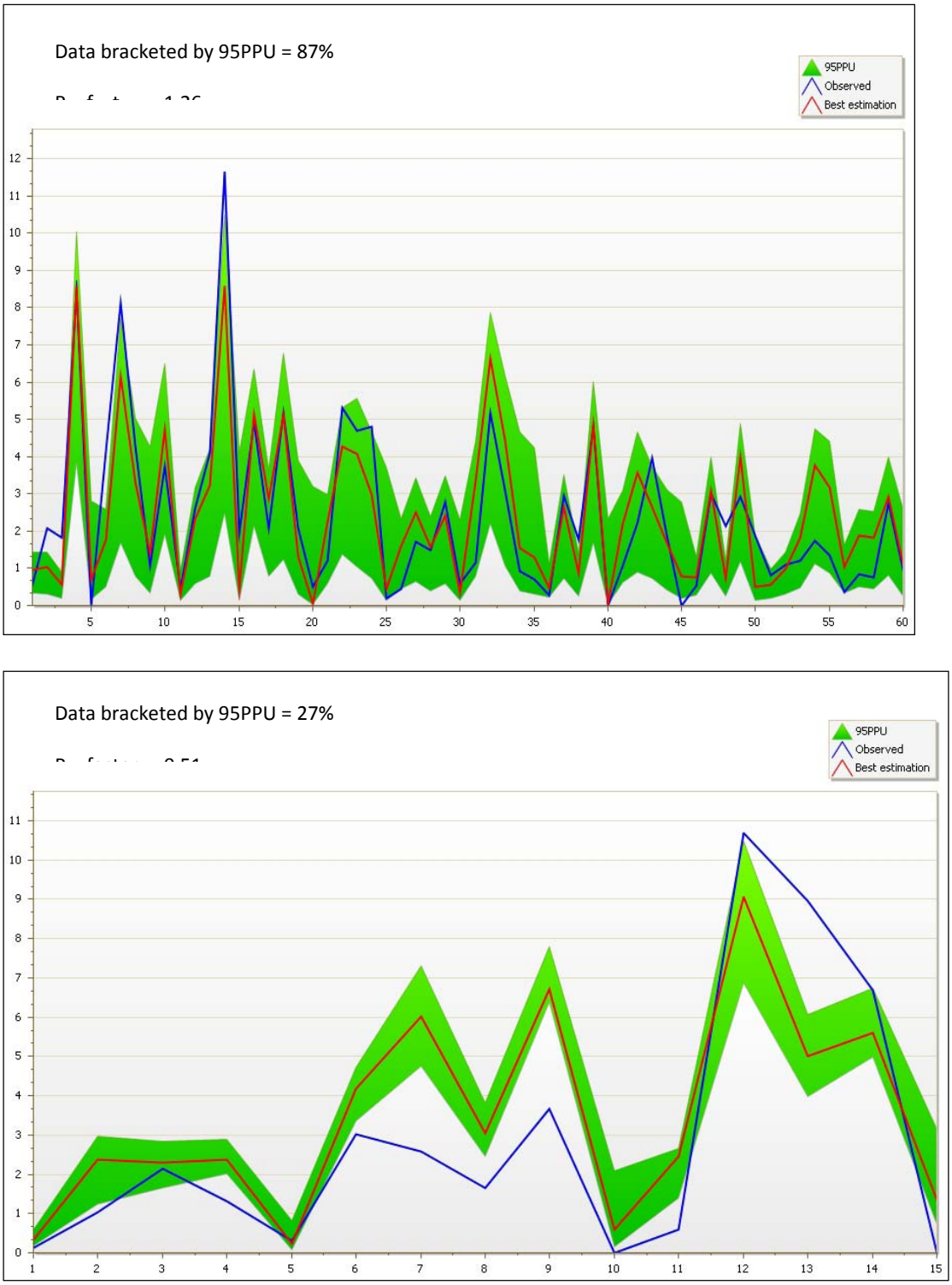

Fig. 2. 95% prediction uncertainty intervals along with the measured and simulated stream flow for SWAT Model during calibration (top) and validation (bottom) periods.

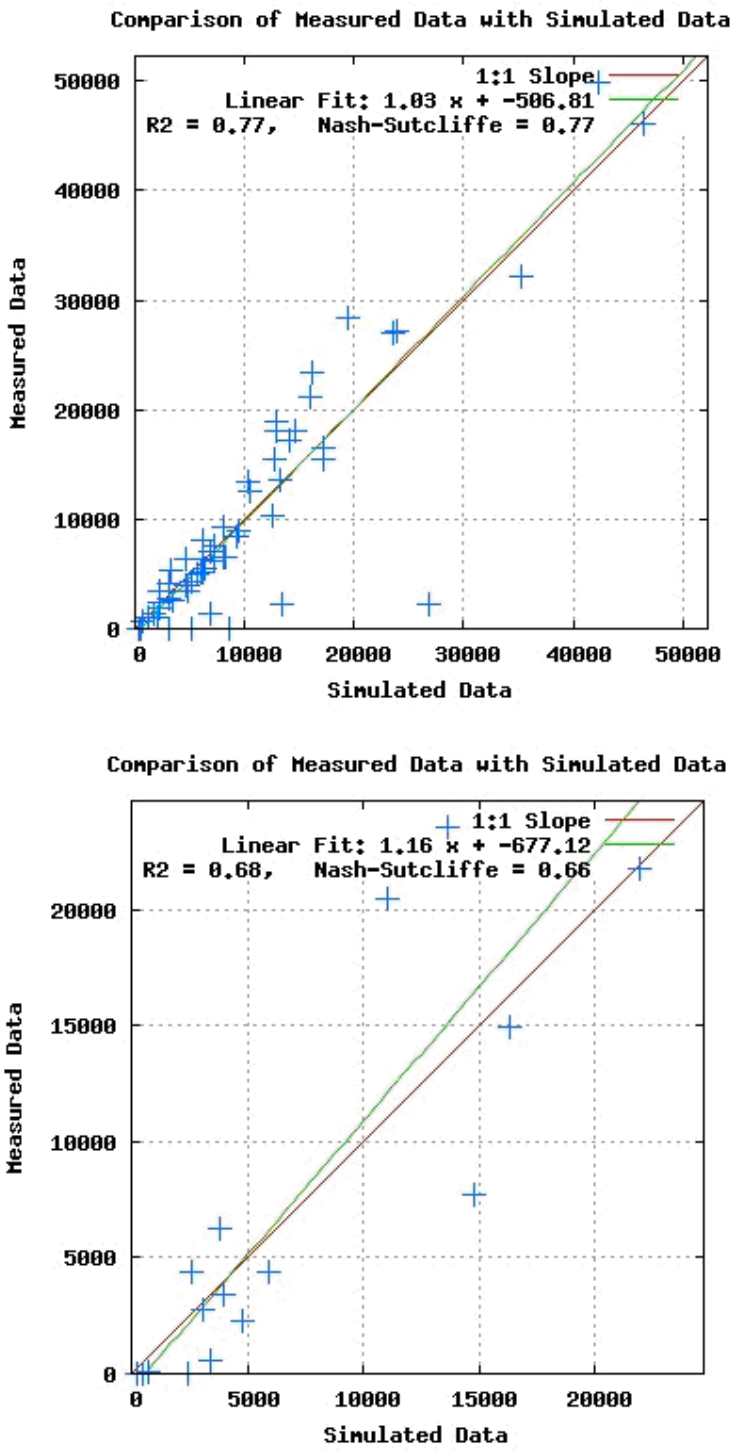

Fig. 3. Scatter plots of monthly measured and SWAT simulated sediment yield (ton) for calibration (top) and validation (bottom) periods.

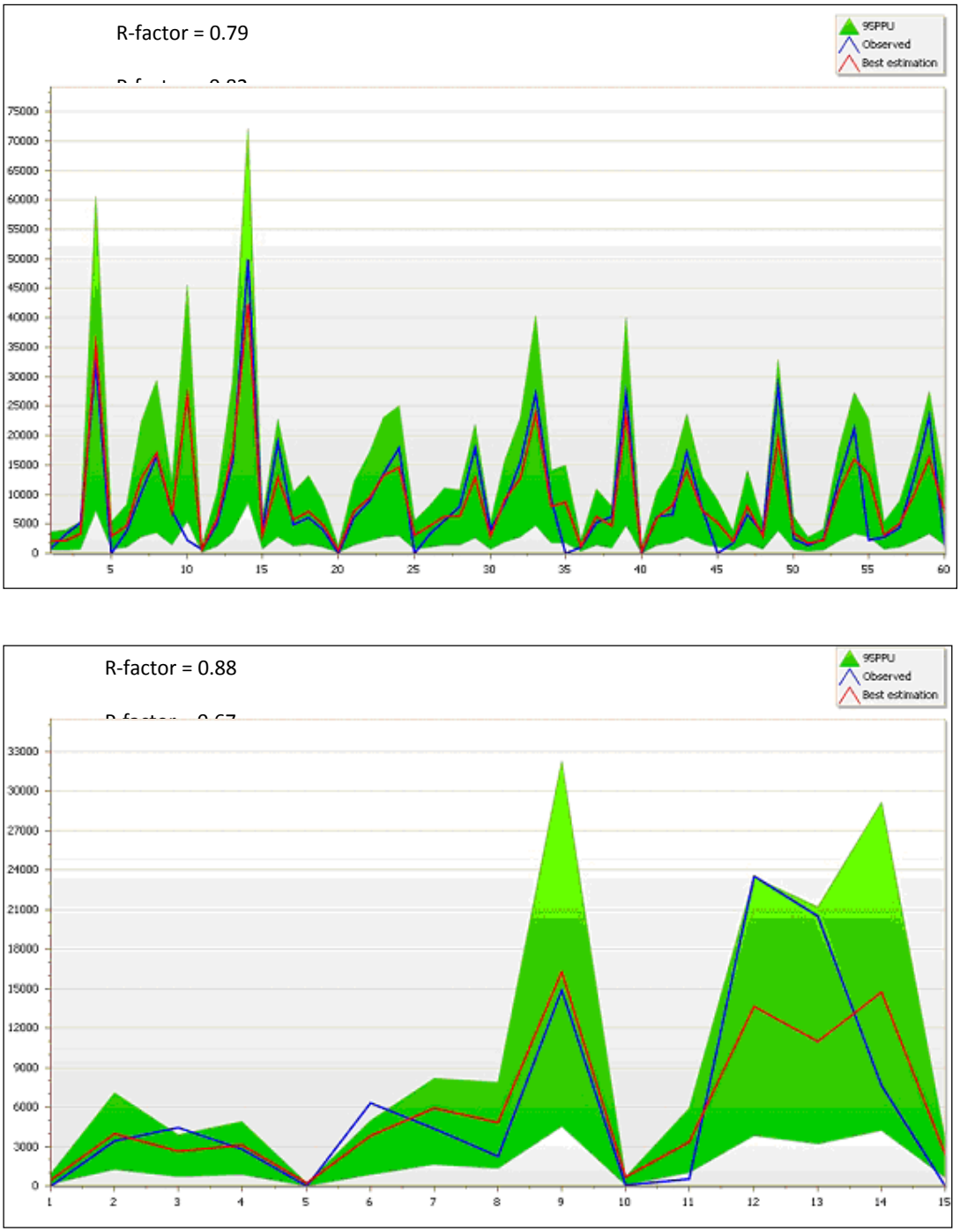

Fig. 4. 95PPU for observed and SWAT simulated monthly sediment yield (ton) at the watershed outlet during calibration periods (1993–2004) and validation periods (2005–2007) shown above and bottom.

than rainfall characteristics. The model performed quite well during validation with R^2 and NSE values as 0.68 and 0.66, respectively. The average R-factor and P-factor were found to be as 0.79 and 0.82 during calibration of SWAT model (Fig. 4), and R – factor and P - factor were observed as 0.88 and 0.67, respectively, during validation. On the basis of calibration and validation results, it can be inferred that ArcSWAT (Version 2009.93.4) can be successfully applied for the management options of soil and water conservation as well as for the identification of best management practices for the study watershed.

Conclusions

In the present study, an attempt was made to calibrate and validate the SWAT, a process based model for simulation of stream flow and sediment yield for a watershed where erosion and water quality problems exists. Monthly simulated stream flow and sediment yield were compared with observed values collected at the Nagwa watershed gauging station for calibration and validation periods. Monthly simulations show good agreement between measured and simulated values of stream flow and sediment yield. The value of R-factor in the SWAT model was found to be as 1.26 which means a wider prediction interval. The value of P-factor in SWAT model was observed as 87% which indicates that the model has been able to bracket 87 of the measured stream flow data within 95PPU. The model predicted closely to the measured values during calibration and validation. Overall, the SWAT model offers the most comprehensive representation of hydrological processes that can be of great help in taking decisions on the land use management alternatives impacting downstream water quality. SWAT model predictions were quite good keeping in view the approximations and spatial variability involved in simulating the complex hydrological processes.

Acknowledgements

The author would like to acknowledge the Department of Soil and Water Conservation, Damodar Valley Corporation, Hazaribagh, Jharkhand, India for sharing their data for this research work.

References

Abbaspour, K. C. 2007. User Manual for SWAT-CUP, SWAT Calibration and Uncertainty Analysis Programs. Swiss Federal Institute of Aquatic Science and Technology, Eawag, Dübendorf, Switzerland.

Abbaspour, K.C. 2008. SWAT-CUP user manual. Federal Institute of Aquatic Science and Technology (Eawag), Swiss

Abbaspour, K.C., M. Vejdani, and R. Srinivasan.2010. SWAT-CUP: A Calibration and Uncertainty Analysis Program for SWAT, *International SWAT Conference*, Seoul, Korea, August 14-16, pp 21.

Arnold, J. G., and J.R.Williams.1987. Validation of SWRRB: Simulator for water resources in rural basins, *J. Water Resour. Plan. Manage*, 113(2): 243-256.

Arnold, J.G., R. Srinivasan, R.S. Muttiah, and J.R.Williams.1998. Large area hydrologic modelling and assessment part I: model development. *J. American Water Resour. Assoc.*, 34(1): 73–89.

Arnold, J. G., and P.M. Allen.1999. Automated methods for estimating base flow and groundwater recharge from stream flow records. *J. American Water Resour. Assoc*., 35(2): 411-424.

ASCE. 1993. Criteria for evaluation of watershed models. *J. Irrigation Drainage Eng.* 119(3):429-442.

Beven, K., and A. Binley.1992. The future of distributed models—model calibration and uncertainty prediction. *Hydrol.Processes*, 6(3): 279–298.

Cao, W., B. W. Bowden, T. Davie, and A. Fenemor.2008. Modelling impacts of land cover change on critical water resources in the Motueka River catchment, New Zealand, *Water Resour. Manag*., 23(1): 137–151.

Jacobs, J.H., and R. Srinivasan.2005. Application of SWAT in developing countries using readily available data. In: *3rd International SWAT Conference*, Zurich, July 11–15.

Kaur, R., O. Singh, R. Srinivasan, S.N. Das, and K. Mishra.2004. Comparison of a subjective and a physical approach for identification of priority areas for soil and water management in a watershed: A case study of Nagwan watershed in Hazaribagh District of Jharkhand, India. *Environ. Model. Assess*, 9(2): 115-127.

Kuczera, G., and E. Parent.1998. Monte Carlo assessment of parameter uncertainty in conceptual catchment models: the Metropolis algorithm. *J. Hydrol,* 211(1–4): 69–85.

Legates, D. R. and G. J. McCabe.1999. Evaluating the use of "goodness-of-fit" measures in hydrologic and hydroclimatic model validation, *Water Resources Res*. 35(1): 233-241.

Mishra, A., S. Kar, and V.P. Singh.2007. Prioritizing structural management by quantifying the effect of land use and land cover on watershed runoff and sediment yield, *Water Resour. Manag*, 21:1899–1913.

Nash, J. E., and J. V. Sutcliffe.1970. River flow forecasting through conceptual models: Part I. A discussion of principles, *J. Hydrol*, 10(3): 282-290.

Neitsch, S.L., J.G. Arnold, J.R. Kiniry, J.R. Williams, and K.W. King.2002. Soil and Water Assessment Tool Theoretical Documentation (Version 2000). Grassland, soil and Water Research Laboratory, Agricultural Research Service, Temple, TX.

Neitsch, S.L., J.G. Arnold, J.R. Kiniry, and J.R. Williams.2005. Soil and Water Assessment Tool (SWAT), Theoretical Documentation. Blackland Research Center, Grassland, Soil and Water Research Laboratory, Agricultural Research Service: Temple, TX.

Saleh, A., J.G. Arnold, P.W. Gassman, L.W. Hauck, W.D. Rosenthal, J.R. Williams, and A.M.S. McFarland.2000. Application of SWAT for the upper North Bosque River watershed. *Trans. ASAE*, 43(5):1077-1087.

Santhi, C., J.G. Arnold, J.R. Williams, W.A. Dugas, and L. Hauck.2001a. Validation of the SWAT model on a large river basin with point and non point sources, *J. Am. Water Resour. As*., 37(5): 1169–1188.

Setegn, S.G., B. Dargahi, R. Srinivasan, A.M. Melesse.2010. Modeling of sediment yield from Anjeni-Gauged watershed, Ethiopia using SWAT Model. *Journal of the American Water Resources Association*, 46(3):514-526.

Srinivasan, R., T.S. Ramanarayanan, J.G. Arnold, and S.T. Bednarz.1998. Large area hydrologic modeling and assessment part II: model application, *J. American Water Resour. Assoc,* 34(1):91– 101.

Talebizadeh, M., S. Morid, S.A.Ayyoubzadeh, and M.Ghasemzadeh.2009. Uncertainty analysis in sediment load modeling using ANN and SWAT model. *Water Resources Management.* 24 (9):1747-1761.

Tripathi, M. P., R.K. Panda, and N.S. Raghuwanshi. 2003. Identification and prioritisation of critical sub-watersheds for soil conservation management using the SWAT model. *Biosys. Eng,* 85(3): 365-379.

Van Griensven, A., and T. Meixner.2006. Methods to quantify and identify the sources of uncertainty for river basin water quality models. *Water Sci. Techno,* 53(1): 51–59.

Van Liew, M. W., and J. Garbrecht (2003), Hydrologic simulation of the Little Washita River experimental watershed using SWAT, *J. American Water Resour. Assoc*. 39(2), 413-426.

Van Liew, M. W, Arnold GJ (2005) Downstream sediment response to conservation practice implementation. In: 3th international SWAT conference, Zurich, 11–15 July 2005

Yang, J., Reichert, P., Abbaspour, K. C., Xia, J. and Yang, H. (2008) Comparing uncertainty analysis techniques for a SWAT application to the Chaohe Basin in China. *Journal of Hydrology*, 358, 1– 23.

Adaptation of Multi-Purpose Dam Operation for Representative Dam in South Korea to the Future Climate Change

Jong-Yoon Park, Doctoral candidate
Dept. of Civil and Environmental System Eng., Konkuk University, 1 Hwayang dong, Gwangjin-gu, Seoul143-701, South Korea, E-mail: bellyon@konkuk.ac.kr

In-Kyun Jung, Ph.D.
Dept. of Civil and Environmental System Eng., Konkuk University, 1 Hwayang dong, Gwangjin-gu, Seoul143-701, South Korea, E-mail: nemoik@konkuk.ac.kr

Cheol-HeeJang, Researcher
Korea Institute of Construction Technology, 2311 Daehwa dong, Ilsan-gu, Goyang-si,

Gyeonggi-do411-712,South Korea, E-mail: chjang@kict.re.kr

Seong-Joon Kim*, Professor
* Dept. of Civil and Environmental System Eng., Konkuk University, 1 Hwayang dong, Gwangjin-gu, Seoul143-701, South Korea, Corresponding author, E-mail: kimsj@konkuk.ac.kr

Abstract

The impacts of climate change on long-term reservoir operations for water resource system of the Chungju multi-purpose dam in South Korea were evaluated with monthlyimpact indicators. The climatic data predicted by ECHAM5-OM, HadCM3, and MIROC3.2 HiResoutputs for three time periods (2020s, 2050s, and 2080s) were downscaled using the stochastic weather generator (LARS-WG). The MIROC3.2 HiRes A1B 2080s temperature and precipitation showed an increase of +4.2°C and 37.7%, respectively, basedon the 1990-2009 dataBy applying the climate prediction to Soil and Water Assessment Tool (SWAT), the dam inflow was evaluated. Hydrologic Engineering Center – Reservoir System Simulation (HEC-ResSim) was used to simulate water supply by dam operation in the future. The purpose of linking the hydrologic and reservoir operation models was to predict changes in water supply and hydropower production resulting with the future climate change scenarios.The projections indicate an increase in annual dam inflow,later peaks and greater volumes during the flood season.According to simulation results bydam operation rule in the future, the tendency is for anincrease in average annual water supply anda reduction in spills, depending on dam inflow change. The main results indicate that average annual water supply and hydropowerwould change by +19.8 to +56.5% and +33.9 to 92.3% in the 2080s, respectively. Model simulations suggest that, under theA1B and B1 emission scenarios of the three GCM models, water supply reliability is generally improved as a consequence of increased dam inflow.

Keywords: Climate change; Hydropower; Reservoir operation; Water management; SWAT

Introduction

Climate change is now an unequivocal truth, andit is expected to strongly affect the hydrologic cyclein the coming decades (Milly et al., 2005; Gedney et al., 2006). Even though climatechange would accelerate water cycles and thereforefreshwater resources may be less limited in the nextcentury, risk of water related problems will be stillremaining in the future due to changes in seasonalpatterns and increased extreme events (Oki and Kanae, 2006; Betts et al., 2007).The change inthe streamflow regime results in a substantial impact on regional water resources andseasonal water supplies (Li et al., 2010).South Korea has 15 multi-purpose dams. There are located in upstream areas of the five major rivers (Han, Keum, Nakdong, Yeongsam, and Seomjin Rivers) and the priority for water supply is given to domestic and industrial uses, though the greatest amount of water is still consumed by agricultural purposes. The total reservoir capacity of the developed multi-purpose dams is 11.3 billion m^3 this provides an annual water supply of 10,461 m^3, flood control of 2.03 billion m^3, and 1 million KW of electricity. Operation of multi-purpose dams obviously is sensitive to watershed hydrology depends on climate change. Therefore, as a result of watershed environmental changes such as climate, land use and vegetation change, and human activity causes, affect the frequency and intensity of drought and flood, the existing dam operation rules may need to change.When operation rules are determined based on regional climate condition, we need to evaluate the water supply capacity by hydrologic impact assessment in the future with water demand.

Water managers can adapt to climate variability by structural change, such as increasing the size or number of dams, building desalination plants and transferring water between catchments; however, a broader set of alternatives with multiple beneficial outcomes for society and the environment should be explored (Watts el al., 2011). On the other hand, we will be able to establish anadaptation strategy to climate change by nonstructural change, such asmodifying dam operations (e.g. flood management, hydropower or water supply). The aim of this study is to evaluate the future potential climate change impacts on multi-purpose dam operation. For Chungjudam of 2.75 billion m^3 storage capacity with watershed of 6,642 km^2, a reservoir simulation model was adopted to predict water supply capacity related to dam operation using the HEC-ResSim model with the Soil and Water Assessment Tool (SWAT) simulated results (Park et al., 2011) of future dam inflow by applying the GCMs output data as HEC-ResSim boundary conditions.

Material and Method

Reservoir simulation model

HEC-ResSim is one such reservoir simulation model. It has been developed by the Hydrologic Engineering Center (HEC) of the US Army Corps of Engineers (USACE) to aid engineers and planners in predicting the behavior of reservoir systems in water management studies, and to help reservoir operators plan releases in real time during day-to-day and emergency operations. HEC-ResSim is unique among reservoir simulation models because it

attempts to reproduce the decision making process that human reservoir operators must use to set releases. The program represents the physical behavior of reservoir systems with a combination of hydraulic computations for flows through control structures, and hydrologic routing to represent the lag and attenuation of flows through segments of streams.

HEC-ResSim uses an original rule-based approach to mimic the actual decision-making process that reservoir operators must use to meet operating requirements for flood control, power generation, water supply, and environmental quality. Parameters that may influence flow requirements at a reservoir include time of year, hydrologic conditions, water temperature, and simultaneous operations by other reservoirs in a system. The reservoirs designated to meet the flow requirements may have multiple and/or conflicted constraints on their operation. HEC-ResSim describes these flow requirements and constraints for the operating zones of a reservoir using a separate set of prioritized rules for each zone. Basic reservoir operating goals are defined by flexible at-site and downstream control functions and multi-reservoir system constraints (Klipsch and Hurst, 2007).

Study area and HEC-ResSim modeling data descriptions

Figure 1 show the Chungjudam watershed, which has a total area of 6,642 km^2 and is located in the northeast of South Korea. The watershed elevation ranges from 115 m to 1559 m, with an average hillslope of 36.9% and elevation of 609 m. More than 82.3% (5,469 km^2) of the watershed area is forested and 12.2% is cultivated. The average annual precipitation is 1,261 mm, with a mean temperature over the last 30 years of 9.4℃. A Chungju multi-purpose dam is located at the watershed outlet, 97.5 m in height, 447 m in length, and with a volume of 2.75 billion m^3, is one of the most important dam which provides energy (412MW of capacity) and water for Seoul (metropolitan city of South Korea) and adjacent urban areas, and irrigation of 22,000 hectares, and flood protection for rural area, and 334 million m^3/year water for stream maintenance. The flood water level (FWL) is 145.0 EL.m, the normal high water level(HWL) is 141.0EL.m, the lowestwater level (LWL) is 110.0 EL.m, and the dead water level (DWL) is 86.0 EL.m. Reservoir is spread to the directions of the east and the west with the maximum depth of 22.0 m, and the average depth of 14.6 m. The detail spatial information of land use and soil, and description of study watershed is found in Park et al. (2011).

The HEC-ResSim model setup of the watershed will include major inflows to the Chungju dam where time-series flow data is available including the Han River, and Jaecheon, Gogyo, Dongdal and Gwang streams, as well as cumulative local inflows (fig. 1a). For calibration and validation of theHEC-ResSim model, the 21 years (1990-2010) of daily dam release (water supply and spillway), storage and water level data were obtained from Korea Water Resources Corporation (K-water). The characteristic parameters of the Chungju dam are shown in figure 1b.

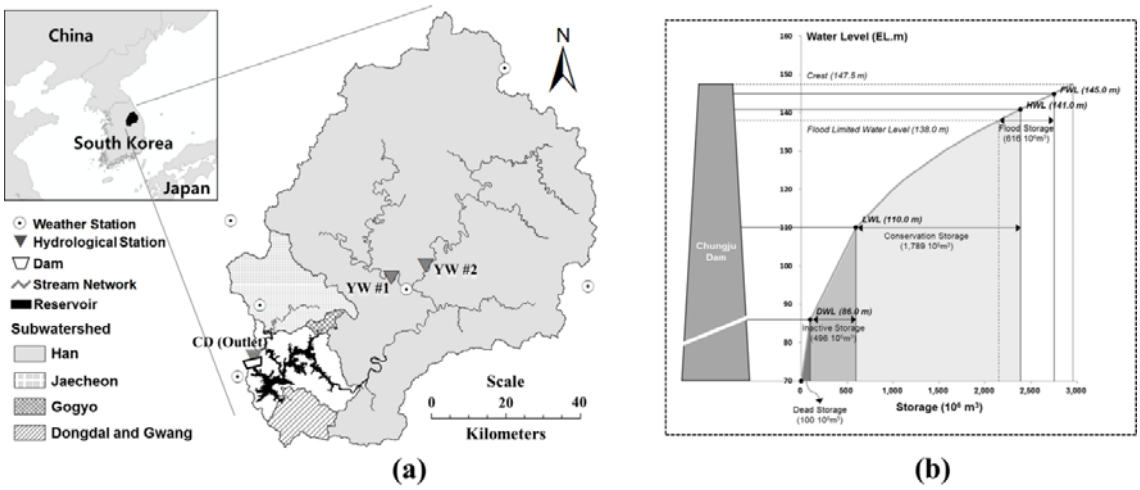

Figure 29. Location of Chungju multi-purpose dam and its watershed: (a) weather and hydrological stations in the watershed, and (b) reservoir storage zones and index levels.

The calibrated SWAT and HEC-ResSim models were linked so that output (daily dam inflow) from the SWAT model became input for the HEC-ResSim model.SWAT is a physically-based continuous, long-term, distributed-parameter watershed model designed to predict the effects of land management practices on the hydrology, sediment and contaminant transport in agricultural watersheds under varying soils, land use and management conditions (Arnold et al., 1998). Further details can be found in the SWAT theoretical documentation (Neitsch et al., 2002).

The SWAT model was calibrated for six years (1998-2003) and validated for another seven years (2004-2010) using daily streamflow data at three locations (YW #1, YW #2 located upstream, and CD at the watershed outlet: shown in Figure 1a) with 0.24 ~ 0.80 Nash and Sutcliffe (1970) model efficiencies. Table 1 shows a statistical summary of the SWAT model calibration and validation. Detailed calibrated parameters and model results can be found in Park et al. (2011).

Table 11.SWAT calibration and validation results of streamflowat three locations.[a]

Static		YW #1		YW #2		CD (Outlet)	
		Cal.	Val.	Cal.	Val.	Cal.	Val.
Rainfall (mm/yr)		1573.2	1374.1	1573.2	1618.1	1573.2	1374.1
Streamflow (mm/yr)	Obs.	765.1	860.3	914.2	964.7	873.5	848.7
	SWAT	850.5	838.4	871.3	1351.2	857.3	800.0
Runoff ratio (%)	Obs.	48.1	62.0	57.0	59.0	53.8	60.6
	SWAT	52.2	60.2	53.9	82.9	53.3	57.3
Evaluation criteria[b]	RMSE	2.59	4.16	2.83	3.22	1.80	4.27
	NSE	0.71	0.47	0.62	0.24	0.80	0.60
	R^2	0.74	0.56	0.72	0.67	0.88	0.64

[a]Cal. = calibration period (1998-2003) and Val. = validation period (2004-2010).

[b] RMSE = the root mean square error (mm/day), NSE = the Nash and Sutcliffe (1970) model efficiency, and R^2 = the coefficient of determination.

The future climate and inflow scenarios for dam operation

The general circulation model (GCM) data source used for this study is future climatedata, which were obtained from the ECHAM5-OM, HadCM3 andMIROC3.2 HiRes, model outputs.TheECHAM5-OM model, developed at the Max Planck Institutefor Meteorology in Germany, has a spatial resolution ofapproximately 1.9°. The HadCM3 model, developed atthe UK Meteorological Office, has a spatial resolution ofapproximately 3.7°.The MIROC3.2 HiRes model, developedat the National Institute for Environmental Studies in Japan,has a spatial resolution of approximately 1.1°. We adopted the three GCM data for 1900 to 2100 using two(A1B and B1) Special Reported on Emissions Scenarios (SRES) of the Intergovernmental Panel on Climate Change (IPCC) Fourth Assessment Report(AR4).

In this study, the downscaling was performed in two steps. First, biascorrections were carried out for each weather station by applyingthe Alcamo et al. (1997) and Droogers and Aerts(2005) method. The temperature and precipitation data of three GCM data were corrected by fitting the 20C3M (20thcentury simulations, 1979-2010) data with the observed data(1979-2010) to give similar statistical properties.This method is generally accepted within the globalchange research community (IPCC-TGCIA, 1999). The detailed procedures can be found in Park et al. (2011). Second, the three GCM data were downscaled using the Long Ashton Research Station – Weather Generator (LARS-WG) stochastic weather generator. LARS-WG is based on the series weather generatordescribed in Racsko et al. (1991) and in Semenov and Barrow (1997).Using LARS-WG and the output from the three GCMs, We generated daily weather (temperature and precipitation) for four time periods: the baseline representing 1990–2009,the 2020s (2010-2039), the 2050s (2040-2069) and the 2080s (2070-2099) for sixground meteorological stationsnear or within the study area.

Figure 3 shows the annual changes in the 2020s, 2050s and 2080s downscaled temperature and precipitation based on the 1990-2009(baseline) data. The increases in temperature vary from approximately 0.5 to 1.1°C, 1.5 to 2.8°C and 2.5 to 4.3°C for the 2020s, 2050s and 2080s, respectively. The future 2080s temperature increased by 3.3°C in winter (December-February), 2.6°C in autumn (September-November), 4.1°C in summer (June-August) and 4.1°C in spring (Mar-May) for three GCMs. Among the three GCMs, the biggest change of temperature were +7.7°C in summer of 2080s HadCM3 A1B scenario. Meanwhile, the downward tendencies of temperature were also appeared in winter of HadCM3 A1B and B1 scenarios.The future annual precipitation of the three GCMs increased 2.8 to 22.2% for2020s, 7.1 to 38.0% for 2050s, and 8.6 to 37.7% for 2080s,respectively. The future precipitationin the spring, autumn and winter seasons showed an increase regardlessof the all the three GCMs. In contrast, for the summer season, future precipitation showed a tendency to decrease in the ECHAM5-OM A1B and B1 scenarios. Among the three GCMs, the biggest changein precipitation was +88.2% in the winter season of the 2080sunder the MIROC3.2 HiResB1 scenario.

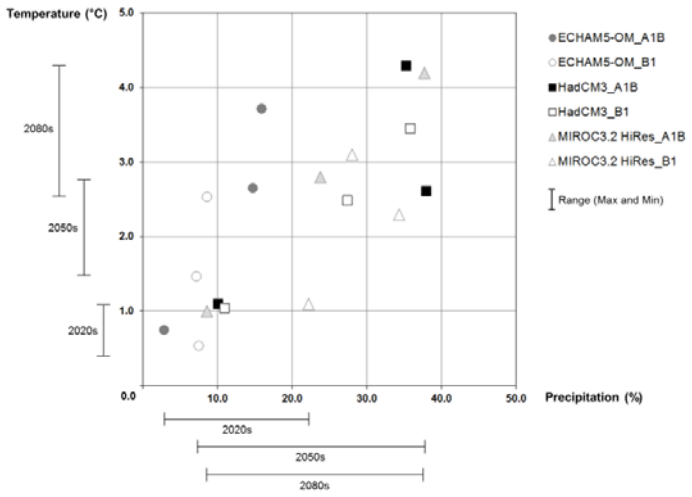

Figure 30. Scatter plots of annual temperature and precipitation changes for three GCMs.

By applying the future ECHAM5-OM, HadCM3, and MIROC3.2 HiRes downscaled climate change scenarios, SWAT was run to evaluatethe future impact of climate change on dam inflow.The future annual dam inflow showeda large range of changes, between -4.7% and +9.5% under the A1B scenario of ECHAM5-OM, between +8.3% and +44.0% under the B1 scenario of HadCM3, and between +3.6% and +40.9%, underthe A1B scenario of MIROC3.2 HiRes.Lookingat the monthly results, as shown in figure 3, we can detectsimilar characteristics for future rainfall-runoffrelation betweenthe HadCM3 and MIROC3.2 HiRes. However,in the case of the2020s A1B scenario of ECHAM5-OM, considerable inflowchanges, within -12.4% and -20.6%, was predicted for spring and summer seasons because of the futurerainfall decrease and evapotranspiration increase.The magnitude of the inflow peaks in the study area will be bigger, and there will be a marked shift in the timing as flood season (from June to September) become warmer and autumn precipitation increase. The future dam inflow in the autumn and winter seasons showed an increase regardless of the three GCM data.

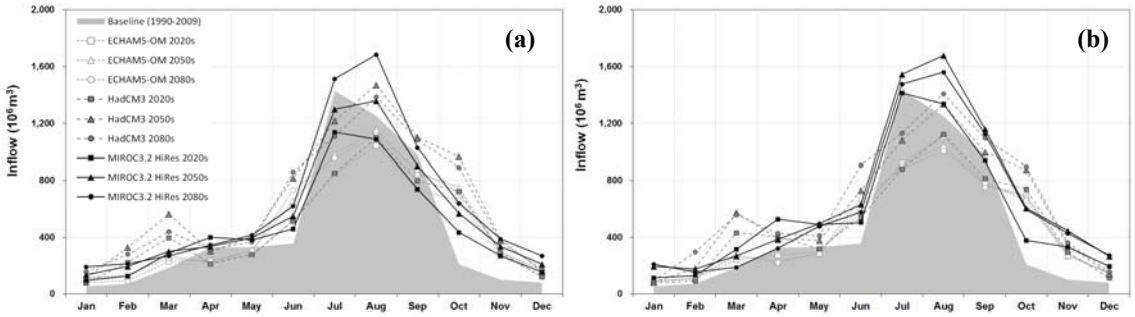

Figure 31. The future monthly dam inflow under (a) A1Band (b) B1 scenarios of ECHAM5-OM, HadCM3, and MIROC3.2 HiRes in the 2020s, 2050s, and 2080s for HEC-ResSim evaluation.

Dam operation rules and impact indicators

The Chungju multi-purpose dam was planned to supply water annually, in 2,731 million m^3 for municipal and industrial purpose, in 315 million m^3 for irrigation, and 334 million m^3 for the environment. Current annual operations are divided into two periods: dry season(September 21 to June 20) and flood season (June 21 to September 20). During dry season, dam release is modulated to ensure a stable supply of water and power within conservation storage. Duringflood season, the water level is managed according to the anticipatedsummer flood. The operations are carried out according to a monthly targetrelease for controlled reservoir. In the rice growing period during April 1 to September 30,irrigation water is managed according to the irrigation requirements for paddy area.The future waterdemand is assumed to be the same withthe climate changes and with the baseline period.Climate change impacts on the Chungju multi-purpose dam operation of this water resourcesystem are evaluated by entering each of future inflows simulated with SWAT under 6 projectionsof climatic changes into the simulation model, while preservingthe current operation rules. Those simulations werecompared with the simulations of the baseline period.

The performance ofthereservoirwas evaluatedintermsofreliabilityandvulnerabilitycriteriaunderbothexistingandfutureclimateconditions. The reliabilityand vulnerability areused here as indices to evaluate the performance of a waterresources system in meeting demand (Hashimoto et al.,1982; Fowler et al., 2003). Reliabilityisameasureofthefrequencyofthereservoirtofailtosupplywaterforalldemands.Vulnerabilityisameasureofthesignificance offailure.Moy et al. (1986) and Simonovic et al. (1992) further developed the conceptof vulnerability. For example, vulnerability may be defined as the magnitude ofthe largest deficit of water during the period of operation.

Results and Discussion

HEC-ResSim model calibration

The calibration and validation of HEC-ResSim model was performed for 21 years (1990-2010) ofdaily inflow, release and water level data from Chungju dam. This is the only period for which both observed inflowsand water level data were available.The inflow data include losses of pool seepage and reservoir evaporation. The model was modified to adjust the references to the specified release and the model was allowed to make the release determination for each period. The accounting of releases includes water supply and spillway from the reservoir, losses through reservoir evaporation, and losses through the reservoir's pool seepage. Figure 4 shows comparison of the observed and simulated water levels and releases. The simulation results at this point appear reasonable. Meanwhile, several factors should be considered when comparing the water levels. For example, we can infer from human element, uncertainty of inflow data, and pool elevation-storagecurve that factors led to the errors.

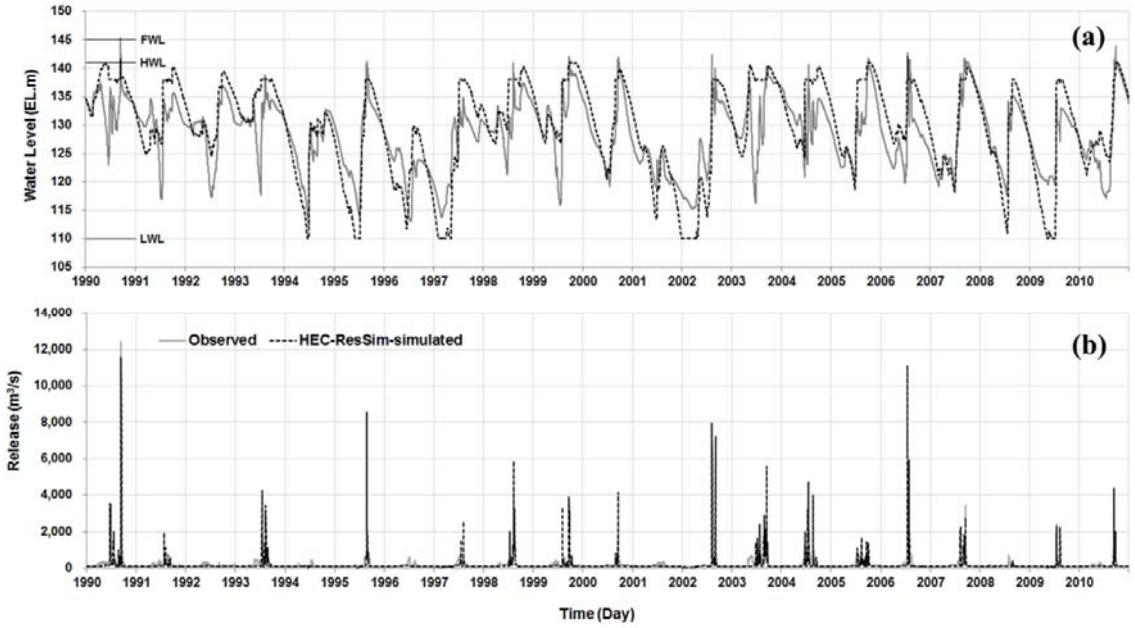

Figure 32.Comparison of the observed and HEC-ResSim-simulated daily (a) water levels and (b) releases from Chungju dam.

Climate change impacts on the water resource system

By applying the future downscaled climate change scenarios, HEC-ResSim was run to evaluate the future impacts of climate change on the water resource system (specifically water system indicators, water supply capacity, and hydropower plant). The reliability and vulnerability are applied to the baseline period and future climate change scenarios. For each

scenario, demand is assumed to be the same as the baseline. Table 2 shows the summary of water resource system performanceresults in the future.Under the baselinescenario the reliability of water supplies within thesystem is generally high, but vulnerability is low as a result. On the other hand, Model simulations suggest that, under the three GCM scenarios, water supply reliability is generally improved as a consequence of increased dam inflow. Meanwhile, the reservoir was vulnerable under four scenarios. Supply vulnerability is decreased in general, with the longest duration of failure being 5 months (2080s of the ECHAM5-OM B1) compared 6 months for baseline period.

Figure 5 shows the simulated monthly water supply for baseline, 2020s, 2050s, and 2080s climate conditions. Water supply capacity is increased in the future for which the reliability is improved as shown in table 2. The future water supply showed a tendency to greatly increase in summer and autumn seasons, depending on the dam inflow change. In spite of the increased dam inflow and water supply, the future decrease in the total spills (releases that do not generate hydropower) may be explained by the overall decrease in the peak runoff. The future water supply showed a general tendency to increase in the A1B and B1 scenarios of the three GCM models. The average annual spills showed a change between -76.0% and +9.3% under the MIROC3.2 HiRes scenarios.

Table 12.Water system indicators for the A1B and B1 scenarios of the ECHAM5-OM, HadCM3, and MIROC3.2 HiRes data in the 2020s, 2050s, and 2080s.

Scenario		Reliability (%)				Vulnerability (10^6 m^3)			
		Baseline	2020s	2050s	2080s	Baseline	2020s	2050s	2080s
ECHAM5-OM	A1B	89.3	100.0	100.0	98.1	59.6	0.0	0.0	113.8
	B1		99.4	100.0	98.1		29.0	0.0	126.4
HadCM3	A1B		99.7	100.0	100.0		1.3	0.0	0.0
	B1		100.0	100.0	100.0		0.0	0.0	0.0
MIROC3.2 HiRes	A1B		100.0	100.0	100.0		0.0	0.0	0.0
	B1		100.0	100.0	100.0		0.0	0.0	0.0

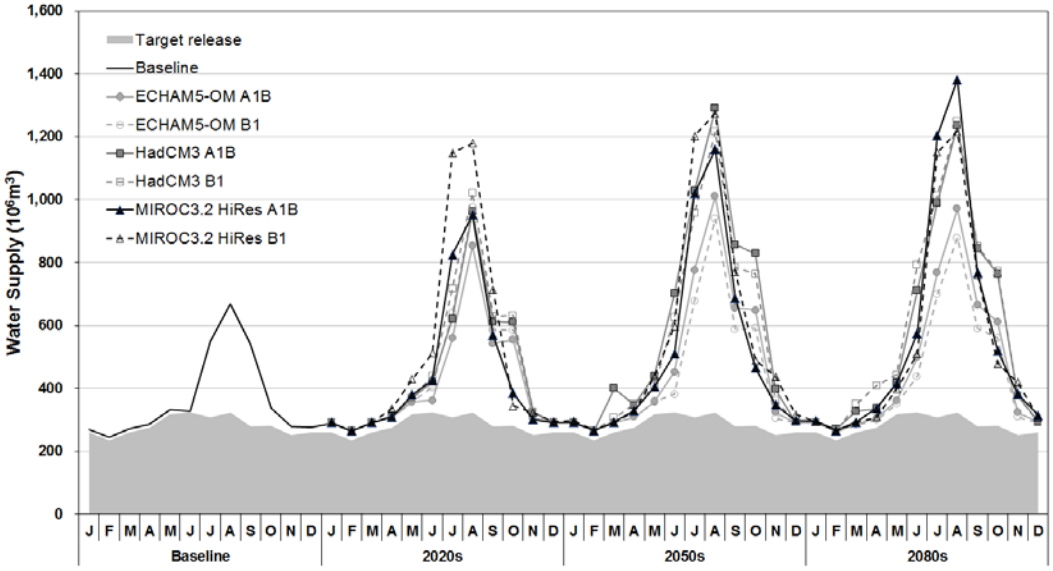

Figure 33.Change in future predicted water supply from Chungju dam under climate change scenarios.

Table 3.Summary of the future simulated annual releases and hydropower productions by climate change scenarios

Performance index	Baseline	2020s		2050s		2080s	
		A1B	B1	A1B	B1	A1B	B1
Average annual precipitation (mm)	1,361	1,459	1,546	1,708	1,673	1,764	1,689
Average annual inflow (10^6m^3)	5,378	5,426	6,004	6,766	6,791	6,965	6,851
Total average annual release (10^6m^3)	5,426	5,400	5,972	6,758	6,788	6,963	6,850
Average annual release to water supply (10^6m^3)	4,386	5,216	5,678	6,297	6,209	6,421	6,257
Average annual spills (10^6m^3)	1,040	184	294	461	579	541	593
Number of spills (months)	31	56	66	90	97	101	108
Number of water supply (months)	240	360	360	360	360	360	360
Average annual production (GWh)	599	799	887	1,000	988	1,023	994
Average annual surplus production (GWh)	87	144	170	270	241	281	253
Average annual deficit production (GWh)	282	160	134	134	109	165	171

Table 3 shows the simulation results when the dam operates by climate change scenarios. The future results indicate that in all the three GCM scenarios the total average annual release is just slightly above 5,400 × 10^6m^3. The actual release to water supply (turbine) range from 5,216 × 10^6m^3 to 6,421 × 10^6m^3 annually, depending on the dam inflow increased.Also, in all scenarios considered there are no months when releases are not made to the water supply. Therefore, the future dam operations always guarantee hydropower production at all times.The baseline simulation produced an annual average production output of 599 GWh

while minimum annual production was 354GWh and maximum was 942 GWh. The average production outputs during 2080s period showed a change between +33.9% and +92.3% under the three GCM scenarios. Due to higher water supply and lower spillway outflow, the results show that it is the production at the Chungju dam power plant that influences the overall tendency toward increased production.

Conclusions

This study was tried to assess the potential impact of climate change on multi-purpose dam operation using hydrological (SWAT) and reservoir simulation (HEC-ResSim) models with EHCAM5-OM, HadCM3, and MIROC3.2 HiRes scenarios.The most significant impacts of the future, projected climate change at Chungjudam are changes in hydrologic conditions and water resource system by applying the current operating rules.

Hydrology output from the SWAT by downscaled climate change scenarios suggests a significant increase in the amount of dam inflow due to precipitation increase. Especially, changes in dam inflow from the watershed will be affected water use such as water supply, hydropower, irrigation, flood control and mitigation, water quality enhancement into the downstream, and recreation. Therefore, to mitigate negative hydrologic impacts and utilize positive impacts, climate change should be considered in water resource planning for the multi-purpose dam watersheds. The future monthly dam inflow change gave us the clue for the future adjustment of dam operation rule for both efficient water use and flood control. For example, without adaptations, projections of the A1B and B1 emission scenarios of three GCM data indicate that hydropower production may increase up to 92.3%. Assuming current operation rule, these changes in system performance may result in increases in economic value of water supply and hydropower production.Therefore, we need to evaluate the monthly water supply for profit maximization based evaluation of optimal reliability of dam operation system. Also, we can consider the adjustment of flood limited water level and flood period due to changes in peak flow and seasonal patterns of runoff.

Finally, a limitation of this study is the current water demandused in the HEC-ResSim. The prediction of water demand is essential to assess future water resource system.To enable adaptation due to climate change as a widely accepted future occurrence, watershed decision makers require quantitative results for the establishment of adaptation strategies.

Acknowledgements

This work was supported by the National Research Foundation of Korea (NRF) grant funded by the Korea government (MEST) (No. 2011-0029851).

References

Alcamo, J., Döll, P., Kaspar, F., and Siebert, S. 1997. Global change and global scenarios of water use and availability: an application of Water GAP 1.0. Report A9701, Kassel, Germany: University of Kassel, Center for Environmental Systems Research.

Arnold, J. G., R. Srinivasan, R. S. Muttiah, and J. R. Williams. 1998. Large area hydrologic modeling and assessment part I: model development. Journal of American Water Resource Association 34(1): 73-89.

Betts, R.A., O.Boucher, M.Collins, P.M. Cox, P.D.Falloon, N.Gedney, D.L.Hemming, C.Huntingford, C.D.Jones, D.M.H.Sexton, and M.J.Webb. 2007. Projected increase in continental runoff due to plant responses to increasing carbon dioxide, Nature 448: 1037-1041.

Droogers, P., and J. Aerts. 2005. Adaptation strategies to climate change and climate variability: A comparative study between seven contrasting river basins. Physics and Chemistry of the Earth 30: 339-346.

Gedney, N., P.M.Cox, R.A.Betts, O.Boucher, C.Huntingford, and P.A. Stott. 2006. Detection of a direct carbon dioxide effect in continental river runoff records, Nature 439: 835-838.

Hashimoto, T., J. R.Stedinger, and D. P.Loucks. 1982. Reliability, resilience, and vulnerability criteriafor water resources system performance evaluation. Water Resources Research 18: 14-20.

Klipsch, J. D., and M. B. Hurst. 2007. HEC-ResSim reservoir system simulation user's manual version 3.0. USACE, Davis, CA.

Li, L, H. Xu, X. Chen, and S. P. Simonovic. 2010. Streamflow forecast and reservoir operation performance assessment under climate change. Water Resource Management 24: 83-104.

Milly, P.C.D., K.A.Dunne, and A.V.Vecchia. 2005. Globalpattern of trends in streamflow and water availability in achanging climate, Nature 438: 347-350.

Moy, W. S., J. L.Cohon, andC. ReVelle. 1986. A programming model for analysis of the reliability, resilience andvulnerability of a water supply reservoir. Water Resources Research 22: 489-498.

Nash, J.E., and J.V. Sutcliffe.1970. River flow forecasting through conceptual models Part I: A discussion of principles. Journal of Hydrology 10(3): 282-290.

Neitsch, S. L., J. G. Arnold, J. R. Kiniry, J. R. Williams, and K. W.King. 2002. Soil and Water Assessment Tool: TheoreticalDocumentation, Version 2000. TWRI Report TR-191. CollegeStation, Tex.: Texas Water Resources Institute.

Oki, T., and S.Kanae. 2006. Global hydrological cycles and world water resources, Science 313: 1068-1072.

Park, J. Y., M. J. Park, H. K. Joh, H. J. Shin, H. J. Kwon, R. Srinivasan, and S. J. Kim. 2011. Assessment of MIROC3.2HiRes climate and CLUE-s land use change impacts onwatershed hydrology using SWAT. Transactions of the ASABE 54(5): 1713-1724.

Racsko, P., L.Szeidl, andM. Semenov. 1991. A serial approach to local stochastic weather models.Ecological Modelling 57: 27-41.

Semenov, M.A., andE. M. Barrow. 1997. Use of a stochastic weather generator in the development ofclimate change scenarios. Climatic Change 35: 397-414.

Simonovic, S. P.,H. D. Venema, and D. H. Burn. 1992. Riskbasedparameter selection for short-termreservoir operation, Journal of Hydrology 131: 269–291.

Watts, R. J., B. D. Richter, J. J. Opperman, and K. H. Bowmer. 2011. Dam reoperation in an era of climate change. Marine and Freshwater Research 62(3): 321-327.

Assessment of Future Climate Change Impacts on Snowmelt and Its Water Quality for a Mountainous Watershed using SWAT

S.B.Kim, Graduate student

Konkuk University, Dept. of Civil and Environmental System Eng., 1 Hwayang dong, Gwangjin-gu, Seoul143-701, South Korea

H. J. Shin, Post-doctoral researcher

Water Analysis & Research Center, K-water, 6-2 San, Yeonchukdong, Daeduck-gu, Daejeon 306-711, SouthKorea

M. J. Park, Post-doctoral researcher

Massachusetts Amherst University, Dept. of Civil and Environmental Eng., Marston Hall, MA01003, U.S.A

S.J. Kim*, Professor

Konkuk University, Dept. of Civil and Environmental System Eng., 1 Hwayang dong, Gwangjin-gu, Seoul143-701, South Korea

Abstract

This study is to assess the future climate change impact on snowmelt and stream water quality of a 6,642.0km^2 mountainous dam watershed in South Korea using Soil and Water Assessment Tool (SWAT). The model was calibrated and validated for 2000-2010 using daily streamflow data at one location and monthly stream water quality data at two locations. The 6 snowmelt parameters of snowfall temperature, maximum and minimum melt rate, snowmelt temperature, initial snow water content and snow areal depletion curve (SADC) were considered and the multiple sets of Terra MODIS (MODerate resolution Imaging Spectroradiometer) snow cover data were used for SADC parameter of the watershed. The SWAT Nash-Sutcliffe model efficiency (NSE) for annual (November to October) and snowmelt period (November to April) was 0.60 and 0.80 respectively. The snowmelt discharge covered 10.1% for the annual. The 3GCMs (MIROC3.2 HiRes, ECHAM5-OM, and HadCM3) were corrected for each bias of weather data and downscaled by LARS-WG (Long Ashton Research Station-Weather Generator) model. The future impact on stream water quality by snowmelt will be discussed for two periods; 2020-2059 (2040s), 2060-2099 (2080s) and compared with baseline period; 1981-2010 (30 years).In the future, the amount of snowmelt runoff for January-March is most a lot of things in the baseline. For snowmelt period, future water quality components showed a general tendency to increase except in the 2040s and 2080s under the ECHAM5-OM data. The streamflow contributed by the melted snow especially at the mountainous area can be unignorable water resources. Climate *change*

can affect various water resources. The hydrological changes in the winter will cause a spring drought, in-stream ecological conditions.

Keywords: Climate Change, Terra MODIS, Snowmelt, Water quality, SWAT

Introduction

Snowmelt hydrology is important in the winter and spring flow of mountainous area as it can effect water availability, water quality and streamflow. The water by snowmelt is an important resource to water scarce area of downstream. Snowmeltingthe future impacts are sensitive to changes in temperature and precipitation.In South Korea, heavy snowfall occurs at 3 regions of southwest plain area, northeast mountainous area, and far-east island area from November to March (April at mountainous area). At present, the streamflow by snowmelt occupies less than usually 5 % of the total. Thinking over the future climate change with temperature rise, the streamflow contributed by the melted snow especially at the mountainous area can be unignorable water resources. The importance and complexity of snowmelt in hydrology has led to widespread development and application of snowmelt algorithms in comprehensive hydrologic modeling (Rango and Martinec, 1994, 1995). The MODerate resolution Imaging Spectroradiometer (MODIS) snow product (Hall et al., 1995) now generates global snow cover mask. Wang and Melease (2005) evaluated the performance of the SWAT (Soil and Water Assessment Tool) snowmelt component for simulating streamflow predominantly from melting snow in watershed. Shin and Kim (2007) assessed the climate change impact on snowmelt in two mountainous watersheds using SLURP (Semi-distributed Land Use-based Runoff Process) model.The objective of this study is to evaluate the future climate change impact on snowmelt and stream water quality for mountainous dam watershed using SWAT and ground meteorological data.

Materials and Methods

Study Area and Data for Model Evaluation

Figure 1(a) showsthe heavy snowfall area that the number of heavy snowfall (≥20cm) using interpolated snow depth of 76 weather station in South Koreaduring 30 years (1981-2010) is ranged from 1 to 92, theaverage annual snowfall is more than 80 cm which is heavy snow region in the South Korea. Figure 1(b) shows the Chungju dam watershed, a total area of 6,640 km^2 within the latitude-longitude range of 127.9°E–129.0°E and 36.8°N–37.8°N.The elevation ranges from 112 m to 1,562 m, with average slope of 36.9%. The annual average precipitation is 1,261 mm, and mean temperature is 9.4℃ over the last 30 years.

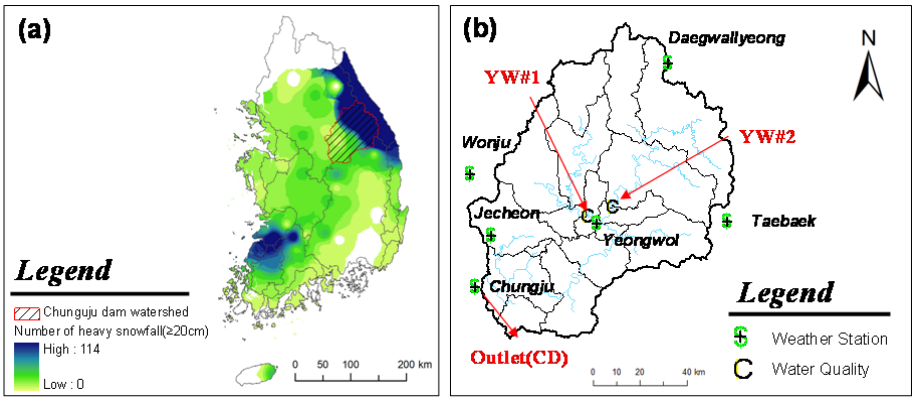

Fig. 1The study area: (a)heavy snowfall area and frequency and (b)Chungju dam watershed.

The spatial data for the watershed (i.e. elevation, land use and soils) were prepared for SWAT. Elevation data was rasterized from a vector map of 1:5,000 scale that was supplied by the Korea National Geography Institute (KNGI). Soil data were rasterized from a vector map of 1:25,000 scale that was supplied by the Korea Rural Development Administration (KRDA). The 2000 year land uses were obtained from Water Resources Management Information System (WAMIS). The 2000 year land uses were obtained from Water Resources Management Information System (Park et al., 2011).Thirty years (1981-2010) of daily weather data obtained for the Korea Meteorological Administration were collected from six ground stations. In addition, continuous daily streamflow data were obtained from a gauging station (CD at the watershed outlet) of the Han River Flood Control Office, and discontinuous (once per month) stream water quality data (sediment, T-N, and T-P) were obtained at two sites (YW#1 and YW#2) of the Korean Ministry of Environment. Nine years (1998-2006) of point-source data for the modeling was prepared from each point-source facility, including discharge rates and nutrient loads (Park et al., 2011).

SWAT Model Description

In SWAT, snowmelt hydrology is realized on an HRU (Hydrologic response unit) basis. Depending on data availability and modeling accuracy, one subbasin may have one or several HRUs defined. When the mean daily air temperature variable, SFTMP, the precipitation within an HRU is classified as snow and the liquid water equivalent of the snow precipitation is added to the snowpack. The snowpack increases with additional snowfall, but decreases with snowmelt or sublimation. The mass balance for the snow pack is:

(1)

where *SNO* is the water content of the snow pack on a given day (mm H_2O), R_{day} is the amount of precipitation on a given day (added only if$\bar{T}_{av} \leq T_{s-r}$) (mm H_2O), E_{sub} is the amount of sublimation on a given day (mm H_2O), and SNO_{mlt} is the amount of snow melt on a given day (mm H_2O).

The areal depletion curve requires a threshold depth of snow, SNOCOVMX, to be defined above which there will always be 100% cover. The threshold depth will depend on factors such as vegetation distribution, wind loading of snow, wind scouring of snow, interception and aspect, and will be unique to the watershed of interest. The areal depletion curve is based on a natural logarithm. The areal depletion curve equation is:

$$sno_{cov} = \frac{SNO}{SNO_{100}} \cdot \left(\frac{SNO}{SNO_{100}} + exp\left(cov_1 - cov_2 \cdot \frac{SNO}{SNO_{100}} \right) \right)^{-1} \quad (2)$$

where sno_{cov} is the fraction of the HRU area covered by snow, *SNO* is the water content of the snow pack on a given day (mm H_2O), SNO_{100} is the threshold depth of snow at 100% coverage (mm H_2O), cov_1 and cov_2 are coefficients that define the shape of the curve.

Climate Change Scenarios and GCM Data

As 3GCMs data, the MIOROC3.2 hires, ECHAM5-OM, and HadCM3 by Special Report on Emissions Scenarios (SRES) climate change scenarios (A1B and B1) of the Intergovernmental Panel on Climate Change (IPCC) AR4 were adopted. The A2 is the "high" is the "middle" GHG emission scenario, and B1 is the "low" GHG emission scenario.

HadCM3 is a coupled atmosphere-ocean general circulation model (AOGCM) developed at the Hadley Centre and described by Gordon et al (2000) and Pope et al (2000). TheA1B and B1 scenarios were considered in this study. The future weather data were generated using the bias correction and estimated over 100-year simulated periods using the LARS-WG (Long Ashton Research Station-Weather Generator) stochastic weather generator. LARS-WG is based on the series weather generatordescribed in Racsko et al. (1991) and in Semenov &Barrow (1997).Firstly, the GCMs data was corrected to ensure that 30 years ovserved data (1979-2010, baseline). Thismethod is generally accepted within the global change researchcommunity (IPCC-TGCIA, 1999).

For temperature, the absolutechanges between historical and future GCM time slices areadded to measured values.

$$\mathrm{T}'_{GCM,fut} = T_{meas} + (\bar{T}_{GCM,fut} - \bar{T}_{GCM,his}) \quad (3)$$

where, $\mathrm{T}'_{GCM,fut}$is the transformed future temperature,$T_{meas}$is themeasured temperature for the 30 years baseline period,$\bar{T}_{GCM,fut}$is the average future GCM temperature and $\bar{T}_{GCM,his}$is theaverage historical GCM temperature. For precipitation, therelative changes between historical data and GCM output areapplied to measured historical values.

$$\mathrm{P}'_{GCM,fut} = P_{meas} \times (\bar{P}_{GCM,fut}/\bar{P}_{GCM,his}) \quad (4)$$

where, $\mathrm{P}'_{GCM,fut}$is the transformed future precipitation, $P_{meas}$is themeasured precipitation, $\bar{P}_{GCM,fut}$is the average future GCMprecipitation and $\bar{P}_{GCM,his}$is the average historical GCMprecipitation.LARS-WG is based on the weather series generator described by Racsko et al. (1991).

Snow cover for model calibration using Terra MODIS and snow depth dtribution with ground measured snowfall data

The snow cover data from Terra MODIS satellite image (2000-2010) during the snowmeltseason (November to April) were prepared. Because the snow cover of the watershed was usually started from November and maintained to April, and almost disappeared in April. The products (MOD10A1) at 500 m spatial resolution and at a day interval were downloaded from the Earth Observing System Data Gateway (EOS).

The snow depth distribution for the MODIS extracted snow cover area was generated using the 6 ground measured snowfall data by applying Inverse Distance Weight (IDW) interpolation method.

Results and Discussions

Depletion Curve

The areal depletion curve requires a threshold depth of snow, SNO_{100}, to be defined above which there will always be 100% cover. The cov_1 and cov_2 are determined by solving equation (2) using two points, one point is 95% coverage at fraction of SNO_{100}

and another point is 50% coverage at fraction of SNO_{100}. As the value for SNO_{100} increases, the influence of the areal depletion curve will assume more importance in snow melt processes. For model calibration, the depletion curve information of the watersheds during the snowmeltseason was obtained by analyzing Terra MODIS images.Figure 2 shows the snow depletion curves from the fraction of snow cover area and snow volume of each data set (2000-2010) using the Terra MODIS and snow depth distribution. The 50% coverage at a fraction of SNO_{100} is range of 0.4 to 0.7. The average 50% coverage of SNO100 is 0.47.

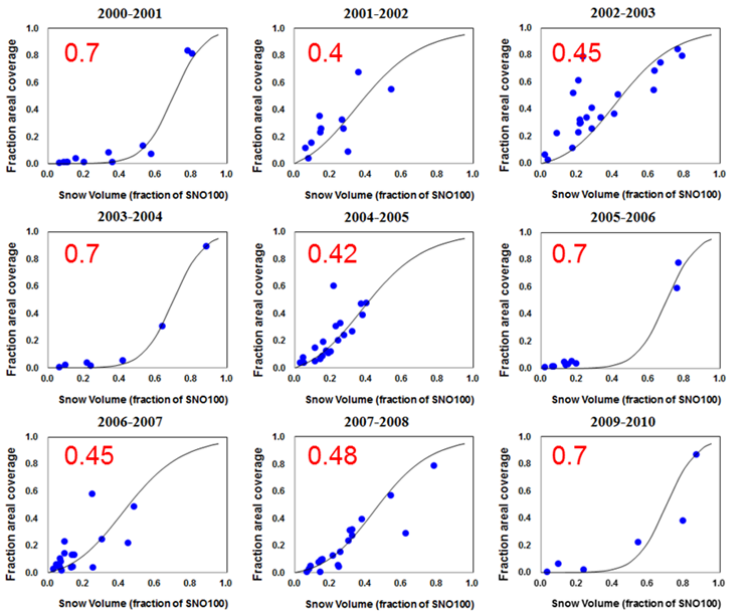

Fig. 2The annual depletion curve of snow cover area (2000-2010).

SWAT Model Calibration and Validation

The daily streamflow at three sites (YW#1, YW#2 and CD) and the monthly streamwater quality (sediment, T-N, and T-P) at two sites(YW#1 and YW#2) were usedfor model setup. The SWAT model was calibration and validation for 10 years (2000-2010) of daily streamflow data using the average annual depletion curve value. For SWAT model calibration, the 6 snowmelt parameters of snowfall temperature (SFTMP), maximum and minimum melt rate (SMFMX and SMFMN), snowmelt temperature (SMTMP), snow pack temperature lag factor (TIMP), the areal snow coverage thresholds at 50% and 100% (SNO50COV and SNOCOVMX) were considered for model calibration.Table 3 shows the statistical summary of model calibration (2000-2005) and validation (2005-2010)result for annual and snowmelt season.The average Nash & Sutcliffe (1970) model efficiency (NSE) for streamflow of snowmelt and annual season was 0.60 and 0.80 respectively. For the snowmelt season,

the discharge covered 10.1% for the annual season.Figures 3 showsthe calibration results for the stream water quality. The average NSE for sediment, T-N, T-P of YW#1 and YW#2 was0.72, 0.70, 0.85 and 0.54, 0.75, 0.70 respectively.

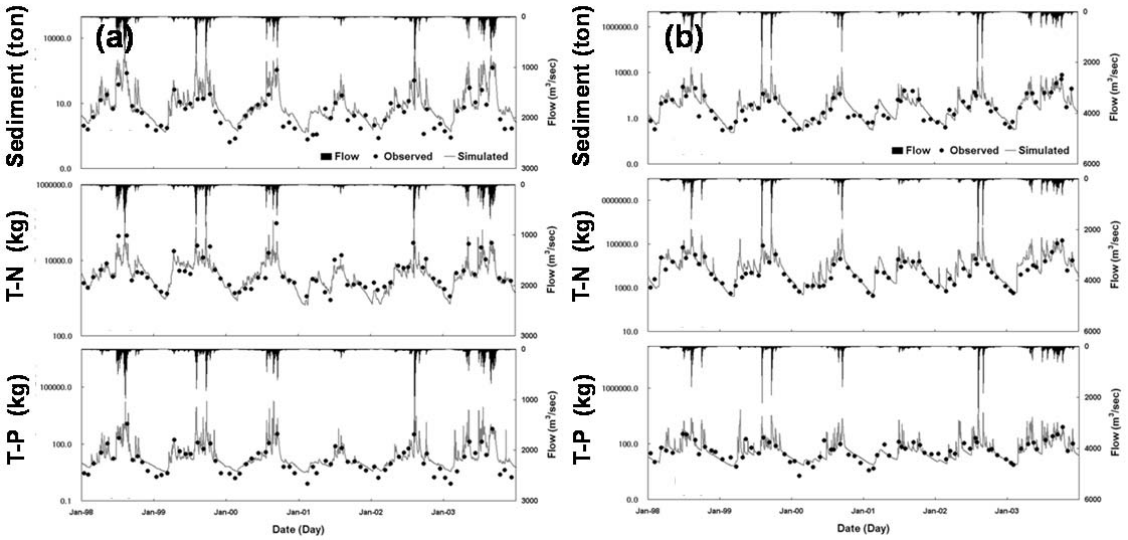

Fig. 3Comparison of the observed and SWAT-simulated sediment, T-N, and T-P at two locations (a)YW#1 and (b)YW#2.

Table 13. Summary of validated statistics for annual season (2000-2010, Nov-Oct)[a].

Year	Season	Snow depth	P	Q (mm)		QR (%)		RMSE	NSE	QRA/ QRS
		(cm)	(mm)	Obs.	Sim.	Obs.	Sim.	*(mm/day)*		
2000-2001	Annual	128.6	831.2	309.4	344.9	37.2	41.5	0.82	0.57	18.2
	Snowmelt		177.2	90.7	62.6	51.2	35.3	0.49	0.37	
2001-2002	Annual	56.5	1238.0	836.7	863.0	67.6	69.7	2.95	0.83	6.6
	Snowmelt		242.0	83.5	56.8	34.5	23.5	0.41	0.96	
2002-2003	Annual	129.7	1590.5	1032.2	1167.6	64.9	73.4	2.56	0.64	13.0
	Snowmelt		270.0	191.6	151.8	71.0	56.2	0.66	0.92	
2003-2004	Annual	59.6	1375.9	931.0	995.6	67.7	72.4	3.38	0.72	8.9
	Snowmelt		187.9	103.5	88.8	55.1	47.3	0.48	0.95	
2004-2005	Annual	86.9	1260.0	741.4	750.5	58.8	59.6	2.33	0.50	6.3
	Snowmelt		175.0	101.3	46.9	57.9	26.8	0.68	0.83	
2005-2006	Annual	52.2	1870.0	953.0	1015.9	51.0	54.3	5.50	0.64	5.6
	Snowmelt		218.0	105.0	57.2	48.2	26.3	0.69	0.90	
2006-2007	Annual	49.7	1538.0	1019.5	963.5	66.3	62.6	3.29	0.65	10.8
	Snowmelt		265.0	131.3	103.6	49.6	39.1	0.54	0.95	
2007-2008	Annual	80.5	1083.0	472.9	458.3	43.7	42.3	4.02	0.38	10.1
	Snowmelt		162.0	83.0	46.4	51.3	28.6	0.44	0.80	
2008-2009	Annual	33.1	1263.0	596.7	539.4	47.2	42.7	3.32	0.70	5.4
	Snowmelt		202.0	55.3	29.4	27.4	14.5	0.29	0.95	
2009-2010	Annual	92.5	1250.3	819.7	684.5	65.6	54.7	3.16	0.64	16.6
	Snowmelt		260.3	181.4	113.6	69.7	43.7	0.80	0.76	
Mean	Annual	76.9	1330.0	76.9	771.2	57.3	57.0	3.10	0.60	10.1
	Snowmelt		215.9	112.7	75.7	51.6	34.1	0.50	0.80	

[a] P: Precipitation,Q : Streamflow, QR : Runoff ratio, QRA : Runoff ratio for annual season , QRS : Runoff ratio for snowmelt season , and RMSE : Root mean square error.

Assessment of Streamflow and Its Water quality Impact

The SWAT model was applied to evaluatethe future (2040s and 2080s) climate change impacts on snowmelt runoff and its water quality using the 3GCMs data by two SRES A1B and B1. Figure 4 shows comparison of the future predicted snowmelt runoff during 2040s and 2080s on the baseline. The data were evaluated by long-term average proportions of each month. The results showed generally increased for the MIROC3.2 and HadCM3 in November-February.Especially, the amount of snowmelt runoff for January-March is most a lot of things in the baseline. However, there is most a lot of snowmelt runoff for December-February in the future. As temperature rises, it starts for dissolving than baseline quickly.Table 2 summarizes the future predicted streamflow and water quality components for the A1B and B1 scenarios.The results showed range of 24.6 % to 39.8 % precipitation increase and range of 3.1 % to 31.8 % decrease of streamflow and range of 185.8 % to 359.3 % increase of sediment.

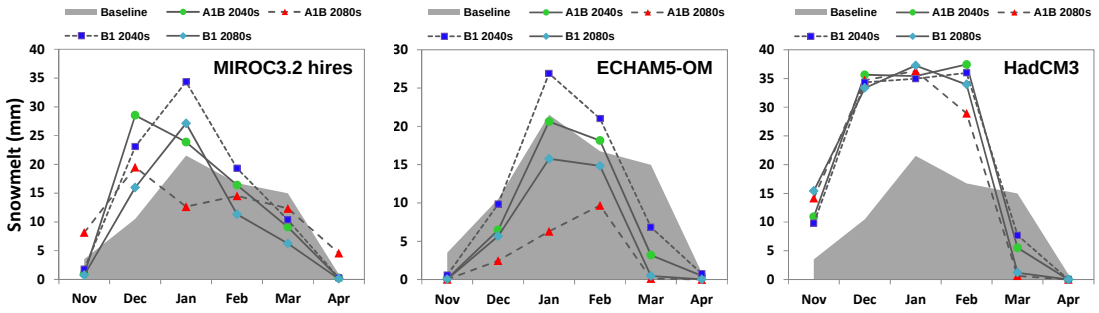

Fig. 4Change in the future predicted snowmelt runoff under the A1B and B1 scenarios of 3GCMs in the baseline, 2040s and 2080s.

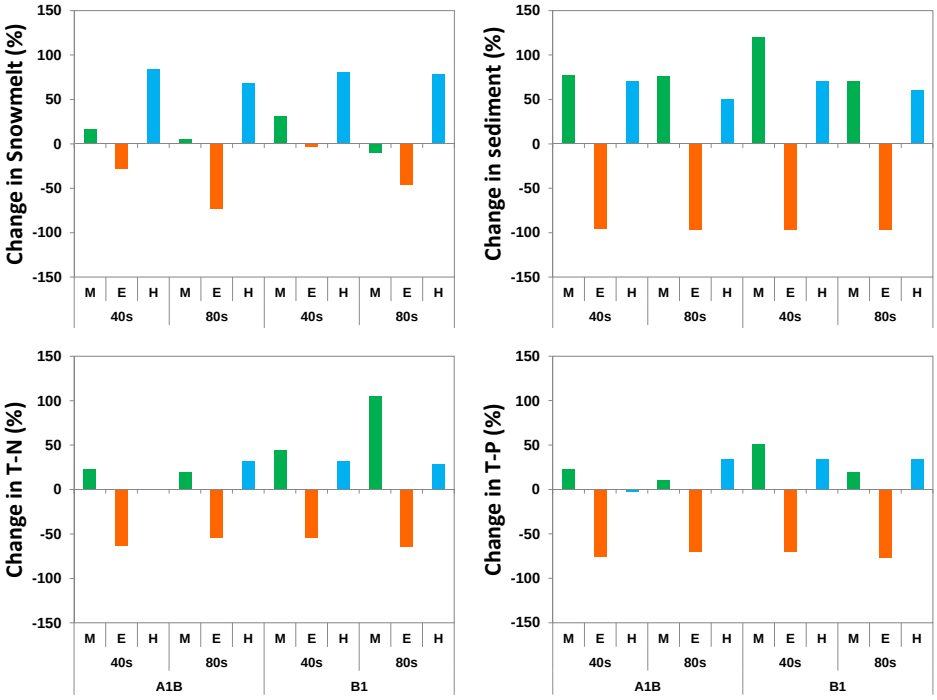

Fig. 5Change in the future predicted snowmelt runoff and water quality under the A1B and B1 scenarios of 3GCMs in the baseline, 2040s and 2080s.

Table 14. Summary of the future predicted annual hydrologic and snowmelt for 3 GCMs.

GCM	Scenarios	Year	Period	PCP (mm)	Q (mm)	QR (%)	SS (ton)	QRA/QRS
Baseline(1981-2010)			Annual	1361.2	637.7	46.8	3392.3	12.9
			Snowmelt	260.2	82.5	31.7	474.3	
MIROC3.2 hires	A1B	2040s	Annual	1579.8	771.0	48.8	1364.8	27.4
			Snowmelt	418.5	211.2	50.5	383.5	
		2080s	Annual	1666.6	897.6	53.9	1832.7	24.4
			Snowmelt	460.9	219.0	47.5	380.6	
	B1	2040s	Annual	1539.7	908.5	59.0	1906.5	26.1
			Snowmelt	409.0	237.0	57.9	540.2	
		2080s	Annual	1579.6	972.1	61.5	2484.1	23.3
			Snowmelt	437.8	226.4	51.7	662.9	
ECHAM5-	A1B	2040s	Annual	1772.	702.5	39.6	1581.	11.9

OM				3			8	
			Snowmelt	470.3	83.6	17.8	349.6	
		2080s	Annual	1993.8	721.3	36.2	1613.8	10.9
			Snowmelt	552.0	78.5	14.2	345.0	
	B1	2040s	Annual	1732.5	721.3	41.6	1613.8	10.9
			Snowmelt	460.4	78.5	17.0	345.0	
		2080s	Annual	1965.8	675.5	34.4	1440.2	12.0
			Snowmelt	543.9	81.3	14.9	333.9	
HadCM3	A1B	2040s	Annual	1690.8	856.2	50.6	2141.7	28.7
			Snowmelt	489.5	245.7	50.2	681.3	
		2080s	Annual	1911.3	963.6	50.4	2456.8	27.7
			Snowmelt	540.3	266.6	49.3	774.2	
	B1	2040s	Annual	1855.0	963.6	51.9	2456.8	27.7
			Snowmelt	558.6	266.6	47.7	774.2	
		2080s	Annual	1904.3	953.9	50.1	2408.8	28.1
			Snowmelt	554.2	268.2	48.4	787.5	

As shown in Table2, the future streamflow for annual and snowmelt periodincreased by MIROC3.2 hires and HadCM3 under A1B, B1 scenarios. The future precipitation increased in all period, especially showing big increases in HadCM3 for snowmelt period. For the future snowmelt period, the biggest discharge covered 28.7% for the annual season. After evaluation of the hydrologic impact, the impact of climate change on stream water quality was evaluated in terms of sediment, T-N and T-P at the watershed outlet.Figure 5 shows change in the future predicted snowmelt runoff and water quality under the A1B and B1 scenarios of 3GCMs.For snowmelt period, future water quality components showed a general tendency to increase except in the 2040s and 2080s under the ECHAM5-OM data. The biggest change for MIROC3.2 hires and ECHAM5-OM in sediment load were +120.0% and -96.0% on snowmelt period, respectively. The future T-N load showed a general tendency to increase except in the 2040s and 2080s under the ECHAM5-OM data. The biggest changes for MIROC3.2 hires and ECHAM5-OM in T-N load were +51.0% and -77.1% on snowmelt period, respectively. The biggest changes for MIROC3.2 hires and ECHAM5-OM in T-P load were 000 and 000% on snowmelt period, respectively. The future T-P load showed comparatively little change.

Conclusions

This study applied to assess the snowmelt impacts of mountainous watershed using SWAT model. The model was calibrated using spatially distributed snow cover and snow depth from Terra MODIS images. The average NSE of model during the snowmelt season (November-April) was 0.80.For the snowmelt season, the discharge covered 10.1% for the annual season. In the future, the snowmelt runoff will be increased about two times and the water quality will be increased greatly. Especially, the amount of snowmelt runoff for January-March is most a lot of things in the baseline.

The streamflow contributed by the melted snow especially at the mountainous area can be unignorable water resources. Climate change can affect various water resources. The hydrological changes in the winter will cause a spring drought, in-stream ecological conditions.The evaluation results could be useful to get the reliable future amount of snowmelt and water quality in mountainous area of our country.

Acknowledgements

This work was supported by the National Research Foundation of Korea(NRF) grant funded by the Korea government(MEST) (No. 2011-0029851).

References

Arnold, J. G., R.Srinivasan, R. S. Muttiah, and J. R. Williams. 1998. Large-area hydrologic modeling and assessment: Part I. Model development. J. American Water Resources Assoc. 34(1): 73-89.

Hall, D., G.Riggs,and V. V.Salomonson.1995. Development of methods for mapping global snow cover using moderate resolution imaging spectroradiometer (MODIS) data. Remote Sensing. 54:127-140.

IPCC-TGCIA, 1999. Guidelines on the use of scenario data for climate impact and adaptation assessment, version 1. Prepared by Carter, T.R., Hulme, M., Lal, M. Intergovernmental Panel on Climate Change, Task Group on Scenarios for Climate Impact Assessment, 69.

Nash, J. E., and J. V. Sutciffe. 1970. River flow forecasting through conceptual models; Part 1 – A discussion of principles. J. Hydrol. 10(3): 282-290.

Park, J. Y., M. J. Park, H. K. Joh, H. J. Shin, H. J. Kwon, R. Srinivasan, and S. J. Kim. 2011. Assessment of MIROC3.2 Hires climate and CLUE-s land use change impacts on watershed hydrology using SWAT. Trans. ASABE. 54(5): 1713-1324.

Park, M. J., J. Y. Park, H. J. Shin, M. S.Lee, G. A.Park, I. K.Jung, and S. J. Kim. 2010. Projection of future climate change impacts on nonpoint source pollution loads for a forest dominant dam watershed by reflecting future vegetation canopy in a Soil and Water Assessment Tool model. Water Sci. Technol. 61(8) : 1975-1986.

Racsko, P., L. Szeidl, and M. Semenov. 1991. A serial approach to local stochastic weather models. Ecol. Model. 57(1-2) : 27-41.

Rango, A., J. Martinec. 1994. Model accuracy in snowmelt runoff forecasts extending from 1 to 20 days. Water Resources bull. 30(3): 463-470.

Rango, A., J. Martinec. 1995. Revisiting the degree-day method for snowmelt computations. Water Resources bull. 31(4): 657-669.

Semenov M. A., and E. M. Barrow (1997) Use of a stochastic weathergenerator in the development of climate change scenarios.Climate Change. 35:397–414.

Shin, H. J., and S. J. Kim.2007. Assessment of Climate Change Impact on Snowmelt in the Two Mountainous Watersheds Using CCCma CGCM2. KSCE. J. Civil Eng. 11(6): 311-319.

Wang, X., and A. M. Melesse.2005. Evaluation of the SWAT model's snowmelt hydrology in a northwestern Minnesota watershed. Trans. ASABE. 48(4): 1359-1376.

Pope, V. D., Gallani, M. L., Rowntree, P. R. and Stratton, R. A. 2000. The impact of new physical parametrizations in the Hadley Centre climate model-HadAM3. Clim. Dynam, 16: 123-146.

Gordon, C., Cooper, C., Senior, C. A., Banks, H., Gregory, J. M., Johns, T. C., Mitchell, J. F. B. and Wood, R. A. 2000. The simulation of SST, sea ice extents and ocean heat transports in a version of the Hadley Centre coupled model without flux adjustments. Clim. Dynam. 16: 147-168.

Assessing Water discharge in Be River Basin, Vietnam using SWAT model

Nguyen Kim Loi
Department of Applied Geomatics, Nong Lam University,
Linh Trung Ward, Thu Duc District, Ho Chi Minh City, Vietnam
nguyenkimloi@gmail.com

Nguyen Duy Liem
Department of Applied Geomatics, Nong Lam University,
Linh Trung Ward, Thu Duc District, Ho Chi Minh City, Vietnam
nguyenduy1133@gmail.com

Abstract

The water discharge is an important hydrological parameter because it defines the shape, size and course of the stream. The results of monitoring flow discharge can be useful information for flood forecasting, predicting sediment loads and assessing the impact of climate change to water resource. The study focused to quantify the impact of topography, land use, soil and climatic condition on water discharge in Be River Basin, Vietnam using GIS technology and SWAT model. In this integration, GIS supplies input data included elevation, soil properties, land use and weather data and creates graphical user interface for SWAT, while SWAT operates input data, delineates watershed, simulates different physical processes, displays output data as discharge. The simulation results in the period 1979 to 2007 represented fluctuation of discharge relatively well with both R^2 and NSI values were above 0.7 in the period 1979 to 1994. This result can be used for predicting the effect of land use change and management practices on water discharge within the basin, helping to water quantity and quality assessment.

Keywords: SWAT, Water discharge, GIS, Be River Basin

Introduction

Water discharge is the volume of water moving past a cross-section of a stream over a set period of time. It is usually measured in cubic meter per second (m^3/s). For river basins, water discharge is an important hydrological parameter because it defines the shape, size and course of the stream. The results of monitoring water discharge can be useful information for flood forecasting, predicting sediment loads and assessing the impact of climate change to water resource.

Nowadays, together with the development of GIS (Geographic Information System), there are many hydrological models to help calculate the water discharge more accurately, easily and quickly than the traditional measurement methods. One of them is SWAT (Soil and Water Assessment Tool). This is a basin-scale model integrated with GIS technology which helps improve the accuracy of simulated result of water discharge from rainfall and physical properties of the basin. In this integration, GIS supplies input data and creates graphical user interface for SWAT, while SWAT operates input data to simulate different physical processes in the basin.

This study aims to assess fluctuations and find out the rule of water discharge in Be river basin through simulating the stream flow from digital elevation model (DEM), land use, soil and weather data using SWAT model and GIS technology.

Materials and methods

Study area description

Be river basin, with an area of 7,650km^2 and water discharge of 255m^3/s, is one of the four main tributaries of Dong Nai watershed. It is located between 11^{o}06'-12^{o}22' north latitude and 106^{o}35'-107^{o}31' east longitude. Administratively, Be river basin passes through four provinces of Vietnam, including Binh Phuoc, Binh Duong, Dong Nai, Dac Nong and a small part of Cambodia (Figure 1).

The terrain of Be river basin changes very complex with many forms of topographical formation: mountainous, midlands interspersed some small narrow plains and some cauldrons. The height of Be river basin decreases gradually in northeast - southwest direction from 750 - 1,000m in the upstream down to 80 - 100m in the downstream and increases from 80 - 150m in the west to 250 - 700m in the east.

In aspect of climate, Be river basin has tropical monsoon climate with the average annual temperature ranging from 25.5 – 26.7^{0}C, and average yearly precipitation from 2,200 - 2,600mm.

The various soils in this basin are rhodic ferralsols (54.21%), ferralic acrisols (18.4%), xanthic ferralsols (8.30%), and the others (Dystric Fluvisols, Chromic Luvisols, Dystric Gleysols, Haplic Andosols, Umbric Gleysols and rivers, lakes) (1.59%).

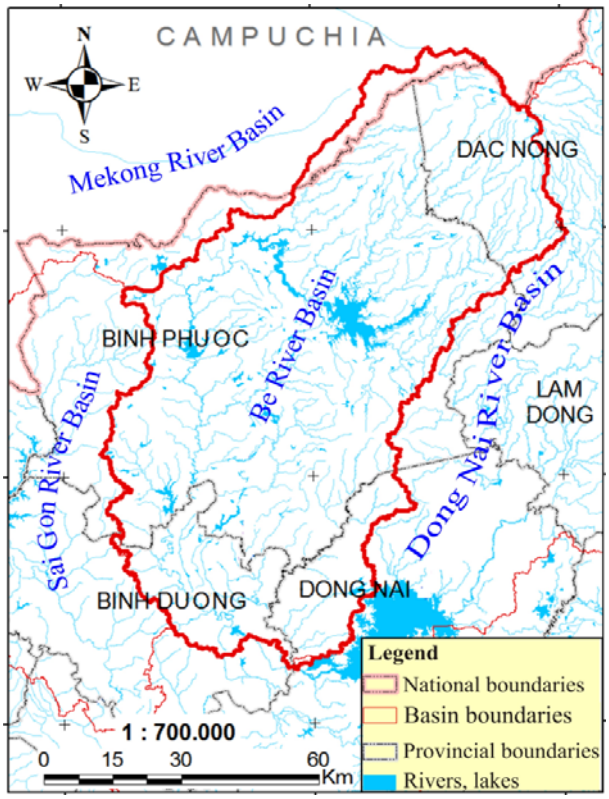

Figure 1. *Overview of Be river basin*

Brief description of SWAT

Soil and Water Assessment Tool (SWAT) is a river basin, or watershed, scale model developed by Dr. Jeff Arnold for the USDA Agricultural Research Service (ARS) in the early

1990s (Susan L. Neitsch et al., 2009). This model is designed to predict the impact of land management practices on water, sediment, and agricultural chemical yields in large complex watersheds with varying soils, land use and management conditions over long periods of time. The model is a set of regression calculations to show relationship between value of input parameters and output parameters. SWAT allows a number of different physical processes to be simulated in a watershed. For modeling purposes, a watershed may be partitioned into a number of subbasins, which are then further subdivided into HRUs that consist of homogeneous land use, management, and soil characteristics.

Data collection

Data required for this study were collected from the local source (Southern Institute For Water Resources Planning) and global source (METI/NASA, FAO) including topography, land use, soil, weather and observed discharge.

DEM data was extracted from ASTER Global Digital Elevation Model (ASTER GDEM) of METI/NASA, with a spatial resolution of 30m;

Land use map was obtained from Southern Institute For Water Resources Planning including 14 land use/ land cover classes: Broadleaf evergreen closed natural forest, Broadleaf evergreen closed planted forest, Broadleaf evergreen closed-open natural forest, Broadleaf evergreen open natural forest, Bamboo closed natural forest, Mixed closed natural forest, Grasslands/shrublands, Sparse woodland, Mixed perennial crops/residential land, Mixed annual crops/residential land, Mixed upland crops/residential land, Residential land, Natural lakes and Artificial lakes;

Soil map was taken from the global soil map of FAO (1995) at 10km spatial resolution. In the research watershed, there are five types of soil, including Ferralic Acrisols, Gleyic Acrisols, Rhodic Ferralsols, Thionic Fluvisols and Pellic Vertisols;

For weather data, based on distribution characteristics, duration and data quality of meteorological monitoring stations in Be river basin and its surrounding areas, eight gages as Bu Nho, Chon Thanh, Dac Nong, Dong Phu, Loc Ninh (Song Be), Phuoc Hoa, Phuoc Long, and So Sao were used. The data was obtained from Southern Institute For Water Resources Planning.

Discharge data was prepared at two monitoring stations named Phuoc Long and Phuoc Hoa in the basin. The data was furnished by Southern Institute For Water Resources Planning.

Model setup

The SWAT model approach applied to the case study area of Be river basin is shown in Figure 2. According to that, the procedure includes such main steps as: watershed delineator, HRU analysis, write input tables, run SWAT and model evaluation.

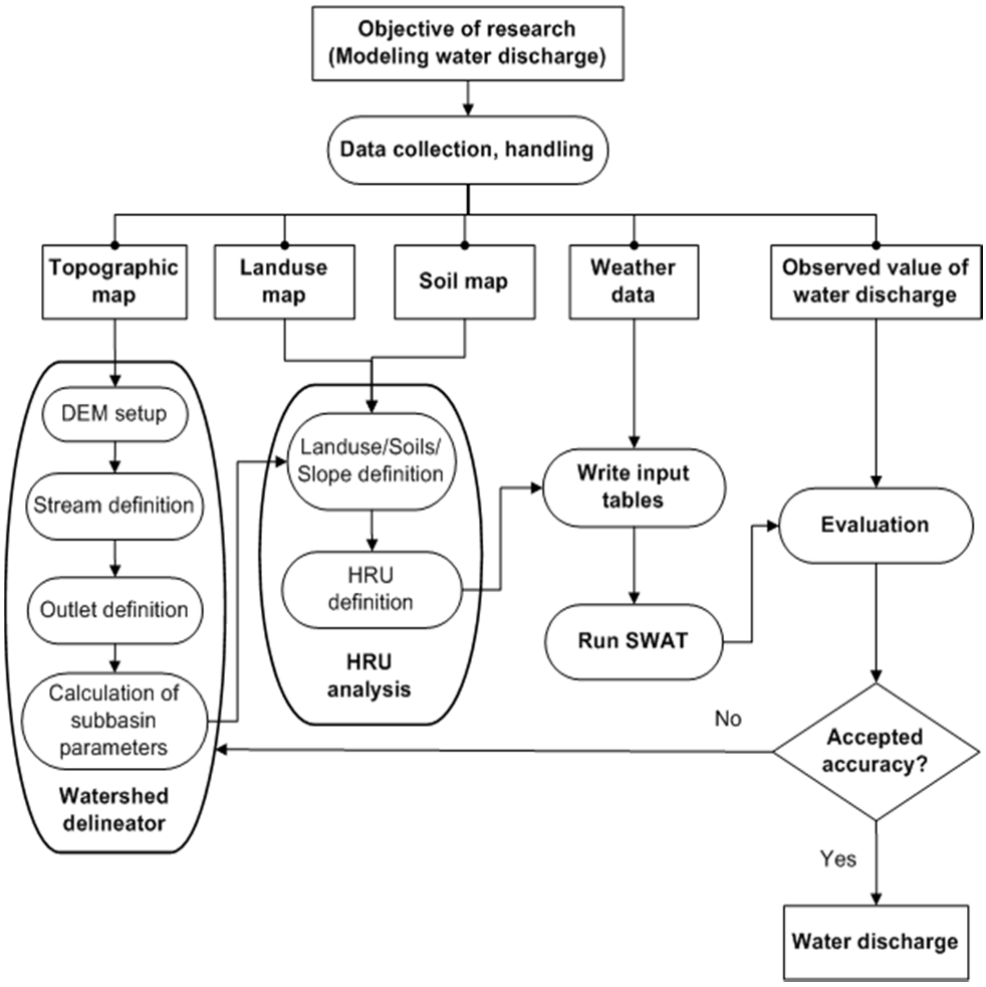

Figure 2. *Flow chart of modeling water discharge in Be river basin*

Model performance evaluation

The SWAT model was evaluated using observed discharge data. The coefficient of determination (R^2) (P. Krause et al., 2005) and Nash – Sutcliffe Index (NSI) (Nash, J.E. and J.V. Sutcliffe, 1970) were used to evaluate the model performance. R^2 value ranges from 0 – 1, shows the correlation between the observed versus the simulated values. NSI value ranges from -∞ to 1, indicates how well the plot of the observed versus the simulated values fits the 1:1 line. If the R^2 and NSI values are less than or very close to zero, the model performance is considered unacceptable or poor. In contrast, if the values are equal to one, then the model prediction is considered to be perfect.

The formula for R^2 and NSI calculations are as follows:

$$R^2 = \left(\frac{\sum_{i=1}^{n}(O_i - \bar{O})(P_i - \bar{P})}{\sqrt{\sum_{i=1}^{n}(O_i - \bar{O})^2}\sqrt{\sum_{i=1}^{n}(P_i - \bar{P})^2}} \right)^2$$

$$NSI = 1 - \frac{\sum_{i=1}^{n}(O_i - P_i)^2}{\sum_{i=1}^{n}(O_i - \bar{O})^2}$$

where O_i is the observed discharge at time i, $\overline{O}$ is the average observed discharge, P_i is the simulated discharge at time i, $\overline{P}$ is the average simulated discharge, and n presents the number of registered discharge data.

Results and discussions

Model evaluation

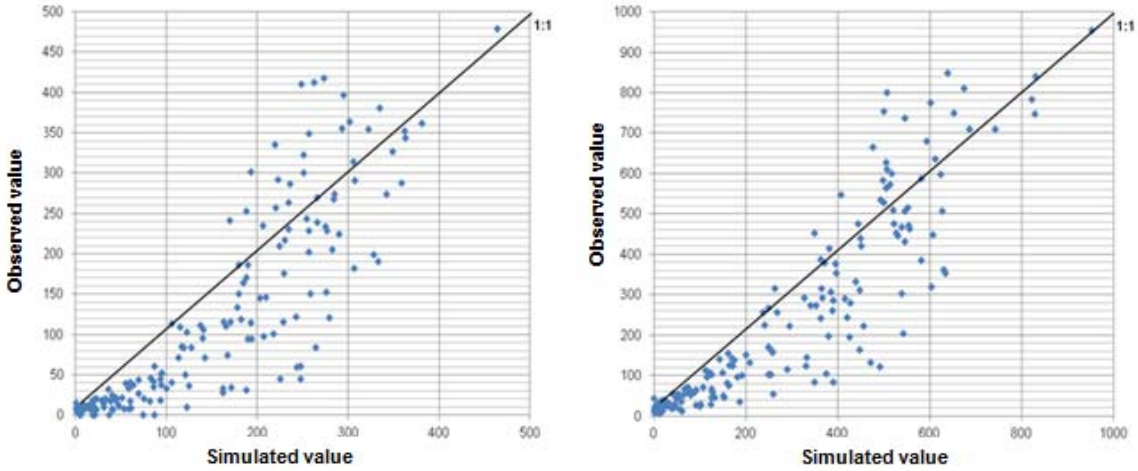

Figure 3. *Observed vs simulated discharge at Phuoc Long (left) and Phuoc Hoa (right)*

Comparing the observed with simulated discharge at two subbasins as Phuoc Long and Phuoc Hoa during the period of 1979 - 1994 shows that the simulation results were relatively well. In this stage, the R2 was 0.769 at Phuoc Long, 0.822 at Phuoc Hoa and NSI of 0.720; 0.794 were Phuoc Long, Phuoc Hoa, respectively. Distribution chart of observed and simulated discharge at two stations is shown as Figure 3.

Discharge variation

Based on Figure 4, obviously, the overall pattern of discharge variation at Phuoc Long, Phuoc Hoa is determined by the fluctuation of precipitation. During months of heavy rain, the discharge is usually greater. Almost, the discharge at Phuoc Long was less than about twice the discharge at Phuoc Hoa although the precipitation at Phuoc Long was greater.

General model of water discharge at two subbasins reaches the peak twice during the rainy season, the rest (especially during the dry season) the discharge is very small. However, water discharge values differ for each year. In particular, during the simulation period (1979 - 1994), on both subbasins, there were 3 years when the water discharge reaches maximum, including August 1986, August 1992 and September 1994. At Phuoc Long, the values were 463.8; 380.4 and 358.3 m^3/s, respectively. At Phuoc Hoa, the values were 951.9; 830.5; 822.6 m^3/s, respectively.

In general, the flood season on both sub-basins usually lasts from June to November with an average water discharge of 224.55 m^3/s (Phuoc Long) and 458.53 m^3/s (Phuoc Hoa). In the dry season (from December to May of the following year), water discharge was low, reaching only 30.85 m^3/s (Phuoc Long) and 60.49 m^3/s (Phuoc Hoa).

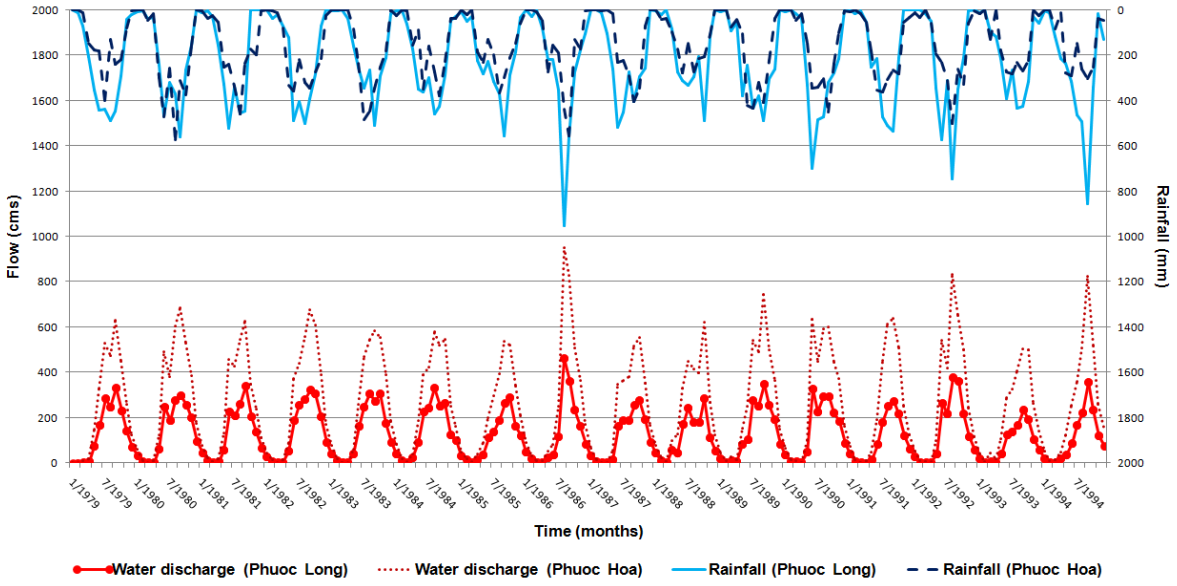

Figure 4. *The variations of rainfall and water discharge at Phuoc Long and Phuoc Hoa*

Conclusions

The study simulated the water discharge of Be river basin in the period from 1979 – 2007 by SWAT model with relatively well results (R^2 and NSI values were above 0.7 in the period from 1979 – 1994). From those results, the flood season on both sub-basins was defined as lasting from June to November with an average water discharge of 224.55 m^3/s (Phuoc Long) and 458.53 m^3/s (Phuoc Hoa). In the dry season (from December to May of the following year), water discharge was low, reaching only 30.85 m^3/s (Phuoc Long) and 60.49 m^3/s (Phuoc Hoa). The results proved that it is suitable to integrate GIS technology and SWAT model for simulating the water discharge in Be river basin and can be applied for other river basins.

A future direction for this study is to calibrate and validate the model again to identify the appropriate parameters for water discharge which can predict accurately changes of water discharge in the basin.

References

FAO, 1995. The digital soil map of the world and derived soil properties. CD-ROM Version 3.5, Rome.

Nash, J. E. and J.V. Suttcliffe, 1970. River flow forecasting through conceptual models, Part 1. A discussion of principles. *Journal of Hydrology* 10 (3): 282-290.

P. Krause et al., 2005. Comparison of different efficiency criteria for hydrological model assessment. *Advances in Geosciences* 5: 89–97.

S.L. Neitsch et al., 2005. Soil and Water Assessment Tool theoretical documentation version 2005. Available at: http://swatmodel.tamu.edu. Accessed 9 Jun 2011.

Susan L. Neitsch et al., 2009. Overview of Soil and Water Assessment Tool (SWAT) Model. In: *Soil and Water Assessment Tool (SWAT): Global Applications. Special Publication No. 4.,*3-23. Arnold, J et al.: Funny Publishing.

Requirements of Hydrological Models for Climate Change Impact Assessment

Raj Kachroo.
Aman Satya KachrooTrust, 689 Sector 23, Gurgaon, India

Abstract

This paper takes a 'Back to the Basics' approach to look at the suitability of operational hydrological models for use in Climate Change impact assessment. Given that SWAT is increasingly used for impact assessment, mostly incorrectly, SWAT is compared with other operational hydrological models, not at computational level but, at the level of principles. Optimizing parameters to minimize a least squares function and suitability of Nash Sutcliffe Criteria for model evaluation is questioned. Impact of climate change on extreme events is discussed at philosophical level.

BACK TO THE BASICS

A hydrological forecasting model, typically, comprises 2 components, namely the Water Balance Component and the Routing Component. The Water Balance component estimates the Effective Rainfall. It is the part of the observed rainfall that contributes to runoff. The total volume of effective rainfall should normally be equal to the total volume of the river flow. The Water Balance Component preserves the mean flow or the first moment of the observed flow. The Routing Component is required to diffuse/route the time series of effective rainfall into a time series of flow. It preserves the higher moments, i.e., the Variance, Skewness etc. of the observed flow.

The Unit Hydrograph: In early 20th Century Sherman devised a procedure to estimate the Effective Rainfall and then he used a Unit hydrograph to route the effective rainfall into, what he called Direct Surface Run off . He then added the Base Flow to the Direct Surface Run off to estimate the river flow. The water balance part the Unit Hydrograph model that separates the effective rainfall from observed rainfall is very subjective and event based.

About 25 years later, Irish hydrologists, namely Dooge and Nash made attempts to put mathematics behind the humble Unit Hydrograph. Nash introduced the concepts of Instantaneous Unit Hydrograph (IUH) , the Convolution Integral and established the concept of Unit Hydrograph in the context of Systems mathematics. He represented a catchment by a Linear Reservoir and then showed

that a conceptual model comprising 'n' linear reservoirs of 'K' Storage coefficients, operating as a cascade has an Instantaneous Unit Hydrograph of incomplete Gamma Function. This is what we know as the Classical Nash Model. He estimated the parameters n and k by equating moments of effective rainfall and the Direct Surface Run off and with the help of a m2:m3 diagram he showed that the gamma function IUH was an optimum choice. We have since realized that it was not only the Irish Hydrologists who were busy developing algebra of the IUH but it was also Russian hydrologists, namely, Klenin and Milikov, who were developing similar mathematics. But because their publications were in the Russian Language the English speaking world never got to know about it until much later.

The Simple Linear Model: The transformation of the humble unit hydrograph into very elegant systems algebra was very exciting for hydrologists. It opened many possibilities which resulted in a number of publications.

Then like with every thing else the next turning point came about with the availability of computing power. Nash & many others argued that there was no need for hydrologists to restrict themselves to isolated events as they could handle large sets of data with comfort. Nash and Foley introduced the Simple Linear Model (SLM) which related time series of observed rainfall with the time series of observed river flow through Eq. 1.

$$Y_i = \sum_{j=1}^{m} R_{i-J+1}.h_j + e_i \qquad \text{Eq. 1}$$

Where

Yi is the observed river flow time series. hj is the Pulse Response function which can be estimated by ordinary least squares. Ri is the observed rainfall time series. The water balance in the SLM is achieved by multiplying the observed rainfall by a constant factor G, given by Eq. 2.

$$G = \sum y_i \Big/ \sum R_i \qquad \textbf{Eq. 2}$$

Where

Ri is the observed rainfall.

Equation 1 is the discrete equivalent of the convolution integral which describes the process of routing or diffusion. This equation is fundamental to applied hydrological modeling.

Linear Systems Models: In a useful generalization of the Nash's work on SLM Liang showed how such models can also be used for multiple inputs, thus permitting, for example, the application of the linear technique to relate the observed out flows at the down stream point to corresponding inflows observed further upstream on the main channel, and on principal tributaries and, if desired, to rainfall observed on the intervening catchment. He showed that where suitable data exists almost 100% efficiencies can be obtained with such multiple input/Single out put routing models on medium to large catchments. The parameters of the Linear model are obtained by minimizing a least squares function. Model evaluation is done by the Nash Sutcliffe Criteria.

The Simple Linear Model and its several variations are suitable for real time forecasting and for data reconstruction. For real time flood forecasting applications these models are operated with an additional error updating model which is often an Autoregressive Model. The Linear Transfer function model (LTFM) of the Box and Jenkins type combines, elegantly, the basic transformation model and the error updating components. The Muskingum flow routing model is a special case of the LTFM where there is one Auto regressive term and 2 moving average terms. The classical Nash Model is a parametric form of the Simple Linear Model.

The work done at Galway and Dar es Salaam and at several other places over two decades endorses the adequacy of the Linear model for flood routing, both in transformation of a hydrograph and in the combination of synchronous hydrographs, particularly for data of daily duration. It would seem unnecessary, hence forth, to use complex non linear elements in flow routing component for models.

Non Linear Systems Models: Well known, Non Linear Systems models, for example, The Linear Perturbation Model, Multi Linear Model, Constrained Linear Systems model , the Seasonally Varying Run off Coefficient model or Linearly Varying Run off Coefficient model are all variations of the Simple Linear Model. The SLM turns into a Seasonally Varying Run off Coefficient Model if G, the Gain factor, is allowed to vary through the year in a systematic manner. The Linearly Varying Gain factor model allows the Gain factor to vary linearly as a function of the antecedent moisture conditions. The same effect is achieved, much more elegantly in LPM when perturbations of rainfall and perturbations of Run off are related by a linear model. The Multi Linear Model and the Constrained Linear Systems model, essentially differ in the manner in which the model parameters are estimated. The model structure is the same in both cases. These models allow the Gain factor and the shape of the pulse response function to vary according to the antecedent moisture conditions in 3 thresholds.

These non linear models can , some times, give better results than the Simple Linear Model in rainfall run off modeling. They are particularly suitable for real time forecasting and for data

reconstruction. The parameters are obtained by minimizing the least squares function. Model evaluation is done by the Nash Sutcliffe Criteria. The procedures of application of these models are well established.

Lumped Conceptual Models: The river flow at any given time is dependent not only on recent rainfall falling upstream of the discharge gauging station , but also, on the evaporation, particularly the amount occurring since the previous rainfall. The effect of evaporation, in the absence of rainfall, is neither immediate nor obvious. Over a prolonged period of time, it creates a soil moisture deficit which in turn controls the volume of the generated run off from a subsequent rainfall storm. This effect can not be allowed for by direct relationship (linear or non linear) between the discharge series as dependent variable and the two series, of rainfall and potential evaporation, for instance, as independent inputs in a systems type of a model. It can, only be accounted for by a series of water balance operations.

SMAR Model: This model was developed in 1960's as a training model. In its 2 parameter version SMAR water balance is given by Eq. 3.

$$S(d) = S(d-1) + R(d) - Ea(d) - X(d) \qquad \text{Eq. 3}$$

Where

S (d) Is the soil moisture on day d

R (d) Is the rainfall of day d

Ea (d) Is the actual evaporation on day d

X(d) Is the run off volume generated on day (d). This is the proportion of the rainfall that contributes to run off and in the UH Terminology it is called the effective Rainfall. This component of the Water Balance equation is routed to estimate the time series of flow.

The calculations are performed, on a daily basis, by assuming that on a day when rainfall (R) occurs and if it exceeds the potential rate of evaporation (PE) a fraction H' of the excess contributes to the effective rainfall by x1. The fraction H' is taken as being proportional to the available soil moisture content of the first five layers of soil so that H' = H (available soil moisture content in 125 mms of the top soil). Therefore x1(d) = H' * (R(d) – PE(d)) provided R(d) – PE(d) is positive and is greater than zero. The parameter H controls the run off generation.

The remaining rainfall ((R(d)-x1(d)) enters the soil moisture storage and restores each layer to the field capacity from the first layer downwards until the rainfall is exhausted or until all the layers are at field capacity. Any surplus rainfall denoted by x2 contributes to the Effective Rainfall.

On a day, when potential for evaporation exceeds the amount of rainfall, the model evaporates water from the soil moisture storage using a form of the Penman actual evaporation model. The model assumes that actual evaporation is a function of the soil moisture deficit. The actual loss due to evaporation is equal to the potential rate only when soil is at field capacity and it diminishes, thereafter, in an exponential manner to almost nil value when the soil is at wilting point. SMAR assumes that the soil moisture storage comprises a huge vertical stack of horizontal layers, initially full, and where each layer contains 25 mms of water at field capacity. Evaporation occurs from the top layer at potential rate and from the second layer only on exhaustion of the first, at the remaining potential multiplied by a parameter C. On exhaustion of the second layer, evaporation from the 3rd layer occurs at the potential rate multiplied by C2 and so on. Thus a constant potential rate applied to the basin would reduce the soil moisture storage in a roughly exponential manner.

Having determined the total volume of effective rainfall (x1 + x2) by means of the water balance component just described , the routing effect of the catchment may be described by a simple Linear Model described earlier by equation 1.

Complex Lumped Conceptual Models: All operational lumped conceptual models, for example, Sacremento model; The HBV model; the SSARR model, NAM model, CEQUEAU, SRM, Xinanjiang , PDM etc. are extensions of the SMAR model. All of them follow, by and large, the same principle, i.e., the observed rainfall is converted into effective rainfall by water balance calculations and then the effective rainfall is routed to generate the river flow. The differences in these models lies in the complexity of the water balance component. Diffusion/ Routing, by and large, comprises a linear systems model.

The Lumped Conceptual Models help improve the accuracy of model forecasts when compared with the Systems type of Models. This is generally true of semi arid regions. But there is no rule that can tell us as to when a Lumped Conceptual model is likely to out perform a Systems type of model. For catchments where seasonality in the flow is dominant the Linear Perturbation model outperforms the Lumped Conceptual models. These models are suitable for real time forecasting and data reconstruction. The model parameters are estimated by minimizing a least squares function and model accuracy is evaluated by Nash Sutcliffe Criteria.

Model Evaluation Criteria: While it is desirable that a model should represent as closely as possible the actual physical processes occurring within the catchment, it is essential that it should represent accurately the transformation of the input into the output. The primary utility of an operational model is reflected in the extent to which it satisfies this practical objective, which may be

called ‘model accuracy’. The second requirement is that of ‘model consistency’ whereby the level of accuracy and the estimates of the parameter values persist through different sample sets of the data. The third requirement is that of ‘model versatility’. A versatile model may be defined as one which is accurate and consistent when subject to diverse applications involving model evaluation criteria that are not directly based on the objective function used to calibrate the model. Operational hydrologists, often, ignore the versatility requirements of a model and concentrate only on the practical objective for which the model is being applied, i.e., the purpose of application of the model. There are not, any operational models, that can truly claim to be versatile in the sense that they would be suitable for all applications and at all locations. Physical Process Models are versatile but such models do not exist as is explained later.

Nash Sutcliffe Criteria: The accuracy of a model reflects the extent to which it satisfies its purpose of application. Therefore, for different applications there must be different criteria of model accuracy. Nash and Sutcliffe Criteria, based on the Least Squares objective function, is a good overall indicator of model accuracy and hence it is one of the most commonly used criteria in River Flow Forecasting. But it is not suitable for every application and in every situation and at times it can be misleading. Pitman argued that the function of models of stream flow synthesis is not to reproduce exactly the history of run off at a particular site. The use of historical data in water resources design does not imply that history will repeat itself but that the behavior of the river in the future will have much the same pattern as in the past. When model parameters are estimated according to the least squares criterion there is a consistent tendency for the extreme flow values to be under estimated and for extreme low flow values to be over estimated. This leads to a synthesized flow sequence will have lower standard deviation than the actual runoff. Pitman argued correctly that this can lead to underestimation of storage capacity of reservoirs.

Stream Flow Synthesis: Although Pitman’s argument against the use of Nash-Sutcliffe Criteria came about in the context of his work which was to synthesize stream flow for design of reservoirs these comments are also valid for applications of impact assessment or for evaluation of models that form core of an integrated decision support systems. These applications too deal with design and/or planning.

There is a difference between Data Reconstruction and Data Synthesis. Reconstruction refers to a situation when historical data are missing and we wish to reconstruct those missing data. For instance, if we have rainfall records of 3rd January, 1960 then we can estimate river flow on the 3rd of January 1960. Data Reconstruction is a purely deterministic exercise. Data Synthesis refers to a

process where deterministic models are used to generate river flow data for design of structures. Synthetic flow data series are not estimates of historical flow but possible sequences of flow that the structure is likely to face during its operation.

Ungauged Catchments: Models of stream flow synthesis or impact assessment, unlike those for data reconstruction, can not be calibrated at the location of interest. It is because there are no historical flow data to calibrate such models. Parameters of such models are estimated from empirical relationships that are developed from studies involving a number of gauged catchments. The acceptability of Pitman model for stream flow synthesis in South Africa is based on the satisfactory results that were achieved in his study conducted in 1973. There are no means of quantifying the accuracy of the model forecast even when the location of the ungauged catchment is within South Africa.

There is an additional source of error in models that are used for stream flow synthesis on ungauged catchments. This error is associated with the empirical relationships that estimate model parameters from catchment characteristics, i.e., the accuracy of the regression model. The accuracy of empirical relationships diminishes further when these relationships are used in locations other than those where the relationships were developed. For instance, if the Pitman model is used for ungauged locations outside the region of Southern African then the likelihood is that the estimated model parameters will be less accurate than those in South Africa unless, of course, new or modified relationships are made available for the region of interest. The same arguments apply to the Soil Conservation Services Curve Number model. This model was developed for use in the USA.

Physically Based Models: A true " Physical Process Model" is one where model parameters have a direct physical interpretation so that those parameters can be measured from laboratory and/or field measurements. This is an important requirement for ' impact assessment' . For example, if we want to know what will happen to flow in the river if we convert a forest land into agricultural land or vice versa then all that we have to do is to replace parameters of forest cover by parameters of an agricultural field. The difference in the estimated flow with two sets of parameters will quantify the impact of change on the River Flow as a result of change.

Physicists and hydrologists have developed such models with fair degree of success for each component of the process of conversion of rainfall into runoff but they have failed to extrapolate that success from the laboratory scale to real catchment scale and also from one process in isolation to a combination of processes. Various attempts have been made by several Research Clusters to put together such components to form a single model which would account for every drop of water in the

catchment in its space and in time but they have so far failed. Systems Hydrologic European , often known as SHE model, was one such failed but brave and an admirable attempt. SHE model could not deliver what it was meant to deliver.

There are several reasons for failure of such models. The primary amongst them is the accumulation of errors. The exit boundary condition of process 1 becomes the initial boundary condition of process 2. And if the process starts with an incorrect initial boundary condition errors multiply in following processes and the overall error accumulation gets out of control. Another reason is that we are not able, at least not yet, to measure catchment characteristics from which we can estimate model parameters at catchment scale. We have achieved a fair degree of success at experimental and laboratory scale but not at catchment scale.

Distributed Condition: Change of Climate or Deforestation does not only impact the amount of water that flows in the river but it triggers a long chain of impacts . Changed quantity of water can have an effect on the eco system within the catchment and on the sociology and economics of populations dependent on the river system. A full assessment of such impacts requires an interconnected suite of models where each model deals with a separate aspect of ecosystem and socioeconomics. But at the core of this interlinked system of models is a hydrological model that feeds the necessary water related information to all the peripheral models. The core hydrological model, in this case, does not only estimate the river flow at the outlet of the catchment but it also estimates the distribution of soil moisture content as a function of space and time. Other state variables are also estimated such as the depth of water as a function of time at different points in the channel network. Peak flows are important for Sediment Transport and so on. These state variables form the link between the core and the peripheral models in an integrated system of models.

Semi Distributed Conceptual Models: The core hydrological model must ideally be a 'Physical Process Model' but in the absence of such models we use a Semi Distributed Conceptual Model, as the next best available option. In this option we divide a catchment into a number of small sub catchments where each sub catchment is represented by a Lumped Conceptual Model and the flows are then routed through a channel network that resembles the actual Channel network in the catchment. Some developers use simple conceptual models to represent their sub catchments and some use very complex conceptual models. In each case the overall look of the model is that of a 'Physical Process Model' but in reality these models are only inspired by 'Physical Processes because their parameters are estimated and not measured. The parameters are estimated from Catchment Characteristics like in the case of ungauged catchments.

Soil Water Assessment Tool: SWAT is not a single model but a system of many interconnected models operating within the frame work of a single computer program. At the core of this computer program is a Flow Forecasting Model of a Semi Distributed Conceptual type which means that a catchment is divided into a number of small sub catchments and flow generated from each sub catchment is routed down through a channel network that resembles the actual drainage network of a catchment.

The core hydrological model of SWAT also comprises, like all other systems/conceptual models, two components. The first is for the water balance and the second for diffusion or routing. The routing/diffusion component of the SWAT model uses linear systems routing models like all other models do. The water balance component is based on Eq. 4.

$$S(d) = S(d-1) + R(d) - Ea(d) - G(d) - x1(d) - x2(d) \qquad \text{Eq. 4.}$$

Where

S (d) Is the soil moisture on day d

R (d) Is the rainfall of day d

Ea (d) Is the actual evaporation on day d

G (d) Is the amount of aquifer recharge

x1(d) Is the run off volume generated on day (d).

x2(d) is the part of the rainfall that appears in the river as base flow.

The sum of x1(d) + x2 (d) is the proportion of the rainfall that contributes to run off and in the UH terminology it is called the Effective Rainfall. This component is routed to estimate the time series of flow.

Clearly SWAT model is not much different from the SMAR model except that the parameters of SMAR, C&H, are optimized to maintain that the total volume of the effective rainfall is equal to the total volume of the observed flow but in the case of SWAT there are no constraints imposed. The run off generated x1(d) is given by the Soil Conservation Services Curve Number method. The parameter CN is not optimized but estimated from catchment characteristics. Similarly there is a procedure for estimation of Actual evaporation.

The essential difference is that the parameters of SWAT can be estimated whereas parameters of the SMAR must be optimized. If , however, one optimizes the parameters of the SWAT then SWAT offers no advantages what so ever except that the computer program of SWAT System is convenient

to use. That is, of course a great advantage but the draw back is equally serious. One does not know whether the results obtained are realistic or not?

Climate Change Methodology: Hydrologists are engaged in two types of impact assessment. One is that of change in climate and second is the classical case of change in the catchment characteristics; deforestation being one of the biggest concerns of the day. Assessing the impact of climate change on river flow comprises the following steps.

Step 1: To generate possible sequences of changed climatic variables, as a result of increased global temperature. This is done by a Global Circulation Models (GCM). This is in the domain of a meteorologist.

Step 2: To express the output of a GCM as a time series of daily precipitation, daily temperature, daily relative humidity etc. This is also generally done by a Meteorologist with the help of a statistician.

Step 3: To use these time series data in a hydrological forecasting model to estimate changes in river flow and other state variables such as the soil moisture, depth of water in a tributary etc. This is within the domain of a hydrologist.

If we assume, for instance, the annual rainfall for catchment X is likely to increase from 1000 mms per year to 1200 mms per year then the climate change impact problem is to know how much will be the increase in the river flow? Will it be proportional, i.e., will the flow also increase by 20% or will it be less or more? We understand that it will not be 20% but will it be 25% or 15% can only be determined with the help of a 'Physical Process model' or by a very good Conceptual Model.

Again, for assessing the impact of deforestation the ideal choice would be a Physical Process model where the parameters have a physical significance and those parameters can be measured. Given that such models do not exist the next best option is a Conceptual Model, like the Pitman Model, whose parameters can be estimated from catchment characteristics.

SWAT AND CLIMATE CHANGE IMPACT.

There are various problems in application of SWAT and/or other models of the same category for climate change impact assessment.

Data Synthesis: The impact of Climate Change is a design and planning problem. The data generated by a GCM that becomes input to a hydrological model is not a weather forecast and the hydrological model used for converting it into run off is not a real time forecasting model. GCM out put is synthetic data. It is a stochastic time series that is not likely to be experienced in the

future. A series that has a similar character in terms of its moments is likely to be experienced. The out put of the hydrological model too is, naturally, synthetic data. There is no problem with this as long as we understand that the usefulness of a hydrological model in this context depends on its ability to predict the moments, i.e., mean, variance etc. as accurately as possible and not necessarily the exact sequence of flows.

The problem of climate change impact is, therefore, to estimate how much would be the corresponding increase in the mean annual run off if the mean annual rainfall increases by let us say X%. The SWAT model can not and should not be used to answer this question if the performance of SWAT model is poor. In Sub Saharan Africa that is the case and I have no reason to believe it will be any different in India. If the magnitude of error in a model is much larger compared to the magnitude of change to be predicted then in that situation such a model can not be used. It is like trying to make measurements in grams on a scale that has a margin of error of kilos.

Calibrated Parameters: When model accuracy measured by the Nash Sutcliffe criteria is poor SWAT parameters are optimized to minimize a sum of squares function. Once that is done the usefulness of SWAT is lost. This model can no longer be used for Impact assessment, neither for Climate Change nor for Deforestation.

Once model parameters are calibrated to match the historical data then the optimized parameters loose their physical meaning and can no longer be estimated from Regression equations. As a result one does not know what value a given parameter should be assigned after catchment changes are assumed. For instance, if a forest is replaced by a rice farm, then what should be the new value of Curve Number CN if CN used under the forested conditions was optimized. Because the CN after optimization would not reflect the conditions of a forest. After calibration CN of SWAT model is the same as H of the SMAR model. It is just a number that was arrived at by minimizing the sum of differences between the observed flow and the estimated flow. In the case of climate change impact analysis optimization of parameters to minimize a sum of squares function ensures that the historical runoff coefficient is maintained. That automatically means that for x% increase in the rainfall the corresponding increase in the run off will also be x %. Once that is done the entire purpose of modeling is defeated.

Insensitivity of Parameters: Sensitivity analysis of optimized parameters of SWAT often reveals that only a few, a small number of parameters, are sensitive to the sums of squares function. Amongst them, often at the top is the Curve Number CN, i.e., the parameter that generates the run

off. It is quite understandable because this is the parameter that generates the Effective Rainfall. The sum of the effective rainfall is the mean flow.

Now let us for the sake of argument assume that in a given catchment only CN was sensitive and the rest were all insensitive parameters. This means that parameters other than CN have no role to play other than enable the computer program to operate. In other words one can assign any reasonable value to these parameters and the results of the computer program will not vary. If that is the case then let us say a non sensitive parameter NP is assigned a value of V for sub catchment 1 and the same value is assigned to it in sub catchments 2 and so on then the distributed character of the model has no meaning. Assigning distributed values to insensitive parameters and then optimizing the over all model to minimize a sum of squares function does not only not make any sense but it can also give a false impression that variations within the catchment are being taken care and the results obtained from the peripheral models will all be incorrect.

Integrated Water Resources Management: If SWAT can give reasonably accurate results without the need for its parameters to be optimized then SWAT would indeed be useful for assessing the impact of Climate Change in the context of Integrated Water Resources Management because it would allow you to assess the impact not only on river flow but also on Sedimentation, Water Quality, Nutrient transport etc. and then in turn on Sociology, Economics etc.

But because the accuracy of forecasts by SWAT prior to estimation of parameters is poor and because after optimization model parameters are mostly insensitive the advantages of SWAT in terms of its distributed character are completely lost. The results of peripheral models, like the nutrient transport model, whose initial conditions are derived from the boundary conditions of the hydrological core model, can not be relied upon. If estimates of boundaries of the core model are all incorrect every thing that follows is incorrect.

Extreme Events

Analysis of extreme events in hydrology is done for design of civil engineering structures. We assume extreme events have a probability density function and based on the mean, variance and skewness of the sample we estimate the parameters of the probability density function and assign a Probability of Exceedence (Return Period) to an event of magnitude Q. With the change in climatic conditions the form of the probability density function will not change but its parameters will change.

For instance, If rainfall is likely to increase in a given area due to climate change then there is a possibility that floods of a magnitude Q will become more frequent than before. It means that the

Probability of Exceedence of magnitude Q will increase or its Return Period will decrease. But it does not mean that the flood of magnitude Q would not have occurred if the climate change had not taken place. The problem of impact on climate change on extreme events is a statistical problem rather than one of deterministic modeling.

SUMMARY & CONCLUSIONS

All hydrological models comprise a Water Balance component that controls the mean flow and a Routing/Diffusion component that controls the higher moments. There is sufficient evidence to prove that Linear Routing models of the systems type are sufficient for routing river flow and are also suitable for diffusion or routing of effective rainfall generated by the Water Balance in Lumped/Semi Distrusted Conceptual Models.

Non Linear Systems models, like LPM, SVRC, LVGFM, CLS etc. are all variations of the Simple Linear Model. They are useful for Real Time Forecasting and Data Reconstruction. Parameters of these models are optimized and model evaluation is done by Nash Sutcliffe Criteria.

Lumped Conceptual Models takes into account the effect of evaporation on river flow. They provide better results than the Systems models but there is no rule that can tell us as to when a Lumped Conceptual model is likely to out perform a Systems type of model. Like the systems models they are useful for Real Time Forecasting and Data Reconstruction. Parameters of these models are optimized.

Pitman argued that the use of historical data in water resources design does not imply that history will repeat itself but that the behavior of the river in the future will have much the same pattern as in the past. There is a difference between Data Reconstruction and Data Synthesis. Reconstruction refers to a situation when historical data are estimated whereas Synthesis refers to a process where river flow data are generated for design of structures.

When there are no historical data to calibrate models parameters are estimated from empirical relationships that are developed from studies involving a number of gauged catchments. Such models, known as un gauged catchment models, are also useful for assessing the impact of changes in catchment characteristics.

A true " Physical Process Model" is one where model parameters have a direct physical interpretation so that parameters can be measured from laboratory and/or field measurements. This condition is a necessary requirement for ' impact assessment'. But such models do not exist.

Change of Climate or Deforestation does not only impact the amount of water that flows in the river but it triggers a long chain of impacts . A full assessment of such impacts requires an interconnected suite of models where each model deals with a separate aspect of ecosystem and socioeconomics.

But at the core of this interlinked system of models is a hydrological model that feeds the necessary water related information to all the peripheral models. The core hydrological model for impact assessment must ideally be a 'Physical Process Model' but in the absence of such models we use a Semi Distributed Conceptual Model, as the next best available option.

SWAT is an example of such a system of models. It is a system of many interconnected models operating within the frame work of a single computer program. At the core of this computer program is a Flow Forecasting Model of a Semi Distributed Conceptual type and not a physically based type. However, there are various problems in application of SWAT in climate change impact assessment. The data generated by a GCM that becomes input to a hydrological model are not a weather forecast and the hydrological model that is used to generate the output is not a real time forecasting model. GCM out put is synthetic data. The out put of the hydrological model too is synthetic data.

The results of SWAT model are often poor. The magnitude of error is much larger compared to the magnitude of change that needs to be predicted. It amounts to weighing in grams on a scale that has margin of error in Kilos.

The parameters of SWAT are often optimized to minimize a sum of squares function. By doing so the purpose of use of a model like SWAT is lost. The model can no longer be used for impact assessment, neither for climate change nor for deforestation. Once model parameters are calibrated to match the historical data then the optimized parameters loose their meaning. As a result one does not know what value a given parameter should be assigned after catchment changes are assumed.

Sensitivity analysis of the optimized parameters of SWAT often reveals that only a few, parameters, are sensitive. Therefore assigning distributed values to insensitive parameters does not make any sense. It can also give a false impression that variations within the catchment are being taken care.

Because of parameter optimization and insensitivity of parameters advantages of SWAT in terms of its distributed character and its usefulness in the context of Integrated Water Resources Management is lost. The results of peripheral models, like the nutrient transport model, whose initial conditions are derived from the boundary conditions of the hydrological core model, can not be relied upon. If estimates of boundaries of the core model are all incorrect every thing that follows is incorrect.

Analysis of extreme events is done for design of civil engineering structures. One can not say that event of magnitude Q would not have happened before the climate change happened. All that one can say is that the probability of exceedence of a given flood has changed. The problem of impact on climate change on extreme events is a statistical problem rather than one of deterministic modeling.

AN INTEGRATED HYDROLOGIC MODELING FRAMEWORK FOR COUPLING SWAT WITH MODFLOW

J.A. Guzman
Grazinglands Research Laboratory, USDA-ARS, El Reno, OK

D.N. Moriasi
Grazinglands Research Laboratory, USDA-ARS, El Reno, OK

P.H. Gowda
Conservation and Production Research Laboratory, USDA-ARS, Bushland, TX

J.L. Steiner
Grazinglands Research Laboratory, USDA-ARS, El Reno, OK

J.G. Arnold
Grassland Soil and Water Research Laboratory, USDA-ARS, Temple, TX

R. Srinivasan
Texas A&M, Spatial Science Laboratory, College Station, TX

P.J. Starks
Grazinglands Research Laboratory, USDA-ARS, El Reno, OK

Abstract

The Soil and Water Assessment Tool (SWAT), Modular Three-Dimensional Finite-Difference Groundwater Flow (MODFLOW), and Energy Balance based Evapotranspiration (EB_ET) models are extensively used to estimate different components of the hydrological cycle. Surface and subsurface hydrological processes are modeled in SWAT but limited to the extent of shallow aquifers while MODFLOW concentrate on groundwater movement. Therefore, neither SWAT nor MODFLOW can independently simulate the full extent of the hydrological cycle at the watershed scale. Further, spatially variable recharge inputs to MODFLOW are normally assumed constant and estimated as a percentage of rainfall, which is does not realistically represent this spatial and temporally variable and management responsive process. In this study, a framework coupling SWAT (v. 477) and the Newton Formulation for MODFLOW-2005 (MODFLOW-NWT) was developed to allow interaction of fluxes between SWAT hydrological units (HRUs) and MODFLOW-NWT grids at user defined time steps. Also, a set of new tools were developed using DELPHI programming language in Windows environment to assist users to create the MODFLOW project and linkage with SWAT. The integrated SWAT-MODFLOW-NWT model system will be evaluated using the Fort Cobb experimental watershed dataset for the period 2005-2010. Measured groundwater levels from the underlying Rush Spring aquifer and flow data at daily time-step from four USGS gauges located within the watershed were used for this purpose. Calibration and validation results from this study is presented and discussed. The next phase

involves incorporating an EB_ET model that can provide improved evapotranspiration (ET) estimates to calibrate or substitute for ET in SWAT model.

Keywords: SWAT, MODFLOW, EB_ET, Integrated hydrological modeling, hydrologic model

INTRODUCTION

The hydrological responses at the watershed scale are sensitive to changes occurring in both the surface and subsurface systems. These two systems are closely related and water and solute fluxes can propagate in one or more directions as a function of the local or regional hydrological cycle. Assessing the impact of anthropogenic and naturally driven changes in the hydrological responses and transport requires comprehensive modeling approaches in which surface and subsurface processes can be realistically modeled. The Soil and Water Assessment Tool (SWAT; Arnold et al., 1998) and the Modular Three-Dimensional Finite-Difference Groundwater Flow (MODFLOW; McDonald and Harbaugh, 1988) are surface and subsurface models, respectively, that are used in numerous studies around the world. SWAT and MODFLOW follow different approaches to represent the physical world with advantages and disadvantages when simulating the hydrological processes and use of computational resources. SWAT simulate processes at the hydrological response unit (HRU) level, which is a function of slope, land use and soil properties while MODFLOW focus on simulating processes occurring at the continuum volume defined by cells and hydrogeological properties. Both SWAT and MODFLOW can capture the space and temporal variability commonly found in hydrologic problems and incorporate flow and transport computations at daily, monthly and yearly time-steps. Integrated or coupled applications for SWAT-MODFLOW can be found in the literature (Sophocleous et al., 1999 and 2000; Conan et al., 2002; Kim et al., 2008), however, no comprehensive modeling framework available and use has been limited.

In addition to surface-subsurface water flux interaction, the atmosphere plays an import role through evapotranspiration (ET) in the hydrological cycle accounting for a large portion of the water budget on specific areas (Starks and Moriasi, 2009; Moriasi and Starks, 2009). As an illustration, Hanson (1991) estimated the mean annual ET for Oklahoma to be approximately 85% of the total annual rainfall. In cases in which observations of the driving ET mechanisms are absent or spatial variability is present, the energy balance evapotranspiration (EB_ET) algorithms can serve to accurately estimate ET at regional scales (Jackson 1984; Gowda et al., 2008). For example, Gowda et al., (2008) concluded from literature review that remote sensing based algorithms can be used to estimate ET within accuracy of 67% to 97%. EB_ET algorithms are based on remote sensing observations of the surface visible and near-infrared electromagnetic spectrum reflectance and radiometric surface temperature measured in an infrared thermal band (Gowda et al., 2008). These properties provide advantages when ET estimations are needed at the watershed scale, as satellite images are commonly available today.

In this paper, an integrated hydrologic modeling framework that has been developed for coupling SWAT and MODFLOW and integrating an EB_ET model with SWAT is presented. Implementation of the framework was done in three steps: (1) development of conceptual framework, (2) development of new application tools for coupling/integrating models and to assist users to create and manipulate cell oriented maps (i.e. GRIDs) necessary to create a MODFLOW project and the necessary linking files, and (3) development and insertion of hard-coded routines to the SWAT and MODFLOW codes to interface the models. Although the EB_ET model integration is not described in detail in this paper, it is presented in the general description to provide the reader a general overview. Note that the EB_ET model will be integrated to SWAT (i.e., executed in batch without output model interaction at each time steep) while MODFLOW was coupled (i.e., execute on the same time framework with models output interaction at each time steep).Finally, implementation of the modeling framework for deriving model input and dynamically linking SWAT and MODFLOW is demonstrated using a watershed dataset from southwestern Oklahoma.

INTEGRATED HYDROLOGIC MODELING FRAMEWORK

Coupled SWAT-MODFLOW model

Figure 1 summarizes the conceptual framework and side-to-side application for the coupling SWAT-MODFLOW and integrated SWAT-EB_ET models. The Newton formulation for MODFLOW 2005 (NWT v. 1.0.4) was coupled with SWAT (v. 477). MODFLOW code was rearranged and compiled with SWAT using Intel visual FORTRAN composer XE 2011 version 12.1 (Intel Corporation, Santa Clara, CA[1]) in visual studio 2010 (Microsoft Corporation, Redmond, WA[1]). Note that MODFLOW-NWT maintains MODFLOW 2005 capabilities but some optional packages may not be compatible with the NWT solver. In addition, a series of interfacing routines were developed allowing SWAT to interact in real-time with MODFLOW and pass simulated results (e.g. recharge) dynamically during execution. Two new application tools (i.e., SPELLmap and SWATmf) were developed in DELPHI XE2 (Embarcadero, San Francisco, CA[1]) to assist modelers create the MODFLOW project and configure the models when coupled or integrated with SWAT.

1 Reference to any non-government products in this paper does not constitute an endorsement. The United States Department of Agriculture (USDA) cannot and will not endorse any private organization. USDA does not affiliate itself with, nor does it warranty in any way the respective software or files created by these applications.

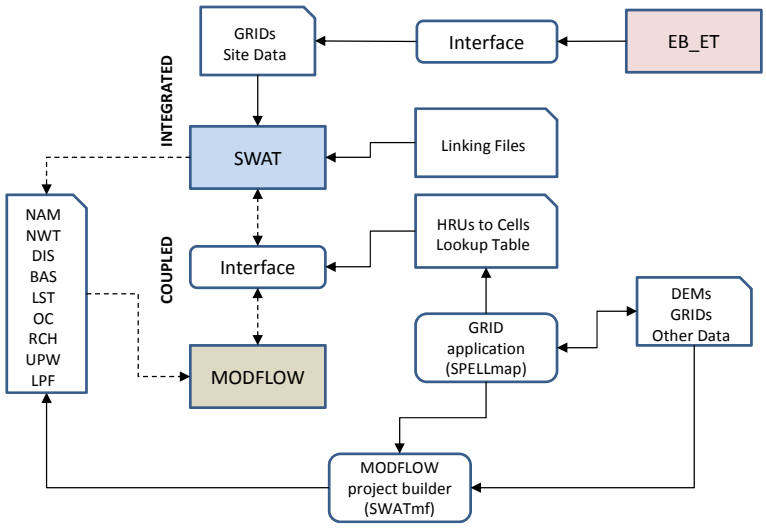

Figure 34. A conceptual integrated modeling framework. Dotted lines represent running time flow of data (coupled approach) and solid lines batch applications (integrated approach).

The SWAT and MODFLOW were coupled by fragmenting the MODFLOW source code into three modules controlling the launch, execution and closing of MODFLOW. Minimum changes in SWAT and MODFLOW code were necessary but some variables and new routines were inserted to make the modeling framework more robust. All new FORTRAN codes were object oriented and developed and interfaced within the SWAT daily cycle simulation (i.e., simulate.f). Two new input options were added to SWAT through the *.cio file allowing activation/deactivation of the MODFLOW or EB_ET model. Also, paths to the linking files were included. The linking files provide SWAT with specific MODFLOW or EB_ET model configuration while maintaining code independence. For example, for MODFLOW, the linking file contains the necessary project folder, file paths and specific variables needed to setup the MODFLOW project in run-time and to exchange results. Note that model interaction occurs through native files and was not hard coded.

SWAT to MODFLOW linkage

The SPELLmap application was developed to provide users the capability to create the MODFLOW project equipped with GIS capabilities. It allows users to perform cell-to-cell manipulation and visualization and other GRID-based operations needed in a common MODFLOW three dimensional project. The SPELLmap produce geo-referenced ASCII GRIDs with ESRI compatible format that can be integrated into MODFLOW projects when using SWATmf application. Note that two-dimensional spatial data in MODFLOW is described by the U2DREL or U2DINT meta-variable along the different packages. Conceptually, spatial discretization in SWAT and MODFLOW is different. Therefore, SWAT-derived hydrologic response units (HRUs) must be spatially represented in a GRID format. Also, HRUs must be able to propagate fluxes to MODFLOW cells (linked). The HRUs in SWAT and GRIDSs in MODFLOW are not geographically but spatially located. In the other hand, ArcSWAT coupling SWAT and ArcGIS (ESRI Corporation, Redlands, CA[1])

operates in a geo-referenced environment. Moreover, planar dimension of HRUs are variable in ArcSWAT while cells in MODFLOW are fixed with rectangular definition. In Figure 2, a general view of the SWAT-MODFLOW linkage is illustrated. The lookup table serves to connect (i.e., indexing) the two models in a GRID-to-GRID fashion. The lookup table was built using the *FullHRU* feature class created by ArcSWAT after developing the HRUs for the SWAT project without using the refinement option and then, converted to raster with equivalent cell size of the original DEM. Extractions of the HRU ID, DEM cell ID, area fraction, and projection to the MODFLOW GRID extent was implemented in SPELLmap (Figure 2). Note that HRUs when converted to GRID are spatially located and identified by the GRID cell position (i.e., vectoring position).

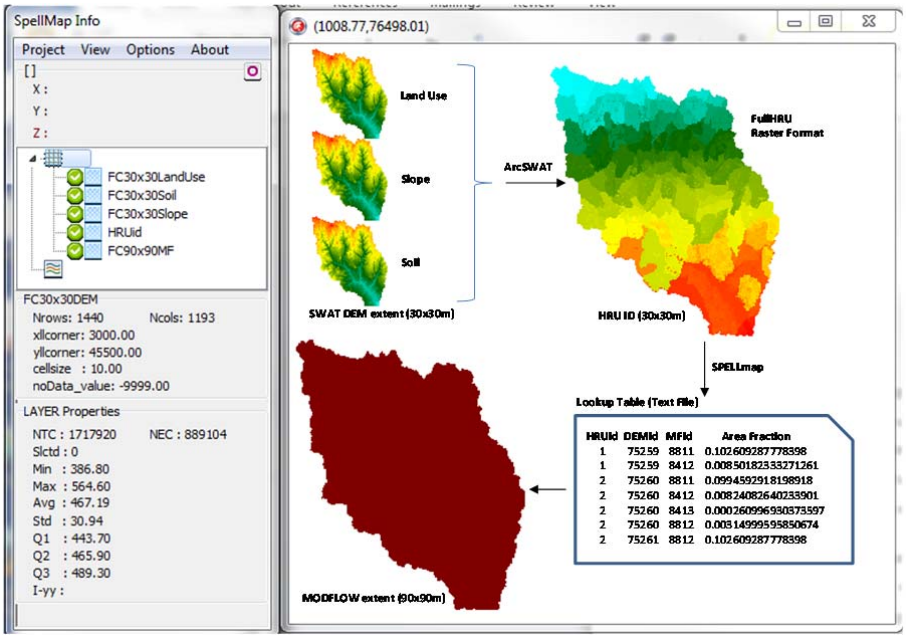

Figure 35. SPELLmap application illustrating the SWAT-MODFLOW linkage through the lookup table.

SWATmf Application

The SWATmf application was developed to assist users in building a MODFLOW project (e.g., basic package–BAS, discretization file–DIS and Newton solver–NWT), setting-up optional packages (e.g., recharge package–RCH, upstream weight package–UPW, output control-OC, list file-LST and layer property flow package–LPF), and to create the SWAT-MODFLOW linking file. Note that MODFLOW projects can be created with any other available application or manual input. In Figure 3, an example of the SWATmf graphical user interface indicating the discretization file for a MODFLOW project with 10 layers is shown.

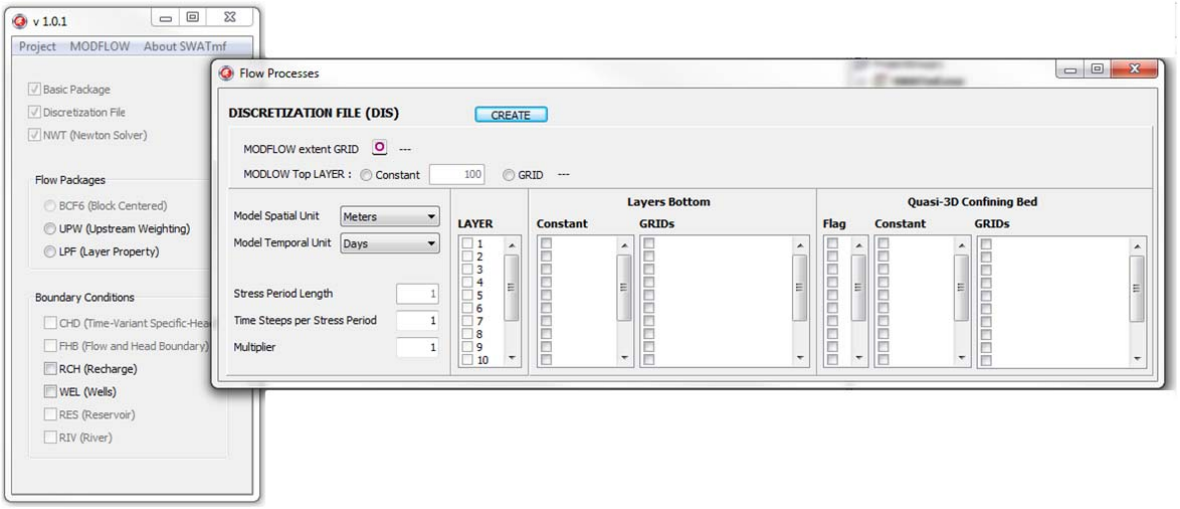

Figure 36. SWATmf development to assist user create the MODFLOW project and linkage with SWAT model.

STUDY CASE

Study area

Located in the southwestern Oklahoma, the Fort Cobb reservoir experimental watershed (FCREW) lay on the Rush Spring aquifer (RSA) on approximately 780 km^2. The land use is predominantly agriculture (56%, about one-third is irrigated) followed by pasture and rangeland (33%), forest and shrub (5%), water (2%) and miscellaneous uses (4%), with low density homesteads (Steiner, 2008). A hilly topography is found in the FCREW with elevations ranging from 380 to 560 m over the mean sea level. Soils are heterogeneous and erosive with fine sandy loam in the eastern part, fine sandy loams and loamy soils in the north central and south central portions of the watershed, and silt loams in the western (Steiner, 2008). A reservoir located close to the watershed outlet serves to regulate stream flow, sediments and nutrient concentrations downstream. The FCREW subsurface watershed is part of the RSA which encompasses more than 6,200 km^2 in the west-central Oklahoma. The RSA is mainly an unconfined aquifer constituted with fine-grained cross-bedded sandstone with irregular dolomite or gypsum lenses (OWRB, 1965, 1965; Becker 1998) from the Permian age. This aquifer is usually less than 75m thick but in some areas it can reach over 90 m. The RSA is the main source of water for irrigation, domestic and public supply in the FCREW that laid on the Marlow formation. The Marlow formation is moderated to well-cemented unit acting as a vertical boundary flow control with extremely low permeability (Becker, 1998).

A network of fifteen observation sites (MICRONET; http://ars.mesonet.org/) collects surface (rainfall, air temperature, relative humidity, and solar radiation) and subsurface (soil temperature and volumetric water content) data at 5, 15 and 30 minute intervals in the FCREW. Additional observation sites were available from the Oklahoma MESONET (http://www.mesonet.org/index.php) and the National Weather Service (NWS). Daily stream

flow from four US Geological Survey sites (USGS, Water Science Center, OK; http://ok.water.usgs.gov/) and two groundwater monitoring wells from the Oklahoma Water Resources Board (OWRB; http://www.owrb.ok.gov/) serve to evaluate the simulated hydrological response.

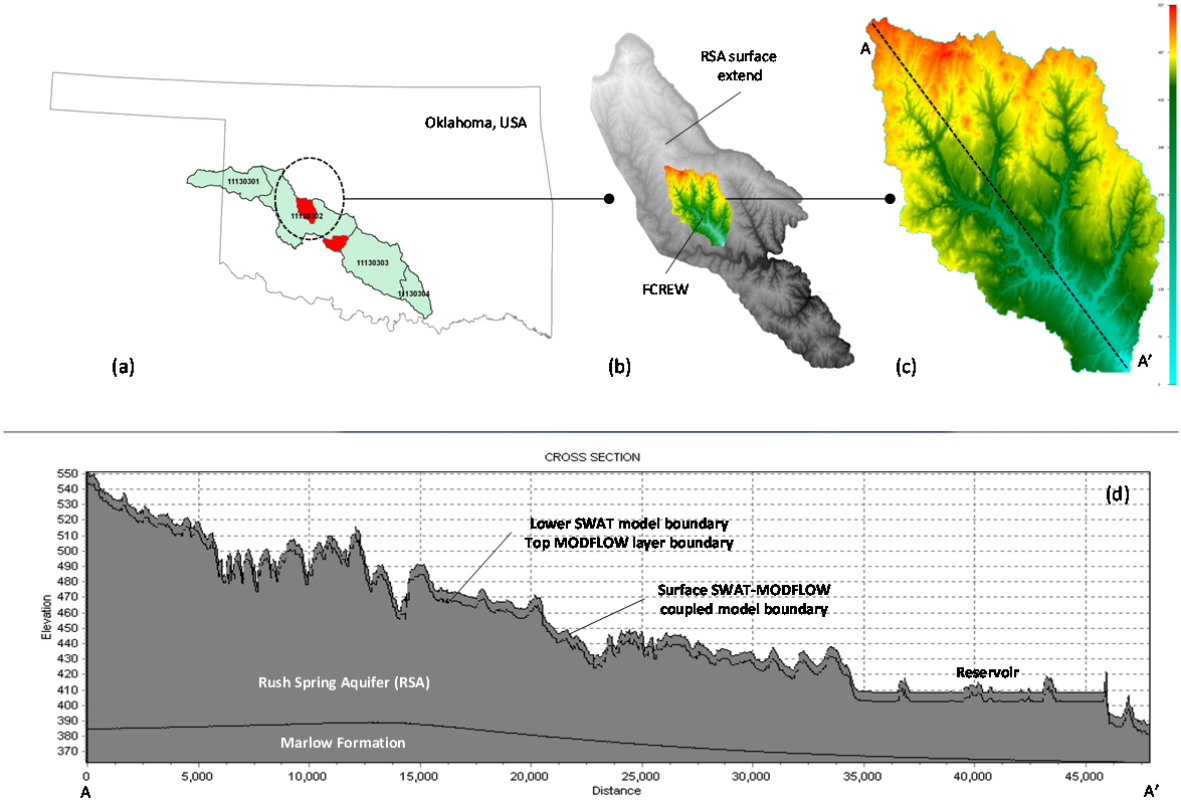

Figure 37. Study area. a) Study case location within USA. b) Surface and groundwater watersheds extend indicated on a surface digital elevation model. c) Fort Cobb Reservoir Experimental Watershed (FCREW) digital elevation model. d) Cross section and major hidrological units.

Model Physical Conceptualization and Model Parameterization

SWAT and MODFLOW models were initially developed separately and then coupled. SWAT model was built from a 30 x 30 m digital elevation model (USGS Seamless Data Distribution System; http://seamless.usgs.gov/viewer.htm) using ArcSWAT application without HRU refinements. In addition to the weather data inputs, soils from the SSURGO database, and land use and coverage from 30 m Landsat 5 Thematic Mapper image was used. The land use layer was complemented with a study conducted in the area in 2005. The watershed delineation and HRU definition were defined to capture the available spatial variability from the combined soil, land use, slope and DEM layers. Weather data, management, crop yields, and flow data were used to complete calibration of the models. More details on the SWAT model setup for the FCREW are described in Starks and Moriasi (2009) and Moriasi and Starks (2009).

The MODFLOW project was developed to represent the unconfined RSA within the FCREW surface extent based on one layer and square 90 x 90 m cells size. This spatial discretization resulted on a GRID of 399 columns by 481 rows and 99,848 active cells. In contrast, the SWAT-derived HRUs were represented in a GRID of 1,193 columns by 1,440 rows, 30 x 30 m cells size with a total of 889,140 active cells. These GRID cell sizes were selected to represent the spatial variability present at the surface and subsurface. The available hydrogeological data for the RSA is very coarse and the RSA hydrogeological properties were considered spatially homogenously distributed but further investigation is needed. The large number of existing extraction wells plays an important role in defining the spatial variability of the groundwater table and was a major consideration on defining the MODFLOW model cell size. The major hydrologial units such as the Marlow formation boundary, and the top MODFLOW boundary layer were interpolated and extracted from USGS observations and SWAT model, respectively. Core samples extracted approximately 20 years ago from the RSA and Magers, (2011) hydrogeological description served to define the top Marlow formation boundary and parameterize the RSA hydrogeological unit.

Discussion

SWAT-MODFLOW coupled Model

SWAT and MODFLOW models have been extensively used for modeling and managing surface and groundwater resources and separately validated at different scales. Also, both models hold a dynamic modeling community and had been constantly improved over years. Use of coupled SWAT-MODFLOW takes advantage of both models capabilities leading to inputting relatively accurate and spatially variable recharge rates to MODFLOW as a function of land use, slope, and water and crop management practices. The proposed modeling framework extends the models capabilities to the full hydrological cycle at the watershed scale. In the coupled model, SWAT controls the MODFLOW horizontal extent. This is a common limitation found in integrated hydrologic models as surface and subsurface watersheds do not necessarily share the same horizontal boundaries. This model restriction requires modelers to assess aquifer boundary conditions (e.g., fluxes or groundwater table slope) base on observations or by modeling extended areas. Also, note that SWAT controls MODFLOW *stress periods* and cycle simulation when coupled. In general, it is recommended that modelers initially assess model parameterization, boundary and initial conditions in each model separately before performing the coupled simulations.

Although the coupled model was compiled for both 32-bit and 64-bit machines, it is recommended that 64-bit architectures be used due to large storage and memory demands. In addition, during execution SWAT or MODFLOW can create files exceeding the 2 GB thresholds found in 32-bit system. Therefore, modelers need to evaluate the trade-offs between the spatial variability representation (e.g., SWAT HRUs and MODFLOW GRID resolution, observations, and physical conceptualization) with model output accuracy, computational resources, and model response time.

Summary

Modeling result from model simulations will be incorporated later in the manuscript as we still working in the framework, applications and models. Also, conclusion will be added.

ACKNOWLEDGEMENTS

The authors would like to thank Shana Mashburn and Mark Becker from the U.S. Geological Survey and Christopher R. Neel and Jessica S. Magers from the Oklahoma Water Resource Board for data provided, access to core samples and general overview of the study area. We also grateful Alan Verser for his contribution to the SWAT model setup and tips and discussions for SWAT data extraction.

REFERENCES

Alley, P.B., and J.W. Naney. 1991. Hydrology of the Little Washita River Watershed, Oklahoma: Data and analysis. ARS-90. USDA Agricultural Research Service.

Arnold, J.G., R. Srinivasan, R.S. Muttiah and J.R. William. 1998. Large area hydrologic modeler and assessment part I: model development. J. Am. Water Resour. As. 34: 73-89.

Becker, M. 1998. Steady-state simulation of ground-water flow in the Rush Spring Aquifer, Western Oklahoma. Water-resources investigations report 98-4082. USGS, Denver, CO.

Conan, C., F. Bouraoui, N. Turpin, G. de Marsily and G. Bidoglio. 2002. Modeling Flow and Nitrate Fate at Catchment Scale in Brittany (France). 32(6): 2026-2032.

Gowda, P.H., J.L. Chavez, P.D. Colaizzi, S.R. Evett, T.A. Howell and J.A. Tolk. 2008. ET mapping for agricultural water management: present status and challenges. Irrig Sci 26:223-237.

Hanson, R.L. 1991. Evapotranspiration and Droughts. In R.W. Paulson et al. (Eds.): National Water Summary 1988-1989, Hydrologic Events and Floods and Droughts. 99-104. USGS Water-Supply Paper 2375.

Jackson, R.D. 1984. Remote sensing of vegetation characteristics for farm management. SPIE 475:81–96.

Kim, N.W., I.M. Chung, Y.S. Won, J.G., Arnold. 2008. Development and application of the integrated SWAT–MODFLOW model. Journal of Hydrology, 356: 1-16

Magers, J.S. 2001. Occurrence of arsenic in the Rush Spring Aquifer sandstone and its implications on groundwater chemistry: Caddo County, Oklahoma. Master thesis. Oklahoma State University, OK.

Moriasi, D.N and P.J. Starks. 2009. Effects of soil dataset resolution on SWAT2005 streamflow calibration parameters and simulation accuracy. Journal of the Soil and Water Conservation Service 65(2):63-78.

Sophocleous, M.A., J.K. Koelliker, R.S. Govindaraju, T. Birdie, S.R. Ramireddygari and S.P. Perkins. 1999. Integrated numerical modeling for basin-wide water management: The case of the Rattlesnake Creek basin in south-central Kansas. Journal of Hydrology, 214: 179-196.

Sophocleous, M., and S.P. Perkins. 2000. Methodology and application of combined watershed and ground-water models in Kansas. Journal of Hydrology, 236: 185-201.

Starks, P.J. and D.N. Moriasi. 2009. Spatial resolution effect of precipitation data on SWAT calibration and performance: implications for CEAP. Transactions of the ASABE 52(4):1171-1180.

Steiner, J.L., P.J. Starks, J.A. Daniel, J.D. Garbrecht, D. Moriasi, S. McIntyre, and S. Chen. 2008. Environmental effects of agricultural conservation: A framework for research in two watershed in Oklahoma's upper Washita river basin. Journal of Soil and Water Conservation, 63:443-452.

OWRB. 1965. Ground water in the Rush Spring Sandstone Caddo county area: Publication No 11. 1965. Oklahoma Water Resource Board, Oklahoma City, OK

OWRB. 1966. Ground water in the Rush Spring Sandstone Caddo county area: Publication No 15. 1966. Oklahoma Water Resource Board, Oklahoma City, OK.

A comparison of stream flow prediction using station and gridded meteorological datasets in IRAN

Sepideh Ramezani
IUT, Isfahan University of Technology, Email: s.ramezani@na.iut.ac.ir

Monireh Faramarzi
IUT, Isfahan University of Technology, Dept. of Natural Resources, 84156-83111, Isfahan, Iran

Saeed Soltani
IUT, Isfahan University of Technology, Dept. of Natural Resources, 84156-83111, Isfahan, Iran

Karim C. Abbaspour
EAWAG, Swiss Federal Institute for Aquatic Science and Technology, P.O. Box 611, 8600 Dübendorf, Switzerland.

Abstract

Accuracy and precision of hydrological simulations depend on the quality and quantity of the input requirements, mainly climatic data. This paper focuses on comparing the effect of two different climate datasets on the prediction of river discharges across Iran. Soil and Water Assessment Tool (SWAT) in combination with SUFI-2 program was used for simulation of the eight main hydrologic regions (HR) in Iran. The two climate datasets were: i) the observed data of 150 synoptic stations obtained from the public Weather Service of the Iranian Meteorological Organization (WSIMO), and ii) the gridded climate data of Climatic Research Unit, University of East Anglia (CRU TS3.0 global), with 0.5 degree resolution (about 1200 grid points covering entire country). The study period was 1987-2002 considering 3 years of warm-up period. Four SWAT projects were created to address the effect of two climate datasets and two different discretizations delineating 506 and 1269 subbasins. The results showed that compare to the local observational datasets (150 stations) the CRU gridded dataset (1200 stations) performed well when simulating river discharge in most of the HRs in Iran. The improvement was significant when more subbasins were delineated using SWAT model. We concluded that the CRU high resolution grid dataset is useful for the hydrological simulation in Iran, but a balance must be reached between the number of stations and the resolution of the subbasins delineation. This study conveys the important message that the global CRU climate data can be used in regions of climate data scarcity with high confidence.

Keywords: SWAT, CRU, subbasins, hydrologic modeling, IRAN.

Introduction

Hydrological models are useful for understanding of the natural processes occurring at the watershed scale and to analyze the impact of different management practices. Precision in the simulation of hydrological processes depends highly on the quality and quantity of climate datasets, especially precipitation. Several studies have focused on the impact of characteristics of spatial datasets such as the resolution of DEM, landuse and soil maps on the simulation of hydrological processes (e.g. Wood et al., 1988; Zhang and Montgomery, 1994; Bloschl and Sivapalan, 1995; Chaplot, 2005; Wu et al., 2007). Numerous precipitation datasets have been developed in the last two decades including: Climate Research Unit of University of East Anglia (CRU) (New et al. 1999), Willmott–Matsuura (WM) (Willmott and Matsuura, 2001), Global Precipitation Climate Center (GPCC) (Rudolf et al. 1994), Global Precipitation Climatology Project (GPCP) (Susskind et al. 1997), Tropical Rainfall Measuring Mission (TRMM) (Huffman et al. 1997), University of Delaware (UDEL) (Matsuura, 2011), Variability Analysis of Surface Climate Observations (VASClimO) (Beck et al. 2005) and NCEP– Department of Energy (DOE) Atmospheric Model Inter comparison Project (AMIP-II) Reanalysis (NCEP-2) (Kistler et al. 2001; Kalnay et al. 1996). Few studies have assessed performance of different climate datasets on the simulation of discharge at local scale.

Iran with an area of about 1648000 km^2 is located in arid and semi-arid region. Hydrogeological conditions are heterogeneous across the country. Except for the north and western parts, the climate data availability is poor for most of the regions in the center and southern area. This creates a large uncertainty in hydrological modeling and decision making for future planning (Faramarzi et al., 2009).

The Soil and Water Assessment Tool (SWAT) was used in this study to create two hydrologic models for entire Iran. For this the observational climate dataset from 150 synoptic stations and the CRU gridded dataset with 0.5 degree resolution were fed into the model, separately. The main goal was to investigate the goodness of the gridded high resolution dataset in the prediction of the river discharge at different hydrologic regions of Iran. If the freely available gridded dataset performs well in the prediction of stream flow, it can be recommended for use in regions of scarce climate data. Objectives of this study were 1) to compare the effect of two climate datasets (observed and gridded) on the prediction of the stream flow, and 2) to show the relationship between resolution of the rain gauge network and subbasin size using SWAT model.

Materials and methods

Study area: Iran is located between 25 and 40 degrees north latitude and 44 to 63 degrees east longitude. The altitude varies from -40 m to 5670 m, which has pronounced influence in the diversity of the climate. Although most parts of the country could be classified as arid and semi-arid, it has a wide spectrum of climatic conditions. The northern and western parts of the country are richer in terms of water availability and precipitation while in eastern and southern regions water scarcity is critical due to inadequate precipitation, high temperature, and improper management of water resources. Iranian Ministry of Energy and Iranian Meteorological Organization are in charge of measuring wide range of climatic variables for which a denser gauge network has been established in the northern and western parts but fewer gauges in number are launched to measure data in central and southern regions.

Input data: A set of digital maps including DEM, landuse, and soil maps were used to setup the hydrologic SWAT model of Iran (see Faramarzi et al., 2009 for more detail). Climate datasets consist of daily precipitation and maximum and minimum temperature obtained from

two different sources: the public Weather Service of the Iranian Meteorological Organization (WSIMO) which provides observational data for more than 150 synoptic stations, and the Climate Research Unit (CRU) which provides global gridded data with a 0.5 degree spatial and daily temporal resolution (available at www.cru.uea.ac.uk), We obtained daily river discharge data of 80 hydrometric stations to compare with SWAT's predictions in the eight hydrologic regions which were defined by the Iranian Ministry of Energy (MOE), (see Figure1). Table 1 gives more detail about the study area and the eight hydrologic regions.

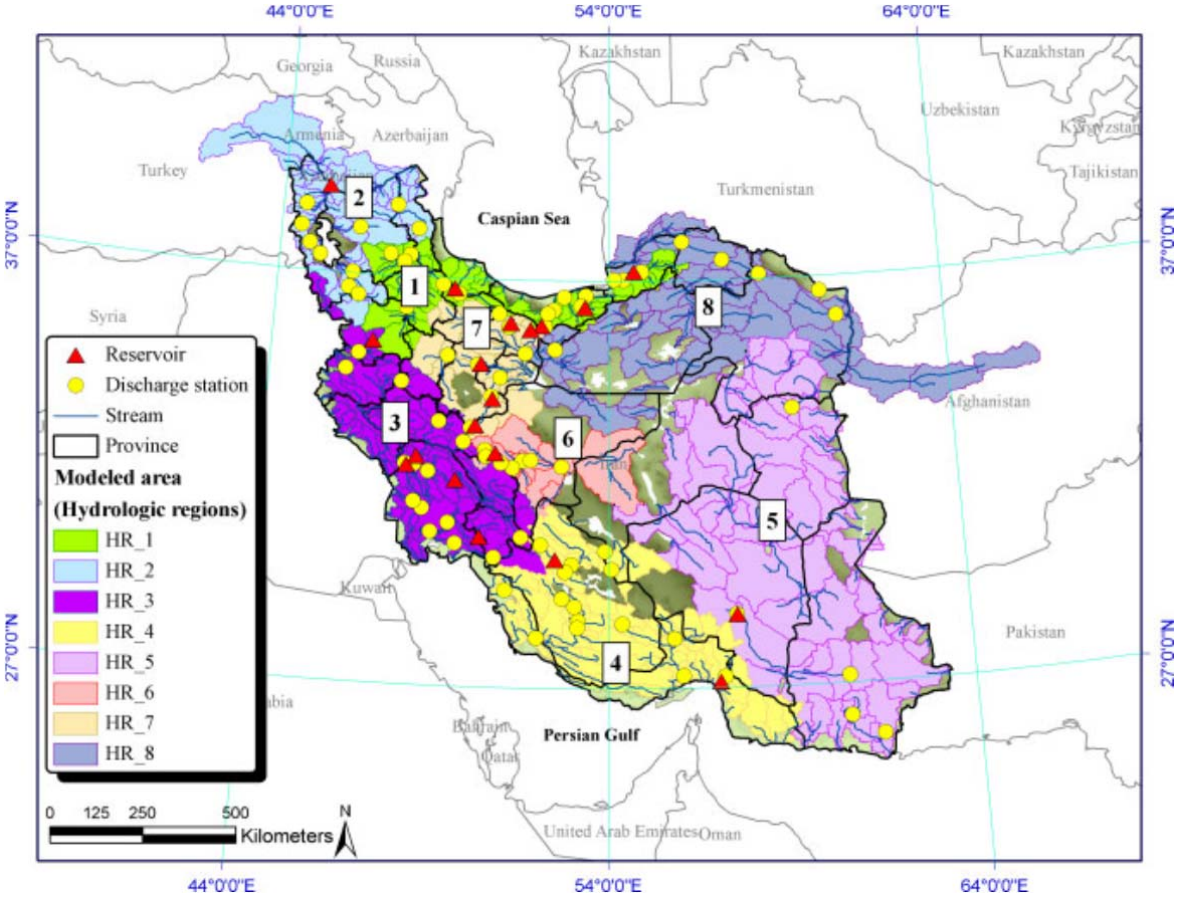

Figure1. Study area and the main hydrologic regions. The dark green areas in the background include wetlands, lakes and marshes which needed to be cut from the DEM in order to have a correct river pattern (not included in the model), (Adapted from Faramarzi et al. 2009)

Table1: Watershed characteristics of the eight main hydrologic regions in Iran

Hydrologic regions	Area[a] (km^2)	Mean precipitation[b]	Number of subbasins		Number of hydrometric stations
			Scenarios 1-3	Scenarios 2-4	
HR1	97,478	599	66	81	16
HR2	131,973	399	57	99	10
HR3	185,042	545	92	173	15

HR4	196,329	278	87	165	15
HR5	459,309	132	68	411	5
HR6	66,654	152	26	54	7
HR7	82,268	287	43	88	7
HR8	256,553	197	67	198	5

[a] Modeled area: area of subbasins delineated in each HR were aggregated.
[b] Available from Iranian Ministry of Energy (1998) report.

Scenario and Model setup: In this paper first we created two SWAT projects using observed and gridded climate data sets. Further we changed the minimum size of threshold area in each project to test the effect of number of the subbasins and climate network resolution. Overall, we created four projects (which we so called four scenarios) with the following characteristics:

Scenario 1: 506 subbasins using observed climate dataset of WSIMO
Scenario 2: 1269subbasins using observed climate dataset of WSIMO
Scenario 3: 506 subbasins using CRU gridded climate dataset
Scenario4: 1269subbasinsusing CRU gridded climate dataset

The number of subbasins at different scenarios and hydrologic regions is addressed in Table1.We used dominant landuse, soil and slope for characterization of the hydrologic response units. The Curve Number (CN) method was used to predict river discharge while potential evapotranspiration (PET) was simulated using Hargreaves method (Hargreaves et al., 1985). To compare the simulated river discharges with those of observed values, we used the SWATCUP package (Abbaspour et al., 2011) but did not calibrate the model for any of the above scenarios as the impact of climate data would then be convoluted by the calibrated parameters.

Results and discussion

The performance of the predictions was evaluated using Nash-Sutcliffe Efficiency (NSE) value. Comparison of the simulated monthly discharges with that of observed values, showed a better prediction in HR3 and HR4 in both scenarios 1 and 3 (Figure 2). A low NSE value in other HRs is related to the initial model parameters which were not calibrated in this study. As shown in Table 2, the NSE values are different at different HRs. Overall; the weighted average value of NSE for the 80 stations, with number of hydrometric station in every HR, in the entire country was -18.45 and -16.33 in scenario 1 and scenario 3, respectively. Keeping all conditions constant, the change of climate input from observed to gridded dataset resulted NSE value of -13.67 and -5.52 for scenarios 2 and 4, respectively. The difference between NSE values of Hydrological regions may be due to number of hydrometric stations in each HR, for example in HR 1, 2, 3 and 4 about 70% of hydrometric stations were located. Also in HR 1, 2 and 3 NSE values show better performance in comparison of other HRs because mean precipitation of these HRs are higher than the others (see Table 1).

The significant improvement in the scenarios with CRU dataset is related to its high spatial resolution, with which, subbasins can better capture proper climate data from the closest grid point. Therefore a balance between the number of subbasins and the resolution of the climate data network is required for optimizing the model performance in the prediction of the hydrological processes. It must be pointed out that improvement of NSE value in Scenario 4

was not similar in all HRs but more significant in HR6 where Zayandehrud, one of the most important rivers in Iran is located. This study lays the basis to use gridded high resolution climate datasets for advanced studies (e.g. water-food-climate change) in data scarce regions of Iran.

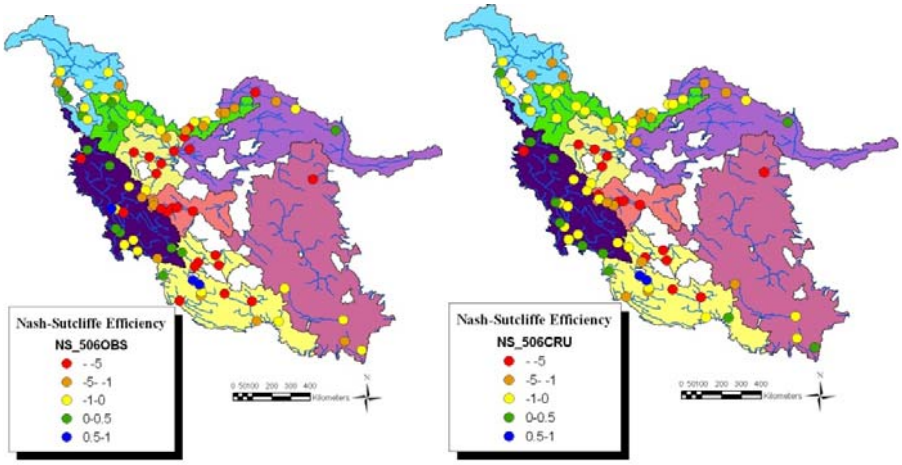

Figure 2. Distribution of NSE values across the country using observed station climate data and gridded CRU climate datasets when 506 subbasins are delineated in SWAT model.

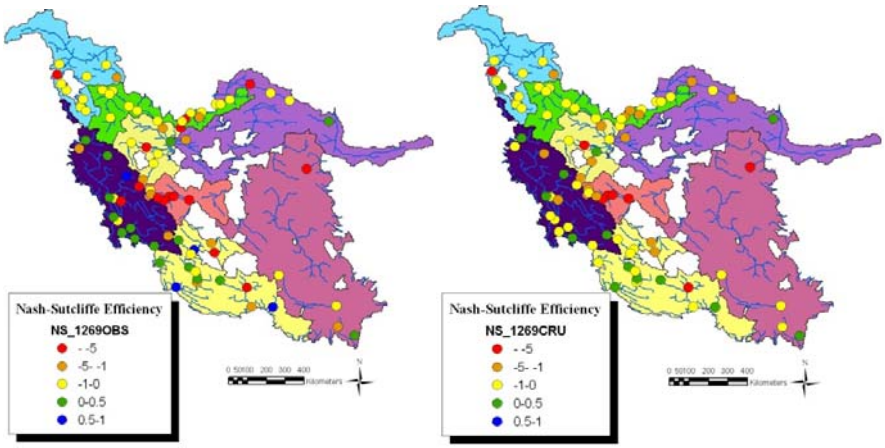

Figure 3. Distribution of NSE values across the country using observed station climate data and gridded CRU climate datasets when 1269 subbasins are delineated in SWAT model

Table2: Performance of the SWAT prediction when 506 subbasins are delineated

	NSE (station climate data)	NSE (CRU)
HR1	-1.97	-0.68
HR2	-0.40	-0.90
HR3	-1.69	-1.34
HR4	-29.25	-5.68
HR5	-87.25	-153.54
HR6	-53.33	-16.64
HR7	-19.83	-41.01
HR8	-5.76	-2.00
Weighted Average	-18.45	-16.33

Table3: Performance of the SWAT prediction using when 1269 subbasins are delineated

	NSE (station climate data)	NSE (CRU)
HR1	-1.52	-0.76
HR2	-0.36	-0.50
HR3	-0.53	-0.22
HR4	-8.34	-3.52
HR5	-10.40	-11.52
HR6	-116.46	-18.17
HR7	-7.46	-25.26
HR8	-2.11	-1.36
Weighted Average	-13.67	-5.52

Conclusions and future work

The hydrologic model SWAT was used to compare the effect of two different climate datasets in the prediction of stream flow while delineating 506 and 1269 subbasins in SWAT model. When delineating 1269 subbasins, the model performance (addressed by NSE) was improved significantly in the prediction of stream flow in most of the hydrologic regions in Iran.

References

Abbaspour, K.C., 2011. SWAT-CUP4, SWAT Calibration and UncertaintyPrograms. A User Manual, EAWAG.Zurich, Switzerland.

Beck, C., J. Grieser and B. Rudolf., 2005. A New Monthly Precipitation Climatology for the Global Land Areas for the Period 1951 to 2000. Published in Climate Status Report 2004, pp. 181 – 190, German Weather Service, Offenbach, Germany.

Blöschl, G., Sivapalan, M., 1995. Scale issues in hydrological modeling: a review. *Hydrological Processes* 9, 251–290.

Chaplot, V., 2005. Impact of DEM mesh size and soil map scale on SWAT runoff, sediment, and NO3-N loads predictions. *Journal of Hydrology* 312 (1-4), 207-222.

CRU, cited 2011: Climate Research Unit, University of East Anglia. [Available online at http://www.cru.uea.ac.uk.]

Faramarzi, M., Abbaspour, K.C., Schulin, R. and Yang, H., 2009. Modelling blue and green water resources availability in Iran. *Hydrological Processes* 23 (3), 486-501.
Hargreaves GL, Hargreaves GH, Riley JP. 1985. Agricultural benefits for Senegal River Basin. *Journal of Irrigation and Drainage Engineering* 111, 113–124.
Huffman, G. J., 1997: Estimates of root-mean-square random error for finite samples of estimated precipitation. *Journal of Applied Meteorology* 36, 1191–1201.
Iran, M.O.E.O., 1998. An overview of natural water plannig of Iran, Tehran.
Kalnay, E., and Coauthors, 1996: The NCEP/NCAR 40-Year Reanalysis Project. *Bulletin of the American Meteorological Society* 77, 437–472.
Kistler, R., and Coauthors, 2001: The NCEP/NCAR 50-Year Reanalysis: Monthly means CD-ROM and documentation. *Bulletin of the American Meteorological Society* 82, 247–267.
Matsuura, K. cited 2011: Terrestrial air temperature and precipitation: Monthly and annual time series (1950–1999) Version 1.02. [Available online at http://climate.geog.udel.edu/ climate.]
New, M., M. Hume, and P. Jones, 1999: Representing twentieth century space–time climate variability: I. Development of a 1961–1990 mean monthly terrestrial climatology, *Journal of climatology* 12, 829–856.
Rudolf, B.,W. Rueth, and U. Schneider, 1994: Terrestrial precipitation analysis: Operational method and required density of point measurements. Global Precipitation and Climate Change, M. Desbois and F. Desahmond, Eds., Springler-Verlag, 173–186.
Susskind, J., P. Piraino, L. Rokke, L. Iredell, and A. Mehta, 1997: Characteristics of the TOVS Pathfinder Path A dataset. *Bulletin of the American Meteorological* Society 78, 1449–1472.
Willmott, C. J., and S. M. Robeson, 1995: Climatologically Aided Interpolation (CAI) of terrestrial air temperature. *International Journal of Climatology* 15, 221–229.
Wood, E.F., Sivapalan, M., Beven, K., B and, L., 1988. Effects of spatial variability andscale with implication to hydrologic modeling. *Journal of Hydrology* 102, 29–47.
Wu, S., Li, J., Huang, G., 2007. Modeling the effects of elevation data resolution onthe performance of topography-based watershed runoff simulation. *Environmental Modeling and Software* 22, 1250–1260.
Zhang, W., Montgomery, D.R., 1994. Digital elevation model grid size, landscape and representation, hydrologic simulations. *Water Resource Research* 30, 1019–1028.

Comparison of Grid-based and SWAT HRU Modeling Approaches for Evaluating the Climate Change Impact on Watershed Hydrology

H.Jung, Graduate student
Konkuk University, Dept. of Civil and Environmental System Eng., 1 Hwayang dong, Gwangjin-gu, Seoul 143-701, South Korea

W. Y.Hong, Researcher
Korea Environment Institute, Korea Adaptation Center for Climate Change, 290 Jinheungno, Eunpyeong-gu,, Seoul 122-706, South Korea

H. G. Jeong, Meteorological Research Scientist
Han River Flood Control Office, Ministry of Land, Transport and Maritime Affairs, Seoul 137-049, South Korea

S.J. Kim*, Professor
Konkuk University, Dept. of Civil and Environmental System Eng., 1 Hwayang dong, Gwangjin-gu, Seoul 143-701, South Korea

Abstract

The aim of this study is to compare the results of grid-based and Soil and Water Assessment Tool (SWAT) HRU (hydrologic response unit)-based modeling for evaluating the climate change impact on watershed hydrology. The grid-based model is a typical distributed hydrological model which divides the watershed as a cell base and calculates the water balance of each cell by constructing 3 vertical layers of surface, subsurface and groundwater flow. SWAT is a well-known hydrologic response units (HRUs)-based model, which are portions of a subbasin that possess unique land use, management, and soil attributes. For a 930.4 km2 YongdamDam watershed located in the middle of South Korea,the two models was calibrated for five years (2002-2006) and validated for another three years (2007-2009) daily streamflow data at multiple locations including couple of year soil moisture and evapotranspiration data. Nash-Sutcliffe model efficiency (NSE)for streamflow were 0.34 – 0.83, soil moisture were 0.15 – 0.86.For the future climate change scenario, the MIROC3.2 hires A1B scenario were prepared for 2040s (2020-2059) and 2080s (2060-2099) using the Long Ashton Research Station – Weather Generator (LARS-WG) model.The MIROC3.2 hires A1B 2080s temperature and precipitation showed an increase of 4.6 and 13.8%, respectively, based on the 1980-2009 data. The impacts of projected future climate change scenarios on the streamflow, evapotranspiration, and soil moisture were increases of SWAT model +13.8%, +10.8%, and 0.7%, Grid-based model -37.7%, +47.9%, and +1.2%. Distribution map for each hydrology component in the two models were compared. Evapotranspiration and soil moisture content was affected by effective soil depth. And there component increase in precipitation has been affected. Grid-based model has interception under the influence of evapotranspiration is larger, runoff is smaller tends to be simulated. SWAT model simulation results were keeping up the trend of the precipitation.

Keywords: Grid-based, SWAT, HRU, Climate change, MIROC3.2 hires, LARS-WG, Watershed, Hydrology

Introduction

A few studies that compare the performance of the SWAT model (Arnold et al.,1993) with other types of models. Most studies with reference to the SWAT model (Srinivasan et al., 1993,1998; Arnold and Allen, 1996; Arnold et al., 1999a,b) are related to model applications. In a number ofpublications reference is made to the SWAT model in combination with other models to obtain more detailedor specific outputs. Sophocleous et al. (1999) linked SWAT with MODFLOW (McDonald and Harbaugh,1988) in order to have a more precise description of the shallow aquifer. Weber et al. (2001) used SWATin a joint modelling exercise with two other models (ELLA, Weber et al., 1999) and (ProLand, Möller andKuhlmann, 1999) using GIS to examine the effects of land use changes in the Aar watershed.

Some authors tend to criticize the use of distributed models. Their main concern is the many parametersthat can be altered during the calibration phase. Beven (1989, 1996) considers such models, which claim to bedistributed and physically based, as being lumped conceptual models with an excessive amount of parameters.According to Beven (1996), a key characteristic of distributed models is the problem of overparameterization.In response, Refsgaard and Storm (1996) emphasize that a rigorous parameterization procedure might help toovercome the problems faced in calibrating and validating fully distributed physically based models.

The main purpose of this study is to compare the performance of two physically basedmodels, the fully distributed Grid-based model and the semi-distributed SWAT model. In that scope we used two models which were designed with a focus on distributed and semi-distributed model.

Study Area and Data

The study area is Yongdamdam watershed (930 km2) which is located within N35˚35′~36˚00′ and E127˚20′~127˚45′ (Figure 1). Daily weather data obtained from Korea Meteorological Administration. The daily streamflow and GIS data were obtained from Water management Information System (WAMIS, http://www.wamis.go.kr), and the soil moisture data were obtained from Agricultural Weather Information Service (AGWI, http://weather.rda.go.kr).

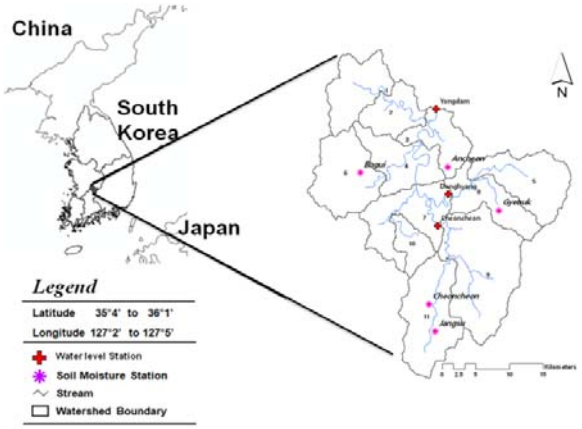

Fig. 1 Location of the Yongdamdam watershed and the water level stations and soil moisture stations.

Methods

Downscaling Technique by LARS-WG

The GCM data were downscaled by two steps for the study watershed. As the first step, to ensure that the historical data (30 years from 1971 to 2000) of ground stations and GCM output have similar statistical properties, the bias correction method by Alcamo et al. (1997) was used. This method is generally accepted within the global change research community (IPCC, 1999). Secondly, the monthly GCM data were generated into daily data using the Long Ashton Research Station – Weather Generator (LARS-WG) stochastic weather generator. LARS-WG was also found to produce better precipitation and minimum, maximum and mean temperature results for diverse climates than other weather generators (Semenov et al., 1998).

Semi Distributed SWAT HRU model

Soil and Water Assessment Tool (SWAT) is a physically based, continuous-time, long-term, semi-distributed, conceptual river basin scale model with spatial distributed parameters developed to predict the effects of land management practices in large, complex watersheds on the hydrology, sediment, and contaminant transport in agricultural watersheds under varying soils, land use, and management conditions (Arnold et al., 1998). It is a public domain model supported by the U.S. Dept of Agriculture Agricultural Research Service (USDA-ARS) at the Grassland, Soil, and Water Research Laboratory in Temple, Texas, USA.

To predict runoff generation, SWAT uses a modified version of Soil Conservation Service Curve Number (SCS-CN) method (USDA-SCS, 1972). The hydrologic cycle as simulated by SWAT is based on the water balance equation:

$$SW_t = SW_0 + \sum_{i=0}^{t} \left(R_{day} - Q_{surf} - E_a - W_{seep} - Q_{gw}\right)$$

where SW*t*is the final soil water content (mm), SW*0* is the initial soil water content on day *i* (mm), *t* is the time (d), R*day* is the amount of precipitation on day *i* (mm), Q*surf* is the amount of surface runoff on day *i* (mm), E*a* is the amount of evapotranspiration on day *i* (mm), W*seep* is the amount of water entering the vadose zone from the soil profile on day *i* (mm), and Q*gw* is the amount of return flow on day *i* (mm) (Neitsch et al., 2001).

Fully Distributed Grid-based model

Grid-based model is a physically based model by cells. The watershed is divided into rectangular cells, and the cell profile is divided into three layered flow components: a surface layer, a subsurface unsaturated layer, and a saturated layer. In the model, surface runoff is simulated by the available storage of soil moisture, Evapotranspiration is calculated by Penman-Monteith method considering Leaf Area Index (LAI), and soil moisture is routed by soil water balance equation. The six parameters viz. surface lag coefficient, soil percolation ratio, lateral flow recession curve slope, lateral flow basin lag time, base flow recession curve slope, and base flow basin lag time, are important for model calibration.

Table 1. Comparison of Grid-based and SWAT HRU Model description and method.

	SWAT model	Grid-based model
Equation		
Water Balance	Water balance equation (USDA-SCS, 1972)	Water balance equation (USDA-SCS, 1972)
Evapotranspiration	Penman-Monteith method	Penman-Monteith method
Infiltration	SCS method	$\text{Infilt} = \text{Prec} - Q_{surf} - ET$
Channel Routing	Muskingum	-

Results and Discussion

Future Climate Data

Precipitation is increase by 7.5-13.9 % compared to the baseline, maximum temperature is 2.5-4.6℃, and minimum temperature is 2.7-4.6℃, respectivelyThe uncertainty of the future precipitation causes evaluation difficulties for the prediction of future hydrologic component. Overall, the MIROC3.2 hiresdata demonstrate to reproduce when compared with the observed data.

Comparison of Calibrated Grid-based and SWAT HRU models

The model was calibrated and validated for daily streamflow data at 3 locations (Yongdam, Donghyang, and Cheoncheon) and daily soil moisture data at 5 locations (Jangsu, Ancheon, Cheoncheon, Gyeobuk, and Bugui).
In this study, nine (ALPHA_BF, CANMX, CH_N1, CH_N2, CH_K1, CH_K2, ESCO, GW_DELAY, SOL_AWC) and seven parameters (Soil percolation ratio, Surface lag coefficient, Lateral flow recession curve slope, Lateral basin lag time, Base flow recession curve slope, Base basin lag time, Interception) were selected for calibration of watersheds by SWAT model and Grid-based Model.The streamflow calibration was carried out using five years (2002 to 2007) and validation was using three years (2008 to 2010) of data. The soil moisture calibration and validation was carried out using five years (2004 to 2008) and four month (May 2008 to August 2008) of data. The average NSE for streamflow were 0.34-0.83, soil moisture were 0.15-0.86, respectively. Tables 4,5 show the statistical summary of streamflow and soil moisture modeling results.Figure 4 show the distribution map of hydrology component modeling results by respectively.

Table 4. Statistical summary of the model calibration and validation results (Streamflow).

Gauging station		Yongdam		Cheoncheon		Donghyang	
		SWAT	Grid-based	SWAT	Grid-based	SWAT	Grid-based
Rainfall (mm/yr)		1371.1		1373.6		1375.3	
Streamflow (mm/yr)	Obs.	878.8		845.7		945.8	
	Sim.	841.4	811.7	781.6	832.4	818.1	817.2
Runoff Ratio (%)	Obs.	61.41		59.04		66.87	
	Sim.	59.74	58.05	55.06	59.37	57.67	58.09

Evaluation Criteria (mm/day)	NSE* (C**)	0.67	0.83	0.78	0.64	0.62	0.62
	NSE (V***)	0.44	0.69	0.63	0.57	0.34	0.56

*NSE: The average Nash and Sutcliffe efficiency, **C: Calibration(2002-2006), ***V: Validation(2007-2009),

Table5.Statistical summary of the model calibration and validation results (Soil Moisture).

Station	Period	R^2		NSE	
		SWAT	Grid-based	SWAT	Grid-based
Jangsu	2004~2008	0.49	0.36	0.42	0.44
Ancheon	2008/05~2008/08	0.76	0.86	0.65	0.52
Cheoncheon	2008/05~2008/08	0.40	0.47	0.20	0.18
Gyeobuk	2008/05~2008/08	0.47	0.67	0.47	0.38
Bugui	2008/05~2008/08	0.27	0.59	0.15	0.58
Average	-	0.48	0.59	0.38	0.42

Assessment of Model Performance for Watershed Hydrology under Climate Change Scenario

To evaluate the climate change impact on hydrologic components the model was run with the future downscaled climate data based on the 1980-2009 data.Tables 6 show the statistical summary of streamflow and soil moisture modeling results respectively.The future increase of evapotranspiration ruled the decrease of dam inflow.

Table 6.Summary of future predicted hydrologic components for A1B scenarios of the MIROC3.2 hires in the 2040s and 2080s.

GCM	Period	Model	DI (mm)	ET (mm)	SM (%)
Baseline	1980-2009	SWAT	816.1	467.9	21.4
		Grid-based	766.4	756.5	19.0
MIROC3.2 hires (A1B)	2040s	SWAT	869.1(+6.5)	496.5(+6.1)	22.0(+0.6)
		Grid-based	449.2(-41.4)	972.9(+28.6)	20.4(+1.4)
	2080s	SWAT	929.0(+13.8)	518.3(+10.8)	22.1(+0.7)
		Grid-based	477.7(-37.7)	1118.8(+47.9)	20.2(+1.2)

*DI: Dam Inflow, **ET: Evapotranspiration, ***SM: Soil Moisture, () : percentage,

Conclusions

This study tried to evaluate the future impact of climate change on hydrological components in watershed by using semi-distributed SWAT HRU model and distributed Grid-based model.Grid-based model is smaller than streamflow of SWAT model, evapotranspiration largely tend to be simulated. But two models are some differences value in that soil moisture. Part of the difference, through modification of the Grid-based model can be improved. SWAT model has Rainfall, runoff and evapotranspiration, which appear similar to the increase.

Distribution map for each hydrology component in the two models were compared. Evapotranspiration and soil moisture content was affected by effective soil depth. Low effective soil depth values can contain less moisture. By affecting evapotranspiration has

amount is less simulated value. Its impact on the distribution maps are identified in the bright parts. Distribution of soil moisture and value difference is showing map. The reason of the results is SWAT model was adoptedsoil series, Grid-based model was adopted soil texture.
SWAT model simulation results were keeping up the trend of the precipitation. But Grid-based model has interception under the influence of evapotranspiration is larger, runoff is smaller tends to be simulated.
The results showed that the future precipitation ruled the hydrologic components of the study watershed than future temperature. This kind of information of future quantitative and estimated hydrologic components would allow appropriate decisions on water resource management for a watershed. Grid-based model is channel routing module should be added. And interception for further studies will be needed.

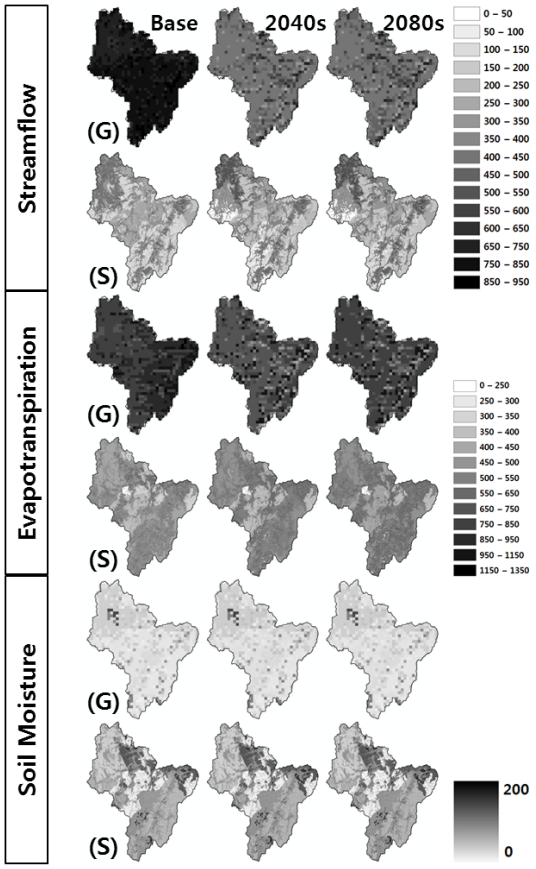

Fig. 2Future predicted hydrologic component distribution map for SWAT model (S) and Grid-based model (G).

References

Alcamo, J., P. Döll,F. Kasper, and S. Siebert 1997. Global change and global scenarios of water use and availability: and application of Water GAP 1.0. Report A9701: Center for Environ. System Research, University of Kassel, Germany.

Amell, N.W. 2003. Relative effects of multi-decadal climatic variability and changes in the mean and variability of climate due to global warming: Future streamflows in Britain. Journal of Hydrology. 270:195-213.

Amell, N.W. 2004. Climate-change impacts on river flows in Britain The UKCIP02 scenarios. J. Chartered Inst. Water Environ. Mgmt. 18:112-117.

Arnold, J.G., and P. M. Allen 1996. Estimating hydrologic budgets for three Illinois watersheds. Journal of Hydrology 176: 55-77.
Arnold, J.G.,P. M. Allen, and G. Bernhardy 1993. A comprehensive surface-groundwater flow model. Journal of Hydrology 142(1-4): 47-69.
Arnold, J. G., R. Srinivasan, R. S. Muttiah, and J. R. Williams 1998. Large-area hydrologic modeling and assessment: Part I. Model development. Journal of American Water Resources Association. 34(1): 73-89.
Arnold, J.G., R. Srinivasan, and B. A. Engelel 1999a. Flexible watershed configurations for simulating models. Hydrological Science and Texhnology 10: 5-14.
Arnold, J.G., R. Srinivasan, R. S. Muttiah, and P. M. Allen 1999b. Continental scale simulation of the hydrologic balance. Journal of the American Water Resources Association 35(5): 1037-1052.
Beven, K. 1989. Changing ideas in hydrology-the case of physically based models. Journal of Hydrology 105: 157-172.
Beven, K. 1996. A discussion of distributed hydrological modeling. In Distributed Hydrological Modelling, 255-278. Abbott MB, Refsgaard JC eds. Kluwer Academic: Dordrecht.
Carter, T.R., M. Hulme, and M. Lal 1999. Guidelines on the use of scenario data for climate impact and adaptation assessment, Version 1. ed. Intergovernmental Panel on Climate Change. Task Group on Scenarios for Climate Impact Assessment. Available via DIALOG. http://www.ipcc-data.org/guidelines/TGICA_guidance_sdciaa_v1_final.pdf. Accessed Dec 1999.
Daly, E., and A. Porporato 2005. A review of soil moisture dynamecs: from rainfall infiltration to ecosystem response. Environ. Eng. Sci. 22:9-24.
El-Nasr, A.A., J. G. Arnold, J. Feyen, and J. Berlamont 2005. Modelling the hydrology of a catchment using a distributed and a semi-distributed model. Hydrological processes 19: 573-587.
Etchevers, P., C. Golaz, F. Habets, and J. Noihan 2002. Impact of a climate change on the Rhone river catchment hydrology. Journal of Geophysical Research 107: 4293-4310.
Ficklin, D.L., Y. Luo, E. Luedelin, and M. Zhang 2009. Climate change sensitivity assessment of a highly agricultural watershed using SWAT. Journal of Hydrology 374:16-29.
Hong, W.Y. 2010. Development of a distributed daily soil moisture routing model and evaluation of its applicability. Konkuk Univ.
Lee, J.Y., and K. K. Lee 2000. Use of hydrologic time series data for identification of recharge mechanism in a fractured bedrock aquifer system. Journal of Hydrology 229:190-201.
Korea Meteorological Administration. 2009. Available at:http://web.kma.go.kr/eng.
Kim, S.J., H. J. Kwon,G. A. Park,and M. S. Lee 2005. Assessment of land-use impact on streamflow via a grid-based modeling approach including Paddy Fiels. Hydrology Prosesses 19:3801-3717.
Kim, S.J., and H. W. Chung, 1994. Field Evaluation of layered Green-Ampt infiltration model considering temporal variation of physical properties. Transaction of the ASAE 37(6):1845-1852.
McDonald, M.G., and A. W. Harbaugh 1988. A modular three-dimensional finite-differences groundwater flow model. In Techniques of Water-Resources Investigations. US Geological Survey: Book 6, Ch. Al, 586.
Möller, D., and F. Kuhlmann 1999. ProLand: a new approach to generate and evaluate land use options. In IX European Congress of Agriculture Economists, Warsaw, Poland August 24-28. 1998.
Nash, J.E., and J. V. Sutclifee 1970. River flow forecasting through conceptual models, Part

I-A discussion of principles. Journal of Hydrology 10:283-290.
Neitsch, S. L., J. G. Arnold, J. R. Kiniry, and J. R. Williams 2001. Soil and Water Assessment Tool Theoretical Documentation, Version 2000. Draft (April 2001). Temple, Tex.: USDA-ARS Grassland, Soil, and Water Research Laboratory, Blackland Research Center.
Refsgaard, J.C., and J. Knudsen 1996. Operational validation and intercomparison of different types of hydrological models. Water Resources Research 32(7): 2189-2202.
Salomonk, S., D. Qin, M. Mannign, Z. Chen, M. Marquis, K. B. Averyt, M. Tignor, and H. L. Miller 2007. Climate change 2007: The physical science basis, contribution of working group I to the fourth assessment report of the Intergovernmental Panel on Climate Change.UK and NY, USA: Cambridge University Press, Cambridge.
Semenov, M.A., and E. M. Barrow 1997. Use of a stochastic weather generator in the development of climate change scenarios. Climatic Change 35(4):397-414.
Semenov, M.A., R. J. Brooks, E. M. Barrow, and C. W. Richardson 1998. Comparison of WGEN and LARS-WG stochastic weather generators for diverse climates. Climate Research 10:95-107.
Sharpley, A.N., and J. R. Williams 1990. Erosion/Productivity impact calculator, 1. Model documentation. USDA-ARS Technical Bulletin 1768.
USDA-SCS 1972. Section 4: Hydrology. In National Engineering Handbook. Washington, D.C.: USDA Soil Conservation Service.
Sophocleous, M.A., J. K. Koelliker, R. S. Govindaraju, T. Birdie, S. R. Ramireddygari, and S. P. Perkins 1999. International numerical modeling for basin-wide water management: the case of the Rattlesnake Creek basin in South Central Kansas. Journal of Hydrology 214: 179-196.
Srinivasan, R. J. G. Arnold, W. Rosenthal, and R. S. Muttiah1993. Hydrologic modeling of Texas Gulf basin using GIS. In Proceedings of Second International GIS and Evironmental Modeling, National Center for Geographic Information and Analysis, Breckenridge, CO; 213-217.
Wever, A. M. Hoffmann, V. Wolters, and W. Köhler 1999. Ein habitateignungsmodell für die feldlerche (Alauda arvensis) basierend auf einem zellulären automaten. Verhandlungen der Gesellschaft fuer Oekologie 29: 329-336.
Weber, A., N. Fohrer, and D. Möller 2001. Long-term land use change in a mesoscale watershed due to socio-economic factors-effects on landscape structures and functions. Ecological Modelling 140: 125-140.
Wilby, R.L., B. Greenfield, and C. Glenny 1994. A coupled synoptic-hydrological model for climate change impact assessment. Journal of Hydrology 153:265-290.

Using ArcSWAT for Evaluation of Water Productivity and Economics of Crops in Canal Irrigation Command

R.T. Thokal
Ph D student and Chief Scientist, AICRP on Water Management,
Dr. B.S. Konkan Krishi Vidyapeeth, Dapoli, Dist.Ratnagiri, Maharashtra State, INDIA
rtt1966@yahoo.com

S.D. Gorantiwar
Head, Dept. of Irrigation and Drainage Engineering
Dr. A. S. College of Agril Engg., Mahatma Phule Krishi Vidyapeeth, Rahuri,
Dist. Ahmednagar, Maharashtra State, INDIA
sdgorantiwar@rediffmail.com

Mahesh Kothari
Assistant Professor, Department of Soil & Water Engg.
College of Technology & Engineering
Maharana Pratap University of Agri. & Tech., Udaipur, Rajasthan State, INDIA

S.R. Bhakar
Head, Department of Soil & Water Engg.
College of Technology & Engineering
Maharana Pratap University of Agri. & Tech., Udaipur, Rajasthan State, INDIA

R.C. Purohit
Head, Department of Soil & Water Engg.
College of Technology & Engineering
Maharana Pratap University of Agri. & Tech., Udaipur, Rajasthan State, INDIA

Abstract

Crop water use efficiency (WUE, yield per unit of water use) is the key for agricultural production with limited resources. Policymakers and water resource managers working at all scales need to address the multitudinous scenarios in which cropping systems and amounts, timing and methods of irrigation may be changed to improve WUE while meeting yield and harvest quality goals. Experimentation cannot address all scenarios, but accurate simulation models may fill in the gaps. Implementing real water saving measures in irrigated agriculture is only possible if all the components of the current water balance are clearly understood. However, measurement of all the terms in the water balance is infeasible on a spatial and temporal scale, but hydrological simulation models can fill the gap between measured and required data. To obtain all the terms of the water balance for Sina irrigation command in Maharashtra state, India, GIS based SWAT model was used to evaluate crop response to different irrigation depths, estimate the crop yield and water productivity. The water productivity was calculated and net crop returns of different crops grown in different soils of irrigation command were critically analyzed for limited water application.

Keywords: SWAT, deficit irrigation, water productivity, GIS, simulation model, crop economics, irrigation command, rotational irrigation system

Introduction

Water is expected to be one of the most critical natural resources in the twenty-first century. The use of water for irrigation is by far the greatest consumer of fresh water globally. Although irrigated regions of the planet occupy approximately 17% of the cultivated regions, they consume more than 70% of the world's water resources (Wolff, 1999). It is therefore not surprising that irrigated agriculture is perceived in those areas as the primary source of water, especially in emergency drought situations. Saving just a small amount of the water destined for irrigation and using it for other purposes instead, (mainly drinking use) could improve the living conditions of millions of people. Because agriculture is the main consumer of freshwater, increasing irrigation efficiencies seem to be the practical way to save water.

Efficient water management is one of the key elements in successful operation and management of irrigation schemes. Irrigation water management involves determining when to irrigate, the amount of water to apply at each irrigation event and during each stage of plant, and operating and maintaining the irrigation system. The main management objective is to manage a production system for profit without compromising environment and in agreement with water availability. A major management activity involves irrigation scheduling or determining when and how much water to apply, considering the irrigation method and other field characteristics such as soil and its variation in the irrigation command.

Under limitations in water availability, it is required to develop new irrigation scheduling approaches focused on to ensure optimal use of available water, and not based on full crop water requirements. The determination of these efficient and effective irrigation schedules (including deficit irrigation strategies) requires the accurate determination of water requirements for the main crops, in order to assist the farmers in deciding when and how much to irrigate their crops. However, in the irrigation command with rotational water supply system, the water allocation is based on applying a fixed depth of water with every irrigation irrespective of the crops, their growth stages, and soils on which these crops are grown (Gorantiwar and Smout, 2003).

The study was undertaken for the irrigation command where the rotational water supply system is adopted with fixed time of on and off. Under the situation of spatial soil variability and mixed cropping pattern, to decide the deficit irrigation strategy and increase water productivity and net crop benefit is complex job. Thus, GIS based SWAT model was used to critically analyze the effect of spatial variation of soils on the crops yields so as to decide

which crop to grow and up to what extent and how to do the water management for achieving higher economic returns from the crops.

Material and Methods

Development of tool framework

A GIS-based tool framework for irrigation scheduling with deficit irrigation under rotational distribution system was used for this study. This tool framework mainly comprises three modules: allocation rules, SWAT modules and economic module. The water allocation formulated initially depending upon water availability in the reservoir at the beginning of season, is the additional input to SWAT. The canal network, their commanded areas, deficit ratio, canal releases are also additional inputs to SWAT. The SWAT runs over growth periods of crops under study and estimates output parameters such as Potential Evapotranspiration (ET_p), Actual Evapotranspiration (ET_a), etc. The yield reduction considering the effect of water deficit at the different crop growth stages of various crops were estimated by using water production function proposed by Stewart *et al*. (1976).

$$\frac{Y_a}{Y_m} = 1 - \sum_{s=1}^{ns} K_{y_s} \left(\frac{ET_{m_s} - ET_{a_s}}{ET_{m_s}} \right) \quad \ldots 1$$

Where K_{ys} is Stewart's moisture stress yield reduction coefficient. This module utilizes ET_p, ET_a values obtained from SWAT and estimates the reduction in crop yield compared to potential yield due to pre-specified allocation rule. The tool eventually estimates the total crop production, yield reduction due to specific water allocation, benefits from the crops, grown on all soils, in all allocation units in the irrigation command. The tool framework is able to estimate daily updates of the reservoir storage on the basis of inflow to reservoir, outflow (water release) and losses from reservoir. The model runs daily for maximum 365 days, for crop season and each soil type. After 365 days cycle of run, it terminates and estimates the carry over storage in the reservoir. It also terminates if the reservoir storage is less than the dead storage or predefined stage. The model is able to give spatial output such as allocation unit wise irrigation amount, its allocation, crop yield, cost estimates, net benefit, etc.

Description of Study Area

A case study for Sina Medium Irrigation Project was selected to describe the ability and applicability of the framework. The project is located on river Sina, a tributary of river

Bhima in Krishna basin, at Nimgaon Gangarda village of Ahmednagar district, Maharshtra state, India (latitude 18°49'0"N and longitude 74°57'0"E) spread over the topo-sheets of 47 J/13, 47 J/14, 47 N/1 and 47 N/2. The location map is shown in Fig. 1.

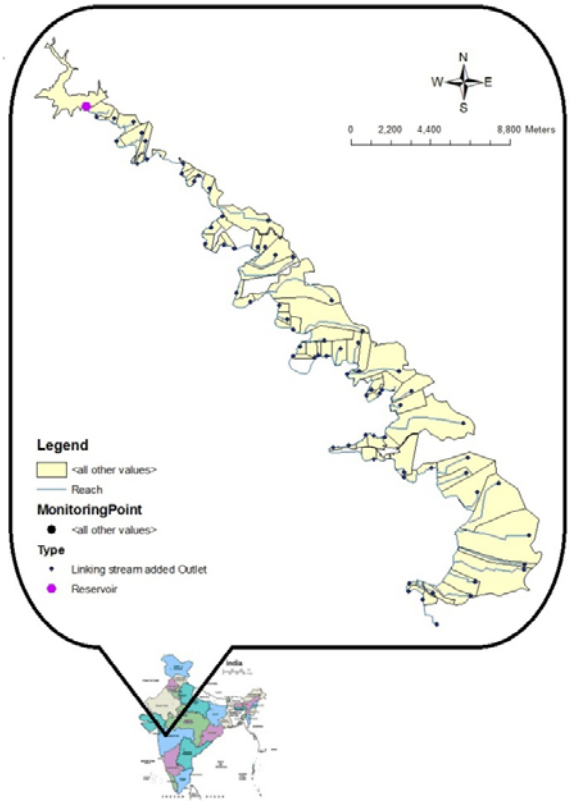

Fig. 1. Stream network and command area with location map of Sina Medium irrigation project

Canal Water Distribution System:

The rotational water supply is being followed in the canal command area of Sina Irrigation Project with an irrigation rotation of 10 days. The rotation is based on 5 days on and 5 days off period. As a routine practice, water demand for each rotation is estimated by collecting the demand of water on the basis of cops grown by the farmers in the command area. The total amount of water release is decided after considering demands of water from each sub-division, before the start of each rotation. Tail to Head water distribution system is followed in the outlet command i.e. the tail end farmers receive water first, then water is delivered to farmers whose lands are located towards the head of the outlet. This type of water distribution is called as *Shejpali* system and is generally adapted in all the irrigation projects of Maharashtra State. In this system, the concerned authorities display the water distribution schedules before the release of each rotation. Each farmer in the command gets prior

intimation of water delivery i.e. date, time and amount of water according to his request for water demand. The water demand is mainly estimated by the thumb rule and is not based on the soil and crops type. Thus, it leads to either excess water to some crops and soils and sometimes the crops remain under stress in certain soils. This in turn leads to either more release of water, which empties the reservoir earlier or low water releases lead to non-uniformity of water distribution in the irrigation command.

Soil and Water Assessment Tool (SWAT) module:

A GIS-based hydrological simulation model, Soil and Water Assessment Tool (SWAT) (Arnold *et al*., 1998; Neitsch *et al*., 2002, www.brc.tamus.edu/swat), developed by the USDA Agricultural Research Service (USDA-ARS). SWAT is a physically based simulation model operating on a daily time step. It was developed to simulate land management processes and soil-water balance with a high level of spatial detail by allowing watershed to be divided into sub-basins. Each sub-basin is divided into several land use and soil combinations, called hydrologic response units (HRUs). The sub-basin simulation processes of SWAT include major components such as hydrology, weather, erosion, soil temperature, crop growth, and agricultural management. As the study is related to irrigation management, the watershed is treated as the irrigation command, area commanded by each outlet was treated as one sub-basin and the HRUs were treated as Allocation Units (AUs).

GIS Input Files:

The basin layout, soil, land use, topography and discretize maps were incorporated into ArcGIS® and then applied to the SWAT model, through the use of the SWAT ArcView interface.

Elevation data: Topo-sheets of 1:50000 ratio were available for the study area and the contour lines passing through the area of interest were of larger intervals, only few lines could be digitized to form the Digital Elevation Map (DEM), which were insufficient to get the elevation data. Thus, images downloaded from Spectral Radar Topographic Mission (SRTM) were used as DEM in this study. As the area of interest was divided in two images of SRTM, these images (SRTM_51_091 and SRTM_52_091) were downloaded and mosaiced to form one DEM input for the project.

Land Cover/Land Use File: Information on land use and land cover for the study was obtained from Indian Regional Remote Sensing Service Centre (IRRSSC), Nagpur. The shape file of the imagery taken from LISS III with a 23x23 metre resolution and a date of

pass (DOP) during the study period was used in this study. Both the land use and soil themes were projected using the soil and crop shapefiles prior to the execution of the *Land Use and Soil Classification* tool. Fig. 2 illustrates the diversity and spread of land use in the study area.

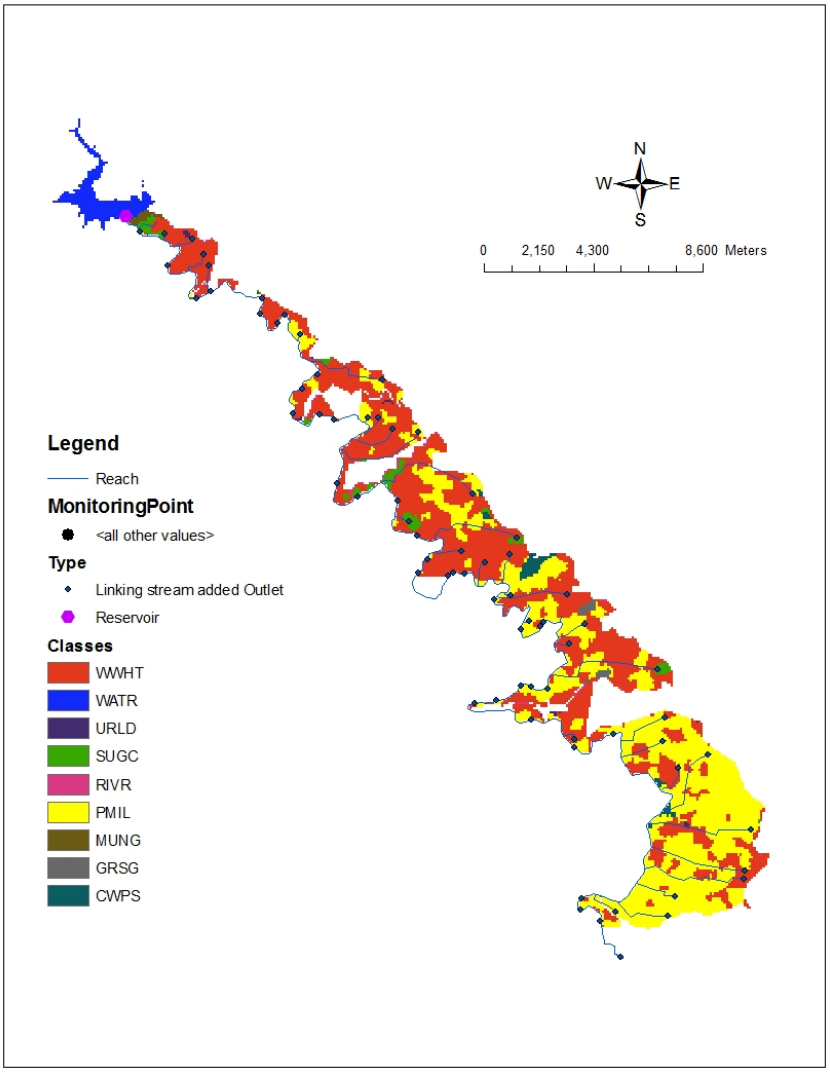

Fig. 2. Land cover presenting diversity of land use throughout the area

The GIS files and other input data required for this study obtained from various governmental agencies are listed in Table 1.

Table 1. Various inputs and sources of information for the required data set of Sina Irrigation Project

Subject area	*Data basis*	**Source and map scale**
Basic data	Boundaries of the command area, administrative boundaries, stream network	Survey of India (SoI); 1:50,000
Climatic data	Mean monthly and daily precipitation, maximum and minimum temperature, relative humidity, wind speed, evaporation	Meteorological observatory, Irrigation Department, Sina Irrigation Project, Mirajgaon
Soil-physical data	Soil series map, soil characteristics (silt, sand, clay, rocks), field capacity, wilting point, hydraulic conductivity, depth to water table, properties for different soil layers varying with depth, organic content, EC, pH, etc.	National Bureau of Soil Survey and Land Use Planning (NBSS&LUP); 1:2,50,000 and its reports from Command Area Development Authority (CADA), Ahmednagar
Land use data	Ground cover, seasonal cropping pattern, land use data imageries	CADA, SoI, State Agriculture Department, IRRSSC, Nagpur
Topography data	Elevation contours, digital elevation map (DEM)	SRTM data (SRTM_51_091 and SRTM_52_091)
Command area	Irrigation canal network	Irrigation Research & Development Wing, Pune
Reservoir storage data	Gauge readings at dam	Sina Irrigation Project, Mirajgaon
Canal release data	Gauge readings at the head of canal network	Sina Irrigation Project, Mirajgaon

Soil Data: Soil map and data for study area were obtained from Command Area Development Authority (CADA), Ahmednagar and reports of National Bureau of Soil Survey and Land Use Planning land use (NBSSLU&P), Nagpur. The shape file of command area was prepared from the map and detailed information on classification in the attribute was added from available data. The soil classification was based on NBSS&LUP. The soil class distribution in the irrigation command is presented in Fig. 3. The major soil series in the study area are Mirajgaon, Ratanjan, Ghumari and Nagalwadi with the texture class of clay, clay loam, silt clay and silt loam respectively. The soil characteristics are tabulated in Table 2 and their extent in the irrigation command are iterated in Table 3.

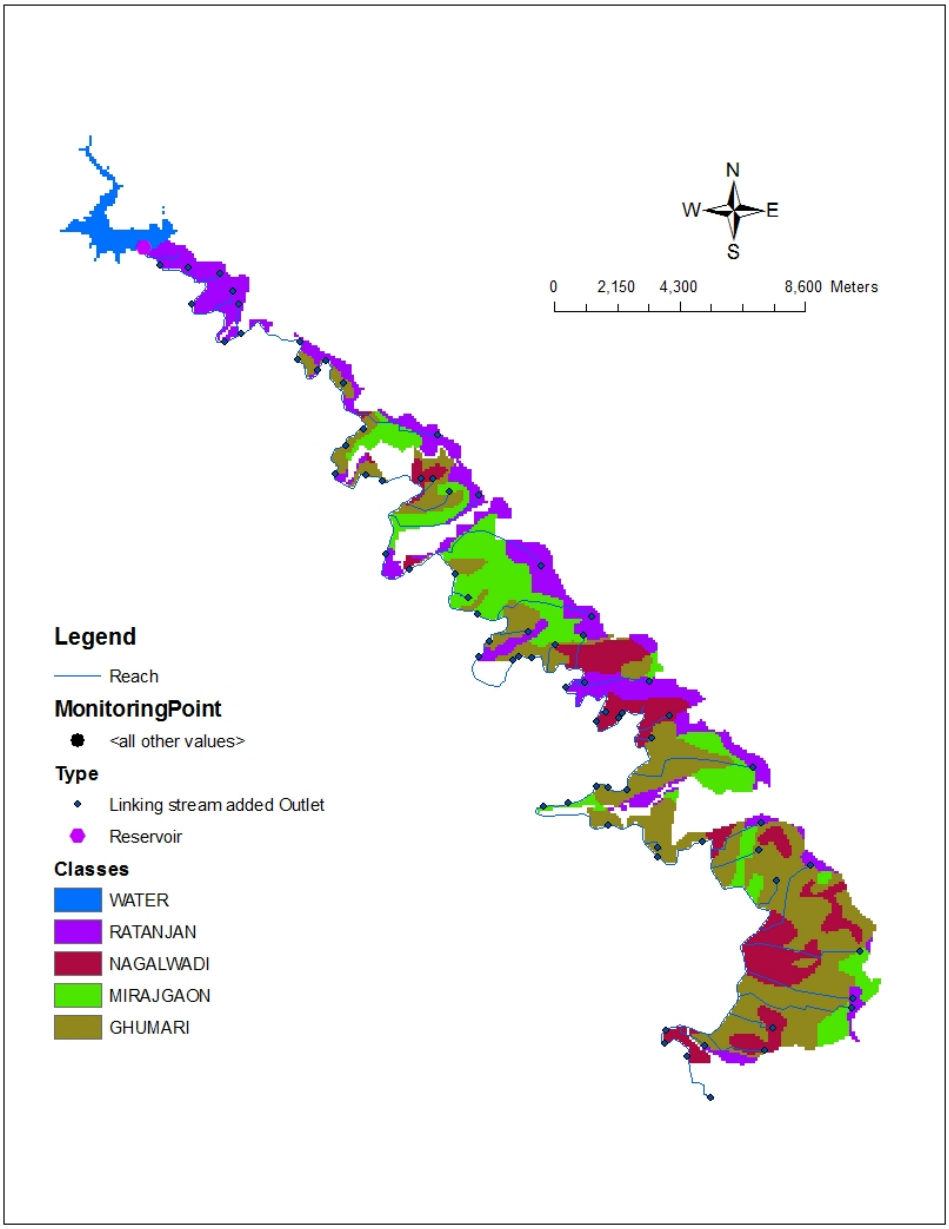

Fig. 3. Soil class distribution in Sina Irrigation Command

The soil database for the irrigation command was created with the information on soil properties including texture, bulk density, water holding capacity, organic carbon content, and horizon depths. The irrigation command of study area has specifically four major soil series. The soil characteristics are iterated below in Table 2.

Table 2. Soil characteristics in Sina irrigation command

Soil name:		Mirajgaon series				Texture of soil:			Clay	
Hydrologic group:		D				Infiltration rate:			1.30 mm/hr	
Max. rooting depth of soil profile (mm):		1500 mm				Number of layers:			6	
Layer No.	Depth from surface (mm)	Particle size distribution				Single value constant			Chemical parameters	
		Clay (%)	Silt (%)	Sand (%)	Rock (%)	Bulk density (kg/dm^3)	AWC (%)	K_{sat} (mm/h)	EC (dS/m)	Organic Carbon (%)
1	190	50.5	22.5	1.7	22.0	1.16	16.5	0.131	0.96	0.32
2	400	58.0	15.0	0.8	19.1	1.25	14.7	0.131	1.01	0.28
3	600	53.0	27.5	4.6	8.6	1.19	15.4	0.131	1.09	0.36
4	810	55.0	27.5	2.5	2.5	1.09	14.3	0.131	1.25	0.48
5	1080	59.2	18.7	1.5	9.8	1.21	15.0	0.131	1.56	0.16
6	1500	55.5	22.5	1.8	10.0	1.19	15.4	0.131	0.18	0.05
Soil name:		Ratanjan series				Texture of soil:			Silt clay	
Hydrologic group:		D				Infiltration rate:			1.80 mm/hr	
Max. rooting depth of soil profile (mm):		1050 mm				Number of layers:			5	
Layer No.	Depth from surface (mm)	Particle size distribution				Single value constant			Chemical parameters	
		Clay (%)	Silt (%)	Sand (%)	Rock (%)	Bulk density (kg/dm^3)	AWC (%)	K_{sat} (mm/h)	EC (dS/m)	Organic Carbon (%)
1	180	45.0	41.8	2.1	3.5	1.19	15.0	0.0554	1.11	0.26
2	320	48.0	37.0	3.4	3.4	1.09	14.7	0.0554	1.97	0.17
3	520	75.0	9.3	2.3	2.1	1.06	13.6	0.0554	1.32	0.17
4	720	62.0	17.3	20.2	2.1	1.05	16.4	0.0554	1.61	0.17
5	1050	55.5	31.5	0.8	1.9	1.11	15.3	0.0554	1.62	0.12
Soil name:		Ghumari series				Texture of soil:			Clay loam	
Hydrologic group:		D				Infiltration rate:			2.30 mm/hr	
Max. rooting depth of soil profile (mm):		350 mm				Number of layers:			2	
Layer No.	Depth from	Particle size distribution				Single value constant			Chemical parameters	

	surface (mm)	Clay (%)	Silt (%)	Sand (%)	Rock (%)	Bulk density (kg/dm^3)	AWC (%)	K_{sat} (mm/h)	EC (dS/m)	Organic Carbon (%)
1	200	41.2	25.0	21.2	2.4	1.08	14.5	0.357	0.18	1.05
2	350	45.8	13.0	30.4	4.4	1.17	14.5	0.357	0.12	1.41
Soil name:			Nagalwadi series			Texture of soil:			Silt loam	
Hydrologic group:			C			Infiltration rate:			6.30 mm/hr	
Max. rooting depth of soil profile (mm):			200 mm			Number of layers:			1	
Layer No.	Depth from surface (mm)	Particle size distribution				Single value constant			Chemical parameters	
		Clay (%)	Silt (%)	Sand (%)	Rock (%)	Bulk density (kg/dm^3)	AWC (%)	K_{sat} (mm/h)	EC (dS/m)	Organic Carbon (%)
1	200	31.0	6.5	40.8	11.9	1.19	15.0	0.3359	0.16	0.52

User-defined and Canal/Stream Network File: Shape file of canal/stream network was prepared by using the map procured from Irrigation Research & Development Wing (IRDW), Pune. SWAT is capable of calculating estimated stream positions with the use of an elevation grid file alone, however, the limited resolution of the file, particularly with low lying flat areas, makes the incorporation of the stream delineation of added advantage. Also the canal network may not follow all-the-way the same path as per the elevation grid. For this reason, the "user-defined watersheds and stream" option was chosen for delineation process to define accurately the areas commanded under each canal outlet.

Climate Record File: The weather data of 19 years record procured from meteorological observatory, was used to calculate statistical parameters for weather generator input file. The meteorological observatory for study area is located at Nimgaon Gangarda village in the command area with the location of 18^{o}49'1.24" N latitude, 74^{o}57'31.62" E longitude and altitude of 585.945m. Other input files for climatic parameters were also created for SWAT.

Canal Irrigation Component

A canal irrigation routine of SWAT model was used to simulate canal irrigation. In this framework approach, area under each outlet was considered as a sub-watershed. The crop fields within the sub-basin were represented by HRUs within the sub-watershed. In this module, SWAT estimates evaporation and seepage losses on daily basis.

Crop Irrigation Scheduling

The user can input a schedule (specifying the depth of irrigation, time, and source of irrigation) for irrigating the crop in an AU, in which the irrigation schedule was planned with the irrigation depth of 50mm, 70mm and 90mm and the irrigation frequency was varied according to the season i.e. 14 days interval for summer, 21 days interval for winter and 28 days interval for monsoon season. The management operations like planting, irrigation, fertilizer application, harvest and kill (termination) were scheduled by date. The potential evapotranspiration (PET) was estimated with SWAT by using modified Penman-Monteith (Monteith, 1965; Allen, *et al*., 1989). Irrigation water applied to a crop AU was used to fill the soil layers to field capacity beginning with the soil surface layer and working downward until all the water applied was used or the soil profile reached field capacity. Soil depth was based on soil horizon and irrigation water was applied only to rooting depth maximum up to depth of soil horizon.

Results and Discussion

Allocation Units Analysis

SWAT divided total irrigable command area (ICA) of 7656ha and created total 305 AUs within 72 sub-basins, the first sub-basin was allocated as the reservoir. The combination of the distribution of crop-soil and slope in the ICA of the study area created by SWAT is presented in Table 3. The results indicated that an existing cropping pattern in the command area has maximum area during the *kharif* season occupied under pearl millet (41.34%), while that in *rabi* season under wheat (51.81%). The area occupied in the irrigation command by Ghumari soil series (clay loam), Ratanjan soil series (silt clay), Mirajgaon soil series (clay) and Nagalwadi soil series (silt loam) are 3083ha, 1821ha, 1571ha and 1185ha, respectively. The distribution of slope among the sub-basins showed that the irrigation command has a gentle slope varying from 0-3% and more than 99% is area occupied under this category of slope, while very few area (0.49%) is having stiff slope (3% and above).

Table 3. Distribution of combination of crop-soil and slope created by SWAT

Soil series / class	Slope					
	0-0.5%	0.5-1%	1-3%	3-5%	Above 5%	Total
Mirajgaon (clay)	39.6	491.9	1034.4	0.0	0.0	1565.9
Ghumari (clay loam)	11.4	358.3	2714.2	0.3	0.0	3084.2
Ratanjan (silt clay)	21.0	328.5	1433.0	36.4	1.9	1820.8
Nagalwadi (silt loam)	2.8	97.6	1083.8	1.1	0.0	1185.3
Total	74.8	1276.3	6265.4	37.8	1.9	7656.2

Soil	Crop					
	Wheat	Sugarcane	Pearl millet	Mung bean	Sorghum	Total
Mirajgaon (clay)	1206.5	22.4	337.1	0.0	0.0	1566.0
Ghumari (clay loam)	1204.8	5.3	1874.0	0.0	0.0	3084.1
Ratanjan (silt clay)	1499.9	46.7	23.1	26.5	14.4	1820.7
Nagalwadi (silt loam)	243.2	3.7	875.9	62.6	0.0	1185.4
Total	4154.4	78.1	3110.1	89.1	14.4	7656.2
Slope	Crop					
	Wheat	Sugarcane	Pearl millet	Mung bean	Sorghum	Total
0-0.5%	62.3	2.8	9.7	0.0	0.0	74.8
0.5-1%	874.4	8.6	393.2	0.0	0.0	1276.2
1-3%	3186.4	58.7	2916.8	89.1	14.4	6265.4
3-5%	31.4	6.2	0.3	0.0	0.0	37.9
Above 5%	0.0	1.9	0.0	0.0	0.0	1.9
Total	4154.5	78.2	3320.0	89.1	14.4	7656.2

The data indicated that more that 80% of the area lies under the slope category of 1-3% followed by 0.5-1% slope. The distribution of wheat was maximum in both clay and clay loam soils. The sugarcane crop was more concentrated in silt clay followed by clay soil. The maximum pearl millet was grown in clay loam followed by silt loam soil. However, the crops like mung beans and sorghum (*rabi*) are very less in the irrigation command and are more concentrated in silt clay and silt loam soils. Most of the crops are more concentrated in the slope category of 1-3% followed by 0.5-1% slope.

Crop Response to Water Application and Soil Types

The crops response in terms of crop yield, economic returns and water use efficiency were analyzed for different irrigation depths and soils. The soil moisture status for the irrigation applications in different soils was also evaluated to verify soil moisture availability during the growing period of crops. For the sake of brevity, the detail analysis of the soil moisture status is presented for only wheat crop. The variation of soil moisture in the root zone of wheat crop grown in different types of soils in the irrigation command and irrigated with different depths of irrigation is shown in Fig. 4.

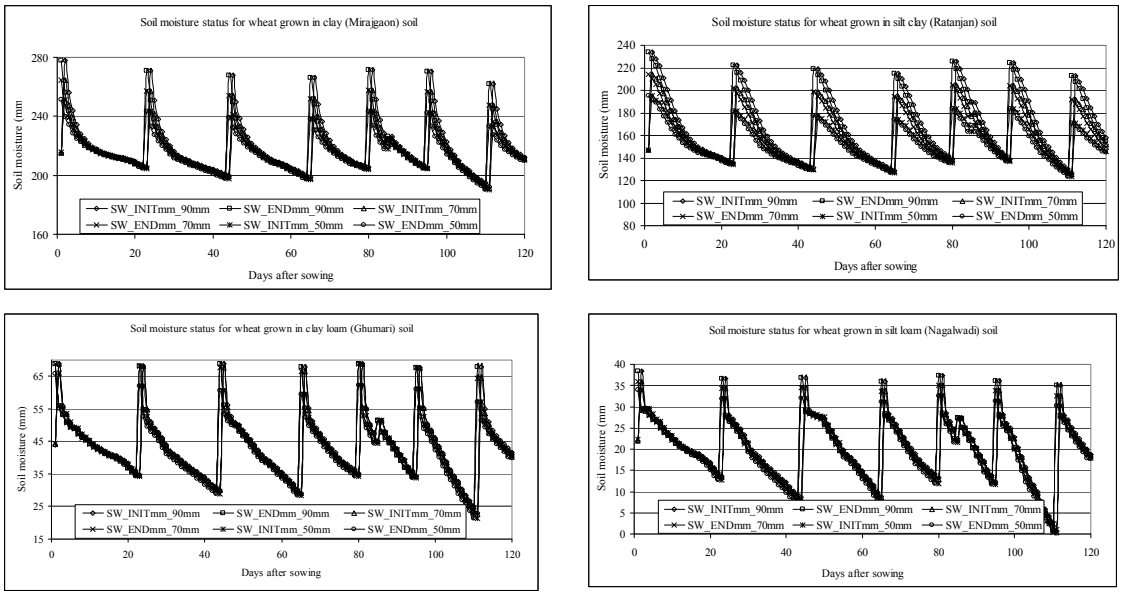

Fig. 4. Soil moisture in the root zone of wheat irrigated with different depths and grown in different types of soils

The wheat crop was irrigated with 50mm, 70mm and 90mm depths in total seven irrigations according to the rotation of irrigation water in the irrigation command. The output from SWAT regarding the daily soil moisture status in root zone of wheat in different soils indicated that the depletion of soil moisture in loam soils was very fast and many times it reached below available moisture before irrigation resulting in the water stress before irrigation also in case of higher irrigation depths (Fig. 4). This indicated the need of irrigation during these periods of crop. The major impact of soil depth on the soil moisture depletion was also observed. For higher soil depths, the soil moisture was well within the available moisture content, indicating the less stress in case of less water application per irrigation. The crop yield may not be affected in clay and silt clay soils, which has more soil depth; however, the yield may be affected due to moisture stress in the soil with shallow depth and lower application of water.

Yield response of crops grown in different soils to irrigation application

The estimated yields of crops were compared to the potential yields of the respective crops and the reduction in crop yield due to moisture stress in the different soils was analyzed to evaluate the effect of amount of irrigation water. Percent yield reduction due to irrigation water application for crops grown on different soils in the study area are presented in Fig. 5.

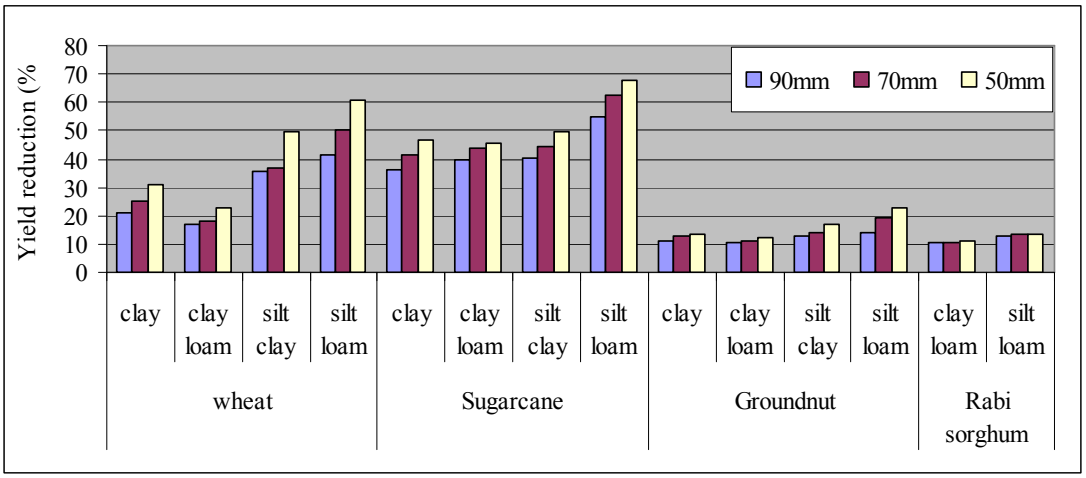

Fig. 5. Percent yield reduction due to deficit water application to crops grown in different soils of Sina irrigation command

The yield reduction of sugarcane was found to be very high in all types of soils and irrigation depths, which was in the range of 36 to 55 per cent in the soils even with application of 90mm irrigation depth. This was still more and varied from the range of 46 to 68% in all soils with the application of 50mm irrigation depth (Fig. 5). The highest reduction of sugarcane yield was observed in the silt loam soil. Results also indicated that sugarcane grown in silt loam soil could not sustain the moisture depletion due to limited water application. The yield reduction was least in groundnut and *rabi* sorghum in the clay and clay loam soils. The irrigation depth played here the vital role in influencing the yield of groundnut particularly in silt and silt loam soils. The decrease in irrigation depth reduced the yield in these soils. The highest yield of wheat grain was obtained in clay loam soil. The yield reduction in wheat grain was highest in silt loam soil. Results from Fig. 4 also confirmed that the least availability of soil moisture in this soil during the crop growth period and thus wheat grown in silt loam soil could not sustain the moisture depletion due to limited water application.

Water Use Efficiency (WUE) and Irrigation Water Use Efficiency (IWUE)

The WUE is the capacity of crop to produce the yield per unit of total water applied including the precipitation. In case of IWUE, the capacity of crop is considered per unit water applied through irrigation. The WUE and IWUE for crops irrigated with different depths and grown in different soils were worked out and are presented in Table 4. The results from Table 4 revealed that WUE and IWUE of crops grown in clay and clay loam soils are higher as compared to that of crops grown in silt clay and silt loam soils. It was also seen that the WUE and IWUE increased with decrease in irrigation depth in most of the crops and soils. This indicated that crops can be sustained with 50mm irrigation depth in all soils in case of water

scarcity period. The highest WUE was observed in groundnut grown in clay, clay loam and silt clay soils with 50mm water application. This indicates that the soil depth more than 350mm can produce good productivity per unit of water application. Patel *et al*. (2008) also indicated the same results stating that maximum soil moisture extraction (49.88%) by groundnut roots is from upper 300mm. Similar results have been report by *Gulati et al*. (2001). The prominent response to limited water application was observed in *rabi* sorghum crop. The significant difference could be seen between WUE and IWUE for sugarcane crop, which was grown for the whole year. Thus, the IWUE was significantly higher in case of sugarcane as compared to WUE. There was very scanty rainfall during the *rabi* season thus, there was no prominent difference in values of WUE and IWUE.

Table 4. Water Use Efficiency (WUE) and Irrigation Water Use Efficiency (IWUE) of crops grown in different soils and irrigated with different depths

Crop	Soil	Water Use Efficiency (kg/ha-cm)		
		90mm	70mm	50mm
Wheat	Clay	56.51	68.05	86.34
	Clay loam	59.55	74.49	96.83
	Silt clay	46.11	57.62	63.30
	Silt loam	42.07	45.13	48.95
Sugarcane	Clay	287.89	307.02	334.35
	Clay loam	276.02	297.65	341.78
	Silt clay	271.42	291.46	312.63
	Silt loam	203.42	197.25	200.82
Groundnut	Clay	29.42	36.68	49.84
	Clay loam	29.70	37.42	50.51
	Silt clay	35.21	45.43	47.65
	Silt loam	28.43	33.81	44.28
Rabi sorghum	Clay loam	64.48	80.83	107.29
	Silt loam	62.89	78.36	104.71

		Irrigation Water Use Efficiency (kg/ha-cm)		
Wheat	Clay	58.50	71.14	91.83
	Clay loam	61.66	77.88	103.00
	Silt clay	47.74	60.24	67.33
	Silt loam	43.55	47.18	52.07
Sugarcane	Clay	465.05	549.99	704.86
	Clay loam	445.91	525.67	719.81
	Silt clay	438.48	522.11	659.05
	Silt loam	328.62	353.35	423.31
Groundnut	Clay	30.85	38.98	54.20
	Clay loam	31.15	39.76	54.92
	Silt clay	38.63	49.97	51.82
	Silt loam	29.81	35.93	48.15
Rabi sorghum	Clay loam	71.04	91.40	126.94
	Silt loam	69.28	88.61	123.88

Crop Economics

The crop economics was worked out based on the crop yields in 305 allocation units comprising different soil were estimated for the different amounts of water applied in different soils. The benefits from yield of each crop were worked out taking into consideration the cost of crop cultivation as well as cost of water for crop production. The cost of water was calculated from known prices as per Government norms for each crop. The Govt. costs for irrigation water is based on the crop per ha. This cost was converted into cost of irrigation water on volumetric basis so as to view how much cost of irrigation water is required for production of each crop. Net returns worked out for different crops grown in different soils and irrigated with different depths and are presented in Fig. 6.

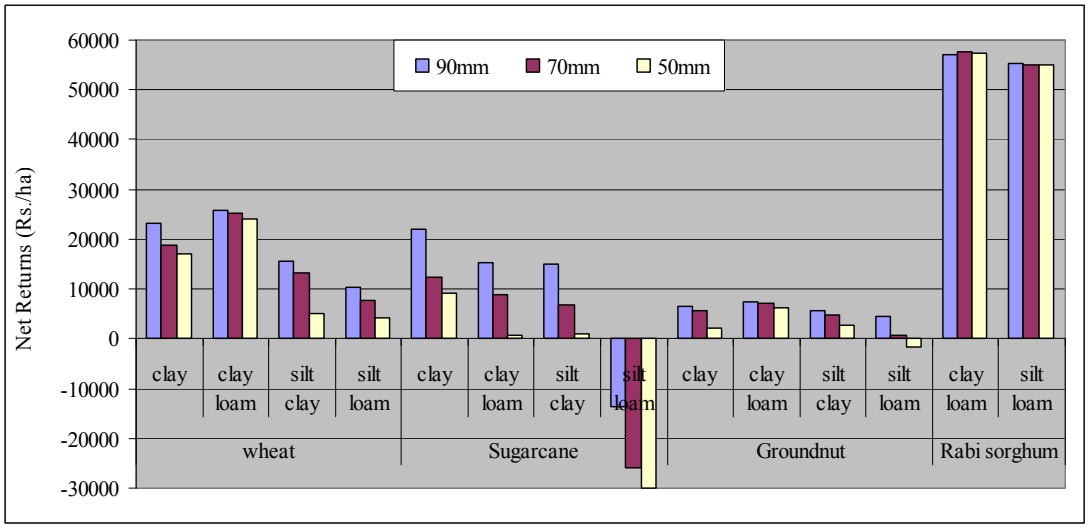

Fig. 6. Net returns of crops irrigated with different depths and grown in different soil of Sina irrigation command

The results in Fig. 6 indicated that the *rabi* sorghum fetched the highest returns. It also revealed that *rabi* sorghum can be cultivated profitably by irrigating the crop with minimum (50mm) depth in clay loam and silt loam soils. This case could not be observed for other crops. The silt loam soil was found to be less productive for other crops even with higher irrigation depths also. The wheat crop was observed to be second profitable crop, however grown in clay loam and clay soils with irrigation depth not less than 70mm. The net return was highest in clay and clay loam soil for 90mm irrigation depth. The significant reduction in net returns of wheat grown in all soils except in clay loam soil was found due to decrease in depth of water application. The loss was observed in sugarcane grown in silt loam soil even with 90mm irrigation depth. Also, irrigation less than 70mm for groundnut grown in silt loam soil was not profitable.

Conclusions:

The GIS based water allocation tool framework was formulated by using SWAT model for increasing the water productivity and net project benefit based on storage availability in the reservoir at the beginning of season. Sina irrigation project in Maharashtra state of India was selected as a case study with irrigable command area of 7656ha. Total 305 AUs were created within 72 sub-basins, the first sub-basin was allocated as the reservoir. As per existing cropping pattern, maximum area during the *kharif* season was occupied by pearl millet (41.34%), while that in *rabi* season under wheat (51.81%). Area occupied by clay loam, silt clay, clay and silt loam soils are 3083ha, 1821ha, 1571ha and 1185ha, respectively. The maximum area (more than 99%) in irrigation command has a gentle slope varying from 0-3%.

The daily soil moisture status in root zone of crops was evaluated for water management strategy in soils, which indicated that the depletion of soil moisture in loam soils was very fast and many times it reached below available moisture before irrigation resulting in the water stress before irrigation also in case of higher irrigation depths. This indicated the need of irrigation during these periods of crop. The major impact of soil depth on the soil moisture depletion was also observed. The yield reduction of sugarcane was found to be in the range of 36 to 55 per cent for different the soils, while it was still more (46 to 68%) in all soils with the application of 50mm irrigation depth. However, WUE was observed to highest with application of 50mm irrigation depth in all soils, indicating in case of water scarcity period, sugarcane can be sustained with limited water application; however, the productivity has to be sacrificed. The highest reduction of sugarcane yield was observed in the silt loam soil. The yield reduction was least in groundnut and *rabi* sorghum in the clay and clay loam soils. The study of WUE and IWUE also concluded that crops grown in clay and clay loam soils were more sustained as compared to that of crops grown in silt clay and silt loam soils. Profitability of the crops grown in different soils in the study area with different irrigation depths was analyzed critically aiming for the water saving and enhancing crop productivity. The study concluded that *rabi* sorghum was most profitable crop in the study area followed by wheat. Also, *rabi* sorghum can be cultivated profitably by irrigating the crop with minimum (50mm) depth in clay loam and silt loam soils. However, other crops could not fetch the handsome profit with limited irrigation (below 70mm) particularly in silt loam and silt clay soils. Sugarcane was found in loss when grown in silt loam soil, while groundnut was also in loss when irrigated with 50mm depth in the same soil.

References:

Allen, R.G.; Jenson, M.E.; Wright, J.L. and Burman, R.D. 1989. Operational estimates of evapotranspiration. *Agron. J.* **81**: 650-662.

Anonymous. 1997. Second Revised Project Report of Sina Medium Irrigation Project. *Report of Irrigation Department, Ahmednagar Irrigation Circle,* Government of Maharashtra – 1996-1997. Vol. I.

Arnold, J. G., Srinivasan R., Muttiah R.S., and Williams, J. R. 1998. Large-area Hydrologic modeling and assessment: Part I. Model development. *J. Am. Water Resour. Asso*. **34**: 73-89.

Dyson, T. 1999. World food trends and prospects to 2025. *Proceedings of the National Academy of Sciences*, USA. 96: 5929-5936.

Fereres, E. and Connor, D.J. 2004. Sustainable water management in agriculture. In Canbera E, Cobacho R, eds. *Challenges of the new water policies for XXI century*. Lisse, The Netherlands: A.A. Balkema, 157-170.

Fereres, E. and Soriano, M.A. 2007. Deficit irrigation for reducing agricultural water use. *J. Exp. Botany* Vol. 58(2): 147-159.

Gorantiwar, S.D. and Smout, I.K. 2003. Allocation of scarce water resources using deficit irrigation in rotational systems. *J. Irrig. & Drain. Engg.* **129**: 155-163.

Gulati, J.M.L.; Lenka, D and Paul, J.C. 2001. Moisture extraction pattern, phasic water use and phasic growth in groundnut (Arachis hypogaea) under varying moisture regimes and ground water table condition. *Indian J. Agronomy*. **46**(2):287-291.

Harrington, G.J. and Heermann, D.F. 1981. State of art irrigation scheduling computer program. In: *Irrigation Scheduling for Water and Energy Conservation in the 80's*. ASAE Publication 23-81: 171-178.

Howard, S.E. and Benn, J.R. 1986. Computer modelling for water management on smallholder irrigation schemes. Report No. OD 74, *Hydraulics Research* Wallingford, UK.

Monteith, J.L. 1965. Evaporation and environment. In: The state and movement of water in living organisms. *19th Symposium, Soc. for Environmental Biology*. Cambridge, UK, Cambridge University Press. 205-234.

Neitsch, S.L.; Arnold, J.G.; Williams, J.R.; Kiniry, J.R. and King, K.W. 2002. Soil and Water Assessment Tool (Version 2000). *Model documentation. GSWRL 02-01, BREC 02-05,TR-191*. College Station, Texas: Texas Water Resources Institute.

Patel, G.N.; Patel, P.T. and Patel, P.H. 2008. Yield, water use efficiency and moisture extraction pattern of summer groundnut as influenced by irrigation schedules, sulful levels and sources. *J. SAT Agric. Research*. **6**: 1-4.

Pereira, L.S.; Teodoro, P.R.; Rodregues, P.N. and Teixerira, J.L. 2003. Irrigation scheduling simulation: the model ISAREG. In *Tools for Drought Mitigation in Mediterranean Regions*. Eds. G. Rossi, A. Cancelliere, L.S. Pereira, T. Oweis, M. Shatanawi and A. Zairi. 161-180. Netherlands: Kluwer Academic Publishers.

Postel, S.L.; Daily, G.C. and Ehrlich, P.R. 1996. Human appropriation renewable freshwater. *Science* **271**: 785-788.

Smith, M. 1992. CROPWAT, A computer program for irrigation planning and management. *FAO Irrigation & Drainage paper 24*. Rome, Italy.

Stewart, J.L.; Hagen, R.M. and Pruit, W.O. 1976. Water production functions and predicted irrigation programs for principal crops as required for water resources planning and increased water use efficiency. University of California. *Dep. Land, Air and Water Resources*, Davis, and USDI/Br, Denver, Co.

Wolff, P. 1999. On the sustainability of water use. *Natural Resources and Development*. **49/50**: 9-28.

Localised variations in water scarcity: a hydrologic assessment using SWAT and spatial techniques

Sathian, K.K.

M.Tech, MBA, PhD, Associate Professor, Department of Land & Water Resources, Kelappaji College of Agrl Engg & Technology, Tavanur, Kerala- 679573. Mob: 9846010324
email: erkksathian@gmail.com

Abstract

Water scarcities of different orders are experienced all over the world. Water availability is not assured even in places with ample receipt of annual rainfall due to the steady decline of natural water conservation as an after effect of unscrupulous changes in land uses and unscientific human interventions under the guise of development. Further, water availability shows high variations between localities with very little geographical separation and almost similar climatic conditions. Major parts of the state of Kerala can be cited as typical examples for the said water paradox.

Hence, a study has been conducted for the Kunthipuzha tributary of Bharathapuzha river basin, one of the major rivers of Kerala, having a catchment area of 822 km^2 to throw scientific insight to the issue of variations in water availability between localities of close geographical proximity. SWAT has been used to delineate the micro-watersheds and to quantify various hydrologic processes on a smaller spatial and temporal scale. GIS has been used to consolidate the water availability in administrative divisions of local self governments (Grama Panchayaths and Block Panchayaths).

The study shows that there is very high variations (more than 70% of the mean value) in different hydrologic processes such as surface runoff, lateral flow and base flow between the micro-watersheds. It is reflected in the water availability within the administrative divisions of local self governments. It is hoped that the study can go a long way to help in giving a scientific framework for water management activities of these institutions.

Key words: watershed model, hydrologic model, SWAT, water balance, Bharathapuzha

Intorduction

Watershed based development is the solution for the socio economic development of a locality. Productive agriculture and agro based industries are the answer for sustainable development of rural areas. One of the major resource constraints for the development of these areas is the water shortage during summer. Water scarcity has become a universal phenomenon. Even high annual rainfall receiving areas face water shortage due to the uneven

distribution of rainfall. It is experienced that different orders of water scarcity is experienced in different micro watersheds of a river basin. Hence, water availability has to be quantified on micro scale using sound hydrological principle. Comparing the demand and availability, the severity of water scarcity can be quantifies at various sub watersheds and this should be the basis for watershed based interventions. Distributed watershed models appear to be the only answer for such an extensive exercise on a micro level. Hence, a study has been undertaken to quantify the water scarcity position in different micro watersheds of a medium sized river basin in the state of Kerala in Indian peninsular.

Study area

A typical river basin from the central part of Kerala State in the Indian peninsular viz. 'Kunthipuzha' has been chosen for the study. Location of the basin and its physical characteristics are presented below.

Kunthipuzha sub basin

Kunthipuzha river is an important tributary of Bharathapuzha river basin, the largest in Kerala. Bharathapuzha originates from the Western Ghats and has a total catchment area of 6400km^2, of which about 70% spread in Kerala and the remaining in Tamilnadu state in India. Kuntipuzha subbasin lies in the North East part of the Bharathapuzha river basin. The sub basin lies in the latitude longitude range of 10^0 53'N, 76^0 04'E to 11^0 14'N, $76^0$41'E and has a total catchment of 940 km^2 at the confluence point with the main river. Catchment area at Pulamanthole river gauging station (10^0 53' 50'' N, 76^0 11'50''E) manned by Central Water Commission, India is 822 km^2. River flow information is available for this gauging station. Elevation of the catchment varies from 20 to 2300m. Mean annual rainfall of the area is 2300mm. About 80% of the total rainfall is received during June to September, 15% from October to November and about 5% during December to May. Mean temperature of the area is 27.3^{0}C. The average daily flow ranged from a minimum of 0.1m^3/s to a maximum of 1020m^3/s during the period of analysis. The mean flow during the period was 53.1m^3/s with a standard deviation 84.9m^3/s. The details of soil and land use and their respective area coverage are presented in table 1.

Data source

Different data required for the study are collected from various departments affiliated to the government of Kerala state and that of the Indian nation. Daily rainfall data have been collected from the Department of water Resources of Kerala State and from various

campuses of Kerala Agricultural University. Climatic parameters such as temperature, humidity, wind velocity and solar radiations have been taken from Kerala Agricultural University. Daily river flows is from Central Water Commission. Digital contour and drainage maps were prepared from Topographic maps made in 1:50,000 scale. Soil map and attributes have come from the National Bureau of Soil Survey and Land Use Planning, Pune. Land use map was generated from multispectral remote sensing imagery of LISS III of IRS P6. Band 1 (0.52 to 0.59μm), band 2 (0.62 to 0.68 μm) and band 3 (0.77 to 0.86 μm) were used for the classification.

GIS and watershed model

Integrated Land and Water Information system (ILWIS) is the GIS software used in the study. The software is an integrated one with image processing capabilities. All the GIS layers required by the watershed model such as digital elevation model, drainage network, soil and land use have been prepared in ILWIS. Watershed model used in the study is Soil and Water Assessment Tool (SWAT) 2005. SWAT is a complex physics based distributed hydrologic model that operates on a daily time step, developed by United States Department of Agriculture (Arnold et al. 1998). SWAT has proven to be an effective tool for assessing water resource and non-point source pollution problems for a wide range of scales and environmental conditions across the globe.

Calibration of the SWAT model

After the sensitivity and uncertainty analysis, the model calibration was attempted on the sensitive parameters, within the range suggested by uncertainty analysis. As daily rainfall data for the basin was available only for 7 years, from 1996 to 2002, the calibration and validation exercise also had to be confined to this period. Out of this, 5 years of data (from 1996 to 2000) has been used for calibration and the rest for validation. First, the calibration has been done for mean annual output values, then it was extended to monthly and ten daily outputs. Further, comparison of simulated base flow with their actual values has been made. There were no exclusive measured base flow values to know its exact quantity. However, the comparison of simulated base flow during summer period and the observed river flow during the same period can give a fair idea about the capability of the model to simulate the base flow separately. Accordingly, summer river flow without any appreciable rainfall events has been considered as sole contribution of base flow. In addition, ET simulated by the model is compared with ET worked out from basin water balance. It is assumed that rainfall minus river flow will be a reasonable estimate of ET for basins having low deep aquifer recharge.

By way of comparison of different component wise watershed hydrology, a better confidence on the model output can be expected than a mere comparison with total river flow as is seen in most studies.

Results and discussion

Catchment characteristics

The digital elevation model of the Kunthipuzha catchment has been generated using GIS software. Terrain elevation ranges from 20 to 2300 m. having a mean elevation of 310 m and a standard deviation of 437 m. Slope of the basin ranges from 3 to 34%. The hypsometric curve of the watershed which shows the area elevation relationship is presented in figure 1. The curve shows that about 70% of the basin lies within an elevation band of 20 to 170m and the remaining 30% area is above 170m and has high relief. Majority of the soils present in the catchment have very high clay and sand content with very low fraction of silt. Surface texture of the soils comes under clayey or clayey loam. The land use map derived through supervised classification of the satellite imagery shows that there are 8 different land use classes. Major land use types present in the watershed are rice, mixed crop, forest, range land and urban settlement. The area coverage of different land use and soil types is shown in table 1.

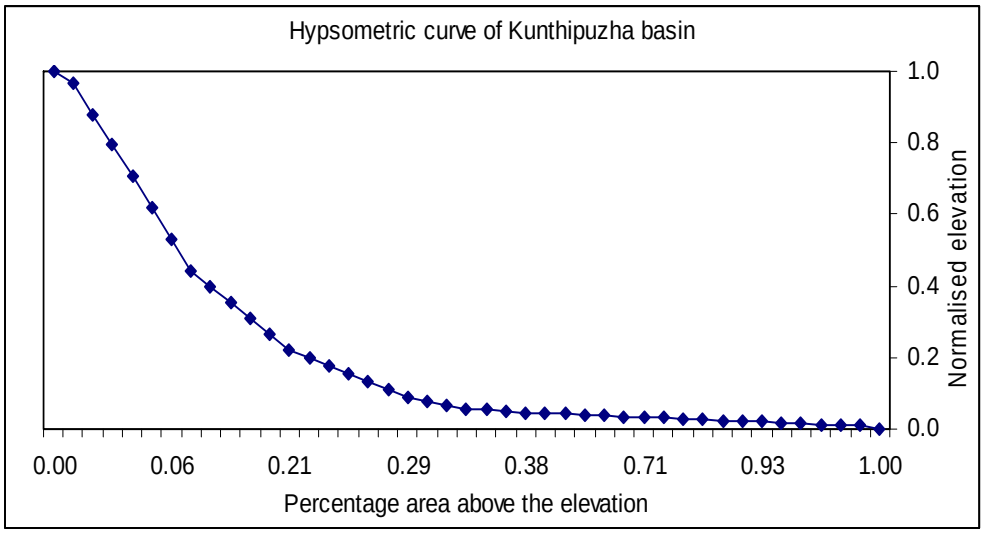

Figure 1. Hypsometric Curve of Kunthipuzha basin

Table 1. Landuse and soil of Kunthipuzha watershed and their area coverage

Land use			Soil		
Class	Area (km^2)	% area of watershed	Series	Area (km^2)	% area of watershed
Barren land	24.06	2.94	Chelikkuzhi	20.30	2.48
Dense mixed forest	42.72	5.22	Kairad	1.93	0.24
Evergreen forest	152.24	18.61	Kalladikkode	168.34	20.56
Garden land	307.27	37.56	Kanchirappuzha	17.53	2.14
Mixed forest	90.88	11.11	Kongad	15.7	1.92
Open scrubs	53.74	6.57	Kottappadi	28.33	3.46
Paddy	41.75	5.10	Manjallor	91.01	11.11
River bed	2.26	0.28	Pallippadi	371.56	45.38
Rubber	99.65	12.18	Perambra	104.11	12.71
Water	3.4	0.42			
Total	817.97	100.00	Total	818.81	100.00

Mean monthly rainfall distribution for the study period is shown in figure 2 and it indicates that temporal variation of rainfall is very significant. The month of June receives the maximum rainfall of about 500 mm out of the annual total of 2300 mm and it is followed by July, October and August (480, 400 350 mm respectively). Practically there is no rainfall from December to March. The monthly temperature variation shows that maximum temperature is received in March, February and May. Lowest temperature is experienced during October to December. Solar radiation is maximum during March to May and is at it's lowest during June to August. Average annual wind velocity of the area is 0.80 m/s. Monthly river flow pattern closely follow the monthly rainfall pattern which lead to the inference that water storage in the basin is poor. It can be observed that 23% of river discharge is taking place during July followed by August (20%), October (17%) and June (12%). River flow in Kunthipuzha is almost nil during February to April.

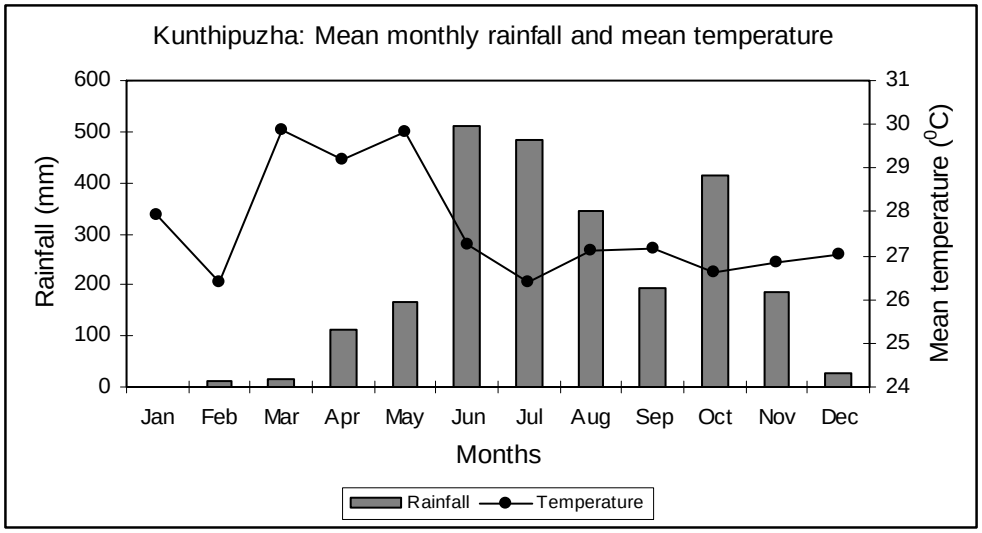

Figure 2. Mean monthly rainfall and temperature of Kunthipuzha

25 subwatersheds have been generated by the SWAT by assigning a threshold limit of 2000 ha for the generation of stream channels. Different subwatersheds and their geographical layout is shown in the figure 3. Important physical characteristics of the various subwatersheds of Kunthipuzha basin is given in table 4.3. Mean elevation of the subwatersheds vary from 52 to 1090 m. Mean slope of various subbasins shows great variations (they vary from 0.03 to 0.34%). It can be seen that all the subwatersheds in the headwater region have high land slope and high drainage density. Mean channel slope of the subbasins vary from 0.1 to 8.3%. High channel slope will lead to fast draining out of water from the subbsains.

Figure 3. Physical properties of sub watersheds

Subwater-shed No	Area (km^2)	Mean elevation (m)	Mean slope (m/m)	Channel length (km)	Channel slope (m/m)
1	27.99	525.9	0.272	11.327	0.067
2	24.62	497.7	0.339	11.095	0.066
3	104.4	1089.7	0.330	31.466	0.068
4	32.54	338.2	0.220	12.549	0.083
5	23.7	343.2	0.314	9.028	0.119
6	46.07	674.8	0.425	17.619	0.114
7	28.37	178.6	0.162	15.494	0.063
8	15.98	75.9	0.030	10.216	0.004
9	18.98	89.9	0.049	13.161	0.001
10	52.72	102.4	0.075	16.898	0.025
11	2.26	70.1	0.042	2.905	0.017
12	3.78	82.0	0.068	3.664	0.023
13	21.74	89.6	0.085	11.140	0.034
14	61.01	74.3	0.047	15.251	0.007
15	8.11	71.0	0.057	6.891	0.003
16	39.93	78.5	0.048	12.243	0.002
17	23.32	59.3	0.079	10.633	0.006
18	20.55	129.3	0.109	8.714	0.046
19	102.31	64.6	0.080	22.956	0.006
20	30.5	76.0	0.038	3.377	0.012
21	39.04	433.2	0.332	15.336	0.073
22	28.07	189.2	0.149	13.659	0.070
23	31.16	72.3	0.066	12.268	0.005
24	52.96	76.3	0.071	15.829	0.009
25	9.56	52.2	0.066	7.982	0.020

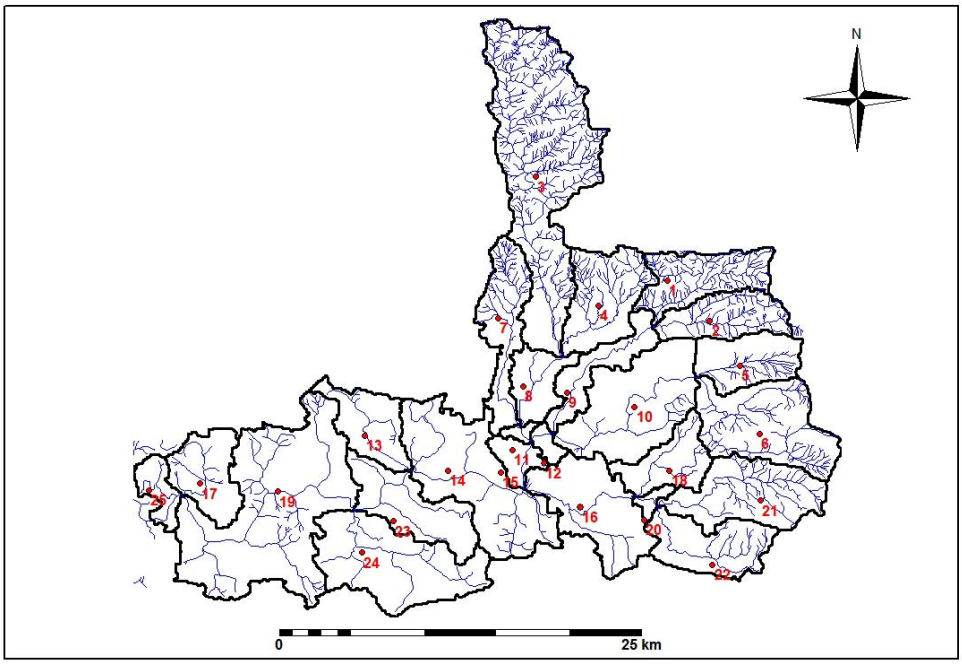

Figure 3. Subbasins of Kunthipuzha with drainage network

Model calibration and validation

The calibration of the model has been carried out by suitably modifying the sensitive parameters, within the range suggested by the uncertainty analysis. It is emphasized here that the calibration effort was very much reduced when the optimum parameter search was limited to the parameters suggested by the sensitivity analysis and their ranges suggested by the uncertainty analysis. First the calibration was attempted to annual time series and then it was extended to monthly and 10 daily basis. the summary statistics of simulated and observed mean annual river flow is presented in table 4. The Nash Sutcliffe Efficiency (NSE) and the coefficient of determination (R^2) were, respectively, 0.72 and 0.84. It is clear that the simulated values closely matched with the observed counterparts as revealed by the time series and the simulation efficiency statistics of NSE and R^2. The relatively lower values of NSE and R^2 may be due to the less number of observations available for annual analysis.

The comparison of monthly average flow for calibration and validation period is shown in figures 4 to 5. Very high NSE of 0.92 and 0.93 and R^2 of 0.96 and 0.99 have been obtained for both the calibration and validation period respectively. However, the simulations under estimate some of the peak values and this under estimation has also been reported by other

researchers (Jayakrishnan et al., 2005;

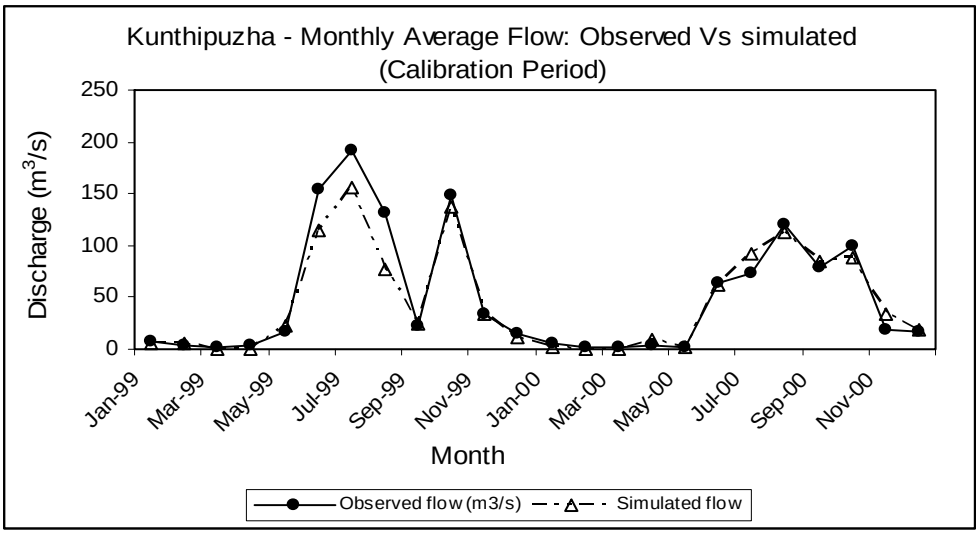

Figure 4. 1. Mean monthly river flow simulation for the calibration period

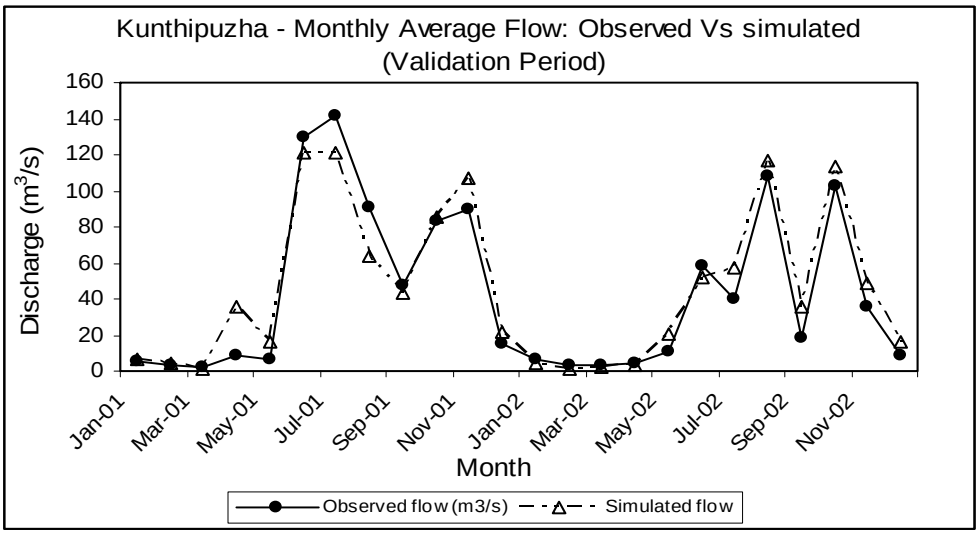

Figure 4. 2. Mean monthly river flow simulation for the validation period

Gassman et al., 2007, Sathian and Syamala, 2009). The same analysis was extended for a 10 days period also to check the model's predictive ability at shorter time scale. The importance of model calibration at different time scales has been reported by Sudheer et al. (2007) and Chabey et al. (2003). The NSE values for the 10 days prediction were 0.86 & 0.89 and R^2 were 0.96 & 0.97 for the calibration and validation periods (table 4).

A ten days average flow prediction has got very important application for Kerala rivers, because, reservoir water balance (reservoir working table) in this region is prepared on a 10 days time interval. So, this flow prediction information can be utilized for the reservoir planning at any section of the stream along its course within the river basin.

Table 4. Summary statistics of calibrated SWAT model on river flow

Statistics	Calibration period		Validation period	
Annual Statistics	Observed flow (m^3/s)	Simulated flow (m^3/s)	Observed flow (m^3/s)	Simulated flow (m^3/s)
Mean	52.58	50.78	-	-
SD	9.65	6.60	-	-
Nash Efficiency	-	0.72	-	-
Coefficient of determination	-	0.84	-	-
Monthly statistics	Observed flow (m^3/s)	Simulated flow (m^3/s)	Observed flow (m^3/s)	Simulated flow (m^3/s)
Mean	50.61	45.75	42.66	45.75
SD	57.06	48.56	44.92	42.28
Nash Efficiency	-	0.92	-	0.93
Coefficient of determination	-	0.96	-	0.99
10 daily statistics	Observed flow (m^3/s)	Simulated flow (m^3/s)	Observed flow (m^3/s)	Simulated flow (m^3/s)
Mean	68.11	64.14	52.14	53.93

SD	79.76	69.52	59.77	69.52
Nash Efficiency	-	0.86	-	0.89
Coefficient of determination	-	0.96	-	0.97

The above said calibration and validation of the model have been done against the total river flow. Since, SWAT has the capability to predict the hydrologic processes component-wise, it may be better, if various predicted hydrologic processes are validated separately with their measured or alternatively computed counterparts. Hence, to validate the model output in a more detailed manner, the simulated base flow was compared with the observed counterparts. As such there is no observed data for base flow. But the summer river flow is considered as the sole contribution of base flow and that has been matched with the simulated one. Very close similarity was observed for all the years under study An NSE of 0.51 and.

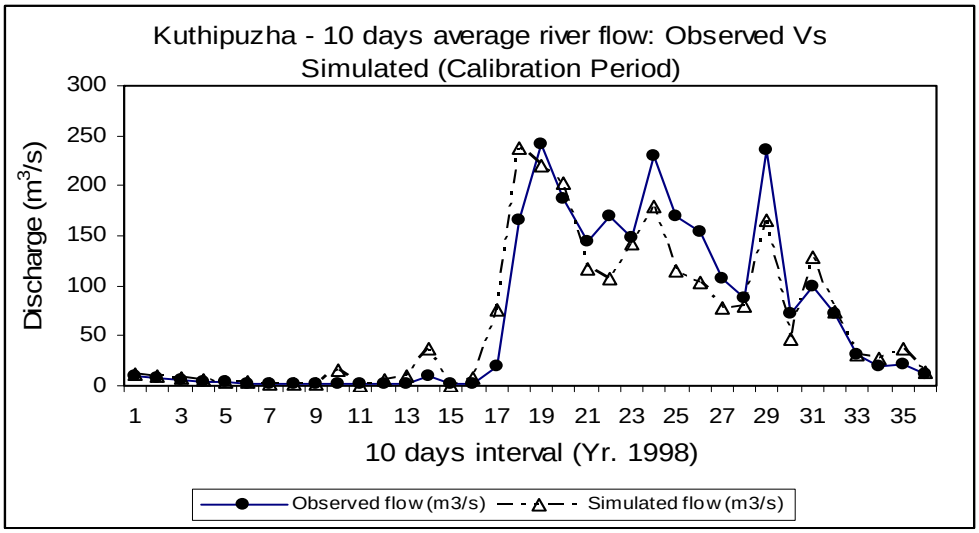

Figure 4. Mean of 10 daily river flow simulation for the calibration period

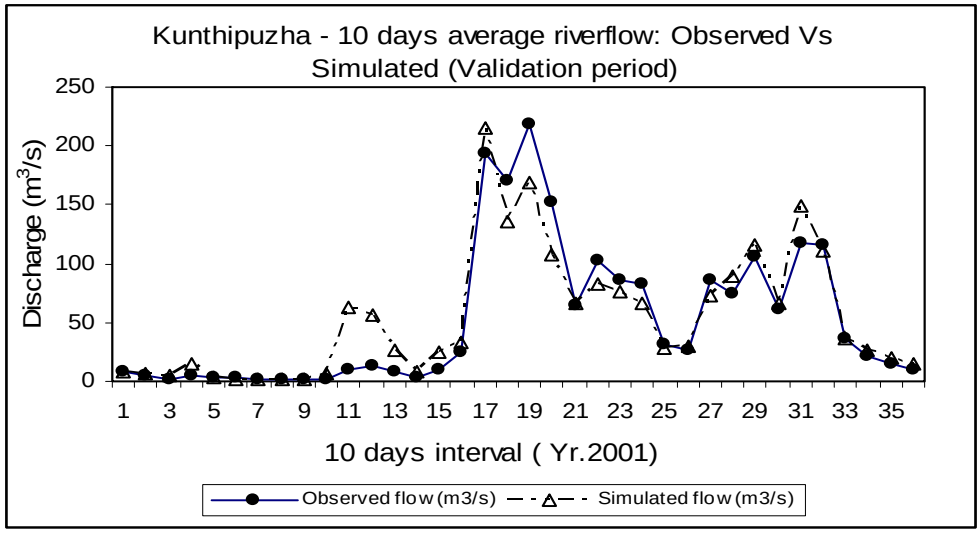

Figure 5. Mean of 10 daily river flow simulation for the validation period

an R^2 of 0.75 is obtained for the base flow simulation. As in the case of annual flow simulation statistics, here also, the relative low value of the above said statistics can be attributed to the smaller sample set.

Similarly, the validity of ET simulation by the model has been evaluated separately. For this, ET was also estimated through a water balance approach. In this case, it is assumed that rainfall minus river flow is equal to ET by neglecting other water losses from the basin such as deep aquifer recharge from the shallow aquifer storage. For the terrain of the state of Kerala, such an assumption can be justified as the deep aquifer recharge in the area is very marginal due to the presence of hard laterite below the shallow aquifer. ET by water balance and ET by SWAT also showed close resemblance. However, the model predicted value was consistently lower than its water balance counter parts. The consistent higher value of ET estimated by water balance is justified as deep aquifer recharge component has also been credited to the ET account. The intention of the comparison was to see that the prediction of ET by the model is reasonable. Hence, it can be inferred that the model simulation has thoroughly been validated and it is predicting different hydrologic components according to their actual or natural physical processes. It can be summarised that the calibration exercise, following the methodology described, was very effective.

Water balance of sub watersheds

SWAT model has got distinct capability to predict the water balance on a micro scale (HRU basis). And for scientific and insitu water management, the water balance of a terrain has to be estimated on micro watershed or sub watershed basis. Though, there is no means of

validating these processes on HRU or sub watershed scale, their relative higher and lower magnitudes between sub basins and HRUs can be justified by correlating the results with the causative physical characteristics.

Water balance of all 25 subwatersheds of Kunthipuzha basin is shown in figures 6 to 7. Majority of the subwatersheds have baseflow and surface runoff as the major flow components and lateral flow is marginal. But for subbasins having high land slope, lateral flow is the major flow component with very marginal baseflow fraction. It shows that in high sloping areas, the potential of shallow groundwater will be very poor. Total runoff does not show much variation between subwatersheds, but in the case of high sloping subwatersheds, total water yield is also higher. Groundwater recharge among less sloping subwatersheds is not varying much. It is very high in least sloping subwatersheds. In high sloping subwatersheds, the GW_R is very low and it gives the reason for poor yield of open wells in sloping terrains despite the high infiltration rate of soil. It can also be seen that ET is also higher in subwatersheds having higher groundwater recharge. The presence of positive correlation between ET and GW_R can be attributed to the presence of vegetation. Both ET and GW_R will be enhanced by vegetation.

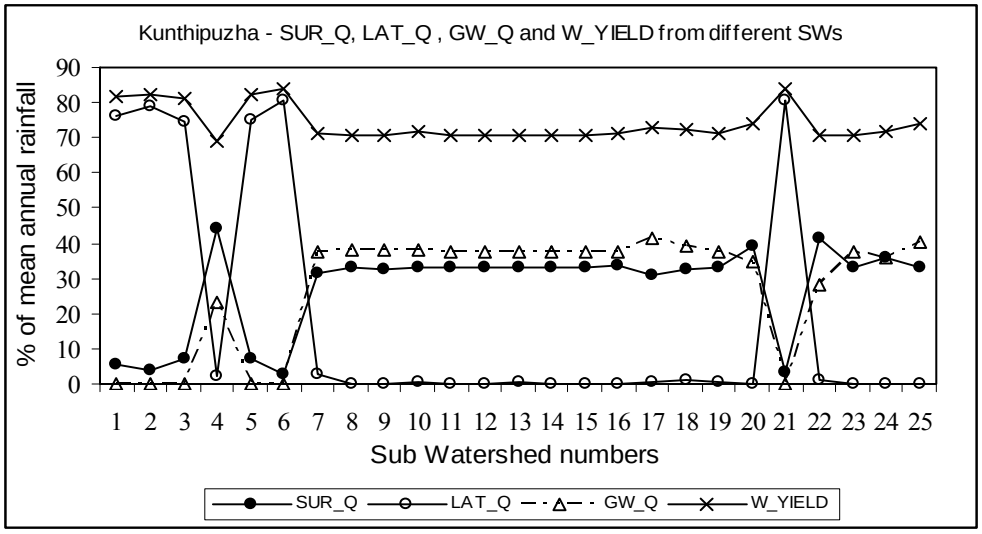

Figure 6. Mean of annual runoff components of various subwatersheds

In the case of HRU water balance also, the total water yield from different HRUs do not vary much (figures 8 to 9). However, high sloping HRUs are yielding more. Lateral flow is very high in high sloping HRUs. GW_Q from these HRUs are very poor indicating low groundwater recharge. GW_R and ET show similar pattern, with higher ET from areas with higher GW_R.

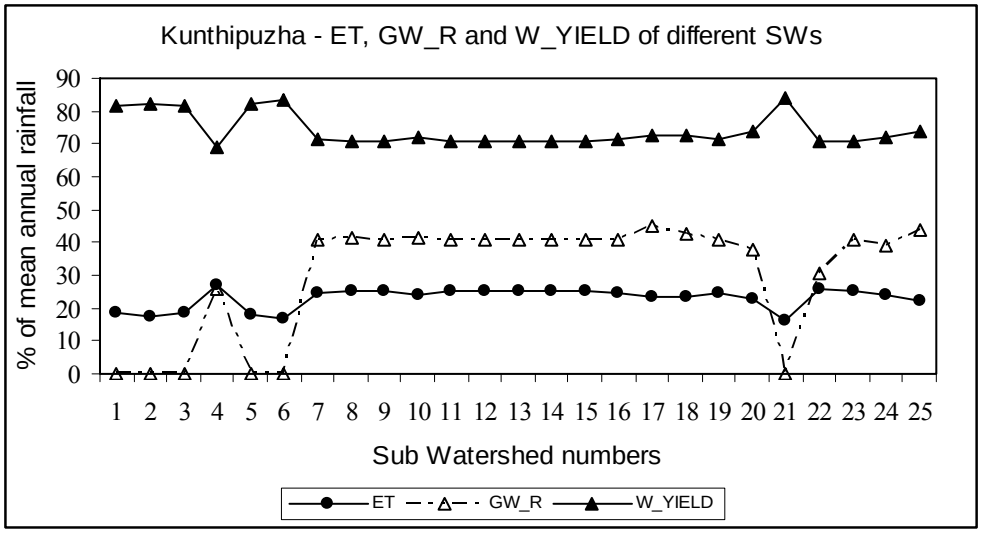

Figure 7. Mean of annual ET and groundwater recharge of various subwatersheds

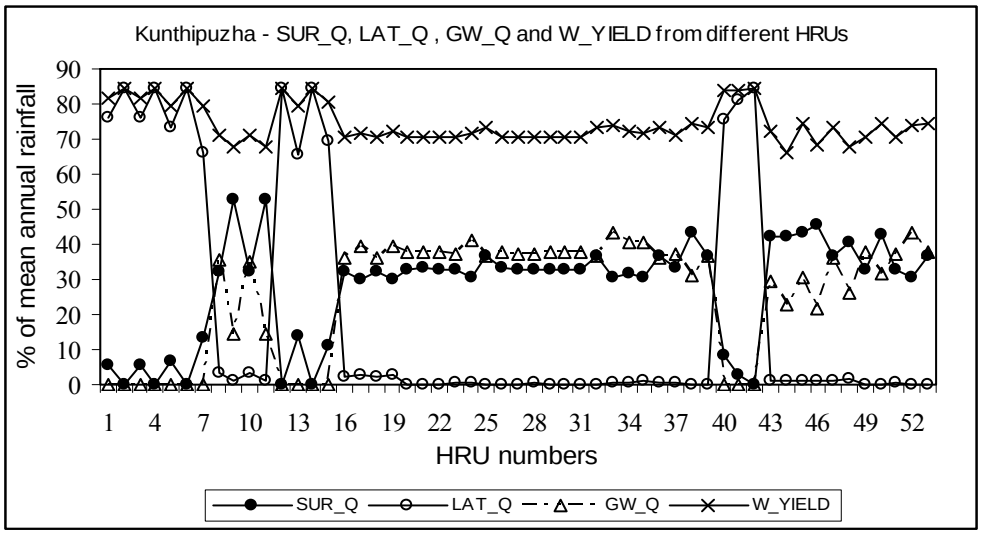

Figure 8. Mean of annual runoff components of various HRUs

HRUs having higher GW_R are those with low land slope and high vegetation. Higher ET from those HRUs is in the expected lines. Between HRUs, the components of hydrological processes are varying greatly and show the importance of micro spatial level water balance studies for insitu water conservation.

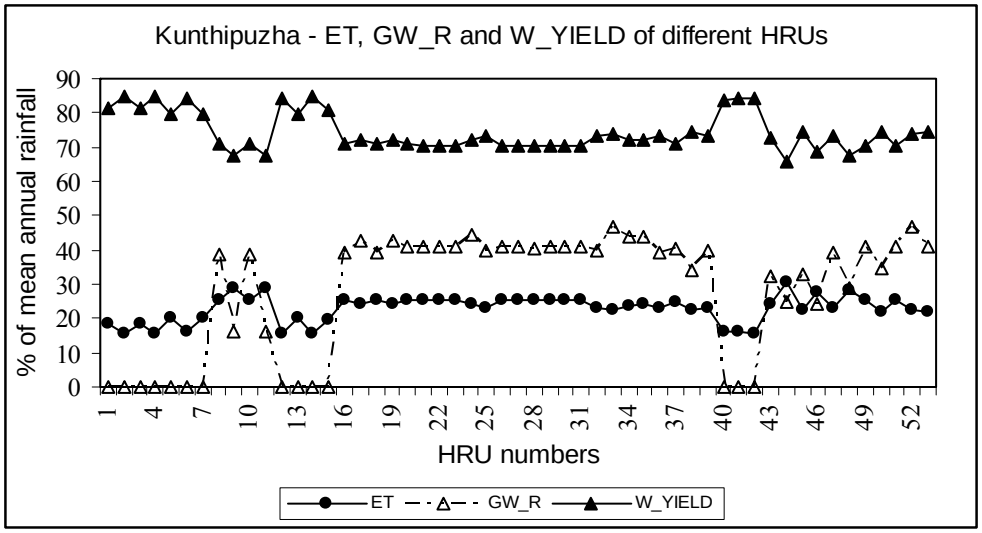

Figure 9. Mean of annual ET and groundwater recharge of various HRUs

Both subbasins and HRU water balance analysis show that in high sloping areas, the shallow groundwater potential is very less and will have negative impact on open well yield. In the study area, open wells are the main source of domestic water requirements. Hence, to improve the open well yield, the lateral flow will have to be checked. Subsurface dike is a feasible measure for the purpose. Positive impact of subsurface dikes has been reported from some places in and around the study area (Suseela and Visalakshi, 2006). The present study can help in identifying the locations suitable for constructing subsurface dikes to improve the shallow groundwater potential.

Water demand Vs availability

Water demand of different sub watersheds have been computed by summing up the requirement for domestic and irrigation. It is computed for the five summer months from December to May. Water availability is taken as the base flow during the summer months. Then the water shortage is worked out as the difference between availability and demand and it is presented as percentage of water demand (table 5). This exercise have been done only for 10 sub watersheds in the river basin due to the unavailability of population data. From the water shortage values of different sub watersheds, it is clear that there is wide variability in the water scarcity position between sub watersheds despite their close geographical locations. Hence, watershed development programmes should keep these points in mind.

Sub watershed no	Total_demand (m3)	Availability (m3)	Water shortage as % of demand
1	419620	0	-100
2	367750	0	-100
3	3292095	0	-100
4	597370	1012684	70
5	1768505	0	-100
6	5579685	0	-100
7	1257650	1443761	15
8	1205670	766151	-36
9	1026330	980219.2	-4
10	2258955	2651683	17

Conclusions

Quantifying water availability at micro watershed scale is the foremost task required in the planning of watershed based development works. To quantify water on a micro scale using hydrologic principles requires the application of physically based distributed watershed models. Hence, an attempt has been made to quantify the hydrologic components of various sub watersheds of river basin using SWAT. It is seen that summer availability of water as reflected by base flow varies greatly between sub watersheds of a river basin. Hence, watershed based development measures should carry out different tailor made measures to address water scarcity issues of various sub watersheds.

References

Arnold, J.G., Srinivasan, R., Muttiah, R.S., Williams, J.R., 1998. Large area hydrological modeling assessment. Journal of the American Water Resources Association 34 (1). 28-42.

Chaubey, I., Costello, T. A., White, K. L., and Cotter, A.S. (2003). Stochastic validation of SWAT model. Proceedings of International Symposium on Total Maximum Daily Load (TMDL) Environmental Regulations–II. Albuquerque, New Mexico, USA. 168-176.

Gassman, P.W., Reyes, M.R., Green, C.H. and Arnold, .G. 2007. The soil and Water Assessment Tool: Historical development, applications and future research directions, Transactions of ASABE 50 (4) 1211 – 1250.

Jayakrishnan, R., Srinivasan,R., Santhi, C. and Arnold, J.G., 2005. Advances in the application of the SWAT model for water resources management. Hydrological Processes. 19(3):749-762.

Sathian,K.K., Syamala,P., 2009. Calibration and validation of a physically based distributed watershed hydrologic model, Indian Journal of Soil Conservation 37(2): 100-105.

Sudheer, K.P., Chaubey, I., Garg, V., Migliaccio, K.W., 2007. Impact of time scale of calibration objective function on the performance of watershed models. Hydrological Processes 21:3409-3419. DOI:10.1002/hyp.6555.

Suseela, P., Visalakshi, K.P., 2006. Subsurface dikes – a case study for its suitability in Kerala. Journal of Agricultural Engineering 43(2) 34- 41.

Simulation of Sub-Daily Runoff for an Indian Watershed Using SWAT Model

T. Reshma
Research Scholar, Department of Civil Engineering/NIT Warangal, Warangal – 506004, Email: talarireshma@yahoo.com

K. Venkata Reddy
Asst Prof, Department of Civil Engineering/NIT Warangal, Warangal – 506004, Email: kvenkatareddy9@rediffmail.com

Deva Pratap
Prof, Department of Civil Engineering/NIT Warangal, Warangal – 506004, Email: prataprec@yahoo.com

Abstract

In India, integrated watershed management has been adopted as a part of the National Water Policy for planning, development and management of water resources. Simulation of sub-daily runoff at watershed level is important to understand the prevailed hydrologic regime of the watershed. This will help in the effective planning and management of water resources at watershed scale. A robust and generic watershed model is required for simulation of runoff at sub-daily time steps by considering the important hydrological processes of the watershed. Soil and Water Assessment Tool (SWAT) model developed by the United States Department of Agriculture is one such widely used model in simulation of hydrologic and water quality parameters. ArcSWAT model is the modified version of SWAT model with can work in the ArcGIS environment. This paper presents the application of ArcSWAT model in simulation of sub-daily runoff of Harsul watershed located in Nashik district, Maharashtra, India. Hourly rainfall data, Land Use (LU)/Land Cover (LC), Soil data and Digital Elevation Model (DEM) data of the watershed has been used to simulate the runoff of the watershed. Model simulation has been verified using the observed runoff data and found to be satisfactory. The methodology presented in this paper will be useful for simulation sub-daily runoff in Indian watersheds using ArcSWAT model.

Keywords: ArcSWAT, GIS, Sub-daily runoff simulation, Watershed.

Introduction

Soil Water Assessment Tool (SWAT) model is a hydro-dynamic and physically-based hydrologic model. Geographic Information System (GIS) provides the framework within

which spatially-distributed data are collected and used to prepare model input files and to evaluate model results. SWAT model with GIS tools, can be used to illustrate the effects of land use practices on runoff, and to support the spatial analysis of hydrologic parameters of the watershed. Watershed computer models have long been an integral part of any assessment, and model types vary with intended application. The application of most hydrological models often requires a large amount of spatially variable input data and a large number of parameters (Srinivasan et al., 2010). One of the most commonly used river basin model is ArcSWAT, a combination of the simulation model SWAT with a Geographical Information System (GIS) user interface. SWAT was developed to predict the impact of land management practices on water, sediment and agricultural chemical yields in large complex watersheds with varying soils, land use and management conditions over long periods of time. The SWAT Model is designed to route water and sediments from individual watersheds, through the river systems. It can incorporate the effects of tanks and the reservoirs/check dam's off-stream as well as on-stream. The agricultural areas can also be integrated with respect to management practices.

The major advantage of the model is that unlike the other conventional conceptual simulation models it does not require much calibration and therefore can be used on ungauged watersheds. For modeling purposes, a macro-watershed or catchment is considered to be made up of a number of watersheds. The use of a number of discrete watersheds in a simulation is particularly beneficial when different areas of the macro-watershed are dominated by land uses or soils different enough in properties to have different impacts on the hydrological response. Within SWAT input information for each watershed is grouped with respect to weather, unique areas of land cover, soil, and management, and is called Hydrologic Response Units (HRUs). Model outputs include all water balance components (surface runoff, evaporation, lateral flow, recharge, percolation, sediment yield, etc.) at the level of each watershed and are available at daily, monthly or annual time steps.

SWAT model includes options for estimation of surface runoff from HRUs, which combine daily or hourly rainfall and USDA Natural Resources Conservation Service (NRCS) curve number (CN) method or Green-Ampt method (Bijan et al., 2008). Water retention on plants is computed by the implicit CN method, while explicit water retention is simulated by Green-Ampt method. Water collection in soil and its runoff lag are computed by the techniques of water redistribution between the soil layers. Penman-Monteith, Priestly-Taylor and Hargreaves methods are used for estimation of potential and real evapotranspiration. Arnold

et al. (2005) describes some recent advances made in the application of SWAT and the SWAT–GIS interface for water resources management and suggested that the model has good potential for application in hydrologic/water quality studies in countries around the world and as a tool to develop time and cost-efficient analyses for watershed/water resources management. SWAT model can be a potential monitoring tool for watersheds in mountainous catchments and the predicted mean daily stream flow was found to be exactly as observed during the water balance simulation (Birhanu et al., 2007). Srinivasan et al. (2010) proposed a framework for developing spatial input data, including hydrography, terrain, land use, soil, tile, weather, and management management practices, for SWAT in the Upper Mississippi River basin (UMRB) and tested the uncalibrated SWAT model for streamflow, base flow, and crop yield simulation. They used annual and monthly streamflow from 11 USGS monitoring gauges to test SWAT, and found that SWAT can capture the amount and variability of annual streamflow very well. Jeong et al. (2010) presents the development and testing of a sub-hourly rainfall–runoff model in SWAT model. Reshma et al. (2011) describes the usefulness of ArcSWAT model over conventional SWAT model in simulating the flow processes of the watershed.

From the above studies, it indicates that SWAT model can be an effective tool for accurately simulating the hydrological processes of the watersheds on different time steps. The present paper describes the application of SWAT model for simulation of sub-daily flows in an Indian watershed.

Study Area and Methodology

Harsul watershed located in Nashik district, Maharashtra, India has been selected as study area to simulate sub-daily flows using ArcSWAT. The watershed has an area of 10.929 sq. km. It is situated between East Longitude of 73º 25´ and 73º 29´ and the North Latitudes of 20º 04´ and 20º 08´. The location map of Harsul watershed is shown in Figure 1. The methodology adopted for the present study in shown in Figure 2. Preparation of DEM, LU/LC maps using remotely sensed data and GIS are explained in Reddy et al. (2011). Parameters like saturated hydraulic conductivity, Manning roughness and sub-daily rainfall data has been used to simulate flow with ArcSWAT model.

SWAT Model Application

The input for SWAT model consists of Digital Elevation Model (DEM), rainfall, soil characteristics, topography, vegetation and other relevant physical parameters. The model has

been used for the sub-daily simulation. Automatic delineation of watershed boundary and other sub-watersheds within the watershed has been carried out using DEM of the watershed in the SWAT model. The watershed boundary with sub-basins is shown in Figure 3. The Land Use/Land Cover map and Soil map which are modified as per the standard Classifications available in the SWAT model are shown in Figure 4 and Figure 5. The soil classes of Harsul watershed are as follows: Loamy (48.01%), Sandy (48.35%) and sandy Loamy (3.63%). LU/LC classes of the watershed are as follows: Agricultural land (50.35%), forest land (40.27%) and waste Land (9.36%). SWAT model requires sub-daily meteorological data that can either be read from a measured data set or generated by a weather generator model. The model setup involves the following five steps: (1) Data preparation (2) Sub-basin discretization (3) HRU definition (4) Weather Generator data (5) Run SWAT.

Figure 1: Location map of the Harsul Watershed

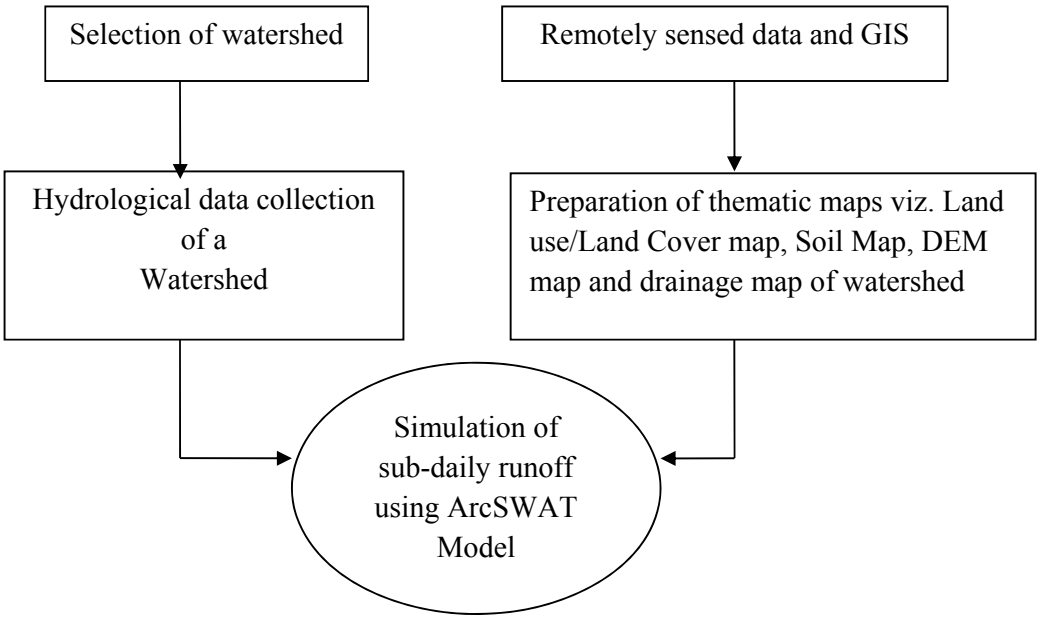

Figure 2: Flow chart showing the methodology followed in the present study

Results and discussion

Three months (July, August and September 1997) rainfall has been used for input for simulation of runoff. The simulated runoff hydrographs for the three months are shown in Figure 6 (a) to (c). Simulations results for the month July, August and September, 1997 are shown in Table 1. From the hydrographs, it is seen that the volume of runoff and time to peak has been simulated within the variation 65-70%. However, the model was not able to capture the peak runoff. There are more than sixty parameters in SWAT model and it is difficult to have exact information on all these parameters. Some physical parameters such as Channel width and Channel depth vary along the channel reaches. These are the some of the reasons for improper simulation of peak runoff. It is observed, that the values of runoff on recession limb of hydrographs are higher than the observed one. The channel roughness and infiltration parameters are may be the reasons for this behavior. The calibration and sensitivity analysis of the model may improve the simulations.

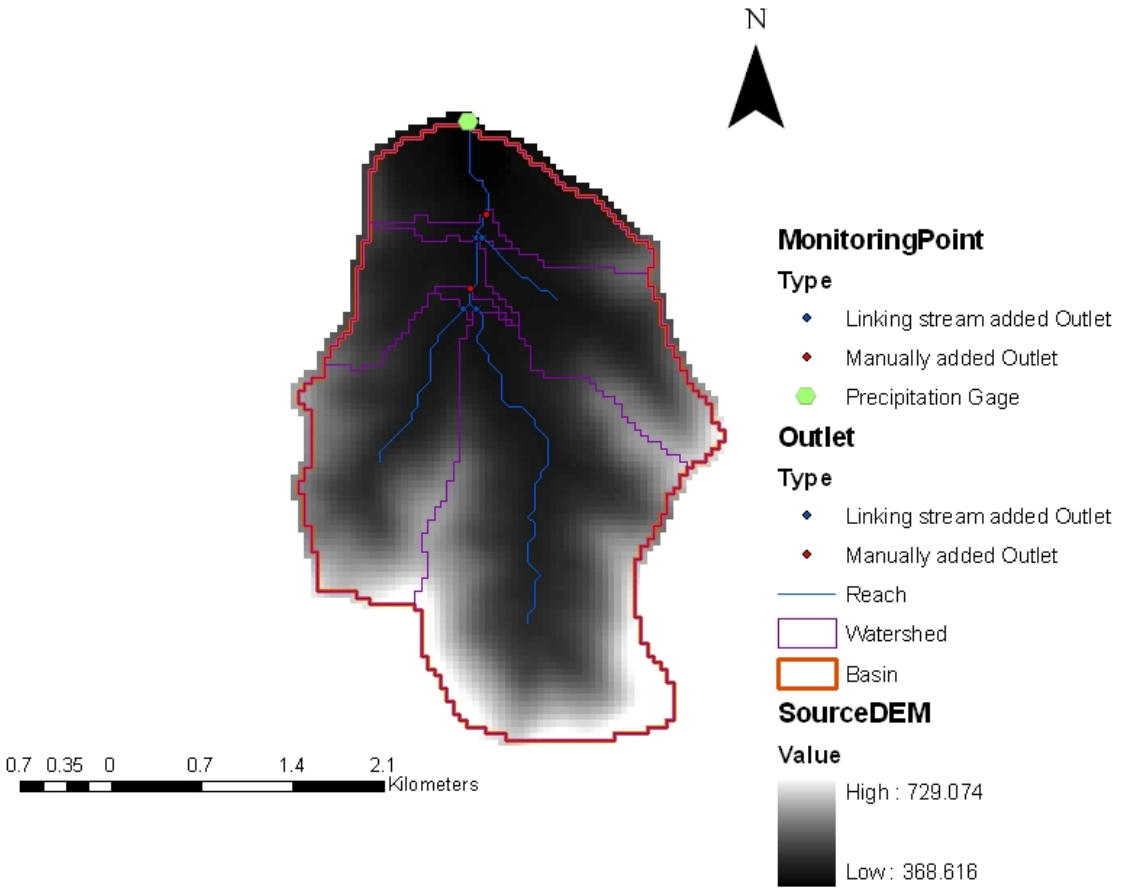

Figure 3: Automatically delineated sub-basins of Harsul watershed

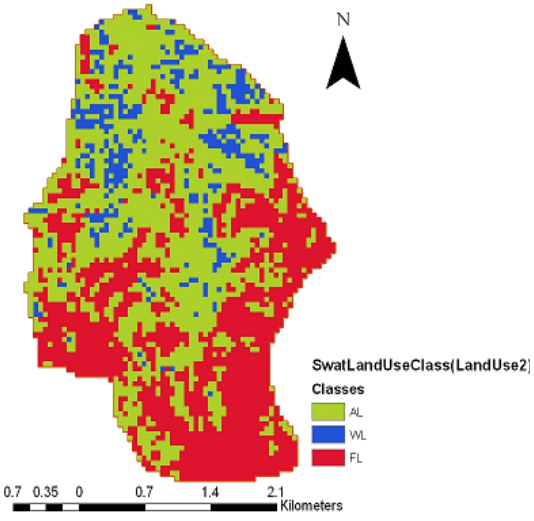

Figure 4: Modified Land use/Land cover map of Harsul Watershed

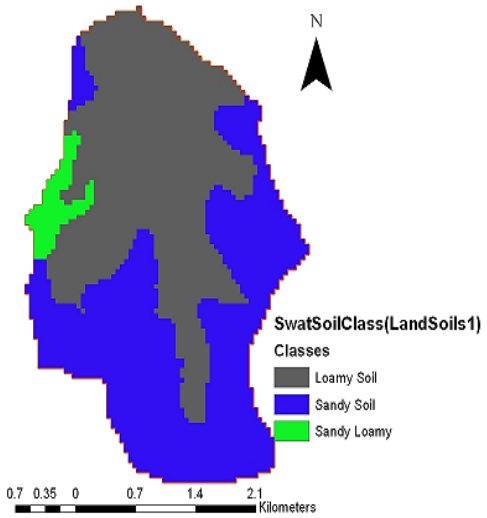

Figure 5: Modified Soil map of of Harsul Watershed

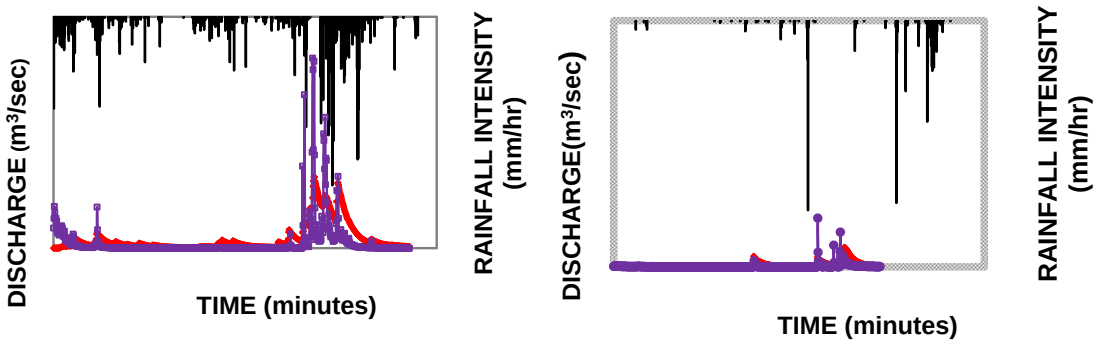

(a) (b)

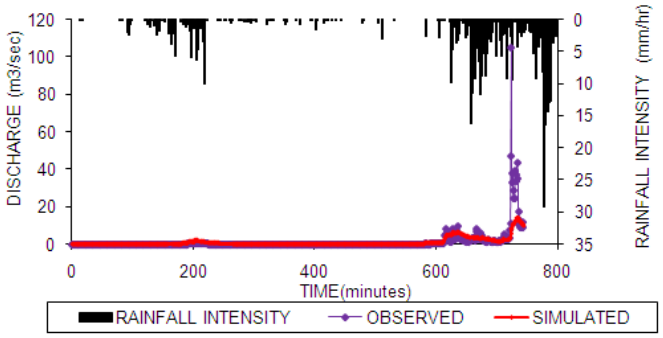

(C)

Figure 6 Simulation runoff hydrograph for the Harsul watershed (a) July 1997 (b) September 1997 (c) August 1997

Table 1.Simulation results for Harsul watershed

Rainfall months	Volume of runoff (mm)		Peak runoff (m^3/sec)		Time to peak (sec)	
	Observed	Simulated	Observed	Simulated	Observed	Simulated
July, 1997	307.76	242.21	104.784	12.9	723	730
August,1997	143.24	247.36	4.437	1.67	91	91
September,1997	16.71447	47.42	5.935	2.37	551	623

Conclusions

This study describes the application of ArcSWAT model for simulation of sub-daily runoff on an Indian watershed. The model has been applied for the three month's rainfall data. From the simulations, it is observed that, the model is able to simulate the volume of runoff and time to peak runoff. But large variations are observed in peak runoff. This may be because of inexactness in the values of parameters. It is also observed that sensitivity analysis has to be carried out to improve the simulation results. The methodology presented in this study is useful to simulate hourly runoff in Indian watersheds using ArcSWAT models.

References

Arnold, J.G., R. Srinivasan, R. Jayakrishnan, and C. Santhi. 2005. Advances in the application of the SWAT model for water resources management. *Hydrological Processes. 19, 749-762.*

Birhanu, B.Z., P.M. Ndomba, and F.W. Mtalo. 2007. Application of SWAT Model for Mountainous Catchment. *Catchment and Lake Research.*

Bijan. D., R. Srinivasan, and G.S. Shimelis. 2008. Hydrological Modelling in the Lake Tana Basin, Ethiopia Using SWAT Model. *The Open Hydrology Journal, 2, 49-62.*

Jeong. J., N. Kannan, J. Arnold, R. Glick, L. Gosselink, and R. Srinivasan.2010. Development and Integration of Sub-hourly Rainfall–Runoff Modeling Capability Within a Watershed model. *Water Resour Manage. Accepted: 6 May.*

Reshma T., K. Venkata Reddy and Deva Pratap. 2011. Simulation of runoff of a watershed using ArcSWAT model. *In Proc. International Conference on Spatial Technologies for Rural Development/Watershed Development*.

Srinivasan, R., X. Zhang, and J. Arnold. 2010. SWAT ungauged: hydrological budget and crop yield predictions in the upper mississippi river basin. *American Society of Agricultural and Biological Engineers. Vol. 53(5): 1533-1546.*

Venkata Reddy. K, Eldho. T. I, Rao. E.P. and Kulkarni, A.T. (2011), FEM-GIS based channel network model for runoff simulation in agricultural watersheds using remotely sensed data, *International Journal of River Basin Management*, 9(1), 17-30.

Acknowledgements

My sincere thanks to Mr. Guy Honore, Project coordinator, Indo German Bilateral Project-Watershed Management, for providing the hydrological data of the Harsul watersheds.

Impact of Agricultural Intensification on the Water Resources in a Semi-Arid Catchment in India

Reshmidevi T.V*
Research Scientist,
Department of Civil Engineering, Indian Institute of Science, Bangalore, India.

D. Nagesh Kumar
Professor,
Department of Civil Engineering, Indian Institute of Science, Bangalore, India

Abstract

Agricultural growth and water resources sustainability are the two critical conflicting issues, particularly in the semi-arid and arid regions in India. In the present study, ArcSWAT (v.2009) has been used to analyze the impact of agricultural intensification on the surface and sub-surface water resources in the Malaprabha catchment in India. The unsustainable cropping pattern of the area, incompatible with the climatology, has given rise to excessive irrigation demand, which is met largely by tapping the aquifer, resulting in a drastic depletion of the groundwater table. The deep aquifer component in SWAT was found to be insufficient to represent this excessive groundwater depletion scenario of the area. Hence, a separate water balance model was developed for the deep aquifer, taking the deep aquifer recharge and irrigation requirement from the SWAT simulation. In order to have a better representation of the catchment climatology, multi-site rainfall data was used as an input to the model. The model parameters were calibrated for the study area using observed monthly stream flow data. Model simulation shows drastic groundwater table depletion in many parts of the catchment. In the context of climate change, where an increase in the temperature and a change in the rainfall pattern is expected, the model can be used to estimate the groundwater recharge and the irrigation demand, so as to develop sustainable agricultural plans for the area.

Key words: ArcSWAT, Groundwater, Irrigation, Sensitivity and Calibration, Malaprabha Catchment, India

Introduction

Agriculture is the largest fresh water consumer in the world. Due to the institutional benefits and the large subsidies available for the farmers, in India the percentage of groundwater irrigated area is much more than the surface water irrigated area, and it is increasing at a faster rate. The unorganized groundwater development has resulted in a drastic depletion of the groundwater table in many parts of India. In this study ArcSWAT (v.2009), which is the Soil and Water Assessment Tool (SWAT) integrated with ArcGIS, has been used to study the impact of excessive groundwater withdrawal on the sub-surface water resources in a semi-arid catchment in India.

SWAT is a conceptual model that takes into account various catchment process in a continuous time scale. It is originally developed from the Simulator for Water Resources in Rural Basins (SWRRB) (Williams et al., 1985; Arnold et al., 1993). In SWAT the watershed is divided into various sub-basins and further into Hydrologic Response Units (HRUs) based on the soil type, land use/ land cover and slope. The land phase is vertically divided into different layers giving four different control volumes viz., surface, root zone, shallow aquifer and deep aquifer (Arnold et al., 1993). SWAT considers the water balance in the four control volumes.

A lumped model is used in SWAT to simulate the groundwater and this has been reported as the main drawback of the SWAT groundwater component (Sophocleous et al., 1999). Integration of SWAT with a fully-distributed groundwater model MODFLOW has been attempted in a few studies to solve this problem. The integrated model takes groundwater recharge as input from the SWAT and run the MODFLOW component to simulate the groundwater table, aquifer evaporation and the stream-aquifer interaction (Sophocleous et al., 1999, Kim et al., 2008). However, such integrated models are not associated with the Geographic Information Systems (GIS) integrated versions of the SWAT like ArcSWAT. Hence in this study the ArcSWAT (v.2009), which is readily available in the public domain, has been used for the analysis assuming that the groundwater processes incorporated in the model are satisfactory for the current level of analysis.

Malaprabha catchment in India is selected as the case study area. This paper presents the problem identified when the ArcSWAT was applied to the study area. In ArcSWAT the shallow aquifer and the deep aquifer are of undefined depths. However, initial storage in

these layers is limited to 1000mm and 3000m, respectively. Qualitative information from the field shows that while drilling bore wells, the depth at which water appeared has increased by around 100m in certain areas over a period of three decades. With the high rate of groundwater extraction happening in the study area, the present values of the maximum initial storage have been found to be insufficient to represent the irrigation scenario of the area. Therefore in the present study, a separate water balance component has been used, taking deep aquifer recharge and irrigation requirement from the SWAT simulation. The following sections describe the integrated use of SWAT and the water balance model for the deep aquifer, and the model calibration and validation for the case study area.

Description of the ArcSWAT

SWAT is a spatially distributed model capable of simulating the flow and nutrient transport processes in a continuous time scale at the basin level. SWAT integrated with ArcGIS, which is called ArcSWAT (Winchell et al., 2007), makes the incorporation of the spatially referenced data much simpler. In SWAT, using different approaches and approximations, the precipitation is partitioned into surface flow, evapotranspiration, lateral flow, percolation, return flow and deep aquifer percolation. SWAT considers hydrologic processes in two phases viz., land phase and channel routing phase. In the land phase, precipitation, after interception at the canopy layer, reaches the soil surface and a part of it becomes surface runoff. The remaining part infiltrates into the soil layer and adds to the soil moisture storage. After making due allowance for the evapotranspiration, a water balance is achieved between the lateral flow and the percolation components. This percolation is added to the shallow groundwater storage.

Water balance in the shallow aquifer is achieved between the percolation, deep aquifer recharge, revap (which is the movement of water from the shallow aquifer to the root zone) and groundwater flow. The model can also consider the withdrawal from the shallow aquifer. The lateral flow from the shallow aquifer is assumed to meet the channel at the sub-basin outlet. Recharge to the deep aquifer is estimated as a fraction of the total percolation reaching the shallow aquifer.

The deep aquifer is defined in such a way that the flow from this layer meets the channel only outside the basin. The flow is therefore considered going out of the system and hence is not

modeled in SWAT. However, SWAT can consider the groundwater extraction from the deep aquifer layer.

ArcSWAT with additional water balance component

In SWAT deep aquifer water balance considers the percolation from the shallow aquifer (or recharge to the deep aquifer, R_i) and the withdrawal (which in this case is the groundwater extraction for irrigation, Irr_i). The water balance equation can be represented as given in Eq. 1.

$$S_{Deep,i} = S_{Deep,i-1} + R_i - Irr_i \tag{1}$$

Where $S_{Deep,i-1}$ and $S_{Deep,i}$ are the storages in the deep aquifer in the previous and the current time steps, respectively. In ArcSWAT the maximum value that can be assigned to the initial deep aquifer storage is limited to 3000mm. Therefore, in order to account for the high extraction rate from the deep groundwater resources, in this study the ArcSWAT is combined with a separate water balance model for the deep aquifer.

In order to assure unlimited water supply for irrigation, the irrigation is assumed to be from outside sources. The estimated irrigation requirement at the HRU level is taken as the first input to the deep aquifer water balance model. The second input is the deep aquifer recharge estimated in ArcSWAT at each HRU. In the water balance model, HRUs in each sub-basin are identified first and the difference in the deep aquifer storage is calculated at sub-basin level using Eq. 2.

$$\nabla WT = \frac{\sum R_i . A_i - \sum Irr_i . A_i . \varepsilon_i}{s . \sum A_i} \tag{2}$$

Where, ε_i is the irrigation efficiency and A_i is the area of the i^{th} HRU in the selected sub-basin. Specific yield of the aquifer in the sub-basin is represented by s. The schematic representation of the model is shown in Fig. 1.

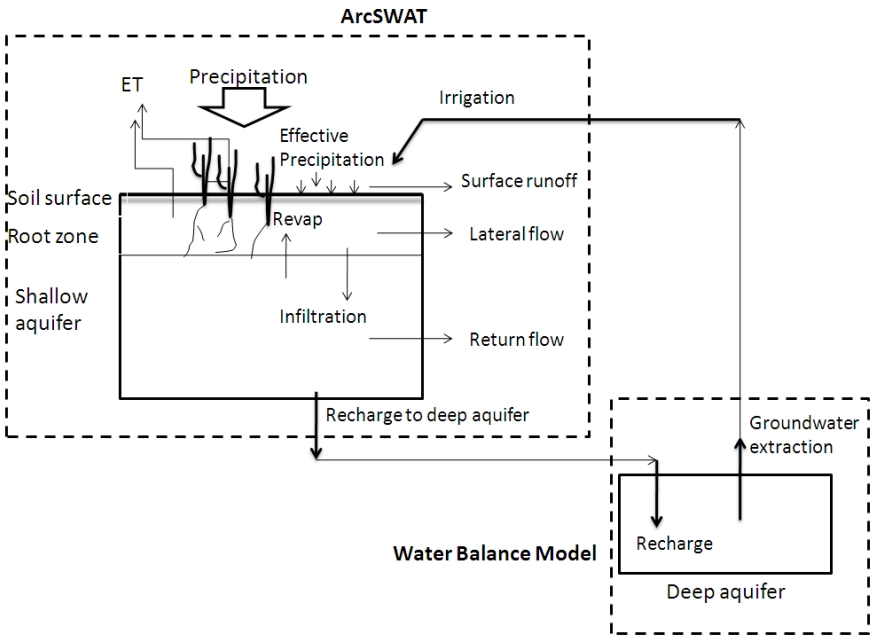

Fig. 1. Schematic representation of the ArcSWAT integrated with the deep aquifer water balance model

Sensitivity, calibration and uncertainty analysis of parameters in ArcSWAT

In ArcSWAT sensitivity analysis can be done automatically by using the Latin Hypercube (LH) and One-factor-At-a-Time (OAT) method. The LH sampling method divides the feasible parameter range into different sub-ranges and assures that each sub-range is sampled only once during the analysis. The model is run by taking different combinations of the input parameters by changing only one parameter at a time. The output therefore shows influence of the parameter that was changed for the run (Van Griensven, 2005).

In ArcSWAT, ParaSol method (Van Griensven and Meixner, 2006), is incorporated for the parameter calibration and uncertainty analysis. In ParaSol, sum of the squares of the residuals (SSQ) between the simulated series and the observed data series is used as the objective function. In cases where observed data for more than one parameter is available, requiring the use of a multiple objective function, a Global Optimization Criterion (GOC) is derived by using the objective functions. Further, the Shuffled Complex Evolution Algorithm (SCE-UA) is used for the optimization (Van Griensven, 2005).

Study area

Malaprabha catchment in Karnataka, India is selected as the case study area for this study. Malaprabha River originates in the Western Ghats in the Belgaum District. The Malaprabha Dam (Navilutheertha Dam) was constructed on this river with a gross storage capacity of 1070 M.cu.m. The catchment area of 2564 sq.km, drained by the Malaprabha River and its tributaries up to the Malaprabha dam, is selected as the present study area. Location map of the catchment is shown in Fig. 2. The boundaries shown in the figure are with reference to the maps published by the Survey of India.

Climatology of the area varies from tropical humid (with rainfall more than 3000mm per year) in the upper catchment, to semi-arid (with rainfall less than 500mm) in the lower catchment. Geological information shows that the area is underlain by Greywacke/ Argillite of the Chitradurga group, pink granite of the Clospet group, and Basalt in a small area.

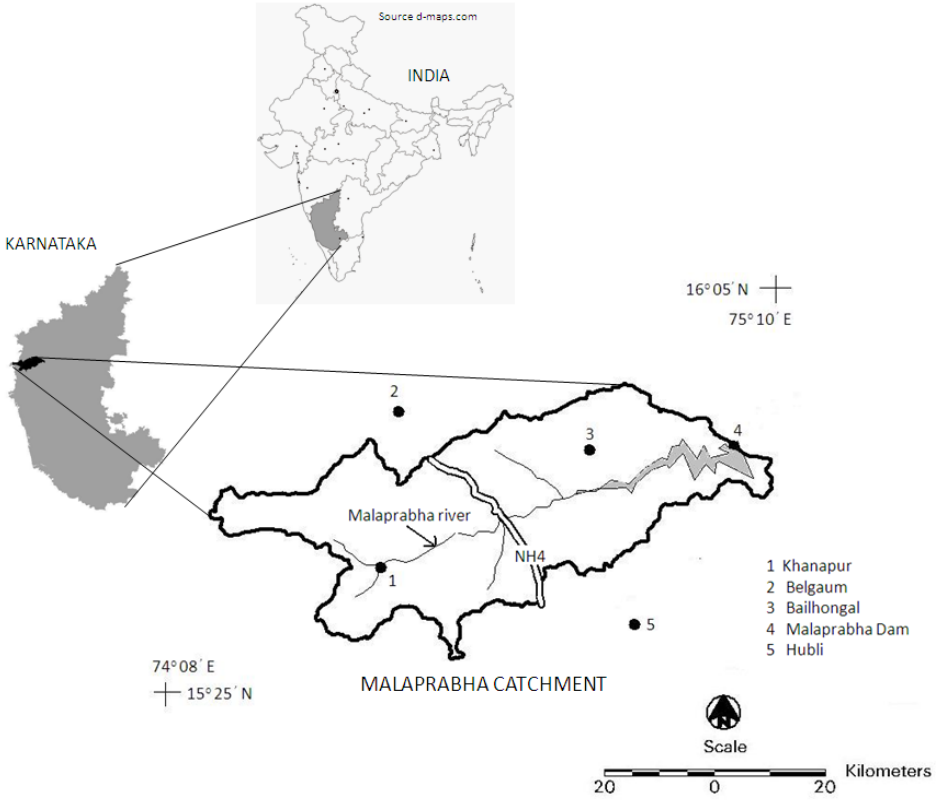

Fig. 2. Location map of the Malaprabha Catchment in India

The study area is an agricultural watershed with paddy, sugarcane, oilseeds, cereals and pulses as the major crops, mostly supported by irrigation. In addition to the cultivation of the

water intensive crops, many areas are cultivated more than once in a year with the help of irrigation. The large irrigation requirement in the area is mainly met from the groundwater resources. According to the statistics of the Directorate of Economics and Statistics, the net irrigated area and the groundwater irrigated area in the study region have been almost doubled in the last three decades. This has resulted in drastic groundwater table depletion in many parts of the catchment. In this study the ArcSWAT combined with the deep aquifer water balance model has been applied to the catchment to study the impact of excessive irrigation on the groundwater resources.

Model setup

Basic data required for the model include the Digital Elevation Model (DEM), soil map, land use/ land cover map, and hydro-meteorological data such as rainfall, temperature, relative humidity and wind speed. DEM of the study area at a spatial resolution of 30m was obtained from the Advanced Space-borne Thermal Emission and Reflection Radiometer (ASTER) Global DEM (GDEM) released by the Japan's Ministry of Economy, Trade and Industry (METI) and NASA. Land use/ land cover (LU/LC) map was generated with the help of Landsat-7 ETM+ imageries. Each of the LU/LC classes in the map was assigned to the corresponding SWAT land use class. Soil map of the area generated by NBSS & LUP was used in this study. Details of each of the soil classes were obtained from an earlier study (Reshmi et al., 2008). In order to incorporate the rainfall spatial variation, data from 9 rain gauge stations in the catchment, obtained from the Directorate of Economics and Statistics, Bangalore, was used in the model. Observed data of daily maximum and minimum temperature, relative humidity, and wind speed from a single observatory in the catchment was also given as an input to the model.

Using the DEM, drainage network of the catchment was generated. Further, 12 sub-basins were delineated using the flow information. Land use/ land cover, soil and slope information were used to define HRUs in each sub-basins. Crop management practices viz., beginning and end of the cropping period, irrigation application etc. were manually defined for each HRU based on field observations. From the different methods available in the ArcSWAT interface, the Curve Number method and the Hargreaves methods were selected for estimation of the surface runoff and the potential evapotranspiration, respectively. The model simulates various hydrologic processes in the root zone and the shallow aquifer, and calculates the recharge to the deep aquifer at each time step at the HRU level. In ArcSWAT

simulation, irrigation application was activated. For this, the irrigated crops were identified and the irrigation was assumed when the plant stress reaches the threshold value of 0.95. The estimated irrigation for each HRU was assumed to be met from the outside source.

The recharge and the irrigation requirement at the HRU level was taken as the input to the water balance model and the deep aquifer water table was simulated. Following the recommendations of the CGWB, specific yield of the rock formations in the area was assumed as 3% (R&D Advisory Committee on Groundwater Estimation, 2009). Also, assuming flood irrigation method, the average irrigation efficiency of 0.4 was assumed for the area (Narayanamoorthy, 2006). The ArcSWAT clubbed with the water balance model was calibrated using the observed stream flow data and the results are presented in the following section.

Results and discussions

Sensitivity analysis and calibration

ArcSWAT was calibrated for the catchment using the monthly values of observed stream flow. The period 1992-1999 was selected as the calibration period. In the first step, parameter sensitivity analysis was performed for the 14 flow and groundwater parameters, by using the LH-OAT method. From the sensitivity analysis, the deep aquifer recharge (RCHRG_DP) was identified as the most sensitive parameter followed by the plant uptake compensation factor (EPCO) and the curve number (CN2).

Further, the sensitive parameters were manually calibrated. Various indices used for the manual calibration were the correlation coefficient, root mean square error (RMSE), normalized mean square error (NMSE), and Nash-Sutcliffe efficiency (NSE). In addition, the qualitative information about the groundwater table depletion was also used to calibrate the model parameters. The set of calibrated parameters and the best values are shown in Table 1.

Table 1. List of parameters, sensitivity rank, calibrated values and uncertainty range of the SWAT parameters for the study area

Rank	Parameter description	Calibrated value	Range for good simulations	% Range
1	Deep aquifer percolation coefficient (RCHRG_DP)	0.01-0.8	0 – 0.8216	82.16
2	Plant uptake compensation factor (EPCO)	1	0 – 0.888	88.82
3	Curve number (CN2)	CN2-20 to CN2+5	CN2-20 to CN2+24*	89.72
4	Baseflow recession coefficient (ALPHA_BF)	0.01	0.01-0.9	91.05
5	Saturated hydraulic conductivity of soil (SOL_K)	2.19-4.86	-23.6 to 22.5 (%)*	92.31
6	Delay time for aquifer recharge (GW_delay)	31	0 – 46.34	92.67
7	Channel hydraulic conductivity (CH_K2)	5.0	0 - 4.75	95.02
8	Manning's roughness coefficient for the channel (CH_N2)	0.03	0 – 0.029	97.51
9	Threshold water level in the shallow aquifer for baseflow (GWQMN)	Default value	0 – 979.2	97.93
10	Available water capacity of soil (SOL_AWC)	0-3 times the observed values	-24.9 to 24.3(%)*	98.60
11	Revaporation coefficient (GW_revap)	0.2-0.5	0 – 0.495	99.06
12	Surface runoff lag coefficient (SURLAG)	4	0.056 – 9.98	99.21
13	Threshold water level in the shallow aquifer for revaporation (REVAPMN)	Default values	0 – 99.43	99.43
14	Soil evaporation compensation factor (ESCO)	0.1	0 – 0.9951	99.51

* Parameter changes are with respect to the calibrated values

The statistical evaluation indices for the calibration period are given in Table 2. The model performance was found to be satisfactory in terms of the monthly stream flow data. The model was then validated for the period 2000-2003. Values of the model evaluation indices for the validation period are given in Table 2. The model performance was found to be satisfactory for the validation period as well.

Table 2. Model performance indices for the Malaprabha catchment

Statistical index	Correlation coefficient	RMSE	NMSE	NSE
Calibration period	0.963	41.34 (M.cu.m)	0.074	0.925
Validation period	0.961	18.10 (M.cu.m)	0.075	0.923

Parameter Uncertainty Analysis

Parameter uncertainty analysis was carried out using the ParaSol method inbuilt in ArcSWAT. The set of 14 parameters related to the stream flow and groundwater were considered for the analysis. Details of the parameters and the range for the good simulations are given in Table 1. For most of the selected parameters, the good simulation covers more than 90% of the feasible range.

Groundwater scenario of the catchment

The irrigation requirement and the deep aquifer recharge from the calibrated model were used in the water balance model and the change in the water table depths at each sub-basin was calculated for the calibration period. Change in the groundwater table depth obtained for the calibration period for each sub-basin is shown in Fig 3. The numbers shows the sub-basin index and the values in the bracket shows the corresponding changes in the groundwater table. Negative values indicate groundwater table depletion. In the upper catchment, variation in the deep aquifer water level was either nil or very small. This upper part, with high rainfall rate, is the main recharge area in the catchment. Also much of the area is forest land and hence irrigation is negligible. On the other hand the semi-arid lower catchment was found to have very high water table depletion.

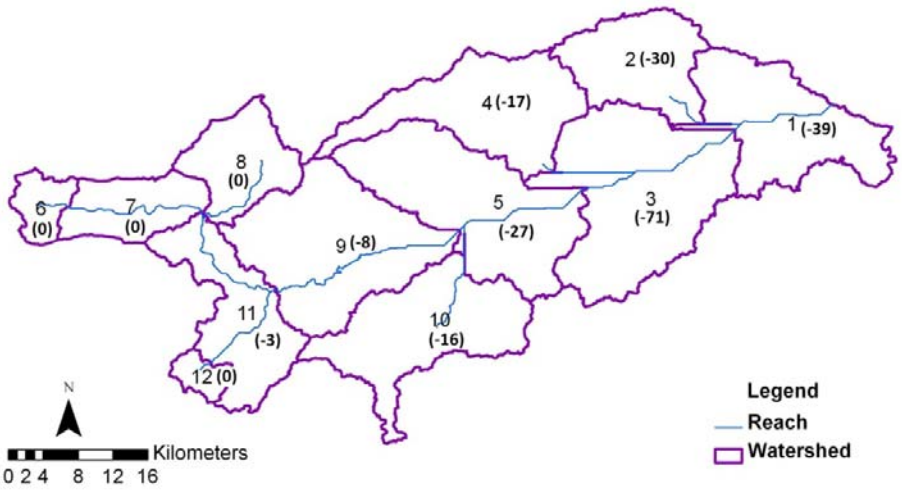

Fig 3. Change in the groundwater table at various sub-basins in the Malaprabha catchment

Field-based information shows 10-15m depletion in the water table depth in sub-basin 9 during the calibration period, which is very well matching with the simulated 14m depletion. The 63m depletion in sub-basin 3 simulated by the model is also in the close range of 70m reported in the field. In sub-basin 5, the model result shows water table depletion of the order of 23 m during the calibration period. Field information shows that the actual depletion exceeds the simulated values. In some villages 20-40m depletion was reported. In sub-basin 4, simulation result shows 14m depletion in the groundwater table, whereas the field reports show around 25m depletion.

The water balance model considers only the recharge and groundwater extraction components, ignoring the lateral movement of groundwater from the upper reaches to the lower reaches. Omission of this groundwater re-distribution component may introduce some error in the water table simulation.

Conclusions

ArcSWAT was used to study the impact of excessive water extraction for irrigation on the groundwater resources. A water balance model was clubbed with the ArcSWAT to overcome the limitation on the maximum initial storage in the deep aquifer. The model was applied to the Malaprabha catchment in India and the model parameters were calibrated with respect to the observed monthly stream flow data and the qualitative information about the groundwater table depletion in the area. The model was found to be giving very good estimate of the

stream flow. The groundwater table simulation shows that in the semi-arid parts of the catchment, due to the excessive groundwater extraction, the water table has been depleted 30-40m, and in some areas around 70m. In the upper parts of the catchment, no such serious water table depletion was observed from the ArcSWAT simulation. The model is helpful to get a general picture of the groundwater scenario in the area.

Acknowledgement

The authors gratefully acknowledge the Department of Science and Technology, Government of India for providing the financial support for this research project under the SERC Fast Track Fellowship Scheme. The authors also acknowledge METI and NASA for providing the ASTER GDEM data used for this study.

References

Arnold, J.G., P. M. Allen, G. Bernhardt. 1993. A comprehensive surface-groundwater flow model. *J. Hydrol*. 142: 47–69.

Kim, N. M., I. M. Chung, Y. S. Won, J. G. Arnold. 2008. Development and application of the integrated SWAT-MODFLOW model. *J.Hydrol.* 356(1-2): 1-16.

Narayanamoorthy, A. 2006. Potential for drip and sprinkler irrigation in India. Draft, IWMI-CPWF Project on Strategic Analysis of India's National River Linking Project, International Water Management Institute, Colombo, Sri Lanka.(URL: http://nrlp.iwmi.org/PDocs/ DReports/Phase_01/12.%20Water%20Savings%20Technologies%20-%20Narayanmoorthy.pdf)

R&D Advisory Committee on Groundwater Estimation. 2009. Status report on review of groundwater resources estimation methodology. Central Ground Water Board, Faridabad.

Reshmi, T.V., A. B. Christiansen, S. Badiger, D. N. Barton. 2008. Hydrology and water allocation: comprehensive database and integrated hydro economic model for selected water services in the Malaprabha River Basin. Report SNO 5695-2008, Norwegian Institute for Water Research, Oslo, Norway.

Sophocleous, M. A., J. K. Koelliker, R. S. Govindaraju, T. Birdie, S. R. Ramireddygari, S. P. Perkins. 1999. Integrated numerical modeling for basin-wide water management: The case of the Rattlesnake Creek Basin in south-central Kansas. *J.Hydol.* 214(1-4): 179-196.

Van Griensven, A. 2005. Sensitivity, auto-calibration, uncertainty and model evaluation in SWAT2005. Unpublished report.

Van Griensven, A., T. Meixner. 2006. Methods to quantify and identify the sources of uncertainty for river basin water quality models. *Water Science and Technology*, 53(1): 51-59.

Williams, J. R., A. D. Nicks, J. G. Arnold. 1985. SWRRB, Simulator for water resources in rural basins. *J. Hydrol. Eng*. ASCE 111 (6): 970–986.

Winchell, M., R. Srinivasan, M. Di Luzio, J. Arnold, J. 2007. ArcSWAT Interface for SWAT2005: User's Guide. Blackland Research Center, Texas Agricultural Experiment Station, Texas and Grassland, Soil and Water Research Laboratory, USDA Agricultural Research Service, Texas.

Analysis of Major Parameters in a Tropical Climate Watershed Case Study: Tabma Sub-basin, Thailand

Orachorn Kamnoet
Environmental Technology Division, The Joint Graduate School of Energy and Environment, King Mongkut's University of Technology Thonburi, Bangkok, Thailand 10140
E-mail address: orchorn.kam@kmutt.ac.th

Chaiyuth Chinnarasri*
Water Resources Engineering & Management Research Center (WAREE), Department of Civil Engineering,
King Mongkut's University of Technology Thonburi, Bangkok, Thailand 10140
*Corresponding Author, E-mail address: chaiyuth.chi@kmutt.ac.th

Abstract

Parameter analysis is an important process in the application of distributed hydrological models. This paper investigates and discusses the analysis method in a SWAT model for a tropical climate, the Tabma sub-basin in Rayong province, Thailand. Thematic maps used for the model are a digital elevation model (DEM), a soil series map, a land-use map, and the drainage network. The data for the calibration and verification processes are from the periods between 2001-2002 and 2003, respectively. Good agreement between the observed and simulated discharge, which was expressed by the Nash-Sutcliffe efficiency (Nash), was found. The most sensitive parameters were: the soil evaporation compensation factor (ESCO), the initial SCS Curve Number II value (CN2), the base flow alpha factor (Alpha BF), saturated hydraulic conductivity in the main alluvium (Sol K), and the available water capacity (Sol AWC).

Keywords: SWAT model, Calibration and Parameters, Sensitivity Analysis.

Introduction

Thailand has a warm, tropical climate affected by an annual monsoon, with a rainy season from June to October and a dry season the rest of the year. Temperatures average 75 to 92 degrees Fahrenheit, with the highest temperatures from March to May and the lowest in December and January. There are three seasons: the cool season (November to February), the hot season (April to May), and the rainy season (June to October), though downpours rarely last more than a couple of hours (FAO, 1997).

In 2005, there were drought problems in Rayong province. These problems caused major difficulties for the industrial sector, which had to be supplied with water from outside the province. The effects of the situation led to social conflict, showing the high priority of water resource management for domestic use, agriculture and industry. Drought problems are caused by rainfall uncertainty, increasing water usage in every section, upstream storage, and the lack of a storage system. In general, the main water storing and transferring systems are reservoirs and rivers, which are inflexible in coping with uncertainty. Therefore, a flexible method is needed to allow a water storage system that can decrease the drought and flood risk.

Parameter analysis is a kind of model response resulting from research on parameter changes, and it is an important method to conduct uncertainty analysis of model parameters. Model sensitivity analysis has been regarded as an effective filtration tool to confirm key

model control parameters at all times (Jia et al., 2005). Sensitivity analysis aims to decrease the number of parameters that need to be adjusted during the period of parameter calibration (Xia et al., 2005), and the parameters that are identified in a given basin have a great influence on simulation precision. Meanwhile, sensitivity analysis can contribute to understanding the model structure or even finding structural defects in the model, and thus the model structure may be improved (Xia et al., 2003). At present, many researchers are applying all kinds of sensitivity analysis methods to different distributed hydrological models (Jia et al., 2005).

An understanding of the relationship between hydrological processes, physical characteristics such as land use and soil, and climate change is important for designing watershed management. At this point, the aim of this research is to investigate the hydrological processes interacting with the physical characteristics. The area covered by this study is the Tabma sub-basin (Fig. 1), which is located in Rayong province. The majority of water demand in Thailand is for use in agriculture; however, Rayong is an area where water is used also for industrial development.

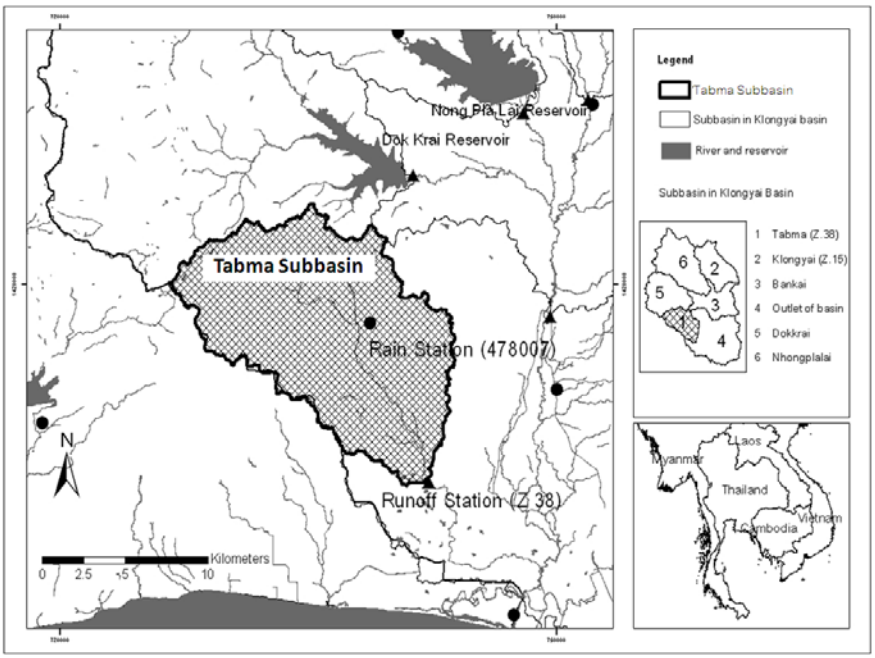

Figure 1 Tabma sub-basin with rain and runoff stations.

Methodology

The Soil Water Assessment Tool (SWAT) is a physically based continuous event hydrologic model developed to predict the impact of land management practices on water, sediment, and agricultural chemical yields in large, complex watersheds with varying soils, land use, and management conditions over long periods of time. The SWAT model is a watershed scale, continuous, long-term, distributed model designed to predict the impact of land management practices on the hydrology, sediment and contaminant transport in agricultural watersheds (Arnold *et al*., 1998). The SWAT subdivides a watershed into different sub-basins connected by a stream network and, further, into hydrological response units (HRUs) to describe spatial heterogeneity in terms of land cover, soil type and slope within a watershed. SUFI-2 (Abbaspour *et al.*, 2004) was used for calibration and uncertainty analysis. The main data

requirements are DEM, weather data, land use data, and soil data. For the calibration of the model, measured river discharge data from a specific river gauge station is needed.

Data Integration

The Digital Elevation Model (DEM) analysis is of equal importance to the rainfall–runoff model, as it constitutes one of the initial stages of the modelling process. In the process of inputting data, use of DEM is important to simulate the physical area in Klongyai Basin. The resolution of the DEM is 90 meters in 2001 from SRTM (Shuttle Radar Topography Mission) (SRTM, 2010) data. Klongyai Basin is an area of Rayong and Chonburi province, located on the east coast of Thailand on the northern shoreline of the Gulf of Thailand.

Land use is an important factor which induces the different hydrologic watershed systems for each area (Heuvelmans *et al.*, 2005). Land use affects the quantity of the surface water lost due to confinement on the surface, and evaporation emission. However, the base flow increases relatively (Fohrer *et al.*, 2001). The increasing change of land use for agriculture influences the quantity of the surface water raised (Lenhart *et al.*, 2003). Land use in 2001 is divided into nine main classifications: crop, para rubber, forest, pineapple, sugarcane, urban, water, cassava and rangeland. The two main land uses are crops (600 km^2) and cassava (580 km^2). Others are para rubber (240 km^2), forest (120 km^2), and pineapple (105 km^2). Especially, the main land uses area in Tabma sub-basin are pineapple (23 km^2), para rubber (24 km^2) and cassava (20 km^2).

Soil series are managed according to the main classification of the related sub-basin which is generated by the model from spatial data. These are Muak Lek (Ml), Don Rai (Dr), Tha Yang (Ty), Chok Chai (Ci), Ban Chong (Bg), Lat Ya (Ly), and Ban Bung (Bbg). Each soil series also shows information about available drainage and percolation.

Historical hydrological data is assessed by the use of rain trend analysis, as shown in Fig. 2, which compares rainfall of station 478007 and runoff of Z.38 Tabma. The discharge data at station Z.38 (Ban Kao Boat) is also shown in Fig. 2. These data were collected by the Royal Irrigation Department (RID) and the Thai Meteorological Department (TMD).

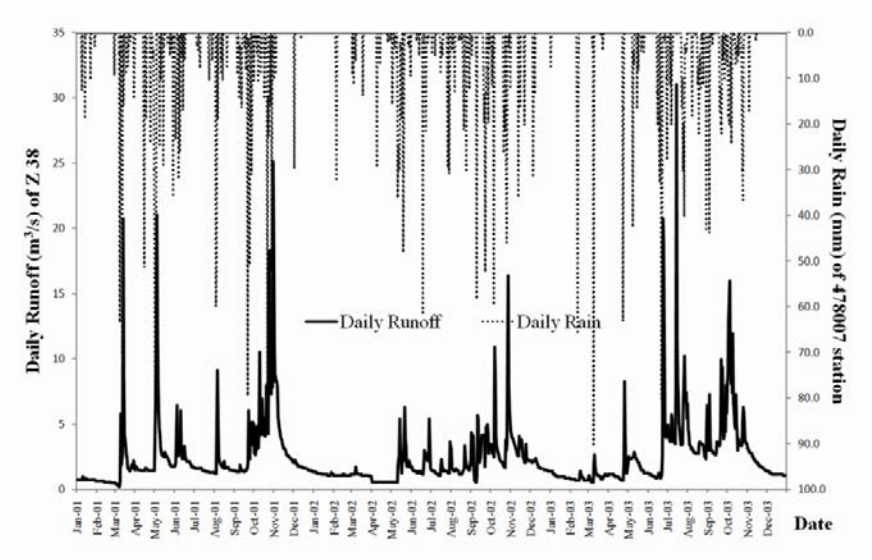

Figure 2 Rain and runoff of Tabma sub-basin (Z 38) in 2001-2003.

Optimization Tools

Optimization tools are useful to identify the best solution. They do not provide information on the uncertainty of parameters and model outputs. Experience has led to the insight that several parameter combinations could give equally good results and has led some to doubt about the concept of an optimal solution and their parameter sets (Beven & Binley, 1992; Beven & Young, 2003). The uncertainty analysis divides the simulations that have been performed by the optimization into "good" and "not good" simulations (Beven & Binley, 1992).

The uncertainty method is efficient in optimizing a model and providing parameter uncertainty estimates without being based on assumptions about prior parameter distributions for the sampling strategy. It is based on statistical techniques to define an objective, statistically based, threshold that is used to subdivide simulations into "good" and "bad" subsets. More specifically, the uncertainty in the model parameters is due to insufficient observed data to identify the free parameters. Other sources of uncertainty include errors in forcing input data (rainfall, temperature, etc.), spatial data errors (GIS data), and model structure (spatial scaling, mathematical equations).

Sensitivity analysis of model parameters provided the main guidelines for the selection of the parameters to be estimated. Of course, there are several parameters that are, undoubtedly, very important for the results, and the sensitivity analysis has only confirmed their importance (Milivojević *et al.*, 2009). Therefore, one of the necessary phases in model calibration and preparation for use is the sensitivity analysis. Sensitivity analysis is a process used to determine the way the results change depending on changes in the model parameters, while inputs and simulation conditions are kept unchanged. Sensitivity analysis is the only reliable way to determine key parameters and the required accuracy of the calibration procedure. Model calibration is a process of parameter estimation performed through continuous comparison of mathematical model results and results of monitoring exercised on the physical model. Finally, model validation is the process of comparison of mathematical model results and monitoring results for a period not used in model calibration. According to Refsgaard (1997), model validation is a process demonstrating the capacity of the subject mathematical model to produce "accurate enough" results relative to the real system.

Simulation

The SWAT simulation methodology consisted of an initial calibration and validation phase followed by a second phase in which the impact of variations in climatic inputs was assessed for the hydrology. The following model options were used for all of the simulations performed in both phases: curve number (CN) method for the partitioning of precipitation between surface runoff and infiltration, Muskingum method for channel routing, and modified Penman-Monteith method for potential evapotranspiration. Manual calibration was conducted to bring the optimized values to better estimated ones that allow the model to represent the real conditions of the area.

Calibration and Validation of the SWAT

The SWAT model was calibrated and validated using measured streamflow data collected at a stream gauge located on the Tabma sub-basin at Klongyai Basin (Station Number Z 38). The total available historical weather data (2001-2003) were divided into two sets: 2 years (2001-2002) for calibration and three years for validation (2003). The watershed characteristics, including land use, soil properties, and anthropogenic effects (e.g.,

agricultural management), were held constant throughout the simulation period. The Root Mean Squared Error (RMSE), Nash-Sutcliffe simulation efficiency (Nash) and Index of Agreement (IA) were used to evaluate the model predictions for both time periods.

Calibration of the water balance and stream flow begins by comparing average annual conditions such as the average annual total base flow, and surface flow. Average annual values are calibrated as the depth of water in millimeters over the drainage area. Once the average annual values are calibrated, the monthly or daily values can be fine-tuned for accuracy.

Model Performance

Nash-Sutcliffe Coefficient (Nash-R^2): In these models, the Nash-Sutcliffe coefficient (Nash and Sutcliffe, 1970) is used as the error criterion to assess the goodness of fit of the flow and head hydrographs. It is used to assess the predictive power of hydrological models, and is defined as

$$\text{Nash} = 1 - \left(\frac{\sum_{i=1}^{n} (Q_{obs} - Q_{sim})^2}{\sum_{i=1}^{n} (Q_{obs} - \overline{Q}_{obs})^2} \right) \tag{1}$$

where Q_{obs} is the observed value, Q_{sim} is the simulated value, and $\overline{Q}_{obs}$ is the mean of observed values. This criterion is always less than unity. A value equal to unity represents a perfect agreement between observed and simulated streamflows.

The Root Mean Squared Error (RMSE): The RMSE is the square root of the squared difference averaging between observed and simulated values. It is a measure of the spread of the observed data. The variance (σ^2) is a measure of the spread of the observed data and RMSE is a measure of the scattering of the simulated values and the departure of the simulated values from the observed values. This method is usually considered to be the best measure of error, if errors are normally distributed. It is defined as

$$\text{RMSE} = \left(\frac{\sum_{i=1}^{N} (Q_{obs} - Q_{sim})^2}{n} \right)^{\frac{1}{2}} \tag{2}$$

where n is the number of days of simulation, Q_{obs} is the observed value, and Q_{sim} is the simulated value. Almost all the parameters of the model need to be calibrated in order to obtain the best fit in flow and head hydrographs. Moreover, the values of these parameters should stay within reasonable limits. For these reasons, the calibration is made step-by-step and only one parameter is calibrated at a time. This is performed in any order and continues until no more improvements are observed.

Index of Agreement (IA) is defined as

$$IA = 1 - \left[\frac{\sum (Q_{obs} - Q_{sim})^2}{\sum \left((Q_{obs} - \bar{Q}) + (Q_{sim} - \bar{Q}) \right)^2} \right] \quad (3)$$

where Q_{obs} is the observed value, Q_{sim} is the simulated value, $\bar{Q}_{obs}$ is the mean of observed values, and $\bar{Q}_{sim}$ is the mean of simulated value. This criterion is always less than unity. A value equal to unity represents a perfect agreement between observed and simulated streamflows.

The Nash (R^2) value is an indicator of the strength of the relationship between the observed and simulated values. The Nash value indicates how well the plot of the observed versus the simulated values fits the 1:1 line. If the R^2 values are close to zero, and the Nash values are less than or close to zero, then the model prediction is unacceptable. If the values equal one, the model predictions are considered perfect.

The selection of parameters for the streamflow calibration and the final calibrated values of those parameters were based on guidelines given in Neitsch *et al.* (2002b) and on previous SWAT streamflow calibration results reported by Santhi *et al.* (2001) and Jha *et al.* (2003). Detailed descriptions of each of the calibration parameters are provided in Neitsch *et al.* (2002a). The parameters were then allowed to vary during the calibration process within suggested ranges across the basin until an acceptable fit between the measured and simulated values was obtained at the watershed outlet. No changes were made to the calibrated parameters during the three years validation simulation.

Results and Discussion

In this process, calibration of the model involves calibrating the parameters to closely match the real spatial data. The observed and simulated data for 2001-2002 are compared to assess the probability of calibration in this model. Validation of the model requires comparison of the model results with an independent data set, without further adjustment. The observed and simulated data in 2003 are compared to assess the probability of the validation of this model.

The model uses one discharge station, Z.38. This was calibrated and validated using the statistical accuracy method, RMSE, Nash (Nash and Sutcliffe, 1970) and the IA (Index of Agreement). These are shown in Fig. 3.

In the calibration process, for comparing the theoretical model values with the measurements, the mean bias and the root mean square error were used and the values of RMSE = 1.493 m^3/s, IA=0.893 and Nash = 0.651 were obtained. In the validation process, the values of RMSE = 2.241 m^3/s, IA=0.803 and Nash = 0.312 were obtained.

In this study, the relative sensitivity values found in the parameter estimation processes were evaluated. Six parameters were found to be sensitive using the relative sensitivity values ranges. Among these, the most sensitive parameters were: soil evaporation compensation factor (ESCO), initial SCS Curve Number II value (CN2), base flow alpha factor (ALPHA_BF) [days], and available water capacity (SOL_AWC). The most sensitive sediment parameters in the Tabma sub-basin are the channel cover factor, the USLE equation support practice factor, the exponent parameter for calculating sediment in channel sediment routing and the minimum value of USLEC factor for land cover/plant. The comparison between the observed and simulated stream flow indicated that there is good agreement between the observed and simulated discharge, which was verified by the coefficient of determination (R^2) and Nash Sutcliffe efficiency (NSE) greater than 0.5.

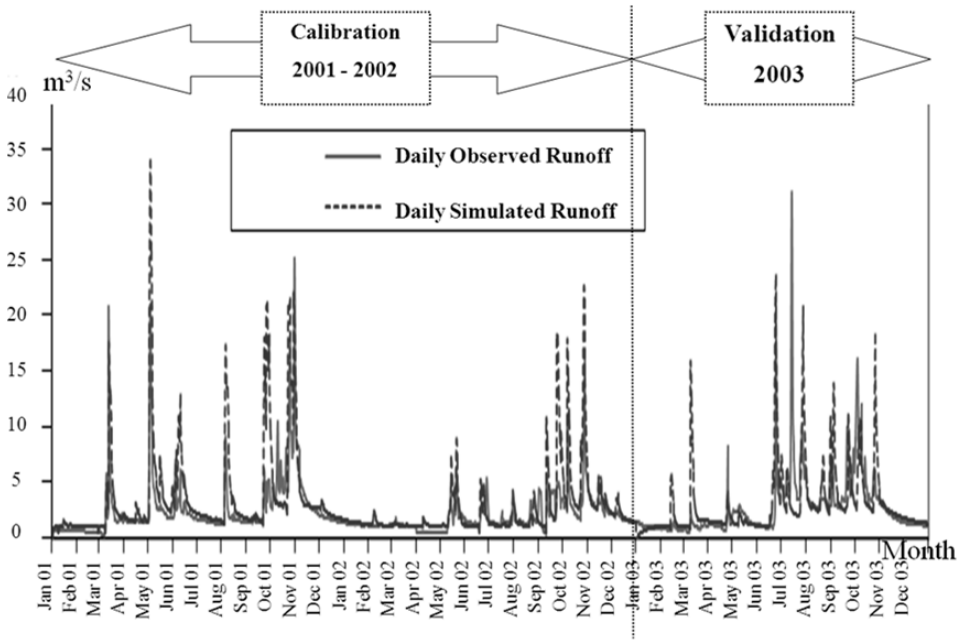

Figure 3 Comparison of observed and simulated data of station Z.38.

The more highly ranked parameters show that the ranking depends on the variable, the location, on the case. However, some generalizations can be made, such as the overall importance of curve number (CN2) and the importance of the groundwater parameter ALPHA_BF. The flow calculations during these low flow periods depend on the groundwater contribution, which in turn depends strongly on the parameter 'ALPHA_BF'. Other generally important parameters for many criteria are the soil water capacity SOL_AWC.

Conclusions

For a small tropical watershed such as Tabma sub-basin, it is found that the most sensitive parameters are: soil evaporation compensation factor (ESCO), initial SCS Curve Number II value (CN2), base flow alpha factor (ALPHA_BF) [days], and available water capacity (SOL_AWC). To develop water resources management, it is a need to investigate the hydrological processes interacting with the physical characteristics and climate change in this watershed.

Acknowledgement

The authors would like to thank the Joint Graduate School of Energy and Environment (JGSEE) and Earth System Sciences Center (ESS) for their financial support for this study.

References

Abbaspour, K.C., Johnson, A., & van Genuchten, M.T. (2004). Estimating uncertain flow and transport parameters using a sequential uncertainty fitting procedure. *Vadose Zone Journal,* 3(4), 1340-1352.

Arnold, J. G., Srinivasan, R., Muttiah, R. S., & Williams, J. R. (1998). Large area hydrologic modelling and assessment, Part 1: model development. *Journal of the American Water Resource Association,* 34(1): 73-89.

Beven, K., & Binley, A. (1992). The future of distributed models: model calibration and uncertainty prediction. *Hydrological Processes,* 6: 279–298.

Beven, K., & Young, P. (2003). Comment on "Bayesian recursive parameter estimation for hydrologic models" by M. Thiemann, M. Torsset, H. Gupta, & S. Sorooshian. *Water Resources Research,* 39 (5), COM1-1–COM1-4.

FAO (1997). *State of the World's Forests*. Food and Agriculture Organization of the United Nations, UK: Oxford.

Heuvelmans, G., Muys, B., & Feyen, J. (2005). Regionalisation of the parameters of a hydrological model: Comparison of linear regression models with artificial neural nets. *Journal of Hydrology,* 357(3-4): 188-206.

Jha, M., Pan, Z., Takle, E. S., & Gu, R. (2004). Impacts of climate change on streamflow in the Upper Mississippi River Basin: A regional climate model perspective. *Journal of Geophysical Research,* 109(D9):D09105, doi: 10.1029/2003JD003686.

Jia, Y.-W., Wang, H., Wang J.-H., Luo, X.-Y., Zhou, Z.-H., Yan, D.-H, & Qin, D.-Y. (2005). Development and verification of distributed hydrological model of Yellow River Basin. *Journal of Natural Resources,* 20(2): 300-308.

Lenhart, T., Fohrer, N., & Frede, H. G. (2003). Effects of land use changes on the nutrient balance in mesoscale catchments. *Physics and Chemistry of the Earth,* 28*:* 1301-1309.

Milivojević, N., Simić, Z., Orlić, A., Milivojević, V., and Stojanović, B. (2009). Parameter estimation and validation of the pProposed SWAT based rainfall-runoff model – methods and outcomes. *Journal of the Serbian Society for Computational Mechanics,* 3(1): 86-110.

Nash, J. E., & Sutcliffe, J. V. (1970). River flow forecasting through conceptual models. *Journal of Hydrology,* 10: 282–290.

Neitsch, S.L., Arnold, J. G., Kiniry, J. R., Williams, J. R., & King, K.W. (2002a). *Soil and Water Assessment Tool Theoretical Documentation, Version 2000*. Blackland Research Center, Texas Agricultural Experiment Station, Temple, Texas. Available at http://www.brc.tamus.edu/swat/downloads/doc/swat2000theory.pdf. Accessed in June 2011.

Neitsch, S.L., Arnold, J.G., Kiniry, J. R., Srinivasan, R., & Williams, J. R. (2002b). *Soil and Water Assessment Tool User's Manual, Version 2000*. Blackland Research Center, Texas Agricultural Experiment Station, Temple, Texas. Available at http://www.brc.tamus.edu/swat/downloads/doc/swatuserman.pdf. Accessed in June 2011.

Refsgaard, J. C. (1997). Parametrisation, calibration and validation of distributed hydrological models. *Journal of Hydrology,* 198: 69-97.

SRTM (2010). SRTM 90m Digital Elevation Database v4.1. Available at http://www.cgiar-csi.org/data/elevation/item/45-srtm-90m-digital-elevation-database-v41. Accessed in Nov 2010.

van Griensven, A., Meixner, T., Grunwald, S., Bishop, T., & Srinivasan, R. (2006). A global sensitivity analysis method for the parameters of multi-variable watershed models. *Journal of Hydrology,* 324(1–4): 10–23.

Xia, J., Ye, A.-Z., & Wang, G.-S. (2005). Distributed time-variant gain hydrological model of Yellow River Basin (I) —principle and structure of the model. *Journal of Wuhan University (engineering),* 38(6): 10-15.

Xia, J., Wang, G.-S., Lu, A.-F., & Tan, G. (2003). Hydrological circulation simulation in distributed time-variant gain basin. *Journal of Geographical Science,* 58(5): 789-796.

Parallelizing SWAT Calibration in Windows using SUFI2 Program

Elham Rouholahnejad*
Eawag, Swiss Federal Institute of Aquatic Science and Technology,
Ueberlandstrasse 133, CH-8600 Duebendorf, Switzerland
elham.rouholahnejad@eawag.ch

Karim Abbaspour
Eawag, Swiss Federal Institute of Aquatic Science and Technology,
Ueberlandstrasse 133, CH-8600 Duebendorf, Switzerland

Mahdi Vejdani
Neprash Technology, 1625 Sundew Pl, Coquitlam, B.C., V3E 2Y4, Canada

Raghavan Srinivasan
Texas A&M University, Texas Agricultural Experimental Station, Spatial Science Lab,
College Station, TX 77845, USA

Abstract

To conduct a large scale hydrological model at high special and temporal resolution, a calibration algorithm was revised utilizing cluster parallel computing. In large-scale hydrologic models time is often a major impediment in the calibration and application of the hydrological models. To overcome this, most projects are run either with a simplified model or by running the models fewer times, resulting in less-than-optimum solutions. In this paper we explain a methodology where a parallel processing scheme is constructed to work in the Windows platform. We have parallelized the calibration of the SWAT (Soil and Water Assessment Tool) hydrological model, where one could submit many simultaneous jobs taking advantage of the capabilities of modern PC and laptops. This offers a powerful alternative to the use of grid or cloud computing. Parallel processing is implemented in SWAT-CUP (SWAT Calibration and Uncertainty Procedures) using the optimization program SUFI2 (Sequential Uncertainty FItting ver. 2). We tested the program with large, medium, and small-size hydrologic models on several computer systems, including PCs, laptops, and servers with up to 24 CPUs. The performance was judged by calculating speedup, efficiency, and CPU usage. In each case, the parallelized version performed much faster than the non-parallelized version, resulting in substantial time saving in model calibration. The results of this study also show that it is feasible to calibrate a large scale hydrological model at high resolution within a reasonable time without demanding significant computing resources.

Keywords: Parallel processing, SWAT-CUP, SUFI2, Hydrologic models

Introduction

The execution time of large hydrological models has always been a major concern, not allowing proper model calibration and uncertainty analysis. For this reason, in the last few years, the use of distributed computing in the form of grid and cloud computing has become increasingly prevalent. In the present study a parallel processing scheme (PPS) was developed to utilize the existing capabilities of the available Windows systems. The PPS works within the SWAT-CUP software package and couples SUFI2 (Abbaspour et al., 2004; 2007) optimization algorithm with SWAT (Arnold et al., 1998). The scheme is ideal for performing hydrologic model calibration and uncertainty analysis. The main advantage of the system we have developed is improving the computational capacity of calibration processes with readily accessible computer recourses without the need for grid or cloud computing. However, for very large models, a powerful computer (e.g., 24-48 CPUs with >24 GB RAM) is needed to take full advantage of parallel processing. With the advancement of new technologies, this is now available at a reasonable cost.

The objective of this paper is to describe the coupling of the PPS with SWAT and to show its operation on different machines. The PPS includes job partitioning and job management, distributed data storage techniques and data exchange among the jobs. We compare the computation time of parallel SUFI2 by applying it to a small, a medium, and a large size SWAT project using different computer systems. The efficiency of the performance of the parallelized algorithm was evaluated by comparing the performance on different multi core machines. This study aims at investigating parallel processing issues rather than performing a meaningful calibration task.

Materials and Methods

SUFI2 Calibration algorithm

In Figure 1 a schematic diagram of the coupling between SUFI2 and SWAT is illustrated. Initially, a Latin hypercube (McKay et al., 1979) procedure draws samples from the spaces defined by user-supplied parameter ranges. The parameter sets thus sampled are independent and for this reason parallel runs could be executed. Theoretically, all samples could be run at once, hence an entire iteration would require only the time that it takes to make one model run. After pre-processing phase, the program copies a set of sampled parameters in their appropriate locations in the SWAT input files. Next, the SWAT model is executed, and the outputs of interest are extracted from SWAT output files (*output.rch*, *output.hru*, *output.sub*). Then post-processing begins with the objective function calculation. Seven different functions including summation and multiplicative forms of mean square error, r^2, Chi square, Nash-Sutcliffe, weighted r^2, and ranked sum of square error aimed at fitting the frequency distributions, are implemented in SUFI2. The use of a "multi-objective" formulation (Duan et al. 2003; Gupta et al., 1998) where different variables are included in the objective function is also included in SWAT-CUP.

Next step is the calculation of the 95% prediction uncertainty. SUFI2 describes parameter uncertainty by means of a multivariate uniform distribution in a parameter hypercube, while the output uncertainty is quantified by the 95% prediction uncertainty band (95PPU). SUFI2 maps all uncertainties on the parameters in the hydrological model. This is achieved when all measurements are bracketed by the 95PPU. Objective of the calibration process thus becomes to bracket most of the data within the 95PPU while minimizing the thickness of the uncertainty band (Fig. 2) (Abbaspour et al., 2007).

After each iteration, the parameters are updated and a subsequent iteration is performed. We assume that all parameters are uniformly distributed within a region bounded by minimum and maximum values. Updated parameters are then calculated as:

$$b'_{j,\min} = b_{j,\text{lower}} - \text{Max}\left(\frac{(b_{j,\text{lower}} - b_{j,\min})}{2}, \frac{(b_{j,\max} - b_{j,\text{upper}})}{2}\right) \quad j = 1,\ldots, p \qquad (1)$$

$$b'_{j,\max} = b_{j,\text{upper}} + \text{Max}\left(\frac{(b_{j,\text{lower}} - b_{j,\min})}{2}, \frac{(b_{j,\max} - b_{j,\text{upper}})}{2}\right) \quad j = 1,\ldots, p \qquad (2)$$

where b' indicate updated values, $b_{j,\text{lower}}$ and $b_{j,\text{upper}}$ are calculated using the best parameter values of the current iteration as well as the confidence intervals around them, $b_{j,\min}$, and $b_{j,\max}$ are the absolute parameter ranges, and p is the number of parameters. The formulation, while producing narrower parameter ranges for the subsequent iteration ensure that the updated parameter ranges are centered on the best estimates of the current iteration.

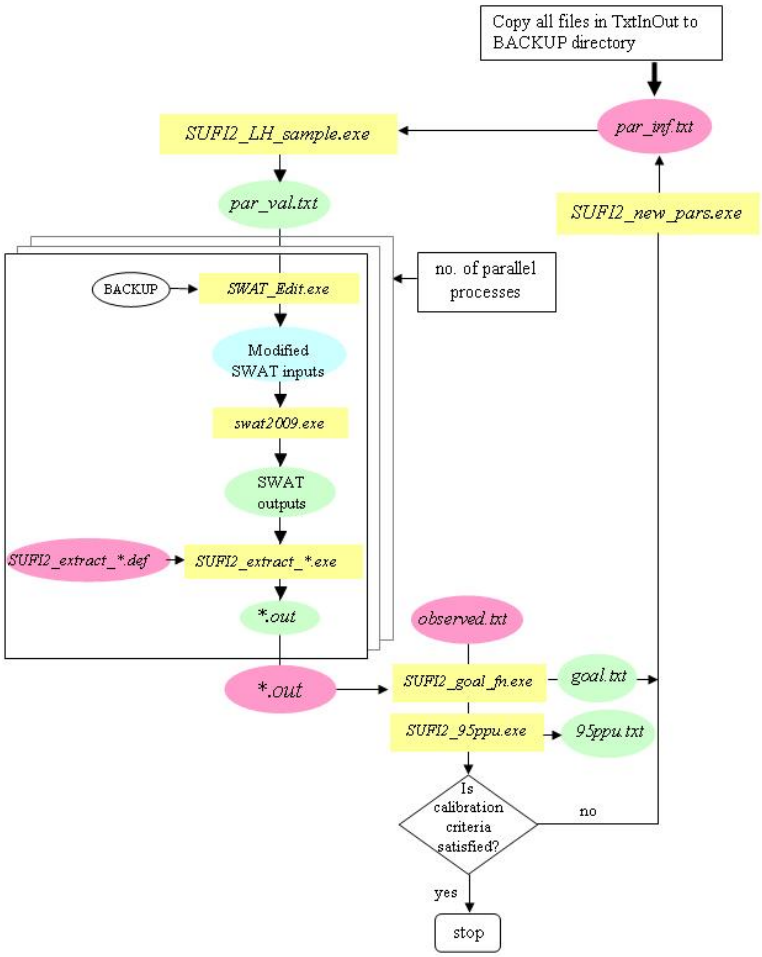

Figure 1. Schematic coupling of SWAT, and SUFI2. The symbol * stands for rch, hru, and sub files.

The process repeats until a satisfactory goodness of fit is obtained, which will be assessed by two measures referred to as the *P-factor* and the *R-factor* (Abbaspour et al., 2004, 2007). The *P-factor* is the percentage of the measured data bracketed by the 95PPU. This index provides a measure of the model's ability to capture uncertainties. The *R-factor,* on the other hand, is a

measure of the quality of calibration and indicates the thickness of the 95PPU. It is calculated as the average distance between the upper and the lower 95PPU divided by the standard deviation of the observed data. The goodness of calibration and prediction uncertainty is judged on the basis of the closeness of the *P-factor* to 1 (i.e., all observations bracketed by the prediction uncertainty) and the *R-factor* to 0 (i.e., measured and simulated values coinciding). The combination of these two indices together indicates the strength of model calibration and uncertainty assessment as these are intimately linked.

Parallelization approach and implementation

The structure of parallel SUFI2 is also schematically shown in Figure 1. The program initially calculates the number of parallel processes that can be submitted to a system by optimizing the number of CPUs against the required RAM to run a project. All attempts were made to speed up the runs while using less memory by changing the SUFI2 algorithm, primarily in the following areas:

- Changes in parameter updating program so that it caches the SWAT input files as a BACKUP where the initial value of the parameters are kept static. The number of SWAT input files can vary from tens to hundreds of thousands depending on the project, but each file is only a few KB in size. We took advantage of this and changed the program so that it loads a number of input files on the system's RAM, makes the necessary changes using the cached BACKUP files, make the relative changes and writes them to the hard disc. Then it deletes them from the RAM to load the next set of files. In this way, we avoid copying the BACK UP to the number of parallel jobs. This reduces memory usage by up to 90%.

- SWAT-CUP functions were split to apply simultaneously on several nodes or parallel jobs. The number of nodes can be the same or fewer than the number of CPUs. Depending on the project size and the available RAM, the program calculates the maximum number of jobs that can be submitted to the system. The parallel processing program does not allow the number of nodes to exceed a certain limit if there is a lack of memory. Hence, having a large system RAM (≥ 24 GB) is an advantage.

- The changes in the SWAT-CUP package include: a) changes in user interface to make the parallel option available to users, b) showing the status of each parallel node while the program is running, c) preventing system freezing by giving priorities to other jobs being simultaneously executed, and d) disallowing SWAT-CUP sub-processes to continue running in the background when the program is stopped for any reason.

After finishing the program set up which includes collecting and deleting unused files, calculation of the utmost possible parallel runs and caching files from the BACKUP, the simulations are divided between different processors.

When the parallel runs are finished, parallel processing clean up starts to work by collecting output files from each parallel processing directory and concatenating them in the SUFI2.OUT of the main project directories. Then all unused files are deleted, and the RAM which was used during the parallel process, including the RAM which was used by caching the BACKUP files are released. Now all is done with the parallel section. The rest is post processing, which is done in the same way as the single calibration run by calculating objective function and measures of goodness.

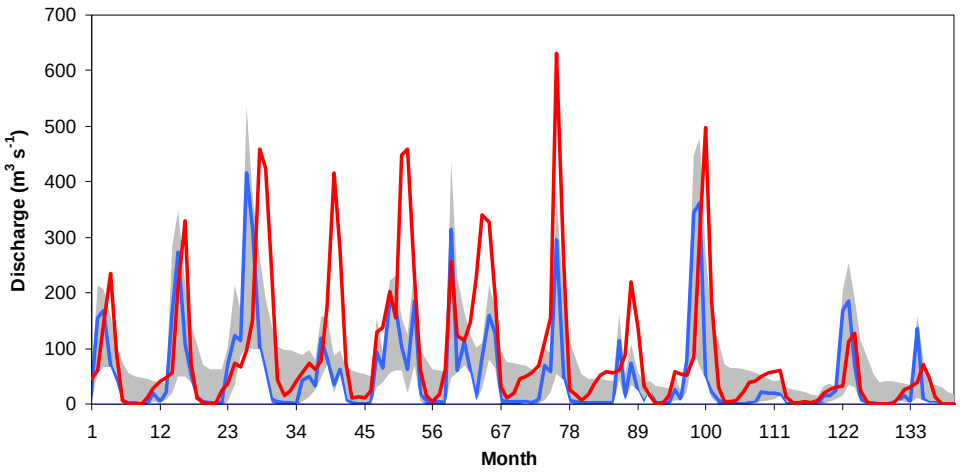

Figure 2. The 95PPU graph in the SWAT-CUP interface. Also shown are the observed signal and the best simulation. The 95PPU is given for every variable considered in the objective function.

Application sites, computer systems and performance measures

Three hydrological models were tested on six different systems to evaluate the functionality of parallel SUFI2. Table 1 has a summary of the attributes of one server, three personal computers, and two laptops used in the study. Three large, medium and small hydrological models were built using the SWAT2009 program over a period of 5 years. The large-size project is the Danube River Basin hydrological model with an area of 801,093 km^2. Danube is Europe's second longest river, flows for a distance of 2,826 km and enters the Black Sea. Using SWAT the Danube basin was divided into 1,224 smaller subbasins taking into account elevation, soil, land use and climatic information. This resulted in 69,875 Hydrological Response Units (HRU) with the unique soil, land use and slop characteristics. Running the calibration program SUFI2, 48 simulations took approximately 2 days to run on the server without using the parallel option. The medium-size project is the Alberta project that covers an area of 661,185 km^2. The region is divided into 938 subbasins resulted in producing 2,689 HRUs. The small-size project is a test example in the SWAT program with only 4 subbasins and 75 Hrus. It should be mentioned that calibration of the hydrological models is not the focus of this study and we only tried to focus on the speed of the calibration process.

We used the two commonly used performance measures to evaluate the parallel computation functionality: *speedup* and *efficiency* (Houstis et al., 1997, Mateos et al., 2010). Speedup for *n* parallel sessions is defined as the computed time of the task when only one processor is used to the computing time when *n* processors are used. The efficiency of a parallel system of *n* processor is defined as the ratio of actual speedup to ideal speedup, where the ideal speed up is equal to the number of processors.

Table 1. Description of the 6 computer systems used to test the parallel Sufi2.

Server 1	**PC 1**
24 CPUs, RAM = 24.0 GB Processors: Intel(R) Xeon(R) CPU L5640@2.27GHz (2 processor) System type = 64-bit OS Windows 7	8 CPUs, RAM = 16.0 GB Process: Intel(R) Core(TM) i7 CPU 860@2.8 GHz System type = 64-bit OS Windows 7
PC 2	**PC 3**
2 CPUs, RAM = 3.46 GB Processor: Intel(R) Core(TM) 2 Duo CPU E8600@3.33GHz System type = 32-bit OS Windows XP	2 CPUs, RAM = 1.00 GB Processor: Intel(R) Pentium(R) D CPU 3.01 GHz System type = 32-bit OS Windows XP
Laptop 1	**Laptop 2**
2 CPUs, RAM = 3.0 GB Processor: Intel(R) Core(TM) 2Duo CPU T960000 @ 2.80 GHz System type = 32-bit OS Windows XP	2 CPUs, RAM = 4.0 GB Processor: Intel(R) Core(TM) 2 Duo CPU P8700 @ 2.53 GHz System type = 64-bit OS Windows 7

Results and Discussion

The three hydrological models were run on different computers using the presented development of Parallel SUFI2. Speedup and efficiency of each system versus the number of processors is shown in Figures 3 and 4, respectively.

Figures 3a and 3b show the speedup of the Danube, the Alberta, and the Test project on machines with 24 and 8 processors, respectively. In the system with 24 CPUs, the speedup of parallel SUFI2 follows closely the ideal speedup up to 8 processors. As the number of the processors increases, the gap between the parallel SUFI2 and the ideal performance grows. As the number of jobs increases, the communication of each CPU with the hard disk increases. The loss of speed is, hence, mostly due to hard disk limitation. The use of Redundant Array of Independent Disks (RAID) or Solid State Drive (SSD) should improve the performance. As the number of parallel processes increases, the speedup decreases for large projects. This is due to a proportionally higher burden of message passing. Hence, Danube shows a smaller speedup than the Alberta or Test project for 24 CPUs (Figure 3a).

The running time of small and medium projects were halved in machines with 2 processors following the ideal speed up (Figures 3 (c,d,e,f)). The small deviations in different machines and projects have to do with the initial state of the computers.

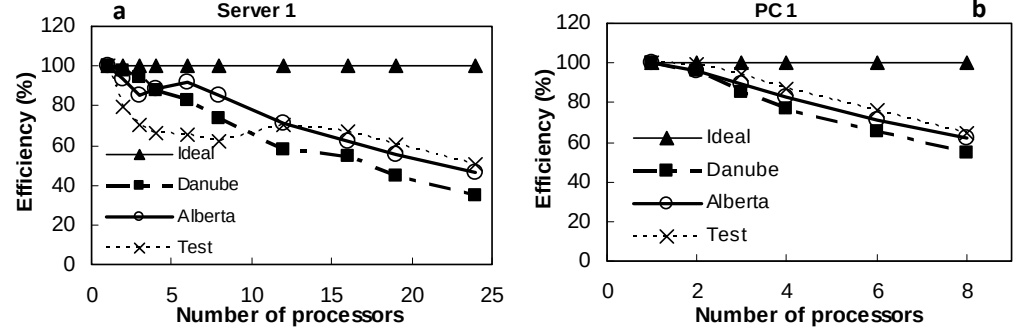
a
Server 1
Efficiency (%)
Number of processors
Ideal
Danube
Alberta
Test

PC 1
b
Efficiency (%)
Number of processors
Ideal
Danube
Alberta
Test

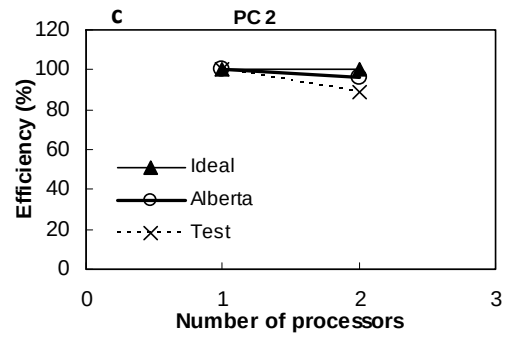
c
PC 2
Efficiency (%)
Number of processors
Ideal
Alberta
Test

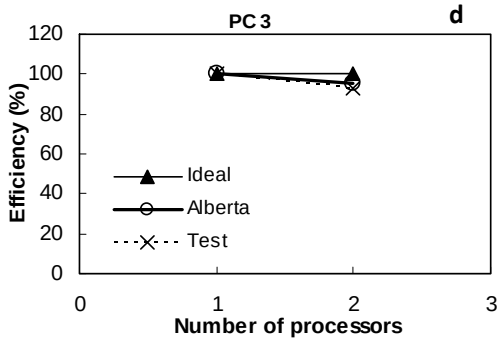
PC 3
d
Efficiency (%)
Number of processors
Ideal
Alberta
Test

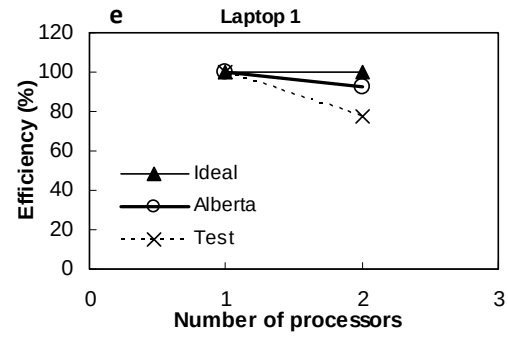
e
Laptop 1
Efficiency (%)
Number of processors
Ideal
Alberta
Test

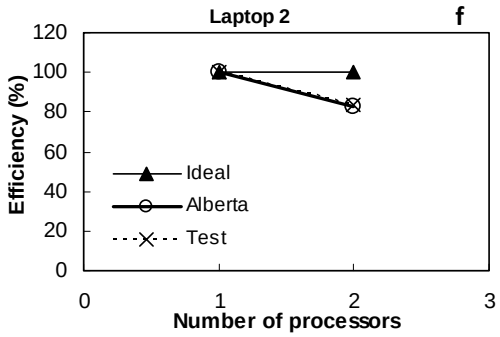
Laptop 2
f
Efficiency (%)
Number of processors
Ideal
Alberta
Test

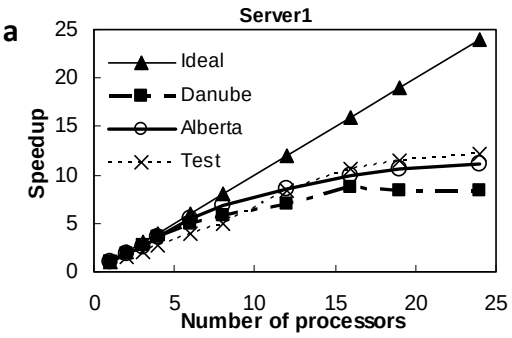
a
Server1
Speedup
Number of processors
Ideal
Danube
Alberta
Test

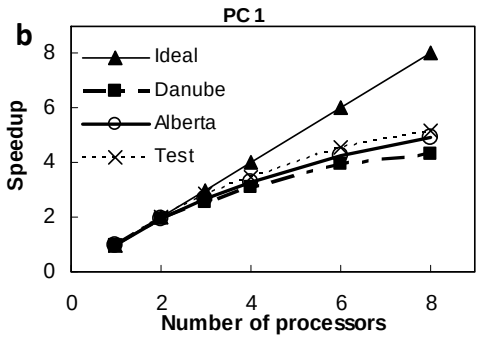
b
PC 1
Speedup
Number of processors
Ideal
Danube
Alberta
Test

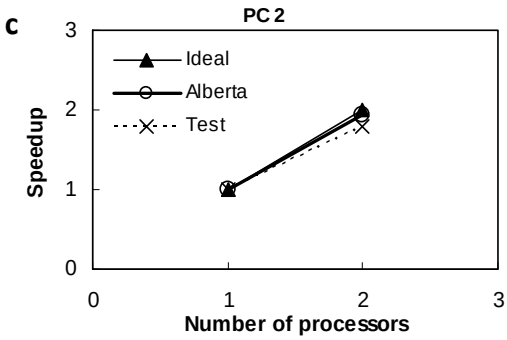
c
PC 2
Speedup
Number of processors
Ideal
Alberta
Test

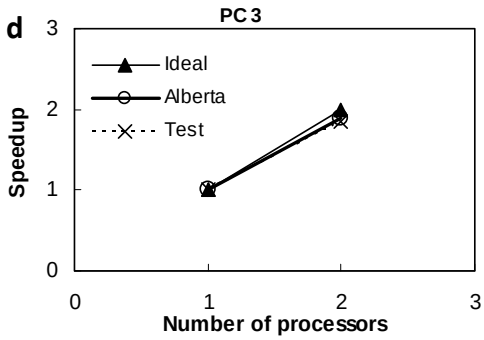
d
PC 3
Speedup
Number of processors
Ideal
Alberta
Test

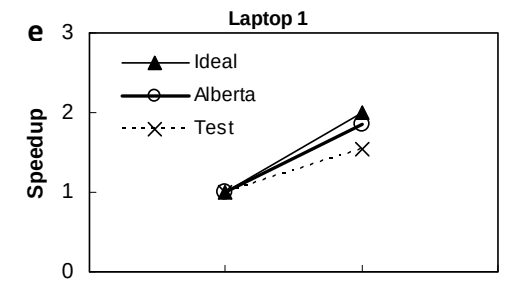
e
Laptop 1
Speedup
Ideal
Alberta
Test

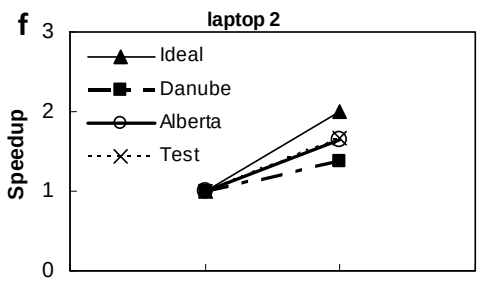
f
laptop 2
Speedup
Ideal
Danube
Alberta
Test

Figure 3. The speedup achieved for different computer systems and SWAT projects. Number of processors on the horizontal axis indicates the number of parallel jobs submitted. The Figure shows that most projects could be run 10 times faster with about 16 processors. Note that PC 2, PC 3, and Laptop 1 could not handle the size of the Danube project for two parallel runs.

It should be noted that the Danube project is missing from Figures 3 c,d,e. This is because the size of the project was too large for these machines to run two parallel processes. Figure 4 illustrates the efficiency of parallel SUFI2. In general, the efficiency of a parallel system is less than unity because of the system overhead such as the resolution of conflicting demands between shared resources, the communication time between processors, and the inability to keep every processor fully busy.

Figure 4. Percentage efficiency calculated for different computer systems and SWAT projects. The decrease in efficiency is a function of the size of the project and the characteristics of the hard disk.

For the ideal case, when the number of processors allocated to a particular task increases, a higher speedup (reduction in computing time) can usually be obtained. The efficiency therefore decreases for the above reasons and the fact that the processors can not be fully utilized. For small requests, such as the Test case in this study, the overhead introduced by the initial model set up is not compensated because the number of processors is too small. This can be seen in Figure 4a, which shows that for very small jobs the server becomes more efficient as the number of processors increase.

Conclusion

In this paper, we presented parallelized SUFI2 optimization program for higher performance calibration purposes. This allows larger scale problems with shorter running time. Performance results with both small and large size projects show that parallel SUFI2 achieves good speedup and reasonable scalability in most cases.

Although the parallel SUFI2 is designed to be used on any system, larger time savings can be achieved with multiple CPUs and larger RAM memory. Note that the emphasis of this research was not on achieving the highest possible speedup and that our current implementation is an early proof-of-concept prototype that does not contain optimization or refinement. Computations based on GPU technology hold the promise of achieving greater speed ups in execution of hydrologic models (Kalyanapu, et al., 2011; Singh, et al., 2011).

Acknowledgments

This project has been funded by the European Commission's Seventh Research Framework through the enviroGRIDS project (Grant Agreement n 226740).

References

Abbaspour, K.C., J. Yang, I. Maximov, R. Siber, K. Bogner, J. Mieleitner, J. Zobrist, R. Srinivasan. 2007. Modelling hydrology and water quality in the pre alpine/alpine Thur watershed using SWAT. Journal of Hydrology 333: 413-430.

Abbaspour, K.C., A. Johnson, M. Th. van Genuchten. 2004. Estimating uncertain flow and transport parameters using a sequential uncertainty fitting procedure. Vadose Zone Journal 3(4): 1340-1352.

Arnold, J.G., R. Srinivasan, R. S. Muttiah, J.R. Williams. 1998. Large area hydrologic modeling and assessment Part I: Model development. Journal of the American Water Res. Association 34(1): 73-89.

Duan, Q. 2003. Global Optimization for Watershed Model Calibration, in Calibration of Watershed Models, edited by Duan, Q., H. V. Gupta, S. Sorooshian, A. N. Rousseau, R. Turcotte. pp. 89-104, AGU, Washington, DC.

Gupta, H.V., S. Sorooshian,P. O. Yapo. 1998. Toward improved calibration of hydrologic models: multiple and non-commensurable measures of information. Water. Resour. Res. 34: 751-763.

Houstis, C., S. Kapidakis, E. P. Markatos, E. Gelenbe. 1997. Execution of computer-intensive applications into parallel machines. Information Sciences 97: 83-124.

Kalyanapu, A. J., S. Shankar, E. R. Pardyjak, D. R. Judi, S. J. Burian. 2011. Assessment of GPU computational enhancement to a 2D flood model. Environmental Modelling and Software 26: 1009-1016.

Mateos, C., A. Zunino, M. Campo. 2010. On the evaluation of gridification effort and runtime aspects of JGRIM applications. Future Generation Computer Systems 26: 797-819.

McKay, M.D., R. J. Beckman, W. J. Conover. 1979. A comparison of three methods for selecting values of input variables in the analysis of output from a computer code. Technometrics 21: 239-245.

Singh, B., E. R.Pardyjak, A. Norgren, P. Willemsen. 2011. Accelerating urban fast response Lagrangian dispersion simulation using inexpensive graphics processor parallelism. Environmental Modelling and Software 26: 739-750.

Assessment of climate change impact on surface water availability in Koshi river basin

Pabitra Gurung

International Water Management Institute (IWMI), Lalitpur, Nepal.

Luna Bharati

International Water Management Institute (IWMI), Lalitpur, Nepal.

Koshi is a largest river in Nepal and it is one of the tributary of Ganges. Taking Chatara as the basin outlet, the Koshi basin has total catchment area of 57,760 km^2. Assessment of surface water availability is a great challenge in Nepal mainly due to data limitations. In this study, the Soil Water Assessment Tool (SWAT) is used to simulate the water availability in the study basin. The impacts of CC projection from average downscaled values from 4 GCM (CNRM-CM3, CSIRO-Mk3.0, ECHam5 and MIROC 3.2) output on the hydrology of the basin are also calculated. Mean annual precipitation in the basin is 1234 mm under current climate scenarios. Under climate change projections, mean annual precipitation is decreasing from 1% to 3% in 2030s and is increasing from 8% to 12% in 2050s. Furthermore, annual maximum temperature is projected to increase by 0.29^0C and 0.26^0C under A2 and B1 scenarios respectively in every ten years within the Koshi basin. Similarly, annual minimum temperature is projected to increase by 0.28^0C and 0.24^0C under A2 and B1 scenario.

Result from model simulation shows that annual flow volume is about 52,731 MCM in the Koshi basin under current climate scenario. Annual flow volume will reduce by 2% under A2 projection scenario in 2030s and increase by 2% in 2050s. Similarly, annual flow volume will increase by 1% under B1 projection scenario in 2030s and by 4% in 2050s. Seasonal simulation result shows that the highest flow reduction will occur in pre-monsoon (16%) under A2 whereas highest flow increase will occur in post-monsoon (25%) under B1 projection scenarios.

Key words: *Water Availability, Climate Change, Hydrological Modelling, Koshi Basin*

Introduction

Water has been identified as the key resource for the development and economic growth of the country (GoN, 2011). There are about 6000 rivers and rivulets in Nepal with total drainage area of 194,471 km^2. All the major river systems of Nepal are snow fed (Kansakar et al., 2004) and are potential source of irrigation and hydropower development. NWPN (2005) indicates that at present some 72% of population has access to safe water, 546MW of hydropower capacity is exploited (out of estimated potential of 83,000 MW) and 'little consideration is being given to environmental requirements". It also sets the aims that by 2017 100% of population has access to water supply, 50% of households have access to electricity and 64% of all irrigable land provided with year-round irrigation. In development of these infrastructures, quantification of water availability at basin and sub-basin level is necessary. At present, developers are using very conventional methods; like catchment correlation and regional method etc.; to generate long term river discharge in these un-gauged locations. The methods consider linear relation among the neighboring catchments and this misleads the results most of the time. So far a countrywide assessment of water availability for all the major river basins has not been done.

Although quantifying water availability for the whole country is out of the scope of this study, this paper reports quantification of the Koshi basin water availability using a physically based hydrological model. In this study, detailed spatial analysis of the hydrology of the Koshi basin under past (1976-2005) as well as future climate projections is conducted. The main objective of the study is to quantify the surface water availability at the sub-basins of Koshi river using SWAT model and then to assess the impact of future climate projection on water availability at sub-basins level.

Climate of Nepal

Nepal's climate varies from arctic to tropical from north to south. Nepal has four seasons; pre-monsoon (March to May), monsoon (June to September), post-monsoon (October to November) and winter (December to February). The weather of pre-monsoon is dry and hot with occasional rain showers; monsoon is very hot with nearly 80% of annual rainfall; post-monsoon is warm and humid; and winter is dry and cold. Rainfall in Nepal varies by altitude; higher altitude experience a lot of drizzle rain and heavy downpours occur in lower altitude.

Koshi River Basin

The Koshi river basin is one of the major snow fed river basins of Nepal. The area considered in this study is the Koshi Basin upstream of Chatara in the mountain and hill region of eastern Nepal and southern Tibet (Figure 38). Taking Chatara as the basin outlet, the Koshi basin has total catchment area of 57,760 km^2. The basin outlet, Chatara, is located at 26.87 degree north and 87.15 degree east. The study area includes the entire mountainous region in the Koshi Basin and is characterized by high climatic and geographical variability. The average elevation of the basin is 3,800 m but varies from 140 m at Chatara to more than 8,000 m in the Great Himalayan Range including Mt. Everest (8848 metres). The basin can be divided into the Tibetan Plateau, Central and Eastern Mountain Regions and the Central and Eastern hill regions. Assessment on water balance in Koshi basin shows that there is large temporal and spatial variability in precipitation, actual evapotranspiration and water yield in the basin (Bharati et al.; 2012). In the hill region of Koshi basin, monsoon is dominated by July rain whereas in mountain region, monsoon is dominated by both July and August rain (Kansakar et al., 2004). The study carried out by Sharma et al., (2000) stated that increasing tendency of temperature and precipitation in Koshi basin and decreasing trends of flow in major tributaries Koshi River.

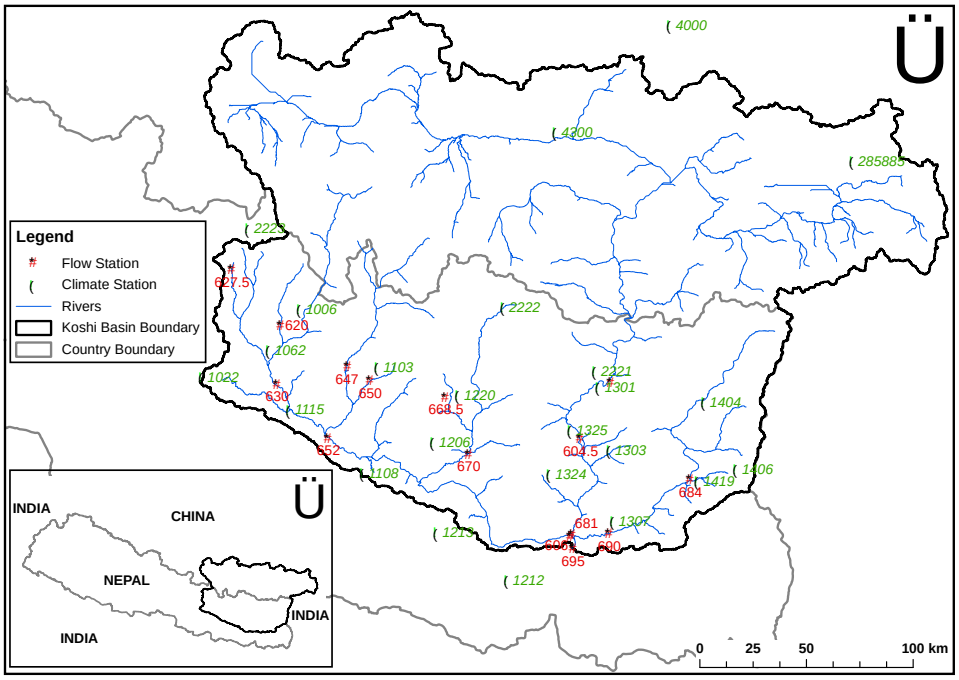

- Figure 38: Map of Koshi Basin showing the location of climate and hydrological stations used in the study (Bharati et al., 2012)

Soil and Water Assessment Tool (SWAT)

SWAT is a continuous, physically based, semi-distributed hydrological public domain model jointly developed by USDA Agricultural Research Service (USDA-ARS) and Texas AgriLife Research, part of The Texas A&M University System. SWAT is a river basin-scale model to quantify impact of land management practices on water quantity, sediment and water quality in large complex watersheds with varying soils, land use and management conditions over a long period of time (Arnold et al., 1998; Neitsch et al., 2005).

Conceptually SWAT divides a basin into sub-basins. Each sub-basin is connected through a stream channel and further divided it to Hydrologic Response Unit (HRU). HRU is a unique combination of a soil, vegetation type and a slope in a sub watershed, and SWAT simulates hydrology, vegetation growth, and management practices at the HRU level. Since the model maintains a continuous water balance, the subdivision of the basin enables the model to reflect differences in evapotranspiration for various crops and soils. Thus runoff is predicted separately for each sub-basin and routed to obtain the total runoff for the basin. This increases the accuracy and gives a much better physical description of the water balance. More detailed descriptions of the model can be found in Arnold et al. (1998) and Srinivasan et al. (1998).

SWAT Model Setup and Flow Simulation

The Soil and Water Assessment Tool (SWAT) model was setup for the Koshi basin. SWAT requires three basic files for delineating the basin into sub-basins and HRUs i.e. Digital Elevation Model (DEM), Soil map and Land Use/Land Cover (LULC) map. For this study 90m Shuttle Radar Topography Mission (SRTM) is used for the DEM. The land use map from Advanced Very High Resolution Radiometer (AVHRR) 1992/93 and the soil map from FAO, 1995 are used for Model setup. Simulated result of model setup for Bharati et al., (2012) is used to carry out this study. Therefore, detail on model setup and hydrological simulations are described in that study report. Bharati et al., (2012) reported that model simulations show very good correlation between simulated and observed flows. The correlation coefficient (r^2) for the monthly simulations is 0.96 during calibration and 0.91 during validation period. The correlation coefficient (r^2) for daily simulations is 0.86 and 0.81 for the calibration and validation period respectively. In the study, the basin was divided into 79 sub-basins. Altogether, data of 24 climate stations and 15 flow stations, obtained from Department of Hydrology and Meteorology (DHM), are used to simulate the flows. The

calibration period was from January, 1996 to December, 2005 and validation period was from January, 2001 to December, 2005.

Downscaled Climate Data and Statistical Adjustment of Biases

In this study, MarkSim weather generator is used to downscale climate data from global circulation model (Jones et al., 2002). Global circulation models (GCM) used to generate time series climate data are CNRM-CM3, CSIRO-Mk3.5, ECHam5, and MIROC3.2 and the projected data are average of these four GCMs. In this study, future projected climate data used for model simulation are under A2 and B1 scenarios of the SRES families. A2 corresponds to a story line of high population growth with slower per capita economic growth and technological change, and B1 corresponds to a story line of population growth to 9 billion in 2050 and then declining with rapid economic growth and moderate technological change by emphasizing on global solutions to economic, social and environmental stability (IPCC, 2000). In the study, period of future simulations is 2030s (average from 2016 to 2045) and 2050s (average from 2036 to 2065), whereas period of base line (BL) is 2000s (average from 1971 to 2000). These time series data include three variables; precipitation, maximum and minimum temperature, and solar radiation. Although, these climate data obtained from MarkSim downscaled techniques still reveal discrepancies with respect to observed meteorological data. Therefore, MarkSim data are adjusted in such a way that, at each 24 station locations, the main statistical properties of adjusted MarkSim output (mean and standard deviation) match those the historical data. The specific adjustment techniques and statistical downscaling approaches are described in Bouwer et al., (2004) and Bharati et al., (2011).

Current Climate and Projected Trend of Climate in Koshi Basin

Mean annual precipitation occurred in the basin was 1234 mm under current climate scenario in the period from 1976 to 2005. Whereas, distribution of mean seasonal precipitation are 223 mm, 856 mm, 59 mm and 96 mm in pre-monsoon, monsoon, post-monsoon and winter seasons respectively. Simulation result shows that maximum mean annual precipitation (3956 mm) was occurred in sub-basin number 64 and minimum precipitation (292 mm) was in sub-basin 7. Under the climate change projection, mean annual precipitation will decrease from 1% to 3% in 2030s and will increase from 8% to 12% in 2050s. Sub-basins wise percentage change in annual precipitation under climate change scenario is presented in Figure 42. Furthermore, in 2030s, sub-basin wise range of change in mean annual precipitation will be

from -37% to +46% under A2 and from -31% to +32% under B1 projection scenarios whereas in 2050s, the range will be from -16% to +52% under A2 and from -31% to +43% under B1 projection scenarios.

Under current climate condition, sub-basins wise range of mean annual maximum temperature was from +7.97^{0}C to +31.42^{0}C whereas range of mean annual minimum temperature was from -12.37^{0}C to +8.82^{0}C. Under the climate change projection, annual maximum temperature is projected to increase by 0.29^{0}C and 0.26^{0}C under A2 and B1 scenario respectively in every ten years within the Koshi basin. Similarly, annual minimum temperature is projected to increase by 0.28^{0}C and 0.24^{0}C under A2 and B1 scenario respectively in every ten years. Further analysis of future climate projections is still ongoing and will be published in a separate report which is in preparation.

Water Availability under Current and Future Projection Scenario

Result from model simulation shows that annual flow volume is about 52,731 MCM in the Koshi basin under current climate scenario. According to simulation results (Figure 39) under current climate condition, 70.8% of total annual flow occurred only in monsoon. Similarly, 13.2% of annual flow is occurred in post-monsoon, 8.1% in winter and 7.9% in pre-monsoon seasons. In the study basin, the simulated result (Figure 39) shows that no significant changes in contribution of monsoon flow on annual flow volume (which is nearly 71%) under current and future climate projections. However, contribution of pre-monsoon and winter flow on annual flow volume is in decreasing trend whereas contribution of post-monsoon flow is in increasing trend under the climate change projection scenarios.

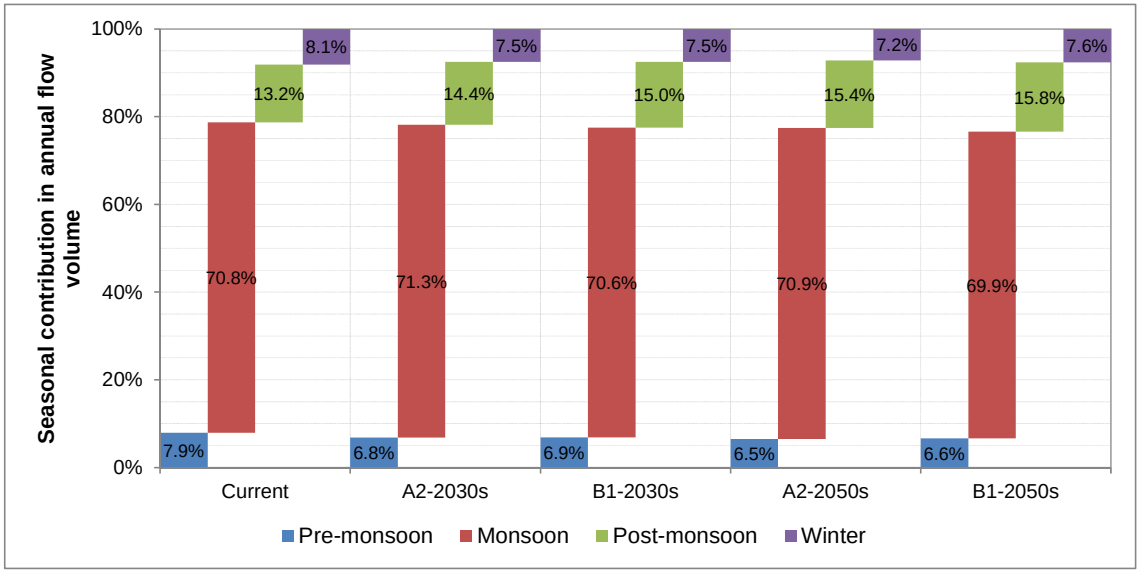

- Figure 39: Seasonal simulated flow volume available at basin outlet Chatara-Kothu under current and future climate projection

Figure 41 represents sub-basin wise seasonal available flow volume under current climate. Model simulation results show that available flow volume at basin outlet is about 4,191 MCM in pre-monsoon. Similarly, available flow volume is about 37,331 MCM in monsoon, about 6,943 MCM in post-monsoon and about 4,266 MCM in winter.

The percentage change in projected flow volume at basin outlet is presented in Table 15. In 2030s, annual flow volume will reduce by 2% under A2 and will increase by 1% under B1 projection scenario. Seasonal projected results show that the highest flow reduction will occur in pre-monsoon (16%) under A2 projection scenario whereas highest flow increase will occur in post-monsoon (15%) under B1 projection scenario. Similarly, in 2050s, annual flow volume will increase by 2% under A2 and by 4% under B1 projection scenario. Seasonal projected results show that maximum flow reduction will occur during pre-monsoon (16%) under A2 whereas maximum flow increase will occur in post-monsoon (25%) under B1 projection scenarios.

- Table 15: Percentage change in projected flow volume at basin outlet Chatara-Kothu

Period	Scenario	Pre-monsoon	Monsoon	Post-monsoon	Winter	Annual
2030s	A2	-16%	-1%	7%	-9%	-2%
	B1	-12%	1%	15%	-7%	1%
2050s	A2	-16%	3%	20%	-9%	2%
	B1	-13%	3%	25%	-2%	4%

Figure 43 represents percentage change in sub-basins wise annual flow volume under A2 and B1 projection scenarios in 2030s and 2050s periods. The figures have three types of representation of percentage change in flow volume; decreasing trend with negative values, no change with zero values and increasing trend with positive values. Sub-basins wise ranges of change in annual flow are from -60% to +30% under A2 and from -20% to +55% under B1 scenario in 2030s whereas the ranges are from -47% to +55% under A2 and from -29% to +107% under B1 scenario in 2050s.

Figure 40 signifies total number of sub-basins that falls in between specified ranges of change in annual flow volume under climate change projections. In 2030s, 63 sub-basins have range of change in annual flow volume from -10% to +10% under A2 scenario and 68 sub-basins have range from -5% to +20% under B1 scenario. Similarly in 2050s, 63 sub-basins have range of change in annual flow from -5% to +20% under A2 scenario and 73 sub-basins have range from -5% to +30% under B1 scenario. Therefore, only few sub-basins have less than -40% and more than +40% of change in annual flow volume.

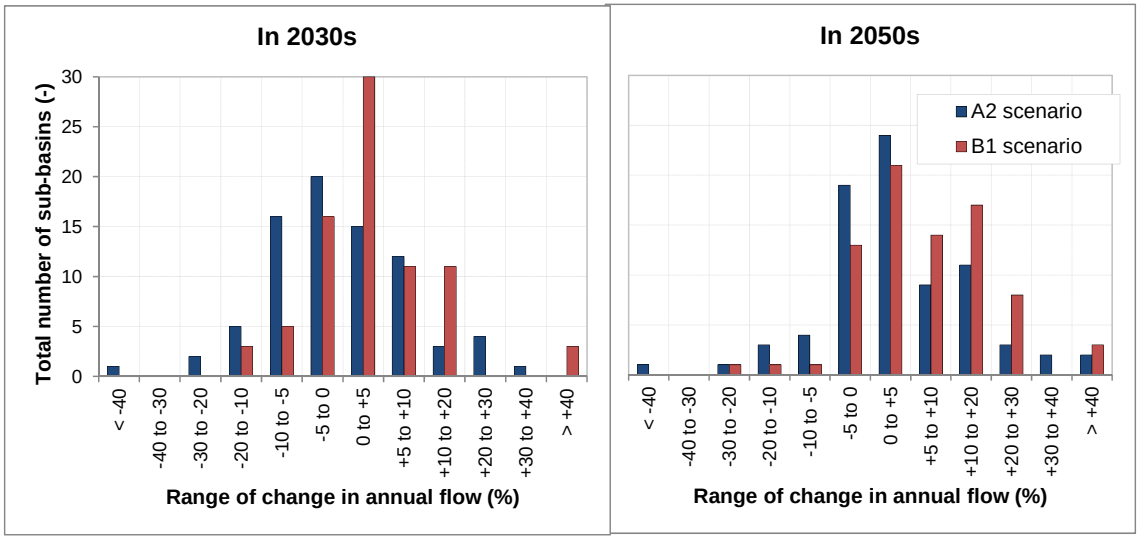

- Figure 40: Histogram for number of sub-basins in the range of percentage change in annual flow volume

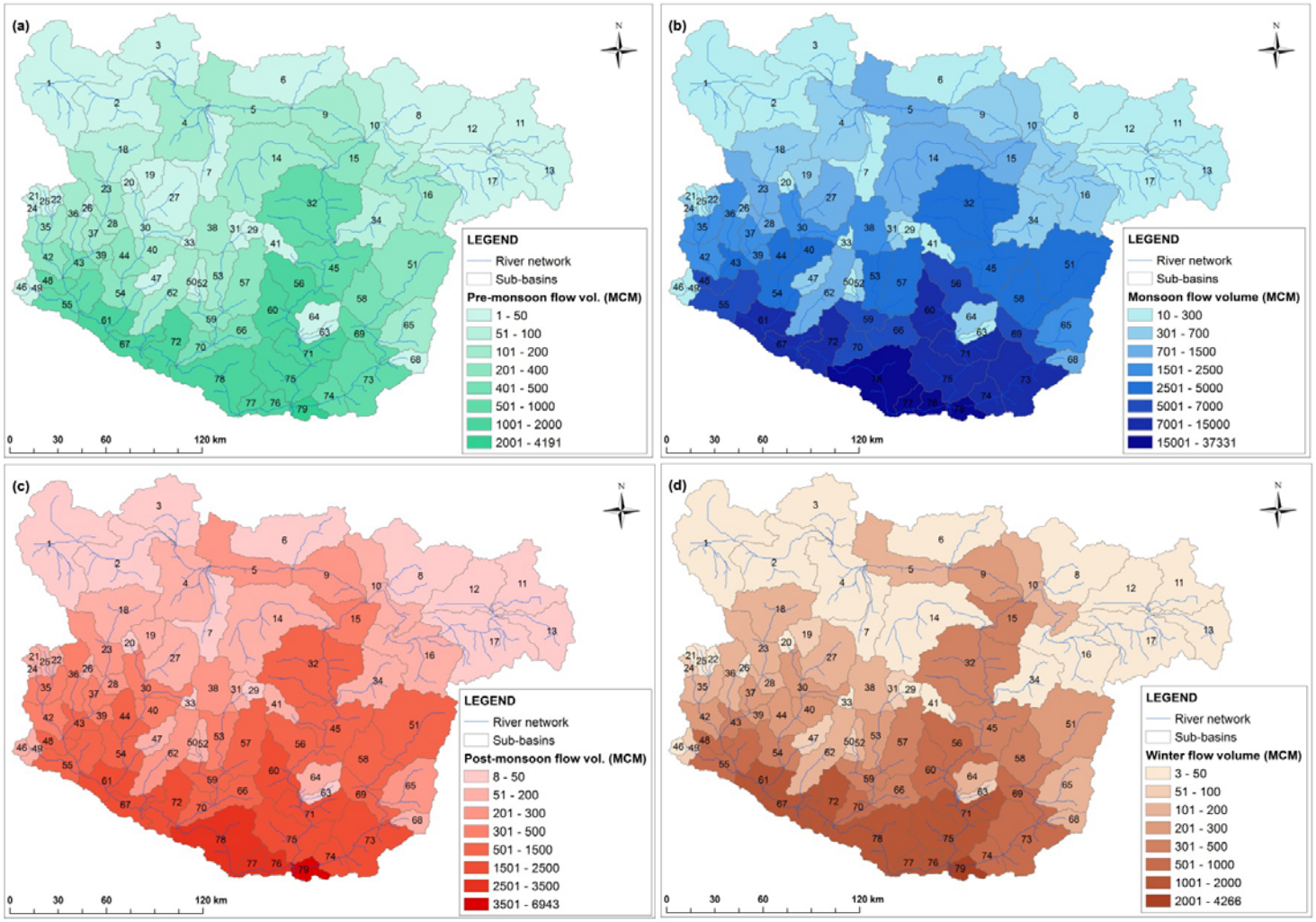

- Figure 41: Seasonal simulated flow volume in sub-basins level under current climate; (a) Pre-monsoon, (b) Monsoon, (c) Post-monsoon, and (d) Winter seasons

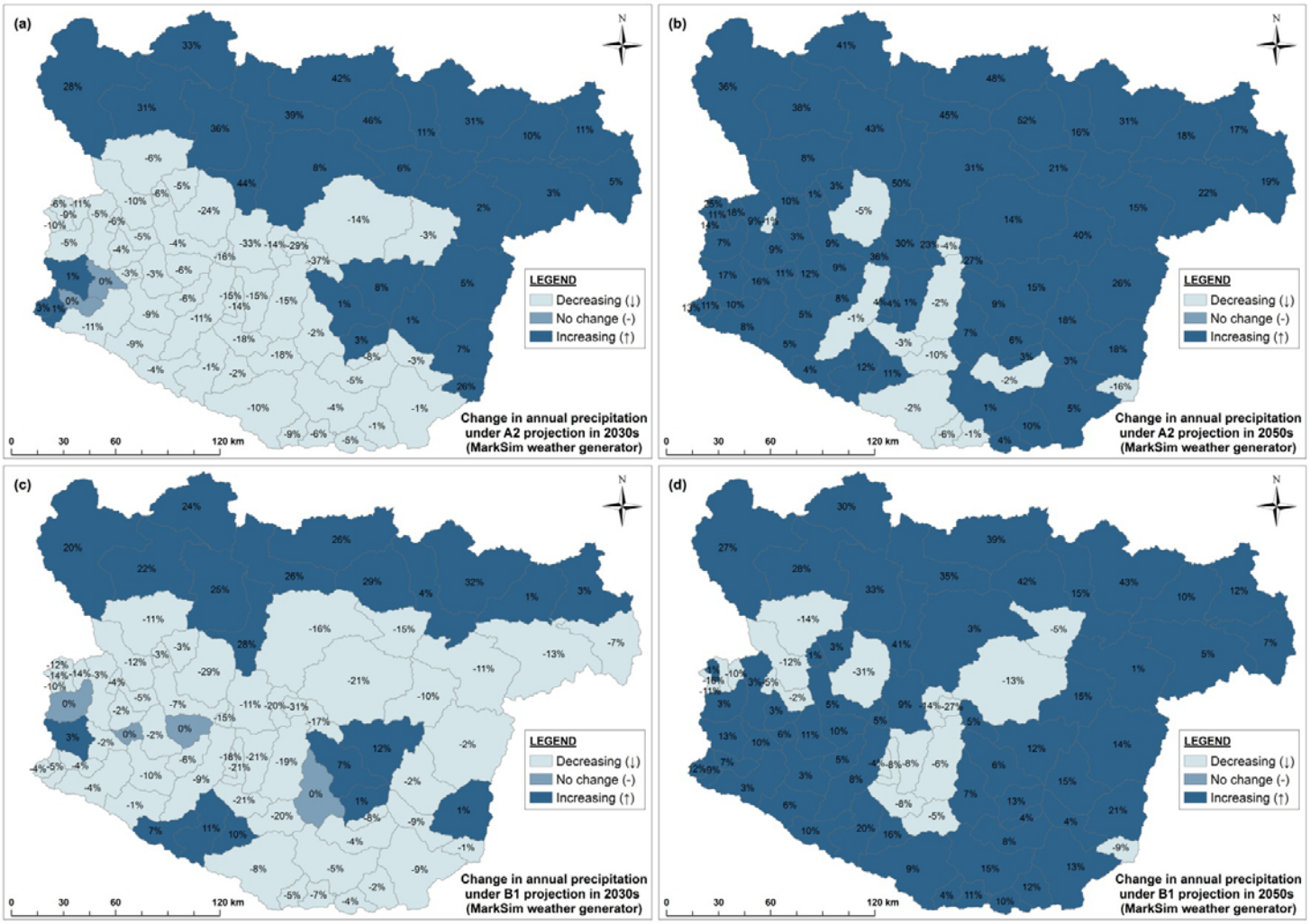

Figure 42: Percentage change (Projected – Current) in annual precipitation under climate change projections; (a) A2 scenario in 2030s, (b) A2 scenario in 2050s, (c) B1 scenario in 2030s, and (d) B1 scenario in 2050s

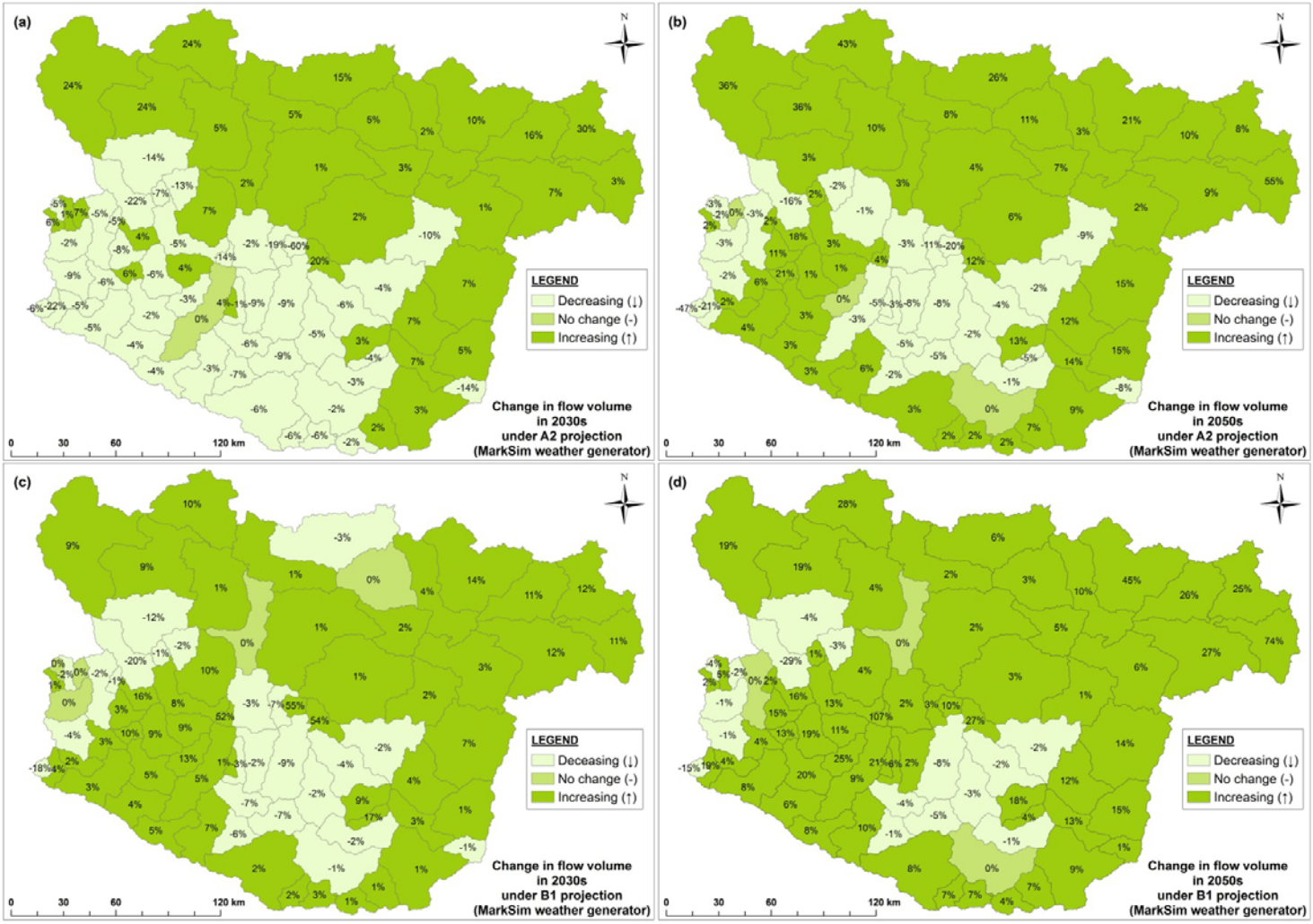

- Figure 43: Percentage change (Projected – Current) in annual flow volume under climate change projections; (a) A2 scenario in 2030s, (b) A2 scenario in 2050s, (c) B1 scenario in 2030s, and (d) B1 scenario in 2050s

Conclusion

The upper sub-basins of the Koshi River are located in trans-mountain region, which is widely known as a rain shadow area of the Koshi basin. Therefore, less precipitation occurred in this region in comparison to lower sub-basins of the Koshi basin. However, increasing trend of precipitation is projected over the trans-mountain region of the Koshi basin under future climate projection (Figure 42). Annual flow volume will increase by 1% under B1 projection scenario in 2030s and by 4% in 2050s. A seasonal simulation result shows that the highest flow reduction will occur in pre-monsoon (16%) under A2 whereas highest flow increase will occur in post-monsoon (25%) under B1 projection scenarios. In general, sub-basins wise flow is decreasing under A2 scenario in period of 2030s than current flow; and slightly increasing in period of 2050s whereas general trend under B1 scenario is in increasing trend. The climate change projection result shows that the sub-basins of trans-mountain region of the basin (northern sub-basins) has trend of increasing flow under both A2 and B1 scenarios. However, due to disagreement among the projected climate under future climate change scenarios, there is still high level of uncertainty in the projected flow availability.

Reference

Arnold, J.G., R. Srinivasan, R.S. Muttiah, and J.R. Williams. 1998. Large area hydrologic modeling and assessment, Part I: Model development. *Journal of the American Water Resources Association*. 34(1): 73-89.

Bharati, L., G. Lacombe, P. Gurung, P. Jayakody, C.T. Hoanh, and V. Smakhtin. 2011. The impacts of water infrastructure and climate change on the hydrology of the Upper Ganges River Basin. *Colombo, Sri Lanka: International Water Management Institute. 36p. (IWMI Research Report 142)*. Doi: 10.5337/2011.210

Bharati, L., P. Gurung, and P. Jayakody. 2012: Hydrologic Characterization of the Koshi Basin and the impact of CC. *Kathmandu, Nepal: National Conference on Water, Food Security and Climate Change (CC) in Nepal, 23-24 November 2011. (In press to publish as a special issue of Hydro Nepal: Journal of Water, Energy and Environment)*

Bouwer, L.M., J.C.J.H Aerts, G.M. van de Coterlet, N. van de Giesen, A. Gieske, and C. Mannaerts. 2004. Evaluating downscaling methods for preparing Global Circulation Model (GCM) Data for Hydrological Impact Modelling. *In: Climate Change in Contrasting River Basins, (eds.) Aerts, J.C.J.H., Droogers, P. Wallingford, UK: CABI Publishing.*

Gon. 2011. Water resources of Nepal in the context of climate change. *Government of Nepal (GoN). Water and Energy Commission Secretariat. Singha Durbar, Kathmandu, Nepal.*

IPCC, 2000. IPCC special report on emission scenarios. Summary for policymakers. *A special report of working group III of the Intergovernmental Panel on Climate Change (IPCC. Geneva, Switzerland: Intergovernmental Panel on Climate Change (IPCC). 20p.*

Jones, P.G., P.K. Thornton, W. Diaz, P.W. Wilkens, and A.L. Jones. 2002. MarkSim – A Computer Tool That Generates Simulated Weather Data for Crop Modeling and Risk Assessment, Version 1.

Kansakar, S.R., D.M. Hannah, J. Gerrard, and G. Rees. 2004. Spatial pattern in the precipitation regime of Nepal. *International Journal of Climatology.* 24: 1645-1659

Neitsch, S.L., J.G. Arnold, J.R. Kiniry, and J.R. Williams. 2005. Soil and Water Assessment Tool Theoretical Documentation. *Grassland, Soil and Water Research Laboratory, Agricultural Research Service, and Blackland Research Center, Texas Agricultural Experiment Station, East Blackland Road: Temple, Texas 76502.*

NWPN. 2005. National Water Plan–Nepal, 27-42. Water and Energy Commission Secretariat, Ministry of Energy, Government of Nepal.

Sharma, K.P., B. Moore III, and C.J. Vorosmarty. 2000. Anthropogenic, Climatic, and Hydrologic Trends in the Kosi basin, Himlalaya. *Kluwer Academic Publishers. Climate Change.* 47: 141 – 165.

Srinivasan, R., T.S. Ramanarayanan, J.G. Arnold, and S.T. Bednarz. 1998. Large area hydrologic modeling and assessment Part II: Model application. *Journal of the American Water Resources Association.* 34(1): 91-101.

Calibration and Validation of QUAL2E model on the Delhi stretch of river Yamuna, India

D.L. Parmar
Associate Professor, Dept. of Civil Engineering, H.B. Technological Institute, Kanpur–208002, India, E mail: d_parmar@rediffmail.com

A.K. Keshari
Professor, Department of Civil Engineering, Indian Institute of Technology, Delhi New Delhi-110016, India, Email: akeshari@hotmail.com

ABSTRACT

The QUAL2E is one of the most popular water quality models used for the purpose of simulation and wasteload allocation studies. However, the applicability of this model for different climate conditions needs to be tested to have accurate prediction by the model. Calibration is one of the most important steps of modeling studies wherein the exact value of reaction parameters to be used in a model is estimated using trail and error method so as to have accurate prediction by the model. In this study, Calibration and Validation of the QUAL2E simulation model has been carried out for the Delhi stretch of river Yamuna, India to find the most sensitive reaction coefficients, namely, the deoxygenration coefficient (K_1) and reaeration coefficient (K_2). The Calibration was accomplished by adjustment of model coefficients using trial and error method, until the best goodness of fit between predicted and observed data is achieved. The model was calibrated to the observed water quality conditions (based on average conditions of March-June 2002) by adjusting parameters that control the water quality in the study stretch. The model was calibrated with the goal of minimizing the error for BOD, DO and temperature. After calibration, the model was applied to February 2003 survey data for the validation. The performance of the model was evaluated in terms of Coefficient of correlation (R^2) and index of agreement (IOA). Results revealed that values of these performance indicators for both, calibration and validation were found to be varying between 0.7142 to 0.9761 thus indicating satisfactory performance. Once the model is calibrated and validated, and its range of accuracy known and judged to be acceptable, it can be used for simulation of water quality.

MODEL PARAMETERS

The presence of dissolved oxygen in water is a primary indicator of water quality. There are various sources and sinks in a water body. For example the BOD of wasteload, respiration, sediment demands etc are the sinks. The photosynthesis, fresh water flow from headwater are the sources of dissolved oxygen. For the water quality simulation, the information about the rates of these processes/sources or sinks (such as deoxygenation, reaeration, sedimentation) is needed. These rates are represented in form of constants known as reaction rate constants. Broadly, there are four types of rate constants. These are: K_1 (deoxygenation constant or CBOD decay rate), the rate of biochemical decomposition of organic matter (per day); K_2 (reaeration constant), the rate at which oxygen enters the water from the atmosphere (per day); K_3 (BOD settling rate), the rate

at which the BOD is removed by sedimentation/settling; and K_4 (Sediment oxygen demand rate, also known as benthic oxygen demand constant), the rate of BOD addition to overlying water from the bottom sediment (usually $gmO_2/m^3/day$). A brief description of the methodology adopted for estimation of these rate constants in this study is given herein. The deoxygenation constant K_1 (BOD decay rate) is the rate of biochemical decomposition of organic matter and has been obtained using the equation (2) (Ortolano 1984) given below.

$$K_1 = \frac{1}{x} \ln \frac{L_0}{L} . V \qquad (2)$$

where,

$L_o =$ BOD at beginning of a reach; $L =$ BOD at end of the reach; $V =$ average velocity of flow in the each; $x =$ distance from beginning to end of the reach

The value of K_1 was found to be varying between 0.23 to 0.55 per day. These values are found to be in good agreement with previous studies on this study stretch (Bhargawa 1983; Kazmi and Agrawal 2005; Paliwal et al. 2007), wherein the range was 0.2-0.5 per day. Another rate constant is the reaeration rate coefficient (K_2) which is extremely important for waste load allocation studies. It is the rate at which oxygen enters the water from the atmosphere (Jha et al. 2000). Some recent modeling studies (Kazmi and Agrawal 2005; Paliwal et al. 2007) on the Delhi stretch have used O'Connor and Dobbins equation (O' Connors and Dobbins 1958) for K_2 estimation. However, Melching and Flores (1999) showed that available equations for K_2 estimation generally yield poor estimates when applied to stream conditions different from those for which the equations were derived. Thus in the present study, a predictive equation for K_2 has been developed for the Delhi stretch of river Yamuna which is given below:

$$K_2 = 4.27 \frac{(V)^{0.47}}{(H)^{2.09}} \qquad (3)$$

It has been reported in the literature (Bhargawa 1983; Kazmi and Agrawal 2005) that in the Delhi stretch of river Yamuna, BOD removal takes place mainly because of settling of organic matter. Thus, the value of K_3, the rate of BOD removal by sedimentation/settling has been adopted as 0.9 per day (Kazmi and Agrawal 2005). This fact has also been supported by the results obtained in sensitivity analysis. Since the benthic oxygen demand (K_4), does not affect the Delhi stretch, this value has been adopted as 0.5 per day from the same literature.

STUDY AREA

The 22 km Delhi stretch of the river starting from the Wazirabad barrage to the Okhla barrage has been considered in the present study. Fig 1 shows the Delhi stretch showing the fifteen drains and the barrages at the ends. Out of the fifteen drains, on the basis of wastewater discharge, the Najafgarh drain (D1) is the largest drain having about 20.68 cumecs (72.68 % of total contribution of 28.46 cumecs of 15 drains) whereas the Moat drain (D8) is the smallest drain having an average discharge of only about 0.001cumecs. Similarly on the basis of BOD load, the Najafgarh drain stands first with an average BOD load of 100.058 tons/day (about 61 %

of the total BOD load of the 15 drains). In addition to the fifteen drains, there are six more drains in the Delhi stretch of the river. The total pollution load in terms of BOD, disposed off into the river by all the 22 drains in Delhi is about 255.75 tons /day. Out of this, 164.05 tones/day BOD load joins the river before Okhla barrage and rest i.e. 91.7 tons /day joins the river/Agra canal downstream of Okhla barrage (CPCB 2005). This implies that total BOD load in whole Delhi stretch is very high resulting in poor water quality.

SIMULATION MODEL

For the purpose of this study, QUAL2E developed by USEPA has been used. QUAL2E is a one dimensional steady state numerical model (USEPA 1995). It uses a finite difference solution to the one dimensional advective-dispersive mass transport and reaction equation. The basic equation solved by QUAL2E is numerically integrated over space and time for each water quality constituent under consideration. This equation includes the effects of advection, dispersion, dilution, constituent reactions and sources/sinks. For any constituent, C, this equation can be written as (Barnwell et al. 2004):

$$\frac{\partial M}{\partial t} = \frac{\partial\left(A_x D_l \frac{\partial C}{\partial x}\right)}{\partial x} dx - \frac{\partial(A_x V C)}{\partial x} dx + (A_x dx) + \frac{dC}{dt} + s \qquad (1)$$

where,

M = mass; x = distance; t = time; C = concentration; A_x = cross sectional area

D_l = dispersion coefficient; and V= mean velocity, s =source/sink

For the purpose of water quality simulation using QUAL2E, the existing 22 km long study reach has been considered. All the existing 15 drains have been considered thus dividing the study stretch into sixteen reaches (R1 to R16). The figure in bracket on the arrows represents the discharges in cumecs (CPCB 2005). The 22 km long study stretch has been considered to be of 21.9 km length so as to fit the QUAL2E requirement of equal size of computational elements in all the reaches. A total of 73 computational elements of size 0.3 km each were considered. The QUAL2E modeling tool uses flow exponent equations to functionally represent the hydraulic routing of the river. These empirical equations relating velocity, depth and width with flow were developed using field data obtained from secondary sources (DJB 2005) and the coefficients and exponents used in the model. The initial conditions of the system were established for temperature, DO, and BOD only. The daily mean flow for the survey dates is also fed as the initial condition. All other initial condition in form of point source water quality inputs were obtained from field data (DJB 2005). The boundary conditions include the point loads and their quality, background flow and concentration. The details of data required for calibration and validation are given elsewhere (Parmar 2006).

CALIBRATION AND VALIDATION OF QUAL2E

The QUAL2E model was calibrated and validated using field data, before it is used for simulating the water quality. Calibration was accomplished by adjustment of model coefficients during successive/iterative model runs, until the best goodness of fit between predicted and

observed data is achieved. The model was calibrated to the observed water quality conditions (based on average conditions of March-June 2002) by adjusting parameters that control the water quality in the study stretch. Although the QUAL2E model has many parameters, only two namely, K_1 and K_2 served as calibration parameters. The goal of model calibration was to accurately simulate observed data using few calibration parameters as possible, and the chosen parameters therefore served as the simplest set that allowed for accurate simulation of various constituents. In general, the model was calibrated with the goal of minimizing the error for BOD, DO and temperature. The performance of the model was evaluated in terms of Coefficient of correlation (R^2) and index of agreement (IOA, Nunnari et al. 2004). R^2 represents the amount of variance in the outcome explained by the model relative to how much variation there was to explain in the observed data. The index of agreement, a bounded relative measure, is capable to measure the degree to which predictions are error free. The denominator accounts for the model's deviation from the mean of the observations as well as to the observations deviation from their mean. With respect to a good model, the index of agreement should approach one. The Index of agreement (IOA) was calculated as,

$$\text{IOA} = 1 - \frac{\sum_{i=1}^{N}(P_i - O_i)^2}{\sum_{i=1}^{N}\left(\left|P_i - \overline{O_i}\right| + \left|O_i - \overline{O}\right|\right)} \qquad (4)$$

where,

P_i = predicted value of output variable

O_i = Observed value of variable

$\overline{P}$ = Average value of predicted output

$\overline{O}$ = Average value of observed variable

After giving all inputs, a number of trials were made to ensure matching of observed and simulated values of BOD and DO. Figures 1a and 1b show the comparison between observed and simulated profiles of BOD. The goodness of fit was measured using the correlation coefficient which was found to be 0.8377 for BOD (Fig.1b). Figures 2a and 2b show the comparison between observed and simulated profiles of DO. The correlation coefficient was found to be 0.8979 for DO (Fig. 2b). Once calibrated, the model was applied to February 2003 survey data for the validation. Only observed inputs were changed for the validation run. A discharge of 1.5 m^3/s was assumed in the headwater. The mean discharge for the river varies from 25.94 m^3/s in R2 to 56.538 m^3/s in R16. Figs. 3a and 3b show the comparison between observed and simulated profiles of BOD for the validation run. Figs. 4a and 4b show the comparison between observed and simulated profiles of DO for validation run. The summary of performance measures obtained for calibration and validation is listed in Table 1. The summary statistics and qualitative comparison of trends show that in general the model is able to reproduce the longitudinal pattern of BOD, DO and temperature and is a realistic representation of the system. Thus the model is acceptable and can therefore be used for water quality simulation.

Table 1 Summary of performance indices

Parameters	Calibration		Validation	
	Coefficient of correlation	Index of agreement	Coefficient of Correlation	Index of agreement
BOD	0.8377	0.8428	0.8487	0.7123
DO	0.8979	0.9761	0.8972	0.9544

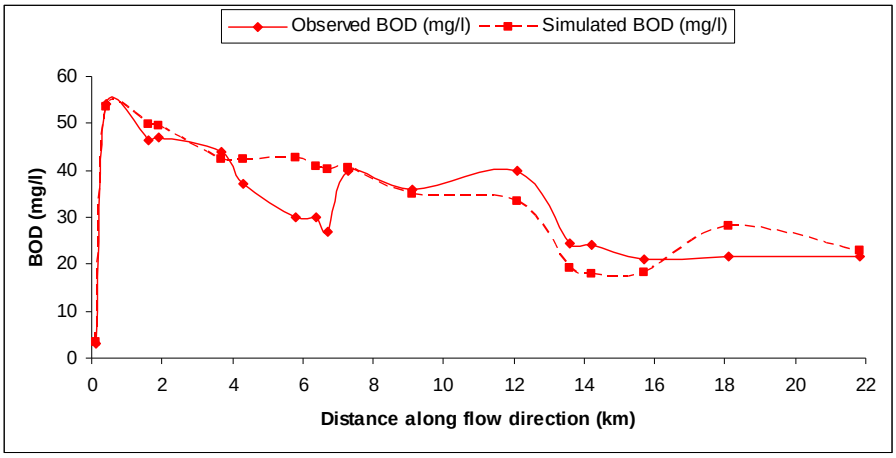

Fig 1a Calibration-Profile of observed and simulated BOD

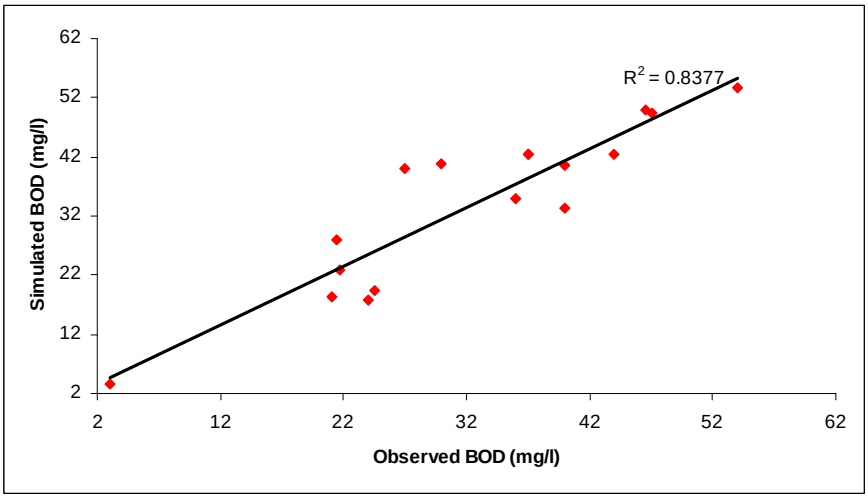

Fig 1b Calibration-Correlation between observed and simulated BOD

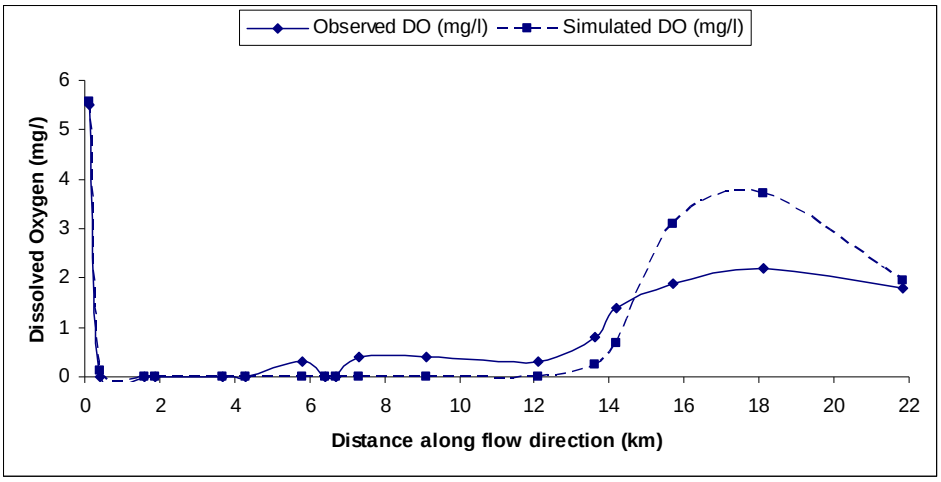

Fig 2a Calibration-Profile of observed and simulated DO

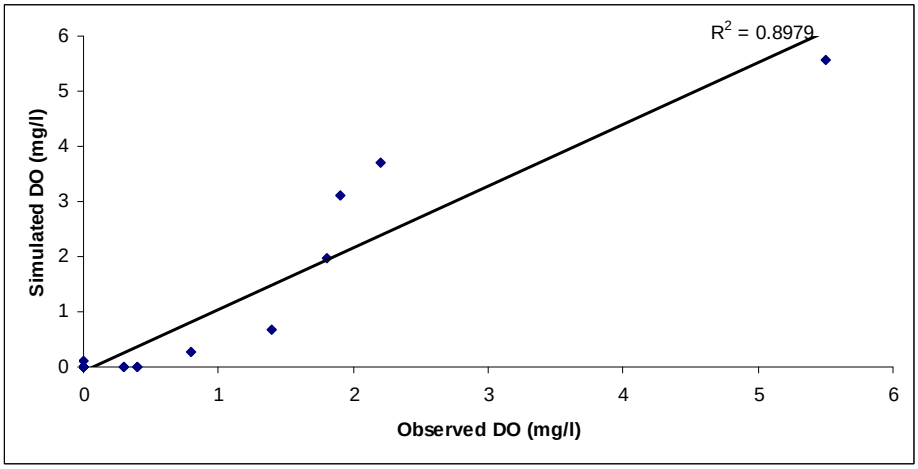

Fig 2b Calibration-Correlation between observed and simulated DO

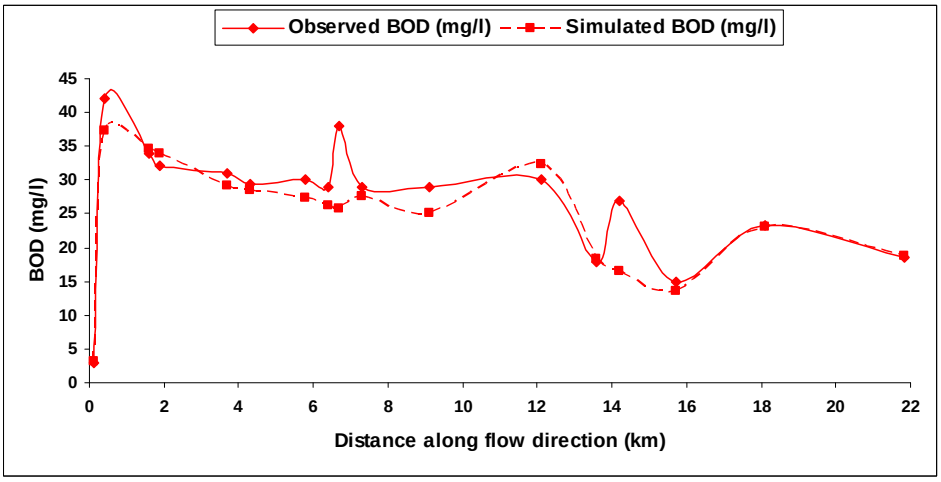

Fig 3a Validation–Profile of observed and simulated BOD

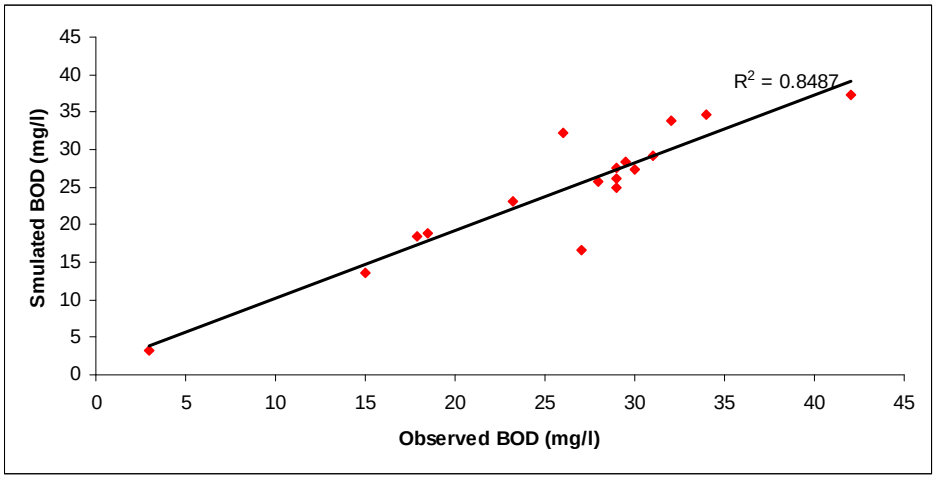

Fig 3b Validation–Correlation between observed vs. simulated BOD

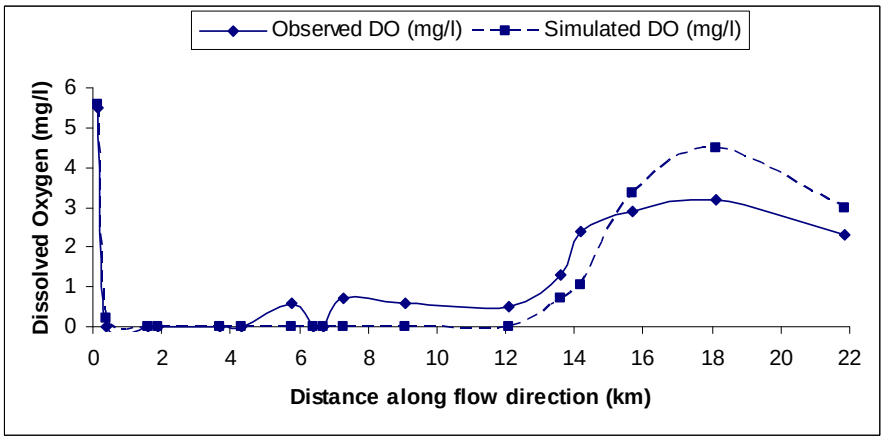

Fig 4a Validation–Profile of observed and simulated DO

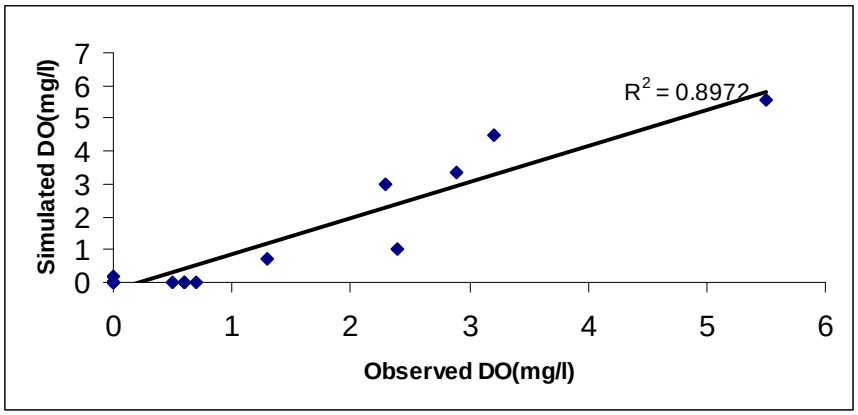

Fig 4b Validation–Correlation between observed vs. simulated DO

CONCLUSIONS

In this paper, Calibration and Validation of the QUAL2E simulation model has been carried out for the Delhi stretch of river Yamuna, India to find the most sensitive reaction coefficients, namely, the deoxygenration coefficient (K_1) and reaeration coefficient (K_2). The Calibration was accomplished by adjustment of model coefficients using trial and error method, until the best goodness of fit between predicted and observed data is achieved. The performance of the model was evaluated in terms of Coefficient of correlation (R^2) and index of agreement (IOA). Results revealed that values of these performance indicators for both, calibration and validation were found to be varying between 0.7142 to 0.9761 thus indicating satisfactory performance. Once the model is calibrated and validated, and its range of accuracy known and judged to be acceptable, it can be used for simulation of water quality. It is suggested that Calibration and validation of models must be done, if they are to be used in different site conditions.

REFERENCES

Bhargava, D. S. (1983). "Most rapid BOD assimilation in Ganga and Yamuna river." Journal of Environmental Engineering, 109(1), 174-188.

Barnwell, T. O., Brown, L. C., and Whittemore, R. C. (2004). "Importance of field data in stream water quality modeling using QUAL2E-UNCAS." Journal of Environmental Engineering, 130(6), 643-647.

C.P.C.B. (2005). "Status of sewage and sewage treatment plants in Delhi." CUPS/57/2005, Central Pollution Control Board, Delhi, India.

Delhi Jal Board (2005). Delhi water supply and sewerage project, Final report-Project preparation study, Part C: Sewerage.

Jha, R., Ojha, C.S.P., Bhatia, K.K.K. (2000). "Development of deoxygenation and reaeration rate coefficients for a small tributary of river Hindon, U.P., India." In: Proc. of International Conference on Integrated Water Resources Management for Sustainable Development, R. Mehrotra, B. Soni, and K.K.S. Bhatia, (eds.), New Delhi, 464-474.

Kazmi, A. A. and Agrawal, L. (2005). "Strategies for water quality management of Yamuna river, India." In: Proc. of third International symposium on South East Asian water environment, Bangkok, 70-80.

Melching, C. S. and Flores, H. E. (1999). “Reaeration equations derived from U.S. Geological Survey database.” Journal of Environmental Engineering, 125(5), 407-414.

Melching, C. S. and Yoon, C. G. (1996). "Key sources of uncertainty in QUAL 2E model of Passaic river.” Journal of Water Resources Planning and management, 122(2), 105-113.

Nunnaari, G., Dorling, S., Schlink, U., Cawley, G., Foxall, R., and Chatterton, T. (2004). “Modeling SO_2 concentrations at a point with statistical approaches.” Environmental Modeling and Software, 19, 887-905.

O’Connor, D.J. and Dobbins, W.E. (1958). “Mechanisms of reaeratio in natural streams.” Trans. American Society Civil Engineers, 123, 641-684

Ortolano, L. (1984). Environmental Planning and Decision Making, John Wiley & Sons, Inc., New York.

Paliwal, R., Sharma, P., and Kansal, A. (2007). “Water quality modeling of the river Yamuna (India) using QUAL2E-UNCAS.” Journal of Environmental Management, 83(2), 131-144.

Parmar, D.L. (2006). “Simulation and Multiobjective Optimization for River Quality Management.” Ph. D. Thesis, I.I.T. Delhi, India.

USEPA. (1995). QUAL2E Windows interface user's guide, United States Environmental Protection Agency, EPA/823/B/95/003.

Estimation of Evapotranspiration in Sardar Sarovar Command Area using WEAP

Rina K. Chokshi
P. G. Student, Civil Engineering Department, The M. S. University of Baroda, Vadodara - 390001, India.

Gopal H. Bhatti
Asso. Professor, Civil Engineering Department, The M. S. University of Baroda, Vadodara - 390001, India.

H. M. Patel
Professor, Civil Engineering Department, The M. S. University of Baroda, Vadodara -390001, India.
Email: haresh_patel@yahoo.com (corresponding author)

ABSTRACT

In India, rainfall is scanty and unevenly distributed over space and time. Irrigation is essential to sustain agricultural productivity for growing population. As the irrigation demand is increasing, surface water and ground water resources are limited; the efficient use of irrigation water is prime concern for water managers. To estimate the adequate crop water requirements, evapotranspiration studies are required. The process of evapotranspiration is dynamic as it is affected by weather parameters, crop related factors, methods of irrigation, management and environmental conditions. Various evapotranspiration estimation models have been developed; Penman Monteith model (P-M model) can reasonably estimate the evapotranspiration. In this study, the P-M model is used to estimate crop water requirement in Region-I of Sardar Sarovar Project command area in Gujarat, India. The study area has semi arid climate and soil texture varies from coarse to moderately fine. The crops grown in this region are cereals, pulses, ground nut, tobacco, cotton, castor, banana, sugarcane etc. As the demand for the canal water is growing for the drinking and industrial requirements, to decide the supply of canal water to agricultural area, reasonable estimation of water requirement for prevailing cropping pattern is necessary for better water management. The objective of the present study is to estimate the actual crop evapotranspiration of maize and wheat crops in the study area. In the present study daily climatological data for the year 2008-09 are used. WEAP modeling tool is used for computing daily ETc value by dual crop coefficient approach. Two different irrigation scheduling strategies, conventional and model decided, are evaluated. The quantity of surface runoff and flow to groundwater due after precipitation and irrigation are also computed. The model suggests better option of irrigation scheduling with less water requirements and ensures stress free condition.

Keywords

Evapotranspiration, Dual Crop Coefficient Approach, WEAP.

INTRODUCTION

In India, rainfall is scanty and unevenly distributed over space and time. Irrigation is essential to sustain agricultural productivity for growing population. As the irrigation demand is increasing, surface water and ground water resources are limited; the efficient use of irrigation water is prime concern for water managers. Irrigation water is to be applied at the right period and in the adequate amount. A good estimation of Evapotranspiration is required for an efficient irrigation water management. The precise estimation of Crop water requirement plays an important role in irrigation design and scheduling. Modified Penman Monteith method in conjunction with dual crop coefficient approach can provide precise estimate of crop water requirement. The recent water evaluation planning system (WEAP software) combines evaporanspiration estimation and irrigation scheduling using MABIA method. The objective of the present study is to estimate the crop water requirement using dual crop coefficient approach and further use it for irrigation scheduling strategy for the study area of Sardar Sarovar Project.

MATERIALS AND METHODS

Soil water balance of root zone needs to be computed on a daily basis and the timing as well as depth of irrigation water can be planned accordingly. Crop water requirement is the amount of water required to compensate the Evapotranspiration losses from the crop field.

Model Description

Water Evaluation and Planning System (WEAP) represents a new generation of water planning software. The design of WEAP is guided by a number of methodological considerations: an integrated and comprehensive planning framework; use of scenario analyses in understanding the effects of different development choices; Demand-management capability; Environmental assessment capability; and Ease of-use (Seiber and Purkey, 2011). It has been applied primarily in a number of studies concerning: Agricultural systems, Municipal systems, Single catchments or complex Trans-boundary river systems. MABIA method uses the dual crop coefficient approach (FAO-56) which is an improvement over CROPWAT which uses single crop coefficient approach.

Method for Estimation of Evapotranspiration

Evapotranspiration depends on:- (1) Weather parameters such as radiation, maximum and minimum temperature, humidity and wind speed; (2) Crop factors such as crop type, development stage, crop height, type of irrigation and (3) Management and environmental

conditions such as soil salinity, application of fertilizers etc. Different climatological methods are used for estimating reference crop evapotranspiration (ETo). Some of these methods are empirical methods e.g. Blaney- Criddle and other methods are based on combination approach which includes radiation term and dynamic terms e.g. Modified Penman Monteith method (FAO – 56).

Reference Evapotranspiration(ETo)

The rate of evapotranspiration from a reference surface is called reference evapotranspiration. Grass is generally used as the reference crop. ETo can be computed from metorological data and crop data. The FAO Penman-Monteith method is recommended as the sole standard method for the definition and computation of the reference evapotranspiration.

Penman Monteith Equation: (Allen et al., 1998; Allen R. G. 2002; Kumar et al.,2011)

$$ETo = \frac{0.408\,\Delta(Rn-G)+\gamma\frac{900}{T+273}U_2(es-ea)}{\Delta+\gamma(1+0.34U_2)} \quad (1)$$

Where, ETo =reference evapotranspiration [mm day-^{1}], Rn =net radiation at the crop surface [MJ m^{-2} day^{-1}], G=soil heat flux density [MJ m^{-2} day^{-1}], T= mean daily air temperature at 2 m height [°C], u_2=wind speed at 2 m height [m s^{-1}], e_s=saturation vapour pressure [kPa], e_a=actual vapour pressure [kPa], e_s-e_a=saturation vapour pressure deficit [kPa], Δ=slope vapour pressure curve [kPa °C^{-1}], γ=psychrometric constant [kPa °C^{-1}].

Potential Evapotranspiration(ETc)

It is the amount of water that would be consumed by evapotranspiration in the catchment if no water restrictions exist i.e.the soil has extensive moisture and it is covered by fully developed vegetation. Crop evapotranspiration (ETc) can be calculated by multiplying the reference ETo by crop coefficient Kc (Allen et al., 1998).

$$ETc = ETo \times Kc \quad (2)$$

After the event of irrigation or significant rainfall, during 'energy limiting stage' of the drying process, topsoil is wet and evaporation occurs at potential rate. In this situation, soil evaporation reduction coefficient (Kr) is maximum. As the soil surface dries, Kr<1 and when no water is available for evaporation in the top soil, Kr=0. Kr is calculated as follows.

$$K_r = \frac{TEW-D_{e,i}}{TEW-REW} \quad \text{for } D_{e,i-1} > REW \quad (3)$$

$$K_r = 1 \quad \text{for } D_{e,i-1} \leq REW$$

Where, TEW= Total evaporable water (mm)

REW= Readily evaporable water (mm)

$De_{,i-1}$ = Cumulative depth of evaporation from the soil surface at end of day i-1(mm)

Ze=Effective rooting depth (m)

Crop Coefficient (Kc)

Crop coefficient (Kc) can be calculated by two approaches – single crop coefficient and dual crop coefficient. In single crop co-efficient, difference in Evaporation and transpiration between field crops and reference grass surface can be integrated in a single crop coefficient (Kc), whereas in dual crop coefficient approach, it is separated into two coefficient – a basal crop (Kcb) and a soil evaporation coefficient (Ke)(Allen et al., 1998; Allen, 2005; Rossa et al., 2012).

$$\mathrm{Kc} = \mathrm{Kcb} + \mathrm{Ke}. \qquad (4)$$

The Basal Crop coefficient represents actual evapotranspiration conditions when the soil surface is dry but sufficient root zone moisture is present to support full transpiration. Soil evaporation coefficient (Ke) calculated when the topsoil dries out, and evaporation is less and evaporation reduces in proportion to the amount of water available in surface soil layer (Allen et al., 1998; Allen R. G. 2002; Allen et al., 2005).

$$Ke = K_r(K_{cmax} - K_{cb}) \leq f_{ew}K_{cmax} \qquad (5)$$

Where, Ke= soil evaporation coefficient, Kcmax=the maximum value of Kc following rain or irrigation, Kr= evaporation reduction coefficient and is dependent on the cumulative depth of evaporated water and few=the fraction of the soil that is both exposed to solar radiation and that is wetted.

Actual Evapotranspiration (ETact)

It is the amount of water that would be consumed by evapotranspiration in the catchment, including water supplied by irrigation also. It is also known as ETadj. The crop is under stress in the dry soil when the potential energy of soil water drops below the threshold value. The effect of soil water stress can be estimated by water stress coefficient (Ks) multiplied with basal crop coefficient (Kcb). The full evapotranspiration requirement is not satisfied by precipitation and irrigation. The soil water content in the root zone is reduced to very low levels to allow plant roots to extract water to satisfy evapotranspiration (Allen et al., 1998; Allen et al.,2005).

$$ET_{act} = (K_s * K_{cb} + K_e) * ETo \qquad (6)$$

When soil is wet, evapotraspiration occurs at potential rate, stress coefficient (Ks) is maximum. If there is precipitation or irrigation, Ks=1. As the soil surface dries, Ks<1 and when no water is available for evapotranspiration in the top soil, Ks=0. To avoid crop water stress, irrigation needs to be applied before or at the moment when Readily Available Water (RAW) is greater than soil moisture depletion (SMD). Ks can be calculated as follows (Allen et al., 1998; Allen R. G. 2002).

$$K_s = 1 \qquad \text{for } D_r \leq RAW$$
$$K_s = \frac{TAW - D_{r,i}}{TAW - RAW} = \frac{TAW - D_{r,i}}{(1-p)TAW} \qquad \text{for } D_r > RAW \qquad (7)$$

Where, TAW= Total Available Water (mm)
RAW= Readily Available water (mm)
Dr,i=root zone depletion at end of day i (mm)

CASE STUDY

Figure 44. Map showing command area under phase-1 of Sardar Sarovar Project

The Sardar Sarovar Project is one of the largest irrigation projects of India which feeds four major states Maharashtra, Madhya Pradesh, Gujarat and Rajasthan. The command area is 18.45 lakh hectares. The SSP command area phase – I; lies between 21^0 15'to 22^0 –53' N latitudes and 72^0–31' to 73^0 – 43' E longitudes. The subsoil water on western part has high salt and not recommended for irrigation use. Therefore Narmada water is only dependable and usable source of irrigation.

Description of Study Area

This paper represents the case study of Naswadi taluka, Vadodara district of Sardar Sarovar Project. The average annual rainfall is 1170 mm, and the rainfall is irregular and non uniform. Most of this area has the clay loam soil. The clay loam soil is having the following properties: saturation-39.00%, field capacity -30.99%, wilting point-16.55%, available water capacity-14.44%. Crops grown in this area are maize, cotton, paddy, bajra, sugarcane, castor, banana, and pulses in Kharif season and wheat, maize, sugarcane, pulses, vegetables in Rabi season. For this study, maize as Kharif crop and wheat as Rabi crop are selected. A crop of maize is sown in July at the onset of the monsoon and harvested on 22nd September. The ground is fallow until the following sowing of the crop wheat which is harvested on 28th February.

Data

For this study, water year starts from 1st March 2008 to 28th February 2009. Depth of surface layer available for drying by evaporation is taken as 100 mm. Due to precipitation or irrigation, the soil is considered at its field capacity. Therefore, initial depletion is taken as zero. Daily climate data of precipitation, wind speed, sunshine hours, maximum and minimum temperature and relative humidity of Naswadi are used. Various options can be worked out for triggering irrigation (fixed interval, % of RAW, %of TAW or fixed depletion). The irrigation amount can be decided as per the available options i.e. (fixed depth, % of RAW, % of TAW, % depletion). For this study two scenarios are considered (i) fixed interval in conjunction with fixed depth (ii) 100% RAW in conjunction with 100% of depletion (Table1). The fraction wetted is taken as 0.8.

Table 16. Irrigation Strategy for Maize and Wheat Crop

CASE NO.	CROP	PLANTING DATE	HARVESTING DATE	IRRIGATION STRATEGY	
				IRRIGATION SCHEDULING	IRRIGATION AMOUNT
I	Maize	5th July	22nd September	18th ,47th, 60th day	25 mm
	Wheat	1st November	28th February	1st, 6th, 11th, 34th, 46th, 58th, 60th, 72nd, 84th day	60 mm
II	Maize	5th July	22nd September	100% RAW	100% Depletion
	Wheat	1st November	28th February	100% RAW	100% Depletion

ANALYSIS AND DISCUSSION

WEAP model was run for maize and wheat crop for two cases. Variation of ETo and Kc in water year 2008-09 is shown in the figure 2 and 3. The values of ETo are found higher during the month of March, April and May due to higher temperature. No crops are grown in this period however the data for this period are supplied to obtain ETo for the whole year using WEAP.

The variation of Soil Moisture Deficit for Case-I and Case-II are shown in figure 4 and 5. It is observed that value of SMD with respect to TEW/TAW and REW/RAW can be classified in three situations.

(1) $REW/RAW \geq SMD$ Where, the crop will have potential evaporation and evapotranspiration.

(2) TEW/TAW $> SMD \geq REW/RAW$ Where the crop will have reduced evaporation and evapotranspiration.

(3) $SMD > TEW/TAW$ Where the crop will have no evaporation and no evapotranspiration. The Soil moisture deficit is greater than TEW. The crop will be under stress condition.

In situation (1), the distribution of moisture in the soil is not so important, since the actual evapotranspiration equals the potential value. In situation (2) and (3), crop stress coefficient (Ks) and evaporation coefficient (Ke) are introduced for allowance of reduced soil moisture(Figure 4). When a significant soil moisture deficit exist and there is substantial rainfall. The moisture is retained near the soil surface. This is most noticeable when the soil has an appreciable clay content, the soil remains moist near the ground surface and crop continue to revive for several days after significant rainfall (Rushton et al., 2005). When the soil is wet, the water has high potential energy; it is relatively free to move and is easily taken up by the plant roots. When the potential energy of the soil water drops below a threshold value, the crop is said to be water stressed. In actual practices, the irrigation is applied before the stress conditions are attained if there is no irrigation. Soil moisture depletion in both the cases is found within the limit of TAW (Figure 5 and 6). The soil reaches at field capacity after precipitation or irrigation. The WEAP computes total amount of irrigation in both the cases as follows.

Case-I, Maize**:** Irrigation depth of 25 mm with 3 watering having total irrigation of 93.75 mm.
Case-II, Maize: Total irrigation with 100% RAW and 100% depletion is 27.12 mm.
Case-I, Wheat: Irrigation depth of 60 mm with 9 watering having total irrigation of 675 mm.
Case-II, Wheat: Total irrigation with 100% RAW and 100% depletion is 436.4 mm.

It can be noticed that more water is applied than required in case-I for maize. While in case-II, for wheat, more water is applied as the irrigation strategy does not allow the crop to be under stress. ET potential and ET actual is same in case I for both the crops (maize and wheat) except in days of initial stage which shows that the soil is slightly under stress during that period. The WEAP has computed potential and actual ET for both the cases (Figure 7 and 8). In case II, potential and actual ET is same throughout the crop season signifying that the crop is not under stress. The maximum ET for maize is reached to 5.09 mm which is quite lower than maximum ET of wheat (7.81mm).

WEAP also computes runoff and deep percolation to ground water under precipitation and irrigation. In case of maize crop, total irrigation, total runoff and total flow to groundwater is marginally higher in case-I compared to case-II indicating that case-II is a better option for irrigation practices. In case of wheat crop, total irrigation, total runoff and total flow to groundwater is appreciably higher in case-I compared to case-II indicating that case-II is a better option for irrigation practices (Table 2, Figure 9 and 10).

Table 2. Runoff and Flow to Groundwater during Irrigation of Maize and Wheat Crop

CASE NO.	CROP	TOTAL ETactual (mm)	TOTAL PRECIPITATION (mm)	TOTAL IRRIGATION* (mm)	TOTAL RUNOFF (mm)	TOTAL FLOW TO GROUND WATER (mm)
1	Maize	251.12	883	75	211.78	508.42
	Wheat	478.13	0	540	352.47	108.31
2	Maize	251.39	883	21.69	178.17	484.23
	Wheat	506.00	0	349.13	0	0

* Effective Irrigation will be total irrigation divided by wetted fraction (0.8)

CONCLUDING REMARKS

The WEAP model is used in this study to find actual evapotranspiration using Penman Monteith Method and dual crop coefficient approach. Conventional irrigation strategy (Case-I) and Model determined irrigation strategy (Case-II) have been evaluated and compared for maize and wheat crops. FAO-56 Penman Monteith model is found very useful to estimate daily potential evapotranspiration using daily climatological data. Further, dual crop coefficient approach of FAO-56 separately computes soil evaporation or surface moisture depletion and transpiration under normal and water stress condition. In maize crop, actual evapotranspiration is found same in Case-I and Case-II as this crop is not under water stress in both the cases. But, in case of wheat crop; the water stress condition has resulted lower value of actual evapotranspiration in Case-I. The model specified irrigation strategy also prevents runoff and deep percolation. Thus saving of water can be achieved by application of WEAP in determining irrigation requirements in real time condition. The prevention of water stress condition by model application also improves yield of crop.

Acknowledgements

The authors wish to acknowledge the technical and data support extended by officers of Sardar Sarovar Narmada Nigam limited, Vadodara and State Water Data Centre, Gandhinagar, Gujarat, India. The authors are also thankful to WEAP developers for providing software and support for this study.

REFERENCES

- Allen R. G., Pereira L.S., Raes D. and Smith M. 1998. Crop evapotranspiration - Guidelines for computing crop water requirements –United Nations Food and Agriculture

Organization, Irrigation and drainage paper 56 Produced by: Natural Resources Management and Environment Department

- Allen R. G. 2002. Evapotranspiration : The FAO-56 Dual Crop Coefficient Method and Accuracy of predictions for Project-wide Evapotranspiration, International meeting on Advances in Drip/Micro Irrigation
- Allen R. G. 2005. FAO-56 Dual crop coefficient Method for estimating Evaporation from soil and application Extensions. Journal of Irrigation and Drainage Engineering ASCE/January/February 2005.
- Kumar R., Vijay Shankar and Mahesh Kumar. Modeling of Crop Reference Evapotranspiration : A Review. Universal journal of Environment Research and Technology, 1(3):239-246
- Rossa R. D., Paredesa P., Rdriguesa G. C., Alvesa I. , Fernandoa R. M., Pereirra L. S. 2012. Implementing the Dual Crop Coefficient approach in interactive software. Agricultural Water Management, 103 : 8-24
- Rushton K. R., Eilers V.H.M., Carter R. C. 2005. Improved soil moisture balance methodology for recharge estimation, Journal of Hydrology 318 (2006): 379-399.
- WEAP 2011. *Tutorial modules & and user guide*, Sieber J., Purkey D., Stockholm Environment Institute (SEI)

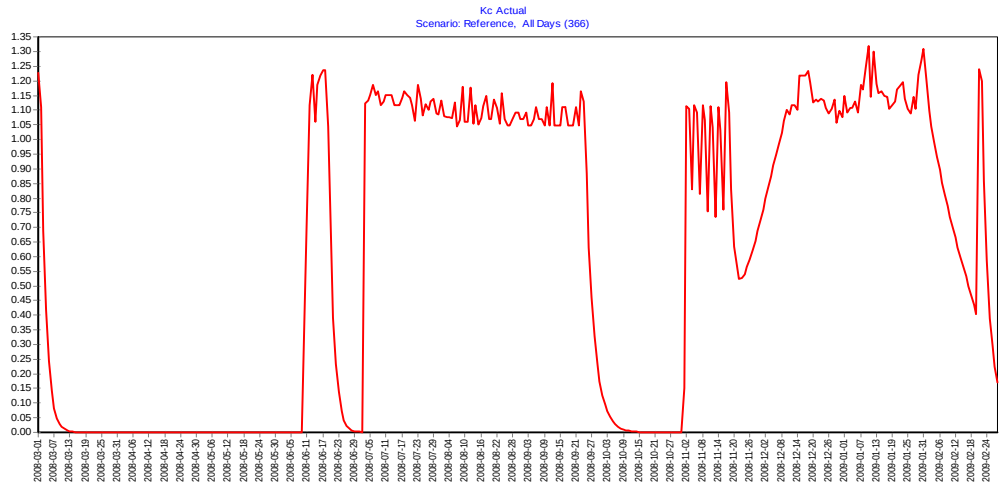

Figure 2. Kc,actual for Maize and Wheat during Water Year 2008-09

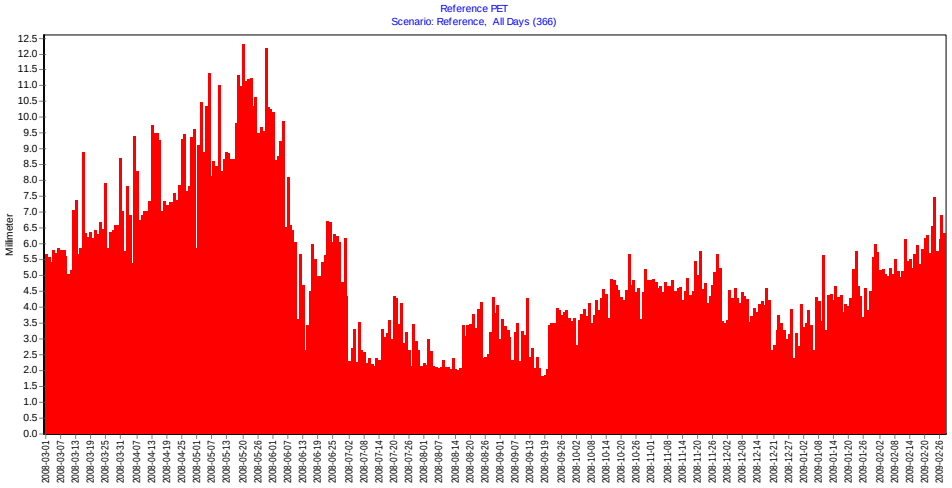

Figure 3. Reference PET (ETo) during Water Year 2008-09

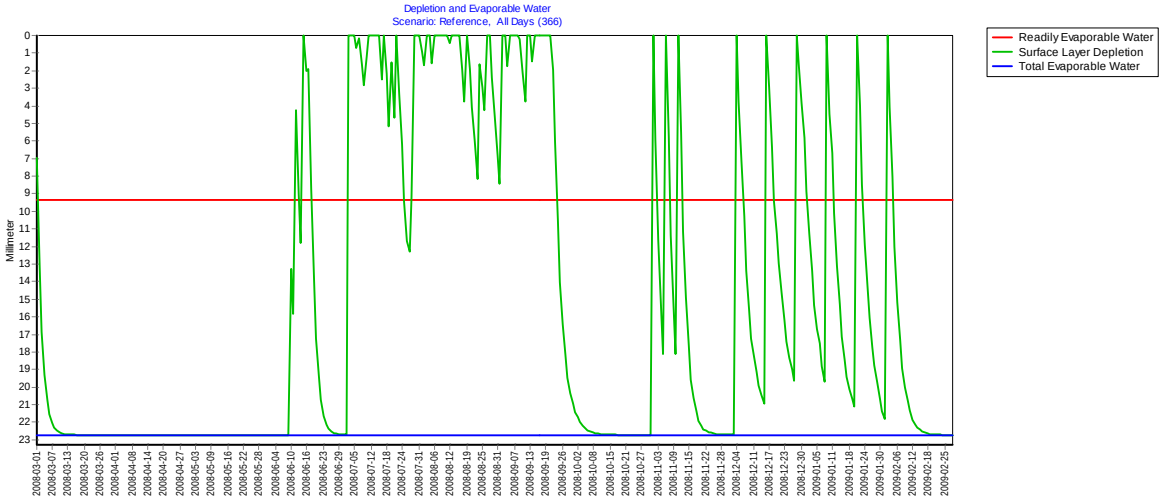

Figure 4. Surface layer depletion

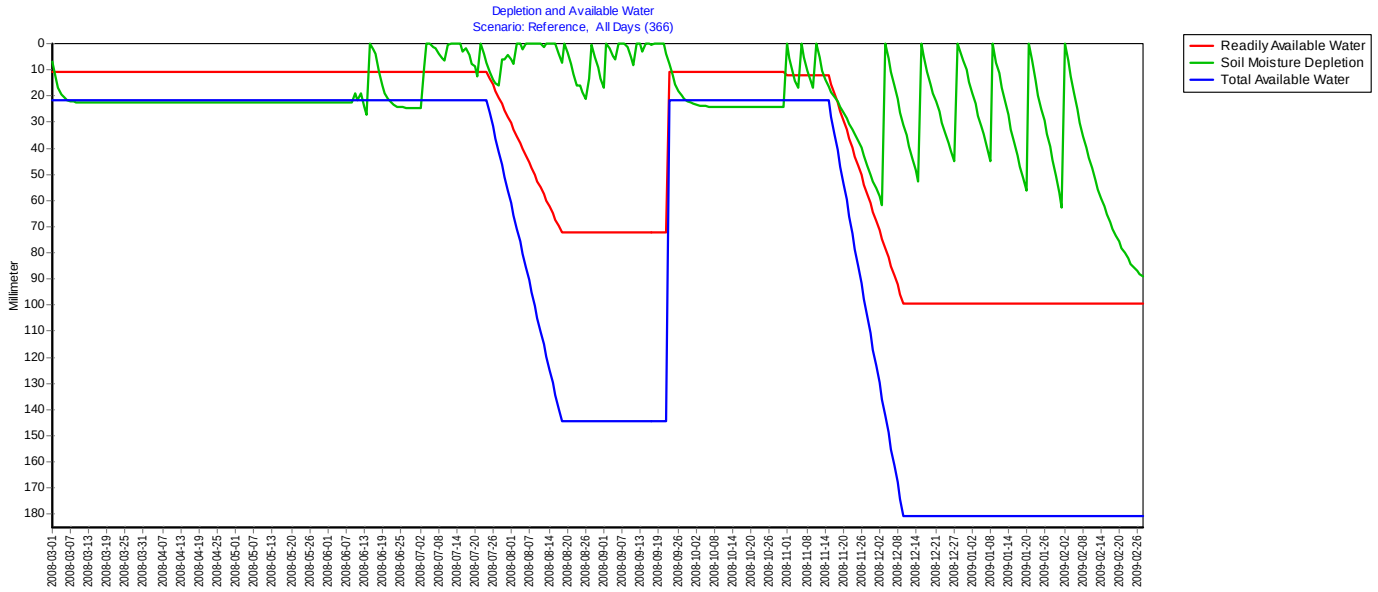

Figure 5. Soil Moisture Depletion, Readily Available Water And Total Available Water(Case-I)

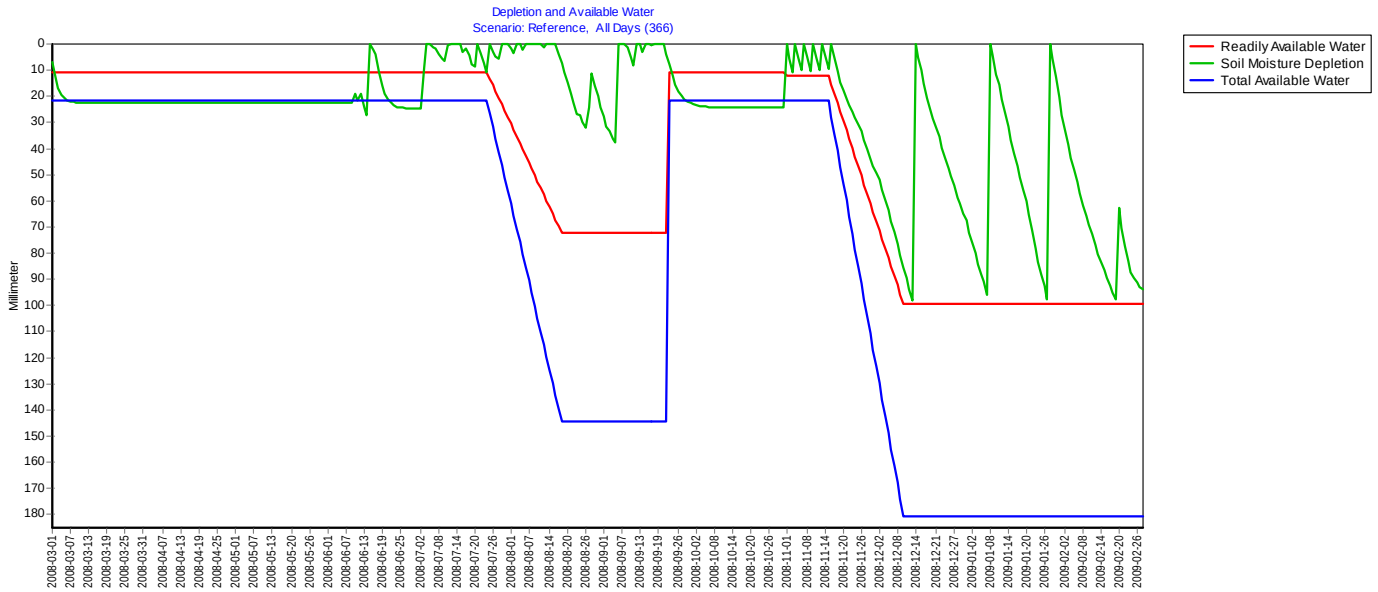

Figure 6. Soil Moisture Depletion, Readily Available Water And Total Available Water(Case-II)

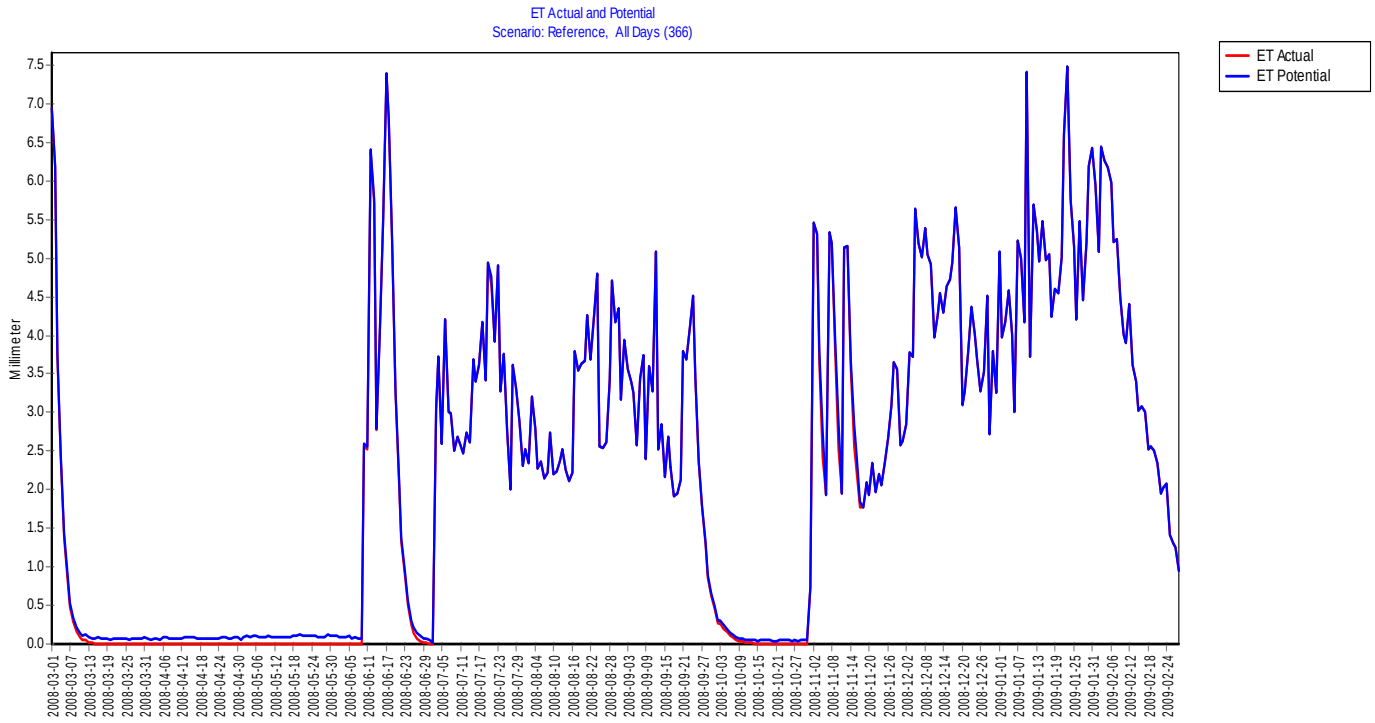

Figure 7 ETpotential and ETactual (Case-I)

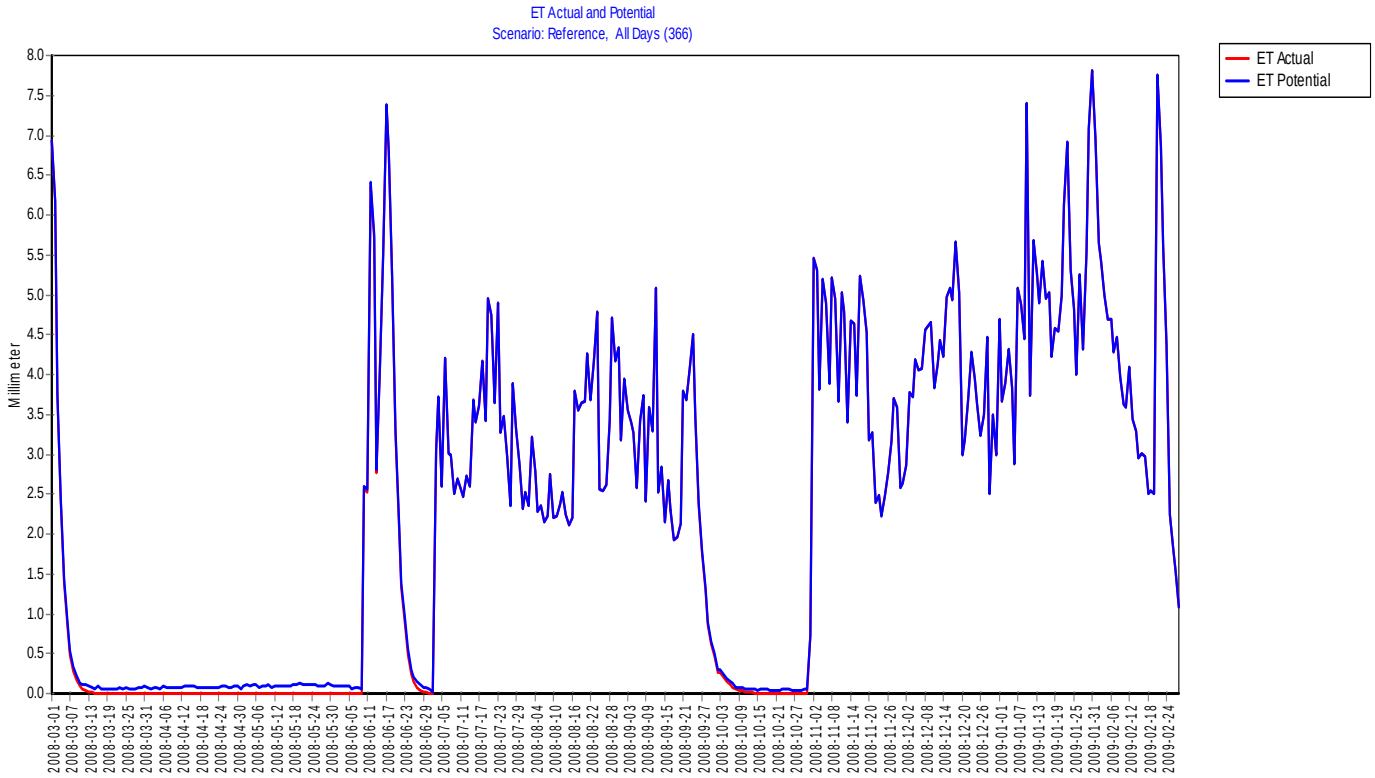

Figure 8 ETpotential and ETactual (Case-II)

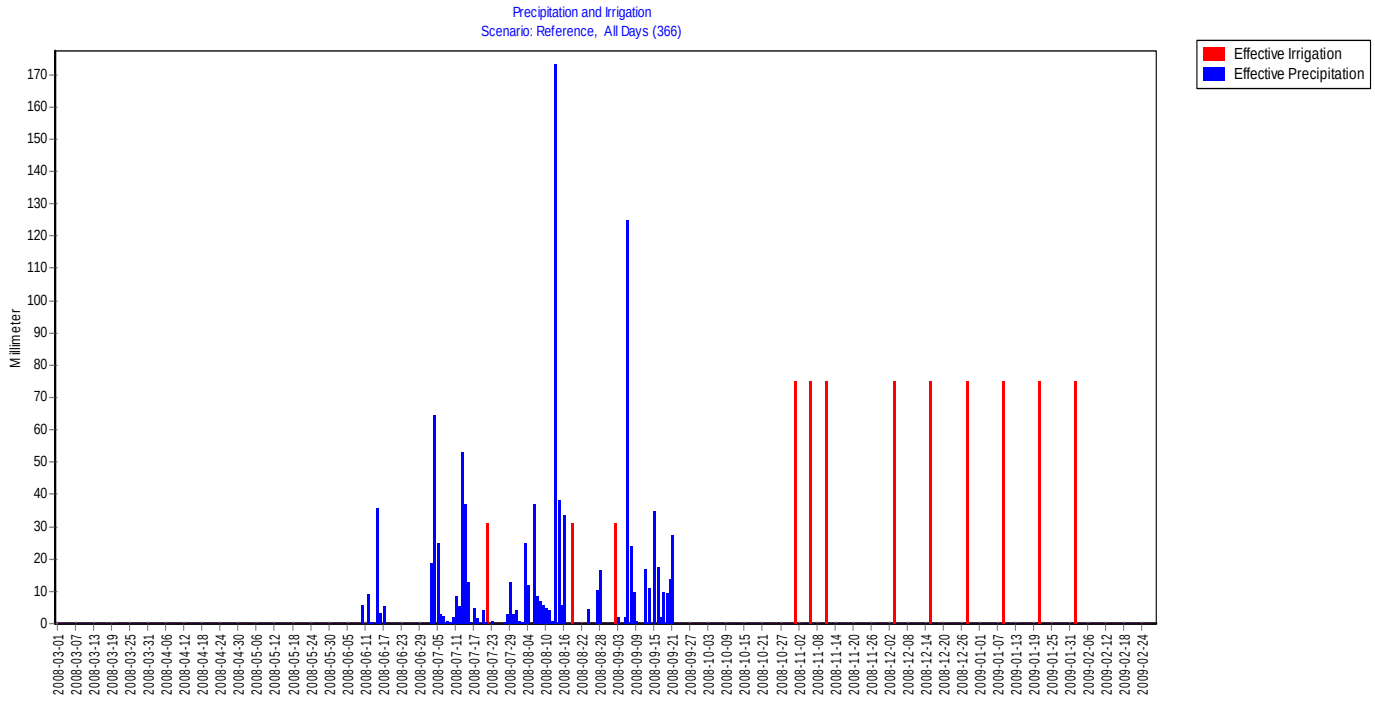

Figure 9. Effective Precipitation and Effective Irrigation (Case-I)

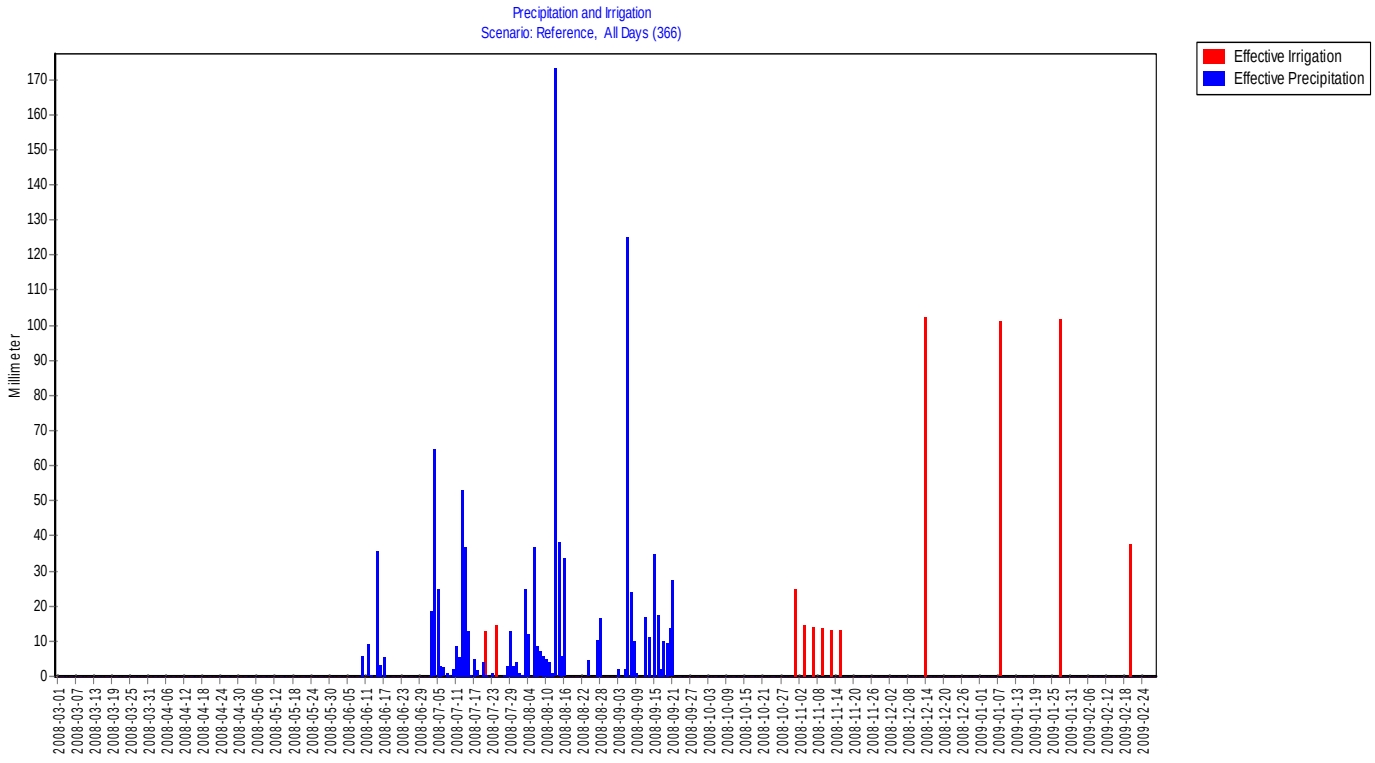

Figure 10. Effective Precipitation and Effective Irrigation (Case-II)

Application of SWAT Model in Runoff Simulation of DMIP 2 Watersheds

K. Venkata Reddy
Asst Prof, Department of Civil Engineering/NIT Warangal, Warangal – 506004, Email: kvenkatareddy9@rediffmail.com

Deva Pratap
Prof, Department of Civil Engineering/NIT Warangal, Warangal – 506004, Email: prataprec@yahoo.com

T. Reshma
Research Scholar, Department of Civil Engineering/NIT Warangal, Warangal – 506004, Email: talarireshma@yahoo.com

V. Revanth
Under Graduate student, Department of Civil Engineering/NIT Warangal, Warangal – 506004, Email: talarireshma@yahoo.com

Abstract

Developments in computer technology have revolutionized the study of hydrologic systems and water resources management. Several computer-based hydrologic/water quality models have been developed for applications in hydrologic modeling and water resources studies. Distributed parameter models, necessary for basin-scale studies, have large input data requirements. Geographic Information Systems (GIS) and model–GIS interfaces aid the efficient creation of input data files required by such models. One such model available for the water resources professionals is the Soil and Water Assessment Tool (SWAT), a distributed parameter model developed by the United States Department of Agriculture. The objective of the study presented in this paper is to evaluate the surface runoff generation for a well monitored experimental watersheds using ArcSWAT model. The model has been applied to the Distributed Model Intercomparison Project Phase –2 (DMIP2) watersheds. Rainfall data, Land Use (LU)/Land Cover (LC), soil data and Digital Elevation Model (DEM) data of the watersheds has been downloaded from the website of the Hydrology Laboratory (HL) of NOAA's National Weather Service (NWS), USA. The down loaded database has been modified in the GIS environment. The simulation of the runoff in watersheds has been carried out and is compared with observed runoff. The hydrologic behavior of watersheds has been studied based on the simulation results.

The present study emphasized the applicability of ArcSWAT models in the watersheds with geospatial database and to understand the hydrologic behavior of the watersheds.

Keywords: ArcSWAT, GIS, runoff simulation, DMIP 2 Watersheds

Introduction

SWAT is the acronym for Soil and Water Assessment Tool, a river basin or watershed scale model developed by Dr. Jeff Arnold for the USDA agricultural research services (ARS). SWAT was developed to predict the impact of land management practices on water, sediment and agricultural chemical yields in large complex watershed with varying soils, land use and management conditions over long periods of time. SWAT is a continuous time model, that is, a long-term yield model having the capability of scenario generation, so as to equip the policy makers with a wider range of options, which makes it the ideal tool to be used for such a study (Singh and Gosain, 2011).

The Hydrology Laboratory (HL) of NOAA's National Weather Service (NWS) initiated the second phase of the Distributed Model Intercomparison Project (DMIP 2). The main aim of DMIP 2 is to invite the academic community and other researchers to guide the NOAA/ NWS's distributed modeling research by participating in a comparison of distributed models applied to test data sets in two vastly different geographic regions. The complete geospatial and hydrological database of DMIP 2 watersheds is kept in the website (http://www.nws.noaa.gov/oh/hrl/dmip/2/) and made it available for public users.

Luzio and Arnold (2005) described the background, formulation and results of an hourly input–output calibration approach proposed for the SWAT watershed model. They applied the methodology for 24 representative storm events occurred during the period between 1994 and 2000 in the Blue River basin, USA. Kalin and Mohammed (2006) described the potential use of Next Generation Weather Radar (NEXRAD) technology as an alternative source of precipitation data to the conventional surface rain gauges. They calibrated and validated the SWAT model for monthly stream flow, base flow and surface runoff. Hydrographs generated from both gauge and NEXRAD driven model simulations compared well with observed flow hydrographs. Pranay et al., (2012) presented the critical hydrologic processes and corresponding SWAT parameters that affect the volume and timing of monthly flow generation in mountainous watersheds and also

suggest a common SWAT parameter set for snow dominated and mountainous watershed and the results justify the applicability of the ArcSWAT model in snow dominated and mountainous watersheds. This paper presents the application of ArcSWAT model in simulation of hourly runoff in the DMIP-2 watersheds.

Study area and Methodology

The ArcSWAT model has been applied to the Blue river basin, USA. It is one of the experimental watersheds of DMIP-2. It has an area of 1233 sq km. The methodology adopted for simulation of flow in the Blue River is shown in Figure 1. Relevant geospatial and hydrological data of the study area has been downloaded from the website of the Hydrology Laboratory (HL) of NOAA's National Weather Service (NWS), USA in ASCII format. The ASCII data is converted to raster data and projected to UTM 14N. Then the geospatial data is clipped to the blue river basin.

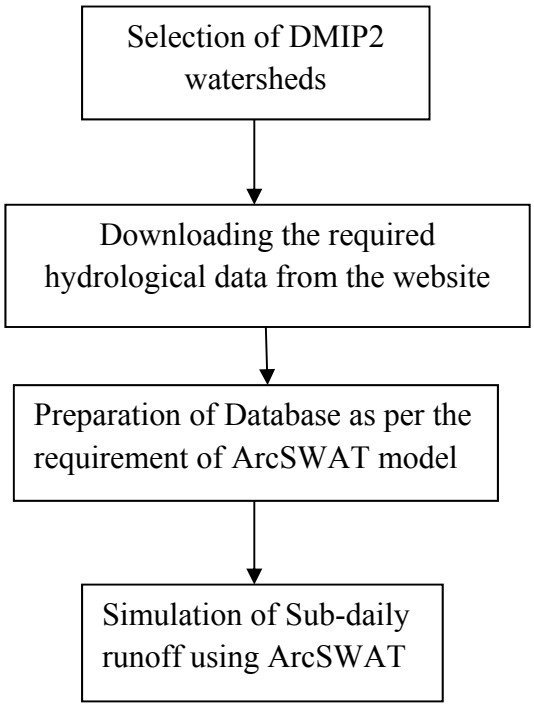

Figure 1: Flow chart showing the methodology followed in the present study

SWAT Model Application

The input for ArcSWAT model consists of Digital Elevation Model (DEM), rainfall, soil characteristics, topography, vegetation and other relevant physical parameters of the watershed. ArcSWAT model is applied for the hourly runoff simulations of the watershed. The model has been used for the sub-daily runoff simulation. The extracted rainfall data of the study area which is in .asc format is converted to raster data using ArcTool box. Then all rainfall files are reprojected to UTM. Automatic delineation of watershed boundary and other sub-watersheds within the watershed has been carried out using DEM of the watershed in the SWAT model. The watershed boundary with sub-basins is shown in Figure 2. The slope map, soil map and Land Use/Land Cover map which are modified as per the standard classifications available in the SWAT model are shown in Figure 3, Figure 4 and Figure 5 respectively. The soil classes of Blue river watershed are as follows: sand (4.17%), Sandy Loam (24.87%), Silt Loam (0.21%), Loam (52.43%), Silt Clay (4.1%) and Clay (14.10%). LU/LC classes of the watershed are as follows: Evergreen Needle leaf Forest (4.2%), Deciduous Broadleaf Forest (13.41%), Mixed Forest (0.96%), Woody Savannah (77.37%), Grasslands (1.97%), Croplands (0.86%), Urban and Built-Up (0.99%) and Cropland/Natural Vegetation Mosaic (0.21%). In SWAT, a watershed can be divided into multiple sub-watersheds, which are then further subdivided into unique soil/land use categories called Hydrologic Response Units (HRUs). In ArcSWAT model, Simulation of flow has to be carried out in the five steps (1) Project set up (2) watershed Delineation (3) HRU definition (4) Weather Generator data (5) Run SWAT.

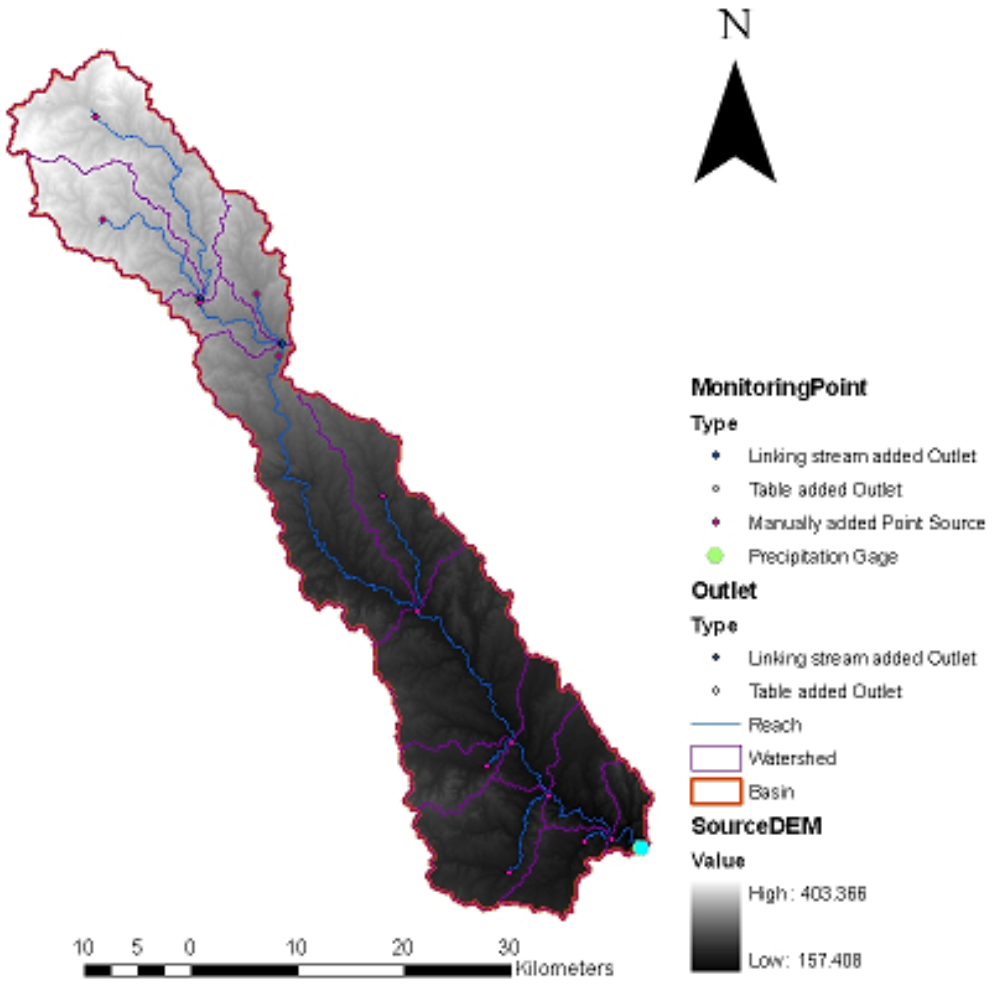

Figure 2: Automatic delineation sub-basins of Blue river basin in ArcSWAT

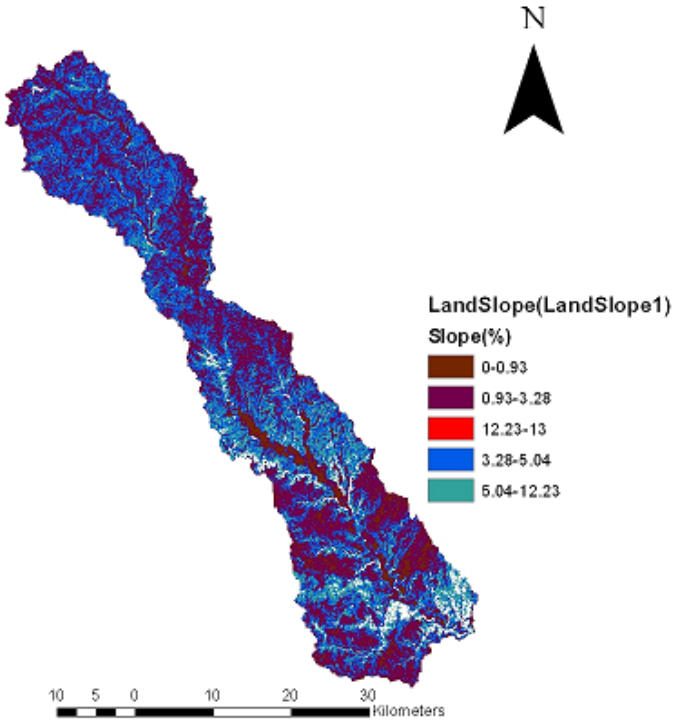

Figure 3. Modified slope map of Blue river basin

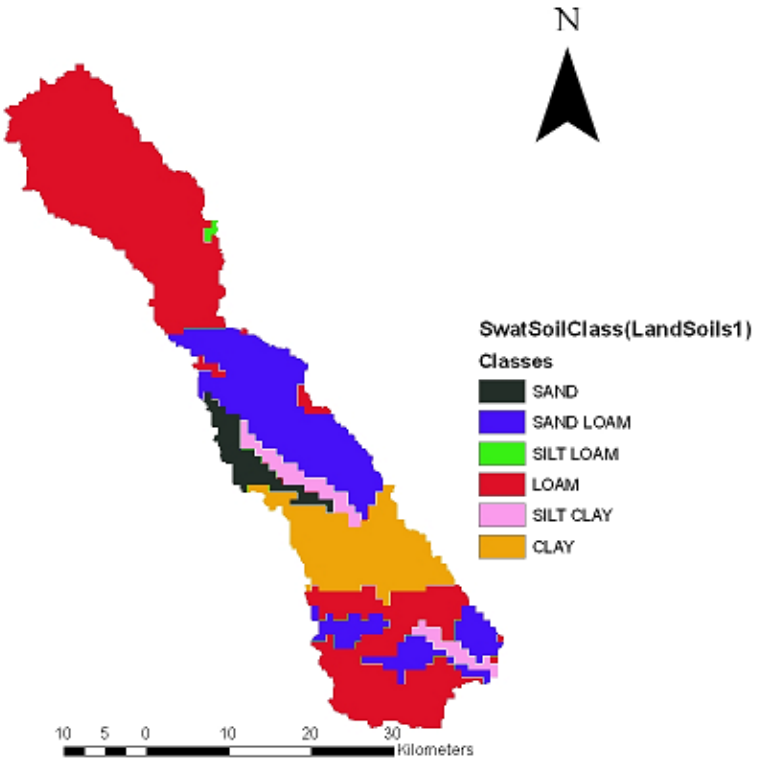

Figure 4. Modified soil map of Blue river basin

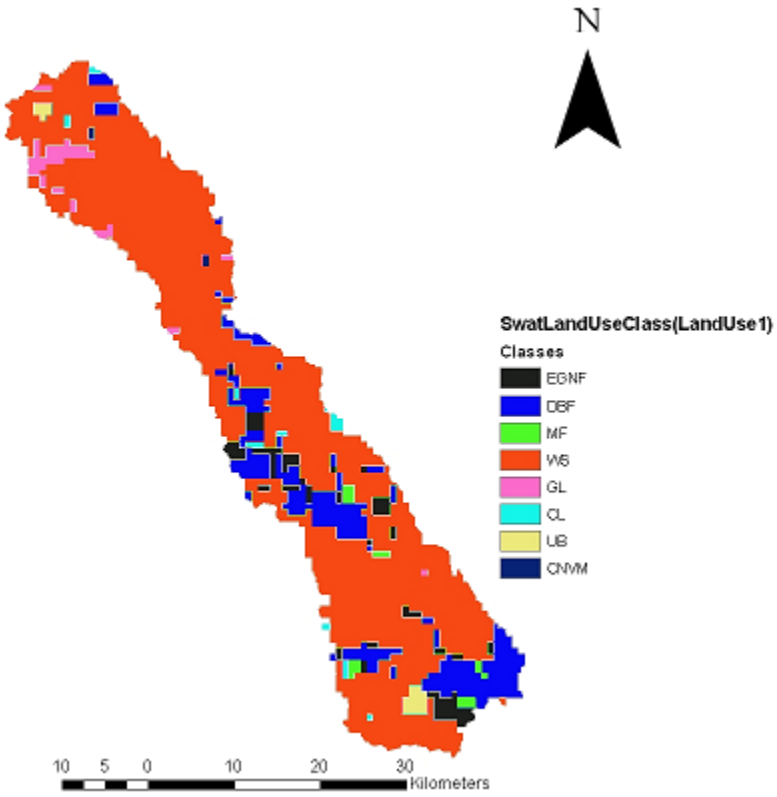

Figure 5. Modified Land use/Land cover map of Blue river basin

Results and Discussions

August, 2002 rainfall has been used as input for simulation of runoff. The simulated runoff hydrograph is shown in Figure 6. Simulation results are shown in Table 1. From the hydrograph, it is seen that the volume of runoff and time to peak has been simulated within the variation 70%. However, the model was not able to capture the peak runoff. There are more than sixty parameters in SWAT model and it is difficult to have exact information on all these parameters. Some physical parameters such as Channel width and Channel depth vary along the channel reaches. These are the some of the reasons for improper simulation of peak runoff. It is observed that, the values of runoff on recession limb of hydrographs are higher than observed one. The channel roughness and infiltration parameters are may be the reasons for this behavior. The calibration and sensitivity analysis of model may improve the simulations.

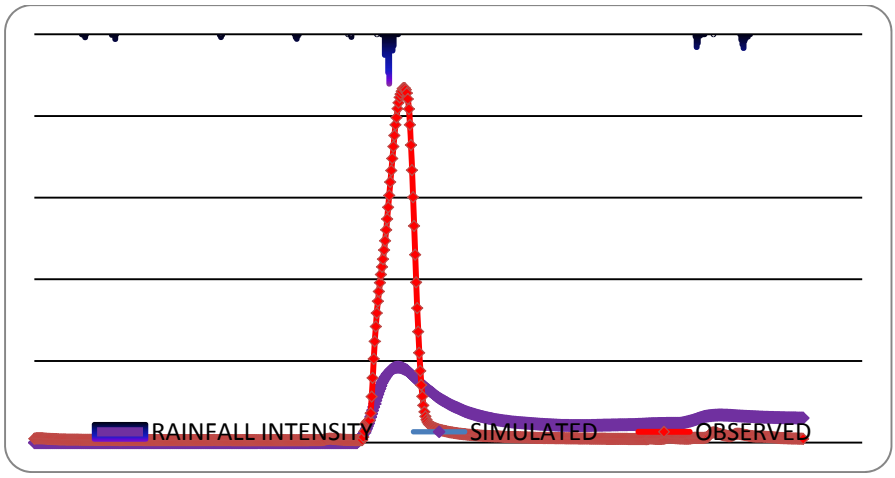

Figure 6. Simulation and observed runoff hydrographs for the Blue river basin for the month of August, 2002

Table 1. Simulation results for Blue River Basin

Rainfall month	Volume of runoff (mm)		Peak runoff (m3/sec)		Time to peak (sec)	
	observed	simulated	observed	simulated	observed	simulated
August, 2002	2596.716	2172.707	217.04	41.6	358	358

Conclusions

This study describes the application of ArcSWAT model for simulation of sub-daily runoff on DMIP 2 watershed. The model has been applied for the August, 2002 rainfall data. From the simulation it is observed that, model is able to simulate the volume of runoff and time to peak runoff, but large variations are observed in peak runoff. This may be because that sensitivity analysis over the model parameters may improve the simulation results. Presently only one rainfall event is simulated to understand the applicability of ArcSWAT model for hourly flow simulation in DMIP-2 watersheds. The simulation of runoff for other rainfall events and study of hydrologic regime of watershed is under progress. The present study emphasized the applicability of ArcSWAT models in the watersheds with complete geospatial dataset and to understand the hydrologic behavior of the watersheds.

References

Luzio, M. Di. and J. G. Arnold. (2004). Formulation of a hybrid calibration approach for a physically based distributed model with NEXRAD data input. *Journal of Hydrology*. 298,136-154.

Kalin, L. and M. M. Hantush. (2006). Hydrologic Modeling of an Eastern Pennsylvania Watershed with NEXRAD and Rain Gauge Data. *Journal of Hydrologic Engineering. Vol. 11(6),555–569.*

Pranay, S., M. Ahmadi, and M. Arabi. (2012). GIS Application of SWAT- Hydrologic modeling in major river basins of Colorado. *AWRA 2012 spring specialty conference new orleans, louisiana,* march 26 – 28.

Singh, A. and A. K. Gosain. (2011). Scenario generation using geographical information system (GIS) based hydrological modelling for a multijurisdictional Indian River basin. *Journal of Oceanography and Marine Science.* 2(6), 140–147.

Acknowledgements

Our sincere thanks to officials of Distributed Hydrologic Model Intercomparison Project - Phase 2 (DMIP 2) for maintaining the geospatial and hydrological data of DMIP 2 watersheds in the public domain through website

(http://www.nws.noaa.gov/oh/hrl/dmip/2/).

A Simplified Channel Routing Scheme Suitable for Adoption in SWAT Model

Muthiah Perumal*, Ph.D.
Department of Hydrology, Indian Institute of Technology Roorkee, Roorkee, India, E-mail: p_erumal@yahoo.com

Bhabagrahi Sahoo, Ph.D.
School of Water Resources, Indian Institute of Technology Kharagpur, Kharagpur, India; Formerly, at ICAR Research Complex for NEH region, Nagaland Centre, Jharnapani, Medzimphema-797106, India, E-mail: bsahoo2003@yahoo.com

C. Madhusudana Rao, Ph.D.
Department of Civil Engineering, National Institute of Technology Jamshedpur, India; Formerly, at Department of Hydrology, Indian Institute of Technology Roorkee, Roorkee, India, E-mail: madhu_chintalacheruvu@yahoo.co.in

Abstract

A suggestion for replacing the existing channel routing schemes adopted in the SWAT model (viz., variable storage routing and classical Muskingum methods), by the variable parameter McCarthy-Muskingum (VPMM) method recently proposed by Perumal and Price (2012) is presented in this study. This fully mass conservative routing method is derived from the Saint-Venant equations and is suitable for routing floods in natural river reaches. The nonlinearity of the routing process is taken care of by varying the parameters of the Muskingum method, which are linked to the channel and flow characteristics, at every computational time and space step levels. The paper also demonstrates using numerical experiments that the performance of the VPMM method is far better than the currently available variable parameter Muskingum-Cunge method and the variable parameter Muskingum-Cunge-Todini method in reproducing the observed hydrographs. Further, this method is fully volume conservative which is independent of the size of the spatial step used. Use of the VPMM method in the channel routing sub-module of the current version of the SWAT model definitely will reduce the model uncertainties significantly.

Keywords: Floods, Hydrograph, Muskingum, Routing, SWAT.

_____ *Conference speaker

Introduction

The Soil Water Transfer Assessment Tool (SWAT) is a semi-physically model that operates at the river basin scale to predict the impact of land management practices on water, sediment and agricultural chemical yield (Neitsch et al., 2011). The various physical processes associated with this model are water movement, sediment movement, crop growth, nutrient cycling etc. To simulate the water movement in the overland and channels, the SWAT model uses the variable storage routing method (Williams, 1969) in which the storage coefficient and travel time are variable; and the classical Muskingum method (Chow et al., 1988) in which the storage coefficient, X and the storage time constant, K are the user-defined constant parameters. However, with the advancement of the hydrological literature in the recent years, which has moved from the linear models with constant parameter to physically-based variable parameter models to deal with the nonlinear dynamism of flow of water, there is a need to upgrade the present version of the SWAT model in this regard.

The linear storage equation proposed by McCarthy (1938), which expresses the storage as a linear weighted function of the inflow and the outflow, forms the basis for the development of the classical Muskingum method. However, in this classical Muskingum equation, the routing parameters remain constant over the entire duration of routing process. Note that the routing parameters of the linear or nonlinear storage equations of the hydrologic methods were estimated using only the inflow, outflow, and the corresponding channel storage information pertaining to a particular flood event without directly involving the physically measurable channel characteristics, viz., the channel geometry and roughness. This limits the applicability and predictive capability of the hydrologic routing methods only to those flood events which are within the range of the events used in the calibration of the parameters.

Moreover, the Muskingum method, conventionally considered as a storage routing method, can be linked to the hydrodynamics-based methods as investigated by Apollov et al. (1964), Cunge (1969), Dooge (1973), and Dooge et al. (1982). With the advent of several variable parameter based simplified hydraulic models in the literature, such as, the variable parameter Muskingum-Cunge (VPMC) method (Ponce and Chaganti, 1994; NERC 1975; Cunge, 1969), variable parameter Muskingum-Cunge-Todini (MCT) method (Todini, 2007), and variable parameter McCarthy-Muskingum (VPMM) method (Perumal and Price, 2012), there is a need to compare all these methods with the classical Muskingum (CM) method built into the SWAT model to decipher their best suitability. Considering this fact in view, in this paper, a numerical experimental study has been carried out to compare the VPMC, MCT and VPMM routing schemes with the CM method.

Model Description

Classical Muskingum (CM) Routing Method

The CM method employs the classical Muskingum routing equation of McCarthy (1938), which is expressed as

$$O_{j+1} = C_1 O_j + C_2 I_j + C_3 I_{j+1} \quad (1)$$

where O = outflow; I =inflow; j = temporal index; and

$$C_1 = \frac{-KX + 0.5\Delta t}{K(1-X) + 0.5\Delta t};\ C_2 = \frac{KX + 0.5\Delta t}{K(1-X) + 0.5\Delta t};\ \text{and}\ C_3 = \frac{K(1-X) - 0.5\Delta t}{K(1-X) + 0.5\Delta t} \quad (2a,b,c)$$

in which the routing parameters *K* and *X* are kept constant at every routing time step of Δt.

VPMC Routing Method

The VPMC method is developed using the concept of matching the numerical diffusion with the physical diffusion. This method employs the same classical Muskingum routing equation of McCarthy (1938) given by equation (1) in which the routing parameters vary at each routing time step given by (Ponce and Chaganti, 1994)

$$K = \Delta x / c;\ X = 0.5 - Q/(2S_o Bc\Delta x) \quad (3,4)$$

where c = wave celerity; Δx = routing space step; Q = reference discharge; S_o = channel bed slope; and B = channel top width.

MCT Routing Method

The model framework of the MCT method can be given by (Todini, 2007)

$$O_{j+1} = \frac{-1 + C^*_{j+1} + D^*_{j+1}}{1 + C^*_{j+1} + D^*_{j+1}} I_{j+1} + \frac{1 + C^*_j - D^*_j}{1 + C^*_{j+1} + D^*_{j+1}} \frac{C^*_{j+1}}{C^*_j} I_j + \frac{1 - C^*_j + D^*_j}{1 + C^*_{j+1} + D^*_{j+1}} \frac{C^*_{j+1}}{C^*_j} O_j \quad (5)$$

where $C^*_j = (c_j / \beta_j)(\Delta t / \Delta x)$; $C^*_{j+1} = (c_{j+1} / \beta_{j+1})(\Delta t / \Delta x)$; $\beta_j = c_j / v_j$; $\beta_{j+1} = c_{j+1} / v_{j+1}$; $D^*_j = Q_j / (\beta_j B S_o c_j \Delta x)$; $D^*_{j+1} = Q_{j+1} / (\beta_{j+1} B S_o c_{j+1} \Delta x)$; c_j and c_{j+1} are the wave celerities at j and $j+1$ time steps, respectively; v_j and v_{j+1} are the wave velocities at j and $j+1$ time steps, respectively; and Q_j and Q_{j+1} are the reference discharges at j and $j+1$ time steps, respectively.

VPMM Routing Method

Recently, Perumal and Price (2012) proposed a physically based, fully mass conservative variable parameter McCarthy-Muskingum method, taking into account the storage concept of McCarthy (1938). This method is derived directly from the Saint-Venant equations governing the laws of continuity and momentum of the one-dimensional unsteady flow, without considering the concept of matching the numerical diffusion with the physical diffusion as in the case of the VPMC method. The method of variation of the VPMM model parameters, which are evaluated using the channel and flow characteristics at every routing time interval, is consistent with the variation built-into the solution of the full Saint-Venant equations, accounting for the slope of water surface. The VPMM method is based on the hypothesis that during steady flow in a river reach having any shape of prismatic cross-section, the stage and, hence, the cross-sectional area of flow at any point of the reach is uniquely related to the discharge at the same

location defining the steady flow rating curve. However, during unsteady flow, the same unique relationship is maintained between the stage and the corresponding steady discharge at any given instant of time, recorded not at the same section, but at a downstream section preceding the corresponding steady stage section (midsection) of the routing reach. The definition sketch of the routing reach of the VPMM method is shown in Figure 1.

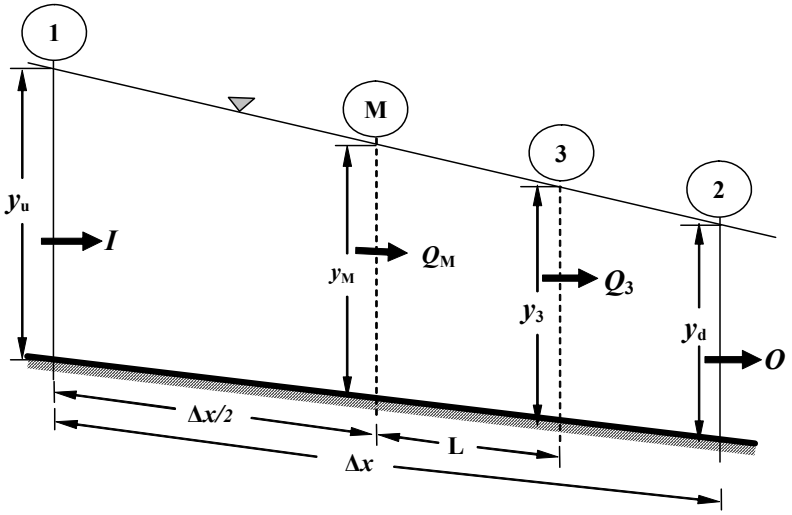

Figure 1. Definition sketch of the VPMM routing method.

The routing equation for the VPMM method can be given by (Perumal and Price, 2012)

$$O_{j+1} = \frac{0.5\Delta t - K_{j+1}X_{j+1}}{0.5\Delta t + K_{j+1}\left(1-X_{j+1}\right)} I_{j+1} + \frac{0.5\Delta t + K_j X_j}{0.5\Delta t + K_{j+1}\left(1-X_{j+1}\right)} I_j + \frac{-0.5\Delta t + K_j\left(1-X_j\right)}{0.5\Delta t + K_{j+1}\left(1-X_{j+1}\right)} O_j \tag{6}$$

where the routing parameters, K and X at the time level $\left(j+1\right)$ are expressed, respectively, as

$$K_{j+1} = \Delta x / V_{Mo,j+1} \tag{7}$$

$$X_{j+1} = 0.5 - Q_{3\,j+1} / \left(2 S_o B_{Mo,j+1}\, c_{Mo,j+1}\, \Delta x\right) \tag{8}$$

where V =velocity of flow; the suffices M and 3 refer to the variables computed at sections 'M' and '3' in Figure 1, respectively; and the suffix M_o associated with a flow variable denotes the normal discharge estimate corresponding to y_M . The discharge $Q_{3,j+1}$ is estimated as

$$Q_{3,j+1} = X_{j+1} I_{j+1} + (1 - X_{j+1}) Q_{j+1} \tag{9}$$

Numerical Application

The performance of the MC, VPMC, MCT and VPMM discharge routing methods were evaluated by routing in different hypothetical prismatic rectangular and trapezoidal cross-section channel reaches characterized by different sets of bed slopes ($So \in \{0.002, 0.001, 0.0008, 0.0005, 0.0004, 0.0002, 0.0001\}$), Manning's roughness coefficients ($n \in \{0.01, 0.02, 0.03, 0.04, 0.05\}$), and channel side slopes ($z \in \{0, 1, 3, 5\}$). Further routing in each of these test channels were carried out for a reach length of 40 km and all these channels were characterized by a bed width of 100m. The routed hydrographs obtained by routing the given hypothetical input discharge hydrographs were compared with the corresponding benchmark solutions of the Saint-Venant equations. The inflow hydrograph estimated at the inlet of the reach was obtained by routing the

given input stage hydrograph using the explicit finite difference scheme of the Saint-Venant equations, and it formed the upstream boundary condition. The given stage hydrograph is used to generate different inflow discharge hydrographs corresponding to each of the channel reach configuration considered. The input stage hydrograph used in the study was of the form of Pearson type III distribution, expressed as

$$y(0,t) = y_b + \left(y_p(t) - y_b\right)\left[\frac{t}{t_p}\right]^{1/(\gamma-1)} \exp\left[\frac{1-t/t_p}{\gamma-1}\right] \tag{10}$$

where $y(0,t)$ = stage at the upstream end ($x = 0$) of the channel reach (m); y_b = initial steady flow depth corresponding to an initial steady discharge of Q_o =100 m^3/s; y_p = peak stage (m) with a corresponding peak discharge of Q_p (m^3/s); t_p = time to peak stage (h); t = time variable; and γ = shape factor. No lateral flow was considered in these numerical experiments

The combination of input stage hydrograph characteristics used in this numerical experimental study are: $y_p \in \{5, 8, 10, 12, 15\}$ and $t_p \in \{5, 10, 15, 20\}$. A spatial step of $\Delta x = 1$ km and a routing time interval of $\Delta t = 5$ minutes were used while routing the input discharge hydrograph using all the simplified routing methods.

Performance Evaluation Measures

The efficacy of all the routing methods considered herein were evaluated using four performance evaluation measures: i) Nash–Sutcliffe criterion of variance explained, η (in %) (Nash and Sutcliffe, 1970; ASCE, 1993); iii) error in volume, *EVOL* (in %); iii) error in peak discharge, q_{per} (in %), expressed as q_{per} = (computed peak discharge/ observed peak discharge – 1) ×100; and iv) error in time to peak discharge, t_{pqer} (in %), expressed as t_{pqer} = (computed time to peak discharge/ observed time to peak discharge – 1) ×100.

Results and Discussion

Figure 2 reveals the variation of the Nash–Sutcliffe criterion of variance explained, η with respect to the maximum value of non-dimensional water surface gradient, $(1/S_o)(\partial y/\partial x)_{\max}$ for all the numerical experiments by all the four routing methods considered herein. It can be surmised from Figure 2 that while the variance explained by the CM and VPMC methods are poor, the MCT and VPMM methods show much better efficiencies. The model efficiency decreases in the sequence of VPMM>MCT>VPMC>MC. Moreover, the VPMM method always perform with more than 95% model efficiency for most of the practical flood routing cases, explained by $(1/S_o)(\partial y/\partial x)_{\max}$. Similarly, Figure 3 illustrates the volume conservation capability of all the routing cases studied herein, which reveals that the CM, MCT and VPMM methods are fully mass conservative; whereas there is always a loss of mass up to 30% by the VPMC method. Hence, the VPMC method has a limited use for various water assessment projects including the inter-basin and intra-basin water transfer purposes where the volume of water plays a major role. However, as far as the error in peaks of the discharge hydrographs, q_{per} are concerned as shown in Figure 4, the CM, MCT and VPMM methods perform almost equally well; while the VPMC method perform poorly with an under-estimation of peak discharge up to 50%. This limits the application of the VPMC method for the purposes of flood forecasting and design flood

estimation. A similar conclusion can also be drawn from Figure 5 illustrating the percentage error in time-to-peaks of the routed discharge hydrographs by all the four methods.

Furthermore, to test the volume conservation capability of the MCT and VPMM routing methods at coarser spatial and temporal resolutions, 222 routing experiments were carried out in a 100 km trapezoidal channel reach having a side slope, z = 3.0, bottom width, b=100 m with varying channel slope and Manning's roughness coefficients; considering Δx = 12.5 km and Δt = 1800 s for routing the same inflow hydrograph. The routing solutions illustrated in Figure 6 clearly reveal that the MCT method is not fully volume conservative, while the VPMM method is fully volume conservative. Hence, these results clearly reveal that the classical Muskingum scheme being used in the SWAT model is not appropriate, and this should be replaced with the VPMM method, which is more accurate as compared to the available simplified models in the recent literature.

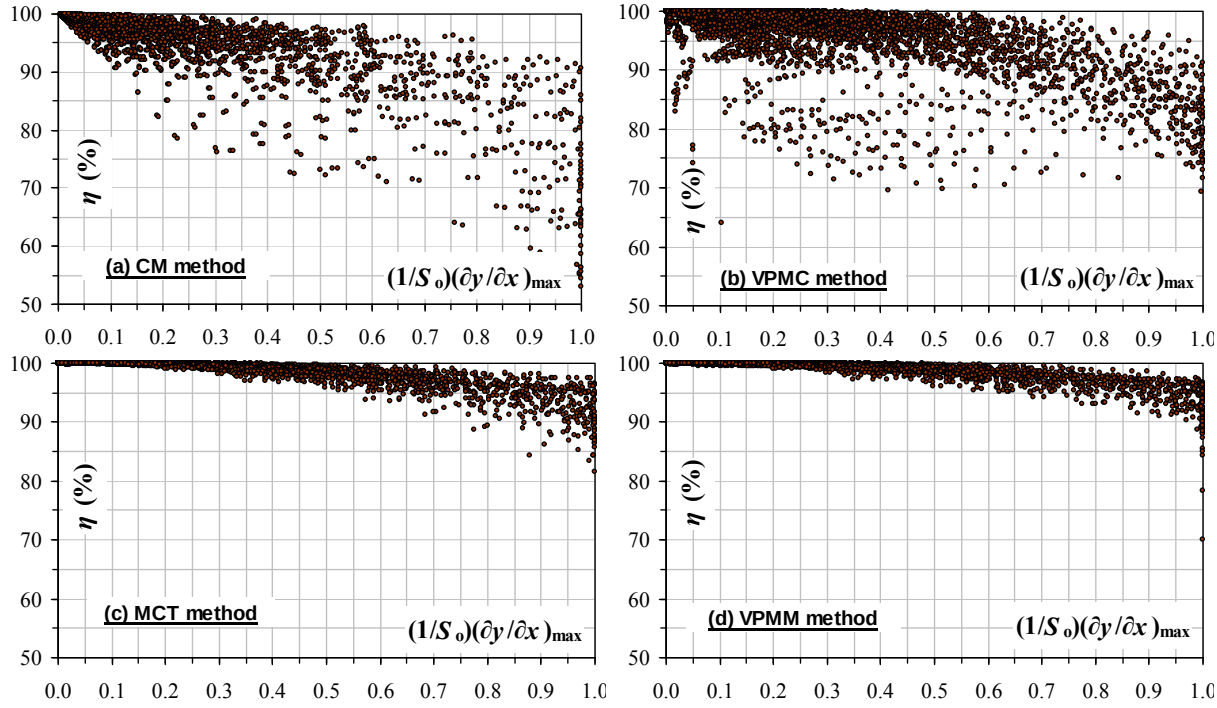

Figure 2. Performance evaluation of the (a) classical Muskingum method, (b) VPMC method, (c) MCT method, and (d) VPMM method using the Nash–Sutcliffe criterion of variance explained.

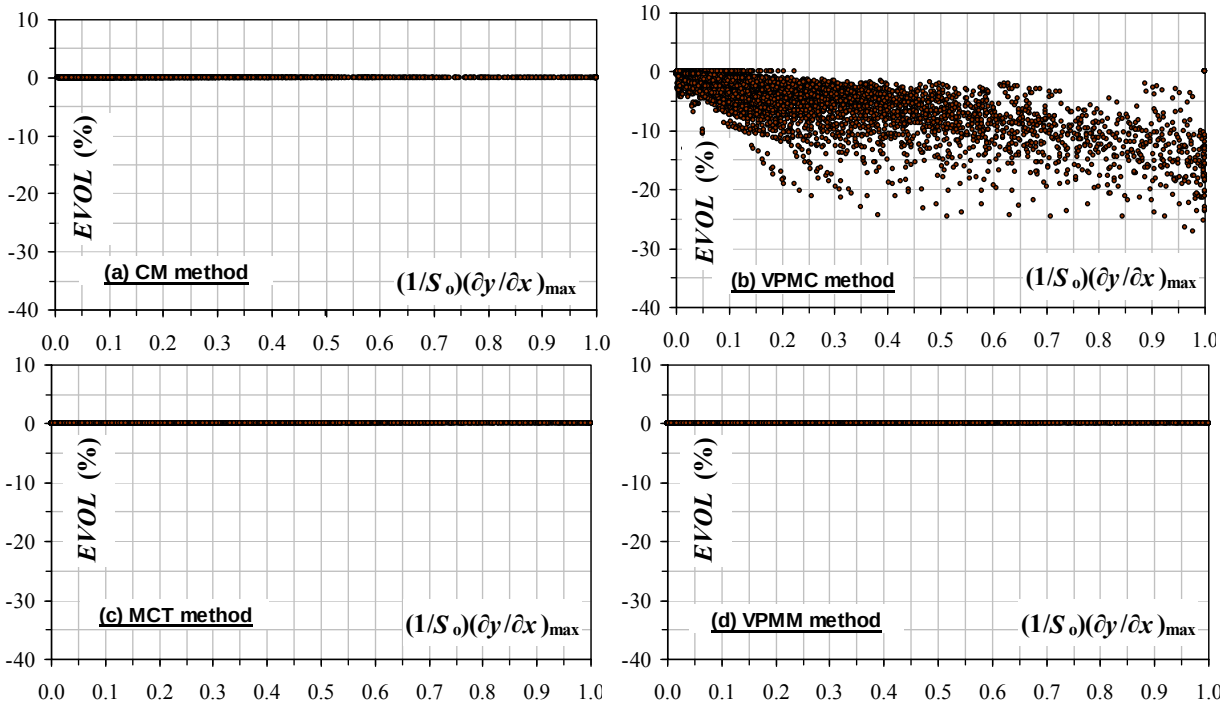

Figure 3. Volume conservation ability of the (a) classical Muskingum method, (b) VPMC method, (c) MCT method, and (d) VPMM method.

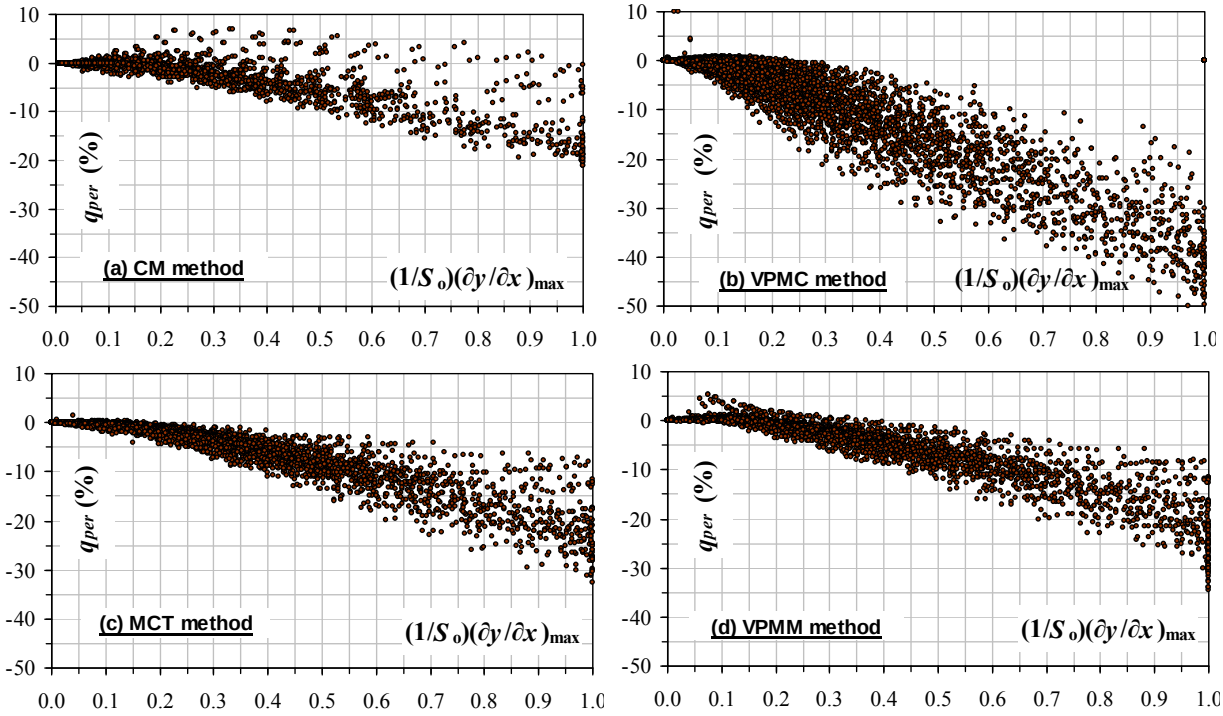

Figure 4. Error in peaks of the routed discharge shown by the (a) classical Muskingum method, (b) VPMC method, (c) MCT method, and (d) VPMM method.

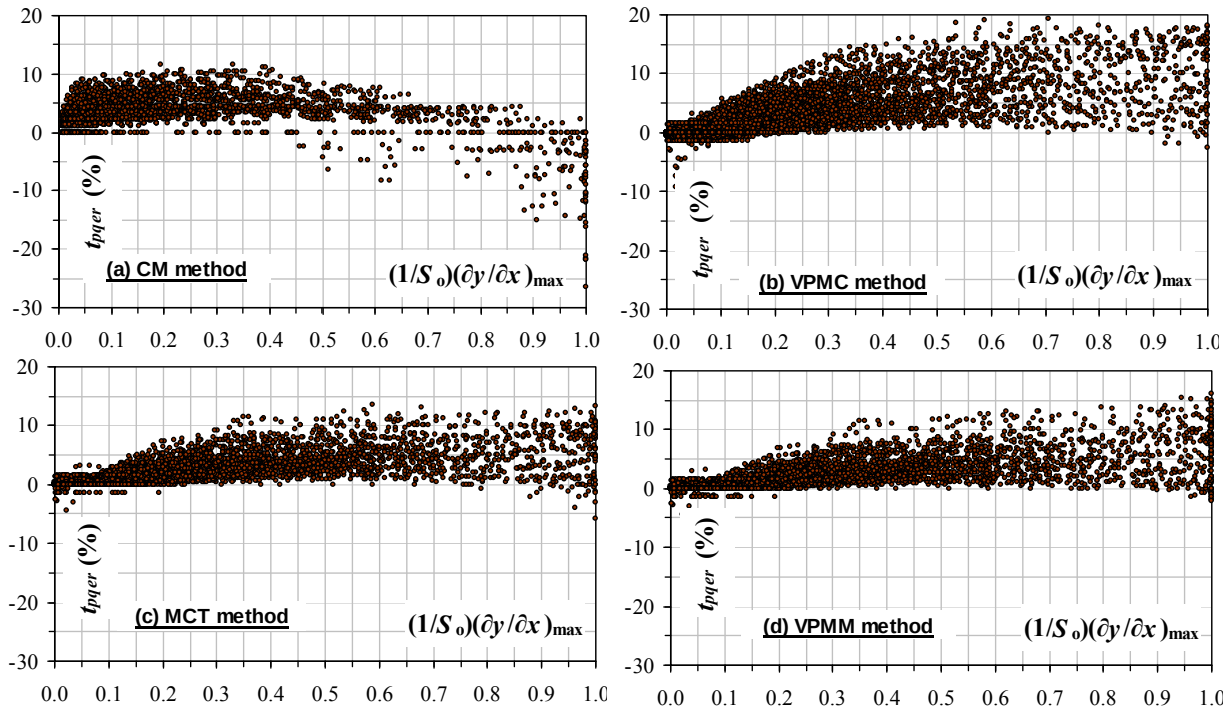

Figure 5. Error in time-to-peaks of the routed discharge shown by the (a) classical Muskingum method, (b) VPMC method, (c) MCT method, and (d) VPMM method.

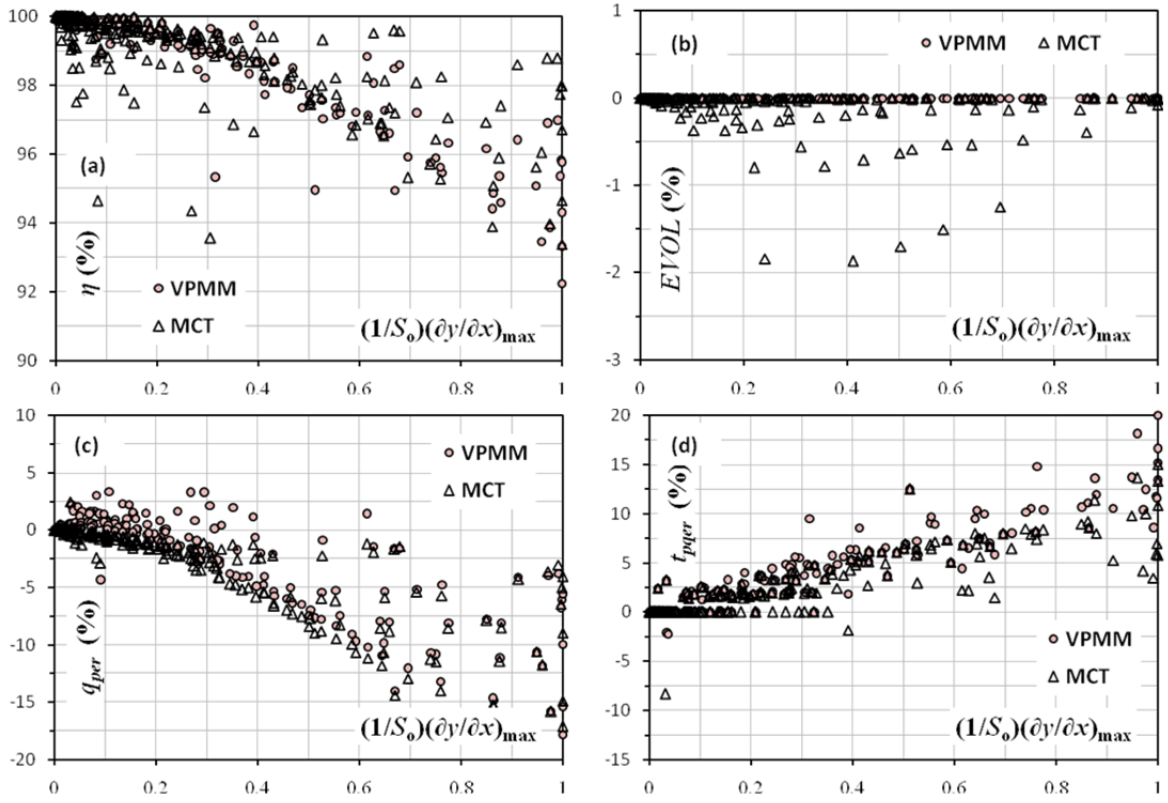

Figure 6. Performance evaluation measures of the MCT and VPMM methods while considering coarser spatial and temporal resolutions of Δx = 12.5 km and Δt = 1800 s.

Conclusion

The SWAT model, which is widely used worldwide to predict the impact of land management practices on water, sediment and agricultural chemical yield, employs the classical Muskingum and variable storage routing methods in the channel routing sub-module. However, these methods have their inherent limitations to model the nonlinear dynamics of river flow accurately. Moreover, with the evolution of simplified and physically-based hydraulic methods, such as the variable parameter McCarthy Muskingum (VPMM) method in the recent hydrological literature, there is need to refine the channel routing sub-module of the SWAT model, which will reduce the model uncertainties significantly. Moreover, the VPMM method is advantageous over all the currently available hydrodynamic-based simplified and physically-based models as it is fully volume conservative with a wider applicability range.

References

Apollov, B.A., G.P. Kalinin, and V.D. Komarov. 1964. *Hydrological forecasting*. Translated from Russian. Israel Program for Scientific Translations, Jerusalem.

ASCE Task Committee on Definition of Criteria for Evaluation of Watershed Models of the Watershed Management Committee, Irrigation and Drainage Division. 1993. Criteria for evaluation of watershed models. *J. Irrig. Drain. Eng., ASCE*. 119(3):429–442.

Chow, V.T., D.R. Maidment, and L.W. Mays. 1988. *Applied Hydrology.* New York, N.Y.: McGraw Hill, Inc.

Cunge, J.A. 1969. On the subject of a flood propagation method (Muskingum Method). *J. Hydraul. Res.*, *IAHR.* 7(2):205–230.

Dooge, J.C.I. 1973. Linear theory of hydrologic systems, USDA. *Agric. Res. Serv., Tech. Bull.,* No.1468.

Dooge, J.C.I., W.G. Strupczewski, and J. J. Napiorkowski. 1982. Hydrodynamic derivation of storage parameters of the Muskingum model. *J. Hydrol*., 54(4):371–387.

McCarthy, G. T. 1938. The unit hydrograph and flood routing. *Conf. North Atlantic Division*. U.S. Army Corps of Engineers, New London, Conn.

Natural Environment Research Council (NERC). 1975. Flood Routing Studies. In: *Flood Studies Report.* Vol. III. Wallingford, U.K.: Institute of Hydrology.

Neitsch, S.L., J.G. Arnold, J.R. Kiniry, and J.R. Williams. 2011. Soil and Water Assessment Tool Theoretical Documentation Version 2009. *Texas Water Resources Institute Technical Report No. 406* (September 2011). College Station, Texas, U.S.A: Texas A&M University System.

Perumal, M., and R.K. Price. 2012. A fully volume conservative variable parameter McCarthy–Muskingum method: Theory and verification. *J. Hydrol.* (under review).

Ponce, V.M., and P.V. Chaganti. 1994. Variable parameter Muskingum–Cunge method revisited. *J. Hydrol.* 162(3–4):433–439.

Todini, E. 2007. A mass conservative and water storage consistent variable parameter Muskingum-Cunge approach. *Hydrol. Earth Syst. Sci.*. 11(5):1645–1659.

Williams, J.R. 1969. Flood routing with variable travel time variable storage coefficients. *Trans. of ASAE.* 12(1):101–103.

EFFECT OF URBANIZATION ON THE MITHI RIVER BASIN IN MUMBAI: A CASE STUDY

P.E. Zope
Research Scholar
Dept. of Civil Engineering, Indian Institute of Technology, Bombay, 400001
Email: pezope@gmail.com

T.I.Eldho
Professor
Dept. of Civil Engineering, Indian Institute of Technology, Bombay, 400001
Email: eldho@civil.iitb.ac.in

V. Jothiprakash
Associate professor
Dept. of Civil Engineering, Indian Institute of Technology, Bombay, 400001
Email: vprakash@iitb.ac.in

ABSTRACT

Land use modifications associated with urbanization such as the reclamations, removal of vegetation, increase in impervious surface area and drainage channel alterations invariably results in the characteristics change of the overall surface runoff hydrograph. Many of the highly populated cities in the developing world that are located on the coast, for example Mumbai, are highly susceptible to urban flooding. In this paper, the Spatio-temporal variations in the urban land use of the Mithi River catchment in Mumbai and its effect on drainage basin are analyzed. The change in land use-land cover (LU-LC) is estimated using toposheet of Survey of India for the year 1966 and satellite images of 2001 and 2009 years through GIS and Remote sensing techniques. The analysis from toposheet and remote sensing data shows adverse human induced influences on the Mithi River Course and its catchment. Around 2001, about 37.81 % of mud flat and main river course area has been encroached by unauthorized slum and infrastructural work compared to 1966, reducing the width of river and its coverage. In 2009, about 45.09 % mud flat area and main river course area are covered by buildings, infrastructural work and slum, reducing the river width drastically. From the analysis, it is also found that there is a rise in built up area of Mithi river catchment from 27.00 to 34.49 % between 1966 and 2009, which is the main cause of increase in impervious surface, which in turn increased the runoff resulting in severe flooding during monsoon season

Keywords: Urbanization, urban flooding, Land use-land cover, GIS and Remote Sensing, Mithi River.

INTRODUCTION

With a concentrated industrial, trading, transport, economic and administrative base, Mumbai has been growing very fast for the last few decades (Samant and Subramanyan, 1998). A city grows not only by population but also by changes in spatial dimensions. The prime factors of

increasing spatial dimension of the city are also the population growth and related requirements of urban life, such as development of transport and communication and others infrastructure facilities.

Urbanization is one the most widespread anthropogenic causes for the loss of arable land, habitat destruction, and the decline in natural vegetation cover. The conversion of rural areas into urban areas through development is currently occurring at an unprecedented rate in recent human history and is having a marked effect on the natural functioning of ecosystems (Turner, 1994, Dewan and Yamaguchi, 2009). Since ecosystems in urban areas are strongly influenced by anthropogenic activities, considerably more attention is currently being directed towards monitoring changes in urban land use and land cover (LULC) (Stow and Chen, 2002). The process of urbanization has induced rapid changes in the land use leading to many infrastructural and environmental problems, one of them being the frequent flooding during rains in major cities across the world (Kamini et. al, 2006). Change in runoff characteristics induced by urbanization is important for understanding the effects of land use and cover change on earth surface hydrological processes. With urban land development, impermeable land surfaces enlarge rapidly, the capability of rainfall detention declines sharply and runoff coefficient increases. Urbanized land usually leads to a decrease in surface roughness; hard road and drainage system can greatly shorten the time of runoff confluence. Therefore, urbanized area would become more susceptible to flood hazard under conditions of high precipitation intensity (Cheng and Feng, 1994, Shi et.al, 2007).

Land use-land cover (LULC) change analysis is an important tool to assess global change at various spatial–temporal scales. In addition, it reflects the dimension of human activities on a given environment. LULC change due to human activities is currently proceeding more quickly in developing countries than in the developed world, and it has been projected that by the year 2020, most of the world's mega cities will be in developing countries (World Bank, 2007). Increasing population in developing cities has caused rapid changes in LULC and increased environmental degradation (Holdgate, 1993). The effect of population is particularly relevant given that the global urban population is projected to almost double by 2050 (UN, 2008).Land use change is a major force altering the hydrological processes over a range of temporal and spatial scales. Land-use and land-cover changes may have four major direct impacts on the hydrological cycle and water quality: they can cause floods, droughts, and changes in river and groundwater regimes, and they can affect water quality. Land use change can affect the runoff generation and concentration by altering hydrological factors such as interception, infiltration and evaporation, and thus causes changes in the frequency and intensity of flooding. Therefore, a better understanding and assessment of land use change impacts on watershed hydrologic process is of great importance for predicting flood potential and the mitigation of hazard, and has become a crucial issue for planning, management, and sustainable development of the watershed drainage system (Chen et al., 2009). Due to encroachment of the flood plain areas, the presence of several structures, and the absence of proper regulations for maintenance, an artificial flood is created (Mohapatra and Singh, 2003). Anthropogenic activities induce floods, which often aggravate their harmful impacts (Istomina et al., 2005). The need for environmental sustainability through proper resource management has prompted accurate and timely monitoring of land cover changes and their interactions within the immediate environments to provide vital information for decision making (Olang and Furst, 2011). Quantification of the effect of land use

and land cover change on the runoff dynamics of a river basin has been an area of interest for hydrologists in recent years.

The integration of remote sensing (RS) and geographic information systems (GIS) has been widely applied and has been recognized as a powerful and effective tool in detecting urban growth. Remote sensing collects multispectral, multiresolution, and multitemporal data, and turns them into information valuable for understanding and monitoring urban land processes and for building urban land-cover data sets. GIS technology provides a flexible environment for entering, analyzing, and displaying digital data from various sources necessary for urban feature identification, change detection, and database development. In hydrological and watershed modeling, remotely sensed data are found to be valuable for providing cost-effective data input and for estimating model parameters (Weng, 2001).

In the present study, the spatio-temporal variations in the urban land use of the Mithi River catchment in Mumbai and its effect on drainage basin are analyzed. The change in land use-land cover (LU-LC) is estimated using toposheet of Survey of India for the year 1966 and satellite images of 2001 and 2009 years through GIS and Remote sensing techniques.

STUDY AREA

Mumbai, formerly called Bombay (Lat 18^0N to 19.20^0N, Long. 72^0E to 73^0E) is the capital of Maharashtra state of India and the commercial and financial centre of India. It generates about 5% of India's gross domestic product (GDP) and contributes to over 25% of the country's tax revenues. Thus, any disaster in Mumbai has roll-on effects on the Indian economy.

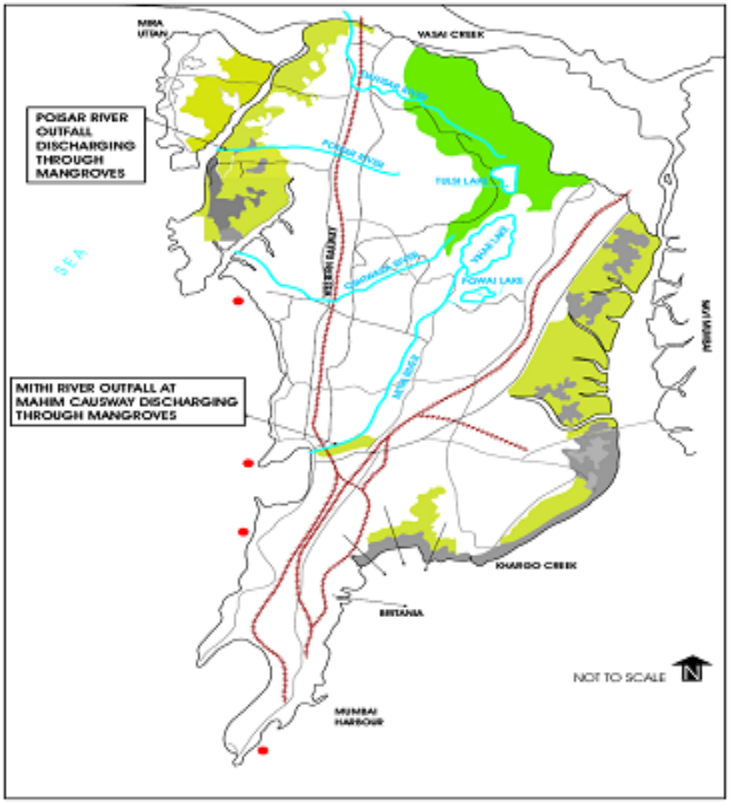

Fig: 1. Main Rivers in Suburban Part of Mumbai City. (FFC, 2006)

Mumbai is lined on the west by Arabian Sea and is intercepted by number of creeks (Mahim, Mahul and Thane creeks), rivers (Mithi, Dahisar, Poisar and Oshiwara rivers, and their tributaries) as shown in Fig. 1 and a complex nallah (drain) system.

Mithi River and its watershed is covered between Latitude 19^0 0' to 19^0 15' North and Longitude at 72^0 45' to 73^0 0'at East. The Mithi River originates downstream of the Vihar and Powai lakes at an altitude of 250 m. in Sanjay Gandhi National Park in Greater Mumbai. It flows southward up to Sion; takes turn watershed to join the Mahim Bay at Mahim Causeway. The location of Mithi river basin catchment is shown in Fig. 1. The total length of river is 17.8 k.m. The river has four distinct reaches with very steep bed gradient from its origin to 12 K.m.of lengths and then flat gradient towards downstream side. On its way the river flows below the airport runway for a distance of about 400 mts. and comes out of airport culvert near Kranti Nagar. The Mithi River flows through the city of Mumbai and forms a principal channel to discharge storm water. The storm water drainage for the Mithi river catchment areas has been disrupted due to the encroachment of hutments in large numbers, storage facilities, processing industries, workshops and scrap yards situated along the banks of the Mithi River that make it difficult even to delineate its path. Direct discharges of untreated sewage, wastewater from the unauthorized settlements, and industrial effluents along the river's course are a cause of concern.

DATA AND METHODOLOGY

Mithi river is covered in Survey of India Topographical sheet no. 47 A/16, however as the toposheet does not contains contours at all over the catchment area of Mithi River, it was not possible to generate precise Digital Elevation model (DEM) for the watershed delineation. Therefore "The Global Digital Elevation Model (GDEM) of Advanced Spaceborne Thermal and Reflection Radiometer (ASTER) of Terra satellite (htpp://asterweb.jpl.nasa.gov)". GDEM from Shuttle Radar Topographic Mission (SRTM) (Htpp://srtm.csi.cgiar.org) has been downloaded for Mumbai region. Also the Cartosat (Stereo) image (28th November 2009) with 2.5 meter resolution was processed to generate digital terrain model (DTM) using the image processing software Leica Photogrammetry Suite (LPS) and the contours were corrected by eliminating the contours running through buildings and again corrected DEM was generated. To delineate the watershed catchment boundry, ARC GIS 9.3.1 software has been used. As per the flow accumulation from DEM generated from Toposheet, ASTER, SRTM and CARTTOSAT superimposing on the stream network of Mithi, delineated from Toposheet, it has been observed that the flow accumulation from DEM generated from CARTOSAT, 2009 gives better results as compared to others and which matches with the Toposheet network as well as in current position of the river alignment. Therefore for further analysis, the DEM of CATOSAT 2009 was considered. The total catchment area of the Mithi River is 68.839 Sq. Km. and it consists of 24 numbers of sub catchments as shown in Fig: 2.

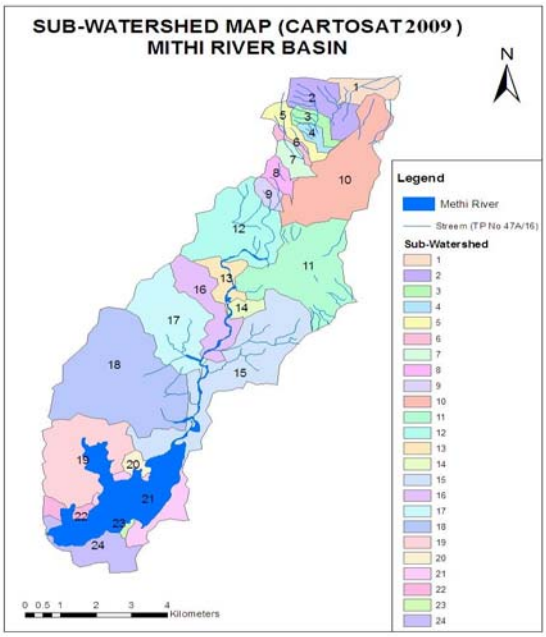

Fig: 2. Sub watershed wise Catchment area of Mithi River

Various satellite images of different years as shown in Table 1 have been used to extract spatio – temporal Land use – Land cover (LU-LC) change of the catchment. The images were geo registered and ortho-rectified on WGS 1984 UTM (Universal Transverse Mercator) 43N

projection system. Supervised classification based on Gaussian Maximum likelihood has been carried out using ERDAS Imagine software 9. This classification method uses the training data as a means of estimating averages and variances of the classes, which are then used to estimate probabilities. The maximum likelihood algorithm assumes that the estimated probabilities are equal for all classes and the histograms of the input bands have normal distributions in order to get a precise outcome. This method considers mean, variances and the variability in brightness values of each class given as a training set. Therefore, accurate training data is required. The main advantage of this technique is, based on the statistics; it provides an estimate of overlap areas (Suriya and Mudgal, 2011).

Table: 1. Details of Satellite Images used in the present study

DD/MM/YY	Satellite/ Sensor	Resolution (m)
27th November 2001	Landsat/ETM+	30
6th March 2009	IRS P6/L-4	5

MAPPING OF LAND USE – LAND COVER CHANGE

The rapid increase in population, urbanization and the change in land use pattern are the major reasons for occurrence of flooding. The time period considered for the land cover- land use change (LU-LC) was from 1966 to 2009. LU-LC classes observed for analysis are Open land, Built-up Land, Water-body, Vegetation and forest. Survey of India Topographic map sheet A-47/16 of the year 1966 was digitized for analysis of above land use classes to find out correct measurements of the LU-LC classes for comparison with the results obtained from the satellite images of year 2001 and 2009.

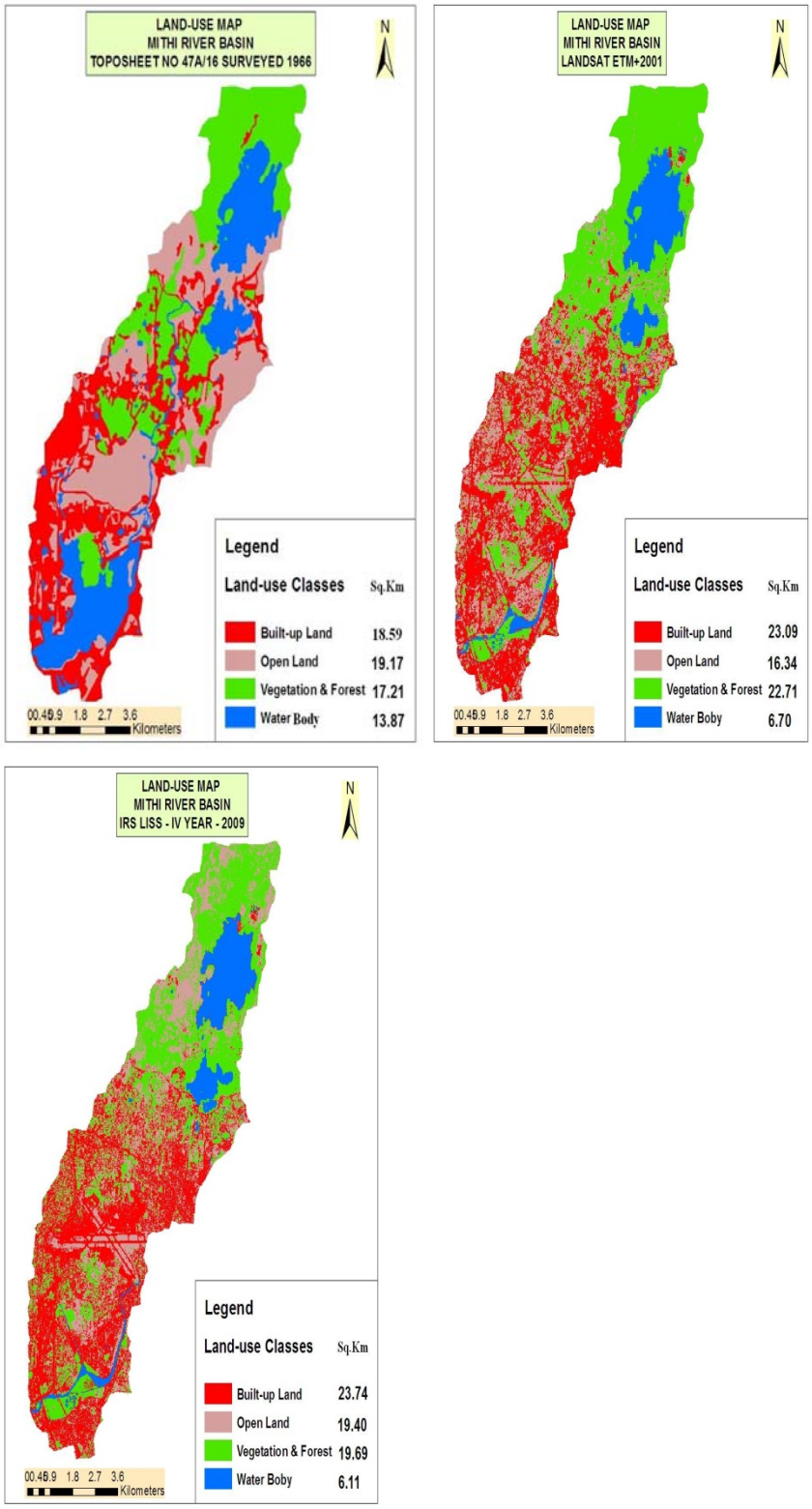

Fig: 3. LU-LC map of Mithi River Basin for the year 1966, 2001 and 2009.

Landsat/Enhanced Thematic mapping plus (ETM+) image of November 2001 and Indian Remote Sensing (IRS) satellite P6/L-4 image of March 2009 has been used to extract the land use-land cover change in Mithi river basin. The Standard False Color Composite (SFCC) was generated from the 3 bands (Green, Red and Infrared) data of the satellite images. Fig: 3 present the LU-LC map for the Mithi river basin for the year1966, 2001 and 2009.

Fig: 4 and Fig: 5 show the comparative graphical representation of change in land use in percent and area of the catchment respectively for the year 1966, 2001 and 2009 for Mithi river basin

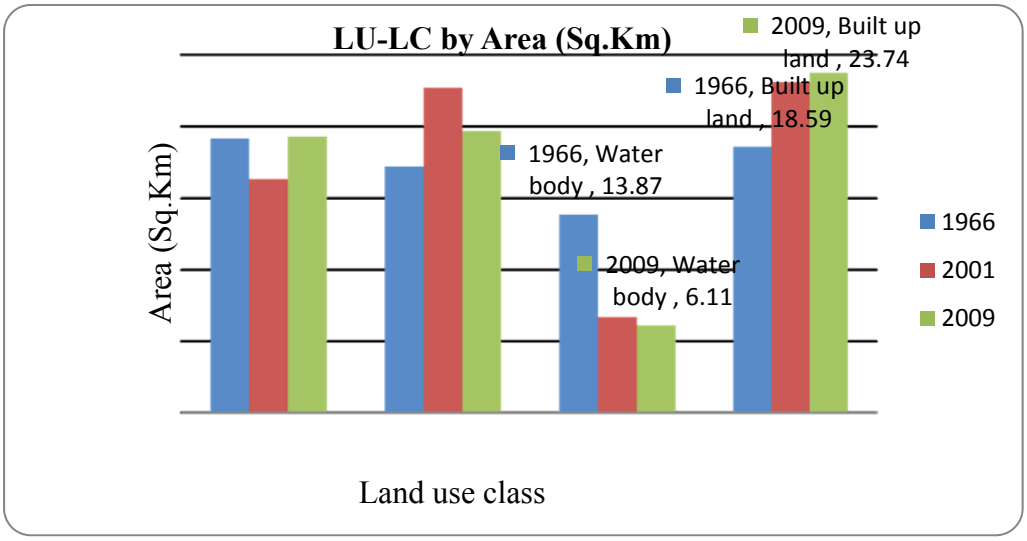

Fig: 4 Land use – Land cover analysis of Mithi River Basin by Area of Catchment

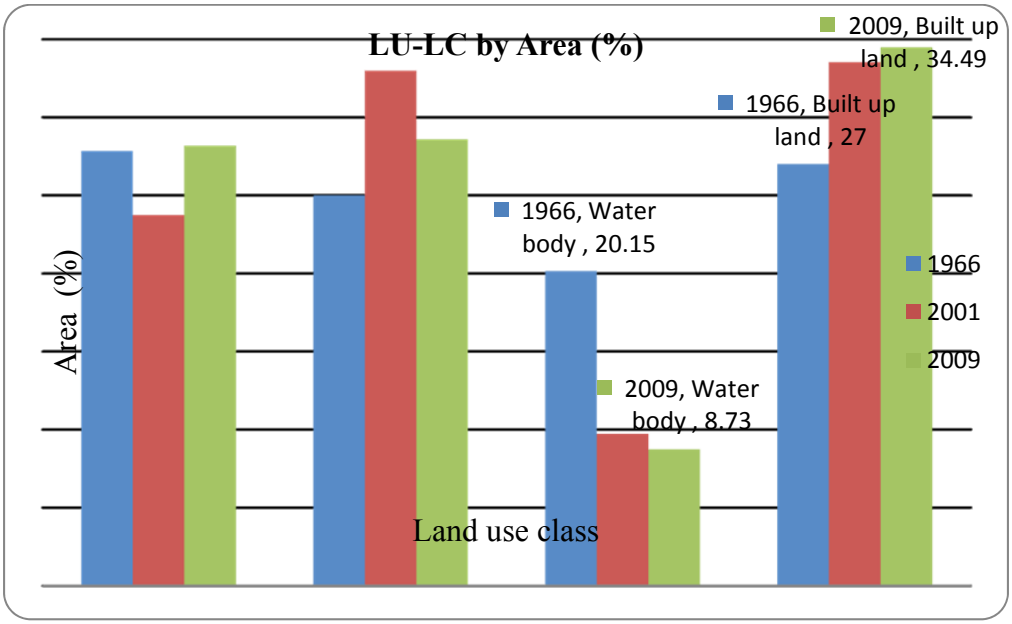

Fig: 5 Land use – Land cover analysis of Mithi River Basin by Percent of Catchment

From above results, it can be concluded that there is substantial land use change as compared to land cover in year 1966. There is increase in built up area from 27% to 35% of the total catchment area and decrease in river course and water body which made the catchment of Mithi vulnerable to flooding. Assessment of the classification accuracy of the derived land cover maps from satellite data was carried out. Error matrices were used to assess the classification accuracy and are summarized for the year, 2001 and 2009 as shown in Table 2.

Table: 2. Summary of classification accuracies (%) for 2001 and 2009

Land Use/Cover class	2001		2009	
	Producer's	User's	Producer's	User's
Built up	90.57	96	91.8	87.55
Water Body	100	96	100	98.44
Vegetation & Forest	95.83	92	90.91	93.75
Open Land	86.27	88	83.08	84.38

The overall accuracy for the year 2001 and 2009 were 93% and 91.02% respectively, with Kappa statistics of 0.9097 and 0.8804.

CHANGE IN RIVER COURSE OF MITHI

Mithi River, being a seasonal stream, primarily flows rapidly during the monsoon on account of the huge rainfall in its catchment area. During the lean months, it discharges the surplus water from Vihar and Powai lakes into the Arabian Sea. Over the last four decades, its course has undergone many changes on account of rapid urbanization in its catchment area. The increased infrastructure in the form of transportation arteries on one hand, and the expansion of airport runway on the other contributed to changes in Mithi river course. Mumbai airport, which is already more than eight-decade old, started in 1920, has expanded primarily along its runway to cater to the increasing air traffic. This has infringed the natural flow course of river Mithi, which is made to flow through a constructed tunnel under the expanded runway at its eastern end. The increase in built-up area, slums and reclamation along the Mahim creek has also contributed to the changes in the river course.

Table: 3. Summary of changes in Mithi River course

Year	Area Encumbered(Sq.Km)	Net River course area including mud flats (Sq.Km)	Type of Changes
1966	nil	6.513	Nil
2001	2.464	4.049	Airport Runway extended, Reclamation at Mahim bay and Bandra Kurla complex area
2009	3.002	3.511	Entire Bandra-Kurla complex area reclaimed, some part of Vakola basin

At downstream side, Poisar River discharges its flow in Mahim creek which is the vital point in terms of tidal variation and high intensity of rainfall being the cause of flooding. Therefore more attention has been given to study the change in land use, river course and width, mud flat area of the creek at downstream side of the river. The river course polygon along with mud flat area was digitized on toposheet of year 1966 and the same digitized polygon was superimposed on satellite image of 2001 and 2009 as shown in Fig: 6. The changes in the course of the river, width, mud flat and land use were observed at various point as shown in Fig: 6 and summarized as in Table 3.

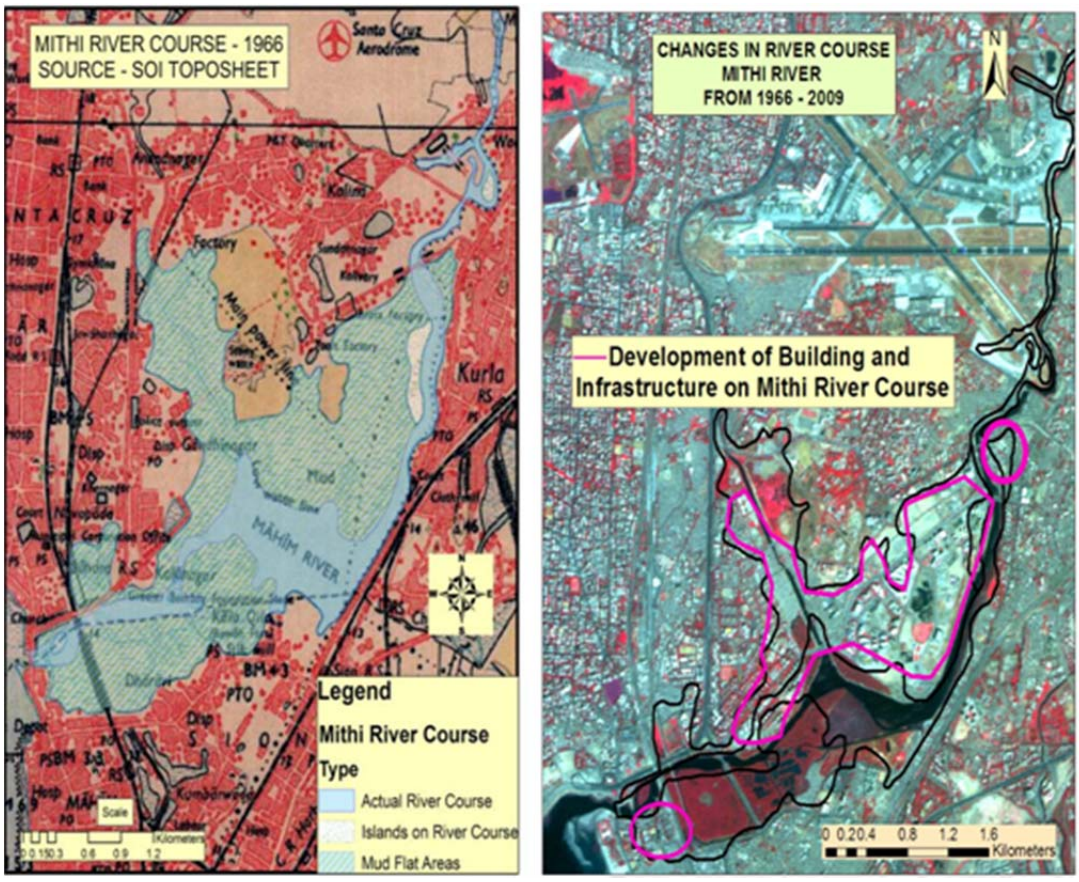

Fig: 6. Change in River course, width, mud flat at downstream side (Year 1966- 2009)

DISCUSSION

Based on the above analysis, the following observations are made.

- In 1966 at downstream side of the river, there was huge open land, mud flat area and wide channel area of river for smooth flow.
- In 2001, about 37.81 % of mud flat area has been encroached by unauthorized slum, construction of building and infrastructural work reducing width of river and smooth river flow.
- In 2009, 45.09 % of mud flat area covered by buildings and slum at Bandra Kurla complex area, reducing the river width and flow drastically.

The analysis from toposheet and remote sensing data shows very adverse human induced influences on the Mithi River Course and its catchment. The increased infrastructure in the form of transportation arteries on one hand, and the expansion of airport runway on the other contributed to changes in Mithi river course. The present analysis shows that due to rapid unplanned urbanization and land use-land cover change in Mithi river basin area, there is an increase in unauthorized slum areas, substantial reduction in open spaces due to infrastructural development and buildings, reducing the river width drastically and about 45% decrease in mud flat area of river due to reclamation. This reclamation has changed the natural hydrologic regime of the coastal/tidal waters in and around the Mahim creek and Mithi river catchment area. Also the expansion of airport runway has contributed the change in Mithi river course drastically.

CONCLUSION

The effect of urbanization on the land use change is major force altering the hydrological process over a range of temporal and spatial scale. Understanding the hydrological effects of urban growth is essential for urban planning i.e., it is necessary to assess land-use change in order to assist urban planning and related decision-making. From the analysis, it is found that there is a rise in built up area from 27.00 to 34.49 % between 1966 and 2009, which is the main cause of increase in impervious surface, which in turn increased the runoff resulting in severe flooding. Mud flat area has been covered by building and slum, reducing the river width and flow drastically in Mithi River basin catchment, which results loss of drainage capacity and resulting in severe flooding. The integration of remote sensing (RS) and geographic information systems (GIS) has been applied as a powerful and effective tool in detecting the urban growth as demonstrated in the study.

REFERENCES

Cheng, X.T., Feng, Z.Y., 1994. "Flood disaster evolution in urbanization and modern society (in Chinese): prospect of Shenzhen from the experiences of Japan". *Journal of Natural Disasters,* 3 (2): 41– 48.

Chen, Y., Youpeng, X. and Yin, Y., 2009, "Impact of land use change scenarios on storm runoff generation in Xitiaoxi basin, China", *Quaternary International*, 208: 121 – 128.

Dewan Ashraf M. and Yamaguchi Yasushi, 2009. "Land use and land cover change in Greater Dhaka, Bangladesh: Using remote sensing to promote sustainable urbanization", *Applied Geography,* 29: 390–401.

Fact Finding Committee on Mumbai (FFC), 2006. "Floods, State Govt Committee Report", 31-130.

Holdgate, M. W. 1993. "The sustainable use of tourism: a key conservation issue". *Ambio*, 22: 481–482.

Istomina, M.N., Kocharyan, A.G., Lebedeva, I.P., 2005. "Floods: genesis, socioeconomic and environmental impacts". *Water Resources*, 32(4): 349–358.

Kamini J., Jayanthi Satish C. and Raghavswami, 2006. "Spatio – Temporal Analysis of Land Use im Urban Mumbai – Using Multi-Sensor Satellite Data and GIS Techaniques", *Journal of the Indian Society of Remote Sensing, Photonirvachak,* 34(4): 385-396

Mohapatra, P.K., Singh, R.D., 2003. "Flood management in India". *Natural Hazards*, 28: 131–143.

Olang L. O. and Furst J., (2011), "Effects of land cover change on flood peak discharges and runoff volumes: model estimates for the Nyando River Basin, Kenya", *Hydrological Processes*, 25: 80–89.

Samant H. P. and Subramanyan V., 1998, "Landuse/Land Cover Change in Mumbai-Navi Mumbai Cities and Its Effects on the Drainage Basins and Channels – A Study Using GIS", *Journal of the Indian Society of Remote Sensing, Photonirvachak*, 26(1&2): 01-06.

Stow, D. A., and Chen, D. M. 2002. "Sensitivity of multi-temporal NOAA AVHRR data of an urbanizing region to land use/cover changes and misregistration". *Remote Sensing of Environment,* 80: 297–307.

Shi Pei-Jun, Yuan Yi, Zheng Jing, Wang Jing-Ai, Ge Yi and Qiu Guo-Yu, 2007., "The effect of land use/cover change on surface runoff in Shenzhen region, China", *Catena*, 69: 31-35.

Suriya S. and Mudgal B.V. 2011. "Impact of urbanization on flooding: The Thirusoolam sub watershed – A case study", *Journal of Hydrology*, article in press.

Turner, B. L., II 1994. Local faces, global flows: the role of land use and land cover in global environmental change. *Land Degradation and Development*, 5: 71–78.

United Nation. 2008. Report of the meeting – urbanization: a global perspective. Proceedings of the expert group meeting on population distribution, urbanization, internal migration and development, 21–23 January, 2008, New York.

Weng Qihao, 2001. "Modeling Urban Growth Effects on Surface Runoff with the Integration of Remote Sensing and GIS". *Environmental Management,* 28(6):737–748.

World Bank. 2007. "Dhaka: Improving living conditions for the urban poor. Sustainable Development Unit, South Asia Region", Report No. 35824-BD.

Estimation of Crop Water Requirement in Mahi Right Bank Canal Command Area

Nidhi J. Shah
P. G. Student, Civil Engineering Department, The M. S. University of Baroda, Vadodara - 390001, India.

H. M. Patel
Professor, Civil Engineering Department, The M. S. University of Baroda, Vadodara -390001, India.
Email: haresh_patel@yahoo.com (corresponding author)

M. H. Kalubarme
Project Director, BISAG, Gandhinagar, India.

ABSTRACT

Water is one of the most important inputs essential for the production of crops. Plants need it continuously during their life and in huge quantities. Both, its shortage and excess affect the growth and development of a plant directly and, consequently, its yield and quality. Hence, reasonable estimate of crop water requirement is a prime concern for irrigation managers. The paper focuses on analyzing the irrigation water requirement of Wheat, Sugarcane and Paddy crop in Mahi Right Bank Canal command area, Gujarat, India. Potential evapotranspiration has been estimated using Penman-Monteith Model (FAO-56). Single crop coefficient values are used for estimating crop evapotranspiration. Effective rainfall is estimated for determining irrigation water requirement in kharif season. Net irrigation water requirement and the volume of water required for crop during the season are estimated using climateological data of the year from 2001 to 2009. Climate variability and rainfall recharge are found as major parameters affecting irrigation water requirements.

Keywords

Evapotranspiration, Single Crop Coefficient Approach, Crop Water Requirement.

INTRODUCTION

Water is one of the most important inputs essential for the production of crops. Plants need it continuously during their life and in huge quantities. Both, its shortage and excess affect the growth and development of a plant directly and, consequently, its yield and quality. In India, however, the frequency distribution and amount of rainfall are not in accordance with the needs of the crops. Irrigation is the only option to meet the food requirements. The goal for water manager is to provide water at the right period and in the adequate amount. The reasonable estimation of evapotranspiration is required for an efficient irrigation water management. Remote sensing and GIS tools are used to handle the geo-spatial and time series data. Objective

of the present study is to estimate the irrigation water requirement in MRBC (Mahi Right Bank Canal) command area of Gujarat.

STUDY AREA

Mahi Right Bank Canal Command Area (Fig.1) lies in Gujarat, India between Latitude of $22^0$65'00" and $22^0$55'00" (north) and Longitude of $72^0$49'00" and $73^0$23'00" (south). Area of the MRBC Command is 4460.34 sq.km. Water to the MRBC command area is supplied from Kadana reservoir in winter and summer seasons. In monsoon supply is provided by Wanakbori weir.

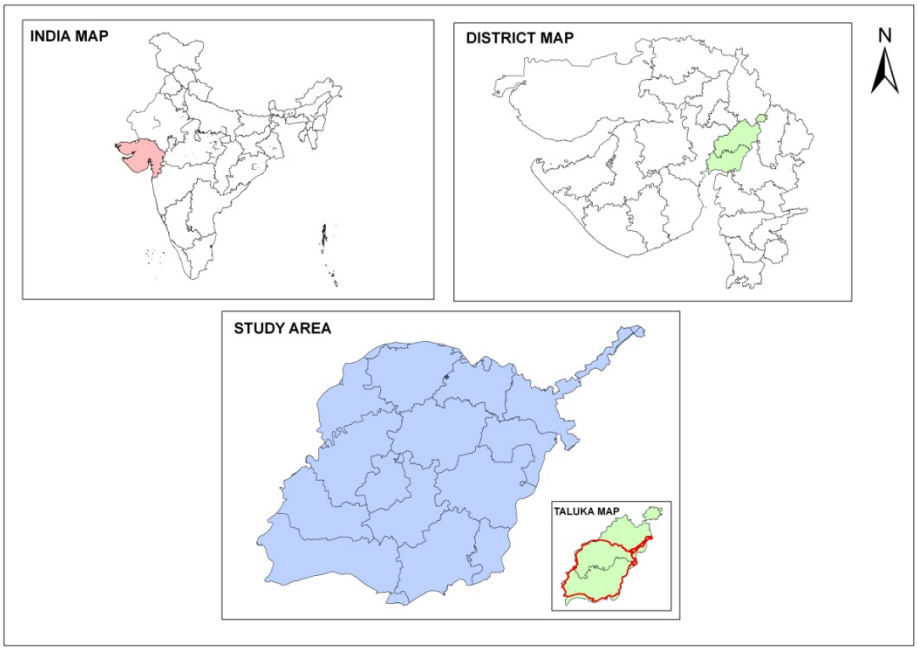

FIG: 1 Index Map of Mahi Right Bank Canal Command Area (source: BISAG)

The Command area covers Kheda and Anand districts. Most of the part of this area is covered with fine loamy texture. Annual rainfall of study area varies from 850mm to 1000mm. The climate of the command area is semi-arid. It is characterized by hot summer and general dryness, except during the south-west monsoon season which experiences heavy rain. In summer day temperature occasionally reaches to 47^0c or more otherwise it very from maximum 41^0c to minimum 26^0c. Kharif, Rabi and hot weather are the crop seasons in study area. Major crops grown in this area are wheat and tobbaco in Rabi season, sugarcane, paddy, bajari, and groundnut in Kharif season and other crops like Cotton, Juwar in hot weather season.

MATERIALS AND METHODS

In order to accomplish the task, meteorological data were obtained for three stations from State Water Data centre, Gujarat. Data consists of daily data of rainfall, maximum and minimum temperature, sunshine, humidity and wind speed recorded from three stations. Also cropping pattern in study area is collected from Mahi Irrigation Circle, Nadiad, Gujarat for the year 2001 to 2010. Wheat, sugarcane and paddy crops are considered for this study method daily Reference

crop evapotranspiration is calculated by using FAO modified Penman-Monteith Method (Allen, et. al, 1998).

POTENTIAL EVAPOTRANSPIRATION OF REFERANCE CROP (ET_O)

The FAO Penman-Monteith equation is a close, simple representation of the physical and physiological factors governing the evapotranspiration process. The mathematical expression for the purpose of calculation is simplified as follow:

$$ETo = \frac{0.408\,\Delta(R_n - G) + \gamma\frac{900}{T+273}U_2(e_s - e_a)}{\Delta + \gamma(1 + 0.34U_2)} \qquad (1)$$

Where,

ET_o = reference evapotranspiration (mm per day)

R_n = net radiation at the crop surface (MJ/m² per day)

G = soil heat flux density (MH/m² per day)

T = mean daily air temperature at 2m height (°c)

U_2 = wind speed at 2m height (m/s)

e_s = saturation vapor pressure (kPa)

e_a = Actual vapor pressure (kPa)

$e_s - e_a$ = saturation vapor pressure deficit (kPa)

Δ = Slope of vapor pressure curve (kPa per °C)

γ = Psychometric constant (kPa per °C)

The equation uses standard meteorological records of solar radiation (sunshine), air temperature, humidity and wind speed. Net radiation if not measured, can be estimated from sunshine data.

Calculation of Potential evapotranspiration of Crop (ETc)

After determining ETo, the ETc can be calculated using the appropriate crop-coefficient (Kc) approach(Allen, 2002; Allen, 2005).

$$ETc = K_c * ETo \qquad (2)$$

Potential evapotranspiration is a measure of the ability of the atmosphere to remove water from the soil and plant surface through the processes of evaporation and transpiration assuming no stress on water supply. Crop coefficient (K_c) is the ratio of actual maximum crop evapotranspiration to reference crop evapotranspiration. Ray and Dadhwal (2001) estimated Kc empirically from the RS derived soil adjusted vegetation index (SAVI) values. In this study, the standard crop coefficient values for various crops are taken from FAO-56.

From the standard value of crop coefficient daily crop coefficient values for the whole season are interpolated. A remote sensing image is used to obtain land use in study area. ArcGIS is used to generate different layers (Fig:2 & 3) and SCS curve numbers are computed for agricultural land use. SCS curve number method (USDA, 1985) is used to find rainfall infiltration. Finally, the net irrigation requirements are computed for each crop for the study period.

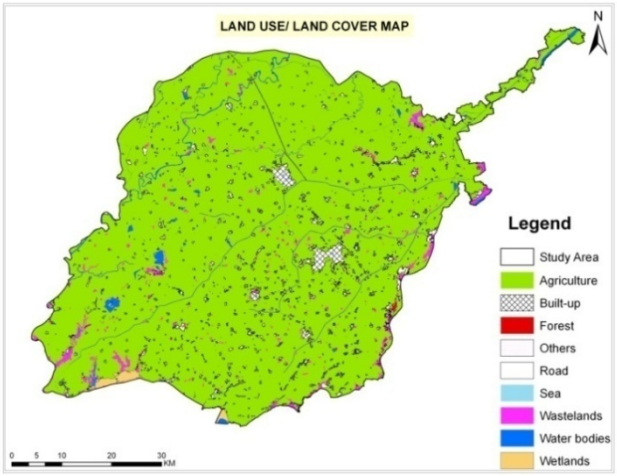

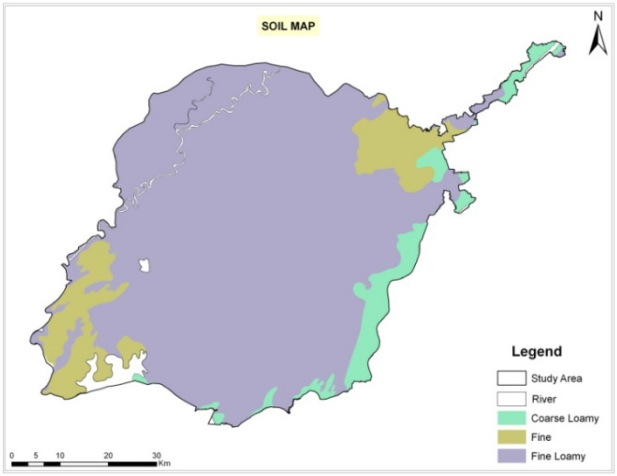

Fig:2- Land use/ land cover map of study area

Fig:3- Soil Map of study area

ANALYSIS AND DISCUSSION

The study area is divided in to three part falling under Bilodra, Gudel and Rasikpura and average monthly ET_o are computed (Table 1). It can be seen that ET_o for the month March to June is higher than the rest of the year. In this period its value exceeds 50 mm. The area falling under Gudel shows higher ET_o than others. ET_c for wheat, sugarcane and paddy are computed for each station area for the years from 2001 to 2010 (Table:2,3 & 4). Using these above values Net Irrigation Required (NIR) is calculated. Year-wise Net Irrigation Requirements are obtained for each crop which are shown in the figure 4, 5 and 6. The NIR values may be further used to estimate the release of canal discharge.

Table 1. Avg. Monthly ET_o for different stations in study area

	ET_o (mm)		
STATION / MONTH	BILODRA	GUDEL	RASIKPURA
January	31.81	36.64	32.06
February	34.91	39.75	34.46
March	51.63	65.93	49.95
April	62.35	79.35	59.18
May	73.30	76.93	70.48
June	58.04	65.53	57.89
July	47.00	56.91	44.66
August	40.20	45.86	42.08
September	39.41	42.69	40.41
October	39.47	39.67	41.21
November	29.00	29.93	31.77
December	25.27	31.03	29.07

Table 2. Season wise ET_c for Wheat

STATION	BILODRA	GUDEL	RASIKPURA
YEAR	ET_c (mm)	ET_c (mm)	ET_c (mm)
2001-02	121	123	118
2002-03	126	171	151
2003-04	134	146	122
2004-05	140	176	152
2005-06	144	181	155
2006-07	144	145	131
2007-08	139	161	135
2008-09	106	75	126
2009-10	111	82	151
AVERAGE	130	135	138

Table: 3 Season wise ET_c for Sugarcane

STATION	BILODRA	GUDEL	RASIKPURA
YEAR	ET_c (mm)	ET_c (mm)	ET_c (mm)
2001-02	559	539	535
2002-03	445	546	492
2003-04	477	544	461
2004-05	475	N.A.	499
2005-06	478	580	506
2006-07	612	622	548
2007-08	563	581	522
2008-09	506	475	540
2009-10	551	584	547
AVERAGE	518	559	517

Table: 4 Season wise ET_c for Paddy

STATION	BILODRA	GUDEL	RASIKPURA
YEAR	ET_c (mm)	ET_c (mm)	ET_c (mm)
2001	229	232	217
2002	201	222	211
2003	231	241	246
2004	212	272	241
2005	219	270	248
2006	209	256	235
2007	220	245	221
2008	203	192	194
2009	230	193	252
AVERAGE	217	231	230

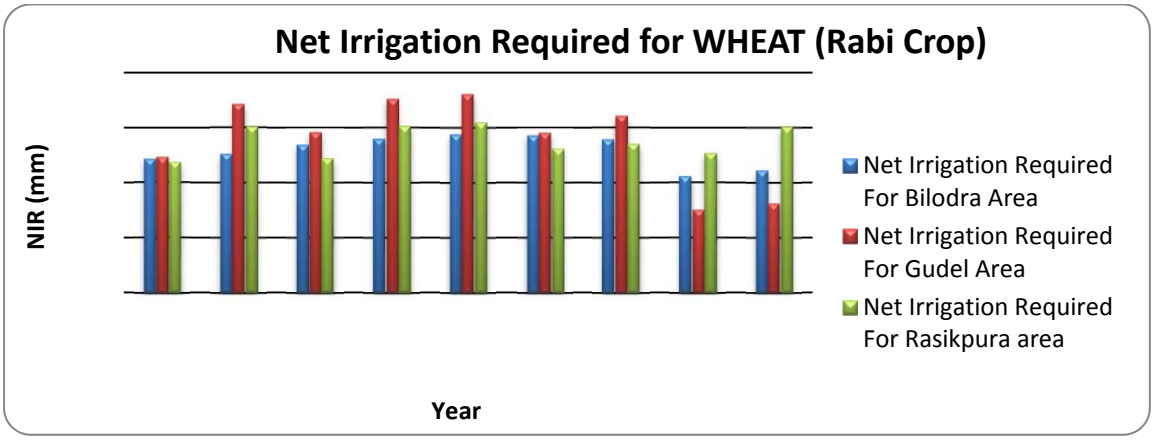

Fig: 4 - Variation of NIR in different areas for wheat crop in MRBC command area

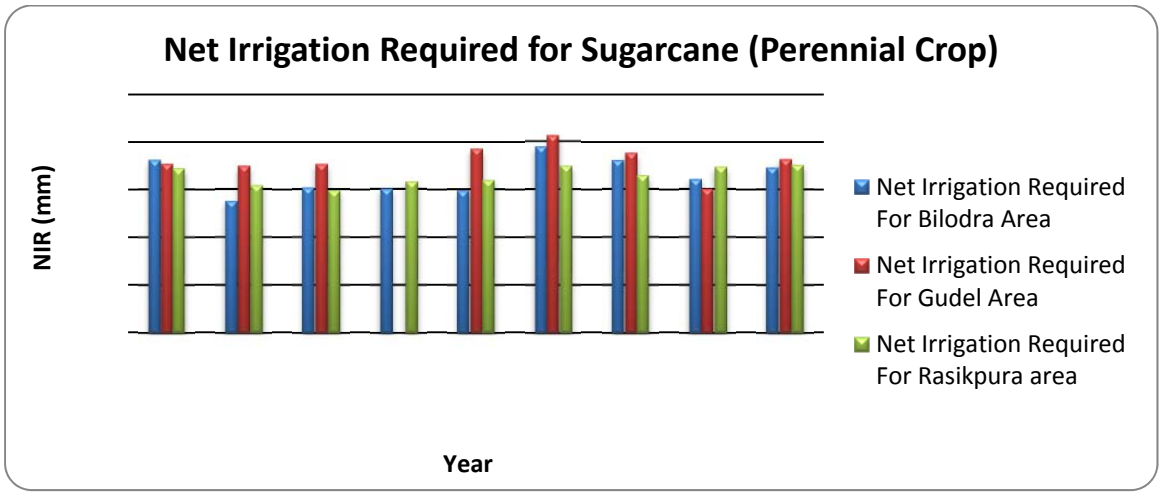

Fig: 5 - Variation of NIR in different areas for Sugarcane crop in MRBC command area

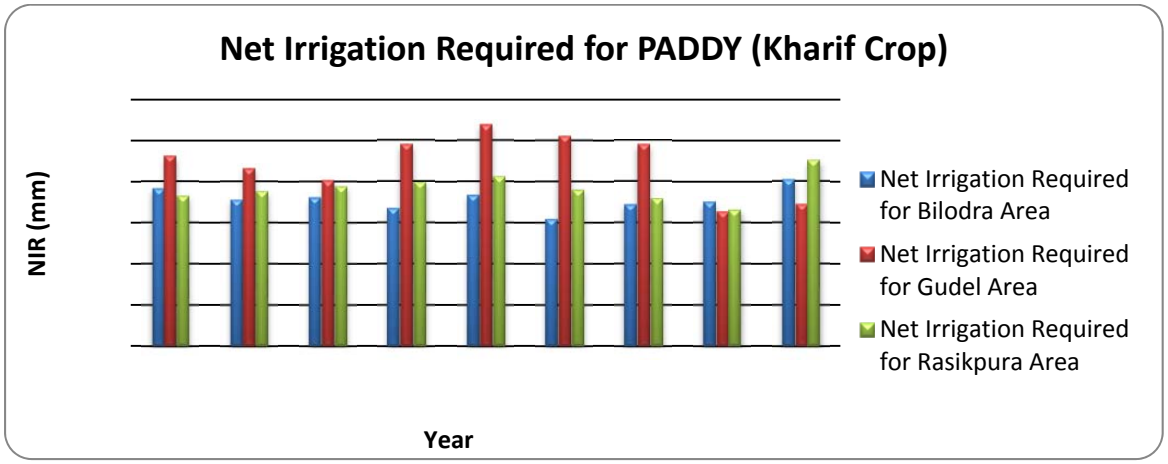

Fig: 6 - Variation of NIR in different areas for Paddy crop in MRBC command area

CONCLUDING REMARKS

Estimation of Crop Water Requirement is very important for managing irrigation water. Remote sensing and GIS tools are found convenient to handle spatial and temporal data and its integration with Penman Monteith Method and SCS curve number method is found very effective approach to precisely predict ET_o considering space and time variability. The average values for ET_o for wheat, sugarcane and paddy are obtained as 135, 526, 226 mm respectively for MRBC area. The estimated values of ET_o and ET_c show sensitivity to climate parameters and

crop growth stages. The methodology adopted in the study fairly estimates NIR which can be further used to evolve irrigation scheduling strategies in command area of irrigation project.

Acknowledgements

The Authors are thankful to State Water Data Centre, Government of Gujarat, Gandhinagar and Mahi Irrigation Circle, Nadiad, Gujarat for providing necessary data for the study. The authors also thankfully acknowledge the support extended by BISAG (Bhaskaracharya Institute of Space Application and Geo-informatics), Gandhinagar for providing facilities in carrying out this study.

REFERENCES

- Allen R. G., Pereira L.S., Raes D. and Smith M. 1998. Crop evapotranspiration - Guidelines for computing crop water requirements –United Nations Food and Agriculture Organization, Irrigation and drainage paper 56 Produced by: Natural Resources Management and Environment Department
- Allen R. G. 2002. Evapotranspiration : The FAO-56 Single Crop Coefficient Method and Accuracy of predictions for Project-wide Evapotranspiration, International meeting on Advances in Drip/Micro Irrigation
- Allen R. G. 2005. FAO-56 Single crop coefficient Method for estimating Evaporation from soil and application Extensions. Journal of Irrigation and Drainage Engineering ASCE/January/February 2005.
- Ray, S. S. and Dadhwal, V. K. 2001. Estimation of crop evapotranspiration of irrigation command area using remote sensing and GIS, Agricultural Water Management, Volume 49, Issue 3, Pages 239–249.
- USDA, 1985. National Engineering Handbook, Soil Conservation Service, USA.

Modeling impacts of climate change on stream flow and sediment yield: implications for adaptive measures on soil and water conservation in north of Iran

M. Azari
Department of Watershed Management Engineering, College of Natural Resources, Tarbiat Modares University (TMU), Noor, Mazandaran Province, Iran, 46417-76489,
azarimahmood@yahoo.com

H.R.Moradi*
Department of Watershed Management Engineering, College of Natural Resources, Tarbiat Modares University (TMU), Noor, Mazandaran Province, Iran, 46417-76489,
morady5hr@yahoo.com

B. Saghafian
Soil Conservation and Watershed Management Research Institute, Tehran, Iran
b.saghafian@gmail.com

M. Faramarzi
Department of Natural Resources, Isfahan University of Technology,
Isfahan, Iran, 84156-83111,
monireh.faramarzi@cc.iut.ac.ir; http://mfaramarzi.iut.ac.ir/

Abstract

Natural earth system confront grand challenges due to climate change. Soil erosion and sediment transport are the key components functioning natural ecosystem. A special report from the Soil and Water Conservation Society indicated that the projected climate changes may increase the overall risk of soil erosion. The amount of change and repercussion is not known for most parts of the world. Iran located in arid and semi-arid part of the world might become one of the most vulnerable regions to climate change. Any change in soil loss and sediment load in the country may have significant implications for water resources development as well as water productivity and food security. A quantitative assessment of climate change impacts on the soil erosion and water resources availability is required to study the potential options in dealing with climate change. The Gorganroud river basin (Golestan Province, northwest of Iran) was considered as the case study. The Soil and Water Assessment Tool (SWAT) was used to simulate the hydrologic regime in this basin. The SUFI-2 algorithm in the SWAT-CUP program was used for parameter optimization using the daily river discharges and sediment loads. Future climate data of multi-model ensembles were downscaled and fed into hydrologic model to predict the impact on hydrologic regime and sediment load, presenting also the uncertainty resulting from structural differences in the global climate models (GCMs), CO2 emission scenarios and uncertainty due to variations in initial conditions or model parameterizations. This study lay the basis to assess feasibility of protecting the soil and water resources and in an advanced study for water productivity and food security issues in the future.

Key words: climate change, SWAT, sediment yield, stream discharge, Iran.

Introduction

Climate change is one of the most significant challenges of the 21st century (Yu and Wang, 2009). Increase of the average global surface air temperature from 1.4 to 5.8 ˚C and further changes in rainfall amount, rainfall intensity as well as the frequency of extreme climatic phenomena are expected (Chaplot, 2007). Climate changes are expected to cause significant impacts on local watershed systems, both to the hydrological and ecological components, with consequences for human activities and welfare (Nunes *et al.*, 2008). Changes in climate are also expected to have noticeable effects on the soil resource since rainfall and runoff are the factors controlling soil erosion and sediment transport within landscapes. The review by the IPCC working group concluded that the following effects were "virtually certain or very likely" to occur in response to increased concentrations of greenhouse gases in the atmosphere:

- Globally averaged mean water vapor evaporation, and precipitation increase.
- Mean precipitation increases in most tropical areas; mean precipitation decreases in most sub-tropical areas; and mean precipitation increases in the high latitudes.
- Intensity of rainfall events increases.
- There is a general drying of the midcontinent areas during summer (decreases in soil moisture).

In addition, it is indicated that the likely increase of precipitation extremes is more than precipitation means and the return period for extreme precipitation events decreases almost everywhere (SWCS, 2003).

With the above background the risk of soil erosion and related environmental consequences is clear, but the actual damage is not known and needs to be assessed. These insights are needed to determine (i) whether a change in the soil and water conservation practices is warranted under changed climate and (ii) what practices should be taken to adequately protect soil and water resources if a change is warranted (Zhang and Nearing, 2005). Though some general conclusions about climate change and their impacts have been drawn, especially at macro-scales, the potential damages of climate change in particular regions or farms need to be assessed under local conditions. Such information is useful for making decisions on how to adapt management practices to mitigate the adverse impacts of climate change (Li *et al.*, 2010). Predictions of runoff and sediment transport support decision makers in developing watershed management plans for better soil and water conservation measures. Iran located in arid and semi-arid part of the world might become one of the most vulnerable regions to climate change. Any change in soil loss and sediment load in this country may have significant implications for water resources development as well as water productivity and food security.

Various studies have been performed to determine the effects of climate change on watershed hydrology and sediment yield. For this purpose, a chain of General Circulation Models (GCM) or Regional Climate Models (RCM) in combination with downscaling techniques and hydrological models are used. For instance Muttiah and Wurbs (2002) used SWAT hydrologic model to simulate the likely impact of climate change on hydrological regime of San Jacinto River basin with 7300 km^2 drainage area in Texas. Rosenberg et al. (2003) simulated the effect of downscaled Hadley Centre Coupled Model version 2 (HadCM2) climate projections on the hydrology of 18 major water resource regions using SWAT hydrologic model, within the

Hydrologic Unit Model of the United State (HUMUS) Framework. Water yields were predicted to change from –11 to 153mm and from 28 to 342mm with respect to baseline conditions in 2030 and 2095, respectively. Aimed at prediction of stream flow in the upper Mississippi River basin Jha et al. (2006) used various global climate models (GCMs). Study results showed a wide range of changes, from a 6% decrease to a 51% increase depending primarily on precipitation patterns. Abbaspour et al. (2009) used SWAT model for studying the impact of future climate on water resources availability in Iran. Future climate scenarios for periods of 2010–2040 and 2070–2100 were generated from the Canadian Global Coupled Model (CGCM 3.1) for A1B, B1, and A2 scenarios. Analysis of daily rainfall intensities indicated more frequent and larger-intensity floods in the wet regions and more prolonged droughts in the dry regions. Nearing et al. (2005) compared runoff and erosion estimates of SWAT with the predictions of six other models in response to six climate change scenarios for the 150 km^2 Lucky Hills watershed in southeastern Arizona. The responses of all seven models were similar across six scenarios. They concluded that climate change could potentially result in significant increase of soil erosion if necessary conservation efforts are not implemented.

Chaplot (2007) determined that water yield was more sensitive to changes in precipitation than temperature or atmospheric CO2. Sediment loads were significantly affected by precipitation changes, while CO2 increases most significantly affected nitrate loadings for the Walnut Creek watershed in Iowa. Marshall and Randhir (2008) determined that climate change results in a significant change in the timing and runoff of sediment loading (20% to 40% increase in October, almost 50% decrease in March) in the Connecticut River watershed. Ficklin et al. (2010) determined the impacts of climate change on agricultural runoff yields in the San Joaquin watershed of California. Nitrate and total phosphorus yield decreased the most in increased temperature scenarios, and phosphorus yields were highly correlated to sediment yield, and therefore to precipitation and surface runoff. Phan et al. (2011) used SWAT model for simulating the impacts of climate change on stream discharge and sediment yield from Song Cau watershed in Northern Viet Nam. The results show that the highest changes in stream discharge (up to 11.4%) and sediment load (15.3%) can be expected in wet season in 2050s according to the high emission scenario (A2), while for the low emission scenario the corresponding changes equal 8.8% and 12.6%, respectively .

Overall, a wide range of SWAT applications underscores that this hydrologic model is a very flexible and robust tool that can be used to simulate a variety of watershed responses. Hence SWAT was selected in this study to simulate regional water flow and erosion dynamics at watershed scale (Gassman *et al.*, 2007). In this study, calibration-validation of the SWAT hydrologic water balance model to Gorganroud river basin as a case study in northern Iran is conducted, followed by processing of future climate change multi-model data. An outline of a linked forecast water and sediment transport modeling system is specified to analyze and test a set of business as usual and proposed watershed management policy options taking into account stakeholder predilections and climate change scenarios. We particularly intend to present the first step of our modeling framework and discuss the challenges faced while performeing the model setup and calibration-validation procedure.

Material and methods

Description of the study area

The Gorganroud river basin has a total area of 7138 km^2, and is located in northeastern Iran, between 36°43′to 37°49′N latitude and 54°42′to 56°28′ E longitude (Fig. 1). The main basin river course has a general west-east direction. Agriculture, range lands and forests dominant the basin's land use. The elevation ranges from 10m at the outlet to 2898 m at the top of highlands in south-west of the basin. The climate in Gorganroud is governed by semiarid in the eastern to wet in the western parts. The annual rainfall varies spatially from 231mm to 848mm. The length of the main stream is 333 km. The average minimum and the maximum temperatures range from 11˚C to 18.1˚C, respectively. High rainfall events in combination with sensitive soils to erosion and intensive land use change from range lands and forest to dry lands has caused more runoff and subsequently high soil losses and sediment yield.

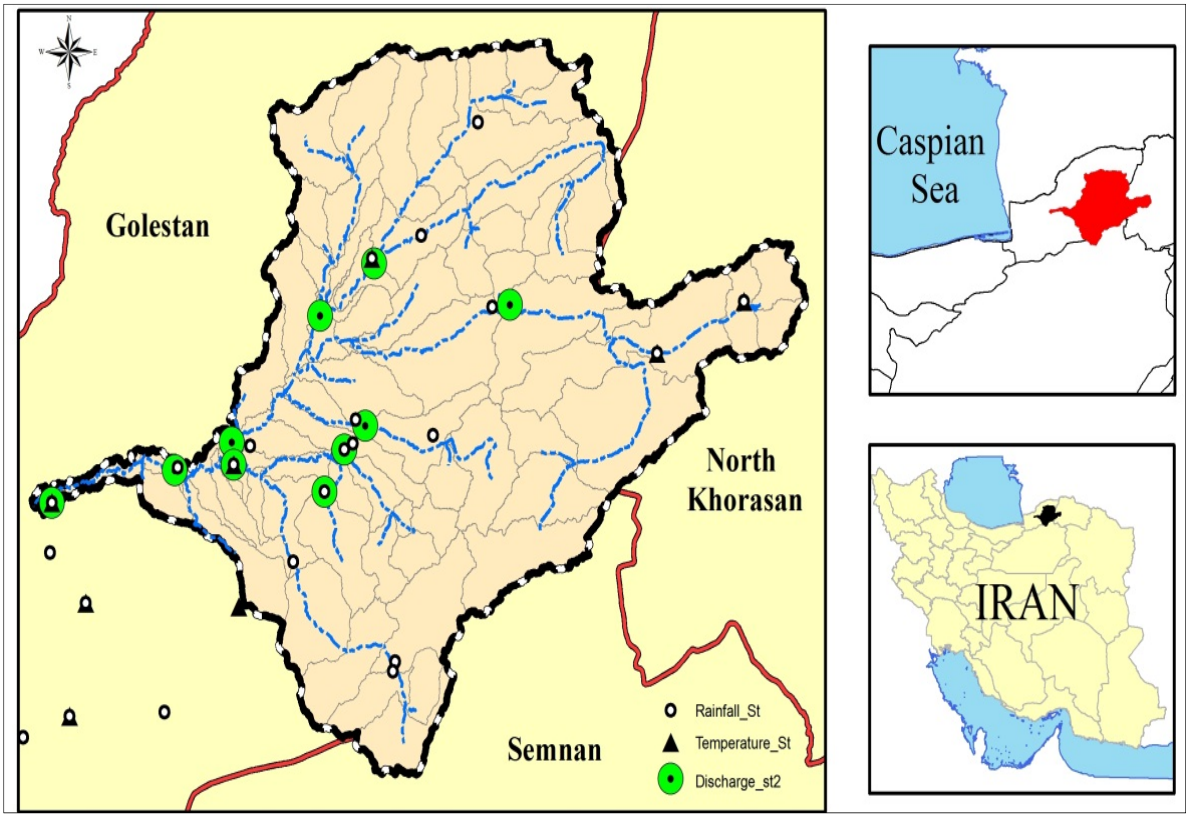

Fig. 1 Location of the Gorganroud basin in Iran.

The hydrologic model

The Soil and Water Assessment Tool (SWAT) is a physical process based model to simulate continuous-time landscape processes at basin scale (Arnold *et al.*, 1998). In this model spatial parameterization is performed by dividing the watershed into subbasins using the digital elevation model (DEM). The subbasins are further divided into hydrological response units (HRUs) based on the soil type, land use and slope classes that allow a high level of spatial detail simulation. The water balance equation is used to simulate hydrological components in each HRU. These include daily precipitation, runoff, evapotranspiration, percolation and return flow components. The surface runoff is estimated in the model using the Natural Resources Conservation Service Curve Number (CN) method and the Green and Ampt method. The percolation through each soil layer is predicted using storage routing techniques combined with the crack-flow model. The evapotranspiration is estimated using Priestley-Taylor, Penman-Monteith and Hargreaves techniques. The flow routing in the river channels is computed using the variable storage coefficient method, or the Muskingum method (Betrie *et al.*, 2011). The Modified Universal Soil Loss Equations (MUSLE) is used in the model to simulate soil erosion. The runoff energy detaches and transports the sediment. The sediment routing in the channel consists of channel degradation using stream power and deposition using fall velocity. Channel degradation is adjusted using USLE soil erodibility and channel cover factors (Arnold *et al.*, 1998).

Model setup

In this study the land use map was extracted from Landsat satellite images of 2010, with a spatial resolution of 30 m, which contains seven different land use classes. Soil texture map was obtained from the Iranian Ministry of Agriculture with a spatial scale of 1:250,000 and includes a set of estimated physical and chemical soil properties. Some nine textures were indentified in the soil map. The DEM at 90m resolution were obtained from the National Cartographic Centre of Iran.

Daily observed climate data including daily precipitation and temperature were obtained for 18 stations from the Iranian Meteorological Organization and the Water Resources Management Organization (WRMO) of Iran. WRMO also provided monthly discharge data from 10 hydrometric stations and a large number of total suspended sediment (TSS) samples for 6 hydrometric stations within the basin. A threshold value of 5000 ha was selected to delineate the basin. Slope (in five classes of 0-5, 5-12, 12-30, 30-60, and >60%), landuse and soil maps were used in the HRU delineation. A total of 79 subbasins and 554 HRUs were delineated in the study area. The selected methods to simulate runoff, evapotranspiration and channel routing were NRCS -CN, Hargreaves, and Muskingum, respectively.

Calibration and analysis

Sensitivity analysis, calibration, validation and uncertainty analysis were performed for the discharge-sediment processes. Based on general recommendations in the literature, some 82 parameters related to discharge and sediment yield were initially selected for calibration. The initially selected parameters are presented in Table 1.

For parameter optimization and uncertainty analysis in this study, we used the Sequential Uncertainty Fitting Program SUFI-2 (Abbaspour, 2007). In this algorithm all uncertainties (parameter, conceptual model, input, etc.) are mapped onto the parameter ranges as the procedure tries to capture most of the measured data within the 95% prediction uncertainty. Two indices were used to quantify the goodness of calibration/uncertainty performance. The P-factor, which is the percentage of data bracketed by the 95PPU band (maximum value 100%), and the R-factor, which is the average width of the band divided by the standard deviation of the corresponding measured variable.

In order to compare the simulated variables with those of observed values, we used coefficient of determination (R2) multiplied by the coefficient of the regression line, bR2. This function allows accounting for the discrepancy in the magnitude of two signals (depicted by b) as well as their dynamics (depicted by R2). The objective function is expressed as:

$$\phi = \begin{cases} |b|R^2 & \text{if} \quad |b| \le 1 \\ |b|^{-1}R^2 & \text{if} \quad |b| > 1 \end{cases} \tag{1}$$

In case of multiple variables, g is defined as:

$$g = \sum_i w_i \phi_i \tag{2}$$

Table1. Initially selected calibration parameters

Parameter name*	Description	Initial range	
		Min	Max
r__CN2.mgt	NRCS runoff curve number for moisture condition II	-0.5	0.5
v__ALPHA_BF.gw	Base flow alpha factor (days)	0	1
v__GW_DELAY.gw	Groundwater delay time (days)	30	450
v__CH_N2.rte	Manning's n value for main channel	0	0.3
v__CH_K2.rte	Effective hydraulic conductivity in the main channel (mm hr 1)	5	130
v__SURLAG.bsn	Surface runoff lag time (days)	1	24
r__SOL_AWC.sol	Soil available water storage capacity (mm H2O/mm soil)	-0.2	0.4
r__SOL_K.sol	Soil conductivity (mm hr 1)	-0.8	0.8
r__SOL_BD.sol	Soil bulk density (g cm 3)	-0.5	0.6
v__SFTMP.bsn	Snowfall temperature (°C)	-5	5
v__SMTMP.bsn	Snowmelt base temperature (°C)	-5	5
v__SMFMX.bsn	Maximum melt rate for snow during the year (mm°C 1 day 1)	0	10
v__SMFMN.bsn	Minimum melt rate for snow during the year (mm°C 1 day 1)	0	10
v__TIMP.bsn	Snow pack temperature lag factor	0.01	1
v__REVAPMN.gw	Threshold depth of water in the shallow aquifer for 'revap' to occur (mm)	0.02	0.2
v__GW_REVAP.gw	Groundwater revap. Coefficient	0	500
v__GWQMN.gw	Threshold depth of water in the shallow aquifer required for return flow to occur (mm)	0	5000
v__RCHRG_DP.gw	Deep aquifer percolation fraction	0	1
v__ESCO.hru	Soil evaporation compensation factor	0.01	1
v__EPCO.hru	Plant uptake compensation factor	0.01	1
r__OV_N.hru	Manning's n value for overland flow	0	0.8
r__SOL_ALB.sol	Moist soil albedo	-0.5	0.5
v__SLSUBBSN.hru	Average slope length	10	150
v__SHALLST.gw	Initial depth of water in the shallow aquifer	0	1000
v__PRF.bsn	Peak factor for sediment routing channel	0	2
v__SPCON.bsn	Linear re-entrainment parameter for channel sediment routing	0.001	0.01
v__SPEXP.bsn	Exponent of re-entrainment parameter for channel sediment routing	1	1.5
v__CH_COV.rte	Channel cover factor	0	1
v__CH_EROD.rte	Channel erodibility factor	0	0.6
r__USLE_K.sol	USLE soil erodibility factor	-0.8	0.8
r__USLE_C.CROP.DAT	USLE land cover factor	-0.5	0.5

* v__: means the default parameter is replaced by a given value, and r__ means the existing parameter value is multiplied by (1 + a given value)

We considered 1979–1991 and 1992–1999 as the simulation periods for calibration and validation, respectively. The first 3 years was considered as a warm-up period in which the model was allowed to initialize and approach reasonable initial values for model state variables.

Future Climate Data

In this study we aim to project discharge and sediment load for the period 2020-2040. The climate data from the Climatic Research Unit, University of East Anglia, under 18 scenarios for monthly fields of maximum temperature, minimum temperature, precipitation, and the number of wet days on a 0.5° grid from 2001 to 2100 are provided (Mitchell et al., 2004). The semi-automated daily weather generator algorithm (dGen), developed by Schuol and Abbaspour (2007), was used to obtain the required daily data from the monthly statistics of precipitation, minimum and maximum temperatures for the emission scenarios. The emission scenarios explore alternative development pathways, covering a wide range of demographic, economic and technological driving forces. The A1 storyline assumes a world of very rapid economic growth, a global population that peaks in mid-century and rapid introduction of new and more efficient technologies. A1FI describes fossil intensive directions of technological change. B1 describes a convergent world, with the same global population as A1 family, but with more rapid changes in economic structures toward a service and information economy. B2 describes a world with intermediate population and economic growth, emphasizing local solutions to economic, social, and environmental sustainability. A2 describes a very heterogeneous world with high population growth, slow economic development and slow technological change. We will use SWAT-SUFI2 to calculate the changes in the variables relative to the corresponding historic simulations during 1979-1999 with respect to different emission scenarios.

Results

Initial SWAT calibration runs indicate that while the river discharge may be simulated well, the reasonable results could not be obtained with respect to the sediment load. The results of runoff and sediment calibration at the main outlet of the basin are presented in Figures 2 and 3. Further effort should be directed at discovering potential reasons for low performance of the simulated sediment. Possible reasons for over-estimation of sediment load and discharge are insufficient accounting of agricultural and industrial water use in the model, constructed flood control measures, land use changes and construction of roads and tunnels that can affect the local hydrology of the basin during the calibration period. Next we will use the calibrated validated model to assess the impact of climate change at the Gorganroud river basin on stream flow and sediment yield.

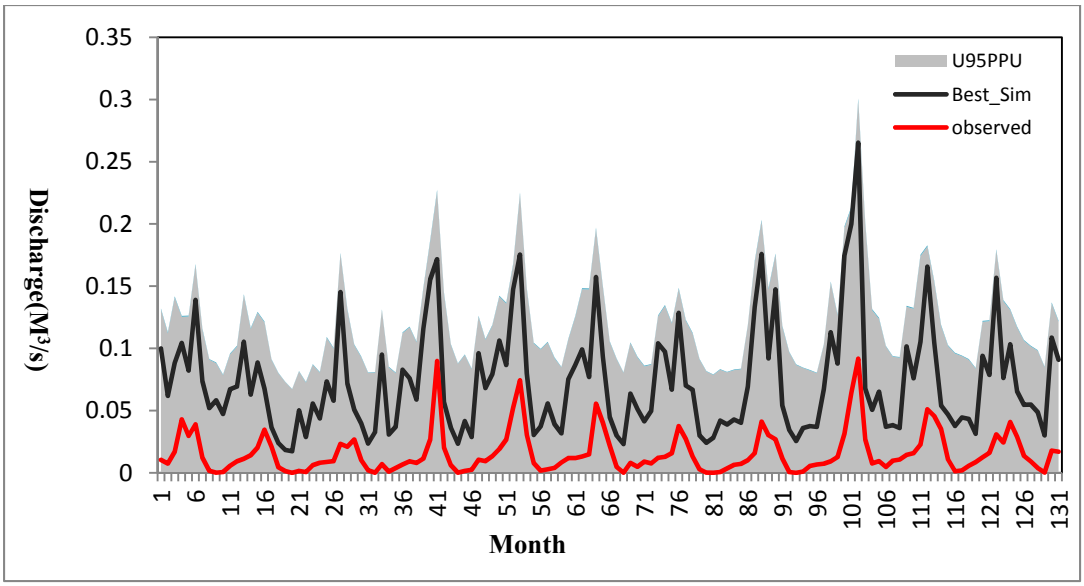

Fig. 2 Result of initial runoff calibration

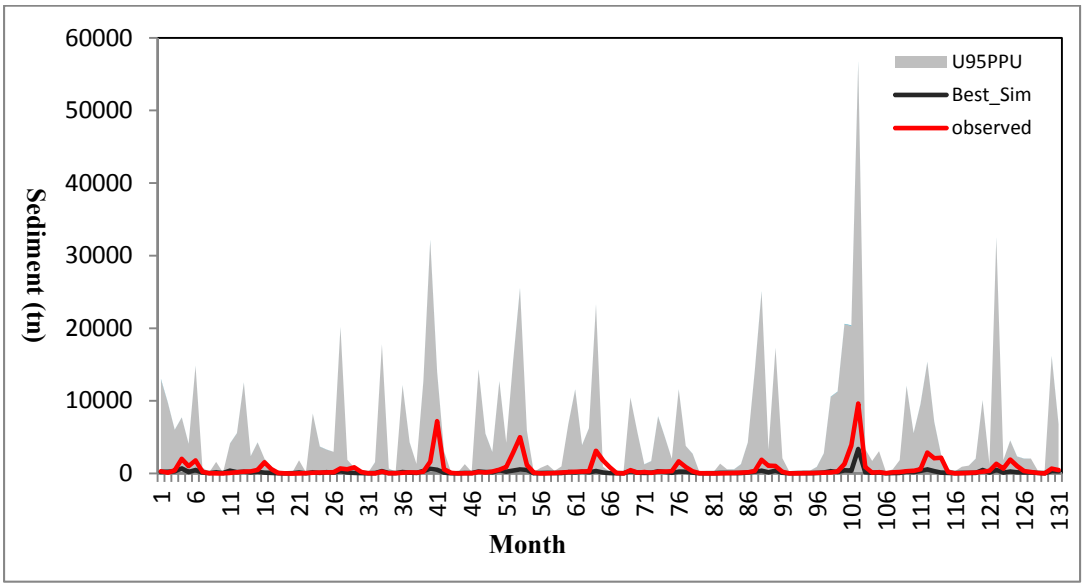

Fig. 3 Results of initial sediment calibration

References

Abbaspour, K.C., 2007. User manual for SWAT-CUP, SWAT calibration and uncertainty analysis programs. Eawag: Swiss Fed. Inst. Of Aquat. Sci. and Technol., Du¨bendorf, Switzerland.

Abbaspour, K.C., Faramarzi, M., Ghasemi, S.S., Yang, H., 2009. Assessing the impact of climate change on water resources in Iran. Water Resources Research 45.

Arnold, J.G., Srinivasan, R., Muttiah, R.S., Williams, J.R., 1998. Large area hydrologic modeling and assessment part I: model development1. Journal of the American Water Resources Association 34, 73-89.

Betrie, G.D., Mohamed, Y.A., van Griensven, A., Srinivasan, R., 2011. Sediment management modelling in the Blue Nile Basin using SWAT model. Hydrol. Earth Syst. Sci. 15, 807-818.

Chaplot, V., 2007. Water and soil resources response to rising levels of atmospheric CO2 concentration and to changes in precipitation and air temperature. Journal of Hydrology 337, 159-171.

Ficklin, D.L., Luo, Y., Luedeling, E., Gatzke, S.E., Zhang, M., 2010. Sensitivity of agricultural runoff loads to rising levels of CO2 and climate change in the San Joaquin Valley watershed of California. Environmental Pollution 158, 223-234.

Gassman, P.W., Reyes, M.R., Green, C.H., Arnold, J.G., 2007. The soil and water assessment tool: Historical development, applications, and future research directions. Trans. ASABE 50, 1211-1250.

Jha, M., Arnold, J.G., Gassman, P.W., Giorgi, F., Gu, R.R., 2006. Climate change sensitivity assessment on upper mississippi river basin streamflows using SWAT. JAWRA Journal of the American Water Resources Association 42, 997-1015.

Li, Z., Liu, W.-Z., Zhang, X.-C., Zheng, F.-L., 2010. Assessing the site-specific impacts of climate change on hydrology, soil erosion and crop yields in the Loess Plateau of China. Climatic Change, 1-20.

Marshall, E., Randhir, T., 2008. Effect of climate change on watershed system: a regional analysis. Climatic Change 89, 263-280.

Muttiah, R.S., Wurbs, R.A., 2002. Modeling the impacts of climate change on water supply reliabilities. Water International 27, 407-419.

Nearing, M.A., Jetten, V., Baffaut, C., Cerdan, O., Couturier, A., Hernandez, M., Le Bissonnais, Y., Nichols, M.H., Nunes, J.P., Renschler, C.S., Souchère, V., Van Oost, K., 2005. Modeling response of soil erosion and runoff to changes in precipitation and cover. CATENA 61, 131-154.

Nunes, J.P., Seixas, J., Pacheco, N.R., 2008. Vulnerability of water resources, vegetation productivity and soil erosion to climate change in Mediterranean watersheds. Hydrological Processes 22, 3115-3134.

Phan, D., Wu, C., Hsieh, S., 2011. Impact of climate change on stream discharge and sediment yield in Northern Viet Nam. Water Resources 38, 827-836.

Rosenberg, N.J., Brown, R.A., Izaurralde, R.C., Thomson, A.M., 2003. Integrated assessment of Hadley Centre (HadCM2) climate change projections on agricultural productivity and irrigation water supply in the conterminous United States: I. Climate change scenarios and impacts on irrigation water supply simulated with the HUMUS model. Agricultural and Forest Meteorology 117, 73-96.

SWCS, 2003. Conservation implications of climate change: soil erosion and runoff from cropland.

Yu, P.-S., Wang, Y.-C., 2009. Impact of climate change on hydrological processes over a basin scale in northern Taiwan. Hydrological Processes 23, 3556-3568.

Zhang, X.C., Nearing, M.A., 2005. Impact of climate change on soil erosion, runoff, and wheat productivity in central Oklahoma. CATENA 61, 185-195.

Preliminary Results from Subsurface Hydrological Investigations of Dehgolan Plain, Kurdistan, Iran using Geophysical Techniques

Payam Sajadi
Remote Sensing Applications Laboratory, School of Environmental Sciences,
Jawaharlal Nehru University, New Delhi, India
Email – Payam.Sajadi@gmail.com

Amit Singh
Remote Sensing Applications Laboratory, School of Environmental Sciences,
Jawaharlal Nehru University, New Delhi, India
Email – amsingh5@gmail.com

Saumitra Mukherjee *
Remote Sensing Applications Laboratory, School of Environmental Sciences,
Jawaharlal Nehru University, New Delhi, India
Email – saumitramukherjee3@gmail.com

Kamran Chapi
Assistant Professor, Department of Rangeland and Watershed Management,
College of Natural Resources, University of Kurdistan, Sanandaj, Iran
Email – K.Chapi@uok.ac.ir

Dehgolan Basin is located in the Kurdistan province, eastern part of Sanandaj City in Iran. This area is known as Dehgolan Basin where eastern part of it is limited by Qorveh-Plain. The entire basin area is estimated to be 2550 square km.

From a geological perspective, Dehgolan plain can be counted as a part of Sanandaj-Sirjan zone which has the same geological history as Iran Central Zone. However, its structure, orientation and layer slope is different, mostly similar to Zagros. Dolomite, shale, quartzite, shale and sandstone found in this area are very important from aquifer transmissivity point of view.

The need for conducting this research is studying conditions for protecting groundwater supplies as a unique source of water for this area. Geoelectrical surveys using the electrical resistivity method were carried out in the Dehgolan-Plain (Kurdistan Province, Iran) to investigate the sub-surface layering and water level. Applying the Schlumberger array, a total of 189 vertical electrical soundings were performed. Bore holes information and lithology data were modelled using Rockwork software to generate 3D sections and groundwater flow regime in the area. This was correlated with geological and geomorphological maps of the area and surface topography data. Ground truth surveys with GPS, soil texture analysis, topographic analysis have also taken place to generate a GIS database, aiding in further correlation and analysis.

Key Words: Hydrological investigations, Schlumberger array, Transmissivity, Rockworks, Kurdistan

Introduction

Hydrological investigations, particularly in arid zones, are becoming a worldwide concern for the need of additional and sustainable water resource. In case of subsurface investigations for groundwater, geophysical techniques such as geo-electrical surveying have been quite successful (Todd and Mays, 2005; Keller and Frischknecht, 1966). Vertical electrical sounding using Schlumberger array has been successfully used over years in various terrain and geological settings (Van Overmeeren, 1989; Urish and Frohlich, 1990; Ebraheem et al., 1997; Sharma and Baranwal, 2005). George et al. (2011) used a combination of Schlumberger array data, and borehole information to gain useful information of subsurface hydrologic condition as well as quantitative aquifer geometry.

The area under study is located in the Kurdistan province and eastern part of Sanandaj City in Iran. This area is known as Dehgolan Basin where eastern part of it is limited by Qorveh-Plain. The whole basin area is estimated to be 2550 square km. Alavi (1994) considers the Sanandaj-Sirjan zone as a sub zone of Zagros. From a geological perspective, Dehgolan plain can be counted as a part of Sanandaj-Sirjan zone which has the same geological history as Iran Central Zone. However, its structure, orientation and layer slope is different, mostly similar to Zagros. Dolomite, shale, quartzite, shale and sandstone found in this area are very important from aquifer transmissivity point of view.

Methodology

Since subsurface investigations in such an area need a large amount of data to be analysed, a multidisciplinary approach was followed integrating datasets and investigations of various types and magnitudes. Data for vertical electrical soundings covering the entire study area, done by applying Schlumberger array, were collected. Before being able to use this whole dataset for studying, predicting and performing subsurface modelling, actual borehole information for a smaller part of the total area was used to perform a preliminary investigation into real existing subsurface hydrological regime and to create necessary templates for GIS investigations. To achieve this, borehole information and lithology data from 12 drillings were modelled using Rockworks software to generate subsurface 3D sections and groundwater flow regime pattern.

This was correlated with geological and geomorphological maps of the area and surface topography data. Ground truth surveys with GPS, soil texture analysis, topographic analysis have also been performed to generate a GIS database, aiding in further correlation with results from remote sensing observations by satellite images.

Results and Discussion

Resistivity Surveys modelling

In total, data for 189 resistivity soundings, performed along various zones spanning the whole drainage basin of Dehgolan plain, was interpreted and modelled to define the possible subsurface lithological layers and associated resistivity (or rather conductivity) differences. This layered information was then stored as a 3D geodatabase to be used later for modelling, and defining the nature of various lithounits in determining hydraulic flow and conductivity for the whole area as well as associated various drainage basins. This information may not be of much physical meaning if not verified by correlating with actual drilling information or other types of indirectly interpreted information about both surface and subsurface hydrological regime.

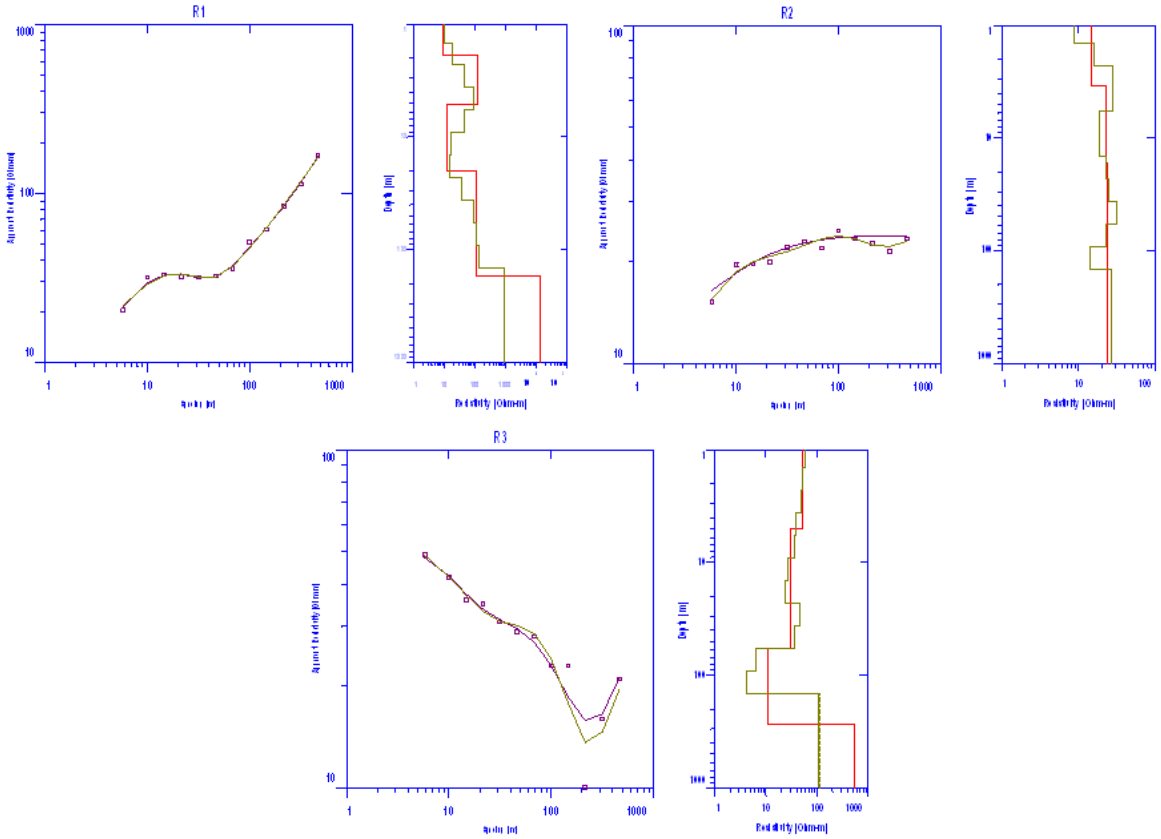

Fig.1 Sample resistivity curves and interpreted layer thickness from study area

Subsurface Modelling

3D Model of Boreholes

A 3 dimensional model of boreholes with respective lithology (Fig. 1) was generated to show their relative positioning in 3D space. The top of individual boreholes is also an indicator of altitude values associated with respective ground surface.

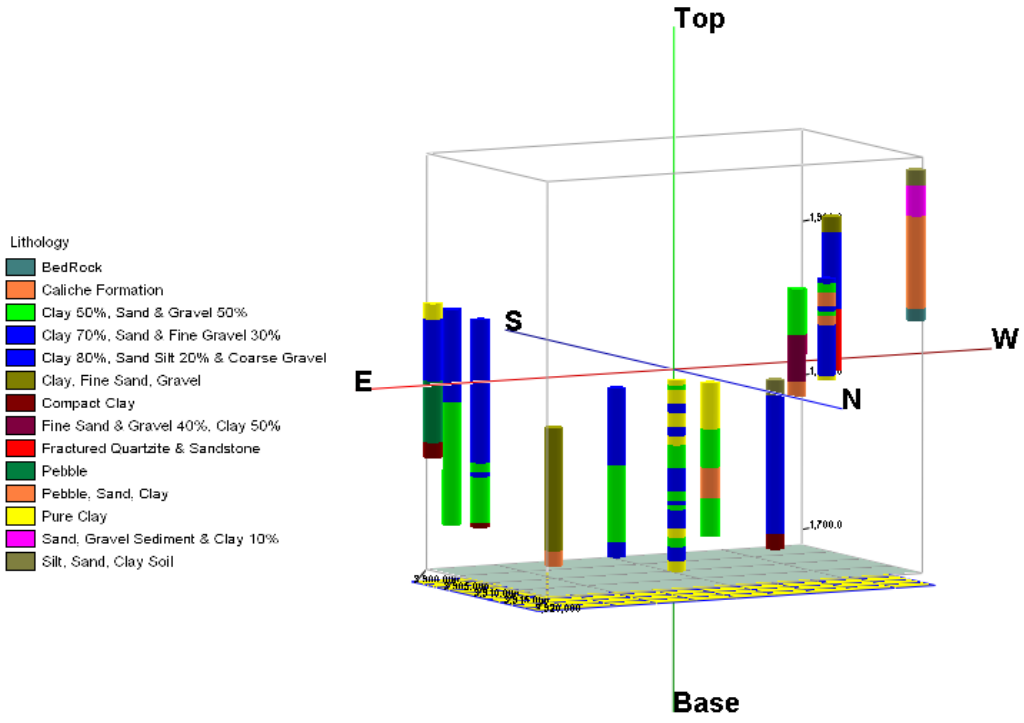

Fig.2 3D representation of 12 boreholes with respective lithology

Hole to Hole Log Section

A section for all boreholes was generated (Fig. 3) for comparing relative positioning of all boreholes from NW to SE direction. Borehole P3 has the highest elevation which refers to an elevated area whereas P8, P6, P2, P7 and P11 were found to be at lowest elevation. In general a decreasing trend in elevation was observed as we move towards eastern side. However, the drilling depth was found to be more in eastern side. This can simply be attributed to the fact that the NW part is dominated by rocky type of lithology whereas the SE aquifers are dominated by loose gravely materials and clay.

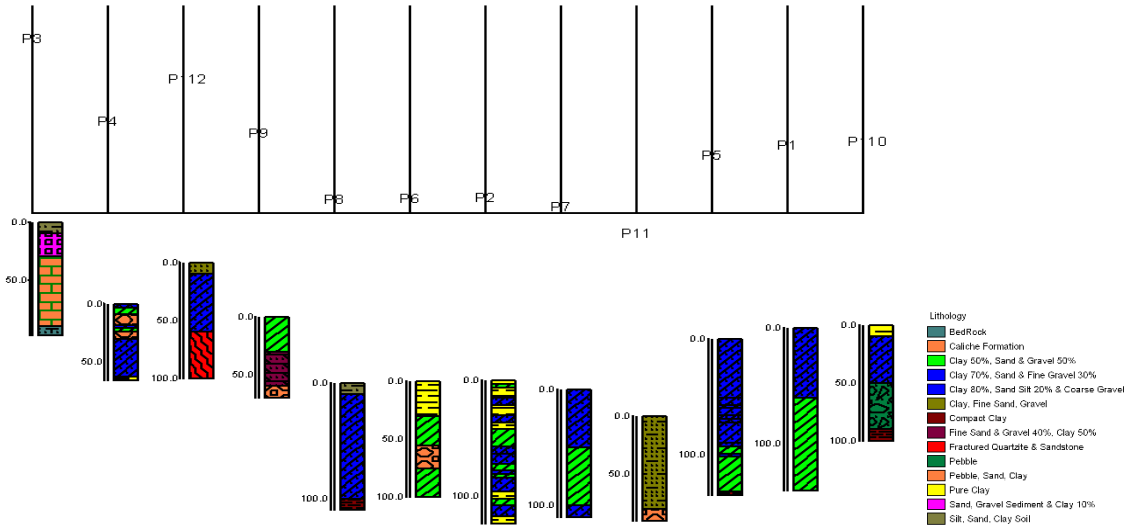

Fig.3 Borehole to borehole cross-section

3D Fence Diagram

Three dimensional fence diagram (Fig. 4) generated for the study area by constructing all possible connections between the 12 boreholes previously modeled. These panels of fence diagram were basically made to connect lithologs together to show which type of lithology could be dominant in between them. As generated model shows that top layers in most parts are predominantly composed by gravel, sand and clay (10%) whereas, the bottom layers are mostly composed of fractured quartzite and sandstone. Also, presence of multi-layered aquifers was detected in NW portions. In such types of multi-layered aquifers, use of slotted pipe arrangement while drilling is expected to increase the overall yield from a borewell. As we move from west to east the thickness of clay increases meaning that the direction of subsurface water flow should possibly be west to east.

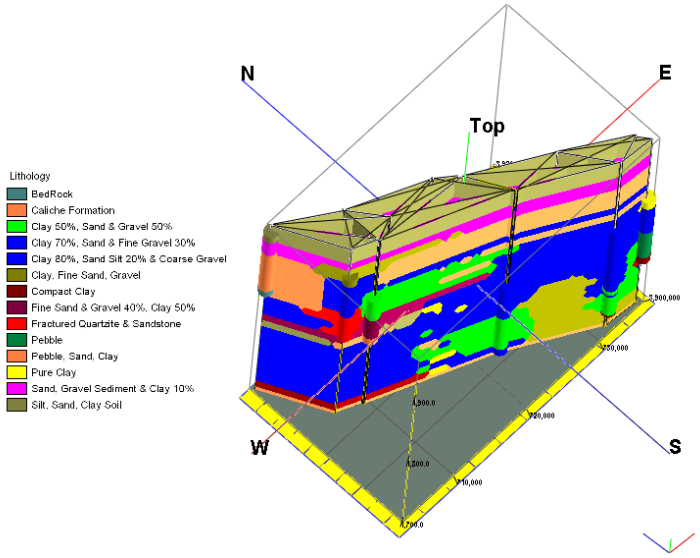

Fig.4 3D Fence Diagram

Lithology Solid Model

Sub-surface lithological information was used to generate a lithology solid model (Fig. 5b) for the area covered by the 12 boreholes. The lithology types along each borehole were identified certain values were assigned to those nodes along the wells. Then “lithoblending” method was used to assign lithology nodes lying between wells (Fig. 5a). Finally, it was extrapolated to the whole subsurface volume covered. Basically the solid model will be helpful later while figuring volumetric coverage by a specific lithology type or while assigning flow characteristics to all or some particular nodes based on lithology while attempting quantitative subsurface hydrological modeling.

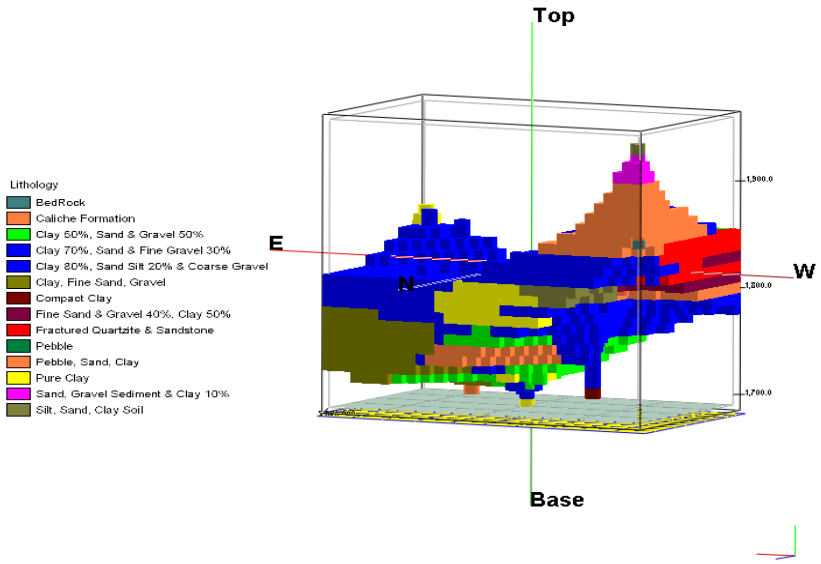

Fig.5a Lithology solid model - initiation

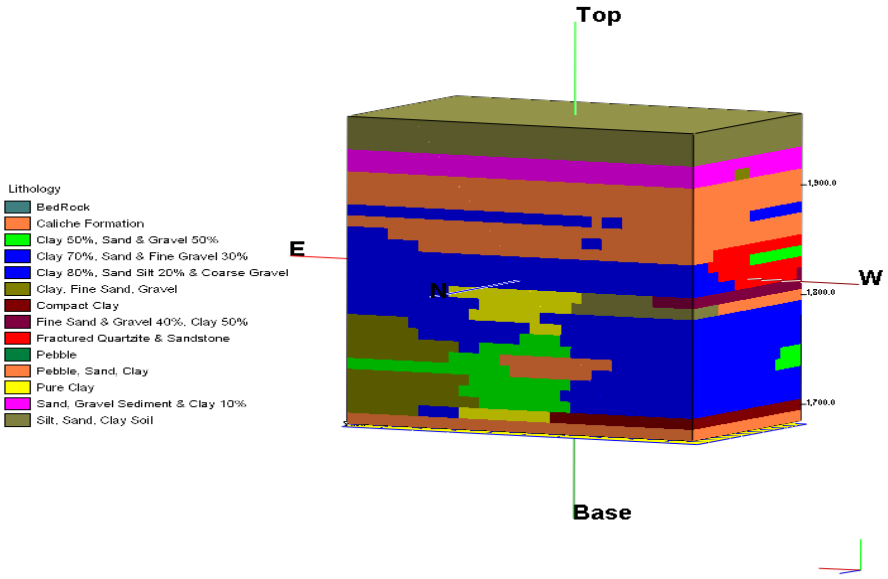

Fig.5b Lithology solid model - final

Aquifer Model

The final output for subsurface modeling was generated in terms of aquifer models for the part of study area covered by lithologs. The generated model illustrates direction of subsurface water flow, aquifers thickness and aquifer behavior in extrapolated domains.

Two types of gridding were used for defining area's interpolated aquifer surface:

1. Type 1 (Fig. 6a) - 8 neighbor first order polyenhancing, inverse distance gridding with weighted exponent equal to 3.0, ran over 10 iterations of densification. This was found mainly suitable for interpolation between boreholes.
2. Type 2 (Fig. 6b) - 16 neighbor exponential variogram fitted krigging. This was found suitable for smoothened outputs for both interpolation and extrapolation of aquifers.

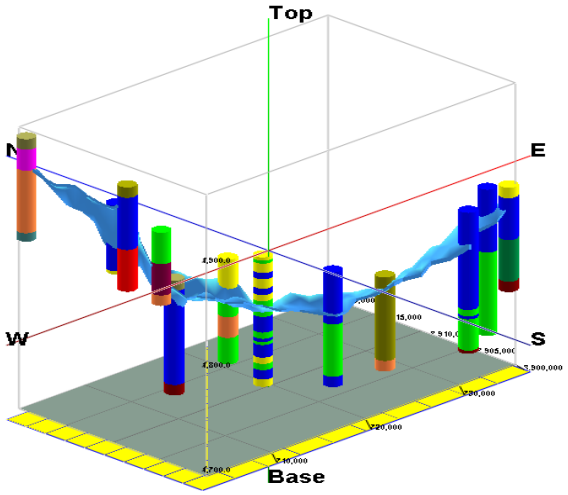

Fig.6a Aquifer model using Inverse Distance Gridding
(Vertical exaggeration = 125, rotated for best view)

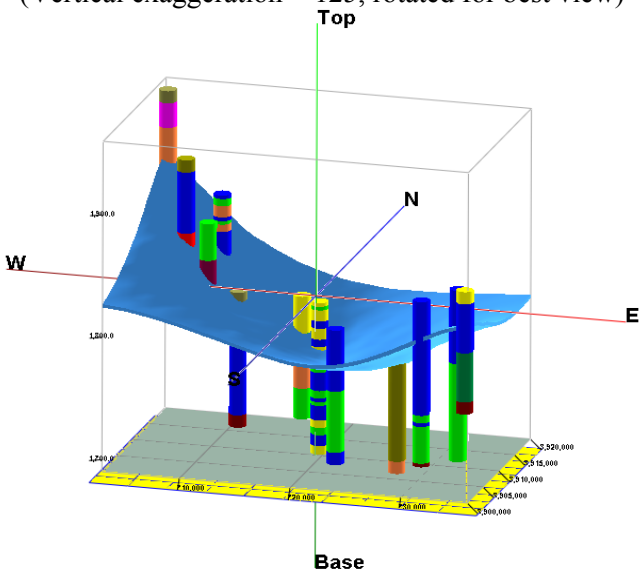

Fig.6b Aquifer model using Krigging
(Vertical exaggeration = 125, rotated for best view)

These models describe the extrapolated water levels of boreholes as a water layer or sheet of water. These models clearly show that the water level and thickness of aquifer is stronger in

West to Northwest Direction rather than East to South-East Direction. These can be used later for simulating specific yields of aquifers or imaginary borehole locations.

Soil Texture Analysis

Ternary diagram for soil texture analysis (Fig. 7a) was made and compared to USGS soil texture triangle (Fig. 7b). The results are shown in Table 1. It was observed that clay loam is distributed from west to north-west and east to south east, and silt clay texture is more seen in west to center of study area and also it is observed in south east. Loamy texture was observed to be more dominant in western part than the eastern part of area, and finally silt loam was equal in terms of distribution in south east and north-west direction of area.

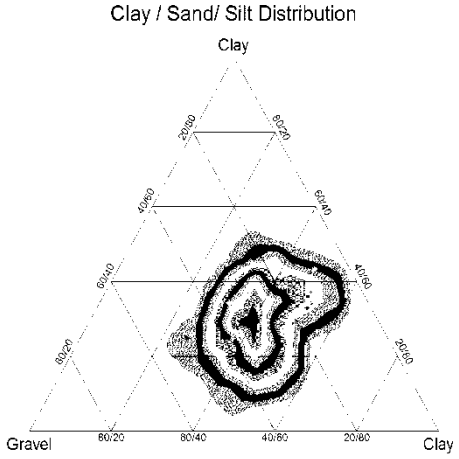

Fig.7a Ternary diagram showing soil texture

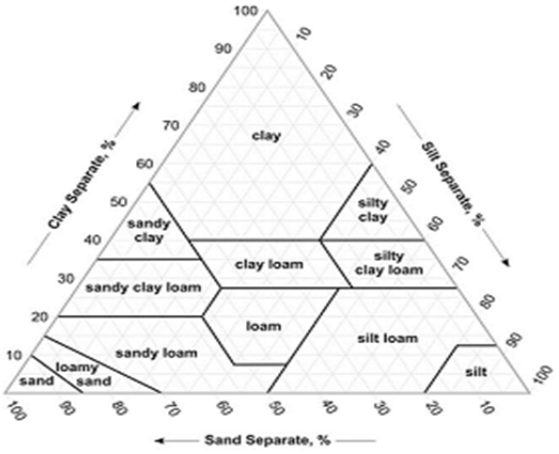

Fig.7b USGS soil texture triangle

Table1. Soil texture analysis results

Location Code	Village	Interpreted Texture
A	Avangan	Clay Loam
B	Kamal Abad	Loam
C	Kazem Abad	Clay Loam
D	Ganji	Clay Loam
E	Dehgolan	Clay Loam
F	Sarab	Silt Clay Loam
G	Talvar	Silt Clay Loam
H	Karondan	Clay
I	Shoorab Ahaji	Loam
J	Ghroochai	Clay Loam
K	Kaka Joob	Silt Loam
L	Miraki	Loam
M	Kani Onaili	Silt Loam
N	Ali Pinak	Clay Loam
O	Dizaj	Loam
P	Ali Abad Moshir	Clay
Q	Taze Abad Ghroochai	Silt Clay Loam
R	Baga Jan	Clay Loam
S	Hussieni	Clay Loam
T	Dehrashid	Silt Clay Loam
U	Asiab Choob	Loam

GIS Data

Drainage maps generated for the area were correlated with observations from Landsat images (of different seasons) along with slope and aspect maps generated from SRTM 90m data.

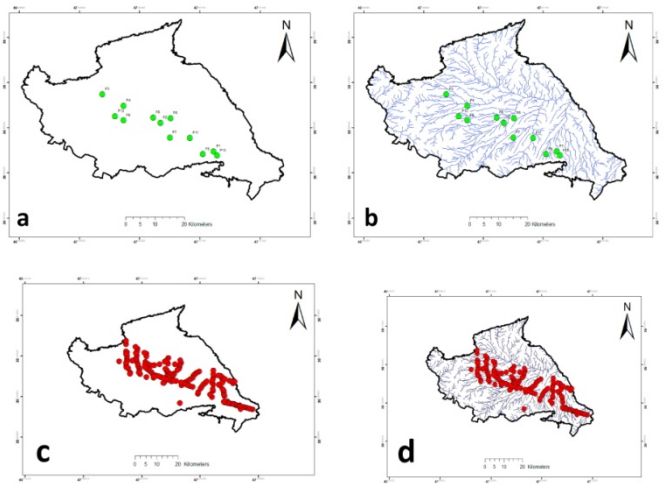

Fig.8 (a) Location of boreholes in area of study, (b) Boreholes distribution along drainage
(c) Resistivity surveys location, (d) Resistivity surveys distribution along drainage

The slope and aspect of a drainage basin are one of the major factors affecting time of overland flow and concentration of water received from rainfall. Generated slope map (Fig. 9) shows that gentle slope for most part of study area with range of 0-30% which is indicated by green colour, the red colour is location of area with steep slope which can be representation of mountainous or hilly area with shorter response time to overland flow and increase in discharge. Aspect map (Fig. 10) shows that the elevated areas have east –west faces which direct preferential flow direction in the drainage basins.

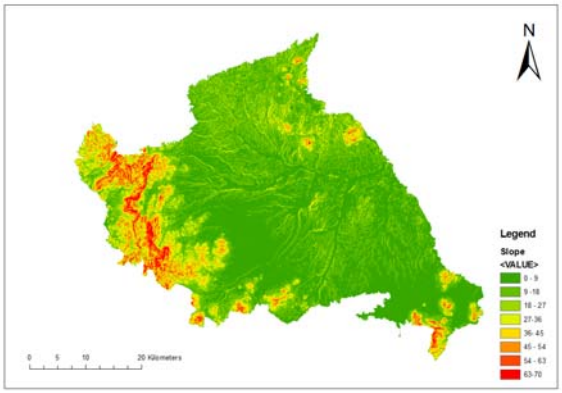

Fig.9 Slope map for study area

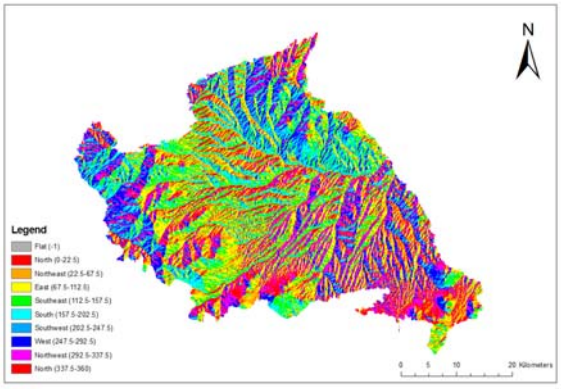

Fig.10 Aspect map for study area

Conclusions

Generated models from boreholes lithology, resistivity surveys and soil texture analysis gives suitable set of information for assessment of water level depth and its behaviour under various geological conditions for a part of the study area. This data set can later be used for validating models created for the whole area and while planning for groundwater exploration with help of remote sensing and GIS techniques or while creating more detailed studies on cumulative water balance in the area.

Acknowledgements

The authors are grateful to the Water Resource Agency of Sanandaj (Kurdistan) for providing requisite data and CGIAR-CSI SRTM 90m Database as the source of elevation data.

Dr. Loghman Namaki, Mr. Salvaty, Mr. Babaie and their colleagues are also acknowledged for their constant help and cooperation.

References

- Alavi M. 1994. Tectonics of the Zagros orogenic belt of Iran: New data and interpretations. *Tectonophysics* 229: 211–38.
- Ebraheem, A.M., Sensosy, M.M., and K.A. Dahab. 1997. Geo-electrical and Hydro-geochemical studies for delineating ground-water contamination due to salt-water intrusion in the northern part of the Nile delta, Egypt. *Ground Water* 35: 216–222.

- George, N.J., Obianwu V.I. and I.B. Obot. 2011. Estimation of groundwater reserve in unconfined frequently exploited depth of aquifer using combined surficial geophysical and laboratory techniques in The Niger Delta, South – South, Nigeria. *Advances in Applied Science Research* 2 (1): 163-177.
- Sharma, S.P. and V.C. Baranwal. 2005. Delineation of groundwater-bearing fracture zones in a hard rock area integrating very low frequency electromagnetic and resistivity data. *Journal of Applied Geophysics* 57(2): 155-166.
- Todd, D.K. and L.W. Mays. 2005. *Groundwater hydrology*. 3rd Ed. John Wiley and Sons
- Urish, D.W. and R.K. Frohlich. 1990. Surface electrical resistivity in coastal groundwater exploration. *Geoexploration* 26: 267–289.
- Van Overmeeren, R.A. 1989. Aquifer boundaries explored by geoelectrical measurements in the coastal plain of Yemen: a case of equivalence. *Geophysics* 54: 38–48.

Sediment Yield Modeling using SWAT and Geospatial Technologies

Prabhanjan A
Former Post Graduate Student, Department of Civil Engineering, IIT Bombay,
a.prabhanjan@gmail.com

Rao E.P. (*)
Associate Professor, Department of Civil Engineering, IIT Bombay, ceepria@iitb.ac.in

Eldho T.I.
Professor, Department of Civil Engineering, IIT Bombay, eldho@iitb.ac.in

Abstract

Extensive soil erosion and its attendant ills have already contributed very significantly to the impoverishment of land and people throughout the world. Essential plant nutrients are lost with soil erosion. The soil lost is deposited in various reservoirs, thereby reducing their capacity. Thus, such a situation demands effective planning and implementation of soil and water conservation measures for which water and sediment yield have to be estimated. In this study, an attempt has been made to use SWAT model, GIS and remotely sensed data for modelling the runoff and sediment yield for Khadakohol watershed in Maharashtra, India. GIS and remotely sensed data are used to develop the required database for the SWAT model. The model's effectiveness has been assessed for its output with default parameters (Prediction in Ungauged Basins) and after scheduling management operations. The model has been calibrated for both runoff and sediment yield for the monsoon months of 2002. Sensitivity analysis, auto and manual calibration have been adopted to get better results. The model has been validated for the monsoon months of 2003 and 2004. The SWAT model, with default parameters has given realistic results, specifically runoff, and the results improved with calibration. It was observed that management parameters have a greater effect on the sediment yield than runoff. Spatio-temporal analysis of sediment yield has also been carried out. Thus, the model has been found to be useful for simulation of runoff and sediment yield even when the calibration data is not available (default parameters) or available for short duration.

Keywords: SWAT model, Remote Sensing, GIS, Runoff, Sediment Yield, Ungauged Basin

Introduction

Soil erosion is a wide spread phenomenon on the earth's surface. Apart from natural soil erosion, accelerated soil erosion due to anthropogenic intervention continues to be a global constraint to economic development. The soil erosion accompanies loss of essential plant nutrients and the soil lost is deposited in various reservoirs, thereby reducing their capacity. As the erosion process is due to complex interaction of various hydrological and geological processes (White, 2005), it is difficult to estimate. Modeling provides an alternative approach for estimation of sediment yield and also a better understanding of sediment movement and delivery. A number of modeling tools have been developed for this purpose like Universal Soil Loss Equation (USLE) and its revised/modified forms, Hydrologic Simulation Program Fortran (HSPF), Water Erosion Prediction Project (WEPP) etc.

Soil and Water Assessment Tool (SWAT) is an integrated hydrologic model used to predict the effect of land management practices on water, sediment and agricultural chemical yields in large complex watersheds (Neitsch et al., 2005). Geospatial technologies are playing a major role in hydrological modeling in the recent years. Remote sensing is being widely used in hydrological modeling as it is capable to generate necessary information in spatio-temporal domain and GIS is used to handle such large data. The purpose of this paper is to assess the applicability of SWAT model combined with the applications of remotely sensed data and GIS in sediment yield modeling for a watershed where some/no data is available (Prediction in an Ungauged Basin context).

Study Area

The Khadakohol watershed lies between East Longitudes of 73° 17' to 73° 20' and North Latitudes of 20° 7' to 20° 9' as shown in Fig. 1. The watershed has an area of 5.468 km^2. The elevation varies from 235m in the north to 530m in south above mean sea level. The watershed is mostly hilly and has undulating to rolling topography. The watershed lies in the western ghats of Deccan plateau and the principal rock formation in the area consists of basaltic trap and amygdaloids and conglomerates underlying hills and terraces (Naik, 2008).The soils in the watershed are mainly sandy silt loam. The area receives rainfall mainly during South-West monsoon and the mean annual rainfall is about 2275mm. Major land class in the watershed is forest

followed by agricultural lands. Crops are grown mainly during Kharif season (June-September). Paddy is the major crop followed by Finger Millet.

Fig. 1. Location map of Khadakohol watershed

Application of SWAT Model

The SWAT model has been applied for modeling the runoff and sediment yield from Khadakohol watershed. The procedure followed has been explained briefly in this section:

Model Input

Basic data used for SWAT modeling are:

1. Digital Elevation Model (DEM): The DEM of cell size 50 m has been derived from the Survey of India toposheet (1:25,000 scale) using Spatial Analyst of ArcGIS and is shown in Fig. 2(a).
2. Remotely sensed data from IRS 1D LISS III imagery of January 13, 1998, with resolution of 23.5 m has been used to prepare the landuse-landcover map as shown in Fig. 2(b). The classes are agriculture (30.82%) and forest (69.18%).
3. As the soil map was not available, information from soil survey report (Wankhede et al., 1984) has been used to derive the map using ArcGIS. The slope map derived from DEM and the LU/LC maps have been combined to obtain the required soil map as shown in Fig. 2(c). The soil series are Galonda and Vinval.
4. The hydrological data (rainfall, runoff, and sediment concentration) were obtained through personal communication (Guy Honore, Project Coordinator, "Indo-German

Bilateral Project on Watershed Management" Ministry of Agriculture, Govt. of India, 2005). The daily weather parameters required are minimum and maximum temperature, relative humidity, wind speed, and solar radiation. All of these, except solar radiation are obtained from IMD. The solar radiation is downloaded from the NCEP/NCAR Reanalysis Project at the NOAA/ESRL Physical Sciences Division (http://www.esrl.noaa.gov/psd/data/reanalysis/reanalysis.shtml).

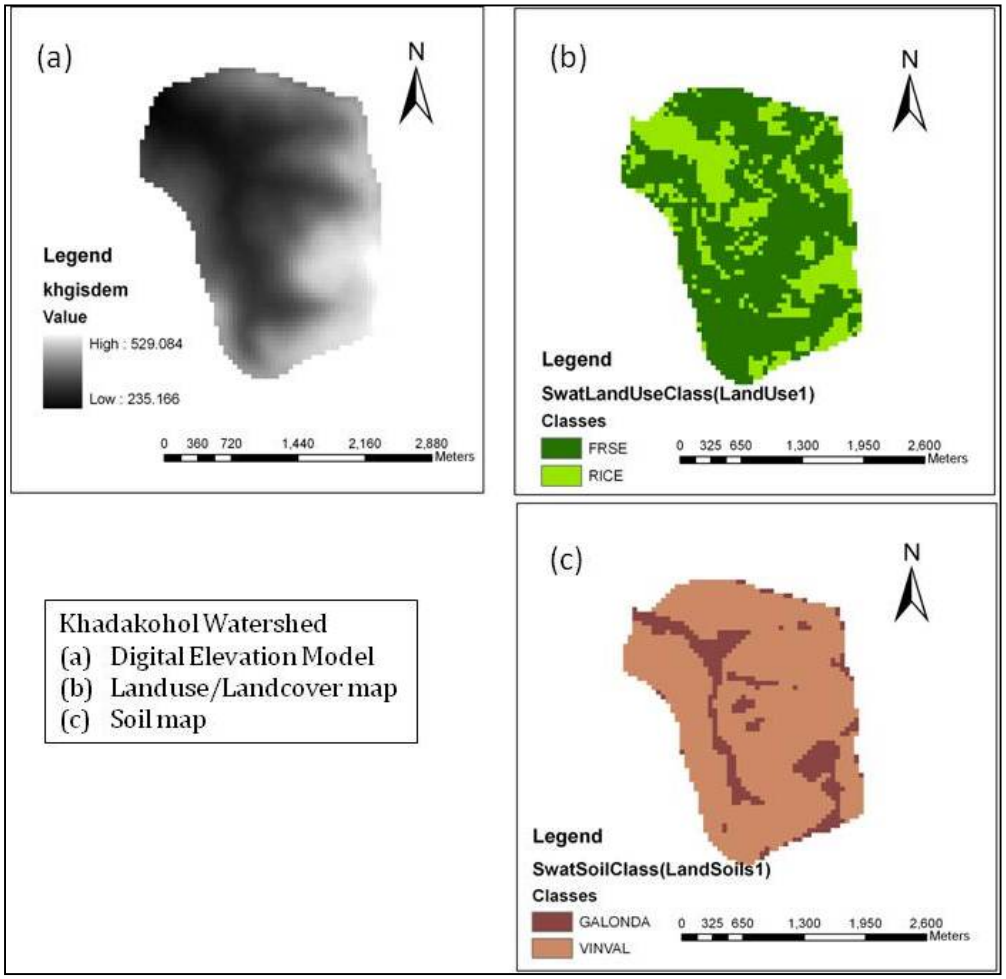

Fig. 2. Khadakohol watershed (a) DEM, (b) LU/LC map and (c) Soil map

Watershed Delineation and HRUs

The derived DEM has been given as input and the watershed delineation has resulted in 23 subbasins. The threshold area to delineate a subbasin was chosen as 10.9 ha by default. The delineated watershed along with reaches is shown in Figure 3(a).

The two land classes (forest and agriculture), two soil classes (Galonda and Vinval) and two slope classes (<10% and >10%) are overlaid to result in unique combinations. A threshold criterion of 10% of area for each landuse, soil and slope classes has been laid to create multiple Hydrological Response Units (HRUs) in a subbasin. This operation resulted in 74 HRUs for Khadakohol watershed as shown in Figure 3(b).

Model Parameterization

For Khadakohol watershed, default model parameters have been used to the extent possible. Manually changed parameters include 0.035 for Manning's 'n' for both main and tributary channels in the *.sub* file, 0.035 and 0.1 respectively for Manning's 'n' for agriculture and forest overland flow in *.hru* file. The cover management factor for agricultural and forest land were 0.2 and 0.01 respectively (Naik, 2008). These values have been incorporated in the *.rte* file.

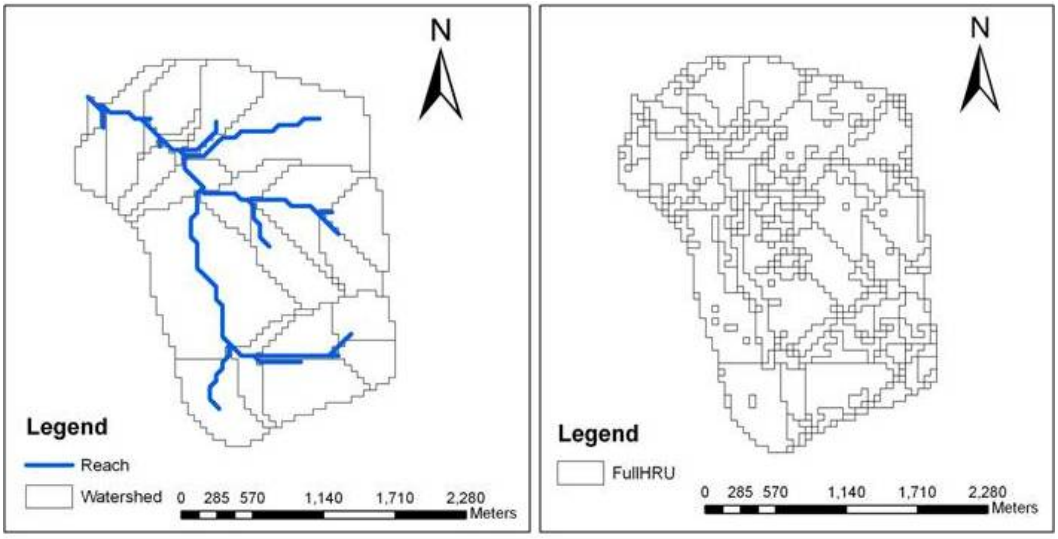

Fig 3. Khadakohol Watershed (a) delineated sub basins and reaches, (b) HRUs

SWAT Model Simulation with Default Parameters

The model has been run for the period 1/6/2002 to 31/7/2002 with default parameters and the management operations scheduled according to heat units (default). The results are tabulated in Table 1.

Table 1. Simulation results with the default parameter set (2002)

2002		Observed		Simulated	
	Rainfall (mm)	Runoff (mm)	Sediment (t/ha)	Runoff (mm)	Sediment (t/ha)
June	682.4	400.29	1.83	369.25	6.72
July	300.8	145.79	0.11	78.50	1.07

Although, for the given rainfall and the catchment hydrology, the simulated runoff seems to be realistic, the simulated sediment yield for the month of June is too high. It may be because; no detail about the soil condition prior to the onset of monsoon is given. All the parameters are set by default and management operations according to heat units. Once the management operations are scheduled by date, the simulations are comparable with the observed data as given in Table 2.

Table 2. Simulation results after scheduling management operations by date (2002)

2002		Observed		Simulated	
	Rainfall (mm)	Runoff (mm)	Sediment (t/ha)	Runoff (mm)	Sediment (t/ha)
June	682.4	400.29	1.83	357.55	1.33
July	300.8	145.79	0.11	74.88	0.19

There is a significant improvement in the simulated sediment yield, but not runoff. Except management operations, rest of the parameter values being still default, it shows that the plant management operations have a greater effect on the sediment yield than runoff. The runoff is under-predicted for both the months. The true representation of catchment hydrology in terms of model parameters is necessary for a good simulation. Hence, the model needs to be calibrated.

Sensitivity Analysis and Calibration of the Model

Since the available information about the catchment hydrology was less, auto-calibration has been preferred before manual calibration. Prior to auto-calibration, a Sensitivity Analysis has been performed for flow and sediment parameters. From the Sensitivity Analysis, 20 parameters are chosen for autocalibration and CN2 and USLE_P have been found to be the most sensitive parameters for flow and sediment respectively. The model has been run with the best parameter set obtained from auto-calibration and the simulation results are shown in Table 3.

Table 3. Simulation results after auto-calibration (2002)

2002		Observed		Simulated	
	Rainfall (mm)	Runoff (mm)	Sediment (t/ha)	Runoff (mm)	Sediment (t/ha)
June	682.4	400.29	1.83	369.38	0.73
July	300.8	145.79	0.11	81.80	0.11

Although there is a little improvement in the runoff, it is still under-predicted and the sediment yield for June is also under-predicted. Overall, the best parameter set from auto-calibration has not given satisfactory results as, in this case, only two monthly outputs are optimized for the Sum of the Squares of the Residuals (SSQs), there might be a possibility that the auto-calibration algorithm has failed to choose the best parameter set. Hence manual calibration has been attempted further and the corresponding simulation results are presented in Table 4.

Table 4. Simulation results after manual calibration (2002)

2002		Observed		Simulated	
	Rainfall (mm)	Runoff (mm)	Sediment (t/ha)	Runoff (mm)	Sediment (t/ha)
June	682.4	400.29	1.83	406.65	1.32
July	300.8	145.79	0.11	102.79	0.19

In general, the outputs are satisfactory after manual calibration. Now, assuming that the parameter set has been optimized to give better simulation results, validation of the model for a fresh data has been opted to test the model.

Validation of the Model

June and July of the year 2003 are chosen for validation of the model. Prior to validation, the model has been run with the default parameters and the results are tabulated in Table 5. Validation results for 2003 are shown in Table 6.

Table 5. Simulation results with default parameter set (2003)

2003		Observed		Simulated	
	Rainfall (mm)	Runoff (mm)	Sediment (t/ha)	Runoff (mm)	Sediment (t/ha)
June	434.40	359.98	0.98	196.78	2.23
July	613.30	570.43	1.82	326.61	6.28

With default parameters, the model has under-predicted runoff and over-predicted sediment yield. High sediment yield could be expected as management operations are not scheduled correctly according to date.

Table 6. Validation results (2003)

2003		**Observed**		**Simulated**	
	Rainfall (mm)	Runoff (mm)	Sediment (t/ha)	Runoff (mm)	Sediment (t/ha)
June	434.40	359.98	0.98	245.10	0.58
July	613.30	570.43	1.82	371.74	0.69

For validation, although the results are improved as compared to those with default parameters, results are under-predicted and are not satisfactory. This could be due to:

1. The best parameter set might not be true representative of the catchment, as the data used for calibration is too small
2. If the best parameter set is assumed to be true representative, it has not worked well for the year 2003 because of different rainfall-runoff conditions. The percentage of observed runoff with respect to rainfall for June and July respectively for 2002 (used for calibration) are 58.66% and 48.33% and for 2003 (used for validation) are 82.87% and 93%.

Since the validation results for 2003 are not satisfactory, it has been tested for another time period i.e., June and July of 2004. The simulation results with default parameter set are shown in Table 7 and validation results are shown in Table 8.

Table 7. Simulation results with default parameter set (2004)

2004		**Observed**		**Simulated**	
	Rainfall (mm)	Runoff (mm)	Sediment (t/ha)	Runoff (mm)	Sediment (t/ha)
June	391.50	193.19	0.22	169.37	2.96
July	604.80	513.44	1.82	297.45	2.87

As expected, the sediment yields are high and the runoff seems to be representative of the watershed, having run the model with default parameters.

Table 8. Validation results (2004)

2004		Observed		Simulated	
	Rainfall (mm)	Runoff (mm)	Sediment (t/ha)	Runoff (mm)	Sediment (t/ha)
June	391.50	193.19	0.22	188.89	0.26
July	604.80	513.44	1.82	341.51	0.23

The validation results show that the model could simulate the runoff and sediment for June month very well. But the results are not matching for the month of July, may be because the observed runoff with respect to rainfall is very high (84.89%). Hence, as discussed earlier, the same reasons hold good for poor simulations.

Spatio-temporal Sediment Yield Distribution

The subbasin-wise monthly sediment yields simulated using SWAT model for Khadakohol watershed is given in Table 9. Using GIS, sediment yield map has been generated for June 2002 and is shown in Fig. 4.

It can be seen from the table that the subbasin 19 has the highest sediment yield rate for all the months. The total agricultural area in the subbasin 19 is 9.75 ha (55.71% of total subbasin area) and 14 ha of the subbasin (80% of total subbasin area) has a slope greater than 10%. The agricultural area, being more prone to erosion, combined with a steep slope has given rise to more sediment yield rate for the subbasin 19.

Table 9. Subbasin wise sediment yield (t/ha) distribution for Khadakohol watershed

Subbasin	Area (ha)	June02	July02	June03	July03	June04	July04
1	2.75	0.655	0.092	0.294	0.337	0.129	0.086
2	27.75	1.672	0.242	0.728	0.863	0.324	0.231
3	21.00	1.519	0.222	0.663	0.791	0.296	0.218
4	12.00	1.647	0.241	0.717	0.862	0.321	0.238
5	5.00	2.322	0.336	1.013	1.208	0.452	0.415
6	11.75	0.952	0.140	0.421	0.505	0.188	0.181
7	2.25	1.859	0.258	0.809	0.918	0.355	0.275
8	25.50	0.996	0.145	0.439	0.515	0.195	0.178
9	0.25	0.837	0.113	0.368	0.406	0.159	0.114
10	71.00	1.571	0.229	0.689	0.820	0.307	0.287
11	16.75	1.671	0.240	0.729	0.855	0.323	0.283
12	19.00	1.784	0.258	0.777	0.923	0.346	0.317
13	35.25	1.529	0.223	0.670	0.800	0.299	0.284
14	22.25	0.925	0.135	0.408	0.485	0.182	0.172
15	16.25	1.579	0.229	0.690	0.819	0.307	0.281
16	26.75	0.705	0.103	0.316	0.371	0.140	0.130
17	103.25	1.004	0.147	0.440	0.523	0.196	0.184
18	15.25	0.332	0.048	0.152	0.176	0.067	0.062
19	17.50	3.529	0.512	1.531	1.815	0.685	0.627
20	17.25	2.090	0.302	0.914	1.085	0.407	0.369
21	13.25	1.819	0.265	0.795	0.954	0.356	0.334
22	32.25	0.941	0.135	0.414	0.481	0.183	0.160
23	32.50	0.479	0.070	0.216	0.250	0.095	0.090

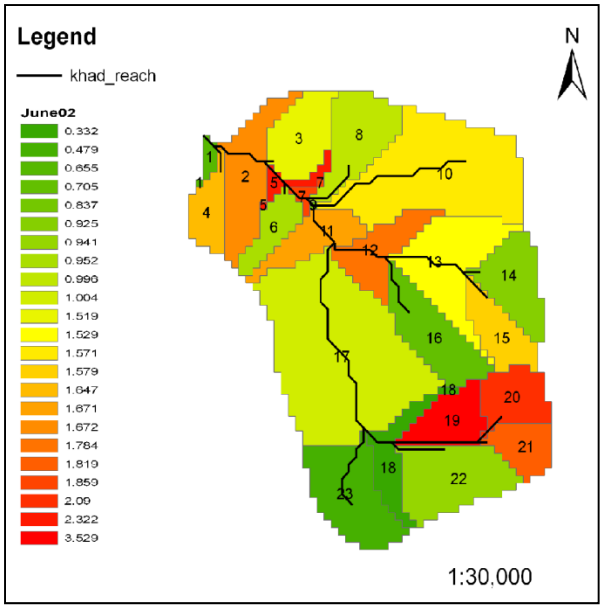

Fig. 4. Sediment yield map for Khadakohol watershed (June, 2002)

Conclusion

Estimation of sediment yield is very important in the effective management of agriculture watersheds. In this study, an attempt has been made to use SWAT model, GIS and remotely sensed data for modelling the runoff and sediment yield of Khadakohol watershed. Based on the SWAT simulation results and its analysis for Khadakohol watershed, the following conclusions are drawn.

1. Computer model such as SWAT integrated with GIS and remote sensing is very effective in runoff and sediment yield simulation of watersheds.

2. The SWAT model gives satisfactory results without even calibration, specifically for runoff as it was observed from several simulations with default parameter sets for various time periods. The results improve with more manual input in the data representative of the watershed. Hence, SWAT model can be used in ungauged watersheds to predict the effect of land management practices on water and sediment.

3. Data of longer duration having wet and dry periods is desirable to calibrate the model. If the data used for auto/manual calibration is too less, the best parameter set obtained will not be representative of the watershed. Hence, the validation results using that parameter set may not match with the observed data.

4. Representation of management practices has a great impact on simulated sediment yield than runoff.

5. The analysis of spatio-temporal distribution of sediment yield show that the subbasins having agricultural areas combined with steep slopes (>10%) yield more sediment.

Further, uncertainty analysis can be carried out to assess the uncertainty associated with the model predictions.

References

Naik, M.G., 2008. Soil erosion and sediment yield modeling of watershed using finite element method, geographical information system and remotely sensed data. Ph.D Thesis, Department of Civil Engineering, Indian Institute of Technology Bombay, Mumbai, India.

Neitsch, S.L., Arnold, J.G., Kiniry, J.R., Williams, J.R., 2005. Soil and Water Assessment Tool Theoretical Documentation, Version 2005, Grassland, Soil and Water Research Laboratory-ARS, and Blackland Research Center, Texas Agricultural Experiment Station, Texas.

White, S., 2005. Sediment yield prediction and modeling. Encyclopedia of Hydrological Sciences, Eds. Anderson, M.G., McDonnell, J.J., Wiley, Chichester, England, 1315-1326.

Wankhede, Z.D.,Dakhole, W.M., Deshmukh, V.S., Shende, N.K., Karale, R.L., 1984. Report on detailed soil survey and land use of sub-watersheds, Damanganga catchment, Peint: Tahsil, Nasik district, Maharashtra, Report No. AGRI-651. All India Soil & Land Use Survey Organization, Ministry of Agriculture, Govt. of India, New Delhi.

Comprehensive Water Stress Indicator

Dr Poonam Ahluwalia

Senior Manager (Environment), TATA Consulting Engineers Limited,

17-18, Zamrudpur Commercial Complex, Kailash Colony extension, New Delhi-110048

Phone: +91 (011) 66169180

Fax: +91 (011) 66169100

Email: poonama@tce.co.in; poonamkahluwalia@yahoo.co.in

Abstract

Water stress refers to economic, social, or environmental problems caused by unmet water needs. The three major sectors exerting water demand are domestic, agriculture and Industry. Each country / region has a different allocation pattern to each of these sectors depending on the landuse and economy. Although several indices have been developed to indicate water stress affected areas, there is a need to modify these for developing nations like India to effectively take into account practical conditions such as intermittent supply hours and increasing use of grey/ recycled water for non potable uses. The current study builds up on the available indices to propose computation of three sector wise water stress indicators (taking into consideration these practical aspects). The advantage of segregating the index sector wise at the initial stage is to get an indication of the sector wise deficit/ surplus to adequately plan for addressing the issue. For example a surplus in agriculture sector could be utilized preferentially for domestic sector as it is perceived to have more influence on the overall water stress in a region. After determining the individual indicators, an overall indicator can be arrived at after assigning suitable weightages (region specific) to each sector.

Key Words: Water Scarcity, Water Stress, Water Demand

Introduction

Water stress and water scarcity occur when the demand for water exceeds the available amount during a certain period or when poor quality restricts its use. Scarcity can be absolute, such as in environments of low precipitation and large evapo-transpiration rates. It can also, however, be induced by economic or political constraints, which do not permit the adequate development of water resources. Critical conditions often arise for economically poor and politically weak communities living in already dry environments. The United Nations' FAO states that by 2025, 1.8 billion people will be living in countries or regions with absolute water scarcity, and two-thirds of the world population could be under stress conditions (FAO, 2012).

A country or region is said to experience "water stress" when annual water supplies drop below 1,700 cubic meters per person per year, according to the Falkenmark Water Stress Indicator (Falkenmark and Lindh, 1976). At levels between 1,700 and 1,000 cubic meters per person per year, periodic or limited water shortages can be expected. When water supplies drop below 1,000 cubic meters per person per year, the country is said to be facing "water scarcity" (Larsen 2012).

According to the UNDP, the population of a country whose renewable fresh water availability falls below 1,700 m3/person/year (m3/ppy) will experience "water stress," and a "chronic water shortage" when availability falls below 1,000m3/ppy (Hinrichsen and Tacio, 1997; Ahmad et al., 2001; Shiva, 2002). The major industrial economies of Australia, India, China, and U.S. are rated as 'high risk' in a new study evaluating the vulnerability of 159 countries to water stress, while the regions of the Middle East and North Africa are at the highest risk.

The average water availability in India in 1951 was 3,540 m^3/person/year (m^3/ppy). By the late 1990s, it had fallen to 1,250 m^3/ppy. By 2050, some project a drop below 750 m^3/ppy (Shiva, 2002). A study has stated that in India, "gross per capita water availability" will decline from around 1,820 cubic metres a year to as low as around 1,140 cubic metres a year in 2050 (Gupta and Deshpande, 2004). Many aquifers have been over-pumped and are not recharging quickly. Quite a few of the available fresh water resources have become polluted, salted, unsuitable or otherwise unavailable for drinking, industry and agriculture.

Experts say incorporating water improvements into economic development is necessary to end the severe problems caused by water stress and to improve public health and advance the economic stability of the region. Because water sources are often cross-border, conflict emerges. Successful transboundary water laws have historically been multilateral and focus on joint management and development of resources. Experts say that regardless of a country's water abundance or scarcity, development is the only means to ease future water stress.

Most municipalities are planning for Improvement and Revamping the Existing Water Supply System to effectively meet the gap between water supply and demand. However, owing to crunch of financial resources and mega size of the project command areas, the authorities are interested to know critical areas where water efficiency/ water resource development has to be taken on priority, to suitably phase out the proposal for revamping/ improvement of water supply systems.

The following section details a few key water stress indicators developed so far.

Indices Developed for Water Stress

The difficulty of characterizing water stress is that there are many equally important facets to water use, supply and scarcity. Selecting the criteria by which water is assessed can be as much a policy decision as a scientific decision. The indices existing can be broadly grouped into the following categories:

1. Indices Based on Human Water Requirements
2. Water Resources Vulnerability Indices
3. Indices Incorporating Environmental Water Requirements
4. Indices based on LCA and Water Footprint

Indices Based on Human Water Requirements

The logic behind these indices is that if the water necessary to meet human demands is known, then the water that is available to each person can serve as a measure of scarcity (Rijsberman,

2006). The Falkenmark indicator (Falkenmark and Lindh, 1976) is perhaps the most widely used measure of water stress. It is defined as the fraction of the total annual runoff available for human use. Water scarcity index has also been developed a water scarcity index as a measurement of the ability to meet all water requirements for basic human needs: drinking water for survival, water for human hygiene, water for sanitation services, and modest household needs for preparing food (Gleick, 1996). Both Falkenmark and Gleick developed a benchmark of 1,000m^3 per capita per year as a standard that has been accepted by the World Bank (Gleick, 1995; Falkenmark and Widstrand, 1992). Building on the Falkenmark indicator, a study (Ohlsson, 2000) integrated the adaptive capacity of a society to consider how economic, technological, or other means affect the overall freshwater availability status of a region. This index is known as UNDP Human Development Index (HDI) which functions as a weighted measure of the Falkenmark indicator in order to account for the ability to adapt to water stress and is also termed the Social Water Stress Index.

The relative water stress index as prepared by Water Systems Analysis Group, University of New Hampshire (UNH) proposed water stress to be computed as ratio of product of domestic water demand (km^3/yr), Industrial water demand (km3/yr) and Agricultural water demand (km3/yr), to water supply (km^3/yr) (Relative Water Stress Index, 2009). Population exposed to water stress was computed by setting a water stress threshold of 0.4 and then summing the number of people in each grid cell that is above or below this threshold. Number of people exposed to water stress was typically presented as number of people (in thousands) per grid cell.

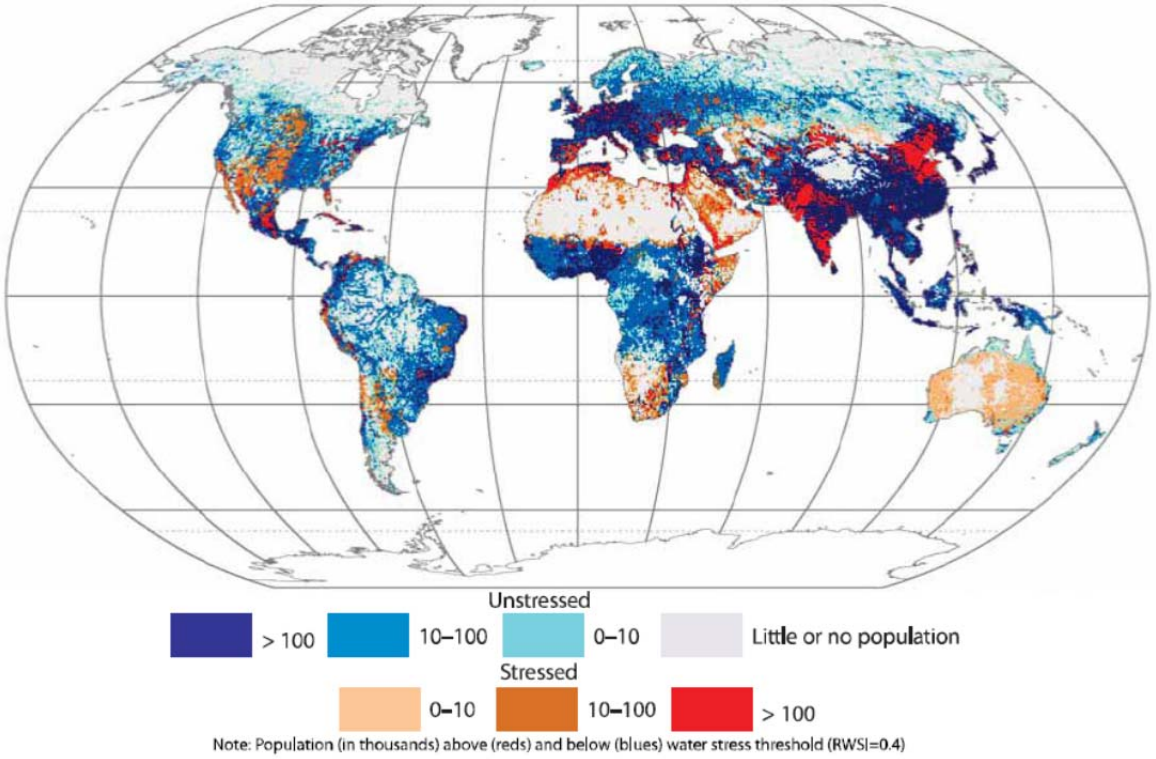

Figure 1: Water Stressed Areas as determined by Relative water stress indicator proposed by Water Systems Analysis Group, University of New Hampshire (UNH)

Water Resources Vulnerability Indices

These indices go one step further than considering human water requirements and water availability and incorporate renewable water supply and national, annual demand for water. The Water Resources Vulnerability Index, sometimes referred to as the WTA ratio, is one such example which was developed as the ratio of total annual withdrawals to available water resources. A country is considered water scarce if annual withdrawals are between 20 and 40% of annual supply, and severely water scarce if withdrawals exceed 40% (Raskin et al., 1997).

A Watershed Sustainability Index (WSI) incorporating hydrology, environment, life, and policy has been proposed which is structured to be watershed or basin specific and intended for a maximum area of 2,500 km^2 (Chaves and Alipaz, 2007) . Larger areas would need to be broken down into smaller sections. The WSI (0-1) is the average of four indicators; the hydrologic indicator H (0-1); the environmental indicator E (0-1); the life (human) indicator L (0-1); and the policy indicator P (0-1). Each parameter is given a score of 0, 0.25, 0.50, 0.75, or 1.0. All indicators are equal in weight, although parameters may vary from basin to basin, and should be chosen by consensus among stakeholders.

A new hydrologic term "Water Supply Stress Index" (WaSSI) has been proposed to quantitatively assess the relative magnitude of water supply and demand at the 8-digit USGS Hydrologic Unit Code (HUC) level (McNulty et al., 2010). WaSSI although similar to the WTA, is unique from other water availability measurement tools in that factors in anthropogenic water demand. Therefore, it is possible to have areas with high annual levels of precipitation to have a high WaSSI value.

International Water Management Institute (IWMI) (Comprehensive Assessment of Water Management in Agriculture, 2007) used a similar water scarcity assessment though on a slightly larger scale across the entire globe. They conducted an analysis that considered the portion of renewable freshwater resources available for human requirements (accounting for existing water infrastructure), with respect to the main water supply. The Analysis labeled countries as "physically water scarce" when more than 75% of river flows are withdrawn for agriculture, industry, and domestic purposes. This implies that dry areas are not necessarily water scarce. Indicators of physical water scarcity include: acute environmental degradation, diminishing groundwater, and water allocations that support some sectors over others. Countries having adequate renewable resources with less than 25% of water from rivers withdrawn for human purposes, but needing to make significant improvements in existing water infrastructure to make such resources available for use, are considered "economically water scarce" (Seckler et al., 1998). The IWMI assessed the global freshwater resources status and mapped the regions indicative of none or little, physical, approaching physical, and economic water scarcity (refer figure below).

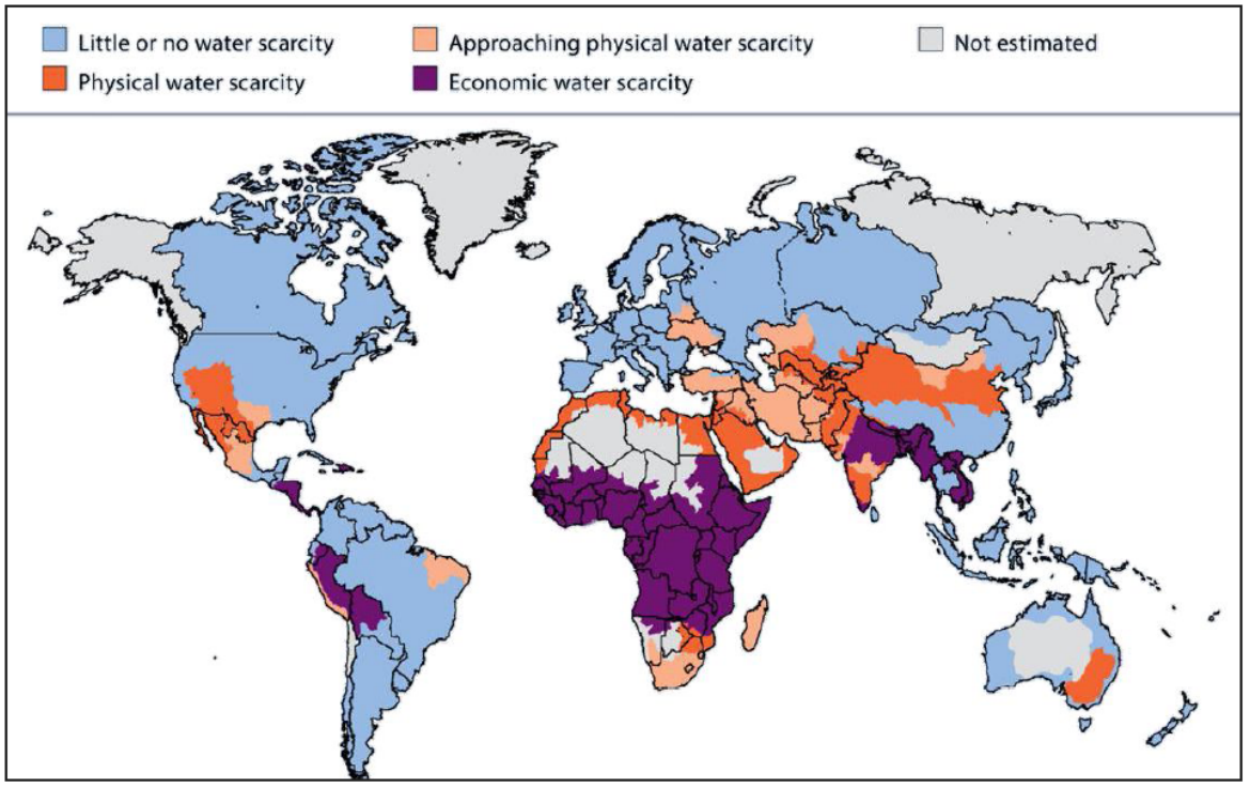

Figure 2: Areas of physical and economical water scarcity on a basin level in 2007 (Comprehensive Assessment of Water Management in Agriculture, 2007)

The Water Stress Index, developed by global risks advisory firm Maplecroft (2010) has identified the risks from water scarcity to governments, population, and business. It has been calculated by evaluating the ratio of a country's total water use from domestic, agriculture, and industrial use, to the renewable supply of water from precipitation, rivers, streams, and groundwater. The index is accompanied by a sub-national map, which utilises GIS technology, pinpointing global water stress down to 50sqkm worldwide (refer Figure 3).

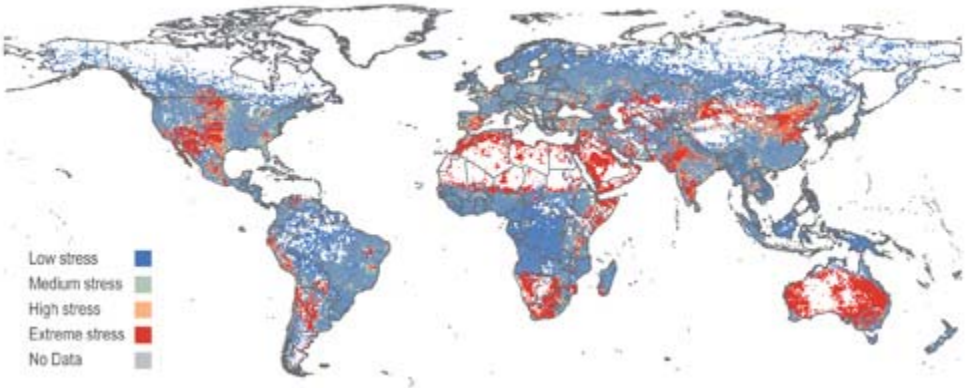

Figure 3: Water Stressed Areas as determined by Water Stress Index proposed by Maplecroft

According to Maplecroft, expanding populations, such as India's, which grew 1.3% in 2009, together with rising global temperatures, indicate that water stress will continue to be a challenge for governments, business and society.

Indices Incorporating Environmental Water Requirements

Every aquatic ecosystem requires a certain amount of water to sustain their ecological processes and their animal and plant communities. Recognition of the need to establish environmental water requirements, has resulted in the development of concepts such as environmental or instream flow requirements, or environmental water allocations. Methods used to estimate environmental water demand range from purely hydrological models to holistic multidisciplinary methodologies.

The Dublin conference in 1992 concluded that "since water sustains all life, effective management of water resources demands a holistic approach, linking social and economic development with protection of natural eco systems" (ICWE, 1992).

It has further been reported that depleted freshwater resources are linked to ecosystem degradation, and therefore, any index of water poverty should include the condition of ecosystems that maintain sustainable levels of water availability (Sullivan, 2002). However, this approach is critically dependent on the development of standardized weights to be applied to each of the variables such as ecosystem productivity, community, human health, and economic welfare. The problem therein lies with the basis of these weights as well as the assumption that the weights hold true for all ecosystems, communities, economies, and cultures.

An Environmental Water Stress Indicator has been proposed based water required for the maintenance of freshwater-dependent ecosystems per river basin (Smakhtin et al., 2005). The water stress indicator provides information/ analysis on the proportion of the utilizable water in world river basins currently withdrawn for direct human use and where this use is in conflict with environmental water requirements. Figure 4 shows the map depicting the results of the same in the form of a Digital Environmental Water Stress Indicator (Available at: http://atlas.gwsp.org) .

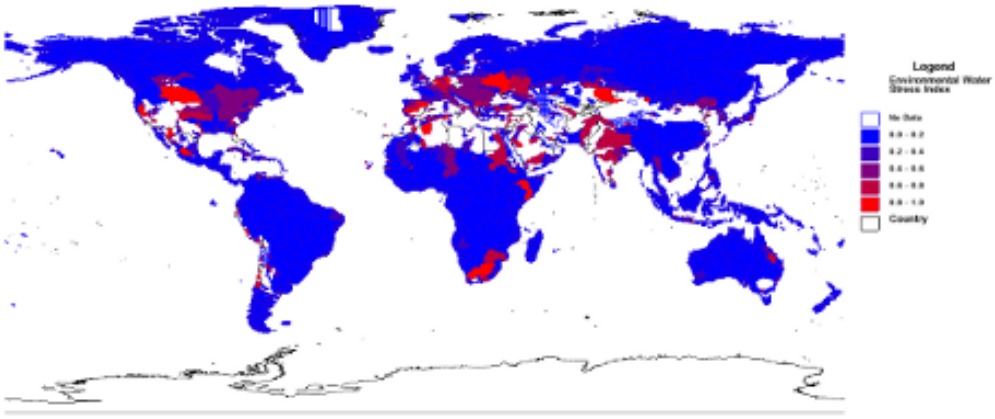

Figure 4: Water Stressed Areas as determined by Environmental Water Stress Indicator

World resources Institute developed a map (refer Figure 5) based on basin-specific information on river discharges and water use simulated by the global water model WaterGAP 2 (Alcamo et al., 2003; Döll et al., 2003) and a simple conceptual rule for estimation of environmental water requirements from simulated hydrological records. In this map, the term environmental water scarcity (represented as a water stress indicator on the map) (EWSI, 2003), refers to cases where the amount of water removed from the system puts the ecosystem at risk by tapping into the environmental water demand-–that is, the amount of water needed to sustain the integrity of the ecosystem. This concept is similar to the human water scarcity measures that put people and development at risk when there is not enough water to meet their needs.

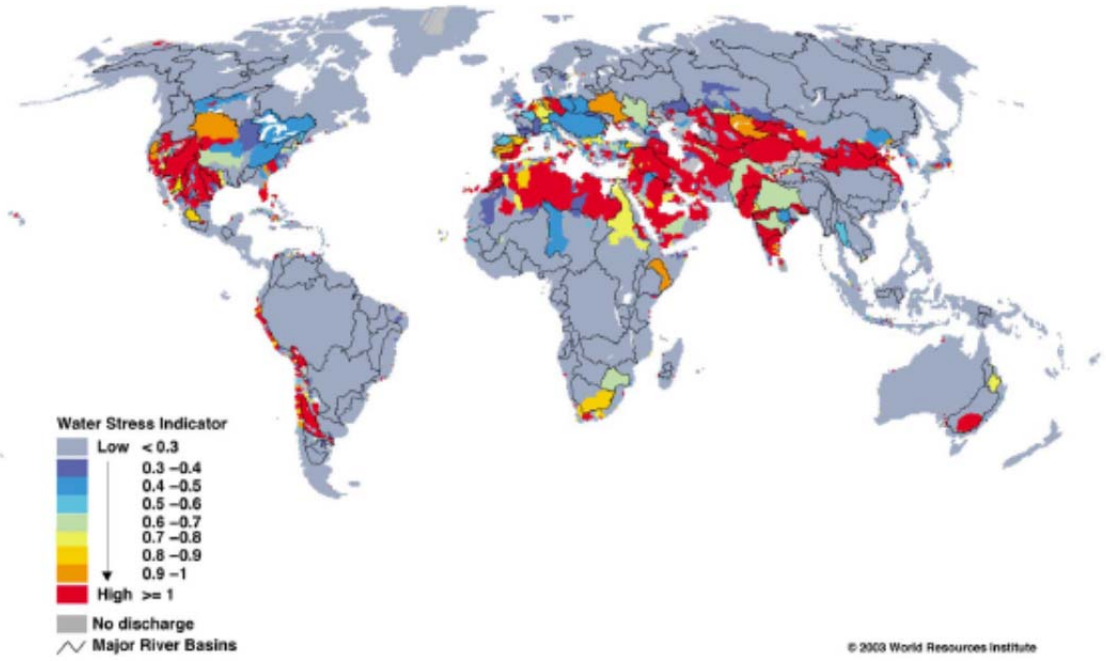

Figure 5: Environmental water scarcity (represented as a water stress indicator) proposed by International World Resources Institute

A study proposed a Water Stress Index (WSI) by referring to theories and indexes already developed and applied in other countries and taking into consideration the appropriate situation and condition of Indonesia in general and Jakarta in particular (Ali, 2010). WSI consisted of 3 (three) components namely Water resources (consisting of three indicators, namely water resources potential/availability, piped water coverage, and water resources continuity); Ecosystem (which described water quality properly used both for the piped water system as well as non-piped water system, i.e., surface water and groundwater) and Water consumption (which described how much water need of the population of a certain area, use of drinking water sources and affordability or ability of the population to obtain supply of water).

Do we need another water stress indicator?

Although several indices have been developed to indicate water stress affected areas, there is a need to modify these to relate more effectively to the urban growth centres. In the context of a an urban or a peri-urban centre of developing nations like India, the water stress indicator has to effectively take into account practical conditions such as intermittent supply hours and increasing use of grey/ recycled water for non potable uses. Also India has typical unique features wrt to

water resources, rapid development, growing population, extreme climate variation and landuse which set it apart from other regions on the global arena.

As compared to 70% of freshwater use being used worldwide for agriculture (Pimentel et al., 2004), in Indian water scenario 88 per cent of water is being utilised for agriculture (Pandey, 2009). As per a world Bank study, of the 27 Asian cities with population of over 10 lakh, Chennai and Delhi were ranked as the worst performing metropolitan cities in terms of water availability per day, while Mumbai was ranked as second worst performer and Calcutta fourth (World Bank, 2001).

The current study builds up from the available indices to suggest a comprehensive indicator for urban and peri-urban growth centres of developing nations like India. The index can provide the authorities with a scientific basis to suitably phase out the proposed revamping/ rehabilitation of water supply projects.

Proposed Water Stress Indicator

The three major sectors exerting water demand in urban and peri-urban areas are domestic, agriculture and Industry. Each country / region has a different allocation pattern to each of these sectors depending on the landuse and economy. However, it would be incorrect to assign equal weightage/ significance to each of these sectors while computing water stress. The current study proposes computation of three sector wise water stress indicators which could be integrated to arrive at a single stress indicator. The methodology for estimating the three sector wise indicators is detailed below:

Domestic Water Stress Indicator (DWSI)

This could be estimated as ratio of domestic water supply of potable quality to domestic water demand. The domestic water demand could be estimated as product of population (in numbers) and the per capita water supply norms as specified by the concerned authority (e.g, CPHEEO in India). The domestic water supply could be further classified as water supply available with desirable quality and that of acceptable quality (refer IS 104500). The water supply meeting the acceptable quality criteria but failing to meet the desirable quality parameters could be multiplied by a factor (say 0.9) to suitably account for water of lower quality standards. Water supply failing to meet the acceptable water quality criteria should not be taken into account as available.

Agriculture Water Stress Indicator (AWSI)

As the demand for agriculture in a region varies significantly with season, this index could be calculated for each prominent crop season. This could be estimated as ratio of seasonal water supply for irrigation (including the supply from both fresh and recycled water meeting the norms for use in irrigation) to the ratio of irrigation demand in that season. Owing to the psychological nature of impacts associated with water scarcity, the least of the values for all seasons should be taken as an indicator of water stress wrt to agriculture in the area

Industrial Water Stress Indicator (AWSI)

This could be estimated as ratio of water allocated for industrial applications (including the supply from both fresh and recycled water) to the ratio of industrial demand in that area.

A value of 1 for the above mentioned indicators implies NIL water stress. A value more than 1 implies surplus water availability and less than 1 implies a condition of water stress (the lesser the value the more the degree of the water stress is implied).

Even though water is a basic need for mankind, there is a general unwillingness to pay for the same. Perception of affordability of water supply also governs the quantum of water stress and hence needs to be taken into account. Being a developing nation with a large population on the negative side of the poverty line, economic water scarcity (limited access to fresh water due to lower affordability) assumes equal, if not, greater importance as that of physical water scarcity. The threshold of affordability needs to defined specific to a sector and can be designated as a value equal to 1 for reasonably affordable level, ranging from 1 to 2 for easily affordable level and 0.5 to 1 depending on the degree of difficulty perceived in affording the allocated supply.

The other significant factor which affects the magnitude of water stress is the reliability of water supply. The stress induced by intermittent supply with fixed/ reliable supply hours is less as compared to intermittent supply with unreliable supply hours. The factor could be taken as 1 for 24 x 7 supply, 0.8 for intermittent but reliable supply for more than 6 hours per day and 0.7 for intermittent but reliable supply of less than 6 hours per day. The factor could be taken as 0.5 for unreliable and intermittent supply.

The advantage of segregating the index sector wise at the initial stage is to get an indication of the sector wise deficit/ surplus to adequately plan for addressing the issue. For example a surplus in agriculture sector should be utilized preferentially for domestic sector as it has more influence on the overall water stress in a region.

The sector wise water stress indicators could be multiplied by affordability and reliability factors specific to their sectors to effectively take these practical considerations into account.

After determining the individual indicators, an overall indicator can be arrived at after assigning suitable weightages to each sector. For example, the weightage assigned to DWSI, AWSI and IWSI could be 40%, 35% and 25% respectively.

Also the current water stress indicator needs to be read in conjunction with future projected/ envisaged water stress, wherein the analysis could be done taking into account the forecasted population, forecasted increase/ decrease in per capita demand for water and forecasted resource availability. This should be done at the sectoral level, before integration into one single future water stress indicator.

Summary and Conclusions

There is a increasing awareness that our freshwater resources are limited and need to be protected both in terms of quantity and quality. This water challenge affects not only the water community, but also decision-makers and every human being. With urbanization and changes in lifestyle, water consumption is bound to increase. The key focus areas are:

- Preserving existing water resources
- Improving access to potable water
- Improving transboundary cooperation

However since the authority managing the water supply system is a different entity for each urban / peri-urban centre, an assessment of water scarcity and its quantification of its psychological impacts in terms of a comprehensive water stress indicator is required at an urban/ peri-urban level. The present study has attempted to develop a comprehensive water stress

indicator which can be utilized to quantify the extent of the problem and identify the high priority areas requiring immediate attention in terms of rehabilitation of water supply systems.

References

Ahmad, Q.K., Biwas, A.K., Rangashari, R., and Sainju, M.M. (Eds) 2001. Ganges-Brahmaputra-Meghna Region: A Framework for Sustainable Development, The University Press, Dhaka.

Alcamo, J., Döll, P., Henrichs, T., Kaspar, F., Lehner, B., Rösch, T., and Siebert, S. 2003. WaterGAP 2: A model for global assessment of freshwater resources. Hydrological Sciences Journal. Vol: 48(3): 317-337.

Ali, F. 2010. Development of water stress index as a tool for the assessment of water stress in metropolitan Jakarta presented at the sixteenth annual international sustainable development research conference, Hongkong. Available at: http://www.kadinst.hku.hk/sdconf10/Papers_PDF/p551.pdf Accessed 15 January 2012.

Chaves, H. M. L., and Alipaz, S. 2007. An Integrated Indicator Based on Basin Hydrology, Environment, Life, and Policy: The Watershed Sustainability Index. *Water Resour Manage* (Springer) 21: 883-895.

Comprehensive Assessment of Water Management in Agriculture. 2007. Water for Food, Water for Life: A Comprehensive Assessment of Water Management in Agriculture. London: Earthscan, and Colombo: International Water Management Institute.

Digital Environmental Water Stress Indicator. Available at: http://atlas.gwsp.org Accessed 20 March 2012.

Döll, P., Kaspar, F., and Lehner, B. 2003. A global hydrological model for deriving water availability indicators: model tuning and validation. J. Hydrol. Vol: 270, Issue: 1-2, Pages: 105-134.

EWSI (Environmental Water Scarcity Index by Basin). 2003. Available at: http://pdf.wri.org/watersheds_2003/gm16.pdf Accessed 20 March 2012.

Falkenmark, M. and Lindh, G. 1976. Quoted in UNEP/WMO. Climate Change 2001: Working Group II: Impacts, Adaptation and Vulnerability. UNEP. Available at: http://www.grida.no/climate/ipcc_tar/wg2/180.htm Accessed 15 January 2012.

Falkenmark, M., and Widstrand, C. 1992. Population and Water Resources: A Delicate Balance. *Population Bulletin, Population Reference Bureau*.

FAO. 2012. Hot issues: Water scarcity. Available at: http://www.fao.org/nr/water/issues/scarcity.html Accessed 20 January 2012.

Gleick, P. 1995. Human Population and Water: To the limits in the 21st Century. Human Population and Water, Fisheries, and Coastal Areas. Washington, D.C.: American Association for the Advancement of Science Symposium.

Gleick, P. H. 1996. Basic Water Requirements for Human Activities: Meeting Basic Needs. *Water International (IWRA)* 21: 83-92.

Gupta, S. K., and Deshpande, R. D. 2004. Water for India in 2050: first-order assessment of available options. *Current Science*, Vol. 86(9): 1216-1224. Available at: http://www.iisc.ernet.in/currsci/may102004/1216.pdf Accessed 15 March 2012.

Hinrichsen, D., and Tacio, H. 1997. The Coming Freshwater Crisis is Already Here. *Finding the Source: The Linkages between Population and Water*, Woodrow Wilson Center, Washington, D.C.

ICWE "International Conference on Water and the Environment". 1992. "The Dublin statement and record of the Conference." WMO. Geneva, Available at: http://www.gdrc.org/uem/water/dublin-statement.html Accessed 20 January 2012.

Larsen, S. T. L. 2012. "Lack of Freshwater Throughout the World". Evergreen State College. Available at: http://academic.evergreen.edu/g/grossmaz/LARSENST/ Accessed 15 March 2012.

Maplecroft. 2010. Key economies of Australia, India, China and USA at 'high risk' from water stress; Middle East and North Africa most at risk dated 11/11/2010. Available at: http://www.maplecroft.com/about/news/water-stress.html Accessed 15 January 2012.

McNulty, S., Sun, G., Myers, J. A. M., Cohen, E., and Caldwell, P. 2010. Robbing Peter to Pay Paul: Tradeoffs between Ecosystem Carbon Sequestration and Water Yield. *Proceedings of the Watershed Management Conference 2010: Innovations in Watershed Management under Land Use and Climate Change*. doi:http://dx.doi.org/10.1061/41143(394)10

Ohlsson, L. 2000. Water Conflicts and Social Resource Scarcity. *Phys. Chem. Earth* 25(3): 213-220.

Pandey, M.M. 2009. Indian Agriculture – An Introduction. Submitted to Fourth Session of the Technical Committee of APCAEM 10-12 February 2009, Chiang Rai, Thailand. Available at: http://www.unapcaem.org/Activities%20Files/A0902/in-p.pdf Accessed 20 January 2012.

Pimentel, D., Berger, B., Filberto, D., Newton, M., Wolfe, B., Karabinakis, E., Clark, S., Poon, E., Abbett, E., and Nandagopal, S. 2004. "Water Resources: Agricultural and Environmental Issues". Bioscience October. Available at: http://ecommons.cornell.edu/bitstream/1813/352/1/pimentel_report_04-1.pdf Accessed 20 January 2012.

Raskin, P., Gleick, P., Kirshen, P., Pontius, G., and Strzepek, K. 1997. Water futures: Assessment of long-range patterns and prospects, Stockholm Environment Institute, Stockholm, Sweden.

Relative Water Stress Index. 2009. . Available at: http://www.unesco.org/new/fileadmin/MULTIMEDIA/HQ/SC/pdf/wwap_A3_Relative_water_stress_index.pdf Accessed 15 March 2012.

Rijsberman, F. R. 2006. Water scarcity: Fact or Fiction? *Agricultural Water Management*, 80: 5-22.

Seckler, D., Molden, D., and Barker, R. 1998. Water Scarcity in the Twenty-First Century. Water Brief 1, International Water Management Institute, Colombo, Sri Lanka: IWMI. Available at: http://pdf.usaid.gov/pdf_docs/PNACH595.pdf Accessed 20 January 2012.

Shiva, V. 2002. Water Wars: Privatization, Pollution, and Profit, South End Press.

Smakhtin, V., Revanga, C., and Doll, P. 2005. Taking into Account Environmental Water Requirements in Globalscale Water Resources Assessments. IWMI The Global Podium. Available at: http://podium.iwmi.org/podium/Doc_Summary.asp Accessed 20 January 2012.

Sullivan, C. A. 2002. Calculating a Water Poverty Index. World Development (Elsevier Science Ltd) 30, no.7: 1195-1210.

World Bank (2001): Background Paper - International Conference on New Perspectives on Water for Urban & Rural India - 18-19 September, 2001, New Delhi, as cited on CSE webnet, Available at: http://www.rainwaterharvesting.org/crisis/Urbanwater-scenario.htm Accessed 20 January 2012.

SWAT 2012
IIT Delhi, India

We would like to thank the following Conference Sponsors

giz Deutsche Gesellschaft für Internationale Zusammenarbeit (GIZ) GmbH

INRM Consultants Pvt Ltd
(Incubatee Company established through TBIU system of IIT Delhi)
Integrated Natural Resource Management - Solutions with Modeling and Geoinformatics

UKaid from the Department for International Development

भाकृअनुप ICAR

COOPERATION
REPUBLIC OF INDIA
FEDERAL REPUBLIC OF GERMANY

एनटीपीसी NTPC

esri India

Green Shakti Foundation

USDA United States Department of Agriculture

ARS

AgriLIFE RESEARCH Texas A&M System

Indian Institute of Technology Delhi
Hauz Khas, New Delhi – 100 016 India
Tel.: +91-11-2659 1241 Fax: +91-11-2658 1117
E-MAIL: hodcivil@admin.iitd.ac.in
Website: http://civil.iitd.ac.in